

The Synthesis, Thermal and Photochemical Properties of Cyclophanedienes and Dihdropyrenes with Different Internal Substituents

by

Khurshid Ayub

B.Sc. University of the Punjab, Lahore, Pakistan, 1999

M.Sc. University of the Punjab, Lahore, Pakistan, 2002

A Dissertation Submitted in Partial Fulfillment of the
Requirements for the Degree of

DOCTOR OF PHILOSOPHY

in the Department of Chemistry

© Khurshid Ayub, 2008
University of Victoria

All rights reserved. This dissertation may not be reproduced in whole or in part, by
photocopy or other means, without the permission of the author.

The Synthesis, Thermal and Photochemical Properties of Cyclophanedienes and Dihydropyrenes with Different Internal Substituents

by

Khurshid Ayub

B.Sc. University of the Punjab, Lahore, Pakistan, 1999

M.Sc. University of the Punjab, Lahore, Pakistan, 2002

Supervisory Committee

Dr. Reginald H. Mitchell, Supervisor

(Department of Chemistry)

Dr. Frank C. J. M. van Veggel, Departmental Member

(Department of Chemistry)

Dr. Robin G. Hicks, Departmental Member

(Department of Chemistry)

Dr. Ben F. Koop, Outside Member

(Biology department, Centre for Biomedical Research)

Supervisory Committee

Dr. Reginald H. Mitchell, Supervisor
(Department of Chemistry)

Dr. Frank C. J. M. van Veggel, Departmental Member
(Department of Chemistry)

Dr. Robin G. Hicks, Departmental Member
(Department of Chemistry)

Dr. Ben F. Koop, Outside Member
(Biology department, Centre for Biomedical Research)

Abstract

A series of cyclophanedienes (CPDs) with different internal functional groups were synthesized. Dicyano CPD **85**, cyano methyl CPD **127** and phenylethynyl/methyl CPD **138** were synthesized from bis-bromomethyl aromatics via a thiacyclophane-thiomethylcyclophane route. Diformyl cyclophanediene **152** and bis(hydroxymethyl) CPD **159** were obtained by the functional group transformation of CPDs **85** and **152** respectively. Cyclophanedienes with internal olefinic groups were obtained by three different routes: the best was the functional group transformations of the dicyano mercaptomethylcyclophane **99** followed by a Hoffmann elimination. Using the best synthetic route, CPDs with substituted vinyl groups such as alkylvinyl (**162**, **163**, **178** and **198**), butadienyl (**184**, **185** and **186**), styryl (**202**, **203** and **204**), nitro-substituted styryl (**210**, **211** and **212**), methoxy-substituted styryl (**218**, **219** and **220**) and methyl-

substituted styryl (**226**, **227** and **228**) were synthesized. Cyclophanediene **235** with an internal ethynyl (alkynyl) group was also synthesized by a similar synthetic route; however, it gave two major interesting side products; vinyl-ethynyl CPD **237** and vinyl-styryl CPD **240**. The cyclophanedienes except dicyano **85**, cyano-methyl **127** and diformyl **152** were converted to their corresponding dihydropyrenes both thermally and photochemically. Dicyano CPD **85** and cyano-methyl CPD **127** were converted photochemically to the DHPs **86** and **128**, respectively. Diformyl CPD **152** underwent decomposition in any attempt to transform it into the DHP **154** either thermally or photochemically. Diphenylethynyl DHPs **141** and **247** were obtained by the Sonogashira coupling of diethynyl DHP **236**. The Eglinton coupling reaction was used to achieve butadiynyl DHPs **257** and **254**. Naphthoyl DHPs **248** and **250** were synthesized by the Friedel-Crafts acylation reaction of DHPs **179** and **167**, respectively. All compounds were characterized by NMR, IR, and UV spectroscopy and mass spectrometry.

Dicyano CPD **85** was quite stable towards thermal isomerization to the dihydropyrene **86** and showed a calculated half life of ~ 36 years (three orders of magnitude higher than that of benzo CPD **53** i.e., 7.3 days) at room temperature, whereas CPDs **127** (cyano methyl), **138** (phenylethynyl/methyl) and **152** (diformyl) showed half lives less than a month at 20 °C. Cyclophanedienes with internal ethynyl and substituted vinyl groups were quite stable thermally and showed half lives of several years (1-16 years) at room temperature. CPDs with *cis* substituted internal vinyl groups were thermally more stable than their *trans* counterparts. Electron withdrawing substituent (NO₂) at the *para* positions of the internal styryl groups accelerate, whereas electron donating groups (MeO, Me) decelerate the thermal return reaction. Naphthoyl CPDs **249**

and **251** isomerized at rates about 6-12 times faster than their non naphthoylated analogues **178** and **166** respectively.

DHPs with internal ethenyl (**167**, **238** and **241**), substituted ethynyl (**139**, **141** and **247**) and *trans* substituted vinyl (**199**, **207**, **215**, **223** and **231**) groups failed to open under visible light irradiation. Dicyano DHP **86**, diethynyl DHP **236** and the unsymmetrical isomers of internal olefinic CPDs (**206**, **214**, **222** and **230**) formed photostationary states (pss). Disubstituted vinyl (**179**) and *cis* substituted vinyl DHPs (**164**, **205**, **213**, **221** and **229**) opened completely; however their opening rates although faster than the parent **43**, were 4-6 times slower than the benzo DHP **47**. Introduction of an electron withdrawing substituent on the internal styryl group decelerated the visible opening reaction whereas electron donating groups accelerated it. 2-Naphthoyl divinyl DHP **250** opened at rates quite comparable to those of benzo DHP **47** whereas 2-naphthoyl diisobutenyl **248** opened about 25 times faster than the benzo DHP.

The [1,5]-sigmatropic rearrangement of the internal nitrile (DHPs **86** and **128**) and formyl (DHP **153**) groups was observed. The sigmatropic rearrangement of the nitrile group in **86** was quite favorable in CDCl₃ ($E_{\text{act}} = 23.4 \pm 0.7$ kcal/mol) compared to benzene ($E_{\text{act}} = 28.6 \pm 1.2$ kcal/mol). Formyl groups showed a much higher migration aptitude and E_{act} is estimated to be < 20 kcal/mol in any solvent.

In this study, the best switch pair obtained was naphthoyl diisobutyl **248/249** which in comparison with previously the best switch pair **47/53** (benzo) showed much higher stability of the cyclophanedienene (two orders of magnitude); moreover, the dihydropyrene opened about 25 times faster as well and is one of the best new photochromes yet.

Table of Contents

Supervisory Committee	ii
Abstract.....	iii
Table of Contents.....	vi
List of Tables	xiv
List of Appendix Tables	xv
List of Figures.....	xxi
List of Schemes.....	xxiii
List of Numbered Compounds	xxviii
List of Symbols, Abbreviations and Nomenclature	xlviii
Acknowledgement	liii
Chapter 1: Introduction.....	1
1.1 Introduction.....	1
1.2 Molecular switches.....	1
1.3 Photochromism	2
1.3.1 <i>Cis-trans (E/Z)</i> isomerization.....	3
1.3.2 Intramolecular hydrogen transfer	5
1.3.3 Intramolecular group transfer.....	6
1.3.4 Dissociation processes.....	6
1.3.5 Oxido-reduction (electron transfer) processes	7
1.3.6 Pericyclic reactions	8
1.3.6.1 Cycloaddition reactions	8
[4 + 4] cycloadditions	9
[2 + 2] Cycloadditions	9
1.3.6.2 Electrocyclic reactions.....	10

Fulgides /Fulgimides/ Fulgenates	11
Spirooxazine and spiropyrans	13
Dithienylethenes	14
1.4 Dihydropyrene photoswitches.....	17
1.4.1 Tedious syntheses.....	18
1.4.2 Quantum yield	19
1.4.3 Decompositions/side reactions	20
1.4.4 Thermal return.....	20
1.5 The nature of the transition state.....	21
1.5.1 Radicals	25
1.5.2 The effect of the internal substituent on the thermal closing	27
1.5.3 The effect of substituents at the 1 and 8 positions on the thermal closing	28
1.5.4 The effect of substituents at other positions.....	29
1.5.5 Substituent effects in other photochromic systems	29
1.6 Thesis Research Objectives.....	31
Chapter 2: Syntheses.....	32
2.1 Synthesis of the CPD/DHP pair 85 , 86 with internal nitrile groups	32
2.1.1 Synthesis of 2,6-bis-bromomethylbenzotrile 102	33
2.1.2 Synthesis of dicyanothiacyclophanes 100 and 108	34
2.1.3 The Stevens rearrangement of the thiacyclophanes	36
2.1.3.1 The Stevens rearrangement of the <i>anti</i> -thiacyclophane 100 into the thiomethylcyclophane 99	37
2.1.4 Formation of the sulfonium salt 111 and the subsequent Hoffmann elimination.....	38
2.1.5 The Stevens rearrangement of the <i>syn</i> -thiacyclophane 108 to the thiomethylcyclophanes.....	41
2.1.6 Synthesis of the <i>cis</i> -DHP 117	42
2.1.7 Pyrene and thiomethylpyrene formation	44

2.1.8 Migration of the nitrile groups over the π system and finally an elimination of HCN	48
2.2 Synthesis of 2-(<i>t</i> -butyl)-10b-methyl-10c-cyano- <i>trans</i> -10b,10c-dihydropyrene 128	49
2.2.1 Synthesis of the cyano-methylthiacyclophanes 130 and 131	50
2.2.2 The Stevens rearrangement of the <i>syn</i> -thiacyclophane 130	51
2.2.3 The Hoffmann elimination of the thiomethylcyclophanes 133 and 134	52
2.2.4 The Stevens rearrangement of the <i>anti</i> -thiacyclophane 131	53
2.2.5 Photochemical isomerization of cyano-methyl CPD 127 into the <i>trans</i> -DHP 128	54
2.2.6 Migration of the internal nitrile in cyano-methyl DHP 128	54
2.3 Synthesis of phenylethynyl/methyl DHP 139	55
2.3.1 Synthesis of the bis(bromomethyl) diphenylacetylene 143	56
2.3.2 Thiacyclophane formation by coupling dibromide 143 and dithiol 129	57
2.3.3 The Wittig rearrangement on the phenylethynylthiacyclophanes	59
2.3.4 Synthesis of CPD 138 by Hoffmann elimination and its isomerization to the DHP 139	60
2.3.5 Synthesis of the <i>cis</i> -DHP 148	62
2.3.6 Attempted syntheses of acyl DHP 149 by Friedel-Crafts acylation ..	63
2.3.7 An anionic approach to the synthesis of the acyl DHP	64
2.4 Chemistry at the internal substituents	65
2.4.1 DIBAL-H reduction of the dinitrile 85	65
2.4.1.1 The [1,5]-sigmatropic rearrangement of the formyl groups ..	66
2.4.2 The attempted synthesis of the acyl substituted CPD 157	67
2.4.3 Reduction of the nitrile 85 into the primary amine 158	68
2.4.4 Reduction the internal formyl groups using NaBH ₄	68
2.4.5 The 2,4-dinitrophenyl hydrazone of the cyclophanediene 152	69
2.4.6 Wittig reaction of the diformyl CPD 152	70

2.4.6.1 A photoswitch with low thermal and migration rates.....	72
2.5 Improved syntheses of the dihydropyrenes with internal olefin groups	73
2.5.1 DIBAL-H reduction-Wittig reaction sequence to synthesize the thiacyclophane 170	74
2.5.2 Synthesis of the divinylcyclophanediene 166	75
2.5.3 Thermal isomerization of the cyclophanediene 166 into the dihydropyrene 167	76
2.5.4 A comparison of the synthetic routes to the olefin substituted CPDs	77
2.5.5 Another improvement in the synthesis of divinyl CPD 166	78
2.5.6 Synthesis of the diisobutenyl CPD 178	79
2.6 .6 Syntheses of the olefinic CPDs with extended conjugation	81
2.6.1 Butadienyl as the internal substituents	81
2.6.1.1 Dihydropyrenes 190-192 by the thermal closure of the CPDs 184-186	85
2.6.2 Extending the conjugation with a triple bond	85
2.6.3 Distyryl CPDs 202-204 , an example of extended conjugation by phenyl rings	87
2.6.4 Synthesis of nitro-styryl CPDs 210-212 , an exploration of the electronic effects on the thermal back reaction	90
2.6.5 <i>para</i> -Methoxy-styryl CPDs 218-220 , an example of an electron rich internal olefin	92
2.6.6 Synthesis of <i>para</i> -methyl-styryl CPDs 226-228	95
2.7 Alkynes as the internal substituents.	97
2.7.1 Synthesis of diethynyl CPD 235	97
2.7.1.1 Unexpected products from Wittig reaction.....	99
2.7.2 Diphenylethynyl DHP	102
2.8 Synthesis of naphthoyl dihydropyrenes	104
2.8.1 2-Naphthoyl diisobutenyl DHP 248	104
2.8.2 Synthesis of 2-naphthoyldivinyl DHP 250 and its photoopening to the CPD 251	108

2.9 Synthesis of dimer, oligomers and polymers	109
2.9.1 Polymerization of the acetylene DHP 236	109
2.9.2 Formation of a dimer by Eglinton coupling	110
2.9.3 Cross coupling between vinyl-ethynyl DHP 238 and diethynyl DHP 236	111
2.9.4 Bis Phenbutadienyl DHP 257	112
Chapter 3: Thermochemical Reaction	114
3.1 Electrocyclic reaction	114
3.1.1 Cyclophanedienes with internal olefin substituents	126
3.1.2 Extension of conjugation by a double bond in the internal substituents	132
3.1.3 Extending the conjugation by a phenyl ring	134
3.1.4 An electronic contribution towards thermal isomerization	135
3.1.5 Alkynes as the internal substituents	136
3.1.6 Unsymmetrical CPDs	139
3.1.7 5-Naphthoylated CPDs 249 and 251	139
3.1.8 DFT Calculations	141
3.2 [1,5]-sigmatropic rearrangement	142
Chapter 4: Photochemical isomerization	147
4.1 Visible light opening	147
4.1.1 Dicyano DHP 86 and diethynyl DHP 236	154
4.1.2 DHPs with alkyl substituted internal vinyl groups	156
4.1.3 Distyryl DHPs 205-207	158
4.1.3.1 Visible light closing of the CPDs <i>E/Z</i> 203 and <i>E/E</i> 204	158
4.1.4 <i>Para</i> substituted styryl DHPs	159
4.1.4.1 A shift in the UV-Vis absorption spectrum	160
4.1.4.2 Electronic effects on the stability of photo excited states.	161
4.1.5 Naphthoyl DHPs 248 and 250	162
4.1.6 Dimer 254	163

4.2 UV Closing	164
Chapter 5: X-Ray Structure Analyses	165
5.1 Dicyano DHPs 86 and 117	167
5.2 <i>Cis</i> -dihydropyrenes	167
5.3 <i>Trans</i> dihydropyrenes	171
5.4 Cyclophanedienes	171
5.5 <i>Anti</i> -thiacyclophanes	174
5.6 Thiomethylcyclophanes	176
Chapter 6: Conclusions.....	177
6.1 Synthesis	177
6.2 Thermal isomerization of cyclophanedienes.....	178
6.3 Thermal rearrangement of dihydropyrenes.....	178
6.4 Photochemical isomerization	179
6.5 Future Work	181
Chapter 7: Experimental.....	184
7.1 General experimental conditions.....	184
7.2 General procedure for crystal growth	185
7.3 Experimental conditions for X-ray crystallographic studies.....	185
7.4 General procedure for S-Methylation	186
7.5 General procedure for the Hoffmann elimination.....	186
7.6 General procedure for the thermal isomerization of cyclophanedienes to dihydropyrenes.....	186
7.7 General procedure for Wittig reaction	187
7.7.1 Procedure A.....	187
7.7.2 Procedure B	187

7.8 General procedure for photoopening (NMR).....	188
7.9 Syntheses.....	188
References.....	291
X-ray structure reports.....	298
X-ray structure for <i>anti</i> -dithiacyclophane 100	298
X-ray structure report for <i>syn</i> -dithiacyclophane 108	308
X-ray structure report for dicyano DHP 86	316
X-ray structure report for <i>cis</i> -dicyano DHP 117	323
X-ray Structure Report for <i>syn</i> -thiacyclophane 130	331
X-ray structure report for <i>anti</i> -thiacyclophane 131	340
X-ray structure report for thiomethylcyclophane 134	349
X-ray structure report for <i>cis</i> -cyano-methyl DHP 136	358
X-ray report for <i>syn</i> -thiacyclophane 145	372
X-ray structure report for thiomethylcyclophane 146	384
X-ray structure report for phenylethynyl DHP 139	394
X-ray structure report for <i>cis</i> -phenylethynyl/methyl DHP 148	403
X-ray structure report for divinyl DHP 167	412
X-ray structure report for diisobutenyl CPD 178	418
X-ray structure report for diisobutenyl DHP 179	426
X-ray structure report for <i>cis</i> -styryl CPD 202	433
X-ray structure report for diethynyl CPD 235	441
X-ray structure report for diethynyl DHP 236	450
X-ray structure report for pyrene 150	459
Appendix B Thermal closing data for cyclophanedienes.....	470

Appendix C: Sigmatropic rearrangement data for dicyano DHP 86	499
Appendix D Photoopening data for dihydropyrenes.....	502
Appendix E: UV closing data for CPDs 53 , 85 , 226 and 249	509
Appendix F: NMR spectra.....	511

.....

List of Tables

Table 1.1	Allowed modes for photochemical and thermal electrocycliations	10
Table 1.2	Half lives of some cyclophanedienes at 20 °C ^{39,41}	23
Table 1.3	Radical stabilizing functional groups and their bond stabilization energies for FG—CH ₂ —H.....	26
Table 3.1	Thermodynamic parameters for the thermal back reaction of cyclophanedienes.....	118
Table 3.2	Half lives of the cyclophanedienes at three different temperatures	120
Table 3.3	A comparison of theoretical and experimental ΔG^\ddagger values (kcal.mol ⁻¹)...	142
Table 3.4	The facial migration modes of 4n and 4n +2 π systems.....	144
Table 3.5	Thermodynamic data for the sigmatropic rearrangement of the internal nitrile group in 86	144
Table 4.1	Visible opening of the dihydropyrenes to the cyclophanedienes	153
Table 4.2	UV closing comparison of cyclophanedienes	164
Table 6.1.	Summary of half lives of cyclophanedienes and visible opening time of their corresponding dihydropyrenes	180

List of Appendix Tables

Table A. 1	Crystal data and structure refinement for 100 (C ₁₈ H ₁₄ N ₂ S ₂).....	302
Table A. 2	Atomic coordinates (x 10 ⁴) and equivalent isotropic displacement parameters (Å ² x 10 ³) for 100 (bt 906).....	303
Table A. 3	Bond lengths [Å] and angles [°] for 100 (bt 906).	304
Table A. 4	Anisotropic displacement parameters (Å ² x 10 ³) for 100 (bt 906).	306
Table A. 5	Hydrogen coordinates (x 10 ⁴) and isotropic displacement parameters (Å ² x 10 ³) for 100 (bt 906).....	307
Table A. 6	Crystal data and structure refinement for 108 (C ₁₈ H ₁₄ N ₂ S ₂).....	311
Table A. 7	Atomic coordinates (x 10 ⁴) and equivalent isotropic displacement parameters (Å ² x 10 ³) for 108 (bt 908t).....	312
Table A. 8	Bond lengths [Å] and angles [°] for 108 (bt 908t)	312
Table A. 9	Anisotropic displacement parameters (Å ² x 10 ³) for 108 (bt 908t)	314
Table A. 10	Hydrogen coordinates (x 10 ⁴) and isotropic displacement parameters (Å ² x 10 ³) for 108 (bt 908t).....	315
Table A. 11	Crystal data and structure refinement for DHP 86 (C ₁₈ H ₁₀ N ₂).....	318
Table A. 12	Atomic coordinates (x 10 ⁴) and equivalent isotropic displacement parameters (Å ² x 10 ³) for 86 (bt 953).....	319
Table A. 13	Bond lengths [Å] and angles [°] for 86 (bt 953)	319
Table A. 14	Anisotropic displacement parameters (Å ² x 10 ³) for 86 bt953.	321
Table A. 15	Hydrogen coordinates (x 10 ⁴) and isotropic displacement parameters (Å ² x 10 ³) for 86 (bt 953).....	321

Table A. 16	Hydrogen bonds for 86 (bt953) [\AA and $^\circ$]	322
Table A. 17	Crystal data and structure refinement for 117 (C18 H10 N2)	325
Table A. 18	Atomic coordinates ($\times 10^4$) and equivalent isotropic displacement parameters ($\text{\AA}^2 \times 10^3$) for 117 (bt 1105)	326
Table A. 19	Bond lengths [\AA] and angles [$^\circ$] for 117 (bt 1105)	327
Table A. 20	Anisotropic displacement parameters ($\text{\AA}^2 \times 10^3$) for 117 (bt 1105)	329
Table A. 21	Hydrogen coordinates ($\times 10^4$) and isotropic displacement parameters ($\text{\AA}^2 \times 10^3$) for 117 (bt 1105)	330
Table A. 22	Crystal data and structure refinement for 130 (C22 H25 N S2)	334
Table A. 23	Atomic coordinates ($\times 10^4$) and equivalent isotropic displacement parameters ($\text{\AA}^2 \times 10^3$) for 130 (bt 907t)	335
Table A. 24	Bond lengths [\AA] and angles [$^\circ$] for 130 (bt 907t)	336
Table A. 25	Anisotropic displacement parameters ($\text{\AA}^2 \times 10^3$) for 130 (bt907t)	338
Table A. 26	Hydrogen coordinates ($\times 10^4$) and isotropic displacement parameters ($\text{\AA}^2 \times 10^3$) for 130 (bt 907t)	339
Table A. 27	Crystal data and structure refinement for 131 (C22 H25 N S2)	343
Table A. 28	Atomic coordinates ($\times 10^4$) and equivalent isotropic displacement parameters ($\text{\AA}^2 \times 10^3$) for 131 (bt 909)	344
Table A. 29	Bond lengths [\AA] and angles [$^\circ$] for 131 (bt 909)	345
Table A. 30	Anisotropic displacement parameters ($\text{\AA}^2 \times 10^3$) for 131 (bt 909)	347
Table A. 31	Hydrogen coordinates ($\times 10^4$) and isotropic displacement parameters ($\text{\AA}^2 \times 10^3$) for 131 (bt 909)	348
Table A. 32	Crystal data and structure refinement for 134 (C24 H29 N S2)	351

Table A. 33	Atomic coordinates ($\times 10^4$) and equivalent isotropic displacement parameters ($\text{\AA}^2 \times 10^3$) for 134 (bt 960).....	352
Table A. 34	Bond lengths [\AA] and angles [$^\circ$] for 134 (bt 960).....	353
Table A. 35	Anisotropic displacement parameters ($\text{\AA}^2 \times 10^3$) for 134 (bt 960).....	356
Table A. 36	Hydrogen coordinates ($\times 10^4$) and isotropic displacement parameters ($\text{\AA}^2 \times 10^3$) for 134 (bt 960).....	357
Table A. 37	Crystal data and structure refinement for 136	362
Table A. 38	Atomic coordinates ($\times 10^4$) and equivalent isotropic displacement parameters ($\text{\AA}^2 \times 10^3$) for 136 (bt 1019).....	363
Table A. 39	Bond lengths [\AA] and angles [$^\circ$] for 136 (bt 1019).....	365
Table A. 40	Anisotropic displacement parameters ($\text{\AA}^2 \times 10^3$) for 136 (bt1019).....	369
Table A. 41	Hydrogen coordinates ($\times 10^4$) and isotropic displacement parameters ($\text{\AA}^2 \times 10^3$) for 136 (bt 1019).....	370
Table A. 42	Crystal data and structure refinement for 145 (C ₂₉ H ₃₀ S ₂).....	376
Table A. 43	Atomic coordinates ($\times 10^4$) and equivalent isotropic displacement parameters ($\text{\AA}^2 \times 10^3$) for 145 (bt 830).....	377
Table A. 44	Bond lengths [\AA] and angles [$^\circ$] for 145 (bt 830).....	378
Table A. 45	Anisotropic displacement parameters ($\text{\AA}^2 \times 10^3$) for 145 (bt 830).....	381
Table A. 46	Hydrogen coordinates ($\times 10^4$) and isotropic displacement parameters ($\text{\AA}^2 \times 10^3$) for 145 (bt 830).....	382
Table A. 47	Crystal data and structure refinement for 146 (C ₃₁ H ₃₄ S ₂).....	386
Table A. 48	Atomic coordinates ($\times 10^4$) and equivalent isotropic displacement parameters ($\text{\AA}^2 \times 10^3$) for 146 (bt 958).....	387
Table A. 49	Bond lengths [\AA] and angles [$^\circ$] for 146 (bt 958).....	388

Table A. 50	Anisotropic displacement parameters ($\text{\AA}^2 \times 10^3$) for 146 (bt 958).	391
Table A. 51	Hydrogen coordinates ($\times 10^4$) and isotropic displacement parameters ($\text{\AA}^2 \times 10^3$) for 146 (bt 958).	392
Table A. 52	Crystal data and structure refinement for 139	396
Table A. 53	Atomic coordinates ($\times 10^4$) and equivalent isotropic displacement parameters ($\text{\AA}^2 \times 10^3$) for 139 (bt 914).	397
Table A. 54	Bond lengths [\AA] and angles [$^\circ$] for 139 (bt 914)	398
Table A. 55	Anisotropic displacement parameters ($\text{\AA}^2 \times 10^3$) for 139 (bt 914).	401
Table A. 56	Hydrogen coordinates ($\times 10^4$) and isotropic displacement parameters ($\text{\AA}^2 \times 10^3$) for 139 (bt 914).	402
Table A. 57	Crystal data and structure refinement for 148	405
Table A. 58	Atomic coordinates ($\times 10^4$) and equivalent isotropic displacement parameters ($\text{\AA}^2 \times 10^3$) for 148 (bt 956).	406
Table A. 59	Bond lengths [\AA] and angles [$^\circ$] for 148 (bt 956)	407
Table A. 60	Anisotropic displacement parameters ($\text{\AA}^2 \times 10^3$) for 148 (bt 956).	410
Table A. 61	Hydrogen coordinates ($\times 10^4$) and isotropic displacement parameters ($\text{\AA}^2 \times 10^3$) for 148 (bt 956).	411
Table A. 62	Crystal data and structure refinement for Divinyl-DHP 167	414
Table A. 63	Atomic coordinates ($\times 10^4$) and equivalent isotropic displacement parameters ($\text{\AA}^2 \times 10^3$) for 167 (bt 1160).	415
Table A. 64	Bond lengths [\AA] and angles [$^\circ$] for 167 (bt 1160).	416
Table A. 65	Anisotropic displacement parameters ($\text{\AA}^2 \times 10^3$) for bt1160 (167).	417
Table A. 66	Hydrogen coordinates ($\times 10^4$) and isotropic displacement parameters ($\text{\AA}^2 \times 10^3$) for 167 (bt1160).	417

Table A. 67	Crystal data and structure refinement for 178 (C ₂₄ H ₂₄)	421
Table A. 68	Atomic coordinates (x 10 ⁴) and equivalent isotropic displacement parameters (Å ² x 10 ³) for 178 (bt 1173).....	422
Table A. 69	Bond lengths [Å] and angles [°] for 178 (bt 1173)	423
Table A. 70	Anisotropic displacement parameters (Å ² x 10 ³) for 178 (bt 1173).....	424
Table A. 71	Hydrogen coordinates (x 10 ⁴) and isotropic displacement parameters (Å ² x 10 ³) for 178 (bt 1173).....	425
Table A. 72	Crystal data and structure refinement for 179	428
Table A. 73	Atomic coordinates (x 10 ⁴) and equivalent isotropic displacement parameters (Å ² x 10 ³) for 179 (bt 1265).....	429
Table A. 74	Bond lengths [Å] and angles [°] for 179 (bt 1265).....	430
Table A. 75	Anisotropic displacement parameters (Å ² x 10 ³) for 179 (bt 1265).....	431
Table A. 76	Hydrogen coordinates (x 10 ⁴) and isotropic displacement parameters (Å ² x 10 ³) for 179 (bt 1265).....	432
Table A. 77	Crystal data and structure refinement for <i>cis</i> -distyryl CPD 202	436
Table A. 78	Atomic coordinates (x 10 ⁴) and equivalent isotropic displacement parameters (Å ² x 10 ³) for 202 (bt 1263).....	437
Table A. 79	Bond lengths [Å] and angles [°] for 202 (bt 1263).....	438
Table A. 80	Anisotropic displacement parameters (Å ² x 10 ³) for 202 (bt 1263).....	439
Table A. 81	Hydrogen coordinates (x 10 ⁴) and isotropic displacement parameters (Å ² x 10 ³) for 202 (bt 1263).....	440
Table A. 82	Crystal data and structure refinement for diethynyl CPD 235	444
Table A. 83	Atomic coordinates (x 10 ⁴) and equivalent isotropic displacement parameters (Å ² x 10 ³) for 235 (bt 1220).....	445

Table A. 84	Bond lengths [\AA] and angles [$^\circ$] for 235 (bt 1220).....	446
Table A. 85	Anisotropic displacement parameters ($\text{\AA}^2 \times 10^3$) for 235 (bt 1220).	448
Table A. 86	Hydrogen coordinates ($\times 10^4$) and isotropic displacement parameters ($\text{\AA}^2 \times 10^3$) for 235 (bt 1220).....	449
Table A. 87	Crystal data and structure refinement for diethynyl DHP 236	455
Table A. 88	Atomic coordinates ($\times 10^4$) and equivalent isotropic displacement parameters ($\text{\AA}^2 \times 10^3$) for 236 (bt 1228).....	456
Table A. 89	Bond lengths [\AA] and angles [$^\circ$] for 236 (bt 1228).....	457
Table A. 90	Anisotropic displacement parameters ($\text{\AA}^2 \times 10^3$) for 236 (bt 1228).	458
Table A. 91	Hydrogen coordinates ($\times 10^4$) and isotropic displacement parameters ($\text{\AA}^2 \times 10^3$) for 236 (bt 1228).	458
Table A. 92	Crystal data and structure refinement for ^t Bu-pyrene 150	461
Table A. 93	Atomic coordinates ($\times 10^4$) and equivalent isotropic displacement parameters ($\text{\AA}^2 \times 10^3$) for 150 (bt 957).....	462
Table A. 94	Bond lengths [\AA] and angles [$^\circ$] for 150 (bt 957).	463
Table A. 95	Anisotropic displacement parameters ($\text{\AA}^2 \times 10^3$) for 150 (bt 957).	466
Table A. 96	Hydrogen coordinates ($\times 10^4$) and isotropic displacement parameters ($\text{\AA}^2 \times 10^3$) for 150 (bt 957).	468

List of Figures

Figure 1.1	Photochromism.....	2
Figure 1.2	Viologens-ruthenium complex dyad 15	8
Figure 1.3	Conrotatory and disrotatory mode of cyclization.....	11
Figure 1.4	Numbering system for description in section 1.5.....	25
Figure 1.5	Substituents' effect on the energies of cyclophanedienes and the TS [‡]	27
Figure 2.1	¹ H NMR spectrum of dicyano CPD 85 in CDCl ₃ at 500 MHz	40
Figure 2.2	¹ H NMR spectrum of dicyano DHP 86 in CDCl ₃ at 500 MHz.....	44
Figure 2.3	¹ H NMR spectrum of naphthoyl DHP 248 in CD ₂ Cl ₂ at 500 MHz.....	106
Figure 2.4	¹ H NMR spectrum of naphthoyl CPD 249 in CD ₂ Cl ₂ at 500 MHz.....	107
Figure 2.5	¹ H NMR spectra of monomer 238 and dimer 254 in CDCl ₃ at 500 MHz.	111
Figure 3.1	Arrhenius plot for the thermal reaction of dicyano CPD 85 in solid phase	122
Figure 3.2	A Combined Arrhenius plot for the internal olefinic cyclophanedienes in toluene	127
Figure 3.3	Structures of CPD (left), TS [‡] (middle) and DHP (right).....	128
Figure 3.4	Combined ¹ H NMR spectra of 167 and 179 in CDCl ₃ at 500 MHz.....	129
Figure 3.5	ORTEP diagrams of divinyl DHP 167 (right) and diisobutenyl DHP 179 (left) showing 30% probability ellipsoids.	131
Figure 3.6	Molecular diagrams of Diisobutenyl DHP 178 (left) and divinyl DHP 167 ... (right) derived from X-ray structures	131
Figure 3.7	Arrhenius plot for the styryl CPDs 202-204 in toluene	134
Figure 3.8	Molecular diagrams of distyryl 202 (left) and diisobutenyl 178 (right) derived from X-ray structures	137
Figure 3.9	Molecular diagram of diethynyl CPD 235 derived from X-ray structure .	137

Figure 4.1	UV-Vis spectrum of the orange and red filters	147
Figure 4.2	Visible light opening experiment setup.....	148
Figure 4.3	Outline of the proposed mechanism for the DHP/CPD photochromism ..	156
Figure 4.4	Combined UV-vis spectrum of styryl CPDs 202 , 203 and 204	159
Figure 4.5	Combined UV-vis spectrum of <i>cis</i> -styryl CPDs 202 , 210 and 226 in	
	CH ₂ Cl ₂	161
Figure 5.1	Molecular diagrams of dicyano DHPs 86 (left) and 117 (right) derived	
	from X-ray structures	167
Figure 5.2	Molecular diagrams of <i>cis</i> -phenylethynyl DHP 148 (left) and <i>cis</i> -cyano-	
	methyl DHP 136 (right) derived from X-ray structures	168
Figure 5.3	Molecular structures of <i>trans</i> -phenylethynyl/methyl DHP 139 and <i>trans</i> -	
	diethynyl DHP 236 derived from X-ray structures	169
Figure 5.4	Molecular diagrams of divinyl DHP 167 (left) and diisobutenyl DHP 179	
	(right) derived from X-ray structures	170
Figure 5.5	Molecular diagram of diethynyl CPD 235 derived from X-ray structure .	172
Figure 5.6	Molecular diagrams of diisobutenyl CPD 178 (left) and distyryl CPD 202	
	(right) derived from X-ray structures	173
Figure 5.7	Molecular diagrams of dicyano- <i>anti</i> -thiacyclophane 100 and cyano/methyl-	
	<i>anti</i> -thiacyclophane 131 derived from X-ray structures.....	174
Figure 5.8	Molecular diagrams of phenylethynyl/methyl- <i>syn</i> -thiacyclophane 145 (top),	
	cyano-methyl- <i>syn</i> -thiacyclophane 130 (bottom right), dicyano- <i>syn</i> -	
	thiacyclophane 108 (bottom left) derived from X-ray structures.....	175
Figure 5.9	Molecular diagrams of phenylethynyl/methylcyclophane 146 (top) and	
	cyano-methylcyclophane 134 (bottom) derived from X-ray structures	176

List of Schemes

Scheme 1.1	<i>Cis-trans</i> isomerization of stilbenes	3
Scheme 1.2	<i>Cis-trans</i> isomerization of azobenzene	4
Scheme 1.3	An azobenzene type photoswitch	4
Scheme 1.4	Phototautomerization	5
Scheme 1.5	Photochemistry of Tinuvin P	5
Scheme 1.6	Acyl migration in a polycyclic quinone	6
Scheme 1.7	Dissociation of triphenylcarbinol to release HO ⁻	7
Scheme 1.8	Electron transfer in viologens	7
Scheme 1.9	The Diels Alder reaction	9
Scheme 1.10	The Photo-dimerization of anthracene	9
Scheme 1.11	The norbornadiene rearrangement.....	10
Scheme 1.12	Photoisomerization of fulgides.....	12
Scheme 1.13	Highly diastereoselective cyclization of ketal fulgide 25	13
Scheme 1.14	Photochromism of spiropyran 31	13
Scheme 1.15	Photochromism of spirooxazine 33	14
Scheme 1.16	Phenanthrene from <i>cis</i> -stilbene	14
Scheme 1.17	Irie's dithienylethene photoswitch	15
Scheme 1.18	Photo-controlled release of saccharide from dithienylethene 39	16
Scheme 1.19	Photoswitching magnetism	17
Scheme 1.20	Photoswitching of dihydropyrene 43	18
Scheme 1.21	A dihydropyrene based photoswitch with CF ₃ internal groups.....	28
Scheme 1.22	A photoswitch with a high calculated activation barrier.....	28

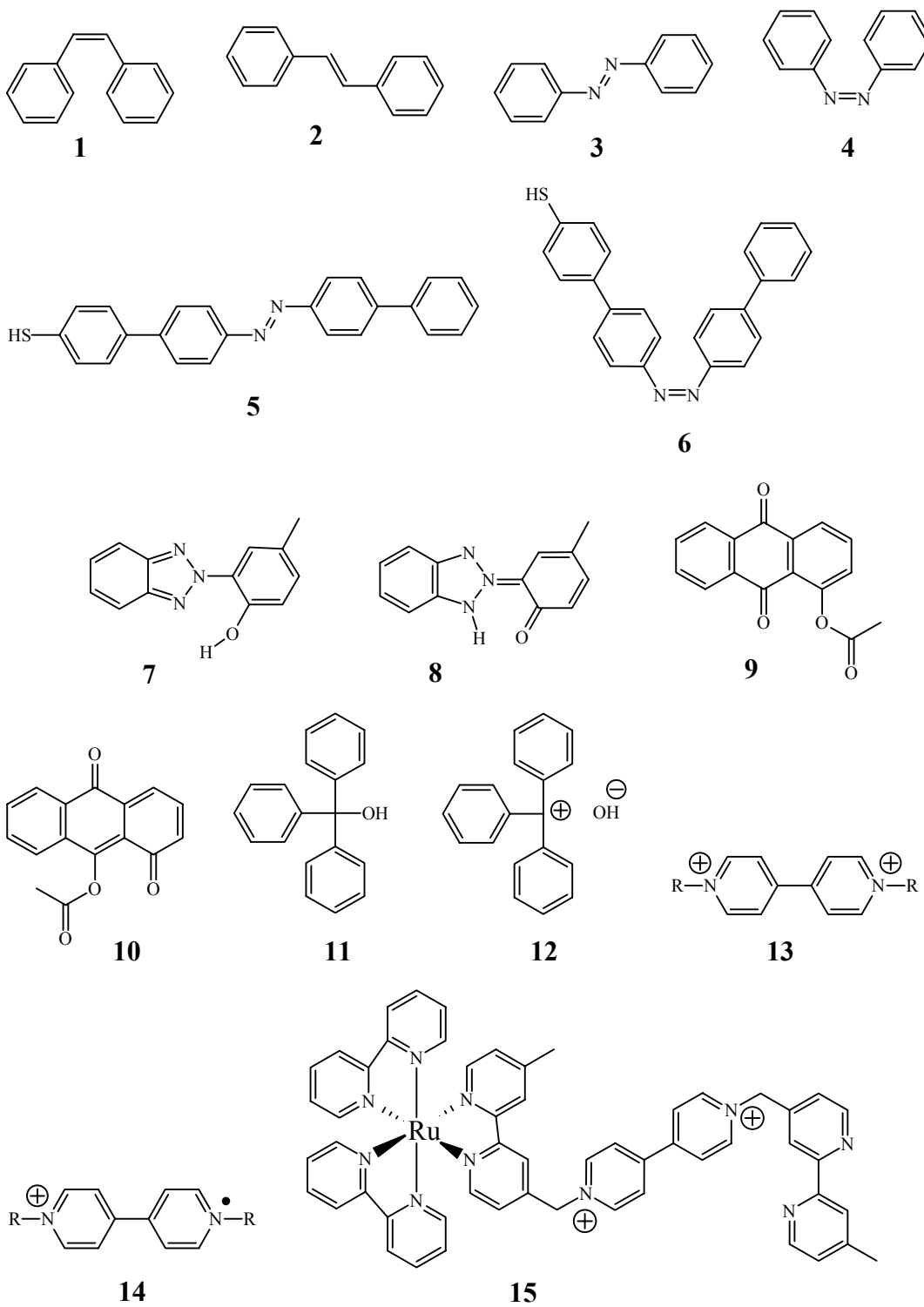
Scheme 1.23 The effect of substituents on the thermal return of merocyanine to spiropyran	30
Scheme 1.24 Switching between a P and T type photochrome	31
Scheme 2.1 Reterosynthetic analysis of dicyano DHP 86	32
Scheme 2.2 Synthesis of 2,6-bis-bromomethylbenzonitrile 102	33
Scheme 2.3 Attempted formation of thiol 101	34
Scheme 2.4 Synthesis of nitrile thiacyclophanes 100 , 108 and 109	35
Scheme 2.5 The Stevens rearrangement of <i>anti</i> -thiacyclophane 100 into the thiomethylcyclophane 99	37
Scheme 2.6 The attempted Hoffmann elimination to synthesize DHP 86	38
Scheme 2.7 The Hoffmann elimination at room temperature.....	39
Scheme 2.8 Stevens rearrangement of <i>syn</i> -thiacyclophane 108 into the thiomethyl cyclophanes	41
Scheme 2.9 The Hoffmann elimination at room temperature.....	42
Scheme 2.10 Attempted thermal closing of dicyano CPD 85	43
Scheme 2.11 Formation of pyrene 112 and thiomethylpyrene 113	45
Scheme 2.12 Mechanism for the formation of the pyrenes	46
Scheme 2.13 Mechanism for the elimination of the internal nitrile groups during the Hoffmann elimination.	47
Scheme 2.14 Migration and elimination of nitrile group.....	48
Scheme 2.15 Synthesis of thiacyclophanes 130 and 131	50
Scheme 2.16 Stevens rearrangement of the <i>syn</i> -thiacyclophane 130	51
Scheme 2.17 The Hoffmann elimination to generate cyano-methyl CPD 127 and <i>cis</i> -DHP 136	52
Scheme 2.18 Generation of 128 by photochemical isomerization	54

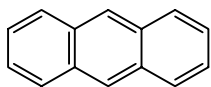
Scheme 2.19 Migration of the internal nitrile group in 128	54
Scheme 2.20 Retrosynthetic analysis of phenylethynyl/methyl CPD 138	56
Scheme 2.21 Synthesis of the dibromide 143	57
Scheme 2.22 Coupling reaction to yield dithiacyclophanes 142 and 145	57
Scheme 2.23 An attempted synthesis of dithiol 147	59
Scheme 2.24 Wittig rearrangement to prepare thiomethylcyclophanes 146	59
Scheme 2.25 Synthesis of the phenylethynyl/methylcyclophanediene 138	61
Scheme 2.26 Thermal closure of phenylethynyl/methyl CPD 138 to the DHP 139	61
Scheme 2.27 Hoffmann elimination of mixed isomers of 147	62
Scheme 2.28 Attempted Friedel-Craft acylation to yield 149	63
Scheme 2.29 Attempted synthesis of 149 involving a bromide intermediate 151	64
Scheme 2.30 Reduction of the dinitrile 85 to the dialdehyde 152	65
Scheme 2.31 Thermal rearrangement of the internal formyl groups	66
Scheme 2.32 Attempted synthesis of the acetyl CPD 157	67
Scheme 2.33 Attempted reduction of nitrile 85 to primary amine 158	68
Scheme 2.34 Reduction of the diformyl CPD 152 to the primary alcohol 159	69
Scheme 2.35 Attempted synthesis of a bis hydrazone.....	70
Scheme 2.36 Wittig reaction of 152 to produce styryl CPDs.....	70
Scheme 2.37 Synthesis of the CPDs with internal propenyl substituents.....	71
Scheme 2.38 Thermal isomerization of 162 to 164	72
Scheme 2.39 A photoswitch with internal vinyl substituents	73
Scheme 2.40 Modified synthesis of CPDs with internal olefin substituents	74
Scheme 2.41 Synthesis of the diformyl- <i>anti</i> -thiacyclophane 168	74
Scheme 2.42 Wittig reaction of 168 to synthesize 169 and 170	75

Scheme 2.43 Wittig rearrangement of the thiacyclopentane 170 and subsequent Hoffmann elimination	76
Scheme 2.44 Synthesis of propenyl DHP 162 via CPD 152	77
Scheme 2.45 Improved synthesis of divinyl CPD 166 starting from thiomethylcyclopentane 99	78
Scheme 2.46 Attempted synthesis of diformyl CPD 152 by the Hoffmann elimination..	79
Scheme 2.47 Synthesis of the diisobutenyl CPD 178	80
Scheme 2.48 The thermal closure of diisobutenyl CPD 178 to the DHP 179	81
Scheme 2.49 Attempted synthesis of butadienyl CPDs 181	82
Scheme 2.50 Attempted synthesis of thiomethylcyclopentane 187	83
Scheme 2.51 Synthesis of CPDs containing methyl substituted butadienyl internal groups	84
Scheme 2.52 Attempted synthesis of pentenynyl CPD by the Wittig reaction-Hoffmann elimination sequence	86
Scheme 2.53 Synthesis of 194 by Wittig reaction of 152	86
Scheme 2.54 Synthesis of CPDs with internal styryl groups 202-204	88
Scheme 2.55 Synthesis of nitro-styryl CPDs 210-212	90
Scheme 2.56 Synthesis of <i>p</i> -methoxy-styryl CPDs 218-220	93
Scheme 2.57 Synthesis of <i>p</i> -methyl-styryl CPDs 226-228	95
Scheme 2.58 Synthesis of diethynyl-thiomethylcyclopentane 233	97
Scheme 2.59 Synthesis of the diethynyl CPD 235	98
Scheme 2.60 Thermal isomerization of diethynyl CPD 235 into DHP 236	98
Scheme 2.61 Mechanism of vinyl and styryl incorporation during the Wittig reaction.	100
Scheme 2.62 Thermal isomerization of the CPD 237 to DHP 238	101
Scheme 2.63 Thermal return of the CPD 240 to the DHP 241	102

Scheme 2.64 Sonogashira coupling to synthesize 141	102
Scheme 2.65 Sonogashira coupling to synthesize 247	104
Scheme 2.66 Friedel-Crafts naphthoylation of diisobutenyl DHP 179	105
Scheme 2.67 Photoopening of DHP 248	106
Scheme 2.68 Synthesis of the naphthoyl DHP 250	108
Scheme 2.69 Visible opening of the DHP 250 to the cyclophanediene	108
Scheme 2.70 Attempted synthesis of the DHP based polymer.....	109
Scheme 2.71 Synthesis of the dimer 254	110
Scheme 2.72 Attempted synthesis of the oligomers	112
Scheme 2.73 Eglinton coupling of the diethynyl DHP 236 with phenylacetylene.....	113
Scheme 3.1 An example of the captodative effect in electrocyclization	124
Scheme 3.2 The Cope rearrangement of 258 to 259	143
Scheme 3.3 The Claisen rearrangement of 260 to 261	143
Scheme 3.4 A [1,5] hydride shift in conversion of 262 to 263	143

List of Numbered Compounds

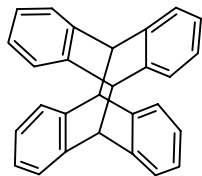




16



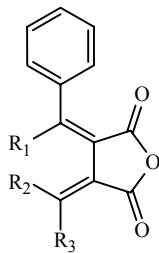
18



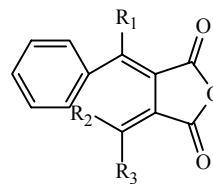
17



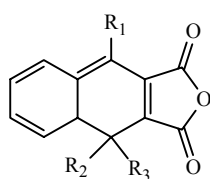
19



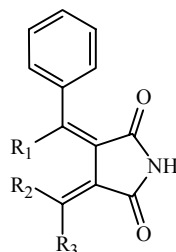
20



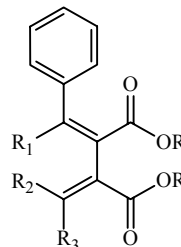
21



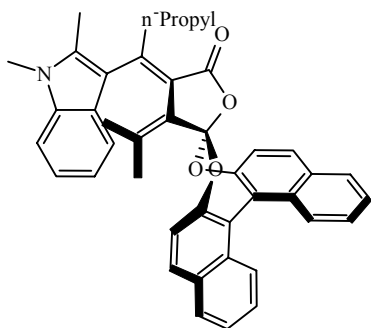
22



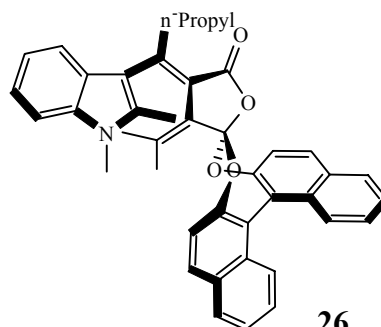
23



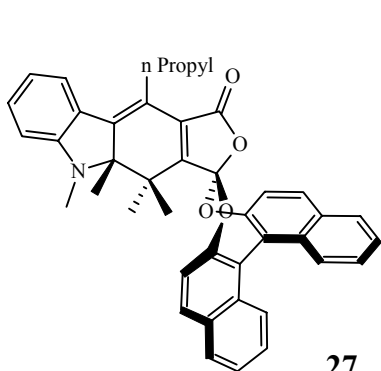
24



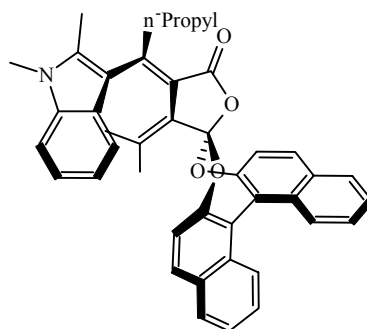
25



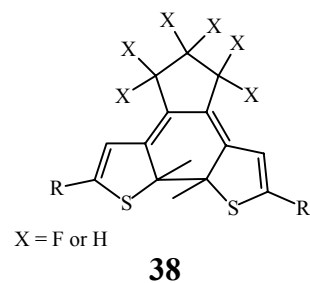
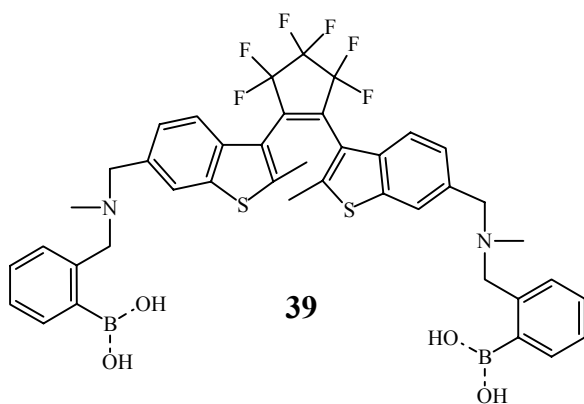
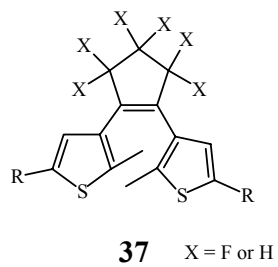
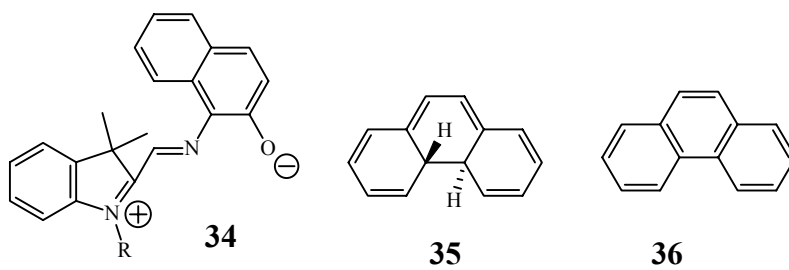
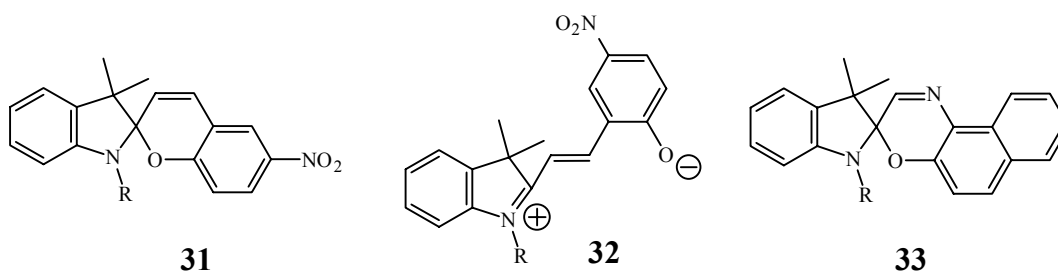
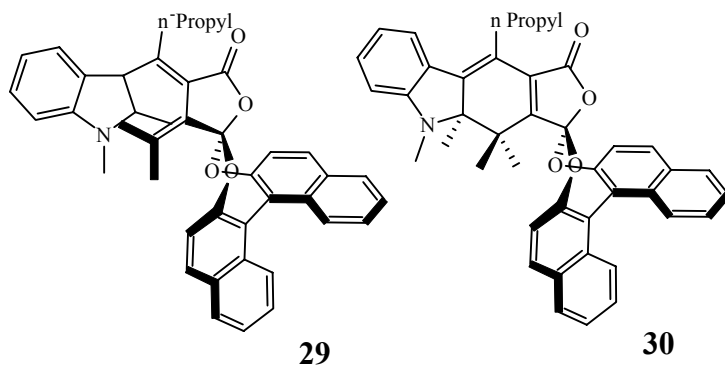
26

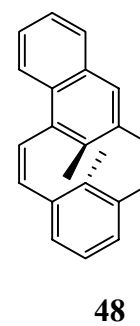
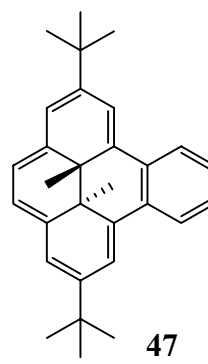
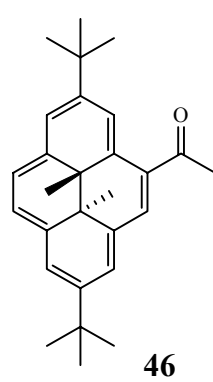
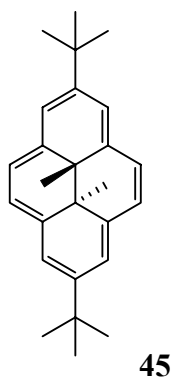
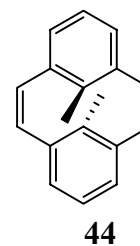
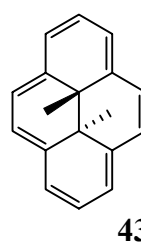
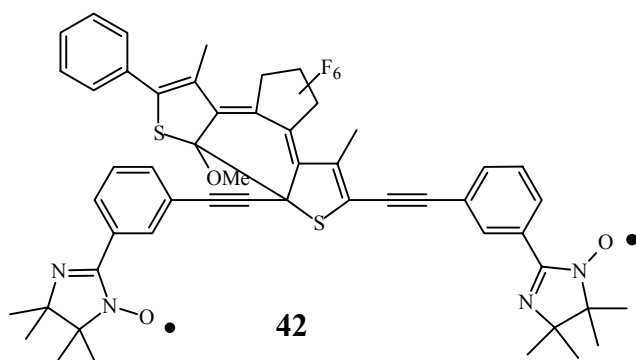
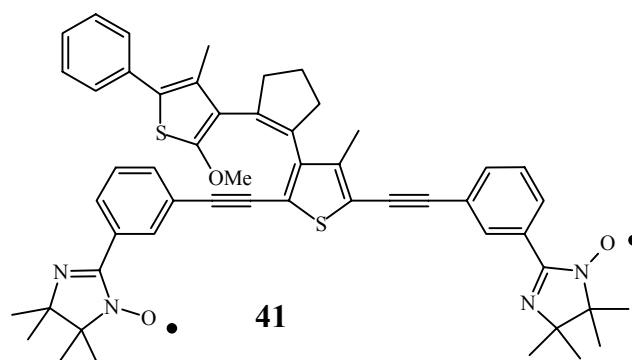
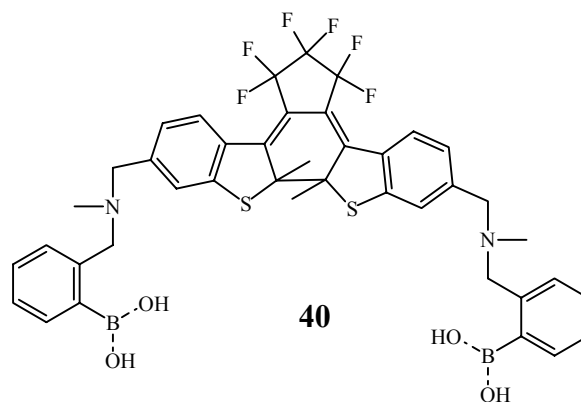


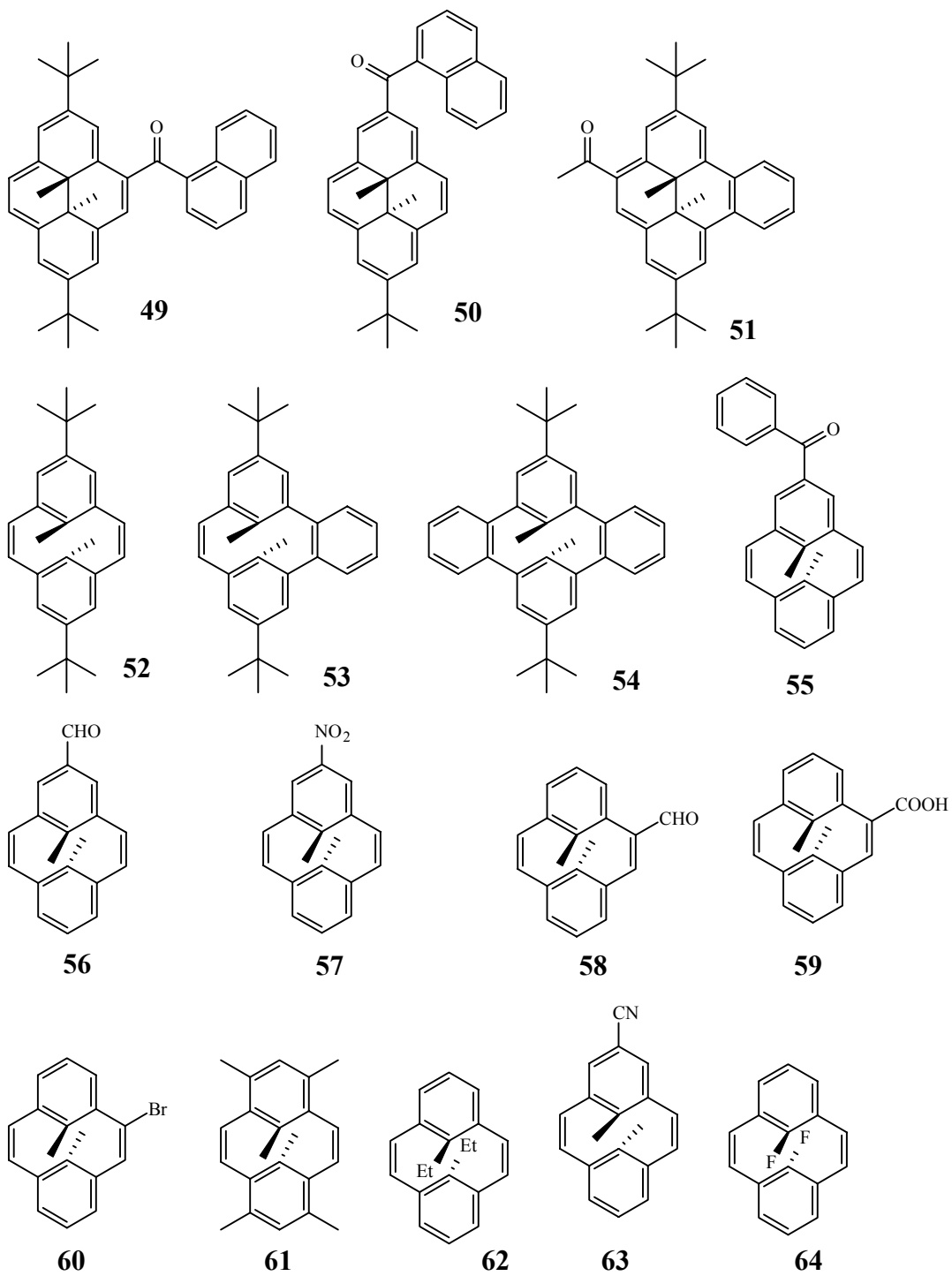
27

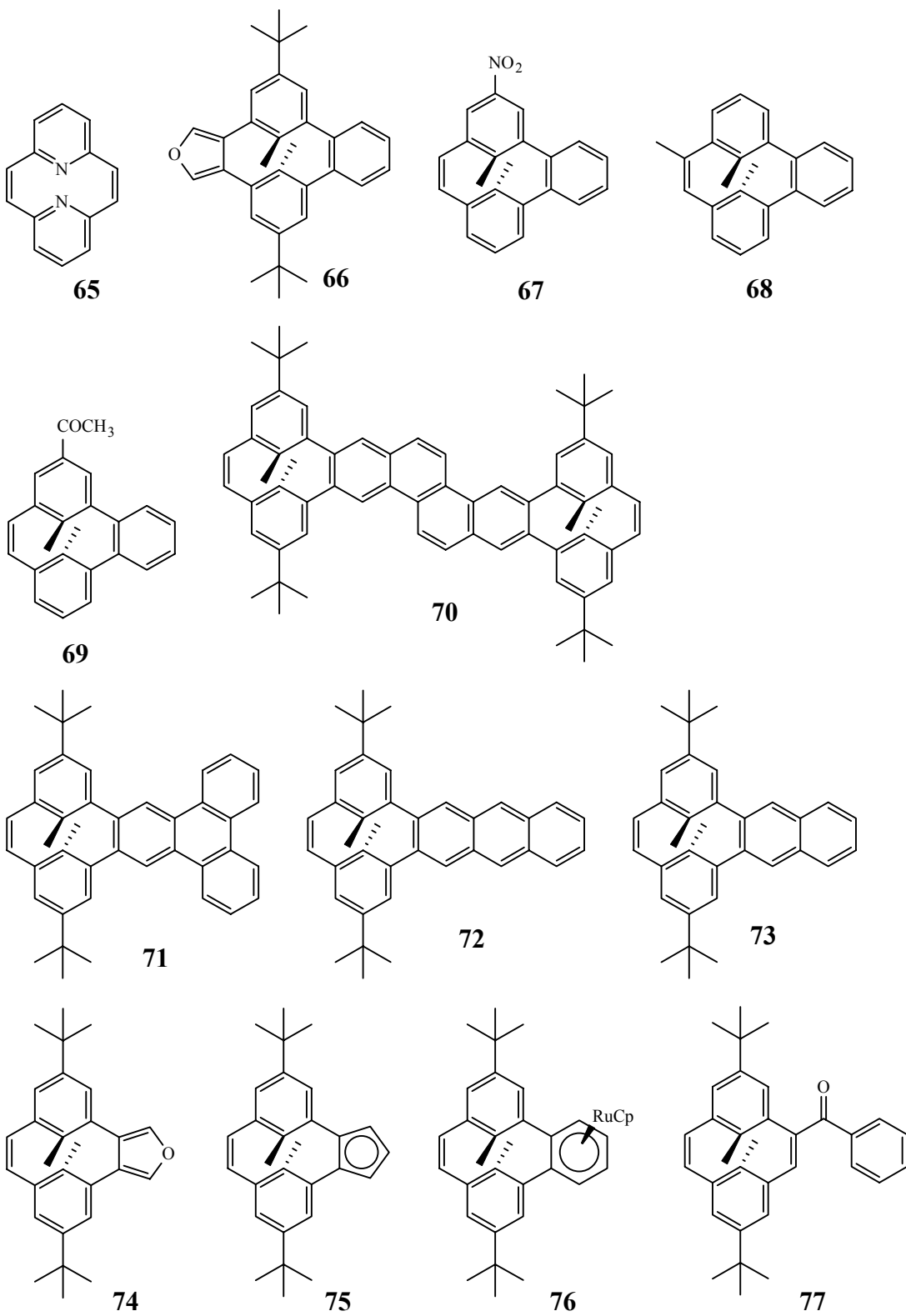


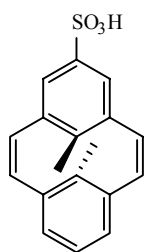
28



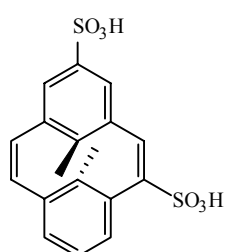




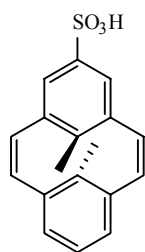




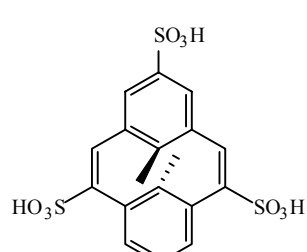
78



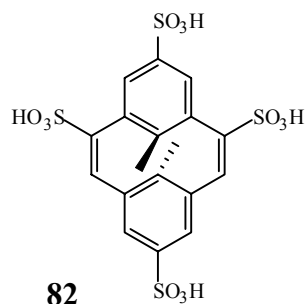
79



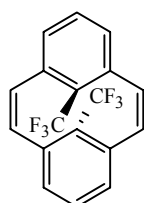
80



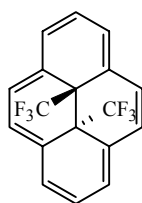
81



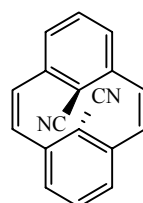
82



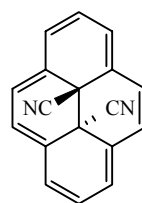
83



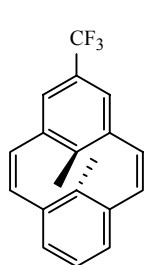
84



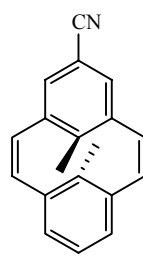
85



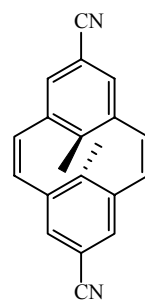
86



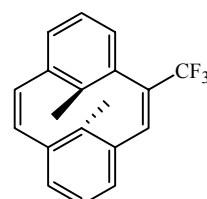
87



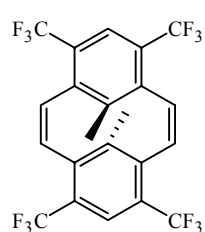
88



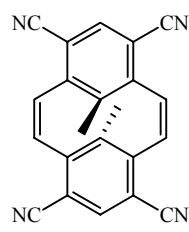
89



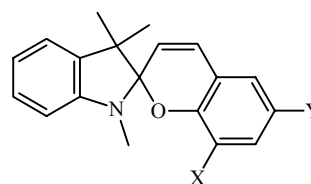
90



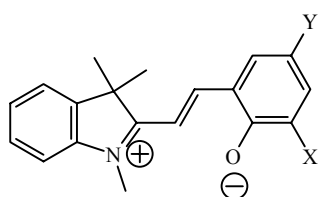
91



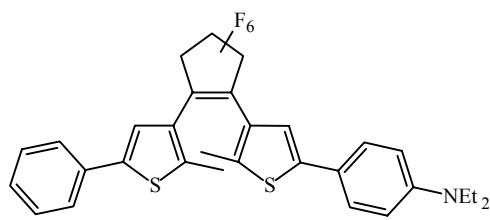
92



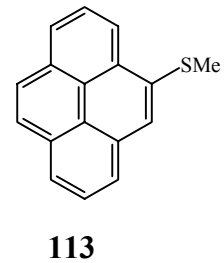
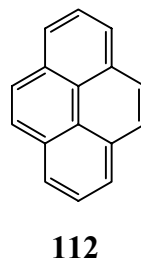
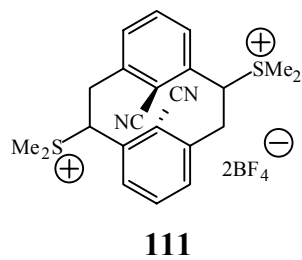
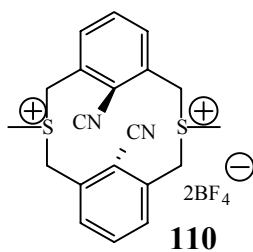
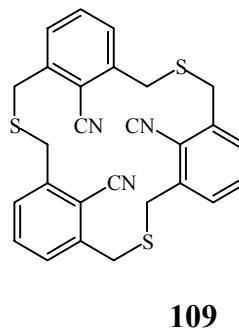
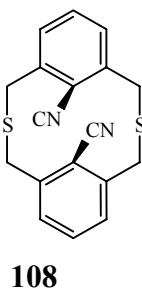
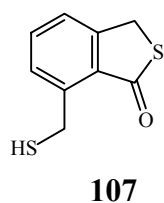
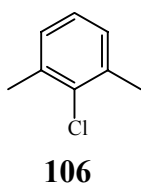
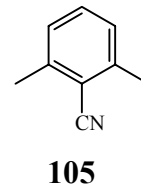
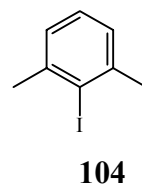
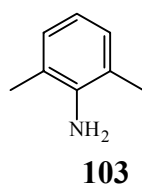
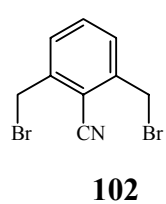
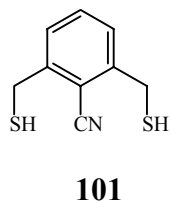
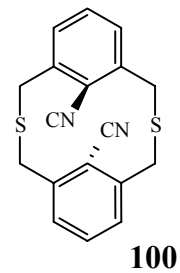
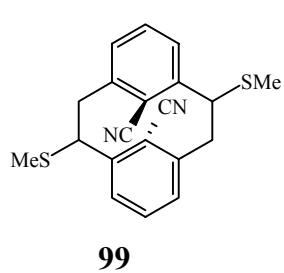
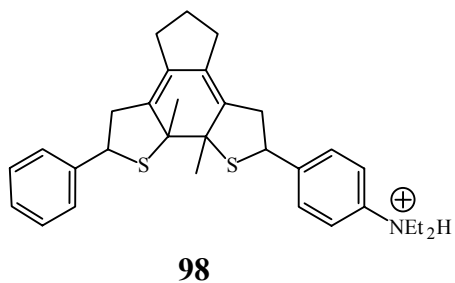
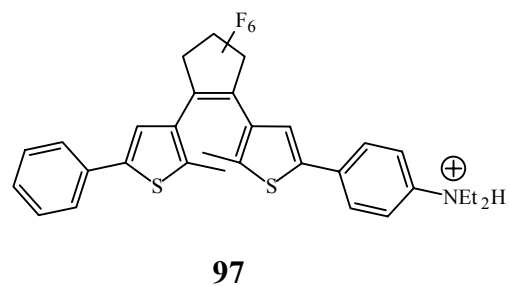
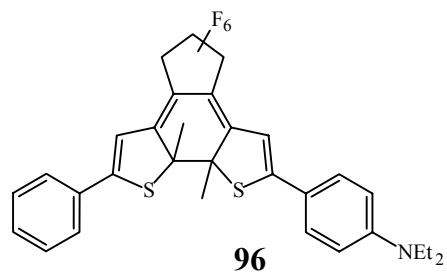
93

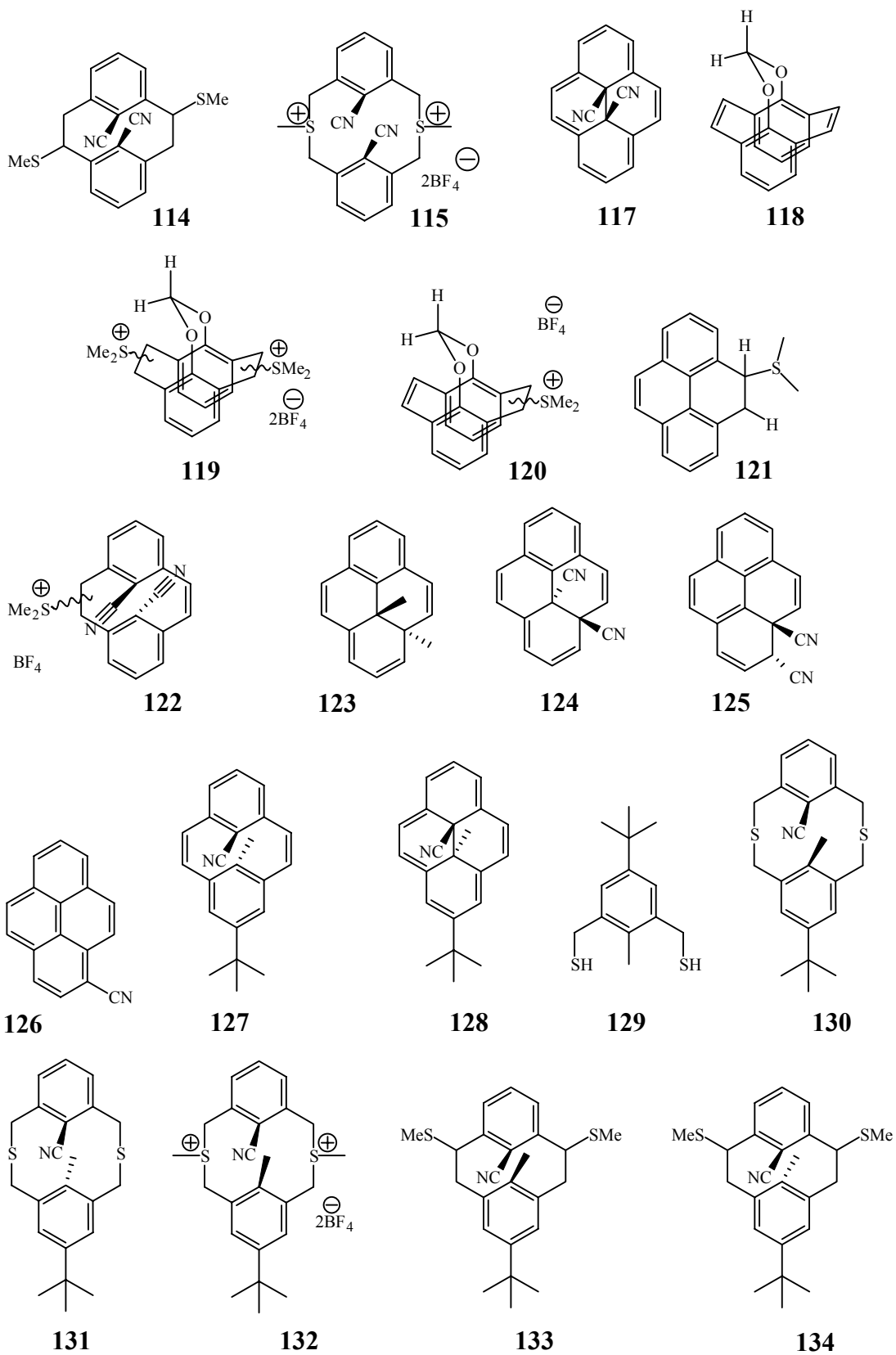


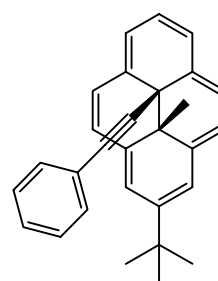
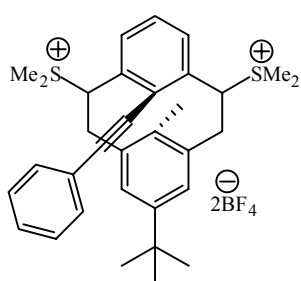
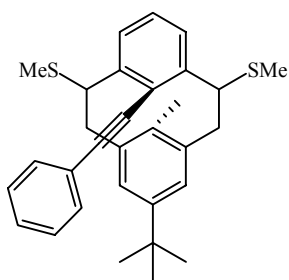
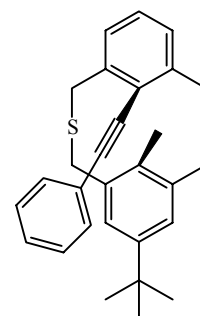
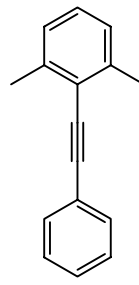
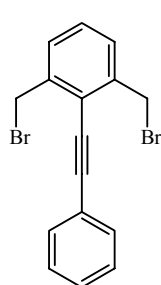
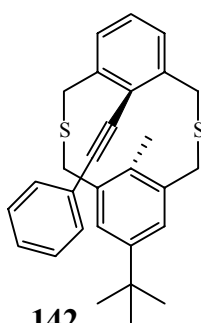
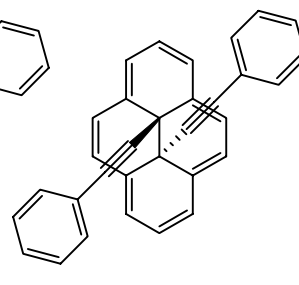
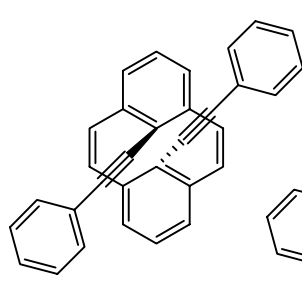
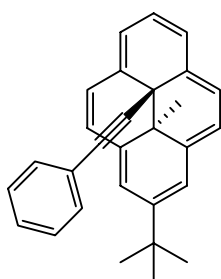
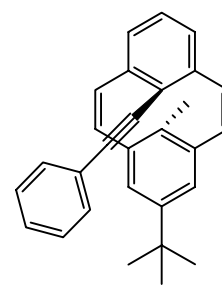
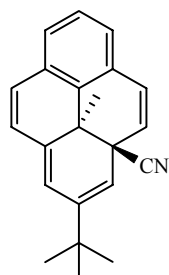
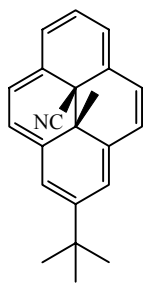
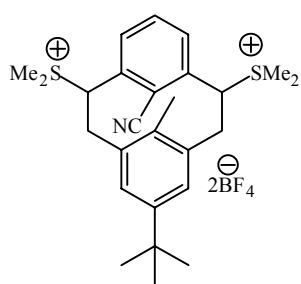
94

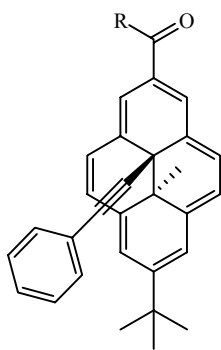


95

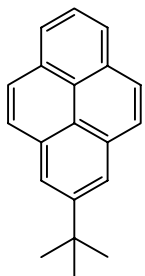




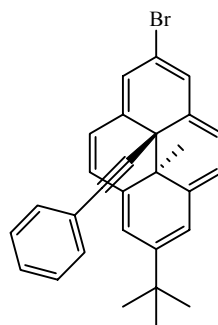




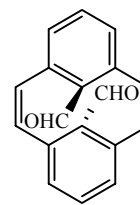
149



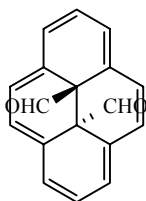
150



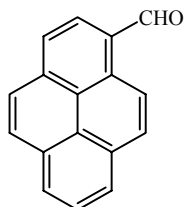
151



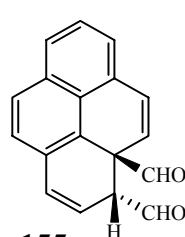
152



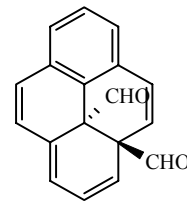
153



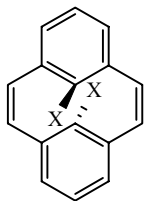
154



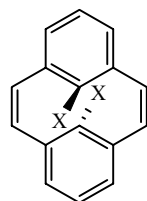
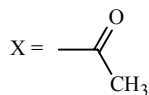
155



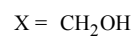
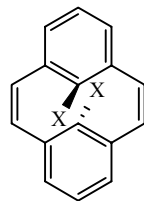
156



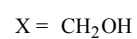
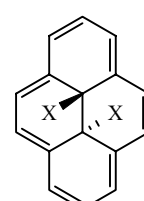
157



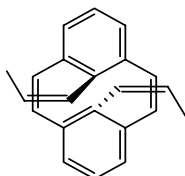
158



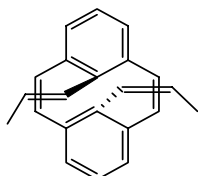
159



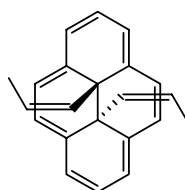
160



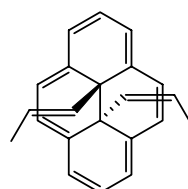
162



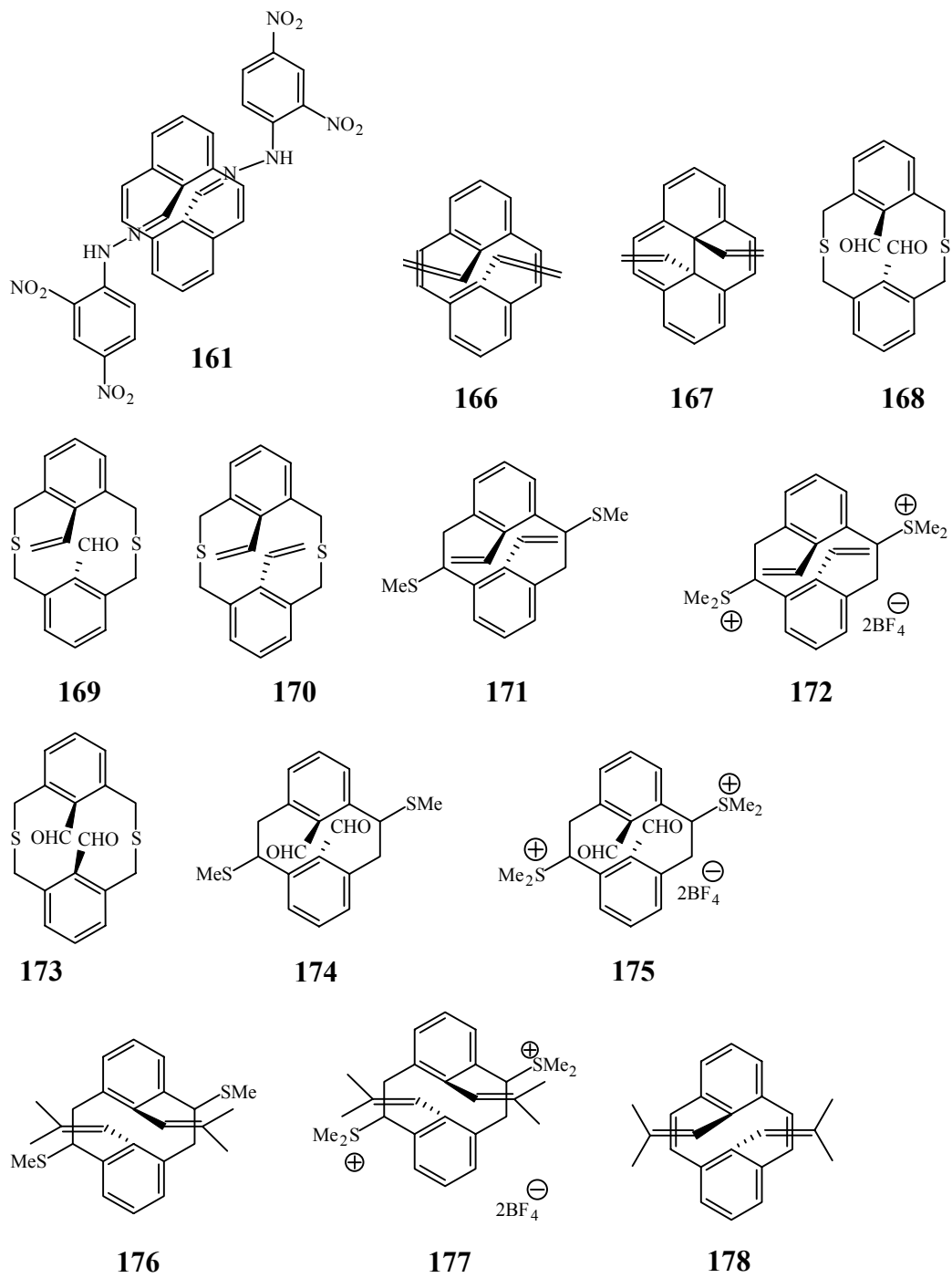
163

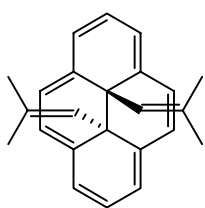
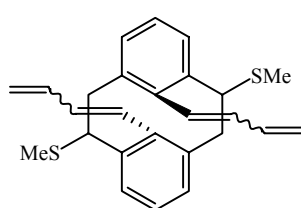
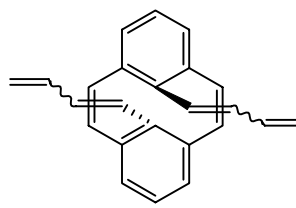
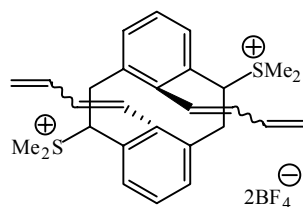
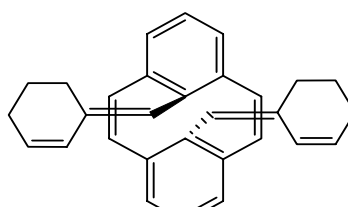
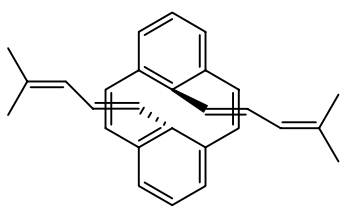
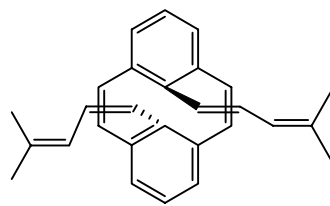
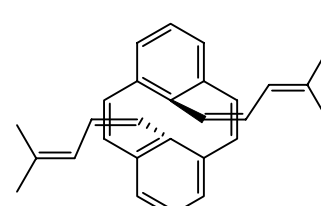
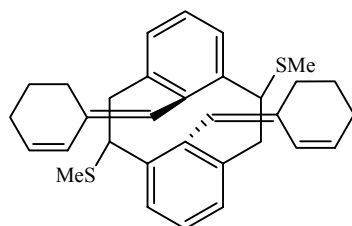
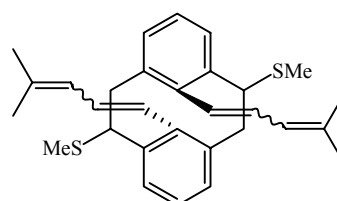
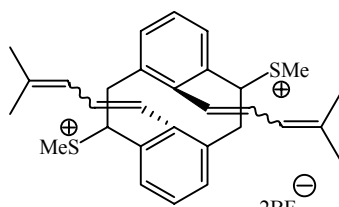
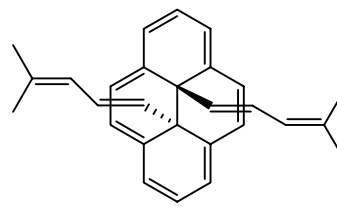


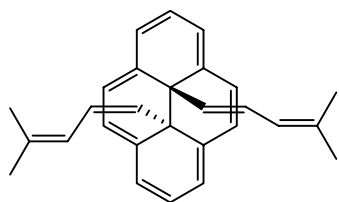
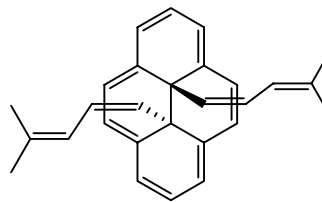
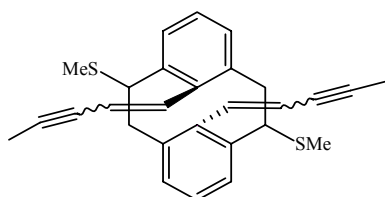
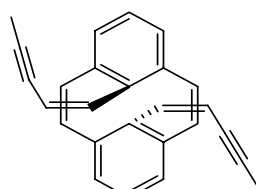
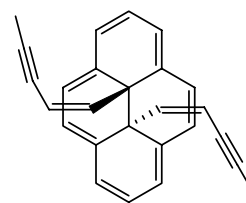
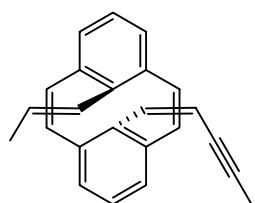
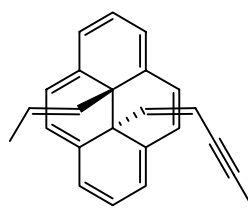
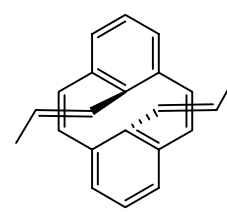
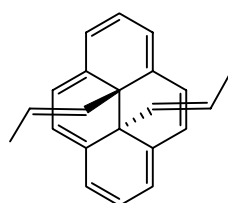
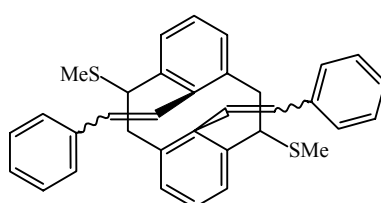
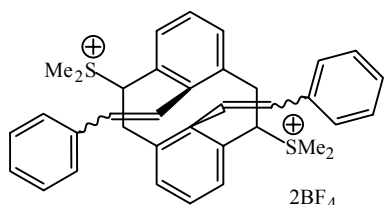
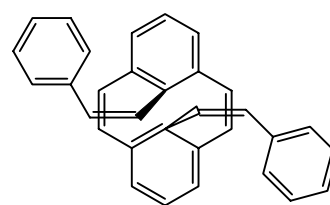
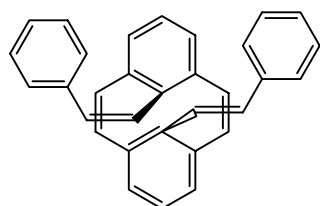
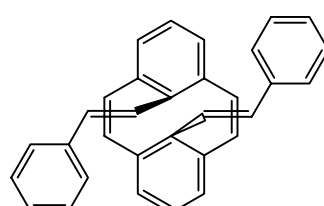
164

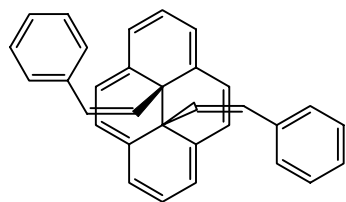
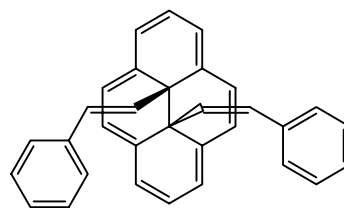
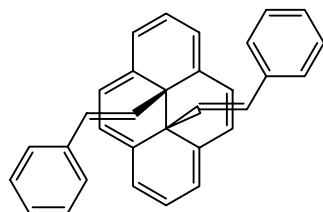
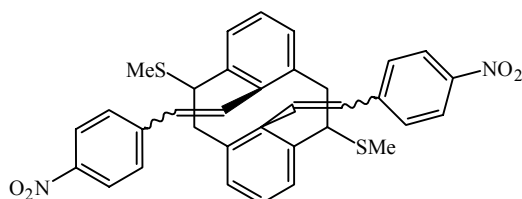
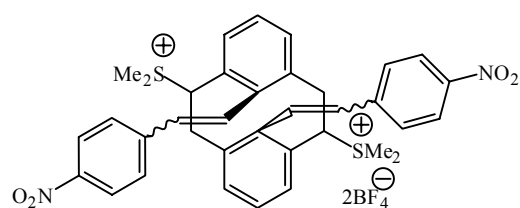
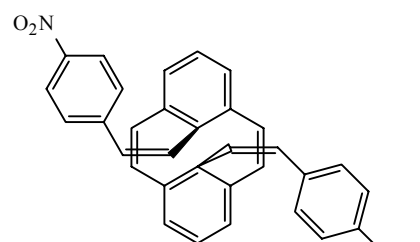
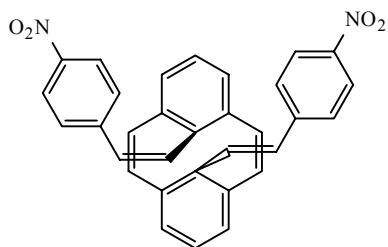
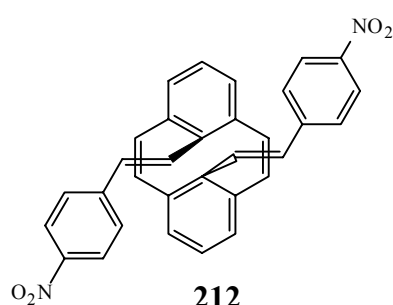
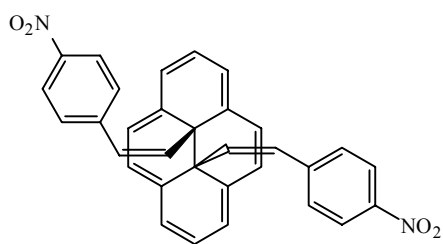
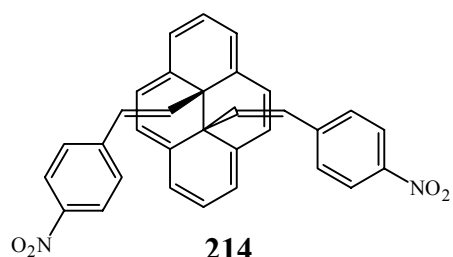


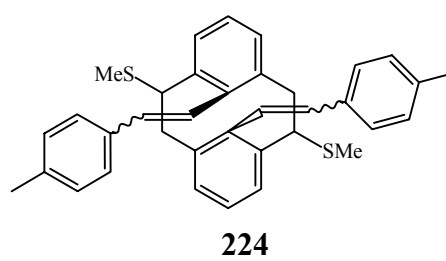
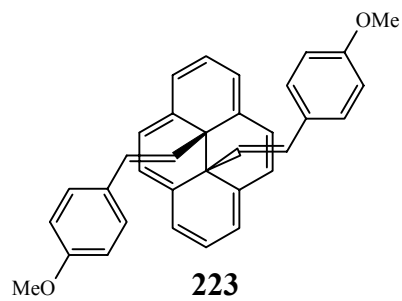
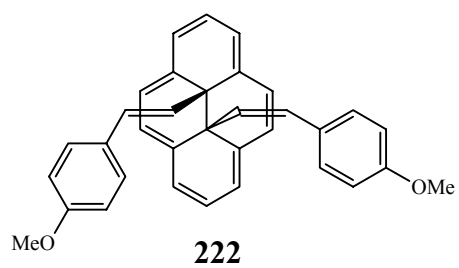
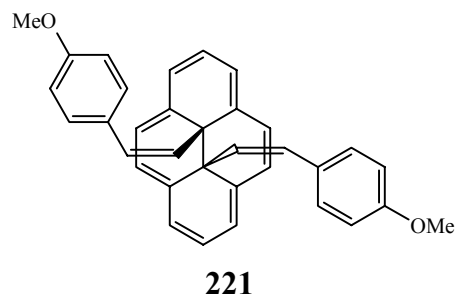
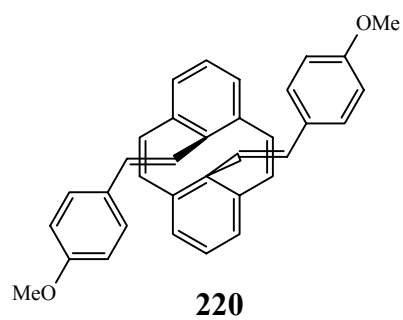
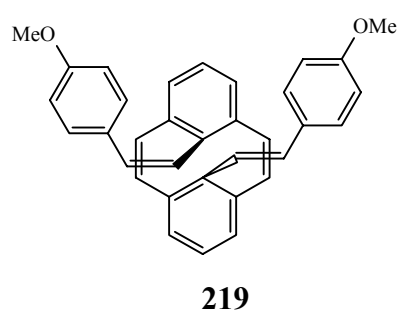
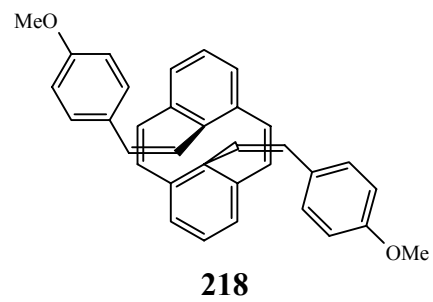
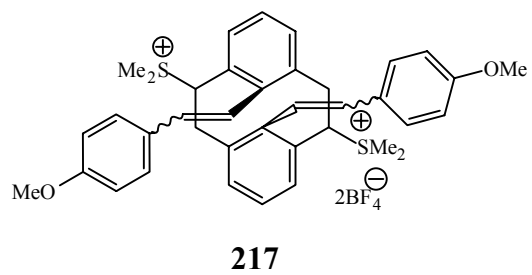
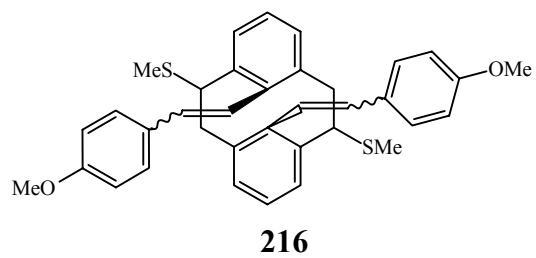
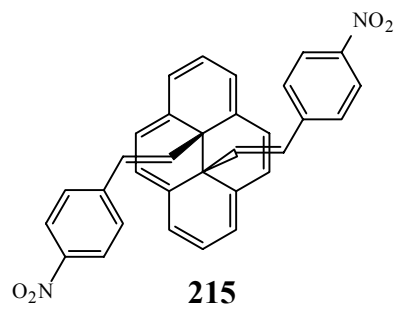
165

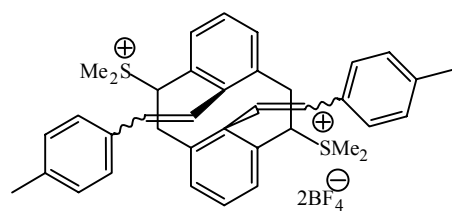
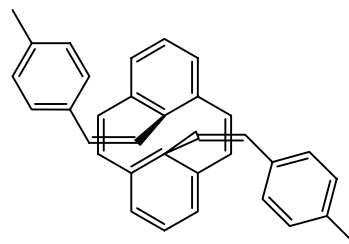
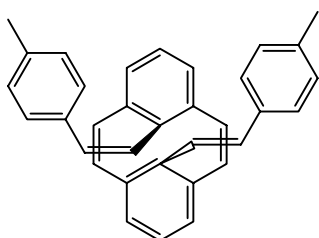
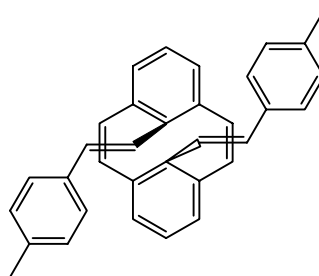
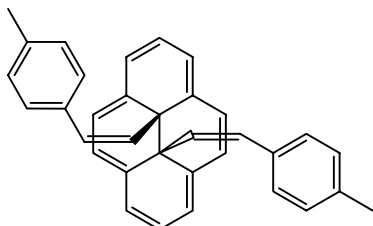
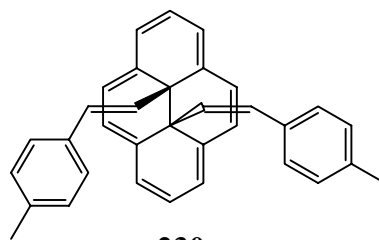
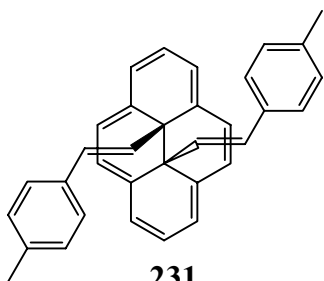
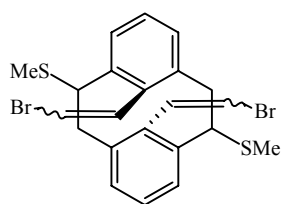
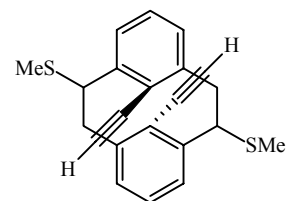
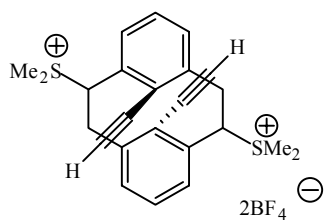
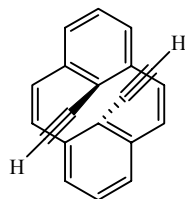
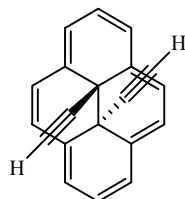
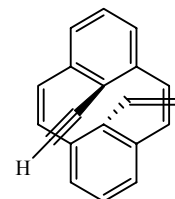


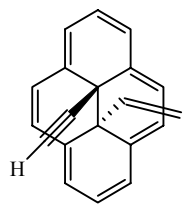
**179****180****181****182****183****184****185****186****187****188****189****190**

**191****192****193****194****195****196****197****198****199****200****201****202****203****204**

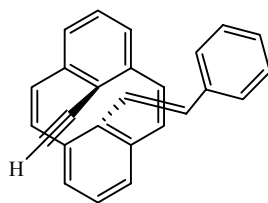
**205****206****207****208****209****210****211****212****213****214**



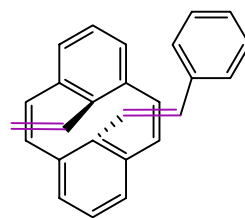
**225****226****227****228****229****230****231****232****233****234****235****236****237**



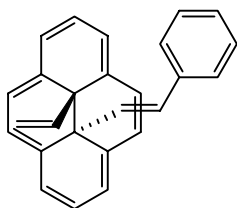
238



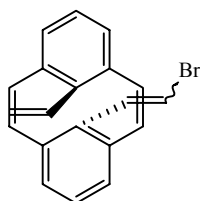
239



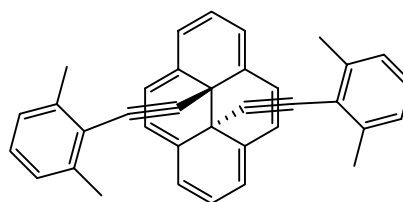
240



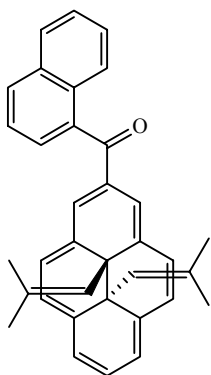
241



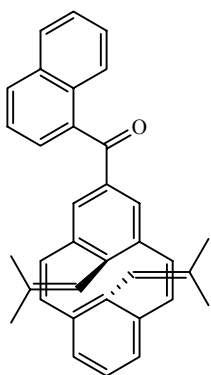
246



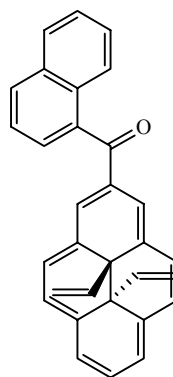
247



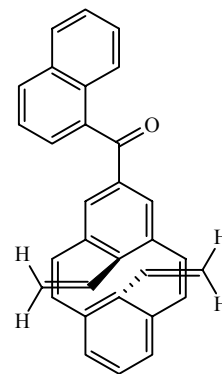
248



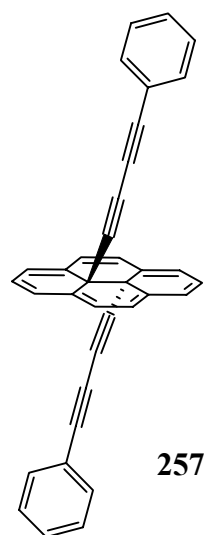
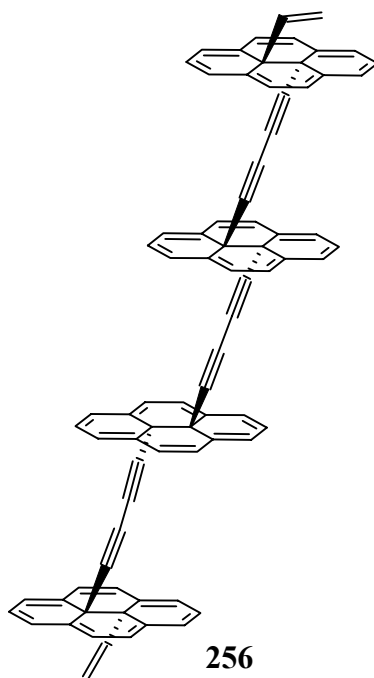
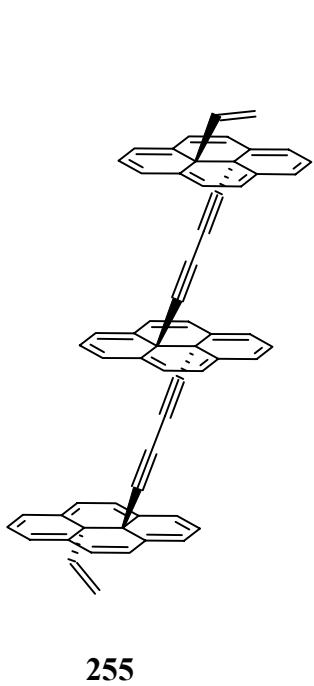
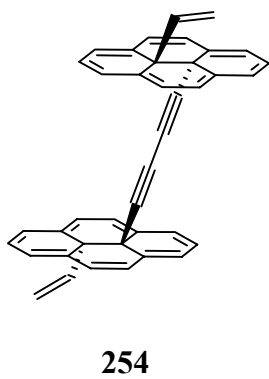
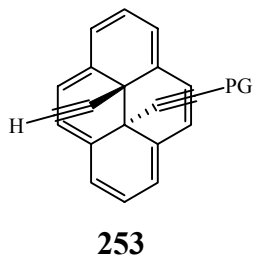
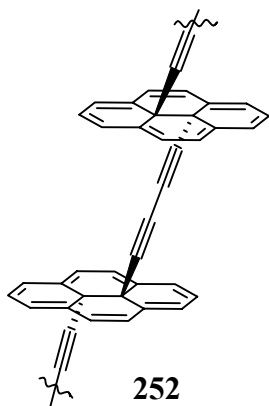
249

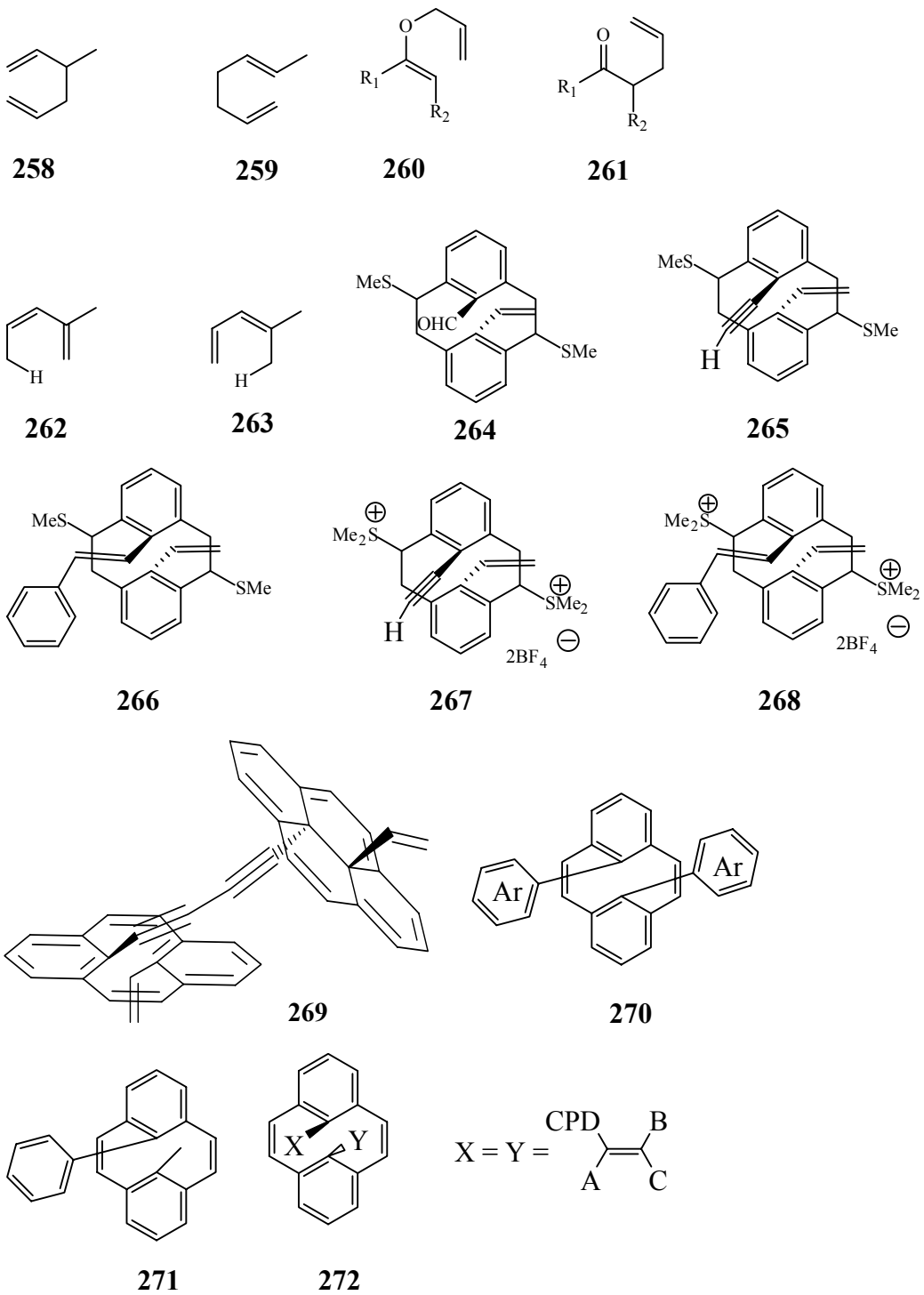


250



251





List of Symbols, Abbreviations and Nomenclature

Symbol	Definition
^{13}C NMR	Carbon-13 nuclear magnetic resonance
^1H NMR	Proton nuclear magnetic resonance
a	Antarafacial
Å	Angstrom
AIBN	Azo-bis(isobutyronitrile)
BDHP	Benzo[e]dimethyldihdropyrene
bp	Boiling point
bs	Broad singlet
c	Closed
CI	Conical intersection
COSY	Correlated spectroscopy
CPD	Cyclophanediene
<i>d</i>	Deuterium
d	Doublet
DCM	Dichloromethane
dd	Doublet of doublets
<i>de</i>	Diastereomeric excess
dec	Decomposition
DEPT	Distortionless enhancement of polarisation transfer (NMR)
DFT	Density functional theory (calculations)

DHP	Dihydropyrene
DMF	Dimethylformamide
EI	Electron impact
Et	Ethyl
EtOAc	Ethyl acetate
EtOH	Ethanol
E	Entgegen (<i>trans</i> orientation of high priority groups on alkene, Cahn-Ingold-Prelog Nomenclature)
ev	Electron volts
E_{act}	Energy of activation
FG	Functional group
g	Grams
GS	Ground state
HMBC	Heteronuclear multiple bond correlation
HRMS	High resolution mass spectrometry
h	Hours
HSQC	Heteronuclear single quantum coherence
Hz	Hertz
IR	Infrared
J	Coupling constant
K	Kelvin
kcal	Kilo calorie
L	Litre

L.A.	Lewis acid
LDA	Lithium diisopropylamide
M	Molecular ion
MeLi	Methyl lithium
Me	Methyl
MeI	Methyl iodide
MeO	Methoxy
MeOH	Methanol
MeS	Thiomethyl
mg	Milligram
min	Minute
MHz	Mega hertz
mL	Milli litre
mp	Melting point
MS	Mass spectrometry
MV	Methylviologen
m/z	Mass per unit charge
NBS	N-bromo succinimide
<i>n</i> -BuLi	<i>normal</i> butyl lithium
nm	Nanometer
NMR	Nuclear magnetic resonance
NMP	<i>N</i> -methylpyrrolidone
NOESY	Nuclear Overhauser enhancement spectroscopy

o	Open
P	Photochemically reversible
P	Positive helicity
Ph	Phenyl
ppm	Parts per million
Pr	Propyl
pss	Photostationary state
q	Quartet (NMR)
R	Rectus (clockwise orientation of high priority groups, Cahn-Ingold-Prelog Nomenclature)
R	alkyl
R _f	Ratio of distance travelled by compound to that of solvent on TLC
r.t.	Room temperature
s	Singlet (NMR) or seconds
S	Sinister (counter clockwise orientation of high priority groups)
s	Suprafacial (pericyclic reactions)
sh	Shoulder
S/N	Signal to noise ratio
t	Triplet (NMR)
T	Thermally reversible photochrome
TEA	Triethyl amine
THF	Tetrahydrofuran
TIN	Tinuvin P

TIPS	Triisopropylsilyl
TLC	Thin layer chromatography
TS [‡]	Transition state
UV	Ultraviolet
vis	Visible
W	Watt
ϵ	Extinction coefficient
λ_{\max}	Maximum wavelength absorption
Δ	Heat
δ	Chemical shift in ppm from standard
π	Pi electron
σ	Sigma electron
Φ	Quantum yield
ΔH^{\ddagger}	Enthalpy of activation
ΔE^{\ddagger}	Energy of activation

Acknowledgement

I would like to express my sincerest gratitude to Dr Reginald H Mitchell for his excellent guidance, suggestions and constant encouragement as well as giving me extraordinary experience throughout the work. I gratefully acknowledge useful discussions with the members of the supervisory committee and with the departmental faculty members during the course of the research. I would like to thank Dr Brendan Twamley (University of Idaho) for X-ray structure determinations. I would also like to thank Dr Richard V. Williams for DFT calculations. My special thanks go to Christine Greenwood for training me on how to operate NMR spectrometers as I benefitted extensively from this facility. I would like to thank David McGillivray for mass spectrometric analysis

I would like to thank my family members who provided a consistent moral support. I also wish to thank all current and former group members with whom I had a chance to work in the lab; Wei Fan, Rui Zhang, Stephen G Robinson, Pengrong Zhang, Yanhong Yang, Olga Sarycheva, Tracy Lohr, Sarah Bennet, Leah Paile, Derek Mendal and Kate Waldie.

Financial support from the University of Victoria and from NSERC Canada is gratefully acknowledged

Words fail me to express my greatest thanks to almighty Allah (God) Who is the source of strength and Whose bounties are countless.

To

All prophets of Allah and in particular to Nooh (Noah), Eesa (Jesus), Moosa (Moses), Ibraheem (Abraham) and above all, Muhammad (peace be upon them all) who were sent as a guidance to mankind.

Chapter 1: Introduction

1.1 Introduction

The active components of future computers and other electronic devices will probably be molecule based because of the massive size reduction using molecules¹ as building blocks compared to conventional silicon based methods. For a molecule based device to be functional there are two important requirements.

1. The molecule must be designed and tuned to give the desired properties.
2. They must be integrated together to form a macro device.

A tremendous amount of research over the past three decades,² has made it possible to screen molecules suitable for molecular devices and successful examples of rectification^{3a}, wiring^{3b}, storage^{3c} and switching processes^{3d} have been reported. It is however, now recognized that it is difficult to obtain communication between molecules in macro devices.

1.2 Molecular switches

Molecular switches are at the core of molecule based devices. A “Molecular Switch” is a broad concept which can be defined as;

“Molecules capable of inducing chemical and physical changes in response to external stimuli such as electrical current, light and heat.”¹

A brief list of external stimuli and the processes associated with them would include:⁴

1. Light: Photochromism, Light induced energy transfer, Phototropism, Heliochromism.
2. Electrical current: Electrochromism

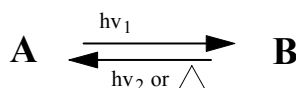
3. Heat: Thermochromism
4. Chemical: Halosolvatochromism, Solvatochromism, Acidochromism, Ionochromism
5. Mechanical: Piezochromism, Tribochromism.

Among the above mentioned phenomena, only photochromism will be described here.

1.3 Photochromism

“Photochromism is a reversible transformation of a chemical species induced in one or both directions by absorption of electromagnetic radiations between two forms A and B having different absorption spectra”⁴

Figure 1.1 Photochromism



P type and T type photochromes

Photochromic chromophores can be divided into two categories based on the stability of the photogenerated species. If the photogenerated species (B) reverts back thermally to the initial state (A) in the dark then it is called T type (thermally reversible). If no such thermal reversion is observed in dark then it is called P type (photochemically reversible). Unfortunately most photochromic chromophores belong to the T type and are thus less generally applicable in photoswitchable molecular systems.

Photochromism can be positive or negative. If λ_{max} of B $>$ λ_{max} of A, then it is called positive photochromism. Most of the photochromic chromophores belong to this division. If λ_{max} B $<$ λ_{max} of A, then it is called negative photochromism.⁴

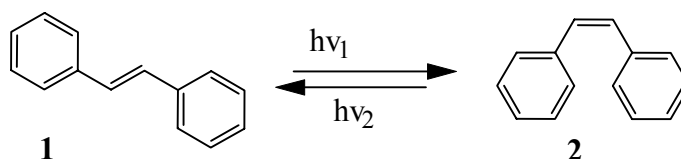
According to the type of the reaction taking place through light, photochromic compounds can be divided into six categories⁴.

1. *Cis-trans (E/Z)* isomerization
2. Intramolecular hydrogen transfer
3. Intramolecular group transfer
4. Dissociation processes
5. Electron transfers (redox)
6. Pericyclic reactions

1.3.1 *Cis-trans (E/Z)* isomerization

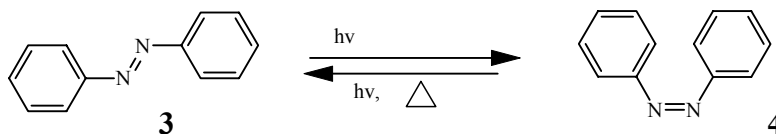
Both *cis* and *trans*-stilbenes interconvert reversibly upon excitation of the double bond (Scheme 1.1). This is one of the best understood photochemical systems but has not yet found applications in memory devices.

Scheme 1.1 *Cis-trans* isomerization of stilbenes



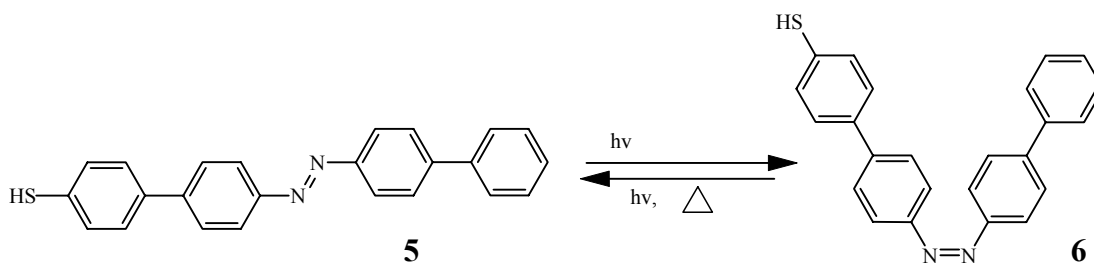
A particularly well-studied example in this category is azobenzene **3** (Scheme 1.2). *trans*-Azobenzene **3** isomerizes into *cis*-azobenzene **4** by irradiation with UV light. The *cis* or *Z*-form **4** is thermally unstable and reverts to the *trans* or *E* form **3**, which renders it unsuitable for memory devices. However, because of the appreciable change in distance between the two ends upon isomerization, this system has gained some unusual applications, some of which are given below.

Scheme 1.2 *Cis-trans* isomerization of azobenzene



Rampie⁵ and coworkers have shown that the change in the structure upon isomerization can be applied to gain mechanical work by use of the biphenyl example shown in Scheme 1.3 below.

Scheme 1.3 An azobenzene type photoswitch



The thiol group was used to anchor to a gold surface. The difference of the distance between two ends in *trans* **5** and *cis* **6** is about 7.0 Å which is almost double that of azobenzene itself (3.5 Å)

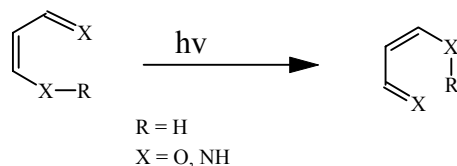
Azobenzene based polymers upon photoisomerization influence polymer swelling properties,^{6a} wettability,^{6b} membrane properties,^{6c} viscosity and solubility.⁷ Azobenzene based photoswitches also have applications in liquid crystals⁸ because of their interesting nonlinear properties.

Other systems which also show *cis-trans* isomerization are overcrowded alkenes,¹ azines, thioindigoids⁴ etc.

1.3.2 Intramolecular hydrogen transfer

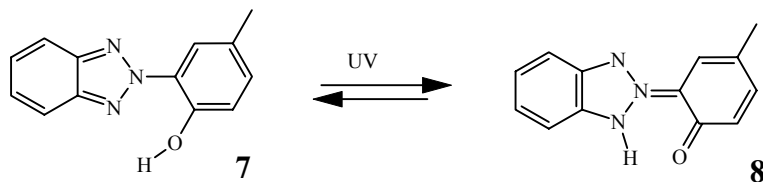
Intramolecular hydrogen transfer takes place from the electronically excited state of a molecule of the type shown in Scheme 1.4. This is also called phototautomerization.

Scheme 1.4 Phototautomerization



Generally the species generated in this process is thermally highly unstable and soon reverts back and dissipates energy in the form of heat. These kinds of molecules are generally used as UV stabilizers for polymers. A commercial UV stabilizer for polymers is 2-(2'-hydroxy-5'-methylphenyl)benzotriazole^{4b} **7** (trade name Tinuvin P (TIN)), which is a benzotriazole based hydrogen transfer system. The process taking place on absorption of UV light is shown in Scheme 1.5. The phenolic hydrogen is transferred to the triazole part on irradiation and generates an ortho-quinoid species **8** which is unstable and reverts back to **7**.

Scheme 1.5 Photochemistry of Tinuvin P

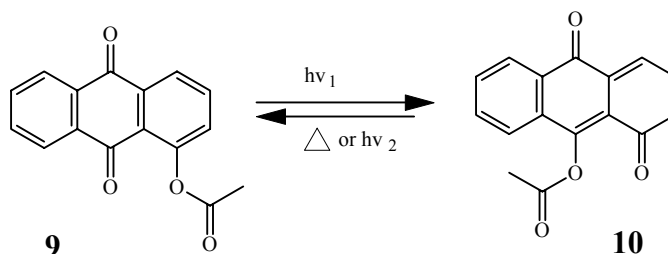


Other families of compounds showing this kind of behavior are anils,⁹ benzylpyridines, aci-nitro compounds, salicylates, oxazoles, and perimidinespiro hexadieneones.¹

1.3.3 Intramolecular group transfer

This is similar to hydrogen transfer except that in this case the migrating group is other than hydrogen. A well known example (Scheme 1.6) is the migration of an acetoxy group in polycyclic quinones (periaryloxyquinones).¹⁰

Scheme 1.6 Acyl migration in a polycyclic quinone



1.3.4 Dissociation processes

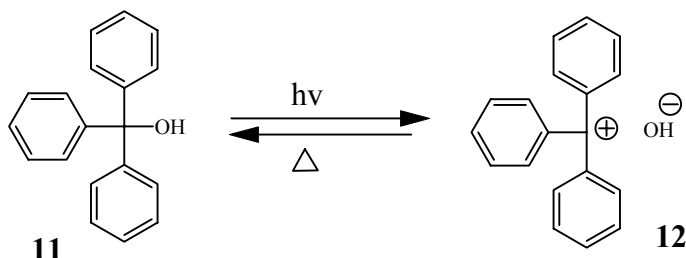
Light can cause homolytic or heterolytic cleavage of a bond to form more or less separated radicals or ion pairs. This dissociation, accompanied by a color change forms the basis of photochromism. Triarylimidazole dimers, tetrachloronaphthalenes, nitroso dimers and triaryl methanes are among the classes of compounds which can show bond dissociation photochromism.

These classes of compounds have gained little interest as photochromic compounds but they have a variety of other industrial applications. For example,

1. Triarylimidazole dimers are used in microlithography and silver free imaging processes.
2. Light mediated C-C cleavage of benzil and benzoin derivatives is used in radical polymer initiation.¹¹

- Malachite green derivatives are UV actinometers and are used in flash blind protection.¹²
- Triphenyl leucohydroxides provide HO^- ions on photoirradiation and thus cause pH to change.¹³ The dissociation process is shown in Scheme 1.7.

Scheme 1.7 Dissociation of triphenylcarbinol to release HO^-

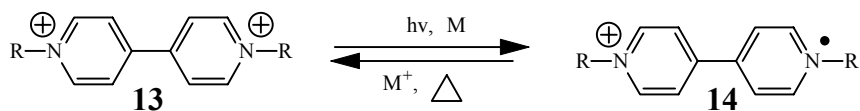


This release of an HO^- group from **11** causes the pH of the medium to change from 5.6 to 10.0 which slowly reduces because of the thermal back reaction.

1.3.5 Oxido-reduction (electron transfer) processes

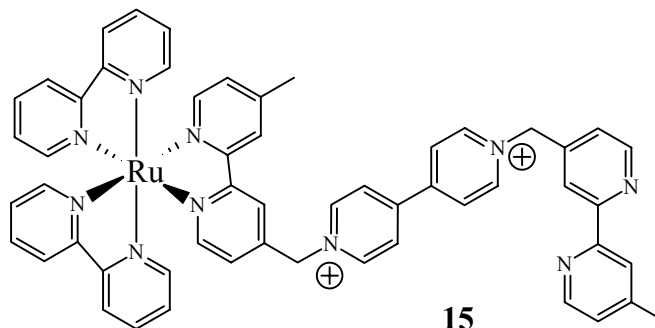
Viologens undergo electron transfer in the presence of metals upon irradiation with light, shown in Scheme 1.8.

Scheme 1.8 Electron transfer in viologens

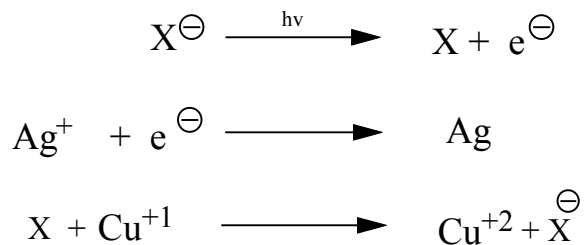


The R group is methyl or other alkyl derivative. Methyl viologens are interesting in their behavior. e.g. Hammarstrom¹⁴ has shown that the MV^{+2} part of **15** oxidizes the excited ruthenium complex, while in the MV^{+1} or the MV^0 state it reduces the complex. So the direction of electron flow can be controlled by an externally applied bias.

Figure 1.2 Viologens-ruthenium complex dyad 15



Another example of a photo redox system is the early photochromic ophthalmic spectacles¹⁵ by Corning. The chemistry involves a redox pair of Ag and Cu. Silver, present as Ag^+ , accepts an electron from halide and forms metallic silver in the presence of light. At the same time Cu^{+1} present in the mixture reduces halogen back to halide.¹⁵ While in dark, Cu^{+2} oxidizes the Ag into Ag^+ and this causes bleaching.



1.3.6 Pericyclic reactions

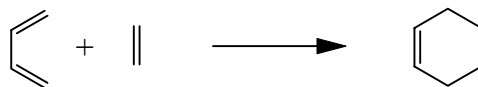
The two common pericyclic reactions in photochromism are cycloaddition reactions and electrocyclic reactions.

1.3.6.1 Cycloaddition reactions

Cycloaddition reactions are defined as: “Reaction in which two or more unsaturated molecules or parts of the same molecule combine with the formation of a cyclic adduct in which there is a net reduction of the bond multiplicity.”¹⁶

Cycloaddition reactions are generally symbolized as $[i + j + \dots]$ where i and j are the number of electron in the interacting units that take part in the formation of the ring. According to this notation the Diels-Alder reaction is described as $[4 + 2]$. Very often symbols “s” and “a” are added as subscripts to these numbers which specifies the stereochemistry of addition of each unit. “s” and “a” stand for suprafacial and antarafacial selectivity respectively. So the Diels-Alder reaction would be $[4s + 2s]$.

Scheme 1.9 The Diels Alder reaction

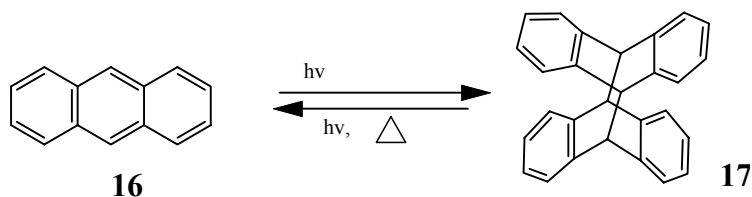


According to selectivity rules, a photochemical $[2+2]$ reaction occurs readily while a thermal $[2+2]$ requires quite drastic conditions. On the other hand, the thermal $[4+2]$ cycloadditions is quite feasible while the photochemical is difficult.¹⁹

$[4 + 4]$ cycloadditions

A well known example of a $[4+4]$ cycloaddition reaction is the dimerization of anthracene (Scheme 1.10).¹⁷

Scheme 1.10 The Photo-dimerization of anthracene

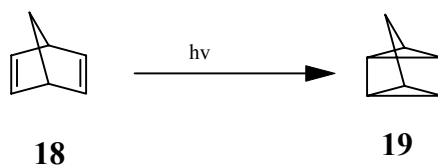


$[2 + 2]$ Cycloadditions

An example of a $[2+2]$ cycloaddition reaction is the norboradiene rearrangement shown in Scheme 1.11. This system has achieved considerable generality including

examples with a variety of functional groups which affect both the UV-vis spectrum and the thermal stability of the photogenerated species¹⁸.

Scheme 1.11 The norbornadiene rearrangement



1.3.6.2 Electrocyclic reactions

“An electrocyclic reaction is characterized by the opening or closing of a ring, within a single molecule leading to the conversion to 2σ electrons to 2π electrons or the reverse.”¹⁹

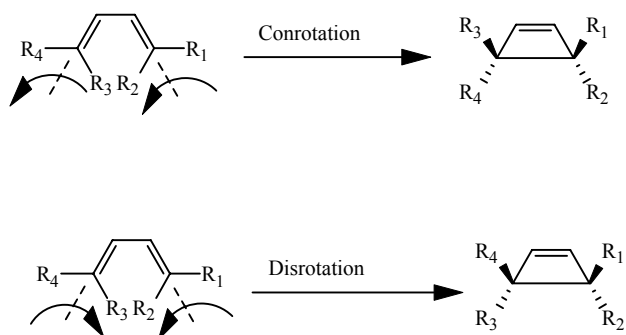
There are two different modes of cyclization, namely conrotatory and disrotatory cyclization. Taking butadiene as an example (Figure 1.3) if both ends move in the same direction, it is called conrotatory cyclization (Conrotation), while movement in opposite directions is termed as disrotatory cyclization (Disrotation).

The general rules for photochemical and thermal electrocyclization

Table 1.1 Allowed modes for photochemical and thermal electrocycliations

Entry	Number of π electrons	Photochemical	Thermal
1	$4n \pi$	Disrotatory	Conrotatory
2	$4n + 2 \pi$	Conrotatory	Disrotatory

Figure 1.3 Conrotatory and disrotatory mode of cyclization

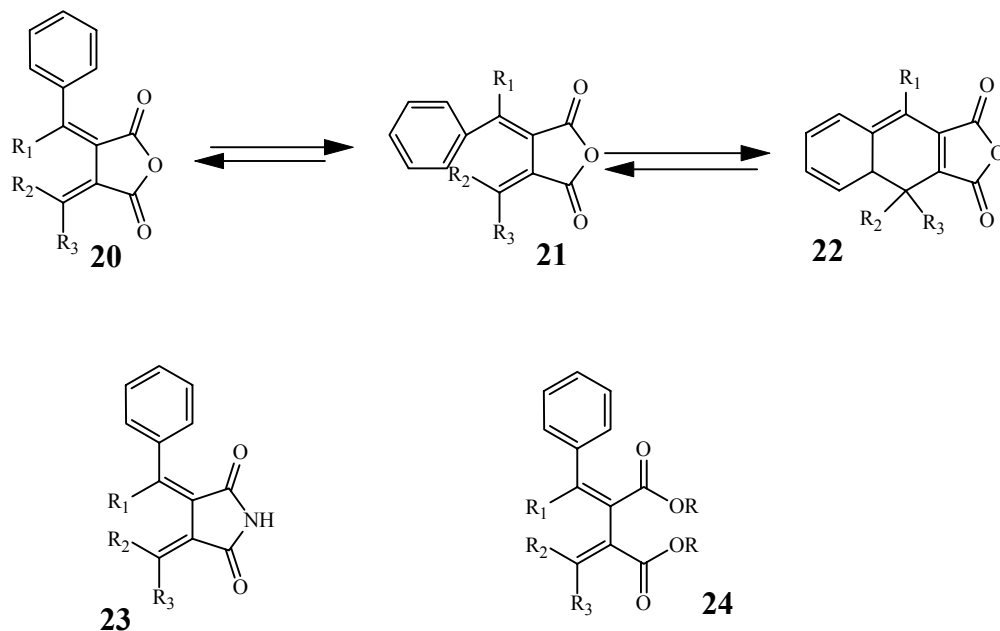


In this section only 6π 6-carbon electrocyclic reactions will be described. Most popular photoswitches for memory devices i.e dithienylethenes and fulgides belong to this class. These two systems generally show thermal irreversibility and are P type photochromes. Other families are spiropyrans, spirooxazines and chromenes. Dihydropyrenes, negative type photochromes, also fall under this category.

Fulgides /Fulgimides/ Fulgenates

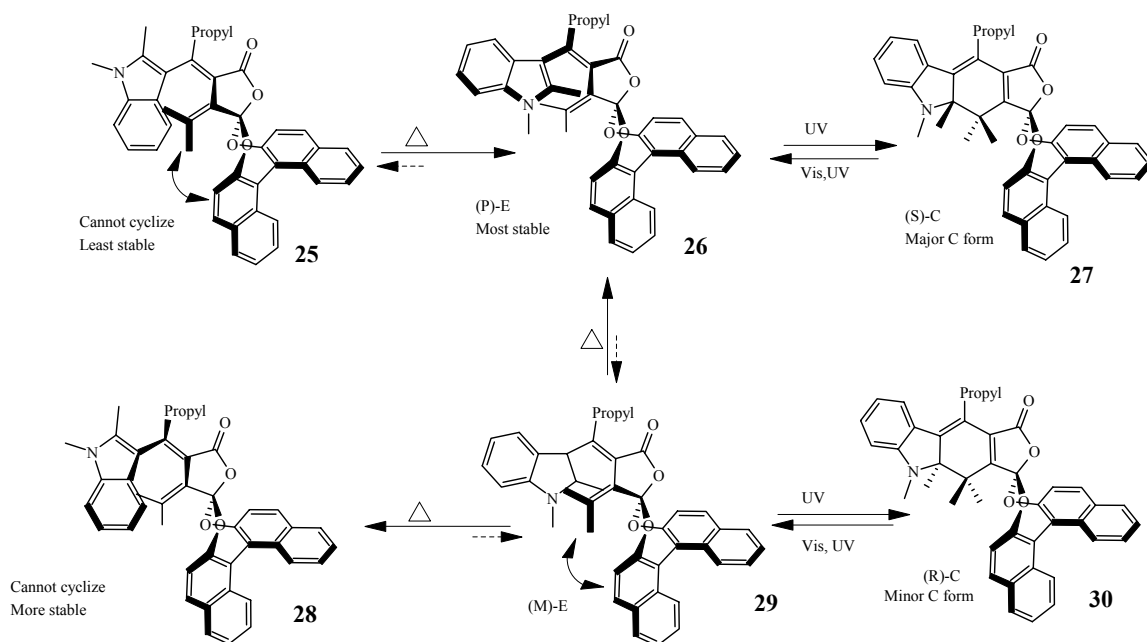
Fulgides, the common name for bismethylenesuccinic anhydrides possessing at least one aromatic ring on the methylene carbon atoms such as molecule **20**, were first synthesized by Stobbe in the early 20th century.²⁰ Upon irradiation with UV light, the colorless form **21** isomerizes into the colored form **22** and to another colorless form **20**. Switching between E-**21** and Z-**20** and between E-**21** and C-**22** continues until the photostationary state is formed. Fulgimides **23** are the imides instead of anhydrides while diesters are called fulgenates **24** (Scheme 1.12).

Scheme 1.12 Photoisomerization of fulgides



Molecule **25** shown in Scheme 1.13 was reported by Yokoyama et al.²¹ as a highly diastereoselective photochromic system. Because of the steric repulsion between one of the binaphthol naphthalene rings and an isopropylidene methyl group pointing away from the molecule, the hexatriene moiety is forced to adopt positive (**P**) helicity **26**. This results in high diastereoselectivity in the closed form (90% de) with the *S* diastereomer predominant. This has application in chiral nematic crystals (liquid crystals). The specific rotation values of hexatriene and its photo stationary state (closed) at the sodium D line are -572° and -186° , respectively. These quite distinct values, along with the fact the sodium D line does not cause a photochromic reaction, provide a tool for non-destructive readout.

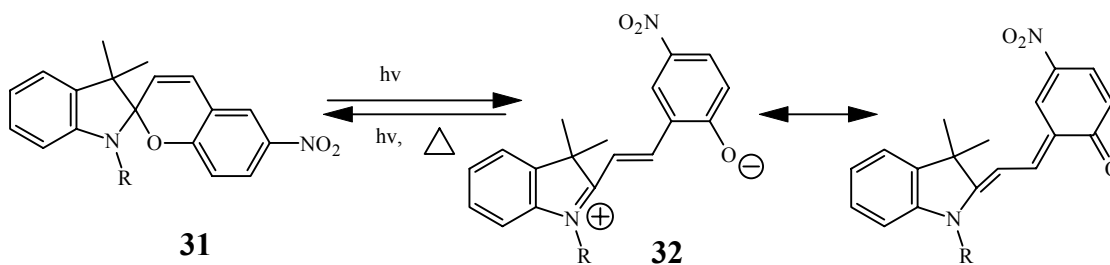
Scheme 1.13 Highly diastereoselective cyclization of ketal fulgide **25**



Spirooxazine and spiropyrans

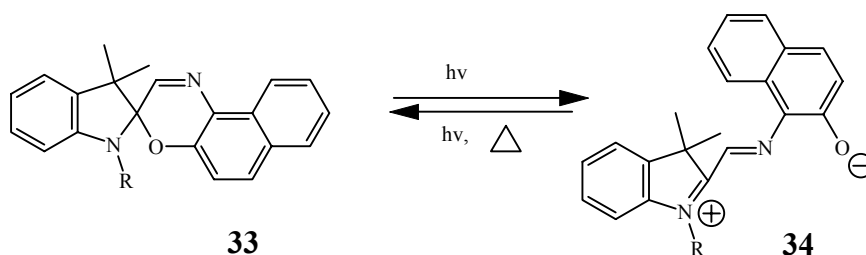
The photochromism of spiropyrans was first observed by Fischer and Hirschberg²² in 1952, even though thermochromism of these compounds has been known since 1921. In solution, spiropyran **31** (Scheme 1.14) shows absorption in the UV region (200-400 nm). Irradiation with light in this region causes the spiropyran to open into a colored species called a merocyanine **32**.

Scheme 1.14 Photochromism of spiropyran **31**



Spirooxazines **33** are structurally similar to spiropyrans except that one of the methine carbons in the spiropyrans is replaced by a nitrogen in the spirooxazine. Both spiropyrans and spirooxazines are T type positive photochromes.

Scheme 1.15 Photochromism of spirooxazine 33

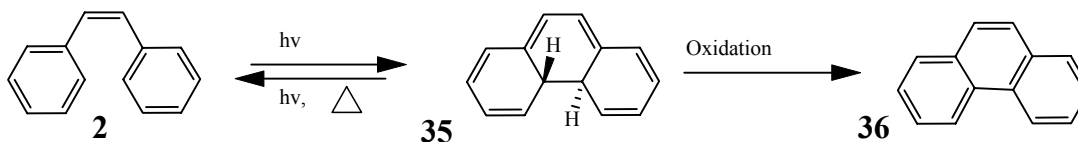


Spiropyrans and spirooxazines have some interesting applications e.g. in self developing photography, actinometry, displays, filters, and lenses of variable optical density including eye protection glasses and more recently in three dimensional optical memories based on two photon conversion.²³

Dithienylethenes

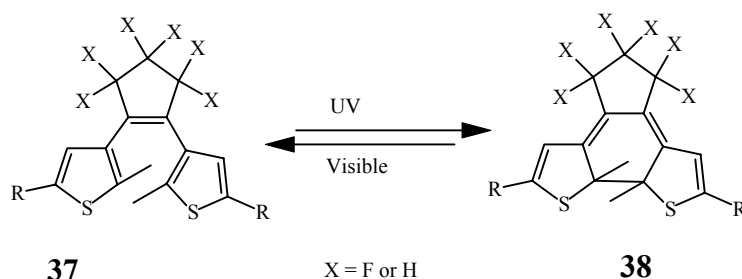
Dithienylethenes belong to the diarylethene class of photoswitches, the parent example of which is the interconversion between *cis*-stilbene **2** and dihydrophenanthrene **35** (Scheme 1.16). The dihydrophenanthrene is quite reactive towards oxidation and irreversibly forms phenanthrene **36**.

Scheme 1.16 Phenanthrene from *cis*-stilbene



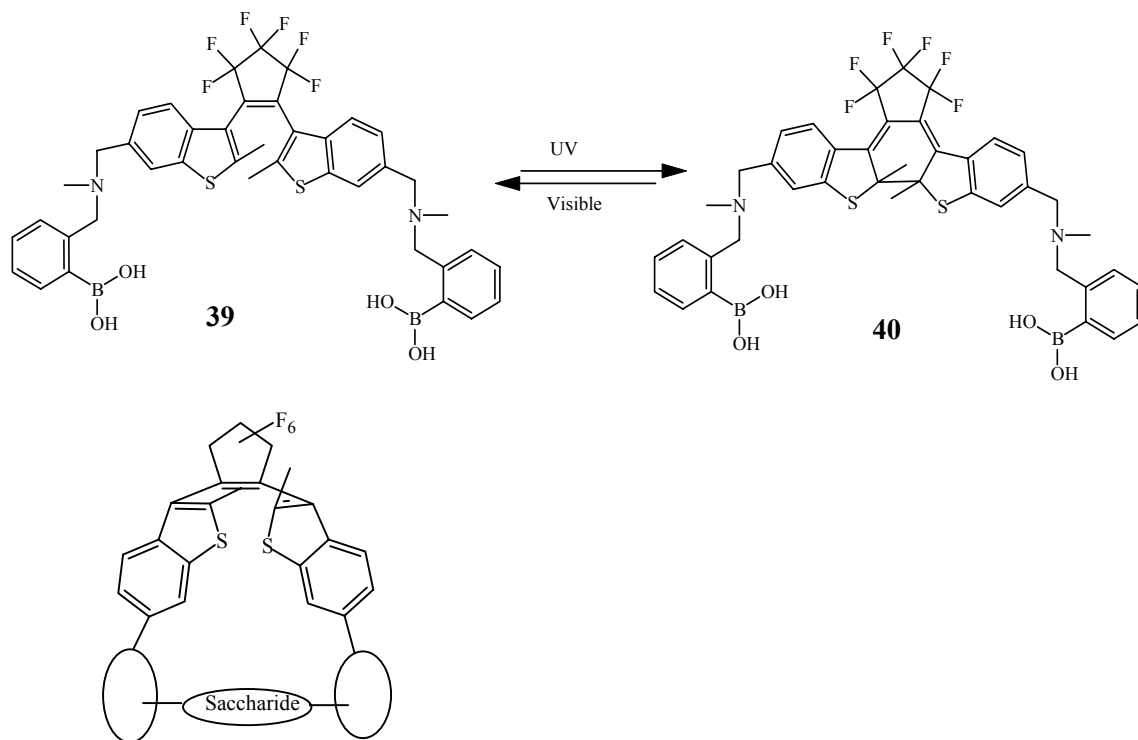
This problematic oxidation reaction can be avoided by replacing the hydrogens with methyl groups. In the parent example, the thermal back reaction is rapid but when the phenyl ring is replaced with a heteroaryl ring such as thiophene, the thermal back reaction is quenched (P type photochromes).

Scheme 1.17 Irie's dithienylethene photoswitch



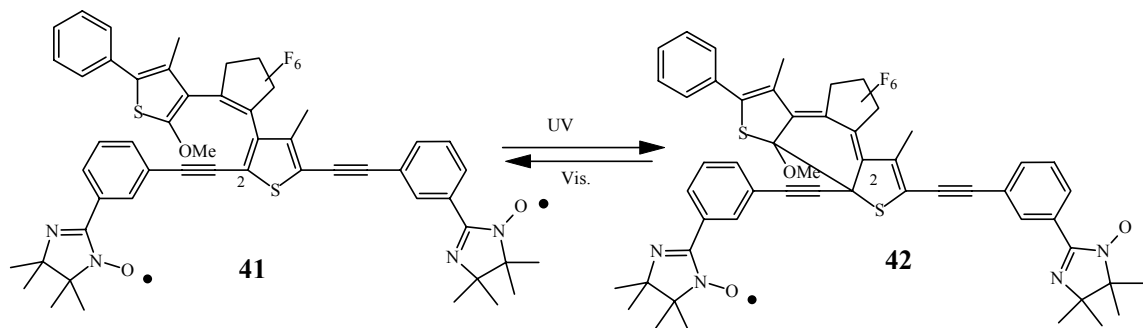
Dithienylethene photoswitches (Scheme 1.17) are characterized by a number of practical advantages including thermal stability of isomers, fatigue resistance (stable up to 10000 cycles) and fast response time which make them suitable for applications in molecular devices.²⁴ This photoisomerization has application not only in molecular devices but also in biology where a molecule or an ion binds selectively to one isomer. One example is the reversible binding of saccharides to molecule **39** which contains two boronic acids functional groups (Scheme 1.18). Open isomer **39** binds to saccharide and forms the complex²⁵ which can be monitored easily by the growth of a CD spectrum. Upon irradiation with UV light, ϵ drops to 40% while the photostationary state contains 60% of the closed isomer, this indicates that the closed form **40** hardly binds to the saccharide at all. The ϵ value returned upon irradiation with visible light.

Scheme 1.18 Photo-controlled release of saccharide from dithienylethene 39



2,5-Bis(arylethynyl)thiophene has been applied for the switching of magnetism when the aryl group contains imino nitroxide radicals (Scheme 1.19). In the open form **41**, the system is fully conjugated and the two radicals interact with each another (“ON” state). Upon UV closing, the conjugation is broken (carbon 2 changes from sp^2 to sp^3) and the switch represents the “OFF” state.²⁶

Scheme 1.19 Photoswitching magnetism

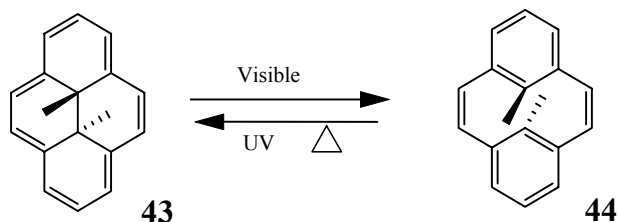


Other applications of dithienylethene photoswitches involve photoelectrochromism,²⁷ gated reactivity,^{28, 24} liquid crystalline switches and many others.²⁴

1.4 Dihydropyrene photoswitches

Dihydropyrene photoswitches are of negative T type²⁹ in which the colored form **43** (closed/DHP) is more stable and isomerizes upon irradiation with visible light into the colorless form, cyclophanediene **44** (Scheme 1.20), which returns back either thermally or photochemically with UV light. Quite analogous to many other photoswitches, the bond forming termini of the 6π electrocyclic system should not contain hydrogen atoms so as to avoid oxidation. 10b,10c-Dimethyldihydropyrene³⁰ **43** and 2,7-di-*tert*-butyl-10b,10c-dimethyldihydropyrene **45** are the molecules in this series which have been studied in some detail.

Scheme 1.20 Photoswitching of dihydropyrene 43



Quite a number of factors were involved for this photoswitch to stay dormant both from a research and a commercial point of view.

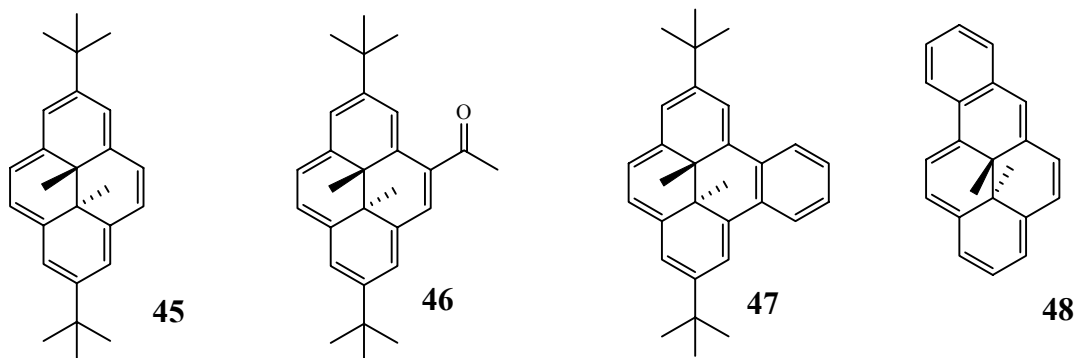
1. Tedious synthesis
2. Poor quantum efficiency for opening
3. Decomposition/side reactions
4. Thermal back reaction.

A brief outline is mentioned towards the success of solving each problem.

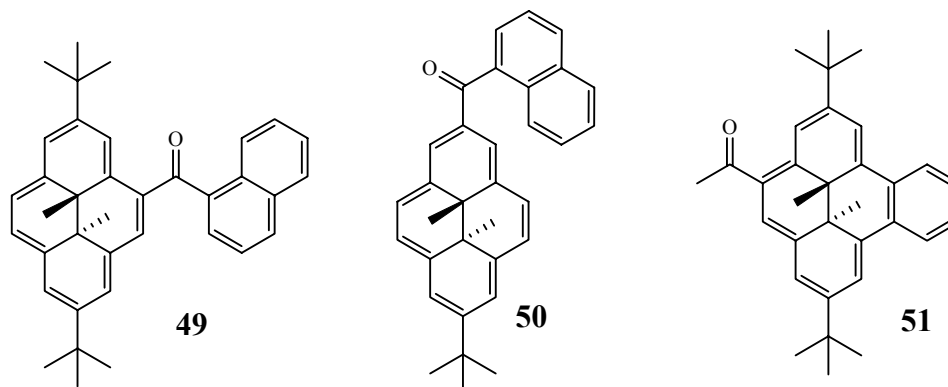
1.4.1 Tedious syntheses

The very first synthesis reported by Boekelheide³¹ involved 14 steps with a 3% overall yield starting from *p*-cresol. This small yield limited the study of dimethyldihydropyrene derivatives. In the 70s, Mitchell³² reported an improved synthesis of dimethyldihydropyrene with 36% yield starting from 2,6-dichlorotoluene. This was a major breakthrough in the chemistry of dimethyldihydropyrene because it allowed the study of these molecules in greater detail. Further improvement came when *t*-butyl derivative³³ 45 was reported in 35-45% yield in just six steps starting from *t*-butyltoluene. This synthesis could provide gram quantities of dihydropyrene 45 in a span of two weeks or less.

1.4.2 Quantum yield



Dimethyldihydropyrene **43** has a low quantum yield for ring opening (0.006) which rendered it inapplicable for practical devices. *t*-Butylated dimethyldihydropyrene **45** has an even poorer quantum yield³⁴ (0.0015), about 4 times less than the parent. Quite a large number of compounds have been scanned for their photophysical properties but the quantum yield for ring opening is generally low. However, introduction of a carbonyl functional group at the 2 and 4 positions or [e]-annulation with a benzene ring (BDHP **47**) enhances the photoopening rates. Dihydropyrenes **46**, **47** and **51** have ring opening quantum yields of 0.0038, 0.042 and 0.095 respectively.³⁴ Robinson³⁵ has reported that the naphthoyl group at the 2-position, dihydropyrene **50**, has even higher ring opening rates but the quantum yield was not reported.

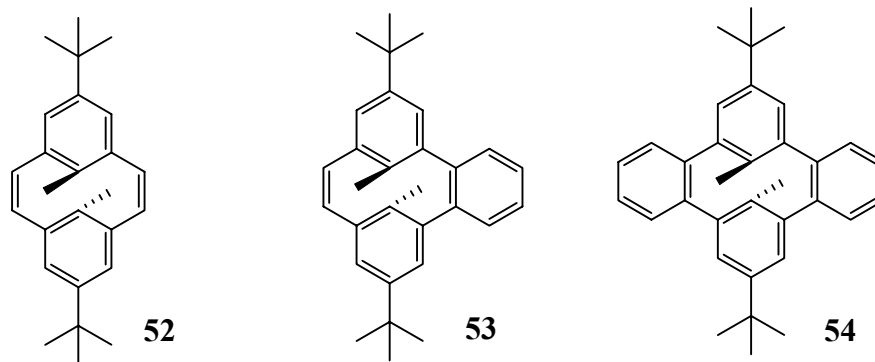


1.4.3 Decompositions/side reactions

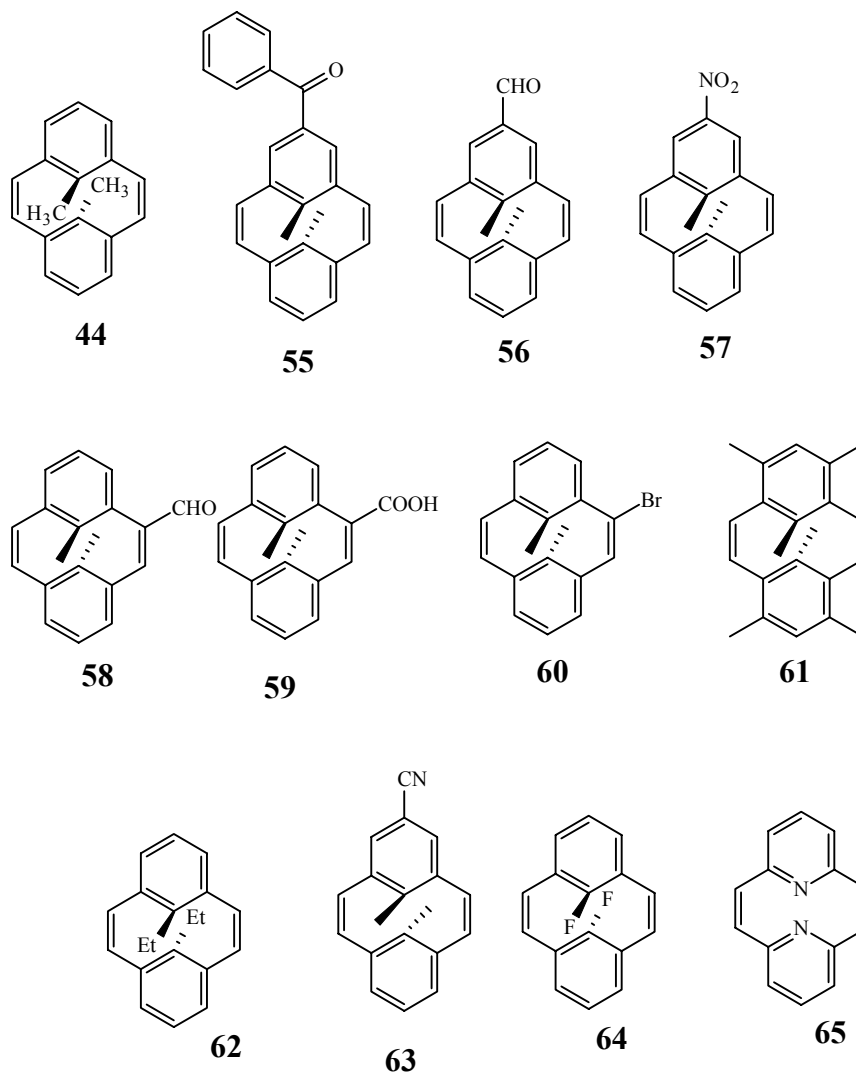
Even though the improved synthesis of dimethyldihdropyrene has opened up a new gate and allowed the synthesis of many derivatives of dihydropyrene, a basic question is still there: how robust is dihydropyrene to different reaction conditions. The answer is not that simple. Dihydropyrenes have been shown to be quite sensitive to mineral and lewis acids.³⁶ Thanks to the patience of Mitchell and other researchers working in this field, a wide variety of reaction can now be carried out with moderate to good yields.

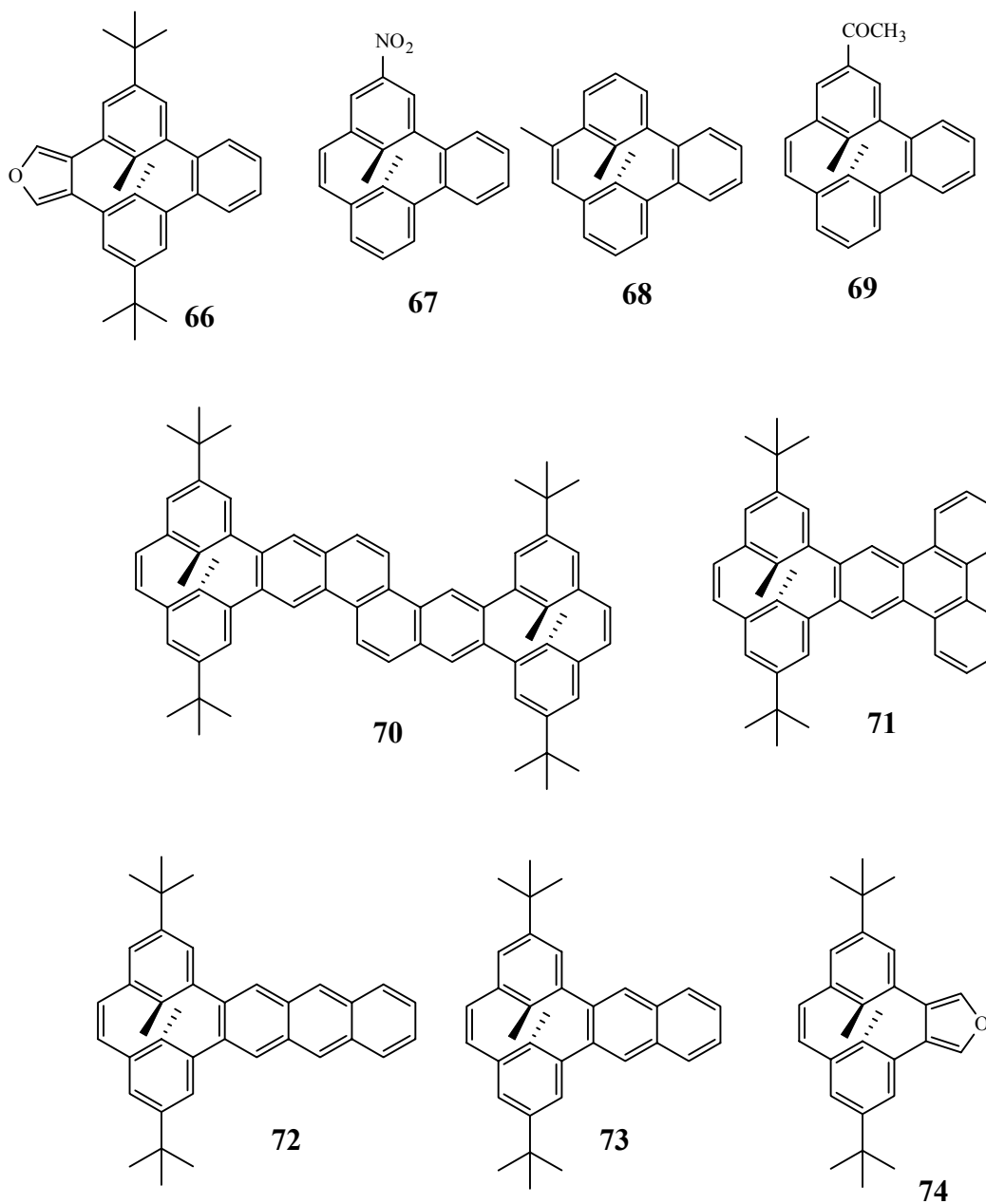
1.4.4 Thermal return

The problem of the thermal instability of the open form, cyclophanediene **43**, is the major cause for these switches not gaining proper attention. This problem still has not yet been solved. For switches and memory purposes, both isomers should be stable enough to store information for a long time. *t*-Butylated cyclophanediene **52**, obtained from photoopening of **45**, has a half life of about 42 hours at room temperature³⁷ (20 °C). [e]-Annelation of one benzene ring **53**³⁴ increases the half life to 7.3 days at 20 °C, but still this number is much smaller than required for practical purposes. Annelating a benzene ring on each side reversed the direction of photochromism, making the open form **54** more stable than the closed form³⁸ (a positive photochrome).



1.5 The nature of the transition state





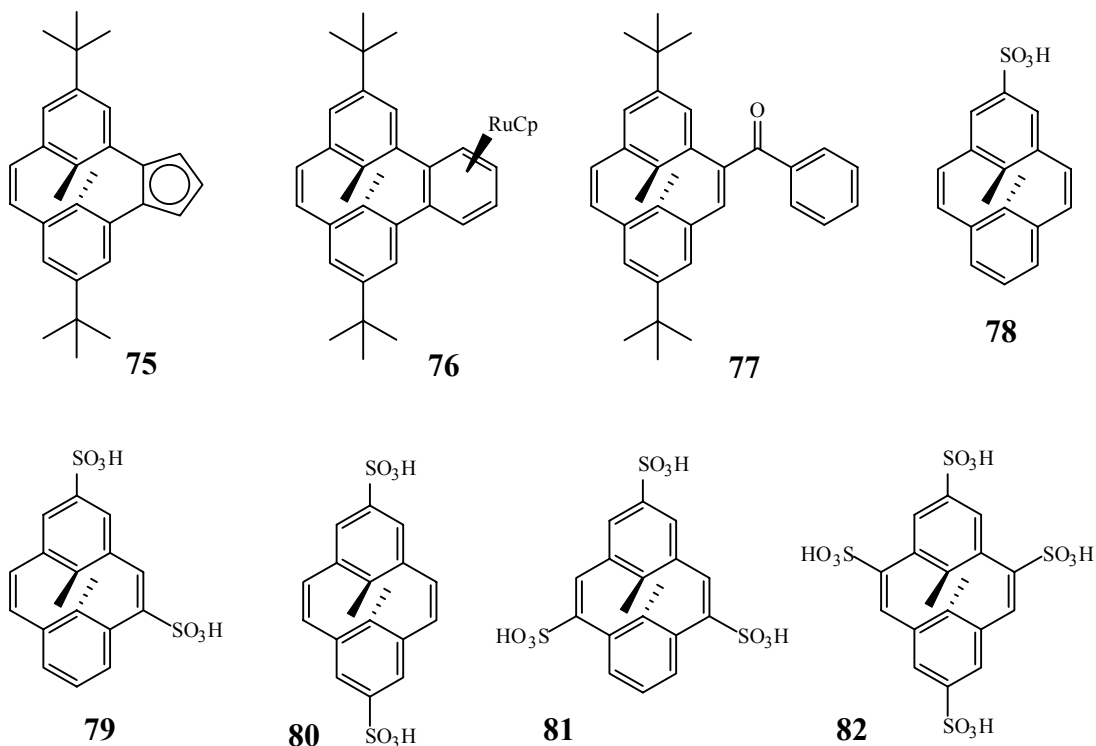
The following table is a partial representation of the thermal closing data which was available at the start of this thesis.

Table 1.2 Half lives of some cyclophanedienes at 20 °C^{39,41}

Entry No.	Compound	$\tau_{1/2}$ *	Entry No.	Compound	$\tau_{1/2}$ *
1	74	90 days	17	72	5 h
2	53	7.3 days	18	61	5 h
3	71	4.5 days	19	57	3h
4	60	83 h	20	55	90 min
5	59	78 h	21	68	51 min (32 °C)
6	70	58 h	22	56	42 min
7	76	55 h	23	67	12 min (32 °C)
8	52	54 h	24	81	6 min (22 °C)
9	58	49 h	25	82	198 s (22 °C)
10	77	45 h	26	79	79 s (22 °C)
11	44	42 h	27	78	25 s (22 °C)
12	75	39 h	28	80	25 s (22 °C)
13	69	27 h (32 °C)	29	54 [§]	-
14	73	25 h	30	66 [§]	-
15	62	2 h (30 °C)	31	65 [#]	-
16	63	2 h (30 °C)	32	64 [#]	-

[#] non photochromic / non thermochemical, § CPD form is more stable than the DHP form

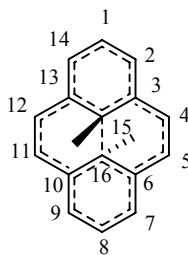
* Errors in half lives, where available, were less than 5%.



Difluorocyclophanedienes **64** and pyridine CPD **65** failed to close thermally but, they are not photochromic as well. Ideally, we would like compounds which show greater thermal stability (i.e., slow/no thermal return of the CPD into the DHP) but are photochromic. We asked Dr. Williams (University of Idaho) to model the transition state for the thermal back reaction.

The thermal back reaction (conrotation, 6π e) is forbidden by Woodward-Hoffmann rules.⁴⁰ For a forbidden reaction, the transition state may involve radical or ionic components so Williams⁴¹ used unrestricted DFT (UB3LYP) calculations involving electron correlations⁴² and found that the transition state has radical character^{43, 44} and shows equal contribution from singlet and triplet states (spin contamination $\langle S^2 \rangle = 1$).

Figure 1.4 **Numbering system for description in section 1.5**



The positions of the highest spin density were carbons 15 and 16 followed by carbons 1 and 8 (Figure 1.4). Based on spin density calculations, a radical destabilizing substituent such as CF_3 at these positions would make the TS^\ddagger higher in energy and would slow down the thermal return.

1.5.1 Radicals

A species that possesses one or more unpaired (“odd” or “single”) electrons is called a free radical. It can be neutral, or positively or negatively charged.⁴⁵

The stability of carbon based radicals is important in understanding the reactions involving radicals as reactants, intermediates or products. Substituents are known to have a remarkable effect on the stability of radicals. Substituted methyl radicals have been studied both theoretically⁴⁶ and experimentally⁴⁷ to unravel the effect of the substituent on the stability of radicals. The stability of radicals is determined by the bond dissociation energy difference between substituted methanes and methane in the gas phase. If the bond dissociation energy is lowered because of the substituent then the substituent is stabilizing, and vice versa. The difference in the bond dissociation energies is a measure of the strength of the substituent.⁴⁷ Radicals are electron deficient, so an electron rich substituent is expected to stabilize the radicals but several studies carried out

on radicals so far reveal that most substituents stabilize radicals either by hyperconjugation or by lone pair participation or by the delocalization of the radical on the π system of the substituent even with electron withdrawing substituents. When the electron withdrawing power of the substituent overcomes the delocalization stability, then the substituent becomes destabilizing and this is true only with either positively charged or highly fluorinated substituents. Examples of radical destabilizing substituents⁴⁸ are $\text{H}_3\text{P}^+ < \text{HSO}_2 < \text{CF}_3 < \text{H}_2\text{S}^+ < \text{H}_3\text{N}^+$. The following table gives a brief summary of the most common functional groups as a substituent in the order of decreasing stability from top to bottom

Table 1.3 Radical stabilizing functional groups and their bond stabilization energies for $\text{FG}-\text{CH}_2\cdots\text{H}$

Sr. No.	Functional group	$\Delta(\text{BDS})$ in kcal/mol
1	NH_2	22
2	$\text{CH}=\text{CH}_2$ etc.	19
3	Ph	17
4	PhS, RS, MeO, CN	12
5	MeCO, HO	11
6	MeOCO	10
7	PhSe	8
8	Me, NO_2	7
9	PhSO_2 , Me_3Si	6
10	Cl	4

11	F	3
12	H	0

1.5.2 The effect of the internal substituent on the thermal closing

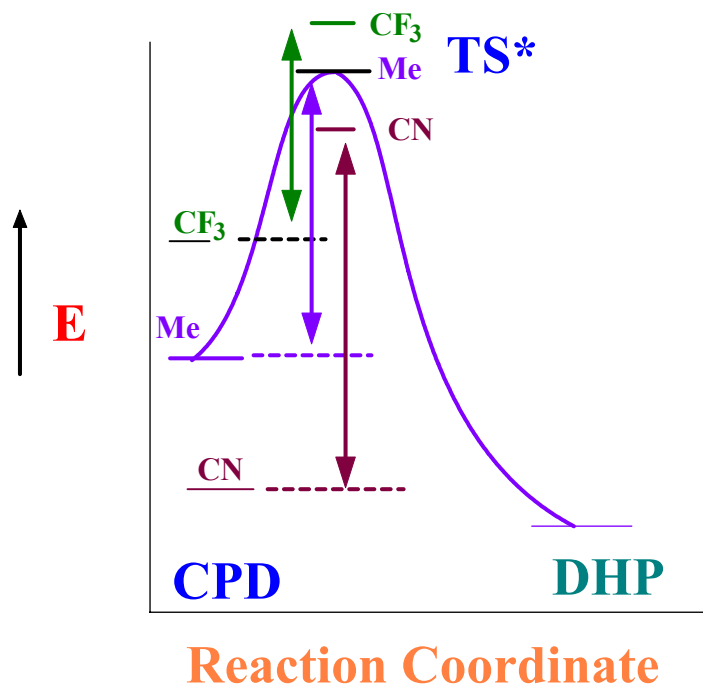
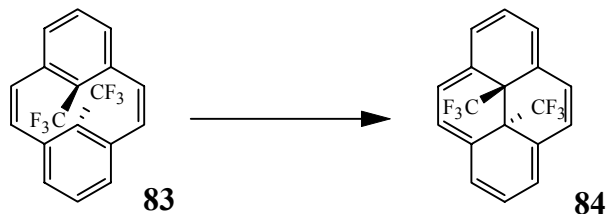


Figure 1.5 Substituents' effect on the energies of cyclophanedienes and the TS[‡]

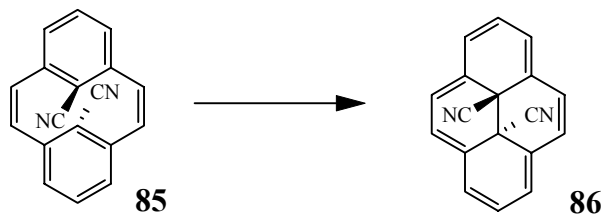
Williams studied computationally two internal substituents i.e., CF₃ and CN. CF₃ is a radical destabilizing group and is expected to increase the energy of the TS[‡] and thus E_{act}. In reality the E_{act} is calculated to decrease, which is counter-intuitive. The explanation is that it destabilizes the TS[‡] but at the same time it also destabilizes the CPD (Figure 1.5) and the destabilization for CPD is more than that for the TS[‡], so the activation barrier for the conversion of **83** into **84** (Scheme 1.21) is lower compared to the conversion of **44** into **43**.

Scheme 1.21 A dihydropyrene based photoswitch with CF₃ internal groups

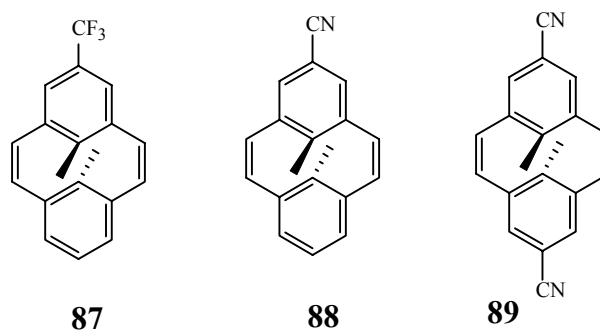


The radical stabilizing group, nitrile was also investigated by Williams at the internal position and it stabilizes the CPD more than the TS[‡] which would increase the activation barrier for the thermal back reaction.

Scheme 1.22 A photoswitch with a high calculated activation barrier



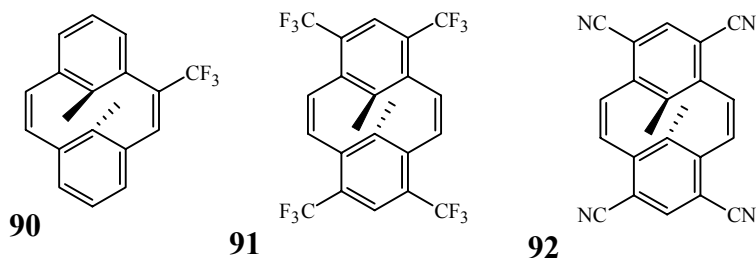
1.5.3 The effect of substituents at the 1 and 8 positions on the thermal closing



The next highest spin density is calculated to be at positions 1 and 8 (Figure 1.4). A radical stabilizing substituent at these positions should lower the energy of activation, e.g. compounds **88** and **89** shown above lower the calculated activation barrier from the CPD to the TS[‡] by 1 and 2 kcal/mol respectively, an additive effect. In **87**, the CF₃ group

at the 1 or 8 positions surprisingly has no effect on E_{act} . This implies that direct radical stabilization is not the only principle factor in determining the activation barrier.

1.5.4 The effect of substituents at other positions



Williams's calculations suggested that.

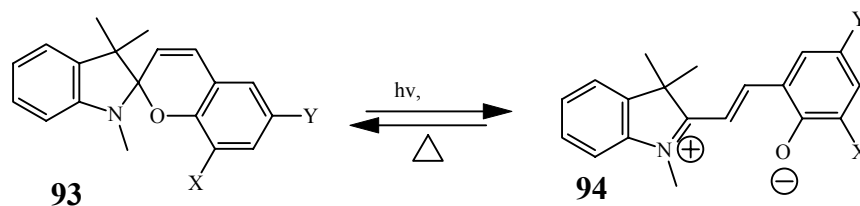
1. Nitrile groups at the 2,7,9,14 positions, **92** would have almost no effect on E_{act} .
2. A CF_3 group at the 4 position in **90** would have no effect.
3. CF_3 groups at positions 2,7,9,14 in **91** should increase the activation barrier by 2 kcal/mol.

Though these calculations gave no obvious trend in activation barrier with regards to both, the nature and the position of the substituents, these calculations were useful enough to identify the positions of the greatest effect, i.e 15 and 16 (Figure 1.4).

1.5.5 Substituent effects in other photochromic systems

Substituents have been shown to have great influence on the thermal stability of a variety of other photoswitches as well. An early example dates back to 1959 when Berman⁴⁹ showed that substituents X and Y (Scheme 1.23) in the spiropyran-merocyanine photoswitch can affect the rate of thermal closing by more than three orders of magnitude.

Scheme 1.23 The effect of substituents on the thermal return of merocyanine to spiropyran

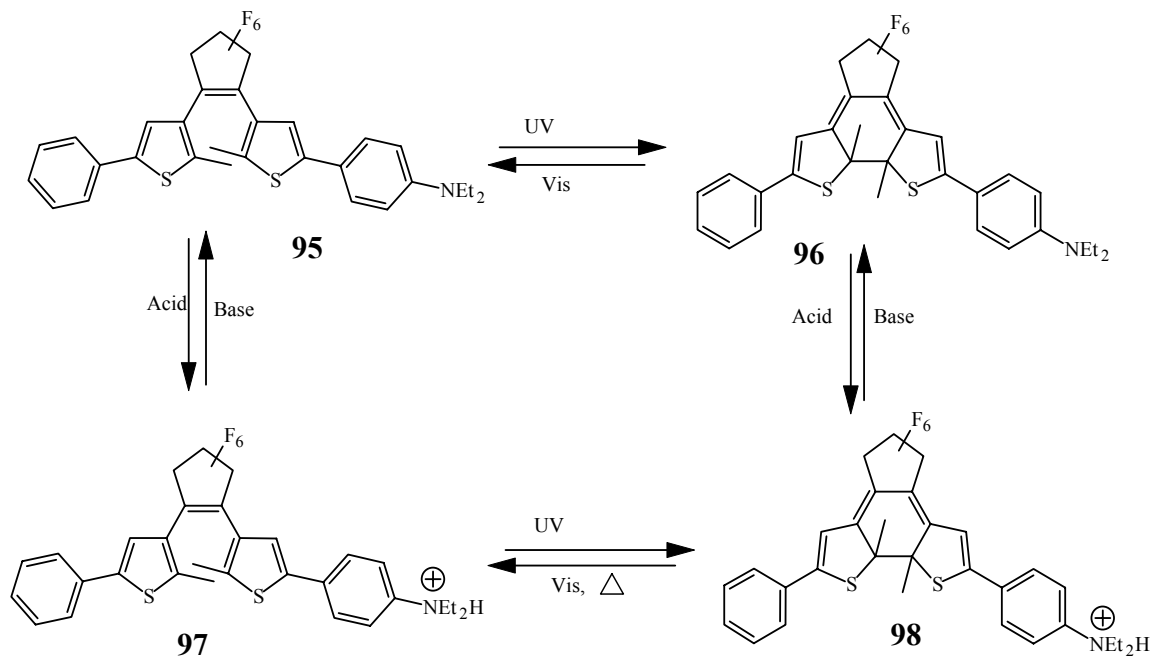


$$X = \text{F}, Y = \text{NO}_2 \quad \text{rate} = 6.33 \times 10^{-6} \text{s}^{-1}$$

$$X = \text{NO}_2, Y = \text{OMe} \quad \text{rate} = 1.32 \times 10^{-2} \text{s}^{-1}$$

Substituent change can also convert a P type chromophore into a T type chromophore as shown in Scheme 1.24. Dithienylethenes are P type chromophores provided they have an electron donating group on the phenyl ring such as the NEt_2 in molecule **95**. Upon acidification, the NEt_2 is transformed into an $^+\text{NEt}_2\text{H}$, an electron withdrawing group, and this change of functional group makes the photoswitch **97** a T type. This switching between the P and T types can be controlled by acid or base.⁵⁰

Scheme 1.24 Switching between a P and T type photochrome



Substituents not only affect the thermal back reaction but also affect other physical properties such as shifting of the UV-vis spectrum to longer or shorter wavelength, improving the quantum yield for photophysical processes etc.^{51,52}

1.6 Thesis Research Objectives

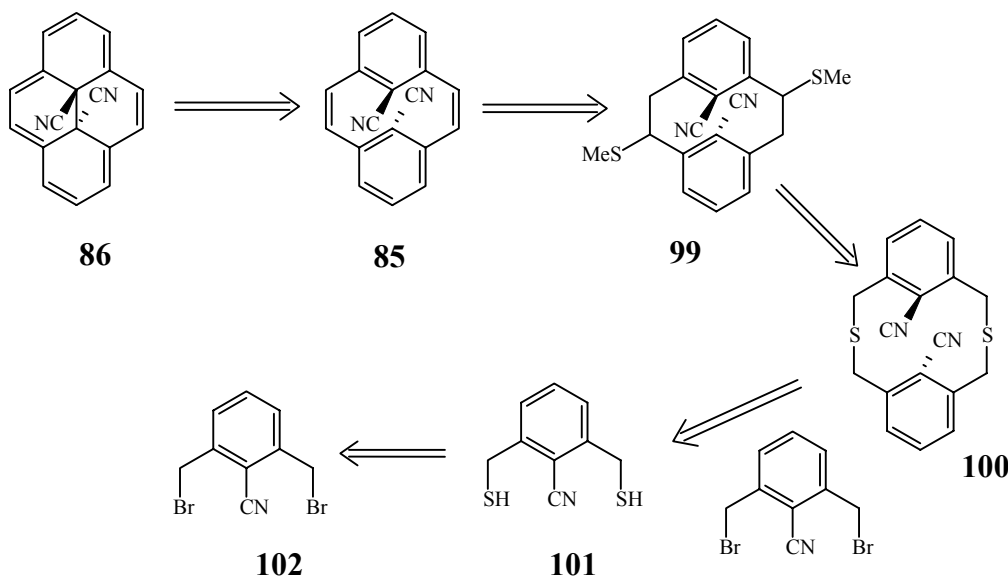
Given the calculations discussed above, the first objective was to synthesize and study the dinitrile switch pair **85/86**, and then, depending on the results obtained, to investigate the effect of other internal substituents such as ethynyl, vinyl and formyl, on the thermal and photochemical properties. The next objective was to synthesize naphthoyl (carbonyl) derivatives to improve photoopening properties once thermal stability has been attained.

Chapter 2: Syntheses

2.1 Synthesis of the CPD/DHP pair **85**, **86** with internal nitrile groups

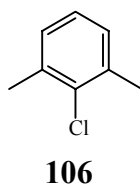
Calculations suggested that internal nitrile groups should slow down the thermal return of the cyclophanediene **85** into the dihydropyrene **86**, thus we decided to synthesize these two species. The retrosynthetic analysis of **86** is shown in Scheme 2.1 and it involves thiacyclophane **100** as an intermediate. Thiacyclophanes are key intermediates^{31,32,33} in the synthesis of dihydropyrenes and can be synthesized either by coupling dibromide with dithiol or by reacting dibromide with sodium sulfide. Generally, Wittig rearrangement followed by Hoffmann elimination converts the thiacyclophanes into the cyclophanedienes. However, a nitrile group is sensitive to the BuLi used in the Wittig rearrangement,⁵³ so in this case the Stevens rearrangement⁵⁴ is preferred which uses a two step process to convert **100** into **99**.

Scheme 2.1 Retrosynthetic analysis of dicyano DHP **86**

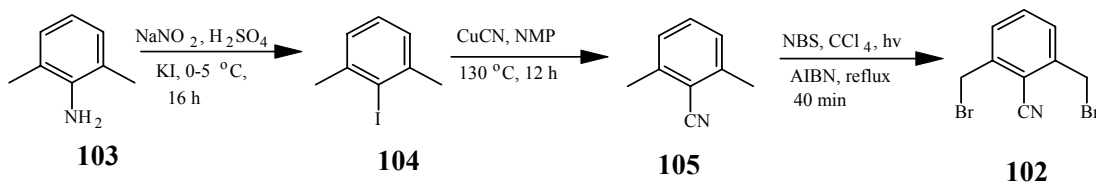


2.1.1 Synthesis of 2,6-bis-bromomethylbenzonitrile **102**

Dibromide **102** was synthesized according to the literature procedure⁵⁵ with slight improvements. Diazotization of **103** using H₂SO₄/NaNO₂ followed by treatment with KI gave **104** in 67% yield (Scheme 2.2). When HCl was used, a 3:1 mixture of 2,6-dimethyliodobenzene **104** and 2,6-dimethylchlorobenzene **106** was obtained. This was surprising because chloride generally does not incorporate under these conditions unless cuprous salts are used.⁵⁶ 2,6-Dimethyl-chlorobenzene formation was confirmed from a control experiment, when KCl was used instead of KI, the chloro product was obtained although in relatively small quantities.



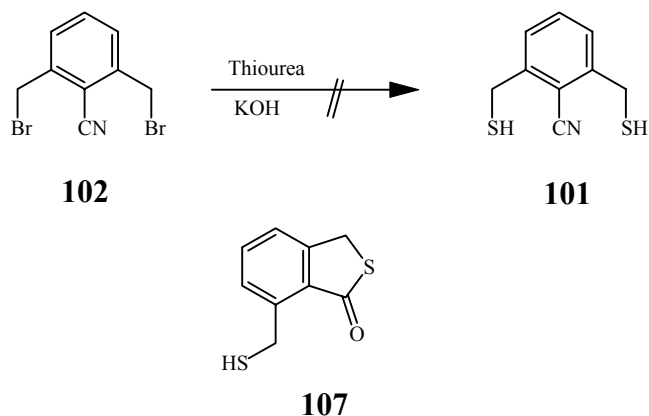
Scheme 2.2 Synthesis of 2,6-bis-bromomethylbenzonitrile **102**



Reaction of 2,6-dimethyliodobenzene with CuCN in NMP at 120 °C overnight gave almost quantitatively 2,6-dimethylbenzonitrile **105**. The reaction could be carried out in greater than 97% yield even on the large scale (200 g). Then, free radical benzylic bromination of **105** using NBS gave 56% of dibromide **102** (Scheme 2.2). The reaction gave four or five products with very close R_f values on TLC. The desired product crystallized out cleanly from the product mixture using cyclohexane:dichloromethane (4:

1) as recrystallizing solvent mixture. Attempts were made to purify the side products using column chromatography, but these were unsuccessful.

Scheme 2.3 Attempted formation of thiol **101**

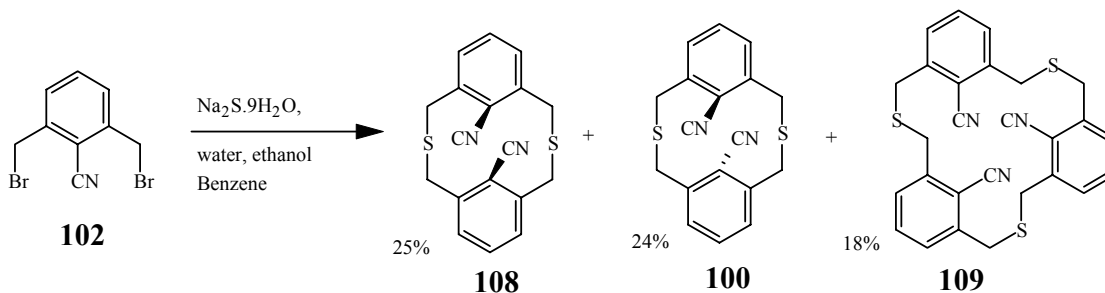


The functional group interconversion of bromide **102** to thiol **101** (Scheme 2.3) using thiourea and then KOH was unsuccessful. The pale yellow product mixture changed to orange red in a few minutes after the work up. Probably, the thiol formed reacted with the nitrile group to give a product, tentatively assigned as **107**. Change of the reaction conditions including temperature, KOH concentration, acid concentration during the acidification step and protection of the product from air also did not help to isolate the desired product.

2.1.2 Synthesis of dicyanothiacyclophanes **100** and **108**

Although the synthesis of most dithiacyclophanes involved bis-thiol-bis-bromide coupling, many have been made by coupling dibromide with $\text{Na}_2\text{S}\cdot 9\text{H}_2\text{O}$, even the parent.³²

Scheme 2.4 Synthesis of nitrile thiacyclophanes **100**, **108** and **109**



Bodwell⁵⁷ has reported that use of the reagent $\text{Na}_2\text{S}\cdot 9\text{H}_2\text{O}/\text{Al}_2\text{O}_3$ avoids high dilution conditions which are usually required. Addition of dibromide in small portions to $\text{Na}_2\text{S}\cdot 9\text{H}_2\text{O}/\text{Al}_2\text{O}_3$ gives moderate yields of thiacyclophanes (13-65%). The reaction is quite sensitive to the size of the internal groups. When hydrogens are the internal substituents, the yield is > 60% but it drops dramatically to 13% for the methyl analogue. Since a nitrile group is linear and sterically less demanding, it was anticipated to give a moderate yield. Bodwell's method, when tried on the small scale (sub millimolar quantities), gave 25-30% yield of the dicyanothiacyclophanes as a mixture of *syn*-**108** and *anti*-**100** isomers, however a gram scale reaction gave a very poor yield.

Under high dilution conditions, reaction of dibromide **102** and $\text{Na}_2\text{S}\cdot 9\text{H}_2\text{O}$ by slow addition from two dropping funnels in ethanol-benzene-water gave a 1:1 mixture of the *syn*- and *anti*-isomers **108** and **100** in 50% yield (Scheme 2.4). The major side product was the trimer **109**. Because of low atom efficiency, a 30 g scale reaction gave less than 8 g of the thiacyclophanes. Vogtle⁵⁸ first made this thiacyclophane in the seventies but little experimental data was reported, and so he may have obtained one or both isomers. We were able to purify each isomer and the trimeric species. Purification was a tedious job because these compounds were not soluble in most useful solvents

except dichloromethane, in which they were partially soluble. The low bp of dichloromethane ruled out recrystallization or selective dissolution. Separation was achieved by column chromatography but it required a long column and much solvent.

The assignment of structure for the *syn*- and *anti*-isomers was quite apparent from their ^1H NMR spectra. Aromatic protons in the *syn*-isomer were shielded³² to δ 7.15-7.07 vs. 7.66-7.60 in the *anti*-isomer because both benzene rings of **108** are parallel and experience each other's ring current. The aliphatic bridge protons of **108** showed a more widely spaced AB quartet at δ 4.55-3.81 while a closely spaced AB quartet at δ 3.94-3.88 was observed for **100**. The trimer **109** showed a singlet in the aliphatic region because of freely tumbling bridge protons while the aromatic protons were at δ 7.46-7.39. X-ray crystallographic analysis confirmed the *syn* and *anti* orientation in **108** and **100** respectively.

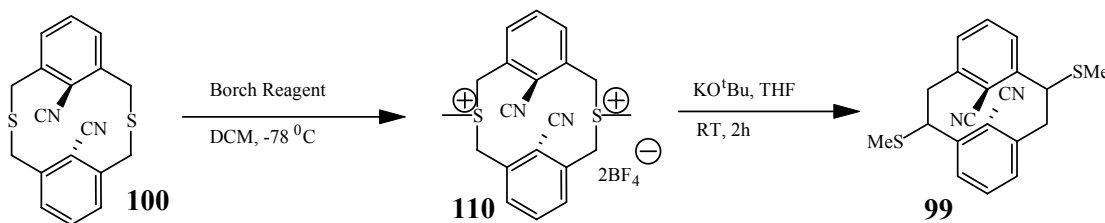
2.1.3 The Stevens rearrangement of the thiacyclophanes

The Wittig rearrangement is generally preferred for the conversion of thiacyclophanes to thiomethylcyclophanes. A nitrile group is sensitive to BuLi and thus LDA was used as the base to affect the Wittig rearrangement but it failed to give the desired product. The Stevens rearrangement involves the formation of a sulfonium salt intermediate which upon treatment with relatively mild base usually rearranges to the thiomethylcyclophanes as shown in Scheme 2.5. The Stevens rearrangement was carried out separately on the *syn*- and *anti*-thiacyclophanes.

2.1.3.1 The Stevens rearrangement of the *anti*-thiacyclophane **100** into the thiomethylcyclophane **99**

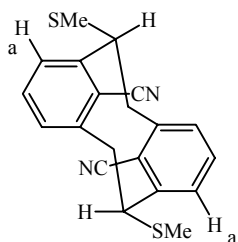
Methylation of **100** with dimethoxycarbonium fluoroborate⁵⁹ gave almost quantitatively the bis-sulfonium salt **110** (Scheme 2.5). The ¹H NMR spectrum showed all peaks deshielded relative to the thiacyclophane starting material. The methyl protons appeared at δ 3.45. The bridge aliphatic protons were four doublets between δ 5.2 and 4.2 while the aromatic protons were at δ 7.97 (d) and δ 8.14 (t). The sulfonium salt **110**, when reacted with potassium *tert*-butoxide in THF gave a mixture of the thiomethyl-*anti*-cyclophanes **99**.

Scheme 2.5 The Stevens rearrangement of *anti*-thiacyclophane **100** into the thiomethylcyclophane **99**



The major isomer could be obtained in 48% yield by careful chromatography over silica using 60:40 dichloromethane:hexanes as eluant. This isomer, based on its ¹H NMR spectrum, was assigned to contain both thiomethyl groups equatorially orientated.³² The thiomethyl protons appeared as singlet at δ 2.17 while the bridge protons appeared as three doublets of doublets between δ 2.8 and 4.3. Complete assignment of the structure was made through HMBC, HSQC, COSY and NOESY experiments and is given in the experimental section. The IR spectrum confirmed the presence of the nitrile group by a

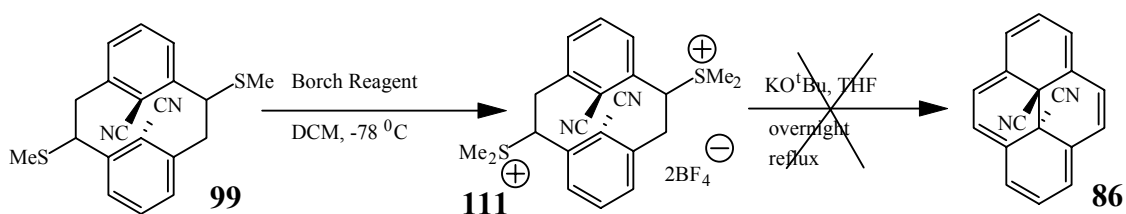
band at 2215 cm^{-1} . Cyclophane **99** had the expected HRMS at m/z 350.0902 (calculated 350.0911)



2.1.4 Formation of the sulfonium salt **111** and the subsequent Hoffmann elimination

In the subsequent steps, the single isomer of **99** was employed; however the reactions could be carried out on the mixture of isomers. The pure isomer, on treatment with dimethoxycarbonium fluoroborate gave the bis-sulfonium salt **111** in quantitative yield (Scheme 2.6). The ^1H NMR chemical shifts of **111** were similar to those of **99** but were deshielded because of the positive charge. The aliphatic protons alpha to the positive sulfur atoms were most deshielded and appeared at δ 4.92 while the other aliphatic protons appeared at δ 4.0 and 3.2.

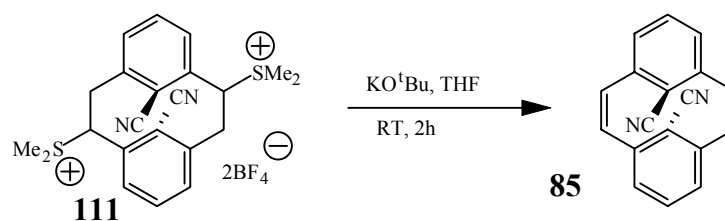
Scheme 2.6 The attempted Hoffmann elimination to synthesize DHP **86**



Sulfonium salt **111**, on reaction with *t*-BuOK in refluxing THF failed to give the dihydropyrene **86** (Scheme 2.6). TLC analysis of the reaction showed a mixture of

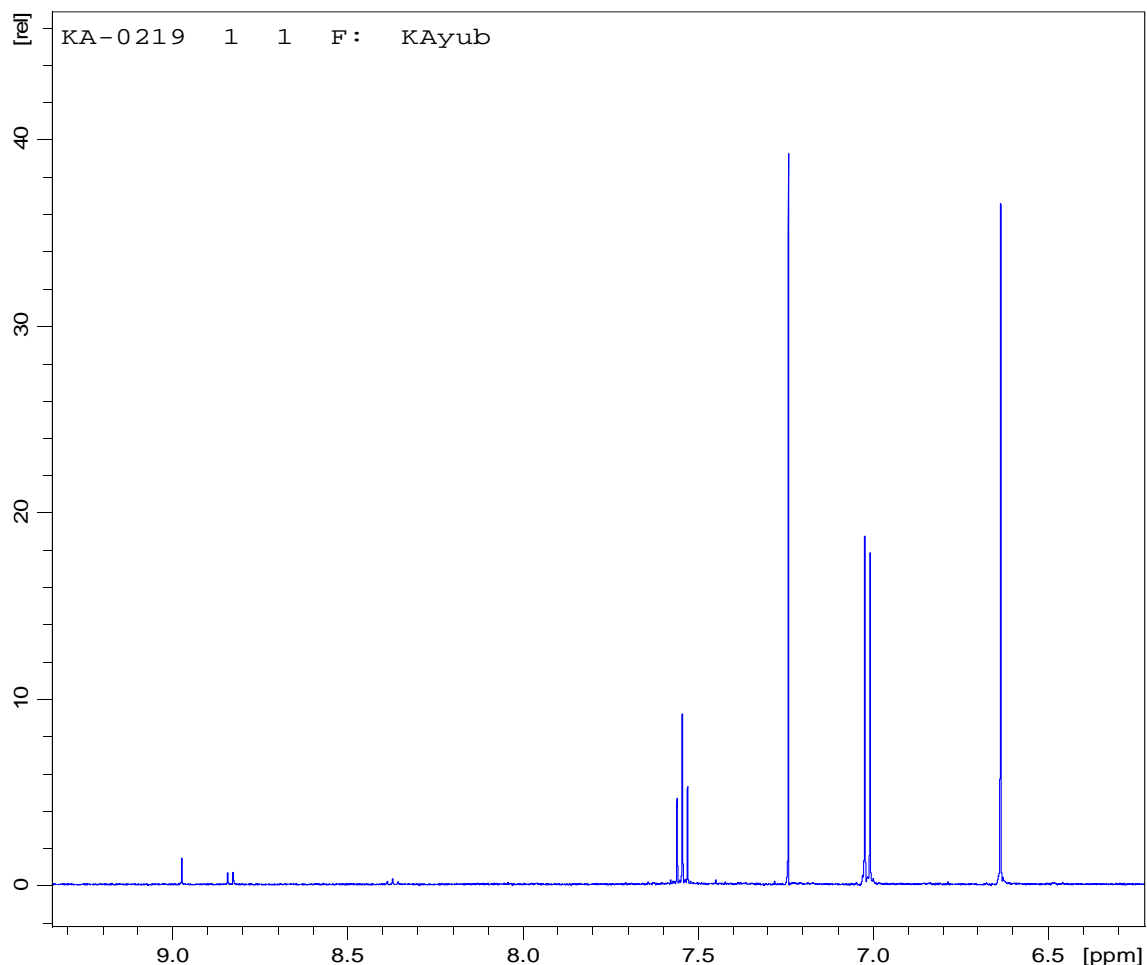
fluorescent compounds which were thought to be pyrenes based on the chemical shifts in the ^1H NMR spectrum. KH in refluxing THF also yielded a mixture of pyrenes; different from the one obtained using *t*-BuOK. NaH failed to give any products under similar conditions. Surprisingly, carrying out the reaction at room temperature gave the dicyano CPD **85** in > 90% as pale yellow crystals (Scheme 2.7) along with ~ 6% yield of **99**, obtained by demethylation. The course of the reaction was monitored using TLC. A pale yellow spot appeared immediately after the addition of *t*-BuOK to the suspension of sulfonium salt **111** in THF. This pale yellow product increased with time and stabilized after 20 minutes, so the reaction was quenched after a total of 30 min.

Scheme 2.7 The Hoffmann elimination at room temperature

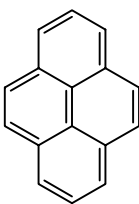


The cyclophanediene **85** had poor solubility in most solvents except for dichloromethane and chloroform where it was soluble enough to obtain NMR spectra or to perform column chromatography. The ^1H NMR spectrum of **85** (Figure 2.1), as expected because of symmetry, showed only three peaks, a singlet at δ 6.63 corresponding to the bridge alkene protons, a doublet at δ 7.01 and a triplet at δ 7.54. The nitrile group was confirmed by the IR band at 2215 cm^{-1} . Mass spectrometry gave the correct molecular ion peak at m/z 254.

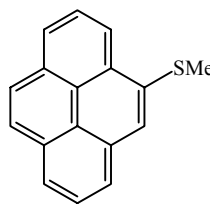
Figure 2.1 ^1H NMR spectrum of dicyano CPD **85** in CDCl_3 at 500 MHz



The mixture of isomers **99** when subjected to the S-methylation-Hoffmann elimination sequence also gave predominantly the cyclophanediene **85**. Pyrene **112** and the thiomethylpyrene **113** were also obtained in variable quantities and sometimes the only products of the reaction; however a small scale reaction at low temperature minimized the formation of the side products.



112

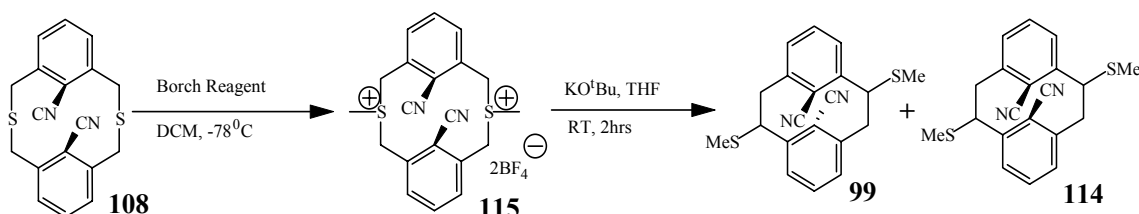


113

2.1.5 The Stevens rearrangement of the *syn*-thiacyclophane **108** to the thiomethylcyclophanes

Stevens' rearrangement of *syn*-**108** gave predominantly the *anti*-cyclophane **99** as a mixture of isomers. A small amount of the *syn*-isomers **114** was also obtained, which eventually gave the *cis*-DHP (Scheme 2.8) when this mixture was used directly in the subsequent steps. The fact that the *syn*-thiacyclophane yields a mixture of the *syn*- and *anti*-thiomethylcyclophanes is probably because of the high degree of steric strain in the *syn*- isomer which is relieved upon isomerization. The sulfonium salt **115**, formed by the methylation of **108**, showed methyl protons at δ 3.4 in the ^1H NMR spectrum. Aliphatic bridge protons appeared as two doublets at δ 4.10 and δ 4.22 while aromatic protons were at δ 7.1- 7.5.

Scheme 2.8 Stevens rearrangement of *syn*-thiacyclophane **108** into the thiomethyl cyclophanes

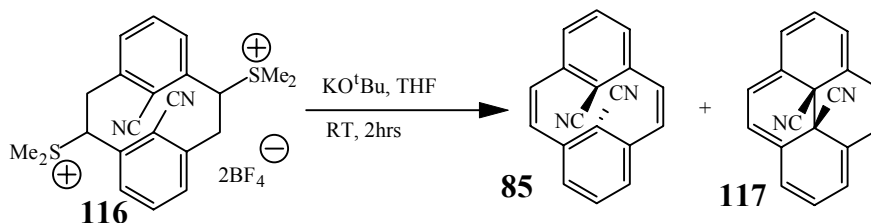


Attempts were made to obtain more of the *syn*-cyclophane (**114**) but were not successful. Low temperature or change of base e.g., LDA or NaH instead of *t*-BuOK gave more or less the same results.

2.1.6 Synthesis of the *cis*-DHP 117

The mixture of *syn*- and *anti*-isomers was methylated to yield the bis(dimethylsulfonium) fluoroborate salt **116** which on reaction with *t*-BuOK in THF at 20 °C gave 90% of the *anti*-cyclophanediene **85** and 5% of the green *cis*-dihydropyrene **117**, mp 192 °C (Scheme 2.9). The dihydropyrene showed three peaks in the ¹H NMR spectrum, a singlet at δ 8.97, a doublet at δ 8.66 and a triplet at δ 8.10. The *cis* relationship of the internal nitrile groups was established by the X-ray structure determination.

Scheme 2.9 The Hoffmann elimination at room temperature



The *anti*-cyclophanediene **85** could not be cyclized thermally into the *trans*-dihydropyrene **86** in useful yields because of the subsequent migrations of the nitrile groups (Scheme 2.10). However irradiation with UV light converted **85** into the green *trans*-dihydropyrene **86** quantitatively (Scheme 2.10). Presence of the *trans*-dihydropyrene was quite apparent from its ¹H NMR spectrum which showed a singlet at δ 8.97, a doublet at δ 8.83 and a triplet at δ 8.37 (Figure 2.2). The aromatic protons are strongly deshielded by the aromatic ring current from those of CPD **85**. The IR stretch at 2227 cm⁻¹ confirmed the presence of a nitrile group. The structure was confirmed by X-ray analysis.

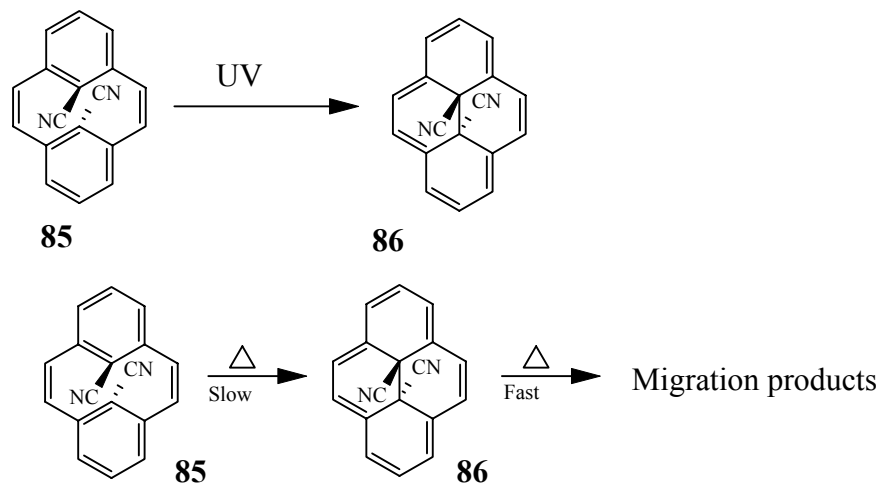
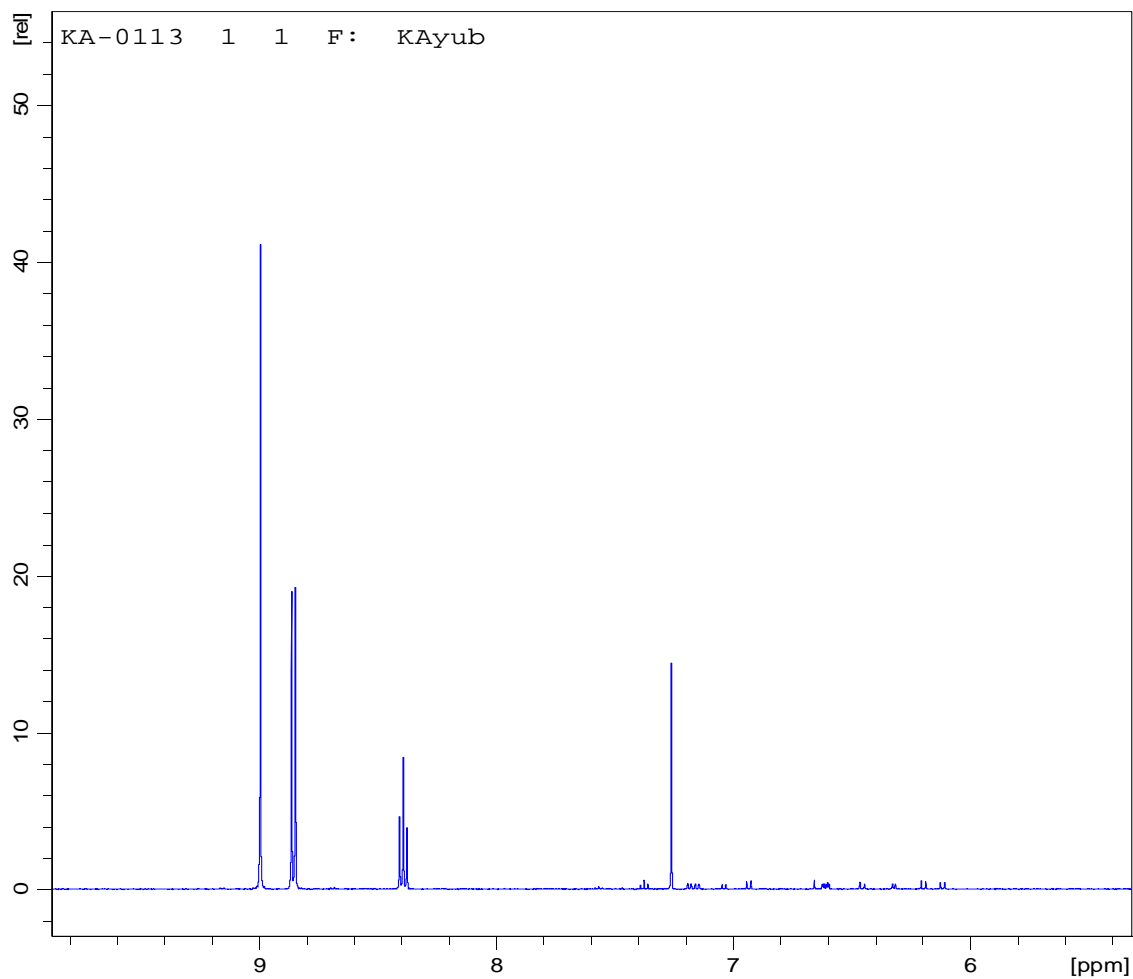
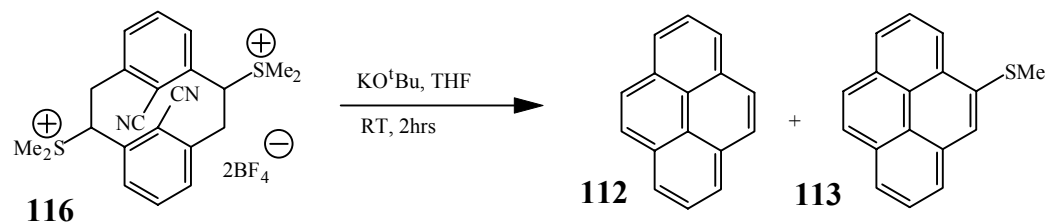
Scheme 2.10 Attempted thermal closing of dicyano CPD **85**

Figure 2.2 ^1H NMR spectrum of dicyano DHP **86** in CDCl_3 at 500 MHz



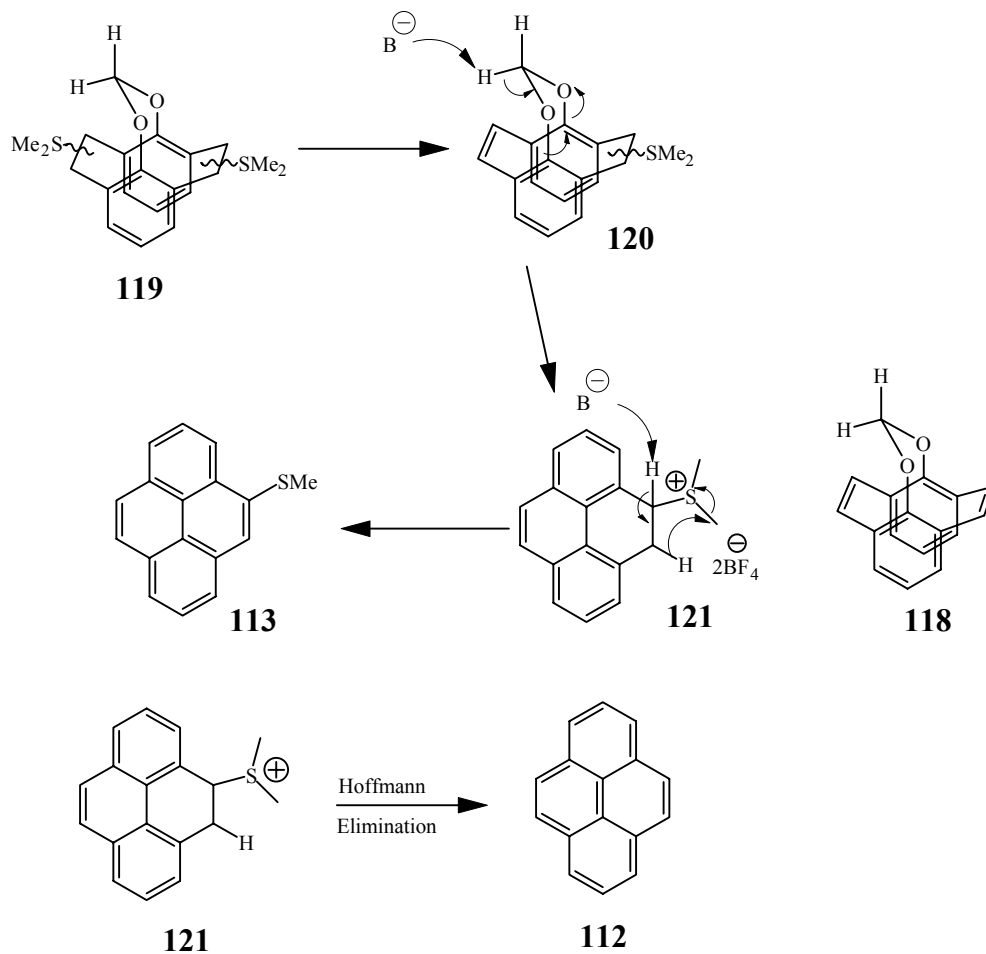
2.1.7 Pyrene and thiomethylpyrene formation

A nuisance in the Hoffmann elimination to prepare cyclophanediene **85** was the formation of pyrenes **112** and **113** in variable quantities (Scheme 2.11). Sometimes these pyrenes were the only products.

Scheme 2.11 Formation of pyrene 112 and thiomethylpyrene 113

Lai and Eu⁶⁰ have reported that pyrene **112** and 4-methylthiopyrene **113** are the only products in an attempted synthesis of the cyclophanediene **118**. The postulated mechanism is shown in Scheme 2.12 which involves an initial Hoffmann elimination in **119** to generate **120**.

Scheme 2.12 Mechanism for the formation of the pyrenes



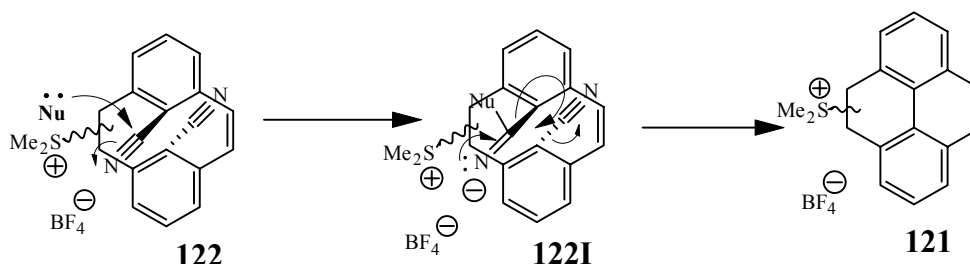
A proton abstraction from the central methylenedioxy bridge drives the extrusion of the internal substituents and forms a closed ring species **121** which upon Hoffmann elimination gives pyrene. Alternatively, abstraction of the most acidic proton in **121**, next to the positive sulfur atom, followed by a 1,4-hydride transfer and concomitant elimination of a methane molecule generates the 4-methylthiopyrene **113**.

In our case, the problem arose when;

1. The reaction was carried out on a large scale, one gram or more of the sulfonium salt **116**.

2. Crude thiomethylcyclophane **99** was employed directly in the formation of the sulfonium salt without purification on the column. This effect was more pronounced when NaH was used to affect the Stevens rearrangement (Scheme 2.5 & 2.8).
3. Neutral (non acidic) work up was used.

Scheme 2.13 Mechanism for the elimination of the internal nitrile groups during the Hoffmann elimination.

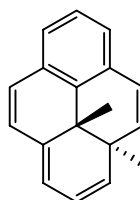


Thiomethylpyrene **113** was the major product in the first two cases while in the third case, only pyrene **112** was formed.

A mechanism involving abstraction of a proton from the internal substituent is excluded when nitriles are the internal substituents. A plausible mechanism could be the attack of a nucleophile on the nitrile in **122** to form the intermediate **122I**. Then, the electronically driven elimination of the internal substituents would form **121** as shown in Scheme 2.13. Monoene **121** would eventually lead to the pyrenes via Lai's mechanism⁶⁰ (Scheme 2.12).

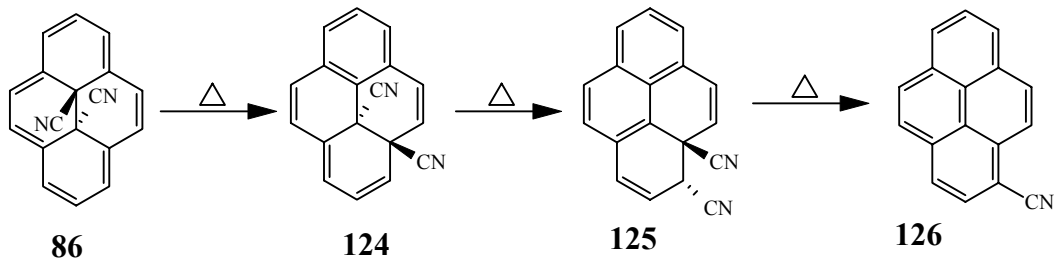
2.1.8 Migration of the nitrile groups over the π system and finally an elimination of HCN

When the *anti*-DHP **86** was left at room temperature for a week, partial decomposition was observed (TLC showed a new colorless spot). EI MS indicated that this new product was isomeric with **86**. Heating the NMR sample of **86** at 70 °C for 30 minutes gave a clean spectrum of this isomeric colorless product.



123

Scheme 2.14 Migration and elimination of nitrile group



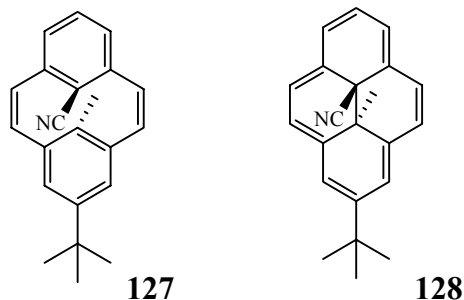
Boekelheide⁶¹ reported that the internal methyl-substituted DHP **43** rearranged on heating at 200 °C to **123**. With other internal groups such as Et, Pr and H, lower isomerization temperatures have been observed.⁶² The spectrum of our isomerization product was consistent with structure **124**, analogous to **123**. The presence of the nitrile groups was confirmed by the IR band at 2227 cm^{-1} and by the ^{13}C NMR peaks at δ 116.65 and 116.15. The relative orientation of the two nitrile groups is based on the Woodward-Hoffmann rules.

When this 1st migration product **124** was heated at 70 °C for 4 days, formation of another isomeric colorless product **125** was observed (Scheme 2.14). This product, in contrast to its isomeric **124**, was quite sensitive to chromatography using silica as adsorbent and decomposed to 1-cyanopyrene **126**. The 2nd migration product **125**, which contains a naphthalene skeleton, has its ¹H NMR peaks somewhat downfield compared to the 1st migration product **124**. The aliphatic CH bearing the CN group appeared at δ 3.92 as doublet of doublets. In its IR spectrum, the nitrile band was at 2224 cm⁻¹. Once again the *anti* relationship of the nitriles was based on the Woodward-Hoffmann rules. Each proton and carbon in isomeric products **124** and **125** were assigned using NOESY, COSY, HMBC and HSQC techniques.

The 2nd migration product when heated at 110 °C for 8 hrs or passed through a silica column gave 1-cyanopyrene **126**, which is commercially available and showed identical physical properties (mp, ¹H NMR data) to literature values.⁶³

2.2 Synthesis of 2-(*t*-butyl)-10b-methyl-10c-cyano-*trans*-10b,10c-dihydropyrene **128**

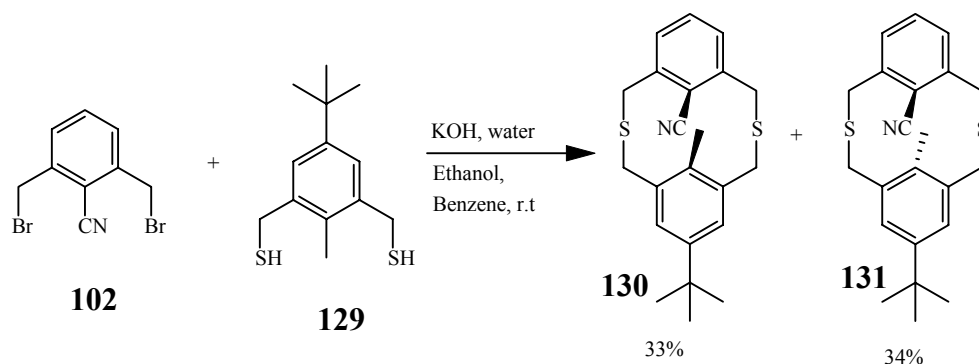
Introduction of the internal nitrile groups has enhanced the thermal stability of the cyclophanediene **85** but the migration of the nitriles in the DHP **86** prohibits its use as a photoswitch. A requirement for a photoswitch is the stability of both isomers. It was, however, of interest to synthesize the switch pair **127/128** to see how does a combination of a nitrile and a methyl as the internal substituents affect the properties of the photoswitch.



2.2.1 Synthesis of the cyano-methylthiacyclophanes **130** and **131**

Under high dilution conditions, coupling of dibromide **102** and dithiol^{33,64} **129** gave a 1:1 mixture of the *syn*-**130** and *anti*-**131** thiacyclophanes in 67% yield (Scheme 2.15).

Scheme 2.15 Synthesis of thiacyclophanes **130** and **131**



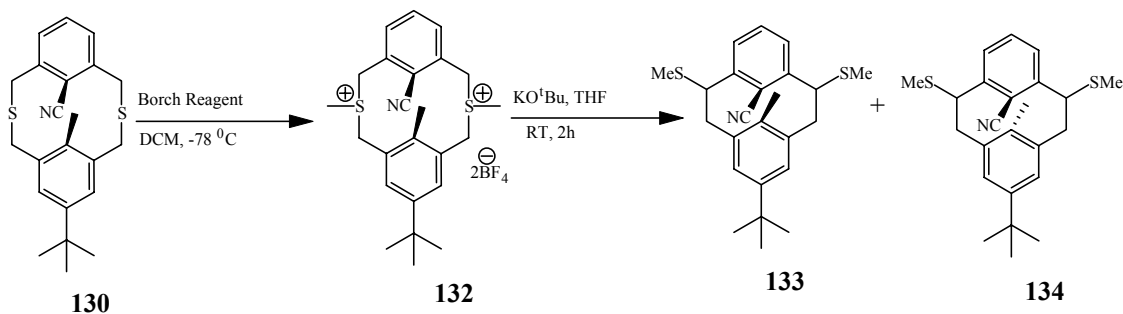
The *ant*- and *syn* isomers were separated by column chromatography on silica using 35:65 and 45:55 dichloromethane:hexanes respectively. Both isomers were readily identified by their ¹H NMR spectra. The aromatic protons in **130** were shielded and appeared at δ 6.9-7.1 whereas in the *anti*-isomer they appeared at δ 7.5. The internal methyl protons in **130** appeared at δ 2.56 whereas in **131** they were shielded by the opposite aromatic ring and appeared at δ 1.43. The IR stretches at 2217 cm⁻¹ and 2214 cm⁻¹ in **131** and **130**, respectively, confirmed the presence of the internal nitrile groups.

Satisfactory elemental analyses were obtained for both isomers. Finally, both isomers were confirmed by X-ray structures. The Stevens rearrangement was then carried out separately on each of the *syn*- and *anti*-thiacyclophanes.

2.2.2 The Stevens rearrangement of the *syn*-thiacyclophane **130**

Treatment of *syn*-dithiacyclophane **130** with dimethoxycarbonium fluoroborate afforded the bis-sulfonium salt **132** quantitatively which underwent the Stevens rearrangement in the presence of *t*-BuOK to give a mixture of the *syn*- and *anti*-thiomethylcyclophanes, **133** and **134**, respectively (Scheme 2.16). In the ^1H NMR spectrum, the protons of the internal methyl group of **134** appeared at δ 0.5-0.8 compared to δ 2.0-2.2 in **133**. In addition, the aromatic protons in the *syn*- isomer were shielded to δ 6.3-7.2 when compared to the *anti*-isomers, δ 7.0-8.0.

Scheme 2.16 Stevens rearrangement of the *syn*-thiacyclophane **130**



An *anti*-isomer of **134** could be purified by careful chromatography over silica using 30:70 dichloromethane:hexanes. This isomer, based on its ^1H -NMR spectrum was assigned to contain two equatorial thiomethyl groups. The internal methyl protons showed an upfield signal at δ 0.54 (singlet) while the aromatic protons were at δ 7.2-8.0.

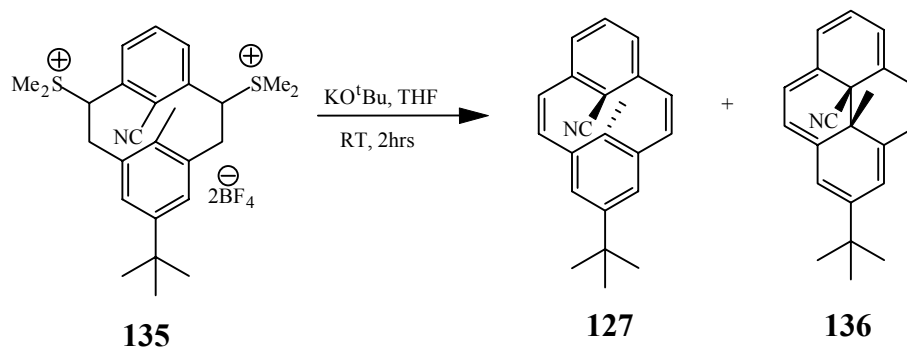
The IR spectrum confirmed the presence of the nitrile by a stretch at 2216 cm^{-1} . Finally, X-ray analysis established the structure.

2.2.3 The Hoffmann elimination of the thiomethylcyclophanes **133** and **134**

The mixture of thiomethylcyclophanes was methylated to give the air sensitive sulfonium salt **135** which on Hoffmann elimination with *t*-BuOK in THF at room temperature gave 60% of the *cis*-dihydropyrene **136** and 28% of the *anti*-cyclophanediene **127** (Scheme 2.17). Both products were separated by column chromatography on silica gel.

Cyano-methyl CPD **127**, as expected because of its symmetry, showed a total of seven peaks in the ^1H NMR spectrum. The bridge alkene protons showed an AB pattern at δ 6.6-6.3 with a coupling constant of 11.3 Hz. The aromatic protons appeared as a triplet δ 7.28, a doublet at δ 6.85 and a singlet at δ 6.79. The peak corresponding to the protons of the internal methyl was a singlet at δ 1.57, a characteristic of *anti*-cyclophanedienes. A peak at δ 115.92 in the ^{13}C NMR spectrum indicated the presence of the nitrile which was confirmed by a band at 2215 cm^{-1} in the IR spectrum.

Scheme 2.17 The Hoffmann elimination to generate cyano-methyl CPD **127** and *cis*-DHP **136**



The mass spectrum showed the correct molecular ion peak at m/z 299. A satisfactory elemental analysis could not be obtained probably because of higher percentages of carbon. Extended combustion using V_2O_5 also failed to give the correct analysis.

The *cis*-DHP **136** was obtained as dark green crystals, mp 108-109 °C. A peak at δ -1.60 in the 1H NMR spectrum corresponding to the internal methyl protons indicated the *cis* relationship of the internal substituents. *Cis*-dihydropyrenes are generally saucer shaped which results in different chemical shifts for the external and internal protons when compared with their *trans* counterparts. Moreover, the internal methyl group is farther away from the center of the ring than in the *trans*-DHP and appears relatively downfield at $\sim \delta$ -2.0 (*trans*-DHP $\sim \delta$ -4.0). The dihydropyrene protons were between δ 7.8 and 9.0. The *cis*-DHP had the expected HRMS at m/z 299.1670 (calculated 299.1674). All peaks in the 1H and ^{13}C NMR spectrum of the cyano-methyl CPD **127** and *cis*-DHP **136** could be assigned.

2.2.4 The Stevens rearrangement of the *anti*-thiacyclophane **131**

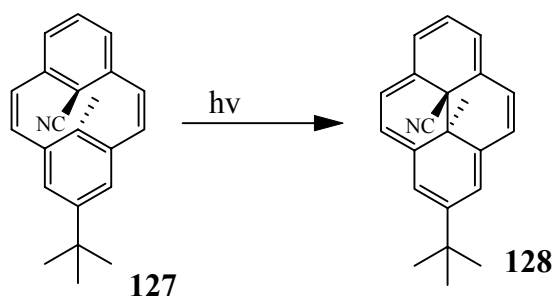
The Stevens rearrangement-Hoffmann elimination sequence starting from thiacyclophane **131** gave the *anti*-CPD **127** exclusively. Lai and Zhou⁶⁵ have reported that in the non *t*-butylated analogue, the *anti*-thiacyclophane gives *cis*-DHP through the Stevens rearrangement-Hoffmann elimination sequence. However we did not see any such isomerization.

2.2.5 Photochemical isomerization of cyano-methyl CPD **127** into the *trans*-DHP

128

Cyano-methyl DHP **128** was obtained photochemically from the CPD **127** (Scheme 2.18); an attempted thermal closure gave the migration product **137** (Scheme 2.19). Facile migration of the internal nitrile of **128** at room temperature did not permit obtaining clean NMR spectra of **128**. The *trans*-dihydropyrene nucleus was readily identified by a peak at -4 ppm in the ^1H NMR spectrum corresponding to the internal methyl protons. The DHP protons appeared at δ 8.6 -7.7.

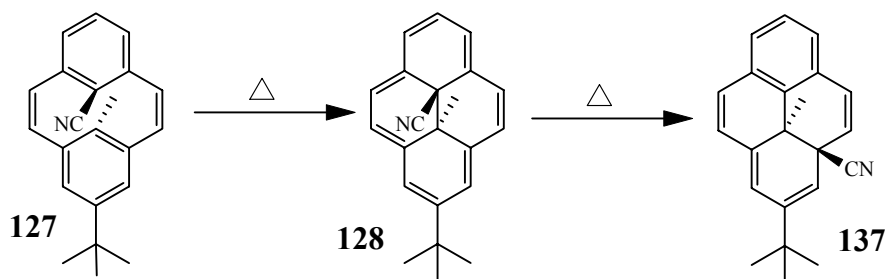
Scheme 2.18 Generation of **128** by photochemical isomerization



2.2.6 Migration of the internal nitrile in cyano-methyl DHP **128**

Cyclophanediene **127**, when heated at 70 °C for three hours gave the migration product **137**.

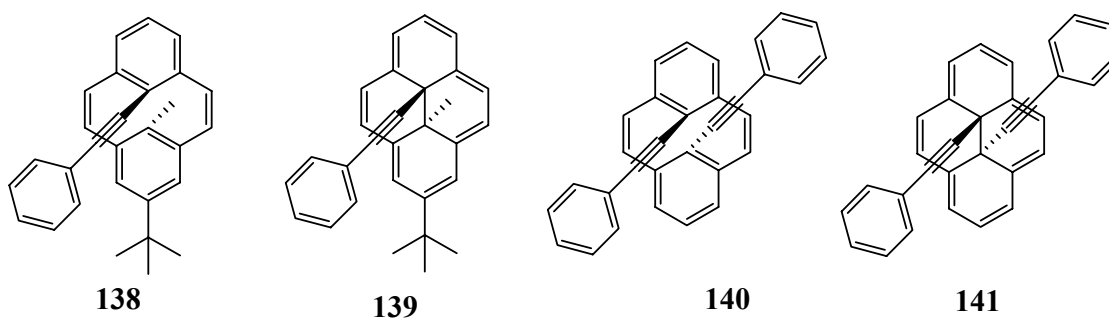
Scheme 2.19 Migration of the internal nitrile group in **128**



The cyclophanediene **127** closes thermally to the dihydropyrene **128** which rapidly decomposes to **137** by a [1,5]-sigmatropic shift of the nitrile. Complete assignment of all protons and carbons was made in the DHP **128** and in the migration product **137**.

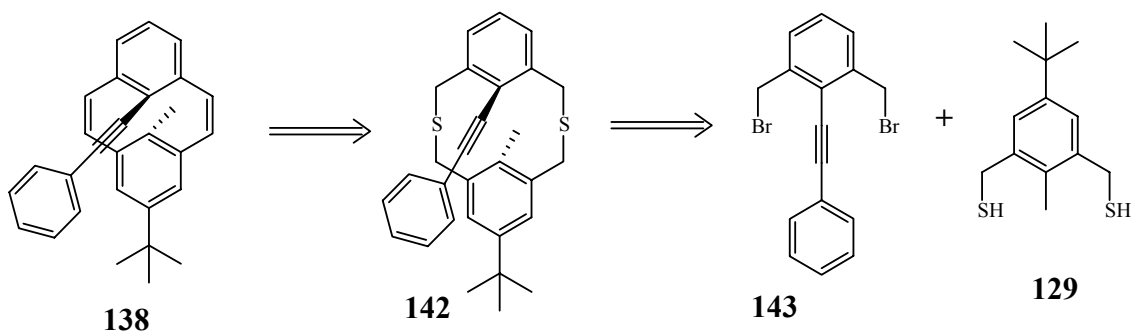
2.3 Synthesis of phenylethynyl/methyl DHP **139**

The cyano-methyl switch pair **127/128** showed much higher migration and thermal closing rates when compared with the dinitrile switch pair **85/86**. Both switch pairs were more stable to the thermal return than the methyl parent, **52/45**. Nitrile groups at the internal positions reduce the thermal closing rates of the CPDs to the DHPs but they have much higher migration aptitude compared to the methyl groups. Replacement of the nitrile group in **127/128** by a phenylethynyl substituent was anticipated to slow down the migration of the internal group in phenylethynyl/methyl DHP **139**. The choice of the phenylethynyl group was based on its structural similarity with the nitrile; both groups are rod-like in nature. The switch pair **138/139** was preferred over the pair **140/141** because of the ease of the synthesis of the former.



Our approach towards the synthesis of **138** was based on the synthesis of the thiacyclophane intermediate **142**. The thiacyclophane in turn can be made from dibromide **143** by coupling with **129** (Scheme 2.20).

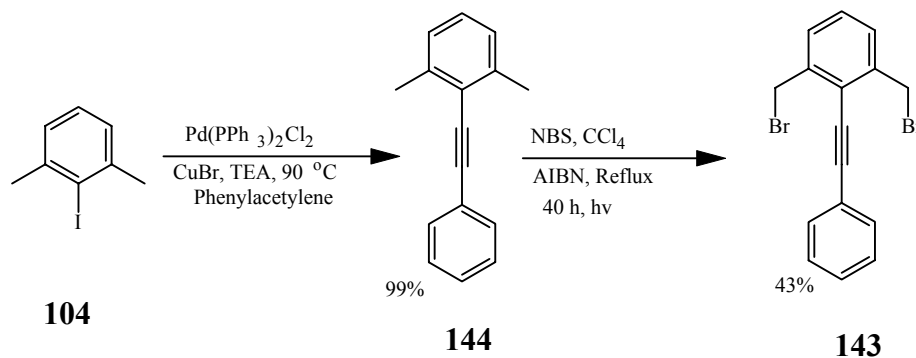
Scheme 2.20 Reterosynthetic analysis of phenylethynyl/methyl CPD 138



2.3.1 Synthesis of the bis(bromomethyl) diphenylacetylene 143

Dibromide **143** was prepared as shown in Scheme 2.21. Sonogashira coupling of the iodide **104** with phenylacetylene using $\text{Pd}(\text{PPh}_3)_2\text{Cl}_2$ as a catalyst in refluxing TEA gave the diphenylethynyl derivative **144** in quantitative yields. Alkyne **144** was brominated at the benzylic positions with NBS in refluxing CCl_4 under photochemical conditions to give **143** in ~ 43% yield. The reaction was sluggish and required relatively large quantities of the AIBN catalyst. Fortunately, the desired product could be selectively crystallized from a mixture of five or six compound with very close R_f values on TLC. The mp and the NMR data of **143** were identical to the literature values.⁶⁶

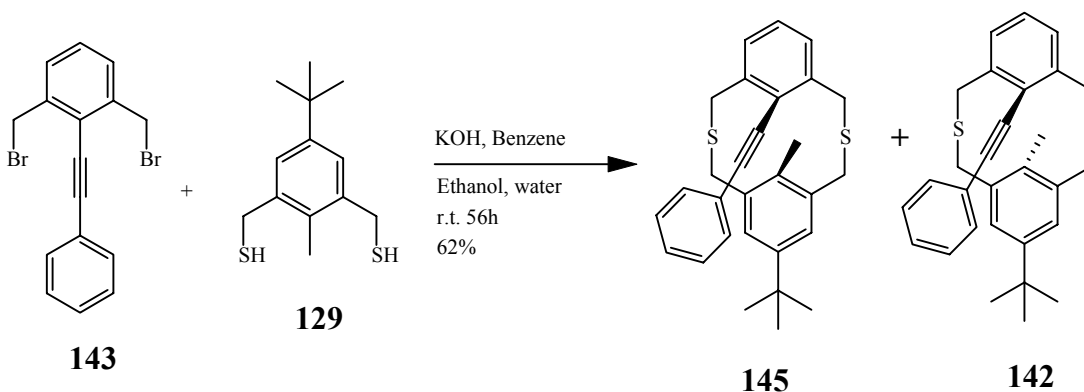
Scheme 2.21 Synthesis of the dibromide 143



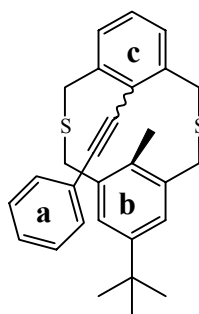
2.3.2 Thiacyclophane formation by coupling dibromide 143 and dithiol 129

Slow addition (one drop per seven seconds) of dibromide **143** and dithiol **129** in ethanol-benzene-water containing KOH under high dilution conditions gave a 3:1 mixture of the *syn*- and *anti*-dithiacyclophanes in 62% yield (Scheme 2.22). The slow drop rate was required probably due to the sterically demanding phenylethynyl group. The *syn*- isomer could be crystallized selectively from cyclohexane while the purification of the *anti*-isomer required multiple columns using column chromatography on silica gel.

Scheme 2.22 Coupling reaction to yield dithiacyclophanes 142 and 145



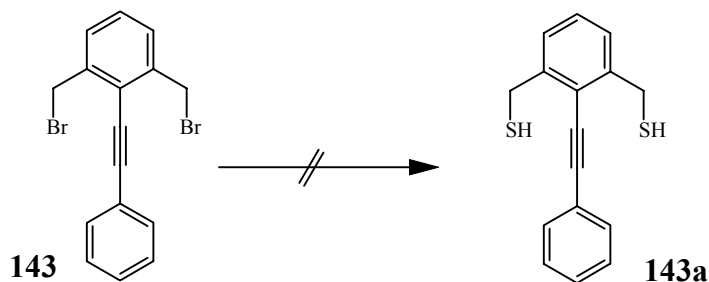
. The protons of the internal methyl group of *anti*-**142** showed an upfield shift due to the ring current of ring “c” and appear at δ 1.42 in the ^1H NMR spectrum whereas the corresponding protons in **145** were normal and appeared at δ 2.54.



In addition, the aromatic protons of **142** showed the normal *anti*-thiacyclopentane pattern and appeared at δ 7.40-7.27 where as the aromatic protons of **145** were shifted upfield to δ 7.00. Moreover, in the *anti*-isomer **142**, protons from the phenylethynyl aromatic ring (ring **a**) experience the shielding effect of ring **b** and appear at δ 7.43-7.31 when compared with the *syn*-isomer, δ 7.62-7.44 and this close spatial orientation was further supported by an NOE interaction of the *meta* protons of ring **a** with the aromatic protons of ring **b**.

The *sp*-carbons of the phenylethynyl group in both isomers were confirmed by ^{13}C NMR spectroscopy by peaks at δ 100-87. All protons and carbons in **145** could be assigned but in **142**, complete assignment in the ^1H NMR spectrum was not possible because of overlapping peaks. The correct structures were indicated by HRMS at m/z 442.1782 and 442.1779 for **145** and **142** (calculated 442.1788). The structure of the *syn*-isomer was also confirmed by X-ray analysis.

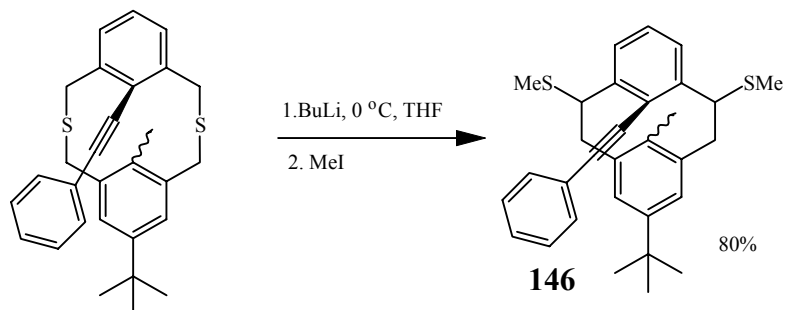
Scheme 2.23 An attempted synthesis of 2,6-bis-(thiomethyl)diphenylacetylene



An attempted reaction to convert dibromide **143** to dithiol **143a** (Scheme 2.23) using thiourea and then KOH was unsuccessful. Quite analogous to the reaction of **102**, an orange red product was obtained.

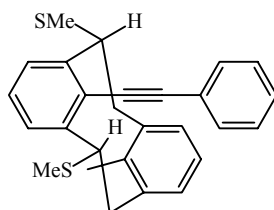
2.3.3 The Wittig rearrangement on the phenylethynylthiacyclophanes

Scheme 2.24 Wittig rearrangement to prepare thiomethylcyclophanes 146



Wittig rearrangement of the thiacyclophanes (mixture of isomers) using BuLi in THF followed by MeI gave a mixture of *syn*- and *anti*-thiomethylcyclophanes **146** in 80% yield (Scheme 2.24). The Wittig rearrangement was accomplished successfully on the smaller scale (less than a millimole); however a large scale reaction gave an insoluble gum like material.

The product mixture consisted mostly of *anti*-isomers. This inference is based on the comparison of the peaks at δ 2.5 for the internal methyl groups in the *syn*-isomers with those of the *anti*-isomers at δ 0.6 in the ^1H NMR spectrum. The major isomer of **146** was purified by column chromatography using hexane:dichloromethane 7:1 and was fully characterized. X-ray structure determination confirmed the geometry shown in **146a**.

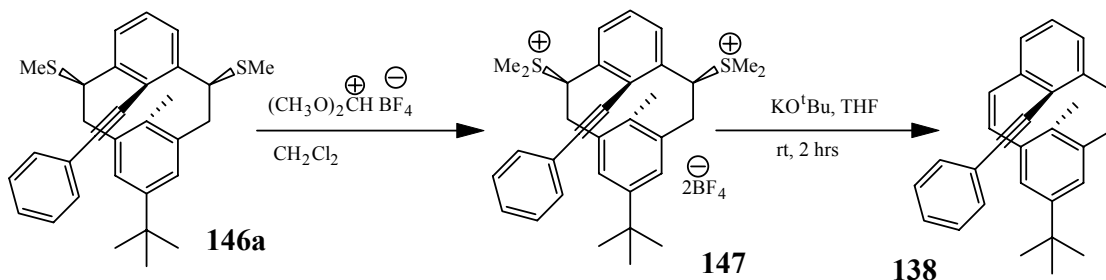


146a

2.3.4 Synthesis of CPD **138** by Hoffmann elimination and its isomerization to the DHP **139**

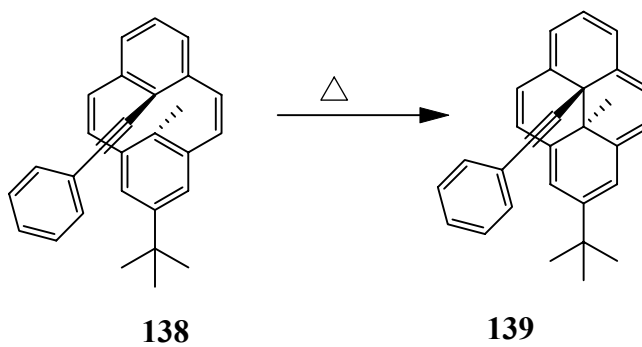
Isomer **146a** when reacted with dimethoxycarbonium fluoroborate afforded the sulfonium salt **147** which on Hoffmann elimination gave the *anti*-cyclophanediene **138** (Scheme 2.25). These two steps were carried out in greater than 90% yield. To avoid thermal return, cyclophanediene **138** was chromatographed in a jacketed column with ice water flowing through it. In its ^1H NMR spectrum, the phenylethynyl protons were at δ 7.25. Protons from the CPD nucleus showed seven peaks at δ 7.12-6.32. The internal methyl protons appeared at δ 1.65, characteristic of *anti*-CPDs. The ethynyl carbons were confirmed by the ^{13}C NMR peaks at δ 89.98 and 95.13.

Scheme 2.25 Synthesis of the phenylethynyl/methylcyclophanediene 138



Diene **138** was isomerized thermally into the green *trans*-DHP **139**, mp 112-113 °C (Scheme 2.26). The transformation could be monitored by the growth of the peak at δ -4 in the ^1H NMR spectrum, corresponding to the internal methyl protons. The DHP protons were at δ 8.72-8.07. A decrease in the diatropic ring current of the DHP with distance was shown by the chemical shifts of the phenylethynyl protons. The *ortho* protons are close to the DHP ring and are shielded to δ 6.04 when compared with the *meta* (δ 6.72) or *para* (δ 6.83) protons. The ethynyl spacer was confirmed by the ^{13}C NMR spectrum in which the carbons appeared significantly shielded at δ 84.61 and 75.41 as compared to those of CPD **138** (δ 95.13 and 89.98). Besides spectral data, the structure of the *trans*-DHP **139** was also confirmed by a crystal structure.

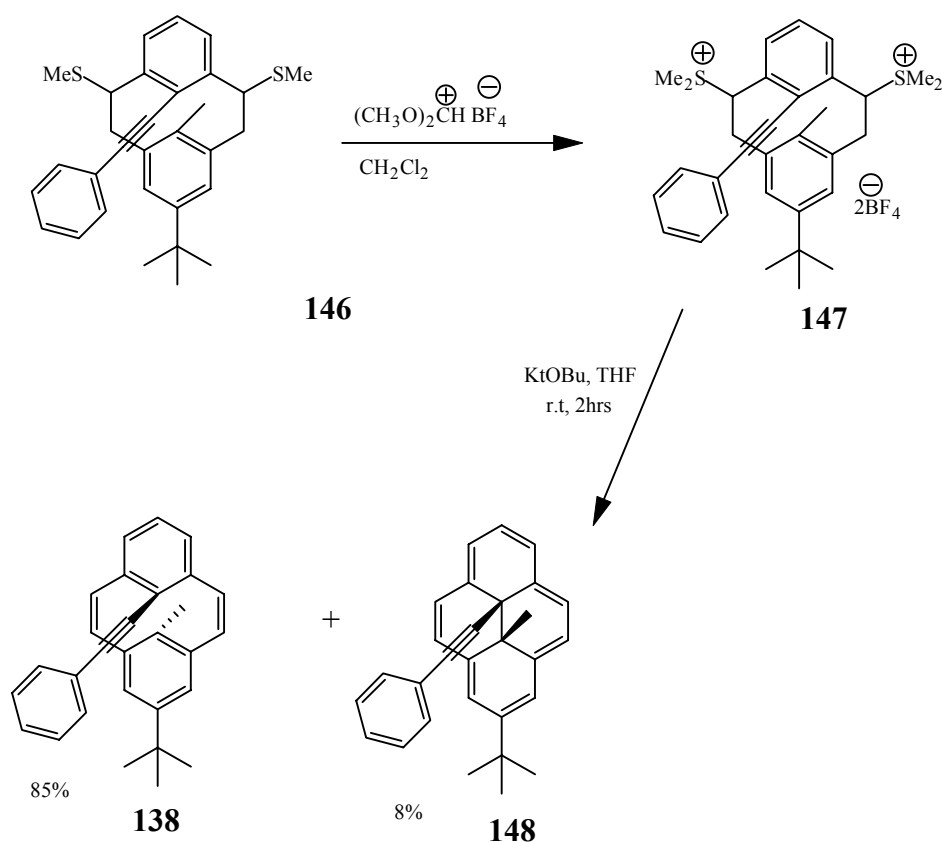
Scheme 2.26 Thermal closure of phenylethynyl/methyl CPD 138 to the DHP 139



2.3.5 Synthesis of the *cis*-DHP 148

Methylation of **146** (mixture of *syn*- and *anti*-isomers) with Borch⁵⁹ reagent gave the sulfonium salt mixture **147** (Scheme 2.27) which underwent Hoffmann elimination to afford **138** as the major product (85% yield) along with an 8% yield of the green *cis*-DHP **148**, mp 159-160 °C.

Scheme 2.27 Hoffmann elimination of mixed isomers of 147

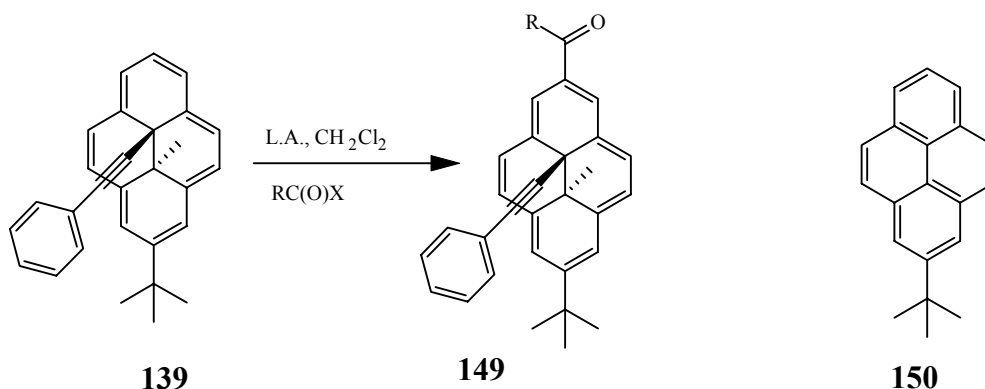


The *cis* orientation of the internal groups in the DHP **148** was easily established by a peak at δ -1.55 in the ^1H NMR spectrum. The *ortho* protons of the phenylethynyl ring were shielded to δ 6.67 when compared with the *meta* and *para* protons, δ 6.97-7.00. The structure of the *cis*-DHP **148** was confirmed by an X-ray structure determination.

2.3.6 Attempted syntheses of acyl DHP 149 by Friedel-Crafts acylation

Phenylethynyl/methyl DHP **139** was quite stable and did not decompose to any migration product(s) when heated at 70 °C. Moreover, the cyclophanediene **138** isomerized to the DHP **139** at slower rates when compared with the benzo CPD **53** (for details see Chapter 3). But an attempted photobleaching of **139** did not produce **138** at all. Carbonyl functionality at the 2- and 4- positions of DHP is known to enhance the visible opening rates.⁶⁷ We became interested in installing an acyl group at the C-2 position of DHP **139**.

Scheme 2.28 Attempted Friedel-Craft acylation to yield 149

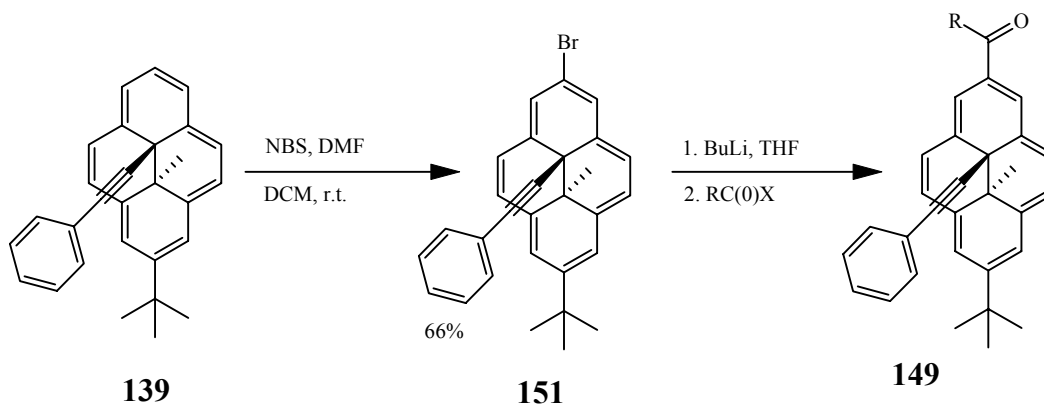


Different combinations of Lewis acids (L.A.) ($\text{BF}_3 \cdot \text{Et}_2\text{O}$, AlCl_3) and acylating agents (acetic anhydride, benzoyl chloride, naphthoyl chloride) were tried to prepare **149** but were unsuccessful. The green color of the dihydropyrene faded to pale yellow in a few minutes after the addition of Lewis acid which indicated its decomposition. The major isolated product was *t*-butylpyrene **150** which is formed probably by the migration and subsequent eliminations of the internal groups.

2.3.7 An anionic approach to the synthesis of the acyl DHP

An alternative approach to synthesize **149** is shown in Scheme 2.29 which avoids the use of Lewis acids. Phenylethynyl/methyl DHP **139** was brominated to **151** using NBS in dry DMF and dry DCM in variable yields. Robinson³⁵ has reported that carrying out the bromination reaction at room temperature gives high yields and the results are quite reproducible. We failed to gain reproducible results under similar conditions and the yield varied between 0-66%. A 1:1 ratio of M and M+2 peaks in the mass spectrum of **151** confirmed the presence of a bromine atom. Bromide **151** was lithiated with *n*-BuLi in THF to generate an anion of the DHP which on treatment with benzoyl bromide afforded a product probably the desired one.

Scheme 2.29 Attempted synthesis of **149** involving a bromide intermediate **151**



This product could not be purified by column chromatography from a co-eluting side product. Selective recrystallization also failed. No further attempts were made to prepare **149**; rather attention was diverted towards the synthesis of other photoswitches.

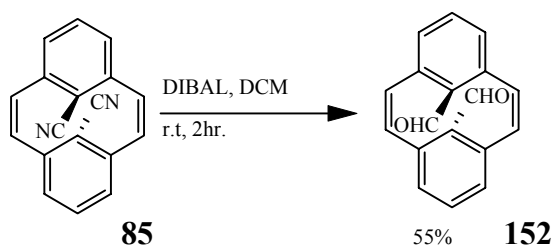
2.4 Chemistry at the internal substituents

The switch pairs **85/86** (dicyano), **127/128** (cyano-methyl) and **138/139** (phenylethynyl), though synthesized successfully, required lengthy and time consuming syntheses. Each of them required the synthesis of a new thiacyclophane. If FG transformations could be performed on a preformed cyclophanediene or dihydropyrene nucleus then it would generate a new switch pair in a single step. For this purpose, switch pair **85/86** was chosen. Dicyano CPD **85** was preferred over the DHP **86** for its use in a chemical reaction because it is thermally stable. Moreover, the CPDs formed from the reaction would allow performing kinetic analysis even if the corresponding DHPs are not photochromic.

2.4.1 DIBAL-H reduction of the dinitrile **85**

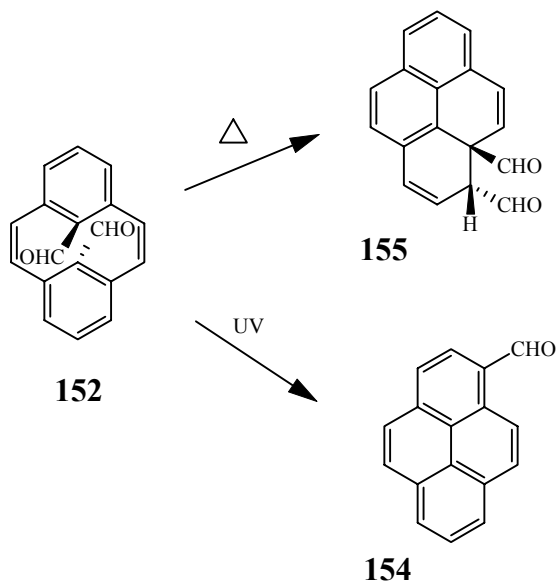
DIBAL-H reduction of **85** in DCM (Scheme 2.30) at room temperature gave **152** in 56% yield. The desired product could be purified either by crystallization from methanol or by column chromatography using EtOAc:DCM 1:9 as eluant.

Scheme 2.30 Reduction of the dinitrile **85** to the dialdehyde **152**

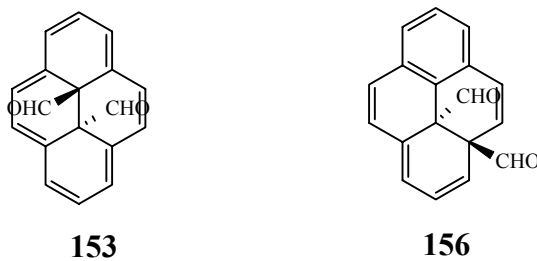


The aldehyde group was identified by the ^1H NMR and ^{13}C NMR peaks at δ 9.35 and 185.77 respectively. The IR bands at 2768 and 1712 cm^{-1} confirmed the aldehyde group. The side products were minimized at lower temperature.

Scheme 2.31 Thermal rearrangement of the internal formyl groups



When diformyl CPD **152** was irradiated with UV light (254 nm), it gave 1-formylpyrene, **154** (Scheme 2.31) instead of the DHP **153** while the attempted thermal isomerization gave the migration product **155**.



2.4.1.1 The [1,5]-sigmatropic rearrangement of the formyl groups

An NMR sample of **152** in CDCl_3 , when heated at 70°C for one hour gave the migration product **154**. No traces of the first migration product **156** analogous to **123** or **124** (Scheme 2.14, page # 48) could be found by ^1H NMR spectroscopy. This could be either due to the simultaneous migration of both formyl groups in **153** or because of the

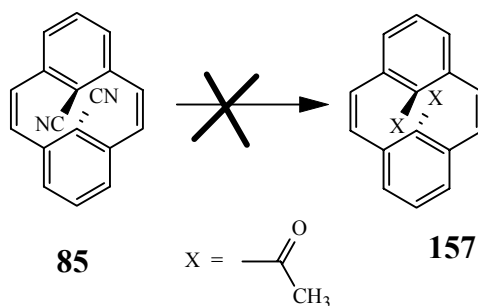
high instability of **156**. Dehydroformylation of **155** was observed on attempted column chromatography giving **154**.

The structure **155** was assigned to the migration product based on its NMR spectroscopic analysis. In the ^1H NMR spectrum, the signals of the two formyl protons were found at δ 9.71 and 9.34. In the ^{13}C NMR spectrum, both formyl carbons were also quite distinct and appeared at δ 198.74 and 190.97. The relative position of the formyl groups was assigned based on the HMBC and HSQC techniques. The IR stretches at 2721 and 1719 cm^{-1} confirmed the presence of the aldehyde groups. The mass spectrum showed molecular ion peak at m/z 260. The base peak at m/z 202 in the mass spectrum indicated decomposition to pyrene **112**.

2.4.2 The attempted synthesis of the acyl substituted CPD **157**

MeLi treatment of **85** was expected to give the methyl ketone **157** (Scheme 2.32), however it failed to furnish the desired product. Pyrene **112** was the only isolated product. The reaction was monitored by TLC and it was revealed that the pyrene formation started at -20 $^\circ\text{C}$ and was complete before the reaction mixture reached room temperature.

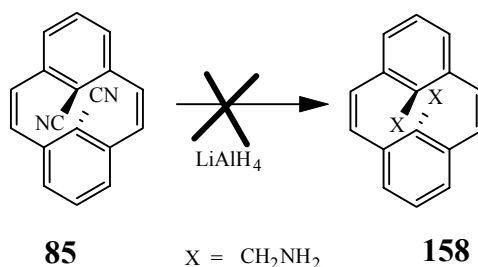
Scheme 2.32 Attempted synthesis of the acetyl CPD **157**



2.4.3 Reduction of the nitrile **85** into the primary amine **158**

Complete reduction of the nitrile **85** using LiAlH_4 to the primary amine **158** failed (Scheme 2.33). Once again pyrene **112** was the major product. Our interest in investigating the chemistry of the internal nitriles was limited by this pyrene formation. Thus we did not endeavor to hydrolyze the nitrile **85** to the corresponding amide or carboxylic acid derivatives because of its sensitivity to many nucleophiles.

Scheme 2.33 Attempted reduction of nitrile **85** to primary amine **158**

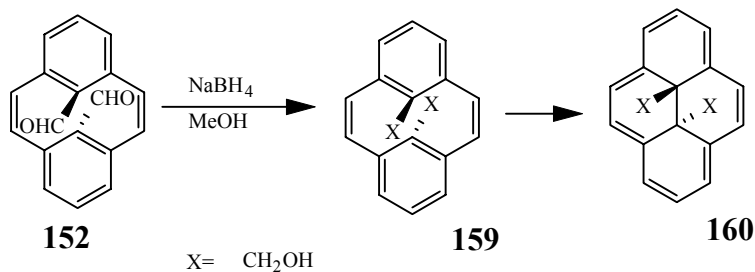


2.4.4 Reduction the internal formyl groups using NaBH_4

Attention was directed towards the chemistry of diformyl CPD **152**. The CPD has relatively short half life (11 days at rt) so a reaction involving mild conditions such as reduction with NaBH_4 would be an ultimate starting point.

Reduction of the aldehyde **152** with NaBH_4 in methanol at room temperature (Scheme 2.34) delivered the primary alcohol **159** in quantitative yields. Hydroxymethyl CPD **159** was thermally unstable and isomerized to the dihydropyrene **160** in less than an hour which subsequently decomposed to pyrene **112** in a few hours at room temperature. Thus characterization was carried out on the non chromatographed sample.

Scheme 2.34 Reduction of the diformyl CPD **152 to the primary alcohol **159****



In the ¹H NMR spectrum, replacement of the aldehyde peak at δ 9.35 by the hydroxymethylene peak at δ 3.80 indicated the formation of the desired product. The peak corresponding to the OH protons was not located. Probably it was broad and unresolved to the base line. The methylene carbons bearing the OH groups were at δ 62.73 in the ¹³C NMR spectrum. The IR spectrum supported the presence of the OH group by a stretch at 3390 cm⁻¹. Mass spectrometry did not show a molecular ion peak, rather a peak at m/z 202 which indicated decomposition to the pyrene **112**.

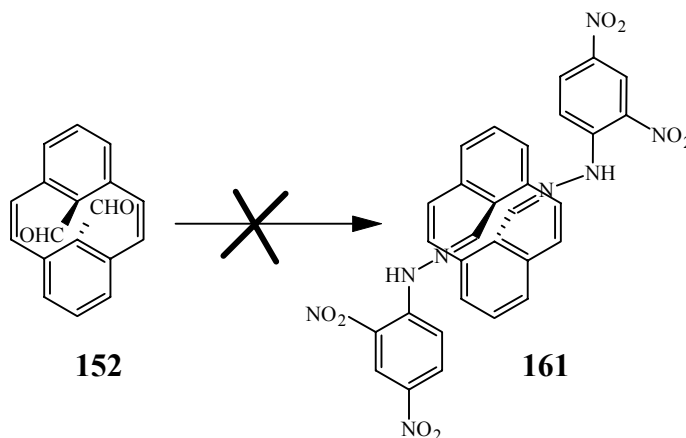
Hydroxymethyl CPD **159** transformed at room temperature to the dihydroxyrene **160** in an hour. The methylene and hydroxyl protons in **160** were at δ -1.77 (doublet) and -2.1 (triplet) respectively in the ¹H NMR spectrum.

2.4.5 The 2,4-dinitrophenyl hydrazone of the cyclophanediene **152**

2,4-Dinitrophenylhydrazone formation is a textbook reaction to test for the presence of an aldehyde or a ketone functional group.⁶⁸ We were quite surprised to know that the **152** when reacted with 2,4-dinitrophenylhydrazine failed to produce the hydrazone **161** (Scheme 2.35). This abnormality in reactivity could be attributed either to the insolubility of the formyl CPD **152** in the methanol-glycerol solvent mixture or to steric constraints associated with the approach of the hydrazine to the hindered carbonyl

functionality. The latter was excluded by a reaction of **152** with hydrazine hydrochloride which also failed to give any products.

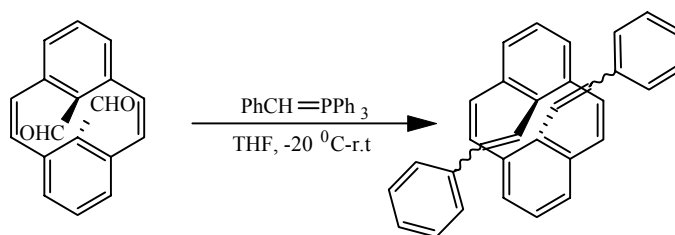
Scheme 2.35 Attempted synthesis of a bis hydrazone



2.4.6 Wittig reaction of the diformyl CPD **152**

Wittig reaction of **152** with benzyltriphenylphosphonium bromide using BuLi in THF at room temperature resulted in the formation of pyrenes. However, when the reaction was carried out at lower temperature, it gave a mixture of four or five pale green to colorless products with very close R_f values on TLC.

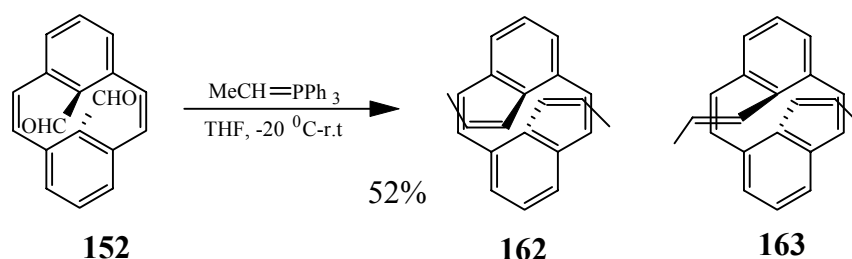
Scheme 2.36 Wittig reaction of **152** to produce styryl CPDs



^1H NMR analysis was complicated by the jumbled peaks at δ 7.5-5.0. Overlap of the styryl protons with the CPD protons with an added effect of the number of isomers at

the double bond would lead to the complicated spectrum. Thus it was predicted that the replacement of the styryl group by an alkyl substituted alkene would simplify the ^1H NMR spectrum, and hence the analysis.

Scheme 2.37 Synthesis of the CPDs with internal propenyl substituents



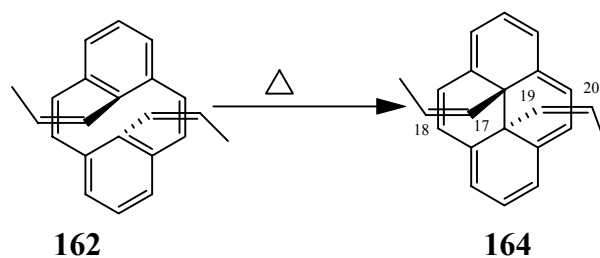
Dialdehyde **152**, when subjected to the ylide derived from ethyltriphenylphosphonium bromide gave a 6:1 mixture of **162** and **163** in 52% yield (Scheme 2.37). The major isomer **162**, as expected, gave a total of six peaks in the ^1H NMR spectrum. The *cis* orientation of the double bond was established by a coupling constant of 12 Hz between the olefinic protons, which was also supported by the IR band at 711 cm^{-1} . The olefinic protons were found as doublets of quartets at δ 6.12 and 5.23 while the methyl protons appeared as a doublet of doublets at δ 1.55. The product was confirmed by mass spectrometry which gave the correct molecular weight of m/z 284.

All protons and carbon in the major isomer (**162**) could easily be accounted for but in the minor isomer **163**, the *cis*-propenyl protons and carbons were obscure. This could be due to overlap with peaks of the major isomer. The *trans*-propenyl internal group in **163** was identified by a coupling constant of 15.4 Hz for the alkene protons at δ 5.94 and by the IR stretch at 962 cm^{-1} .

2.4.6.1 A photoswitch with low thermal and migration rates

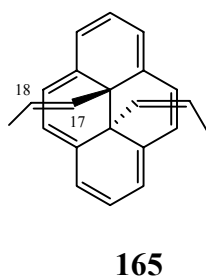
The mixture of propenyl CPDs **162** and **163** when heated at 100 °C for 12 hours furnished the dihydropyrenes **164** and **165** without any *cis-trans* isomerization of the internal olefinic groups. In the ^1H NMR spectrum of **164**, the DHP protons appeared at δ 8.65-8.05. The internal propenyl protons were shielded to different extents depending on their distance from the diatropic ring.

Scheme 2.38 Thermal isomerization of 162 to 164



The protons H-17/19 were the most shielded protons followed by H-18/20 (Scheme 2.38) and appeared at δ 0.09 and δ 3.21 respectively as doublets of quartets. A coupling constant of 12.4 Hz indicated the *cis* geometry of the double bond. The methyl protons were at δ 0.33.

The internal *trans*-propenyl protons in **165**, H-17 and H-18, appeared at δ 0.15 and 2.36 respectively in the ^1H NMR spectrum and indicated a significant shielding of H-18 when compared with the *cis* analogue H-20 at δ 3.14.



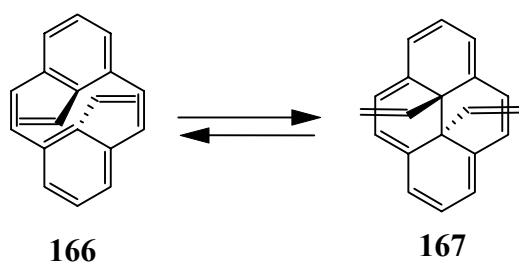
Internal alkene substituted CPD and DHP pairs, **162/164** and **163/165** showed high stability towards:

1. The thermal closure of the cyclophanedienes to the dihydropyrenes
2. The migration of the internal substituents in the DHP.
3. The thermal *cis-trans* isomerization of the internal olefin.

2.5 Improved syntheses of the dihydropyrenes with internal olefin groups

The thermal stability of switch pairs **162/164** and **163/165** fascinated us and it drove our attention towards the synthesis of a series of dihydropyrene photoswitches with different internal olefin substituents. The synthetic strategy for the internal olefin substituted cyclophanedienes had some limitations such as the involvement of small scale and heat sensitive FG transformations (Schemes 2.30 and 2.37), and thus required revision.

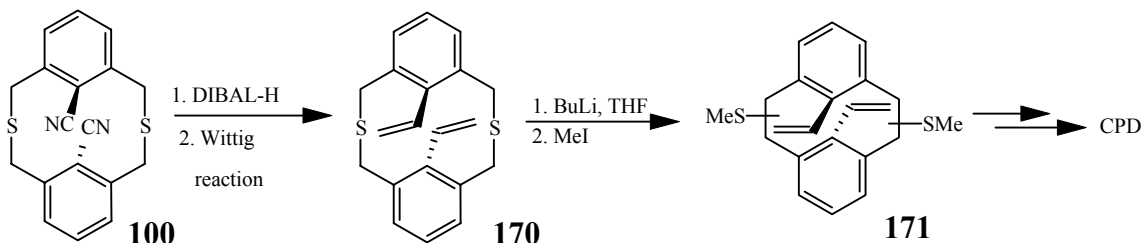
Scheme 2.39 A photoswitch with internal vinyl substituents



FG transformations either in the dicyanothiacyclophane **100** or in the Stevens product **99** and their subsequent conversion to cyclophanedienes was anticipated to improve the yield. In order to eliminate complications arising from the *cis-trans* isomers, the vinyl substituted switch pair **166/167** (Scheme 2.39) was chosen as the synthetic

target. Scheme 2.40 represents a brief outline of the proposed synthetic route with FG transformations in the thiacyclophane **100**.

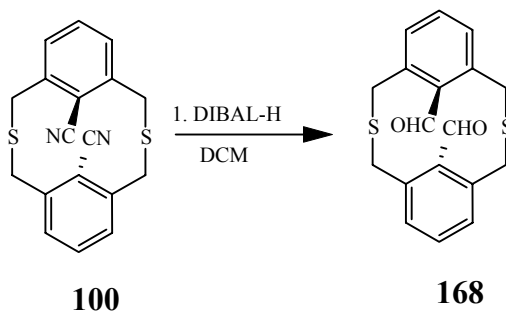
Scheme 2.40 Modified synthesis of CPDs with internal olefin substituents



2.5.1 DIBAL-H reduction-Wittig reaction sequence to synthesize the thiacyclophane **170**

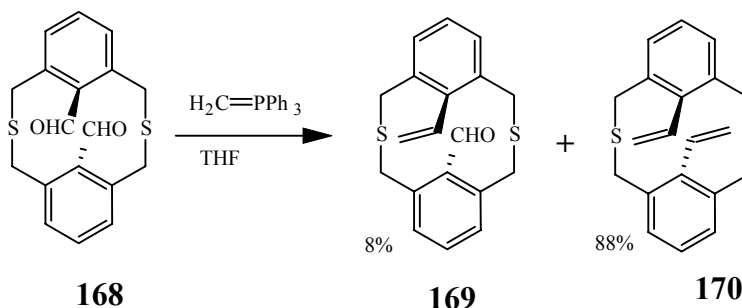
DIBAL-H reduction of **100** at room temperature in DCM gave ~ 90% yield of the diformylthiacyclophane **168** (Scheme 2.41). The formyl protons appeared at δ 9.93 in the ^1H NMR spectrum. The chemical shift of the carbonyl carbon at δ 191.49 in the ^{13}C NMR spectrum and the IR stretches at 2773 cm^{-1} and 1683 cm^{-1} confirmed the aldehyde functional group. The bridge protons in **168** were at δ 4.32-3.79 and were relatively widely spaced when compared with the nitrile analogue **100** (δ 3.94-3.88).

Scheme 2.41 Synthesis of the diformyl-*anti*-thiacyclophane **168**



Thiacyclophane **168**, when treated with the ylide derived from methyltriphenyl phosphonium bromide in THF gave 88% of the divinylthiacyclophane **170** along with 8% of the monovinyl thiacyclophane **169** (Scheme 2.42). Both products were isolated by column chromatography and their assignment was made on the basis of NMR spectroscopy. The replacement of the formyl proton peak at δ 9.93 in the ^1H NMR spectrum by the vinyl proton peaks at δ 5.93-4.68 indicated the formation of the desired product **170**. The ^1H NMR spectrum showed a total of seven peaks as expected because of symmetry. Satisfactory elemental analysis was obtained for **170**.

Scheme 2.42 Wittig reaction of 168 to synthesize 169 and 170



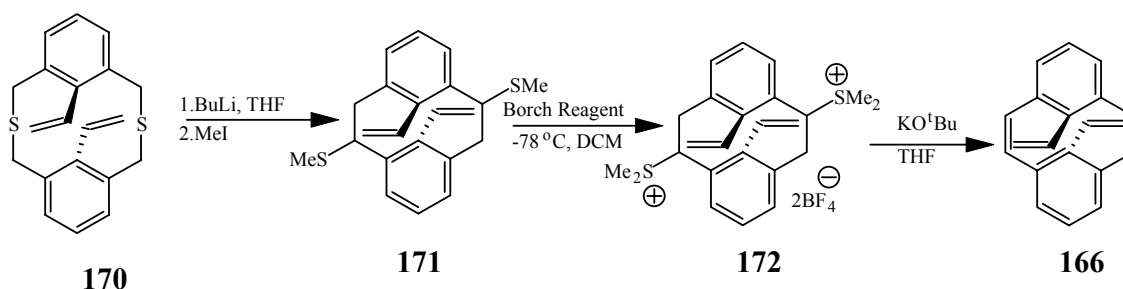
The minor product, **169** indicated the presence of the formyl and vinyl groups by peaks at δ 9.82 and δ 6.00-4.78 respectively in the ^1H NMR spectrum. IR bands at 2780 and 1679 cm^{-1} confirmed the presence of the aldehyde functional group.

2.5.2 Synthesis of the divinylcyclophanediene 166

Wittig rearrangement of the divinylthiacyclophane **170** followed by treatment with MeI gave greater than 90% yield of the thiomethylcyclophanes **171** as a mixture of isomers (Scheme 2.43). The success of the reaction was shown by the appearance of the methyl groups as singlets at δ 2.1 in the ^1H NMR spectrum. The vinyl protons were centered at δ 4.9-4.2. The di-equatorial isomer of **171** was purified using column

chromatography and fully characterized. Mass spectrometry gave the correct molecular mass at m/z 352.

Scheme 2.43 Wittig rearrangement of the thiacyclophane **170 and subsequent Hoffmann elimination**



Mixed isomers of **171**, when treated with dimethoxycarbonium tetrafluoroborate gave the sulfonium salts **172** which on Hoffmann elimination furnished the cyclophanediene **166** in quantitative yield. The desired product could easily be identified by its ¹H NMR spectrum. Protons from the internal vinyl substituent appeared at δ 6.32-4.84 as three doublets of doublets. The molecular ion peak at m/z 256 confirmed the formula.

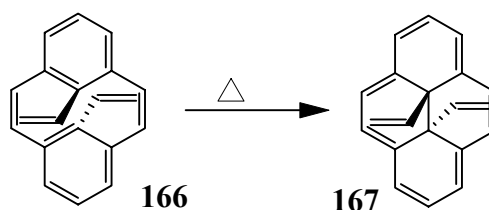
2.5.3 Thermal isomerization of the cyclophanediene **166 into the dihydropyrene**

167

A solution of cyclophanediene **166** in toluene when heated at 100 °C for 8 hours yielded the dihydropyrene **167**. The vinylic -CH=CH₂ was highly shielded and appeared at δ 0.5 as doublet of doublets in the ¹H NMR spectrum. The -CH=CH₂ protons were at δ 2.06 and 2.67 (doublets of doublets). The mass spectrum confirmed the molecular

formula by a peak at m/z 256. A satisfactory elemental analysis was obtained for **167**. Finally an X-ray structure determination confirmed the structure.

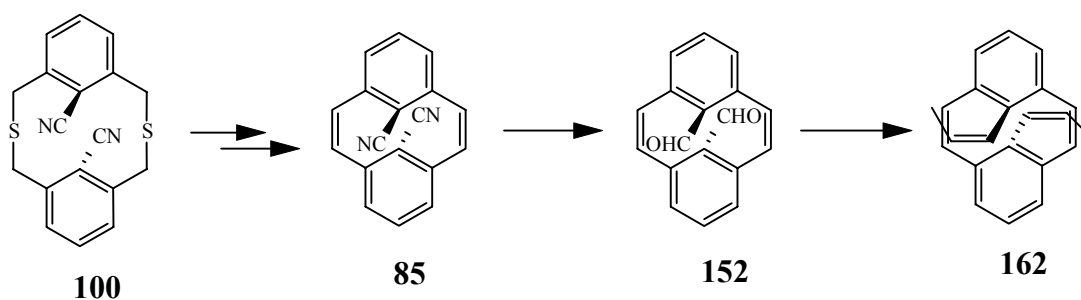
Scheme 2.39 Thermal return of the divinyl CPD 166 to the dihydropyrene 167



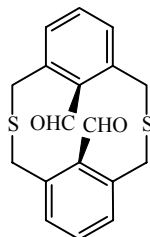
2.5.4 A comparison of the synthetic routes to the olefin substituted CPDs

Starting from the *anti*-thiacyclophane **100**, the sequence of reactions described in Scheme 2.40 gave an overall yield of 72% for divinyl CPD **166**. On the other hand the cyclophanediene route shown in Scheme 2.44 gave ~ 23% of the CPD **162**.

Scheme 2.44 Synthesis of propenyl DHP 162 via CPD 152



However the revised scheme (Scheme 2.40) had some limitation as well. For example, the *syn*-dicyanothiacyclophane **108**, when subjected to the DIBAL-H reduction failed to give any yields of the diformyl-*syn*-thiacyclophane **173**. Moreover, successful reduction of **100** using DIBAL-H was limited to a small scale reaction (sub millimolar scale).

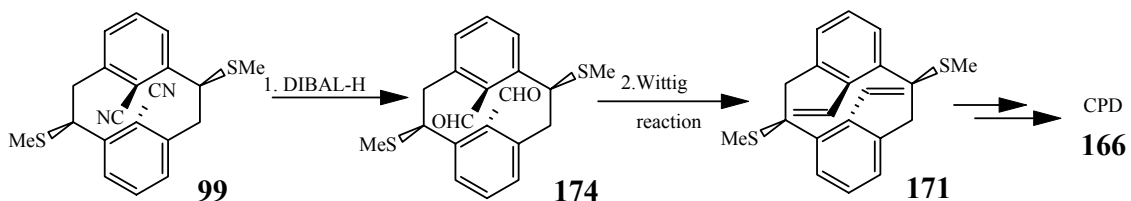


173

2.5.5 Another improvement in the synthesis of divinyl CPD 166

It was expected that the FG transformations in the dicyanothiomethylcyclophanes **99** would eliminate or at least reduce the above mentioned problems because **99** is generally obtained as a mixture of *anti*-isomers. Reduction of **99** (mixed isomers) with DIBAL-H furnished the diformyl MeS-cyclophanes **174** quantitatively. Appearance of singlets at δ 9.1-8.8 in the ^1H NMR spectrum corresponding to the aldehyde protons indicated the success of the reaction. The reaction could be carried out on a two gram scale.

Scheme 2.45 Improved synthesis of divinyl CPD 166 starting from thiomethylcyclophane 99



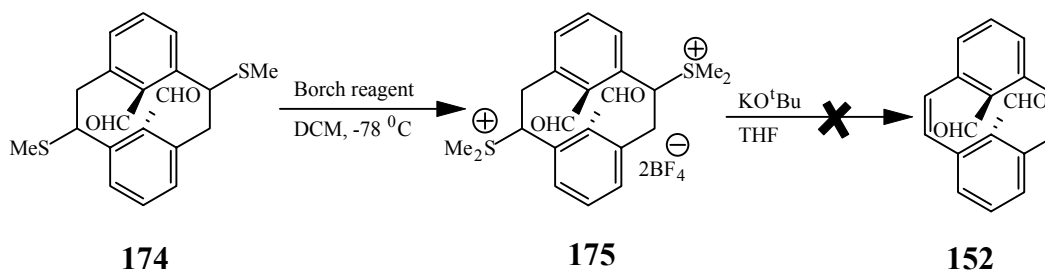
When a single isomer of **99** was employed, it gave **174** as a pure isomer (Scheme 2.45). This isomer of **174** was fully characterized and complete assignment of all the protons and carbon was made. The internal formyl protons appeared at δ 8.95. The aldehyde group was further confirmed by the ^{13}C NMR peak at δ 188.74 and by the IR

stretches at 2786 and 1682 cm^{-1} . The mass spectrum confirmed the molecular formula with m/z 356.

Wittig reaction of **174** with methyltriphenylphosphonium bromide using BuLi as the base generated the olefin substituted thiomethylcyclophane **171** in greater than 90% yield. With this improved methodology, cyclophanediene **166** could be made in gram quantities in > 70% yield starting from the dicyanothiacyclophanes **108** and **100** (*syn*- and *anti*). The above mentioned scheme (Scheme 2.45) served as a standard protocol for the syntheses of a variety of olefin substituted cyclophanedienes.

It was however of interest to see if the diformylcyclophanes **174** could be converted to the cyclophanediene **152**. Sulfonium salt **175** was successfully prepared but the subsequent Hoffmann elimination gave a mixture of pyrenes instead of **152** (Scheme 2.46).

Scheme 2.46 Attempted synthesis of diformyl CPD **152** by the Hoffmann elimination

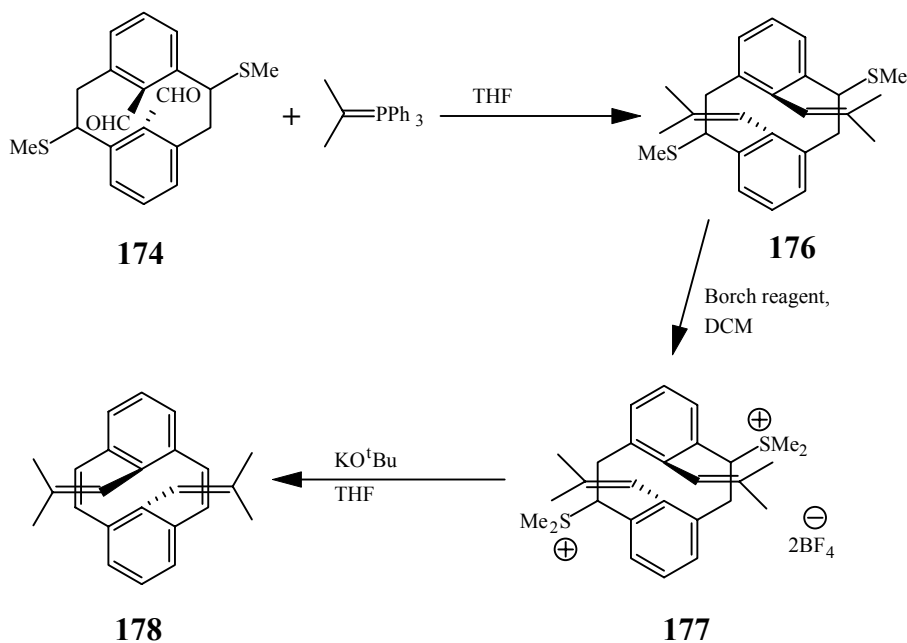


2.5.6 Synthesis of the diisobutenyl CPD **178**

A comparison of the thermal return rates of divinyl (**166**) and dipropenyl (**162**) cyclophanedienes (Chapter 3 for details) revealed that the methyl substituent on the internal olefin had a substantial decelerating effect. Thus, the CPD **178** with two methyls

on the internal olefin substituent was predicted to show even higher thermal stability. Diisobutenyl CPD **178** was successfully synthesized in two steps (Scheme 2.47) starting from the diformylcyclophane **174** in an overall yield of $\sim 70\%$. Isopropyltriphenyl phosphonium bromide,⁶⁹ when reacted with BuOK, generated the ylide that on reaction with **174** gave a 71% yield of **176**. The isobutenyl functional group was confirmed by the methyl protons peaks at δ 0.8-1.6 in the ^1H NMR spectrum. No attempts were made to purify isomers of **176**. Methylation of **176** with Borch reagent delivered **177** quantitatively and subsequent Hoffmann elimination gave the cyclophanediene **178** in 96% yield.

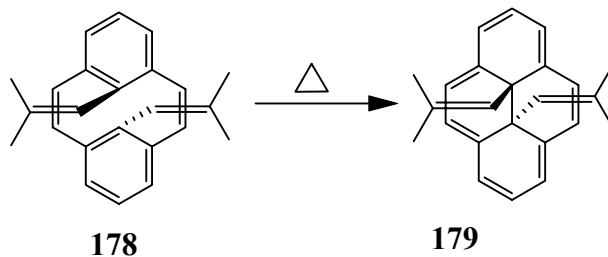
Scheme 2.47 Synthesis of the diisobutenyl CPD 178



The olefinic CH proton of the internal isobutenyl substituent in **178** appeared as septet at δ 5.70 in the ^1H NMR spectrum, and the signal of methyl protons were at δ 1.57. Mass spectrometry showed the correct molecular ion peak at m/z 312. Successive losses of 55 mass units in the mass spectrum further confirmed the presence of the internal

butenyl groups. X-ray structure determination was also obtained for the cyclophanediene **178**, which confirmed its structure.

Scheme 2.48 The thermal closure of diisobutenyl CPD **178 to the DHP **179****



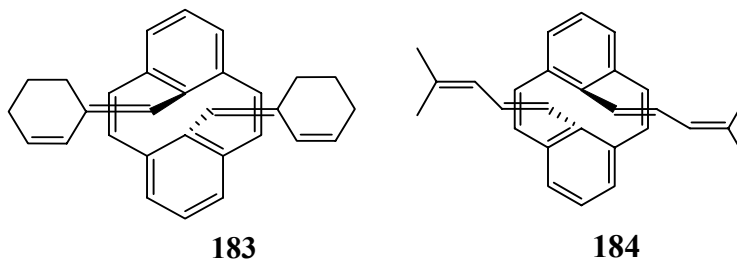
Diisobutenyl DHP **179** was obtained by the thermal closure of **178** at 110 °C for 12 hours (Scheme 2.48). The internal vinyl protons were observed at δ -0.16 in the ^1H NMR spectrum, and the methyl protons were observed as two doublets at δ 0.17 and 0.14. Partial decomposition of the dihydropyrene **179** was seen in deuterated chloroform, probably because of the acid present in it. An X-ray structure was obtained for **179**.

2.6.6 Syntheses of the olefinic CPDs with extended conjugation

The high thermal stability of **178**, as expected, has shown that a slight change in the internal substituent can lead to dramatic effects on the thermal closure reaction. Thus, we became interested in modifying the internal olefin by extending the conjugation by a double or a triple bond and by a phenyl ring (substituted and non-substituted), and study their influence on the photoswitch.

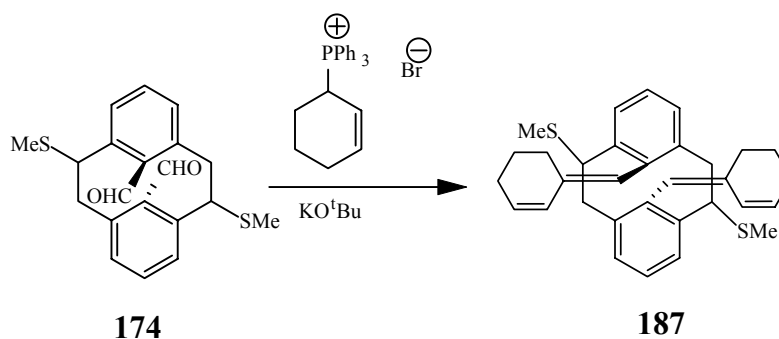
2.6.1 Butadienyl as the internal substituents

Our standard protocol for the synthesis of internal olefin substituted cyclophanedienes starting from **174** through **180** failed to yield **181** at all (Scheme 2.49).



Synthesis of **183** could not be accomplished however, because the Wittig reaction shown in Scheme 2.50 failed to furnish the thiomethylcyclophane **187**. Cyclohexenyl triphenylphosphonium bromide when treated with *t*-BuOK formed globules, probably clusters of ions, which then failed to react with the formylcyclophane **174**. No precedent example of the Wittig reaction from this salt is found in the literature probably because of similar reasons.

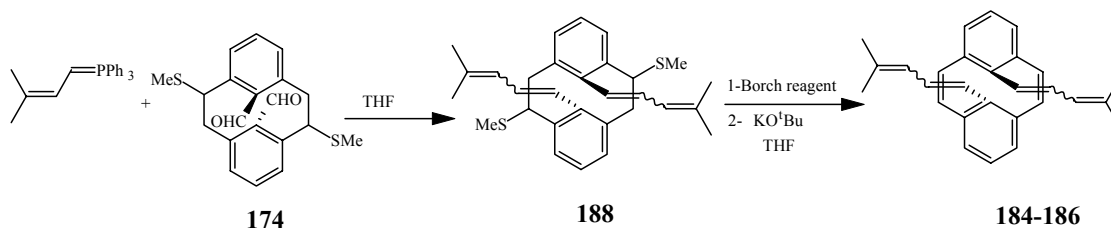
Scheme 2.50 Attempted synthesis of thiomethylcyclophane 187



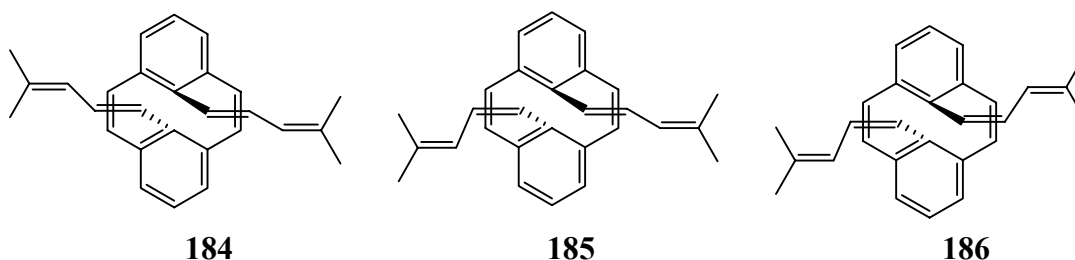
Wittig reaction of **174** with the ylide derived from 3-methyl-2-butenyltriphenyl phosphonium bromide gave 54% of the cyclophane **188** in an unoptimized reaction (Scheme 2.51). The ^1H NMR spectrum revealed the presence of the desired product by the alkene protons at δ 6.2-4.0 and by the methyl protons at δ 2.0-1.5. Butadiene **188**, on treatment with Borch reagent gave the sulfonium salt which on Hoffmann elimination yielded the desired cyclophanediene as a mixture of three isomers. Attempted column

chromatography failed to separate the isomers however fractions rich in one or the other isomer were obtained.

Scheme 2.51 Synthesis of CPDs containing methyl substituted butadienyl internal groups



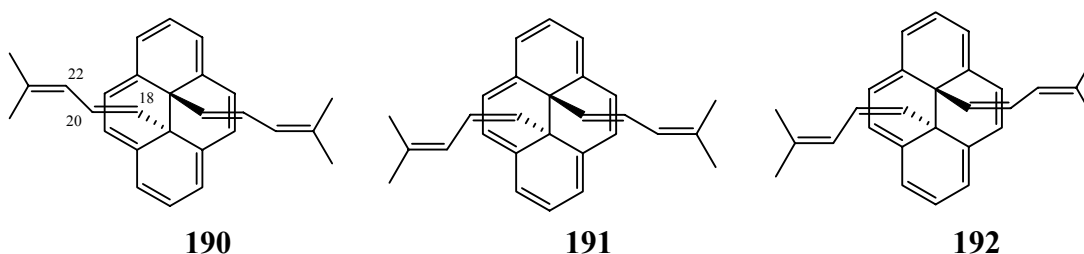
Virtually all protons and carbons in all the isomers could be assigned by NMR spectroscopy. Because of symmetry in the isomers **184** and **186**, a total of eight peaks appeared in their ^1H NMR spectra while the unsymmetrical isomer **185** was found to contain 16 peaks. The all *trans*-isomer **184** was characterized by a coupling constant of 15.4 Hz for the alkene protons at δ 6.80 and 6.09. The methyl protons were observed at δ 1.72 and 1.78 as poorly resolved doublets.



A coupling constant of 12.4 Hz of alkene protons at δ 5.76 indicated the *cis* orientation of double bond in **186**. The methyl protons were observed at δ 1.74 and 1.71.

2.6.1.1 Dihydropyrenes **190-192** by the thermal closure of the CPDs **184-186**

Dihydropyrenes **190-192** were obtained by heating the cyclophanedienes **184-186** respectively in refluxing toluene for 8 hrs. The isomers were purified by column chromatography. In its ^1H NMR spectrum, the *trans*-isomer **190** showed peaks at δ 0.22, 2.95 and 4.04 for the protons 18, 20 and 22, respectively, (shown below) whereas the corresponding protons in the *cis*-isomer **192** appeared at δ -0.02, 3.90 and 4.53. The *trans* orientation of the double bond in **190** was confirmed by the coupling constant of 15 Hz.

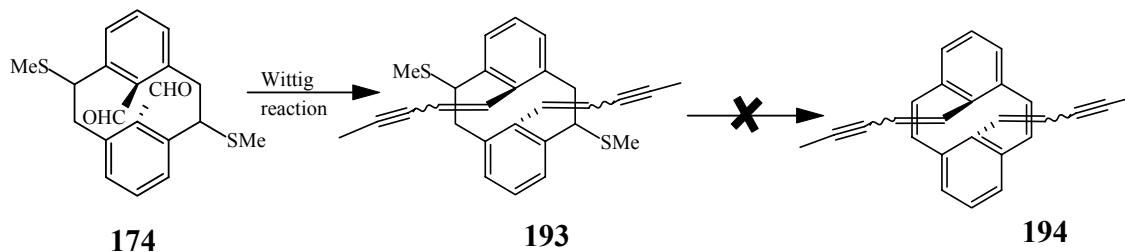


In the unsymmetrical isomer **191**, chemical shifts of the protons from the *cis* and *trans* internal substituent were comparable to those of **192** and **190**, respectively.

2.6.2 Extending the conjugation with a triple bond

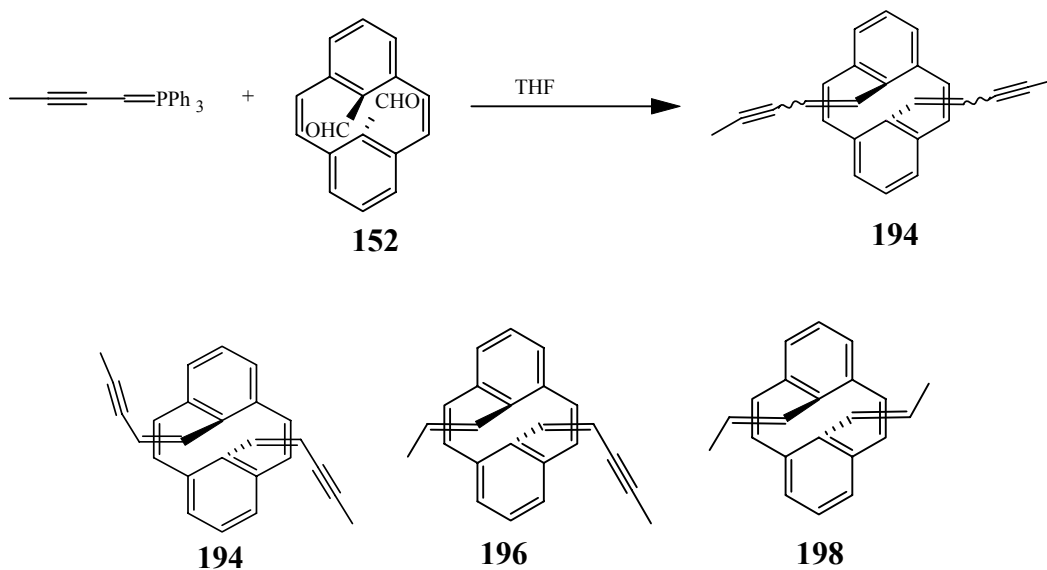
Pentenynyl CPD **194** represents an example of elongation of the internal olefin by a triple bond. The terminal methyl groups were chosen to avoid unfavorable Glaser coupling.⁷⁰ The Glaser coupling is the homocoupling of terminal alkynes to form diynes in the presence of a catalyst and an oxidant. Wittig reaction of **174** delivered the thiomethylcyclophanes **193** in moderate yield but subsequent Hoffmann elimination failed to yield the cyclophanediene **194** (Scheme 2.52). Pyrene **112** was obtained as the product of the reaction.

Scheme 2.52 Attempted synthesis of pentenynyl CPD by the Wittig reaction-Hoffmann elimination sequence



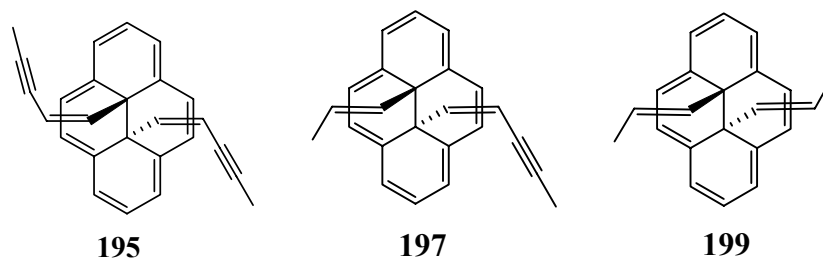
However the Wittig reaction of diformyl **152** (Scheme 2.53) gave the desired product **194** along with two unexpected side products **196** and **198**. Attempts to purify these three products using column chromatography were unsuccessful.

Scheme 2.53 Synthesis of 194 by Wittig reaction of 152



The ^1H NMR spectrum of the cyclophanedienes mixture (**194**, **196** and **198**) was quite complex and it failed to locate the propenyl substituent because of its resemblance with the pentenynyl substituent in terms of number of peaks and associated chemical shifts. However, the ^{13}C NMR spectrum pointed out the absence of the sp carbon atoms

and this was supported by the mass spectrum peaks at m/z 308 and 284 corresponding to **196** and **198**, respectively. The cyclophanediene mixture was heated in toluene overnight to give a mixture of dihydropyrenes.

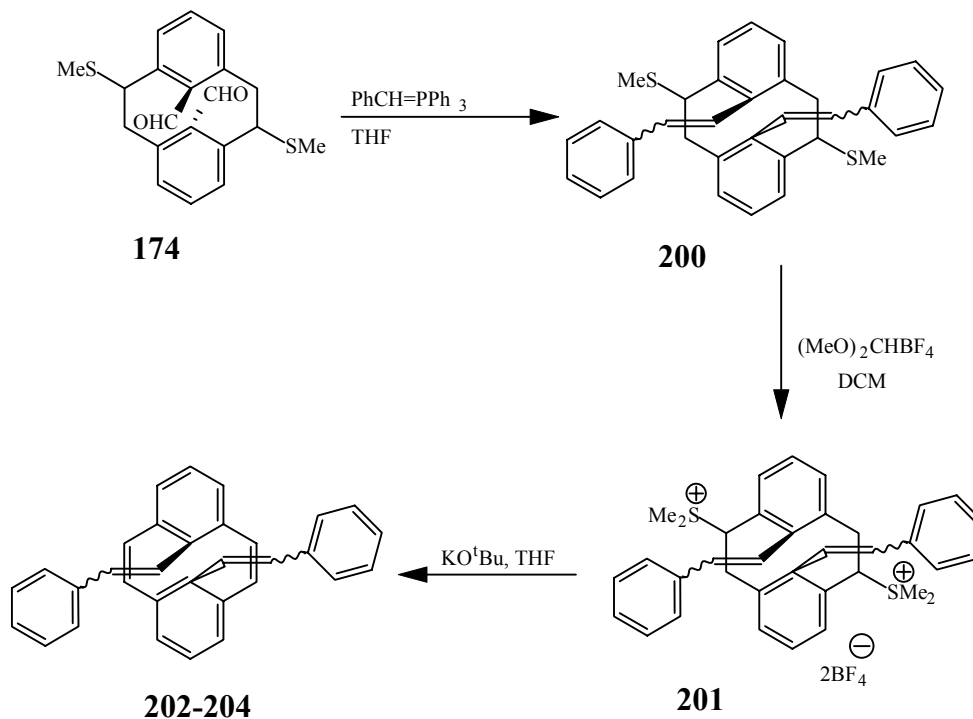


Dihydropyrenes **195**, **197** and **199**, quite contrary to the CPDs, could be separated by column chromatography and showed fairly distinct ^1H NMR chemical shifts for the methyl protons from the propenyl and the pentenynyl groups. The signal of the methyl protons in **199** and **195** were found at δ 0.1 and 1.94 respectively. The upfield chemical shift of the methyl protons in **199** along with a coupling constant of 6.0 Hz with the neighboring alkene proton indicated the presence of the propenyl substituent, which was further corroborated by the absence of the resonances for the sp carbons in the ^{13}C NMR spectrum. A coupling constant of 15.5 Hz indicated the *trans* geometry of the propenyl substituent in **197** and **199**. We are not clear how the *trans* propenyl group was incorporated.

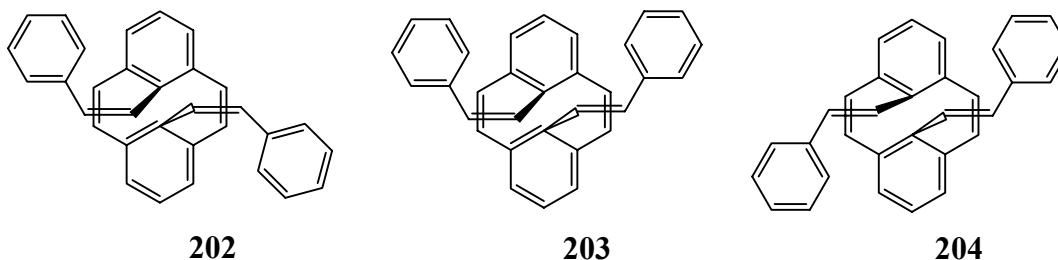
2.6.3 Distyryl CPDs 202-204, an example of extended conjugation by phenyl rings

Mixed isomers **174** on treatment with an ylide derived from benzyltriphenylphosphonium bromide gave 20% of the thiomethylcyclophanes **200** in an unoptimized reaction (Scheme 2.54). The styryl protons of **200** appeared at δ 5.0-7.5 in the ^1H NMR spectrum. The *cis*-styryl group because of its close proximity in space shielded the thiomethyl protons to δ 1.4 when compared with the *anti* analogue at δ 2.3.

Scheme 2.54 Synthesis of CPDs with internal styryl groups 202-204

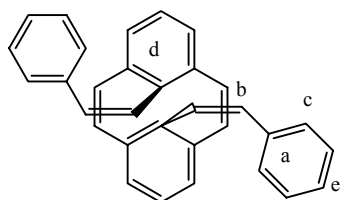


The thiomethylcyclophane **200** on treatment with Borch reagent gave the sulfonium salt **201** which on subsequent elimination provided a mixture of the cyclophanedienes, **202-204** in 80% overall yield. The isomers were separated by column chromatography.

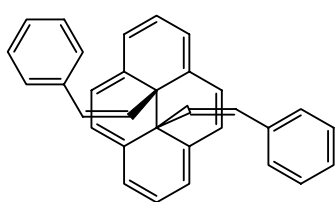
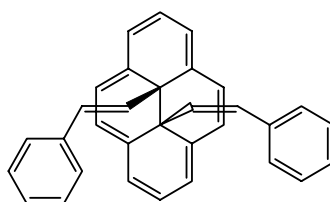
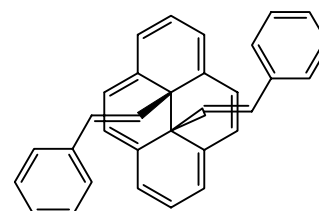


All *cis*-isomer **202** eluted first from the column and showed the CPD bridge alkene protons (proton b) at δ 5.84 in the ^1H NMR spectrum, slightly upfield compared to

δ 6.5 for most of the *anti*-CPDs. PC Model⁷¹ has shown a close spatial relationship of the phenyl ring “a” to the bridge alkene protons “b” which results in mutual shielding and is shown by the chemical shift of protons “c” at δ 6.78, slightly upfield compared to protons “e” at δ 7.05. The structure was further supported by the molecular ion peak at m/z 408 in the mass spectrum and was finally confirmed by X-ray structure determination.

**202**

The styryl aromatic protons in the all *trans*-isomer **204** appeared at δ 7.22-7.20 and the bridge alkene CPD protons were a singlet at δ 6.48.

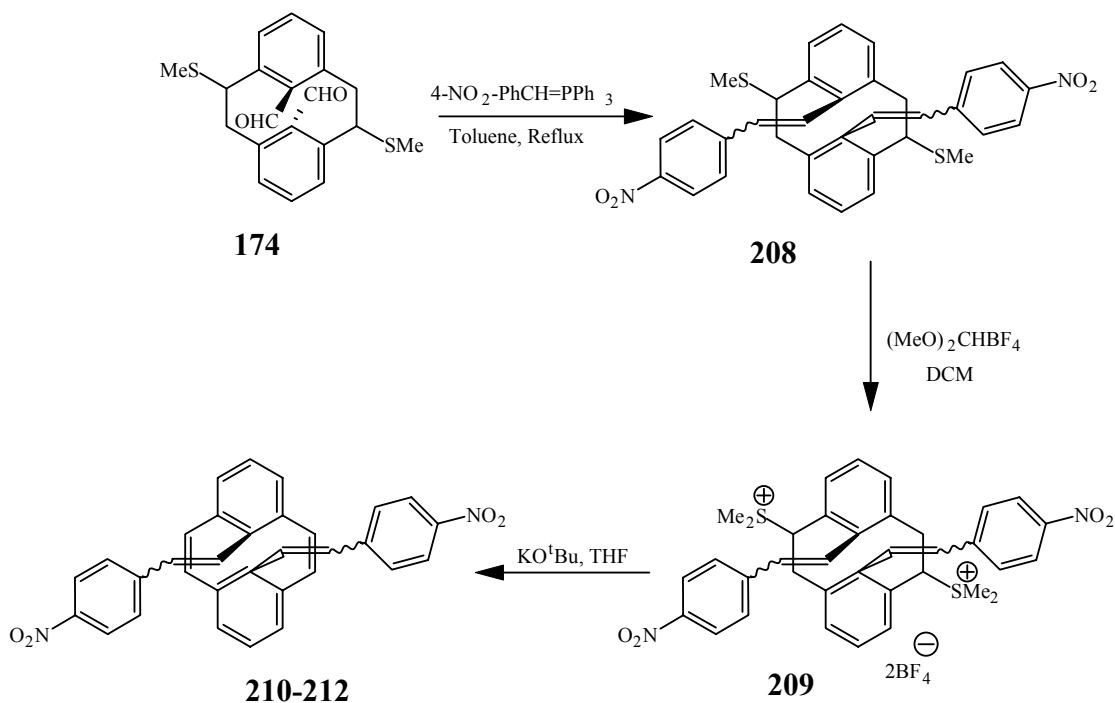
**205****206****207**

The cyclophanediene **202** when heated at 100 °C for 12 hrs yielded the orange dihydropyrene **205**, mp 152-154 °C. The *cis* geometry of the styryl group was confirmed by a coupling constant of 12.6 Hz between olefin protons at δ 4.21 and 0.28 in the ¹H NMR spectrum. Phenyl protons of the styryl ring appeared at δ 7.15 (*p*), 7.03 (*m*) and 6.02 (*o*). Styryl DHPs **206** and **207** were also obtained by the thermal closure of their corresponding CPDs and no *cis-trans* isomerization of the styryl double bond was observed.

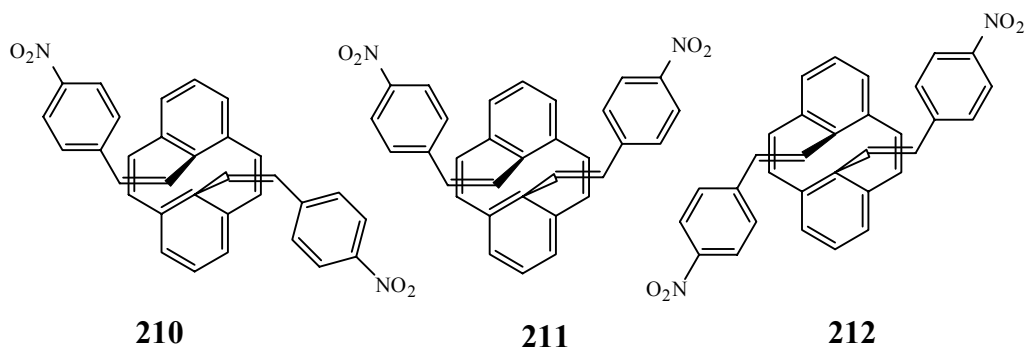
2.6.4 Synthesis of nitro-styryl CPDs 210-212, an exploration of the electronic effects on the thermal back reaction

Wittig reaction of **174** with 4-nitrobenzyl triphenylphosphonium bromide failed to give the desired product **208** when *t*-BuOK was used as the base in THF at room temperature. On addition of base to 4-nitrobenzyl triphenylphosphonium bromide, the solution instantly turned dark purple red which indicated the generation of the anion (ylide). However this anion failed to react with **174** probably because of the stability of the anion by delocalization onto the nitro group. Other bases such as K_2CO_3 in refluxing methanol or NaH in refluxing THF also failed to afford the desired product. Finally, a successful Wittig reaction was carried out in refluxing toluene with *t*-BuOK as base (Scheme 2.55).

Scheme 2.55 Synthesis of nitro-styryl CPDs 210-212



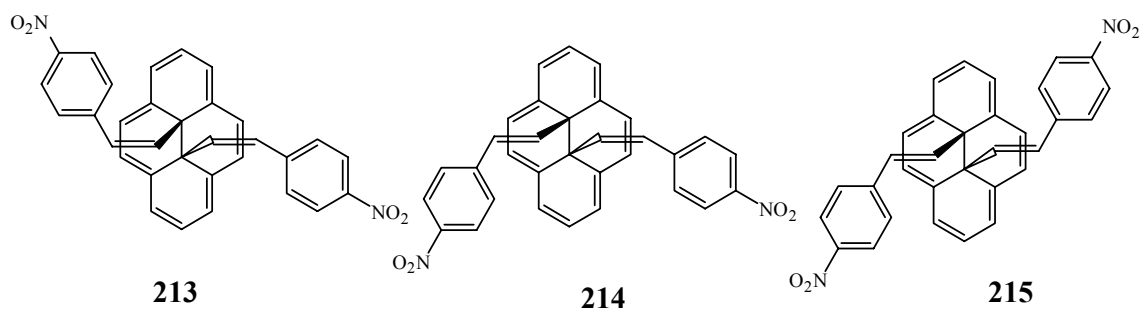
The high temperature Wittig reaction was expected to generate exclusively *trans* double bonds.⁷² However the ¹H NMR analysis of **208** indicated almost 1:1 ratio of *cis* and *trans* double bonds. Protons *ortho* to the nitro group were located as doublets at δ 7.8-8.2 in the ¹H NMR spectrum. The mass spectrum of **208** gave the correct molecular mass of m/z 594.



S-methylation of **208** quantitatively afforded the sulfonium salt **209** which on subsequent Hoffmann elimination gave a 1:2:1 mixture of the cyclophanedienes **210**, **211** and **212** respectively. Column chromatography failed to separate the isomers efficiently. Since nitro-styryl CPDs **210** and **212** were almost insoluble in most common organic solvents except DCM so partial separation by column chromatography followed by washing with toluene or chloroform afforded the cyclophanedienes in reasonable purity.

The CPD alkene bridge protons were shielded to δ 5.84 in the ¹H NMR spectrum of **210**, characteristic of *cis*-styryl CPDs. Doublets at δ 7.94 and 6.91 indicated a *para*-disubstituted phenyl ring which was further supported by a peak at 855 cm^{-1} in the IR spectrum. The expected molecular mass at m/z 498 in the mass spectrum along with two successive losses of 148 mass units confirmed the nitro-styryl internal groups in **210**. Protons from the nitro-styryl ring in the *trans*-isomer **212** appeared as doublets at δ 8.17

and 7.35 in the ^1H NMR spectrum. Almost every proton and carbon in the isomers could be assigned.

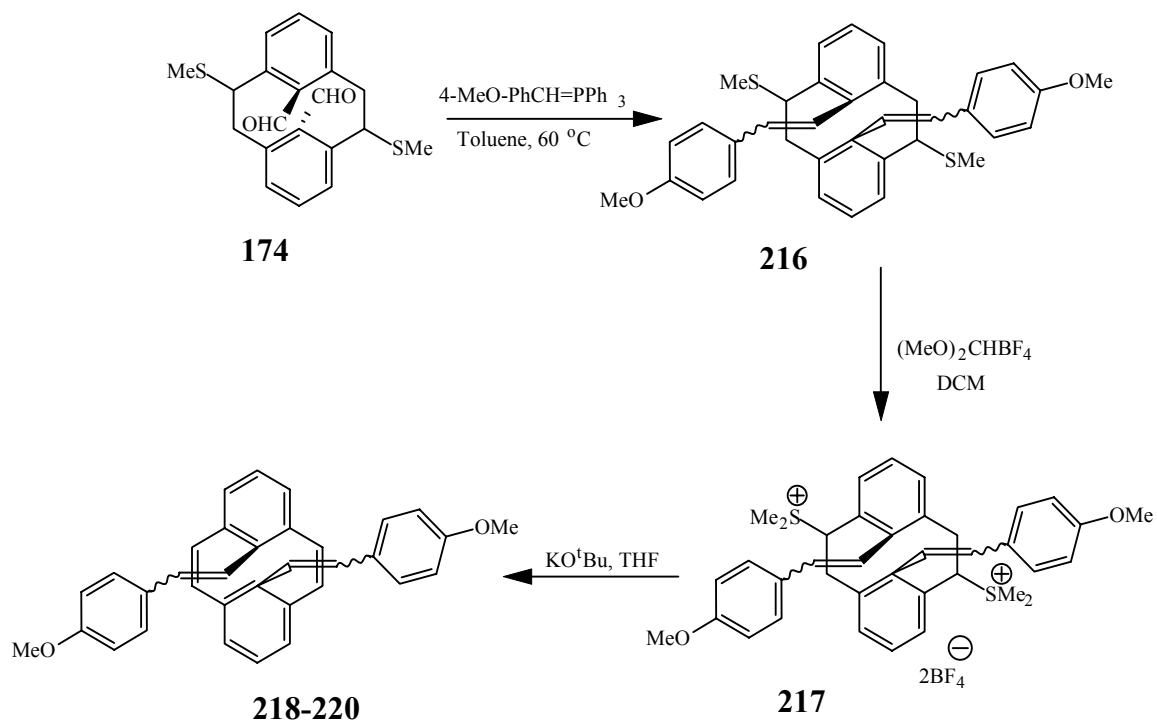


The dihydropyrenes **213-215** were obtained by the thermal closure of their corresponding cyclophanedienes. The all *trans*-isomer, **215** was insoluble in commonly available organic solvents which resulted in its failure to yield a useful ^{13}C NMR spectrum. For example, a high temperature ^{13}C NMR spectrum with scans as high as 40000 failed to show quaternary carbons at all. The other isomers **213** and **214** could be characterized completely even though the *cis*-isomer **213** had poor solubility in most organic solvents.

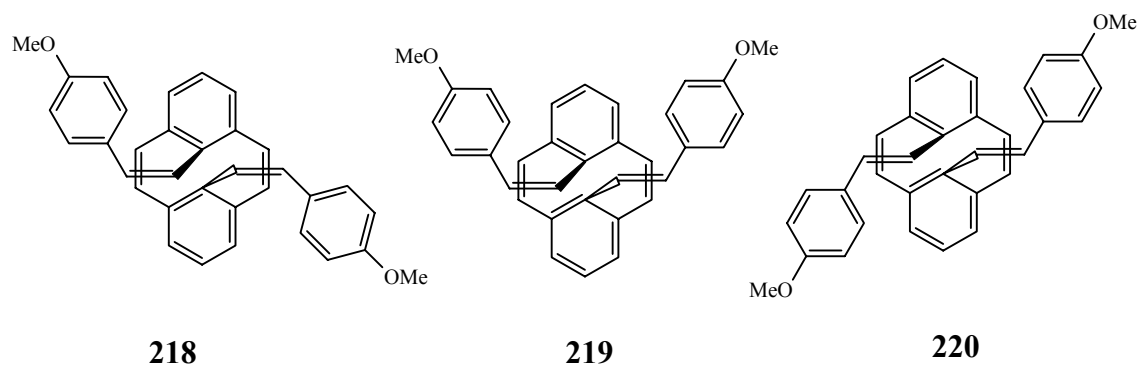
2.6.5 *para*-Methoxy-styryl CPDs **218-220**, an example of an electron rich internal olefin

The nitro-substituted styryl cyclophanedienes **210-212** showed higher thermal closing rates when compared with the non-substituted styryl CPDs **202-204**. Based on these results, it was projected that an electron donating substituent such as methoxy at the *para*-positions of the styryl rings would decelerate the thermal return. Cyclophanedienes with *para*-methoxy-styryl internal substituents were synthesized as shown in Scheme 2.56.

Scheme 2.56 Synthesis of *p*-methoxy-styryl CPDs **218-220**

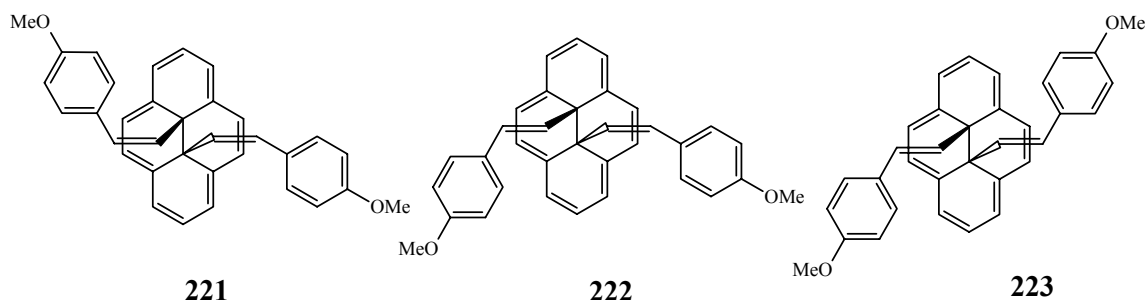


The diformyl MeS-cyclophanes **174** on Wittig reaction in toluene at $60\text{ }^\circ\text{C}$ gave 50% yield of the *p*-methoxy-styrylcyclophanes **216**. Appearance of singlets at δ 3.9-3.6 in the ^1H NMR spectrum indicated the formation of the desired product. S-Methylation of **216** and the subsequent elimination on the sulfonium salt generated the *p*-methoxy-styryl CPDs **218-220**.



The isomeric cyclophanedienes could be purified by column chromatography and showed distinct peaks for methoxy groups in the ^1H and ^{13}C NMR spectra. The protons of the methoxy groups in **218** appeared at δ 3.74 and, the methyl carbons at δ 55.34 in the ^1H and ^{13}C NMR spectra, respectively, slightly shielded when compared with the *trans*-isomer **220** (δ 3.81 and 55.49). In the unsymmetrical isomer **219**, the protons of the methoxy substituents were found at δ 3.82 and 3.75 in the ^1H NMR spectrum and the corresponding carbons at δ 55.47 and 55.33 in the ^{13}C NMR spectrum. The presence of the methoxy groups was further confirmed by the C-O stretches at 1252 and 1032 cm^{-1} in the IR spectrum.

Cyclophanedienes **218-220** were thermally isomerized to the dihydropyrenes **221-223** at rates slower than those of non substituted styryl CPDs **202-204**, as expected, with no observable *cis-trans* isomerization of the styryl double bond.

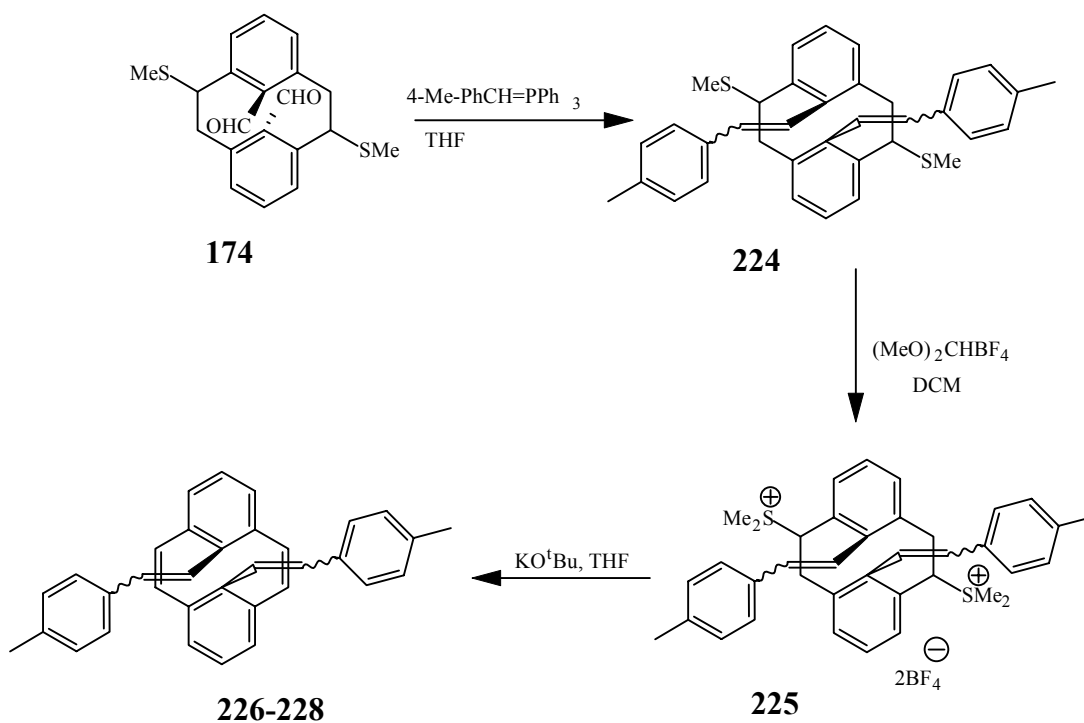


The methoxy protons were also quite distinct in different isomers **221-223** besides the general differences in the DHP protons. The methoxy protons and carbons in the all *cis*-isomer **221** appeared at δ 3.83 and 55.74, respectively, compared to δ 3.51 and 55.49 for the all *trans* isomer **223**.

2.6.6 Synthesis of *para*-methyl-styryl CPDs 226-228

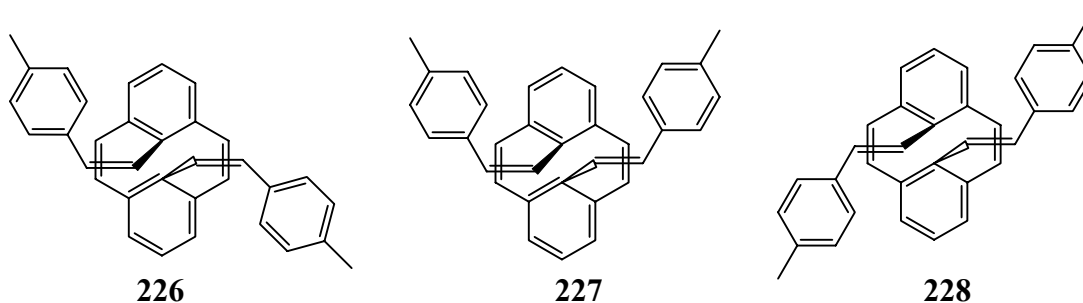
A comparison of the nitro- and methoxy-substituted cyclophanedienes revealed that an electron withdrawing substituent on the phenyl ring of internal styryl group has accelerated the thermal closure whereas an electron donating group has slowed it down. We were interested in studying the behavior of the more electronically neutral methyl substituent at the *para*-position of styryl group.

Scheme 2.57 Synthesis of *p*-methyl-styryl CPDs 226-228



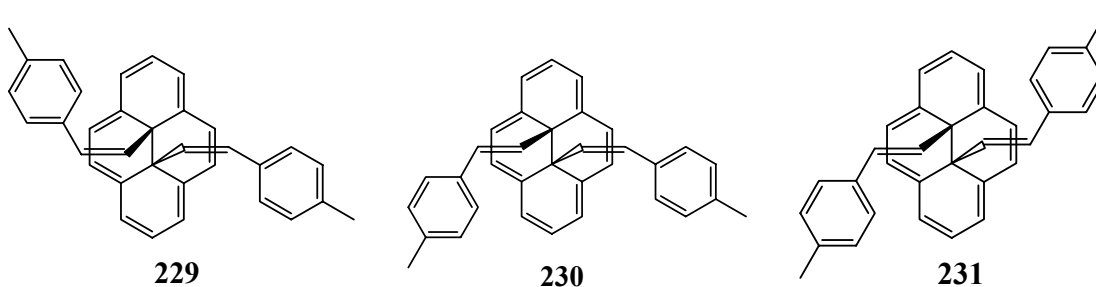
Wittig reaction of **174** in THF at room temperature afforded the thiomethylcyclophanes **224** in >57% yield (Scheme 2.57). The desired product **224** was identified by the ¹H NMR peaks at δ 2.4-2.0 corresponding to the benzylic protons. Methylation of **224** with Borch reagent gave **225** and the subsequent Hoffmann

elimination gave a 5:2:1 mixture of cyclophanedienes **226:227:228** in 38% combined yield. The isomeric CPDs were purified by column chromatography over silica gel.



The all *cis*-isomer **226**, eluted first from the column, was the major product of the reaction and was easily identified by its ^1H NMR spectrum. The protons of the methyl group in **226** appeared at δ 2.25 and, the corresponding carbon at 21.36 in the ^1H and ^{13}C NMR spectra respectively, slightly shielded when compared with the *trans*-isomer **228** (δ 2.34 and 21.49). In the unsymmetrical isomer **227**, protons of the methyl substituents were found at δ 2.32 and 2.24 in the ^1H NMR spectrum and, the corresponding carbons at δ 21.48 and 21.38 in the ^{13}C NMR spectrum.

Cyclophanedienes **226-228** were thermally isomerized to the dihydropyrenes **229-231** at rates quite comparable to those of methoxy CPDs **218-220**.



The methyl protons were also quite distinct in different isomers besides the general differences in the DHP protons. The methyl protons and carbons in the all *cis*-

isomer **229** appeared at δ 2.34 and 21.47 respectively compared to 1.99 and 21.04 for the all *trans*-isomer **231**.

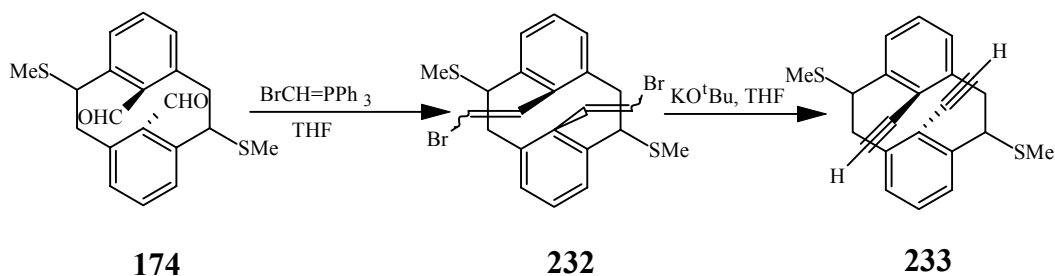
2.7 Alkynes as the internal substituents.

2.7.1 Synthesis of diethynyl CPD **235**

Internal olefin substituted cyclophanedienes have shown slow rates for the unwanted thermal return. Moreover, dihydropyrenes are stable and show no tendency towards migration which makes them excellent candidates as photoswitches. We became interested in introducing alkyne substituents at both internal positions. A cyclophanediene with one internal alkyne substituent, **138** has already been described but it was postulated that a cyclophanediene with two internal alkyne substituents, for example **235** or **140** would behave quite differently and this was based on the comparison of the behavior of pairs **127/128** and **85/86**.

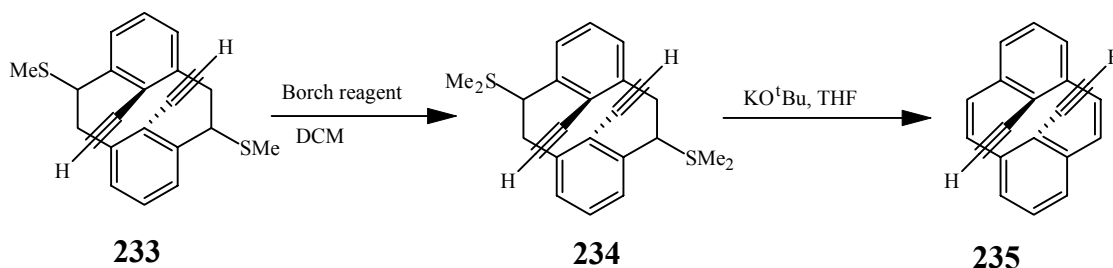
The thiomethylcyclophane **233**, required for the synthesis of the CPD **235** could be generated from the diformyl MeS-cyclophane **174** in one pot (Scheme 2.58). Wittig reaction of **174** with the ylide afforded **232** which eliminated HBr in-situ to give the desired products **233**.

Scheme 2.58 Synthesis of diethynyl-thiomethylcyclophane **233**



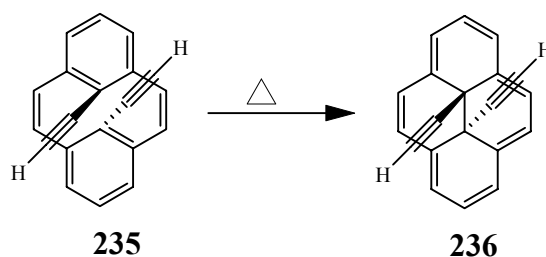
The ethynyl group in **233** was identified by peaks at δ 2.3 and δ 86.94 in the ^1H and ^{13}C NMR spectra, respectively. Thiomethylcyclophanes **233** when treated with dimethoxycarbonium tetrafluoroborate gave 63% of the sulfonium salt mixture **234** which on Hoffmann elimination using *t*-BuOK as base in THF afforded the desired product **235** in variable yields, the origin of what will be discussed in the next section. (Scheme 2.59).

Scheme 2.59 Synthesis of the diethynyl CPD **235**



Diethynyl CPD **235** was purified by column chromatography and could easily be identified by its ^1H NMR spectrum. The ethynyl protons appeared at δ 2.84. The ethynyl group was further supported by the ^{13}C NMR peaks at δ 83.39 and 81.84 and finally confirmed by the IR stretches at 3293 and 2578 cm^{-1} . An X-ray analysis established the structure **235**.

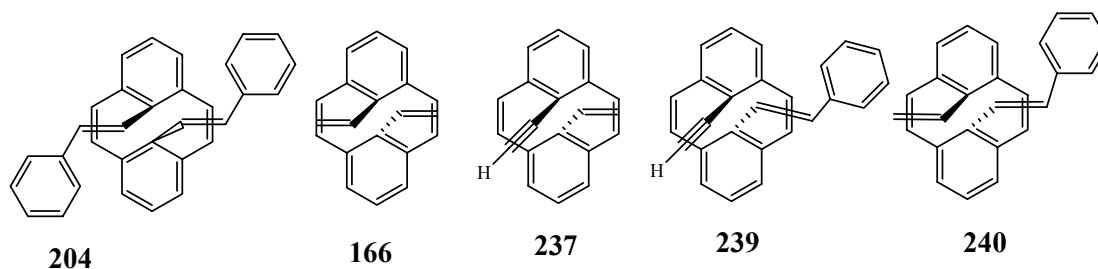
Scheme 2.60 Thermal isomerization of diethynyl CPD **235** into DHP **236**



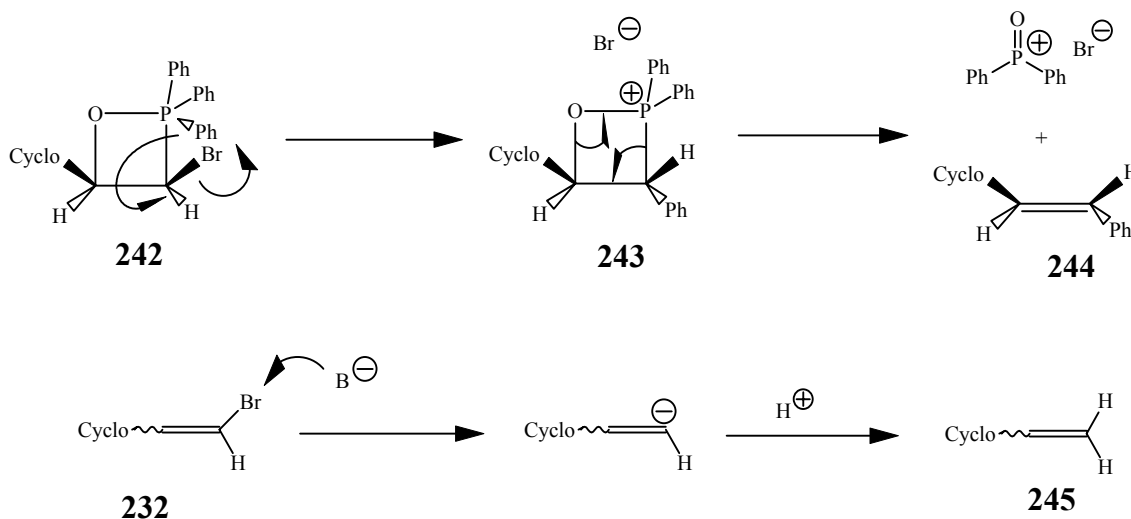
The dihydropyrene **236** was obtained by thermal isomerization of **235** (Scheme 2.60) and showed its internal ethynyl protons shielded to δ -0.09 in the ^1H NMR spectrum. The ethynyl carbons also appeared highly shielded at δ 65.00 and 75.36 in the ^{13}C NMR spectrum. The alkyne C-H stretch at 3264 cm^{-1} confirmed the ethynyl group. Mass spectrometry gave the correct molecular mass of m/z 252 and the structure was finally established by X-ray analysis.

2.7.1.1 Unexpected products from Wittig reaction

It has already been stated that the CPD **235** was obtained in variable yields. The side products of the reaction involved one or more of the following cyclophanedienes. Divinyl CPD **166** was the most common side product. CPDs **166** and **204** (*trans*-distyryl) were identified by comparison of spectral data. The cyclophanedienes **237** and **240** were purified and fully characterized while structure was tentatively assigned to **239**. A large excess of base and high temperature were key factors in the formation of the side products.



Scheme 2.61 Mechanism of vinyl and styryl incorporation during the Wittig reaction



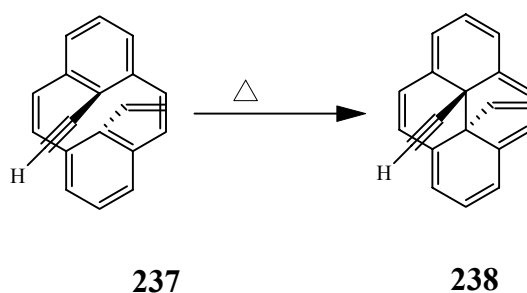
A plausible mechanism for the formation of the vinyl and styryl cyclophanedienes is shown in Scheme 2.61. The Wittig reaction of the aldehyde **174** and the ylide generates betaine **242**. A phenyl group attached to the phosphorous atom undergoes a 1,2 migration and expels the bromine atom in an S_N2 fashion and generates **243** which upon elimination generates the *trans*-styryl olefin **244**. The phenyl group attacks the bromide *anti* to the cyclophane (cyclo) probably because of steric reasons which results in the *trans* double bond in the resulting olefin.

The vinyl group is generated probably through the bromide abstraction-protonation sequence shown in Scheme 2.61. Although a mixture of *t*-BuOK/ DMSO⁷³ has been shown to abstract a vinylic bromide, we are not certain how *t*-BuOK itself abstracts the bromide.

A ¹H NMR signal at δ 2.80 indicated the presence of an ethynyl group in **237** which was supported by the ¹³C chemical shifts at δ 82.28 and 81.96. The ethynyl group

was confirmed by the IR stretch at 3303 cm^{-1} . Protons from the vinyl group were observed as three doublets of doublets at δ 6.32, 5.45 and 4.80 in the ^1H NMR spectrum. The CPD alkene bridge protons were found as an AB quartets at δ 6.55-6.33 with a coupling constant of 11.4 Hz. Mass spectrometry confirmed the formula by the molecular ion peak at m/z 254.

Scheme 2.62 Thermal isomerization of the CPD 237 to DHP 238

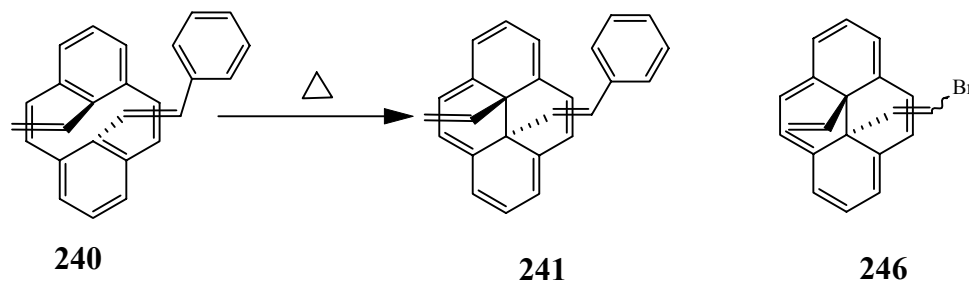


The internal ethynyl and vinyl group were quite distinct in the dihydropyrene **238** and could easily be accounted for. The proton of ethynyl group expressed itself as a singlet in the ^1H NMR spectrum at δ -0.14. In the ^{13}C NMR spectrum, signals at δ 63.44 and 77.23 further supported the presence of the ethynyl group, which was finally corroborated by a band at 3267 cm^{-1} in the IR spectrum. A molecular ion at m/z 254 in the mass spectrum confirmed the molecular formula.

Vinyl-styryl CPD **240** was initially considered to be **246** and this conclusion was based on the analysis of the 300 MHz ^1H NMR spectrum. Phenyl protons at δ 7.24 were masked by the residual CDCl_3 peak. However, phenyl protons became more obvious in the 500 MHz NMR spectrum. An AB quartet at δ 6.43 with 15.4 Hz coupling constant indicated the *trans* orientation of the double bond. Mass spectrometry confirmed the

molecular formula by a peak at m/z 332. The loss of the styryl and ethenyl groups was suggested by peaks at $[M-103]^+$ and $[M-130]^+$ in the mass spectrum.

Scheme 2.63 Thermal isomerization of the CPD 240 to the DHP 241

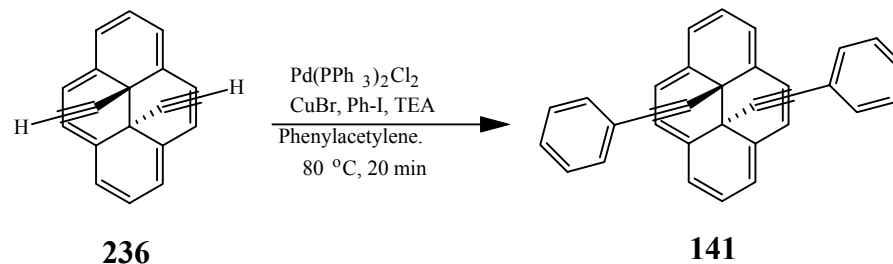


The vinyl and styryl groups were more obvious in the dihydropyrene **241** (Scheme 2.63). The olefin protons at δ 0.84 and 3.21 showed a coupling constant of 16 Hz, confirming the *trans*-styryl group.

2.7.2 Diphenylethynyl DHP

The high stability of switch pair **235/236** refreshed our interest in the bis(phenylethynyl) DHP **141**. We realized that **141** might be synthesized in one step from **236** by Sonogashira coupling with phenyl iodide.

Scheme 2.64 Sonogashira coupling to synthesize 141



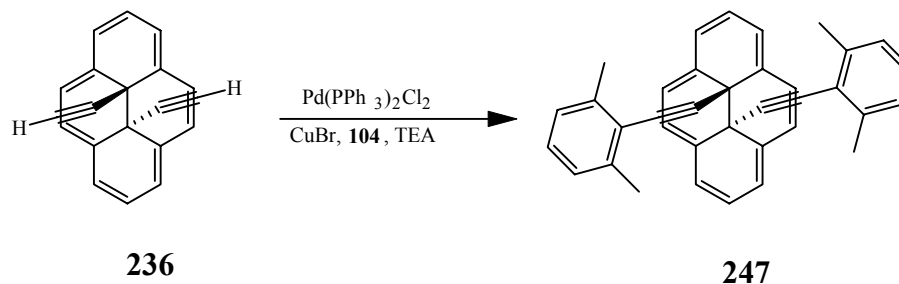
The Sonogashira coupling of **236** with iodobenzene in refluxing TEA using $\text{Pd}(\text{PPh}_3)_2\text{Cl}_2$ as a catalyst failed to furnish the desired product **141**. Variation of the

reaction conditions including temperature, catalyst loading or concentration gave either the starting material or the pyrene **112**. It was noticed that a diluted reaction at higher temperature gave pyrene instantly. Moreover, high catalyst loading was detrimental as well.

In the Sonogashira coupling⁷⁴, acetylene reacts with the Pd⁺² catalyst and forms an acetylide complex which undergoes reductive elimination of the bis-acetylene to generate an active Pd(0) catalyst. We thought that this Pd(0) generation step is the main source of pyrene formation under high catalyst loading conditions. If Pd(0) could be generated by some other acetylene such as phenylacetylene, then the Sonogashira coupling of **236** with phenyl iodide would yield the desired product **141**.

Thus, Pd(0) was generated by reacting the Pd⁺² catalyst with phenylacetylene at 80 °C in TEA in the presence of iodobenzene. This Pd(0), on reaction with **236** afforded the desired product in ~ 70% yield in less than 20 minutes (Scheme 2.64). A 15% yield of the pyrene **112** was also obtained. Phenylethynyl DHP **141** was purified by column chromatography. The phenylethynyl group was identified in the ¹H NMR spectrum by peaks at δ 6.06, 6.78 and 6.89 corresponding to *ortho*, *meta* and *para* protons respectively. The ethynyl carbon resonances were found at δ 81.55 and 76.96 in the ¹³C NMR spectrum. DHP **247**, a dimethyl derivative of **141** was also prepared by the Sonogashira coupling of **236** with 2,6-dimethyliodobenzene **104** in 25% yield (Scheme 2.65).

Scheme 2.65 Sonogashira coupling to synthesize 247



2.8 Synthesis of naphthoyl dihydropyrenes

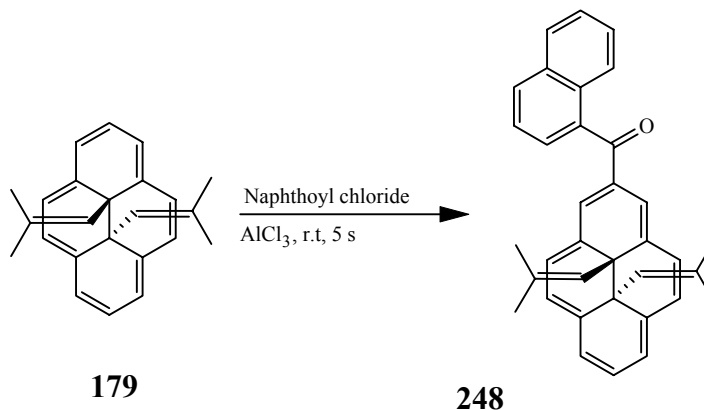
Slow thermal return along with the stability of both isomers render the pair **178/179** as an excellent cyclophanediene/dihydropyrene based photoswitch. However the photoopening of the isobutenyl DHP **179** is relatively slow when compared with the benzo-DHP. It has already been stated that introduction of carbonyl functional groups can accelerate the photoopening reaction of dihydropyrenes. Robinson³⁵ has reported that a naphthoyl substituent at the two position of DHP can accelerate the photoopening reaction up to two orders of magnitude; however it speeds up the thermal return as well.

2.8.1 2-Naphthoyl diisobutenyl DHP 248

Addition of AlCl_3 to the mixture of DHP **179** and naphthoyl chloride afforded the naphthoylated DHP **248** instantly. The desired product could only be isolated in useful yields if the reaction was quenched within 10 seconds of the addition of AlCl_3 (Scheme 2.66). Longer reaction times gave a mixture of at least five or six pyrenes as revealed by fluorescent spots on TLC. The formation of pyrenes could also be visualized by change in color from purple to orange and finally to pale yellow. Column chromatography using alumina failed to separate **248** from a co-eluting pyrene, while use of silica resulted in the

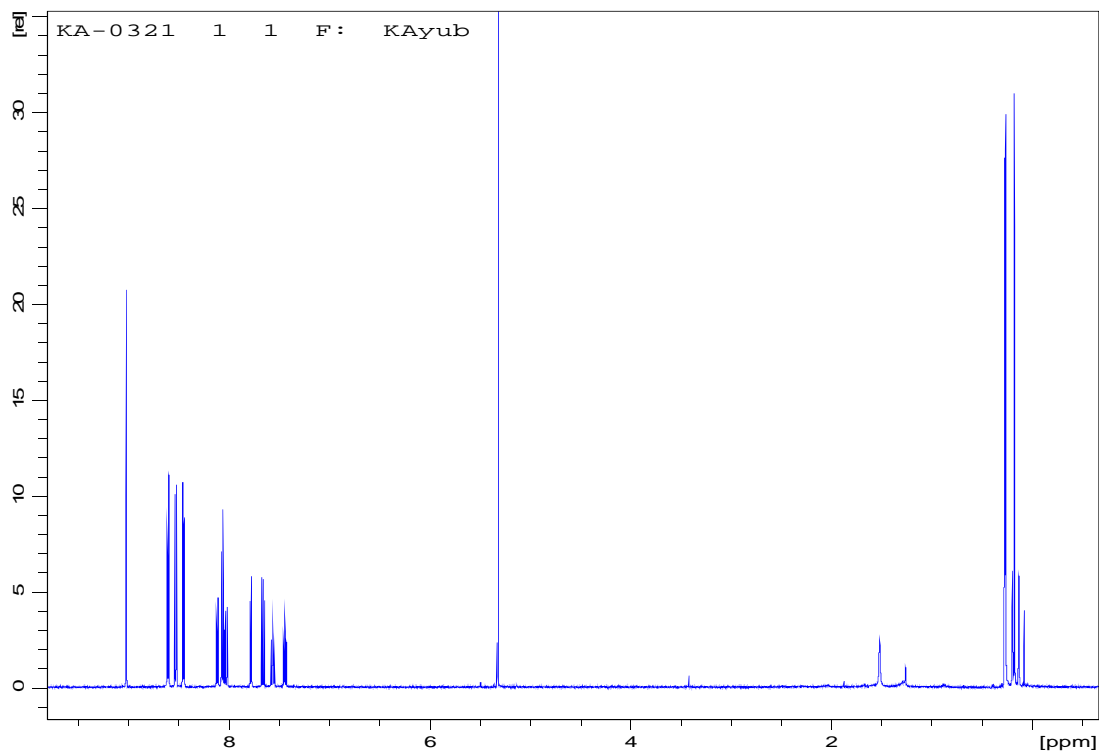
decomposition of the DHP. Recrystallization from methanol yielded nice purple crystals of **248**, mp 179-180 °C.

Scheme 2.66 Friedel-Crafts naphthoylation of diisobutenyl DHP 179

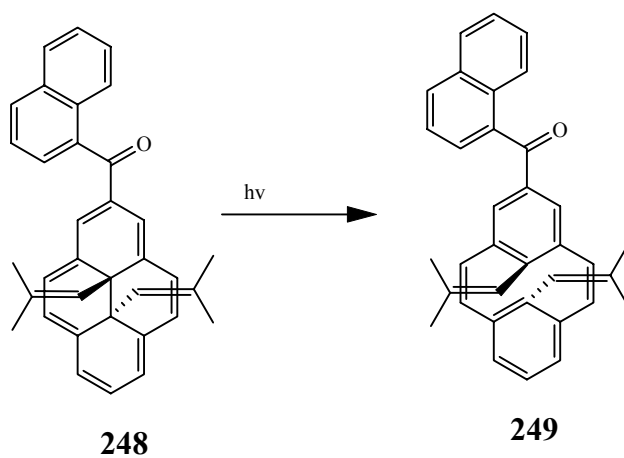


In the ¹H NMR spectrum (Figure 2.3), appearance of five peaks from the DHP protons indicated the naphthoyl group at the two position, an assignment that was further supported by a downfield singlet at δ 9.06 corresponding to H-1,3, the protons *ortho* to the naphthoyl substituent. The position of the naphthoyl group was confirmed by HMBC and HSQC experiments. The naphthoyl protons appeared at δ 8.08-7.46 and were completely assigned. The ¹³C NMR signal at δ 198.30 indicated the carbonyl functional group which was confirmed by the IR stretch at 1637 cm⁻¹, a highly conjugated ketone.

Figure 2.3 ^1H NMR spectrum of naphthoyl DHP **248** in CD_2Cl_2 at 500 MHz



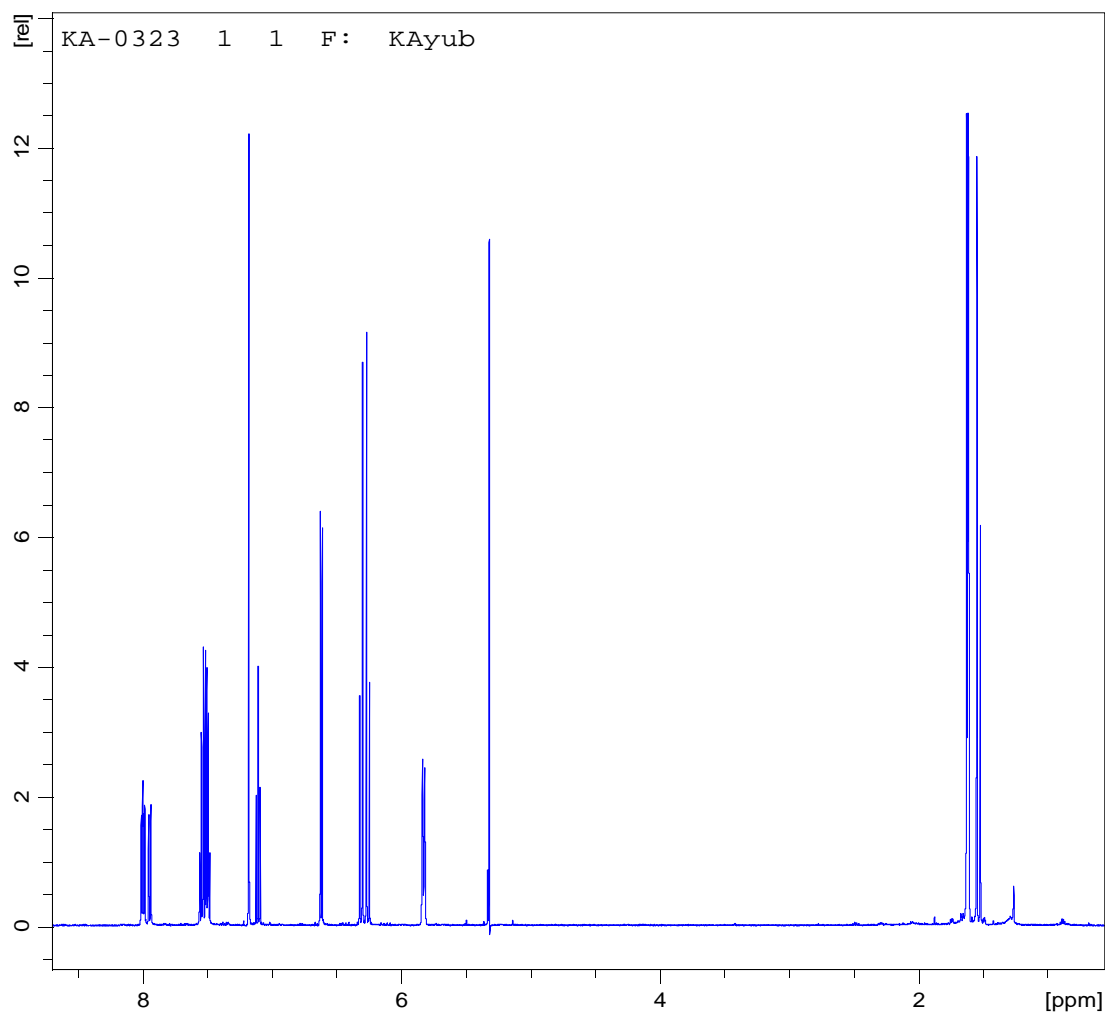
Scheme 2.67 Photoopening of DHP **248**



The naphthoyl dihydrophenanthrene, when irradiated with visible light, opened instantaneously to the cyclophanediene **249** (For details; see chapter 4). The carbonyl carbon was identified by the ^{13}C NMR chemical shift at 196.73 ppm, and the presence of

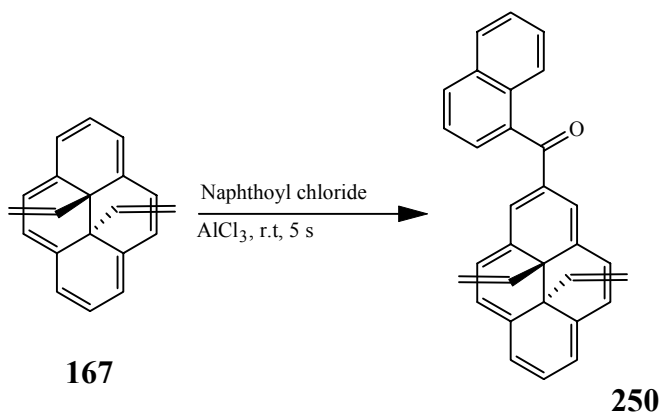
a carbonyl was supported by the IR band at 1653 cm^{-1} . The cyclophanediene had the expected HRMS signal at m/z 466.2292 (calculated 466.2296)

Figure 2.4 ^1H NMR spectrum of naphthoyl CPD 249 in CD_2Cl_2 at 500 MHz



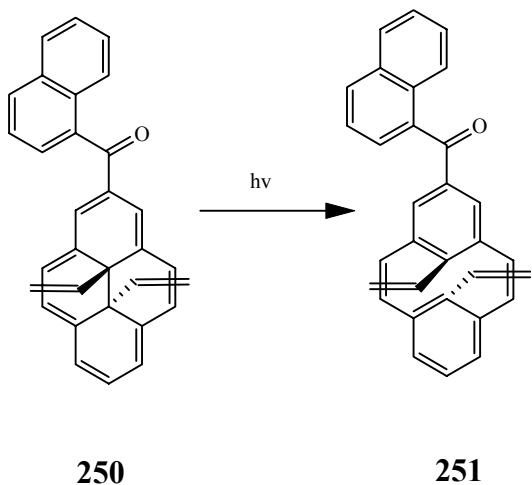
2.8.2 Synthesis of 2-naphthoyldivinyl DHP **250** and its photoopening to the CPD **251**

Scheme 2.68 Synthesis of the naphthoyl DHP **250**



Friedel-Crafts naphthoylation of **167** gave 67% of the dark maroon **250** (Scheme 2.68). Photoirradiation of the DHP afforded the cyclophanediene **251**. All protons and carbons in DHP **250** could be assigned. However in the CPD, naphthoyl protons were not fully assigned because they overlapped with each other.

Scheme 2.69 Visible opening of the DHP **250** to the cyclophanediene



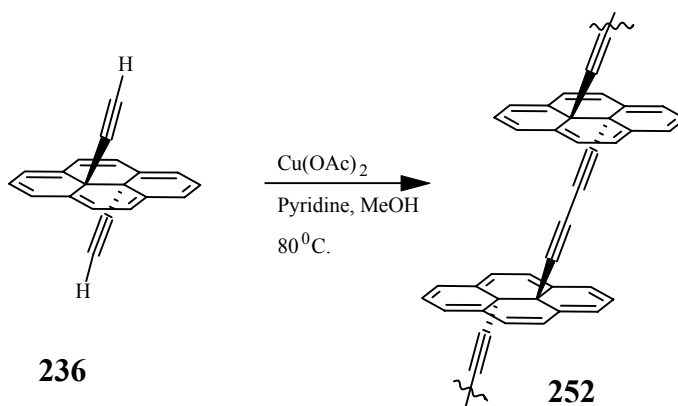
2.9 Synthesis of dimer, oligomers and polymers

Practical applications of photoswitches require that they can be used in the solid phase, either crystalline or in a polymeric phase⁷⁵. Literature^{1,76} suggests that most of the examples involve a photoswitch pendant on a polymer backbone. We became interested in the synthesis of a polymer in which the monomer unit itself is a photoswitch. An example of a DHP based polymer is shown in Scheme 2.70.

2.9.1 Polymerization of the acetylene DHP 236

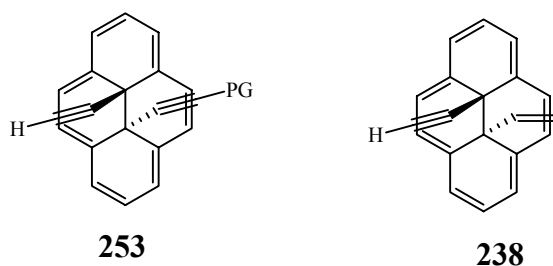
Eglinton⁷⁷ coupling of the diethynyl DHP **236** using $\text{Cu}(\text{OAc})_2$ in pyridine/methanol at 80 °C gave an olive green solid, practically insoluble in all common solvents (Scheme 2.70). Its UV-vis spectrum in dichloromethane showed the characteristic DHP absorption bands at 470 and 385 nm which suggested the formation of the desired product. A ^1H NMR spectrum could not be obtained, because of the insolubility of the polymer and also due to the presence of paramagnetic copper species.

Scheme 2.70 Attempted synthesis of the DHP based polymer

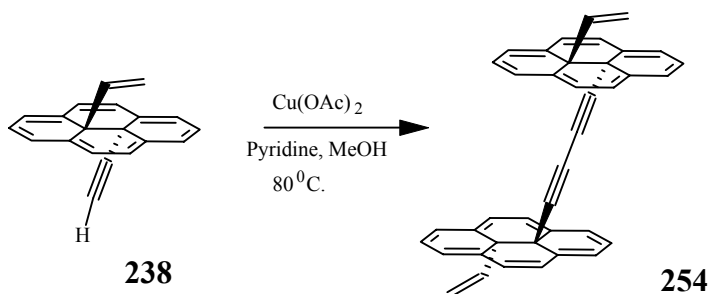


2.9.2 Formation of a dimer by Eglinton coupling

Eglinton coupling of mono protected DHP **253** was expected to give a dimer which would be easy to characterize. We realized that the vinyl-ethynyl DHP **238**, already available to us, can function like a mono-protected DHP **253**.

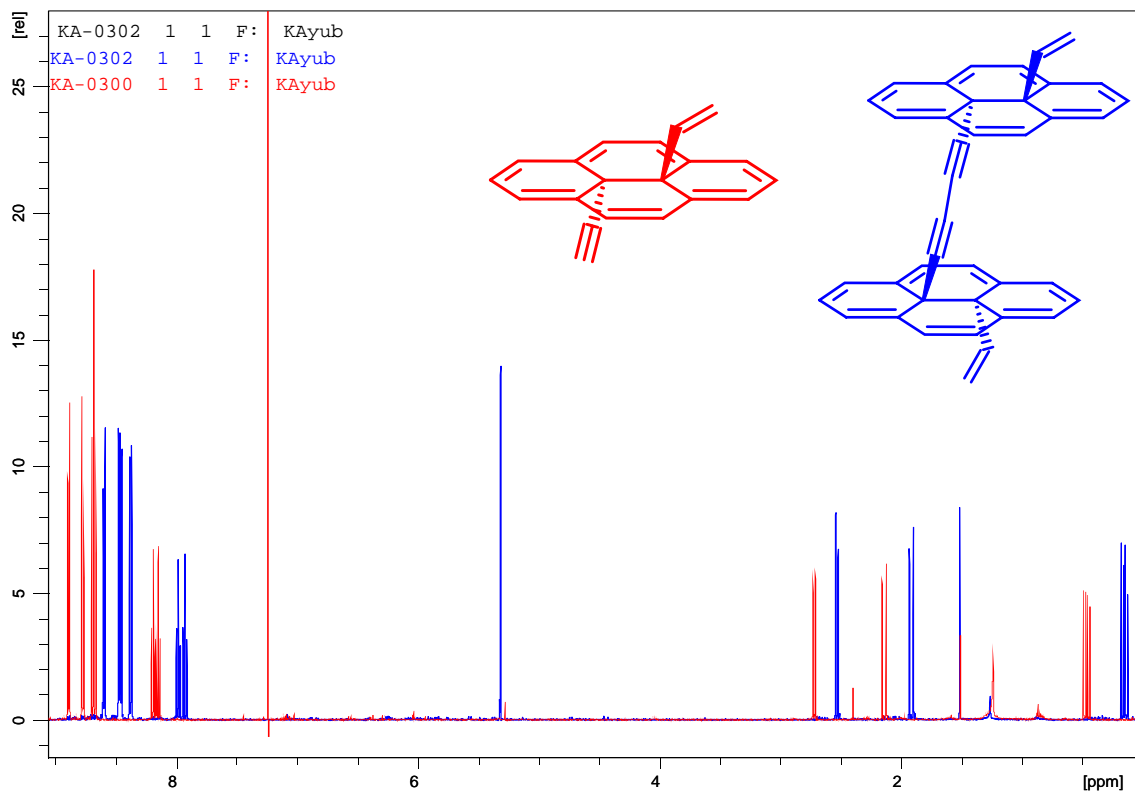


Scheme 2.71 Synthesis of the dimer **254**



The self Eglinton coupling of **238** using Cu(OAc)_2 in pyridine/methanol at 80°C gave >90% yield of the dimer **254** (Scheme 2.71). The product was purified by column chromatography. The disappearance of the ethynyl peak at $\delta -0.14$ in the ^1H NMR spectrum (Figure 2.5) suggested formation of the desired product. All protons in the dimer were shielded by 0.2-0.3 ppm when compared with the monomer. In the ^{13}C NMR spectrum, the ethyl carbons were found at $\delta 70.90$ and 58.95 .

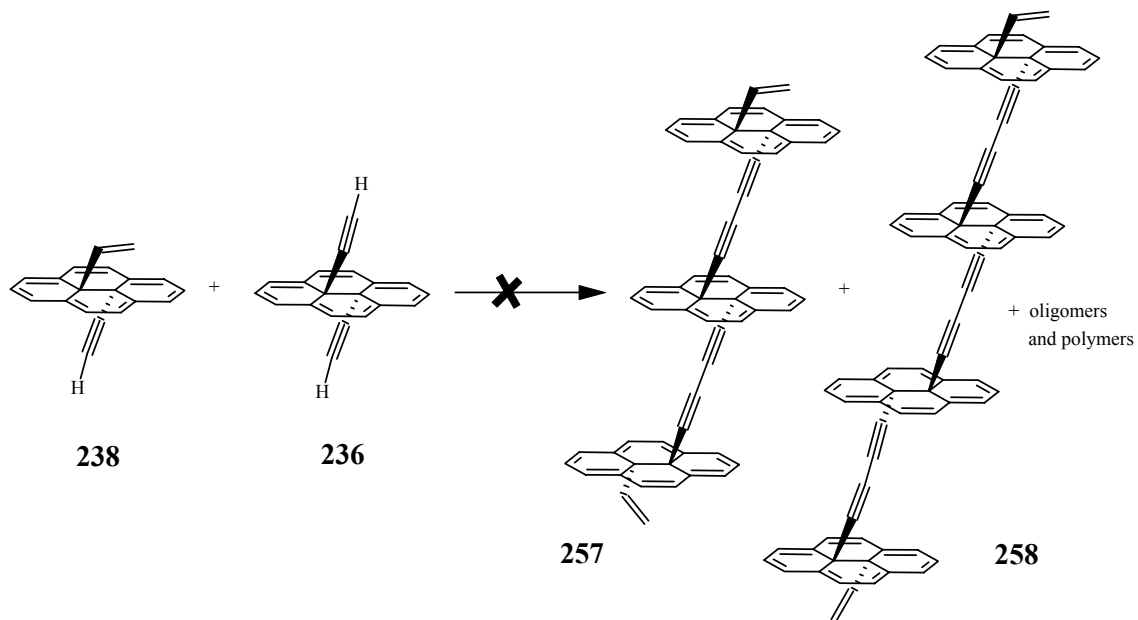
Figure 2.5 ^1H NMR spectra of monomer **238** and dimer **254** in CDCl_3 at 500 MHz



2.9.3 Cross coupling between vinyl-ethynyl DHP **238** and diethynyl DHP **236**

A cross coupling of the dihydropyrenes **238** and **236** in equimolar quantities failed to afford the oligomers **255** and **256**. Analysis of the product mixture indicated unreacted **238**, the dimer **254** and some long chain oligomers/polymers with no unreacted **236** which indicated the low reactivity of **238**. We are not certain how the vinyl substituent in **238** decelerates the Eglinton coupling even though it is electronically and sterically isolated from the ethynyl group.

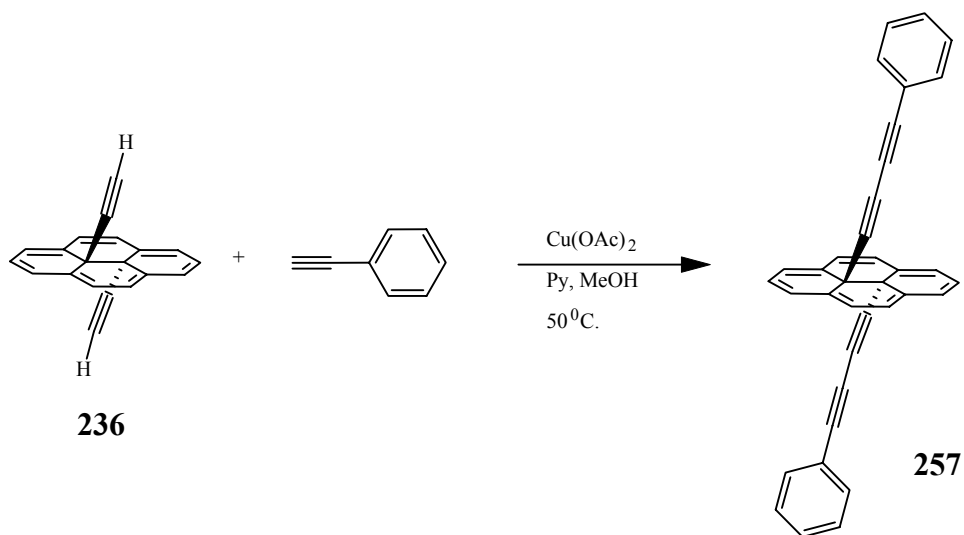
Scheme 2.72 Attempted synthesis of the oligomers



An Eglinton coupling with three to four fold excess of **238** also failed to afford the oligomers in useful yields. TLC indicated two or three spots with R_f values slightly lower than the dimer **254** but these compounds comprised less than 5% of the product mixture. Other modifications such as higher temperature or change of the acetylene to TIPS-acetylene gave pyrene **112**.

2.9.4 Bis Phenbutadienyl DHP 257

Eglinton coupling of diethynyl DHP **236** with a large excess of phenylacetylene afforded a ~30% yield of the diene DHP **257** (Scheme 2.73). The desired product was purified from the starting material and the mono-coupled product by repeated washing with dichloromethane.

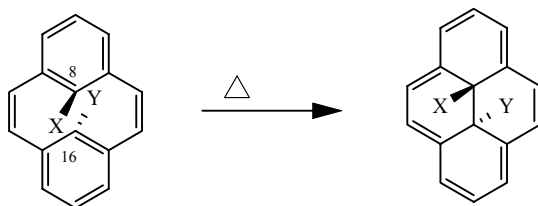
Scheme 2.73 Eglinton coupling of the diethynyl DHP 236 with phenylacetylene

The phenyl protons were found at δ 6.99 (*o*), 7.09 (*m*) and 7.19 (*p*) in the ^1H NMR spectrum. The alkyne carbons appeared in the ^{13}C NMR spectrum at δ 62.15, 72.32, 74.93 and 76.44 but their complete assignment was not possible.

Chapter 3: Thermochemical Reaction

3.1 Electrocyclic reaction

Williams⁴¹ has shown by DFT calculations that the transition state for the unfavorable thermal reaction of cyclophanedienes has biradical character with most of the spin density at the 8-, and 16- internal positions. A change in functional group at these positions was calculated to have a marked influence on the magnitude of the activation barrier for the thermal isomerization, thus a series of cyclophanedienes with different internal substituents were prepared as outlined in Chapter 2. A schematic representation of the thermal reaction is given below.



The thermal reaction of the cyclophanedienes was monitored by ¹H NMR spectroscopy. Diformyl CPD **152** and *cis*-dipropenyl CPD **162** were studied by variable temperature (VT) NMR spectroscopy. For other CPDs except **85**, as a general procedure, an NMR sample was held at the experiment temperature for the desired time interval, immersed in ice-water to quench the thermal reaction, and its ¹H NMR spectrum was then taken as quickly as possible. Dicyano CPD **85**, practically insoluble in all useful organic solvents, was studied in the solid phase. Six NMR samples containing ~2 mg each were held at the reaction temperature, taken out one by one at desired intervals, dissolved in CDCl₃ and then the ¹H NMR spectrum was obtained. The NMR samples were wrapped in aluminum foil in order to prevent the photochemical reaction.

Corresponding hydrogens in the cyclophanediene and dihydropyrene were chosen for integration purposes, except in the cases of CPDs **85** (dicyano), **127** (cyano-methyl) and **152** (diformyl), where the dihydropyrenes decomposed into the migration products. However, integration of the corresponding protons in the CPD and in the migration products gave acceptable results. Moreover, multiple protons in the CPD and DHP/migration products were integrated and averaged in order to reduce the errors arising from integration.

First order rate constants (k) were obtained by plotting $\ln[\text{CPD}/\text{CPD}+\text{DHP}]$ against time. These rate constants were used in the Arrhenius equation (3.2) to obtain E_{act} from the slope of $\ln(k)$ vs. $1/T$ plot and $\ln(A)$ from the intercept. The slope and intercept in the Eyring plot of $\ln(k/T)$ vs. $1/T$ (equation 3.5), were used to calculate ΔH^\ddagger and ΔS^\ddagger respectively.

$$k = Ae^{-E_{\text{act}}/RT} \quad 3.1$$

$$\text{From (3.1)} \quad \ln(k) = \ln(A) - E_{\text{act}}/RT \quad 3.2$$

$$k = (k_b \cdot T/h)e^{-\Delta H^\ddagger/RT} \cdot e^{\Delta S^\ddagger/R} \quad 3.3$$

$$\text{From (3.3)} \quad \ln k = \ln(k_b \cdot T/h) - \Delta H^\ddagger/R \cdot T + \Delta S/R \quad 3.4$$

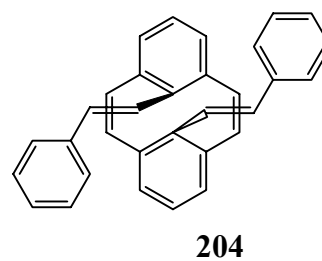
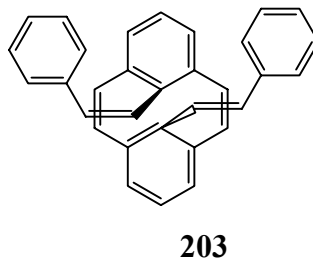
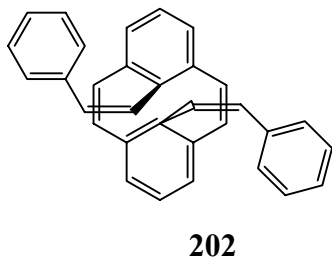
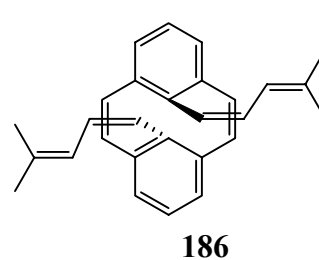
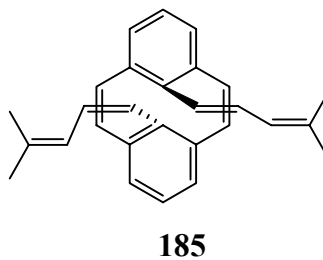
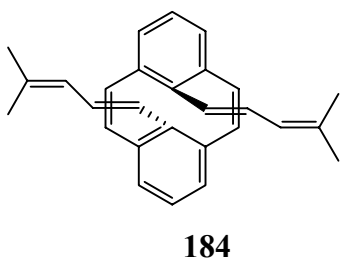
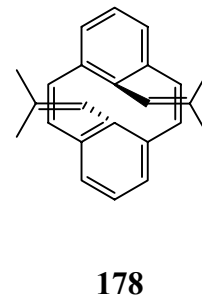
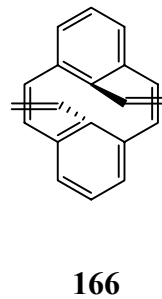
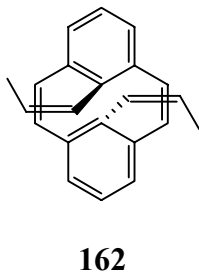
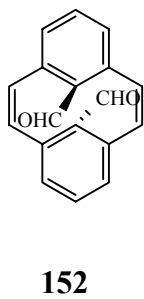
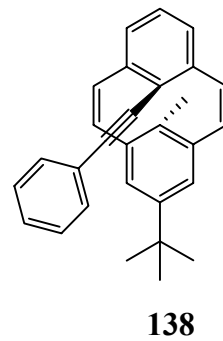
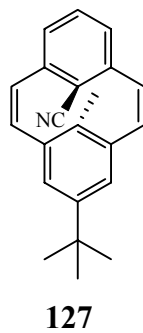
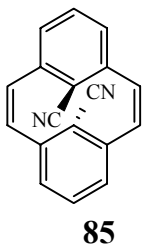
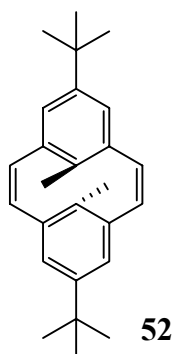
or

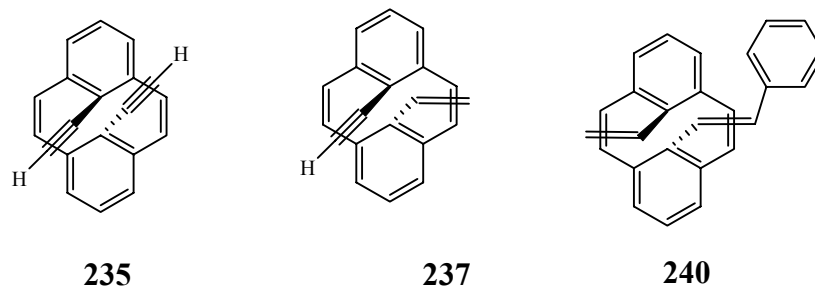
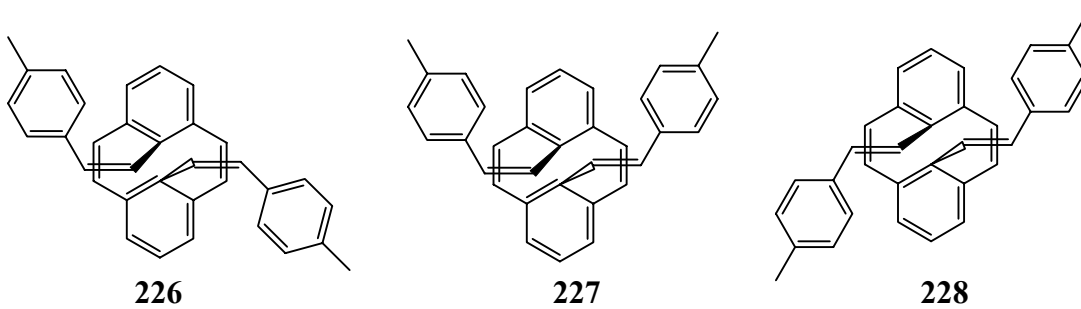
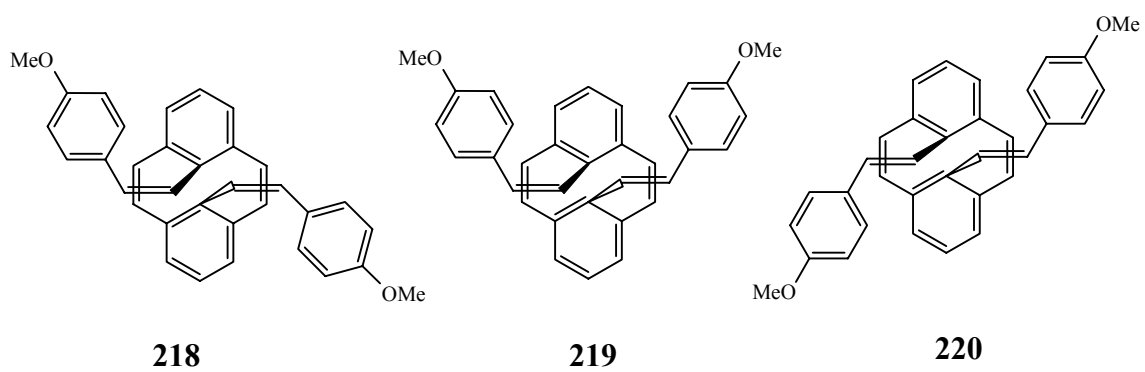
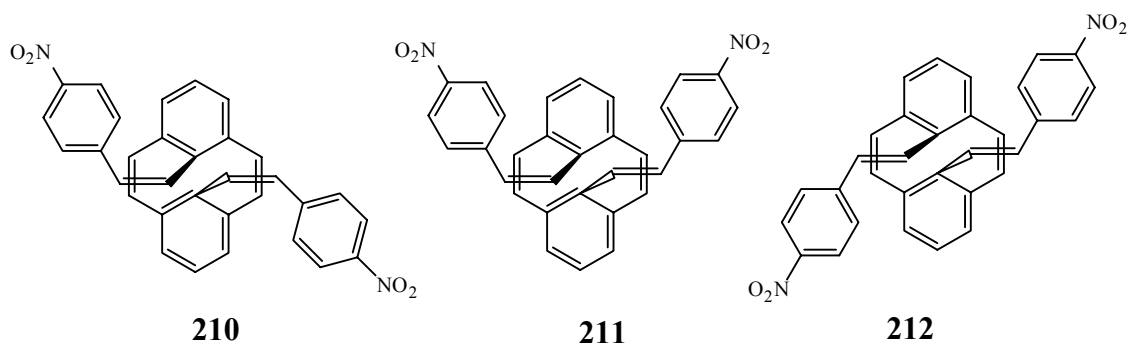
$$\ln(k/T) = \ln(k_b/h) - \Delta H^\ddagger/RT + \Delta S/R \quad 3.5$$

$k_b = 1.381 \times 10^{-23} \text{ J K}^{-1}$ (Boltzmann constant)

$R = 8.314 \text{ J K}^{-1} \text{ mol}^{-1}$ (gas constant), $h = 6.626 \times 10^{-34} \text{ Js}$ (Planks constant)

The following cyclophanedienes were studied for their thermal closure to the dihydropyrenes and the results are shown in Tables 3.1 and 3.2.





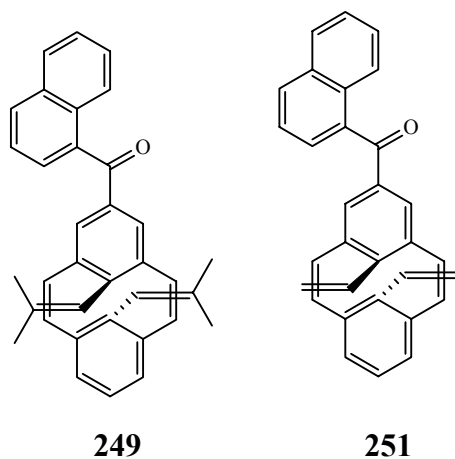


Table 3.1 **Thermodynamic parameters for the thermal back reaction of cyclophanedienes**

Compound	E_{act} kcal/mol	ΔH^{\ddagger} kcal/mol	ΔS^{\ddagger} cal/mol	$\ln A$
52	20 ± 2	20 ± 2	15 ± 6	22.8 ± 3
85[§]	30 ± 1	29.1 ± 1	-1 ± 2.5	30.2 ± 1.3
127[*]	24 ± 0.6	23.2 ± 0.5	-7.6 ± 1.4	26.9 ± 0.8
127[#]	23.8 ± 0.2	23.0 ± 0.2	-7.8 ± 0.6	26.8 ± 0.2
138[*]	24.4 ± 0.3	23.7 ± 0.3	-7.6 ± 1	26.7 ± 0.5
152[#]	26.2 ± 0.3	25.6 ± 0.3	0.6 ± 0.8	30.8 ± 0.4
162[∞]	29.9 ± 0.6	29.2 ± 0.6	1.3 ± 1.6	31.3 ± 0.8
166[∞]	25.0 ± 0.9	24.4 ± 1	4.3 ± 3	26.8 ± 1.4
178[∞]	28.2 ± 0.5	27.5 ± 0.5	-5.4 ± 1.2	28.0 ± 0.6
184[∞]	26.7 ± 0.2	26.0 ± 0.2	-5.8 ± 0.5	27.8 ± 0.2
185[∞]	27.6 ± 0.1	26.8 ± 0.1	-4.9 ± 0.1	28.4 ± 0.1

186[∞]	26.8 ± 0.6	26.1 ± 0.6	-7.5 ± 1.6	26.9 ± 0.8
202[∞]	27.2 ± 0.6	26.5 ± 0.6	-5.9 ± 1.5	27.7 ± 0.8
203[∞]	26.9 ± 0.1	26.2 ± 0.1	-6.3 ± 0.3	27.5 ± .1
204[∞]	26.3 ± 0.6	25.6 ± 0.6	-6.7 ± 1.5	27.3 ± 0.8
210[∞]	25.7 ± 0.1	25 ± 0.1	-9.6 ± 0.3	25.8 ± 0.1
211[∞]	26.4 ± 0.5	25.6 ± 0.5	-7.3 ± 1.2	26.9 ± 0.6
212[∞]	26.3 ± 0.4	25.6 ± 0.4	-7.4 ± 1	27 ± 0.5
218[∞]	27.4 ± 0.1	26.7 ± 0.1	-6.4 ± 0.1	27.6 ± 0.1
219[∞]	26.6 ± 0.2	25.9 ± 0.2	-7.5 ± 0.6	26.9 ± 0.3
220[∞]	26.4 ± 0.2	25.7 ± 0.2	-7.4 ± 0.4	27 ± 0.2
226[∞]	26.9 ± 0.3	26.1 ± 0.3	-7.6 ± 0.8	26.9 ± 0.4
227[∞]	26.2 ± 0.5	25.3 ± 0.5	-8.8 ± 1.4	26.2 ± 0.7
228[∞]	25.9 ± 0.1	25.1 ± 0.1	-8.8 ± 0.2	26.2 ± 0.1
235[∞]	28.4 ± 0.8	27.7 ± 0.6	-3.2 ± 1.6	29 ± 1.1
237[∞]	25.7 ± 0.5	25 ± 0.5	-7.4 ± 1.4	27 ± 0.7
240[∞]	26.1 ± 0.1	25.4 ± 0.1	-5.8 ± 0.1	27.7 ± 0.1
249[∞]	27.3 ± 1	26.6 ± 1	-4.1 ± 2.9	28.6 ± 1.4
251[#]	24.2 ± 0.8	23.5 ± 0.8	-5.2 ± 2.6	28 ± 1.3

[∞] = Toluene, # = CDCl₃, * = Benzene, § = Solid phase

Table 3.2 Half lives of the cyclophanedienes at three different temperatures

Compound	$\tau_{1/2}$ (20 °C)*	$\tau_{1/2}$ (50 °C)*	$\tau_{1/2}$ (100 °C)
85	~ 36 years	107 days	5 h
178	16 years	65 days	4.5 h
162	10 years	33 days	94 min
235	8 years	49 days	124 min
218	6 years	27.7 days	130 min
226	5 years	25 days	132 min
186	4.5 years	23 days	115 min
202	4.3 years	20 days	91 min
185	4 years	18 days	82 min
219	3.1 years	16.4 days	92 min
203	2.8 years	14 days	73 min
227	2.5 years	14 days	87 min
220	2 years	11 days	64 min
249	2 years	8.5 days	43 min
210	1.9 years	11.3 days	77 min
211	1.8 years	9.8 days	59 min
228	1.7 years	10 days	63 min
212	1.7 years	9.2 days	55 min
184	1.6 years	8.5 days	45 min
204	1.2 years	6.3 days	40 min

237	200 days	80 h	24 min
240	197 days	74 h	23 min
198	-	-	~15 min
166	56 days	24 h	7.7 min
138	30 days	15.2 h	-
127 (benzene)	12.3 days	6.7 h	-
152	11 days	4.2 h	-
127 CDCl₃	9.5 days	5.2 h	-
251	5.8 days	3 h	-

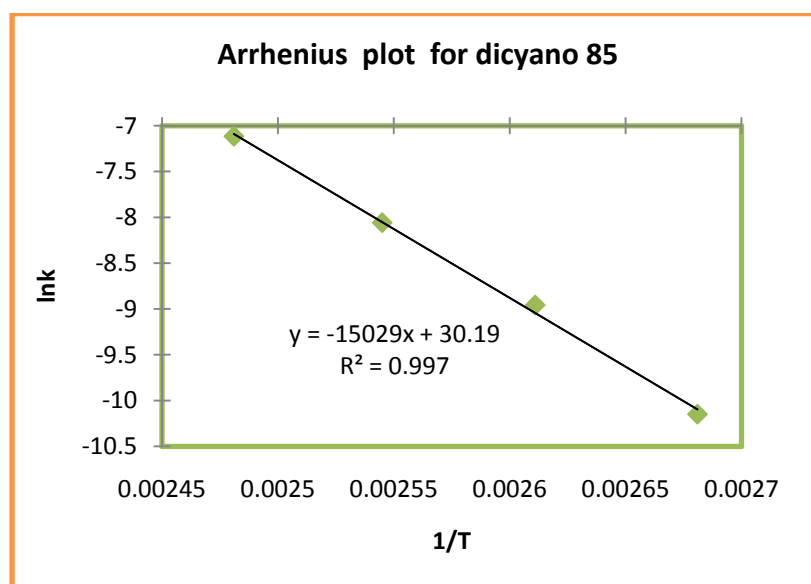
* Errors estimated are < 5%

The dicyano CPD **85** was calculated by Williams, to have an activation barrier of about 25-27 kcal/mol for the thermal closure. The nitrile group is a radical stabilizing group and was anticipated to lower the activation barrier however conjugation of the aryl rings with the nitriles stabilizes the CPD more than the TS[‡] and thus increases the activation barrier.

Nitrile **85** when heated at 70 °C for 12 hours failed to isomerize to the dihydropyrene **86** which indicated its high activation barrier, quite consistent with Williams' calculations. However, heating **85** at 100 °C did not lead to **86** as the only product, rather a mixture of *trans*-DHP **86**, migration and elimination products **124**, **125** and **126** was observed. The mole fraction of the CPD [**85/85+86+124+125+126**] when plotted against time gave rate constants of 3.90, 12.9, 31.6 and 81.3 x 10⁻⁵ s⁻¹ at 100, 110, 120 and 130 °C respectively. The Arrhenius plot yielded E_{act} ~ 30 kcal/mol. The Eyring plot gave ΔH[‡] ~ 29.3 kcal/mol. The activation barrier was about 3-5 kcal/mol higher than

the calculated value. This high activation barrier should be viewed cautiously since there could be a temperature lag in the solid phase. However we believe that the temperature lag, if any, cannot account for 3-5 kcal/mol. We thought that the entropy change might be unfavorable in the solid phase and thus has resulted in the slow thermal return. However the ΔS^\ddagger value obtained for **85** was -1.0 ± 2.5 cal mol⁻¹ K⁻¹, considerably higher and favorable than the methyl analogue **52** (-15 ± 6) cal K⁻¹ mol⁻¹). Thus, while the DFT calculations were quite successful in predicting a high activation barrier for the cyano CPD **85**, they did underestimate the value.

Figure 3.1 Arrhenius plot for the thermal reaction of dicyano CPD **85** in the solid phase



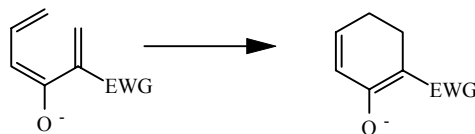
Dicyano CPD **85** has a calculated half life of > 30 years at 20 °C which is about three orders of magnitude higher than for the benzo-CPD **53** (7.3 days) which previously was the best switch. The high stability of the cyclophanediene **85** however was flawed by a relatively facile migration of the internal nitrile groups of the dihydropyrene **86** (for details see, Chapter 3 sigmatropic rearrangements).

The cyano-methylcyclophanediene **127** was made with anticipation that the migration and thermal return rates would be an average of those for **52** and **85**. This turned out to be the case for the thermal return; however migration rates were higher than **85**. The thermodynamic data was obtained in benzene and in CDCl_3 in order to determine the solvent effect on the thermal closure. The rates were slightly higher in CDCl_3 (~ 20%) although other thermodynamic parameters were quite comparable. Cyano-methyl CPD **127** has calculated half lives of 12 and 10 days at 20 °C in benzene and CDCl_3 respectively, slightly higher than that of the benzo-CPD **53** (7.3 days).

It was anticipated that the replacement of the nitrile group in **127** with a phenylethynyl group (CPD **138**) would have little effect on the thermal return because both groups are structurally similar and are rod like in nature. However the thermal return of **138** to **139** is approximately 3 times slower than **127** to **128** and has a calculated half life of ~ 30 days in benzene at 20 °C. The energy of activation was ~ 24.3 kcal/mol for **138** and was quite comparable to **127** (24 kcal/mol). The phenylethynyl group is better at stabilizing radicals than the nitrile and should make the transition state lower in energy and hence E_{act} ; however this is not the case. The relatively fast thermal return of **127** can be explained by the “captodative effect”⁷⁸ of the internal substituents.

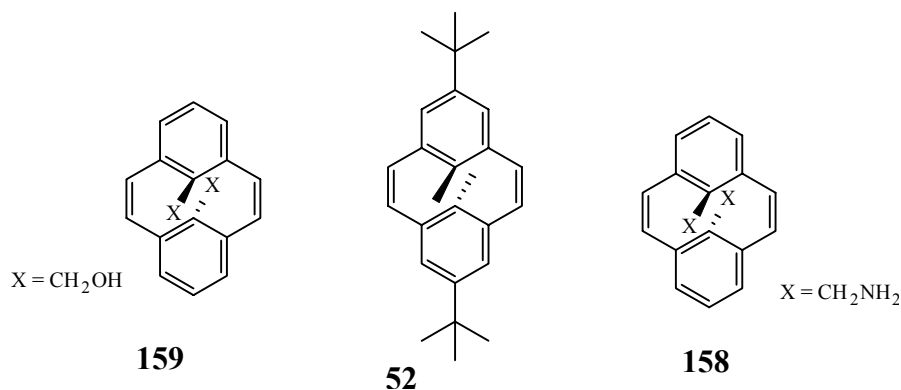
The word “captodative” is generally used to describe the combined effect of electron withdrawing (captor) and electron donating (dative) substituents, both attached to the radical centre or unsaturated compounds. An elegant example of the captodative effect in thermal 6π electrocyclic reactions is reported by Megomedov⁷⁹ et al. and is shown in Scheme 3.1. The presence of electron withdrawing groups at C-2 of the 3-oxido hexatrienes enormously lowers E_{act} , making the reaction feasible at -78 °C.

Scheme 3.1 An example of the captodative effect in electrocyclicization



Since nitrile is an electron withdrawing group, and the methyl is a weak electron donor through hyperconjugation, the captodative effect could be a possible explanation. Alternatively, it may be possible that the TS^\ddagger has some anionic character as well, which might not have been pointed out by the DFT calculations. Nitrile, an electron withdrawing group would favor an anionic transition state and would decrease E_{act} .

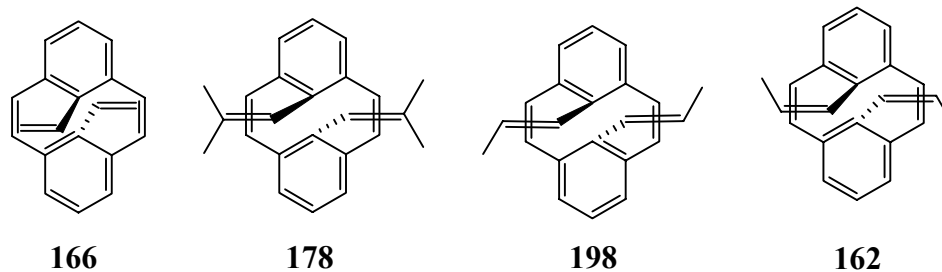
Diformyl CPD **152** is expected to close thermally at rates comparable to those of **85** because both groups, nitrile and aldehyde, stabilize radicals to a comparable extent. Moreover, the captodative effect would also be comparable: however the formylcyclophanediene **152** has a much faster thermal return ($\tau_{1/2} = 11$ days at 20°C) than **85** ($\tau_{1/2} = \sim 36$ years at 20°C). A number of factors may be contributing towards the fast thermal reaction of **152**. The formyl groups in **152** may not be in plane with the phenyl rings which would result in decreased conjugation. A low stability of the CPD due to the decreased conjugation would facilitate the thermal isomerization. Alternatively, the formyl group with its more electronegative oxygen atom can better stabilize the anionic transition state, as we proposed earlier, than a nitrile. Dihydropyrenes are electron rich in nature so it may be possible that an electron withdrawing substituent may favour the TS^\ddagger by delocalizing the electron density.



Reduction of the formyl CPD **152** gave **159** which is thermally unstable and isomerizes to the dihydropyrene with a half life less than an hour at 20 °C, much shorter than the parent methyl analogue **52** ($\tau_{1/2} = 42$ hours at 20 °C). The high instability of **159** not only demonstrates the importance of conjugation at the internal positions but also supports the notion that the internal electron withdrawing groups accelerate the thermal reaction. However, we failed to obtain **158** which would give us a better understanding of the effect of electron withdrawing groups at the internal positions. It is anticipated that the aminomethyl CPD **158**, once formed, would have a half life higher than that of **159**. We did not explore the captodative effect in detail. However it may be of considerable significance in accelerating the electrocyclic reaction.

Kinetic data of the above mentioned CPDs suggests that a conjugated internal group without any electron withdrawing atoms/substituents would slow down the thermal return. It was realized that alkenes and alkynes might fulfil this criteria.

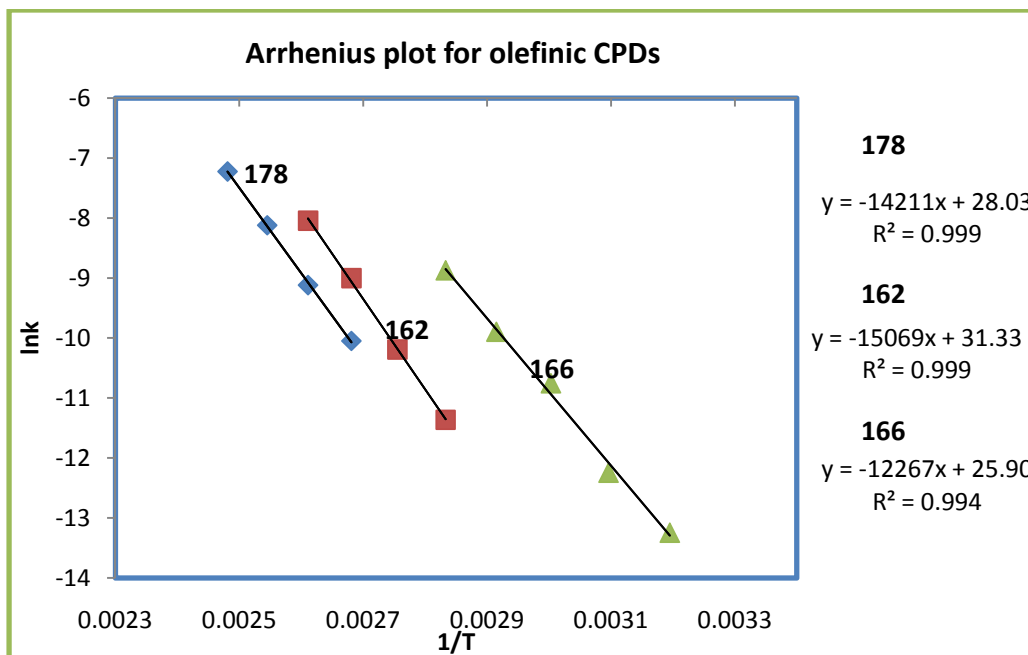
3.1.1 Cyclophanedienes with internal olefin substituents



As it was anticipated, cyclophanedienes with internal olefinic substituents have high stability towards thermal isomerization. The energy of activation is somewhat misleading in this series and this is probably due to variation in the pre-exponential factor A , thus half-lives give more useful comparison. In our series, diisobutenyl CPD **178** shows the best thermal stability and has a calculated half life of ~ 16 years at $20\text{ }^{\circ}\text{C}$ whereas CPDs **162** and **166** have half lives ~ 10 years and 56 days respectively. Why the thermal return of **178** to **179** is slow in this series is not immediately obvious. The high stability of the methyl substituted cyclophanedienes, however, cannot be explained only on the basis of radicaloid TS^{\ddagger} because the methyl substituents at the terminal olefin carbon would be expected to stabilize somewhat the radicaloid transition state, thus lowering E_{act} .

A comparison of the rate constants of the olefinic CPDs reveals that introduction of the *trans* methyl groups (**198**) decelerates the thermal return by a factor of two to three whereas the *cis* methyl groups have a twelvefold effect (**162**). Introduction of both *cis* and *trans* methyl groups (**178**) have an even more pronounced effect, i.e., the thermal reaction is slowed by a factor of ~ 34 . A significant difference in the behaviour of the *cis*- and *trans* methyl groups strongly suggests the involvement of steric factors.

Figure 3.2 A Combined Arrhenius plot for the internal olefinic cyclophanedienes in toluene



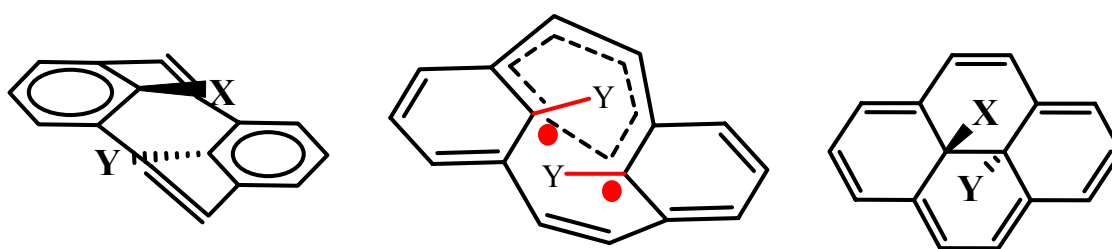
A number of factors may contribute:

1. The TS^\ddagger may be destabilized due the steric effects arising from the additional methyl groups.
2. The CPDs are additionally stabilized by hyperconjugation from the methyl groups.
3. The methyl groups destabilize the anionic TS^\ddagger (as we proposed earlier) by hyper conjugation.

DFT calculations by Williams⁴¹ suggest that the structure of the TS^\ddagger is intermediate between those of cyclophanediene and dihydropyrene for a variety of internal groups (see

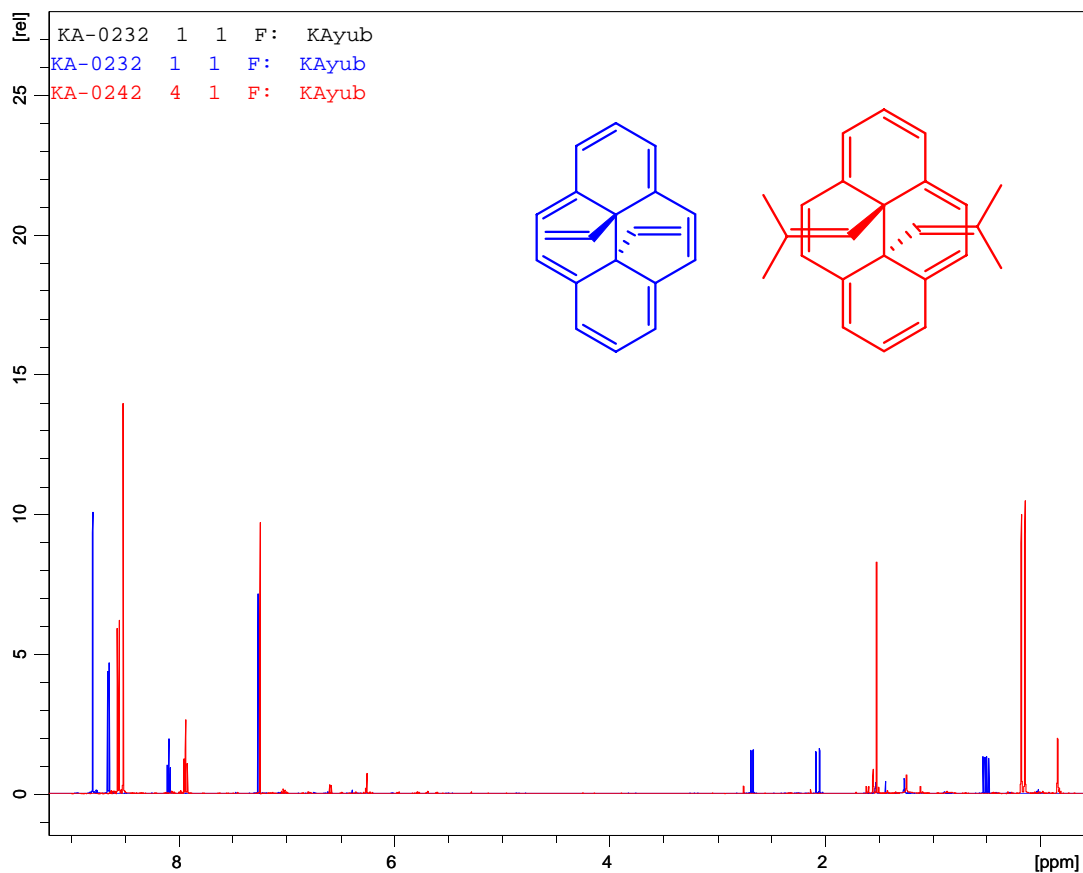
Figure 3.3), thus any unfavorable steric effect in the TS^\ddagger due to the movement of the internal groups is expected to be apparent in the product as well. Divinyl DHP **167** and diisobutenyl DHP **179** were compared in their 1H NMR spectra and X-ray structures to untangle the steric effect due to the methyl groups.

Figure 3.3 Structures of CPD (left), TS^\ddagger (middle) and DHP (right)

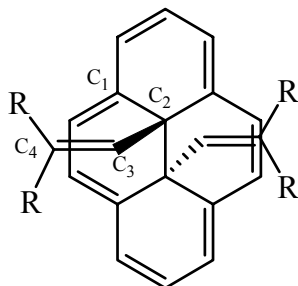


1H NMR analysis revealed that the DHP protons in **179** are relatively upfield (Figure 3.4, shown in red) compared to those of **167** (blue). This upfield shift could be either due to the decreased diatropic ring current (decreased planarity) or because of the anisotropic effect of the internal double bond. X-ray structure analysis revealed a difference in the orientation of the internal olefins in **167** and **179** as shown in Figure 3.5 and 3.6. The olefinic double bond in **167** resides at angle < 45 degree to the DHP nucleus whereas in **179**; it is deflected away and is almost perpendicular to the DHP ring

Figure 3.4 Combined ^1H NMR spectra of **167** and **179** in CDCl_3 at 500 MHz



^1H NMR analysis revealed that the DHP protons in **179** are relatively upfield (Figure 3.4, shown in red) compared to those of **167** (blue). This upfield shift could be either due to the decreased diatropic ring current (decreased planarity) or because of the anisotropic effect of the internal double bond. X-ray structure analysis revealed a difference in the orientation of the internal olefins in **167** and **179** as shown in Figure 3.5 and 3.6. The olefinic double bond in **167** resides at angle < 45 degree to the DHP nucleus whereas in **179**; it is deflected away and is almost perpendicular to the DHP ring.



The deflection is shown by marked differences in some of the bond angles. The $C_1-C_2-C_3$ angle is 103.71° in the case of **167** ($R = H$) whereas in **179** ($R = Me$), it is 111.34° . Moreover, $C_2-C_3-C_4$ angle is 127.01° in **167** whereas the corresponding angle in **179** is 132.87° .

Although the crystal structure does not have to be the solution structure, there are no strong polar effects at work and so it is probably not so different.

This deflection of the internal olefin in **179** results in the close spatial alignment of the olefinic CH proton to the DHP nucleus and is seen in the 1H NMR spectrum where it appears at $\delta -0.1$, shielded by 0.6 ppm compared to the olefinic CH in **167** ($\delta 0.5$). Moreover, the X-ray structure has shown that the 14-annulene **179** is significantly stepped compared to **167** and this is quite consistent with the upfield shift of the DHP protons in the former than the latter due to the reduced diatropicity.

Figure 3.5 ORTEP diagrams of divinyl DHP **167** (right) and diisobutenyl DHP **179** (left) showing 30% probability ellipsoids.

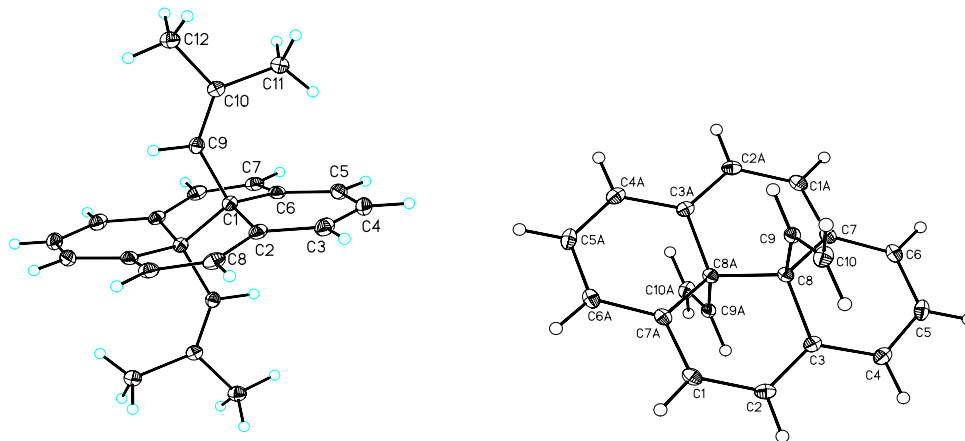
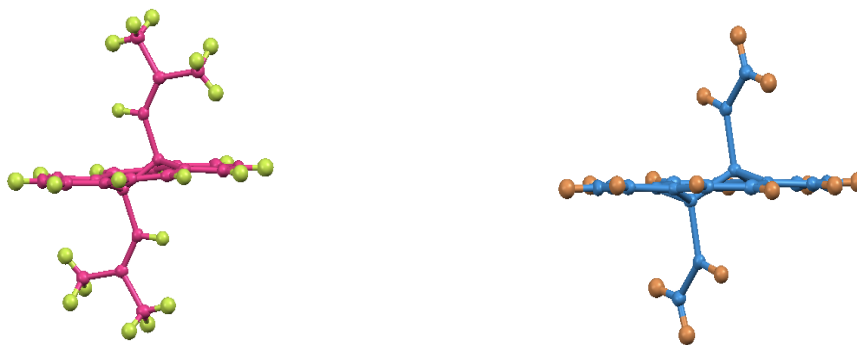


Figure 3.6 Molecular diagrams of diisobutenyl DHP **178** (left) and divinyl DHP **167** (right) derived from X-ray structures



The internal olefinic group in **179** aligns away from the DHP nucleus probably because of the repulsion between C-11 methyl and the DHP ring (C-1 to C-6) (Figure 3.5 left). A somewhat similar repulsion is also expected in **164** and is quite apparent from its ^1H NMR spectrum where the chemical shifts of the DHP protons and the internal olefin proton appeared between those of **179** and **167**; however we failed to obtain an X-ray

structure for **164**. This repulsion is probably the principle factor for the slow thermal return of the cyclophanedienes **162** and **178**.

How much CPDs are stabilized or destabilized by the methyl groups present on the olefinic substituents is not clear. ^1H NMR analysis did not yield any fruitful conclusions. Moreover X-ray crystal structures were not obtained for **162** and **166**. X-ray analysis of **178** indicates that the methyl groups cause the internal olefinic group to move away from the plane of the aromatic rings and thus would decrease the activation barrier which is quite contrary to the observations. The X-ray analysis of diisobutenyl CPD **178** will be discussed in detail later in section 3.1.5

The *trans*-methyl groups in **178** and **198** are far away from the DHP nucleus and are considered not to have any steric effects as seen for the *cis* analogue. Thus, these compounds probably would give a better estimate of the electronic effects. A comparison of **166** and **198** or **162** and **178** indicates that the *trans* methyl groups decelerate the thermal reaction by a factor of 2-3. On the other hand *cis*-methyl groups have twelve to 15-fold effects.

3.1.2 Extension of conjugation by a double bond in the internal substituents

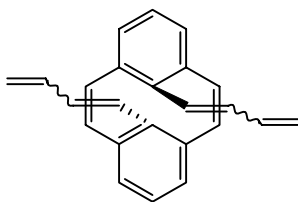
The aforementioned examples reveal that the conjugation in the internal substituent stabilizes the cyclophanedienes. In order to further elaborate the conjugation effects, butadienyl CPDs **184-186** were synthesized and studied for their behaviour in the thermal reaction.

The thermal return experiments in this series were performed on the mixture of isomers as the peaks corresponding to each isomer in the ^1H NMR spectrum could be easily identified both in the cyclophanediene and in the dihydropyrene. The experimental

design was useful not only in saving time but also confirmed that the rate differences in different isomers are not due to experimental errors.

The all *cis*-isomer **186** has the slowest thermal return among the three isomers, probably because of the steric interactions in the TS[‡], quite similar to those mentioned earlier for **164** or **179**. It is also supported by the fact that the DHP protons in **192** were slightly shielded when compared with the *trans*-isomer **190**. A comparison of the rate constants for **166** and **184** indicates that the additional *trans* double bond (with minimum steric contribution) slows down the thermal reaction by a factor of six. The rate constants gradually decrease along the series **184-186**.

Cyclophanedienes **184-186** contain terminal methyl groups and thus do not give a true estimate of extended conjugation by a double bond. The terminal methyl groups may have accelerating or decelerating effects and so non-methylated butadienyl CPD **181** would give a more accurate estimate. Unfortunately, we failed to prepare it. The thermodynamic data of the cyclophanedienes **184-186** clearly demonstrate that the terminal methyl groups do not have as marked effect as seen in the cases of **162** and **178**.



181

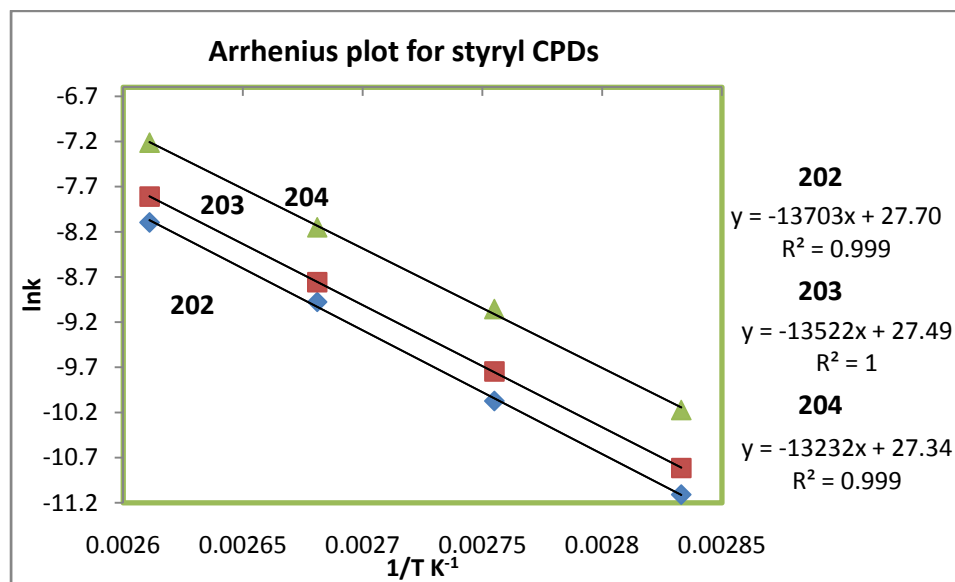
A comparison of the methyl substituted CPDs **162**, **198** and **178** with the butadienyl CPDs **184-186** indicate that steric effects play a major role in slowing down the thermal reaction in the former series whereas in the latter series, electronic effect are dominant.

We did not attempt to further extend the conjugation by another double bond due to several reasons such as complications arising from the increasing number of isomers in the hexatriene and its photo and thermal chemistry interfering with the cyclophanediene-dihydropyrene photoswitch properties.

3.1.3 Extending the conjugation by a phenyl ring

Quite analogous to the butadiene series, rates of the thermal return decrease upon extending the conjugation by a phenyl ring. The rate constants obtained at 100 °C for **202**, **203** and **204** are 7.5, 9.4 and 17 x 10⁻³ min⁻¹ respectively. The relative rate comparison indicates that the butadienyl group in **184-186** has more pronounced decelerating effect than the styryl groups in **202-204**. A possible explanation could be the effect of the terminal methyl groups in the former series absent in the latter.

Figure 3.7 Arrhenius plot for the styryl CPDs **202-204** in toluene



The DHP protons in the all *cis*-isomer **205** appeared at δ 8.2-8.3 and are more shielded than the DHP protons in **179** (δ 8.5). The shielding is believed to arise not only

from steric crowding (stepped DHP nucleus) but also from the ring current associated with the phenyl group. This shielding, if arising only from the stepped DHP nucleus, would be expected to make the thermal return of **202** slower than **178**; however this is not the case.

3.1.4 An electronic contribution towards thermal isomerization

In order to explore the electronic effects on the thermal return, *para* substituted styryl CPDs were studied. The effect was studied on all the geometrical isomers. The *para* position was chosen in order to have minimal contribution from the steric effects. Nitro and methoxy groups were chosen as representative examples of electron withdrawing and electron donating groups respectively. The electron neutral methyl group was also studied because of its anomalous behavior in the thermal back reactions.

The symmetrical nitro-styryl CPDs **210** and **212** had poor solubility in common organic solvents whereas the unsymmetrical isomer **211** was fairly soluble in toluene or in CDCl₃. In order to overcome the solubility problem, a larger number of scans (84 instead of 16 in ¹H NMR) were taken so as to increase the S/N ratio. Moreover, kinetic experiments were performed on the mixture of isomers as peaks corresponding to each isomer could easily be identified in the ¹H NMR spectrum.

In the cases of **210** and **211**, a relatively fast thermal reaction is observed compared to the non-substituted styryl CPDs **202** and **203** respectively, however the *trans*-nitro-styryl CPD **212** is thermally more stable when compared with the styryl parent CPD **204**. The thermodynamic data for the **212** may be misleading because of the poor solubility of its closed isomer, **215**. We did not observe any precipitate formation, but it may be possible that the dihydropyrene **215** formed suspensions which are invisible

in the colored solution. In this series, the most reliable data is for **211** which shows an accelerated thermal closure over that for **203**.

An electron donating methoxy substituent at the *para* position increases the thermal stability of the cyclophanedienes **218-220** compared to the corresponding non-substituted CPDs **202-204**. *cis*-Styryl CPD **218** has a half life of 130 minutes at 100 °C, considerably higher than that of **202**, 90 minutes. A comparison of the relative rates reveals that electron donating substituents at the *para* position of the styryl group decelerate the thermal return whereas electron withdrawing substituents promote the thermal reaction. Surprisingly, introduction of a virtually electron neutral methyl groups enhances the thermal stability of the cyclophanedienes **226-228** and the effect of the methyl is almost comparable to that of the methoxy substituent. The dramatic effect of the methyl groups can be attributed to hyperconjugation.

p-Methyl-styryl CPD **226** has a relatively low E_{act} (26.9 ± 0.3 kcal/mol) relative to *p*-methoxy-styryl **218** (27.4 ± 0.1 kcal/mol), even though the former is more stable at higher temperatures. The low E_{act} of **226** manifests itself in the relatively short half life at room temperature. Calculated half-lives at 20 °C for **226** and **218** are approximately 5 and 6 years respectively. It is already mentioned that the calculations by Williams suggest a radical transition state for the thermal isomerization, but our data, once again, supports anionic character in the TS[‡].

3.1.5 Alkynes as the internal substituents

Diethynyl CPD **235** isomerizes thermally to the DHP **236** at rates slower than those of dipropenyl **162** and divinyl **166**; however it closes faster than diisobutenyl **178**. The ethynyl group is linear and is not expected to exert any steric effects in the TS[‡]. The

high stability of **235** is probably because of a better conjugation in the cyclophanediene. Crystal structures were obtained for three cyclophanedienes; diisobutenyl **178**, distyryl **202** and diethynyl **235**, and their analyses reveal that the degree of bending of the internal carbons from planarity increases with increasing steric bulk.

Figure 3.8 Molecular diagrams of distyryl **202** (left) and diisobutenyl **178** (right) derived from X-ray structures

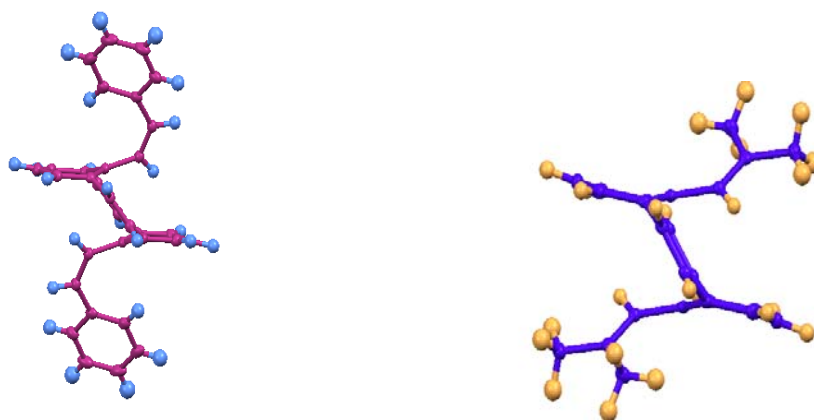
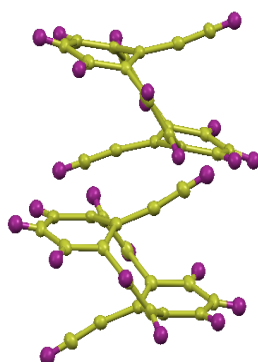
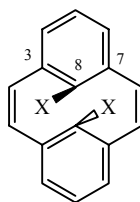


Figure 3.9 Molecular diagram of diethynyl CPD **235** derived from X-ray structure

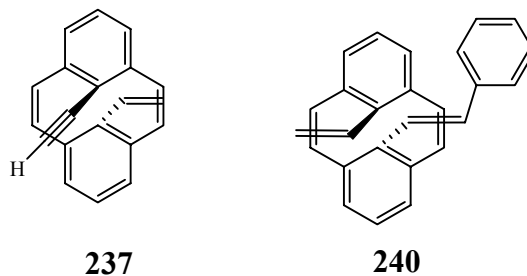


Diethynyl CPD **235** contained the least bending of the phenyl ring and the angle found is 118.40° ($C_3-C_8-C_7$) whereas the corresponding angles in **202** and **178** are 117.61° and 116.49° respectively. The high planarity of **235** and thus better conjugation are probably the reasons for its slow thermal return. Diisobutenyl CPD **178** is the most sterically unstable of all the three CPDs shown above and it should isomerize easily; but the steric repulsion in the transition state, as mentioned earlier, seems to exert an overwhelming effect.



Diethynyl CPD **235**, when compared to the dicyano CPD **85** has a fast thermal return and it is in contradiction to our proposed anionic transition state. However, as we mentioned earlier that the results from the solid phase kinetics of **85** should be taken with caution and it should not be compared with results from solution kinetics to draw some conclusions. However, it may be possible that the nitrile with a smaller nitrogen atom is sterically even less demanding and stabilizes the cyclophanediene **85** more than the ethynyl group stabilizes CPD **235**. We failed to get an X-ray structure of **85** to support this argument.

3.1.6 Unsymmetrical CPDs

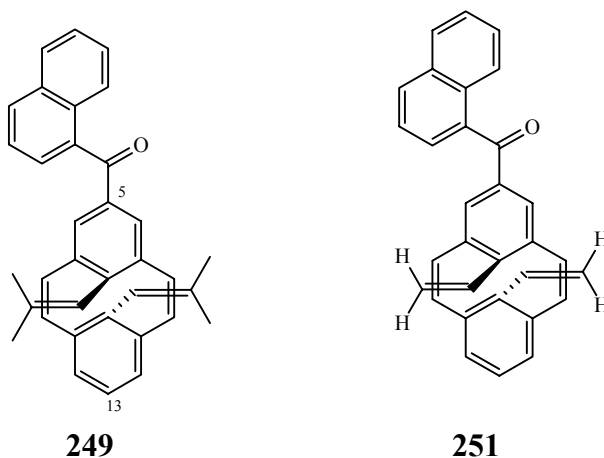


Thermodynamic data was obtained for the thermal closing reaction of the unsymmetrical CPDs **237** and **240**. CPD **237**, containing a vinyl and an ethynyl group was anticipated to isomerize thermally at an average rate of those for **166** and **235**. The thermal return of **237** to **238** is approximately 3 times slower than **166** to **167**, but more than five times faster than **235** to **236**. The data suggests that both ethynyl groups are required in order to slow down the thermal return. On the other hand, replacing one styryl group in **204** with a vinyl group, **240**, accelerates the thermal return only by a factor of < 2.

3.1.7 5-Naphthoylated CPDs **249** and **251**

A naphthoyl group at the 5 position of cyclophanedienes is known to accelerate the thermal return and this is also observed in the cases of **249** and **251**. Rate constants obtained at 100 °C are 16.2 and $2.59 \times 10^{-3} \text{ min}^{-1}$ for **249** and its non-naphthoylated analogue **178** respectively, which indicates that the incorporation of a naphthoyl group accelerates the thermal return approximately by a factor of six. This acceleration in the rate is accompanied by a drop in E_{act} by 1 kcal/mol. Introduction of a naphthoyl group at the 5 position in the divinyl CPD **166** has an even more profound effect on the thermal reaction. The thermal reaction of **251** to **250** is approximately 12 times faster than **166** to

167, although the drop in E_{act} is still about 1 kcal/mol. The origin of this extra acceleration of the thermal reaction in **251** is not clear. One contributing factor may be solvent. Thermodynamic data for **250** was obtained in CDCl_3 whereas **166** was studied in toluene. It is already mentioned that CDCl_3 accelerates the thermal return by $\sim 20\%$.



Williams' calculations suggest that the 5- and 13- positions of cyclophanedienes (shown above) are the sites of second highest spin density in the TS^\ddagger , thus any radical stabilizing group, such as naphthoyl, is expected to accelerate the thermal return and this is consistent with our experimental observations. However, the rest of our data suggest an anionic character in the TS^\ddagger and thus we tried to interpret these results accordingly. The naphthoyl group, besides being a radical stabilizer, is also an electron withdrawing group and it can stabilize the anion as well and it should accelerate the thermal reaction based on the anionic TS^\ddagger .

The radical spin density at positions 5 and 13 is strongly negated by the sulfonated CPDs **78-82**. A radical destabilizing SO_3H would be expected to slow down the thermal return but the sulfonated CPDs are highly unstable thermally as evident by their half lives (Table 1.2, pg 23). Most of the 5-substituted CPDs reported in the

literature have faster thermal returns than the corresponding non substituted parent CPDs and contain electron withdrawing groups at this position. A radical stabilizing but electron donating group at these positions can discriminate the anionic vs. radical TS[‡]. A limitation towards this study is the electron rich nature of the dihydropyrene nucleus which prohibits installation of electron donating groups at the 5 and 13 positions.

The thermal return data along with the X-ray structure analysis suggests that the principle factors include

1. A drop in steric bulk at the internal positions of CPD slows down the thermal return.
2. Conjugation at the internal position enhances the half-life of the CPD
3. Steric crowding in the transition state resists the thermal closure.
4. Electron withdrawing groups accelerate while electron donating groups decelerate the thermal return

3.1.8 DFT Calculations

We asked Dr Williams (University of Idaho) to perform DFT calculation on some of the thermally stable cyclophanedienes, namely diisobutenyl **178**, dipropenyl **162**, *cis*-distyryl **202**, *trans*-distyryl **204** and divinyl **166**. A comparison of ΔG^\ddagger values is given in Table 3.3. The experimental ΔG^\ddagger values are calculated at 100 °C using Equation 3.5.

$$\Delta G^\ddagger = \Delta H^\ddagger - T \Delta S^\ddagger$$

Equation 3.5

Table 3.3 A comparison of theoretical and experimental ΔG^\ddagger values (kcal.mol⁻¹)

Compound	Theoretical ΔG^\ddagger	Experimental ΔG^\ddagger
Divinyl 166	23.2	22.5
<i>trans</i> -Distyryl 204	24.0	28.0
Dipropenyl 162	26.6	28.6
<i>cis</i> -Distyryl 202	27.0	28.7
Diisobutenyl 178	27.5	29.4

Even though the calculated values are lower (except **166**) than the experimental values, the relative order of theoretical values perfectly agrees with that of the experimental ones. This underestimation of the activation barrier has already been observed in the case of dicyano cyclophanediene **85**.

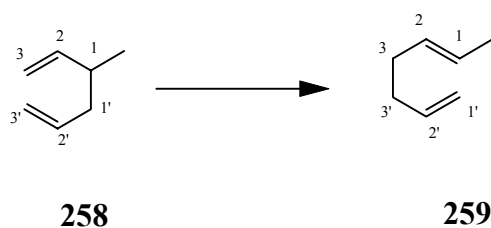
3.2 [1,5]-sigmatropic rearrangement

A sigmatropic rearrangement can be defined as: “A molecular rearrangement that involves both the formation of a new σ bond and the concomitant breakage of the existing σ bond with a concurrent relocation of π bonds in the molecule, but the total number of σ and π bonds does not change” Or “a pericyclic reaction wherein the net result is one σ bond changed to another σ bond”

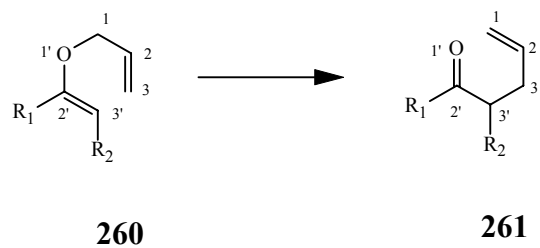
Sigmatropic rearrangements are classified by the substituent that moves and the order of the rearrangement, which is given in brackets [i, j] where i and j denote the number of carbons atoms at each terminus of the sigma bond that moves. Well known

examples of sigmatropic rearrangements are the Cope rearrangement, Claisen rearrangement and [1,5]-hydride shifts. The Cope rearrangement is a [3,3]-sigmatropic rearrangement of 1,5-dienes. The Claisen rearrangement is also a [3,3]-sigmatropic rearrangement of allyl vinyl ethers to give a γ, δ unsaturated carbonyls

Scheme 3.2 The Cope rearrangement of 258 to 259



Scheme 3.3 The Claisen rearrangement of 260 to 261



Scheme 3.4 A [1,5] hydride shift in conversion of 262 to 263

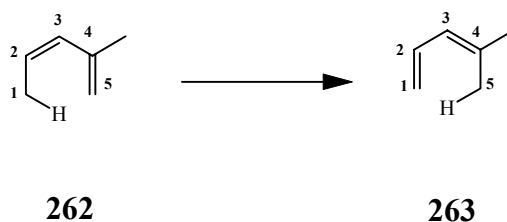
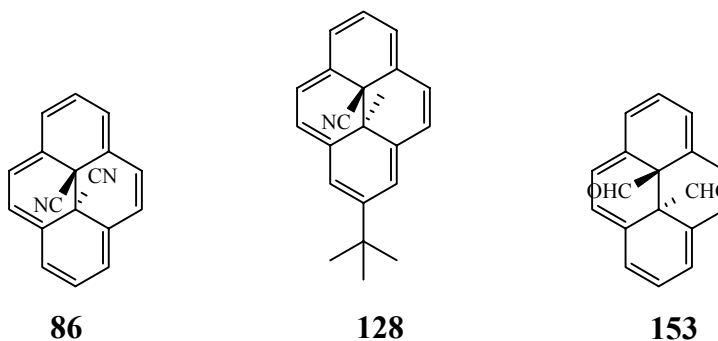


Table 3.4 The facial migration modes of $4n$ and $4n + 2$ π systems

π electrons	Photochemically	Thermally	Examples
$4n$	Suprafacial	Antarafacial	[1,3]-shift, [1,7]-shift
$4n + 2$	Antarafacial	Suprafacial	[1,5]-shift, [3,3]-shift

The following three compounds will be discussed. Dicyano DHP **86** was studied quantitatively and the data are reported in Table 3.5. Sigmatropic rearrangements of the internal nitrile and formyl groups in DHPs **128** and **153**, respectively, will be discussed qualitatively.

**Table 3.5** Thermodynamic data for the sigmatropic rearrangement of the internal nitrile group in **86**

	E_{act} kcal/mol	$\ln A$	ΔH^{\ddagger} kcal/mol	ΔS^{\ddagger} cal/mol	$\tau_{(1/2)}^*$ 20 °C	$\tau_{(1/2)}^*$ 50 °C
CDCl_3	23.4 ± 0.7	25.9 ± 1	22.8 ± 0.7	-9.22 ± 2.0	15 days	8.3 h
Benzene	28.6 ± 1.2	31.9 ± 1.9	27.9 ± 1.2	2.3 ± 4.0	266 days	66 h
Solid phase	28.6 ± 1.8	33.2 ± 2.8	27.9 ± 1.8	5.41 ± 5.6	24 days	13 h

* Errors estimated are less than 5%

The sigmatropic rearrangement of the internal groups showed first order kinetics, as expected. Equation 3.2 was used to calculate E_{act} and the pre-exponential factor A whereas the Eyring equation (3.5) gave the enthalpy and entropy of activation.

Rearrangement of the internal methyl groups has a high energy of activation and requires an elevated temperature (~ 200 °C). However, the sigmatropic rearrangement of the internal nitriles is quite facile at 50 °C in CDCl_3 (E_{act} 23.4 kcal/mol). This rearrangement is more favorable in CDCl_3 than in benzene or in the solid phase. We believe that this difference arises because of the acid content present in CDCl_3 since both mineral and Lewis acid catalysis in sigmatropic rearrangements is a well known phenomenon.⁸⁰

Boekelheide et al.^{61,62} concluded that these rearrangement proceed through a 1,5-sigmatropic rearrangement. However, nitriles can also undergo a 1,3-sigmatropic rearrangement with a radical intermediate.⁸¹ We thought that the 1,5-sigmatropic rearrangement may be a sum of two 1,3-sigmatropic rearrangements. However, we did not observe any products arising from a single 1,3-sigmatropic rearrangement. To address this problem further, DFT calculations were performed, which strongly suggested a 1,5-sigmatropic rearrangement. The activation barrier for the arrangement of the nitrile are quite consistent with the experimental values and are about 7 kcal/mol less than that for the rearrangement of the internal methyl group.

The driving force for the rearrangement may be the formation of a benzene ring. Migration of the second nitrile generates a naphthalene derivative from a benzene one and this migration is expected to be more difficult. The second sigmatropic shift probably has $E_{\text{act}} > 30$ kcal/mol; however this migration was not studied quantitatively.

Cyano-methyl DHP **128** transformed into the migration product **137** at a much faster rate than the dinitrile DHP **86** and had a half life of a few hours at room temperature. E_{act} is estimated $\sim 20\text{-}22$ kcal/mol in benzene whereas in CDCl_3 , E_{act} is much lower. The first migration product is quite stable and no further migration was observed even if the sample was heated at > 110 °C.

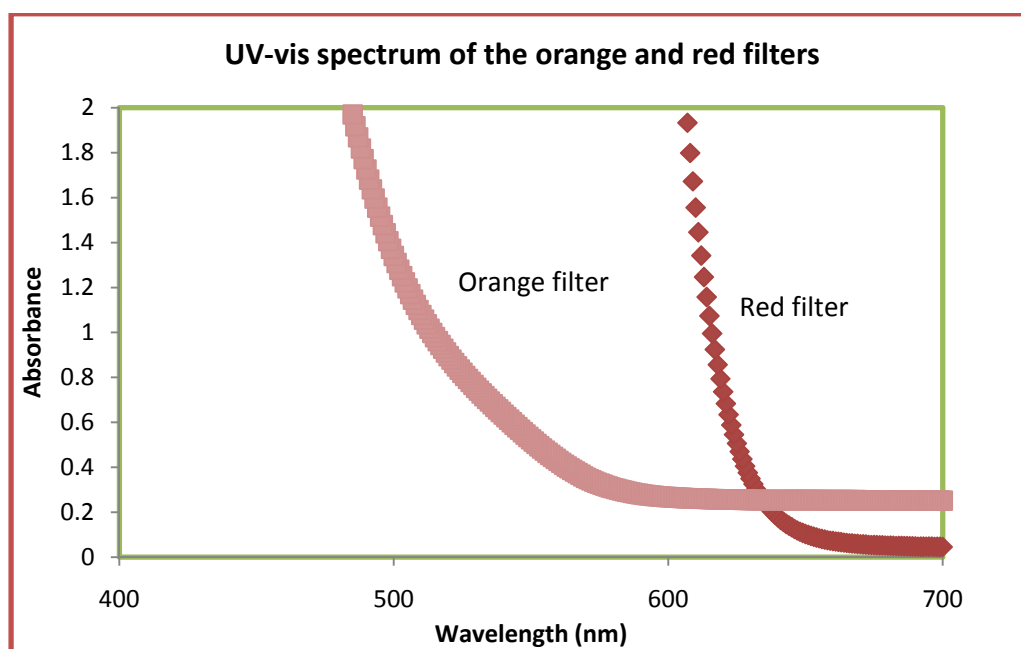
The [1,5]-sigmatropic rearrangement of diformyl DHP **153** was extremely fast. When a sample of cyano-methyl CPD **152** was heated to isomerize it into the DHP **153**, no traces of the DHP and the first migration product **156** could be seen by ^1H NMR spectroscopy, rather it transformed directly into the 2nd migration product **155**. This finding suggests that the energies of activation for both rearrangement processes are much lower than 26 kcal/mol (E_{act} of the thermal isomerization of diformyl CPD **152** into DHP **153**). DFT calculations suggest that the sigmatropic rearrangement of the internal carbonyls would have $E_{\text{act}} \sim 17$ kcal/mol.

Chapter 4: Photochemical isomerization

4.1 Visible light opening

Visible light opening studies were performed using a 500 W tungsten light with a 490 nm cut off filter (Figure 4.1), and the reaction was monitored by ^1H NMR spectroscopy. A d_8 -toluene solution (unless otherwise mentioned) of dihydropyrene (1-2 mg) in an NMR tube, cooled by a small cold water bath was irradiated until the sample solution was colorless or photostationary state was reached

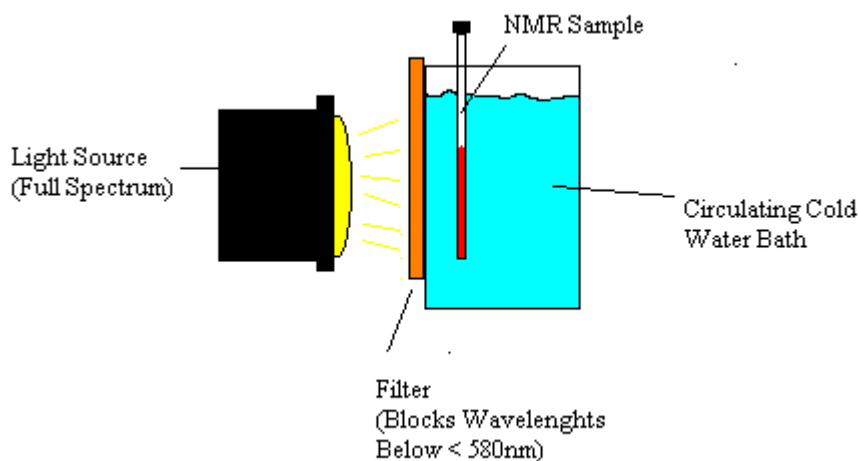
Figure 4.1 UV-vis spectrum of the orange and red filters



Benzo DHP **47** was chosen as a standard for the comparison of the visible opening rates. However the compounds studied, except **250**, have either very low or very high opening rates compared to the benzo DHP **47**, thus a direct rate comparison was not possible. For slow opening compounds *p*-methyl-styryl DHP **229**, a DHP with moderately fast opening rate, was calibrated against the benzo DHP **47** and thus used as a

standard. Both, sample and the standard were irradiated side by side and had approximately equal concentration. Rate comparison against the parent dimethyldihydropyrene **43** is reported as well.

Figure 4.2 Visible light opening experiment setup



The rate law of a photoopening reaction is typically second order; first order both in photons of light $[\gamma]$ and in concentration of the dihydropyrene molecule A (4.1). If a large excess of light photons are used then $[\gamma]$ becomes constant and the reaction rate law becomes a pseudo first order reaction (4.2). Rearrangement of the differential equation (4.3) and subsequent integration yields equation 4.4. However, a first order kinetic equation did not give the best fit of data for the visible opening experiment. Robinson³⁵ has reported that a zero order kinetic equation gives the best fit of data when ^1H NMR spectroscopy is used to monitor the reaction. This is due to the fact that NMR samples are concentrated and have little surface area exposed to the light source. Moreover, dihydropyrene molecules are highly colored. Even using a bright light source, only surface molecules are irradiated. As the photochemical reaction proceeds and the outer

molecules open to the cyclophanedienene, the inner molecules are exposed to the visible light. At any time, the number of molecules being exposed to the light source is constant and the rate equation becomes independent of the dihydropyrene concentration, i.e, it is a pseudo zero order reaction (4.5). After rearrangement of the differential equation (4.6) and integration (4.7), it can be seen that a plot of $[A]$ vs time yields rate constant (k'').

$$\text{Rate} = k[A][\gamma] \quad 4.1$$

$$\text{Rate} = k'[A] \quad 4.2$$

$$\text{Rate} = -d[A]/dt = k'[A] \quad 4.3$$

$$-d[A]/[A] = k'dt$$

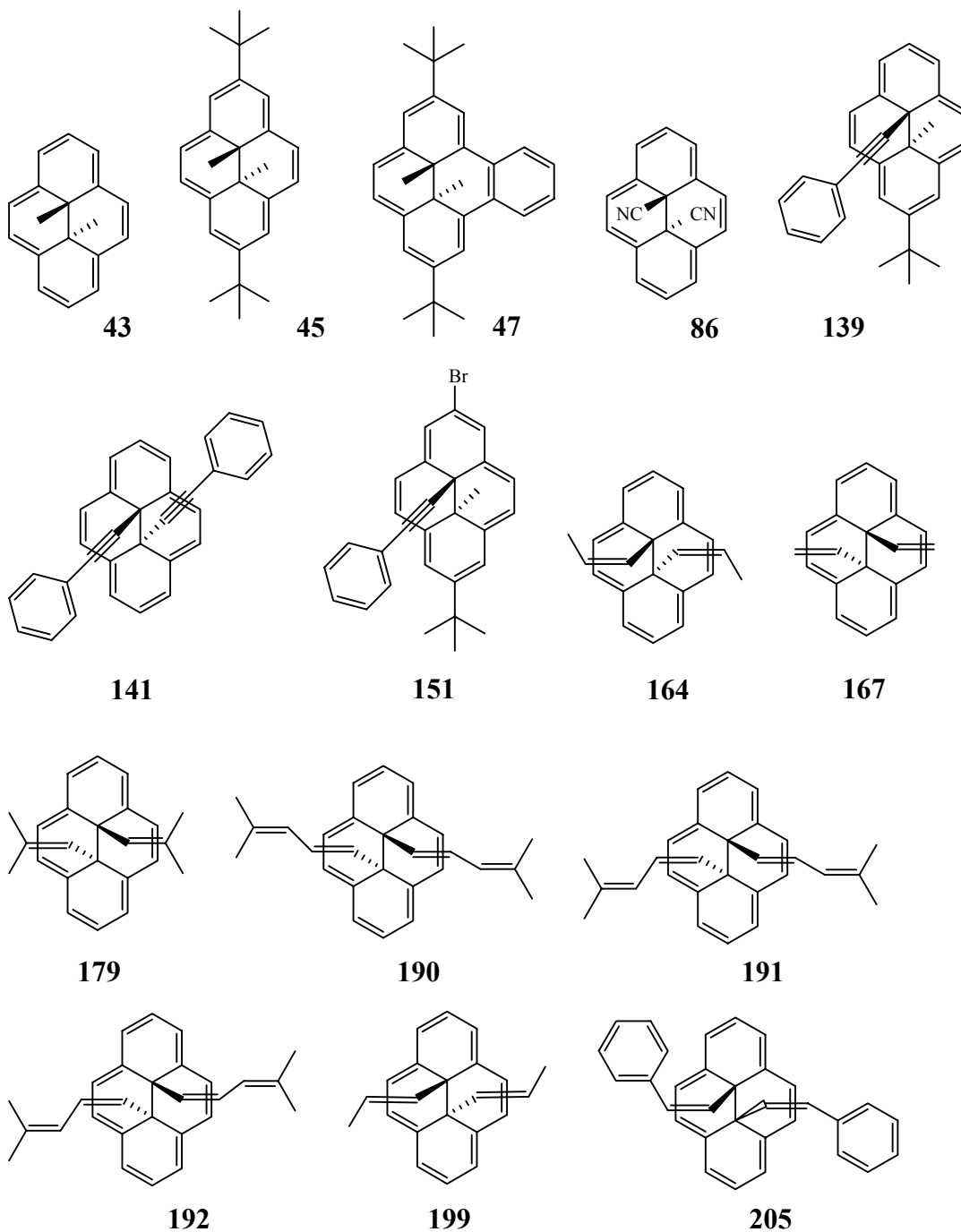
$$\ln[A] = -k't + \ln[A_0] \quad 4.4$$

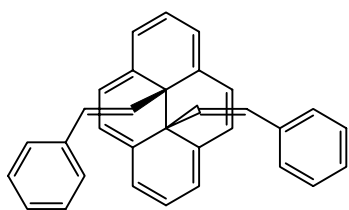
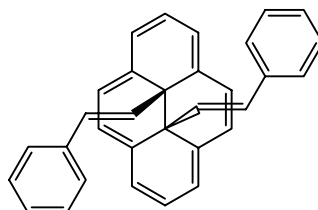
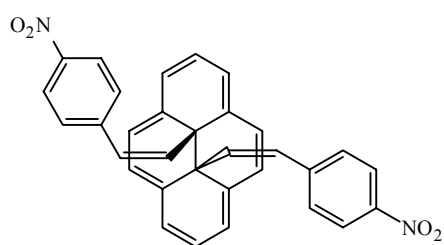
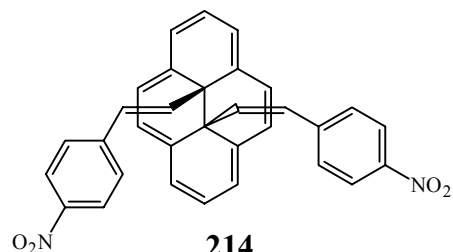
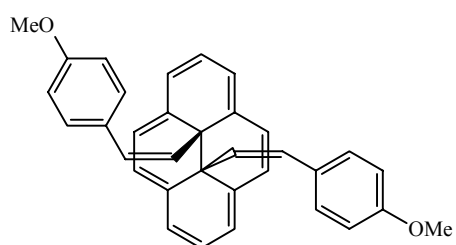
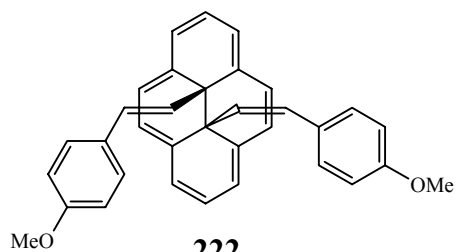
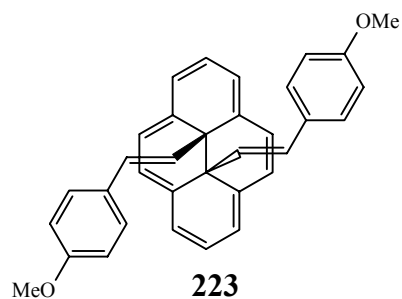
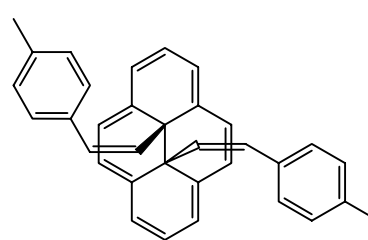
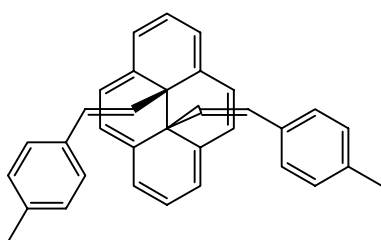
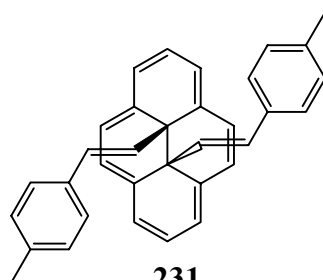
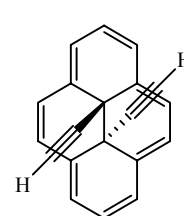
$$\text{Rate} = k'' \quad 4.5$$

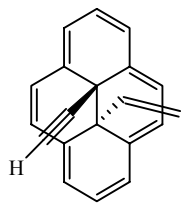
$$\text{Rate} = -d[A]/dt = k'' \quad 4.6$$

$$A = -k''t + [A_0] \quad 4.7$$

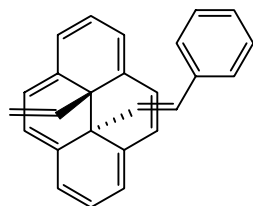
The following dihydropyrenes were studied for visible light isomerization to the cyclophanedienes and the results are shown in Table 4.1.



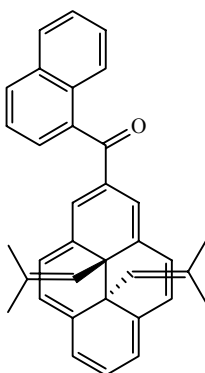
**206****207****213****214****221****222****223****229****230****231****236**



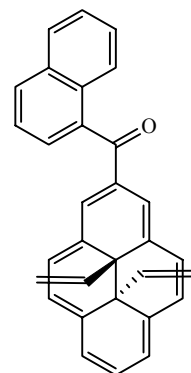
238



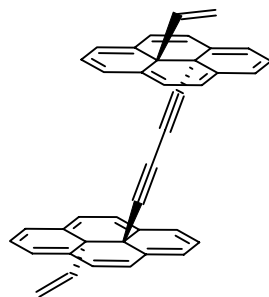
241



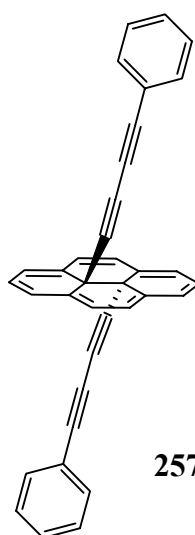
248



250



254



257

Table 4.1 Visible opening of the dihydropyrenes to the cyclophanedienes

Compound	Relative rates# vs DHP 43 (1000)	Relative rates vs benzo DHP 47 (1000)
139	Failed to open	Failed to open
141	Failed to open	Failed to open
151	Failed to open	Failed to open
190	Failed to open	Failed to open
199	Failed to open	Failed to open
207	Failed to open	Failed to open
223	Failed to open	Failed to open
231	Failed to open	Failed to open
238	Failed to open	Failed to open
241	Failed to open	Failed to open
257	Failed to open	Failed to open
167	Slow opening (dec.)	Slow opening (dec.)
191	Isomerized to 190	Isomerized to 190
192	Isomerized to 190	Isomerized to 190
86*	~ 6	~ 1
236*	65	4
164	180	11
214*	200	12
206*	740	45

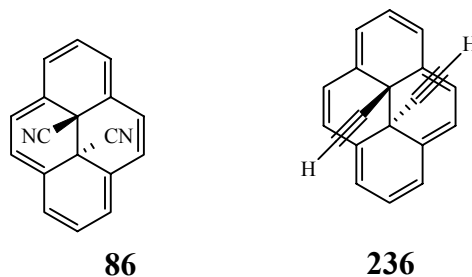
230*	980	60
222*	1130	69
254	200	12
205	2500	150
221	2900	180
229 (calibrant)	2900	180
179	3900	240
250	18000	1100
248	~ 410000	~ 25000

*photostationary state. # Errors estimates are less than 5%

Discussion of the results

4.1.1 Dicyano DHP **86** and diethynyl DHP **236**

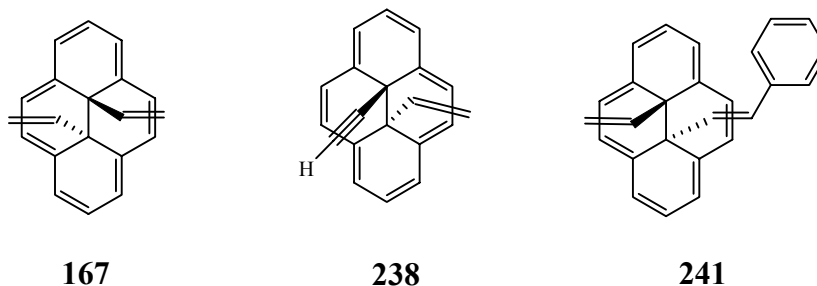
The parent dihydropyrene **43** and its *t*-butylated analogue **45** have poor quantum yields of photoopening reactions, 0.006 and 0.0015 respectively. Activators such as [e]-Annelation or addition of a carbonyl group at the 2- or 4- positions of the dihydropyrene, accelerate the photoopening reaction. We were not sure if dicyano DHP **86**, without any activator would open or not. The photoopening reaction was quite slow; however it did open and equilibrated to a photostationary state, CPD:DHP 60:40. An NMR sample of the dihydropyrene **86** in CDCl₃ was irradiated overnight before the photostationary state was reached. No decomposition of the dihydropyrene was observed in the chlorinated solvent. Diethynyl DHP **236** showed a similar behavior, however the photostationary state (CPD: DHP 60:40) was reached relatively rapidly.



Robb⁸², using high level *ab initio* calculations, has shown that the photoopening reaction of the parent DHP **43** occurs through a conical intersection between a biradical excited state and the ground state. For a highly efficient DHP based photochrome, this biradical excited state needs to be populated. However, calculations suggest that the radical excited state is not the lowest energy excited state. Moreover, excitation to this biradical excited state is symmetry forbidden.

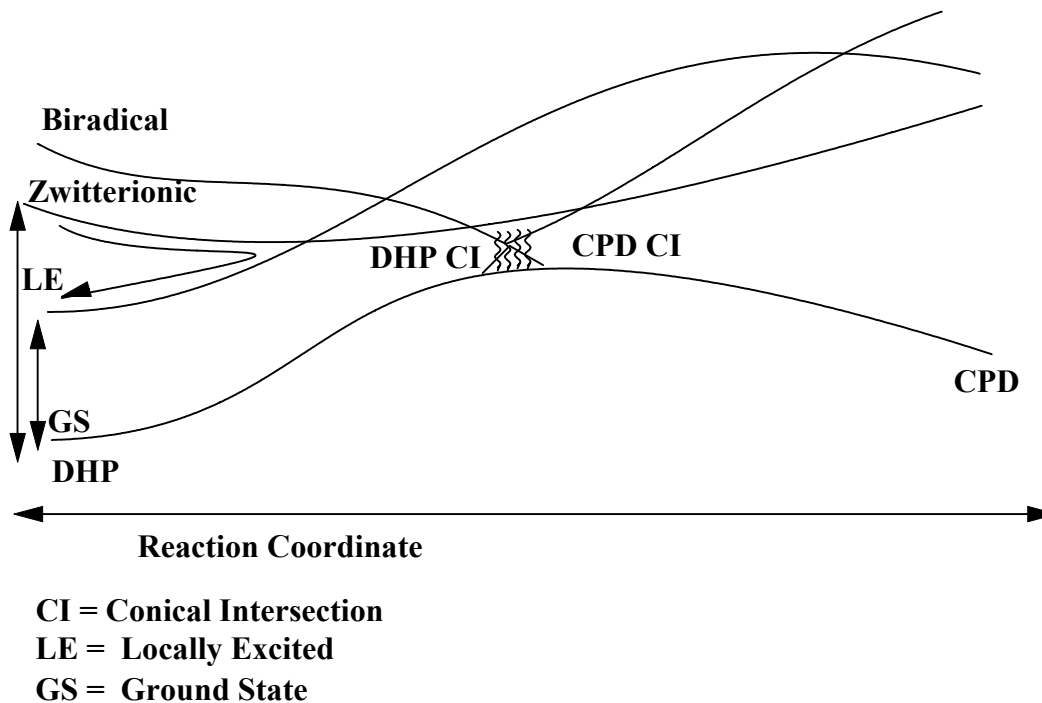
Stabilization of the biradical excited state or destabilization of the highly populated zwitterionic excited state is expected to accelerate the photoopening reaction of dihydropyrene based switches. It could be possible that the biradical excited state of the dihydropyrene **236**, bearing a radical stabilizing ethynyl group, is more highly populated than that of **86** which is responsible for its relatively fast photoopening. Introduction of phenyl or additional ethynyl groups (DHPs **139**, **141** and **257**) at the termini of the ethynyl substituents shuts down the photoopening reaction. The exception is the dimer **254** which will be discussed later. We are not sure what factors are responsible for this behavior.

4.1.2 DHPs with alkyl substituted internal vinyl groups



Divinyl DHP **167** failed to open to any appreciable extent and it decomposes on prolonged irradiation. The unsymmetrical DHPs containing a vinyl group such as **238** and **241** failed to open at all, however no decomposition was observed. Once again the exception to this generalization is the dimer **254**.

Figure 4.3 Outline of the proposed mechanism for the DHP/CPD photochromism



A vinyl group is as good as an ethynyl group in terms of stabilizing a radical. On the basis of this fact, divinyl DHP **167** was expected to open as fast as **236**; however this is not the case. This strongly suggests that the population of the biradical excited state is not the only factor. Robb⁸² has shown that there are two different conical intersections along the CPD-DHP isomerization reaction coordinate namely CPD CI and DHP CI residing on the CPD and DHP sides of potential energy surfaces respectively (Figure 4.3). A decay of the excited state at the CPD CI can lead to both photo products, i.e., CPD and DHP ground states whereas DHP CI decays only to DHP GS. It could be possible that excited states of DHPs **236** and **167** are decaying from different conical intersections.

Alternatively, if both DHPs are decaying from a common CPD CI then probably the relative stability of CPDs and DHPs is playing a major role. As mentioned earlier in Chapter 3 that the diethynyl CPD **235** is more stable than the vinyl counterpart which may be a driving force for the excited state arising from divinyl DHP **236** to drop into the diethynyl CPD **235** with a greater probability than in the case of divinyl CPD **166**.

DHP **199** containing a *trans* methyl substituted vinyl group failed to open at all, whereas DHP **164**, which contains a *cis*-methyl group, quantitatively opens to the cyclophanediene **162**. The opening rate is roughly 1% of that of benzo DHP **47**. Visible opening of diisobutenyl DHP **179**, containing two methyl groups, although four times faster than the parent **43**, was four times slower than that of the benzo DHP **47**. The fast opening of the dihydropyrenes containing *cis* substituted olefinic groups, **164** and **179** can be attributed to the steric instability of the dihydropyrenes (see Chapter 3) which drives CPD CI to decay into CPDs **162** and **178** respectively with a higher probability.

4.1.3 Distyryl DHPs 205-207

In the styryl CPD series, a trend is seen quite analogous to the alkyl substituted vinyl CPDs series. The all *cis*-DHP **205** opens at a rate ~15% of that of benzo DHP **47**, whereas the unsymmetrical DHP **206** opens at a much slower rate and forms a photostationary state. The all *trans*-isomer **207** failed to open at all. The difference in the behavior can be explained either by the steric instability factor (similar to one described for **164** and **179**) or by the visible light closing of the corresponding cyclophanedienes.

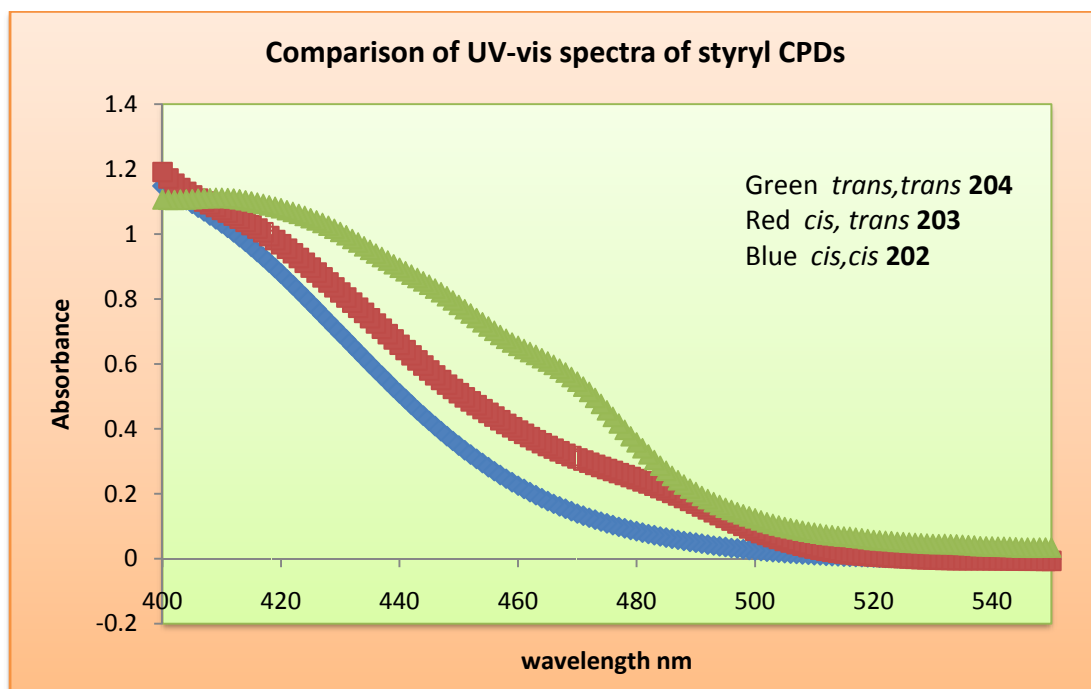
4.1.3.1 Visible light closing of the CPDs *E/Z* **203** and *E/E* **204**.

When a cyclophanediene has a tail which extends to the visible region of the absorption spectrum around 480 nm then there is a possibility that during the visible opening experiment of a dihydropyrene, the open form converts back to the closed dihydropyrene form. *trans*-Styryl CPD **204** shows a tail in the UV-vis spectrum ~ 550 nm, thus it may be possible that the DHP **207** opens to the cyclophanediene but closes back to the DHP at a much faster rate under the experimental conditions. An orange filter with cut-off wavelength 490 nm was used which is not sufficient to completely stop the absorption of the CPD **204** (see Figure 4.4). In a control experiment, irradiating a sample of the *t*-distyryl CPD **204** under the experimental conditions (visible light with orange filter) converted it into DHP **207** which is quite consistent with our proposed hypothesis. Irradiation of a sample of the dihydropyrene using a 590 nm cut-off red filter also failed to generate the open form.

The *cis*, *trans*-DHP **206**, upon photoirradiation, forms a photostationary state. This is not surprising because the corresponding open form **203** shows a small absorption beyond 490 nm in its UV-vis spectrum (Figure 4.4). The all *cis*-CPD **202** does not absorb

beyond 490 nm and thus the DHP **205** is expected to open completely and this is observed upon photoirradiation.

Figure 4.4 Combined UV-vis spectrum of styryl CPDs **202**, **203** and **204**



4.1.4 *Para* substituted styryl DHPs

A comparison of photoopening of the unsubstituted styryl DHPs **205-207** with those of *para* substituted DHPs reveal that:

1. For the all *cis* styryl isomers, a nitro group at the *para* position decelerates the photoopening reaction whereas a methyl or a methoxy group accelerates it relative to unsubstituted analogue.
2. The amount of the open form in the photostationary states for the unsymmetrical isomers **214**, **222** and **230** increases on going from electron withdrawing substituent to electron donating substituents

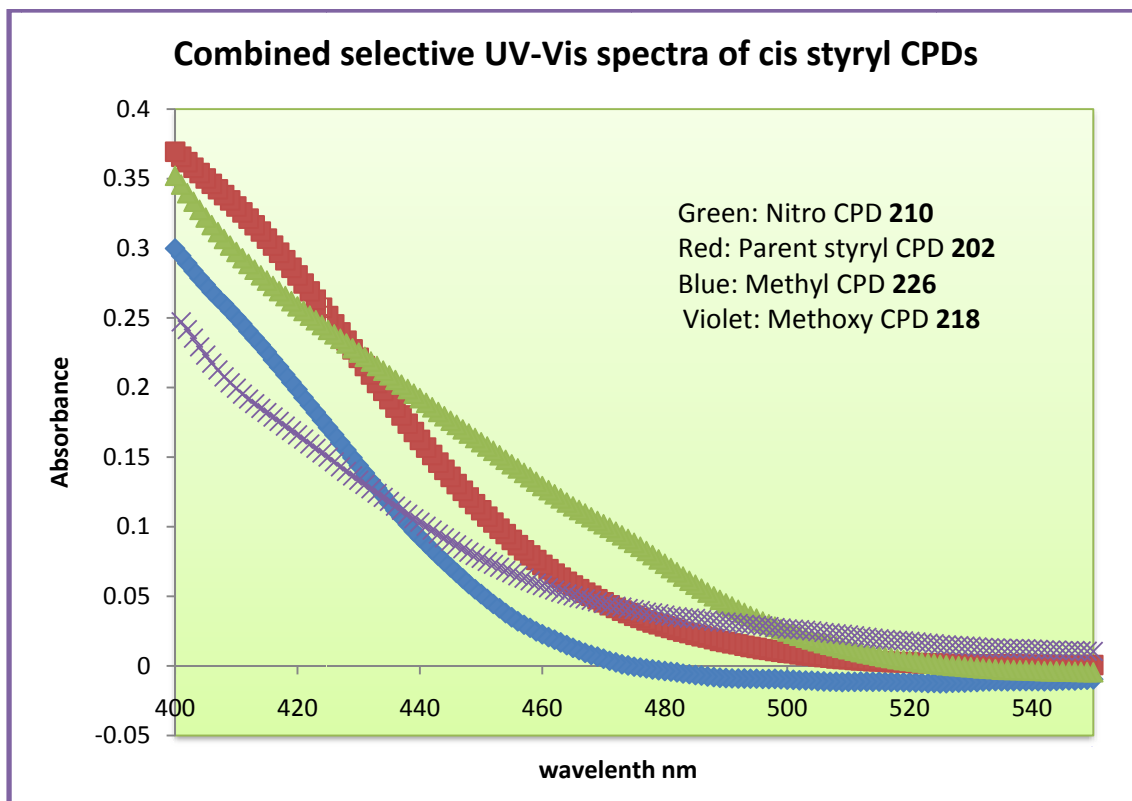
3. The all *trans* isomers failed to open in all cases.

Although quantitative measurement of the rate of photoopening of **213** could not be made (because of its poor solubility), qualitatively, its photoopening is slower than the non substituted styryl DHP **205**. On the other hand, DHPs with a virtually electron neutral methyl group or with an electron donating methoxy groups open faster than the non-substituted styryl DHP **205**. This is explained below.

4.1.4.1 A shift in the UV-Vis absorption spectrum

Introduction of a methyl or a methoxy group at the *para* position of the *cis*-styryl group shifts the tail of the UV-vis absorption spectrum to a shorter wavelength (blue shift), ~ 470 nm (Figure 4.5) whereas the nitro group shifts it towards the red (~ 520 nm) compared to the parent non substituted styryl CPD **202** (~ 495 nm).

Figure 4.5 Combined UV-vis spectrum of *cis*-styryl CPDs 202, 210 and 226 in CH_2Cl_2



Based on the absorption spectrum of cyclophanedienes, it is expected that the methyl substituted DHP **229** should open faster than **205** which, in turn, should open faster than **213** and this is quite consistent with the experimental results.

4.1.4.2 Electronic effects on the stability of photo excited states.

As mentioned earlier, Robb⁸² has shown by high level *ab initio* calculations that a DHP based photoswitch can photo open effectively provided the biradical excited state is highly populated compared to the normal zwitterionic one. Both methyl and methoxy groups are good at stabilizing radicals and can make the radicaloid excited state lower in energy and accelerate the photoopening reaction. However, a similar explanation cannot

be given for a nitro group because a nitro group is also a radical stabilizer and would be expected to accelerate the photoopening reaction.

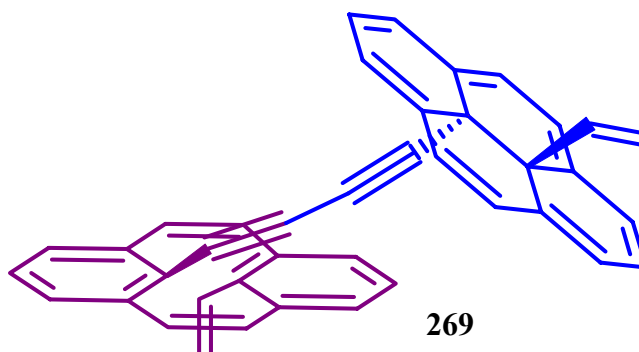
4.1.5 Naphthoyl DHPs **248** and **250**

A carbonyl functional group at the 2- and 4- positions of dihydropyrene is known to increase the photoopening rate.⁶⁷ Robinson³⁵ has shown that a naphthoyl group at the 2-position of a DHP has the most profound effect, thus we synthesized the naphthoyl derivative of the most thermally robust photoswitch **179** and studied its photochemical properties. The naphthoylation enhanced the photoopening rate by approximately two orders of magnitude. Naphthoyl diisobutenyl DHP **248** was almost 25 times faster than BDHP **47**. This relative rate should be adopted with caution because there could be large errors due to very short irradiation interval, i.e., a few seconds. Moreover, in a comparable time, BDHP was open less than 4%, a level of accuracy not provided through analysis of the NMR spectrum. The naphthoyl group probably stabilizes the radical excited state by delocalizing it over the π system and thus increases the photoopening rate.

Naphthoyl divinyl DHP **250**, quite contrary to its non naphthoylated analogue **167**, is quite stable to irradiation and opens at a rate comparable to BDHP **47**. This stability could be due to the short time required for the photoopening. Divinyl **250** forms a photostationary state in cyclohexane whereas in DCM or toluene, it opens completely. Formation of the solvent dependant photostationary state has already been reported in the cases of naphthoylated DHPs.³⁵

4.1.6 Dimer 254

Dimer **254**, despite the fact that it contains a vinyl and a butadiynyl internal group opens under visible opening conditions. Formation of the mono open product **269** can easily be seen by monitoring the NMR spectrum, however prolonged irradiation yielded a pale yellow colorless precipitate which could be the fully open form, however, we failed to obtain an NMR spectrum. Photoopening of the dimer was quite slow.



Another common factor among all the compounds, which fully opened or showed exceptional behavior, was the upfield shift of the DHP protons in their ^1H NMR spectra, examples include the all *cis* isomers of vinyl substituted dihydropyrenes and the dimer **254**. In the dimer, protons were shielded by 0.3-0.5 ppm in comparison to the monomer **237**. We are not sure if this upfield shift is an accident or it has some implications in understanding the photoopening process.

In conclusion, most of the compounds studied either failed to open or formed a photostationary state. However, some generalization could be made:

1. Dihydropyrenes **86** and **236** containing internal nitrile and ethynyl groups respectively (sp carbons substituents) formed photostationary states (60: 40 open: closed), however any extension of the internal alkyne substituents (DHPs **139**, **141** and **257**) shuts down the photoopening except in the case of DHP **254**.

2. The all *cis* isomers of the internal olefinic dihydropyrenes (**164**, **205**, **213**, **221**, **229**) opened to 100% completion.
3. The unsymmetrical (geometrical) isomers of internal styryl/*p*-substituted styryl dihydropyrenes (**206**, **214**, **222** and **230**) formed photostationary states.
4. The all *trans* isomers of the internal olefinic dihydropyrenes (**190**, **199**, **207**, **215**, **223** and **231**) failed to open at all.
5. Dihydropyrenes containing one or two internal ethenyl (vinyl) group such as **167**, **238** and **241** practically failed to open.

4.2 UV Closing

Cyclophanedienes **85** (dicyano), **229** (*p*-methoxystyryl) and **249** (naphthoyl diisobutenyl) were studied for the UV isomerization into the corresponding dihydropyrenes and comparative rates are given in Table

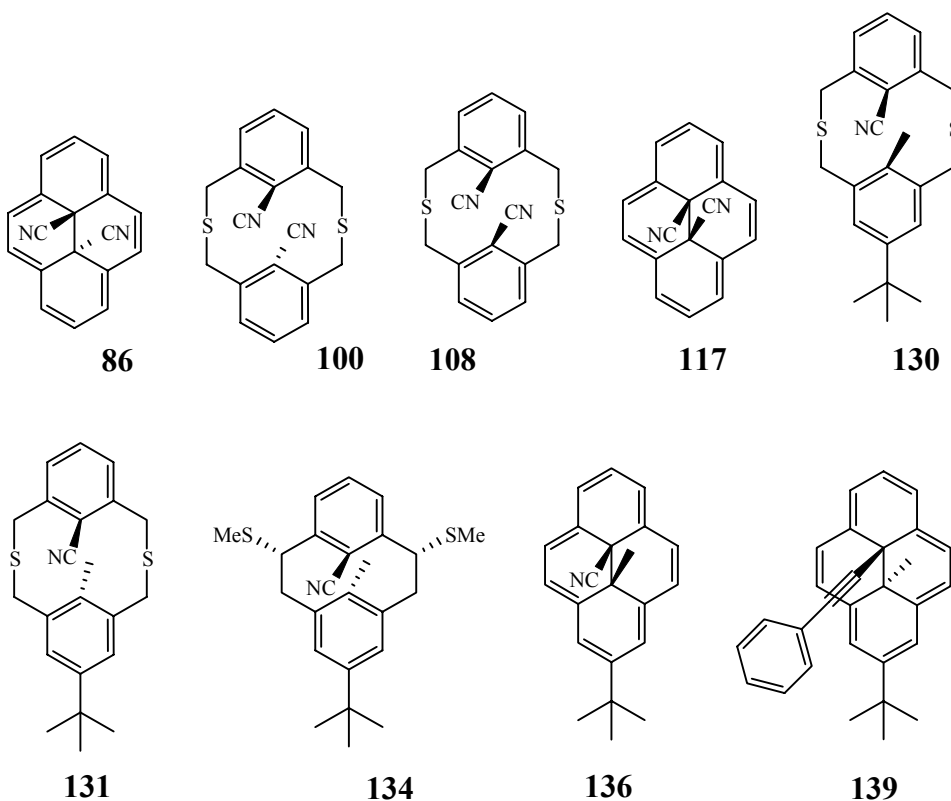
Table 4.2 UV closing comparison of cyclophanedienes

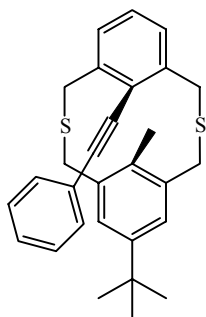
Benzo CPD 53	1
Dicyano CPD 85	0.6
<i>p</i> -Methyl-styryl CPD 229	1
Naphthoyl CPD 249	1.2

The UV closing rates of the cyclophanedienes were quite comparable to that of benzo CPD **53**. Dicyano CPD **85** isomerized slower than benzo CPD **53** whereas naphthoyl CPD **249** closed slightly faster. Robinson³⁵ and Bandyopadhyay⁸³ have concluded in a similar study that the UV isomerization rates of cyclophanedienes are generally quite comparable.

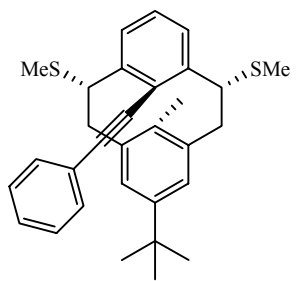
Chapter 5: X-Ray Structure Analyses

X-ray crystallography is the most reliable method for characterizing the atomic structure of materials as it gives information about the size and shape of molecules and complexes, as well as bond lengths and types of chemical bond. X-ray crystallography generally discerns materials which appear quite similar by other experiments (spectroscopic techniques). The technique besides providing insight into the structures of molecules, has also guided the direction of new research, e.g., the X-ray structure of ferrocene initiated scientific studies of sandwich compounds.⁸⁴ The following compounds were studied by X-ray crystallography as a part of this thesis research and the data was obtained by Dr Brendan Twamley (University of Idaho).

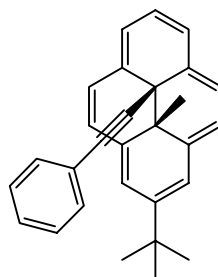




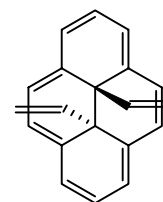
145



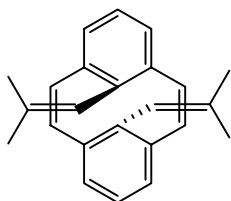
146



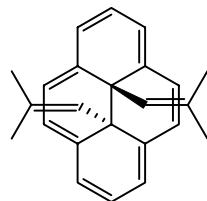
148



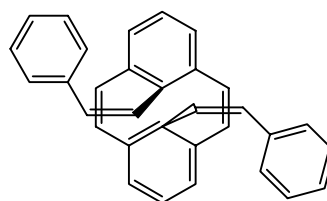
167



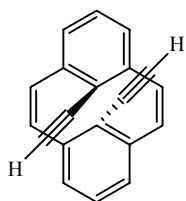
178



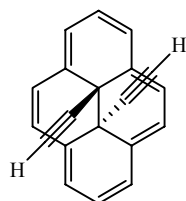
179



202



235

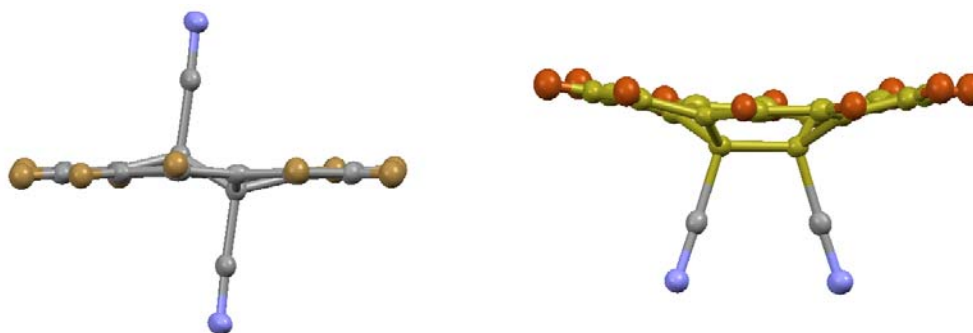


236

5.1 Dicyano DHPs 86 and 117.

It has already been stated that X-ray crystallography can discriminate molecules which appear quite similar by other spectroscopic techniques; examples are the *cis* and *trans* isomers of dicyanodihydropyrene, **117** and **86**, respectively. Both isomers have an equal number of peaks in each of their the ^1H and ^{13}C NMR spectra. Moreover, 2D NMR techniques fail to indicate the relative orientation of the cyano groups. An X-ray structure was obtained for each isomer (Figure 5-1) and the geometry was thus confirmed unambiguously.

Figure 5.1 Molecular diagrams of dicyano DHPs **86** (left) and **117** (right) derived from X-ray structures



5.2 *Cis*-dihydropyrenes

cis-Dicyano DHP **117**, as shown by its X-ray structure (Figure 5.1), is a saucer shaped molecule, a characteristic of *cis*-dihydropyrenes. A similar structure was also found for *cis*-phenylethyl DHP **148** (Figure 5.2, left) and *cis*-cyano-methyl DHP **136** (Figure 5.2, right).

Figure 5.2 Molecular diagrams of *cis*-phenylethynyl/methyl DHP 148 (left) and *cis*-cyano/methyl DHP 136 (right) derived from X-ray structures

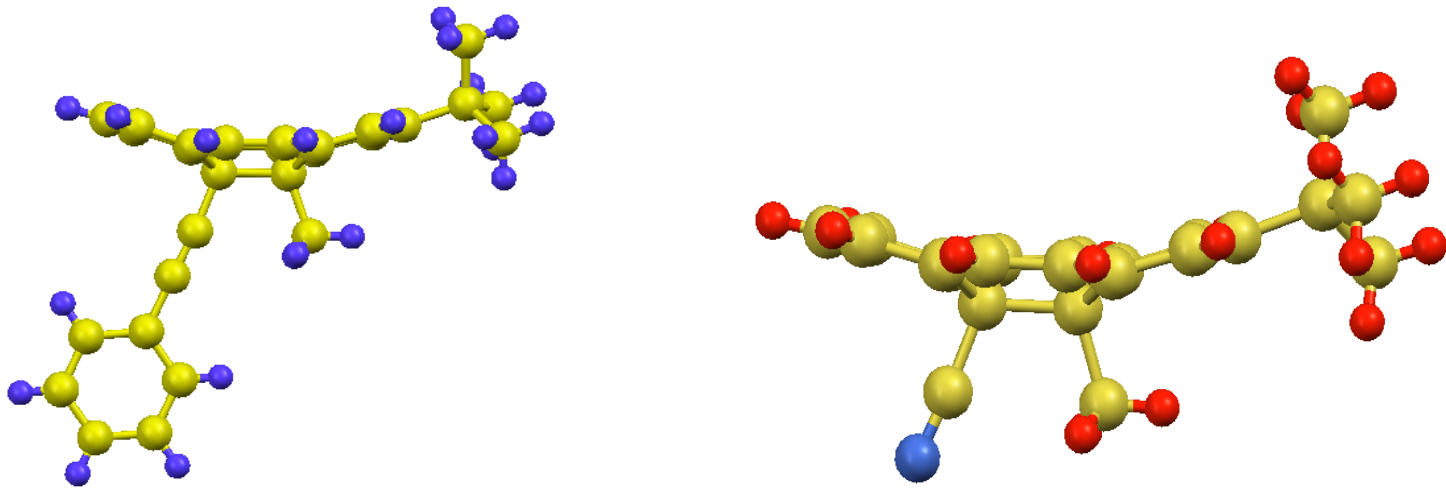


Figure 5.3 Molecular structures of *trans*-phenylethynyl/methyl DHP 139 and *trans*-diethynyl DHP 236 derived from X-ray structures

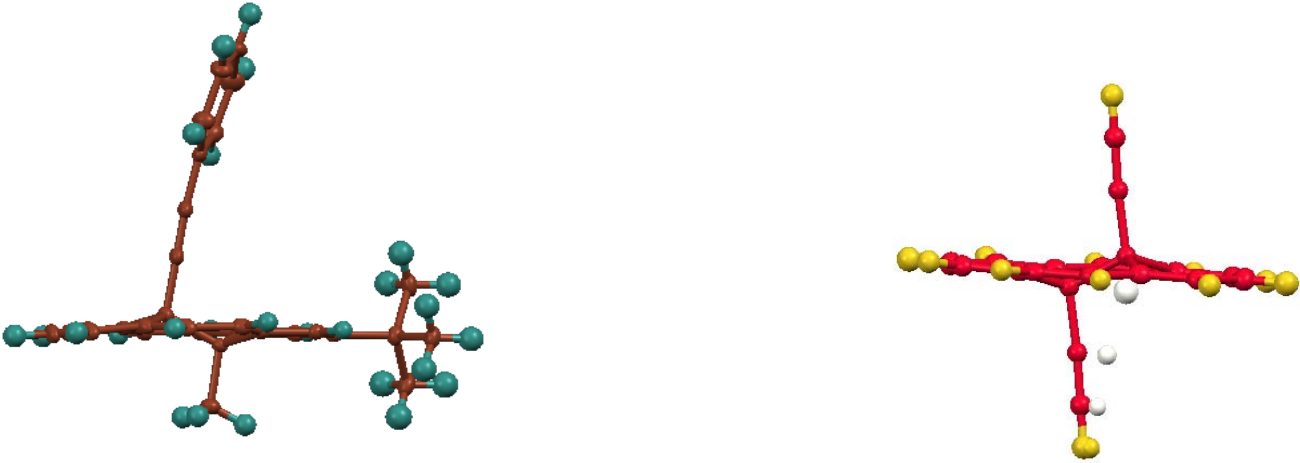
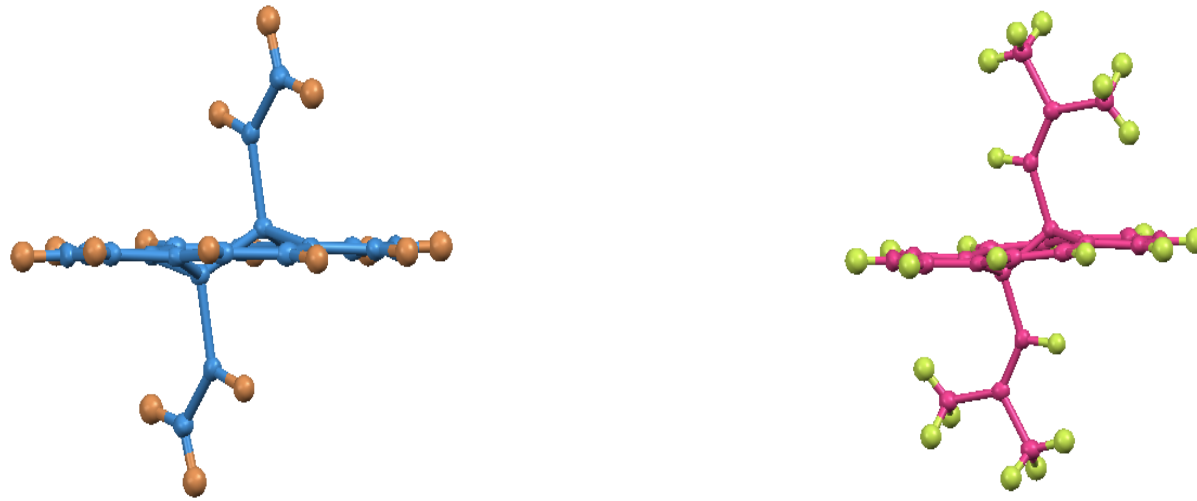


Figure 5.4 Molecular diagrams of divinyl DHP 167 (left) and diisobutenyl DHP 179 (right) derived from X-ray structures



5.3 *Trans* dihydropyrenes

The X-ray structures of the *trans*-dihydropyrenes not only indicate the orientation of the internal groups but they also give mechanistic insight into the thermal return reaction.

The *trans* dihydropyrene nuclei of dicyano DHP **86** (Figure 5.1 left), phenylethynyl/methyl DHP **139** (Figure 5.3 right), divinyl DHP **167** (Figure 5.4 left) and diethynyl DHP **236** (Figure 5.3 right) did not show any appreciable deviation from planarity probably because of the linear and sterically less demanding internal groups. However in the cases of internal diisobutenyl DHP **179**, the dihydropyrene skeleton was significantly stepped which suggests a reason for the slow thermal return of the cyclophanediene **178** (for details, see Chapter 3, pg 128).

5.4 Cyclophanedienes

Cyclophanedienes are thermally unstable compounds; moreover, they also convert to dihydropyrenes photochemically using the common household tungsten bulb. Thus, the crystal growth and the analysis are not trivial. We synthesized some thermally stable cyclophanedienes and thus we decided to obtain X-ray structures. The X-ray structures of diethynyl CPD **235** (Figure 5.5), distyryl CPD **202** (Figure 5.6 right) and diisobutenyl CPD **178** (Figure 5.6 left) were obtained which not only proved the stepped nature of the cyclophanediene but also gave valuable information regarding the mechanism of the thermal return. Cyclophanediene **235** showed better conjugation of the phenyl rings with sterically less demanding ethynyl groups. This conjugation is probably a reason for the high thermal stability of the CPD (for details: see Chapter 3, pg 127).

Figure 5.5 Molecular diagram of diethynyl CPD 235 derived from X-ray structure

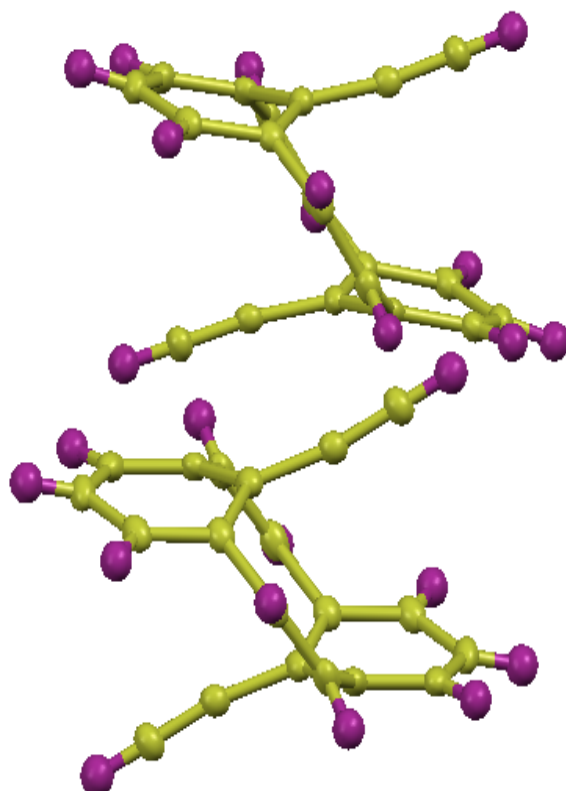
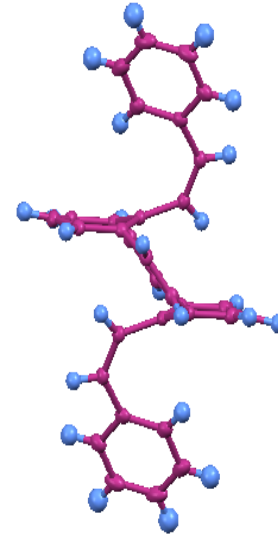
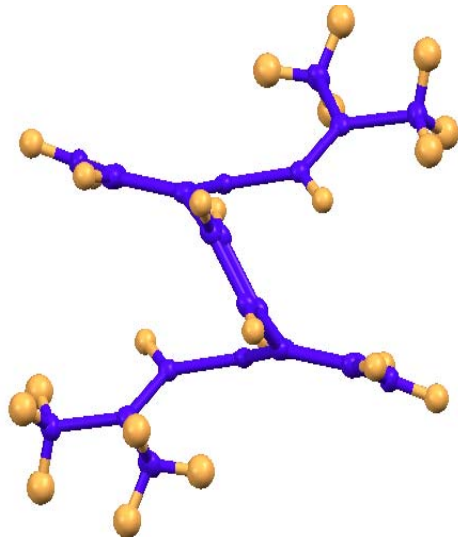
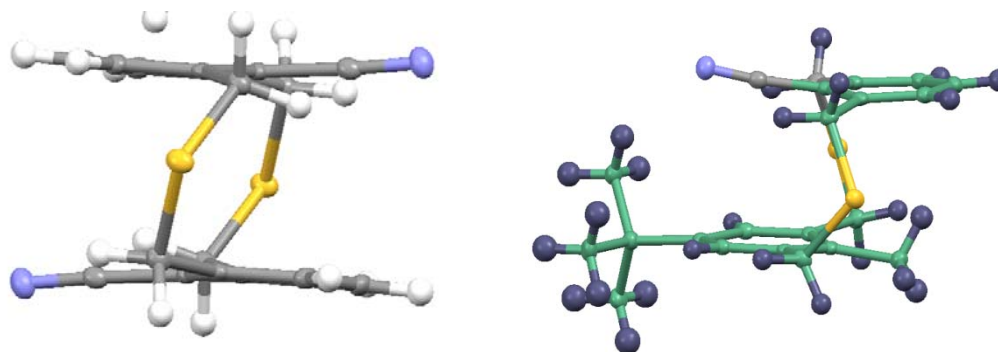


Figure 5.6 Molecular diagrams of diisobutenyl CPD 178 (left) and distyryl CPD 202 (right) derived from X-ray structures



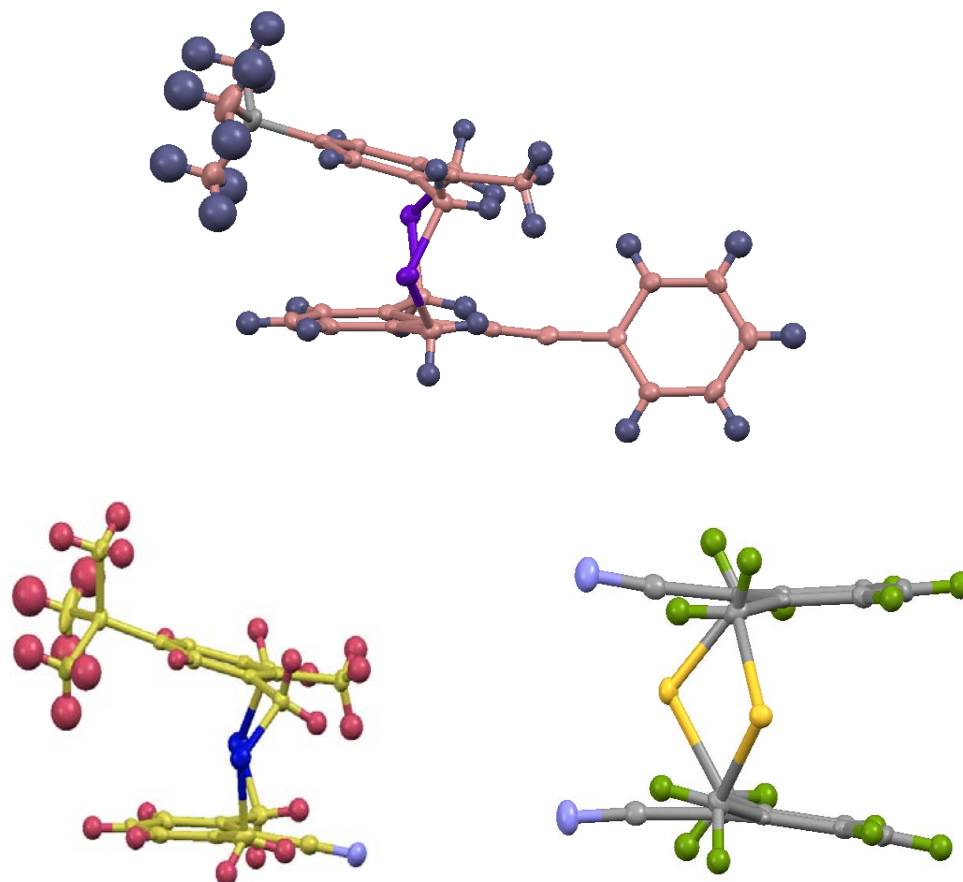
5.5 *Anti*-thiacyclophanes

Figure 5.7 Molecular diagrams of dicyano-*anti*-thiacyclophane **100** and cyano-methyl-*anti*-thiacyclophane **131** derived from X-ray structures



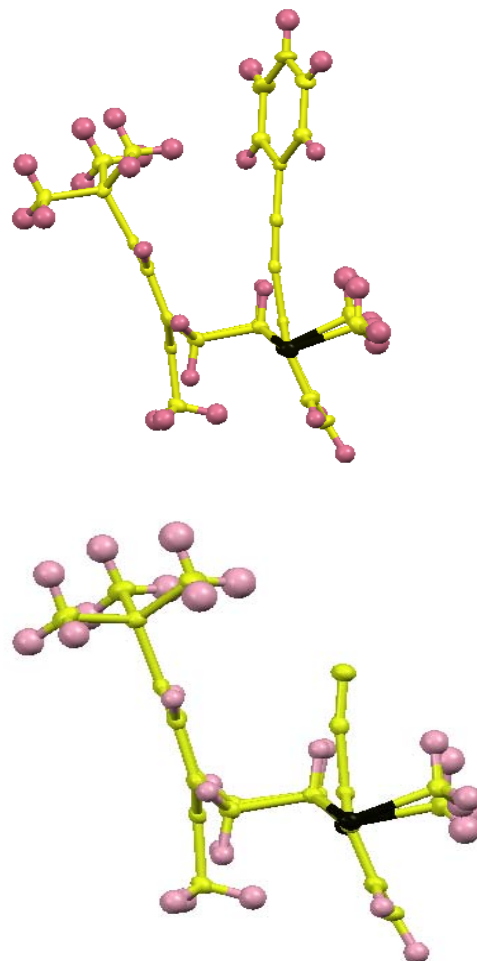
A comparison of dicyano *anti*-thiacyclophane **100** and cyano-methyl *anti*-thiacyclophanes **131** in their X-ray structures (Figure 5.7) does not indicate any observable difference in bond lengths and inter-plane distance. Generally, with increasing steric bulk at the internal positions, the phenyl rings of the thiacyclophane nucleus bend away from the planarity so as to minimize the steric interaction. However a nitrile group is not significantly different from a methyl group which explains why the structures are similar.

Figure 5.8 Molecular diagrams of phenylethynyl/methyl-*syn*-thiacyclophane **145** (top), cyano-methyl-*syn*-thiacyclophane **130** (bottom right), dicyano-*syn*-thiacyclophane **108** (bottom left) derived from X-ray structures



Syn-thiacyclophanes, on the other hand, show considerable differences in the inter-plane distances among the three cyclophanes studied, dicyano **108**, cyano-methyl **130** and phenylethynyl/methyl **145**. The deviation from planarity in dicyano *syn*-thiacyclophane **108** is much less than that for cyano-methyl **130** and phenylethynyl/methyl **145**. However, this difference is believed to arise not from the internal groups but from the *tert*-butyl group present at C-6.

Figure 5.9 Molecular diagrams of phenylethynyl/methylcyclophane **146** (top) and cyano-methylcyclophane **134** (bottom) derived from X-ray structures



5.6 Thiomethylcyclophanes

The NMR data of the pure isomers of different thiomethylcyclophane (dicyano **114**, cyano-methyl **134**, phenylethynyl/methyl **146**, diformyl **174** and divinyl **171**) was indicative of the di-equatorial orientation of the thiomethyl groups. In order to confirm this assignment, X-ray structure for cyano-methyl cyclophane **134** and phenylethynyl/methyl thiomethyl-cyclophane **146** were obtained (Figure 5.9) which is quite consistent with our supposition.

Chapter 6: Conclusions

6.1 Synthesis

Synthesis of a series of cyclophanedienes with different internal groups was accomplished successfully. CPDs **85** (dicyano), **127** (cyano-methyl) and **138** (phenylethynyl/methyl) were synthesized in 25-35% overall yield from bis-bromomethyl starting material via thiacyclophane-thiomethylcyclophane intermediates. Diformyl CPD **152** and bis(hydroxymethyl) CPD **159** were obtained by the reduction of dicyano CPD **85** and diformyl CPD **152** respectively. Cyclophanedienes with internal olefinic (substituted/non-substituted) groups such as alkylvinyl (**162**, **178** and **198**), butadienyl (**184**, **185** and **186**), styryl (**202**, **203** and **204**), nitro-substituted styryl (**210**, **211** and **212**), methoxy-substituted styryl (**218**, **219** and **220**) and methyl substituted styryl (**226**, **227** and **228**) were synthesized in moderate to good yields starting from dicyano thiomethylcyclophane **99** i.e functional group interconversions in **99** followed by Hoffmann elimination. Internal ethynyl substituted cyclophanedienes **235** and **237** were also synthesized by this route. Two other routes for the synthesis of the internal olefinic CPDs were also developed; FGIs in cyclophanedienes, and FGIs in dicyano thiacyclophane **100** followed by Wittig rearrangement-Hoffmann elimination sequence; although these routes provided lower yields

Phenylethynyl DHPs **141** and **247** were obtained by the Sonogashira coupling of diethynyl DHP **236**. The Eglinton coupling reaction was used to achieve butadiynyl DHPs **257** and **254**. Naphthoyl DHPs **248** and **250** were synthesized by the Friedel-Crafts acylation reaction of DHP **179** and **167** respectively.

6.2 Thermal isomerization of cyclophanedienes

Dicyano CPD **85** was quite stable towards its thermal isomerization to the dihydropyrene **86** and showed a calculated half life of ~36 years at room temperature, a number three orders of magnitude higher than that of benzo CPD **53** (7.3 days). Cyano-methyl (**127**), phenylethynyl/methyl (**138**) and diformyl CPDs (**152**) showed half lives less than a month at 20 °C. Cyclophanedienes with internal ethynyl and substituted vinyl groups were quite stable thermally and showed half lives of several years (1-16 years) at room temperature. Substituents on the internal vinyl group have quite remarkable effects on the half lives of cyclophanedienes, e.g. $\tau_{1/2}$ at 100 °C for divinyl CPD **166** (7 min), *cis*-dipropenyl CPD **162** (94 min), diisobutenyl CPD **178** (270 min). CPDs with *cis* substituted internal vinyl groups were thermally more stable than their *trans* counterparts, e.g. $\tau_{1/2}$ at 100 °C for *cis*-**162** and *trans*-**198** propenyl CPDs are 94 and 15 min respectively. Electron withdrawing substituents (NO₂) accelerate whereas electron donating (MeO, Me) decelerate the thermal return reaction of all the geometrical isomers of *p*-substituted styryl CPDs. Naphthoyl CPDs **249** and **251** isomerized at rates about 6-12 faster than their non-naphthoylated analogues **178** and **166** respectively.

6.3 Thermal rearrangement of dihydropyrenes

The [1,5]-sigmatropic rearrangement of internal nitrile (DHPs **86** and **128**) and formyl (DHP **153**) groups were observed. The sigmatropic rearrangement of nitrile in **86** was quite favourable in CDCl₃ (E_{act} 23.4 kcal/mol) compared to benzene (E_{act} 28.6 kcal/mol). The sigmatropic rearrangement of nitrile in the unsymmetrical DHP **128** was much more facile when compared with dicyano DHP **86**. Formyl groups showed a much higher migration aptitude and E_{act} is estimated to be < 20 kcal/mol in any solvents.

6.4 Photochemical isomerization

Disubstituted vinyl (**179**) and *cis* substituted vinyl DHPs (**164**, **205**, **213**, **221** and **229**) opened completely; however their opening rates although much faster than parent **43** were 4-6 times slower than the benzo DHP **47**, a standard for comparison. Dicyano DHP **86**, diethynyl DHP **236** and the unsymmetrical isomers of internal olefinic DHPs (**206**, **214**, **222** and **230**) formed photostationary states (pss) in the photoopening experiment. DHPs with internal ethenyl (**167**, **238** and **241**), substituted ethynyl (**139**, **141** and **247**) and *trans* substituted vinyl (**199**, **207**, **215**, **223** and **231**) groups failed to open in visible light irradiation experiment. In brief, introduction of a *trans* substituent on the internal olefinic group did not assist in photoopening whereas a *cis* substituent or both *cis* and *trans* substituents favoured photoopening of dihydropyrenes. Moreover, introduction of an electron withdrawing substituent on the internal styryl group decelerated the visible opening reaction (DHPs **213** and **214**) whereas electron donating groups accelerated it (DHPs **221** and **222**). Naphthoyl DHP **250** opened at rates quite comparable to that of benzo DHP **47** whereas naphthoyl diisobutenyl DHP **248** opened about 25 times faster than the benzo DHP and is one of the best new photochromes yet.

The following table gives a brief summary of the thermal and photochemical data of all the compounds.

Table 6.1. Summary of half lives of cyclophanedienes and visible opening time of their corresponding dihydropyrenes

No.	Cyclophanediene	$\tau_{1/2}$ (100 °C)*	Dihydropyrene	Visible opening time
1	85	5 h	86	Overnight [#]
2	178	4.5 h	179	13 min
3	162	94 min	164	3 h
4	235	124 min	236	7 h [#]
5	218	130 min	221	17 min
6	226	132 min	229	17 min
7	186	115 min	192	Isomerized to 190
8	202	91 min	205	20 min
9	185	82 min	191	Isomerized to 190
10	219	92 min	222	43 min [#]
11	203	73 min	206	66 min [#]
12	227	87 min	230	50 min [#]
13	220	64 min	223	Failed to open
14	249	43 min	248	4-5 s
15	210	77 min	213	30 min
16	211	59 min	214	~ 3h [#]
17	228	63 min	231	Failed to open

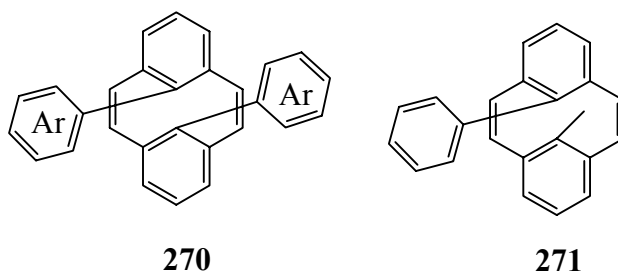
18	212	55 min	215	Failed to open
19	184	45 min	190	Failed to open
20	204	40 min	207	Failed to open
21	237	24 min	238	Failed to open
22	240	23 min	241	Failed to open
23	198	~15 min	199	Failed to open
24	166	7.7 min	167	Slow (dec)
25	138	15.2 h (50 °C)	139	Failed to open
26	127 (benzene)	6.7 h (50 °C)	128	Unstable (dec.)
27	152	4.2 h (50 °C)	153	Decomposes
28	127 CDCl ₃	5.2 h (50 °C)	128	Unstable (dec.)
29	251	3 h (50 °C)	250	2 min
30	158	~ 1 h (20 °C)	159	Decomposes
31			141	Failed to open
32			247	Failed to open
33			257	Failed to open
34			254	~ 3h
35			151	Failed to open

Photostationary state was formed * Errors estimated are less than 5%

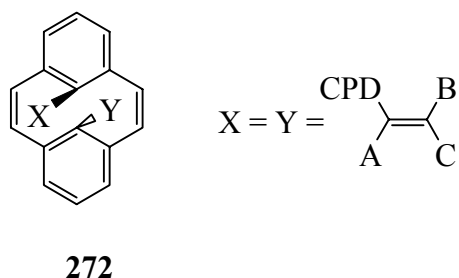
6.5 Future Work

A series of thermally stable cyclophanedienes have been synthesized during the course of this project, however there is still a great potential of research in this field both from a mechanistic and a practical application (commercial) point of view. Substituted

vinyl cyclophanedienes have shown a good compromise between the thermal stability and photoopening. However a closely related series in which the internal vinyl group is a part of aromatic ring e.g. diphenyl CPD **270** or similar compounds with other internal aromatic rings such as furan, thiophene and pyridine needs to be studied. Monophenyl photoswitch **271** has already been made and studied, however the previous synthesis of **270** failed probably because of steric overcrowding⁸⁵. However, if it could be made, we believe that **270** would behave quite differently (compare dicyano **85** and cyano-methyl **127**). Synthesis of **270** and similar compounds is challenging because of increased steric crowding at the internal positions.

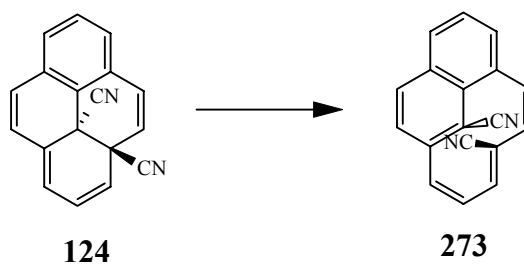


We synthesized several substituted vinyl cyclophanedienes but none of them had a strong electron donating or electron withdrawing group attached directly (groups A, B and C in **272**) to the vinyl group. A study of these vinyl cyclophanedienes would give further insight into the relative contribution of steric and electronic effects absent in this study.



All the olefinic CPDs studied contained hydrogen as group A (CPD **272**). Introduction of methyl, phenyl and styryl groups at this position may have some strong favourable steric effects. Diisobutenyl pair **178/179** (B and C are methyl groups in **272**) showed great thermal stability because of the steric contributions from the methyl groups, however replacement of the methyl groups with ethyl, isopropyl, *t*-butyl would be an interesting project to see the upper limit of steric tolerance.

In the substituted styryl series, electronic effects were studied only at the *para* position; however a study of electronic and steric effects at the *ortho* and *meta* positions would help in designing more sophisticated photoswitches.



We realized that the products of sigmatropic rearrangement (dicyano **124**, cyano-methyl **137**) can also behave as a photoswitch because they still contains a hexadiene moiety. An example of the reaction is shown above. The reaction would be an uphill process, as expected, however by modeling the reaction, suitable substituents may be found to favour this process. Once it is successful it will help in multimode high density storage devices with both permanent and erasable memories CPD \rightarrow DHP \rightarrow mig. prod. \rightarrow mig. open etc.

Investigation of the captodative effect in the Woodward-Hoffmann forbidden reaction and the sigmatropic rearrangements would aid in understanding the mechanism of these reactions as well as in designing the multimode photoswitches mentioned above.

Chapter 7: Experimental

7.1 General experimental conditions

Melting points were determined on a Reichert 7905 melting point apparatus integrated to an Omega Engineering model 199 Chromel-alumel thermocouple. ^1H and ^{13}C NMR spectra were recorded, unless otherwise specified, on a Bruker Avance 500 MHz spectrometer (500.1 MHz for ^1H , 125.7 MHz for ^{13}C). Spectra were calibrated based on the solvent residual peak (5.32 and 54.00 ppm for CD_2Cl_2 , 7.26 and 77.23 ppm for CDCl_3 , 7.16 and 128.39 ppm for C_6D_6). NMR assignments were made on the basis of 2D COSY/NOESY experiments for ^1H and HSQC and HMBC experiments for ^{13}C . The numbering for the structures shown in experimental is for NMR peak identification. H-1,2 means H-1 and H-2; H-1/2 means H-1 or H-2; H-1-3 means H-1, H-2 and H-3. Expanded data sets were used to obtain coupling constant data. Kinetic data were obtained using a Bruker AC 300 MHz or Bruker AV 300 MHz (unless otherwise specified) spectrometer.

Infrared spectra, calibrated with polystyrene, were recorded on a Thermo Nicolet IR 200 spectrometer as KBr pellets or thin film from dichloromethane on NaCl plates and only the major bands are reported. UV-vis spectra were recorded on a Cary 5 UV-vis-NIR spectrometer. Units of ϵ_{max} are $\text{L mol}^{-1} \text{cm}^{-1}$. Mass spectra were recorded on a Finnigan 3300 gas chromatography-mass spectroscopy system using methane as a carrier gas for chemical ionization or electron impact (EI) at 70 eV. Exact mass measurements were obtained on a Kratos Concept-H instrument using perfluorokerosene as the standard. Elemental analyses were performed by Canadian Microanalytical Services Ltd., Vancouver, B.C. All evaporation were carried out under reduced pressure on a rotary

evaporator, or by using an oil pump and liquid nitrogen condenser. Silica gel refers to Merck silica gel, 60-200 mesh. Alumina refers to Aldrich Aluminum oxide, activated neutral, Brockmann I, standard grade, ~ 150 mesh. Tetrahydrofuran (THF) was dried by distillation from potassium benzophenone ketyl. DCM and DMF were dried over calcium hydride. Toluene was used directly without drying; water contents less than 0.03%. Salts used in the Wittig reaction, except methyl triphenylphosphonium bromide and ethyl triphenylphosphonium bromide, were prepared according to the literature procedure and confirmed by their spectral data.

7.2 General procedure for crystal growth

10-20 mg of the sample was dissolved in 2-3 ml of an organic solvent (DCM for **100**, **108**, **86**, **117**, **235**, **236**, **134**; cyclohexane for **130**, **131**, **134**, **167**, **178**; isopropanol for **148**; acetone for **179**, and benzene for **136**) and the solvent was allowed to evaporate slowly. In the cases of thiacyclophanes **130** and **131**, cyclohexane was heated to boiling and the resulting solution, when cooled down to room temperature, yielded nice crystals instantly. Crystals of Phenylethynyl/ methyl DHP **139** were obtained when methanolic solution (5 mg in 4-5 ml) was placed in a freezer for a week.

7.3 Experimental conditions for X-ray crystallographic studies

Crystals of the compound were removed from the flask, a suitable crystal was selected, attached to a glass fiber and data was collected at 90(2) K using a Bruker/Siemens SMART APEX instrument (Mo K α radiation, $\lambda = 0.71073 \text{ \AA}$) equipped with a Cryocool NeverIce low temperature device. Absorption corrections were applied using SADABS. The structure was solved by direct methods and refined by least squares

method on F² using the SHELXTL program package. All non-hydrogen atoms were refined anisotropically.

7.4 General procedure for S-Methylation

Mixed isomers of thiomethyl-*m*-cyclophane (1.00 mmol) in dry CH₂Cl₂ (20 mL) was added slowly to (MeO)₂CHBF₄⁵⁹ (80% oil, 600 mg, 3 mmol) at -78 °C with stirring under nitrogen. The mixture was then stirred at 20 °C for 3 h. The CH₂Cl₂ was decanted and ethyl acetate (40 mL) was added and stirring (trituration) was continued for a further 3 h. Decantation followed by more ethyl acetate and stirring was used if required. The white precipitate was then collected and dried to give bis-sulfonium salt in greater than 90% yield (unless otherwise specified). This was used directly in the next step.

7.5 General procedure for the Hoffmann elimination

[Note: to avoid photochemical conversion of the cyclophanediene product to the dihydropyrene, these operations should be carried out under minimal light] *t*-BuOK (280 mg, 2.50 mmol) was added to a stirred suspension of mixed isomers of bis-sulfonium salt (1 mmol), in THF (25 mL) under argon at 20 °C. After stirring for 30 minutes, water (unless otherwise specified) was added and then dichloromethane (120 mL). The extract was washed, dried and evaporated. The residue was chromatographed over silica gel to give 50-90% yield of cyclophanediene(s).

7.6 General procedure for the thermal isomerization of cyclophanedienes to dihydropyrenes

Cyclophanediene (5-25 mg) in toluene (1-2 mL) was sealed in a glass tube under argon and heated at 100 °C until it isomerized completely to the dihydropyrene. The

reaction was monitored by ^1H NMR spectroscopy. No *cis-trans* isomerization of the internal olefinic substituents was observed during the thermal return experiment. Dicyano DHP **86** and cyano-methyl DHP **128** were obtained by photochemical isomerization. Bis(hydroxymethyl) dihydropyrene **160** was obtained from the bis(hydroxymethyl) CPD **159** at room temperature.

7.7 General procedure for Wittig reaction

7.7.1 Procedure A

BuLi (1.6 mL of 2.5M in hexanes, 4.0 mmol) was added dropwise to a suspension of alkyl triphenylphosphonium bromide (3.22 mmol) in THF (20 mL) under argon at 0 °C and the mixture was stirred for 20 minutes. After that time, a clear and orange to red solution was obtained. To this solution, diformylthiomethylcyclophane **174** (1.46 mmol) was added and the reaction mixture was allowed to stir for 1.5 h and then quenched with water. The resulting solution was extracted with CH_2Cl_2 (4 x 20 mL), dried over anhydrous MgSO_4 and evaporated. The crude mixture was chromatographed over silica gel.

7.7.2 Procedure B

t-BuOK (14.3 mmol) was added to a suspension of alkyl triphenylphosphonium bromide (10.2 mmol) in THF (40 mL) under argon at room temperature and the solution was stirred for 20 minutes. After that time, a clear and dark orange red solution was obtained. To this solution, diformylthiomethylcyclophane **174** (4 mmol) was added and the reaction mixture was allowed to stir for an hour at room temperature and then quenched with water. The resulting solution was extracted with CH_2Cl_2 (4 x 40 mL),

dried over anhydrous MgSO_4 and evaporated. The crude mixture was chromatographed over silica gel.

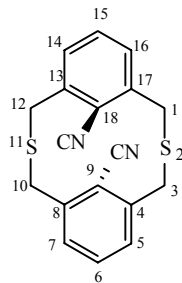
7.8 General procedure for photoopening (NMR)

1-2 mg of the dihydropyrene sample was dissolved in NMR solvent. The NMR tube was capped and wrapped with Teflon film. The sample was irradiated with light using a 500W household tungsten-halogen lamp (8500 lumens) as the light source and a 490 nm cut off filter. Irradiation was continued until color faded or a photo stationary state is reached. Irradiation was stopped after 16 h if no change is observed in the ^1H NMR spectrum.

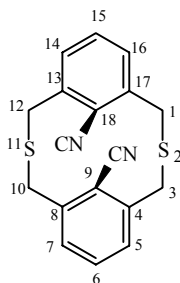
7.9 Syntheses

9,18-Dicyano-2,11-dithia[3.3]cyclophane

The bis(bromomethyl)nitrile⁵⁴ **102** (28.0 g, 97 mmol) in de-aerated benzene (700 mL) in one dropping funnel was added at the same drop rate (~ 1 every 2-3 seconds) as $\text{Na}_2\text{S}\cdot 9\text{H}_2\text{O}$ (23.2 g, 97 mmol) in de-aerated water (700 mL) in a second funnel to a mixture of vigorously stirred ethanol (95%, 2333 mL) and water (367 mL) under nitrogen. The addition took about 8 hours. The solvent was then evaporated and the residue was dissolved in CH_2Cl_2 and washed with water. The organic layer was washed, dried and evaporated, and the residue was chromatographed on silica gel using CH_2Cl_2 -hexanes (6:4) as eluant.

**anti -100**

Eluted first was 3.3 g (21%) of *anti*-**100** as colorless crystals from dichloromethane: mp ~ 220 °C dec; ^1H NMR (CDCl_3) δ 7.66-7.60 (m, 6H, ArH), 3.94 and 3.88 (AB, $J = 14.4$ Hz, 8H, $-\text{CH}_2-$); ^{13}C NMR (CDCl_3) δ 140.80 (C-4,8,13,17), 134.44 (C-6,15), 130.73 (C-5,7,14,16), 115.38 (CN), 114.53 (C-9,18), 32.19 (C-1,3,10,12); IR ν (KBr) 2216, 1588, 1464, 1445, 1408, 1237, 810, 801, 752 cm^{-1} ; UV (CH_2Cl_2) λ_{max} (ϵ_{max}) 305 nm (3400); EI MS m/z 322 (M^+). X-Ray structure- see Appendix A

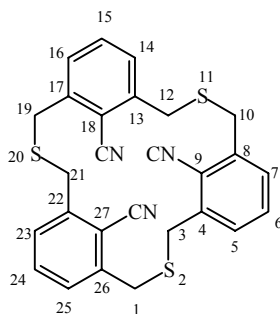
**syn -108**

Eluted second was 3.4 g (22%) of *syn*-**108** as colorless crystals from dichloromethane: mp ~ 220 °C dec; ^1H NMR (CDCl_3) δ 7.15 (triplet, $J = \sim 7.3$ Hz, 4H, H-5,7,14,16), 7.07 (triplet, $J = \sim 7.3$ Hz, 2H, H-6,15), 4.55 and 3.81 (AB, $J = 15.5$ Hz, 8H, $-\text{CH}_2-$); ^{13}C NMR (CDCl_3) δ 141.96 (C-4,8,13,17), 132.97 (C-6,15), 129.51 (C-5,7,14,16), 116.69 (CN), 113.13 (C-9,18), 35.90 (C-1,3,10,12); IR ν (KBr) 2212, 1590, 1466, 1452,

1414, 794, 751 cm^{-1} ; UV (CH_2Cl_2) λ_{max} (ϵ_{max}) 298 nm (5800); EI MS m/z 322 (M^+). X-

Ray structure: see Appendix A

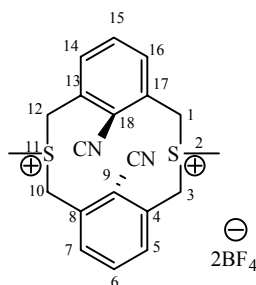
9,18,27-Tricyano-2,11,20-trithia[3.3.3]metacyclophane **109**



109

Eluted third was 3.2 g (21%) of the trimer **109** as colorless crystals from dichloromethane: mp ~ 220 °C dec. ^1H NMR δ 7.46-7.39 (m, 9H, ArH), 3.79 (s, 12H, - CH_2 -); ^{13}C NMR δ 141.78 (C-4,8), 132.73 (C-6,15), 128.61 (C-5,7), 115.19 (CN), 114.05 (C-9), 33.78 (C-1,3); IR ν (KBr) 2213, 1590, 1466, 795, 754 cm^{-1} ; UV-Vis (CH_2Cl_2) λ_{max} nm ϵ_{max} 295 (4700); EI MS m/z 483 (M^+).

Bis-sulfonium salt **110**

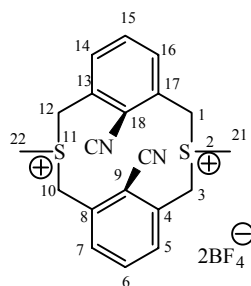


110

anti-Thiacyclophane **100** (400 mg, 1.24 mmol) in dry CH_2Cl_2 (15 mL) was added slowly to $(\text{MeO})_2\text{CHBF}_4$ (80% oil, 550 mg, 2.7 mmol) at -78 °C with stirring under nitrogen. The mixture was then stirred at 20 °C for 3 h. The CH_2Cl_2 was decanted and

ethyl acetate (40 mL) was added and stirring (trituration) was continued for a further 3 h. The white precipitate was then collected and dried to give 650 mg (quant.) of bis-sulfonium salt **110**. This was used directly in the next step. ^1H NMR (DMSO- d_6) δ 8.14-8.12 (m, 2H), 7.98-7.97 (m, 4H), 5.14 and 4.27 (AB, $J = 14.7$ Hz, 4H $-\text{CH}_2-$), 5.01 and 4.92 (AB, $J = 14.1$ Hz, 4H, $-\text{CH}_2-$), 3.46 (s, 6H, $-\text{CH}_3$).

Bis-sulfonium salt **115**



115

syn-Thiacyclophane **108** under the same conditions used for the synthesis of **110** gave the sulfonium salt **115** in quantitative yield.

^1H NMR (DMSO- d_6) δ 8.0-7.8 (m), 7.52 (s), 7.48 (t, $J = 7.8$ Hz), 7.26 (d, $J = 7.7$ Hz), 7.20-7.12 (m), 5.44 (d, $J = 14.0$ Hz), 5.19 (s), 5.15-5.05 (m), 4.22 and 4.11 (AB, $J = 15$ Hz), 3.45-3.40 (m), 3.32 (br s).

2, 10-Bis(thiomethyl)-8,16-dicyano-*anti*-[2.2]cyclophane

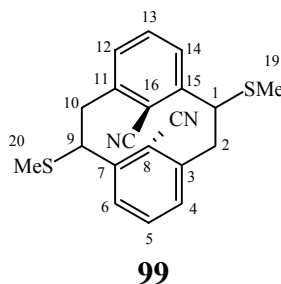
t-BuOK (330 mg, 2.94 mmol) was added to a stirred suspension of mixed isomers of salt **110** (600 mg, 1.15 mmol) in THF (25 mL) under argon at 20 °C. After stirring for 3 h, water was added and then dichloromethane (120 mL). The extract was washed, dried and evaporated. The residue was chromatographed over silica gel using CH_2Cl_2 -hexane

(6:4) as eluant to give 385 mg (98%) of product **99** as a mixture of isomers, EI MS m/z 350 (M^+ , 100%). These could be used directly in the next step.

Mixture of *anti* isomers

^1H NMR (CDCl_3) δ 8.14-8.12 (m), 8.07-8.04 (m), 7.7 -7.40 (m), 6.64 (s), 6.23 (d, $J = 9.0$ Hz), 5.89-5.85 (m), 5.67 (s), 5.29, 5.26 (s), 4.69-4.65 (m), 4.44-4.41 (m), 4.21-4.16 (m), 3.77-3.71 (m), 3.57-3.34 (m), 2.95-2.89 (m), 2.53, 2.39, 2.35, 2.20, 2.19, 2.18, 2.17, 2.16 (s).

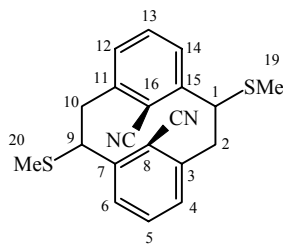
For characterization, re-chromatography yielded a single isomer of **99**, in which the 1,9-thiomethyl groups are pseudo-equatorial (48%).



mp \sim 215 dec. ^1H NMR (CDCl_3) δ 8.05-8.03 (m, 2H, H-6,14), 7.58-7.56 (m, 4H, H-4,5,12,13), 4.17 (dd, $J = 11.5, 3.6$ Hz, 2H, H-1,9), 3.53 (dd, $J = 12.8, 3.6$ Hz, 2H, H-2_{eq},10_{eq}), 2.87 (dd, $J = 12.8, 11.5$ Hz, 2H, H-2_{ax},10_{ax}), 2.17 (s, 6H, -SMe); ^{13}C NMR (CDCl_3) δ 141.00 (C-3,11), 140.29 (C-7,15), 134.56 (C-5,13), 130.78 (C-4,12), 127.31 (C-6,14), 119.75 (C-8,16), 114.92 (CN), 54.54 (C-1,9), 44.60 (C-2,10), 15.82 (CH_3); IR ν (KBr) 2215, 1579, 1460, 1440, 1431, 806, 766, 743, 580, 497 cm^{-1} ; UV (CH_2Cl_2) λ_{max} (ϵ_{max}) 303 nm (1270); EI MS m/z 350 (M^+); HR MS Calcd for $\text{C}_{20}\text{H}_{18}\text{N}_2\text{S}_2$: 350.0911. Found: 350.0902. Anal. Calcd: C, 68.55; H, 5.18; N, 8.00. Found: C, 67.69; H, 5.24; N, 7.79.

Mixture of *cis*-isomers **114**

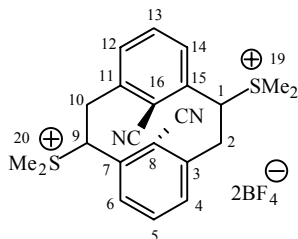
Bis-sulfonium salt **115** under the Stevens rearrangement conditions gave < 10% yield of the *syn*-cyclophane **114** as a mixture of isomers along with ~ 90% yield of the *anti*-isomers **99**. Column chromatography over silica gel using hexanes: DCM 4:6 eluted *trans*-isomers **99**. Hexanes: DCM 3:7 eluted **114** as a mixture of *syn*-isomers



114

$^1\text{H NMR}$ (CDCl_3) δ 8.12-8.09 (m), 8.04-8.01 (m), 7.60-7.40 (m), 7.21 (d, $J = 7.4$ Hz), 7.16 (d, $J = 7.7$ Hz), 7.14 (d, $J = 7.5$ Hz), 6.91 (t, $J = 7.4$ Hz), 6.83 (t, $J = 7.6$ Hz), 6.73 (t, $J = 7.5$ Hz), 6.60 (d, $J = 7.6$ Hz), 6.49 (d, $J = 7.4$ Hz), 5.20-5.14 (m), 4.54 (d, $J = 15.4$ Hz), 4.25-4.14 (m), 3.82-3.72 (m), 3.55-3.38 (m), 2.91-2.61 (m), 2.43-2.37 (dd, $J = 14.1, 8.0$ Hz), 2.21, 2.19, 2.17, 2.16, 2.15, 2.14, 2.13 (s).

2, 10-Bis(thiomethyl)-8,16-dicyano-*anti*-[2.2]cyclophane bis-sulfonium salt **111**

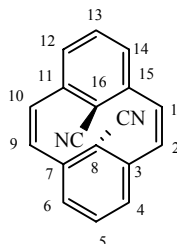


111

Using procedure 7.3 and the pure 1,9-diequatorial-thiomethyl isomer of **99** (350 mg, 1.00 mmol) gave the product **111** as a single isomer, $^1\text{H NMR}$ ($\text{DMSO-}d_6$) δ 8.18-

7.81 (m, 6H, ArH), 4.92 (dd, $J = 11.5, 3.6$ Hz, 2H, H-1,9), 4.01 (dd, $J = 12.8, 3.6$ Hz, 2H, H-2_{eq}, 10_{eq}) and 3.19 (~ t, $J = \sim 12$ Hz, 2H, H-2_{ax}, 10_{ax}), 3.46 and 3.07 (s, 6H, -SMe₂).

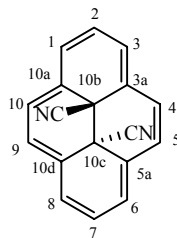
8,16-Dicyano-*anti*-[2.2]metacyclophane-1,9-diene 85



85

Using procedure 7.4 and then column chromatography over silica gel using CH₂Cl₂ as eluant gave (190 mg, 0.75 mmol, 75%) of cyclophanediene **85** as colorless crystals, which on attempted mp determination converts into DHP **86** and migration products: ¹H NMR δ 7.54 (t, $J = 7.6$ Hz, 2H, H-5,13), 7.01 (d, $J = 7.6$ Hz, 4H, H-1,3,6,8), 6.63 (s, 4H, H-1,2,9,10); ¹³C NMR δ 140.66 (C-3,7,11,15), 135.91 (C-5,13), 134.81 (C-1,2,9,10), 128.52 (C-4,6,12,14), 120.11 (C-8,16), 115.81 (CN); IR ν (KBr) 2215, 1560, 1442, 859, 810, 757, 570 cm⁻¹; UV (CH₂Cl₂) λ_{max} (ε_{max}) 225 (30,000), 282 (9800), 330 (4800), 367(1600); EI MS m/z 254 (M⁺); HR MS Calcd for C₁₈H₁₀N₂: 254.0843. Found: 254.0833.

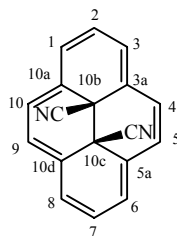
***trans*-10b,10c-Dicyano-10b,10c-dihydropyrene 86.**



86

Irradiation of a solution of cyclophanediene **85** in CH₂Cl₂ (concentration is not critical, 5 mg/mL is convenient) with a UV source with output 254 nm quickly converts **85** in to **86** quantitatively; however, **86** slowly converts thermally in to **124**, even at room temperature (see below), and so irradiation should not be continued unnecessarily. Careful evaporation of the dichloromethane yields green crystals of product **86**. On attempted mp determination, these turn colorless (from ~ 70 °C up, depending upon the rate of heating, and finally melt at 142-144 °C, corresponding to **124**). Slow evaporation (in dark) from CH₂Cl₂ yielded X-ray suitable crystals of **86**. (see Appendix A); ¹H NMR δ 8.97 (s, 4H, H-4,5,9,10), 8.83 (d, *J* = 7.8 Hz, 4H, H-1,3,6,8), 8.37 (t, *J* = 7.8 Hz, 2H, H-2,7); ¹³C NMR δ 127.45 (C-3a,5a,10a,10d), 126.71 (C-4,5,9,10), 126.30 (C-2,7), 125.46 (C-1,3,6,8), 108.64 (CN), 30.76 (C-10b,10c). IR ν (KBr) 2227, 1351, 1254, 974, 930, 855, 767, 620 cm⁻¹; UV (CH₂Cl₂) λ_{max} (ε_{max}) 331 (87,300), 367 (34,300), 442 (6400), 528 (80), 599 (130), 640 (770); EI MS *m/z* 254 (M⁺); HR MS Calcd for C₁₈H₁₀N₂: 254.0843. Found: 254.0832. Anal. Calcd: C, 85.02; H, 3.96; N, 11.02. Found: C, 84.22; H, 4.07; N, 10.91.

***cis*-10b,10c-Dicyano-10b,10c-dihydropyrene 117.**

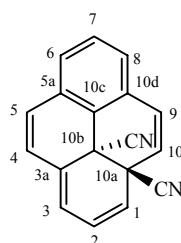


117

If a mixture of *syn*- and *anti*-cyclophane **114** and **99** is employed in the *S*-methylation and Hoffmann elimination reaction sequence, then *cis*-DHP **117** is obtained in a 5% yield along with > 90% of dicyano CPD **85**. The *cis*-dihydropyrene **117** was

obtained as dark green crystals from dichloromethane, mp 192 °C (dec); ^1H NMR (CDCl_3) δ 8.97 (4H, s, H-4,5,9,10), 8.66 (4H, d, $J = 7.8$ Hz, H-1,3,6,8), 8.10 (2H, t, $J = 7.8$ Hz, H-2,7); ^{13}C NMR (CDCl_3) δ 129.22 (C-4,5,9,10), 126.14 (C-1,3,6,8), 124.97 (C-3a,5a,10a,10d), 124.04 (C-2,7), 115.28 (CN), 33.15 (C-10b,10c); IR ν (KBr) 3046, 2925, 2227, 1654, 1593, 1261, 970, 852, 630 cm^{-1} ; UV (CH_2Cl_2) λ_{max} (ϵ_{max}) 331 (67100), 360 (21600), 438 (5700), 635 (670); EI MS m/z 254 (M^+); HR MS Calcd for $\text{C}_{18}\text{H}_{10}\text{N}_2$: 254.0843. Found: 254.0839. Anal. Calcd: C, 85.02; H, 3.96; N, 11.02. Found: C, 80.83; H, 3.93; N, 9.77.

***trans*-10a,10b-Dicyano-10a,10b-dihdropyrene 124.**

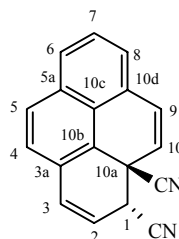


124

Dihdropyrene **86** (10mg) was sealed in a glass tube under argon and heated at 70 °C for 30 min (or until completely colorless), which quantitatively converted it into colorless **124**; evaporation gave crystals: mp 143-145 °C; ^1H NMR δ 7.35 (t, $J = 7.7$ Hz, 1H, H-7), 7.16 (dd, $J = 7.7, 1.1$ Hz, 1H, H-8), 7.13 (dd, $J = 7.7, 1.0$ Hz, 1H, H-6), 6.91 (d, $J = 9.2$ Hz, 1H, H-9), 6.60-6.57 (m, 2H, H-2,5), 6.43 (d, $J = 9.7$ Hz, 1H, H-4), 6.30 (dd, $J = 5.7, 0.6$ Hz, 1H, H-3), 6.17 (d, $J = 9.2$ Hz, 1H, H-10), 6.09 (d, $J = 9.2$ Hz, 1H, H-1); ^{13}C NMR δ 132.74 (C-3a,9), 132.13 (C-5a), 131.82 (C-10a), 130.81 (C-2), 130.75 (C-7), 129.74 (C-5), 128.55 (C-6), 127.73 (C-8), 125.49 (C-4), 125.06 (C-10), 124.42 (C-10c), 124.32 (C-3), 124.09 (C-1), 116.65 (10b-CN), 116.15 (10c-CN), 42.68 (C-10b), 40.63

(C-10a); IR ν (KBr) 2227, 1578, 1467, 974, 909, 882, 828, 801, 757, 731, 708 cm^{-1} ; UV (CH_2Cl_2) λ_{max} (ϵ_{max}) 257 (22,000), 298 (5400), 311 (5400), 333 (5100), 348 (4300), 368 (3500), 385 (4100), 405 (2800); EI MS m/z 254 (M^+); HR MS Calculated for $\text{C}_{18}\text{H}_{10}\text{N}_2$: 254.0843. Found: 254.0834. Anal. Calcd: C, 85.02; H, 3.96; N, 11.02. Found: C, 82.49; H, 4.46; N, 10.05.

***trans*-1,10a-Dicyano-1,10a-dihydropyrene 125**



125

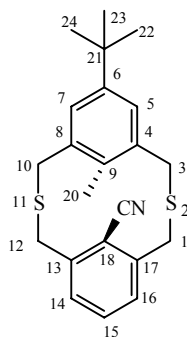
Dihydropyrene **86** (10 mg) in CDCl_3 (0.8 ml) was sealed in a glass tube under argon and heated at 70 $^\circ\text{C}$ for 4 days, which converted it into **125**. Evaporation gave colorless solid which decomposed on attempted chromatography but was pure enough to obtain the following data:

^1H NMR (CDCl_3) δ 7.86 (d, $J = 8.4$ Hz, 1H, H-5), 7.74 (dd $J = 0.9, 8.3$ Hz, 1H, 1H, H-6), 7.45 (dd, $J = 7, 8.4$ Hz, 1H, H-7), 7.41 (d, $J = 8.3$ Hz, 1H, H-4), 7.32 (dd, $J = 6.9, 0.8$ Hz, 1H, H-8), 7.08 (d, $J = 9.5$ Hz, 1H, H-9), 7.05 (d, $J = 9.4$ Hz, 1H, H-3), 6.11 (dd, $J = 9.4, 6.2$ Hz, 1H, H-2), 6.04 (1H, d, $J = 9.5$ Hz, H-10), 3.92 (dd, $J = 6.2, 0.6$ Hz, 1H, H-1); ^{13}C NMR (CDCl_3) δ 133.36 (C-5a), 133.15 (C-9), 132.87 (C-3), 129.91 (C-3a), 129.87 (C-5), 129.36 (C-6), 128.40 (C-10d), 127.53 (C-7), 126.95 (C-8), 126.55 (C-10c), 126.24 (C-4), 121.55 (C-10b), 120.84 (C-10), 117.92 (10a-CN), 117.62 (C-2), 114.53 (1-CN), 34.9 (C-10a), 29.9 (C-1); IR ν (KBr) 3055, 2918, 2224, 1590, 1503, 924,

905, 841, 789, 766, 690, 656 cm^{-1} UV (dichloromethane) λ_{max} , nm (ϵ_{max}) 262 (29700), 272 (37900), 342 (4420), 354 (4330), 373 (2200), 407 sh (240); EI MS m/z 254 (M^+) HR MS calcd for $\text{C}_{18}\text{H}_{10}\text{N}_2$: 254.0843. Found: 254.0829.

6-*t*-Butyl-18-Cyano-9-methyl-2,11-dithia[3.3]metacyclophanes **130** and **131**

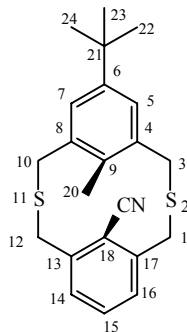
A solution of 2,6-bis(bromomethyl)benzonitrile⁵⁴ **102** (4.4 g, 15.2 mmol) and 2,6-bis-thiomethyl-4-*tert*-butyltoluene⁶⁴ **129** (3.80 g, 15.2 mmol) in de-aerated benzene (700 mL) was added drop wise to ethanolic KOH solution { prepare by adding KOH (4.83 g) in de-aerated water (230 mL) and ethanol (2090 mL) followed by addition of sodium borohydride (0.9 g)} under nitrogen. The drop rate was crucial (~ 1 every 3-4 seconds) and the addition took 44 hours. The solvent was then evaporated and the residue was dissolved in DCM and extracted with water, dried over MgSO_4 and evaporated. The residue was chromatographed on silica gel using CH_2Cl_2 -hexanes 3.5: 6.5 as eluant to give 1.9 g (5.17 mmol, 34%) of **131** as colorless crystals



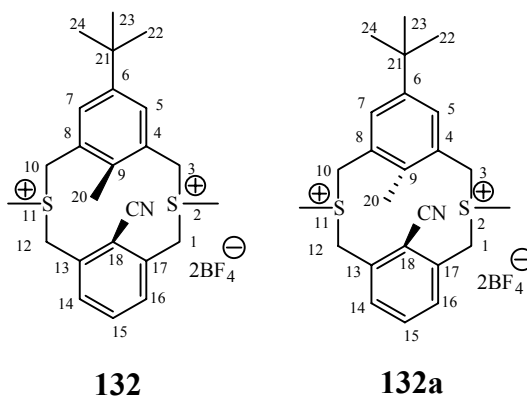
131

from cyclohexane: mp 147-148 $^{\circ}\text{C}$; $^1\text{H-NMR}$ (CDCl_3) δ 7.42-7.45 (m, 3H, H-14,15,16), 7.43 (s, 2H, H-5,7), 3.92 and 3.72 (AB, $J = 14.4$ Hz, 4H, H-1,12), 3.82 and 3.74 (AB, $J = 14.0$ Hz, 4H, H-3,10), 1.43 (s, 3H, Me), 1.39 (s, 9H, $\text{C}(\text{CH}_3)_3$); $^{13}\text{C NMR}$ δ 149.34 (C-6), 141.54 (C-13,17), 136.58 (C-9), 133.46 (C-4,8), 131.89 (C-15), 129.57 (C-14,16), 128.16

(C-5,7), 115.38 (CN), 115.12 (C-18), 34.58 ($\underline{\text{C}}(\text{CH}_3)_3$), 33.01 (C-3,10), 31.62 (C-1,12), 31.26 ($\text{C}(\underline{\text{C}}\text{H}_3)_3$), 15.37 (C-20); IR ν (KBr) 3027, 2954, 2217, 1588, 1483, 1464, 1417, 1236, 877, 804, 794, 755 cm^{-1} ; UV(cyclohexane) λ_{max} nm (ϵ_{max}) 297 (1410), 307 (1390); EI MS m/z 367 (100); HR MS Calcd for $\text{C}_{22}\text{H}_{25}\text{NS}_2$: 367.1428. Found: 367.1413. Anal. Calcd: C, 71.89; H, 6.86; N, 3.81. Found: C, 71.52; H, 6.87; N, 3.69.

**130**

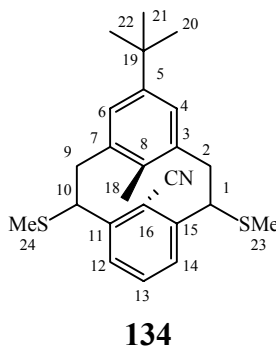
Eluted second using CH_2Cl_2 -hexanes 4.5:5.5 was 1.9 g (4.90 mmol, 32%) of the *syn*-thiacyclophane **130** as colorless crystals from cyclohexane, mp 166-167 $^\circ\text{C}$; ^1H NMR (CDCl_3) δ 7.07 (br s, 3H, H-14-16), 6.96 (s, 2H, H-5,7), 4.36 and 3.75 (AB, $J = 15.1$ Hz, 4H, H-1,12), 4.36 and 3.67(AB, $J = 15$ Hz, 4H, H-3,10), 2.56 (s, 3H, Me), 1.18 (s, 9H, $\text{C}(\underline{\text{C}}\text{H}_3)_3$); ^{13}C NMR δ 147.41 (C-6), 142.54 (C-13,17), 135.85 (C-4,8), 132.88 (C-15), 132.21 (C-9), 128.72 (C-14,16), 126.29 (C-5,7), 117.72 (CN), 111.65 (C-18), 35.79 (C-1,12), 34.94 (C-3,10), 34.27 ($\underline{\text{C}}(\text{CH}_3)_3$), 31.17 ($\text{C}(\underline{\text{C}}\text{H}_3)_3$), 17.00 (C-20); IR ν (KBr) 3040, 2962, 2214, 1592, 1478, 1225, 1185, 871, 746 cm^{-1} ; UV (cyclohexane) λ_{max} nm (ϵ_{max}) 292 (2320), 311 (1210); EI MS m/z 367 (M^+); HR MS Calcd for $\text{C}_{22}\text{H}_{25}\text{NS}_2$: 367.1428. Found: 367.1419. Anal. Calcd: C, 71.89; H, 6.86; N, 3.81. Found: C, 71.56; H, 6.52; N, 3.70.

Sulfonium salt **132/132a**

syn-Thiacyclophane **130** (1.4g, 3.8 mmol) in dry CH_2Cl_2 (12 mL) was added slowly to $(\text{MeO})_2\text{CHBF}_4$ (80% oil, 2.0 g, 9.8 mmol) at $-78\text{ }^\circ\text{C}$ with stirring under nitrogen. The mixture was then stirred at $20\text{ }^\circ\text{C}$ for 3 h. The CH_2Cl_2 was decanted and ethyl acetate (50 mL) was added and stirring (trituration) was continued for a further 3 h. The white precipitate was then collected and dried to give 2.0 g (quant.) of bis-sulfonium salt **132**. This was used directly in the next step. ^1H NMR ($\text{DMSO}-d_6$) δ 7.45-7.58 (m), 7.23-7.17 (m), 6.94 (d, $J = 8.1$ Hz), 5.37-4.73 (m), 3.27-3.25 (m), 2.67, 2.69 (2 s), 1.12, 1.14, 1.18 (3 s).

anti-Thiacyclophane **131** under similar conditions gave bis-sulfonium salt **132a** in quantitative yield. ^1H NMR ($\text{DMSO}-d_6$). δ 8.14-8.13 (m), 7.74-7.69 (m), 7.61-7.53 (m), 5.35-5.31 (m), 5.16 (d, $J = 13.1$ Hz), 4.99-4.93 (m), 4.85-4.81 (m), 4.64 (d), 4.34 (d, $J = 14.2$ Hz), 4.10 (d, $J = 14.5$ Hz), 3.84 (s), 3.38 (s), 3.33 (s), 2.94 (s), 2.34 (s), 1.98 (s), 1.34 (s), 1.27 (s), 1.17 (s).

1,10-Bis(thiomethyl)-5-*t*-butyl-16-cyano-8-methyl-*anti*-[2,2]metacyclophane **134**



t-BuOK (0.87 g, 7.7 mmol) was added to a stirred suspension of mixed isomers of salt **132a** (2g, 3.5 mmol) in THF (35 mL) under argon at 20 °C. After stirring for 3 h, water was added and then dichloromethane (120 mL). The extract was washed, dried and evaporated. The residue was chromatographed over silica gel using CH₂Cl₂-hexane (3.5: 6.5) to give 1.27 g of product **134** as a mixture of isomers, EI MS *m/z* 395 (M⁺). These could be used directly in the next step.

Mixture of *anti*-thiomethylcyclophane isomers **134**

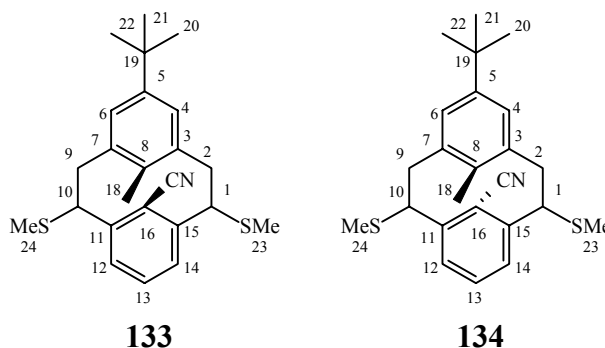
¹H NMR (CDCl₃) δ 7.96 (d, *J* = 7.7 Hz), 7.92-7.84 (d), 7.58-7.21 (m), 7.08 (d, *J* = 8.3 Hz), 6.2(s), 5.9 (s), 5.02 (d, *J* = 11.2 Hz), 4.54-4.48 (m), 4.32-4.28 (dd, *J* = 11.3, 4.4 Hz), 4.10-4.06 (dd, *J* = 11.2, 4.2 Hz) , 3.74-3.70 (m), 3.55 (d, *J* = 2.1 Hz), 3.32-3.23 (m), 2.70-2.62 (m), 2.46, 2.35, 2.27 (3 singlet), 2.13 (m), 2.08 (s), 1.84-1.81 (m), 1.70 (s), 1.34, 1.32, 1.17 (3s), 0.54, 0.51, 0.49 (3 singlet).

For characterization, re-chromatography yielded 170 mg (12%) of a single isomer of **134** in which the 1,10-thiomethyl groups are pseudo-equatorial: mp 139-140 °C; ¹H NMR (CDCl₃) δ 7.97 (d, *J* = 7.7 , 2H, H-12,14), 7.39 (t, *J* = 7.7, 1H, H-13), 7.28 (s, 2H, C-4,6), 4.09 (dd, *J* = 11.2, 4.2 Hz, 2H, H-1,10), 2.67 (dd, *J* = 12.6, 4.2, 2H, H-2_{eq}, 9_{eq}), 2.67 (dd, *J* = 11.4, 12.6 Hz, 2H, H-2_{ax},9_{ax}), 2.13 (s, 6H, S-Me) , 1.33 (s, 9H,

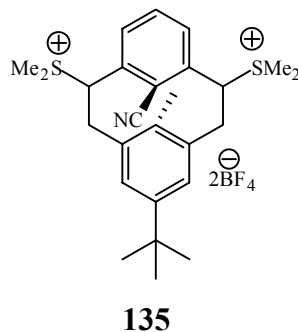
$C(\underline{CH}_3)_3$, 0.54 (s, 3H, Me); ^{13}C NMR δ 150.23 (C-5), 140.88 (C-8), 140.33 (C-11,15), 134.89 (C-3,7), 130.77 (C-13), 126.63 (C-12,14), 126.35 (C-4,6), 119.58 (C-16), 114.40 (CN), 54.8 (C-1,10), 42.75 (C-2,9), 34.23 ($\underline{C}(\underline{CH}_3)_3$), 31.25 ($C(\underline{CH}_3)_3$), 15.52 (S-Me), 14.49 (C-17); IR ν (KBr) 3049, 2951, 2864, 2216, 1598, 1479, 1455, 866, 792, 743, 578 cm^{-1} ; UV (cyclohexane) λ_{max} nm (ϵ_{max}) 274 (3040), 295 (3530); EI MS m/z 395(M^+ , 100%); HR MS Calcd for $C_{24}H_{29}NS_2$: 395.1741. Found: 395.1747. Anal. Calcd: C, 72.86; H, 7.39; N, 3.54. Found: C, 72.41; H, 7.02; N, 3.50.

Mixture of *syn*- and *anti*-thiomethylcyclophanes **133** and **134**

Sulfonium salt **132** under the Stevens rearrangement conditions gave a mixture of *syn*- and *anti*-thiomethylcyclophanes which gave following 1H NMR data.



1H NMR ($CDCl_3$) δ 7.97 (d, $J = 7.8$ Hz), 7.88 (d, $J = 7.7$ Hz), 7.84 (d, $J = 1.8$ Hz), 7.42-7.25 (m), 7.12 (d, $J = 7.6$ Hz), 6.90-6.75 (m), 6.53 (d), 6.47 (d), 6.42 (m), 6.29, 6.17, 6.11, 6.02 (4 singlet), 5.04-4.97 (m), 4.88 (t, $J = 8.6$ Hz), 4.53-4.47 (m), 4.12-3.24 (m), 2.80-2.60 (m), 2.40-2.35 (m), 2.22-2.14 (6 singlets), 1.38, 1.35, 1.32, 1.02, 0.97 (5 singlets), 0.54, 0.51, 0.49 (3 singlets).

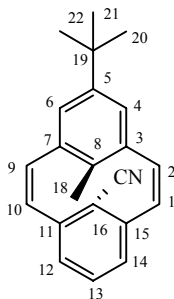
Bis-sulfonium salt 135

Using procedure 7.3, cyclophane **134** (2.8 g, 7.00 mmol) and Borch reagent (4.50 g, 22 mmol) in DCM (25 mL) gave 77% (3.24 g, 5.39 mmol) yield of an air sensitive bis-sulfonium salt **135**.

^1H NMR (DMSO- d_6) δ 8.00 (t, $J = 8.0$ Hz), 7.91-7.84 (m), 7.75-7.61 (m), 7.51 (d, $J = 11.5$ Hz), 7.49 (s), 7.37-7.27 (m), 7.09-7.05 (m), 6.60, 6.40 (s), 5.57 (d, $J = 5.5$ Hz), 5.43 (d, $J = 3.0$ Hz), 5.54, 5.37 (s), 4.74-4.66 (m), 4.25 (d, $J = 2.8$ Hz), 3.45-3.3 (m), 3.05 (d, $J = 8.0$ Hz), 2.96, 2.90, 2.84, 2.81, 2.59 (5 singlet), 1.33-1.31, 1.22, 1.04 (5 singlet), 0.69, 0.63, 0.56 (3 singlet)

If a mixture of **133** and **134** was used, the salt showed following ^1H NMR data:
 ^1H NMR (DMSO- d_6) δ 8.02 (d, $J = 7.9$ Hz), 7.91-7.85 (m), 7.75-7.62 (m), 7.49, 7.50 (singlets), 7.35-7.27 (m), 7.22-7.12 (m), 7.08 (t, $J = 6.5$ Hz), 6.63, 6.60 (s), 5.84-5.54 (m), 4.85-4.74 (m), 4.73-4.67 (m), 3.45-3.30 (m), 3.10-2.92 (m), 1.34-1.30 (singlets), 1.11, 1.04, 0.97, 0.69, 0.63, 0.56 (s).

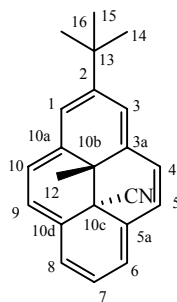
5-(*tert*-Butyl)-16-cyano-8-methyl-*anti*-[2.2]metacyclophane-1,9-diene **127**



127

Using procedure 7.4, a reaction of *t*-BuOK (0.87 g 7.7 mmol) and sulfonium salt **135** (2.0 g, 3.35 mmol) in THF (35 mL) followed by column chromatography using CH₂Cl₂-hexanes 4:6 as eluant gave 710 mg (70% yield) of **127** as colorless crystals from cyclohexane, which on attempted mp determination converts into DHP **128** and the migration product **137**: ¹H NMR (CDCl₃) δ 7.28 (t, *J* = 7.5 Hz, 1H, H-13), 6.85 (d, *J* = 7.5 Hz, 2H, H-12,14), 6.79 (s, 2H, H-4,6), 6.62 (d, *J* = 11.3 Hz, 2H, H-2,9), 6.30 (d, *J* = 11.3 Hz, 2H, H-1,10), 1.57 (s, 3H, Me), 1.31 (s, 9H, -C(CH₃)₃); ¹³C NMR (CDCl₃) δ 154.04 (C-5), 141.46 (C-8), 140.95 (C-11,15), 137.71 (C-2,9), 136.24 (C-3,7), 133.30 (C-13), 129.95 (C-1,10), 126.64 (C-12,14), 124.64 (C-4,6), 120.02 (C-16), 115.92 (CN), 34.45 (-C(CH₃)₃), 31.51 (-C(CH₃)₃), 19.84 (C-18); IR ν (KBr) 3048, 3009, 2964, 2904, 2867, 2215, 1571, 1476, 1443, 1217, 1154, 873, 843, 808, 768, 679, 660, 583, 556, 490 cm⁻¹; UV (cyclohexane) λ_{max} nm (ε_{max}) 225 (31100), 287 (12440), 337 (14970), 375 (6800); EI MS *m/z* 299 (M⁺); HR MS Calcd for C₂₂H₂₁N: 299.1674. Found: 299.1669; Anal. Calcd: C, 88.25; H, 7.07; N, 4.68. Found: C, 86.79; H, 6.96; N, 4.34.

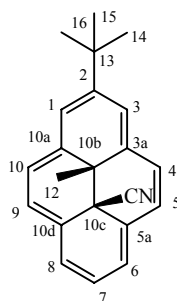
2-(*tert*-Butyl)-10c-cyano-10b-methyl-*trans*-10b,10c-dihydropyrene 128



128

Irradiation of an NMR sample of cyclophanediene **127** in benzene with a UV source with output 254 nm quickly converts **127** in to **128** in ~ 75% yield as a dark green solid: ^1H NMR (CDCl_3) δ 8.56 (s, 2H, H-1,3), 8.42 (AB, $J = 7.9$ Hz, 4H, H-4,5,9,10), 8.30 (d, $J = 7.8$ Hz, 2H, H-6,8), 7.75 (t, $J = 7.8$ Hz, H-7), 1.49 (s, 9H, $-\text{C}(\text{CH}_3)_3$, ^tBu), - 3.97 (s, 3H, Me); ^{13}C NMR (CDCl_3) δ 150.01 (C-2), 140.02 (C-10a,3a), 126.26 (C-5,9), 125.66 (C-5a,10d), 124.72 (C-6,8), 124.52 (C-4,10), 122.80 (C-7), 122.45 (C-1,3), 112.74 (CN), 36.56 ($-\text{C}(\text{CH}_3)_3$), 33.20 (C-10c), 32.00 ($-\text{C}(\text{CH}_3)_3$), 30.2 (C-10b), 12.03 (C-12); IR ν (thin film) 3040, 2964, 2867, 2217, 1601, 1576, 1478, 1463, 1231, 965, 878, 843, 825, 757, 736, 716 cm^{-1} ; UV (cyclohexane) λ_{max} nm (ϵ_{max}) 203 (50300), 274 (7500), 339 (43600), 377 (5600), 463 (3340), 533 (40), 575 (105), 600 (50).

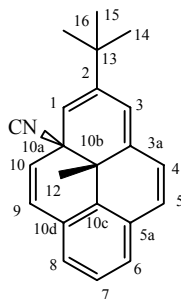
2-(*tert*-Butyl)-10c-cyano-10b-methyl-*cis*-10b,10c-dihydropyrene 136



136

When the sulfonium salt mixture (obtained from the cyclophanes **133** and **134**) was employed in the Hoffmann elimination, it gave 60% yield of the *cis*-DHP **136**. The product was purified by column chromatography using hexanes-CH₂Cl₂ 55: 45 as dark green crystals from benzene: mp 108-109 °C; ¹H NMR (CDCl₃) δ 8.86 & 8.78 (AB, *J* = 8.4 Hz, 4H, H-4,5,9,10), 8.50 (d, *J* = 7.8 Hz, 2H, H-6,8), 8.42 (s, 2H, H-1,3), 7.88 (t, *J* = 7.8 Hz, 1H, H-7), 1.62 (s, 9H, -C(CH₃)₃), -1.60 (s, 3H, Me); ¹³C NMR (CDCl₃) δ 145.10 (C-2), 139.32 (3a,10a), 129.64 (C-5,9), 128.08 (C-4,10), 125.09 (C-6,8), 122.87 (C-5a,10d), 121.39 (C-1,3), 121.25 (C-7), 115.82 (CN), 37.77 (C-12), 35.74 (-C(CH₃)₃), 35.18 (C-10c), 31.87 (-C(CH₃)₃), 30.95 (C-10b); IR ν (KBr) 2960, 2865, 2214, 1235, 818 cm⁻¹; UV (cyclohexane) λ_{max} nm (ε_{max}) 245 (4250), 275 (2710), 334 (85800), 340 (49300), 361 (41300), 404 (3890), 447 (10670), 515 (80), 556 (160), 614 (264); EI MS *m/z*. 299 (M⁺) HR MS Calcd for C₂₂H₂₁N: 299.1674. Found: 299.1670; Anal. Calcd: C, 88.25; H, 7.07; N, 4.68. Found: C, 85.41; H, 7.00; N, 4.44.

2-(*tert*-Butyl)-10a-cyano-10b-methyl-*trans*-10a,10b-dihydropyrene **137**



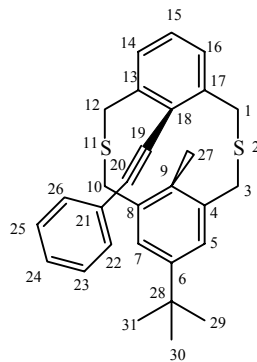
137

Cyclophanediene **127** (10 mg) was sealed in a glass tube under argon and heated at 70 °C for 3 hours (or until completely colorless), which quantitatively converted it into colorless crystals of **137**; evaporation gave crystals: mp 82-84 °C; ¹H NMR (CDCl₃) δ 7.18 (dd, *J* = 7.6, 1H, H-7), 7.04 (m, 2H, H-6,8), 6.72 (d, *J* = 9.1, 1H, H-9), 6.50 & 6.34

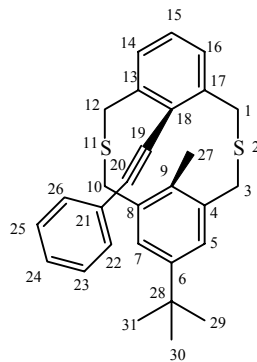
(AB, $J = 9.5$, 1H, H-4,5), 6.13 (s, 1H, H-3), 5.99 (d, $J = 9.1$ Hz, 1H, H-10), 5.53 (s, 1H, H-1), 1.157 (s, 3H, Me), 1.153 (s, 9H, $-\text{C}(\underline{\text{CH}}_3)_3$); ^{13}C NMR (CDCl_3) δ 150.61 (C-2), 143.22 (C-3a), 136.17 (C-10c), 131.67 (C-5a), 130.86 (C-10d), 128.98 (C-5), 127.75 (C-7), 127.39 (C-6), 126.83 (C-8), 126.57 (C-4), 125.65 (C-10), 121.52 (CN), 121.48 (C-3), 113.74 (C-1), 43.17 (C-10b), 40.84 (C-10a), 34.69 ($-\underline{\text{C}}(\text{CH}_3)_3$), 28.88 ($-\text{C}(\underline{\text{C}}\text{H}_3)_3$), 17.44 (C-12); IR ν (KBr) 3038, 2961, 2904, 2867, 2217, 1625, 1577, 1477, 1465, 1367, 1210, 966, 865, 825, 813, 756, 746, 661 cm^{-1} ; UV (dichloromethane) λ_{max} nm (ϵ_{max}) 259 nm (12200), 273 (8870), 289 (4380), 301 (4520), 315 (3870), 339 (3660), 353 (3750); EI MS m/z 299 (M^+) HR MS Calcd for $\text{C}_{22}\text{H}_{21}\text{N}$: 299.1674. Found: 299.1674; Anal. Calcd: C, 88.25; H, 7.07; N, 4.68. Found: C, 84.13; H, 6.84; N, 4.32.

6-(*tert*-Butyl)-9-methyl-18-phenylethynyl-2,11-dithia[3.3]metacyclophanes 142 and 145

A solution of bis-bromomethyl-2-phenylethynylbenzene (3.9 g, 10.7 mmol) and 2,6 bis-thiomethyl-4-*tert*-butyltoluene (2.57 g, 10.7 mmol) in deaerated benzene (500 ml) was added drop wise to ethanolic KOH solution {prepare by adding KOH (3.4 g) in deaerated water (160 mL) and ethanol (1470 mL) followed by addition of sodium borohydride (0.64 g)}. Drop rate was very crucial, optimum result were obtained with a drop per 5-6 second and this addition took 56 hours. The solvent was then evaporated and the residue was dissolved in DCM and extracted with water, dried over MgSO_4 and evaporated. The residue was chromatographed on silica gel using CH_2Cl_2 -hexanes 1.5: 8.5 as eluant.

**142**

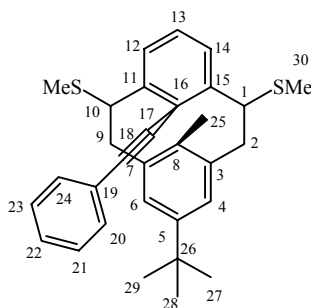
Eluted first was 700 mg (1.58 mmol, 15%) of *anti* **142** as colorless crystals from cyclohexane: mp 148-149 °C; ^1H NMR (CDCl_3) δ 7.43 (m, 2H, H-22, 26), 7.40 (d, $J = 7.6$ Hz, 2H, H-14,16), 7.33-7.31 (m, 3H, H-23,24,25), 7.27 (s, 2H, H-5,7), 7.22 (t, $J = 7.6$ Hz, 1H, H-15), 4.16 and 3.72 (AB, $J = 14.1$ Hz, 4H, H-1, 12), 3.76 (AB, $J = 13.9$ Hz, 4H, H-3,10), 1.42 (s, 3H, Me), 0.98 (s, 9H, $-\text{C}(\text{CH}_3)_3$); ^{13}C NMR (CDCl_3) δ 148.26 (C-6), 139.26 (C-13,17), 135.90 (C-9), 134.14 (C-4,8), 131.64 (C-22,26), 129.07 (C-14,16), 128.51 (C-23,25), 128.45 (C-24), 127.84 (C-15), 127.32 (C-5,7), 125.74 (C-18), 123.97 (C-21), 100.19 (C-20), 86.19 (C-19), 34.08 ($-\text{C}(\text{CH}_3)_3$), 32.4 (C-3,10), 32.13 (C-1,12), 31.08 ($-\text{C}(\text{CH}_3)_3$), 15.27 (C-27); IR ν (KBr) 3057, 2959, 2904, 2862, 1594, 1477, 1488, 1440, 756. 7477, 691 cm^{-1} ; UV (cyclohexane) λ_{max} nm (ϵ_{max}) 288 (10100) 303 (11700), 318 (11900); EI MS m/z 442 (M^+); HR MS calculated for $\text{C}_{29}\text{H}_{30}\text{S}_2$: 442.1788. Found: 442.1779; Anal. Calcd: C, 78.68; H, 6.83. Found: C, 75.81; H, 7.0.

**145**

Eluted second was 2.2 g (4.77 mmol, 47%) of *syn*-**145** as colorless crystals from cyclohexane, mp 170-171 °C; ^1H NMR (CDCl_3) δ 7.62 (dd, $J = 7.8, 1.8$ Hz, 2H, H-22,26), 7.40-7.44 (m, 3H, H-23,24,25), 7.02 (d, $J = 7.6$, 2H, H-14,16), 7.01 (s, 2H, H-5,7), 6.86 (t, $J = 7.6$ Hz, 1H, H-15), 4.65 and 3.67 (AB, $J = 14.8$ Hz, 4H, H-1,12), 4.41 and 3.62 (AB, $J = 14.8$ Hz, 4H, H-3,10), 2.54 (s, 3H, Me) 1.22 (s, 9H, $-\text{C}(\text{CH}_3)_3$); ^{13}C NMR (CDCl_3) δ 147.15 (C-6), 140.41 (C-13,17), 136.01 (C-4,8), 132.15 (C-9), 131.41 (C-22,26), 129.01 (C-15), 128.84 (C-23,25), 128.75 (C-24), 128.04 (C-14,16), 126.02 (C-5,7), 123.56 (C-21), 121.65 (C-18), 99.15 (C-20), 87.83 (C-19), 35.75 (C-1,12), 34.74 (C-3,10), 34.34 ($-\text{C}(\text{CH}_3)_3$), 31.29 ($-\text{C}(\text{CH}_3)_3$), 17.15 (C-27); IR ν (thin film, KBr) 3057, 2961, 2906, 2864, 1596, 1489, 1478, 1461, 1361, 1261, 872, 792, 755, 748, 691 cm^{-1} ; UV (cyclohexane) λ_{max} nm (ϵ_{max}) 258 (16100), 297 (13600), 319 (11000); EI MS m/z 442 (M^+); HR MS Calcd for $\text{C}_{29}\text{H}_{30}\text{S}_2$: 442.1788. Found: 442.1786; Anal. Calcd: C, 78.68; H, 6.83. Found: C, 77.71; H, 6.54.

**1,10-Bis(thiomethyl)- 5-*t*-butyl-8-methyl-16-phenylethynyl-*anti*-[2,2]metacyclophane
146**

BuLi (2.5 mmol) was added dropwise to a solution of mixed thiacyclophanes **142** and **145** (300 mg, 0.68 mmol) in dry THF (30 mL) at 0 °C. The solution was allowed to warm up to room temperature over 10 minutes where dark purple solution turned pale yellow. MeI (0.4 mL, mmol) was added and allowed to stir for another 10 minutes. The reaction was quenched using water (5 mL) and then extracted with dichloromethane (3 x 25 mL). The combined organic extracts were dried over MgSO₄ and evaporated. The residue was chromatographed over silica gel using CH₂Cl₂-hexanes (12:88) as eluant to afford 290 mg (80%) of **146** as a mixture of isomers. Re-chromatography yielded 150 mg of a single isomer of **146** in which the 1,10 thiomethyl groups are pseudo-equatorial.



146

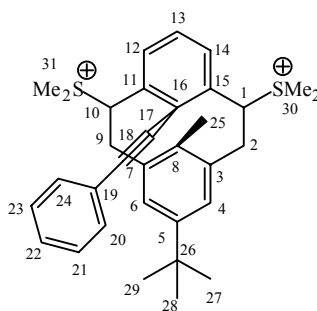
mp 203-204 °C; ¹H NMR (CDCl₃) δ 7.86 (d, *J* = 7.6 Hz, 2H, H-12,14), 7.28 (tt, *J* = 6.4, 1.5 Hz, 1H, H-22), 7.27-7.17 (m, 4H, H-20,21,23,24), 7.21 (t, *J* = 7.6 Hz, 1H, H-13), 7.14 (s, 2H, H-4,6), 4.45 (dd, *J* = 11.4, 4.1 Hz, 2H, H-1_{ax},10_{ax}), 3.24 (dd, *J* = 12.4, 4.1 Hz, 2H, H-2_{eq},9_{eq}), 2.74 (dd, *J* = 12.2, 11.6 Hz, 2H, H-2_{ax},9_{ax}), 2.18 (s, 6H, S-Me), 0.91 (s, 9H, -C(CH₃)₃), 0.63 (s, 3H, Me); ¹³C NMR (CDCl₃) δ 148.44 (C-5), 140.02 (C-8), 138.83 (C-11,15), 135.19 (C-3,7), 131.66 (C-13), 130.21 (C-16), 128.31 (C-22), 127.29, 128.48 (C-20,21,23,24), 125.78 (C-12,14), 125.15 (C-4,6), 123.63 (C-19), 92.78

(C-18), 86.17 (C-17), 54.63 (C-1,10), 43.50 (C-2,9), 34.05 ($-\underline{C}(\text{CH}_3)_3$), 31.23 ($-\underline{C}(\text{CH}_3)_3$), 15.89 (C-30,31), 14.93 (C-25); IR (thin film, KBr) 3044, 2952, 2913, 1596, 1490, 1425, 754, 745, 690 cm^{-1} ; UV (cyclohexane) λ_{max} nm (ϵ_{max}) 280 (13000), 293 (13500), 320 (12600); EI MS m/z 470 (M^+); HR MS Calcd for $\text{C}_{31}\text{H}_{34}\text{S}_2$: 470.2102. Found: 470.2104. Anal. Calcd: C, 79.09; H, 7.28. Found: C, 79.35; H, 7.01.

A mixture of *syn*- and *anti* isomers showed following NMR data:

^1H NMR (CDCl_3) δ 7.8 (d, $J = 7.6$ Hz), 7.7 (br s), 7.6-7.5 (m), 7.4-7.2 (m), 7.1-7.0 (m), 6.91 (d, $J = 7.5$ Hz), 6.8 (t, $J = 7.6$ Hz), 6.6 (t, $J = 7.6$ Hz), 6.4 (d, $J = 7.3$ Hz), 6.3, 6.2 (br s), 6.35 (s), 5.4 (m), 5.23 (t, $J = 8.7$ Hz), 5.15 (t, $J = 8.4$ Hz), 4.8 (d, $J = 14.1$ Hz), 4.44 (dd, $J = 11.3, 4.1$ Hz), 4.35 (d, $J = 15.0$ Hz), 4.1-3.9 (m), 3.7 (t, $J = 13.4$ Hz), 3.3 (m), 3.1 (t, $J = 11.7$ Hz), 2.7 (t, $J = 11.6$ Hz), 2.5 (s), 2.2 (four singlets), 1.17 (s), 1.12 (s), 0.92 (s), 0.64 (s).

1, 10-Bis(thiomethyl)-8-methyl-16-phenylethynyl-*anti*-[2.2]metacyclophane bis-sulfonium salt 147



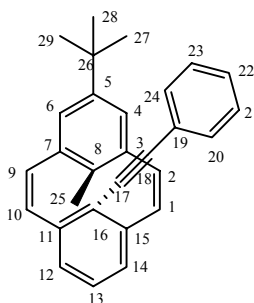
147

Using procedure 7.3, the pure 1,10-diequatorial-thiomethyl isomer of **146** (1 g, 2.12 mmol) on reaction with Borch reagent (1 g, 4.8 mmol) in CH_2Cl_2 (7 mL) gave the product as a single isomer (1.4g, quantitative): ^1H NMR ($\text{DMSO}-d_6$) δ 7.87 (d, $J = 7.8$ Hz, 2H, H-12,14), 7.58 (dd $J = 7.8, 2.3$ Hz, 2H, H-20,24), 7.47 (t, $J = 7.76$ Hz, 1H, H-

13), 7.41 (m, 3H, H-21-23), 7.35 (s, 2H, H-4,6), 4.66 (dd, $J = 12.0, 4.2$ Hz, 2H, H- $1_{ax}, 10_{ax}$), 3.60 (dd, $J = 12, 4.2$ Hz, 2H, H- $2_{eq}, 9_{eq}$), 3.46 (s, 6H, S-Me₂), 3.17 (triplet, $J = 12$ Hz, 2H, H- $2_{ax}, 9_{ax}$), 3.04 (s, 6H, S-Me₂), 0.89 (s, 9H, -C(CH₃)₃), 0.75 (s, 3H, Me).

When the mixture of cyclophane isomers **146** were used in the *S*-methylation, following NMR data was obtained: ¹H NMR (DMSO-*d*₆) δ 7.88-7.34 (m), 7.0-6.8 (m), 6.6 (br s), 5.83-5.55 (m), 4.8-4.6 (m), 4.04-3.00 (m), 2.26, 1.98 (s), 1.18, 0.78 (9 singlets).

5-(*tert*-Butyl)-8-methyl-16-phenylethynyl-*anti*-[2.2]metacyclophane-1,9-diene **138**



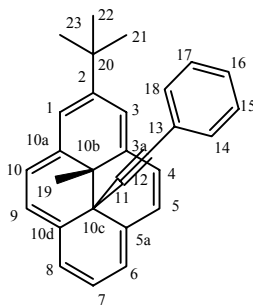
138

Using procedure 7.4, a reaction of sulfonium salt **147** (300 mg, 0.45 mmol) and *t*-BuOK (120 mg, 1.07 mmol) in THF (10 mL) followed by chromatography over silica gel in a jacketed column using hexanes: CH₂Cl₂ (80: 20) as eluant gave **138** (quantitative) as colorless crystals, which on attempted mp determination converts into DHP **139**: ¹H NMR (C₆D₆) δ 7.28 (dd, $J = 7.1, 1.5$ Hz, 2H, H-20,24), 6.92-6.98 (m, 3H, H-21-23), 6.86 (t, $J = 7.4$ Hz, 1H, H-13), 6.73 (s, 2H, H-4,6), 6.54 (d $J = 7.4$ Hz, 2H, H-12,14), 6.42 and 6.23 (AB, $J = 11.3$ Hz, 2H, H-1,2,9,10), 1.83 (s, 3H, Me), 0.93 (s, 9H, -C(CH₃)₃); ¹³C NMR (C₆D₆) δ 150.90 (C-5), 142.47 (C-8), 141.15 (C-11,15), 138.11 (C-3,7), 135.40 (C-2,9), 132.30 (C-20,24), 131.99 (C-1,10), 131.13 (C-16), 129.79 (C-13), 128.68 (C-21,23), 128.12 (C-22), 126.32 (C-12,14), 125.47 (C-19), 123.68 (C-4,6), 95.85 (C-18), 91.03 (C-17), 34.19 (-C(CH₃)₃), 31.72 (-C(CH₃)₃), 20.76 (C-25); IR ν (thin film) 3041, 3004, 2867,

2962, 1597, 1491, 1442, 871, 772, 757, 737, 690, 673 cm^{-1} ; UV (cyclohexane) λ_{max} nm (ϵ_{max}) 288 nm (13500), 339 (15000), 377 (6700);

^1H NMR (CDCl_3) δ 7.25-7.23 (m, 5H), 7.12 (t, $J = 7.4$ Hz, 1H), 6.77 (d, $J = 7.4$ Hz, 2H), 6.58 (s, 2H), 6.49 (d, $J = 11.3$ Hz, 2H), 6.36 (d, $J = 11.3$ Hz, 2H), 1.65 (s, 3H, Me), 0.80 (s, 9H, $\text{C}(\text{CH}_3)_3$, $t\text{-Bu}$); ^{13}C NMR (CDCl_3) δ 150.58, 141.70, 137.42, 131.34, 130.23, 129.39, 128.26, 127.80, 125.90, 124.61, 123.07, 95.13 (sp), 89.98 (sp), 33.03 (C-26), 30.67 ($-\text{C}(\text{CH}_3)_3$) 20.22 (Me).

2-(*tert*-Butyl)-10b-methyl-10c-phenylethynyl-*trans*-10b,10c-dihydropyrene 139

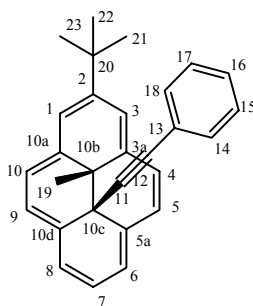


139

$t\text{-BuOK}$ (140 mg, 1.2 mmol) was added to a stirred suspension of mixed isomers of bis-sulfonium salt **147** (350 mg, 0.52 mmol), in THF (10 mL) under argon at 20 °C. After refluxing for 6 h, water was added and then dichloromethane (90 mL). The extract was washed, dried over MgSO_4 and evaporated. The residue was chromatographed over silica gel using hexanes: CH_2Cl_2 (85:15) as eluant to give 160 mg (85%) of the dihydropyrene **139** as green crystals from methanol: mp 112-113 °C; ^1H NMR (CDCl_3) δ 8.72 and 8.65 (AB, $J = 7.8$ Hz, 2H, H-4,5,9,10), 8.69 (s, 2H, H-1,3), 8.62 (d, $J = 7.8$ Hz, 2H, H-6,8), 8.07 (t, $J = 7.8$ Hz, 1H, H-7), 6.83 (tt, $J = 7.8, 1.8$ Hz, 1H, H-16), 6.72 (dd, $J = 7.8, 7.5$ Hz, 2H, H-15,17), 6.04 (dd, $J = 7.4, 1.8$ Hz, 2H, H-14,18), 1.74 (s, 9H, -

$C(\underline{CH}_3)_3$, -4.00 (3H, s, Me); ^{13}C NMR ($CDCl_3$) δ 148.15 (C-2), 139.95 (C-3a,10a), 131.08 (C-14,18), 130.06 (C-5a,10d), 127.39 (C-15,17), 125.11 (C-5,9), 126.99 (C-16), 123.46 (C-4,10), 123.33 (C-6,8), 122.49 (C-13), 121.95 (C-7), 121.30 (C-1,3), 84.61 (C-12) 75.41 (C-11), 36.41 ($-C(\underline{CH}_3)_3$), 32.13 ($-C(\underline{CH}_3)_3$), 31.18 (C-10b), 30.48 (C-10c), 12.86 (C-19); IR ν (thin film) 3036, 2963, 1597, 1489, 1478, 1442, 1230, 874, 822, 755, 737, 691, 682, 628 cm^{-1} ; UV (cyclohexane) λ_{max} nm (ϵ_{max}) 250 (41200), 339 (1.64×10^5), 377 (73200), 467 (14900), 577 (380), 639 (300); EI MS 374 (M^+); HR MS Calcd for $C_{29}H_{26}$: 374.2034. Found: 374.2036. Anal. Calcd: C, 93; H, 7. Found: C, 91.47; H, 7.21.

2-(*tert*-Butyl)-10b-methyl-10c-phenylethynyl- *cis*-10b,10c-dihydropyrene 148

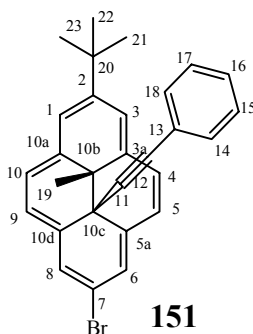


148

Mixed isomers of sulfonium salts (**147**) in the Hoffmann elimination (procedure and quantities same as for **139**) gave an 8% yield of the *cis*-DHP **148**. The product was purified by column chromatography using hexane-DCM 8: 2 to give dark green crystals from isopropanol: mp 159-160 °C; 1H NMR ($CDCl_3$) δ 8.85-8.78 (AB, $J = 8.3$, 2H, H-4,5,9,10), 8.40 (d, $J = 7.6$, 2H, H-6,8), 8.39 (s, 2H, H-1,3), 7.75 (t, $J = 7.6$ Hz, 1H, H-7), 7.01-6.97 (m, 3H, H-15-17), 6.67 (dd, $J = 7.2, 1.2$ Hz, 2H, H-14,18), 1.65 (s, 9H, $-C(\underline{CH}_3)_3$), -1.55 (s, 3H, Me); ^{13}C NMR ($CDCl_3$) δ 143.61 (C-2), 139.38 (C-10a,3a), 131.10 (C-14,18), 129.50 (C-5a,10d), 129.14 (C-5,9), 127.84 (C-15,17), 127.82 (C-4,10),

127.33 (C-16), 124.08 (C-6,8), 123.27 (C-13), 120.67 (C-1,3), 112.14 (C-7), 89.61 (C-11), 77.38 (C-12), 36.25 (C-19), 35.51 ($-\underline{\text{C}}(\text{CH}_3)_3$), 32.90 (C-10c), 32.03 (C-10b), 31.99 ($-\text{C}(\underline{\text{C}}\text{H}_3)_3$); IR ν (KBr) 3022, 2973, 2863, 1594, 1486, 1438, 1234, 874, 867, 822, 755, 690, 647, 632 cm^{-1} ; UV (cyclohexane) λ_{max} nm (ϵ_{max}) 342 (5.07×10^4), 364 (38200), 428 (6755) 447 (13200), 591 (130), 614 nm (160); EI MS m/z 374 (M^+); HR MS Calcd for $\text{C}_{29}\text{H}_{26}$: 374.2034. Found: 374.2033. Anal. Calcd: C, 93; H, 7. Found: C, 90.27; H, 7.05.

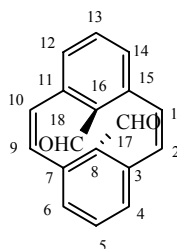
7-Bromo-2-(*tert*-butyl)-10b-methyl-10c-(2-phenylethynyl)-*trans*-10b,10c-dihydropyrene 151



NBS (24 mg, 0.135 mmol) in DMF (4 mL) was added drop wise to a solution of DHP **139** (50 mg, 0.134 mmol) in CH_2Cl_2 (20 mL) at 0 °C and stirred at room temperature for one hour. Reaction mixture was poured into hexanes (200 mL) in a separatory funnel and washed with 4x50 ml of water. The organic green layer was dried over MgSO_4 and evaporated. Column chromatography over silica using CH_2Cl_2 : hexanes (15: 85) as eluant gave the bromo DHP **151** (40 mg, 0.09 mmol, 66%) as green crystals from cyclohexane: mp 120-121 °C; ^1H NMR (CDCl_3) δ 8.72 (s, 2H, H-6,8), 8.67 (s, 2H, H-1,3), 8.62 (s, 4H, H-4,5,9,10), 6.84 (tt, $J = 7.5, 1.5$ Hz, 1H, H-16), 6.74 (dd, $J = 7.8, 7.5$ Hz, 2H, H-15,17), 6.06 (dd, $J = 7.8, 1.5$ Hz, 2H, H-14,18), 1.72 (s, 9H, $-\text{C}(\underline{\text{C}}\text{H}_3)_3$), -3.95 (s, 3H, Me); ^{13}C NMR (CDCl_3) δ 148.74 (C-2). 139.99 (C-3a,10a), 131.09 (C-14,18),

130.12 (C-5a,10d), 127.47 (C-15,17), 127.24 (C-16), 125.53 (C-6,8), 124.63 (C-4,10), 124.31 (C-5,9), 122.45 (C-1,3), 122.18 (C-13), 116.72 (C-7), 75.49, 83.70 (C-11,12), 36.49 ($-\underline{C}(\underline{CH}_3)_3$), 32.01 ($-\underline{C}(\underline{CH}_3)_3$), 31.48 (C-10b), 29.38 (C-10c), 12.84 (C-19); IR ν (thin film) 3043, 2963, 1596, 1489, 1462, 1230, 879, 827, 755, 738, 691, 682 cm^{-1} ; UV (cyclohexane) λ_{max} nm (ϵ_{max}) 343 (24030), 379 (33970), 475 (10360), 581 (290), 640 (340); EI MS m/z 452 (M^+); HR MS Calcd for $C_{29}H_{25}Br$: 452.1139. Found: 452.1130. Calcd. Anal: C, 76.82; H, 5.55. Found: C, 77.35; H, 5.80.

8,16-Diformyl-*anti*-[2.2]metacyclophane-1,9-diene **152**

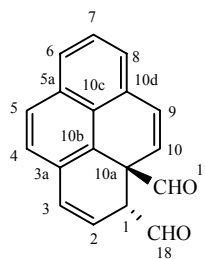


152

DIBAL (2.5 mmol, 2.5 ml of 1 M solution in cyclohexane) was added dropwise to a solution of dicyano CPD **85** (250 mg, 1 mmol) in dry dichloromethane (12 mL) at room temperature, over a period of 6 minutes. It was stirred for 5 h at room temperature, after which it was slowly added to methanol (5 mL) and stirred for half an hour. Then HCl (10 mL, 1M) was added carefully and the resulting solution was extracted with dichloromethane (3 x 30 mL). The organic layer was dried over anhydrous $MgSO_4$, evaporated and column chromatographed over silica using ethyl acetate: DCM (1:9) as eluant to yield 8,16-diformylcyclophanediene **152** (146 mg, 56%) as colorless crystals from methanol, which on attempted mp determination converts into migration products **155**: 1H NMR ($CDCl_3$) δ 9.35 (s, 2H, H-17,18), 7.39 (t, $J = 7.4$ Hz, 2H, H-5,13), 6.85 (d,

$J = 7.4$ Hz, 4H, H-4,6,12,14), 6.73 (s, 4H, H-1,2,9,10); ^{13}C NMR (CDCl_3) δ 185.77 (C-17,18), 145.41(C-8,16), 140.03 (C-3,7,11,15), 135.35 (C-1,2,9,10), 135.29 (C-5,13), 128.84 (C-4,6,12,14); IR ν (KBr) 3056, 3011, 2924, 2869, 2768, 1712, 1683, 1559, 1445, 1222, 1181, 816, 761, 628 cm^{-1} ; UV (dichloromethane), λ_{max} nm (ϵ_{max}) 245 nm (8500), 274 (8600), 338 (4150), 345 (4130), 395 sh (1500); EI MS m/z 260 (M^+).

1,10a-Diformyl-*trans*-1,10a-dihydropyrene **155**



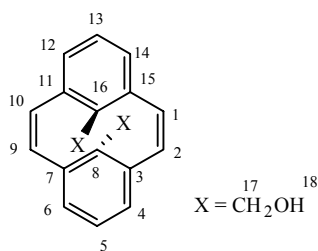
155

Cyclophanedienone **152** (10 mg) in CDCl_3 (1 mL) was sealed in a glass tube under argon and heated at 70 $^{\circ}\text{C}$ for 1 h, which converted it into **155**. Evaporation gave colorless solid which decomposed on attempted chromatography but was pure enough to obtain the following data:

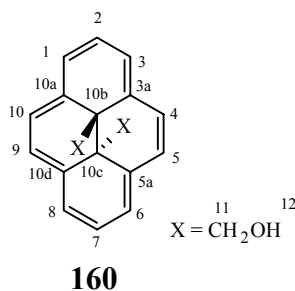
^1H NMR (CDCl_3) δ 9.71 (d, $J = 3.4$ Hz, 1H, H-18), 9.34 (s, 1H, H-17), 7.69 (d, $J = 8.3$ Hz, 1H, H-5), 7.61 (d, $J = 8.4$ Hz, 1H, H-6), 7.32 (dd, $J = 6.9, 8.4$ Hz, 1H, H-7), 7.28 (d, $J = 8.3$ Hz, 1H, H-4), 7.11 (d, $J = 6.8$ Hz, 1H, H-8), 6.9 (d, $J = 9.6$ Hz, 1H, H-9), 6.7 (d, $J = 9.9$ Hz, 1H, H-3), 5.91 (dd, $J = 9.6, 6.2$ Hz, 1H, H-2), 5.68 (d, $J = 9.6$ Hz, 1H, H-10), 3.76 (dd, $J = 6.3, 3.5$ Hz, 1H, H-1); ^{13}C NMR (CDCl_3) δ 198.74 (C-18), 190.97(C-17), 133.50 (C-5a), 132.94 (C-9), 131.29 (C-3), 131.16 (C-3a), 130.45 (C-10d), 128.62 (C-6), 128.41 (C-10c), 128.23 (C-5), 127.14 (C-7), 126.10 (C-4), 125.59 (C-10b), 125.25 (C-8), 122.71 (C-10), 122.02 (C-2), 55.93 (C-10a), 51.08 (C-1); IR ν (thin film) 3048, 2927,

2820, 2721, 1719, 1685, 1590, 1569, 1502, 1174, 842, 770, 734 cm^{-1} ; UV (dichloromethane) λ_{max} nm (ϵ_{max}) 208 (850), 243 (13500), 274 (24600), 322 (3600), 322 (3600), 338 (4100), 402 (2130), 470 *sh* (460); EI MS m/z 260 (M^+)

8,16-Bis(hydroxymethyl)-*anti*-[2.2]metacyclophane-1,9-diene 159



NaBH_4 (9 mg, 0.236 mmol) was added to a solution of diformylcyclophanediene **152** (18 mg, 0.0692 mmol) in methanol (4 mL) at room temperature under argon and stirred for five minutes, then quenched with HCl (0.5 mL of 1M solution). The resulting solution was extracted between dichloromethane and water. The organic layer was dried over MgSO_4 and evaporated in cold to give 17 mg (0.0644 mmol, 93%) of **159** as colorless solid, which on attempted mp determination converts into DHP **160** and pyrene **112**: ^1H NMR (CDCl_3) δ 7.21 (t, $J = 7.4$ Hz, H-5,13), the OH protons are not located, 6.80 (d, $J = 7.4$ Hz, H-4,6,12,14), 6.48 (s, 4H, H-1,2,9,10), 3.80 (s, 2H, H-17,19); ^{13}C NMR (CDCl_3) δ 148.2 (C-8,16), 136.7 (C-3,7,11,15), 133.43 (C-1,2,9,10), 130.00 (C-5,13), 127.33 (C-4,6,12,14), 62.73 (C-17,19); IR ν (thin film) 3049, 2921, 1653, 1438, 1265, 997, 772, 735 cm^{-1} ; UV (dichloromethane) λ_{max} (ϵ_{max}) 236 (11400), 276 (8500) EI MS 202 (M^+ - $\text{C}_2\text{H}_6\text{O}_2$).

10b,10c-Bis(hydroxymethyl)-*trans*-10b,10c-dihydropyrene 160

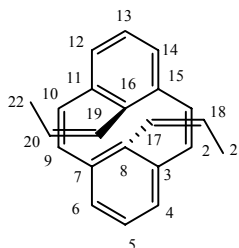
An NMR sample of cyclophanediene **159** was held at room temperature which converted it into dihydropyrene **160** in ~ 80% yield. If the sample was held for longer time, the dihydropyrene gradually decomposed into pyrene **112**: ^1H NMR (CDCl_3) δ 8.80 (s, 4H, H-4,5,9,10), 8.74 (d, $J = 7.5$ Hz, 4H, H-1,3,6,8), 8.07 (t, $J = 7.6$ Hz, 2H, H-2,7), -1.77 (d, $J = 7.1$ Hz, 4H, 11, 13), -2.1 (t, $J = 7.1$ Hz, 2H, H-12,14); ^{13}C NMR (CDCl_3) δ 132.59 (C-3a,5a,10a,10d), 125.90 (C-1,3,6,8), 125.31 (C-4,5,9,10), 124.07 (C-2,7), 61.25 (C-11,13), 34.01 (C-10b,10c); IR ν (thin film) 3048, 2924, 1338, 1261, 852, 630 cm^{-1} ; UV (dichloromethane) λ_{max} nm (ϵ_{max}) 243 (8000), 388 (4200), 482 (950), 636 (40).

8,16-Bis(prop-1-enyl)-*anti*-[2.2]metacyclophane-1,9-dienes 162 and 163

BuLi (0.35 mL of 2.5M in hexanes, 0.9 mmol) was added dropwise to a suspension of ethyltriphenylphosphonium bromide (240 mg, 0.65 mmol) in THF (5 mL) under argon at 0 °C and the mixture was stirred for 20 minutes. After that time, clear and orange to red solution was obtained. At -30 °C, diformylcyclophanediene **152** (70 mg, 0.269 mmol) was added and the reaction mixture was allowed to warm to room temperature over 30 minutes and then quenched with water. The resulting solution was extracted with CH_2Cl_2 (4 x 20 mL), dried over anhydrous MgSO_4 and evaporated. The crude mixture was chromatographed over silica gel. Hexanes eluted firstly pyrene **112**

and then 8,16-dipropenyl cyclophanedienes as a mixture of **162** and **163** (40 mg, 0.14 mmol, 52%).

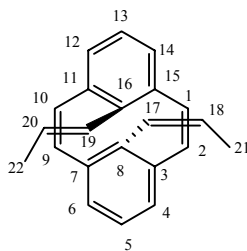
8,16-Bis((1Z)-Prop-1-enyl)-anti-[2.2]metacyclophane-1,9-diene 162 (major isomer)



162

The melting point could not be determined because the sample was a mixture of isomers. $^1\text{H NMR}$ (CDCl_3) δ 6.94 (t, $J = 7.4$ Hz, 2H, H-5,13), 6.46 (d, $J = 7.4$ Hz, 4H, H-4,6,12,14), 6.12 (qd, $J = 12.0, 1.8$ Hz, 2H, H-17,19), 6.09 (s, 4H, H-1,2,9,10), 5.23 (qd, $J = 12.0, 7.2$ Hz, 2H, H-18,20), 1.55 (dd, $J = 7.3, 1.8$ Hz, 6H, H-21,22); $^{13}\text{C NMR}$ (CDCl_3) δ 142.31 (C-8,16), 136.88 (C-3,7,11,15), 131.98 (C-1,2,9,10), 129.37 (C-17,19), 128.20 (C-5,13), 125.98 (C-18,20), 125.45 (C-4,6,12,14), 15.35 (C-21,22); IR ν (thin film) 3036, 3001, 2930, 2848, 1599, 1561, 1434, 962, 929, 858, 842, 771, 711, 665 cm^{-1} ; UV (cyclohexane) λ_{max} nm (ϵ_{max}) 215 (25000), 243 (26200), 277 (11500), 340 (~ 2500); EI MS m/z 284 (M^+); HR MS Calcd for $\text{C}_{22}\text{H}_{20}$: 284.1565. Found: 284.1562.

16-((1*E*)-Prop-1-enyl)-8-((1*Z*)prop-1-enyl)-*anti*-[2.2]metacyclophane-1,9-diene **163**
(minor isomer)



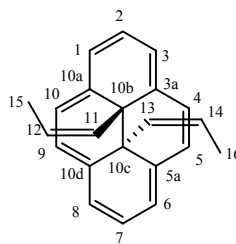
163

The melting point could not be determined because the sample was a mixture of isomers. ¹H NMR (CDCl₃) 6.98 (t, *J* = 7.4 Hz, 1H, H-13), 6.86 (t, *J* = 7.4 Hz, 1H, H-5), 6.44 (d, *J* = 7.4 Hz, 2H, H-12,14), 6.42 (d, *J* = 7.4 Hz, 2H, H-4,6), 6.11(AB*, 4H, H-1,2,9,10), 5.94 (dq, *J* = 15.4, 6.7 Hz, H-20), 1.57 (dd, *J* = 1.9 Hz, *J* = 6.6 Hz, 3H, H-21), 1.52 (dd, *J* = 6.6, 1.6 Hz, 3H, H-22) H-17-19*; ¹³C- NMR (CDCl₃) δ 145.92 (C-8), 141.30 (C-16), 137.40 (C-11,15), 135.10 (C-3,7), 132.56 (C-2,9), 131.80 (C-17), 130.80 (C-19), 129.77 (C-20), 128.49 (C-13), 127.76 (C-5), 126.16 (C-4,6), 125.35 (C-12,14), 18.23 (C-22), 15.32 (C-21), C-1,10,18*

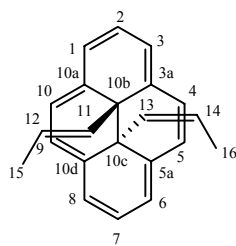
*Indicates when peaks are not distinct (overlapped by the major isomer)

Closed isomers

Using procedure 7.5, a mixture of cyclophanedienes **162** and **163** (10 mg) was converted into a mixture of dihydropyrenes **164** and **165**.

10b,10c-Bis((1Z)prop-1-enyl)-trans-10b,10c-dihydropyrene 164 (major isomer)**164**

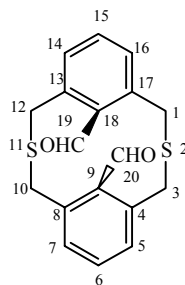
The melting point could not be determined because the sample was a mixture of isomers. ^1H NMR (CDCl_3) δ 8.64 (d, $J = 7.6$ Hz, 4H, H-1,3,6,8), 8.63 (s, 4H, H-4,5,9,10), 8.05 (t, $J = 7.6$ Hz, 2H, H-2,7), 3.21 (qd, $J = 12.4, 7.3$ Hz, 2H, H-12, 14), 0.33 (dd, $J = 7.3, 1.8$ Hz, 6H, H-15,16), 0.09 (qd, $J = 12.4, 1.8$ Hz, 2H, H-11,13); ^{13}C -NMR (CDCl_3) δ 135.27 (C-3a,5a,10a,10d), 126.07 (C-4,5,9,10), 125.35 (C-1,3,6,8), 123.61 (C-12,14), 123.59 (C-2,7), 121.87 (C-11,13), 11.45 (C-15,16); EI MS m/z 284 (M^+). HR MS Calcd for $\text{C}_{22}\text{H}_{20}$: 284.1565. Found: 284.1557.

10b-((1E)prop-1-enyl)-10c-((1Z)prop-1-enyl)-trans-10b,10c-dihydropyrene 165**165**

The melting point could not be determined because the sample was a mixture of isomers. ^1H NMR (CDCl_3) δ 8.71 (d, $J = 7.7$ Hz, 2H, H-4,10), 8.67 (d, $J = 7.6$ Hz, 2H, H-6,8), 8.66 (d, $J = 7.6$ Hz, 2H, H-5,9), 8.58 (d, $J = 7.7$ Hz, 2H, H-1,3), 8.07 (t, $J = 7.8$ Hz, 1H, H-7), 8.02 (t, $J = 7.7$ Hz, 1H, H-2), 3.14 (qd, $J = 12.4, 7.3$ Hz, 1H, H-14), 2.36 (qd, $J = 15.1, 6.5$ Hz, 1H, H-12), 0.32 (dd, $J = 7.2, 1.8$ Hz, 3H, H-15), 0.17 (dd, $J = 6.7, 1.5$ Hz,

3H, H-16), 0.15 (m, 2H, H-11,13); ^{13}C - NMR (CDCl_3) δ 135.15 (C-5a,10d), 134.77 (C-10a,3a), 126.10 (C-5,9), 125.21 (C-4,10), 125.10 (C-6,8), 124.24 (C-1,3), 123.44 (C-2), 123.39 (C-7), 123.00 (C-13), 122.81 (C-14), 120.62 (C-11), 120.32 (C-12), 16.41 (C-15), 11.09 (C-16); IR ν (KBr) 3018, 2923, 2852, 1365, 836, 797, 692 cm^{-1} ; UV (cyclohexane) λ_{max} nm (ϵ_{max}) 346 nm (46600), 369 (12700), 390 (21100), 482 (4500), 626 (120); Calcd Anal.: C, 92.91; H, 7.09. Found: C, 82.91; H, 7.10.

***anti*-9,18-Diformyl-2,11-dithia-[3.3]metacyclophane 168**

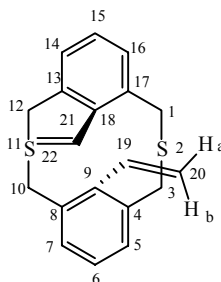


168

DIBAL (5 mL of 1M solution in hexane, 5 mmol) was added dropwise over three minutes to a solution of dicyano-*anti*-thiacyclophane **100** (500 mg, 1.55 mmol) in dichloromethane (10 mL) at room temperature under argon. The reaction mixture was allowed to stir for 3.5 hours and then cooled to 0 °C, treated with excess methanol and stirred for 30 minutes. Then 1N HCl (10 mL) was added and the reaction was stirred for 1hr. The resulting solution was extracted between dichloromethane and water. The organic layer was dried over K_2CO_3 and evaporated. Column chromatography over silica using dichloromethane gave 452 mg (1.38 mmol, 89%) of **168** as colorless crystals from dichloromethane: mp ~ 150 °C dec. ^1H NMR (CDCl_3) δ 9.93 (s, 2H, H-19,20), 7.40 (s, 6H, H-5,6,7,14,15,16), 4.32 and 3.79 (AB, $J = 14.6$ Hz, 4H, H-1,3,10,12); ^{13}C NMR (CDCl_3) δ 191.49 (C-19,20), 140.20 (C-9,18), 135.07 (C-4,8,13,17), 132.88 (C-6,15),

132.18 (C-5,7,14,16), 30.50 (C-1,3,10,12); IR ν (KBr) 3061, 3019, 2903, 2773, 1683, 1584, 1572, 1461, 1401, 1172, 1295, 884, 831, 800, 741 cm^{-1} ; UV (dichloromethane) λ_{max} nm (ϵ_{max}) 235 (12930), 314 (3350).

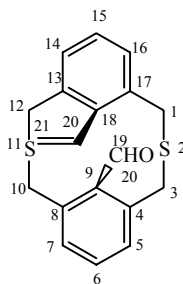
***anti*-9,18-Diethenyl-2,11-dithia-[3.3]metacyclophane 170**



170

Using procedure 7.6 A, a reaction of diformylthiacyclophane **168** (480 mg, 1.46 mmol) with ylide {prepared by reaction of BuLi (1.6 mL of 2.5 M in hexanes, 4 mmol) and methyltriphenylphosphonium bromide (1.15 g, 3.22 mmol) in THF (20 mL)} followed by column chromatography using hexanes: dichloromethane (7:3) as eluant gave divinylthiacyclophane **170** (87.6%) as colorless crystals from cyclohexane: mp \sim 184 $^{\circ}\text{C}$ dec. ^1H NMR (CDCl_3) δ 7.35 (d, $J = 7.6$ Hz, 4H, H-5,7,14,16), 7.17 (t, $J = 7.6$ Hz, 2H, H-6,15), 5.93 (dd, $J = 17.8, 11.3$ Hz, 2H, H-19,21(- $\underline{\text{CH}}=\text{CH}_2$)), 5.16 (dd, $J = 11.3, 2.1$ Hz, 2H, H-20a,22a*), 4.68 (dd, $J = 17.8, 2.1$ Hz, 2H, H-22b,20b*), 3.79 and 3.64 (AB, $J = 14$ Hz, 4H, H-1,3,10,12); ^{13}C NMR (CDCl_3) δ 142.08 (C-9,18), 134.84 (C-4,8,13,17), 134.72 (C-19,21), 130.07 (C-5,7,14,16), 127.09 (C-6,15), 120.34 (C-20,22), 31.94 (C-1,3,10,12); IR ν (KBr) 3080, 2924, 1458, 924, 762 cm^{-1} ; UV (cyclohexane), λ_{max} nm, (ϵ_{max}) 215 (33500), 247 (11000); EI MS m/z 324 (M^+); HR MS Calcd for $\text{C}_{20}\text{H}_{20}\text{S}_2$ 324.1006. Found: 324.1005; Anal. Calcd: C, 74.02; H, 6.21. Found: C, 73.66; H, 6.23.

* "a" stands for the *trans*-vinyl protons whereas "b" stands for the *cis*-vinyl proton.

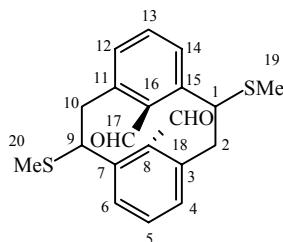


169

Hexanes:dichloromethane 4:6 eluted **169** (8%) as colorless crystals from cyclohexane: mp 169-171 °C; H NMR(CDCl₃) δ 9.82 (s, 1H, -CHO), 7.41 (m, 3H, H-5,6,7), 7.33 (d, $J = 7.6$ Hz, 2H, H-14,16), 7.20 (t, $J = 7.6$ Hz, 1H, H-15), 6.00 (dd, $J = 17.8, 11.3$ Hz, 1H, H-20 (-CH=CH₂)), 5.22 (dd, $J = 11.4, 1.9$ Hz, 1H, H-21a), 4.78 (dd, $J = 17.7, 1.9$ Hz, 1H, H-21b), 4.27 and 3.72 (AB, $J = 14.6$ Hz, 2H, H-3,10), 3.80 and 3.72 (AB, $J = 14.1$ Hz, 1H, H-1,12); ¹³C NMR (CDCl₃) δ 191.81 (CHO), 141.61 (C-18), 139.88 (C-4,8), 135.83 (C-9), 134.82 (C-13,17), 133.86 (C-20), 132.28 (C-6), 131.77 (C-5,7), 130.41 (C-14,16), 127.49 (C-15), 121.04 (C-21), 32.20 (C-1,12), 30.09 (C-3,10); IR ν (KBr) 3080, 2938, 2908, 2780, 1679, 1587, 1464, 1009, 940, 771, 751 cm⁻¹; UV (dichloromethane) λ_{max} nm (ε_{max}) 231 (17500), 306 sh (1900); EI MS 326 (M⁺); Anal. Calcd: C, 69.90; H, 5.55. Found: C, 69.25; H, 5.71.

* "a" stands for the *trans*-vinyl protons whereas "b" stands for the *cis*-vinyl proton.

2, 10-Bis(thiomethyl)-8,16-diformyl-*anti*-[2.2]metacyclophane 174



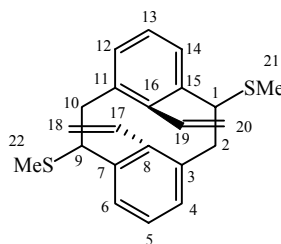
174

DIBAL (20 mL of 1M solution in hexane, 20 mmol) was added dropwise over three minutes to a solution of dicyano-*anti*-thiomethylcyclophane **99** (2.3 g, 6.55 mmol) in dichloromethane (60 mL) at room temperature under argon. The reaction mixture was allowed to stir for 2.5 h and then cooled to 0 °C, treated with excess methanol and stirred for 30 minutes. Then 0.35 N HCl (100 mL) was added and stirred for 1hr. The resulting solution was extracted between dichloromethane and water. The organic layer was dried over K₂CO₃ and evaporated. Column chromatography over silica gel using hexanes-dichloromethane 2:8 gave 2.05 g (5.76 mmol, 88%) of **174** as a mixture of isomers, EI MS m/z 356 (M⁺). These could be used directly in the next step. For characterization, a single isomer of **174**, in which the 1,9-thiomethyl groups are pseudo-equatorial was purified by careful column chromatography: mp 187-192 °C; ¹H NMR (CDCl₃) δ 8.95 (s, 2H, H-17,18), 8.00 (dd, $J = 7.6, 1.0$ Hz, 2H, H-6,14), 7.36 (t, $J = 7.6$ Hz, 2H, H-5,13), 7.27 (dd, $J = 7.5$ Hz, 1.0 Hz, 2H, H-4,12), 5.15 (dd, $J = 11.4, 5.0$ Hz, 2H, H-1_{ax},9_{ax}), 3.36 (dd, $J = 12.8, 5.0$ Hz, 2H, H-2_{eq},10_{eq}), 3.21 (dd, $J = 12.8, 11.4$ Hz, 2H, H-2_{ax},10_{ax}), 2.19 (s, 6H, -SMe); ¹³C NMR (CDCl₃) δ 188.74 (CHO), 143.49 (C-7,15), 142.94 (C-3,11), 141.15 (C-8,16), 133.28 (C-5,13), 131.24 (C-4,12), 127.04 (C-6,14), 50.89 (C-1,9), 42.23 (C-2,10), 15.82 (SMe); IR ν (KBr) 2890, 2889, 2786, 1682, 1580, 1445, 1208, 880, 789,

738, 707 cm^{-1} ; UV (cyclohexane) λ_{max} nm (ϵ_{max}) 227 (5100), 259 (3500), 297 (800); EI MS m/z 356 (M^+); HR MS Calcd for $\text{C}_{20}\text{H}_{20}\text{O}_2\text{S}_2$: 356.0904. Found: 356.0902. Anal. Calcd: C, 67.38; H, 5.65. Found: C, 67.41; H, 5.57.

Mixture of isomers gave following NMR data: ^1H NMR (CDCl_3) δ 9.04, 8.94, 8.91, 8.75 (4s), 8.04 (d, $J = 7.8$ Hz), 7.98 (d, $J = 7.3$ Hz), 7.5-7.2 (m), 5.14 (dd, $J = 11.4$, 5.0 Hz), 4.83 (dd, $J = 11.4$, 4.8 Hz), 4.63 (dd, $J = 7.1$, 1.2 Hz), 4.48 (dd, $J = 11.2$, 4.7 Hz), 4.36 (dd, $J = 14.0$, 7.1 Hz), 3.50 (dd, $J = 12.4$, 11.6 Hz) 3.37-3.33 (m), 3.20 (t), 2.19-2.18 (3 s, S-Me).

2,10-Bis(thiomethyl)-8,16-diethenyl-*anti*-[2.2]metacyclophane 171



171

Using procedure 7.6 A, a reaction of diformylthiomethylcyclophane **174** (1.5 g, 4.21 mmol) with an ylide {prepared by reaction of BuLi (5.3 mL of 2.5M in hexanes, 13.25 mmol) and methyltriphenylphosphonium bromide (3.6 g, 10.08 mmol) in THF (40 mL)} followed by column chromatography using hexanes: dichloromethane (7:3) as eluant gave divinylthiomethylcyclophane **171** (93%) as a mixture of isomers, EI MS m/z 352 (M^+).

Procedure B: Wittig rearrangement.

BuLi (0.9 mL, 2.5M solution in hexanes, 2.25 mmol) was added dropwise to the solution of 9,18-divinylthiacyclophane **170** (250 mg, 0.77 mmol) in THF (12 mL) at 0 $^{\circ}\text{C}$

under argon and brought to room temperature over ten minutes where dark brown solution turned yellow. MeI (excess, 0.5 mL) was added to this reaction mixture and stirred for another 10 minutes. The reaction was quenched with water and extracted with dichloromethane (3 x 20 mL). The organic layer was dried over anhydrous MgSO₄ and evaporated to give desired product **171** (250 mg, 0.71 mmol, 92%) as a mixture of isomers.

Mixture of isomers

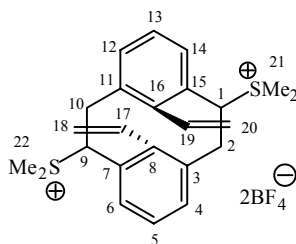
¹H NMR (CDCl₃) δ 7.98 (d, *J* = 7.6 Hz) 7.80 (d, *J* = 7.7 Hz), 7.67-7.62 (m), 7.53-7.51 (m), 7.45-7.42 (m), 7.20-7.16 (m), 7.08-7.05 (m), 6.94 (t, *J* = 7.4 Hz), 4.80-4.60 (complex m), 4.52-4.40 (m), 4.28-4.25 (m), 4.11-4.08 (m), 3.08-3.04 (m), 2.87 (t, *J* = 12.0 Hz), 2.66 (t, *J* = 12.1 Hz), 2.12, 2.08 (s).

These could be used directly in the next step. For characterization, a single isomer of **171**, in which the 1,9-thiomethyl groups are pseudo-equatorial was purified by re-chromatography.

mp 228-229 °C; ¹H NMR (CDCl₃) δ 7.81 (dd, *J* = 7.6, 1.1 Hz, 2H, H-6,14), 7.18 (dd, *J* = 7.5, 1.0 Hz, 2H, H-4,12), 7.07 (t, *J* = 7.5 Hz, 2H, H-5,13), 4.76 and 4.43 (m, 4H, H-19,20,17,18), 4.27 (dd, *J* = 11.6, 4.2 Hz, 2H, H-1,9), 3.06 (dd, *J* = 12.6, 4.2 Hz, 2H, H-2_{eq},10_{eq}), 2.66 (dd, *J* = 12.1, 11.9 Hz, 2H, H-2_{ax},10_{ax}), 2.13 (s, 3H, SMe); ¹³C NMR (CDCl₃) δ 147.02 (C-8,16), 135.70 (C-7,15), 135.24 (C-3,11), 134.98 (C-17, 19), 128.93 (C-4,12), 126.62 (C-5,13), 125.37 (C-6,14), 120.57 (C-18,20), 53.20 (C-1,9), 43.27 (C-2,10), 15.34 (C-21,22); IR ν (KBr) 3078, 2960, 2909, 1438, 1397, 994, 930, 771, 748 cm⁻¹; UV (cyclohexane) λ_{max} nm (ε_{max}) 227 (17300), 288 (3986); EI MS *m/z* 352

(M⁺); HR MS Calcd for C₂₂H₂₄S₂: 352.1319. Found: 352.1319. Anal. Calcd: C, 74.95; H, 6.86. Found: C, 74.48; H, 6.91.

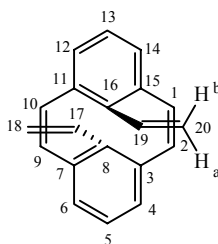
1,10-Bis(thiomethyl)-8-16-divinyl-*anti*-[2.2]metacyclophane bis-sulfonium salt **172**



172

Using procedure 7.3, mixed isomers **171** (360 mg, 1 mmol) on reaction with Borch reagent (80% oil, 580 mg, 2.86 mmol) in CH₂Cl₂ (14 mL) gave the sulfonium salt **172** in 79% yield : ¹H NMR (DMSO-*d*₆) δ 7.72 (d, *J* = 7.8 Hz), 7.58 (d, *J* = 7.4 Hz), 7.54 (d, *J* = 7.3 Hz), 7.41 (d, *J* = 7.6 Hz), 7.28 (t, *J* = 7.6 Hz), 7.13 (t, *J* = 7.4 Hz), 5.2-4.6 (m), 3.46-3.05 (m), 2.90, 2.87(s).

8,16-Divinyl-*anti*-[2.2]metacyclophane-1,9-diene **166**

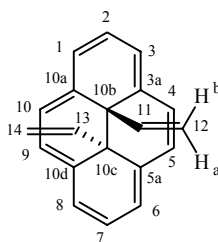


166

Using procedure 7.4, a reaction of bis-sulfonium salt **172** (440 mg, 0.791 mmol) and *t*-BuOK (250 mg, 2.23 mmol) in THF (14 mL) followed by column chromatography over silica gel using hexanes as eluant gave **166** (90%) as colorless crystals from cyclohexane, which on attempted mp determination isomerizes into DHP **167**: ¹H NMR

(CDCl₃) δ 7.07 (t, $J = 7.4$ Hz, 2H, H-5,13), 6.60 (d, $J = 7.4$ Hz, 4H, H-4,6,12,14), 6.38 (s, 4H, H-1,2,9,10), 6.32 (dd, $J = 17.4, 11.0$ Hz, 2H, H-17,19) 5.47 (dd, $J = 17.4, 1.8$ Hz, 2H, H-18,20b), 4.84 (dd, $J = 11.0, 1.8$ Hz, 2H, H-18,20a); ¹³C NMR (CDCl₃) δ 146.42 (C-8,16), 135.83 (3,7,11,15), 135.20 (C-17,19), 133.23 (C-1,2,9,10), 129.54 (C-5,13), 126.68 (C-4,6,12,14), 118.90 (C-18,20); IR ν (KBr) 3077, 3049, 3004, 1618, 1436, 1397, 993, 903, 861, 807, 764, 605 cm⁻¹; UV (cyclohexane) λ_{\max} nm (ϵ_{\max}) 202 (51700), 242 (33170), 279 (12370), 339 (11000), 377 (5710), 390 sh (2100); EI MS m/z 256 (M⁺), 229 (M⁺ -27), 202(100%, M⁺ - 54); HR MS Calcd for C₂₀H₁₆: 256.1252. Found: 256.1255. Calcd. Anal: C, 93.70; H, 6.30. Found: C, 93.51; H, 6.41.

10b,10c-Divinyl- *trans*-10b,10c-dihydropyrene 167

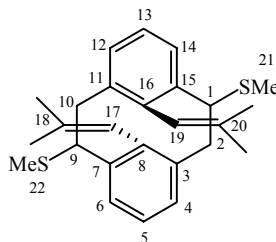


167

Using procedure 7.5, DHP **167** was obtained from cyclophanediene **166** in quantitative yield as dark green crystals from cyclohexane: mp 163-165 °C; ¹H NMR (CDCl₃) δ 8.79 (s, 4H, H-4,5,9,10), 8.65 (d, $J = 7.6$ Hz, 4H, H-1,3,6,8), 8.08 (t, $J = 7.6$ Hz, 2H, H-2,7), 2.67 (dd, $J = 10.3, 1.4$ Hz, 2H, H-12,14b), 2.06 (dd, $J = 17.0, 1.5$ Hz, 2H, H-12,14a), 0.50 (dd, $J = 17.0, 10.3$ Hz, 2H, H-11,13); ¹³C NMR (CDCl₃) δ 133.81 (3a,5a,10a,10d), 128.57 (C-11,13), 125.47 (C-4,5,9,10), 124.42 (C-1,3,6,8), 123.79 (C-2,7), 109.83 (C-12,14), 36.12 (C-10b,10c); IR ν (KBr) 3032, 3007, 1621, 1399, 1295, 912, 841 cm⁻¹; UV (cyclohexane) λ_{\max} nm (ϵ_{\max}) 339 (71300), 377 (30000), 462 (5600),

608 (100); EI MS m/z 256 (M^+), 229 ($M^+ - 27$, 100%), 202. HR MS Calcd for $C_{20}H_{16}$: 256.1252. Found: 256.1251. Calcd. Anal: C, 93.70; H, 6.30. Found: C, 93.92; H, 6.57.

2,10-Bis(thiomethyl)-8,16-bis(2-methyl-1-preopenyl)-anti-[2.2]-cyclophane 176

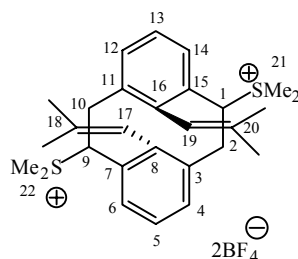


176

Using procedure 7.6 B, a reaction of diformylthiomethylcyclophane **174** (1.0 g, 2.81 mmol) with an ylide {prepared by reaction of *t*-BuOK (2.0 g, 18.6 mmol) and isopropyl triphenylphosphonium bromide (2.75 g, 7.14 mmol) in THF (25 mL)} followed by column chromatography using hexanes: dichloromethane (7:3) as eluant gave diisobutenylthiomethylcyclophane **176** (61%) as a mixture of isomers, EI MS m/z 408 (M^+). These could be used directly in the next step: 1H NMR ($CDCl_3$) δ 7.75 (d, $J = 7.6$ Hz), 7.735 (d, $J = 7.6$ Hz), 7.733 (d, $J = 7.6$ Hz), 7.19 (m), 7.06 (t, $J = 7.5$ Hz), 6.94 (t, $J = 7.4$ Hz), 4.04 (br s), 3.98 (dd, $J = 11.4$, 4.0 Hz), 3.92 (dd, $J = 11.5$, 4.0 Hz), 3.80, 3.69 (br singlets), 3.03 (dd, $J = 12.1$, 4.0 Hz), 2.59 (t, $J = 11.8$ Hz), 2.51 (t, $J = 11.8$ Hz), 2.12, 2.07 (two singlets), 1.43, 1.40, 1.39, 1.07, 0.97, 0.88 (six singlets); ^{13}C NMR ($CDCl_3$) δ 145.77, 144.66, 143.68, 137.45, 137.37, 136.36, 136.21, 136.10, 135.81, 134.86, 134.49, 134.39, 134.36, 134.21, 128.57, 128.04, 128.43, 128.18, 126.05, 125.93, 125.77, 125.36, 125.32, 124.70, 122.48, 122.19, 122.08, 121.997, 53.30, 53.12, 43.87, 43.47, 32.15, 29.92, 29.58, 25.47, 25.27, 25.14, 22.91, 18.70, 18.57, 18.20, 16.11, 15.62, 14.33; IR ν (KBr) 3047, 2962, 2923, 2853, 1654, 1437, 1376, 833, 777, 731, 720 cm^{-1} ;

UV (cyclohexane) λ_{\max} nm (ϵ_{\max}) 230 nm sh (33400); EI MS m/z 408 (M^+); HR MS
Calcd: 408.1945. Found: 408.1950.

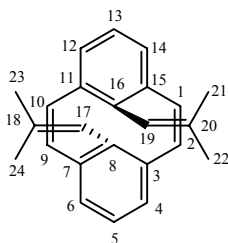
**8,16-Bis(2-methyl-1-propenyl)-1,9-bis(thiomethyl)-*anti*-[2.2]metacyclophane
sulfonium salt **177****



177

Using procedure 7.3, mixed isomers **176** (700 mg, 1.716 mmol) on reaction with Borch reagent ((80% oil, 1.50 g, 7.4 mmol) in CH_2Cl_2 (15 mL) gave the sulfonium salt **177** as a mixture of isomers in 71% yield: ^1H NMR ($\text{DMSO-}d_6$) δ 7.71 (d, $J = 7.8$ Hz), 7.61 (d, $J = 7.3$ Hz), 7.50 (d, $J = 7.2$ Hz), 7.43 (m), 7.29 (t, $J = 7.6$ Hz), 7.14 (t, $J = 7.4$ Hz), 4.56 (dd, $J = 11.6, 3.8$ Hz), 4.41 (dd, $J = 11.6, 4.0$ Hz), 4.22 (s), 3.92 (br s), 3.54 (br s), 3.45 (dd, $J = 12.1, 3.9$ Hz), 3.38 (dd, $J = 12.1, 3.9$ Hz), 3.32 (s, SMe), 2.88 (t), 2.83, 2.82 (singlets), 1.52, 1.49, 1.47, 1.13, 1.03, 0.86 (six broad singlets).

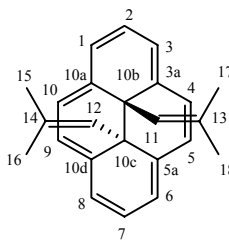
8,16-Bis(2-methylprop-1-enyl)-*anti*-[2.2]metacyclophane-1,9-diene **178**



178

Using procedure 7.4, a reaction of bis-sulfonium salt **177** (640 mg, 1.05 mmol) and *t*-BuOK (400 mg, 3.57 mmol) in THF (25 mL) followed by column chromatography over silica gel using hexanes as eluant gave **178** (96%) as colorless crystals from cyclohexane, which on attempted mp determination isomerizes into DHP **179**: ^1H NMR (CDCl_3) δ 7.04 (t, $J = 7.4$ Hz, 2H, H-5,13), 6.60 (d, $J = 7.4$ Hz, 4H, H-4,6,12,14), 6.26 (s, 4H, H-1,2,9,10), 5.70 (m, 2H, H-17,19), 1.57 (two overlapping doublets, 12H, Me); ^{13}C NMR (CDCl_3) δ 142.80 (C-8,16), 137.45 (C-3,7,11,15), 135.17 (C-18,20), 132.14 (C-1,2,9,10), 127.71 (C-5,13), 125.71 (C-4,6,12,14), 125.47 (C-17,19), 20.64, 26.81 (C-21,22,23,2,4); IR ν (KBr) 3045, 3011, 2956, 2892, 1637, 1444, 1434, 1052, 827, 763, 656, 637 cm^{-1} ; UV (cyclohexane) λ_{max} nm (ϵ_{max}) 229 nm (46000), 254 sh (16900), 299 sh (2400), 355 (2800) EI MS m/z 312 (M^+), 257 (M^+ - isobutenyl), 202 (100%); HR MS Calcd for $\text{C}_{24}\text{H}_{24}$: 312.1878. Found: 312.1876. Calcd. Anal: C, 92.26; H, 7.74. Found: C, 92.00; H, 7.83.

10b,10c-Bis(2-methylprop-1-enyl)-*trans*-10b,10c-dihydropyrene 179

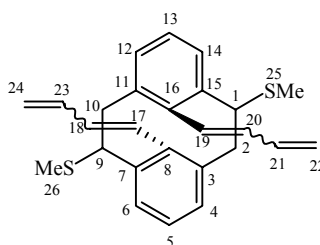


179

Using procedure 7.5, DHP **179** was obtained in quantitative yield from diisobutenyl CPD **178** as orange crystals: mp \sim 142-143 $^{\circ}\text{C}$ dec; decomposed product's mp 175-177 $^{\circ}\text{C}$; ^1H NMR (CDCl_3); δ 8.55 (d, $J = 7.5$ Hz, 4H, H-1,3,6,8), 8.51 (s, 4H, H-4,5,9,10), 7.93 (t, $J = 7.5$ Hz, 2H, H- 2,7), 0.17 (d, $J = 1.1$ Hz, 6H, H-15,17), 0.14 (d, $J =$

1.3 Hz, 6H, H-16,18), -0.16 (m, 2H, H-11,12); ^{13}C NMR (CDCl_3) δ 135.75 (C-3a,5a,10a,10d), 130.73 (C-13,14), 125.89 (C-4,5,9,10), 125.34 (C-1,3,6,8), 123.10 (C-2,7), 116.18 (C-11,12), 36.22 (C-10b,10c), 28.24 (C-15,18), 16.16 (C-16,17); IR ν (KBr) 3020, 2967, 2920, 1654, 1648, 1637, 838, 826, 764 cm^{-1} ; UV (cyclohexane) λ_{max} nm (ϵ_{max}) 205 (32300), 243 (12000), 349 (44400), 371 (14500), 395 (27000), 494 (4200), 644 (130); EI MS m/z 312 (M^+), 257 (M^+ - isobutenyl), 202 (100%); HR MS Calcd for $\text{C}_{24}\text{H}_{24}$: 312.1878. Found: 312.1876. Calcd. Anal: C, 92.26; H, 7.74. Found: C, 85.88; H, 7.21.

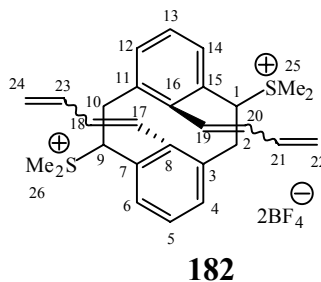
8,16-Bis(buta-1,3-dienyl)-1,9-bis(thiomethyl)-*anti*-[2.2]-cyclophane **180**



180

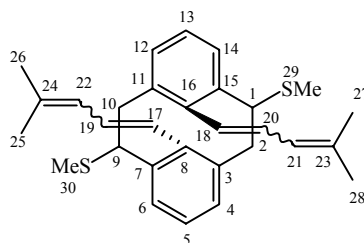
Using procedure 7.6 A, a reaction of diformylthiomethylcyclophane **174** (600 g, 1.68 mmol) with an ylide {prepared by reaction of BuLi (1.7 mL of 2.5M in hexanes, 4.25 mmol) and allyl triphenylphosphonium bromide (1.5 g, 3.24 mmol) in THF (20 mL)} followed by column chromatography using hexanes: dichloromethane (7:3) as eluant gave cyclophane **180** (52%) was obtained as a mixture of isomers by column chromatography using hexanes-DCM 70:30. These could be used directly in the next step: ^1H NMR (CDCl_3) δ 7.88-7.79 (m), 7.25-7.07 (m), 6.0-5.90 (m), 5.68-5.38 (m), 5.03-4.95 (m), 4.87-4.83 (m), 4.72 (d, $J = 15.8$ Hz), 4.31-4.27 (m), 4.13 (d, $J = 9.7$ Hz), 4.01 (dd, $J = 11.5, 4.1$ Hz), 3.07 (dd, $J = 12.8, 4.0$ Hz), 2.70 (t, $J = 12.0$ Hz), 2.54 (t, $J = 12.0$ Hz), 2.50 (t, $J = 12.0$ Hz), 2.17, 2.10, 2.04 (s).

8,16-Bis(buta-1,3-dienyl)-1,9-bis(thiomethyl)-*anti*-[2.2]metacyclophane-bis-sulfonium salt **182**



Using procedure 7.3, mixed isomers **180** (320 mg, 0.8 mmol) on reaction with Borch reagent ((80% oil, 0.6 g, 3 mmol) in CH₂Cl₂ (20 mL) gave 160 mg (0.225 mmol, 33%) of sulfonium salt **182**. The reaction conditions were not optimized. ¹H NMR (DMSO-*d*₆) 7.67 (d, *J* = 7.4 Hz), 7.63 (d, *J* = 7.4 Hz), 7.58 (d, *J* = 7.6 Hz), 7.53 (t, *J* = 7.0 Hz), 7.37 (t, *J* = 7.6 Hz), 7.29 (t, *J* = 7.5 Hz), 5.82 (t, *J* = 10.2 Hz), 5.62-5.50 (m), 5.24 (d, *J* = 16.6 Hz), 5.06 (d, *J* = 10.3 Hz), 4.64 (dd, *J* = 11.4, 3.7 Hz), 4.27 (d, *J* = 11.5 Hz), 4.02 (AB, *J* = 14.3, 7.2 Hz), 3.52-3.47 (m), 3.35-3.29 (4 s), 2.89 (s), 2.82, 2.80, 2.78 (s)

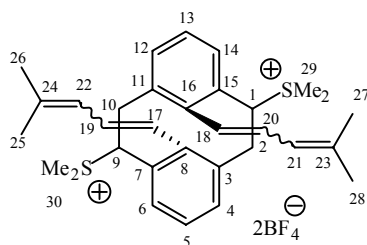
8,16-Bis(4-methylpenta-1,3-dienyl)-1,9-bis(thiomethyl)-*anti*-[2.2]metacyclophane **188**



Using procedure 7.6 B, a reaction of diformylthiomethylcyclophane **174** (680 mg, 1.91 mmol) with an ylide {prepared by reaction of *t*-BuOK (1.60 g, 14.3 mmol) and 3-methylbut-2-enyl triphenylphosphonium bromide (4.2 g, 10.2 mmol) in THF (40 mL)}

followed by column chromatography using hexanes: DCM 75:25 gave the desired product **188** (67%) as a mixture of isomers, $^1\text{H NMR}$ (CDCl_3) δ 7.88-7.78 (m), 7.24-6.89 (m), 5.86-5.56 (m), 5.50-5.40 (m), 5.15-4.91 (m), 4.70-4.56 (m), 4.40-4.32 (m), 4.10-3.95 (m), 3.10-3.00 (m), 2.91-2.83 (m), 2.70-2.50 (m), 2.28 (t, $J = 11.4$ Hz), 2.19, 2.18 (s), 2.13, 2.09 (3 s), 2.06, 2.04, 2.03 (3 s), 1.74, 1.61, 1.60 (br s), 1.53, 1.51 (br s); EI MS m/z 460 (M^+). HR MS Calcd for $\text{C}_{30}\text{H}_{36}\text{S}_2$: 460.2258. Found: 460.2257.

8,16-Bis(4-methylpenta-1,3-dienyl)-1,9-bis(thiomethyl)-*anti*-[2.2]metacyclophane sulfonium salt **189**



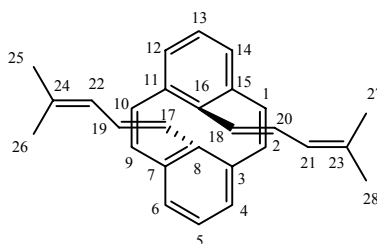
189

Using procedure 7.3, mixed isomers **188** (0.55 g, 1.19 mmol) on reaction with Borch reagent ((80% oil, 0.9 g, 4.4 mmol) in CH_2Cl_2 (8 mL) gave 320 mg (0.48 mmol, 41%) of bis-sulfonium salt **189**: $^1\text{H NMR}$ ($\text{DMSO}-d_6$) 7.77-7.32 (m), 7.26 (t, $J = 7.6$ Hz), 7.10 (t, $J = 7.5$ Hz), 6.08-5.92 (m), 5.82-5.71(m), 5.06 (t, $J = 12.2$ Hz), 4.93-4.74 (m), 4.63-4.42 (m), 4.18 (d, $J = 11.2$ Hz), 4.12 (d, $J = 11.7$ Hz) 4.02 (AB, $J = 14.2, 7.0$ Hz), 3.9 (d, $J = 11.2$ Hz), 3.52-3.10 (m), 3.32-3.29 (overlapping singlets), 2.91-2.76 (6 s), 1.75, 1.64, 1.62, 1.57, 1.55, 1.52 (br s).

8,16-Bis(4-methylpent-1,3-dienyl)-*anti*-[2.2]metacyclophane-1,9-dienes **184-186**

Using procedure 7.4, a reaction of bis-sulfonium salt **189** (300 mg, 1.05 mmol) and *t*-BuOK (400 mg, 3.57 mmol) in THF (20 mL) gave a mixture of cyclophanedienes. The mixture was chromatographed over silica gel using hexanes: DCM 19: 1. Eluted first from column was a mixture of **184** and **185**, and then last the *cis*-isomer **186**.

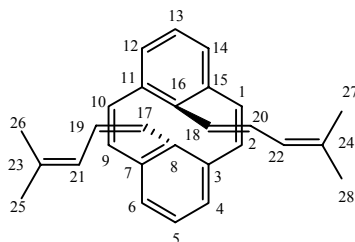
8,16-Bis((*E*) 4-methyl-penta-1,3-dienyl)-*anti*-[2.2]metacyclophane-1,9-diene **184**



184

The melting point could not be determined because the sample was a mixture of isomers. $^1\text{H NMR}$ (CD_2Cl_2) δ 6.98 (t, $J = 7.4$ Hz, 2H, H-5,13), 6.80 (dd, $J = 15.3, 11.0$ Hz, 2H, H-19,20), 6.53 (d, $J = 7.4$ Hz, 4H, H-4,6,12,14), 6.38 (s, 4H, H-1,2,9,10), 6.09 (d, $J = 15.4$ Hz, 2H, H-17,18), 5.60 (dm, $J = 10.8$ Hz, 2H, H-21,22), 1.78 (s, 6H, H-25,28), 1.72 (s, 6H, H-26,27); $^{13}\text{C NMR}$ (CD_2Cl_2) δ 145.99 (C-8,16), 136.44 (C-3,7,11,15), 136.32 (C-23,24), 133.50 (C-1,2,9,10), 130.85 (C-19,20), 129.81 (C-17,18), 128.99 (C-5,13), 127.14 (C-21,22), 126.94 (C-4,6,12,14), 26.45 (C-25,28), 18.71 (C-26,27); EI MS m/z 364 (M^+); HR MS Calcd for $\text{C}_{28}\text{H}_{28}$: 364.2191, Found: 364.2195; Anal. Calcd: C, 92.26; H, 7.74. Found: C, 90.78; H, 7.82.

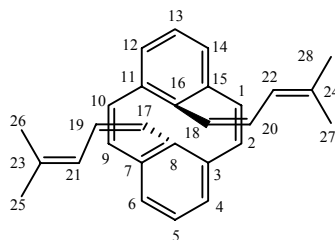
16-Bis((1*E*)-4-methyl-penta-1,3-dienyl)-8-((1*Z*)-4-methyl-penta-1,3-dienyl)-*anti*-[2.2]metacyclophane-1,9-diene 185



185

The melting point could not be determined because the sample was a mixture of isomers. ^1H NMR (CD_2Cl_2) δ 7.09 (t, $J = 7.4$ Hz, 1H, H-13), 6.99 (t, $J = 7.4$ Hz, 1H, H-5), 6.75 (dd, $J = 15.2, 11.0$ Hz, 1H, H-20), 6.58 (d, $J = 7.4$ Hz, 2H, H-12,14), 6.57 (d, $J = 7.4$ Hz, 2H, H-4,6), 6.30 (AB, $J = 11.4$ Hz, 4H, H-1,2,9,10), 6.04 (d, $J = 15.4$ Hz, 1H, H-18), 5.98 (m, 1H, H-21), 5.83 (dd, $J = 12.4, 11.8$ Hz, 1H, H-19), 5.79 (d, $J = 12.4$ Hz, 1H, H-17), 5.60 (dm, $J = 12.5$ Hz, 1H, H-22), 1.78 (s, 3H, H-28), 1.74 (s, 3H, H-25), 1.72 (s, 3H, H-27), 1.71 (s, 3H, H-26); ^{13}C NMR (CD_2Cl_2) δ 147.10 (C-8), 142.36 (C-16), 138.18 (C-11,15), 137.41 (C-23), 136.51 (C-24), 136.20 (C-3,7), 133.10 (C-2,9), 133.01 (C-1,10), 130.93 (C-20), 129.81 (C-13), 129.57 (C-18), 128.36 (C-5), 127.13 (C-22), 126.89 (C-4,6), 126.87 (C-17), 126.42 (C-19), 126.40 (C-12,14), 123.42 (C-21), 26.64 (C-25), 26.45 (C-28), 18.71 (C-27), 18.55 (C-26).

8,16-Bis((1Z)-4-methyl-penta-1,3-dienyl)-*anti*-[2.2]metacyclophane-1,9-diene 186



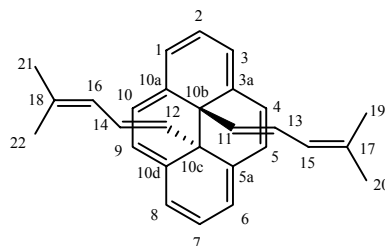
186

The melting point could not be determined because the sample was a mixture of isomers. ^1H NMR (CD_2Cl_2) δ 7.10 (t, $J = 7.4$ Hz, 2H, H-5,13), 6.63 (d, $J = 7.4$ Hz, 4H, H-4,6,12,14), 6.24 (s, 4H, H-1,2,9,10), 5.97 (m, 2H, H-21,22), 5.76 (m, 4H, H-17-20), 1.74 (s, 6H, H-25,28), 1.71 (s, 6H, H-26,27); ^{13}C NMR (CD_2Cl_2) δ 143.43 (C-8,16), 137.92 (C-3,7,11,15), 137.56 (C-23,24), 132.55 (C-1,2,9,10), 129.21 (C-5,13), 126.60, 126.46 (C-17-20), 126.30 (C-4,6,12,14), 26.64 (C-25,28), 18.55 (C-26,27); IR (mix) ν (KBr) 3041, 3002, 2965, 2910, 1636, 1560, 426, 1375, 952, 786, 777, 750 cm^{-1} ; UV (cyclohexane) λ_{max} (ϵ_{max}) 246 (27900), 284 (32600), 390 (5000), 406 sh (4800).

Dihydropyrenes 190-192

A mixture of cyclophanedienes **184-186** (45 mg) in toluene- d_8 (6 mL) was sealed in a glass tube under argon and heated at 110 $^\circ\text{C}$ for 2 h, which converted it into a mixture of dihydropyrenes **190-192**. The mixture was chromatographed over silica gel using hexanes-DCM 9: 1 as eluant. Eluted first was the all *trans*-isomer **190**, then **191** and finally all *cis*-**192**.

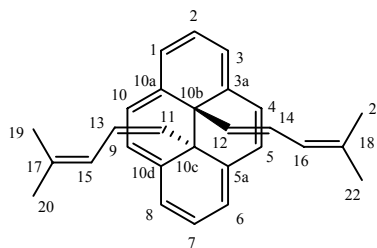
10b,10c-Bis((1E)-4-methylpenta-1,3-dienyl)-trans-10b,10c-dihydropyrene 190



190

mp 188-190 °C; ^1H NMR (CDCl_3) δ 8.76 (s, 4H, H-4,5,9,10), 8.63 (d, $J = 7.8$ Hz, 4H, H-1,3,6,8), 8.06 (t, $J = 7.7$ Hz, 2H, H-2,7), 4.04 (dm, $J = 10.9$ Hz, 2H, H-15,16), 2.95 (dd, $J = 15.0, 10.8$ Hz, 2H, H-13,14), 1.15, 1.10 (s, 12H, Me), 0.22 (d, $J = 15.0$ Hz, 2H, H-11,12); ^{13}C NMR (CDCl_3) δ 134.39 (C-3a,5a,10a,10d), 133.51 (C-17,18), 125.29 (C-4,5,9,10), 124.20 (C-1,3,6,8), 123.84 (C-15,16), 123.66 (C-2,7), 121.75 (C-11,12), 121.38 (C-13,14), 35.75 (C-10b,10c), 25.51, 18.00 (19-22); IR ν (KBr) 3053, 3029, 3003, 1654, 1648, 1441, 1376, 956, 843, 710 cm^{-1} ; UV (cyclohexane) λ_{max} nm (ϵ_{max}) 247 (76200), 338 (78300), 380 (27900), 469 (7900), 609 (135) EI MS m/z 364 (M^+); HR MS Calcd for $\text{C}_{28}\text{H}_{28}$: 364.2191. Found: 364.2195.

10b-((1E)-4-Methylpenta-1,3-dienyl)-10c-((1Z)-4-methylpenta-1,3-dienyl)-trans-10b,10c-dihydropyrene 191

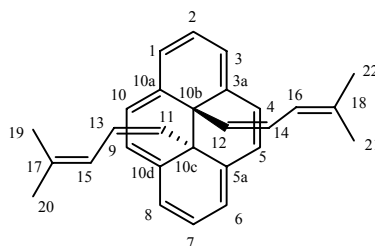


191

The melting point could not be determined because of contamination from **192**.

^1H NMR (CDCl_3) δ 8.70 (AB, $J = 7.7$ Hz, 4H, H-4,5,9,10), 8.69 (d, $J = 7.6$ Hz, 2H, H-6,8), 8.60 (d, $J = 7.8$ Hz, 2H, H-1,3), 8.08 (t, $J = 7.7$ Hz, 1H, H-7), 8.04 (t, $J = 7.8$ Hz, 1H, H-2), 4.50 (dm, $J = 12, 1.3$ Hz, 1H, H-15), 4.06 (dm, $J = 10.8$ Hz 1H, H-16), 3.84 (t, $J = 12.3$ Hz, 1H, H-13), 3.03 (dd, $J = 15.0, 10.8$ Hz, 1H, H-14), 1.52, 1.00 (br s, 6H, H-19,20), 1.16, 1.11 (s, 6H, H-21,22), 0.23 (d, $J = 15.0$ Hz, 1H, H-12), 0.01 (d, $J = 12.4$ Hz, 1H, H-11); ^{13}C NMR 135.93 (C-17,18), 135.31 (C-5a,10d), 134.80 (3a,10a), 126.30 (C-5,9), 125.36 (C-4,10), 125.09 (C-6,8), 124.40 (C-1,3), 123.78 (C-2), 123.84 (C-16), 123.24 (C-7), 122.72 (C-13), 121.92 (C-14), 120.76 (C-12), 119.99 (C-11), 119.36 (C-15), 37.77 (C-10b), 34.75 (C-10c), 26.54, 17.08 (C-19,20), 25.52, 18.03 (C-21,22); IR v (KBr) 3030, 3003, 2926, 2853, 1654, 1438, 1374, 955, 843, 838, 714, 645 cm^{-1} ; UV (cyclohexane) λ_{max} nm (ϵ_{max}) 250 nm (54800), 344 (56400), 389 (30400), 475 (6058), 614 (120).

10b,10c-Bis((1Z)-4-methylpenta-1,3-dienyl)-trans-10b,10c-dihydropyrene 192



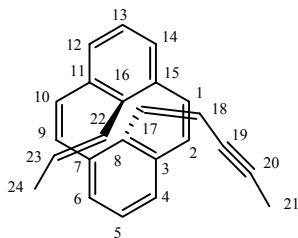
192

The melting point could not be determined because of contamination from **191**.

^1H NMR (CDCl_3) δ 8.65 (d, $J = 7.7$ Hz, 4H, H-1,3,6,8), 8.62 (s, 4H, H-4,5,9,10), 8.08 (2H, H-2,7), 4.53 (dm, $J = 12.2, 1.4$ Hz, 2H, H-15,16), 3.90 (dd, $J = 12.2$ Hz, 2H, H-13,14), 1.52, 1.01 (s, 12H, Me), -0.02 (d, $J = 12.5$ Hz, 2H, H-11,12); ^{13}C NMR (CDCl_3) δ 136.06 (C-17,18), 135.88 (C-3a,5a,10a,10d), 126.31 (C-4,5,9,10), 125.36 (C-1,3,6,8),

123.53 (C-2,7), 123.31 (C-13,14), 119.39 (C-15,16), 119.01 (C-11,12), 36.62 (C-10b,10c), 26.55, 17.11 (C-19-22); IR ν (KBr) 3023, 2965, 1647, 1654, 1438, 1374, 836, 729 cm^{-1} ; UV (cyclohexane) λ_{max} nm (ϵ_{max}) 251 (42900), 347 (38200), 392 (20100), 486 (5000), 627 (137).

(Pent-1-ene-3-ynyl)-anti-[2.2]metacyclophane-1,9-dienes



196

BuLi (1.20 mmol, 0.55 mL of 2.25 M in hexanes) was added dropwise to a suspension of 2-butylnyl triphenylphosphonium bromide (300 mg, 0.8 mmol) in THF (8 mL) at room temperature under argon and allowed to stir for 20 minutes. The reaction mixture was cooled to -20 to -30 °C and diformyl cyclophanediene **174** (120 mg, 0.47 mmol) was added. The reaction mixture was brought to room temperature over 30 minutes and then quenched with acid (15 mL of 1.5 M aq. HCl solution) and extracted with hexanes, dried and evaporated. The crude product was column chromatographed over silica using hexanes as eluant to give a mixture of CPDs **194**, **196** and **198** (20 mg).

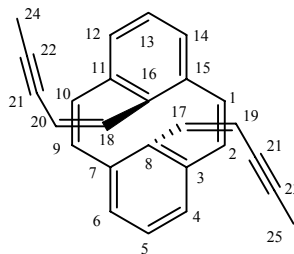
16-((1E)-Propenyl)-8-((1Z)-pent-1-ene-3-ynyl)-anti-[2.2]metacyclophane-1,9-diene

196

The melting point was not determined because the sample was a mixture of products. ^1H NMR (CDCl_3) δ 7.17 (t, $J = 7.4$ Hz, 1H, H-5), 6.97 (t, $J = 7.4$ Hz, H-13), 6.62 (d, $J = 7.4$ Hz, H-4,6), 6.58 (d, $J = 7.4$ Hz, 2H, H-12,14), 6.33 (s, 4H, H-1,2,9,10), 6.28 (d, $J = 11.7$ Hz, 1H, H-17), 5.99 (m, 2H, H-22,23), 5.12 (d, $J = 11.7$ Hz, 1H, H-18),

1.74 (m, 3H, H-21), 1.56 (m, 3H, H-24); ^{13}C NMR (CDCl_3) δ 146.23 (C-16), 140.99 (C-8), 137.80 (C-3,7), 137.73 (C-17), 135.23 (C-11,15), 132.81 (C-2,9), 132.39 (C-1,10), 130.76, 130.65 (C-22,23), 130.02 (C-5), 127.98 (C-13), 126.87 (C-12,14), 125.84 (C-4,6), 109.66 (C-18), 91.28 (C-20), 80.00 (C-19), 18.84 (C-24), 4.88 (C-21).

8,16-Bis((1Z)-pent-1-ene-3-ynl)-anti-[2.2]metacyclophane-1,9-diene 194

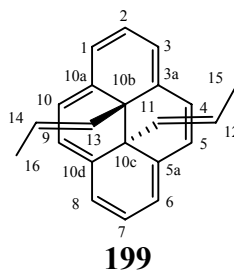


194

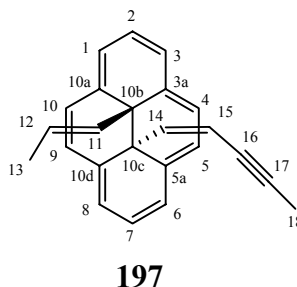
^1H NMR (CDCl_3) δ 7.09 (t, $J = 7.4$ Hz, 2H, H-5,13), 6.65 (d, $J = 7.4$ Hz, 4H, H-4,6,12,14), 6.34 (s, 4H, H-1,2,9,10), 6.30 (d, $J = 11.8$ Hz, 2H, H-17,18) 5.12 (dq, $J = 11.8, 2.5$ Hz, 2H, H-19,20), 1.96 (d, $J = 2.6$ Hz, 6H, Me); ^{13}C NMR (CDCl_3) δ 142.30 (C-8,16), 137.40 (C-3,7,11,15), 133.73 (C-17,18), 132.22 (C-1,2,9,10), 129.76 (C-5,13), 126.10 (C-4,6,12,14), 109.96 (C-19,20), 92.04 (C-23,24), 80.04 (C-21,22), 4.91 (C-25,26); IR ν (thin film) 3044, 2958, 2924, 2852, 1722, 1683, 1436, 1374, 1262, 1095, 785, 768, 738 cm^{-1} ; UV (cyclohexane), λ_{max} nm (ϵ_{max}), 257 (14100), tails up to 500 nm)

(Pent-1-ene-3-ynl)-10b,10c-trans-dihydropyrenes 195, 197 and prop-1-enyl-10b,10c-trans-dihydropyrene 199

Cyclophanediene mixture (**194**, **196** and **198**) was converted to the dihydropyrene mixture (**195**, **197** and **199**). The mixture was column chromatographed over silica gel using hexane-DCM 9:1. Eluted first was 3 mg of DHP **199** as a dark green solid. Eluted second was DHP **197** and the last was DHP **195**.

10b,10c-Bis((1E)-propenyl)-10b,10c-dihydropyrene 199

^1H NMR (CDCl_3) δ 8.73 (s, 4H, H-4,5,9,10), 8.60 (d, $J = 7.5$ Hz, 4H, 1,3,6,8), 8.04 (t, $J = 7.6$ Hz, 2H, H-2,7), 2.26 (dq, $J = 15.1, 6.5$ Hz, 2H, H-12,14), 0.14 (s, 6H, H-15,16), 0.06 (dq, $J = 15.1, 1.6$ Hz, 2H, H-11,13); ^{13}C - NMR (CDCl_3) δ 134.76 (C-3a,5a,10a,10d), 125.17 (C-4,5,9,10), 124.05 (C-1,3,6,8), 123.45 (C-2,7), 121.26 (C-11,13), 119.97 (C-12,14), 35.56 (C-10b,10c); UV (dichloromethane) λ_{max} nm (ϵ_{max}) 274 (7000), 343 (55800), 383 (22700), 468 (4300), 609 (110).

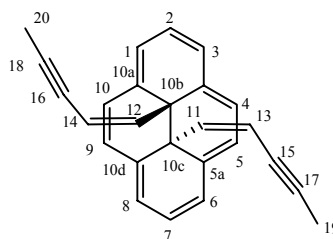
10b-((1E)-Propenyl)-10c-((1Z)pent-1-ene-3-ynyl)-*trans*-10b,10c-dihydropyrene 197

The melting point determination failed because the product was contaminated with **195**. ^1H NMR (CDCl_3) δ 8.71 (s, 4H, H-4,5,9,10), 8.69 (d, $J = 7.8$ Hz, 2H, H-6,8), 8.55 (d, $J = 7.7$ Hz, 2H, H-1,3), 8.10 (t, $J = 7.8$ Hz, 1H, H-7), 8.00 (t, $J = 7.7$ Hz, 1H, H-2), 3.18 (dq, $J = 12.3, 2.7$ Hz, 1H, H-15), 2.38 (dq, $J = 15.5, 6.0$ Hz, 1H, H-12), 1.94 (d, $J = 3.0$ Hz, 3H, H-18), 0.26 (d, $J = 12.4$ Hz, 1H, H-14), 0.18 (d, $J = 6$ Hz, 3H, H-13), 0.16 (d*, 1H, H-11); ^{13}C NMR (CDCl_3) δ 134.80 (C-3a,10a), 132.57 (C-5a,10d), 131.09

(C-14), 126.58 (C-5,9), 125.71 (C-6,8), 125.02 (C-4,10), 123.97 (C-1,3), 123.56 (C-2), 123.50 (C-7), 120.64 (C-12), 120.38 (C-11), 105.43 (C-15), 92.18, 75.31 (C-16,17), 36.63 (C-10b), 35.84 (C-10c), 16.70 (C-13), 4.77 (C-18); IR ν (thin film) 3030, 2957, 2924, 2852, 1727, 1445, 1376, 1348, 1262, 960, 842, 805, 739, 717; UV (cyclohexane) λ_{\max} nm (ϵ_{\max}) 232 (17600), 275 (7300), 343 (60100), 385 (22500), 471 (5200), 608 (130); EI MS m/z 308 (M^+). HR MS Calcd for $C_{24}H_{20}$: 308.1565. Found:308.1570.

* Coupling constant is not clear due to the overlap of peaks.

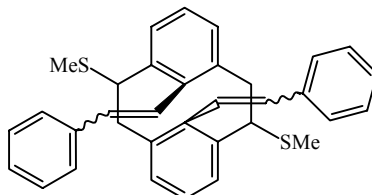
10b,10c-Bis((1Z)pent-1-ene-3-ynyl)-*trans*-10b,10c-dihydropyrene **195**



195

The melting point determination failed because the product was contaminated with **197**. 1H NMR ($CDCl_3$) δ 8.69 (s, 4H, H-4,5,9,10), 8.63 (d, $J = 7.6$ Hz, 4H, H-1,3,6,8), 8.06 (t, $J = 7.6$ Hz, 2H, H-2,7), 3.25 (dq, $J = 12.3, 2.7$ Hz, 2H, H-13,14), 1.93 (d, $J = 2.4$ Hz, 6H, H-19,20), 0.38 (d, $J = 12.3$ Hz, 2H, H-11,12); ^{13}C NMR ($CDCl_3$) δ 132.71 (C-3a,5a,10a,10d), 130.11 (C-11,12), 126.40 (C-4,5,9,10), 125.66 (C-1,3,6,8), 123.66 (C-2,7), 106.02 (C-13,14), 92.50, 75.26 (C-15-18), 36.80 (C-10b,10c), 4.78 (C-19,20); IR ν (KBr) 3003, 2924, 2853, 1637, 1560, 1458, 1261, 1099, 1024, 844, 803; UV (cyclohexane) λ_{\max} nm (ϵ_{\max}) 234 (28500), 278 (10700), 346 (54000), 387 (19800), 475 (5300), 616 (130); EI MS m/z 332 (M^+). HR MS Calcd for $C_{26}H_{20}$: 332.1565. Found 332.1559.

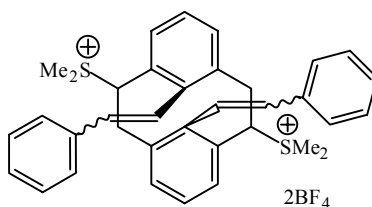
8,16-Bis(2-phenylethenyl)-1,9-bis(thiomethyl)-*anti*-[2.2]metacyclophane 200



200

Using procedure 7.6 B, a reaction of diformylthiomethylcyclophane **174** (1.4 g, 3.93 mmol) with an ylide {prepared by reaction of *t*-BuOK (4.0 g, 35.72 mmol) and benzyl triphenylphosphonium bromide (5.0 g, 11.54 mmol) in THF (30 mL)} followed by column chromatography using hexanes:dichloromethane (7:3) delivered 400 mg (0.8 mmol, 20%) of distyrylthiomethylcyclophane **200** as a mixture of isomers: EI MS m/z 504 (M^+); $^1\text{H NMR}$ (CDCl_3) δ 7.98 (d, $J = 7.7$ Hz), 7.96 (d, $J = 8.0$ Hz), 7.91 (d, $J = 7.6$ Hz), 7.84 (d, $J = 7.6$ Hz), 7.4-6.9 (m), 6.34-6.27 (m), 5.93 (d, $J = 12.4$ Hz), 5.88 (d, $J = 12.4$ Hz), 5.73 (d, $J = 16.4$ Hz), 5.22 (d, $J = 16.4$ Hz), 5.16 (d, $J = 16.4$ Hz) 4.4-4.0 (m), 3.1-3.0 (m), 2.73-2.53 (m), 2.19, 2.18 (s), 1.61, 1.38, 1.37 (3 singlets); EI MS m/z 504 (M^+), 409 (100), HRMS Calcd for $\text{C}_{34}\text{H}_{32}\text{S}_2$: 504.1945. Found: 504.1938.

8,16-Bis(2-phenylethenyl)-1,9-bis(thiomethyl)-*anti*-[2.2]metacyclophane sulfonium salt 201



201

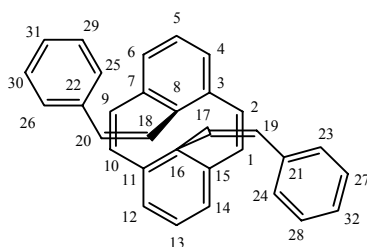
Using procedure 7.3, mixed isomers **200** (600 mg, 1.19 mmol) on reaction with Borch reagent ((80% oil, 1g, 4.94 mmol) in CH_2Cl_2 (10 mL) gave 700 mg (0.99 mmol,

83%) of bis-sulfonium salt **201**: $^1\text{H NMR}$ ($\text{DMSO-}d_6$) δ 7.75-7.18 (m), 7.08-6.96 (m), 6.37-5.91 (m), 5.33 (d, $J = 16.4$ Hz), 4.54 (m), 4.28-3.95 (m), 3.48-3.37 (m), 3.29-3.15 (singlets) 2.98-2.80 (singlets), 2.27, 2.29 (s), 2.14, 1.96 (s).

8,16-Bis(2-phenylethenyl)-*anti*-[2.2]metacyclophane-1,9-dienes **202-204**

Using procedure 7.4, a reaction of bis-sulfonium salt **201** (650 mg, 0.93 mmol) and *t*-BuOK (500 mg, 4.46 mmol) in THF (10 mL) gave a mixture of cyclophanedienes. The product mixture was purified by column chromatography using hexanes-dichloromethane 85: 15 as eluant.

8,16-Bis((1*Z*)-2-phenylethenyl)-*anti*-[2.2]metacyclophane-1,9-diene **202**



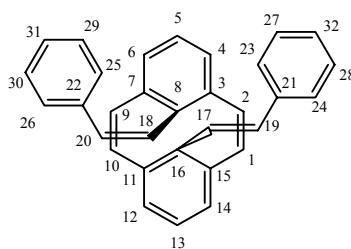
202

Eluted first was 152 mg (41%) of *cis,cis*-distyrylcyclophanediene **202** as pale yellow crystals from cyclohexane, which on melting point determination converts into DHP **205**: $^1\text{H NMR}$ (CD_2Cl_2) δ 7.18 (t, $J = 7.4$ Hz, 2H, H-5,13), 7.05 (m, 6H, H-27-32), 6.78 (m, 4H, 23-26), 6.59 (d, $J = 7.4$ Hz, 4H, H-4,6,12,14), 5.96 (d, $J = 12.4$ Hz, 2H, H-19,20), 5.84 (s, 4H, 1,2,9,10), 5.80 (d, $J = 12.4$ Hz, 2H, H-17,18); $^{13}\text{C NMR}$ (CD_2Cl_2) δ 141.94 (C-8,16), 139.14 (C-21,22), 138.55 (3,7,11,15), 132.69 (C-1,2,9,10), 131.60 (C-19,20), 130.22 (C-5,13), 129.97 (C-17,18), 128.81 (C-23-26), 128.20 (C-31,32), 126.79 (C-27-30), 126.56 (C-4,6,12,14); IR ν (KBr) 3077, 3050, 3005, 1596, 1492, 1448, 1432, 961, 795, 769, 736, 702, 696, 646, 597 cm^{-1} ; UV (cyclohexane) λ_{max} nm (ϵ_{max}) 257

(28900), 280 (23900), 389 (3700); EI MS m/z 408 (M^+), 305 (M^+ - styryl); HR MS Calcd for $C_{32}H_{24}$: 408.1878. Found: 408.1884. Anal. Calcd: C, 94.08; H, 5.92. Found: C, 93.21; H, 6.04.

1H NMR ($CDCl_3$) δ 7.2-7.1 (m, 6H, H-27-32), 7.16 (t, $J = 7.4$ Hz, 2H, H-5,13), 6.81 (m, 4H, H-23-26), 6.56 (d, $J = 7.4$ Hz, 4H, H-4,6,12,14), 5.97 (d, $J = 12.4$ Hz, 2H, H-19,20), 5.84 (d, $J = 12.4$ Hz, 2H, H-17,18), 5.80 (s, 4H, H-1,2,9,10); ^{13}C NMR ($CDCl_3$) δ 141.54 (C-8,16), 138.80 (C-21,22), 138.19 (C-3,7,11,15), 132.35 (C-1,2,9,10), 131.54 (C-19,20), 129.45 (C-17,18), 128.50 (C-23-26), 127.33 (C-5,13), 126.14 (C-4,6,12,14).

8-((1E)-2-Phenylethenyl)-16-((1Z)-2-phenylethenyl)-anti-[2.2]metacyclophane-1,9-diene **203**

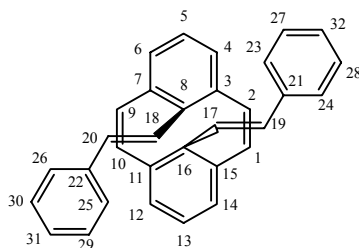


203

Eluted second was 132 mg (35.4%) of the unsymmetrical isomer **203** as pale yellow crystals from cyclohexane, which on attempted melting point determination converts into DHP **206**: 1H NMR ($CDCl_3$) δ 7.24-7.0 (m, 8H, 23,24, 27-32), 7.13 (t, $J = 7.4$ Hz, 1H, H-13), 6.84 (m, 2H, H-25,26), 7.00 (t, $J = 7.4$ Hz, 1H, H-5), 6.77 (AB, $J = 16.3$ Hz, H-17,19), 6.72 (d, $J = 7.4$ Hz, 2H, H-12,14), 6.45 (d, $J = 7.4$ Hz, 2H, H-4,6), 6.33 (d, $J = 11.4$ Hz, H-1,10), 6.06 (d, $J = 12.5$ Hz, 1H, H-20), 5.97 (d, $J = 11.4$ Hz, 2H, H-2,9), 5.92 (d, $J = 12.5$ Hz, 1H, H-18); ^{13}C - NMR ($CDCl_3$) δ 146.12 (C-16), 140.07 (C-

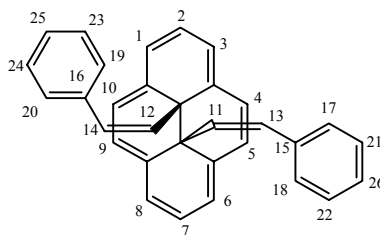
8), 138.83 (C-22), 138.59 (C-3,7), 138.11 (C-21), 136.24 (C-11,15), 133.28 (C-19), 132.96 (C-1,10), 132.74 (C-2,9), 131.54 (C-20), 130.29 (C-5), 129.52 (C-18), 128.82 (C-13), 128.75 (C-17), 128.55 (25,26), 126.80 (C-12,14), 126.33 (C-4,6); IR ν (thin film) 3020, 1597, 1574, 1493, 1448, 960, 793, 763, 737, 691 cm^{-1} ; UV (cyclohexane) λ_{max} nm (ϵ_{max}) 252 (29300), 282 (26500), 408 (1600); EI MS m/z 408 (M^+), 305 (M^+ - styryl); HR MS Calcd for $\text{C}_{32}\text{H}_{24}$: 408.1878. Found: 408.1884.

8,16-Bis((1E)-2-phenylethenyl)-anti-[2.2]metacyclophane-1,9-diene **204**

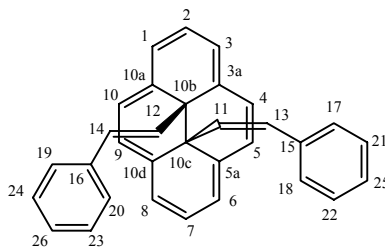


204

Eluted third was 67 mg (18%) of *trans, trans*-distyryl CPD **204**, which on melting point determination converts into DHP **207**: ^1H NMR (CDCl_3) δ 7.22-7.02 (m, 10H, H-23-32), 7.0 (t, $J = 7.4$ Hz, 2H, H-5,13), 6.86 (s, 4H, H-17-20), 6.62 (d, $J = 7.4$ Hz, 4H, H-4,6,12,14), 6.48 (s, 4H, H-1,2,9,10); ^{13}C NMR (CDCl_3) δ 144.58 (C-8,16), 138.18 (C-21,22), 136.66 (C-3,7,11,15), 133.61 (C-19,20), 133.28 (C-1,2,9,10), 129.29 (C-5,13), 128.82 (C-17,18), 127.40 (C-31,32), 126.98 (C-4,6,12,14), 126.78 (C-27,28,29,30), 126.49 (C-23,24,25,26); IR ν (KBr) 3026, 1598, 1492, 1447, 959, 838, 774, 763, 736, 690 cm^{-1} ; UV (cyclohexane) λ_{max} nm (ϵ_{max}) 258 (33000), 284 (33400), 308 (30300), 411 sh (1900).

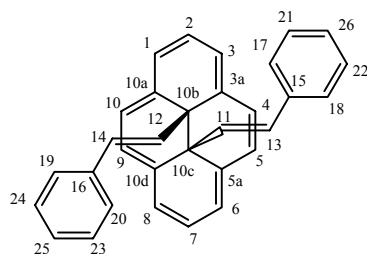
10b,10c-Bis((1Z)-2-phenylvinyl)-*trans*-10b,10c-dihydropyrene 205**205**

Using procedure 7.5, *cis*-styryl DHP **205** was obtained from the *cis*-styryl CPD **202** as orange crystals from cyclohexane, mp 152-154 °C; ^1H NMR (CD_2Cl_2) δ 8.26 (s, 4H, H-4,5,9,10), 8.21 (d, $J = 7.5$ Hz, 4H, H-1,3,6,8), 7.78 (t, $J = 7.5$ Hz, 2H, H-2,7), 7.15 (tt, $J = 6.5, 1.1$ Hz, 2H, H-25,26), 7.03 (m, 4H, H-21-24), 6.02 (m, 4H, H-17-20), 4.21 (d, $J = 12.6$ Hz, 2H, 13,14), 0.28 (d, $J = 12.6$ Hz, 2H, H-11,12); ^{13}C NMR (CD_2Cl_2) δ 136.79 (C-15,16), 134.17 (C-3a,5a,10a,10d), 128.76 (C-17-20), 127.48 (C-13,14), 126.92 (C-4,5,9,10), 126.36 (C-21-26), 125.72 (C-1,3,6,8), 124.12 (C-2,7), 122.47 (C-11,12), 36.72 (C-10b,10c); IR ν (KBr) 3024, 844, 830, 694, 609 cm^{-1} ; UV (cyclohexane) λ_{max} nm (ϵ_{max}) 351 nm (56400), 369 (15300), 395 (25700), 487 (5100), 624 (95); EI MS m/z 408 (M^+); HR MS Calcd for $\text{C}_{32}\text{H}_{24}$: 408.1878. Found: 408.1887. Anal. Calcd: C, 94.08; H, 5.92. Found: C, 93.90; H, 6.02.

10b-((1E)-2-Phenylvinyl)-10c-((1Z)-2-phenylvinyl)-*trans*-10b,10c-dihydropyrene 206**206**

cis, trans-Styryl DHP **206** could not be crystallized (oily film) which resulted in failure to determine melting point. ^1H NMR (CDCl_3) δ 8.72 (d, $J = 7.7$ Hz, 2H, H-4,10), 8.64 (d, $J = 7.7$ Hz, 2H, H-1,3), 8.41 (d, $J = 7.7$ Hz, 2H, H-5,9), 8.27 (d, $J = 7.7$ Hz, 2H, H-6,8), 8.08 (t, $J = 7.6$ Hz, 1H, H-2), 7.81 (t, $J = 7.7$ Hz, 1H, H-7), 7.18 (tt, $J = 7.4$, 1.0 Hz, 1H, H-25), 7.09 (dd, $J = 7.6$, 7.4 Hz, 2H, H-21,22), 6.72 (m, 3H, H-23,24,26), 6.11 (dd, $J = 7.8$, 0.9 Hz, 2H, H-17,18), 5.99 (dd, $J = 7.8$, 1.4 Hz, 2H, H-19,20), 4.31 (d, $J = 12.9$ Hz, 1H, H-13), 3.22 (d, $J = 15.8$ Hz, 1H, H-14), 0.83 (d, $J = 15.9$ Hz, H-12), 0.41 (d, $J = 12.9$ Hz, 1H, H-11); ^{13}C -NMR (CDCl_3) δ 136.50 (C-15), 136.29 (C-16), 134.02 (C-3a,10a), 133.68 (C-5a,10d), 128.55 (C-17,18), 127.79 (C-23,24), 127.17 (C-13), 126.94 (C-5,9), 126.55 (C-26), 126.07 (C-21,22,25), 125.78 (C-6,8), 125.60 (C-19,20), 125.29 (C-4,10), 124.84 (C-14), 124.19 (C-1,3), 123.96 (C-7), 123.73 (C-2), 122.57 (C-11), 120.18 (C-12), 37.29 (C-10b), 15.03(C-10c); IR ν (thin film) 3028, 1733, 1597, 1490, 1441, 1355, 1070, 958, 836, 738, 693, 599 cm^{-1} ; UV (dichloromethane) λ_{max} nm (ϵ_{max}) 256 nm (20000), 348 (54800), 389 (25300), 478 (5780), 609 (106).

10b,10c-Bis((1*E*)-2-phenylvinyl)-*trans*-10b,10c-dihydropyrene **207**



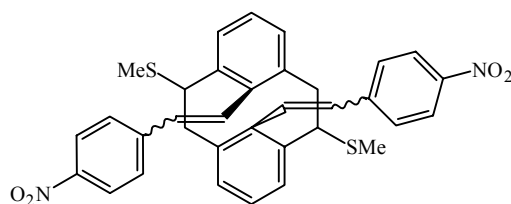
207

Using procedure 7.5, the all *trans*-styryl DHP **207** was obtained from CPD **204** as dark green crystals from cyclohexane, mp 232-234 $^{\circ}\text{C}$; ^1H NMR (CDCl_3) δ 8.85 (s, 4H, H-4,5,9,10), 8.67 (d, $J = 7.7$ Hz, 4H, H-1,3,6,8), 8.08 (t, $J = 7.7$ Hz, 2H, H-2,7), 6.75 (m,

6H, H-21-26), 6.03 (dd, $J = 8.0, 2.5$ Hz, 4H, H-17-20), 3.22 (d, $J = 15.8$ Hz, 2H, H-13,14), 0.87 (d, $J = 15.8$ Hz, 2H, H-11,12); ^{13}C NMR (CDCl_3) δ 136.28 (C-15,16), 133.93 (C-3a,5a,10a,10d), 127.85 (C-21-24), 126.62 (C-25,26), 125.66 (C-17,20), 125.63 (C-4,5,9,10), 124.58 (C-1,3,6,8), 124.56 (C-13,14), 123.97 (C-2,7), 120.82 (C-11,12), 35.91 (C-10b,10c); IR ν (KBr) 3027, 1654, 1636, 1492, 1447, 959, 838, 774, 735, 717, 690 cm^{-1} ; UV (cyclohexane) λ_{max} nm (ϵ_{max}) 257 nm (47900), 342 (58000), 380 (26400), 466 (5770), 597 (165).

8,16-Bis(2-(4-nitro-phenyl)ethenyl)-1,9-bis(thiomethyl)-*anti*-[2.2]metacyclophane

208

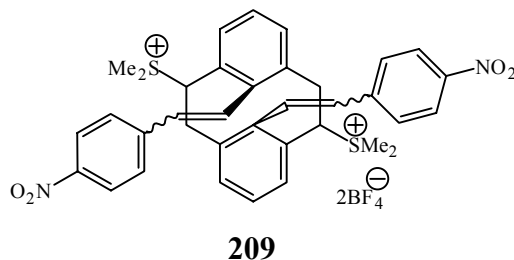


208

To a suspension of 4-nitrobenzyl triphenylphosphonium bromide (4 g, 8.37 mmol) in toluene (50 mL), potassium *tert*-butoxide (1.3g, 11.6 mmol) was added and heated at 50 °C for 1hour and then 8,16-diformylthiomethylcyclophane **174** (1 g, 2.81 mmol) was added. The mixture was heated to reflux over a period of 6 h and stirred overnight. Toluene was evaporated and the crude was extracted between water and dichloromethane (5 x 40 mL). The combined organic layer was dried over anhydrous MgSO_4 and evaporated. The residue was chromatographed over silica gel using dichloromethane-hexane (55: 45) to give 0.9 gram (1.51 mmol, 54%) of yellow orange **208** as a mixture of isomers.

^1H NMR (CDCl_3) δ 8.14 (d, $J = 8.7$ Hz), 7.99 (m), 7.94 (d, $J = 8.6$ Hz), 7.90-7.76 (m), 7.42-7.05 (m), 6.51-6.31 (m), 6.02-5.90 (m), 5.42-5.20 (m), 4.43-4.23 (m), 3.96-3.85 (m), 3.17-3.05 (m), 2.98 (dd, $J = 12.5, 3.9$ Hz), 2.87 (t, $J = 12.2$ Hz), 2.68 (t, $J = 12.5$ Hz), 2.55-2.45 (m), 2.17, 2.11 (4s), 1.63 (s), 1.62 (s), 1.52 (s), 1.47 (s), 1.46 (s); HRMS Calcd for $\text{C}_{34}\text{H}_{30}\text{N}_2\text{O}_4\text{S}_2$: 594.1647. Found: 594.1657.

8,16-Bis(2-(4-nitro-phenyl)ethenyl)-1,9-bis-(thiomethyl)-*anti*-[2.2]metacyclophane sulfonium salt **209**

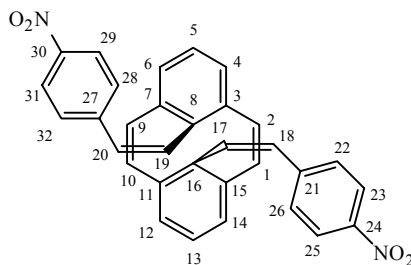


Using procedure 7.3, mixed isomers **208** (900 mg, 1.50 mmol) on reaction with Borch reagent ((80% oil, 0.9 g, 4.44 mmol) in CH_2Cl_2 (22 mL) gave 1.20 g (quantitative) of bis-sulfonium salt **209**: ^1H NMR ($\text{DMSO-}d_6$) δ 8.22 (m), 7.89-7.39 (m), 6.61-6.19 (m), 4.60-4.54 (m), 4.32 (d, $J = 12.6$ Hz), 4.18 (d, $J = 12.4$ Hz), 3.44-3.32 (m), 3.26 (s), 3.25 (s), 3.23 (s), 3.20 (s), 2.95 (s), 2.94 (s), 2.92 (s), 2.87 (s), 2.81 (s).

Bis-2-(4-nitrophenyl)vinyl)-*anti*-[2.2]metacyclophane-1,9-dienes **210-212**

Using procedure 7.4, a reaction of bis-sulfonium salt **209** (1.20 g) and *t*-BuOK (600 mg, 5.35 mmol) in THF (10 mL) gave a mixture of cyclophanedienes **210-212**. The residue was chromatographed over silica gel using hexanes: DCM 60: 40.

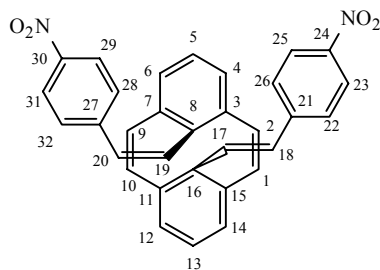
8,16-Bis((1Z)-2-(4-nitrophenyl)vinyl)-*anti*-[2.2]metacyclophane-1,9-diene **210**



210

Eluted first was semi-pure **210** (~75% pure) which was purified by washing with CH₂Cl₂ to yield 88 mg (23%) of the all *cis* isomer as orange crystals, which on attempted melting point determination converts into DHP **213**: ¹H NMR (CDCl₃) δ 7.94 (d, *J* = 8.8 Hz, 4H, H-23,25,29,31), 7.23 (t, *J* = 7.4 Hz, 2H, H-5,13), 6.91 (d, *J* = 8.8 Hz, 4H, H-22,26,28,32), 6.60 (d, *J* = 7.4 Hz, 4H, H-4,6,12,14), 6.00 (s, 4H, H-17-20), 5.84 (s, 4H, H-1,2,9,10); ¹³C-NMR (CDCl₃) δ 146.22 (C-24,30), 145.83 (C-21,27), 140.80 (C-8,16), 138.15 (C-3,7,11,15), 132.56 (C-18,20), 132.51 (C-1,2,9,10), 130.88 (C-5,13), 129.42 (C-17,19), 129.18 (C-22,26,28,32), 126.56 (C-4,6,12,14), 123.30 (C-23,25,29,31); IR ν (KBr) 3045, 3008, 1592, 1512, 1339, 1106, 884, 855, 797, 772, 712 cm⁻¹; UV (dichloromethane) λ_{max} nm (ε_{max}) 254 (14900), 342 (16400), 423 sh (5800); EI MS *m/z* 498 (M⁺), 350 (M⁺ - NO₂-styryl), 202 (M⁺ - 2NO₂ styryl); HR MS Calcd for C₃₂H₂₂N₂O₄: 498.1579. Found: 498.1593; Anal. Calcd: C, 76.78; H, 4.83. Found: C, 72.75; H, 4.19.

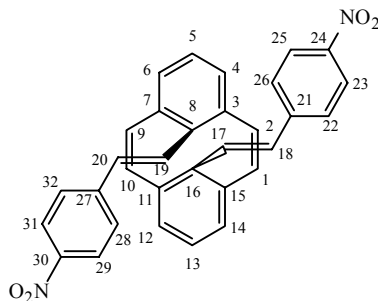
16-((1*E*)-2-(4-Nitrophenyl)vinyl)-8-((1*Z*)-2-(4-nitrophenyl)vinyl)-*anti*-[2.2]metacyclophane-1,9-diene **211**



211

Eluted second was 175 mg (45%) of the unsymmetrical isomer **211** as orange red crystals from dichloromethane, which on attempted melting point determination converts into DHP **214**: ^1H NMR (CDCl_3) δ 8.13 (d, $J = 8.8$ Hz, 2H, H-29,31), 7.96 (d, $J = 8.8$ Hz, 2H, H-23,25), 7.30 (d, $J = 8.8$ Hz, 2H, H-28,32), 7.20 (t, $J = 7.4$ Hz, 1H, H-5), 6.98 (t, $J = 7.4$ Hz, 1H, H-13), 6.96 (d, $J = 8.8$ Hz, 2H, H-22,26), 6.95 (d, $J = 16.2$ Hz, 1H, H-19), 6.86 (d, $J = 16.2$ Hz, 1H, H-20), 6.76 (d, $J = 7.4$ Hz, 2H, H-4,6), 6.45 (d, $J = 7.4$ Hz, 2H, H-12,14), 6.38 (d, $J = 11.4$ Hz, 2H, H-2,9), 6.10 (s, 2H, H-17,18), 6.00 (d, $J = 11.4$ Hz, 2H, H-1,10); ^{13}C NMR (CDCl_3) δ 146.71 (C-30), 146.25 (C-24), 145.75 (C-21), 144.33 (C-27), 144.81 (C-8), 139.611 (C-16), 138.55 (C-11,15), 136.92 (C-3,7), 133.25 (C-2,9), 132.98 (C-1,10), 132.69 (C-18), 132.27 (C-19), 130.93 (C-13), 130.67 (C-20), 130.13 (C-5), 129.60 (C-17), 129.19 (C-22,26), 127.13 (C-4,6), 126.88 (C-28,32), 126.64 (C-12,14), 124.05 (C-29,31), 123.35 (C-23,25); IR ν (KBr) 3007, 1592, 1512, 1339, 1108, 855, 795, 772, 711 cm^{-1} ; UV (dichloromethane) λ_{max} nm (ϵ_{max}) 258 (32100), 340 (25000), 435 sh (9300).

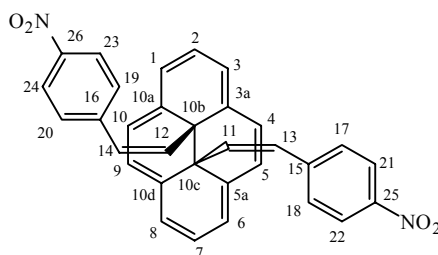
8,16-Bis((1*E*)-2-(4-nitrophenyl)vinyl)-*anti*-[2.2]metacyclophane-1,9-diene **212**



212

Eluted third was 86 mg (22%) of the all *trans*-isomer **212** as red crystals, which on attempted melting point determination converts into *trans*-DHP **215**: ^1H NMR (CDCl_3) δ 8.17 (d, $J = 8.8$ Hz, 4H, H-23,25,29,31), 7.35 (d, $J = 8.8$ Hz, 4H, H-22,26,28,32), 7.05 (d, $J = 16.2$ Hz, 2H, H-17,19), 7.00 (t, $J = 7.4$ Hz, 2H, H-5,13), 6.96 (d, $J = 16.2$ Hz, 2H, H-18,20), 6.63 (d, $J = 7.4$ Hz, 4H, H-4,6,12,14), 6.55 (s, 4H, H-1,2,9,10); ^{13}C NMR (CDCl_3) δ 146.84 (C-24,30), 144.44 (C-21,27), 143.72 (C-8,16), 137.40 (C-3,7,11,15), 133.76 (C-1,2,9,10), 132.54 (C-17,19), 131.10 (C-18,20), 130.30 (C-5,13), 127.27 (C-4,6,12,14), 126.95 (C-22,26,28,32), 124.14 (C-23,25,29,31); IR ν (KBr) 3046, 1588, 1507, 1335, 1108, 965, 863, 817, 761, 745, 688 cm^{-1} ; UV (dichloromethane) λ_{max} nm (ϵ_{max}) 240 (27000), 258 (25400), 285 sh (18100), 369 (28800), 444 sh (13400).

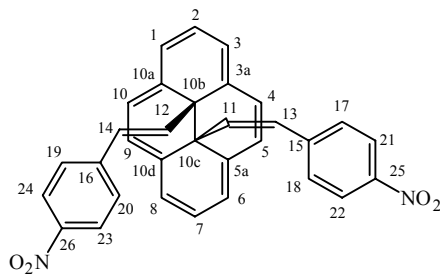
10b,10c-Bis((1*Z*)-2-(4-nitrophenyl)vinyl)-*trans*-10b,10c-dihydropyrene **213**



213

Using procedure 7.5, *cis*-DHP **213** was obtained from CPD **210** as orange crystals from dichloromethane mp 243-244 °C; ^1H NMR (CDCl_3) δ 8.28 (s, 4H, H-4,5,9,10), 8.25 (d, $J = 7.5$ Hz, 4H, H-1,3,6,8), 7.94 (d, $J = 8.6$ Hz, 4H, H-21-24), 7.86 (t, $J = 7.6$ Hz, 2H, H-2,7), 6.20 (dd, $J = 8.7, 0.8$ Hz, 4H, H-17-20), 4.18 (d, $J = 13.2$ Hz, 2H, H-13,14), 0.38 (d, $J = 13.2$ Hz, 2H, H-11,12); ^{13}C NMR (CDCl_3) δ 146.60 (C-25,26), 143.78 (C-15,16), 133.40 (C-3a,5a,10a,10d), 129.19 (C-17-20), 126.91 (C-4,5,9,10), 125.91 (C-1,3,6,8), 125.24 (C-13,14), 124.26 (C-2,7), 123.35 (C-11,12), 121.36 (C-21-24), 36.12 (C-10b,10c); IR ν (KBr) 3074, 3036, 1598, 1515, 1341, 1107, 854, 842 cm^{-1} ; UV (dichloromethane) λ_{max} nm (ϵ_{max}) 281 (19500), 348 (46700), 397 (19500), 484 (5160); EI MS m/z 498 (M^+). HR MS Calcd for $\text{C}_{32}\text{H}_{22}\text{N}_2\text{O}_4$: 498.1580. Found: 498.1586.

10b-((1*E*)-2-(4-Nitrophenyl)vinyl)-10c-((1*Z*)-2-(4-nitrophenyl)vinyl)-*trans*-10b,10c-dihydropyrene **214**

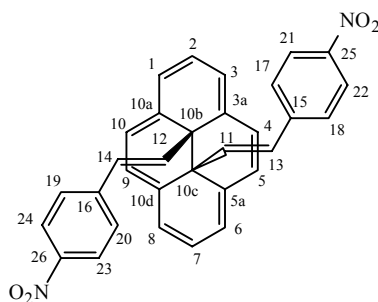


214

Using procedure 7.5, the unsymmetrical DHP **214** was obtained from CPD **211** as olive green crystals from dichloromethane mp 214-216 °C; ^1H NMR (CDCl_3) δ 8.75 (d, $J = 7.8$ Hz, 2H, H-4,10), 8.68 (d, $J = 7.7$ Hz, 2H, H-1,3), 8.40 (d, $J = 7.8$ Hz, 2H, H-5,9), 8.29 (d, $J = 7.7$ Hz, 2H, H-6,8), 8.12 (t, $J = 7.7$ Hz, 1H, H-2), 7.97 (d, $J = 8.6$ Hz, 2H, H-21,22), 7.88 (t, $J = 7.7$ Hz, 1H, H-7), 7.56 (d, $J = 9.0$ Hz, 2H, H-23,24), 6.26 (d, $J = 8.7$

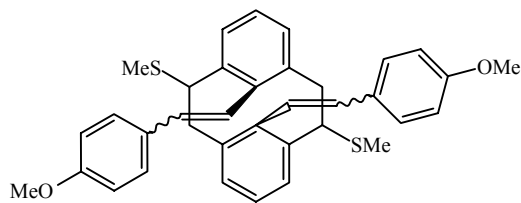
Hz, 2H, H-17,18), 6.08 (d, $J = 9.0$ Hz, 2H, H-19,20), 4.23 (d, $J = 13.1$ Hz, 1H, H-13), 3.25 (d, $J = 15.8$ Hz, 1H, H-14), 0.96 (d, $J = 15.8$ Hz, 1H, H-12), 0.46 (d, $J = 13.1$ Hz, 1H, H-11); ^{13}C NMR (CDCl_3) δ 146.66 (C-25), 146.23 (C-26), 143.76 (C-15), 142.65 (C-16), 133.49 (C-3a,10a), 133.08 (C-5a,10d), 129.24 (C-17,18), 127.19 (C-5,9), 126.09 (C-19,20), 126.06 (C-6,8), 125.59 (C-4,10), 125.11 (C-12), 125.01 (C-13), 124.77 (C-1,3), 124.38 (C-2), 124.30 (C-7), 123.87 (C-11), 123.55 (C-14), 123.25 (C-23,24), 121.40 (C-21,22), 37.39 (C-10b), 34.78 (C-10c); IR ν (KBr) 3031, 1595, 1512, 1341, 846 cm^{-1} ; UV (dichloromethane) λ_{max} nm (ϵ_{max}) 228 (32100), 344 (65800), 387 (25800), 481 (6860), 606 (125).

10b,10c-Bis((1E)-2-(4-nitrophenylvinyl)-trans-10b,10c-dihydropyrene 215

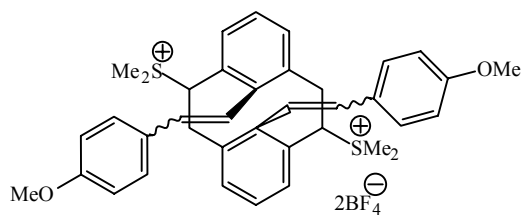


215

Using procedure 7.5, *trans*-DHP **215** was obtained from CPD **212** as dark green crystals from cyclohexane, mp 275-276 °C; ^1H NMR (CDCl_3) δ 8.88 (s, 4H, H-4,5,9,10), 8.71 (d, $J = 7.6$ Hz, 4H, H-1,3,6,8), 8.13 (t, $J = 7.6$ Hz, 2H, H-2,7), 7.60 (d, $J = 8.8$ Hz, 4H, H-21-24), 6.12 (d, $J = 8.9$ Hz, 4H, H-17-20), 3.28 (d, $J = 15.7$ Hz, 2H, H-13,14), 1.05 (d, $J = 15.8$ Hz, 2H, H-11,12); IR ν (KBr) 3032, 1513, 1340, 1109, 850 cm^{-1} ; UV (dichloromethane) λ_{max} nm (ϵ_{max}) 228 (16700), 340 (45900), 375 (16300), 473 (4800).

8,16-Bis((2-(4-methoxyphenyl)ethenyl)-1,9-bis(thiomethyl)-*anti*-[2.2]metacyclophane**216****216**

Using the same procedure as for the synthesis of **208** except warming the reaction to 80 °C overnight gave the cyclophane **216** (50%) as a mixture of isomers. column chromatography over silica gel using dichloromethane-hexane 4:6 eluted the desired products as pale yellow solid: $^1\text{H NMR}$ (CDCl_3) 7.95-7.80 (m), 7.29-7.20 (m), 7.04-6.98 (m), 6.85-6.80 (m), 6.47-6.43 (m), 6.23 (d, $J = 8.8$ Hz), 6.18 (d, $J = 9.0$ Hz), 5.85-5.62 (m), 5.09-5.0 (m), 4.36 (dd), 4.09-3.93 (m), 3.801, 3.80, 3.798 (3 s), 3.66, 3.65 (s), 3.63, 3.62 (3s), 3.12-3.00 (m), 2.91 (t), 2.72 (AB, $J = 12$ Hz), 2.59-2.50 (m), 2.17, 2.16, 2.10, 2.09, 1.64, 1.63, 1.52, 1.45, 1.44 (9 s); EI MS m/z 564 (M^+); HR MS Calcd for $\text{C}_{36}\text{H}_{36}\text{O}_2\text{S}_2$: 564.2157. Found:564.2169.

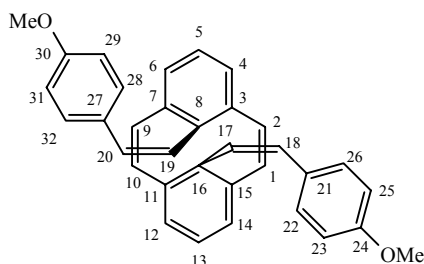
8,16-Bis((2-(4-methoxyphenyl)ethenyl)-1,9-bis(thiomethyl)-*anti*-[2.2]metacyclophane**sulfonium salt 217****217**

Using procedure 7.3, mixed isomers **216** (200 mg, 0.35 mmol) on reaction with Borch reagent (80% oil, 0.5 g, 2.44 mmol) in CH₂Cl₂ (5 mL) gave 275 mg (quantitative) of bis-sulfonium salt **217**: ¹H NMR (DMSO-*d*₆) 7.84-7.34 (m), 7.25-7.17 (m), 6.99-6.91 (m), 6.63-6.55 (m), 6.28-5.88 (m), 4.62-4.52 (m), 3.77, 3.62 (2 s), 3.48-3.20 (6 s), 2.97, 2.94, 2.92 (3 s), 2.36, 2.34, 2.24, 2.23, 1.99 (5 s).

Bis-2-(4-methoxyphenyl)vinyl)-*anti*-[2.2]metacyclophane-1,9-dienes **218-220**

Using procedure 7.4, a reaction of bis-sulfonium salt **217** (200 mg, 0.26 mmol) and *t*-BuOK (250 mg, 2.23 mmol) in THF (10 mL) gave a mixture of cyclophanedienes **218-220**. The residue was chromatographed over silica gel using hexanes: DCM 60:40.

8,16-Bis((1*Z*)-2-(4-methoxyphenyl)vinyl)-*anti*-[2.2]metacyclophane-1,9-diene **218**

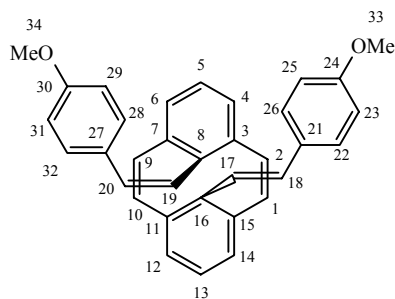


218

Eluted first was 19 mg of **218** (0.04 mmol, 16%) as colorless crystals, which on attempted melting point determination converts into DHP **221**: ¹H NMR (CDCl₃) δ 7.15 (t, *J* = 7.3 Hz, 2H, H-5,13), 6.74 (d, *J* = 8.7 Hz, 4H, H-22,26,28,32), 6.61 (d, *J* = 8.7 Hz, 4H, H-23,25,29,31), 6.57 (d, *J* = 7.3 Hz, 4H, H-4,6,12,14), 5.91 (d, *J* = 12.4 Hz, 2H, H-18,20), 5.86 (s, 4H, H-1,2,9,10), 5.73 (d, *J* = 12.4 Hz, 2H, H-17,19), 3.74 (s, 6H, H-33,34); ¹³C NMR (CDCl₃) δ 158.26 (C-24,30), 141.89 (C-8,16), 138.18 (C-3,7,11,15), 132.37 (C-1,2,9,10), 131.36 (C-21,27), 130.86 (C-18,20), 129.71 (C-22,26,28,32), 129.56 (C-5,13), 128.25 (C-17,19), 126.16 (C-4,6,12,14), 113.32 (C-23,25,29,31), 55.34 (C-

33,34); IR ν (KBr) 3003, 2835, 1605, 1509, 1458, 1303, 1252, 1178, 1032, 832, 812, 784, 739, 517 cm^{-1} ; UV (DCM) λ_{max} nm (ϵ_{max}) 228 (46400), 257 (46100), 372 sh (4160); EI MS m/z 468 (M^+); HR MS Calcd for $\text{C}_{34}\text{H}_{28}\text{O}_2$: 468.2089. Found: 468.2095.

16-((1E)-2-(4-Methoxyphenyl)vinyl)-8-((1Z)-2-(4-methoxyphenyl)vinyl)-anti-[2.2]metacyclophane-1,9-diene **219**

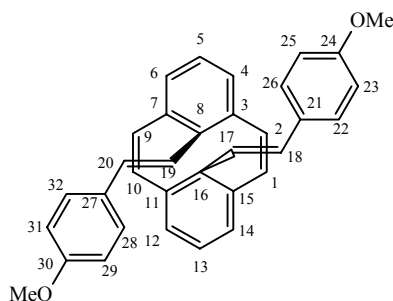


219

Eluted second was 57 mg (0.12 mmol, 47%) of the unsymmetrical isomer **219** as pale yellow solid, which on attempted melting point determination converts into DHP **222**: ^1H NMR (CDCl_3) δ 7.17 (d, $J = 8.8$ Hz, 2H, H-22,26), 7.09 (t, $J = 7.4$ Hz, 1H, H-13), 7.02 (t, $J = 7.3$ Hz, 1H, H-5), 6.82 (d, $J = 8.8$ Hz, 2H, H-23,25), 6.78 (d, $J = 8.7$ Hz, 2H, H-28,32), 6.69 (d, $J = 7.4$ Hz, 2H, H-12,14), 6.68 (AB hidden, 2H, H-17,18), 6.65 (d, $J = 8.6$ Hz, 2H, H-29,31), 6.46 (d, $J = 7.4$ Hz, 2H, H-4,6), 6.32 (d, $J = 11.3$ Hz, 2H, H-1,10), 6.00 (d, $J = 11.3$ Hz, 2H, H-2,9), 5.98 (d, $J = 12.3$ Hz, 1H, H-20), 5.79 (d, $J = 12.3$ Hz, 1H, H-19), 3.82 (s, 3H, H-33), 3.75 (s, 3H, H-34); ^{13}C NMR (CDCl_3) δ 159.20 (C-24), 158.28 (C-30), 146.48 (C-16), 140.32 (C-8), 138.64 (C-3,7), 135.89 (C-11,15), 133.05 (C-2,9), 132.83 (C-18), 132.47 (C-2,9), 131.33 (C-27), 131.10 (C-21), 131.00 (C-17), 130.06 (C-5), 129.78 (C-28,32), 128.01 (C-13), 128.28 (C-19), 128.01 (C-22,26), 126.73 (C-12,14), 126.30 (C-4,6), 113.97 (C-23,25), 113.34 (C-29,31), 55.47 (C-33),

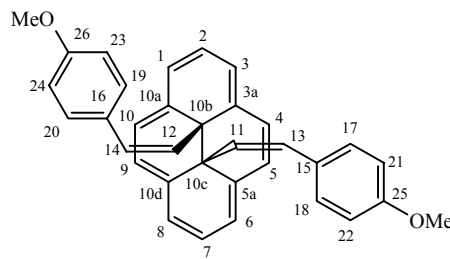
55.33 (C-34); IR ν (KBr) 3031, 3001, 2834, 1604, 1509, 1465, 1250, 1175, 1033, 832, 812, 783 cm^{-1} ; UV (DCM) λ_{max} nm (ϵ_{max}) 227 (44600), 257 (50000), 283 (36300), 417 sh (4900).

8,16-Bis((1*E*)-2-(4-methoxyphenyl)vinyl)-*anti*-[2.2]metacyclophane-1,9-diene **220**



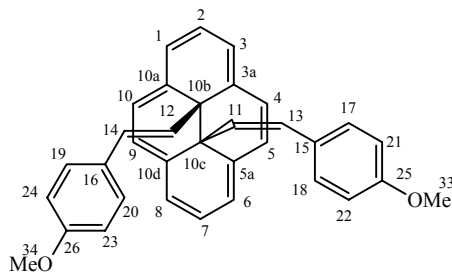
220

Eluted third was 27 mg (0.057 mmol, 22%) of the all *trans*-isomer **220** pale yellow crystals, which on attempted melting point determination converts into DHP **223**: ^1H NMR (CDCl_3) δ 7.20 (d, $J = 8.8$ Hz, 4H, H-22,26,28,32), 6.98 (t, $J = 7.4$ Hz, 2H, H-5,13), 6.84 (d, $J = 8.8$ Hz, 4H, H-23,25,29,31), 6.76 (AB, hidden, 4H, H-17-20), 6.60 (d, $J = 7.4$ Hz, 4H, H-4,6,12,14), 6.45 (s, 4H, H-1,2,9,10), 3.83 (s, 6H, OMe); ^{13}C NMR (CDCl_3) δ 159.24 (C-24,30), 144.84 (C-8,16), 136.41 (C-3,7,11,15), 133.14 (C-18,20), 133.11 (C-1,2,9,10), 131.22 (C-21,27), 128.85 (C-23,25,29,31), 128.28 (C-5,13), 128.01 (C-22,26,28,32), 127.04 (C-17,19), 126.86 (C-4,6,12,14), 55.49 (C-33,34); IR ν (KBr) 3031, 3001, 2833, 1604, 1509, 1465, 1438, 1250, 1174, 1034, 966, 810, 770, 753 cm^{-1} ; UV (DCM) λ_{max} nm (ϵ_{max}) 228 (50600), 263 (45700), 417 sh (6200).

10b,10c-Bis((1Z)-2-(4-methoxyphenyl)vinyl)-*trans*-10b,10c-dihdropyrene 221**221**

Using procedure 7.5, methoxy-styryl DHP **221** was obtained from CPD **218** as orange crystals from DCM, ^1H NMR (CD_2Cl_2) δ 8.28 (s, 4H, H-4,5,9,10), 8.24 (d, $J = 7.6$ Hz, 4H, H-1,3,6,8), 7.79 (t, $J = 7.6$ Hz, 2H, H-2,7), 6.59 (d, $J = 8.6$ Hz, 4H, H-21-24), 5.92 (d, $J = 8.6$ Hz, 4H, H-17-20), 4.12 (d, $J = 12.8$ Hz, 2H, H-13,14), 3.83 (OMe), 0.25 (d, $J = 12.8$ Hz, 2H, H-11,12); ^{13}C NMR (CD_2Cl_2) δ 158.56 (C-25,26), 134.33 (3a,5a,10a,10d), 129.75 (C-17-20), 129.12 (C-15,16), 127.26 (C-13,14), 126.79 (C-4,5,9,10), 125.67 (C-1,3,6,8), 124.02 (C-2,7), 122.94 (C-11,12), 111.82 (C-21,24), 55.74 (OMe), 36.83 (10b,10c); IR ν (thin film) 3030, 2834, 1605, 1574, 1507, 1463, 1243, 1174, 1034, 960, 860, 814, 737, 704 cm^{-1} ; UV (DCM) λ_{max} nm (ϵ_{max}) 228 (34600), 351 (47100), 394 (25200), 486 (5500), 619 (140); EI MS m/z 468 (M^+); HR MS Calcd for $\text{C}_{34}\text{H}_{28}\text{O}_2$: 468.2089. Found: 468.2094. Anal. Calcd: C, 87.15; H, 6.02. Found: C, 82.66; H, 6.20.

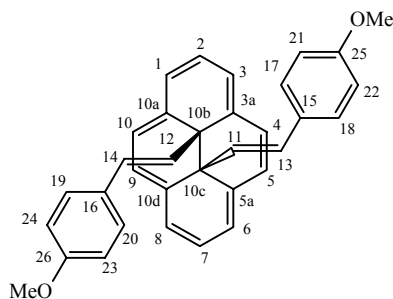
10b-((1E)-2-(4-Methoxyphenyl)vinyl)-10c-((1Z)-2-(4-methoxyphenyl)vinyl)-trans-10b,10c-dihdropyrene **222**



222

Using procedure 7.5, methoxy-styryl DHP **222** was obtained from CPD **219** as olive green solid. Melting point could not be determined because of contamination from **223**. ^1H NMR (CD_2Cl_2) δ 8.72 (d, $J = 7.7$ Hz, 2H, H-4,10), 8.64 (d, $J = 7.7$ Hz, 2H, 1,3), 8.44 (d, $J = 7.7$ Hz, 2H, H-5,9), 8.31 (d, $J = 7.7$ Hz, 2H, H-6,8), 8.06 (t, $J = 7.7$ Hz, 1H, H- 2), 7.83 (t, $J = 7.7$ Hz, 1H, H-7), 6.62 (d, $J = 8.5$ Hz, 2H, H-21,22), 6.25 (d, $J = 8.8$ Hz, 2H, H-23,24), 5.98 (d, $J = 8.4$ Hz, 2H, H-17,18), 5.89 (d, $J = 8.8$ Hz, 2H, H-19,20), 4.20 (d, $J = 12.8$ Hz, 1H, H-13), 3.84 (s, 3H, H-33), 3.48 (s, 3H, H-34), 3.15 (d, $J = 15.8$ Hz, 1H, H-14), 0.65 (d, $J = 15.8$ Hz, 1H, H-12), 0.33 (d, $J = 12.8$ Hz, 1H, H-11); ^{13}C NMR (CD_2Cl_2) δ 158.96 (C-26), 158.57 (C-25), 134.40 (C-3a,10a), 134.09 (C-5a,10d), 129.83 (C-17,18), 127.16 (C-5,9), 127.06 (C-13), 126.79 (C-19,20), 126.01 (C-6,8), 125.67 (C-4,10), 124.43 (C-1,3), 124.25 (C-14), 124.17 (C-7), 123.90 (C-2), 123.41 (C-11), 118.33 (C-12), 113.59 (C-23,24), 111.85 (C-21,22), 55.72 (C-33), 55.47 (C-34), 37.67 (C-10b), 35.55 (C-10c); IR ν (thin film) 3030, 2834, 1606, 1509, 1464, 1440, 1244, 1174, 1034, 959, 842, 815, 736, 704 cm^{-1} ; UV (DCM) λ_{max} nm (ϵ_{max}) 225 (24300), 264 (32300), 346 (42100), 387 (21200), 472 (5400), 607 (120).

10b,10c-Bis((1E)-2-(4-methoxyphenylvinyl)-trans-10b,10c-dihydropyrene 223

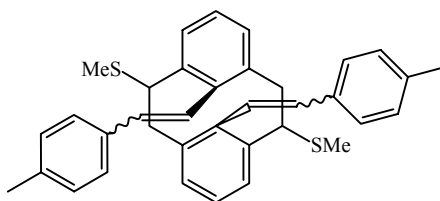


223

Using procedure 7.5, methoxy-styryl DHP **223** was obtained from CPD **220** as dark green solid, **223** could not be crystallized (oily film) which resulted in failure to determine the melting point. ^1H NMR (CD_2Cl_2) δ 8.88 (s, 4H, H-4,5,9,10), 8.70 (d, $J = 7.7$ Hz, 4H, 1,3,6,8), 8.10 (t, $J = 7.7$ Hz, 2H, H-2,7), 6.28 (d, $J = 8.8$ Hz, 4H, H-21-24), 5.95 (d, $J = 8.8$ Hz, 4H, H-17-20), 3.51 (OMe), 3.17 (d, $J = 15.8$ Hz, 2H, H-13,14), 0.70 (d, $J = 15.8$ Hz, 2H, H-11,12); ^{13}C NMR (CD_2Cl_2) δ 159.01 (C-25,26), 134.48 (C-3a,5a,10a,10d), 129.83 (C-15,16), 126.84 (C-17-20), 125.98 (C-4,5,9,10), 124.80 (C1,3,6,8), 124.21 (C-13,14), 124.17 (C-2,7), 118.98 (C-11,12), 113.63 (C-21-24), 55.49 (OMe), 36.35 (C-10b,10c); IR ν (thin film) 3030, 2834, 1606, 1509, 1464, 1440, 1244, 1174, 1034, 959, 842, 815, 736, 704 cm^{-1} ; UV (DCM) λ_{max} nm (ϵ_{max}) 225 (31000), 265 (40200), 343 (46800), 382 (22400), 470 (6400), 606 (130).

8,16-Bis(2-(4-methylphenyl)ethenyl)-1,9-bis(thiomethyl)-anti-[2.2]metacyclophane 224

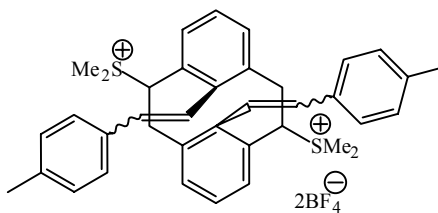
224



224

Using procedure 7.6 B, a reaction of diformylthiomethylcyclophane **174** (0.8 g, 2.25 mmol) with an ylide {prepared by reaction of *t*-BuOK (1.70 g, 15.12 mmol) and 4-methylbenzyl triphenylphosphonium bromide (4.5 g, 10 mmol) in THF (45 mL)} followed by column chromatography using hexanes: dichloromethane (7:3) eluted 685 mg of **224** (1.27 mmol, 57%) as a mixture of isomers: $^1\text{H NMR}$ (CDCl_3) δ 7.88 (d, $J = 7.6$ Hz), 7.84 (d, $J = 7.7$ Hz), 7.83-7.80 (m), 7.44-6.94 (m), 6.76-6.69 (m), 6.24 (d, $J = 8.2$ Hz), 6.20 (d, $J = 8.2$ Hz), 6.16 (d, $J = 8.6$ Hz), 6.14 (d, $J = 8.3$ Hz), 6.10 (d, $J = 8.2$ Hz), 5.92 (d, $J = 12.3$ Hz), 5.87 (d, $J = 12.4$ Hz), 5.82 (d, $J = 12.4$ Hz), 5.68 (d, $J = 16.3$ Hz), 5.23 (d, $J = 16.3$ Hz), 5.10 (d, $J = 16.3$ Hz), 4.35 (dd, $J = 11.5, 4.0$ Hz), 4.15-3.95 (m), 3.14-2.87 (m), 2.75-2.51 (m), 2.36, 2.32, 2.28, 2.26 (4s), 2.17, 2.16, 2.15, 2.12, 2.11, 2.10 (s), 2.03 (s), 1.61, 1.60, 1.42, 1.40 (s); EI MS m/z 532 (M^+); HR MS Calcd for $\text{C}_{36}\text{H}_{36}\text{S}_2$: 532.2258. Found: 532.2253.

8,16-Bis(2-(4-methylphenyl)ethenyl)-1,9-bis(thiomethyl)-*anti*-[2.2]metacyclophane sulfonium salt **225**



225

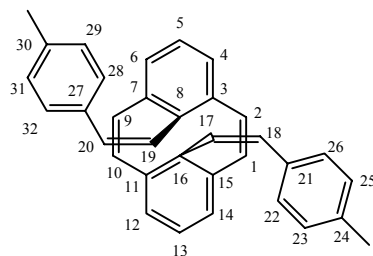
Using procedure 7.3, mixed isomers **224** (650 mg, 1.21 mmol) on reaction with Borch reagent (80% oil, 1.0 g, 4.84 mmol) in CH_2Cl_2 (7 mL) gave 510 mg (0.69 mmol, 57%) of bis-sulfonium salt **225**: $^1\text{H NMR}$ ($\text{DMSO-}d_6$) δ 7.83 (d, $J = 7.7$ Hz), 7.75 (d, $J = 7.6$ Hz), 7.71-7.50 (m), 7.47 (t, $J = 7.6$ Hz), 7.20-7.10 (m), 6.86-6.76 (m), 6.24-6.05 (m),

6.00-5.87 (m), 5.46 (d, $J = 16.4$ Hz), 5.30 (d, $J = 16.6$ Hz), 4.53 (br d), 4.26-3.97 (m), 3.30, 3.22, 3.21, 3.20, 3.18 (s), 2.98-2.78 (m), 2.30, 2.28 (3 s), 2.18, 2.10, 1.96 (4 s).

Bis-2-(4-methylphenyl)vinyl)-*anti*-[2.2]metacyclophane-1,9-dienes **226-228**

Using procedure 7.4, a reaction of bis-sulfonium salt **225** (470 mg, 0.63 mmol) and *t*-BuOK (200 mg, 1.79 mmol) in THF (8 mL) gave a mixture of cyclophanedienes **226-228**. The residue was chromatographed over silica gel using hexanes: DCM 90:10.

8,16-Bis((*Z*)-2-(4-methylphenyl)vinyl)-*anti*-[2.2]metacyclophane-1,9-diene **226**

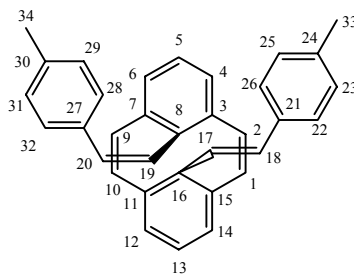


226

Eluted first was 116 mg of **226** (0.27 mmol, 42%) as colorless crystals which on attempted melting point determination converts into DHP **229**: ^1H NMR (CDCl_3) δ 7.16 (t, $J = 7.3$ Hz, 2H, H-5,13), 6.88 (d, $J = 8.0$ Hz, 4H, H-23,25,29,31), 6.70 (d, $J = 8.0$ Hz, 4H, H-22,26,28,32), 6.57 (d, $J = 7.3$ Hz, 4H, H-4,6,12,14), 5.94 (d, $J = 12.4$ Hz, 2H, H-18,20), 5.85 (s, 4H, H-1,2,9,10), 5.78 (d, $J = 12.4$ Hz, 2H, H-17,19), 2.25 (s, 6H, Me); ^{13}C NMR (CDCl_3) δ 141.81 (C-8,16), 138.18 (C-3,7,11,15), 136.01 (C-24,30), 135.84 (C-21,27), 132.37 (C-1,2,9,10), 131.31 (C-18,20), 129.62 (C-5,13), 128.87 (C-17,19), 128.57 (C-23,25,29,31), 128.40 (C-22,26,28,32), 126.13 (C-4,6,12,14), 21.36 (C-33,34); IR ν (KBr) 3041, 3015, 3003, 1560, 1508, 1370, 1405, 1151, 859, 817, 782, 749, 737, 594 cm^{-1} ; UV (cyclohexane) λ_{max} nm (ϵ_{max}) 257 (30100), 277 (24000), 392 (3300); EI MS

m/z 436 (M^+); HR MS Calcd for $C_{34}H_{28}$: 436.2191. Found: 436.2205; Anal. Calcd: C, 93.54; H, 6.46. Found: C, 92.80; H, 6.46.

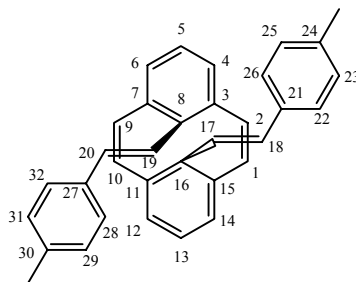
16-((1E)-2-(4-Methylphenyl)vinyl)-8-((1Z)-2-(4-methylphenyl)vinyl)-anti-[2.2]metacyclophane-1,9-diene **227**



227

Eluted second was 105 mg (24 mmol, 38%) of the unsymmetrical isomer **227** as pale yellow crystals from cyclohexane, which on attempted melting point determination converts into DHP **230**: 1H NMR ($CDCl_3$) δ 7.12 (d, $J = 8.3$ Hz, 2H, H-22,26), 7.10 (t, $J = 7.5$ Hz, 1H, H-13), 7.08 (d, $J = 8.4$ Hz, 2H, H-23,25), 7.01 (t, $J = 7.4$ Hz, 1H, H-5), 6.90 (d, $J = 8.0$ Hz, 2H, H-29,31), 6.74 (m, 4H, H-17,18,28,32), 6.71 (d, $J = 7.4$ Hz, 2H, H-12,14), 6.47 (d, $J = 7.4$ Hz, 2H, H-4,6), 6.33 (d, $J = 11.3$ Hz, 2H, H-1,10), 6.02 (d, $J = 12.3$ Hz, H-20), 6.00 (d, $J = 11.4$ Hz, 2H, H-2,9), 5.83 (d, $J = 12.3$ Hz, 1H, H-19). 2.34 (s, 3H, H-33), 2.26 (s, 3H, H-34); ^{13}C NMR ($CDCl_3$) δ 146.34 (C-16), 140.24 (C-8), 137.16 (C-24), 138.58 (C-3,7), 136.09 (C-30), 136.07 (C-11,15), 135.78 (C-27), 133.20 (C-18), 132.98 (C-1,10), 132.64 (C-2,9), 131.47 (C-20), 130.17 (C-5), 129.20 (C-13), 128.90 (C-19), 128.62 (C-29,31), 128.46 (C-28,32), 127.84 (C-17), 126.75 (C-12,14), 126.73 (C-22,26), 126.30 (C-4,6), 21.48 (C-33), 21.38 (C-34) IR ν (thin film) 3045, 3019, 3005, 1510, 1436, 1265, 963, 868, 816, 805, 786, 777, 746, 702, 647 cm^{-1} ; UV (cyclohexane) λ_{max} nm (ϵ_{max}) 252 (60000), 280 (48400), 413 sh (6600).

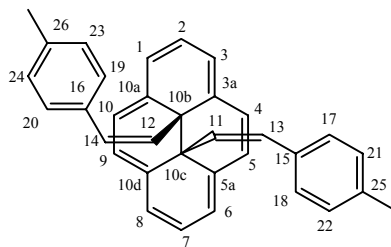
8,16-Bis((1E)-2-(4-methylphenyl)vinyl)-anti-[2.2]metacyclophane-1,9-diene 228



228

Eluted third was 30 mg (0.07 mmol, 11%) of the all *trans*-isomer **228** as pale yellow crystals which on attempted melting point determination converts into DHP **231**: $^1\text{H NMR}$ (CDCl_3) δ 7.16 (AB, $J = 8.1$ Hz, 4H, H-22,26,28,32), 7.10 (AB, $J = 8.1$ Hz, 4H, H-23,25,29,31), 6.98 (t, $J = 7.3$ Hz, 2H, H-5,13), 6.81 (AB, $J = 16.2$, 4H, H-17-20), 6.60 (d, $J = 7.3$ Hz, 4H, H-4,6,12,14), 6.46 (s, 4H, H-1,2,9,10) 2.34 (s, 6H, Me); $^{13}\text{C NMR}$ (CDCl_3) δ 144.70 (C-8,16), 137.21 (C-24,30), 136.53 (C-3,7,11,15), 135.47 (C-21,27), 133.52 (C-18,20), 133.19 (C-1,2,9,10), 129.23 (C-23,25,29,31), 129.06 (C-5,13), 127.93 (C-17,19), 126.90 (C-4,6,12,14), 126.72 (C-22,26,28,32). 21.49 (C-33,34, Me) ; IR ν (KBr) 3045, 3022, 3003, 1560, 1513, 1458, 1429, 960, 797, 755, 653, 631 cm^{-1} ; UV (cyclohexane) λ_{max} nm (ϵ_{max}) 257 (53500), 285 (53000), 313 (48700), 410 sh (6100).

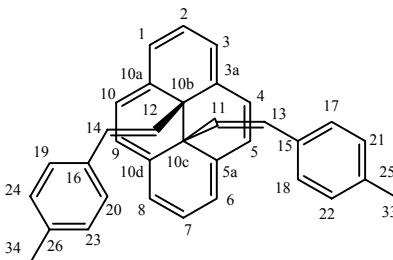
10b,10c-Bis((1Z)-2-(4-methylphenyl)vinyl)-trans-10b,10c-dihydropyrene 229



229

Using procedure 7.5, *cis*-styryl DHP **229** was obtained from CPD **226** as orange crystals from cyclohexane, $^1\text{H NMR}$ (CD_2Cl_2) δ 8.25 (s, 4H, H-4,5,9,10), 8.22 (d, $J = 7.5$ Hz, 4H, H-1,3,6,8), 7.78 (t, $J = 7.5$ Hz, 2H, H-2,7), 6.84 (d, $J = 7.6$ Hz, 4H, H-21-24), 5.89 (d, $J = 7.5$ Hz, 4H, H-17-20), 4.17 (d, $J = 12.9$ Hz, 2H, H-13,14), 2.34 (s, 6H, Me) 0.25 (d, $J = 12.9$ Hz, 2H, H-11,12); $^{13}\text{C NMR}$ (CD_2Cl_2) δ 135.84 (C-25,26), 134.19 (C-3a,5a,10a,10d), 133.70 (C-15,16), 128.60 (17-20), 127.51 (C-13,14), 127.01 (C-21-24), 126.88 (C-4,5,9,10), 125.71 (C-1,3,6,8), 124.04 (C-2,7), 122.47 (C-11,12), 36.72 (C-10b,10c), 21.47 (Me); IR ν (KBr) 3038, 3019, 1507, 1345, 860, 836, 607 cm^{-1} ; UV (cyclohexane) λ_{max} nm (ϵ_{max}) 227 (37500), 353 (68800), 396 (33300), 490 (6300), 624 (130); EI MS m/z 436 (M^+); HR MS Calcd for $\text{C}_{34}\text{H}_{28}$: 436.2191. Found: 436.2197; Anal. Calcd: C, 93.54; H, 6.46. Found: C, 88.69; H, 6.78.

10b-((1E)-2-(4-Methylphenyl)vinyl)-10c-((1Z)-2-(4-methylphenyl)vinyl)-trans-10b,10c-dihdropyrene 230

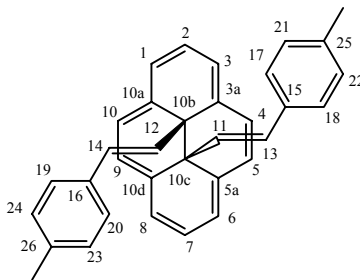


230

Using procedure 7.5, *p*-methyl-styryl DHP **230** was obtained from CPD **227** as olive green solid. The dihydropyrene **230** could not be crystallized (oily film) which resulted in failure to determine the melting point. $^1\text{H NMR}$ (CD_2Cl_2) δ 8.72 (d, $J = 7.7$ Hz, 2H, H-4,10), 8.63 (d, $J = 7.7$ Hz, 2H, H-1,3), 8.41 (d, $J = 7.7$ Hz, 2H, H-5,9), 8.28 (d, $J =$

7.7 Hz, 2H, H-6,8), 8.06 (t, $J = 7.7$ Hz, 1H, H-2), 7.82 (t, $J = 7.7$ Hz, 1H, H-7), 6.89 (d, $J = 7.7$ Hz, 2H, H-21,22), 6.51 (d, $J = 8.1$, 2H, H-23,24), 5.95 (d, $J = 7.4$ Hz, 2H, H-17,18), 5.84 (d, $J = 8.3$ Hz, 2H, H-19,20), 4.22 (d, $J = 12.8$ Hz, 1H, H-13), 3.17 (d, $J = 15.9$ Hz, 1H, H-14), 2.36 (s, 3H, H-33), 1.96 (s, 3H, H-34), 0.73 (d, $J = 15.9$ Hz, 1H, H-12), 0.32 (d, $J = 12.9$ Hz, 1H, H-11); ^{13}C NMR (CD_2Cl_2) δ 136.94 (C-26), 135.91 (C-25), 134.43 (C-3a,10a), 134.10 (C-5a,10d), 133.69 (C-15), 133.57 (C-16), 128.87 (C-23,24), 128.70 (C-17,18), 127.38 (C-13), 127.27 (C-5,9), 127.08 (C-21,22), 126.10 (C-6,8), 125.53 (C-19,20), 124.89 (C-14), 124.44 (C-1,3), 124.31 (C-7), 123.92 (C-2), 122.94 (C-11), 119.57 (C-12), 37.67 (C-10b), 35.47 (C-10c), 21.49 (C-33), 21.03 (C-34); IR ν (thin film) 3025, 2921, 2851, 1637, 1512, 1458, 1123, 962, 840, 801, 711 cm^{-1} ; UV (dichloromethane) λ_{max} nm (ϵ_{max}) 227 (24500), 257 (28900), 347 (42900), 387 (19100), 478 (4300), 607 (100).

10b,10c-Bis((1E)-2-(4-methylphenylvinyl)-trans-10b,10c-dihydropyrene 231

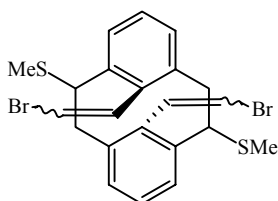


231

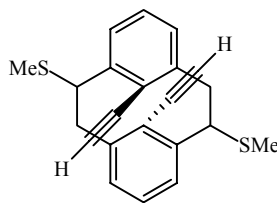
Using procedure 7.5, *trans*-styryl DHP **231** was obtained from CPD **228** as dark green solid. DHP **231** could not be crystallized (oily film) which resulted in failure to determine the melting point. ^1H NMR (CD_2Cl_2) δ 8.88 (s, 4H, H-4,5,9,10), 8.69 (d, $J = 7.6$ Hz, 4H, H-1,3,6,8), 8.10 (t, $J = 7.6$ Hz, 2H, H-2,7), 6.55 (d, $J = 8.2$ Hz, 4H, H-21-24), 5.89 (d, $J = 8.2$ Hz, 4H, H-17-20), 3.19 (d, $J = 15.8$ Hz, 2H, H-13,14), 1.99 (s, Me), 0.79

(d, $J = 15.8$ Hz, 2H, H-11,12); ^{13}C NMR (CD_2Cl_2) δ 137.00 (C-25,26), 134.39 (C-3a,5a,10a,10d), 133.54 (C-15,16), 128.90 (C-21-24), 126.00 (C-4,5,9,10), 125.60 (C-17-20), 124.85 (C-1,3,6,8), 124.67 (C-13,14), 124.25 (C-2,7), 120.13 (C-11,12), 36.33 (C-10b,10c) 21.04 (Me); IR ν (KBr) 3025, 2921, 2851, 1637, 1512, 1458, 962, 840, 801, 711 cm^{-1} ; UV (dichloromethane) λ_{max} nm (ϵ_{max}) 227 (19100), 259 (33700), 343 (40300), 380 (21000), 468 (5400), 593 (170) ;

8,16-Bis(ethynyl)-1,9-bis(thiomethyl)-*anti*-[2.2]metacyclophane 233



232



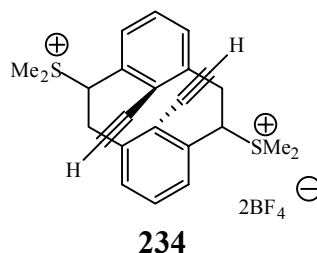
233

Using procedure 7.6 B, a reaction of diformylthiomethylcyclophane **174** (1.0 g, 2.81 mmol) with an ylide {prepared by reaction of *t*-BuOK (3.0 g, 26.8 mmol) and bromomethyl triphenylphosphonium bromide (2.76 g, 6.3 mmol) in THF (25 mL)} followed by column chromatography using hexanes: dichloromethane (7:3) eluted 600 mg of **232/233** as a mixture of isomers.

^1H NMR (CDCl_3) δ 7.86 (d, $J = 7.6$ Hz), 7.84 (d, $J = 7.7$ Hz), 7.67-7.62 (m), 7.55-7.52 (m), 7.47-7.41 (m), 7.30-7.25 (m), 7.19 (t, $J = 7.5$ Hz), 7.06 (t, $J = 7.3$ Hz), 5.83-5.73 (m), 4.58 (d, $J = 7.8$ Hz), 4.54 (d, $J = 7.6$ Hz), 3.89 (dd, $J = 11.5, 4.0$ Hz), 3.80 (dd, $J = 11.5, 3.9$ Hz), 3.17-3.13 (m), 2.55 (t, $J = 12.5$ Hz), 2.44 (t, $J = 12.1$ Hz), 2.17, 2.15, 2.12, 2.10 (4 s); ^{13}C NMR (CDCl_3) δ 144.44, 143.02, 141.72, 141.24, 136.12, 135.9, 135.87, 134.94, 133.17, 132.70, 132.27, 132.14, 132.12, 132.04, 131.42, 130.21, 129.76, 129.58, 129.18, 128.93, 128.75, 128.65, 128.47, 128.36, 127.97, 127.89, 127.59, 127.50,

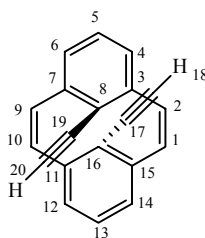
127.26, 127.07, 126.30, 125.92, 125.20, 124.89, 123.49, 110.24, 109.47, 109.32, 109.04, 108.96, 87.24, 54.02, 53.53, 53.31, 52.96, 50.72, 46.15, 44.12, 44.05, 43.59, 29.9, 28.4, 22.89, 21.09, 17.56, 16.86, 16.95, 15.90, 15.62, 14.31.

8,16-Bis(ethynyl)-1,9-bis(thiomethyl)-*anti*-[2.2]metacyclophane sulfonium salts 233



Using procedure 7.3, mixed isomers of **232/233** (600 mg) on reaction with Borch reagent (80% oil, 1.0 g, 4.84 mmol) in CH₂Cl₂ (7 mL) gave 600 mg of bis-sulfonium salt **234**: ¹H NMR (DMSO-*d*₆) δ 7.81 (d, *J* = 7.8 Hz), 7.69 (d, *J* = 7.5 Hz), 7.62 (d, *J* = 7.6 Hz), 7.52 (d, *J* = 7.6 Hz), 7.41 (t, *J* = 7.6 Hz), 7.27 (t, *J* = 7.2 Hz), 6.41 (d, *J* = 7.6 Hz), 6.36 (d, *J* = 7.8 Hz), 6.25 (d, *J* = 8.0 Hz), 5.08 (d, *J* = 7.7 Hz), 4.74 (d, *J* = 7.8 Hz), 4.57 (dd, *J* = 11.2, 3.3 Hz), 4.48-4.42 (m), 3.55-3.50 (m), 3.33, 3.32 (2s), 2.86, 2.84 (s), 2.93-2.74 (m).

8,16-Diethynyl-*anti*-[2.2]metacyclophane-1,9-diene 235

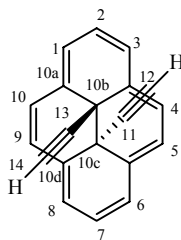


Using procedure 7.4, a reaction of bis-sulfonium salt **234** (650 mg, 1.18 mmol) and *t*-BuOK (600 mg, 5.35mmol) in THF (20 mL) followed by column chromatographed

over silica gel using hexane-CH₂Cl₂ 90: 10 gave diethynyl CPD **235** (100 mg, 0.4 mmol). Other products include **237** and **240** in variable quantities.

On attempted melting point determination, diethynyl CPD **235** isomerizes into diethynyl DHP **236**. ¹H NMR (CDCl₃) δ 7.19 (t, *J* = 7.5 Hz, 2H, H-5,13), 6.75 (d, *J* = 7.5 Hz, 4H, H-4,6,12,14), 6.49 (s, 4H, H-1,2,9,10), 2.84 (H-18,20); ¹³C NMR (CDCl₃) δ 141.11 (C-3,7,11,15), 133.86 (C-1,2,9,10), 131.44 (C-5,13), 129.78 (C-8,16), 126.45 (C-4,6,12,14), 83.39 (C-18,20), 81.84 (C-17,19); IR ν (KBr) 3293, 3050, 3005, 2578, 1727, 1427, 1262, 857, 805, 755, 655 cm⁻¹; UV (dichloromethane) λ_{max} nm (ε_{max}) 235 (35800), 281 (12900); EI MS *m/z* 252 (M⁺, 100%); HR MS Calcd for C₂₀H₁₂: 252.0939. Found: 252.0923.

10b,10c-Diethynyl-*trans*-10b,10c-dihydropyrene **236**

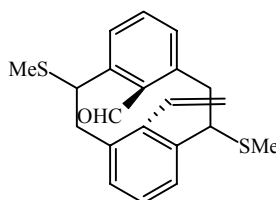


236

Using procedure 7.5, diethynyl DHP **236** was obtained from diethynyl CPD **235** as dark green crystals from DCM, mp 245-250 °C (dec); ¹H NMR (CDCl₃) δ 8.88 (s, 4H, H-4,5,9,10), 8.74 (d, *J* = 7.6 Hz, 4H, H-1,3,6,8), 8.27 (t, *J* = 7.7 Hz, 2H, H-2,7), -0.09 (s, 2H, H-12,14); ¹³C NMR (CDCl₃) δ 132.89 (C-3a,5a,10a,10d), 125.54 (C-4,5,9,10), 124.58 (C-2,7), 123.83 (C-1,3,6,8), 75.36 (C-11,13), 65.00 (C-12,14), 30.00 (C-10b, 10c); IR ν (KBr) 3264, 3042, 1654, 1353, 845, 756, 662 cm⁻¹; UV (dichloromethane) λ_{max} nm (ε_{max}) 223 (2900), 229 (7900), 336 (9700), 372 (42700), 399 (4400), 452 (7200), 535

(100), 596 (130), 639 (210); EI MS m/z 252 (M^+); HR MS Calcd for $C_{20}H_{12}$: 252.0939. Found. 252.0923: Calcd. Anal: C, 95.21; H, 4.79. Found: C, 94.15; H, 4.91.

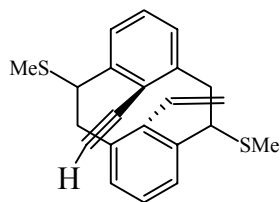
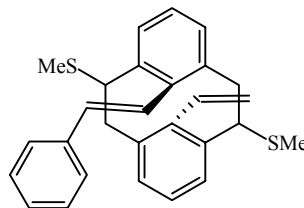
1,9-Bis(thiomethyl)-8-formyl-16-vinyl-*anti*-[2.2]metacyclophane 264



264

BuLi (2.4 mL of 2.5M in hexanes, 6 mmol) was added dropwise to a suspension of methyl triphenylphosphonium bromide (3.6 g, 10.08 mmol) in THF (40 mL) under argon at 0 °C and the mixture was stirred for 20 minutes at room temperature. To this solution, diformylcyclophane **174** (1.5 g, 4.21 mmol) was added and the reaction mixture was allowed to stir for 1.5 h and then quenched with water. The resulting solution was extracted with CH_2Cl_2 (4 x 40 mL), dried over anhydrous $MgSO_4$ and evaporated. The crude mixture was chromatographed over silica gel using hexane: dichloromethane (7:3) to give mono vinyl thiomethylcyclophane **264** (690 mg, 1.95 mmol, 46%) as a mixture of isomers.

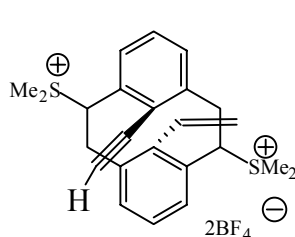
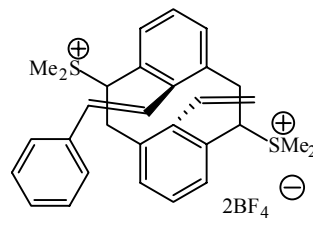
1H NMR ($CDCl_3$) 8.92 (s), 8.72 (s), 8.07-7.72 (m), 7.41-7.07 (m), 5.12 (dd, $J = 11.4, 5.0$ Hz), 4.99 (dd, $J = 11.6, 4.6$ Hz), 4.85-4.45 (m), 4.35-4.25 (m), 4.16-4.07 (m), 3.39-3.09 (m), 2.96-2.54 (m), 2.16, 2.15, 2.146, 2.137, 2.135, 2.131, 2.124, 2.119 (singlets); HR MS Calcd for $C_{21}H_{22}OS_2$: 354.1112. Found: 354.1107.

**265****266**

Using procedure 7.6 B, a reaction of diformylthiomethylcyclophane **174** (0.6 g, 1.7 mmol) with an ylide {prepared by reaction of *t*-BuOK (1.1 g, 10 mmol) and bromomethyl triphenylphosphonium bromide (1.6 g, 3.7 mmol) in THF (25 mL)} followed by column chromatography using hexanes: dichloromethane (7:3) eluted 360 mg of **265** and **266** as a mixture of isomers.

$^1\text{H NMR}$ (CDCl_3) δ 7.88-7.86 (m), 7.84 (d, $J = 7.6$ Hz), 7.78 (d, $J = 7.6$ Hz), 7.75 (m), 7.69 (dd, $J = 7.7, 1.8$ Hz), 7.63 (m), 7.43 (t, $J = 7.6$ Hz), 7.37-6.97 (m), 5.81 (d, $J = 16.4$ Hz), 5.72 (d, $J = 16.4$ Hz), 5.27 (d, $J = 16.3$ Hz), 5.16 (d, $J = 16.4$ Hz), 4.86-3.86 (m), 3.4-2.65 (m), 2.59 (dd, $J = 11.8$ Hz), 2.15-2.17 (9 singlets); EI MS m/z 428(M^+ , **266**), 350(M^+ , **265**); HR MS, Calcd for $\text{C}_{28}\text{H}_{28}\text{S}_2$: 428.1632. Found: 428.1633. Calcd for $\text{C}_{22}\text{H}_{22}\text{S}_2$: 350.1162. Found: 350.1161.

Thiomethylcyclophane sulfonium salts **267** and **268**

**267****268**

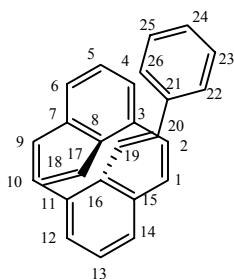
Using procedure 7.3, mixed isomers of **265** and **266** (300 mg) on reaction with Borch reagent (80% oil, 0.5 g, 2.47 mmol) in CH_2Cl_2 (5 mL) gave 280mg of bis-

sulfonium salts **267** and **268**, ^1H NMR (DMSO- d_6) δ 7.80-7.15 (m), 5.95 (two doublets, $J = 16.4$ Hz), 5.53 (d, $J = 16.4$ Hz), 5.36 (d, $J = 16.4$ Hz), 5.13-4.53 (m), 4.42 (two doublets, $J = 11.3$ Hz), 4.22 (m), 3.6-3.0 (m), 3.3 (s), 2.9 (s).

Unsymmetrical cyclophanedienes with internal vinyl groups

Using procedure 7.4, a reaction of bis-sulfonium salt mixture of **267** and **268** (280 mg) and *t*-BuOK (420 mg, 3.75 mmol) in THF (8 mL) followed by column chromatography over silica gel using hexane- CH_2Cl_2 95: 5 first eluted the 8-styryl-16-vinyl cyclophanediene **240** (~ 17%) as colorless crystals from cyclohexane which on attempted melting point determination converts into DHP **241**.

16-((1*E*)-2-Phenylvinyl)-8-vinyl-*anti*-[2.2]metacyclophane-1,9-diene **240**



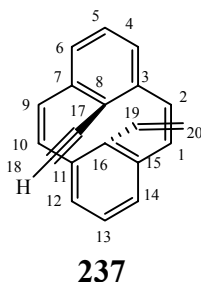
240

^1H NMR (CDCl_3) δ 7.29 (m, 2H, H-23,25), 7.24 (dd, $J = 7.0, 1.5$ Hz, 2H, H-22,26), 7.20 (tt, $J = 7.0, 1.5$ Hz, 1H, H-24), 7.08 (t, $J = 7.4$ Hz, 1H, H-13), 6.99 (t, $J = 7.4$ Hz, 1H, H-5), 6.81 (AB, $J = 16.1$, 2H, H-19,20), 6.64 (d, $J = 7.4$ Hz, 2H, H-12,14), 6.58 (d, $J = 7.4$ Hz, 2H, H-4,6), 6.43 (AB, $J = 11.45$, 4H, H-1,2,9,10), 6.39 (dd, $J = 17.5, 11.0$ Hz, 1H, H-17(- $\underline{\text{CH}}=\text{CH}_2$)), 5.49 (dd, $J = 17.4, 1.7$ Hz, 1H, H-18b*), 4.88 (dd, $J = 11, 1.7$ Hz, 1H, H-18a*); ^{13}C NMR (CDCl_3) δ 145.72 (C-16), 145.25 (C-8), 138.16 (C-21), 136.32 (C-11,15), 136.18 (C-3,7), 135.36 (C-17), 133.64 (C-20), 133.43, 133.09 (C-1,2,9,10), 129.41 (C-5), 129.35 (C-13), 128.66 (C-19), 128.48 (C-23,25), 127.38 (C-24),

126.88 (C-4,6), 126.80 (C-22,26), 126.78 (C-12,14), 118.76 (C-18); IR ν (KBr) 3044, 3007, 1741, 1449, 964, 909, 805, 758, 769, 692 cm^{-1} ; UV (cyclohexane) λ_{max} nm (ϵ_{max}) 261 (28500), 275 (26300), 400 sh (4000); EI MS m/z 332 (M^+), 227 (M^+ - styryl), 202 (100); HR MS Calcd for $\text{C}_{26}\text{H}_{20}$: 332.1565. Found: 332.1568.

* "a" stands for the *trans*-vinyl protons whereas "b" stands for the *cis*-vinyl proton.

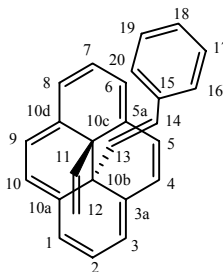
8-Ethynyl-16-vinyl-*anti*-[2.2]metacyclophane-1,9-diene **237**



Hexanes: DCM (92:08) eluted 8-ethynyl-16-vinyl cyclophanediene **237** (~20%) as colorless crystals which on attempted melting point determination converts into DHP **238**: ^1H NMR (CDCl_3) δ 7.19 (t, $J = 7.4$ Hz, 1H, H-5), 7.06 (t, $J = 7.4$ Hz, 1H, H-13), 6.69 (d, $J = 7.3$ Hz, 2H, H-12,14), 6.67 (d, $J = 7.2$ Hz, 2H, H-4,6), 6.56 (d, $J = 11.4$ Hz, 2H, H-1,10), 6.34 (d, $J = 11.4$ Hz, 2H, H-2,9), 6.33 (dd, $J = 17.3, 11.0$ Hz, 1H, H-19, (- $\text{CH}=\text{CH}_2$)), 5.46 (dd, $J = 17.4, 1.7$ Hz, 1H, H-20b*), 4.81 (dd, $J = 11.0, 1.7$ Hz, 1H, H-20a*), 2.81 (s, H-18); ^{13}C NMR (CDCl_3) δ 147.88 (C-16), 141.03 (C-33,7), 136 (C-1,10), 134.77 (C-19), 131.26 (C-5), 131.13 (C-2,9), 129.73 (C-13), 128.81 (C-8), 127.08 (C-12,14), 126.20 (C-4,6), 118.75 (C-20), 82.28, 81.96 (C-17,18); IR ν (KBr) 3303, 3047, 3005, 2580, 1615, 1427, 908, 860, 804, 768, 755, 653, 597 cm^{-1} ; UV (dichloromethane) λ_{max} nm (ϵ_{max}) 239 (24000), 281 (10900), 355 sh (2800); EI MS m/z 254 (M^+); HR MS Calcd for $\text{C}_{20}\text{H}_{14}$: 254.1095. Found: 254.1094.

* "a" stands for the *trans*-vinyl protons whereas "b" stands for the *cis*-vinyl proton.

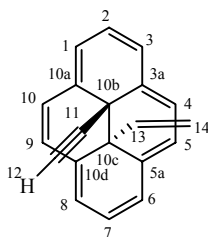
10b-((1E)-2-Phenylvinyl)-10c-vinyl-*trans*-10b,10c-dihydropyrene 241



241

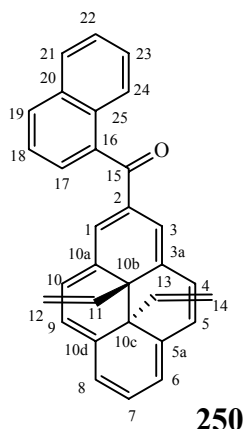
Using procedure 7.5, vinyl-styryl DHP **241** was obtained from CPD **240** as dark green crystals from cyclohexane, mp 147-148 °C; ¹H NMR (CDCl₃) δ 8.83 (AB, *J* = 7.9 Hz, 4H, H-4,5,9,10), 8.68 (d, *J* = 7.7 Hz, 2H, H-1,3), 8.65 (d, *J* = 7.7 Hz, 2H, H-6,8), 8.10 (t, *J* = 7.5 Hz, 1H, H-2), 8.08 (t, *J* = 7.5 Hz, 1H, H-7), 6.73 (m, 3H, H-17,18,19), 6.03 (dd, *J* = 7.5, 1.7 Hz, 2H, H-16,20), 3.21 (d, *J* = 15.6 Hz, 1H, H-14), 2.70 (dd, *J* = 10.3, 1.4 Hz, 1H, H-12a*), 2.08 (dd, *J* = 17.0, 1.5 Hz, 1H, H-12b*), 0.84 (d, *J* = 16.1 Hz, 1H, H-13), 0.54 (dd, *J* = 17.0, 10.3 Hz, 1H, H-11(-CH=CH₂)); ¹³C- NMR (CDCl₃) δ 136.22 (C-15), 133.93 (C-5a,10d), 133.76 (C-3a,10a), 128.64 (C-11), 127.83 (C-17,19), 126.62 (C-18), 125.63 (C-16,20), 125.57, 125.52 (C-4,5,9,10), 124.54 (C-6,8), 124.45 (C-14), 123.87 (C-2,7), 120.70 (C-13), 109.85 (C-12), 36.37 (C-10c), 35.61(C-10b); IR ν (KBr) 3028, 959, 917, 839, 744, 691; UV (cyclohexane) λ_{max} nm (ε_{max}) 253 (18900), 341 (73700), 466 (6400), 609 (110); EI MS *m/z* 332 (M⁺), 227(M⁺ - styryl, 100%); HR MS Calcd for C₂₆H₂₀: 332.1565. Found: 332.1565. Calcd. Anal: C, 93.94; H, 6.06. Found: C, 92.27; H, 6.26.

* "a" stands for the *trans*-vinyl protons whereas "b" stands for the *cis*-vinyl proton.

10b-Ethynyl-10c-vinyl-*trans*-10b,10c-dihdropyrene 238**238**

Using procedure 7.5, vinyl-ethynyl DHP **238** was obtained from CPD **237** as dark green crystals from cyclohexane, mp 216-217 °C; ^1H NMR (CDCl_3) δ 8.91 (AB, $J = 7.8$ Hz, 2H, H-5,9), 8.80 (AB, $J = 7.8$ Hz, H-4,10), 8.70 (overlapping doublets, 4H, H-1,3,6,8), 8.21 (t, $J = 7.7$ Hz, 1H, H-2), 8.17 (t, $J = 7.7$ Hz, 1H, H-7), 2.74 (dd, $J = 10.3$, 1.3 Hz, 1H, H-14a*), 2.16 (dd, $J = 16.9$, 1.3 Hz, 1H, H-14b*), 0.49 (dd, $J = 16.9$, 10.3 Hz, 1H, H-13 ($-\underline{\text{CH}}=\text{CH}_2$)), -0.14 (s, H-12); ^{13}C NMR (CDCl_3) δ 135.20 (C-5a,10a), 131.40 (C-3a,10a), 126.13 (C-13), 125.70 (C-5,9), 125.39 (C-4,10), 124.83 (C-7), 124.63, 123.65 (C-1,3,6,8), 123.57 (C-2), 111.27 (C-14), 77.73 (C-11), 63.44 (C-12), 36.86 (C-10c), 29.47 (C-10b); IR ν (KBr) 3267, 3036, \sim 2560, 841, 632 cm^{-1} ; UV (dichloromethane) λ_{max} nm (ϵ_{max}) 232 (6500), 338 (67000), 375 (29500), 458 (5900), 525 (50), 595 (120), 637 (70); EI MS m/z 254 (M^+); HR MS Calcd for $\text{C}_{20}\text{H}_{14}$: 254.1095. Found: 254.1090. Calcd. Anal: C, 94.45; H, 5.55. Found: C, 92.22; H, 5.70.

* "a" stands for the *trans*-vinyl protons whereas "b" stands for the *cis*-vinyl proton.

10b,10c-Divinyl-2-(1-naphthoyl)-*trans*-10b,10c-dihydropyrene 250

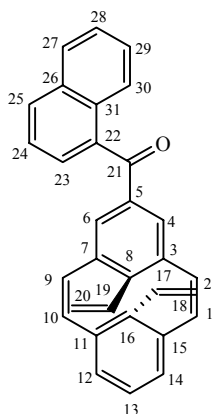
To avoid photo isomerization of the product, this reaction was carried out under minimal light. 15,16-Divinyl-dihydropyrene **167** (60 mg, 0.234 mmol) and naphthoyl chloride (300 mg, 1.574 mmol) were stirred in DCM (10 mL) for 15 minutes. AlCl₃ (160 mg, 1.198 mmol) was added and the reaction mixture was stirred for 10 seconds and then quenched with water. The resulting solution was extracted with DCM (3 x 25 mL), dried over MgSO₄ and evaporated. The crude was column chromatographed over silica gel to give the naphthoylated product **250** (65 mg, 0.16 mmol, 67%) as dark maroon solid from dichloromethane.

¹H NMR (CDCl₃) δ 9.13 (s, 2H, H-1,3), 8.86 (d, *J* = 7.8 Hz, 2H, H-4,10), 8.72 (d, *J* = 7.8 Hz, 2H, H-5,9), 8.58 (d, *J* = 7.7 Hz, 2H, H-6,8), 8.09-8.16 (m, 3H, H-7,19,24), 8.00 (br d, *J* = 8.3 Hz, 1H, H-21), 7.79 (dd, *J* = 7, 1.0 Hz, 1H, H-17), 7.63 (dd, *J* = 8.1, 7.1 Hz, 1H, H-18), 7.56 (dt, *J* = 7.0, 0.9 Hz, 1H, H-22), 7.44 (dt, *J* = 7.0, 1.1 Hz, 1H, H-23), 2.85 (dd, *J* = 10.4, 1.0 Hz, 1H, H-14a*), 2.80 (dd, *J* = 10.3, 1.0 Hz, 1H, H-12a), 2.27 (dd, *J* = 17.0, 1.0, 1H, H-12b), 2.22 (dd, *J* = 17.0, 1.0 Hz, 1H, H-14b*), 0.83 (dd, *J* = 17.0, 10.3 Hz, 1H, H-11), 0.74 (dd, *J* = 17.0, 10.3 Hz, H-13); ¹³C NMR (CDCl₃) δ 199.07 (C-15), 138.05 (C-2), 137.73 (C-10d,5a), 134.02 (C-20), 132.54 (C-10a,3a), 131.53 (C-

25), 131.90 (C-19), 130.29 (C-4,10), 128.86 (C-13), 128.63 (C-21), 128.47 (C-11), 127.93 (C-17), 127.24 (C-23), 127.07 (C-7), 126.63 (C-22), 126.60 (C-1,3), 126.31 (C-24), 125.93 (C-5,9), 124.93 (C-6,8), 124.80 (C-18), 110.90 (C-14), 110.83 (C-12), 37.19 (C-10c), 36.75 (C-10b); IR ν (KBr) 3042, 1637, 1544, 1507, 1462, 1401, 1308, 1236, 1185, 1136, 890, 832, 785 cm^{-1} ; UV (cyclohexane) λ_{max} nm (ϵ_{max}) 222 (75000), 350 (80200), 373 (20000), 397 (25500), 508 (11600), 600 (350), 664 (470); EI MS m/z 410 (M^+); HR MS Calcd for $\text{C}_{31}\text{H}_{22}\text{O}$: 410.1670. Found: 410.1679.

* "a" stands for the *trans*-vinyl protons whereas "b" stands for the *cis*-vinyl proton. C-16 is not clear, probably at δ 137.75.

5-(1-Naphthoyl)-8,16-divinyl-*anti*-[2.2]metacyclophane-1,9-diene **251**

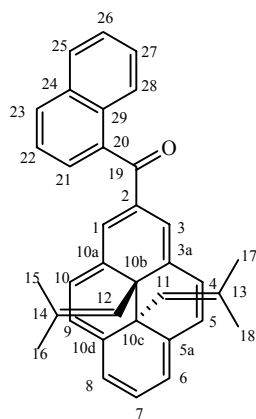


251

Using procedure 5.7, cyclophanediene **251** was obtained quantitatively from the dihydropyrene **250**. On attempted melting point determination, it converts into DHP **250**: ^1H NMR (CDCl_3) δ 8.07 (dd, $J = 7.8, 2.3$ Hz, 1H, H-30), 7.98 (m, 1H, H-25), 7.92 (dd, $J = 7.3, 2.3$ Hz, 1H, H-27), 7.53-7.51 (m, 4H, H-23,24,28,29), 7.16 (s, 2H, H-4,6), 7.13 (t, $J = 7.4$ Hz, 1H, H-13), 6.60 (d, $J = 7.4$ Hz, 2H, H-12,14), 6.45 (dd, $J = 17.4, 11.1$ Hz, 1H, H-17), 6.38 (AB, $J = 11.2$, 4H, H-1,2,9,10), 6.37 (m, 1H, H-19), 5.64 (dd, $J = 17.5, 1.7$

Hz, 1H, H-20b), 5.56 (dd, $J = 17.5, 1.5$ Hz, 1H, H-18b), 4.98 (dd, $J = 11.0, 1.5$ Hz, 1H, H-18a*), 4.97 (dd, $J = 11.1, 1.5$ Hz, 1H, H-20a); ^{13}C NMR (CDCl_3) δ 196.90 (C-21), 152.58 (C-8), 144.41 (C-16), 139.32 (C-5), 137.16 (C-22), 136.32 (C-11,15), 135.94 (C-3,7), 134.89 (C-17), 134.40 (C-19), 133.90 (C-26), 133.62 (C-1,10), 132.93 (C-2,9), 131.08 (C-31), 130.95 (C-25), 130.59 (C-13), 129.16 (C-4,6), 128.59 (C-27), 127.27 (C-29), 126.93 (C-23), 126.76 (C-12,14), 126.63 (C-28), 125.89 (C-30), 124.66 (C-24), 120.87 (C-20), 119.26 (C-18); IR ν (Thin film) 3049, 2924, 2853, 1732, 1651, 1564, 1462, 1291, 806, 785, 768, 741 cm^{-1} ; UV (dichloromethane) λ_{max} nm (ϵ_{max}) 222 (18200), 228 (43700), 250 (36300), 329 (8400), 408 (4200).

10b,10c-Bis(3-methyl-1-propenyl)-2-(1-Naphthoyl)-*trans*-10b,10c-dihdropyrene 248

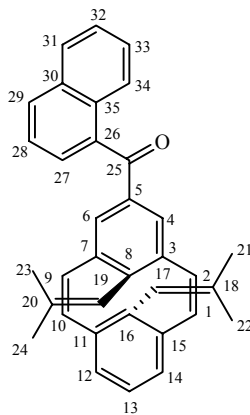


248

Procedure same as for the synthesis of **250** except that the reaction time is 3 s instead of 10 s: mp 179-180 °C; ^1H NMR (CD_2Cl_2) δ 9.04 (s, 2H, H-1,3), 8.63 (AB, $J = 7.8$ Hz, 2H, H- 4,10), 8.52 (d, $J = 7.8$ Hz, 2H, H- 6,8), 8.45 (AB, $J = 7.8$ Hz, H-5,9), 8.06 (m, 4H, H-7,23,25,28), 7.79 (dd, $J = 7.0, 1.2$ Hz, 1H, H-21), 7.65 (dd, $J = 7.0$ Hz, 1H, H-22), 7.55 (td, $J = 6.8, 1.2$ Hz, 1H, H-26), 7.44 (td, $J = 6.7, 1.3$ Hz, 1H, H-27), 0.28, 0.272 (d, $J = 1.2$ Hz, 6H, H-15,16), 0.27 (d, $J = 1.2$ Hz, 3H, H-17), 0.21 (septet, $J = 1.2$ Hz, 1H,

H-12), 0.19 (br s, 3H, H-18), 0.15 (septet, $J = 1.2$ Hz, H-11); ^{13}C NMR (CD_2Cl_2) δ 198.30 (C-19), 140.39 (C-5a,10d), 138.85 (C-20), 134.87 (C-3a,10a), 134.43 (C-24), 132.40 (C-14), 132.27 (C-13), 131.72 (C-29), 131.60 (C-4,10), 131.00 (C-23), 129.03 (C-25), 127.71 (C-1,3), 127.64 (C-21), 127.40 (C-7), 126.96 (C-26), 126.79 (C-5,9), 126.51 (C-27), 126.32 (C-6,8), 125.30 (C-22), 117.19 (C-12), 115.63 (C-11), 37.85 (C-10c), 37.19 (C-10b), 28.37 (C-17), 28.05, 16.44 (C-15,16), 16.54 (C-18)*; IR ν (thin film) 3046, 2963, 2924, 2853, 1637, 1591, 1507, 1461, 1304, 1235, 1185, 1136, 1057, 1028, 883, 829, 785, 736 702, 631 cm^{-1} ; UV (dichloromethane) λ_{max} nm (ϵ_{max}) 228 (20400), 361 (16800), 397 (5590), 421 (6480), 557 (3320), 631 (284); EI MS m/z 466 (M^+); HR MS Calcd: 466.2297. Found: 466.2294. Calcd. Anal: C, 90.09; H, 6.48. Found: C, 88.49; H, 6.55.

C-2 is not clear probably overlapping with the signal at δ 140.39.



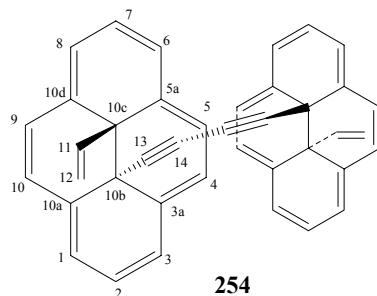
249

Using procedure 5.7, cyclophanediene **249** was obtained quantitatively from the dihydropyrene **248**. On attempted melting point determination transforms into DHP **248**: ^1H NMR (CD_2Cl_2) δ 8.00 (m, 2H, H-31,34), 7.94 (dd, $J = 7.0, 1.3$ Hz, 1H, H-29), 7.52 (m, 4H, H-27,28,32,33), 7.18 (s, 2H, H-4,6), 7.10 (t, $J = 7.4$ Hz, 1H, H-13), 6.62 (d, $J =$

7.4 Hz, H-12,14), 6.25, 6.32 (AB, $J = 11.4$ Hz, 4H, H-1,2,9,10), 5.83 (septet, $J = 1.4$ Hz, H-17), 5.82 (septet $J = 1.4$ Hz, 1H, H-19), 1.63 (d, $J = 1.4$ Hz, 3H, H-24), 1.62 (d, $J = 1.4$ Hz, 3H, H-23), 1.61 (d, $J = 1.4$ Hz, 3H, H-21), 1.55 (d, $J = 1.4$ Hz, 3H, H-22); ^{13}C NMR (CD_2Cl_2) δ 197.43 (CO), 150.56 (C-8), 142.06 (C-16), 139.92 (C-20), 138.93 (C-11,15), 138.61 (C-3,7), 138.60 (C-26), 138.52 (C-5), 135.06 (C-30), 133.52 (C-1,10), 132.69 (C-2,9), 132.12 (C-35), 131.60 (C-31/C-34), 129.86 (C-13), 129.58 (C-29), 129.10 (C-4,6), 128.17, 127.62, 125.69 (C-27,28,32,33) 126.86 (C-31/34), 126.86 (C-12,14), 126.18 (C-17,19), 28.08, 27.90 (C-21,24), 21.95 (C-23), 21.60 (C-22); IR ν (thin film) 3048, 2971, 2927, 1652, 1591, 1507, 1461, 1292, 1234, 1186, 1127, 1056, 1028, 1008, 966, 853, 782, 736; UV (dichloromethane) λ_{max} nm (ϵ_{max}) 231 (24000), 247 (23300), 281 (14500), 325 (6900), 396 sh (3200); EI MS m/z 466 (M^+); HR MS calculated: 466.2297. Found: 466.2294.

10b-[4-(10b-Vinyl(10b,10c-dihdropyrene-10c-yl))buta-1,3-diyndl]-10c-vinyl-10b,10c-dihdropyrene 254

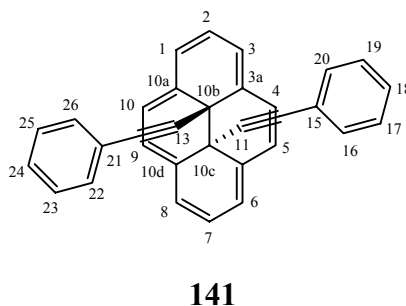
$\text{Cu}(\text{OAc})_2$ (90 mg, 0.5 mmol) was added to a solution of 15-vinyl-16-ethynyldihdropyrne **237** (15 mg) in pyridine: methanol (6 mL:6 mL) solvent mixture. The reaction mixture was heated overnight at 80 °C, cooled to room temperature, solvent was evaporated under vacuum. The crude mixture was chromatographed over silica gel using dichloromethane: hexane (2: 8) to give the dimer **254** (14 mg, 94%) as dark green crystals from benzene.



mp 208-240 °C (dec.) ^1H NMR (CD_2Cl_2) δ 8.60 (d, $J = 7.7$ Hz, 4H, H-5,9), 8.47 (d, $J = 7.7$ Hz, 4H, H-4,10), 8.46 (d, $J = 7.6$ Hz, 4H, H-6,8), 8.38 (d, $J = 7.8$ Hz, 4H, H-1,3), 7.98 (t, $J = 7.7$ Hz, 2H, H-7), 7.93 (t, $J = 7.8$ Hz, 2H, H-2), 2.53 (dd, $J = 10.4, 1.4$ Hz, 2H, H-12a*), 1.92 (dd, $J = 16.9, 1.4$ Hz, 2H, H-12b*), 0.16 (dd, $J = 16.9, 10.3$ Hz, 2H, H-11); ^{13}C NMR (CD_2Cl_2) δ 135.03 (C-5a,10d), 130.32 (C-3a, 10a), 125.93 (C-11), 125.82 (C-5,9), 125.54 (C-4,10), 125.17 (C-7), 124.73 (C-6,8), 123.60 (C-1,3), 123.56 (C-2), 111.30 (C-12), 70.90, 58.95 (C-13,14), 36.57 (C-10c), 30.44 (C-10b); IR ν (KBr) 3035, 1624, 1401, 1349, 917, 838, 743, 685, 630 cm^{-1} ; UV (DCM) λ_{max} nm (ϵ_{max}) 232 (11900), 338 (79300), 377 (32500), 461 (7600), 534 (30), 595 (80), 638 (70); HR MS Calcd for $\text{C}_{20}\text{H}_{14}$: 506.2034. Found: 506.2038; Calcd. Anal: C, 94.82; H, 5.18. Found: C, 90.11; H, 5.14.

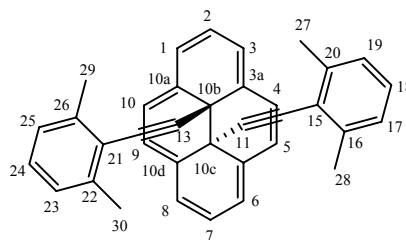
* "a" stands for the *cis*-vinyl proton whereas "b" denotes the *trans*-vinyl proton.

10b,10c-Bis(2-phenylethynyl)-*trans*-10b,10c-dihydropyrene



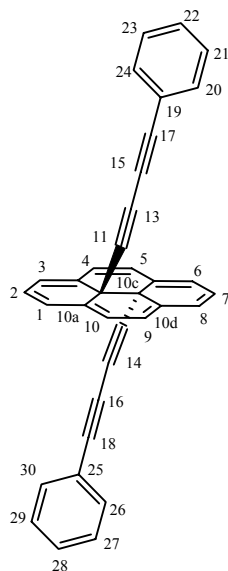
Dichloro-bis-triphenylphosphine palladium (II) (90 mg, 0.13 mmol) and CuBr (30 mg, 0.2 mmol) were added to a solution of iodobenzene (300 mg, 1.47 mmol) and phenyl acetylene (30 mg, 0.29 mmol) in 2.5 mL triethylamine under argon at room temperature. The solution was stirred at 80 °C for 20 min and then 15,16-diethynyldihydropyrene **235** (40 mg, 0.08 mmol) was added and stirring was continued for another 20 minutes. The reaction mixture was cooled to room temperature and TEA evaporated. The crude mixture was extracted between dichloromethane and water. The organic layer was washed three times with aq NaHCO₃ solution, dried over MgSO₄ and evaporated. The product mix was chromatographed over silica gel using hexane: dichloromethane (80: 20) to give the desired prod **141** (42 mg, 66%) as dark green crystals from benzene.

mp 192-193 °C; ¹H NMR (CD₂Cl₂) δ 8.92 (s, 4H, H-4,5,9,10), 8.76 (d, *J* = 7.6 Hz, 4H, H-1,3,6,8), 8.27 (t, *J* = 7.7 Hz, 2H, H-2,7), 6.89 (tt, *J* = 7.5, 1.3 Hz, 2H, H-18,24), 6.78 (m, 4H, H-17,19,23,25), 6.06 (dd, *J* = 8.4, 1.4 Hz, 4H, H-16,20,22,26); ¹³C NMR (CD₂Cl₂) δ 133.66 (C-3a,5a,10a,10d), 131.11 (C-16,20,22,26), 128.09 (C-17,19,23,25), 128.04 (C-18,24), 125.91 (C-4,5,9,10), 124.65 (C-2,7), 123.95 (C-1,3,6,8), 121.89 (C-15,21), 81.55 (C-11,13), 76.96 (C-12,14), 31.66 (C-10b,10c); IR ν (KBr) 3053, 3037, 1596, 1489, 1442, 1351, 1251, 1029, 837, 755, 693, 618 cm⁻¹; UV (DCM) λ_{max} nm (ε_{max}) 245 (35000), 253 (35200), 339 (53000), 375 (30000), 456 (5800), 597 (70), 641 (100); Calcd. Anal: C, 95.01; H, 4.99. Found: C, 92.63; H, 5.48. HR MS Calcd for C₃₂H₂₀: 404.1565. Found: 404.1549.

10b,10c-bis[2-(2,6-dimethylphenyl)ethynyl]-10b,10c-dihydropyrene**247**

Dichloro-bis-triphenylphosphine palladium (II) (20 mg, 0.03 mmol) and CuBr (10 mg, 0.068 mmol) were added to a solution of 2,6-dimethyliodobenzene (46 mg, 0.198 mmol) and 15,16-diethynyldihydropyrene **235** (40 mg, 0.08 mmol) in 2 mL triethylamine under argon at room temperature. The solution was stirred at 90 °C for 1.5 h, cooled to room temperature and TEA evaporated. The crude mixture was extracted between dichloromethane and water. The organic layer was washed three times with aq NaHCO₃ solution, dried over MgSO₄ and evaporated. The product mix was chromatographed over silica gel using hexane: dichloromethane (80: 20) to give the desired prod **247** (15 mg, 20%) as dark green crystals from benzene.

¹H NMR (CDCl₃) δ 8.88 (s, 4H, H-4,5,9,10), 8.71 (d, *J* = 7.7 Hz, 4H, H-1,3,6,8), 8.21 (t, *J* = 7.7 Hz, 2H, H-2,7), 6.46 (d, *J* = 7.5 Hz, 4H, H-17,19,23,25), 6.63 (t, *J* = 7.5 Hz, 2H, H-18,24), 1.17 (s, 12H, Me); ¹³C NMR (CDCl₃) δ 139.74 (C-16,20,22,26), 133.85 (C-3a,5a,10a,10d), 126.89 (C-18,24), 125.87 (C-17,19,23,25), 125.44 (4,5,9,10), 124.07 (C-2,7), 123.43 (1,3,6,8), 121.62 (C-15,21), 89.56, 74.44 (sp carbons), 31.53 (C-10b,10c), 29.92 (Me).

10b,10c-Bis(4-phenylbutadiyny)-*trans*-10b,10c-dihydropyrene 257**257**

$\text{Cu}(\text{OAc})_2$ (500 mg, 2.76 mmol) was added to a solution of phenylacetylene (0.3 g, 0.29 mmol) and diethynyl DHP **235** (10 mg, 0.02 mmol) in pyridine (30 mL). The reaction mixture was heated at 50 °C for 16 h, cooled to room temperature and the solvent was evaporated under vacuum. The crude mixture was chromatographed over silica. hexanes eluted 1,4-diphenylbutadiyne. Dichloromethane: hexane (3: 7) eluted 5 mg of the desired product **257** as green crystals from benzene.

mp ~ 325 °C (dec); ^1H NMR (CD_2Cl_2) δ 8.94 (s, 4H, H-4,5,9,10), 8.78 (d, $J = 7.7$ Hz, 4H, H-1,3,6,8), 8.32 (t, $J = 7.7$ Hz, 2H, H-2,7), 7.19 (tt, $J = 7.5, 1.4$ Hz, 2H, H-22,28), 7.09 (dd, $J = 8.0, 7.6$ Hz, 4H, H-21,23,27,29), 6.99 (dd, $J = 8.1, 1.4$ Hz, 4H, H-20,24,26,30); ^{13}C - NMR (CD_2Cl_2) δ 132.68 (C-22,24,26,30), 132.39 (C-3a,5a,10a,10d), 129.67 (C-22,28), 128.76 (C-21,23,27,29), 126.19 (C-4,5,9,10), 125.23 (C-2,7), 124.33 (C-1,3,6,8), 76.44 (C-17,18), 74.93, 72.32, 62.15 (C-11-16); IR ν (KBr) 1489, 1441, 837, 750, 685 cm^{-1} ; UV (dichloromethane) λ_{max} nm (ϵ_{max}) 229 (40100), 266 (25100), 281

(25600), 298 (17600), 340 (36400), 378 (16700), 457 (4440), 640 (170); EI MS m/z 452 (M^+). HR MS Calcd for $C_{36}H_{20}$: 452.1565. Found: 452.1554; Anal. Calcd: C, 95.55; H, 4.45. Found: C, 89.89; H, 4.16.

References

1. Feringa, B. L. *Molecular Switches*, Wiley-VCH, Weinheim, **2001**.
2. Micheau, J-C.; Yokoyama, Y. *J. Phys. Org. Chem.* **2007**, *20*, 801-1020 and references therein.
3. (a)Waldeck, D. H.; Beratan, D. N. *Science* **1993**, *261*, 576-577; Tour, J. M.; Schumm, J. S. *J. Am. Chem. Soc.* **1991**, *113*, 7064-7066; (b) Patil, A. O.; Heegar, A. J.; Wudl, F. *Chem. Rev.* **1988**, *88*, 183-200 and references therein. Hu, J.; Odom, T. W.; Lieber, C.M. *Acc. Chem. Res.* **1999**, *32*, 434-445; (c) Feringa, B. L.; Jager, W. F.; de Lange, B. *Tetrahedron* **1993**, *49*, 8267-8310; (d). Willner, I.; Willner, B. *J. Mater. Chem.* **1998**, *8*, 2543-2556 and references therein.
4. Bouas-Laurent, H.; Durr, H. *Pure Appl. Chem.* **2001**, *73*, 639-665; (b) *Photochromism: Molecules and Systems*, ed. by H. Durr, H. Bouas-Laurent, Elsevier, Amsterdam, **2003**.
5. Ferri, V.; Elbing, M.; Pace, G.; Dickey, M. D.; Zharnikov, M.; Samori, P.; Mayor, M.; Rampi, M. A. *Angew. Chem. Int. Ed.* **2008**, *47*, 3407-3409.
6. (a) Ichihara, K.; Namada, N.; Kato, S.; Shinohara, I. *J Polymer Sci., Polym. Chem. Ed.* **1984**, *22*, 121-128; (b) Ichihara, K.; Namada, N.; Kato, S.; Shinohara, I. *J. Polymer Sci., Polym. Chem. Ed* **1983**, *21*, 1551-1555; (c) Balasubramaman, D.; Subramani, S.; Kumar, C. *Nature*, **1975**, *254*, 252-254;
7. Irie, M.; Tanaka, H., *Macromolecules*, **1983**, *16*, 210-214.
8. Delaire, J. A.; Nakatani, K. *Chem. Rev.* **2000**, *100*, 1817-1845.
9. Sakagami, S.; Koga, T.; Takase, A. *Liquid crystals*, **2000**, *27*, 1551-1554.

10. Barachevsky, V. A.; Crano, J. C.; Guglielmetti, R. J. *Org. Photochromic Thermo-chromic Compd.* **1999**, 267-314. Plenum Publishing Corp., New York N.Y.
11. Reddy, C. D.; Ramamurthy, V. *J. Org. Chem.* **1987**, 52, 5521-5528.
12. Noakas, J. E.; Culp, R. A. US Pat. (1985) 4,507,226.
13. Irie, M., *J. Am. Chem. Soc.* **1983**, 105, 2078-2079.
14. Lomoth, R.; Haupl, T.; Johanssen, O.; Hammarstrom, L. *Chem. Eur. J.*, **2002**, 8, 102-109.
15. Stookey, S.D. US patent 3252374, Corning Glass Works, **1962**.
16. IUPAC *Compendium of Chemical Terminology*, 2nd Edition, **1997**.
17. Bouas-Laurent, H.; Castellan, A.; Desvergne, J-P. *Pure Appl. Chem.* **1980**, 52, 2633-2648.
18. Sauter, von H.; Hoerster, H.; Prinzbach, H. *Angew. Chem.* **1973**, 85, 1106-1107.
19. Ansari, F. L.; Qureshi, R.; Qureshi, M. L. *Electrocyclic Reactions* 1st ed. Wiley VCH Weinheim, **1999**.
20. Stobbe, H. *Ber.* **1905**, 38, 3673-3682.
21. Yokoyama, Y.; Uchida, S.; Sugawara, Y.; Kurita, Y. *J. Am. Chem. Soc.* **1996**, 118, 3100-3107.
22. Fischer, E.; Hirshberg, Y. *J. Chem. Soc.* **1952**, 4522-4524.
23. Berkovic, G. *Chem. Rev.* **2000**, 100, 1741-1753.
24. Irie, M. *Chem. Rev.*, **2000**, 100, 1685-1716.
25. Takeshita, M.; Irie, M. *J. Chem. Soc. Chem. Comm.* **1996**, 1807-1808.
26. Tanifuji, N.; Irie, M.; Matsuda, K. *Chem. Lett.* **2005**, 34, 1580-1581

27. Gilat, S.L.; Kawai, S. H.; Lehn, J. M. *Chem. Eur. J.* **1995**, *1*, 275-284
28. Samachetty, H. D.; Branda, N. R., *Pure Appl. Chem.* **2006**, *78*, 2351-2359.
29. Mitchell, R.H.; Brkic, Z.; Sauro, V. A.; Berg, D. J. *J. Am. Chem. Soc.*, **2003**, *125*, 7581-7585.
30. Blattman, H. R.; Meuch, D.; Heilbronner, E.; Molyneux, R. G.; Boekelheide, V. *J. Am. Chem. Soc.* **1965**, *87*, 130-131.
31. Boekelheide, V. J.; Phillips, J. *J. Am. Chem. Soc.* **1967**, *89*, 1695-1704.
32. Mitchell, R. H.; Boekelheide, V. *J. Am. Chem. Soc.* **1974**, *96*, 1547-1553
33. Tashiro, M.; Yamato, T, *J. Am. Chem. Soc.* **1982**, *104*, 3701-3707.
34. Sheepwash, M. A. L.; Mitchell, R. H.; Bohne, C. *J. Am. Chem. Soc.*, **2002**, *124*, 4693-4700.
35. Robinson, S. G., Ph.D. Thesis, University of Victoria, **2008**.
36. Mitchell, R. H.; Boekelheide, V. *Tet. Lett*, **1970**, *11*, 1197-1202
37. Ayub, K.; Zhang, R.; Robinson, S. G.; Twamley, B.; Williams, R. V.; Mitchell, R. H. *J. Org. Chem.* **2008**, *73*, 451-456.
38. Mitchell, R. H.; Ward, T. R.; Chen, Y.; Weerawana, S. A.; Dibble, P. W.; Marsella, M. J.; Almutairi, A.; Wang, Z. Q. *J. Am. Chem. Soc.* **2003**, *125*, 2974-2988.
39. Mitchell, R. H.; Brkic, Z.; Sauro, V. A.; Berg, D. J. *J. Am. Chem. Soc.* **2003**, *125*, 7581-7585; Mitchell, R. H.; Yan, J. S. H.; Dingle, T. W. *J. Am. Chem. Soc.* **1982**, *104*, 2551-2559; Cerfontain, H.; Koeberg-Tedler, A.; Bakker, B. H.; Mitchell, R. H.; Tashiro, M. *Leibigs Ann./Recueil* **1997**, 873-878; Mitchell, R. H.; Fan, W.; Lau, D. Y. K.; Berg, D. J. *J. Org. Chem.* **2004**, *69*, 549-554; Mitchell, R. H. *Eur.*

- J. Org. Chem.* **1999**, 2695-2703. Blattman, H. R.; Schmidt, W. *Tetrahedron*, **1970**, 26, 5885-5899.
40. Woodward, R. B.; Hoffmann, R. *The Conservation of Orbital Symmetry*; Verlag Chemie: Weinheim Germany, **1970**; Schmidt, W. *Helv. Chem. Acta.* **1971**, 54, 862-868.
41. Williams, R. V.; Edwards, W. D.; Mitchell, R. H.; Robinson, S. G. *J. Am. Chem. Soc.* **2005**, 127, 16207-16214.
42. Baldwin, J. E. *Org. Chem.* **1977**, 35, 273.
43. Jarzecki, A. A.; Gajewski, J.; Davidson, E. R. *J. Am. Chem. Soc.* **1999**, 121, 6928-6935.
44. Borden, W. T. *Mol. Phys.* **2002**, 100, 337-347.
45. Pryor, W. A. Free Radicals, McGraw Hill. New York. 1960. March, J. *Advanced Org. Chem.* 4th Ed. Wiley Interscience, New York, **1992**, 186-195.
46. Henry, D. J.; Parkinson, C. J.; Mayer, P. M.; Radom, L. *J. Phys. Chem. A*, **2001**, 105, 6750-6756.
47. Pasto, D. J.; Krasnansky, R.; Zercher, C. *J. Org. Chem.* **1987**, 52, 3062-3072. Bordwell, F. G.; Zhang, X.; Alnajjar, M. S. *J. Am. Chem. Soc.* **1992**, 114, 7623-7629.
48. Song, K.; Liu, L.; Guo, Q. *J. Org. Chem.* **2003**, 68, 4604-4607.
49. Berman, E.; Fox, R. E.; Thomson, F. D. *J. Am. Chem. Soc.* **1959**, 81, 5605-5608
50. Kobatake, S.; Terakawa, Y. *Chem. Comm.* **2007**, 17, 1698-1700.
51. Morimitsu, K.; Kobatake, S.; Irie, M. *Mol. Cryst. Liq. Cryst.* **2005**, 431, 151-154.
52. Pu, S.; Zheng, C.; Le, Z.; Liu, G.; Fan, C. *Tetrahedron*, **2008**, 64, 2576-2585.

53. Wittig, G.; Lohmann, L. *Ann.* **1942**, 550, 260
54. Stevens, T. S.; Creighton, E. M.; Gordon, A. B.; MacNicol, M. *J. Chem. Soc.* **1928**, 3193-3197..
55. Bruhin, J.; Gerson, F.; Martin, W. B.; Novotny, H. *J. Am. Chem. Soc.* **1988**, 110, 6377-6384.
56. Sandmeyer, T. *Ber. Dtsch. Chem. Ges.* **1884**, 17, 1633-1635.
57. Bodwell, G. J.; Houghton, T. J.; Koury, H. E.; Yarlagadda, B. *Synlett*, **1995**, 751-752.
58. Vogtle, F.; Zuber, M.; Neumann, P. *Z. Naturforsch.* **1971**, 26b, 707-709.
59. Borch, R. F. *J. Org. Chem.* **1969**, 34, 627-629.
60. Lai, Y.; Eu, H. *J. Chem. Soc. Perkin Trans. 1*, **1993**, 233-237.
61. Boekelheide, V.; Sturm, E. *J. Am. Chem. Soc.* **1969**, 91, 902.
62. Boekelheide, V.; Hylton, T. A. *J. Am. Chem. Soc.* **1970**, 92, 3669.
63. Kitagawa, F.; Murase, M.; Kitamura, N. *J. Org. Chem.* **2002**, 67, 2524-2531
64. Tashiro, M.; Yamato, T. *J. Org. Chem.* **1981**, 46, 1543-1552
65. Lai, Y-H.; Zhou, Z-L. *J. Org. Chem.* **1994**, 59, 8275-8278.
66. Cao, D.; Kolshorn, H.; Meier, H. *Tetrahedron Lett.* **1996**, 37, 4487-4490.
67. Sheepwash, M. A. L.; Mitchell, R. H.; Bohne, C. *J. Am. Chem. Soc.* **2002**, 124, 4693-4700.
68. Brady, O. L.; Eksmie, G. V. *Analyst* 1926, 51, 77-78; (b) *Chemistry in context*, 4th Edition, **2000**, Graham Hill and John Holman.
69. For isopropyl triphenylphosphonium bromide, procedure was adopted from Brovema, S.; Duar, Y. *J. Am. Chem. Soc.* **1990**, 112, 5830-5837. Other

phosphonium bromides were obtained by heating triphenyl phosphine and allylic/benzylic bromide in toluene at 100 °C overnight.

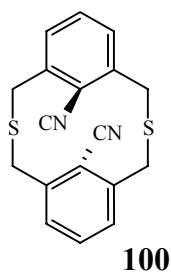
70. Glaser, C. *Ann* **1870**, *154*, 159; Glaser, C. *Ber.* **1869**, *2*, 422-424.
71. PC MODEL for Windows Version 8.50.0, September 2003, Sereena Software.
72. Otero, M.; Herranz, M. A.; Seoane, C.; Martin, N.; Garin, J.; Orduna, J.; Alcalá, R.; Villacampa, B. *Tetrahedron*, **2002**, *58*, 7463-7475.
73. Lamture, J. B.; Suryawanshi, S. N.; Nayak, U. R. *Indian Journal of Chemistry, Section B: Organic Chemistry Including Medicinal Chemistry*, **1981**, *20B*, 957-959.
74. Sonogashira, K.; Tohda, Y.; Hagihara, N. *Tet. Lett.* **1975**, 4467-4470.
75. Kobatake, S.; Takami, S.; Muto, H.; Ishikawa, T.; Irie, M. *Nature*, **2007**, *446*, 778-781.
76. Pieroni, O.; Houben, J. L.; Fissi, A.; Costantino, P.; Ciardelli, F. *J. Am. Chem. Soc.*, **1980**, *102*, 5913-5915.
77. Eglington, G.; Galbraith, A. R. *J. Chem. Soc.* **1959**, 889-896.
78. Yu, T.; Fu, Y.; Liu, L.; Guo, Q. *J. Org. Chem.* **2006**, *71*, 6157-6164.
79. Megamedov, N. A.; Ruggiero, P. L.; Tang, Y. *J. Am. Chem. Soc.* **2004**, *126*, 1624-1625.
80. Nonoshita, K.; Banno, H.; Maruoka, K.; Yamamoto, H. *J. Am. Chem. Soc.* **1990**, *112*, 316-322. and references therein.
81. Bury, A.; Bougeard, P.; Corker, S. J.; Johnson, M. D.; Perlmann, M.; *J Chem Soc Perkin Trans II*, **1982**, 1367-1372.

- 82.** Boggio-Pasqua, M.; Bearpark, M. J.; Bobb, M. A. *J. Org. Chem.* **2007**, *72*, 4497-4503.
- 83.** Bandyopadhyay, S. PhD thesis, University of Victoria, **2004**.
- 84.** Dunitz, J.D.; Orgel, L. E.; Rich, A. *Acta Crystallographica*, **1956**, *9*, 373-375.
- 85.** Anker, W., Ph.D. Thesis, University of Victoria, **1982**.

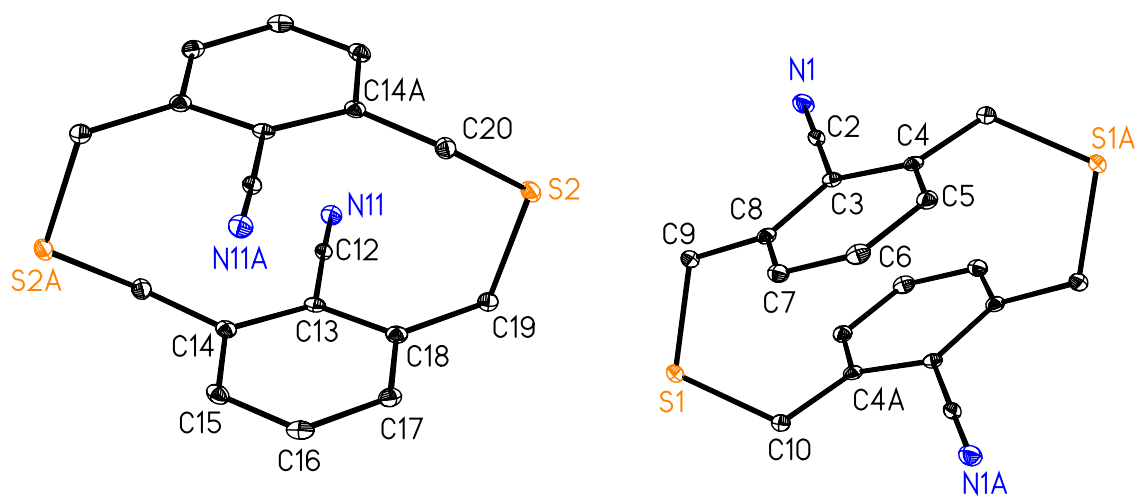
X-ray structure reports

Single-Crystal X-ray Diffraction Laboratory University of Idaho

X-ray structure for *anti*-dithiacyclophane 100



Brendan Twamley



Project name : bt906

5-30-06

Experimental:

Crystals of compound **1** were removed from the flask, a suitable crystal was selected, attached to a MiTeGen fiber and data were collected at 89(2) K using a Bruker/Siemens SMART APEX instrument (Mo K α radiation, $\lambda = 0.71073$ Å) equipped with a Cryocool NeverIce low temperature device. Data were measured using omega scans of 0.3 ° per frame for 30 seconds, and a full sphere of data was collected. A total of 2400 frames were collected with a final resolution of 0.83 Å. Cell parameters were retrieved using SMART¹ software and refined using SAINTPlus² on all observed reflections. Data reduction and correction for Lp and decay were performed using the SAINTPlus software. Absorption corrections were applied using SADABS.³ The structure was solved by direct methods and refined by least squares method on F² using the SHELXTL program package.⁴ The structure was solved in the space group P-1 (# 2) by analysis of systematic absences. All non-hydrogen atoms were refined anisotropically. No decomposition was observed during data collection. Details of the data collection and refinement are given in Table 1. Further details are provided in the Supporting Information.

Acknowledgement

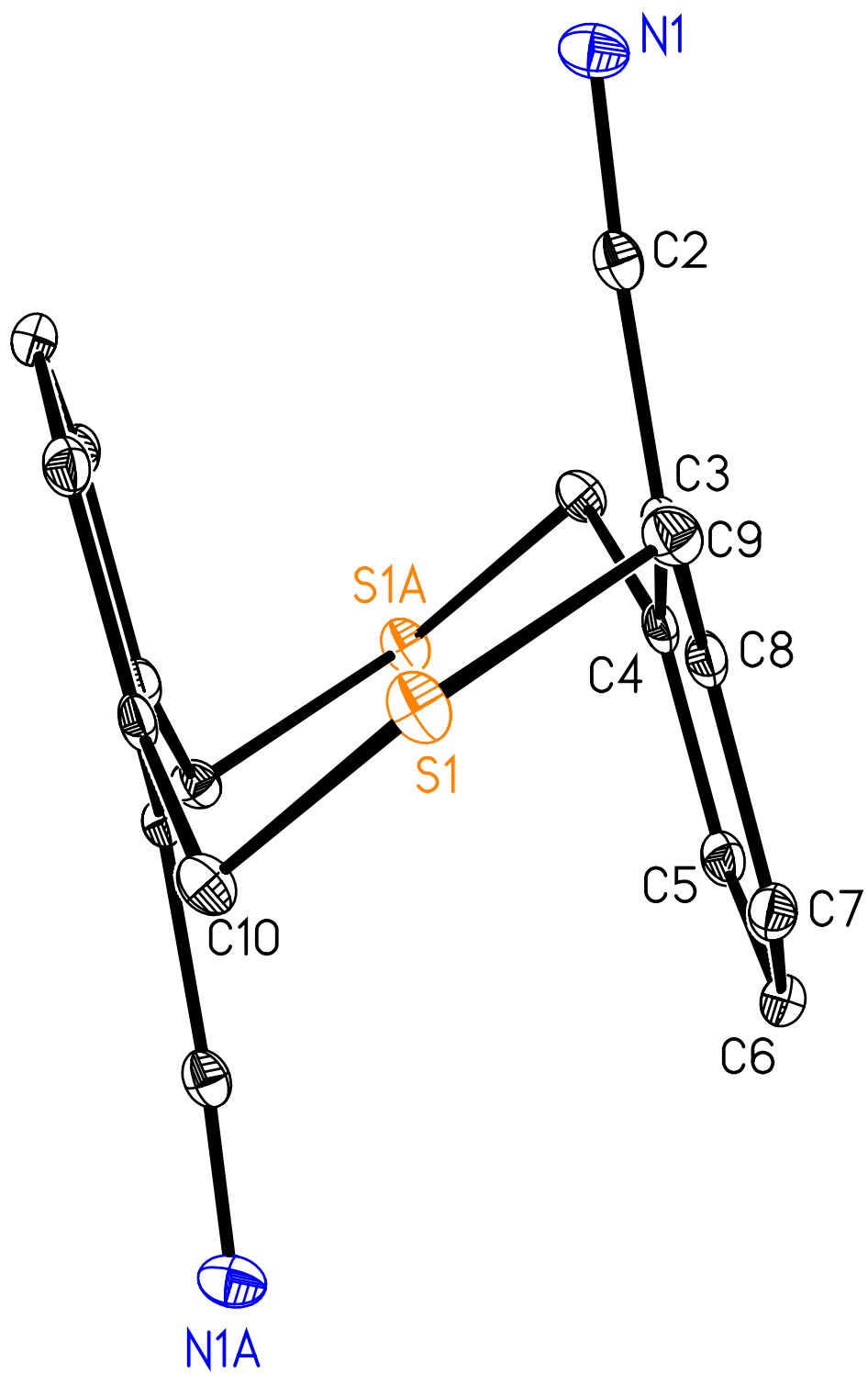
The Bruker (Siemens) SMART APEX diffraction facility was established at the University of Idaho with the assistance of the NSF-EPSCoR program and the M. J. Murdock Charitable Trust, Vancouver, WA, USA.

¹ SMART: v.5.630, Bruker Molecular Analysis Research Tool, Bruker AXS, Madison, WI, **2001**.

² SAINTPlus: v. 7.23a, Data Reduction and Correction Program, Bruker AXS, Madison, WI, **2004**.

³ SADABS: v.2004/1, an empirical absorption correction program, Bruker AXS Inc., Madison, WI, **2004**.

⁴ SHELXTL: v. 6.14, Structure Determination Software Suite, Sheldrick, G.M., Bruker AXS Inc., Madison, WI, **2004**.



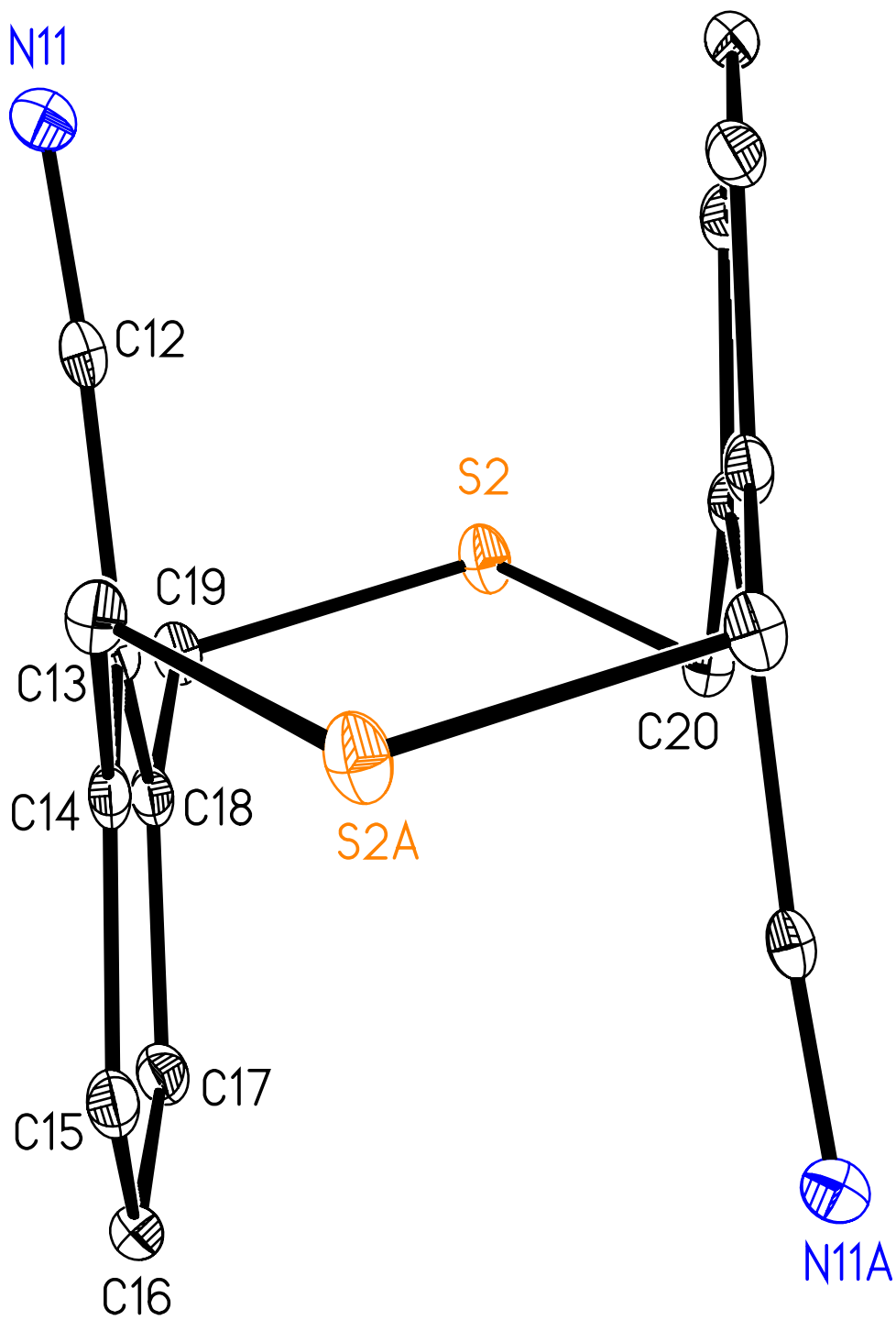


Table A. 1 Crystal data and structure refinement for 100 (C₁₈ H₁₄ N₂ S₂).

Identification code	bt906	
Empirical formula	C ₁₈ H ₁₄ N ₂ S ₂	
Formula weight	322.43	
Temperature	89(2) K	
Wavelength	0.71073 Å	
Crystal system	Triclinic	
Space group	P-1	
Unit cell dimensions	a = 6.8155(10) Å	α = 99.458(2)°.
	b = 7.8620(12) Å	β = 96.368(2)°.
	c = 14.322(2) Å	γ = 106.897(2)°.
Volume	714.01(19) Å ³	
Z	2	
Density (calculated)	1.500 Mg/m ³	
Absorption coefficient	0.369 mm ⁻¹	
F(000)	336	
Crystal size	0.20 x 0.17 x 0.05 mm ³	
Crystal color and habit	colorlessplate	
Diffractometer	Bruker/Siemens SMART APEX	
Theta range for data collection	1.46 to 25.25°.	
Index ranges	-8<=h<=8, -9<=k<=9, -17<=l<=17	
Reflections collected	10494	
Independent reflections	2595 [R(int) = 0.0194]	
Completeness to theta = 25.25°	100.0%	
Absorption correction	Semi-empirical from equivalents	
Max. and min. transmission	0.9818 and 0.9298	
Solution method	Bruker, 2003; XS, SHELXTL v. 6.14	
Refinement method	Full-matrix least-squares on F ²	
Data / restraints / parameters	2595 / 0 / 199	
Goodness-of-fit on F ²	1.062	
Final R indices [I>2sigma(I)]	R1 = 0.0312, wR2 = 0.0791	
R indices (all data)	R1 = 0.0341, wR2 = 0.0821	
Largest diff. peak and hole	0.431 and -0.189 e.Å ⁻³	

Table A. 2 Atomic coordinates ($\times 10^4$) and equivalent isotropic displacement parameters ($\text{\AA}^2 \times 10^3$) for 100 (bt 906)

	x	y	z	U(eq)
C(2)	1243(2)	-2342(2)	4019(1)	14(1)
C(3)	1828(2)	-448(2)	4483(1)	12(1)
C(4)	2772(2)	82(2)	5454(1)	13(1)
C(5)	3513(2)	1931(2)	5861(1)	15(1)
C(6)	3265(3)	3195(2)	5325(1)	16(1)
C(7)	2207(2)	2646(2)	4387(1)	15(1)
C(8)	1448(2)	811(2)	3952(1)	13(1)
C(9)	185(3)	169(2)	2958(1)	15(1)
C(10)	-2834(3)	1334(2)	3958(1)	15(1)
C(12)	2082(2)	2578(2)	-442(1)	13(1)
C(13)	2542(2)	4504(2)	-72(1)	12(1)
C(14)	2982(2)	5726(2)	-690(1)	13(1)
C(15)	3174(2)	7535(2)	-332(1)	16(1)
C(16)	3029(3)	8115(2)	618(1)	16(1)
C(17)	2748(2)	6919(2)	1238(1)	16(1)
C(18)	2481(2)	5085(2)	904(1)	14(1)
C(19)	2170(3)	3778(2)	1570(1)	15(1)
C(20)	6761(3)	4906(2)	1711(1)	15(1)
N(1)	857(2)	-3832(2)	3639(1)	19(1)
N(11)	1618(2)	1039(2)	-732(1)	17(1)
S(1)	-2155(1)	872(1)	2770(1)	16(1)
S(2)	4577(1)	3440(1)	2127(1)	18(1)

Table A. 3 Bond lengths [Å] and angles [°] for 100 (bt 906).

C(2)-N(1)	1.148(2)	C(18)-C(19)	1.500(2)
C(2)-C(3)	1.445(2)	C(19)-S(2)	1.8524(17)
C(3)-C(8)	1.407(2)	C(19)-H(19A)	0.9900
C(3)-C(4)	1.407(2)	C(19)-H(19B)	0.9900
C(4)-C(5)	1.391(2)	C(20)-C(14)#2	1.512(2)
C(4)-C(10)#1	1.509(2)	C(20)-S(2)	1.8233(17)
C(5)-C(6)	1.388(2)	C(20)-H(20A)	0.9900
C(5)-H(5)	0.9500	C(20)-H(20B)	0.9900
C(6)-C(7)	1.386(2)		
C(6)-H(6)	0.9500	N(1)-C(2)-C(3)	177.22(17)
C(7)-C(8)	1.392(2)	C(8)-C(3)-C(4)	121.90(15)
C(7)-H(7)	0.9500	C(8)-C(3)-C(2)	119.27(15)
C(8)-C(9)	1.503(2)	C(4)-C(3)-C(2)	118.82(14)
C(9)-S(1)	1.8405(17)	C(5)-C(4)-C(3)	117.89(15)
C(9)-H(9A)	0.9900	C(5)-C(4)-C(10)#1	121.80(15)
C(9)-H(9B)	0.9900	C(3)-C(4)-C(10)#1	120.18(14)
C(10)-C(4)#1	1.509(2)	C(6)-C(5)-C(4)	120.50(16)
C(10)-S(1)	1.8203(17)	C(6)-C(5)-H(5)	119.7
C(10)-H(10A)	0.9900	C(4)-C(5)-H(5)	119.7
C(10)-H(10B)	0.9900	C(7)-C(6)-C(5)	120.95(15)
C(12)-N(11)	1.149(2)	C(7)-C(6)-H(6)	119.5
C(12)-C(13)	1.448(2)	C(5)-C(6)-H(6)	119.5
C(13)-C(14)	1.402(2)	C(6)-C(7)-C(8)	120.40(15)
C(13)-C(18)	1.406(2)	C(6)-C(7)-H(7)	119.8
C(14)-C(15)	1.393(2)	C(8)-C(7)-H(7)	119.8
C(14)-C(20)#2	1.512(2)	C(7)-C(8)-C(3)	118.03(15)
C(15)-C(16)	1.385(2)	C(7)-C(8)-C(9)	121.56(15)
C(15)-H(15)	0.9500	C(3)-C(8)-C(9)	120.37(14)
C(16)-C(17)	1.385(2)	C(8)-C(9)-S(1)	115.99(11)
C(16)-H(16)	0.9500	C(8)-C(9)-H(9A)	108.3
C(17)-C(18)	1.394(2)	S(1)-C(9)-H(9A)	108.3
C(17)-H(17)	0.9500	C(8)-C(9)-H(9B)	108.3

S(1)-C(9)-H(9B)	108.3	C(14)#2-C(20)-H(20B)	108.3
H(9A)-C(9)-H(9B)	107.4	S(2)-C(20)-H(20B)	108.3
C(4)#1-C(10)-S(1)	114.75(11)	H(20A)-C(20)-H(20B)	107.4
C(4)#1-C(10)-H(10A)	108.6	C(10)-S(1)-C(9)	105.06(8)
S(1)-C(10)-H(10A)	108.6	C(20)-S(2)-C(19)	107.68(8)
C(4)#1-C(10)-H(10B)	108.6		
S(1)-C(10)-H(10B)	108.6		
H(10A)-C(10)-H(10B)	107.6		
N(11)-C(12)-C(13)	176.69(17)		
C(14)-C(13)-C(18)	121.92(15)		
C(14)-C(13)-C(12)	119.86(15)		
C(18)-C(13)-C(12)	118.20(14)		
C(15)-C(14)-C(13)	117.87(15)		
C(15)-C(14)-C(20)#2	121.24(15)		
C(13)-C(14)-C(20)#2	120.89(14)		
C(16)-C(15)-C(14)	120.72(15)		
C(16)-C(15)-H(15)	119.6		
C(14)-C(15)-H(15)	119.6		
C(17)-C(16)-C(15)	120.71(15)		
C(17)-C(16)-H(16)	119.6		
C(15)-C(16)-H(16)	119.6		
C(16)-C(17)-C(18)	120.46(16)		
C(16)-C(17)-H(17)	119.8		
C(18)-C(17)-H(17)	119.8		
C(17)-C(18)-C(13)	118.03(15)		
C(17)-C(18)-C(19)	120.88(15)		
C(13)-C(18)-C(19)	121.08(15)		
C(18)-C(19)-S(2)	115.16(11)		
C(18)-C(19)-H(19A)	108.5		
S(2)-C(19)-H(19A)	108.5		
C(18)-C(19)-H(19B)	108.5		
S(2)-C(19)-H(19B)	108.5		
H(19A)-C(19)-H(19B)	107.5		
C(14)#2-C(20)-S(2)	115.73(11)		
C(14)#2-C(20)-H(20A)	108.3		
S(2)-C(20)-H(20A)	108.3		

Symmetry transformations used to generate equivalent atoms:

#1 -x,-y,-z+1 #2 -x+1,-y+1,-z

Table A. 4 Anisotropic displacement parameters ($\text{\AA}^2 \times 10^3$) for 100 (bt 906).

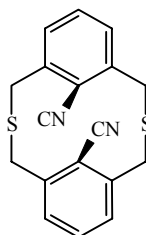
	U11	U22	U33	U23	U13	U12
C(2)	13(1)	19(1)	14(1)	6(1)	3(1)	8(1)
C(3)	9(1)	12(1)	15(1)	3(1)	4(1)	4(1)
C(4)	8(1)	17(1)	17(1)	5(1)	5(1)	6(1)
C(5)	10(1)	18(1)	15(1)	2(1)	2(1)	5(1)
C(6)	12(1)	13(1)	21(1)	2(1)	5(1)	2(1)
C(7)	13(1)	15(1)	20(1)	7(1)	5(1)	5(1)
C(8)	10(1)	16(1)	16(1)	5(1)	5(1)	5(1)
C(9)	17(1)	16(1)	16(1)	6(1)	4(1)	8(1)
C(10)	15(1)	19(1)	14(1)	4(1)	3(1)	9(1)
C(12)	10(1)	19(1)	13(1)	6(1)	2(1)	7(1)
C(13)	9(1)	13(1)	16(1)	3(1)	0(1)	5(1)
C(14)	7(1)	15(1)	16(1)	5(1)	0(1)	4(1)
C(15)	11(1)	16(1)	22(1)	8(1)	1(1)	4(1)
C(16)	12(1)	12(1)	24(1)	1(1)	2(1)	5(1)
C(17)	13(1)	18(1)	16(1)	1(1)	2(1)	7(1)
C(18)	9(1)	17(1)	17(1)	4(1)	1(1)	5(1)
C(19)	13(1)	19(1)	16(1)	5(1)	3(1)	7(1)
C(20)	13(1)	16(1)	15(1)	5(1)	2(1)	4(1)
N(1)	23(1)	17(1)	19(1)	2(1)	1(1)	10(1)
N(11)	19(1)	16(1)	18(1)	5(1)	4(1)	8(1)
S(1)	15(1)	22(1)	13(1)	6(1)	2(1)	9(1)
S(2)	15(1)	22(1)	20(1)	12(1)	5(1)	7(1)

Table A. 5 Hydrogen coordinates ($\times 10^4$) and isotropic displacement parameters ($\text{\AA}^2 \times 10^3$) for 100 (bt 906).

	x	y	z	U(eq)
H(5)	4194	2331	6510	17
H(6)	3827	4454	5604	19
H(7)	1999	3528	4040	18
H(9A)	-247	-1175	2801	18
H(9B)	1092	617	2499	18
H(10A)	-1865	2522	4317	18
H(10B)	-4252	1441	3885	18
H(15)	3405	8380	-743	19
H(16)	3125	9346	846	20
H(17)	2736	7352	1897	19
H(19A)	1217	2587	1208	18
H(19B)	1478	4218	2087	18
H(20A)	6599	6129	1772	18
H(20B)	8056	5029	2143	18

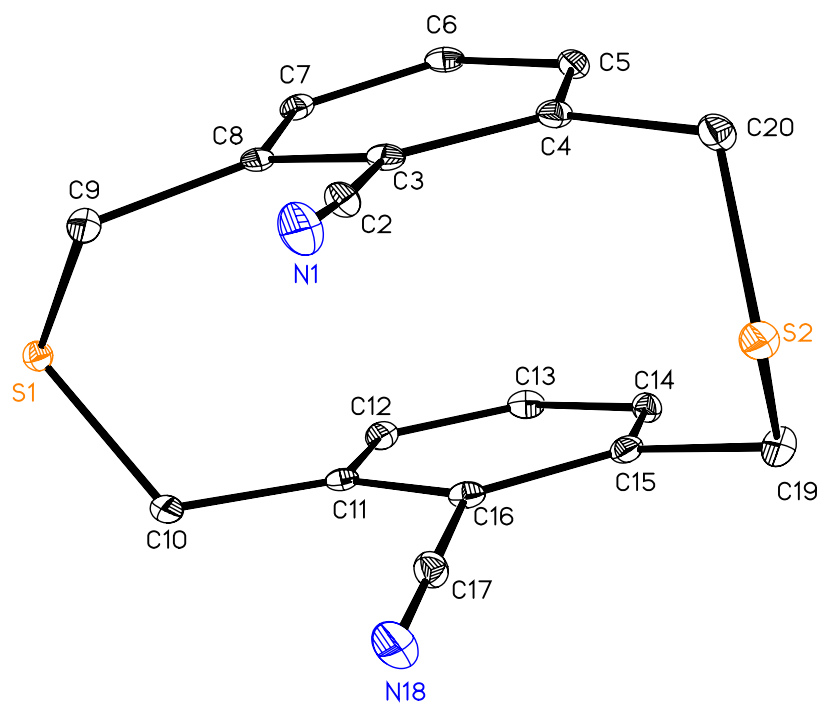
Single-Crystal X-ray Diffraction Laboratory
University of Idaho

X-ray structure report for *syn*-dithiacyclophane 108



108

Brendan Twamley



Project name : bt908t

5-31-06

Experimental:

Crystals of compound **1** were removed from the flask, a suitable crystal was selected, attached to a MiTeGen fiber and data for **1** were collected at 89(2) K using a Bruker/Siemens SMART APEX instrument (Mo K α radiation, $\lambda = 0.71073$ Å) equipped with a Cryocool NeverIce low temperature device. Data were measured using omega scans of 0.3 ° per frame for 5 seconds, and a full sphere of data was collected. A total of 2400 frames were collected with a final resolution of 0.83 Å. Cell parameters were retrieved using SMART⁵ software. The data were rotationally twinned and were deconvoluted using CELL_NOW⁶ giving a two component twin relationship: 179.9° rotation about the reciprocal axis 1.000, 0.006, -0.995, with a refined twinning ratio of 0.285(1). The matrix used to relate both orientations to the first domain are:

0.383 0.003 -0.621

0.006 -1.000 -0.007

-1.375 0.000 -0.383

Each cell component was refined using SAINTPlus⁷ on all observed reflections. Data reduction and correction for Lp and decay were performed using the SAINTPlus software. Absorption corrections were applied using TWINABS.⁸ The structure was solved by direct methods and refined by least squares method on F² using the SHELXTL program package.⁹ The structure was solved in the space group P2(1)/n (# 14) by analysis of systematic absences. All non-hydrogen atoms were refined anisotropically. No

⁵ SMART: v.5.630, Bruker Molecular Analysis Research Tool, Bruker AXS, Madison, WI, **2002**.

⁶ CELL_NOW: Sheldrick, G.M., **2002**.

⁷ SAINTPlus: v. 6.45a, Data Reduction and Correction Program, Bruker AXS, Madison, WI, **2001**.

⁸ TWINABS: v.1.05, an empirical absorption correction program, Sheldrick, G.M., Bruker AXS Inc., Madison, WI, **2002**.

⁹ SHELXTL: v. 6.14, Structure Determination Software Suite, Sheldrick, G.M., Bruker AXS Inc., Madison, WI, **2003**.

decomposition was observed during data collection. Details of the data collection and refinement are given in Table 1. Further details are provided in the Supporting Information.

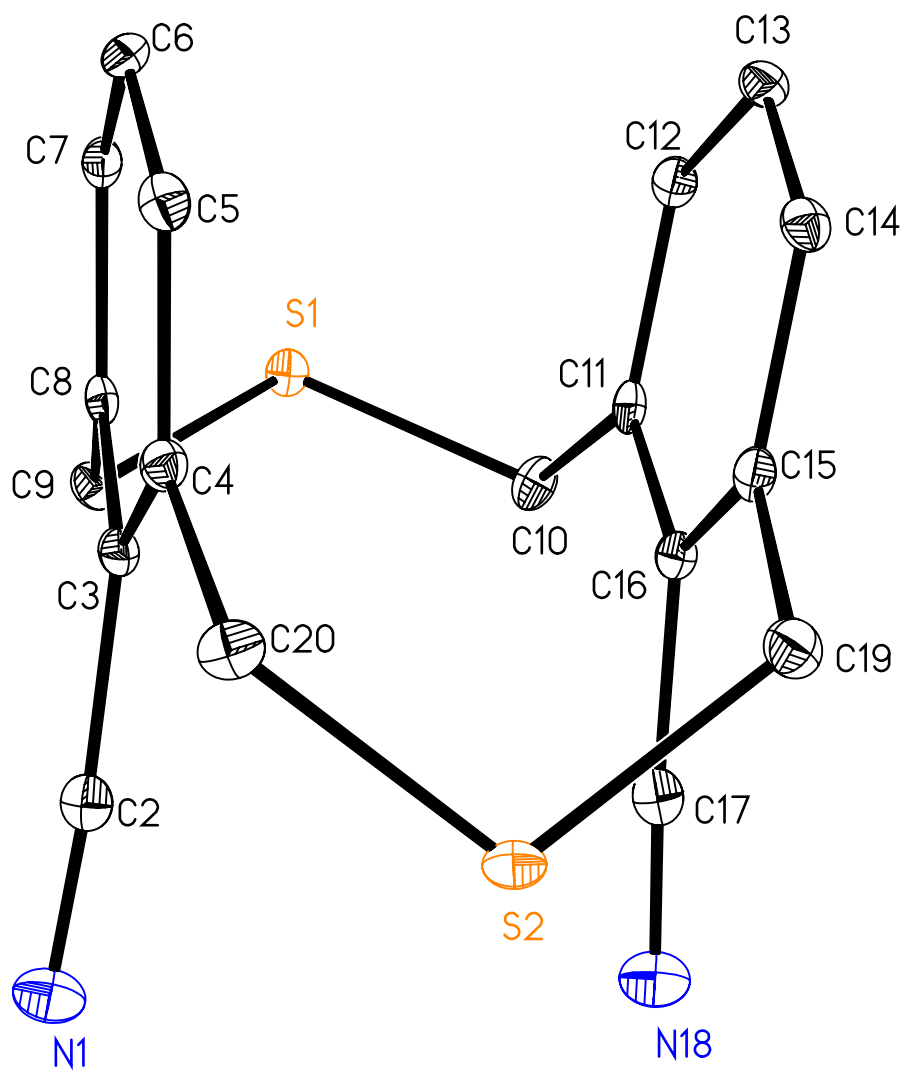


Table A. 6 Crystal data and structure refinement for 108 (C₁₈ H₁₄ N₂ S₂)

Identification code	bt908t	
Empirical formula	C ₁₈ H ₁₄ N ₂ S ₂	
Formula weight	322.43	
Temperature	89(2) K	
Wavelength	0.71073 Å	
Crystal system	Monoclinic	
Space group	P2(1)/n	
Unit cell dimensions	a = 8.653(2) Å	α = 90°.
	b = 14.262(4) Å	β = 100.058(4)°.
	c = 11.980(3) Å	γ = 90°.
Volume	1455.7(6) Å ³	
Z	4	
Density (calculated)	1.471 Mg/m ³	
Absorption coefficient	0.362 mm ⁻¹	
F(000)	672	
Crystal size	0.55 x 0.21 x 0.12 mm ³	
Crystal color and habit	colorlessblock	
Diffractometer	Bruker/Siemens SMART APEX	
Theta range for data collection	2.24 to 25.25°.	
Index ranges	-10 ≤ h ≤ 10, 0 ≤ k ≤ 17, 0 ≤ l ≤ 14	
Reflections collected	34520	
Independent reflections	3182 [R(int) = 0.0000]	
Completeness to theta = 25.25°	100.0%	
Absorption correction	Semi-empirical from equivalents	
Max. and min. transmission	0.9578 and 0.8256	
Solution method	Bruker, 2003; XS, SHELXTL v. 6.14	
Refinement method	Full-matrix least-squares on F ²	
Data / restraints / parameters	3182 / 0 / 200	
Goodness-of-fit on F ²	1.083	
Final R indices [I > 2σ(I)]	R1 = 0.0332, wR2 = 0.0831	
R indices (all data)	R1 = 0.0389, wR2 = 0.0851	
Largest diff. peak and hole	0.344 and -0.266 e.Å ⁻³	

Table A. 7 Atomic coordinates ($\times 10^4$) and equivalent isotropic displacement parameters ($\text{\AA}^2 \times 10^3$) for 108 (bt 908t)

	x	y	z	U(eq)
C(2)	8843(2)	2107(1)	3950(2)	14(1)
C(3)	7771(2)	2734(1)	4374(1)	12(1)
C(4)	7985(2)	3705(1)	4302(2)	12(1)
C(5)	7076(2)	4285(1)	4838(1)	13(1)
C(6)	5955(2)	3912(1)	5413(2)	14(1)
C(7)	5682(2)	2967(1)	5406(2)	13(1)
C(8)	6569(2)	2356(1)	4874(1)	11(1)
C(9)	6185(2)	1326(1)	4810(2)	14(1)
C(10)	3917(2)	1387(1)	2764(2)	16(1)
C(11)	4044(2)	2418(1)	2541(1)	13(1)
C(12)	2984(2)	3032(1)	2891(2)	14(1)
C(13)	3121(2)	3980(1)	2748(2)	15(1)
C(14)	4357(2)	4343(1)	2290(1)	13(1)
C(15)	5445(2)	3757(1)	1938(2)	13(1)
C(16)	5226(2)	2786(1)	2014(2)	13(1)
C(17)	6193(2)	2146(1)	1508(2)	16(1)
C(19)	6810(2)	4185(1)	1496(2)	17(1)
C(20)	9096(2)	4123(1)	3616(2)	16(1)
N(1)	9733(2)	1608(1)	3671(1)	21(1)
N(18)	6859(2)	1614(1)	1063(1)	22(1)
S(1)	4136(1)	1079(1)	4255(1)	13(1)
S(2)	8771(1)	3774(1)	2126(1)	15(1)

Table A. 8 Bond lengths [\AA] and angles [$^\circ$] for 108 (bt 908t)

C(2)-N(1)	1.140(2)	C(4)-C(20)	1.494(2)
C(2)-C(3)	1.443(2)	C(5)-C(6)	1.389(2)
C(3)-C(8)	1.395(2)	C(5)-H(5)	0.9500
C(3)-C(4)	1.402(2)	C(6)-C(7)	1.368(2)
C(4)-C(5)	1.375(2)	C(6)-H(6)	0.9500

C(7)-C(8)	1.387(2)	C(4)-C(5)-C(6)	120.46(16)
C(7)-H(7)	0.9500	C(4)-C(5)-H(5)	119.8
C(8)-C(9)	1.505(2)	C(6)-C(5)-H(5)	119.8
C(9)-S(1)	1.8165(18)	C(7)-C(6)-C(5)	120.60(16)
C(9)-H(9A)	0.9900	C(7)-C(6)-H(6)	119.7
C(9)-H(9B)	0.9900	C(5)-C(6)-H(6)	119.7
C(10)-C(11)	1.502(2)	C(6)-C(7)-C(8)	120.80(16)
C(10)-S(1)	1.8162(19)	C(6)-C(7)-H(7)	119.6
C(10)-H(10A)	0.9900	C(8)-C(7)-H(7)	119.6
C(10)-H(10B)	0.9900	C(7)-C(8)-C(3)	117.95(16)
C(11)-C(12)	1.385(2)	C(7)-C(8)-C(9)	120.10(15)
C(11)-C(16)	1.395(2)	C(3)-C(8)-C(9)	121.91(15)
C(12)-C(13)	1.371(2)	C(8)-C(9)-S(1)	113.61(12)
C(12)-H(12)	0.9500	C(8)-C(9)-H(9A)	108.8
C(13)-C(14)	1.385(2)	S(1)-C(9)-H(9A)	108.8
C(13)-H(13)	0.9500	C(8)-C(9)-H(9B)	108.8
C(14)-C(15)	1.379(2)	S(1)-C(9)-H(9B)	108.8
C(14)-H(14)	0.9500	H(9A)-C(9)-H(9B)	107.7
C(15)-C(16)	1.402(2)	C(11)-C(10)-S(1)	114.39(12)
C(15)-C(19)	1.506(2)	C(11)-C(10)-H(10A)	108.7
C(16)-C(17)	1.442(2)	S(1)-C(10)-H(10A)	108.7
C(17)-N(18)	1.141(2)	C(11)-C(10)-H(10B)	108.7
C(19)-S(2)	1.8292(19)	S(1)-C(10)-H(10B)	108.7
C(19)-H(19A)	0.9900	H(10A)-C(10)-H(10B)	107.6
C(19)-H(19B)	0.9900	C(12)-C(11)-C(16)	118.37(16)
C(20)-S(2)	1.8279(18)	C(12)-C(11)-C(10)	119.51(16)
C(20)-H(20A)	0.9900	C(16)-C(11)-C(10)	122.09(16)
C(20)-H(20B)	0.9900	C(13)-C(12)-C(11)	120.63(17)
		C(13)-C(12)-H(12)	119.7
N(1)-C(2)-C(3)	176.4(2)	C(11)-C(12)-H(12)	119.7
C(8)-C(3)-C(4)	121.58(16)	C(12)-C(13)-C(14)	120.56(17)
C(8)-C(3)-C(2)	119.05(15)	C(12)-C(13)-H(13)	119.7
C(4)-C(3)-C(2)	119.35(15)	C(14)-C(13)-H(13)	119.7
C(5)-C(4)-C(3)	118.21(16)	C(15)-C(14)-C(13)	120.64(16)
C(5)-C(4)-C(20)	119.51(16)	C(15)-C(14)-H(14)	119.7
C(3)-C(4)-C(20)	122.20(15)	C(13)-C(14)-H(14)	119.7

C(14)-C(15)-C(16)	118.14(16)	S(2)-C(19)-H(19B)	108.1
C(14)-C(15)-C(19)	118.77(16)	H(19A)-C(19)-H(19B)	107.3
C(16)-C(15)-C(19)	123.09(16)	C(4)-C(20)-S(2)	115.12(12)
C(11)-C(16)-C(15)	121.28(16)	C(4)-C(20)-H(20A)	108.5
C(11)-C(16)-C(17)	118.46(16)	S(2)-C(20)-H(20A)	108.5
C(15)-C(16)-C(17)	120.22(16)	C(4)-C(20)-H(20B)	108.5
N(18)-C(17)-C(16)	175.00(19)	S(2)-C(20)-H(20B)	108.5
C(15)-C(19)-S(2)	116.93(13)	H(20A)-C(20)-H(20B)	107.5
C(15)-C(19)-H(19A)	108.1	C(10)-S(1)-C(9)	103.90(8)
S(2)-C(19)-H(19A)	108.1	C(20)-S(2)-C(19)	106.82(9)
C(15)-C(19)-H(19B)	108.1		

Table A. 9 Anisotropic displacement parameters ($\text{\AA}^2 \times 10^3$) for 108 (bt 908t)

	U11	U22	U33	U23	U13	U12
C(2)	14(1)	13(1)	16(1)	0(1)	2(1)	-4(1)
C(3)	10(1)	14(1)	11(1)	-1(1)	-1(1)	0(1)
C(4)	11(1)	14(1)	11(1)	-1(1)	1(1)	-1(1)
C(5)	13(1)	11(1)	15(1)	0(1)	0(1)	-2(1)
C(6)	14(1)	17(1)	10(1)	-4(1)	2(1)	2(1)
C(7)	10(1)	18(1)	10(1)	2(1)	1(1)	-1(1)
C(8)	10(1)	13(1)	10(1)	1(1)	-3(1)	0(1)
C(9)	11(1)	14(1)	17(1)	3(1)	2(1)	0(1)
C(10)	20(1)	15(1)	12(1)	-1(1)	2(1)	-5(1)
C(11)	14(1)	15(1)	8(1)	1(1)	-3(1)	-2(1)
C(12)	11(1)	19(1)	13(1)	2(1)	2(1)	-2(1)
C(13)	11(1)	18(1)	15(1)	-1(1)	1(1)	3(1)
C(14)	15(1)	10(1)	15(1)	1(1)	1(1)	0(1)
C(15)	13(1)	16(1)	10(1)	2(1)	1(1)	-1(1)
C(16)	13(1)	15(1)	10(1)	-1(1)	0(1)	1(1)
C(17)	14(1)	14(1)	18(1)	2(1)	1(1)	-4(1)
C(19)	16(1)	17(1)	18(1)	5(1)	5(1)	1(1)
C(20)	16(1)	15(1)	17(1)	-2(1)	5(1)	-3(1)

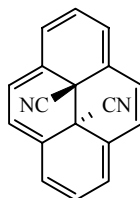
N(1)	20(1)	14(1)	29(1)	-1(1)	9(1)	0(1)
N(18)	22(1)	17(1)	29(1)	-4(1)	8(1)	-2(1)
S(1)	13(1)	13(1)	14(1)	2(1)	2(1)	-3(1)
S(2)	13(1)	16(1)	17(1)	-1(1)	6(1)	0(1)

Table A. 10 Hydrogen coordinates ($\times 10^4$) and isotropic displacement parameters ($\text{\AA}^2 \times 10^3$) for 108 (bt 908t)

	x	y	z	U(eq)
H(5)	7215	4945	4815	16
H(6)	5373	4317	5813	17
H(7)	4876	2726	5771	15
H(9A)	6458	1052	5578	17
H(9B)	6844	1015	4321	17
H(10A)	4732	1053	2432	19
H(10B)	2881	1162	2371	19
H(12)	2154	2794	3233	17
H(13)	2363	4392	2965	18
H(14)	4456	5003	2217	16
H(19A)	6775	4872	1605	20
H(19B)	6659	4068	669	20
H(20A)	10178	3945	3967	19
H(20B)	9020	4814	3655	19

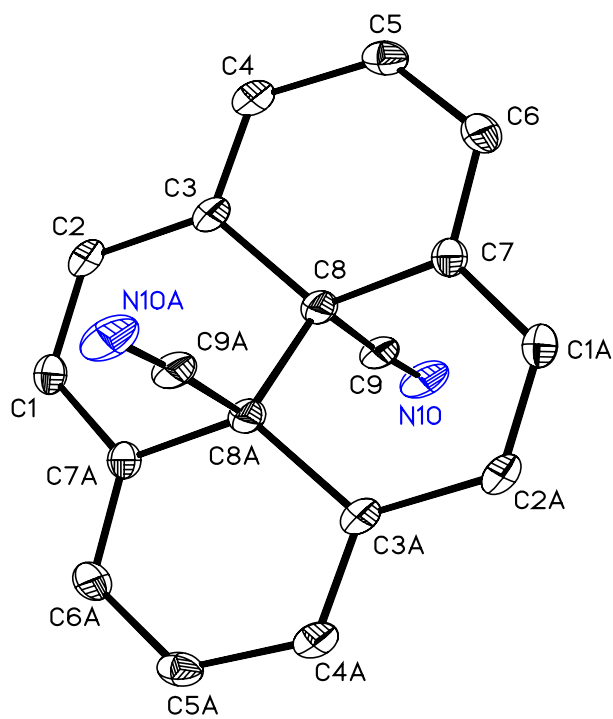
Single-Crystal X-ray Diffraction Laboratory
University of Idaho

X-ray structure report for dicyano DHP 86



86

Brendan Twamley



Project name : bt953

8-15-06

Experimental:

Crystals of compound **1** were removed from the flask, a suitable crystal was selected, attached to a glass fiber and data were collected at 90(2) K using a Bruker/Siemens SMART APEX instrument (Mo K α radiation, $\lambda = 0.71073$ Å) equipped with a Cryocool NeverIce low temperature device. Data were measured using omega scans of 0.3 ° per frame for 50 seconds, and a partial sphere of data was collected. A total of 953 frames were collected with a final resolution of 0.83 Å. Cell parameters were retrieved using SMART¹⁰ software and refined using SAINTPlus¹¹ on all observed reflections. Data reduction and correction for Lp and decay were performed using the SAINTPlus software. Absorption corrections were applied using SADABS.¹² The structure was solved by direct methods and refined by least squares method on F² using the SHELXTL program package.¹³ The structure was solved in the space group Pbc_a (# 61) by analysis of systematic absences. All non-hydrogen atoms were refined anisotropically. No decomposition was observed during data collection. Details of the data collection and refinement are given in Table 1. Further details are provided in the Supporting Information.

Acknowledgement

The Bruker (Siemens) SMART APEX diffraction facility was established at the University of Idaho with the assistance of the NSF-EPSCoR program and the M. J. Murdock Charitable Trust, Vancouver, WA, USA.

¹⁰ SMART: v.5.630, Bruker Molecular Analysis Research Tool, Bruker AXS, Madison, WI, **2001**.

¹¹ SAINTPlus: v. 7.23a, Data Reduction and Correction Program, Bruker AXS, Madison, WI, **2004**.

¹² SADABS: v.2004/1, an empirical absorption correction program, Bruker AXS Inc., Madison, WI, **2004**.

¹³ SHELXTL: v. 6.14, Structure Determination Software Suite, Sheldrick, G.M., Bruker AXS Inc., Madison, WI, **2004**.

Table A. 11 Crystal data and structure refinement for DHP 86 (C₁₈ H₁₀ N₂)

Identification code	bt953	
Empirical formula	C ₁₈ H ₁₀ N ₂	
Formula weight	254.28	
Temperature	90(2) K	
Wavelength	0.71073 Å	
Crystal system	Orthorhombic	
Space group	Pbca	
Unit cell dimensions	a = 7.8663(12) Å	α = 90°.
	b = 11.7838(18) Å	β = 90°.
	c = 13.402(2) Å	γ = 90°.
Volume	1242.3(3) Å ³	
Z	4	
Density (calculated)	1.360 Mg/m ³	
Absorption coefficient	0.081 mm ⁻¹	
F(000)	528	
Crystal size	0.41 x 0.38 x 0.08 mm ³	
Crystal color and habit	greenplate	
Diffractometer	Bruker/Siemens SMART APEX	
Theta range for data collection	3.04 to 25.23°.	
Index ranges	-6<=h<=9, -14<=k<=14, -9<=l<=16	
Reflections collected	7085	
Independent reflections	1126 [R(int) = 0.0378]	
Completeness to theta = 25.23°	100.0%	
Absorption correction	Semi-empirical from equivalents	
Max. and min. transmission	0.993 and 0.963	
Solution method	Bruker, 2003; XS, SHELXTL v. 6.14	
Refinement method	Full-matrix least-squares on F ²	
Data / restraints / parameters	1126 / 0 / 91	
Goodness-of-fit on F ²	1.043	
Final R indices [I>2sigma(I)]	R1 = 0.0450, wR2 = 0.1103	
R indices (all data)	R1 = 0.0579, wR2 = 0.1182	
Largest diff. peak and hole	0.295 and -0.226 e.Å ⁻³	

Table A. 12 Atomic coordinates ($\times 10^4$) and equivalent isotropic displacement parameters ($\text{\AA}^2 \times 10^3$) for 86 (bt 953).

	x	y	z	U(eq)
C(1)	-2339(2)	8555(2)	356(1)	25(1)
C(2)	-957(2)	8213(2)	927(1)	24(1)
C(3)	552(2)	8839(2)	976(1)	22(1)
C(4)	1974(2)	8545(2)	1521(1)	25(1)
C(5)	3439(3)	9215(2)	1510(1)	27(1)
C(6)	3589(2)	10166(2)	909(1)	26(1)
C(7)	2266(2)	10541(2)	314(1)	23(1)
C(8)	522(2)	10008(2)	481(1)	22(1)
C(9)	-381(2)	10795(2)	1199(1)	25(1)
N(10)	-993(2)	11388(1)	1771(1)	35(1)

Table A. 13 Bond lengths [\AA] and angles [$^\circ$] for 86 (bt 953)

C(1)-C(2)	1.389(3)	C(8)-C(8)#1	1.529(4)
C(1)-C(7)#1	1.394(3)	C(9)-N(10)	1.144(2)
C(1)-H(1)	0.9500		
C(2)-C(3)	1.399(3)	C(2)-C(1)-C(7)#1	122.96(18)
C(2)-H(2)	0.9500	C(2)-C(1)-H(1)	118.5
C(3)-C(4)	1.380(3)	C(7)#1-C(1)-H(1)	118.5
C(3)-C(8)	1.529(3)	C(1)-C(2)-C(3)	122.45(17)
C(4)-C(5)	1.398(3)	C(1)-C(2)-H(2)	118.8
C(4)-H(4)	0.9500	C(3)-C(2)-H(2)	118.8
C(5)-C(6)	1.385(3)	C(4)-C(3)-C(2)	125.42(17)
C(5)-H(5)	0.9500	C(4)-C(3)-C(8)	117.93(16)
C(6)-C(7)	1.384(3)	C(2)-C(3)-C(8)	116.23(16)
C(6)-H(6)	0.9500	C(3)-C(4)-C(5)	121.38(18)
C(7)-C(1)#1	1.394(3)	C(3)-C(4)-H(4)	119.3
C(7)-C(8)	1.525(3)	C(5)-C(4)-H(4)	119.3
C(8)-C(9)	1.513(3)	C(6)-C(5)-C(4)	122.27(18)

C(6)-C(5)-H(5)	118.9
C(4)-C(5)-H(5)	118.9
C(7)-C(6)-C(5)	121.95(18)
C(7)-C(6)-H(6)	119.0
C(5)-C(6)-H(6)	119.0
C(6)-C(7)-C(1)#1	125.73(18)
C(6)-C(7)-C(8)	117.42(17)
C(1)#1-C(7)-C(8)	116.51(17)
C(9)-C(8)-C(7)	105.25(15)
C(9)-C(8)-C(8)#1	106.98(18)
C(7)-C(8)-C(8)#1	111.39(18)
C(9)-C(8)-C(3)	106.47(14)
C(7)-C(8)-C(3)	114.90(15)
C(8)#1-C(8)-C(3)	111.25(19)
N(10)-C(9)-C(8)	176.6(2)

Symmetry transformations used to generate
equivalent atoms:

#1 -x,-y+2,-z

Table A. 14 Anisotropic displacement parameters ($\text{\AA}^2 \times 10^3$) for 86 bt953.

	U11	U22	U33	U23	U13	U12
C(1)	26(1)	22(1)	26(1)	-3(1)	7(1)	-7(1)
C(2)	34(1)	15(1)	21(1)	0(1)	8(1)	0(1)
C(3)	30(1)	17(1)	18(1)	0(1)	6(1)	2(1)
C(4)	35(1)	22(1)	18(1)	1(1)	4(1)	4(1)
C(5)	29(1)	31(1)	21(1)	-3(1)	-2(1)	4(1)
C(6)	24(1)	30(1)	24(1)	-6(1)	2(1)	-3(1)
C(7)	26(1)	20(1)	22(1)	-5(1)	2(1)	-3(1)
C(8)	25(1)	20(1)	21(1)	1(1)	1(1)	-1(1)
C(9)	31(1)	21(1)	23(1)	3(1)	2(1)	2(1)
N(10)	51(1)	26(1)	27(1)	0(1)	7(1)	11(1)

Table A. 15 Hydrogen coordinates ($\times 10^4$) and isotropic displacement parameters ($\text{\AA}^2 \times 10^3$) for 86 (bt 953).

	x	y	z	U(eq)
H(1)	-3381	8156	426	30
H(2)	-1040	7528	1297	28
H(4)	1956	7872	1911	30
H(5)	4365	9011	1928	32
H(6)	4632	10573	905	31

Table A. 16 Hydrogen bonds for 86 (bt953) [\AA and $^\circ$].

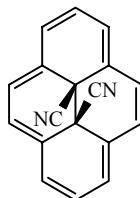
D-H...A	d(D-H)	d(H...A)	d(D...A)	$\angle(\text{DHA})$
C(4)-H(4)...N(10)#2	0.95	2.60	3.507(3)	160.1

Symmetry transformations used to generate equivalent atoms:

#1 $-x, -y+2, -z$ #2 $-x, y-1/2, -z+1/2$

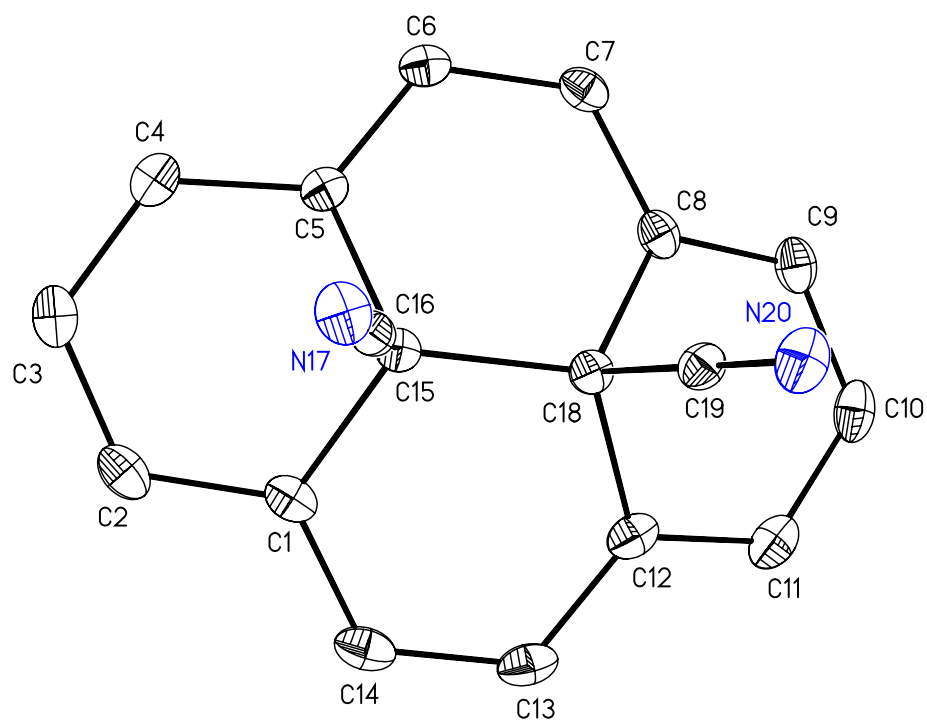
Single-Crystal X-ray Diffraction Laboratory
University of Idaho

X-ray structure report for *cis*-dicyano DHP 117



117

Brendan Twamley



Project name : Bt1105

5-9-07

Experimental:

Crystals of compound **1** were removed from the flask, a suitable crystal was selected, attached to a glass fiber and data were collected at 90(2) K using a Bruker/Siemens SMART APEX instrument (Mo K α radiation, $\lambda = 0.71073 \text{ \AA}$) equipped with a Cryocool NeverIce low temperature device. Data were measured using omega scans 0.3° per frame for 30 seconds, and a full sphere of data was collected. A total of 2400 frames were collected with a final resolution of 0.83 \AA . Cell parameters were retrieved using SMART¹⁴ software and refined using SAINTPlus¹⁵ on all observed reflections. Data reduction and correction for Lp and decay were performed using the SAINTPlus software. Absorption corrections were applied using SADABS.¹⁶ The structure was solved by direct methods and refined by least squares method on F^2 using the SHELXTL program package.¹⁷ The structure was solved in the space group Pbc a (# 61) by analysis of systematic absences. All non-hydrogen atoms were refined anisotropically. No decomposition was observed during data collection. Details of the data collection and refinement are given in Table 1. Further details are provided in the Supporting Information.

Acknowledgement

The Bruker (Siemens) SMART APEX diffraction facility was established at the University of Idaho with the assistance of the NSF-EPSCoR program and the M. J. Murdock Charitable Trust, Vancouver, WA, USA.

¹⁴ SMART: v. 5.632, Bruker AXS, Madison, WI, **2005**.

¹⁵ SAINTPlus: v. 7.23a, Data Reduction and Correction Program, Bruker AXS, Madison, WI, **2004**.

¹⁶ SADABS: v.2004/1, an empirical absorption correction program, Bruker AXS Inc., Madison, WI, **2004**.

¹⁷ SHELXTL: v. 6.14, Structure Determination Software Suite, Sheldrick, G.M., Bruker AXS Inc., Madison, WI, **2004**.

Table A. 17 Crystal data and structure refinement for 117 (C₁₈ H₁₀ N₂).

Identification code	bt1105	
Empirical formula	C ₁₈ H ₁₀ N ₂	
Formula weight	254.28	
Temperature	90(2) K	
Wavelength	0.71073 Å	
Crystal system	Orthorhombic	
Space group	Pbca	
Unit cell dimensions	a = 13.0508(6) Å	α = 90°.
	b = 11.7608(6) Å	β = 90°.
	c = 16.0871(8) Å	γ = 90°.
Volume	2469.2(2) Å ³	
Z	8	
Density (calculated)	1.368 Mg/m ³	
Absorption coefficient	0.082 mm ⁻¹	
F(000)	1056	
Crystal size	0.45 x 0.33 x 0.03 mm ³	
Crystal color and habit	green fragment	
Diffractometer	Bruker/Siemens SMART APEX	
Theta range for data collection	2.53 to 25.25°.	
Index ranges	-15 ≤ h ≤ 15, -14 ≤ k ≤ 14, -19 ≤ l ≤ 19	
Reflections collected	35893	
Independent reflections	2234 [R(int) = 0.0599]	
Completeness to theta = 25.25°	99.9%	
Absorption correction	None	
Max. and min. transmission	0.993 and 0.964	
Solution method	XS, SHELXTL v. 6.14 (Bruker, 2003)	
Refinement method	Full-matrix least-squares on F ²	
Data / restraints / parameters	2234 / 0 / 181	
Goodness-of-fit on F ²	1.036	
Final R indices [I > 2σ(I)]	R1 = 0.0334, wR2 = 0.0861	
R indices (all data)	R1 = 0.0436, wR2 = 0.0906	
Largest diff. peak and hole	0.248 and -0.147 e.Å ⁻³	

Table A. 18 Atomic coordinates ($\times 10^4$) and equivalent isotropic displacement parameters ($\text{\AA}^2 \times 10^3$) for 117 (bt 1105).

	x	y	z	U(eq)
C(1)	-371(1)	6469(1)	2834(1)	25(1)
C(2)	-225(1)	5967(1)	2066(1)	29(1)
C(3)	687(1)	5439(1)	1840(1)	29(1)
C(4)	1460(1)	5279(1)	2418(1)	27(1)
C(5)	1407(1)	5729(1)	3217(1)	22(1)
C(6)	2064(1)	5417(1)	3852(1)	24(1)
C(7)	1860(1)	5632(1)	4683(1)	26(1)
C(8)	983(1)	6187(1)	4951(1)	24(1)
C(9)	650(1)	6188(1)	5773(1)	29(1)
C(10)	-292(1)	6630(1)	5999(1)	32(1)
C(11)	-1001(1)	6974(1)	5405(1)	31(1)
C(12)	-775(1)	7002(1)	4565(1)	26(1)
C(13)	-1502(1)	7125(1)	3940(1)	31(1)
C(14)	-1312(1)	6868(1)	3119(1)	30(1)
C(15)	591(1)	6653(1)	3371(1)	21(1)
C(16)	1080(1)	7670(1)	2984(1)	22(1)
N(17)	1480(1)	8422(1)	2668(1)	28(1)
C(18)	371(1)	6926(1)	4336(1)	22(1)
C(19)	753(1)	8092(1)	4529(1)	22(1)
N(20)	1045(1)	8978(1)	4707(1)	31(1)

Table A. 19 Bond lengths [\AA] and angles [$^\circ$] for 117 (bt 1105)

C(1)-C(2)	1.383(2)		
C(1)-C(14)	1.392(2)	C(2)-C(1)-C(14)	124.00(13)
C(1)-C(15)	1.5385(18)	C(2)-C(1)-C(15)	116.69(12)
C(2)-C(3)	1.390(2)	C(14)-C(1)-C(15)	119.19(12)
C(2)-H(2)	0.9500	C(1)-C(2)-C(3)	122.76(13)
C(3)-C(4)	1.385(2)	C(1)-C(2)-H(2)	118.6
C(3)-H(3)	0.9500	C(3)-C(2)-H(2)	118.6
C(4)-C(5)	1.3924(19)	C(4)-C(3)-C(2)	120.63(13)
C(4)-H(4)	0.9500	C(4)-C(3)-H(3)	119.7
C(5)-C(6)	1.3821(19)	C(2)-C(3)-H(3)	119.7
C(5)-C(15)	1.5411(18)	C(3)-C(4)-C(5)	122.13(13)
C(6)-C(7)	1.386(2)	C(3)-C(4)-H(4)	118.9
C(6)-H(6)	0.9500	C(5)-C(4)-H(4)	118.9
C(7)-C(8)	1.3859(19)	C(6)-C(5)-C(4)	123.38(13)
C(7)-H(7)	0.9500	C(6)-C(5)-C(15)	119.84(12)
C(8)-C(9)	1.391(2)	C(4)-C(5)-C(15)	116.74(12)
C(8)-C(18)	1.5412(19)	C(5)-C(6)-C(7)	122.99(13)
C(9)-C(10)	1.384(2)	C(5)-C(6)-H(6)	118.5
C(9)-H(9)	0.9500	C(7)-C(6)-H(6)	118.5
C(10)-C(11)	1.391(2)	C(8)-C(7)-C(6)	123.01(13)
C(10)-H(10)	0.9500	C(8)-C(7)-H(7)	118.5
C(11)-C(12)	1.385(2)	C(6)-C(7)-H(7)	118.5
C(11)-H(11)	0.9500	C(7)-C(8)-C(9)	123.68(13)
C(12)-C(13)	1.389(2)	C(7)-C(8)-C(18)	119.57(12)
C(12)-C(18)	1.5426(18)	C(9)-C(8)-C(18)	116.58(12)
C(13)-C(14)	1.378(2)	C(10)-C(9)-C(8)	121.90(14)
C(13)-H(13)	0.9500	C(10)-C(9)-H(9)	119.0
C(14)-H(14)	0.9500	C(8)-C(9)-H(9)	119.0
C(15)-C(16)	1.4903(18)	C(9)-C(10)-C(11)	121.32(13)
C(15)-C(18)	1.6116(19)	C(9)-C(10)-H(10)	119.3
C(16)-N(17)	1.1472(17)	C(11)-C(10)-H(10)	119.3
C(18)-C(19)	1.4920(19)	C(12)-C(11)-C(10)	122.42(14)
C(19)-N(20)	1.1462(17)	C(12)-C(11)-H(11)	118.8

C(10)-C(11)-H(11)	118.8
C(11)-C(12)-C(13)	124.27(13)
C(11)-C(12)-C(18)	115.99(13)
C(13)-C(12)-C(18)	119.71(13)
C(14)-C(13)-C(12)	123.17(13)
C(14)-C(13)-H(13)	118.4
C(12)-C(13)-H(13)	118.4
C(13)-C(14)-C(1)	123.28(13)
C(13)-C(14)-H(14)	118.4
C(1)-C(14)-H(14)	118.4
C(16)-C(15)-C(1)	103.20(11)
C(16)-C(15)-C(5)	101.76(10)
C(1)-C(15)-C(5)	112.00(11)
C(16)-C(15)-C(18)	108.57(10)
C(1)-C(15)-C(18)	114.98(11)
C(5)-C(15)-C(18)	114.69(11)
N(17)-C(16)-C(15)	177.16(14)
C(19)-C(18)-C(8)	102.17(10)
C(19)-C(18)-C(12)	102.76(11)
C(8)-C(18)-C(12)	112.48(11)
C(19)-C(18)-C(15)	108.91(11)
C(8)-C(18)-C(15)	114.46(11)
C(12)-C(18)-C(15)	114.51(11)
N(20)-C(19)-C(18)	177.63(14)

Table A. 20 Anisotropic displacement parameters ($\text{\AA}^2 \times 10^3$) for 117 (bt 1105).

	U11	U22	U33	U23	U13	U12
C(1)	24(1)	20(1)	29(1)	5(1)	-6(1)	-4(1)
C(2)	33(1)	25(1)	29(1)	5(1)	-10(1)	-9(1)
C(3)	42(1)	23(1)	23(1)	1(1)	1(1)	-8(1)
C(4)	31(1)	21(1)	29(1)	1(1)	7(1)	-2(1)
C(5)	20(1)	19(1)	26(1)	2(1)	4(1)	-3(1)
C(6)	20(1)	20(1)	32(1)	2(1)	1(1)	-1(1)
C(7)	25(1)	22(1)	30(1)	2(1)	-7(1)	-2(1)
C(8)	28(1)	20(1)	24(1)	-1(1)	-4(1)	-5(1)
C(9)	40(1)	23(1)	25(1)	-2(1)	-2(1)	-6(1)
C(10)	44(1)	24(1)	27(1)	-5(1)	9(1)	-12(1)
C(11)	30(1)	24(1)	40(1)	-6(1)	12(1)	-6(1)
C(12)	23(1)	18(1)	37(1)	-2(1)	6(1)	-2(1)
C(13)	20(1)	25(1)	47(1)	1(1)	3(1)	1(1)
C(14)	23(1)	26(1)	42(1)	6(1)	-8(1)	-2(1)
C(15)	20(1)	19(1)	24(1)	1(1)	-1(1)	-2(1)
C(16)	21(1)	22(1)	22(1)	-2(1)	-3(1)	1(1)
N(17)	32(1)	24(1)	26(1)	1(1)	-1(1)	-5(1)
C(18)	21(1)	19(1)	24(1)	-1(1)	0(1)	-2(1)
C(19)	20(1)	24(1)	23(1)	0(1)	4(1)	-1(1)
N(20)	35(1)	26(1)	31(1)	-3(1)	7(1)	-7(1)

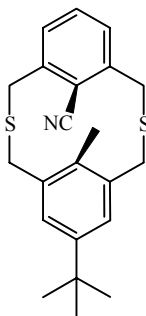
Table A. 21 Hydrogen coordinates ($\times 10^4$) and isotropic displacement parameters ($\text{\AA}^2 \times 10^3$) for 117 (bt 1105).

	x	y	z	U(eq)
H(2)	-771	5984	1675	35
H(3)	780	5185	1285	35
H(4)	2046	4848	2264	32
H(6)	2683	5039	3712	29
H(7)	2343	5388	5087	31
H(9)	1081	5875	6190	35
H(10)	-457	6700	6572	38
H(11)	-1665	7199	5583	37
H(13)	-2162	7400	4087	37
H(14)	-1849	6969	2728	36

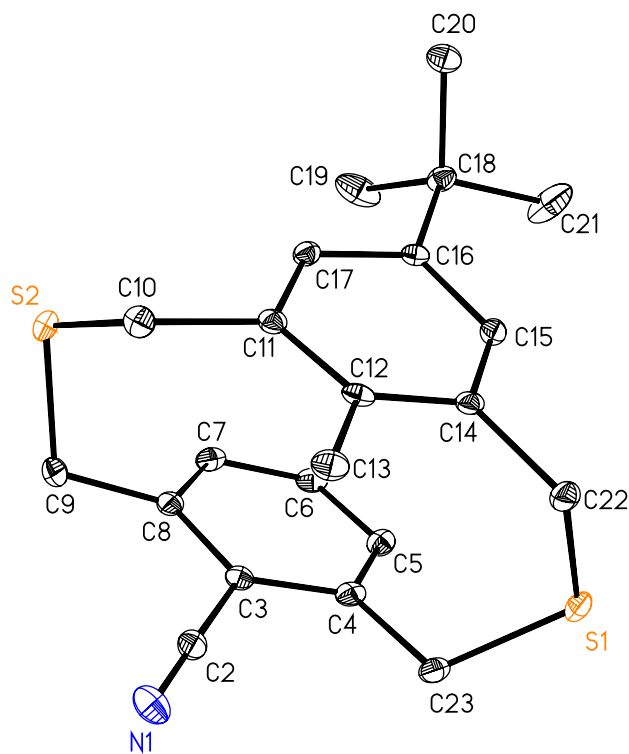
Single-Crystal X-ray Diffraction Laboratory
University of Idaho

X-ray Structure Report for *syn*-thiacyclophane **130**

Brendan Twamley



130



Project name : bt907t

5-30-06

Experimental:

Crystals of compound **1** were removed from the flask, a suitable crystal was selected, attached to a MiTeGen fiber and data for **1** were collected at 89(2) K using a Bruker/Siemens SMART APEX instrument (Mo K α radiation, $\lambda = 0.71073$ Å) equipped with a Cryocool NeverIce low temperature device. Data were measured using omega scans of 0.3 ° per frame for 30 seconds, and a full sphere of data was collected. A total of 2400 frames were collected with a final resolution of 0.83 Å. Cell parameters were retrieved using SMART¹⁸ software. The data were rotationally twinned and were deconvoluted using CELL_NOW¹⁹ giving a two component twin relationship: 180° rotation about the reciprocal axis 0.001, -0.003, 1.000, with a refined twinning ratio of 0.447(1). The matrix used to relate the second orientation to the first domain is:

-0.999 0.000 0.001

-0.001 -1.000 -0.006

0.909 0.002 0.999

Each cell component was refined using SAINTPlus²⁰ on all observed reflections. Data reduction and correction for Lp and decay were performed using the SAINTPlus software. Absorption corrections were applied using TWINABS.²¹ The structure was solved by direct methods and refined by least squares method on F² using the SHELXTL program package.²² The structure was solved in the space group P2(1)/c (# 14) by analysis of systematic absences. All non-hydrogen atoms were refined anisotropically.

¹⁸ SMART: v.5.630, Bruker Molecular Analysis Research Tool, Bruker AXS, Madison, WI, **2002**.

¹⁹ CELL_NOW: Sheldrick, G.M., **2002**.

²⁰ SAINTPlus: v. 6.45a, Data Reduction and Correction Program, Bruker AXS, Madison, WI, **2001**.

²¹ TWINABS: v.1.05, an empirical absorption correction program, Sheldrick, G.M., Bruker AXS Inc., Madison, WI, **2002**.

²² SHELXTL: v. 6.14, Structure Determination Software Suite, Sheldrick, G.M., Bruker AXS Inc., Madison, WI, **2003**.

No decomposition was observed during data collection. Details of the data collection and refinement are given in Table 1. Further details are provided in the Supporting Information.

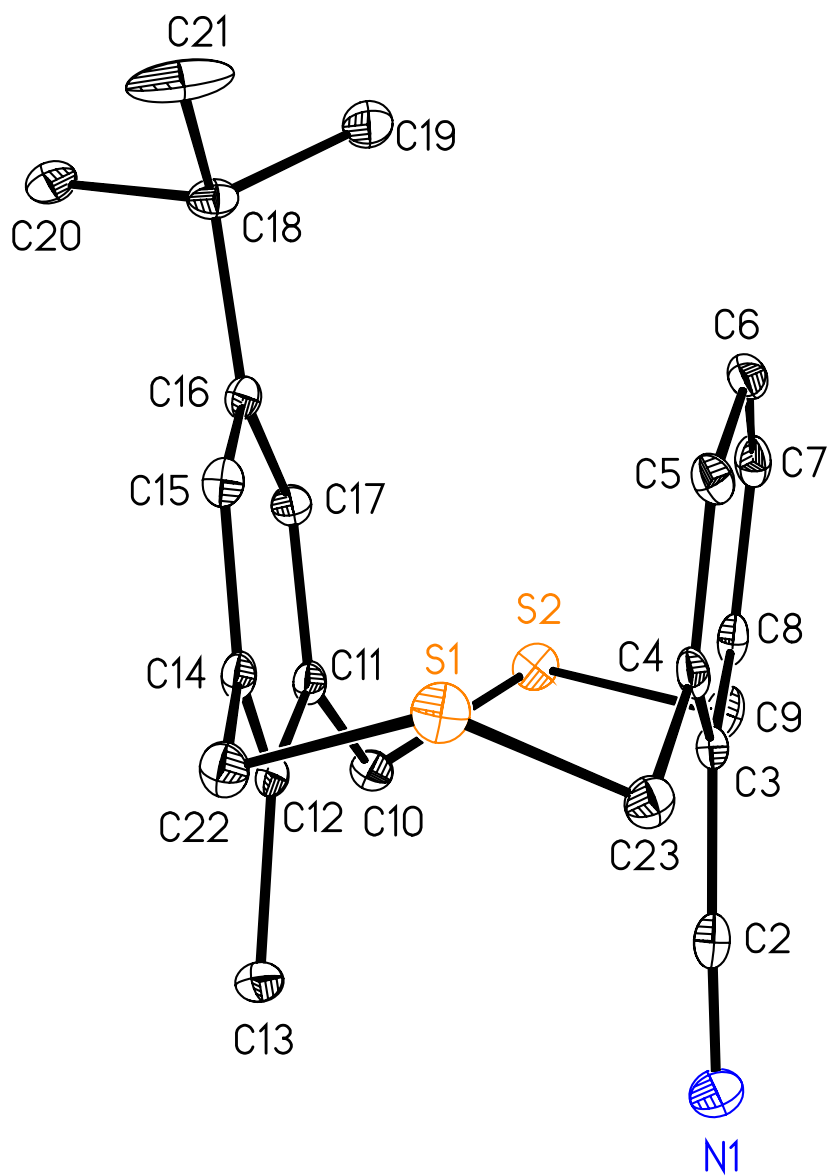


Table A. 22 Crystal data and structure refinement for 130 (C₂₂ H₂₅ N S₂).

Identification code	bt907t	
Empirical formula	C ₂₂ H ₂₅ N S ₂	
Formula weight	367.55	
Temperature	89(2) K	
Wavelength	0.71073 Å	
Crystal system	Monoclinic	
Space group	P2(1)/c	
Unit cell dimensions	a = 7.1512(13) Å	α = 90°.
	b = 15.903(3) Å	β = 100.734(3)°.
	c = 17.304(3) Å	γ = 90°.
Volume	1933.5(6) Å ³	
Z	4	
Density (calculated)	1.263 Mg/m ³	
Absorption coefficient	0.280 mm ⁻¹	
F(000)	784	
Crystal size	0.33 x 0.13 x 0.08 mm ³	
Crystal color and habit	colorless plate	
Diffractometer	Bruker/Siemens SMART APEX	
Theta range for data collection	1.75 to 25.25°.	
Index ranges	-8 ≤ h ≤ 8, 0 ≤ k ≤ 19, 0 ≤ l ≤ 20	
Reflections collected	40892	
Independent reflections	5056 [R(int) = 0.0000]	
Completeness to theta = 25.25°	99.8%	
Absorption correction	Semi-empirical from equivalents	
Max. and min. transmission	0.9780 and 0.9133	
Solution method	Bruker, 2003; XS, SHELXTL v. 6.14	
Refinement method	Full-matrix least-squares on F ²	
Data / restraints / parameters	5056 / 6 / 231	
Goodness-of-fit on F ²	0.997	
Final R indices [I > 2σ(I)]	R1 = 0.0411, wR2 = 0.1122	
R indices (all data)	R1 = 0.0500, wR2 = 0.1155	
Largest diff. peak and hole	0.332 and -0.236 e.Å ⁻³	

Table A. 23 Atomic coordinates ($\times 10^4$) and equivalent isotropic displacement parameters ($\text{\AA}^2 \times 10^3$) for 130 (bt 907t).

	x	y	z	U(eq)
C(2)	1296(3)	-637(1)	3969(1)	20(1)
C(3)	534(3)	-277(1)	3207(1)	16(1)
C(4)	423(3)	-772(1)	2531(1)	18(1)
C(5)	-482(3)	-437(1)	1823(1)	19(1)
C(6)	-1239(3)	364(1)	1780(1)	20(1)
C(7)	-1017(3)	864(1)	2447(1)	20(1)
C(8)	-99(3)	560(1)	3167(1)	19(1)
C(9)	288(3)	1126(1)	3873(1)	23(1)
C(10)	4288(3)	1260(1)	3840(1)	21(1)
C(11)	4402(3)	837(1)	3063(1)	16(1)
C(12)	4967(3)	-4(1)	3025(1)	16(1)
C(13)	5886(3)	-477(1)	3765(1)	22(1)
C(14)	4711(3)	-382(1)	2284(1)	17(1)
C(15)	4146(3)	91(1)	1606(1)	18(1)
C(16)	3787(3)	948(1)	1630(1)	16(1)
C(17)	3871(3)	1294(1)	2374(1)	16(1)
C(18)	3323(3)	1505(1)	899(1)	20(1)
C(19)	1525(3)	2024(2)	910(2)	38(1)
C(20)	4985(3)	2107(1)	891(1)	25(1)
C(21)	3041(5)	993(2)	137(1)	48(1)
C(22)	4949(3)	-1317(1)	2185(1)	22(1)
C(23)	1264(3)	-1648(1)	2570(1)	21(1)
N(1)	1853(3)	-934(1)	4571(1)	29(1)
S(1)	2711(1)	-1870(1)	1829(1)	22(1)
S(2)	2160(1)	1899(1)	3833(1)	21(1)

Table A. 24 Bond lengths [\AA] and angles [$^\circ$] for 130 (bt 907t)

C(2)-N(1)	1.144(3)	C(17)-H(17)	0.9500
C(2)-C(3)	1.448(3)	C(18)-C(20)	1.529(3)
C(3)-C(4)	1.400(3)	C(18)-C(21)	1.530(3)
C(3)-C(8)	1.404(3)	C(18)-C(19)	1.531(3)
C(4)-C(5)	1.380(3)	C(19)-H(19A)	0.9800
C(4)-C(23)	1.514(3)	C(19)-H(19B)	0.9800
C(5)-C(6)	1.380(3)	C(19)-H(19C)	0.9800
C(5)-H(5)	0.9500	C(20)-H(20A)	0.9800
C(6)-C(7)	1.387(3)	C(20)-H(20B)	0.9800
C(6)-H(6)	0.9500	C(20)-H(20C)	0.9800
C(7)-C(8)	1.383(3)	C(21)-H(21A)	0.9800
C(7)-H(7)	0.9500	C(21)-H(21B)	0.9800
C(8)-C(9)	1.502(3)	C(21)-H(21C)	0.9800
C(9)-S(2)	1.828(2)	C(22)-S(1)	1.830(2)
C(9)-H(9A)	0.9900	C(22)-H(22A)	0.9900
C(9)-H(9B)	0.9900	C(22)-H(22B)	0.9900
C(10)-C(11)	1.520(3)	C(23)-S(1)	1.826(2)
C(10)-S(2)	1.828(2)	C(23)-H(23A)	0.9900
C(10)-H(10A)	0.9900	C(23)-H(23B)	0.9900
C(10)-H(10B)	0.9900		
C(11)-C(17)	1.387(3)	N(1)-C(2)-C(3)	178.1(2)
C(11)-C(12)	1.403(3)	C(4)-C(3)-C(8)	121.57(19)
C(12)-C(14)	1.397(3)	C(4)-C(3)-C(2)	119.50(18)
C(12)-C(13)	1.524(3)	C(8)-C(3)-C(2)	118.93(19)
C(13)-H(13A)	0.9800	C(5)-C(4)-C(3)	117.99(18)
C(13)-H(13B)	0.9800	C(5)-C(4)-C(23)	120.78(19)
C(13)-H(13C)	0.9800	C(3)-C(4)-C(23)	121.24(18)
C(14)-C(15)	1.389(3)	C(6)-C(5)-C(4)	121.2(2)
C(14)-C(22)	1.510(3)	C(6)-C(5)-H(5)	119.4
C(15)-C(16)	1.388(3)	C(4)-C(5)-H(5)	119.4
C(15)-H(15)	0.9500	C(5)-C(6)-C(7)	120.1(2)
C(16)-C(17)	1.390(3)	C(5)-C(6)-H(6)	120.0
C(16)-C(18)	1.530(3)	C(7)-C(6)-H(6)	120.0

C(8)-C(7)-C(6)	120.73(19)	C(14)-C(15)-H(15)	118.9
C(8)-C(7)-H(7)	119.6	C(15)-C(16)-C(17)	116.13(18)
C(6)-C(7)-H(7)	119.6	C(15)-C(16)-C(18)	123.78(18)
C(7)-C(8)-C(3)	118.09(19)	C(17)-C(16)-C(18)	120.09(18)
C(7)-C(8)-C(9)	120.57(19)	C(11)-C(17)-C(16)	123.08(19)
C(3)-C(8)-C(9)	121.27(19)	C(11)-C(17)-H(17)	118.5
C(8)-C(9)-S(2)	113.39(14)	C(16)-C(17)-H(17)	118.5
C(8)-C(9)-H(9A)	108.9	C(20)-C(18)-C(16)	108.77(17)
S(2)-C(9)-H(9A)	108.9	C(20)-C(18)-C(21)	107.59(19)
C(8)-C(9)-H(9B)	108.9	C(16)-C(18)-C(21)	112.23(18)
S(2)-C(9)-H(9B)	108.9	C(20)-C(18)-C(19)	108.57(18)
H(9A)-C(9)-H(9B)	107.7	C(16)-C(18)-C(19)	110.84(17)
C(11)-C(10)-S(2)	114.95(14)	C(21)-C(18)-C(19)	108.7(2)
C(11)-C(10)-H(10A)	108.5	C(18)-C(19)-H(19A)	109.5
S(2)-C(10)-H(10A)	108.5	C(18)-C(19)-H(19B)	109.5
C(11)-C(10)-H(10B)	108.5	H(19A)-C(19)-H(19B)	109.5
S(2)-C(10)-H(10B)	108.5	C(18)-C(19)-H(19C)	109.5
H(10A)-C(10)-H(10B)	107.5	H(19A)-C(19)-H(19C)	109.5
C(17)-C(11)-C(12)	119.63(19)	H(19B)-C(19)-H(19C)	109.5
C(17)-C(11)-C(10)	118.53(18)	C(18)-C(20)-H(20A)	109.5
C(12)-C(11)-C(10)	121.81(18)	C(18)-C(20)-H(20B)	109.5
C(14)-C(12)-C(11)	117.57(18)	H(20A)-C(20)-H(20B)	109.5
C(14)-C(12)-C(13)	121.42(18)	C(18)-C(20)-H(20C)	109.5
C(11)-C(12)-C(13)	120.98(19)	H(20A)-C(20)-H(20C)	109.5
C(12)-C(13)-H(13A)	109.5	H(20B)-C(20)-H(20C)	109.5
C(12)-C(13)-H(13B)	109.5	C(18)-C(21)-H(21A)	109.5
H(13A)-C(13)-H(13B)	109.5	C(18)-C(21)-H(21B)	109.5
C(12)-C(13)-H(13C)	109.5	H(21A)-C(21)-H(21B)	109.5
H(13A)-C(13)-H(13C)	109.5	C(18)-C(21)-H(21C)	109.5
H(13B)-C(13)-H(13C)	109.5	H(21A)-C(21)-H(21C)	109.5
C(15)-C(14)-C(12)	120.72(19)	H(21B)-C(21)-H(21C)	109.5
C(15)-C(14)-C(22)	117.32(19)	C(14)-C(22)-S(1)	113.67(14)
C(12)-C(14)-C(22)	121.91(18)	C(14)-C(22)-H(22A)	108.8
C(16)-C(15)-C(14)	122.13(19)	S(1)-C(22)-H(22A)	108.8
C(16)-C(15)-H(15)	118.9	C(14)-C(22)-H(22B)	108.8
S(1)-C(22)-H(22B)	108.8	C(4)-C(23)-H(23B)	108.6

H(22A)-C(22)-H(22B)	107.7	S(1)-C(23)-H(23B)	108.6
C(4)-C(23)-S(1)	114.72(14)	H(23A)-C(23)-H(23B)	107.6
C(4)-C(23)-H(23A)	108.6	C(23)-S(1)-C(22)	104.20(10)
S(1)-C(23)-H(23A)	108.6	C(10)-S(2)-C(9)	103.96(10)

Table A. 25 Anisotropic displacement parameters ($\text{\AA}^2 \times 10^3$) for 130 (bt907t).

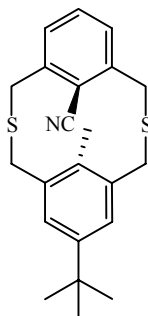
	U11	U22	U33	U23	U13	U12
C(2)	19(1)	21(1)	22(1)	-2(1)	6(1)	-2(1)
C(3)	10(1)	18(1)	19(1)	1(1)	3(1)	-2(1)
C(4)	10(1)	17(1)	27(1)	1(1)	3(1)	-3(1)
C(5)	15(1)	19(1)	23(1)	-2(1)	1(1)	-2(1)
C(6)	14(1)	21(1)	24(1)	4(1)	0(1)	-2(1)
C(7)	14(1)	14(1)	34(1)	2(1)	8(1)	2(1)
C(8)	14(1)	18(1)	27(1)	-2(1)	10(1)	-3(1)
C(9)	24(1)	24(1)	26(1)	-5(1)	14(1)	-2(1)
C(10)	19(1)	23(1)	19(1)	1(1)	2(1)	-1(1)
C(11)	13(1)	17(1)	20(1)	0(1)	5(1)	-2(1)
C(12)	12(1)	18(1)	20(1)	5(1)	4(1)	-2(1)
C(13)	22(1)	21(1)	21(1)	7(1)	3(1)	1(1)
C(14)	13(1)	14(1)	25(1)	2(1)	8(1)	0(1)
C(15)	17(1)	18(1)	20(1)	-2(1)	5(1)	-2(1)
C(16)	14(1)	16(1)	19(1)	2(1)	4(1)	-4(1)
C(17)	17(1)	13(1)	20(1)	1(1)	4(1)	0(1)
C(18)	25(1)	16(1)	17(1)	2(1)	1(1)	-2(1)
C(19)	27(1)	47(2)	39(2)	26(1)	8(1)	7(1)
C(20)	28(1)	23(1)	23(1)	8(1)	5(1)	0(1)
C(21)	100(2)	22(1)	16(1)	2(1)	-8(1)	-11(1)
C(22)	21(1)	15(1)	30(1)	1(1)	8(1)	3(1)
C(23)	21(1)	14(1)	26(1)	2(1)	5(1)	-2(1)
N(1)	29(1)	38(1)	21(1)	4(1)	6(1)	1(1)
S(1)	26(1)	14(1)	26(1)	-5(1)	6(1)	0(1)
S(2)	27(1)	16(1)	22(1)	-6(1)	6(1)	-1(1)

Table A. 26 Hydrogen coordinates ($\times 10^4$) and isotropic displacement parameters ($\text{\AA}^2 \times 10^3$) for 130 (bt 907t).

	x	y	z	U(eq)
H(5)	-585	-764	1358	23
H(6)	-1912	572	1292	24
H(7)	-1501	1422	2409	24
H(9A)	660	777	4351	28
H(9B)	-899	1426	3919	28
H(10A)	5422	1623	3993	25
H(10B)	4341	821	4249	25
H(13A)	4924	-823	3950	32
H(13B)	6419	-74	4175	32
H(13C)	6904	-839	3645	32
H(15)	4000	-180	1109	21
H(17)	3549	1870	2412	20
H(19A)	1271	2385	443	56
H(19B)	1710	2374	1384	56
H(19C)	443	1646	909	56
H(20A)	6120	1785	834	37
H(20B)	5240	2425	1384	37
H(20C)	4661	2498	448	37
H(21A)	1991	596	128	72
H(21B)	4211	683	109	72
H(21C)	2742	1374	-315	72
H(22A)	5554	-1559	2698	26
H(22B)	5819	-1412	1811	26
H(23A)	212	-2061	2512	25
H(23B)	2059	-1730	3098	25

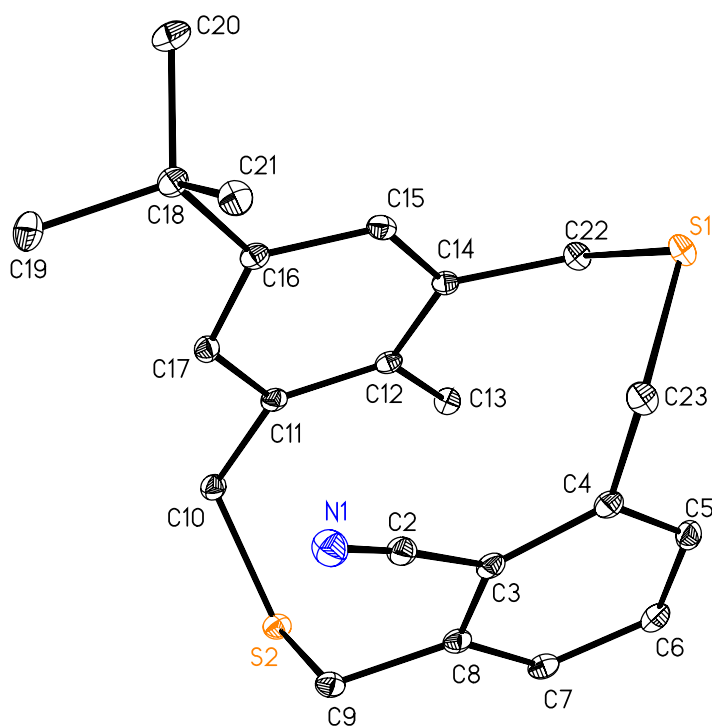
Single-Crystal X-ray Diffraction Laboratory
University of Idaho

X-ray structure report for *anti*-thiacyclophane 131



131

Brendan Twamley



Project name : bt909

5-31-06

Experimental:

Crystals of compound **1** were removed from the flask, a suitable crystal was selected, attached to a MiTeGen fiber and data were collected at 89(2) K using a Bruker/Siemens SMART APEX instrument (Mo K α radiation, $\lambda = 0.71073$ Å) equipped with a Cryocool NeverIce low temperature device. Data were measured using omega scans of 0.3 ° per frame for 10 seconds, and a full sphere of data was collected. A total of 2400 frames were collected with a final resolution of 0.83 Å. Cell parameters were retrieved using SMART²³ software and refined using SAINTPlus²⁴ on all observed reflections. Data reduction and correction for Lp and decay were performed using the SAINTPlus software. Absorption corrections were applied using SADABS.²⁵ The structure was solved by direct methods and refined by least squares method on F² using the SHELXTL program package.²⁶ The structure was solved in the space group C2/c (# 15) by analysis of systematic absences. All non-hydrogen atoms were refined anisotropically. No decomposition was observed during data collection. Details of the data collection and refinement are given in Table 1. Further details are provided in the Supporting Information.

Acknowledgement

The Bruker (Siemens) SMART APEX diffraction facility was established at the University of Idaho with the assistance of the NSF-EPSCoR program and the M. J. Murdock Charitable Trust, Vancouver, WA, USA.

²³ SMART: v.5.630, Bruker Molecular Analysis Research Tool, Bruker AXS, Madison, WI, **2001**.

²⁴ SAINTPlus: v. 7.23a, Data Reduction and Correction Program, Bruker AXS, Madison, WI, **2004**.

²⁵ SADABS: v.2004/1, an empirical absorption correction program, Bruker AXS Inc., Madison, WI, **2004**.

²⁶ SHELXTL: v. 6.14, Structure Determination Software Suite, Sheldrick, G.M., Bruker AXS Inc., Madison, WI, **2004**.

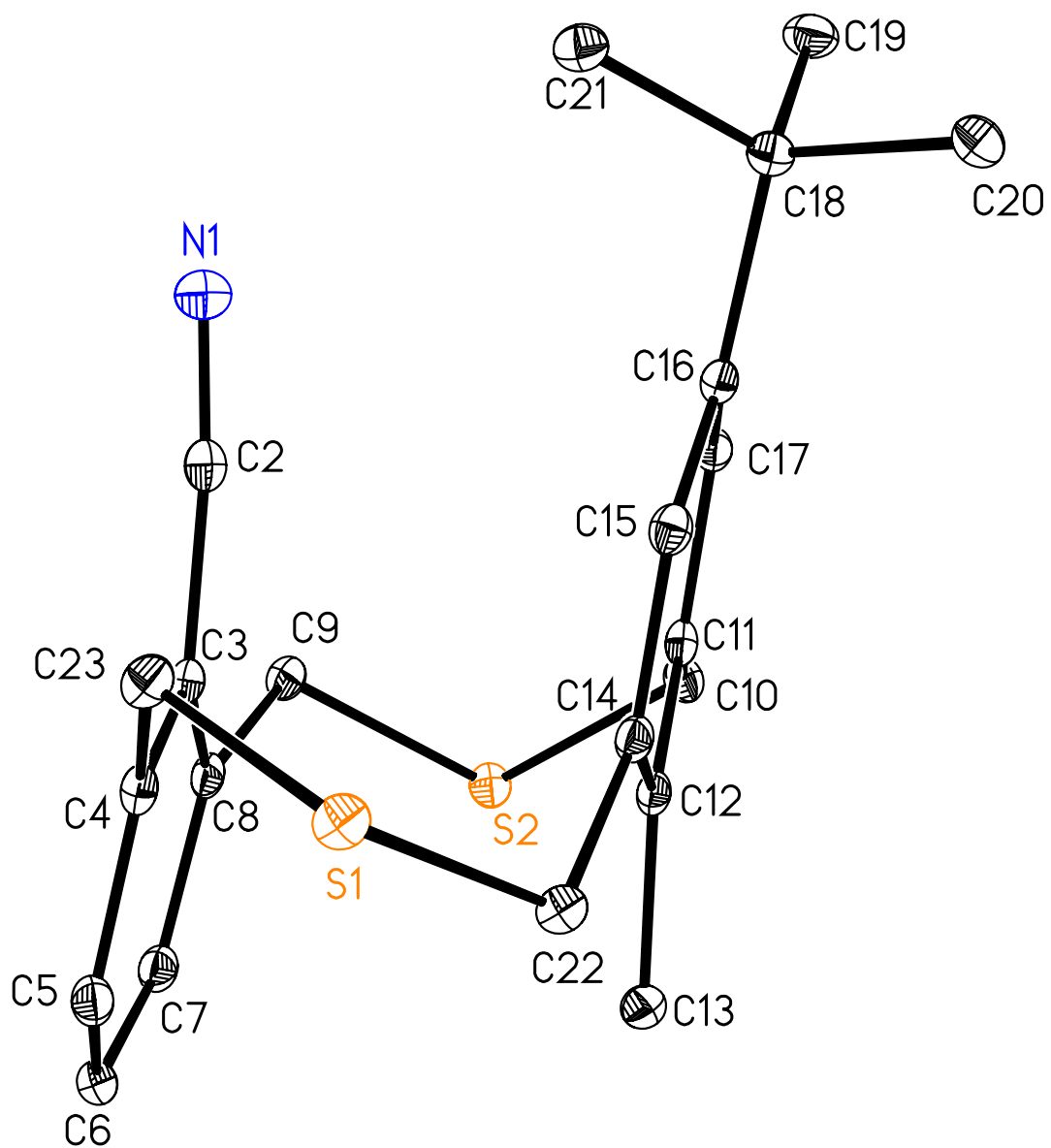


Table A. 27 Crystal data and structure refinement for 131 (C₂₂ H₂₅ N S₂).

Identification code	bt909	
Empirical formula	C ₂₂ H ₂₅ N S ₂	
Formula weight	367.55	
Temperature	89(2) K	
Wavelength	0.71073 Å	
Crystal system	Monoclinic	
Space group	C2/c	
Unit cell dimensions	a = 29.829(4) Å	α = 90°.
	b = 7.2157(9) Å	β = 122.036(1)°.
	c = 20.565(3) Å	γ = 90°.
Volume	3752.3(9) Å ³	
Z	8	
Density (calculated)	1.301 Mg/m ³	
Absorption coefficient	0.288 mm ⁻¹	
F(000)	1568	
Crystal size	0.48 x 0.25 x 0.19 mm ³	
Crystal color and habit	colorlessblock	
Diffractometer	Bruker/Siemens SMART APEX	
Theta range for data collection	1.61 to 25.25°.	
Index ranges	-35 ≤ h ≤ 35, -8 ≤ k ≤ 8, -24 ≤ l ≤ 24	
Reflections collected	27816	
Independent reflections	3403 [R(int) = 0.0221]	
Completeness to theta = 25.25°	100.0%	
Absorption correction	Semi-empirical from equivalents	
Max. and min. transmission	0.9473 and 0.8740	
Solution method	Bruker, 2003; XS, SHELXTL v. 6.14	
Refinement method	Full-matrix least-squares on F ²	
Data / restraints / parameters	3403 / 0 / 230	
Goodness-of-fit on F ²	1.084	
Final R indices [I > 2σ(I)]	R1 = 0.0291, wR2 = 0.0770	
R indices (all data)	R1 = 0.0307, wR2 = 0.0784	
Largest diff. peak and hole	0.352 and -0.215 e.Å ⁻³	

Table A. 28 Atomic coordinates ($\times 10^4$) and equivalent isotropic displacement parameters ($\text{\AA}^2 \times 10^3$) for 131 (bt 909).

	x	y	z	U(eq)
C(2)	1761(1)	936(2)	4797(1)	16(1)
C(3)	1501(1)	721(2)	5221(1)	15(1)
C(4)	993(1)	-74(2)	4854(1)	16(1)
C(5)	785(1)	-509(2)	5301(1)	18(1)
C(6)	1071(1)	-173(2)	6084(1)	18(1)
C(7)	1555(1)	731(2)	6426(1)	17(1)
C(8)	1771(1)	1242(2)	5995(1)	15(1)
C(9)	2266(1)	2410(2)	6354(1)	16(1)
C(10)	1903(1)	6199(2)	5879(1)	16(1)
C(11)	1472(1)	5507(2)	5098(1)	14(1)
C(12)	989(1)	4780(2)	4945(1)	14(1)
C(13)	844(1)	4796(2)	5545(1)	16(1)
C(14)	642(1)	4034(2)	4213(1)	14(1)
C(15)	746(1)	4226(2)	3635(1)	15(1)
C(16)	1203(1)	5108(2)	3759(1)	14(1)
C(17)	1568(1)	5666(2)	4506(1)	14(1)
C(18)	1286(1)	5383(2)	3092(1)	16(1)
C(19)	1813(1)	6349(2)	3351(1)	21(1)
C(20)	837(1)	6604(2)	2478(1)	22(1)
C(21)	1281(1)	3487(2)	2745(1)	18(1)
C(22)	160(1)	2950(2)	4062(1)	16(1)
C(23)	675(1)	-346(2)	3998(1)	18(1)
N(1)	1985(1)	963(2)	4484(1)	22(1)
S(1)	30(1)	804(1)	3522(1)	17(1)
S(2)	2175(1)	4623(1)	6699(1)	16(1)

Table A. 29 Bond lengths [Å] and angles [°] for 131 (bt 909)

C(2)-N(1)	1.1472(19)	C(18)-C(19)	1.5339(19)
C(2)-C(3)	1.4495(19)	C(18)-C(21)	1.5388(19)
C(3)-C(8)	1.4011(19)	C(18)-C(20)	1.5401(19)
C(3)-C(4)	1.408(2)	C(19)-H(19A)	0.9800
C(4)-C(5)	1.389(2)	C(19)-H(19B)	0.9800
C(4)-C(23)	1.5059(19)	C(19)-H(19C)	0.9800
C(5)-C(6)	1.388(2)	C(20)-H(20A)	0.9800
C(5)-H(5)	0.9500	C(20)-H(20B)	0.9800
C(6)-C(7)	1.388(2)	C(20)-H(20C)	0.9800
C(6)-H(6)	0.9500	C(21)-H(21A)	0.9800
C(7)-C(8)	1.3946(19)	C(21)-H(21B)	0.9800
C(7)-H(7)	0.9500	C(21)-H(21C)	0.9800
C(8)-C(9)	1.5096(19)	C(22)-S(1)	1.8234(14)
C(9)-S(2)	1.8252(14)	C(22)-H(22A)	0.9900
C(9)-H(9A)	0.9900	C(22)-H(22B)	0.9900
C(9)-H(9B)	0.9900	C(23)-S(1)	1.8301(14)
C(10)-C(11)	1.5132(18)	C(23)-H(23A)	0.9900
C(10)-S(2)	1.8287(14)	C(23)-H(23B)	0.9900
C(10)-H(10A)	0.9900		
C(10)-H(10B)	0.9900	N(1)-C(2)-C(3)	174.33(15)
C(11)-C(17)	1.3961(19)	C(8)-C(3)-C(4)	121.67(12)
C(11)-C(12)	1.4038(19)	C(8)-C(3)-C(2)	119.04(12)
C(12)-C(14)	1.4062(19)	C(4)-C(3)-C(2)	119.24(12)
C(12)-C(13)	1.5088(18)	C(5)-C(4)-C(3)	117.93(13)
C(13)-H(13A)	0.9800	C(5)-C(4)-C(23)	121.22(13)
C(13)-H(13B)	0.9800	C(3)-C(4)-C(23)	120.77(12)
C(13)-H(13C)	0.9800	C(6)-C(5)-C(4)	120.92(13)
C(14)-C(15)	1.3872(19)	C(6)-C(5)-H(5)	119.5
C(14)-C(22)	1.5173(18)	C(4)-C(5)-H(5)	119.5
C(15)-C(16)	1.3978(19)	C(7)-C(6)-C(5)	120.23(13)
C(15)-H(15)	0.9500	C(7)-C(6)-H(6)	119.9
C(16)-C(17)	1.3901(19)	C(5)-C(6)-H(6)	119.9
C(16)-C(18)	1.5319(18)	C(6)-C(7)-C(8)	120.63(13)
C(17)-H(17)	0.9500	C(6)-C(7)-H(7)	119.7

C(8)-C(7)-H(7)	119.7	C(17)-C(16)-C(18)	123.11(12)
C(7)-C(8)-C(3)	118.05(13)	C(15)-C(16)-C(18)	120.05(12)
C(7)-C(8)-C(9)	119.89(12)	C(16)-C(17)-C(11)	122.42(12)
C(3)-C(8)-C(9)	121.98(12)	C(16)-C(17)-H(17)	118.8
C(8)-C(9)-S(2)	111.71(9)	C(11)-C(17)-H(17)	118.8
C(8)-C(9)-H(9A)	109.3	C(16)-C(18)-C(19)	111.81(11)
S(2)-C(9)-H(9A)	109.3	C(16)-C(18)-C(21)	109.49(11)
C(8)-C(9)-H(9B)	109.3	C(19)-C(18)-C(21)	108.76(11)
S(2)-C(9)-H(9B)	109.3	C(16)-C(18)-C(20)	108.86(11)
H(9A)-C(9)-H(9B)	107.9	C(19)-C(18)-C(20)	108.11(12)
C(11)-C(10)-S(2)	119.07(10)	C(21)-C(18)-C(20)	109.79(11)
C(11)-C(10)-H(10A)	107.5	C(18)-C(19)-H(19A)	109.5
S(2)-C(10)-H(10A)	107.5	C(18)-C(19)-H(19B)	109.5
C(11)-C(10)-H(10B)	107.5	H(19A)-C(19)-H(19B)	109.5
S(2)-C(10)-H(10B)	107.5	C(18)-C(19)-H(19C)	109.5
H(10A)-C(10)-H(10B)	107.0	H(19A)-C(19)-H(19C)	109.5
C(17)-C(11)-C(12)	119.81(12)	H(19B)-C(19)-H(19C)	109.5
C(17)-C(11)-C(10)	116.61(12)	C(18)-C(20)-H(20A)	109.5
C(12)-C(11)-C(10)	123.56(12)	C(18)-C(20)-H(20B)	109.5
C(11)-C(12)-C(14)	117.93(12)	H(20A)-C(20)-H(20B)	109.5
C(11)-C(12)-C(13)	121.38(12)	C(18)-C(20)-H(20C)	109.5
C(14)-C(12)-C(13)	120.69(12)	H(20A)-C(20)-H(20C)	109.5
C(12)-C(13)-H(13A)	109.5	H(20B)-C(20)-H(20C)	109.5
C(12)-C(13)-H(13B)	109.5	C(18)-C(21)-H(21A)	109.5
H(13A)-C(13)-H(13B)	109.5	C(18)-C(21)-H(21B)	109.5
C(12)-C(13)-H(13C)	109.5	H(21A)-C(21)-H(21B)	109.5
H(13A)-C(13)-H(13C)	109.5	C(18)-C(21)-H(21C)	109.5
H(13B)-C(13)-H(13C)	109.5	H(21A)-C(21)-H(21C)	109.5
C(15)-C(14)-C(12)	120.46(12)	H(21B)-C(21)-H(21C)	109.5
C(15)-C(14)-C(22)	119.73(12)	C(14)-C(22)-S(1)	115.76(9)
C(12)-C(14)-C(22)	119.77(12)	C(14)-C(22)-H(22A)	108.3
C(14)-C(15)-C(16)	121.92(13)	C(14)-C(22)-H(22B)	108.3
C(14)-C(15)-H(15)	119.0	S(1)-C(22)-H(22B)	108.3
C(16)-C(15)-H(15)	119.0	H(22A)-C(22)-H(22B)	107.4
C(17)-C(16)-C(15)	116.82(12)	C(4)-C(23)-S(1)	113.47(10)
		S(1)-C(23)-H(23B)	108.9

C(4)-C(23)-H(23A)	108.9	H(23A)-C(23)-H(23B)	107.7
S(1)-C(23)-H(23A)	108.9	C(22)-S(1)-C(23)	103.62(6)
S(1)-C(22)-H(22A)	108.3	C(9)-S(2)-C(10)	105.68(6)
C(4)-C(23)-H(23B)	108.9		

Table A. 30 Anisotropic displacement parameters ($\text{\AA}^2 \times 10^3$) for 131 (bt 909).

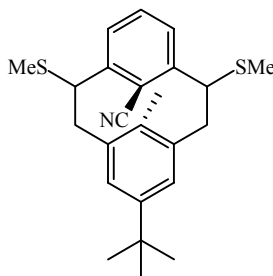
	U11	U22	U33	U23	U13	U12
C(2)	16(1)	14(1)	16(1)	0(1)	6(1)	0(1)
C(3)	17(1)	11(1)	18(1)	3(1)	10(1)	4(1)
C(4)	18(1)	11(1)	19(1)	1(1)	9(1)	3(1)
C(5)	16(1)	13(1)	25(1)	1(1)	12(1)	0(1)
C(6)	23(1)	14(1)	23(1)	5(1)	16(1)	4(1)
C(7)	21(1)	15(1)	17(1)	2(1)	10(1)	5(1)
C(8)	16(1)	11(1)	19(1)	2(1)	9(1)	4(1)
C(9)	15(1)	16(1)	17(1)	0(1)	8(1)	3(1)
C(10)	18(1)	14(1)	15(1)	0(1)	7(1)	-2(1)
C(11)	16(1)	9(1)	15(1)	1(1)	7(1)	2(1)
C(12)	16(1)	11(1)	15(1)	2(1)	8(1)	4(1)
C(13)	17(1)	16(1)	17(1)	-1(1)	10(1)	0(1)
C(14)	13(1)	12(1)	16(1)	2(1)	7(1)	3(1)
C(15)	14(1)	14(1)	13(1)	0(1)	5(1)	2(1)
C(16)	16(1)	12(1)	16(1)	1(1)	9(1)	3(1)
C(17)	14(1)	12(1)	18(1)	1(1)	9(1)	1(1)
C(18)	18(1)	16(1)	15(1)	1(1)	10(1)	1(1)
C(19)	25(1)	21(1)	23(1)	-2(1)	17(1)	-4(1)
C(20)	27(1)	23(1)	17(1)	5(1)	13(1)	5(1)
C(21)	19(1)	20(1)	17(1)	-2(1)	11(1)	-1(1)
C(22)	15(1)	17(1)	16(1)	-2(1)	8(1)	0(1)
C(23)	17(1)	18(1)	20(1)	-3(1)	10(1)	0(1)
N(1)	21(1)	26(1)	21(1)	0(1)	12(1)	0(1)
S(1)	13(1)	18(1)	17(1)	-4(1)	6(1)	-3(1)
S(2)	19(1)	16(1)	12(1)	-1(1)	6(1)	0(1)

Table A. 31 Hydrogen coordinates ($\times 10^4$) and isotropic displacement parameters ($\text{\AA}^2 \times 10^3$) for 131 (bt 909).

	x	y	z	U(eq)
H(5)	443	-1043	5066	21
H(6)	935	-563	6388	22
H(7)	1740	1005	6959	21
H(9A)	2364	2641	5971	20
H(9B)	2560	1724	6788	20
H(10A)	1763	7297	6003	20
H(10B)	2200	6631	5833	20
H(13A)	480	5245	5315	25
H(13B)	1086	5616	5967	25
H(13C)	871	3537	5741	25
H(15)	501	3744	3140	18
H(17)	1895	6174	4617	17
H(19A)	1813	7586	3548	31
H(19B)	1859	6461	2915	31
H(19C)	2105	5618	3757	31
H(20A)	495	6022	2311	32
H(20B)	878	6740	2038	32
H(20C)	851	7828	2695	32
H(21A)	1564	2707	3141	27
H(21B)	1338	3663	2322	27
H(21C)	939	2885	2553	27
H(22A)	-155	3760	3779	19
H(22B)	202	2648	4561	19
H(23A)	620	-1690	3886	22
H(23B)	879	137	3781	22

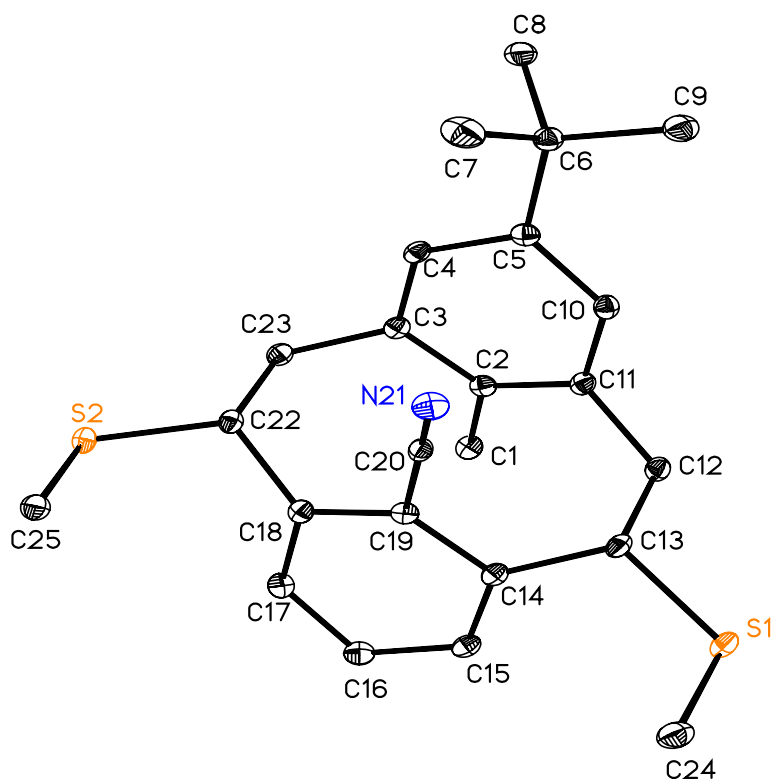
Single-Crystal X-ray Diffraction Laboratory
University of Idaho

X-ray structure report for thiomethylcyclophane 134



134

Brendan Twamley



Project name : bt960

8-21-06

Experimental:

Crystals of compound **1** were removed from the flask, a suitable crystal was selected, attached to a glass fiber and data were collected at 89(2) K using a Bruker/Siemens SMART APEX instrument (Mo K α radiation, $\lambda = 0.71073$ Å) equipped with a Cryocool NeverIce low temperature device. Data were measured using omega scans of 0.3 ° per frame for 10 seconds, and a full sphere of data was collected. A total of 2400 frames were collected with a final resolution of 0.83 Å. Cell parameters were retrieved using SMART²⁷ software and refined using SAINTPlus²⁸ on all observed reflections. Data reduction and correction for Lp and decay were performed using the SAINTPlus software. Absorption corrections were applied using SADABS.²⁹ The structure was solved by direct methods and refined by least squares method on F² using the SHELXTL program package.³⁰ The structure was solved in the space group P2(1)/c (# 14) by analysis of systematic absences. All non-hydrogen atoms were refined anisotropically. No decomposition was observed during data collection. Details of the data collection and refinement are given in Table 1. Further details are provided in the Supporting Information.

Acknowledgement

The Bruker (Siemens) SMART APEX diffraction facility was established at the University of Idaho with the assistance of the NSF-EPSCoR program and the M. J. Murdock Charitable Trust, Vancouver, WA, USA.

²⁷ SMART: v.5.630, Bruker Molecular Analysis Research Tool, Bruker AXS, Madison, WI, **2001**.

²⁸ SAINTPlus: v. 7.23a, Data Reduction and Correction Program, Bruker AXS, Madison, WI, **2004**.

²⁹ SADABS: v.2004/1, an empirical absorption correction program, Bruker AXS Inc., Madison, WI, **2004**.

³⁰ SHELXTL: v. 6.14, Structure Determination Software Suite, Sheldrick, G.M., Bruker AXS Inc., Madison, WI, **2004**.

Table A. 32 Crystal data and structure refinement for 134 (C₂₄ H₂₉ N S₂).

Identification code	bt960	
Empirical formula	C ₂₄ H ₂₉ N S ₂	
Formula weight	395.60	
Temperature	89(2) K	
Wavelength	0.71073 Å	
Crystal system	Monoclinic	
Space group	P2(1)/c	
Unit cell dimensions	a = 12.1190(10) Å	α = 90°.
	b = 10.0317(8) Å	β = 104.752(1)°.
	c = 18.1594(14) Å	γ = 90°.
Volume	2134.9(3) Å ³	
Z	4	
Density (calculated)	1.231 Mg/m ³	
Absorption coefficient	0.258 mm ⁻¹	
F(000)	848	
Crystal size	0.52 x 0.41 x 0.25 mm ³	
Crystal color and habit	colorless block	
Diffractometer	Bruker/Siemens SMART APEX	
Theta range for data collection	1.74 to 25.25°.	
Index ranges	-14 ≤ h ≤ 14, -12 ≤ k ≤ 12, -21 ≤ l ≤ 21	
Reflections collected	31239	
Independent reflections	3858 [R(int) = 0.0277]	
Completeness to theta = 25.25°	100.0%	
Absorption correction	Semi-empirical from equivalents	
Max. and min. transmission	0.9383 and 0.8775	
Solution method	Bruker, 2003; XS, SHELXTL v. 6.14	
Refinement method	Full-matrix least-squares on F ²	
Data / restraints / parameters	3858 / 0 / 250	
Goodness-of-fit on F ²	1.042	
Final R indices [I > 2σ(I)]	R1 = 0.0340, wR2 = 0.0853	
R indices (all data)	R1 = 0.0364, wR2 = 0.0870	
Largest diff. peak and hole	0.459 and -0.175 e.Å ⁻³	

Table A. 33 Atomic coordinates ($\times 10^4$) and equivalent isotropic displacement parameters ($\text{\AA}^2 \times 10^3$) for 134 (bt 960)

	x	y	z	U(eq)
C(1)	4936(1)	7620(2)	8212(1)	19(1)
C(2)	5979(1)	8167(2)	8005(1)	16(1)
C(3)	6336(1)	9490(2)	8184(1)	16(1)
C(4)	7136(1)	10056(2)	7849(1)	16(1)
C(5)	7655(1)	9337(2)	7370(1)	17(1)
C(6)	8476(1)	10050(2)	6984(1)	19(1)
C(7)	9475(2)	10637(2)	7594(1)	32(1)
C(8)	7842(2)	11191(2)	6493(1)	25(1)
C(9)	8957(2)	9118(2)	6475(1)	26(1)
C(10)	7443(1)	7971(2)	7319(1)	17(1)
C(11)	6645(1)	7370(2)	7649(1)	17(1)
C(12)	6670(1)	5869(2)	7756(1)	19(1)
C(13)	7531(1)	5463(2)	8530(1)	18(1)
C(14)	7219(1)	6126(2)	9202(1)	16(1)
C(15)	6494(1)	5567(2)	9600(1)	18(1)
C(16)	6064(1)	6339(2)	10100(1)	20(1)
C(17)	6229(1)	7707(2)	10137(1)	18(1)
C(18)	6944(1)	8310(2)	9745(1)	16(1)
C(19)	7540(1)	7467(2)	9360(1)	15(1)
C(20)	8530(1)	7970(2)	9140(1)	15(1)
C(22)	6965(1)	9803(2)	9605(1)	16(1)
C(23)	6057(1)	10196(2)	8853(1)	17(1)
C(24)	8590(2)	3324(2)	9431(1)	27(1)
C(25)	7975(1)	10372(2)	11095(1)	21(1)
N(21)	9391(1)	8299(1)	9045(1)	22(1)
S(1)	7529(1)	3651(1)	8554(1)	23(1)
S(2)	6709(1)	10819(1)	10373(1)	18(1)

Table A. 34 Bond lengths [Å] and angles [°] for 134 (bt 960)

C(1)-C(2)	1.510(2)	C(14)-C(15)	1.390(2)
C(1)-H(1A)	0.9800	C(14)-C(19)	1.409(2)
C(1)-H(1B)	0.9800	C(15)-C(16)	1.391(2)
C(1)-H(1C)	0.9800	C(15)-H(15)	0.9500
C(2)-C(11)	1.405(2)	C(16)-C(17)	1.386(2)
C(2)-C(3)	1.408(2)	C(16)-H(16)	0.9500
C(3)-C(4)	1.390(2)	C(17)-C(18)	1.393(2)
C(3)-C(23)	1.518(2)	C(17)-H(17)	0.9500
C(4)-C(5)	1.397(2)	C(18)-C(19)	1.408(2)
C(4)-H(4)	0.9500	C(18)-C(22)	1.521(2)
C(5)-C(10)	1.393(2)	C(19)-C(20)	1.449(2)
C(5)-C(6)	1.532(2)	C(20)-N(21)	1.148(2)
C(6)-C(9)	1.531(2)	C(22)-C(23)	1.571(2)
C(6)-C(8)	1.532(2)	C(22)-S(2)	1.8169(15)
C(6)-C(7)	1.535(2)	C(22)-H(22A)	1.0000
C(7)-H(7A)	0.9800	C(23)-H(23A)	0.9900
C(7)-H(7B)	0.9800	C(23)-H(23B)	0.9900
C(7)-H(7C)	0.9800	C(24)-S(1)	1.8044(18)
C(8)-H(8A)	0.9800	C(24)-H(24A)	0.9800
C(8)-H(8B)	0.9800	C(24)-H(24B)	0.9800
C(8)-H(8C)	0.9800	C(24)-H(24C)	0.9800
C(9)-H(9A)	0.9800	C(25)-S(2)	1.8024(16)
C(9)-H(9B)	0.9800	C(25)-H(25A)	0.9800
C(9)-H(9C)	0.9800	C(25)-H(25B)	0.9800
C(10)-C(11)	1.398(2)	C(25)-H(25C)	0.9800
C(10)-H(10)	0.9500		
C(11)-C(12)	1.517(2)	C(2)-C(1)-H(1A)	109.5
C(12)-C(13)	1.576(2)	C(2)-C(1)-H(1B)	109.5
C(12)-H(12A)	0.9900	H(1A)-C(1)-H(1B)	109.5
C(12)-H(12B)	0.9900	C(2)-C(1)-H(1C)	109.5
C(13)-C(14)	1.519(2)	H(1A)-C(1)-H(1C)	109.5
C(13)-S(1)	1.8180(15)	H(1B)-C(1)-H(1C)	109.5
C(13)-H(13)	1.0000	C(11)-C(2)-C(3)	117.58(14)

C(11)-C(2)-C(1)	121.54(14)	C(5)-C(10)-H(10)	118.9
C(3)-C(2)-C(1)	120.85(14)	C(11)-C(10)-H(10)	118.9
C(4)-C(3)-C(2)	119.52(14)	C(10)-C(11)-C(2)	119.54(14)
C(4)-C(3)-C(23)	118.81(13)	C(10)-C(11)-C(12)	119.32(14)
C(2)-C(3)-C(23)	120.39(13)	C(2)-C(11)-C(12)	120.05(14)
C(3)-C(4)-C(5)	122.40(14)	C(11)-C(12)-C(13)	110.94(12)
C(3)-C(4)-H(4)	118.8	C(11)-C(12)-H(12A)	109.5
C(5)-C(4)-H(4)	118.8	C(13)-C(12)-H(12A)	109.5
C(10)-C(5)-C(4)	116.41(14)	C(11)-C(12)-H(12B)	109.5
C(10)-C(5)-C(6)	123.99(14)	C(13)-C(12)-H(12B)	109.5
C(4)-C(5)-C(6)	119.44(14)	H(12A)-C(12)-H(12B)	108.0
C(9)-C(6)-C(8)	108.49(13)	C(14)-C(13)-C(12)	111.07(12)
C(9)-C(6)-C(5)	112.49(13)	C(14)-C(13)-S(1)	114.63(11)
C(8)-C(6)-C(5)	109.06(13)	C(12)-C(13)-S(1)	105.94(10)
C(9)-C(6)-C(7)	108.53(14)	C(14)-C(13)-H(13)	108.3
C(8)-C(6)-C(7)	108.68(14)	C(12)-C(13)-H(13)	108.3
C(5)-C(6)-C(7)	109.53(13)	S(1)-C(13)-H(13)	108.3
C(6)-C(7)-H(7A)	109.5	C(15)-C(14)-C(19)	117.25(14)
C(6)-C(7)-H(7B)	109.5	C(15)-C(14)-C(13)	124.06(14)
H(7A)-C(7)-H(7B)	109.5	C(19)-C(14)-C(13)	117.97(13)
C(6)-C(7)-H(7C)	109.5	C(14)-C(15)-C(16)	120.34(14)
H(7A)-C(7)-H(7C)	109.5	C(14)-C(15)-H(15)	119.8
H(7B)-C(7)-H(7C)	109.5	C(16)-C(15)-H(15)	119.8
C(6)-C(8)-H(8A)	109.5	C(17)-C(16)-C(15)	120.68(14)
C(6)-C(8)-H(8B)	109.5	C(17)-C(16)-H(16)	119.7
H(8A)-C(8)-H(8B)	109.5	C(15)-C(16)-H(16)	119.7
C(6)-C(8)-H(8C)	109.5	C(16)-C(17)-C(18)	120.41(14)
H(8A)-C(8)-H(8C)	109.5	C(16)-C(17)-H(17)	119.8
H(8B)-C(8)-H(8C)	109.5	C(18)-C(17)-H(17)	119.8
C(6)-C(9)-H(9A)	109.5	C(17)-C(18)-C(19)	117.22(14)
C(6)-C(9)-H(9B)	109.5	C(17)-C(18)-C(22)	123.58(13)
H(9A)-C(9)-H(9B)	109.5	C(19)-C(18)-C(22)	118.42(13)
C(6)-C(9)-H(9C)	109.5	C(14)-C(19)-C(18)	121.64(13)
H(9A)-C(9)-H(9C)	109.5	C(14)-C(19)-C(20)	118.75(13)
H(9B)-C(9)-H(9C)	109.5	C(18)-C(19)-C(20)	119.59(13)
C(5)-C(10)-C(11)	122.14(14)	N(21)-C(20)-C(19)	171.71(16)

C(18)-C(22)-C(23)	110.75(12)
C(18)-C(22)-S(2)	114.25(11)
C(23)-C(22)-S(2)	107.93(10)
C(18)-C(22)-H(22A)	107.9
C(23)-C(22)-H(22A)	107.9
S(2)-C(22)-H(22A)	107.9
C(3)-C(23)-C(22)	109.23(12)
C(3)-C(23)-H(23A)	109.8
C(22)-C(23)-H(23A)	109.8
C(3)-C(23)-H(23B)	109.8
C(22)-C(23)-H(23B)	109.8
H(23A)-C(23)-H(23B)	108.3
S(1)-C(24)-H(24A)	109.5
S(1)-C(24)-H(24B)	109.5
H(24A)-C(24)-H(24B)	109.5
S(1)-C(24)-H(24C)	109.5
H(24A)-C(24)-H(24C)	109.5
H(24B)-C(24)-H(24C)	109.5
S(2)-C(25)-H(25A)	109.5
S(2)-C(25)-H(25B)	109.5
H(25A)-C(25)-H(25B)	109.5
S(2)-C(25)-H(25C)	109.5
H(25A)-C(25)-H(25C)	109.5
H(25B)-C(25)-H(25C)	109.5
C(24)-S(1)-C(13)	101.41(8)
C(25)-S(2)-C(22)	97.93(7)

Table A. 35 Anisotropic displacement parameters ($\text{\AA}^2 \times 10^3$) for 134 (bt 960).

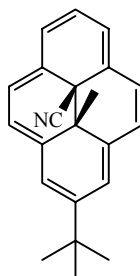
	U11	U22	U33	U23	U13	U12
C(1)	15(1)	19(1)	22(1)	-1(1)	2(1)	-2(1)
C(2)	14(1)	18(1)	15(1)	1(1)	0(1)	-1(1)
C(3)	13(1)	16(1)	17(1)	1(1)	1(1)	3(1)
C(4)	16(1)	13(1)	18(1)	1(1)	1(1)	1(1)
C(5)	14(1)	19(1)	15(1)	2(1)	0(1)	1(1)
C(6)	19(1)	19(1)	20(1)	1(1)	6(1)	-1(1)
C(7)	25(1)	42(1)	28(1)	1(1)	6(1)	-14(1)
C(8)	32(1)	20(1)	27(1)	5(1)	14(1)	4(1)
C(9)	26(1)	23(1)	32(1)	4(1)	15(1)	3(1)
C(10)	16(1)	17(1)	16(1)	-1(1)	3(1)	2(1)
C(11)	18(1)	16(1)	16(1)	-1(1)	0(1)	-2(1)
C(12)	21(1)	16(1)	20(1)	-3(1)	6(1)	-2(1)
C(13)	19(1)	11(1)	24(1)	-1(1)	8(1)	-1(1)
C(14)	13(1)	14(1)	19(1)	0(1)	2(1)	1(1)
C(15)	16(1)	14(1)	24(1)	1(1)	4(1)	-2(1)
C(16)	15(1)	22(1)	23(1)	2(1)	7(1)	-3(1)
C(17)	14(1)	21(1)	19(1)	-2(1)	5(1)	1(1)
C(18)	13(1)	16(1)	16(1)	-1(1)	0(1)	-1(1)
C(19)	12(1)	17(1)	16(1)	2(1)	2(1)	-1(1)
C(20)	17(1)	13(1)	16(1)	-1(1)	3(1)	1(1)
C(22)	14(1)	16(1)	19(1)	-2(1)	6(1)	-1(1)
C(23)	16(1)	16(1)	20(1)	0(1)	5(1)	1(1)
C(24)	28(1)	22(1)	32(1)	6(1)	11(1)	5(1)
C(25)	21(1)	20(1)	20(1)	-1(1)	4(1)	-2(1)
N(21)	17(1)	24(1)	26(1)	2(1)	6(1)	-2(1)
S(1)	29(1)	13(1)	27(1)	-1(1)	8(1)	0(1)
S(2)	17(1)	17(1)	21(1)	-4(1)	6(1)	0(1)

Table A. 36 Hydrogen coordinates ($\times 10^4$) and isotropic displacement parameters ($\text{\AA}^2 \times 10^3$) for 134 (bt 960).

	x	y	z	U(eq)
H(1A)	4632	6866	7879	29
H(1B)	4354	8319	8148	29
H(1C)	5144	7320	8743	29
H(4)	7338	10965	7951	20
H(7A)	10007	11078	7346	48
H(7B)	9872	9920	7923	48
H(7C)	9184	11288	7900	48
H(8A)	7549	11813	6815	37
H(8B)	7203	10828	6099	37
H(8C)	8366	11661	6252	37
H(9A)	8327	8703	6097	38
H(9B)	9420	8423	6788	38
H(9C)	9433	9630	6214	38
H(10)	7853	7430	7050	20
H(12A)	6900	5438	7328	23
H(12B)	5896	5549	7753	23
H(13)	8311	5769	8517	21
H(15)	6291	4652	9530	22
H(16)	5653	5924	10418	23
H(17)	5852	8236	10432	21
H(22A)	7737	10037	9540	19
H(23A)	5285	9935	8891	21
H(23B)	6064	11173	8778	21
H(24A)	8316	3648	9862	40
H(24B)	9301	3784	9423	40
H(24C)	8731	2362	9484	40
H(25A)	7991	9405	11172	31
H(25B)	7970	10822	11573	31
H(25C)	8652	10646	10931	31

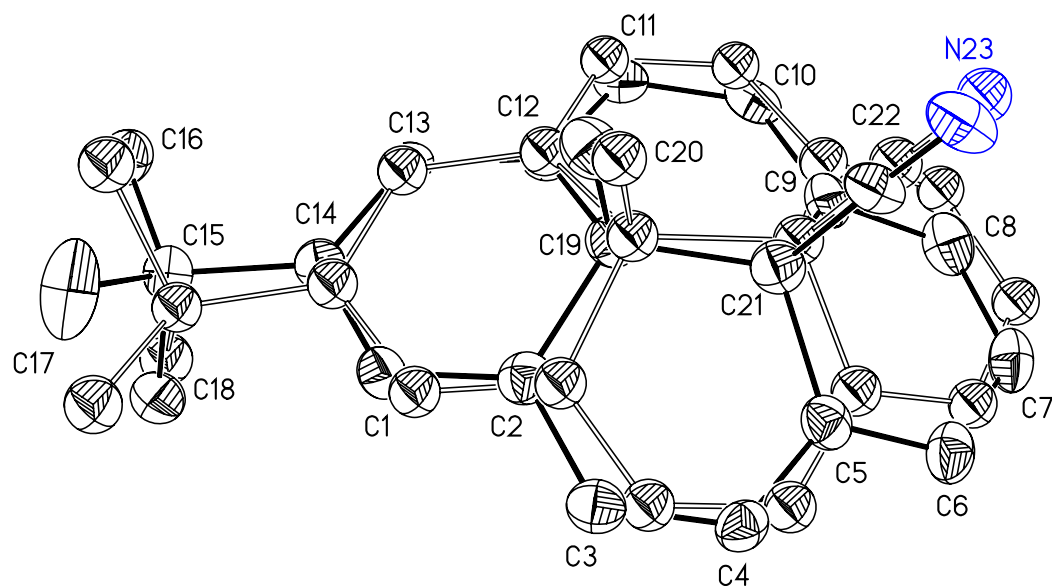
Single-Crystal X-ray Diffraction Laboratory
University of Idaho

X-ray structure report for *cis*-cyano-methyl DHP 136



136

Brendan Twamley



Project name : Bt1019

12-15-06

Experimental:

Crystals of compound **1** were removed from the flask, a suitable crystal was selected, attached to a glass fiber and data were collected at 90(2) K using a Bruker/Siemens SMART APEX instrument (Mo K α radiation, $\lambda = 0.71073$ Å) equipped with a Cryocool NeverIce low temperature device. Data were measured using omega scans 0.3 ° per frame for 60 seconds, and a total of 2366 frames were collected. Cell parameters were retrieved using SMART³¹ software and refined using SAINTPlus³² on all observed reflections. Data reduction and correction for Lp and decay were performed using the SAINTPlus software. Absorption corrections were applied using SADABS.³³ The structure was solved by direct methods and refined by least squares method on F² using the SHELXTL program package.³⁴ The structure was solved in the space group P2(1)/c (# 14) by analysis of systematic absences. The data exhibited whole molecule disorder and was refined in two positions with occupancies of 85:15%. The first moiety was refined anisotropically, the second held isotropic. Coordinates for the second moiety were generated from the major moiety and were refined as a rigid group. Restraints were applied to the tBu bond lengths of the minor moiety to stabilize the refinement. The diffraction was very weak and the data were truncated to a resolution of 0.93 Å. No decomposition was observed during data collection. Details of the data collection and refinement are given in Table 1. Further details are provided in the Supporting Information.

³¹ SMART: v. 5.632, Bruker AXS, Madison, WI, **2005**.

³² SAINTPlus: v. 7.23a, Data Reduction and Correction Program, Bruker AXS, Madison, WI, **2004**.

³³ SADABS: v.2004/1, an empirical absorption correction program, Bruker AXS Inc., Madison, WI, **2004**.

³⁴ SHELXTL: v. 6.14, Structure Determination Software Suite, Sheldrick, G.M., Bruker AXS Inc., Madison, WI, **2004**.

Acknowledgement

The Bruker (Siemens) SMART APEX diffraction facility was established at the University of Idaho with the assistance of the NSF-EPSCoR program and the M. J. Murdock Charitable Trust, Vancouver, WA, USA.

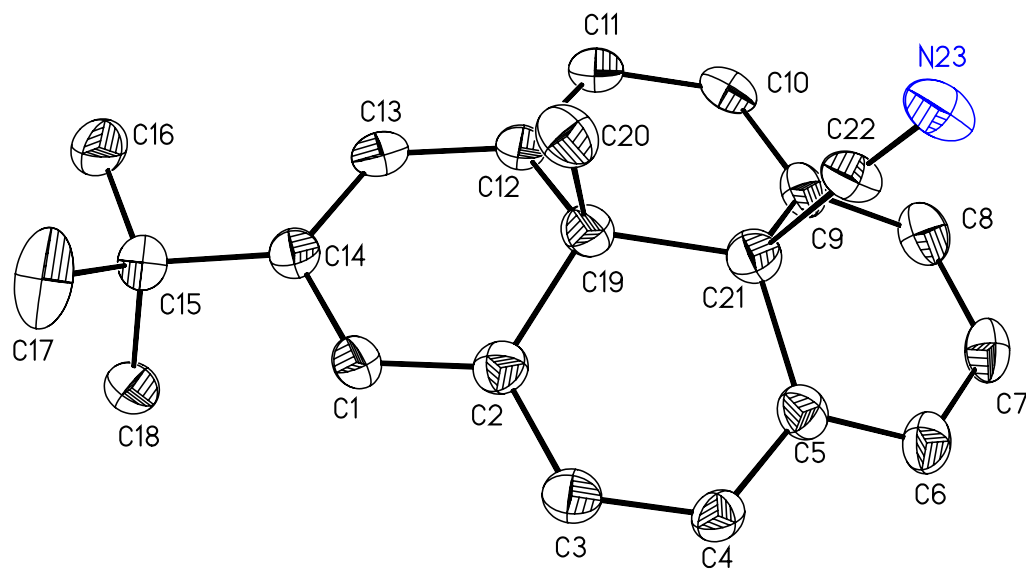


Figure 1a. Thermal ellipsoid plot (30%) of the major moiety in 1 (85%). This moiety was refined anisotropically.

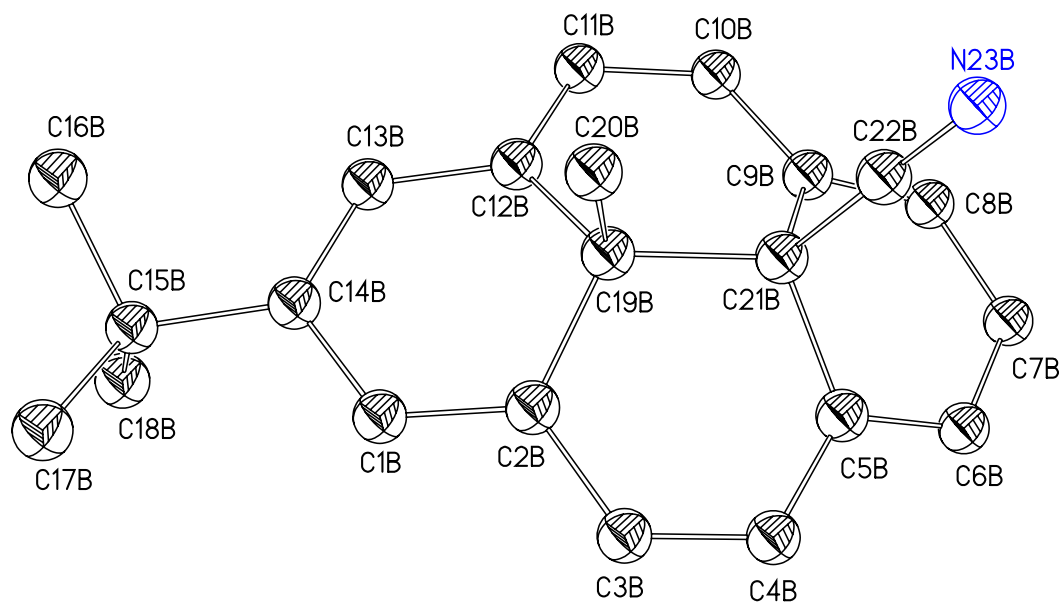


Figure 1b. Thermal ellipsoid plot (30%) of the minor moiety in 1 (15%). This moiety was refined isotropically using coordinates from the major moiety.

Table A. 37 Crystal data and structure refinement for 136

Identification code	bt1019	
Empirical formula	C ₂₂ H ₂₁ N	
Formula weight	299.40	
Temperature	90(2) K	
Wavelength	0.71073 Å	
Crystal system	Monoclinic	
Space group	P2(1)/c	
Unit cell dimensions	a = 14.2537(11) Å	$\alpha = 90^\circ$.
	b = 8.6909(7) Å	$\beta = 104.395(2)^\circ$.
	c = 13.8551(11) Å	$\gamma = 90^\circ$.
Volume	1662.4(2) Å ³	
Z	4	
Density (calculated)	1.196 Mg/m ³	
Absorption coefficient	0.069 mm ⁻¹	
F(000)	640	
Crystal size	0.44 x 0.25 x 0.10 mm ³	
Crystal color and habit	brown/green block	
Diffractometer	Bruker/Siemens SMART APEX	
Theta range for data collection	2.77 to 22.50°.	
Index ranges	-15 ≤ h ≤ 15, -9 ≤ k ≤ 9, -14 ≤ l ≤ 14	
Reflections collected	17683	
Independent reflections	2169 [R(int) = 0.0413]	
Completeness to theta = 22.50°	99.7%	
Absorption correction	Semi-empirical from equivalents	
Max. and min. transmission	0.992 and 0.979	
Solution method	Bruker, 2003; XS, SHELXTL v. 6.14	
Refinement method	Full-matrix least-squares on F ²	
Data / restraints / parameters	2169 / 6 / 231	
Goodness-of-fit on F ²	1.085	
Final R indices [I > 2σ(I)]	R1 = 0.0737, wR2 = 0.1938	
R indices (all data)	R1 = 0.0911, wR2 = 0.2083	
Largest diff. peak and hole	0.296 and -0.194 e.Å ⁻³	

Table A. 38 Atomic coordinates ($\times 10^4$) and equivalent isotropic displacement parameters ($\text{\AA}^2 \times 10^3$) for 136 (bt 1019).

	x	y	z	U(eq)
C(1)	2113(3)	7888(5)	4896(3)	46(1)
C(2)	2720(3)	9004(5)	5410(3)	44(1)
C(3)	3321(3)	8761(5)	6369(3)	45(1)
C(4)	4124(3)	9639(5)	6745(3)	41(1)
C(5)	4418(3)	10856(5)	6229(3)	43(1)
C(6)	5332(3)	11475(5)	6475(4)	51(1)
C(7)	5652(3)	12516(6)	5860(4)	52(1)
C(8)	5089(4)	12855(6)	4924(4)	54(1)
C(9)	4154(3)	12280(5)	4574(3)	44(1)
C(10)	3614(3)	12371(5)	3589(3)	45(1)
C(11)	2799(3)	11481(5)	3219(3)	44(1)
C(12)	2460(3)	10441(5)	3799(3)	41(1)
C(13)	1841(3)	9240(6)	3364(3)	46(1)
C(14)	1638(3)	7980(5)	3878(3)	48(1)
C(15)	1017(3)	6622(6)	3361(4)	55(1)
C(16)	546(4)	6899(6)	2299(4)	73(2)
C(17)	252(4)	6313(9)	3930(5)	93(2)
C(18)	1694(5)	5205(7)	3429(5)	67(2)
C(19)	2716(3)	10586(5)	4919(3)	44(1)
C(20)	1829(3)	11405(6)	5162(4)	51(1)
C(21)	3672(3)	11609(5)	5354(3)	46(1)
C(22)	3404(4)	13081(5)	5796(4)	46(1)
N(23)	3249(4)	14250(5)	6122(4)	58(1)
C(15B)	1068(12)	6605(19)	3773(13)	40
C(14B)	1678(10)	8036(16)	4167(11)	40
C(1B)	2284(10)	8051(15)	5141(10)	40
C(2B)	2892(9)	9241(15)	5534(8)	40
C(3B)	3611(11)	9106(17)	6430(9)	40
C(4B)	4397(11)	10058(18)	6667(9)	40

C(5B)	4552(9)	11259(15)	6050(9)	40
C(6B)	5434(9)	11949(17)	6142(11)	40
C(7B)	5611(9)	12966(17)	5429(13)	40
C(8B)	4921(10)	13202(16)	4543(12)	40
C(9B)	4006(10)	12544(15)	4348(10)	40
C(10B)	3347(12)	12525(18)	3425(10)	40
C(11B)	2555(11)	11561(18)	3203(10)	40
C(12B)	2356(9)	10540(16)	3882(9)	40
C(13B)	1747(9)	9270(18)	3567(10)	40
C(19B)	2761(8)	10801(14)	4989(9)	40
C(20B)	1930(9)	11569(17)	5364(14)	40
C(21B)	3709(8)	11947(13)	5242(9)	40
C(22B)	3443(10)	13401(14)	5706(13)	40
N(23B)	3290(12)	14587(16)	6024(17)	40
C(16B)	170(16)	7180(30)	3015(17)	50
C(17B)	728(19)	5730(30)	4572(17)	50
C(18B)	1610(30)	5550(50)	3230(30)	50

Table A. 39 Bond lengths [\AA] and angles [$^\circ$] for 136 (bt 1019).

C(1)-C(2)	1.375(6)	C(16)-H(16B)	0.9800
C(1)-C(14)	1.406(6)	C(16)-H(16C)	0.9800
C(1)-H(1A)	0.9500	C(17)-H(17A)	0.9800
C(2)-C(3)	1.407(6)	C(17)-H(17B)	0.9800
C(2)-C(19)	1.533(6)	C(17)-H(17C)	0.9800
C(3)-C(4)	1.367(6)	C(18)-H(18A)	0.9800
C(3)-H(3A)	0.9500	C(18)-H(18B)	0.9800
C(4)-C(5)	1.398(6)	C(18)-H(18C)	0.9800
C(4)-H(4A)	0.9500	C(19)-C(20)	1.558(6)
C(5)-C(6)	1.373(6)	C(19)-C(21)	1.614(6)
C(5)-C(21)	1.544(6)	C(20)-H(20A)	0.9800
C(6)-C(7)	1.394(7)	C(20)-H(20B)	0.9800
C(6)-H(6A)	0.9500	C(20)-H(20C)	0.9800
C(7)-C(8)	1.377(7)	C(21)-C(22)	1.508(6)
C(7)-H(7A)	0.9500	C(22)-N(23)	1.155(5)
C(8)-C(9)	1.393(7)	C(15B)-C(18B)	1.515(19)
C(8)-H(8A)	0.9500	C(15B)-C(17B)	1.519(17)
C(9)-C(10)	1.393(6)	C(15B)-C(16B)	1.523(17)
C(9)-C(21)	1.532(6)	C(15B)-C(14B)	1.5381
C(10)-C(11)	1.384(6)	C(14B)-C(13B)	1.3759
C(10)-H(10A)	0.9500	C(14B)-C(1B)	1.4098
C(11)-C(12)	1.374(6)	C(1B)-C(2B)	1.3719
C(11)-H(11A)	0.9500	C(1B)-H(1BA)	0.9500
C(12)-C(13)	1.402(6)	C(2B)-C(3B)	1.4043
C(12)-C(19)	1.509(6)	C(2B)-C(19B)	1.5409
C(13)-C(14)	1.376(6)	C(3B)-C(4B)	1.3644
C(13)-H(13A)	0.9500	C(3B)-H(3BA)	0.9500
C(14)-C(15)	1.542(6)	C(4B)-C(5B)	1.4015
C(15)-C(16)	1.477(7)	C(4B)-H(4BA)	0.9500
C(15)-C(17)	1.521(7)	C(5B)-C(6B)	1.3691
C(15)-C(18)	1.552(7)	C(5B)-C(21B)	1.5449
C(16)-H(16A)	0.9800	C(6B)-C(7B)	1.3946

C(6B)-H(6BA)	0.9500	C(3)-C(2)-C(19)	119.2(4)
C(7B)-C(8B)	1.3838	C(4)-C(3)-C(2)	122.2(4)
C(7B)-H(7BA)	0.9500	C(4)-C(3)-H(3A)	118.9
C(8B)-C(9B)	1.3874	C(2)-C(3)-H(3A)	118.9
C(8B)-H(8BA)	0.9500	C(3)-C(4)-C(5)	123.8(4)
C(9B)-C(10B)	1.3862	C(3)-C(4)-H(4A)	118.1
C(9B)-C(21B)	1.4985	C(5)-C(4)-H(4A)	118.1
C(10B)-C(11B)	1.3780	C(6)-C(5)-C(4)	123.8(4)
C(10B)-H(10B)	0.9500	C(6)-C(5)-C(21)	117.0(4)
C(11B)-C(12B)	1.3731	C(4)-C(5)-C(21)	119.2(4)
C(11B)-H(11B)	0.9500	C(5)-C(6)-C(7)	122.5(4)
C(12B)-C(13B)	1.4047	C(5)-C(6)-H(6A)	118.8
C(12B)-C(19B)	1.5160	C(7)-C(6)-H(6A)	118.8
C(13B)-H(13B)	0.9500	C(8)-C(7)-C(6)	120.8(4)
C(19B)-C(20B)	1.5571	C(8)-C(7)-H(7A)	119.6
C(19B)-C(21B)	1.6444	C(6)-C(7)-H(7A)	119.6
C(20B)-H(20D)	0.9800	C(7)-C(8)-C(9)	122.3(4)
C(20B)-H(20E)	0.9800	C(7)-C(8)-H(8A)	118.9
C(20B)-H(20F)	0.9800	C(9)-C(8)-H(8A)	118.9
C(21B)-C(22B)	1.5075	C(10)-C(9)-C(8)	124.6(4)
C(22B)-N(23B)	1.1628	C(10)-C(9)-C(21)	118.6(4)
C(16B)-H(16D)	0.9800	C(8)-C(9)-C(21)	116.7(4)
C(16B)-H(16E)	0.9800	C(11)-C(10)-C(9)	122.6(4)
C(16B)-H(16F)	0.9800	C(11)-C(10)-H(10A)	118.7
C(17B)-H(17D)	0.9800	C(9)-C(10)-H(10A)	118.7
C(17B)-H(17E)	0.9800	C(12)-C(11)-C(10)	122.5(4)
C(17B)-H(17F)	0.9800	C(12)-C(11)-H(11A)	118.8
C(18B)-H(18D)	0.9800	C(10)-C(11)-H(11A)	118.8
C(18B)-H(18E)	0.9800	C(11)-C(12)-C(13)	120.9(4)
C(18B)-H(18F)	0.9800	C(11)-C(12)-C(19)	121.1(4)
		C(13)-C(12)-C(19)	118.0(4)
C(2)-C(1)-C(14)	124.3(4)	C(14)-C(13)-C(12)	124.1(4)
C(2)-C(1)-H(1A)	117.9	C(14)-C(13)-H(13A)	117.9
C(14)-C(1)-H(1A)	117.9	C(12)-C(13)-H(13A)	117.9
C(1)-C(2)-C(3)	122.7(4)	C(13)-C(14)-C(1)	117.0(4)
C(1)-C(2)-C(19)	118.1(4)	C(13)-C(14)-C(15)	122.6(4)

C(1)-C(14)-C(15)	120.0(4)	C(4B)-C(3B)-H(3BA)	118.8
C(16)-C(15)-C(17)	109.7(5)	C(2B)-C(3B)-H(3BA)	118.8
C(16)-C(15)-C(14)	113.9(4)	C(3B)-C(4B)-C(5B)	123.3
C(17)-C(15)-C(14)	107.2(4)	C(3B)-C(4B)-H(4BA)	118.3
C(16)-C(15)-C(18)	108.2(5)	C(5B)-C(4B)-H(4BA)	118.3
C(17)-C(15)-C(18)	110.1(5)	C(6B)-C(5B)-C(4B)	123.4
C(14)-C(15)-C(18)	107.6(4)	C(6B)-C(5B)-C(21B)	115.4
C(12)-C(19)-C(2)	110.8(3)	C(4B)-C(5B)-C(21B)	121.2
C(12)-C(19)-C(20)	105.0(3)	C(5B)-C(6B)-C(7B)	122.4
C(2)-C(19)-C(20)	103.2(3)	C(5B)-C(6B)-H(6BA)	118.8
C(12)-C(19)-C(21)	113.3(3)	C(7B)-C(6B)-H(6BA)	118.8
C(2)-C(19)-C(21)	114.8(3)	C(8B)-C(7B)-C(6B)	120.5
C(20)-C(19)-C(21)	108.9(3)	C(8B)-C(7B)-H(7BA)	119.8
C(22)-C(21)-C(9)	99.6(3)	C(6B)-C(7B)-H(7BA)	119.8
C(22)-C(21)-C(5)	103.6(3)	C(7B)-C(8B)-C(9B)	122.6
C(9)-C(21)-C(5)	111.9(4)	C(7B)-C(8B)-H(8BA)	118.7
C(22)-C(21)-C(19)	110.1(3)	C(9B)-C(8B)-H(8BA)	118.7
C(9)-C(21)-C(19)	115.5(3)	C(10B)-C(9B)-C(8B)	125.0
C(5)-C(21)-C(19)	114.3(3)	C(10B)-C(9B)-C(21B)	119.5
N(23)-C(22)-C(21)	175.8(5)	C(8B)-C(9B)-C(21B)	115.3
C(18B)-C(15B)-C(17B)	110.7(19)	C(11B)-C(10B)-C(9B)	122.9
C(18B)-C(15B)-C(16B)	107.2(19)	C(11B)-C(10B)-H(10B)	118.6
C(17B)-C(15B)-C(16B)	107.5(16)	C(9B)-C(10B)-H(10B)	118.6
C(18B)-C(15B)-C(14B)	111(2)	C(12B)-C(11B)-C(10B)	122.5
C(17B)-C(15B)-C(14B)	113.7(12)	C(12B)-C(11B)-H(11B)	118.7
C(16B)-C(15B)-C(14B)	106.6(11)	C(10B)-C(11B)-H(11B)	118.7
C(13B)-C(14B)-C(1B)	116.9	C(11B)-C(12B)-C(13B)	120.8
C(13B)-C(14B)-C(15B)	122.3	C(11B)-C(12B)-C(19B)	120.3
C(1B)-C(14B)-C(15B)	120.3	C(13B)-C(12B)-C(19B)	118.9
C(2B)-C(1B)-C(14B)	124.3	C(14B)-C(13B)-C(12B)	123.8
C(2B)-C(1B)-H(1BA)	117.8	C(14B)-C(13B)-H(13B)	118.1
C(14B)-C(1B)-H(1BA)	117.8	C(12B)-C(13B)-H(13B)	118.1
C(1B)-C(2B)-C(3B)	122.6	C(12B)-C(19B)-C(2B)	109.5
C(1B)-C(2B)-C(19B)	118.7	C(12B)-C(19B)-C(20B)	105.8
C(3B)-C(2B)-C(19B)	118.6	C(2B)-C(19B)-C(20B)	102.9
C(4B)-C(3B)-C(2B)	122.5	C(12B)-C(19B)-C(21B)	113.1

C(2B)-C(19B)-C(21B)	115.8
C(20B)-C(19B)-C(21B)	108.8
C(19B)-C(20B)-H(20D)	109.5
C(19B)-C(20B)-H(20E)	109.5
H(20D)-C(20B)-H(20E)	109.5
C(19B)-C(20B)-H(20F)	109.5
H(20D)-C(20B)-H(20F)	109.5
H(20E)-C(20B)-H(20F)	109.5
C(9B)-C(21B)-C(22B)	102.4
C(9B)-C(21B)-C(5B)	113.8
C(22B)-C(21B)-C(5B)	104.4
C(9B)-C(21B)-C(19B)	114.8
C(22B)-C(21B)-C(19B)	108.6
C(5B)-C(21B)-C(19B)	111.7
N(23B)-C(22B)-C(21B)	174.3
C(15B)-C(16B)-H(16D)	109.5
C(15B)-C(16B)-H(16E)	109.5
H(16D)-C(16B)-H(16E)	109.5
C(15B)-C(16B)-H(16F)	109.5
H(16D)-C(16B)-H(16F)	109.5
H(16E)-C(16B)-H(16F)	109.5
C(15B)-C(17B)-H(17D)	109.5
C(15B)-C(17B)-H(17E)	109.5
H(17D)-C(17B)-H(17E)	109.5
C(15B)-C(17B)-H(17F)	109.5
H(17D)-C(17B)-H(17F)	109.5
H(17E)-C(17B)-H(17F)	109.5
C(15B)-C(18B)-H(18D)	109.5
C(15B)-C(18B)-H(18E)	109.5
H(18D)-C(18B)-H(18E)	109.5
C(15B)-C(18B)-H(18F)	109.5
H(18D)-C(18B)-H(18F)	109.5
H(18E)-C(18B)-H(18F)	109.5

Table A. 40 Anisotropic displacement parameters ($\text{\AA}^2 \times 10^3$) for 136 (bt1019).

	U11	U22	U33	U23	U13	U12
C(1)	42(3)	41(2)	54(3)	7(2)	10(2)	-6(2)
C(2)	38(2)	48(3)	46(2)	3(2)	11(2)	2(2)
C(3)	49(3)	47(3)	42(2)	4(2)	15(2)	2(2)
C(4)	44(3)	42(2)	35(2)	-6(2)	4(2)	5(2)
C(5)	51(3)	36(2)	42(2)	-6(2)	14(2)	0(2)
C(6)	46(3)	47(3)	58(3)	-16(2)	9(2)	-2(2)
C(7)	42(3)	51(3)	63(3)	-15(2)	16(2)	-12(2)
C(8)	56(3)	49(3)	64(3)	-8(2)	28(3)	-8(2)
C(9)	48(3)	34(2)	52(3)	-9(2)	18(2)	-3(2)
C(10)	57(3)	33(2)	52(3)	10(2)	27(2)	8(2)
C(11)	44(3)	44(3)	44(2)	6(2)	12(2)	9(2)
C(12)	39(2)	36(2)	47(2)	1(2)	8(2)	6(2)
C(13)	42(3)	51(3)	43(3)	5(2)	5(2)	11(2)
C(14)	40(2)	41(3)	60(3)	2(2)	5(2)	2(2)
C(15)	47(3)	50(3)	61(3)	4(3)	4(3)	-7(2)
C(16)	67(3)	55(3)	79(4)	-8(3)	-14(3)	-2(3)
C(17)	72(4)	117(5)	95(5)	-40(4)	31(3)	-38(4)
C(18)	66(4)	42(4)	81(5)	4(3)	-3(4)	0(3)
C(19)	44(2)	42(3)	47(3)	6(2)	12(2)	-2(2)
C(20)	57(3)	44(3)	58(3)	-3(2)	22(2)	3(2)
C(21)	51(3)	47(3)	40(2)	2(2)	13(2)	-1(2)
C(22)	57(3)	35(3)	47(3)	5(2)	16(2)	8(2)
N(23)	84(3)	40(3)	55(3)	6(2)	26(2)	8(2)

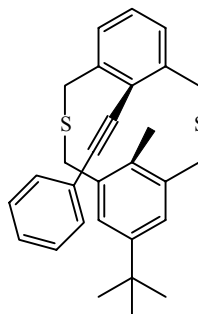
Table A. 41 Hydrogen coordinates ($\times 10^4$) and isotropic displacement parameters ($\text{\AA}^2 \times 10^3$) for 136 (bt 1019).

	x	y	z	U(eq)
H(1A)	2007	6997	5251	55
H(3A)	3164	7959	6768	55
H(4A)	4505	9409	7395	49
H(6A)	5764	11183	7087	61
H(7A)	6265	12998	6090	62
H(8A)	5347	13504	4502	65
H(10A)	3814	13072	3153	54
H(11A)	2461	11593	2540	53
H(13A)	1544	9300	2671	56
H(16A)	110	7785	2240	109
H(16B)	173	5987	2016	109
H(16C)	1041	7108	1936	109
H(17A)	-136	7244	3932	140
H(17B)	568	6023	4617	140
H(17C)	-171	5474	3608	140
H(18A)	2197	5428	3079	100
H(18B)	1314	4314	3122	100
H(18C)	1997	4981	4131	100
H(20A)	1742	12420	4844	77
H(20B)	1941	11525	5885	77
H(20C)	1245	10784	4908	77
H(1BA)	2271	7180	5552	48
H(3BA)	3549	8324	6889	48
H(4BA)	4862	9898	7281	48
H(6BA)	5943	11727	6712	48
H(7BA)	6210	13501	5552	48
H(8BA)	5080	13839	4050	48
H(10B)	3446	13206	2923	48
H(11B)	2130	11605	2556	48

H(13B)	1361	9263	2901	48
H(20D)	1374	10869	5252	60
H(20E)	1735	12529	4997	60
H(20F)	2157	11793	6077	60
H(16D)	365	7873	2543	75
H(16E)	-251	7724	3360	75
H(16F)	-180	6296	2652	75
H(17D)	283	4908	4261	75
H(17E)	394	6434	4926	75
H(17F)	1288	5276	5045	75
H(18D)	1289	4543	3130	75
H(18E)	2277	5428	3620	75
H(18F)	1605	5998	2577	75

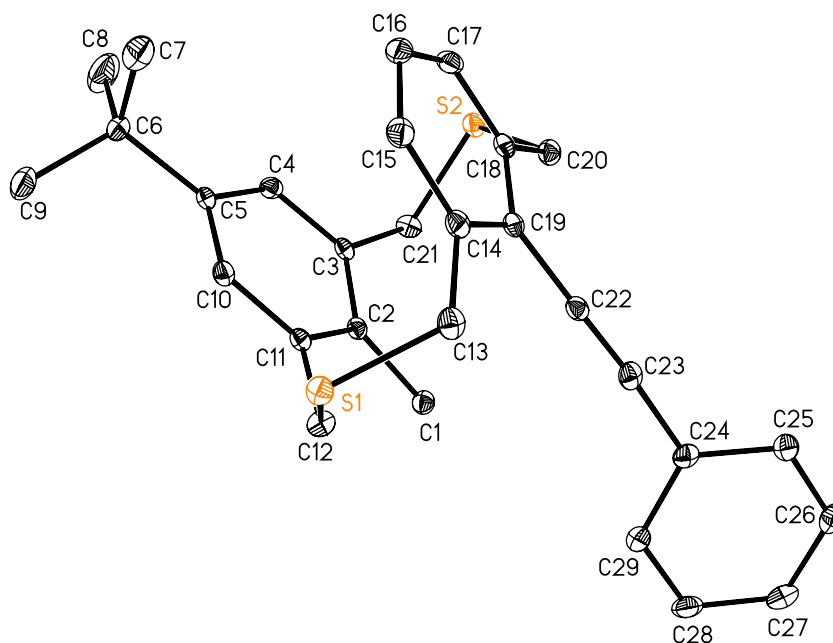
Single-Crystal X-ray Diffraction Laboratory
University of Idaho

X-ray report for *syn*-thiacyclophane 145



145

Brendan Twamley



Project name : bt830

11-29-05

Experimental:

A crystal of compound **1** was removed from the flask and covered with a layer of hydrocarbon oil. A suitable fragment was selected, attached to a MiTeGen fiber and placed in the low-temperature nitrogen stream.³⁵ Data for **1** were collected at 89(2) K using a Bruker/Siemens SMART APEX instrument (Mo K α radiation, $\lambda = 0.71073$ Å) equipped with a Cryocool NeverIce low temperature device. Data were measured using omega scans of 0.3 ° per frame for 10 seconds, and a full sphere of data was collected. A total of 2400 frames were collected with a final resolution of 0.83 Å. The first 50 frames were recollected at the end of data collection to monitor for decay. Cell parameters were retrieved using SMART³⁶ software and refined using SAINTPlus³⁷ on all observed reflections. Data reduction and correction for Lp and decay were performed using the SAINTPlus software. Absorption corrections were applied using SADABS.³⁸ The structure was solved by direct methods and refined by least squares method on F² using the SHELXTL program package.³⁹ The structure was solved in the chiral space group P2(1) (# 4) by analysis of systematic absences. All non-hydrogen atoms were refined anisotropically. No decomposition was observed during data collection. Details of the data collection and refinement are given in Table 1. Further details are provided in the Supporting Information.

Acknowledgement

³⁵ Hope, H. *Prog. Inorg. Chem.*, **1994**, *41*, 1.

³⁶ SMART: v.5.626, Bruker Molecular Analysis Research Tool, Bruker AXS, Madison, WI, **2002**.

³⁷ SAINTPlus: v. 6.45a, Data Reduction and Correction Program, Bruker AXS, Madison, WI, **2003**.

³⁸ SADABS: v.2.01, an empirical absorption correction program, Bruker AXS Inc., Madison, WI, **2004**.

³⁹ SHELXTL: v. 6.10, Structure Determination Software Suite, Sheldrick, G.M., Bruker AXS Inc., Madison, WI, **2001**.

The Bruker (Siemens) SMART APEX diffraction facility was established at the University of Idaho with the assistance of the NSF-EPSCoR program and the M. J. Murdock Charitable Trust, Vancouver, WA, USA.

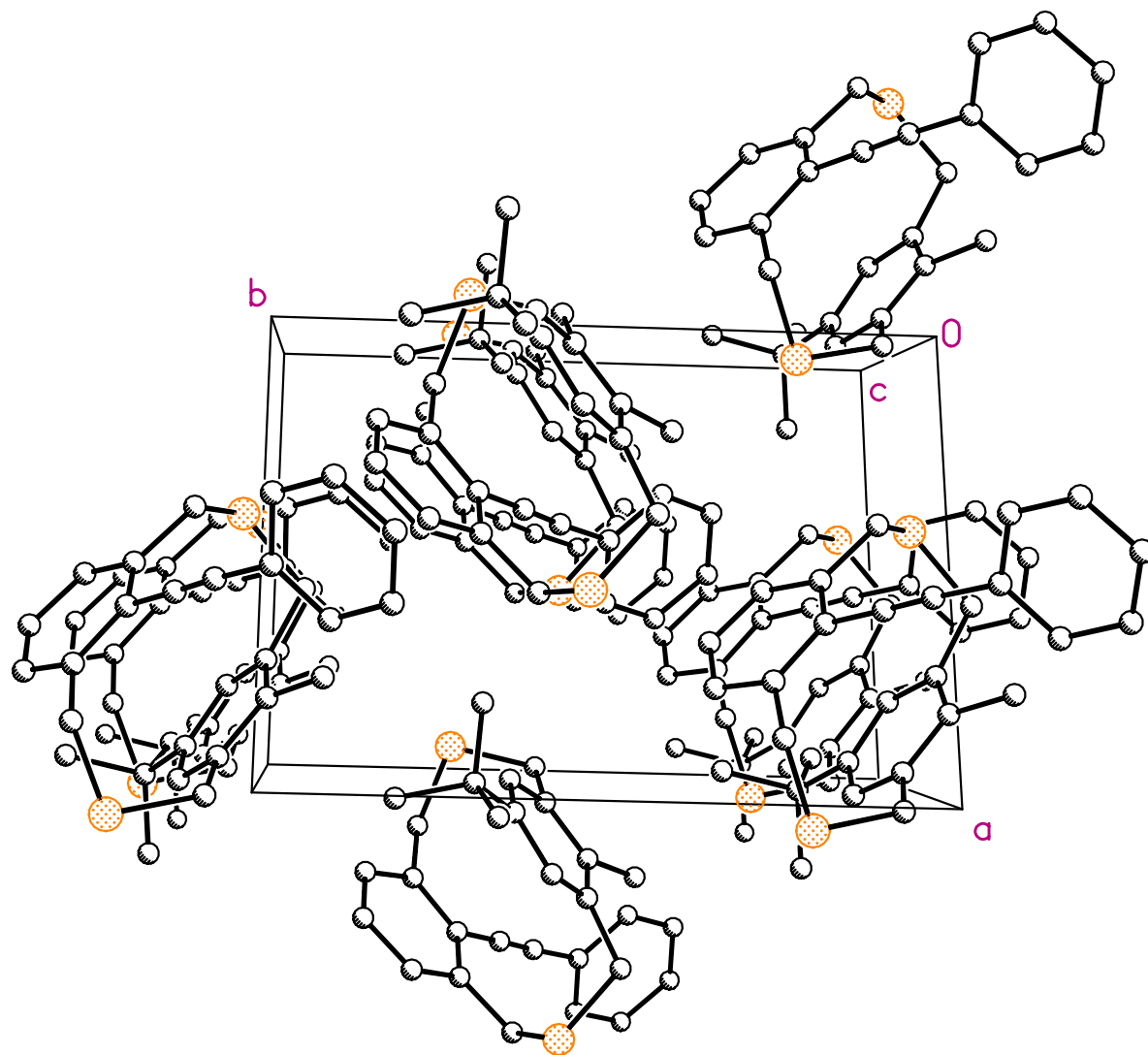


Table A. 42 Crystal data and structure refinement for 145 (C₂₉H₃₀S₂).

Identification code	bt830	
Empirical formula	C ₂₉ H ₃₀ S ₂	
Formula weight	442.65	
Temperature	89(2) K	
Wavelength	0.71073 Å	
Crystal system	Monoclinic	
Space group	P2(1)	
Unit cell dimensions	a = 9.7279(14) Å	α = 90°.
	b = 12.5775(17) Å	β = 116.703(2)°.
	c = 10.6452(15) Å	γ = 90°.
Volume	1163.6(3) Å ³	
Z	2	
Density (calculated)	1.263 Mg/m ³	
Absorption coefficient	0.243 mm ⁻¹	
F(000)	472	
Crystal size	0.36 x 0.32 x 0.22 mm ³	
Crystal color and habit	colorless needle	
Diffractometer	Bruker/Siemens SMART APEX	
Theta range for data collection	2.14 to 25.25°.	
Index ranges	-11 ≤ h ≤ 11, -15 ≤ k ≤ 15, -12 ≤ l ≤ 12	
Reflections collected	17126	
Independent reflections	4196 [R(int) = 0.0204]	
Completeness to theta = 25.25°	100.0%	
Absorption correction	Semi-empirical from equivalents	
Max. and min. transmission	0.946 and 0.914	
Solution method	XS, Bruker SHELXTL v. 6.12	
Refinement method	Full-matrix least-squares on F ²	
Data / restraints / parameters	4196 / 1 / 284	
Goodness-of-fit on F ²	1.047	
Final R indices [I > 2σ(I)]	R1 = 0.0311, wR2 = 0.0864	
R indices (all data)	R1 = 0.0313, wR2 = 0.0867	
Absolute structure parameter	0.03(5)	
Largest diff. peak and hole	0.559 and -0.212 e.Å ⁻³	

Table A. 43 Atomic coordinates ($\times 10^4$) and equivalent isotropic displacement parameters ($\text{\AA}^2 \times 10^3$) for 145 (bt 830)

	x	y	z	U(eq)
C(1)	2315(2)	4066(2)	9404(2)	19(1)
C(2)	1836(2)	4881(1)	8235(2)	16(1)
C(3)	2607(2)	4934(1)	7399(2)	17(1)
C(4)	2003(2)	5532(2)	6162(2)	18(1)
C(5)	667(2)	6126(2)	5749(2)	17(1)
C(6)	-29(2)	6775(2)	4377(2)	25(1)
C(7)	360(3)	7964(2)	4771(3)	47(1)
C(8)	612(3)	6445(3)	3369(3)	51(1)
C(9)	-1773(3)	6684(2)	3640(2)	38(1)
C(10)	21(2)	6167(2)	6679(2)	18(1)
C(11)	580(2)	5566(1)	7908(2)	16(1)
C(12)	-149(2)	5694(2)	8901(2)	20(1)
C(13)	1352(2)	7539(2)	10493(2)	22(1)
C(14)	2481(2)	7608(2)	9888(2)	20(1)
C(15)	2282(2)	8373(2)	8875(2)	24(1)
C(16)	3221(2)	8389(2)	8217(2)	23(1)
C(17)	4346(2)	7614(2)	8526(2)	23(1)
C(18)	4603(2)	6845(1)	9540(2)	19(1)
C(19)	3698(2)	6877(1)	10278(2)	17(1)
C(20)	5813(2)	5999(2)	9837(2)	22(1)
C(21)	4149(2)	4396(2)	7836(2)	21(1)
C(22)	4015(2)	6158(2)	11435(2)	18(1)
C(23)	4295(2)	5573(2)	12412(2)	20(1)
C(24)	4601(2)	4775(2)	13483(2)	19(1)
C(25)	5988(2)	4771(2)	14733(2)	25(1)
C(26)	6314(2)	3944(2)	15680(2)	27(1)
C(27)	5286(3)	3117(2)	15425(2)	27(1)
C(28)	3904(3)	3125(2)	14204(2)	30(1)
C(29)	3548(2)	3956(2)	13250(2)	25(1)
S(1)	-548(1)	7051(1)	9243(1)	20(1)
S(2)	5729(1)	5336(1)	8282(1)	21(1)

Table A. 44 Bond lengths [Å] and angles [°] for 145 (bt 830)

C(1)-C(2)	1.516(3)	C(13)-S(1)	1.832(2)
C(1)-H(1A)	0.9800	C(13)-H(13A)	0.9900
C(1)-H(1B)	0.9800	C(13)-H(13B)	0.9900
C(1)-H(1C)	0.9800	C(14)-C(15)	1.393(3)
C(2)-C(3)	1.400(3)	C(14)-C(19)	1.407(3)
C(2)-C(11)	1.405(2)	C(15)-C(16)	1.378(3)
C(3)-C(4)	1.396(3)	C(15)-H(15)	0.9500
C(3)-C(21)	1.516(3)	C(16)-C(17)	1.391(3)
C(4)-C(5)	1.388(3)	C(16)-H(16)	0.9500
C(4)-H(4)	0.9500	C(17)-C(18)	1.386(3)
C(5)-C(10)	1.392(3)	C(17)-H(17)	0.9500
C(5)-C(6)	1.539(3)	C(18)-C(19)	1.419(3)
C(6)-C(9)	1.520(3)	C(18)-C(20)	1.511(3)
C(6)-C(8)	1.521(3)	C(19)-C(22)	1.445(3)
C(6)-C(7)	1.553(4)	C(20)-S(2)	1.8230(19)
C(7)-H(7A)	0.9800	C(20)-H(20A)	0.9900
C(7)-H(7B)	0.9800	C(20)-H(20B)	0.9900
C(7)-H(7C)	0.9800	C(21)-S(2)	1.825(2)
C(8)-H(8A)	0.9800	C(21)-H(21A)	0.9900
C(8)-H(8B)	0.9800	C(21)-H(21B)	0.9900
C(8)-H(8C)	0.9800	C(22)-C(23)	1.201(3)
C(9)-H(9A)	0.9800	C(23)-C(24)	1.447(3)
C(9)-H(9B)	0.9800	C(24)-C(29)	1.394(3)
C(9)-H(9C)	0.9800	C(24)-C(25)	1.406(3)
C(10)-C(11)	1.393(3)	C(25)-C(26)	1.382(3)
C(10)-H(10)	0.9500	C(25)-H(25)	0.9500
C(11)-C(12)	1.522(2)	C(26)-C(27)	1.383(3)
C(12)-S(1)	1.8227(19)	C(26)-H(26)	0.9500
C(12)-H(12A)	0.9900	C(27)-C(28)	1.388(3)
C(12)-H(12B)	0.9900	C(27)-H(27)	0.9500
C(13)-C(14)	1.504(3)	C(28)-C(29)	1.389(3)

C(28)-H(28)	0.9500	C(6)-C(8)-H(8C)	109.5
C(29)-H(29)	0.9500	H(8A)-C(8)-H(8C)	109.5
		H(8B)-C(8)-H(8C)	109.5
C(2)-C(1)-H(1A)	109.5	C(6)-C(9)-H(9A)	109.5
C(2)-C(1)-H(1B)	109.5	C(6)-C(9)-H(9B)	109.5
H(1A)-C(1)-H(1B)	109.5	H(9A)-C(9)-H(9B)	109.5
C(2)-C(1)-H(1C)	109.5	C(6)-C(9)-H(9C)	109.5
H(1A)-C(1)-H(1C)	109.5	H(9A)-C(9)-H(9C)	109.5
H(1B)-C(1)-H(1C)	109.5	H(9B)-C(9)-H(9C)	109.5
C(3)-C(2)-C(11)	117.94(16)	C(11)-C(10)-C(5)	122.53(17)
C(3)-C(2)-C(1)	119.98(16)	C(11)-C(10)-H(10)	118.7
C(11)-C(2)-C(1)	122.01(16)	C(5)-C(10)-H(10)	118.7
C(4)-C(3)-C(2)	120.45(16)	C(10)-C(11)-C(2)	119.61(16)
C(4)-C(3)-C(21)	117.95(16)	C(10)-C(11)-C(12)	119.19(16)
C(2)-C(3)-C(21)	121.53(16)	C(2)-C(11)-C(12)	121.16(16)
C(5)-C(4)-C(3)	121.71(17)	C(11)-C(12)-S(1)	116.42(13)
C(5)-C(4)-H(4)	119.1	C(11)-C(12)-H(12A)	108.2
C(3)-C(4)-H(4)	119.1	S(1)-C(12)-H(12A)	108.2
C(4)-C(5)-C(10)	116.92(16)	C(11)-C(12)-H(12B)	108.2
C(4)-C(5)-C(6)	122.39(16)	S(1)-C(12)-H(12B)	108.2
C(10)-C(5)-C(6)	120.57(17)	H(12A)-C(12)-H(12B)	107.3
C(9)-C(6)-C(8)	109.4(2)	C(14)-C(13)-S(1)	113.61(13)
C(9)-C(6)-C(5)	111.25(17)	C(14)-C(13)-H(13A)	108.8
C(8)-C(6)-C(5)	112.30(18)	S(1)-C(13)-H(13A)	108.8
C(9)-C(6)-C(7)	107.0(2)	C(14)-C(13)-H(13B)	108.8
C(8)-C(6)-C(7)	109.0(2)	S(1)-C(13)-H(13B)	108.8
C(5)-C(6)-C(7)	107.73(17)	H(13A)-C(13)-H(13B)	107.7
C(6)-C(7)-H(7A)	109.5	C(15)-C(14)-C(19)	119.00(18)
C(6)-C(7)-H(7B)	109.5	C(15)-C(14)-C(13)	119.81(18)
H(7A)-C(7)-H(7B)	109.5	C(19)-C(14)-C(13)	121.12(17)
C(6)-C(7)-H(7C)	109.5	C(16)-C(15)-C(14)	120.71(19)
H(7A)-C(7)-H(7C)	109.5	C(16)-C(15)-H(15)	119.6
H(7B)-C(7)-H(7C)	109.5	C(14)-C(15)-H(15)	119.6
C(6)-C(8)-H(8A)	109.5	C(15)-C(16)-C(17)	120.05(18)
C(6)-C(8)-H(8B)	109.5	C(15)-C(16)-H(16)	120.0
H(8A)-C(8)-H(8B)	109.5	C(17)-C(16)-H(16)	120.0

C(18)-C(17)-C(16)	121.36(18)	C(29)-C(28)-H(28)	119.7
C(18)-C(17)-H(17)	119.3	C(27)-C(28)-H(28)	119.7
C(16)-C(17)-H(17)	119.3	C(28)-C(29)-C(24)	120.23(19)
C(17)-C(18)-C(19)	118.17(17)	C(28)-C(29)-H(29)	119.9
C(17)-C(18)-C(20)	120.35(17)	C(24)-C(29)-H(29)	119.9
C(19)-C(18)-C(20)	121.49(17)	C(12)-S(1)-C(13)	102.90(9)
C(14)-C(19)-C(18)	120.32(17)	C(20)-S(2)-C(21)	102.79(9)
C(14)-C(19)-C(22)	119.24(17)		
C(18)-C(19)-C(22)	120.44(17)		
C(18)-C(20)-S(2)	114.78(13)		
C(18)-C(20)-H(20A)	108.6		
S(2)-C(20)-H(20A)	108.6		
C(18)-C(20)-H(20B)	108.6		
S(2)-C(20)-H(20B)	108.6		
H(20A)-C(20)-H(20B)	107.5		
C(3)-C(21)-S(2)	113.12(13)		
C(3)-C(21)-H(21A)	109.0		
S(2)-C(21)-H(21A)	109.0		
C(3)-C(21)-H(21B)	109.0		
S(2)-C(21)-H(21B)	109.0		
H(21A)-C(21)-H(21B)	107.8		
C(23)-C(22)-C(19)	178.9(2)		
C(22)-C(23)-C(24)	173.82(19)		
C(29)-C(24)-C(25)	118.84(18)		
C(29)-C(24)-C(23)	119.83(18)		
C(25)-C(24)-C(23)	121.23(17)		
C(26)-C(25)-C(24)	120.06(19)		
C(26)-C(25)-H(25)	120.0		
C(24)-C(25)-H(25)	120.0		
C(25)-C(26)-C(27)	120.92(19)		
C(25)-C(26)-H(26)	119.5		
C(27)-C(26)-H(26)	119.5		
C(26)-C(27)-C(28)	119.31(19)		
C(26)-C(27)-H(27)	120.3		
C(28)-C(27)-H(27)	120.3		
C(29)-C(28)-C(27)	120.6(2)		

Table A. 45 Anisotropic displacement parameters ($\text{\AA}^2 \times 10^3$) for 145 (bt 830).

	U11	U22	U33	U23	U13	U12
C(1)	21(1)	18(1)	18(1)	0(1)	7(1)	0(1)
C(2)	15(1)	15(1)	16(1)	-2(1)	5(1)	-2(1)
C(3)	14(1)	17(1)	17(1)	-4(1)	4(1)	-4(1)
C(4)	20(1)	20(1)	17(1)	-2(1)	10(1)	-3(1)
C(5)	14(1)	19(1)	14(1)	-2(1)	3(1)	-5(1)
C(6)	21(1)	34(1)	18(1)	7(1)	7(1)	-1(1)
C(7)	44(1)	44(2)	38(1)	15(1)	5(1)	-4(1)
C(8)	47(2)	81(2)	29(1)	18(1)	20(1)	14(1)
C(9)	29(1)	59(2)	23(1)	15(1)	10(1)	6(1)
C(10)	14(1)	21(1)	18(1)	0(1)	5(1)	1(1)
C(11)	14(1)	16(1)	16(1)	-3(1)	5(1)	-3(1)
C(12)	25(1)	17(1)	21(1)	0(1)	12(1)	2(1)
C(13)	22(1)	24(1)	20(1)	-5(1)	9(1)	1(1)
C(14)	20(1)	18(1)	18(1)	-6(1)	7(1)	-4(1)
C(15)	25(1)	18(1)	23(1)	-1(1)	7(1)	-1(1)
C(16)	28(1)	17(1)	21(1)	1(1)	8(1)	-6(1)
C(17)	24(1)	23(1)	22(1)	-4(1)	11(1)	-10(1)
C(18)	18(1)	19(1)	17(1)	-5(1)	5(1)	-7(1)
C(19)	19(1)	17(1)	14(1)	-5(1)	5(1)	-6(1)
C(20)	21(1)	26(1)	18(1)	-3(1)	8(1)	-2(1)
C(21)	21(1)	18(1)	26(1)	-2(1)	13(1)	0(1)
C(22)	17(1)	17(1)	18(1)	-5(1)	7(1)	-4(1)
C(23)	22(1)	22(1)	17(1)	-6(1)	9(1)	0(1)
C(24)	26(1)	19(1)	18(1)	-4(1)	14(1)	0(1)
C(25)	27(1)	25(1)	21(1)	-2(1)	10(1)	-5(1)
C(26)	27(1)	33(1)	18(1)	3(1)	8(1)	5(1)
C(27)	38(1)	25(1)	27(1)	6(1)	22(1)	3(1)
C(28)	40(1)	29(1)	28(1)	0(1)	22(1)	-11(1)
C(29)	26(1)	31(1)	18(1)	-2(1)	10(1)	-6(1)
S(1)	18(1)	22(1)	20(1)	0(1)	10(1)	4(1)
S(2)	16(1)	28(1)	20(1)	-3(1)	10(1)	-1(1)

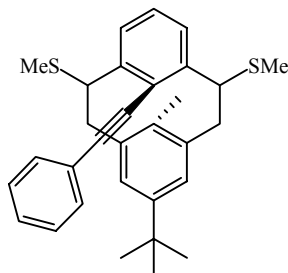
Table A. 46 Hydrogen coordinates ($\times 10^4$) and isotropic displacement parameters ($\text{\AA}^2 \times 10^3$) for 145 (bt 830).

	x	y	z	U(eq)
H(1A)	2367	3362	9034	29
H(1B)	1559	4054	9777	29
H(1C)	3327	4255	10158	29
H(4)	2519	5532	5587	22
H(7A)	-69	8187	5404	70
H(7B)	-85	8398	3916	70
H(7C)	1480	8057	5242	70
H(8A)	1730	6549	3821	77
H(8B)	142	6879	2515	77
H(8C)	378	5693	3122	77
H(9A)	-2065	5942	3368	57
H(9B)	-2187	7133	2798	57
H(9C)	-2190	6917	4278	57
H(10)	-834	6623	6467	22
H(12A)	542	5361	9811	24
H(12B)	-1128	5291	8508	24
H(13A)	1235	8254	10823	27
H(13B)	1776	7061	11320	27
H(15)	1491	8889	8635	28
H(16)	3100	8930	7553	28
H(17)	4951	7611	8031	27
H(20A)	5705	5456	10461	26
H(20B)	6841	6329	10354	26
H(21A)	4086	3935	7058	25
H(21B)	4371	3936	8659	25
H(25)	6701	5337	14927	30
H(26)	7257	3945	16519	32

H(27)	5524	2549	16077	33
H(28)	3195	2557	14020	36
H(29)	2582	3967	12434	30

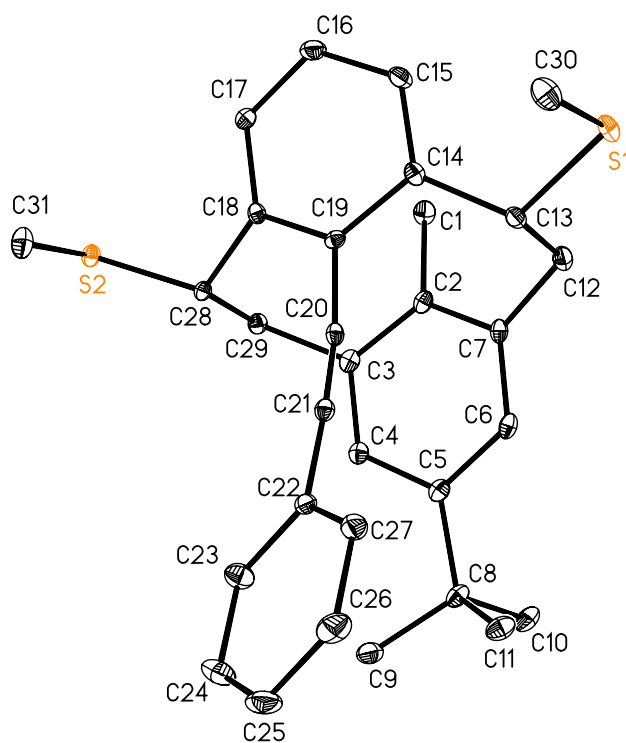
Single-Crystal X-ray Diffraction Laboratory University of Idaho

X-ray structure report for thiomethylcyclophane 146



146

Brendan Twamley



Project name : bt958

8-20-06

Experimental:

Crystals of compound **1** were removed from the flask, a suitable crystal was selected, attached to a MiTeGen fiber and data were collected at 90(2) K using a Bruker/Siemens SMART APEX instrument (Mo K α radiation, $\lambda = 0.71073$ Å) equipped with a Cryocool NeverIce low temperature device. Data were measured using omega scans of 0.3 ° per frame for 10 seconds, and a full sphere of data was collected. A total of 2400 frames were collected with a final resolution of 0.83 Å. Cell parameters were retrieved using SMART⁴⁰ software and refined using SAINTPlus⁴¹ on all observed reflections. Data reduction and correction for Lp and decay were performed using the SAINTPlus software. Absorption corrections were applied using SADABS.⁴² The structure was solved by direct methods and refined by least squares method on F² using the SHELXTL program package.⁴³ The structure was solved in the space group P2(1)/c (# 14) by analysis of systematic absences. All non-hydrogen atoms were refined anisotropically. No decomposition was observed during data collection. Details of the data collection and refinement are given in Table 1. Further details are provided in the Supporting Information.

Acknowledgement

The Bruker (Siemens) SMART APEX diffraction facility was established at the University of Idaho with the assistance of the NSF-EPSCoR program and the M. J. Murdock Charitable Trust, Vancouver, WA, USA.

⁴⁰ SMART: v.5.630, Bruker Molecular Analysis Research Tool, Bruker AXS, Madison, WI, **2001**.

⁴¹ SAINTPlus: v. 7.23a, Data Reduction and Correction Program, Bruker AXS, Madison, WI, **2004**.

⁴² SADABS: v.2004/1, an empirical absorption correction program, Bruker AXS Inc., Madison, WI, **2004**.

⁴³ SHELXTL: v. 6.14, Structure Determination Software Suite, Sheldrick, G.M., Bruker AXS Inc., Madison, WI, **2004**.

Table A. 47 Crystal data and structure refinement for 146 (C₃₁H₃₄S₂)

Identification code	bt958	
Empirical formula	C ₃₁ H ₃₄ S ₂	
Formula weight	470.70	
Temperature	90(2) K	
Wavelength	0.71073 Å	
Crystal system	Monoclinic	
Space group	P2(1)/c	
Unit cell dimensions	a = 12.1876(19) Å	α = 90°.
	b = 21.210(3) Å	β = 110.925(2)°.
	c = 10.6355(17) Å	γ = 90°.
Volume	2567.9(7) Å ³	
Z	4	
Density (calculated)	1.218 Mg/m ³	
Absorption coefficient	0.225 mm ⁻¹	
F(000)	1008	
Crystal size	0.50 x 0.43 x 0.09 mm ³	
Crystal color and habit	colorless plate	
Diffractometer	Bruker/Siemens SMART APEX	
Theta range for data collection	1.79 to 25.25°.	
Index ranges	-14 ≤ h ≤ 14, -25 ≤ k ≤ 25, -12 ≤ l ≤ 12	
Reflections collected	37760	
Independent reflections	4658 [R(int) = 0.0331]	
Completeness to theta = 25.25°	100.0%	
Absorption correction	Semi-empirical from equivalents	
Max. and min. transmission	0.9801 and 0.8960	
Solution method	Bruker, 2003; XS, SHELXTL v. 6.14	
Refinement method	Full-matrix least-squares on F ²	
Data / restraints / parameters	4658 / 0 / 304	
Goodness-of-fit on F ²	1.086	
Final R indices [I > 2σ(I)]	R1 = 0.0380, wR2 = 0.0904	
R indices (all data)	R1 = 0.0414, wR2 = 0.0924	
Largest diff. peak and hole	0.434 and -0.221 e.Å ⁻³	

Table A. 48 Atomic coordinates ($\times 10^4$) and equivalent isotropic displacement parameters ($\text{\AA}^2 \times 10^3$) for 146 (bt 958).

	x	y	z	U(eq)
C(1)	6564(2)	6329(1)	-404(2)	20(1)
C(2)	6872(1)	5874(1)	766(2)	16(1)
C(3)	5999(1)	5573(1)	1119(2)	15(1)
C(4)	6286(1)	5047(1)	1963(2)	16(1)
C(5)	7433(1)	4824(1)	2532(2)	16(1)
C(6)	8310(1)	5209(1)	2376(2)	16(1)
C(7)	8052(1)	5740(1)	1554(2)	16(1)
C(8)	7756(1)	4200(1)	3301(2)	19(1)
C(9)	6731(2)	3911(1)	3616(2)	24(1)
C(10)	8124(2)	3731(1)	2423(2)	23(1)
C(11)	8790(2)	4287(1)	4642(2)	22(1)
C(12)	8996(1)	6229(1)	1703(2)	18(1)
C(13)	8995(1)	6741(1)	2772(2)	16(1)
C(14)	7814(1)	7068(1)	2406(2)	15(1)
C(15)	7509(2)	7608(1)	1622(2)	19(1)
C(16)	6350(2)	7814(1)	1121(2)	21(1)
C(17)	5465(1)	7439(1)	1253(2)	17(1)
C(18)	5734(1)	6888(1)	2006(2)	14(1)
C(19)	6929(1)	6755(1)	2733(2)	13(1)
C(20)	7236(1)	6308(1)	3814(2)	13(1)
C(21)	7456(1)	6010(1)	4833(2)	14(1)
C(22)	7653(1)	5664(1)	6047(2)	14(1)
C(23)	6805(2)	5243(1)	6132(2)	22(1)
C(24)	6990(2)	4904(1)	7299(2)	30(1)
C(25)	8013(2)	4983(1)	8399(2)	29(1)
C(26)	8853(2)	5407(1)	8335(2)	27(1)
C(27)	8678(2)	5745(1)	7166(2)	20(1)
C(28)	4830(1)	6378(1)	1897(2)	14(1)
C(29)	4808(1)	5880(1)	795(2)	16(1)
C(30)	10178(2)	7743(1)	4338(2)	25(1)

C(31)	3479(2)	7074(1)	2992(2)	26(1)
S(1)	10221(1)	7267(1)	2956(1)	19(1)
S(2)	3334(1)	6666(1)	1457(1)	16(1)

Table A. 49 Bond lengths [Å] and angles [°] for 146 (bt 958)

C(1)-C(2)	1.512(2)	C(12)-H(12A)	0.9900
C(1)-H(1A)	0.9800	C(12)-H(12B)	0.9900
C(1)-H(1B)	0.9800	C(13)-C(14)	1.517(2)
C(1)-H(1C)	0.9800	C(13)-S(1)	1.8187(16)
C(2)-C(3)	1.402(2)	C(13)-H(13)	1.0000
C(2)-C(7)	1.412(2)	C(14)-C(15)	1.388(2)
C(3)-C(4)	1.397(2)	C(14)-C(19)	1.411(2)
C(3)-C(29)	1.514(2)	C(15)-C(16)	1.389(2)
C(4)-C(5)	1.392(2)	C(15)-H(15)	0.9500
C(4)-H(4)	0.9500	C(16)-C(17)	1.387(2)
C(5)-C(6)	1.401(2)	C(16)-H(16)	0.9500
C(5)-C(8)	1.532(2)	C(17)-C(18)	1.388(2)
C(6)-C(7)	1.390(2)	C(17)-H(17)	0.9500
C(6)-H(6)	0.9500	C(18)-C(19)	1.413(2)
C(7)-C(12)	1.515(2)	C(18)-C(28)	1.520(2)
C(8)-C(9)	1.532(2)	C(19)-C(20)	1.434(2)
C(8)-C(10)	1.537(2)	C(20)-C(21)	1.199(2)
C(8)-C(11)	1.541(2)	C(21)-C(22)	1.429(2)
C(9)-H(9A)	0.9800	C(22)-C(23)	1.393(2)
C(9)-H(9B)	0.9800	C(22)-C(27)	1.394(2)
C(9)-H(9C)	0.9800	C(23)-C(24)	1.382(2)
C(10)-H(10A)	0.9800	C(23)-H(23)	0.9500
C(10)-H(10B)	0.9800	C(24)-C(25)	1.382(3)
C(10)-H(10C)	0.9800	C(24)-H(24)	0.9500
C(11)-H(11A)	0.9800	C(25)-C(26)	1.381(3)
C(11)-H(11B)	0.9800	C(25)-H(25)	0.9500
C(11)-H(11C)	0.9800	C(26)-C(27)	1.385(2)
C(12)-C(13)	1.573(2)	C(26)-H(26)	0.9500

C(27)-H(27)	0.9500	C(6)-C(7)-C(2)	119.35(15)
C(28)-C(29)	1.570(2)	C(6)-C(7)-C(12)	119.71(14)
C(28)-S(2)	1.8185(15)	C(2)-C(7)-C(12)	119.93(14)
C(28)-H(28)	1.0000	C(9)-C(8)-C(5)	112.84(13)
C(29)-H(29A)	0.9900	C(9)-C(8)-C(10)	108.16(14)
C(29)-H(29B)	0.9900	C(5)-C(8)-C(10)	108.09(13)
C(30)-S(1)	1.7993(18)	C(9)-C(8)-C(11)	107.85(14)
C(30)-H(30A)	0.9800	C(5)-C(8)-C(11)	111.13(13)
C(30)-H(30B)	0.9800	C(10)-C(8)-C(11)	108.67(13)
C(30)-H(30C)	0.9800	C(8)-C(9)-H(9A)	109.5
C(31)-S(2)	1.7993(18)	C(8)-C(9)-H(9B)	109.5
C(31)-H(31A)	0.9800	H(9A)-C(9)-H(9B)	109.5
C(31)-H(31B)	0.9800	C(8)-C(9)-H(9C)	109.5
C(31)-H(31C)	0.9800	H(9A)-C(9)-H(9C)	109.5
		H(9B)-C(9)-H(9C)	109.5
C(2)-C(1)-H(1A)	109.5	C(8)-C(10)-H(10A)	109.5
C(2)-C(1)-H(1B)	109.5	C(8)-C(10)-H(10B)	109.5
H(1A)-C(1)-H(1B)	109.5	H(10A)-C(10)-H(10B)	109.5
C(2)-C(1)-H(1C)	109.5	C(8)-C(10)-H(10C)	109.5
H(1A)-C(1)-H(1C)	109.5	H(10A)-C(10)-H(10C)	109.5
H(1B)-C(1)-H(1C)	109.5	H(10B)-C(10)-H(10C)	109.5
C(3)-C(2)-C(7)	117.34(14)	C(8)-C(11)-H(11A)	109.5
C(3)-C(2)-C(1)	121.47(14)	C(8)-C(11)-H(11B)	109.5
C(7)-C(2)-C(1)	121.19(14)	H(11A)-C(11)-H(11B)	109.5
C(4)-C(3)-C(2)	119.75(14)	C(8)-C(11)-H(11C)	109.5
C(4)-C(3)-C(29)	119.32(14)	H(11A)-C(11)-H(11C)	109.5
C(2)-C(3)-C(29)	120.06(14)	H(11B)-C(11)-H(11C)	109.5
C(5)-C(4)-C(3)	122.15(15)	C(7)-C(12)-C(13)	110.61(12)
C(5)-C(4)-H(4)	118.9	C(7)-C(12)-H(12A)	109.5
C(3)-C(4)-H(4)	118.9	C(13)-C(12)-H(12A)	109.5
C(4)-C(5)-C(6)	116.20(14)	C(7)-C(12)-H(12B)	109.5
C(4)-C(5)-C(8)	123.44(14)	C(13)-C(12)-H(12B)	109.5
C(6)-C(5)-C(8)	120.36(14)	H(12A)-C(12)-H(12B)	108.1
C(7)-C(6)-C(5)	122.36(15)	C(14)-C(13)-C(12)	112.09(13)
C(7)-C(6)-H(6)	118.8	C(14)-C(13)-S(1)	114.54(11)
C(5)-C(6)-H(6)	118.8	C(12)-C(13)-S(1)	106.73(10)

C(14)-C(13)-H(13)	107.7	C(25)-C(26)-H(26)	119.9
C(12)-C(13)-H(13)	107.7	C(27)-C(26)-H(26)	119.9
S(1)-C(13)-H(13)	107.7	C(26)-C(27)-C(22)	120.33(16)
C(15)-C(14)-C(19)	118.16(14)	C(26)-C(27)-H(27)	119.8
C(15)-C(14)-C(13)	123.87(14)	C(22)-C(27)-H(27)	119.8
C(19)-C(14)-C(13)	117.40(14)	C(18)-C(28)-C(29)	110.74(12)
C(14)-C(15)-C(16)	120.46(15)	C(18)-C(28)-S(2)	114.38(11)
C(14)-C(15)-H(15)	119.8	C(29)-C(28)-S(2)	106.62(10)
C(16)-C(15)-H(15)	119.8	C(18)-C(28)-H(28)	108.3
C(17)-C(16)-C(15)	120.16(15)	C(29)-C(28)-H(28)	108.3
C(17)-C(16)-H(16)	119.9	S(2)-C(28)-H(28)	108.3
C(15)-C(16)-H(16)	119.9	C(3)-C(29)-C(28)	111.08(12)
C(16)-C(17)-C(18)	120.57(15)	C(3)-C(29)-H(29A)	109.4
C(16)-C(17)-H(17)	119.7	C(28)-C(29)-H(29A)	109.4
C(18)-C(17)-H(17)	119.7	C(3)-C(29)-H(29B)	109.4
C(17)-C(18)-C(19)	118.00(14)	C(28)-C(29)-H(29B)	109.4
C(17)-C(18)-C(28)	122.72(14)	H(29A)-C(29)-H(29B)	108.0
C(19)-C(18)-C(28)	118.48(13)	S(1)-C(30)-H(30A)	109.5
C(14)-C(19)-C(18)	120.02(14)	S(1)-C(30)-H(30B)	109.5
C(14)-C(19)-C(20)	120.37(14)	H(30A)-C(30)-H(30B)	109.5
C(18)-C(19)-C(20)	119.60(14)	S(1)-C(30)-H(30C)	109.5
C(21)-C(20)-C(19)	169.68(16)	H(30A)-C(30)-H(30C)	109.5
C(20)-C(21)-C(22)	176.74(16)	H(30B)-C(30)-H(30C)	109.5
C(23)-C(22)-C(27)	118.95(15)	S(2)-C(31)-H(31A)	109.5
C(23)-C(22)-C(21)	119.87(14)	S(2)-C(31)-H(31B)	109.5
C(27)-C(22)-C(21)	121.17(15)	H(31A)-C(31)-H(31B)	109.5
C(24)-C(23)-C(22)	120.29(16)	S(2)-C(31)-H(31C)	109.5
C(24)-C(23)-H(23)	119.9	H(31A)-C(31)-H(31C)	109.5
C(22)-C(23)-H(23)	119.9	H(31B)-C(31)-H(31C)	109.5
C(25)-C(24)-C(23)	120.41(17)	C(30)-S(1)-C(13)	99.74(8)
C(25)-C(24)-H(24)	119.8	C(31)-S(2)-C(28)	99.45(8)
C(23)-C(24)-H(24)	119.8		
C(26)-C(25)-C(24)	119.83(16)		
C(26)-C(25)-H(25)	120.1		
C(24)-C(25)-H(25)	120.1		
C(25)-C(26)-C(27)	120.18(17)		

Table A. 50 Anisotropic displacement parameters ($\text{\AA}^2 \times 10^3$) for 146 (bt 958).

	U11	U22	U33	U23	U13	U12
C(1)	19(1)	27(1)	14(1)	1(1)	5(1)	2(1)
C(2)	18(1)	17(1)	14(1)	-4(1)	5(1)	2(1)
C(3)	14(1)	17(1)	12(1)	-5(1)	1(1)	0(1)
C(4)	15(1)	15(1)	16(1)	-4(1)	5(1)	-1(1)
C(5)	17(1)	15(1)	14(1)	-5(1)	4(1)	1(1)
C(6)	13(1)	20(1)	15(1)	-5(1)	3(1)	3(1)
C(7)	16(1)	20(1)	15(1)	-5(1)	8(1)	1(1)
C(8)	16(1)	17(1)	19(1)	-1(1)	1(1)	2(1)
C(9)	23(1)	20(1)	26(1)	5(1)	5(1)	1(1)
C(10)	21(1)	18(1)	26(1)	-4(1)	3(1)	4(1)
C(11)	22(1)	19(1)	20(1)	1(1)	0(1)	3(1)
C(12)	16(1)	23(1)	18(1)	1(1)	8(1)	1(1)
C(13)	13(1)	19(1)	16(1)	3(1)	6(1)	-2(1)
C(14)	14(1)	18(1)	13(1)	-1(1)	4(1)	-2(1)
C(15)	18(1)	19(1)	21(1)	3(1)	7(1)	-4(1)
C(16)	22(1)	17(1)	22(1)	6(1)	6(1)	1(1)
C(17)	15(1)	18(1)	18(1)	3(1)	5(1)	3(1)
C(18)	15(1)	15(1)	12(1)	-1(1)	6(1)	0(1)
C(19)	16(1)	11(1)	12(1)	-1(1)	5(1)	1(1)
C(20)	11(1)	14(1)	15(1)	-3(1)	5(1)	-1(1)
C(21)	13(1)	15(1)	15(1)	-2(1)	6(1)	0(1)
C(22)	17(1)	14(1)	13(1)	1(1)	7(1)	3(1)
C(23)	23(1)	22(1)	20(1)	1(1)	6(1)	-3(1)
C(24)	37(1)	25(1)	30(1)	6(1)	17(1)	-7(1)
C(25)	43(1)	26(1)	21(1)	10(1)	14(1)	6(1)
C(26)	28(1)	31(1)	17(1)	4(1)	2(1)	7(1)
C(27)	19(1)	22(1)	20(1)	2(1)	6(1)	0(1)
C(28)	10(1)	15(1)	14(1)	2(1)	3(1)	2(1)
C(29)	14(1)	17(1)	15(1)	0(1)	3(1)	1(1)

C(30)	25(1)	30(1)	21(1)	-3(1)	8(1)	-7(1)
C(31)	22(1)	30(1)	27(1)	-7(1)	11(1)	2(1)
S(1)	14(1)	24(1)	20(1)	0(1)	7(1)	-5(1)
S(2)	12(1)	18(1)	18(1)	1(1)	4(1)	2(1)

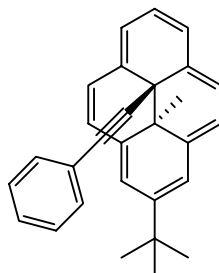
Table A. 51 Hydrogen coordinates ($\times 10^4$) and isotropic displacement parameters ($\text{\AA}^2 \times 10^3$) for 146 (bt 958).

	x	y	z	U(eq)
H(1A)	6415	6747	-108	31
H(1B)	5859	6180	-1130	31
H(1C)	7219	6354	-731	31
H(4)	5679	4834	2156	19
H(6)	9110	5104	2850	20
H(9A)	6983	3515	4106	36
H(9B)	6075	3829	2773	36
H(9C)	6477	4205	4169	36
H(10A)	8749	3917	2166	35
H(10B)	7446	3634	1611	35
H(10C)	8411	3342	2932	35
H(11A)	9492	4414	4461	33
H(11B)	8943	3888	5141	33
H(11C)	8592	4613	5179	33
H(12A)	8856	6434	824	22
H(12B)	9774	6021	1990	22
H(13)	9157	6522	3653	19
H(15)	8096	7839	1427	23
H(16)	6164	8212	688	25
H(17)	4667	7560	823	21
H(23)	6095	5189	5384	27
H(24)	6411	4614	7346	35
H(25)	8138	4747	9198	35

H(26)	9552	5466	9094	32
H(27)	9260	6035	7126	24
H(28)	5056	6156	2784	16
H(29A)	4215	5552	741	19
H(29B)	4578	6090	-93	19
H(30A)	9441	7981	4060	38
H(30B)	10843	8036	4608	38
H(30C)	10228	7470	5100	38
H(31A)	3764	6781	3751	38
H(31B)	2712	7242	2932	38
H(31C)	4038	7422	3127	38

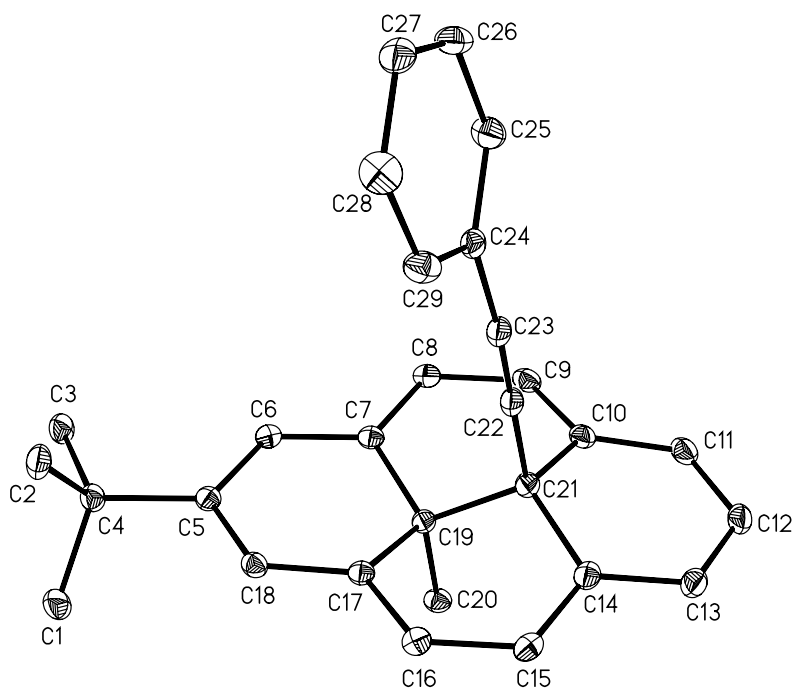
Single-Crystal X-ray Diffraction Laboratory
University of Idaho

X-ray structure report for phenylethynyl DHP 139



139

Brendan Twamley



Project name : bt914

6-10-06

Experimental:

Crystals of compound **1** were removed from the flask, a suitable crystal was selected, attached to a glass fiber and data were collected at 89(2) K using a Bruker/Siemens SMART APEX instrument (Mo K α radiation, $\lambda = 0.71073$ Å) equipped with a Cryocool NeverIce low temperature device. Data were measured using omega scans of 0.3 ° per frame for 30 seconds, and a full sphere of data was collected. A total of 2400 frames were collected with a final resolution of 0.83 Å. Cell parameters were retrieved using SMART⁴⁴ software and refined using SAINTPlus⁴⁵ on all observed reflections. Data reduction and correction for Lp and decay were performed using the SAINTPlus software. Absorption corrections were applied using SADABS.⁴⁶ The structure was solved by direct methods and refined by least squares method on F² using the SHELXTL program package.⁴⁷ The structure was solved in the space group Pbc_a (# 61) by analysis of systematic absences. All non-hydrogen atoms were refined anisotropically. No decomposition was observed during data collection. Details of the data collection and refinement are given in Table 1. Further details are provided in the Supporting Information.

Acknowledgement

The Bruker (Siemens) SMART APEX diffraction facility was established at the University of Idaho with the assistance of the NSF-EPSCoR program and the M. J. Murdock Charitable Trust, Vancouver, WA, USA.

⁴⁴ SMART: v.5.630, Bruker Molecular Analysis Research Tool, Bruker AXS, Madison, WI, **2001**.

⁴⁵ SAINTPlus: v. 7.23a, Data Reduction and Correction Program, Bruker AXS, Madison, WI, **2004**.

⁴⁶ SADABS: v.2004/1, an empirical absorption correction program, Bruker AXS Inc., Madison, WI, **2004**.

⁴⁷ SHELXTL: v. 6.14, Structure Determination Software Suite, Sheldrick, G.M., Bruker AXS Inc., Madison, WI, **2004**.

Table A. 52 Crystal data and structure refinement for 139

Identification code	bt914	
Empirical formula	C ₂₉ H ₂₆	
Formula weight	374.50	
Temperature	89(2) K	
Wavelength	0.71073 Å	
Crystal system	Orthorhomibc	
Space group	Pbca	
Unit cell dimensions	a = 15.3244(16) Å	α = 90°.
	b = 13.3476(14) Å	β = 90°.
	c = 20.633(2) Å	γ = 90°.
Volume	4220.4(7) Å ³	
Z	8	
Density (calculated)	1.179 Mg/m ³	
Absorption coefficient	0.066 mm ⁻¹	
F(000)	1600	
Crystal size	0.55 x 0.26 x 0.04 mm ³	
Crystal color and habit	greenplate	
Diffractometer	Bruker/Siemens SMART APEX	
Theta range for data collection	1.97 to 25.24°.	
Index ranges	-18<=h<=18, -16<=k<=16, -24<=l<=24	
Reflections collected	62517	
Independent reflections	3818 [R(int) = 0.0380]	
Completeness to theta = 25.24°	100.0%	
Absorption correction	Semi-empirical from equivalents	
Max. and min. transmission	0.9974 and 0.9644	
Solution method	Bruker, 2003; XS, SHELXTL v. 6.14	
Refinement method	Full-matrix least-squares on F ²	
Data / restraints / parameters	3818 / 0 / 266	
Goodness-of-fit on F ²	1.033	
Final R indices [I>2sigma(I)]	R1 = 0.0390, wR2 = 0.0926	
R indices (all data)	R1 = 0.0463, wR2 = 0.0973	
Largest diff. peak and hole	0.277 and -0.170 e.Å ⁻³	

Table A. 53 Atomic coordinates ($\times 10^4$) and equivalent isotropic displacement parameters ($\text{\AA}^2 \times 10^3$) for 139 (bt 914).

	x	y	z	U(eq)
C(1)	4199(1)	6279(1)	4972(1)	31(1)
C(2)	4701(1)	5679(1)	3881(1)	28(1)
C(3)	4870(1)	7467(1)	4184(1)	27(1)
C(4)	4277(1)	6548(1)	4250(1)	23(1)
C(5)	3359(1)	6732(1)	3979(1)	19(1)
C(6)	3133(1)	7615(1)	3664(1)	19(1)
C(7)	2295(1)	7798(1)	3423(1)	19(1)
C(8)	2063(1)	8648(1)	3076(1)	22(1)
C(9)	1210(1)	8796(1)	2848(1)	25(1)
C(10)	582(1)	8054(1)	2873(1)	23(1)
C(11)	-298(1)	8178(1)	2708(1)	28(1)
C(12)	-903(1)	7420(1)	2797(1)	30(1)
C(13)	-676(1)	6501(1)	3077(1)	26(1)
C(14)	169(1)	6284(1)	3261(1)	22(1)
C(15)	423(1)	5417(1)	3595(1)	22(1)
C(16)	1265(1)	5284(1)	3819(1)	21(1)
C(17)	1892(1)	6054(1)	3801(1)	18(1)
C(18)	2737(1)	5952(1)	4018(1)	20(1)
C(19)	1572(1)	7088(1)	3615(1)	18(1)
C(20)	1154(1)	7537(1)	4238(1)	22(1)
C(21)	898(1)	7006(1)	3065(1)	20(1)
C(22)	1330(1)	6564(1)	2482(1)	22(1)
C(23)	1673(1)	6204(1)	2016(1)	24(1)
C(24)	2143(1)	5756(1)	1486(1)	21(1)
C(25)	2386(1)	6313(1)	945(1)	28(1)
C(26)	2898(1)	5891(1)	464(1)	31(1)
C(27)	3183(1)	4917(1)	517(1)	29(1)
C(28)	2939(1)	4354(1)	1046(1)	33(1)
C(29)	2411(1)	4761(1)	1523(1)	27(1)

Table A. 54 **Bond lengths [\AA] and angles [$^\circ$] for 139 (bt 914)**

C(1)-C(4)	1.5370(19)	C(14)-C(21)	1.5303(19)
C(1)-H(1A)	0.9800	C(15)-C(16)	1.3826(19)
C(1)-H(1B)	0.9800	C(15)-H(15)	0.9500
C(1)-H(1C)	0.9800	C(16)-C(17)	1.4063(18)
C(2)-C(4)	1.532(2)	C(16)-H(16)	0.9500
C(2)-H(2A)	0.9800	C(17)-C(18)	1.3774(18)
C(2)-H(2B)	0.9800	C(17)-C(19)	1.5140(18)
C(2)-H(2C)	0.9800	C(18)-H(18)	0.9500
C(3)-C(4)	1.5328(19)	C(19)-C(21)	1.5390(17)
C(3)-H(3A)	0.9800	C(19)-C(20)	1.5565(17)
C(3)-H(3B)	0.9800	C(20)-H(20A)	0.9800
C(3)-H(3C)	0.9800	C(20)-H(20B)	0.9800
C(4)-C(5)	1.5333(18)	C(20)-H(20C)	0.9800
C(5)-C(6)	1.3902(18)	C(21)-C(22)	1.4937(18)
C(5)-C(18)	1.4147(18)	C(22)-C(23)	1.1967(19)
C(6)-C(7)	1.3985(18)	C(23)-C(24)	1.4399(19)
C(6)-H(6)	0.9500	C(24)-C(25)	1.392(2)
C(7)-C(8)	1.3883(18)	C(24)-C(29)	1.392(2)
C(7)-C(19)	1.5116(18)	C(25)-C(26)	1.384(2)
C(8)-C(9)	1.4031(19)	C(25)-H(25)	0.9500
C(8)-H(8)	0.9500	C(26)-C(27)	1.377(2)
C(9)-C(10)	1.383(2)	C(26)-H(26)	0.9500
C(9)-H(9)	0.9500	C(27)-C(28)	1.376(2)
C(10)-C(11)	1.4001(19)	C(27)-H(27)	0.9500
C(10)-C(21)	1.5321(19)	C(28)-C(29)	1.385(2)
C(11)-C(12)	1.384(2)	C(28)-H(28)	0.9500
C(11)-H(11)	0.9500	C(29)-H(29)	0.9500
C(12)-C(13)	1.400(2)		
C(12)-H(12)	0.9500	C(4)-C(1)-H(1A)	109.5
C(13)-C(14)	1.3798(19)	C(4)-C(1)-H(1B)	109.5
C(13)-H(13)	0.9500	H(1A)-C(1)-H(1B)	109.5
C(14)-C(15)	1.401(2)	C(4)-C(1)-H(1C)	109.5

H(1A)-C(1)-H(1C)	109.5	C(9)-C(10)-C(21)	116.34(12)
H(1B)-C(1)-H(1C)	109.5	C(11)-C(10)-C(21)	118.38(13)
C(4)-C(2)-H(2A)	109.5	C(12)-C(11)-C(10)	121.73(14)
C(4)-C(2)-H(2B)	109.5	C(12)-C(11)-H(11)	119.1
H(2A)-C(2)-H(2B)	109.5	C(10)-C(11)-H(11)	119.1
C(4)-C(2)-H(2C)	109.5	C(11)-C(12)-C(13)	121.97(13)
H(2A)-C(2)-H(2C)	109.5	C(11)-C(12)-H(12)	119.0
H(2B)-C(2)-H(2C)	109.5	C(13)-C(12)-H(12)	119.0
C(4)-C(3)-H(3A)	109.5	C(14)-C(13)-C(12)	121.98(14)
C(4)-C(3)-H(3B)	109.5	C(14)-C(13)-H(13)	119.0
H(3A)-C(3)-H(3B)	109.5	C(12)-C(13)-H(13)	119.0
C(4)-C(3)-H(3C)	109.5	C(13)-C(14)-C(15)	124.66(13)
H(3A)-C(3)-H(3C)	109.5	C(13)-C(14)-C(21)	118.72(13)
H(3B)-C(3)-H(3C)	109.5	C(15)-C(14)-C(21)	116.55(11)
C(2)-C(4)-C(3)	108.05(11)	C(16)-C(15)-C(14)	122.01(12)
C(2)-C(4)-C(5)	109.18(11)	C(16)-C(15)-H(15)	119.0
C(3)-C(4)-C(5)	112.47(11)	C(14)-C(15)-H(15)	119.0
C(2)-C(4)-C(1)	109.77(12)	C(15)-C(16)-C(17)	122.33(13)
C(3)-C(4)-C(1)	108.69(11)	C(15)-C(16)-H(16)	118.8
C(5)-C(4)-C(1)	108.66(11)	C(17)-C(16)-H(16)	118.8
C(6)-C(5)-C(18)	118.86(12)	C(18)-C(17)-C(16)	124.18(12)
C(6)-C(5)-C(4)	122.38(12)	C(18)-C(17)-C(19)	118.48(11)
C(18)-C(5)-C(4)	118.65(11)	C(16)-C(17)-C(19)	116.81(11)
C(5)-C(6)-C(7)	122.91(12)	C(17)-C(18)-C(5)	122.89(12)
C(5)-C(6)-H(6)	118.5	C(17)-C(18)-H(18)	118.6
C(7)-C(6)-H(6)	118.5	C(5)-C(18)-H(18)	118.6
C(8)-C(7)-C(6)	124.19(12)	C(7)-C(19)-C(17)	113.64(10)
C(8)-C(7)-C(19)	117.37(11)	C(7)-C(19)-C(21)	110.03(10)
C(6)-C(7)-C(19)	118.07(11)	C(17)-C(19)-C(21)	109.87(10)
C(7)-C(8)-C(9)	121.86(13)	C(7)-C(19)-C(20)	106.06(10)
C(7)-C(8)-H(8)	119.1	C(17)-C(19)-C(20)	105.97(10)
C(9)-C(8)-H(8)	119.1	C(21)-C(19)-C(20)	111.16(10)
C(10)-C(9)-C(8)	122.30(13)	C(19)-C(20)-H(20A)	109.5
C(10)-C(9)-H(9)	118.8	C(19)-C(20)-H(20B)	109.5
C(8)-C(9)-H(9)	118.8	H(20A)-C(20)-H(20B)	109.5
C(9)-C(10)-C(11)	125.20(13)	C(19)-C(20)-H(20C)	109.5

H(20A)-C(20)-H(20C)	109.5
H(20B)-C(20)-H(20C)	109.5
C(22)-C(21)-C(14)	106.71(11)
C(22)-C(21)-C(10)	107.08(11)
C(14)-C(21)-C(10)	114.32(11)
C(22)-C(21)-C(19)	108.97(10)
C(14)-C(21)-C(19)	109.81(11)
C(10)-C(21)-C(19)	109.77(11)
C(23)-C(22)-C(21)	179.58(16)
C(22)-C(23)-C(24)	175.58(14)
C(25)-C(24)-C(29)	118.34(13)
C(25)-C(24)-C(23)	121.45(13)
C(29)-C(24)-C(23)	120.10(13)
C(26)-C(25)-C(24)	120.64(14)
C(26)-C(25)-H(25)	119.7
C(24)-C(25)-H(25)	119.7
C(27)-C(26)-C(25)	120.39(14)
C(27)-C(26)-H(26)	119.8
C(25)-C(26)-H(26)	119.8
C(28)-C(27)-C(26)	119.59(13)
C(28)-C(27)-H(27)	120.2
C(26)-C(27)-H(27)	120.2
C(27)-C(28)-C(29)	120.47(14)
C(27)-C(28)-H(28)	119.8
C(29)-C(28)-H(28)	119.8
C(28)-C(29)-C(24)	120.50(13)
C(28)-C(29)-H(29)	119.8
C(24)-C(29)-H(29)	119.8

Table A. 55 Anisotropic displacement parameters ($\text{\AA}^2 \times 10^3$) for 139 (bt 914).

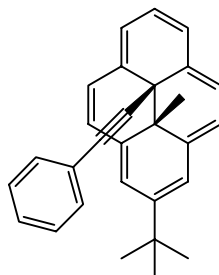
	U11	U22	U33	U23	U13	U12
C(1)	26(1)	38(1)	28(1)	7(1)	-9(1)	-6(1)
C(2)	18(1)	28(1)	39(1)	3(1)	-4(1)	1(1)
C(3)	21(1)	31(1)	30(1)	3(1)	-7(1)	-5(1)
C(4)	20(1)	24(1)	24(1)	3(1)	-4(1)	-2(1)
C(5)	19(1)	22(1)	16(1)	-2(1)	0(1)	-1(1)
C(6)	21(1)	18(1)	18(1)	-2(1)	1(1)	-2(1)
C(7)	22(1)	19(1)	15(1)	-3(1)	2(1)	1(1)
C(8)	25(1)	22(1)	20(1)	1(1)	3(1)	0(1)
C(9)	29(1)	25(1)	21(1)	6(1)	3(1)	8(1)
C(10)	23(1)	31(1)	16(1)	2(1)	2(1)	6(1)
C(11)	26(1)	38(1)	21(1)	6(1)	0(1)	12(1)
C(12)	18(1)	49(1)	22(1)	1(1)	-1(1)	7(1)
C(13)	19(1)	39(1)	22(1)	-3(1)	1(1)	-1(1)
C(14)	19(1)	30(1)	18(1)	-5(1)	2(1)	0(1)
C(15)	20(1)	24(1)	24(1)	-3(1)	3(1)	-4(1)
C(16)	22(1)	19(1)	23(1)	-1(1)	2(1)	0(1)
C(17)	20(1)	19(1)	15(1)	-2(1)	2(1)	1(1)
C(18)	22(1)	18(1)	19(1)	2(1)	0(1)	3(1)
C(19)	16(1)	20(1)	16(1)	-1(1)	1(1)	2(1)
C(20)	25(1)	22(1)	19(1)	-1(1)	3(1)	2(1)
C(21)	17(1)	26(1)	18(1)	0(1)	1(1)	3(1)
C(22)	16(1)	29(1)	21(1)	-1(1)	-3(1)	0(1)
C(23)	16(1)	33(1)	21(1)	-2(1)	-2(1)	0(1)
C(24)	16(1)	30(1)	18(1)	-4(1)	-2(1)	0(1)
C(25)	32(1)	27(1)	24(1)	1(1)	2(1)	8(1)
C(26)	34(1)	38(1)	21(1)	2(1)	6(1)	2(1)
C(27)	28(1)	36(1)	24(1)	-11(1)	3(1)	4(1)
C(28)	41(1)	22(1)	34(1)	-7(1)	0(1)	3(1)
C(29)	32(1)	26(1)	24(1)	0(1)	0(1)	-8(1)

Table A. 56 Hydrogen coordinates ($\times 10^4$) and isotropic displacement parameters ($\text{\AA}^2 \times 10^3$) for 139 (bt 914).

	x	y	z	U(eq)
H(1A)	3821	5691	5022	46
H(1B)	3948	6846	5209	46
H(1C)	4779	6127	5146	46
H(2A)	4350	5072	3938	42
H(2B)	5290	5564	4049	42
H(2C)	4733	5846	3419	42
H(3A)	5442	7320	4373	41
H(3B)	4606	8036	4410	41
H(3C)	4941	7633	3724	41
H(6)	3567	8117	3610	23
H(8)	2493	9142	2990	27
H(9)	1059	9429	2669	30
H(11)	-485	8799	2530	34
H(12)	-1489	7527	2664	35
H(13)	-1118	6012	3143	32
H(15)	4	4906	3668	27
H(16)	1426	4651	3992	25
H(18)	2910	5330	4202	24
H(20A)	1593	7569	4583	33
H(20B)	668	7112	4379	33
H(20C)	937	8213	4146	33
H(25)	2199	6988	905	34
H(26)	3053	6277	94	37
H(27)	3545	4634	191	35
H(28)	3135	3681	1085	39
H(29)	2229	4358	1878	33

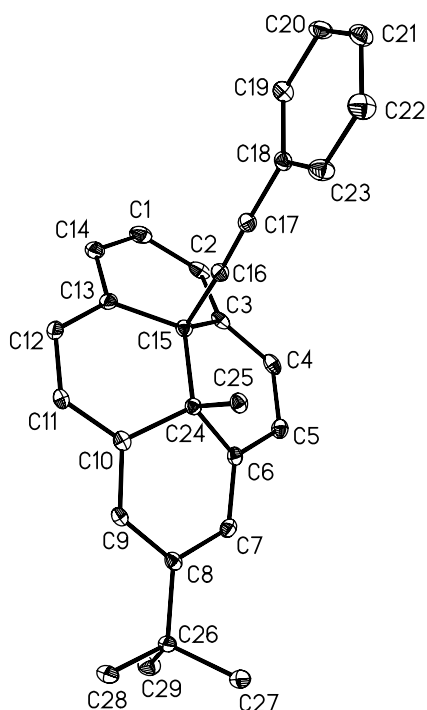
Single-Crystal X-ray Diffraction Laboratory
University of Idaho

X-ray structure report for *cis*-phenylethynyl/methyl DHP 148



148

Brendan Twamley



Project name : bt956

8-17-06

Experimental:

Crystals of compound **1** were removed from the flask, a suitable crystal was selected, attached to a glass fiber and data were collected at 89(2) K using a Bruker/Siemens SMART APEX instrument (Mo K α radiation, $\lambda = 0.71073$ Å) equipped with a Cryocool NeverIce low temperature device. Data were measured using omega scans of 0.3 ° per frame for 10 seconds, and a full sphere of data was collected. A total of 2400 frames were collected with a final resolution of 0.83 Å. Cell parameters were retrieved using SMART⁴⁸ software and refined using SAINTPlus⁴⁹ on all observed reflections. Data reduction and correction for Lp and decay were performed using the SAINTPlus software. Absorption corrections were applied using SADABS.⁵⁰ The structure was solved by direct methods and refined by least squares method on F² using the SHELXTL program package.⁵¹ The structure was solved in the space group P2(1)2(1)2(1) (# 19) by analysis of systematic absences. The structure was refined as a racemic twin. All non-hydrogen atoms were refined anisotropically. No decomposition was observed during data collection. Details of the data collection and refinement are given in Table 1. Further details are provided in the Supporting Information.

Acknowledgement

The Bruker (Siemens) SMART APEX diffraction facility was established at the University of Idaho with the assistance of the NSF-EPSCoR program and the M. J. Murdock Charitable Trust, Vancouver, WA, USA.

⁴⁸ SMART: v.5.630, Bruker Molecular Analysis Research Tool, Bruker AXS, Madison, WI, **2001**.

⁴⁹ SAINTPlus: v. 7.23a, Data Reduction and Correction Program, Bruker AXS, Madison, WI, **2004**.

⁵⁰ SADABS: v.2004/1, an empirical absorption correction program, Bruker AXS Inc., Madison, WI, **2004**.

⁵¹ SHELXTL: v. 6.14, Structure Determination Software Suite, Sheldrick, G.M., Bruker AXS Inc., Madison, WI, **2004**.

Table A. 57 Crystal data and structure refinement for 148

Identification code	bt956	
Empirical formula	C ₂₉ H ₂₆	
Formula weight	374.50	
Temperature	89(2) K	
Wavelength	0.71073 Å	
Crystal system	Orthorhombic	
Space group	P2(1)2(1)2(1)	
Unit cell dimensions	a = 8.1094(6) Å	α = 90°.
	b = 13.9234(11) Å	β = 90°.
	c = 18.4052(14) Å	γ = 90°.
Volume	2078.1(3) Å ³	
Z	4	
Density (calculated)	1.197 Mg/m ³	
Absorption coefficient	0.067 mm ⁻¹	
F(000)	800	
Crystal size	0.50 x 0.34 x 0.15 mm ³	
Crystal color and habit	red needle	
Diffractometer	Bruker/Siemens SMART APEX	
Theta range for data collection	1.83 to 25.25°.	
Index ranges	-9<=h<=9, -16<=k<=16, -22<=l<=22	
Reflections collected	30885	
Independent reflections	2163 [R(int) = 0.0279]	
Completeness to theta = 25.25°	100.0%	
Absorption correction	Semi-empirical from equivalents	
Max. and min. transmission	0.9900 and 0.9671	
Solution method	Bruker, 2003; XS, SHELXTL v. 6.14	
Refinement method	Full-matrix least-squares on F ²	
Data / restraints / parameters	2163 / 0 / 267	
Goodness-of-fit on F ²	1.096	
Final R indices [I>2sigma(I)]	R1 = 0.0369, wR2 = 0.0923	
R indices (all data)	R1 = 0.0377, wR2 = 0.0929	
Largest diff. peak and hole	0.231 and -0.144 e.Å ⁻³	

Table A. 58 Atomic coordinates ($\times 10^4$) and equivalent isotropic displacement parameters ($\text{\AA}^2 \times 10^3$) for 148 (bt 956).

	x	y	z	U(eq)
C(1)	623(3)	11085(2)	3344(1)	28(1)
C(2)	2214(3)	11460(2)	3369(1)	24(1)
C(3)	3560(3)	10966(2)	3107(1)	20(1)
C(4)	5090(3)	11399(2)	3005(1)	21(1)
C(5)	6253(3)	11055(2)	2526(1)	21(1)
C(6)	5975(3)	10225(2)	2114(1)	18(1)
C(7)	6871(3)	10040(2)	1488(1)	20(1)
C(8)	6456(3)	9304(2)	996(1)	18(1)
C(9)	5008(3)	8796(1)	1122(1)	17(1)
C(10)	4011(3)	8935(1)	1735(1)	17(1)
C(11)	2438(3)	8556(2)	1766(1)	19(1)
C(12)	1247(3)	8906(2)	2240(1)	21(1)
C(13)	1563(3)	9661(2)	2711(1)	20(1)
C(14)	306(3)	10216(2)	3003(1)	25(1)
C(15)	3353(3)	9890(2)	2925(1)	17(1)
C(16)	3503(3)	9424(2)	3653(1)	19(1)
C(17)	3525(3)	9081(2)	4246(1)	20(1)
C(18)	3593(3)	8667(2)	4964(1)	20(1)
C(19)	2557(3)	9012(2)	5513(1)	23(1)
C(20)	2657(3)	8636(2)	6209(1)	26(1)
C(21)	3782(3)	7916(2)	6364(1)	29(1)
C(22)	4800(3)	7564(2)	5824(1)	33(1)
C(23)	4704(3)	7937(2)	5125(1)	28(1)
C(24)	4735(3)	9482(1)	2375(1)	16(1)
C(25)	5823(3)	8723(2)	2774(1)	20(1)
C(26)	7467(3)	9177(2)	299(1)	19(1)
C(27)	9310(3)	9095(2)	487(1)	26(1)
C(28)	6989(3)	8264(2)	-115(1)	26(1)
C(29)	7180(3)	10049(2)	-195(1)	28(1)

Table A. 59 Bond lengths [\AA] and angles [$^\circ$] for 148 (bt 956)

C(1)-C(14)	1.386(4)	C(18)-C(19)	1.399(3)
C(1)-C(2)	1.393(4)	C(19)-C(20)	1.386(3)
C(1)-H(1)	0.9500	C(19)-H(19)	0.9500
C(2)-C(3)	1.378(3)	C(20)-C(21)	1.385(4)
C(2)-H(2)	0.9500	C(20)-H(20)	0.9500
C(3)-C(4)	1.392(3)	C(21)-C(22)	1.382(4)
C(3)-C(15)	1.544(3)	C(21)-H(21)	0.9500
C(4)-C(5)	1.377(3)	C(22)-C(23)	1.389(3)
C(4)-H(4)	0.9500	C(22)-H(22)	0.9500
C(5)-C(6)	1.400(3)	C(23)-H(23)	0.9500
C(5)-H(5)	0.9500	C(24)-C(25)	1.560(3)
C(6)-C(7)	1.385(3)	C(25)-H(25A)	0.9800
C(6)-C(24)	1.522(3)	C(25)-H(25B)	0.9800
C(7)-C(8)	1.409(3)	C(25)-H(25C)	0.9800
C(7)-H(7)	0.9500	C(26)-C(28)	1.533(3)
C(8)-C(9)	1.391(3)	C(26)-C(29)	1.534(3)
C(8)-C(26)	1.532(3)	C(26)-C(27)	1.538(3)
C(9)-C(10)	1.401(3)	C(27)-H(27A)	0.9800
C(9)-H(9)	0.9500	C(27)-H(27B)	0.9800
C(10)-C(11)	1.381(3)	C(27)-H(27C)	0.9800
C(10)-C(24)	1.521(3)	C(28)-H(28A)	0.9800
C(11)-C(12)	1.389(3)	C(28)-H(28B)	0.9800
C(11)-H(11)	0.9500	C(28)-H(28C)	0.9800
C(12)-C(13)	1.387(3)	C(29)-H(29A)	0.9800
C(12)-H(12)	0.9500	C(29)-H(29B)	0.9800
C(13)-C(14)	1.387(3)	C(29)-H(29C)	0.9800
C(13)-C(15)	1.538(3)		
C(14)-H(14)	0.9500	C(14)-C(1)-C(2)	121.0(2)
C(15)-C(16)	1.493(3)	C(14)-C(1)-H(1)	119.5
C(15)-C(24)	1.614(3)	C(2)-C(1)-H(1)	119.5
C(16)-C(17)	1.193(3)	C(3)-C(2)-C(1)	122.3(2)
C(17)-C(18)	1.442(3)	C(3)-C(2)-H(2)	118.9
C(18)-C(23)	1.391(3)	C(1)-C(2)-H(2)	118.9

C(2)-C(3)-C(4)	122.5(2)	C(16)-C(15)-C(13)	102.50(17)
C(2)-C(3)-C(15)	118.3(2)	C(16)-C(15)-C(3)	102.65(16)
C(4)-C(3)-C(15)	119.2(2)	C(13)-C(15)-C(3)	111.06(18)
C(5)-C(4)-C(3)	123.09(19)	C(16)-C(15)-C(24)	110.68(17)
C(5)-C(4)-H(4)	118.5	C(13)-C(15)-C(24)	114.94(16)
C(3)-C(4)-H(4)	118.5	C(3)-C(15)-C(24)	113.72(18)
C(4)-C(5)-C(6)	121.6(2)	C(17)-C(16)-C(15)	175.6(2)
C(4)-C(5)-H(5)	119.2	C(16)-C(17)-C(18)	178.7(2)
C(6)-C(5)-H(5)	119.2	C(23)-C(18)-C(19)	119.1(2)
C(7)-C(6)-C(5)	121.3(2)	C(23)-C(18)-C(17)	120.8(2)
C(7)-C(6)-C(24)	118.86(18)	C(19)-C(18)-C(17)	120.1(2)
C(5)-C(6)-C(24)	119.78(19)	C(20)-C(19)-C(18)	120.1(2)
C(6)-C(7)-C(8)	123.0(2)	C(20)-C(19)-H(19)	119.9
C(6)-C(7)-H(7)	118.5	C(18)-C(19)-H(19)	119.9
C(8)-C(7)-H(7)	118.5	C(19)-C(20)-C(21)	120.2(2)
C(9)-C(8)-C(7)	117.64(19)	C(19)-C(20)-H(20)	119.9
C(9)-C(8)-C(26)	122.21(18)	C(21)-C(20)-H(20)	119.9
C(7)-C(8)-C(26)	119.66(19)	C(22)-C(21)-C(20)	120.1(2)
C(8)-C(9)-C(10)	123.49(19)	C(22)-C(21)-H(21)	119.9
C(8)-C(9)-H(9)	118.3	C(20)-C(21)-H(21)	119.9
C(10)-C(9)-H(9)	118.3	C(21)-C(22)-C(23)	120.0(2)
C(11)-C(10)-C(9)	120.95(19)	C(21)-C(22)-H(22)	120.0
C(11)-C(10)-C(24)	120.99(19)	C(23)-C(22)-H(22)	120.0
C(9)-C(10)-C(24)	118.02(19)	C(22)-C(23)-C(18)	120.4(2)
C(10)-C(11)-C(12)	122.30(19)	C(22)-C(23)-H(23)	119.8
C(10)-C(11)-H(11)	118.9	C(18)-C(23)-H(23)	119.8
C(12)-C(11)-H(11)	118.9	C(10)-C(24)-C(6)	110.56(17)
C(13)-C(12)-C(11)	122.0(2)	C(10)-C(24)-C(25)	104.13(16)
C(13)-C(12)-H(12)	119.0	C(6)-C(24)-C(25)	103.61(17)
C(11)-C(12)-H(12)	119.0	C(10)-C(24)-C(15)	113.25(17)
C(12)-C(13)-C(14)	121.9(2)	C(6)-C(24)-C(15)	114.69(16)
C(12)-C(13)-C(15)	119.47(19)	C(25)-C(24)-C(15)	109.61(16)
C(14)-C(13)-C(15)	118.62(19)	C(24)-C(25)-H(25A)	109.5
C(1)-C(14)-C(13)	121.7(2)	C(24)-C(25)-H(25B)	109.5
C(1)-C(14)-H(14)	119.2	H(25A)-C(25)-H(25B)	109.5
C(13)-C(14)-H(14)	119.2	C(24)-C(25)-H(25C)	109.5

H(25A)-C(25)-H(25C)	109.5
H(25B)-C(25)-H(25C)	109.5
C(8)-C(26)-C(28)	112.13(18)
C(8)-C(26)-C(29)	108.89(17)
C(28)-C(26)-C(29)	108.89(18)
C(8)-C(26)-C(27)	109.88(17)
C(28)-C(26)-C(27)	107.21(19)
C(29)-C(26)-C(27)	109.82(19)
C(26)-C(27)-H(27A)	109.5
C(26)-C(27)-H(27B)	109.5
H(27A)-C(27)-H(27B)	109.5
C(26)-C(27)-H(27C)	109.5
H(27A)-C(27)-H(27C)	109.5
H(27B)-C(27)-H(27C)	109.5
C(26)-C(28)-H(28A)	109.5
C(26)-C(28)-H(28B)	109.5
H(28A)-C(28)-H(28B)	109.5
C(26)-C(28)-H(28C)	109.5
H(28A)-C(28)-H(28C)	109.5
H(28B)-C(28)-H(28C)	109.5
C(26)-C(29)-H(29A)	109.5
C(26)-C(29)-H(29B)	109.5
H(29A)-C(29)-H(29B)	109.5
C(26)-C(29)-H(29C)	109.5
H(29A)-C(29)-H(29C)	109.5
H(29B)-C(29)-H(29C)	109.5

Table A. 60 **Anisotropic displacement parameters ($\text{\AA}^2 \times 10^3$) for 148 (bt 956).**

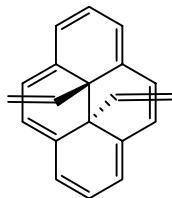
	U11	U22	U33	U23	U13	U12
C(1)	28(1)	35(1)	20(1)	-1(1)	4(1)	11(1)
C(2)	34(1)	23(1)	14(1)	-1(1)	1(1)	8(1)
C(3)	29(1)	18(1)	12(1)	0(1)	-2(1)	3(1)
C(4)	31(1)	14(1)	18(1)	-2(1)	-6(1)	1(1)
C(5)	21(1)	18(1)	23(1)	1(1)	-3(1)	-3(1)
C(6)	17(1)	19(1)	18(1)	1(1)	-4(1)	2(1)
C(7)	16(1)	21(1)	22(1)	2(1)	-1(1)	-3(1)
C(8)	20(1)	18(1)	16(1)	1(1)	-3(1)	4(1)
C(9)	21(1)	16(1)	15(1)	-1(1)	-3(1)	2(1)
C(10)	21(1)	12(1)	18(1)	1(1)	-3(1)	3(1)
C(11)	21(1)	17(1)	17(1)	-2(1)	-4(1)	-1(1)
C(12)	17(1)	27(1)	19(1)	2(1)	-2(1)	-3(1)
C(13)	18(1)	25(1)	17(1)	5(1)	1(1)	-2(1)
C(14)	22(1)	35(1)	18(1)	2(1)	1(1)	3(1)
C(15)	18(1)	18(1)	16(1)	1(1)	-1(1)	1(1)
C(16)	20(1)	19(1)	19(1)	-3(1)	0(1)	-1(1)
C(17)	21(1)	19(1)	20(1)	-2(1)	0(1)	-1(1)
C(18)	22(1)	20(1)	17(1)	0(1)	-2(1)	-5(1)
C(19)	26(1)	22(1)	21(1)	-1(1)	-1(1)	2(1)
C(20)	31(1)	30(1)	18(1)	-3(1)	7(1)	-2(1)
C(21)	35(1)	32(1)	20(1)	7(1)	-2(1)	-2(1)
C(22)	36(1)	31(1)	33(1)	9(1)	0(1)	10(1)
C(23)	31(1)	29(1)	25(1)	2(1)	5(1)	7(1)
C(24)	17(1)	17(1)	16(1)	0(1)	-1(1)	1(1)
C(25)	20(1)	20(1)	19(1)	-1(1)	-4(1)	4(1)
C(26)	19(1)	24(1)	15(1)	0(1)	2(1)	1(1)
C(27)	23(1)	34(1)	22(1)	-1(1)	3(1)	2(1)
C(28)	28(1)	31(1)	18(1)	-3(1)	4(1)	1(1)
C(29)	31(1)	31(1)	23(1)	7(1)	2(1)	2(1)

Table A. 61 Hydrogen coordinates (x 10⁴) and isotropic displacement parameters (Å²x 10³) for 148 (bt 956).

	x	y	z	U(eq)
H(1)	-258	11428	3563	33
H(2)	2376	12079	3575	28
H(4)	5344	11957	3280	25
H(5)	7267	11389	2473	25
H(7)	7809	10427	1387	24
H(9)	4677	8330	774	20
H(11)	2161	8037	1454	22
H(12)	183	8620	2241	25
H(14)	-800	9996	2968	30
H(19)	1783	9506	5409	28
H(20)	1952	8872	6580	32
H(21)	3854	7664	6842	35
H(22)	5566	7067	5930	40
H(23)	5402	7691	4755	34
H(25A)	5123	8200	2952	29
H(25B)	6384	9028	3185	29
H(25C)	6644	8466	2435	29
H(27A)	9495	8518	780	39
H(27B)	9654	9664	762	39
H(27C)	9955	9052	38	39
H(28A)	7167	7702	197	38
H(28B)	7670	8207	-553	38
H(28C)	5824	8297	-254	38
H(29A)	7829	9976	-641	42
H(29B)	7522	10635	59	42
H(29C)	6007	10093	-319	42

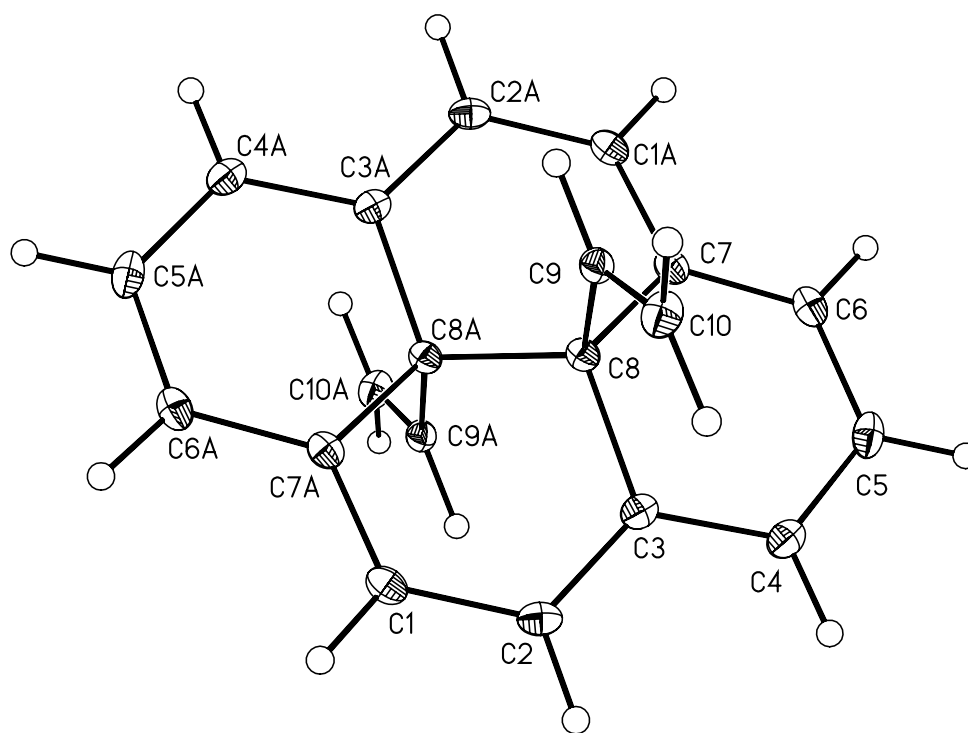
Single-Crystal X-ray Diffraction Laboratory
University of Idaho

X-ray structure report for divinyl DHP 167



167

Brendan Twamley



Project name : Bt1160

8-9-07

Experimental:

Crystals of compound **1** were removed from the flask, a suitable crystal was selected, attached to a glass fiber and data were collected at 90(2) K using a Bruker/Siemens SMART APEX instrument (Mo K α radiation, $\lambda = 0.71073$ Å) equipped with a Cryocool NeverIce low temperature device. Data were measured using omega scans 0.3° per frame for 10 seconds, and a full sphere of data was collected. A total of 2400 frames were collected with a final resolution of 0.83 Å. Cell parameters were retrieved using SMART⁵² software and refined using SAINTPlus⁵³ on all observed reflections. Data reduction and correction for Lp and decay were performed using the SAINTPlus software. Absorption corrections were applied using SADABS.⁵⁴ The structure was solved by direct methods and refined by least squares method on F² using the SHELXTL program package.⁵⁵ The structure was solved in the space group Pbc_a (# 61) by analysis of systematic absences. All non-hydrogen atoms were refined anisotropically. No decomposition was observed during data collection. Details of the data collection and refinement are given in Table 1. Further details are provided in the Supporting Information.

Acknowledgement

The Bruker (Siemens) SMART APEX diffraction facility was established at the University of Idaho with the assistance of the NSF-EPSCoR program and the M. J. Murdock Charitable Trust, Vancouver, WA, USA.

⁵² SMART: v. 5.632, Bruker AXS, Madison, WI, **2005**.

⁵³ SAINTPlus: v. 7.23a, Data Reduction and Correction Program, Bruker AXS, Madison, WI, **2004**.

⁵⁴ SADABS: v.2004/1, an empirical absorption correction program, Bruker AXS Inc., Madison, WI, **2004**.

⁵⁵ SHELXTL: v. 6.14, Structure Determination Software Suite, Sheldrick, G.M., Bruker AXS Inc., Madison, WI, **2004**.

Table A. 62 Crystal data and structure refinement for Divinyl-DHP 167.

Identification code	bt1160	
Empirical formula	C ₂₀ H ₁₆	
Formula weight	256.33	
Temperature	90(2) K	
Wavelength	0.71073 Å	
Crystal system	Orthorhombic	
Space group	Pbca	
Unit cell dimensions	a = 12.1187(7) Å	α = 90°.
	b = 7.1498(4) Å	β = 90°.
	c = 15.2530(9) Å	γ = 90°.
Volume	1321.62(13) Å ³	
Z	4	
Density (calculated)	1.288 Mg/m ³	
Absorption coefficient	0.073 mm ⁻¹	
F(000)	544	
Crystal size	0.34 x 0.26 x 0.06 mm ³	
Crystal color and habit	colorless plate	
Diffractometer	Bruker/Siemens SMART APEX	
Theta range for data collection	2.67 to 25.25°.	
Index ranges	-14 ≤ h ≤ 14, -8 ≤ k ≤ 8, -18 ≤ l ≤ 18	
Reflections collected	19365	
Independent reflections	1203 [R(int) = 0.0425]	
Completeness to theta = 25.25°	100.0%	
Absorption correction	Semi-empirical from equivalents	
Max. and min. transmission	0.991 and 0.971	
Solution method	XS, SHELXTL v. 6.14 (Bruker, 2003)	
Refinement method	Full-matrix least-squares on F ²	
Data / restraints / parameters	1203 / 0 / 91	
Goodness-of-fit on F ²	1.097	
Final R indices [I > 2σ(I)]	R1 = 0.0496, wR2 = 0.1302	
R indices (all data)	R1 = 0.0537, wR2 = 0.1343	
Largest diff. peak and hole	0.395 and -0.207 e.Å ⁻³	

Table A. 63 Atomic coordinates ($\times 10^4$) and equivalent isotropic displacement parameters ($\text{\AA}^2 \times 10^3$) for 167 (bt 1160).

	x	y	z	U(eq)
C(1)	5552(1)	13128(2)	682(1)	20(1)
C(2)	4914(1)	12227(2)	1311(1)	20(1)
C(3)	4527(1)	10401(2)	1192(1)	17(1)
C(4)	3872(1)	9444(2)	1789(1)	21(1)
C(5)	3456(1)	7671(2)	1605(1)	23(1)
C(6)	3624(1)	6802(2)	796(1)	21(1)
C(7)	4275(1)	7623(2)	152(1)	17(1)
C(8)	4957(1)	9342(2)	398(1)	16(1)
C(9)	6103(1)	8525(2)	625(1)	17(1)
C(10)	6611(1)	8599(2)	1389(1)	22(1)

Table A. 64 Bond lengths [\AA] and angles [$^\circ$] for 167 (bt 1160).

C(1)-C(2)	1.391(2)	C(5)-C(4)-H(4)	119.3
C(1)-C(7)#1	1.396(2)	C(4)-C(5)-C(6)	122.08(14)
C(1)-H(1)	0.9500	C(4)-C(5)-H(5)	119.0
C(2)-C(3)	1.399(2)	C(6)-C(5)-H(5)	119.0
C(2)-H(2)	0.9500	C(7)-C(6)-C(5)	121.32(14)
C(3)-C(4)	1.390(2)	C(7)-C(6)-H(6)	119.3
C(3)-C(8)	1.5197(19)	C(5)-C(6)-H(6)	119.3
C(4)-C(5)	1.393(2)	C(6)-C(7)-C(1)#1	124.55(14)
C(4)-H(4)	0.9500	C(6)-C(7)-C(8)	118.17(13)
C(5)-C(6)	1.395(2)	C(1)#1-C(7)-C(8)	116.90(13)
C(5)-H(5)	0.9500	C(3)-C(8)-C(7)	114.31(11)
C(6)-C(7)	1.391(2)	C(3)-C(8)-C(8)#1	110.29(14)
C(6)-H(6)	0.9500	C(7)-C(8)-C(8)#1	109.55(14)
C(7)-C(1)#1	1.396(2)	C(3)-C(8)-C(9)	108.51(11)
C(7)-C(8)	1.5280(19)	C(7)-C(8)-C(9)	103.71(11)
C(8)-C(8)#1	1.540(3)	C(8)#1-C(8)-C(9)	110.26(14)
C(8)-C(9)	1.5467(19)	C(10)-C(9)-C(8)	127.01(13)
C(9)-C(10)	1.319(2)	C(10)-C(9)-H(9)	116.5
C(9)-H(9)	0.9500	C(8)-C(9)-H(9)	116.5
C(10)-H(10A)	0.9500	C(9)-C(10)-H(10A)	120.0
C(10)-H(10B)	0.9500	C(9)-C(10)-H(10B)	120.0
		H(10A)-C(10)-H(10B)	120.0
C(2)-C(1)-C(7)#1	122.25(14)		
C(2)-C(1)-H(1)	118.9		
C(7)#1-C(1)-H(1)	118.9		
C(1)-C(2)-C(3)	121.90(13)		
C(1)-C(2)-H(2)	119.1		
C(3)-C(2)-H(2)	119.1		
C(4)-C(3)-C(2)	124.43(14)		
C(4)-C(3)-C(8)	118.22(13)		
C(2)-C(3)-C(8)	117.03(13)		
C(3)-C(4)-C(5)	121.49(14)		
C(3)-C(4)-H(4)	119.3		

Table A. 65 Anisotropic displacement parameters ($\text{\AA}^2 \times 10^3$) for bt1160 (167).

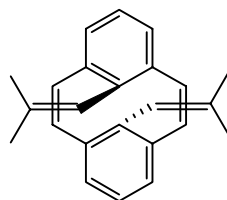
	U11	U22	U33	U23	U13	U12
C(1)	19(1)	16(1)	24(1)	-1(1)	-5(1)	0(1)
C(2)	19(1)	21(1)	19(1)	-5(1)	-3(1)	4(1)
C(3)	15(1)	22(1)	14(1)	0(1)	-2(1)	4(1)
C(4)	19(1)	27(1)	17(1)	2(1)	0(1)	6(1)
C(5)	17(1)	29(1)	22(1)	10(1)	2(1)	0(1)
C(6)	17(1)	18(1)	27(1)	4(1)	-3(1)	-1(1)
C(7)	15(1)	16(1)	21(1)	2(1)	-3(1)	2(1)
C(8)	15(1)	15(1)	18(1)	0(1)	-1(1)	0(1)
C(9)	16(1)	16(1)	20(1)	1(1)	3(1)	0(1)
C(10)	17(1)	28(1)	21(1)	4(1)	0(1)	2(1)

Table A. 66 Hydrogen coordinates ($\times 10^4$) and isotropic displacement parameters ($\text{\AA}^2 \times 10^3$) for 167 (bt1160).

	x	y	z	U(eq)
H(1)	5882	14294	825	23
H(2)	4735	12870	1837	24
H(4)	3704	10011	2337	25
H(5)	3045	7034	2042	27
H(6)	3286	5627	684	25
H(9)	6483	7902	165	21
H(10A)	6269	9205	1872	26
H(10B)	7319	8047	1456	26

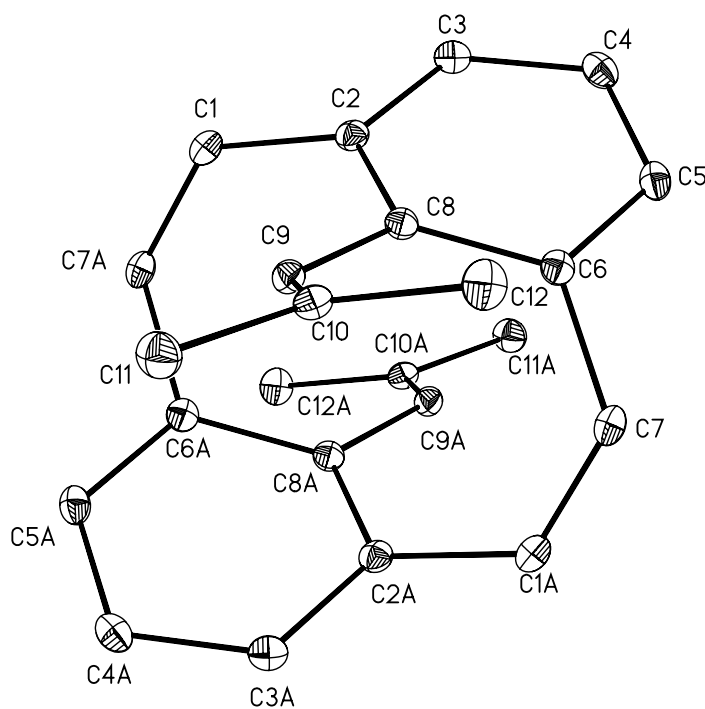
Single-Crystal X-ray Diffraction Laboratory
University of Idaho

X-ray structure report for diisobutenyl CPD 178



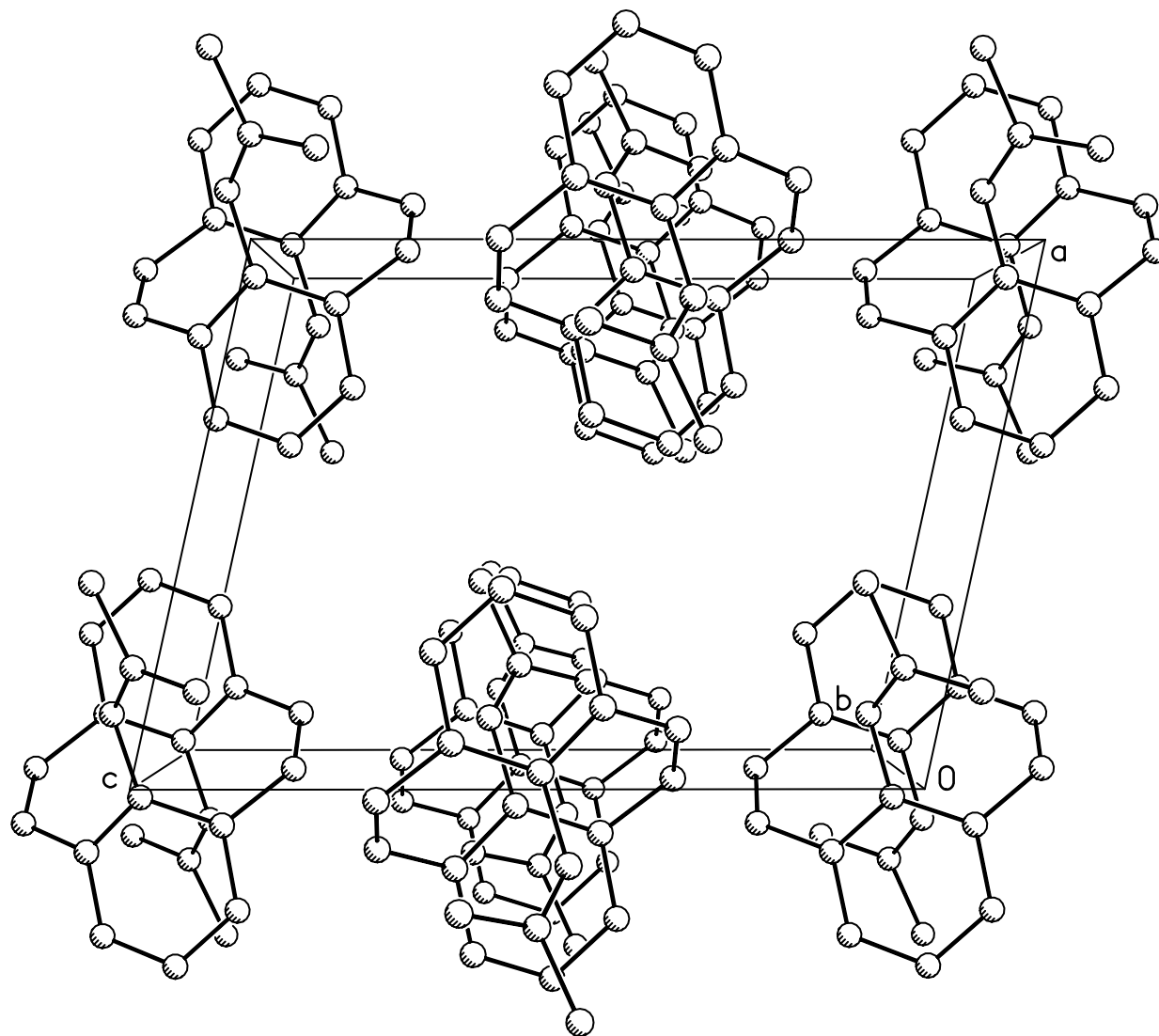
178

Brendan Twamley



Project name : Bt1173

8-29-07



Experimental:

Crystals of compound **1** were removed from the flask, a suitable crystal was selected, attached to a glass fiber and data were collected at 90(2) K using a Bruker/Siemens SMART APEX instrument (Mo K α radiation, $\lambda = 0.71073 \text{ \AA}$) equipped with a Cryocool NeverIce low temperature device. Data were measured using omega scans 0.3° per frame for 5 seconds, and a full sphere of data was collected. A total of 2400 frames were collected with a final resolution of 0.77 \AA . Cell parameters were retrieved using SMART⁵⁶ software and refined using SAINTPlus⁵⁷ on all observed reflections. Data reduction and correction for Lp and decay were performed using the SAINTPlus software. Absorption corrections were applied using SADABS.⁵⁸ The structure was solved by direct methods and refined by least squares method on F^2 using the SHELXTL program package.⁵⁹ The structure was solved in the space group P2(1)/c (# 14) by analysis of systematic absences. No decomposition was observed during data collection. Details of the data collection and refinement are given in Table 1. Further details are provided in the Supporting Information.

Acknowledgement

The Bruker (Siemens) SMART APEX diffraction facility was established at the University of Idaho with the assistance of the NSF-EPSCoR program and the M. J. Murdock Charitable Trust, Vancouver, WA, USA.

⁵⁶ SMART: v. 5.632, Bruker AXS, Madison, WI, **2005**.

⁵⁷ SAINTPlus: v. 7.23a, Data Reduction and Correction Program, Bruker AXS, Madison, WI, **2004**.

⁵⁸ SADABS: v.2004/1, an empirical absorption correction program, Bruker AXS Inc., Madison, WI, **2004**.

⁵⁹ SHELXTL: v. 6.14, Structure Determination Software Suite, Sheldrick, G.M., Bruker AXS Inc., Madison, WI, **2004**.

Table A. 67 Crystal data and structure refinement for 178 (C₂₄ H₂₄)

Identification code	bt1173
Empirical formula	C ₂₄ H ₂₄
Formula weight	312.43
Temperature	90(2) K
Wavelength	0.71073 Å
Crystal system	Monoclinic
Space group	P2(1)/c
Unit cell dimensions	a = 8.6932(3) Å α = 90°. b = 8.2751(3) Å β = 102.388(1)°. c = 12.2713(4) Å γ = 90°.
Volume	862.21(5) Å ³
Z	2
Density (calculated)	1.203 Mg/m ³
Absorption coefficient	0.067 mm ⁻¹
F(000)	336
Crystal size	0.44 x 0.34 x 0.15 mm ³
Crystal color and habit	orange block
Diffractometer	Bruker/Siemens SMART APEX
Theta range for data collection	2.40 to 27.50°.
Index ranges	-11 ≤ h ≤ 11, -10 ≤ k ≤ 10, -
	15 ≤ l ≤ 15
Reflections collected	12814
Independent reflections	1988 [R(int) = 0.0218]
Completeness to theta = 27.50°	100.0%
Absorption correction	Semi-empirical from equivalents
Max. and min. transmission	0.992 and 0.907
Solution method	XS, SHELXTL v. 6.14 (Bruker, 2003)
Refinement method	Full-matrix least-squares on F ²
Data / restraints / parameters	1988 / 0 / 111
Goodness-of-fit on F ²	1.074
Final R indices [I > 2σ(I)]	R1 = 0.0438, wR2 = 0.1241
R indices (all data)	R1 = 0.0468, wR2 = 0.1280
Largest diff. peak and hole	0.396 and -0.239 e.Å ⁻³

Table A. 68 Atomic coordinates ($\times 10^4$) and equivalent isotropic displacement parameters ($\text{\AA}^2 \times 10^3$) for 178 (bt 1173).

	x	y	z	U(eq)
C(1)	8914(1)	-32(1)	6724(1)	16(1)
C(2)	8454(1)	979(1)	5701(1)	15(1)
C(3)	6848(1)	1122(1)	5228(1)	18(1)
C(4)	6328(1)	1659(1)	4134(1)	19(1)
C(5)	7422(1)	1831(1)	3465(1)	18(1)
C(6)	9038(1)	1694(1)	3924(1)	15(1)
C(7)	10094(1)	1298(1)	3156(1)	16(1)
C(8)	9564(1)	1569(1)	5099(1)	14(1)
C(9)	11184(1)	1941(1)	5687(1)	15(1)
C(10)	12122(1)	3123(1)	5449(1)	16(1)
C(11)	13715(1)	3387(1)	6201(1)	21(1)
C(12)	11740(1)	4276(1)	4484(1)	21(1)

Table A. 69 Bond lengths [Å] and angles [°] for 178 (bt 1173)

C(1)-C(7)#1	1.3452(16)	C(4)-C(3)-C(2)	121.04(10)
C(1)-C(2)	1.4905(15)	C(4)-C(3)-H(3)	119.5
C(1)-H(1)	0.9500	C(2)-C(3)-H(3)	119.5
C(2)-C(3)	1.3974(15)	C(5)-C(4)-C(3)	118.66(10)
C(2)-C(8)	1.4220(15)	C(5)-C(4)-H(4)	120.7
C(3)-C(4)	1.3936(16)	C(3)-C(4)-H(4)	120.7
C(3)-H(3)	0.9500	C(4)-C(5)-C(6)	120.47(10)
C(4)-C(5)	1.3915(16)	C(4)-C(5)-H(5)	119.8
C(4)-H(4)	0.9500	C(6)-C(5)-H(5)	119.8
C(5)-C(6)	1.4019(15)	C(5)-C(6)-C(8)	119.44(10)
C(5)-H(5)	0.9500	C(5)-C(6)-C(7)	117.65(9)
C(6)-C(8)	1.4188(15)	C(8)-C(6)-C(7)	121.32(10)
C(6)-C(7)	1.4862(15)	C(1)#1-C(7)-C(6)	124.84(9)
C(7)-C(1)#1	1.3452(16)	C(1)#1-C(7)-H(7)	117.6
C(7)-H(7)	0.9500	C(6)-C(7)-H(7)	117.6
C(8)-C(9)	1.4705(14)	C(6)-C(8)-C(2)	116.49(10)
C(9)-C(10)	1.3445(16)	C(6)-C(8)-C(9)	123.29(10)
C(9)-H(9)	0.9500	C(2)-C(8)-C(9)	120.15(9)
C(10)-C(12)	1.5014(15)	C(10)-C(9)-C(8)	127.41(10)
C(10)-C(11)	1.5061(15)	C(10)-C(9)-H(9)	116.3
C(11)-H(11A)	0.9800	C(8)-C(9)-H(9)	116.3
C(11)-H(11B)	0.9800	C(9)-C(10)-C(12)	126.26(10)
C(11)-H(11C)	0.9800	C(9)-C(10)-C(11)	119.59(10)
C(12)-H(12A)	0.9800	C(12)-C(10)-C(11)	114.15(10)
C(12)-H(12B)	0.9800	C(10)-C(11)-H(11A)	109.5
C(12)-H(12C)	0.9800	C(10)-C(11)-H(11B)	109.5
		H(11A)-C(11)-H(11B)	109.5
C(7)#1-C(1)-C(2)	125.37(9)	C(10)-C(11)-H(11C)	109.5
C(7)#1-C(1)-H(1)	117.3	H(11A)-C(11)-H(11C)	109.5
C(2)-C(1)-H(1)	117.3	H(11B)-C(11)-H(11C)	109.5
C(3)-C(2)-C(8)	118.97(10)	C(10)-C(12)-H(12A)	109.5
C(3)-C(2)-C(1)	117.46(9)	C(10)-C(12)-H(12B)	109.5
C(8)-C(2)-C(1)	122.75(9)	H(12A)-C(12)-H(12B)	109.5

C(10)-C(12)-H(12C)	109.5	H(12B)-C(12)-H(12C)	109.5
H(12A)-C(12)-H(12C)	109.5		

Symmetry transformations used to generate equivalent atoms:

#1 -x+2,-y,-z+1

Table A. 70 **Anisotropic displacement parameters ($\text{\AA}^2 \times 10^3$) for 178 (bt 1173)**

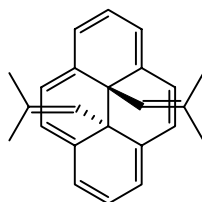
	U11	U22	U33	U23	U13	U12
C(1)	19(1)	18(1)	14(1)	-1(1)	5(1)	-3(1)
C(2)	18(1)	13(1)	15(1)	-2(1)	4(1)	0(1)
C(3)	18(1)	16(1)	20(1)	-1(1)	6(1)	-1(1)
C(4)	16(1)	18(1)	23(1)	0(1)	1(1)	1(1)
C(5)	20(1)	15(1)	16(1)	2(1)	0(1)	0(1)
C(6)	18(1)	12(1)	16(1)	1(1)	3(1)	-1(1)
C(7)	20(1)	16(1)	12(1)	1(1)	3(1)	-4(1)
C(8)	17(1)	11(1)	15(1)	0(1)	3(1)	1(1)
C(9)	17(1)	14(1)	13(1)	-1(1)	2(1)	1(1)
C(10)	18(1)	16(1)	15(1)	-3(1)	4(1)	1(1)
C(11)	18(1)	22(1)	22(1)	-2(1)	2(1)	-2(1)
C(12)	23(1)	18(1)	21(1)	2(1)	4(1)	-4(1)

Table A. 71 Hydrogen coordinates ($\times 10^4$) and isotropic displacement parameters ($\text{\AA}^2 \times 10^3$) for 178 (bt 1173)

	x	y	z	U(eq)
H(1)	8470	241	7343	20
H(3)	6098	848	5658	21
H(4)	5248	1904	3852	23
H(5)	7072	2042	2690	21
H(7)	10066	1991	2535	20
H(9)	11617	1270	6305	18
H(11A)	13914	2543	6774	31
H(11B)	13740	4448	6559	31
H(11C)	14529	3342	5759	31
H(12A)	12276	3929	3898	31
H(12B)	12097	5364	4737	31
H(12C)	10600	4288	4189	31

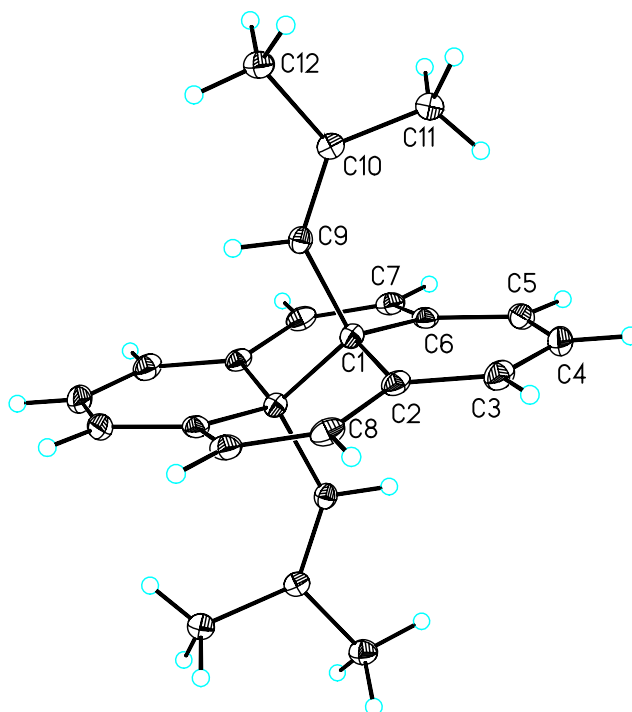
Single-Crystal X-ray Diffraction Laboratory
University of Idaho

X-ray structure report for diisobutenyl DHP 179



179

Brendan Twamley



Project name : Bt1265

3-31-0

Experimental:

Crystals of compound **1** were removed from the flask, a suitable crystal was selected, attached to a glass fiber and data were collected at 90(2) K using a Bruker/Siemens SMART APEX instrument (Mo K α radiation, $\lambda = 0.71073$ Å) equipped with a Cryocool NeverIce low temperature device. Data were measured using omega scans 0.3 ° per frame for 30 seconds, and a full sphere of data was collected. A total of 2400 frames were collected with a final resolution of 0.83 Å. Cell parameters were retrieved using SMART⁶⁰ software and refined using SAINTPlus⁶¹ on all observed reflections. Data reduction and correction for Lp and decay were performed using the SAINTPlus software. Absorption corrections were applied using SADABS.⁶² The structure was solved by direct methods and refined by least squares method on F² using the SHELXTL program package.⁶³ The structure was solved in the space group P2(1)/c (# 14) by analysis of systematic absences. All non-hydrogen atoms were refined anisotropically. Hydrogen atoms associated with C11 were refined with mild distance restraints. No decomposition was observed during data collection. Details of the data collection and refinement are given in Table 1. Further details are provided in the Supporting Information.

Acknowledgement

The Bruker (Siemens) SMART APEX diffraction facility was established at the University of Idaho with the assistance of the NSF-EPSCoR program and the M. J. Murdock Charitable Trust, Vancouver, WA, USA.

⁶⁰ SMART: v. 5.632, Bruker AXS, Madison, WI, **2005**.

⁶¹ SAINTPlus: v. 7.23a, Data Reduction and Correction Program, Bruker AXS, Madison, WI, **2004**.

⁶² SADABS: v.2007/4, an empirical absorption correction program, Bruker AXS Inc., Madison, WI, **2007**.

⁶³ SHELXTL: v. 6.14, Structure Determination Software Suite, Sheldrick, G.M., Bruker AXS Inc., Madison, WI, **2004**.

Table A. 72 Crystal data and structure refinement for 179.

Identification code	bt1265	
Empirical formula	C ₂₄ H ₂₄	
Formula weight	312.43	
Temperature	90(2) K	
Wavelength	0.71073 Å	
Crystal system	Monoclinic	
Space group	P2(1)/c	
Unit cell dimensions	a = 8.9436(19) Å	α = 90°.
	b = 13.044(3) Å	β = 107.758(4)°.
	c = 7.5887(16) Å	γ = 90°.
Volume	843.1(3) Å ³	
Z	2	
Density (calculated)	1.231 Mg/m ³	
Absorption coefficient	0.069 mm ⁻¹	
F(000)	336	
Crystal size	0.28 x 0.13 x 0.04 mm ³	
Crystal color and habit	orange plate	
Diffractometer	Bruker/Siemens SMART APEX	
Theta range for data collection	2.39 to 25.25°.	
Index ranges	-10 ≤ h ≤ 10, -15 ≤ k ≤ 15, -9 ≤ l ≤ 9	
Reflections collected	12281	
Independent reflections	1527 [R(int) = 0.0615]	
Completeness to theta = 25.25°	100.0%	
Absorption correction	None	
Solution method	XS, SHELXTL v. 6.14 (Bruker, 2003)	
Refinement method	Full-matrix least-squares on F ²	
Data / restraints / parameters	1527 / 3 / 119	
Goodness-of-fit on F ²	0.832	
Final R indices [I > 2σ(I)]	R1 = 0.0415, wR2 = 0.0939	
R indices (all data)	R1 = 0.0659, wR2 = 0.1053	
Largest diff. peak and hole	0.274 and -0.254 e.Å ⁻³	

Table A. 73 Atomic coordinates ($\times 10^4$) and equivalent isotropic displacement parameters ($\text{\AA}^2 \times 10^3$) for 179 (bt 1265).

	x	y	z	U(eq)
C(1)	4256(2)	5213(1)	9267(2)	20(1)
C(2)	4797(2)	5896(1)	7923(2)	22(1)
C(3)	3978(2)	5864(2)	6058(3)	29(1)
C(4)	2857(2)	5109(2)	5316(3)	31(1)
C(5)	2518(2)	4343(2)	6415(3)	28(1)
C(6)	3217(2)	4316(1)	8320(2)	22(1)
C(7)	3031(2)	3523(1)	9461(3)	25(1)
C(8)	6071(2)	6540(1)	8690(3)	26(1)
C(9)	3389(2)	5923(1)	10263(2)	20(1)
C(10)	1884(2)	6192(1)	9896(2)	20(1)
C(11)	497(2)	5854(2)	8320(3)	27(1)
C(12)	1442(2)	6956(1)	11144(3)	27(1)

Table A. 74 Bond lengths [Å] and angles [°] for 179 (bt 1265)

C(1)-C(6)	1.531(2)	C(9)-C(1)-C(1)#1	108.18(17)
C(1)-C(2)	1.539(2)	C(3)-C(2)-C(8)	123.87(17)
C(1)-C(9)	1.545(2)	C(3)-C(2)-C(1)	119.05(17)
C(1)-C(1)#1	1.554(3)	C(8)-C(2)-C(1)	117.05(15)
C(2)-C(3)	1.381(3)	C(2)-C(3)-C(4)	121.79(18)
C(2)-C(8)	1.393(3)	C(2)-C(3)-H(3)	119.1
C(3)-C(4)	1.395(3)	C(4)-C(3)-H(3)	119.1
C(3)-H(3)	0.9500	C(5)-C(4)-C(3)	121.66(17)
C(4)-C(5)	1.393(3)	C(5)-C(4)-H(4)	119.2
C(4)-H(4)	0.9500	C(3)-C(4)-H(4)	119.2
C(5)-C(6)	1.390(3)	C(6)-C(5)-C(4)	122.04(18)
C(5)-H(5)	0.9500	C(6)-C(5)-H(5)	119.0
C(6)-C(7)	1.391(3)	C(4)-C(5)-H(5)	119.0
C(7)-C(8)#1	1.390(3)	C(5)-C(6)-C(7)	124.45(17)
C(7)-H(7)	0.9500	C(5)-C(6)-C(1)	118.98(16)
C(8)-C(7)#1	1.390(3)	C(7)-C(6)-C(1)	116.57(16)
C(8)-H(8)	0.9500	C(8)#1-C(7)-C(6)	122.04(17)
C(9)-C(10)	1.335(3)	C(8)#1-C(7)-H(7)	119.0
C(9)-H(9)	0.9500	C(6)-C(7)-H(7)	119.0
C(10)-C(11)	1.503(3)	C(7)#1-C(8)-C(2)	122.23(17)
C(10)-C(12)	1.507(2)	C(7)#1-C(8)-H(8)	118.9
C(11)-H(11A)	1.017(15)	C(2)-C(8)-H(8)	118.9
C(11)-H(11B)	0.954(15)	C(10)-C(9)-C(1)	132.87(16)
C(11)-H(11C)	0.936(15)	C(10)-C(9)-H(9)	113.6
C(12)-H(12A)	0.9800	C(1)-C(9)-H(9)	113.6
C(12)-H(12B)	0.9800	C(9)-C(10)-C(11)	128.52(17)
C(12)-H(12C)	0.9800	C(9)-C(10)-C(12)	118.94(16)
		C(11)-C(10)-C(12)	112.52(15)
C(6)-C(1)-C(2)	113.60(14)	C(10)-C(11)-H(11A)	108.5(11)
C(6)-C(1)-C(9)	111.34(14)	C(10)-C(11)-H(11B)	111.5(11)
C(2)-C(1)-C(9)	106.48(14)	H(11A)-C(11)-H(11B)	102.6(13)
C(6)-C(1)-C(1)#1	109.06(17)	C(10)-C(11)-H(11C)	118.3(12)
C(2)-C(1)-C(1)#1	107.99(17)	H(11A)-C(11)-H(11C)	104.6(13)

H(11B)-C(11)-H(11C)	109.9(14)	C(10)-C(12)-H(12C)	109.5
C(10)-C(12)-H(12A)	109.5	H(12A)-C(12)-H(12C)	109.5
C(10)-C(12)-H(12B)	109.5	H(12B)-C(12)-H(12C)	109.5
H(12A)-C(12)-H(12B)	109.5		

Symmetry transformations used to generate equivalent atoms:

#1 -x+1,-y+1,-z+2

Table A. 75 Anisotropic displacement parameters ($\text{\AA}^2 \times 10^3$) for 179 (bt 1265).

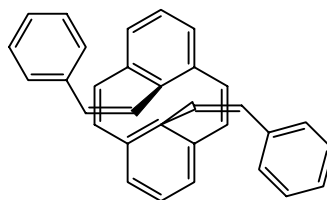
	U11	U22	U33	U23	U13	U12
C(1)	22(1)	20(1)	18(1)	0(1)	7(1)	1(1)
C(2)	26(1)	20(1)	23(1)	1(1)	11(1)	7(1)
C(3)	34(1)	30(1)	24(1)	6(1)	12(1)	9(1)
C(4)	30(1)	41(1)	20(1)	-2(1)	3(1)	10(1)
C(5)	22(1)	31(1)	28(1)	-10(1)	4(1)	3(1)
C(6)	17(1)	22(1)	28(1)	-6(1)	7(1)	2(1)
C(7)	22(1)	22(1)	35(1)	-6(1)	13(1)	-2(1)
C(8)	32(1)	20(1)	32(1)	2(1)	19(1)	1(1)
C(9)	23(1)	19(1)	19(1)	-1(1)	6(1)	-2(1)
C(10)	23(1)	17(1)	23(1)	1(1)	9(1)	-1(1)
C(11)	24(1)	31(1)	26(1)	-1(1)	7(1)	2(1)
C(12)	25(1)	26(1)	30(1)	-1(1)	10(1)	2(1)

Table A. 76 Hydrogen coordinates ($\times 10^4$) and isotropic displacement parameters ($\text{\AA}^2 \times 10^3$) for 179 (bt 1265)

	x	y	z	U(eq)
H(3)	4183	6369	5260	34
H(4)	2312	5118	4028	37
H(5)	1787	3823	5844	34
H(7)	2266	3010	8962	30
H(8)	6337	7039	7924	31
H(9)	4060	6228	11355	24
H(11A)	-130(20)	6486(11)	7740(30)	32
H(11B)	-240(20)	5480(12)	8750(20)	32
H(11C)	690(20)	5507(13)	7330(30)	32
H(12A)	704	6637	11705	32
H(12B)	947	7554	10418	32
H(12C)	2387	7171	12120	32

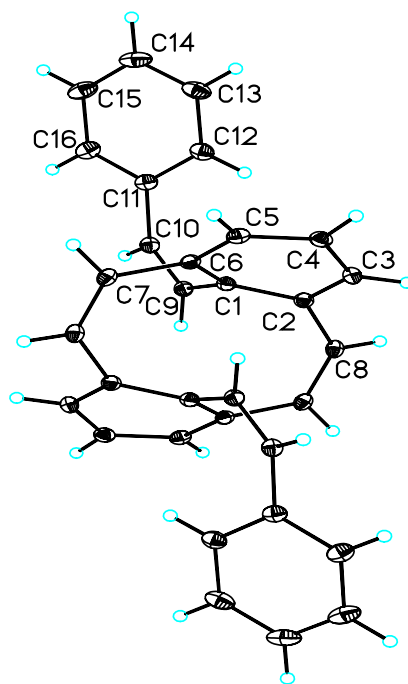
Single-Crystal X-ray Diffraction Laboratory
University of Idaho

X-ray structure report for *cis*-styryl CPD 202



202

Brendan Twamley



Project name : Bt1263

3-23-08

Experimental:

Crystals of compound **1** were removed from the flask, a suitable crystal was selected, attached to a glass fiber and data were collected at 90(2) K using a Bruker/Siemens SMART APEX instrument (Mo K α radiation, $\lambda = 0.71073$ Å) equipped with a Cryocool NeverIce low temperature device. Data were measured using omega scans 0.3 ° per frame for 5 seconds, and a full sphere of data was collected. A total of 2400 frames were collected with a final resolution of 0.77 Å. Cell parameters were retrieved using SMART⁶⁴ software and refined using SAINTPlus⁶⁵ on all observed reflections. Data reduction and correction for Lp and decay were performed using the SAINTPlus software. Absorption corrections were applied using SADABS.⁶⁶ The structure was solved by direct methods and refined by least squares method on F² using the SHELXTL program package.⁶⁷ The structure was solved in the space group P2(1)/n (# 14) by analysis of systematic absences. All non-hydrogen atoms were refined anisotropically. No decomposition was observed during data collection. Details of the data collection and refinement are given in Table 1. Further details are provided in the Supporting Information

Acknowledgement

The Bruker (Siemens) SMART APEX diffraction facility was established at the University of Idaho with the assistance of the NSF-EPSCoR program and the M. J. Murdock Charitable Trust, Vancouver, WA, USA.

⁶⁴ SMART: v. 5.632, Bruker AXS, Madison, WI, **2005**.

⁶⁵ SAINTPlus: v. 7.23a, Data Reduction and Correction Program, Bruker AXS, Madison, WI, **2004**.

⁶⁶ SADABS: v.2007/4, an empirical absorption correction program, Bruker AXS Inc., Madison, WI, **2007**.

⁶⁷ SHELXTL: v. 6.14, Structure Determination Software Suite, Sheldrick, G.M., Bruker AXS Inc., Madison, WI, **2004**.

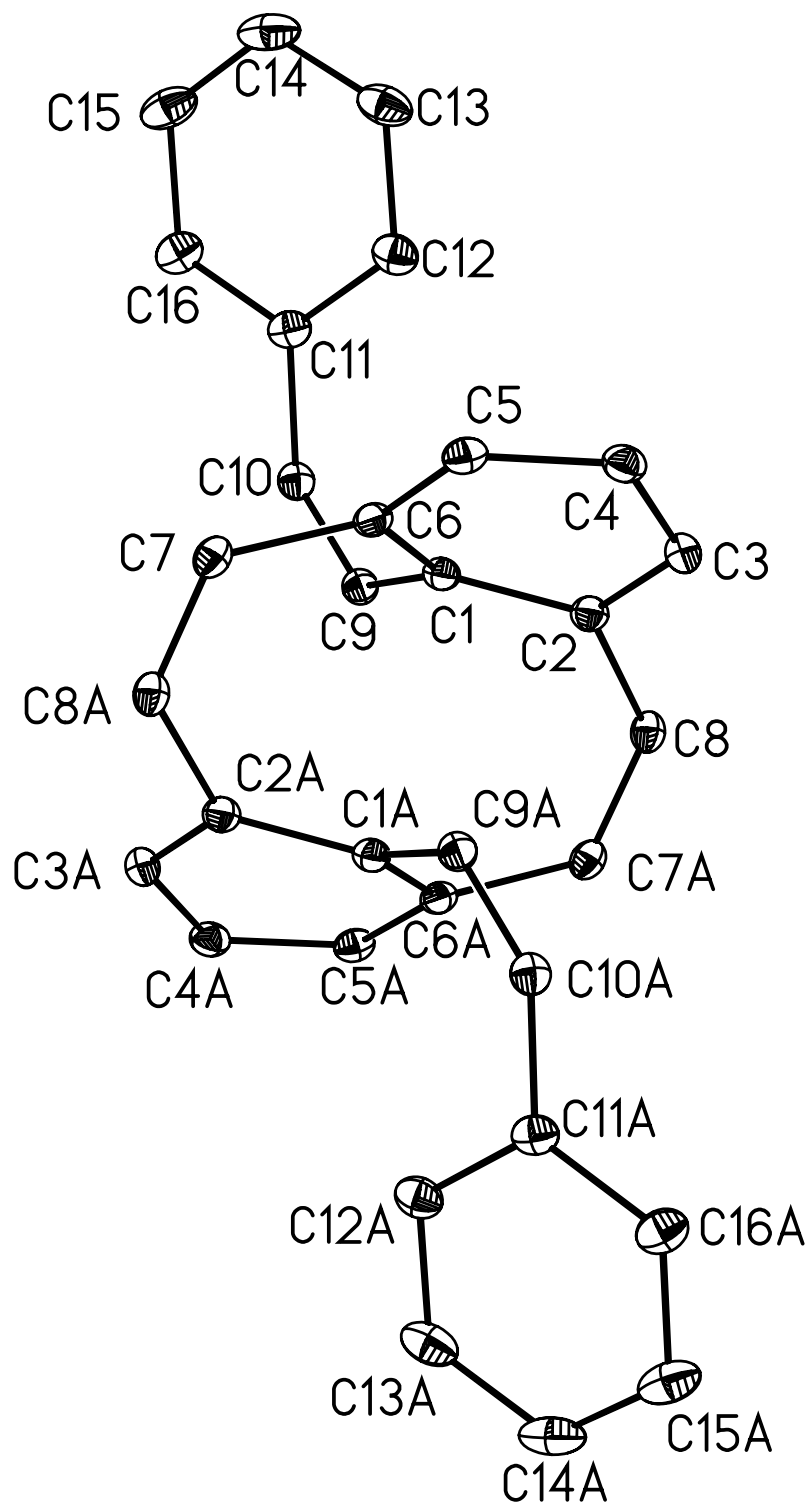


Table A. 77 Crystal data and structure refinement for *cis*-distyryl CPD 202

Identification code	bt1263	
Empirical formula	C ₃₂ H ₂₄	
Formula weight	408.51	
Temperature	90(2) K	
Wavelength	0.71073 Å	
Crystal system	Monoclinic	
Space group	P2(1)/n	
Unit cell dimensions	a = 9.6423(3) Å	α = 90°.
	b = 7.3261(2) Å	β = 100.983(1)°.
	c = 15.3388(5) Å	γ = 90°.
Volume	1063.69(6) Å ³	
Z	2	
Density (calculated)	1.275 Mg/m ³	
Absorption coefficient	0.072 mm ⁻¹	
F(000)	432	
Crystal size	0.34 x 0.23 x 0.17 mm ³	
Crystal color and habit	yellow needle	
Diffractometer	Bruker/Siemens SMART APEX	
Theta range for data collection	2.31 to 27.49°.	
Index ranges	-12 ≤ h ≤ 12, -9 ≤ k ≤ 9, -19 ≤ l ≤ 19	
Reflections collected	15817	
Independent reflections	2447 [R(int) = 0.0303]	
Completeness to theta = 27.49°	100.0%	
Absorption correction	Semi-empirical from equivalents	
Max. and min. transmission	0.984 and 0.902	
Solution method	XS, SHELXTL v. 6.14 (Bruker, 2003)	
Refinement method	Full-matrix least-squares on F ²	
Data / restraints / parameters	2447 / 0 / 145	
Goodness-of-fit on F ²	1.842	
Final R indices [I > 2σ(I)]	R1 = 0.0442, wR2 = 0.1139	
R indices (all data)	R1 = 0.0525, wR2 = 0.1183	
Largest diff. peak and hole	0.302 and -0.202 e.Å ⁻³	

Table A. 78 Atomic coordinates ($\times 10^4$) and equivalent isotropic displacement parameters ($\text{\AA}^2 \times 10^3$) for 202 (bt 1263).

	x	y	z	U(eq)
C(1)	9749(1)	5278(2)	824(1)	19(1)
C(2)	9339(1)	7078(2)	569(1)	20(1)
C(3)	10175(1)	8526(2)	970(1)	23(1)
C(4)	11459(1)	8193(2)	1533(1)	23(1)
C(5)	12003(1)	6436(2)	1598(1)	21(1)
C(6)	11189(1)	4971(2)	1205(1)	19(1)
C(7)	11926(1)	3277(2)	1017(1)	21(1)
C(8)	8215(1)	7507(2)	-214(1)	21(1)
C(9)	8722(1)	3756(2)	694(1)	20(1)
C(10)	8437(1)	2684(2)	1344(1)	21(1)
C(11)	8984(1)	2755(2)	2312(1)	23(1)
C(12)	9455(1)	4367(2)	2768(1)	26(1)
C(13)	9921(1)	4347(2)	3680(1)	33(1)
C(14)	9919(2)	2741(2)	4159(1)	37(1)
C(15)	9426(1)	1156(2)	3723(1)	35(1)
C(16)	8965(1)	1157(2)	2810(1)	28(1)

Table A. 79 Bond lengths [\AA] and angles [$^\circ$] for 202 (bt 1263)

C(1)-C(2)	1.4110(16)	C(2)-C(1)-C(6)	117.61(11)
C(1)-C(6)	1.4171(16)	C(2)-C(1)-C(9)	121.43(10)
C(1)-C(9)	1.4798(16)	C(6)-C(1)-C(9)	120.95(10)
C(2)-C(3)	1.4018(17)	C(3)-C(2)-C(1)	118.57(11)
C(2)-C(8)	1.4897(16)	C(3)-C(2)-C(8)	117.61(11)
C(3)-C(4)	1.3900(17)	C(1)-C(2)-C(8)	122.92(11)
C(3)-H(3)	0.9500	C(4)-C(3)-C(2)	120.65(11)
C(4)-C(5)	1.3864(17)	C(4)-C(3)-H(3)	119.7
C(4)-H(4)	0.9500	C(2)-C(3)-H(3)	119.7
C(5)-C(6)	1.3971(16)	C(5)-C(4)-C(3)	119.17(11)
C(5)-H(5)	0.9500	C(5)-C(4)-H(4)	120.4
C(6)-C(7)	1.4851(16)	C(3)-C(4)-H(4)	120.4
C(7)-C(8)#1	1.3422(17)	C(4)-C(5)-C(6)	120.58(11)
C(7)-H(7)	0.9500	C(4)-C(5)-H(5)	119.7
C(8)-C(7)#1	1.3422(17)	C(6)-C(5)-H(5)	119.7
C(8)-H(8)	0.9500	C(5)-C(6)-C(1)	118.79(11)
C(9)-C(10)	1.3378(16)	C(5)-C(6)-C(7)	118.38(11)
C(9)-H(9)	0.9500	C(1)-C(6)-C(7)	121.32(10)
C(10)-C(11)	1.4795(17)	C(8)#1-C(7)-C(6)	124.57(11)
C(10)-H(10)	0.9500	C(8)#1-C(7)-H(7)	117.7
C(11)-C(16)	1.3998(18)	C(6)-C(7)-H(7)	117.7
C(11)-C(12)	1.4028(18)	C(7)#1-C(8)-C(2)	125.43(11)
C(12)-C(13)	1.3865(18)	C(7)#1-C(8)-H(8)	117.3
C(12)-H(12)	0.9500	C(2)-C(8)-H(8)	117.3
C(13)-C(14)	1.387(2)	C(10)-C(9)-C(1)	124.69(11)
C(13)-H(13)	0.9500	C(10)-C(9)-H(9)	117.7
C(14)-C(15)	1.379(2)	C(1)-C(9)-H(9)	117.7
C(14)-H(14)	0.9500	C(9)-C(10)-C(11)	130.00(11)
C(15)-C(16)	1.3866(18)	C(9)-C(10)-H(10)	115.0
C(15)-H(15)	0.9500	C(11)-C(10)-H(10)	115.0
C(16)-H(16)	0.9500	C(16)-C(11)-C(12)	117.97(12)

C(16)-C(11)-C(10)	118.62(11)	C(15)-C(14)-C(13)	119.50(13)
C(12)-C(11)-C(10)	123.32(11)	C(15)-C(14)-H(14)	120.3
C(13)-C(12)-C(11)	120.38(13)	C(13)-C(14)-H(14)	120.3
C(13)-C(12)-H(12)	119.8	C(14)-C(15)-C(16)	120.27(14)
C(11)-C(12)-H(12)	119.8	C(14)-C(15)-H(15)	119.9
C(14)-C(13)-C(12)	120.74(13)	C(16)-C(15)-H(15)	119.9
C(14)-C(13)-H(13)	119.6	C(15)-C(16)-C(11)	121.11(13)
C(12)-C(13)-H(13)	119.6	C(15)-C(16)-H(16)	119.4
		C(11)-C(16)-H(16)	119.4

Symmetry transformations used to generate equivalent atoms:

#1 -x+2,-y+1,-z

Table A. 80 Anisotropic displacement parameters ($\text{\AA}^2 \times 10^3$) for 202 (bt 1263).

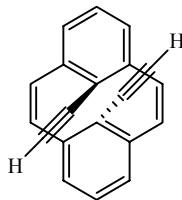
	U11	U22	U33	U23	U13	U12
C(1)	21(1)	20(1)	15(1)	-1(1)	3(1)	-1(1)
C(2)	20(1)	22(1)	18(1)	0(1)	4(1)	1(1)
C(3)	28(1)	18(1)	22(1)	-1(1)	6(1)	2(1)
C(4)	28(1)	23(1)	18(1)	-3(1)	3(1)	-4(1)
C(5)	21(1)	25(1)	17(1)	2(1)	1(1)	-2(1)
C(6)	21(1)	20(1)	15(1)	2(1)	3(1)	0(1)
C(7)	19(1)	21(1)	22(1)	4(1)	0(1)	1(1)
C(8)	19(1)	19(1)	25(1)	1(1)	2(1)	2(1)
C(9)	18(1)	20(1)	19(1)	-1(1)	1(1)	1(1)
C(10)	19(1)	21(1)	22(1)	-1(1)	2(1)	-1(1)
C(11)	16(1)	31(1)	21(1)	2(1)	5(1)	0(1)
C(12)	21(1)	33(1)	25(1)	-3(1)	7(1)	0(1)
C(13)	23(1)	49(1)	26(1)	-10(1)	6(1)	1(1)
C(14)	26(1)	66(1)	19(1)	2(1)	5(1)	3(1)
C(15)	27(1)	52(1)	27(1)	13(1)	7(1)	0(1)
C(16)	22(1)	34(1)	27(1)	5(1)	6(1)	-3(1)

Table A. 81 Hydrogen coordinates ($\times 10^4$) and isotropic displacement parameters ($\text{\AA}^2 \times 10^3$) for 202 (bt 1263)

	x	y	z	U(eq)
H(3)	9860	9747	856	27
H(4)	11959	9158	1869	27
H(5)	12937	6226	1913	26
H(7)	12539	2710	1498	25
H(8)	7541	8411	-138	26
H(9)	8228	3524	107	24
H(10)	7782	1729	1154	25
H(12)	9455	5478	2449	31
H(13)	10245	5445	3981	39
H(14)	10255	2734	4783	45
H(15)	9402	58	4050	42
H(16)	8630	55	2517	33

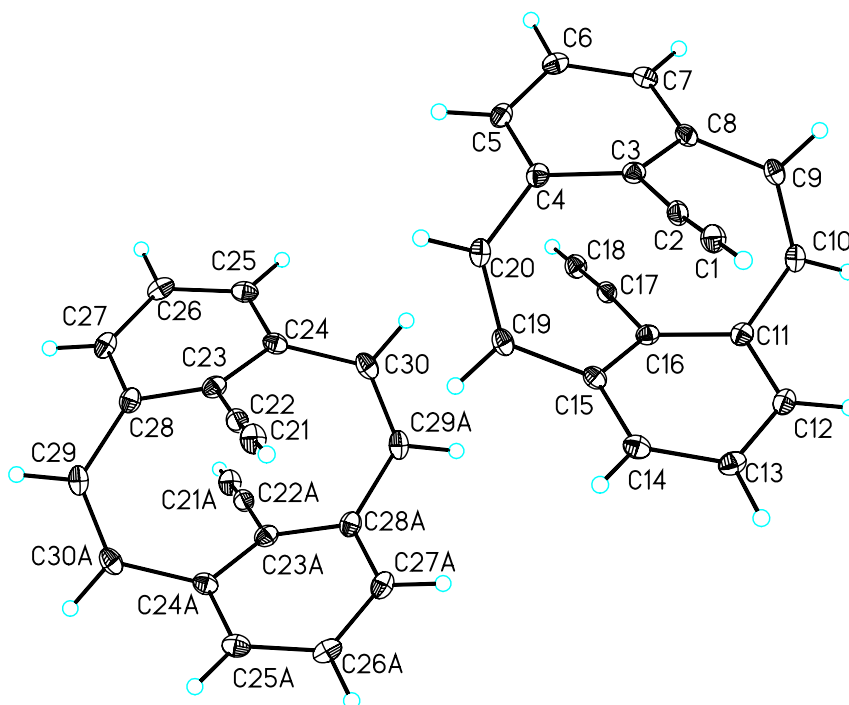
Single-Crystal X-ray Diffraction Laboratory
University of Idaho

X-ray structure report for diethynyl CPD 235



235

Brendan Twamley



Project name : Bt1220

1-17-08

Experimental:

Crystals of compound **1** were removed from the flask, cooled with dry ice, a suitable crystal was selected, attached to a glass fiber and data were collected at 90(2) K using a Bruker/Siemens SMART APEX instrument (Mo K α radiation, $\lambda = 0.71073$ Å) equipped with a Cryocool NeverIce low temperature device. Data were measured using omega scans 0.3° per frame for 10 seconds, and a full sphere of data was collected. A total of 2400 frames were collected with a final resolution of 0.83 Å. Cell parameters were retrieved using SMART⁶⁸ software and refined using SAINTPlus⁶⁹ on all observed reflections. Data reduction and correction for Lp and decay were performed using the SAINTPlus software. Absorption corrections were applied using SADABS.⁷⁰ The structure was solved by direct methods and refined by least squares method on F² using the SHELXTL program package.⁷¹ The structure was solved in the space group P2(1)/n (# 14) by analysis of systematic absences. All non-hydrogen atoms were refined anisotropically. No decomposition was observed during data collection. Details of the data collection and refinement are given in Table 1. Further details are provided in the Supporting Information.

Acknowledgement

The Bruker (Siemens) SMART APEX diffraction facility was established at the University of Idaho with the assistance of the NSF-EPSCoR program and the M. J. Murdock Charitable Trust, Vancouver, WA, USA.

⁶⁸ SMART: v. 5.632, Bruker AXS, Madison, WI, **2005**.

⁶⁹ SAINTPlus: v. 7.23a, Data Reduction and Correction Program, Bruker AXS, Madison, WI, **2004**.

⁷⁰ SADABS: v.2007/4, an empirical absorption correction program, Bruker AXS Inc., Madison, WI, **2007**.

⁷¹ SHELXTL: v. 6.14, Structure Determination Software Suite, Sheldrick, G.M., Bruker AXS Inc., Madison, WI, **2004**.

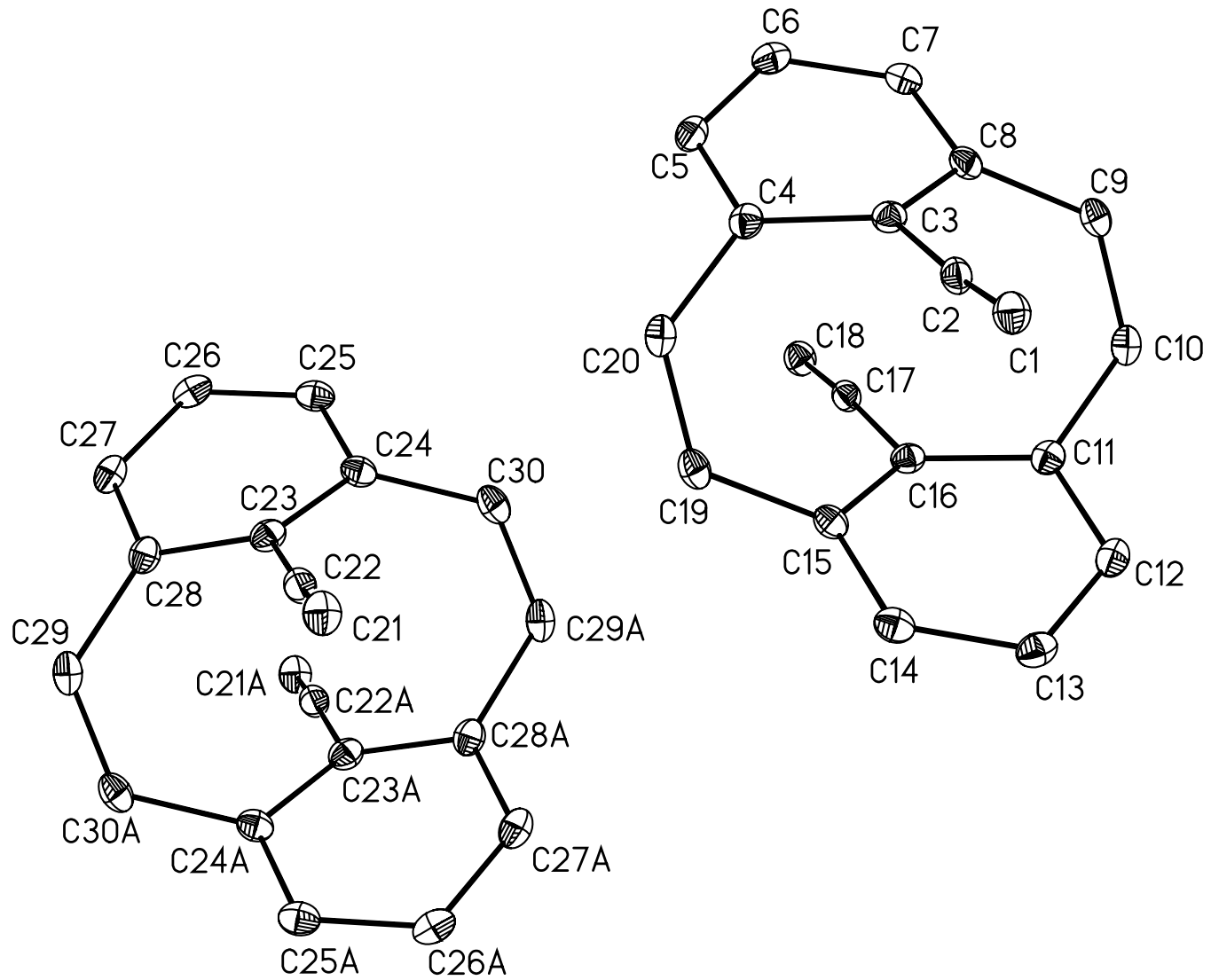


Table A. 82 Crystal data and structure refinement for diethynyl CPD 235

Identification code	bt1220	
Empirical formula	C ₂₀ H ₁₂	
Formula weight	252.30	
Temperature	90(2) K	
Wavelength	0.71073 Å	
Crystal system	Monoclinic	
Space group	P2(1)/n	
Unit cell dimensions	a = 7.4416(3) Å	α = 90°.
	b = 19.6206(7) Å	β = 104.501(1)°.
	c = 13.6665(5) Å	γ = 90°.
Volume	1931.86(13) Å ³	
Z	6	
Density (calculated)	1.301 Mg/m ³	
Absorption coefficient	0.074 mm ⁻¹	
F(000)	792	
Crystal size	0.33 x 0.23 x 0.09 mm ³	
Crystal color and habit	yellow needle	
Diffractometer	Bruker/Siemens SMART APEX	
Theta range for data collection	1.86 to 25.25°.	
Index ranges	-8 ≤ h ≤ 8, -23 ≤ k ≤ 23, -16 ≤ l ≤ 16	
Reflections collected	28655	
Independent reflections	3496 [R(int) = 0.0356]	
Completeness to theta = 25.25°	100.0%	
Absorption correction	Semi-empirical from equivalents	
Max. and min. transmission	0.990 and 0.976	
Solution method	XS, SHELXTL v. 6.14 (Bruker, 2003)	
Refinement method	Full-matrix least-squares on F ²	
Data / restraints / parameters	3496 / 0 / 271	
Goodness-of-fit on F ²	1.012	
Final R indices [I > 2σ(I)]	R1 = 0.0434, wR2 = 0.1129	
R indices (all data)	R1 = 0.0544, wR2 = 0.1228	
Largest diff. peak and hole	0.258 and -0.172 e.Å ⁻³	

Table A. 83 Atomic coordinates ($\times 10^4$) and equivalent isotropic displacement parameters ($\text{\AA}^2 \times 10^3$) for 235 (bt 1220).

	x	y	z	U(eq)
C(1)	3552(2)	539(1)	9121(1)	22(1)
C(2)	2337(2)	936(1)	9104(1)	19(1)
C(3)	790(2)	1396(1)	8937(1)	19(1)
C(4)	909(2)	2051(1)	8524(1)	19(1)
C(5)	-741(2)	2392(1)	8084(1)	22(1)
C(6)	-2441(2)	2126(1)	8143(1)	23(1)
C(7)	-2490(2)	1569(1)	8761(1)	21(1)
C(8)	-859(2)	1218(1)	9219(1)	20(1)
C(9)	-824(2)	789(1)	10117(1)	21(1)
C(10)	419(2)	830(1)	11019(1)	21(1)
C(11)	2193(2)	1213(1)	11225(1)	19(1)
C(12)	3848(2)	884(1)	11696(1)	21(1)
C(13)	5550(2)	1151(1)	11645(1)	23(1)
C(14)	5606(2)	1696(1)	11003(1)	22(1)
C(15)	3974(2)	2039(1)	10524(1)	19(1)
C(16)	2321(2)	1862(1)	10797(1)	18(1)
C(17)	769(2)	2322(1)	10612(1)	19(1)
C(18)	-444(2)	2726(1)	10553(1)	22(1)
C(19)	3944(2)	2470(1)	9629(1)	21(1)
C(20)	2686(2)	2433(1)	8729(1)	21(1)
C(21)	6742(2)	3986(1)	8900(1)	26(1)
C(22)	5653(2)	4398(1)	9031(1)	21(1)
C(23)	4194(2)	4882(1)	9024(1)	21(1)
C(24)	2537(2)	4679(1)	9269(1)	21(1)
C(25)	957(2)	5079(1)	8917(1)	23(1)
C(26)	1067(2)	5696(1)	8438(1)	25(1)
C(27)	2793(2)	5961(1)	8438(1)	24(1)
C(28)	4404(2)	5578(1)	8786(1)	22(1)
C(29)	6224(2)	5928(1)	9077(1)	24(1)

C(30)	2518(2)	4143(1)	10035(1)	24(1)
-------	---------	---------	----------	-------

Table A. 84 Bond lengths [Å] and angles [°] for 235 (bt 1220)

C(1)-C(2)	1.189(2)	C(18)-H(18)	0.9500
C(1)-H(1)	0.9500	C(19)-C(20)	1.348(2)
C(2)-C(3)	1.435(2)	C(19)-H(19A)	0.9500
C(3)-C(4)	1.416(2)	C(20)-H(20A)	0.9500
C(3)-C(8)	1.419(2)	C(21)-C(22)	1.189(2)
C(4)-C(5)	1.395(2)	C(21)-H(21)	0.9500
C(4)-C(20)	1.484(2)	C(22)-C(23)	1.440(2)
C(5)-C(6)	1.389(2)	C(23)-C(24)	1.413(2)
C(5)-H(5A)	0.9500	C(23)-C(28)	1.421(2)
C(6)-C(7)	1.388(2)	C(24)-C(25)	1.395(2)
C(6)-H(6A)	0.9500	C(24)-C(30)	1.487(2)
C(7)-C(8)	1.399(2)	C(25)-C(26)	1.389(2)
C(7)-H(7A)	0.9500	C(25)-H(25A)	0.9500
C(8)-C(9)	1.485(2)	C(26)-C(27)	1.385(2)
C(9)-C(10)	1.345(2)	C(26)-H(26A)	0.9500
C(9)-H(9A)	0.9500	C(27)-C(28)	1.394(2)
C(10)-C(11)	1.484(2)	C(27)-H(27A)	0.9500
C(10)-H(10A)	0.9500	C(28)-C(29)	1.481(2)
C(11)-C(12)	1.396(2)	C(29)-C(30)#1	1.342(2)
C(11)-C(16)	1.415(2)	C(29)-H(29A)	0.9500
C(12)-C(13)	1.389(2)	C(30)-C(29)#1	1.342(2)
C(12)-H(12A)	0.9500	C(30)-H(30A)	0.9500
C(13)-C(14)	1.389(2)		
C(13)-H(13A)	0.9500	C(2)-C(1)-H(1)	180.0
C(14)-C(15)	1.399(2)	C(1)-C(2)-C(3)	172.04(16)
C(14)-H(14A)	0.9500	C(4)-C(3)-C(8)	118.40(13)
C(15)-C(16)	1.416(2)	C(4)-C(3)-C(2)	120.44(13)
C(15)-C(19)	1.483(2)	C(8)-C(3)-C(2)	121.11(13)
C(16)-C(17)	1.437(2)	C(5)-C(4)-C(3)	118.07(14)
C(17)-C(18)	1.188(2)	C(5)-C(4)-C(20)	119.05(13)

C(3)-C(4)-C(20)	121.68(14)	C(15)-C(16)-C(17)	120.85(14)
C(6)-C(5)-C(4)	120.77(14)	C(18)-C(17)-C(16)	173.54(16)
C(6)-C(5)-H(5A)	119.6	C(17)-C(18)-H(18)	180.0
C(4)-C(5)-H(5A)	119.6	C(20)-C(19)-C(15)	125.80(14)
C(7)-C(6)-C(5)	119.60(14)	C(20)-C(19)-H(19A)	117.1
C(7)-C(6)-H(6A)	120.2	C(15)-C(19)-H(19A)	117.1
C(5)-C(6)-H(6A)	120.2	C(19)-C(20)-C(4)	125.63(14)
C(6)-C(7)-C(8)	120.50(14)	C(19)-C(20)-H(20A)	117.2
C(6)-C(7)-H(7A)	119.8	C(4)-C(20)-H(20A)	117.2
C(8)-C(7)-H(7A)	119.8	C(22)-C(21)-H(21)	180.0
C(7)-C(8)-C(3)	118.08(14)	C(21)-C(22)-C(23)	170.96(17)
C(7)-C(8)-C(9)	118.86(14)	C(24)-C(23)-C(28)	118.54(14)
C(3)-C(8)-C(9)	121.78(13)	C(24)-C(23)-C(22)	120.91(14)
C(10)-C(9)-C(8)	126.10(14)	C(28)-C(23)-C(22)	120.55(14)
C(10)-C(9)-H(9A)	116.9	C(25)-C(24)-C(23)	118.02(15)
C(8)-C(9)-H(9A)	116.9	C(25)-C(24)-C(30)	118.98(14)
C(9)-C(10)-C(11)	125.42(14)	C(23)-C(24)-C(30)	121.94(14)
C(9)-C(10)-H(10A)	117.3	C(26)-C(25)-C(24)	120.60(15)
C(11)-C(10)-H(10A)	117.3	C(26)-C(25)-H(25A)	119.7
C(12)-C(11)-C(16)	117.65(14)	C(24)-C(25)-H(25A)	119.7
C(12)-C(11)-C(10)	119.57(13)	C(27)-C(26)-C(25)	119.37(15)
C(16)-C(11)-C(10)	121.73(13)	C(27)-C(26)-H(26A)	120.3
C(13)-C(12)-C(11)	120.79(14)	C(25)-C(26)-H(26A)	120.3
C(13)-C(12)-H(12A)	119.6	C(26)-C(27)-C(28)	121.09(15)
C(11)-C(12)-H(12A)	119.6	C(26)-C(27)-H(27A)	119.5
C(14)-C(13)-C(12)	119.63(14)	C(28)-C(27)-H(27A)	119.5
C(14)-C(13)-H(13A)	120.2	C(27)-C(28)-C(23)	117.47(15)
C(12)-C(13)-H(13A)	120.2	C(27)-C(28)-C(29)	119.45(14)
C(13)-C(14)-C(15)	120.39(15)	C(23)-C(28)-C(29)	122.03(14)
C(13)-C(14)-H(14A)	119.8	C(30)#1-C(29)-C(28)	125.30(14)
C(15)-C(14)-H(14A)	119.8	C(30)#1-C(29)-H(29A)	117.4
C(14)-C(15)-C(16)	117.90(14)	C(28)-C(29)-H(29A)	117.4
C(14)-C(15)-C(19)	119.56(14)	C(29)#1-C(30)-C(24)	125.69(14)
C(16)-C(15)-C(19)	121.51(13)	C(29)#1-C(30)-H(30A)	117.2
C(11)-C(16)-C(15)	118.87(14)	C(24)-C(30)-H(30A)	117.2
C(11)-C(16)-C(17)	120.25(13)		

Symmetry transformations used to generate equivalent atoms:

#1 -x+1,-y+1,-z+2

Table A. 85 **Anisotropic displacement parameters ($\text{\AA}^2 \times 10^3$) for 235 (bt 1220).**

	U11	U22	U33	U23	U13	U12
C(1)	24(1)	19(1)	24(1)	0(1)	8(1)	1(1)
C(2)	24(1)	17(1)	18(1)	1(1)	7(1)	-4(1)
C(3)	20(1)	18(1)	17(1)	-2(1)	3(1)	1(1)
C(4)	23(1)	20(1)	16(1)	-1(1)	7(1)	1(1)
C(5)	28(1)	19(1)	17(1)	2(1)	5(1)	2(1)
C(6)	21(1)	26(1)	19(1)	-2(1)	2(1)	4(1)
C(7)	18(1)	22(1)	21(1)	-5(1)	4(1)	-3(1)
C(8)	22(1)	15(1)	22(1)	-4(1)	5(1)	-2(1)
C(9)	21(1)	15(1)	27(1)	-1(1)	10(1)	-1(1)
C(10)	23(1)	17(1)	24(1)	4(1)	11(1)	2(1)
C(11)	22(1)	20(1)	15(1)	-1(1)	7(1)	2(1)
C(12)	28(1)	18(1)	18(1)	1(1)	7(1)	4(1)
C(13)	23(1)	23(1)	20(1)	-3(1)	2(1)	6(1)
C(14)	20(1)	22(1)	23(1)	-6(1)	6(1)	0(1)
C(15)	21(1)	16(1)	21(1)	-5(1)	5(1)	-2(1)
C(16)	19(1)	19(1)	16(1)	-2(1)	3(1)	1(1)
C(17)	23(1)	16(1)	17(1)	-1(1)	5(1)	-3(1)
C(18)	24(1)	18(1)	25(1)	-1(1)	7(1)	1(1)
C(19)	22(1)	15(1)	29(1)	0(1)	10(1)	0(1)
C(20)	23(1)	18(1)	24(1)	4(1)	11(1)	2(1)
C(21)	30(1)	22(1)	27(1)	-1(1)	11(1)	1(1)
C(22)	24(1)	20(1)	20(1)	-1(1)	7(1)	-4(1)
C(23)	24(1)	22(1)	17(1)	-2(1)	3(1)	2(1)
C(24)	22(1)	19(1)	22(1)	-6(1)	4(1)	-2(1)
C(25)	22(1)	27(1)	21(1)	-7(1)	5(1)	-1(1)
C(26)	24(1)	31(1)	18(1)	0(1)	3(1)	8(1)
C(27)	31(1)	22(1)	19(1)	2(1)	8(1)	5(1)
C(28)	26(1)	22(1)	19(1)	1(1)	9(1)	2(1)

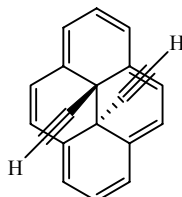
C(29)	29(1)	19(1)	29(1)	4(1)	16(1)	1(1)
C(30)	23(1)	16(1)	35(1)	-2(1)	11(1)	-2(1)

Table A. 86 Hydrogen coordinates ($\times 10^4$) and isotropic displacement parameters ($\text{\AA}^2 \times 10^3$) for 235 (bt 1220)

	x	y	z	U(eq)
H(1)	4522	221	9134	27
H(5A)	-702	2810	7740	26
H(6A)	-3563	2325	7762	27
H(7A)	-3639	1425	8875	25
H(9A)	-1768	453	10049	25
H(10A)	137	594	11569	25
H(12A)	3809	472	12056	25
H(13A)	6669	963	12046	27
H(14A)	6758	1836	10889	26
H(18)	-1413	3048	10506	27
H(19A)	4896	2803	9695	25
H(20A)	2959	2672	8180	25
H(21)	7611	3657	8795	31
H(25A)	-204	4928	9007	28
H(26A)	-31	5935	8112	30
H(27A)	2880	6411	8198	29
H(29A)	6525	6227	8595	29
H(30A)	1529	3823	9882	29

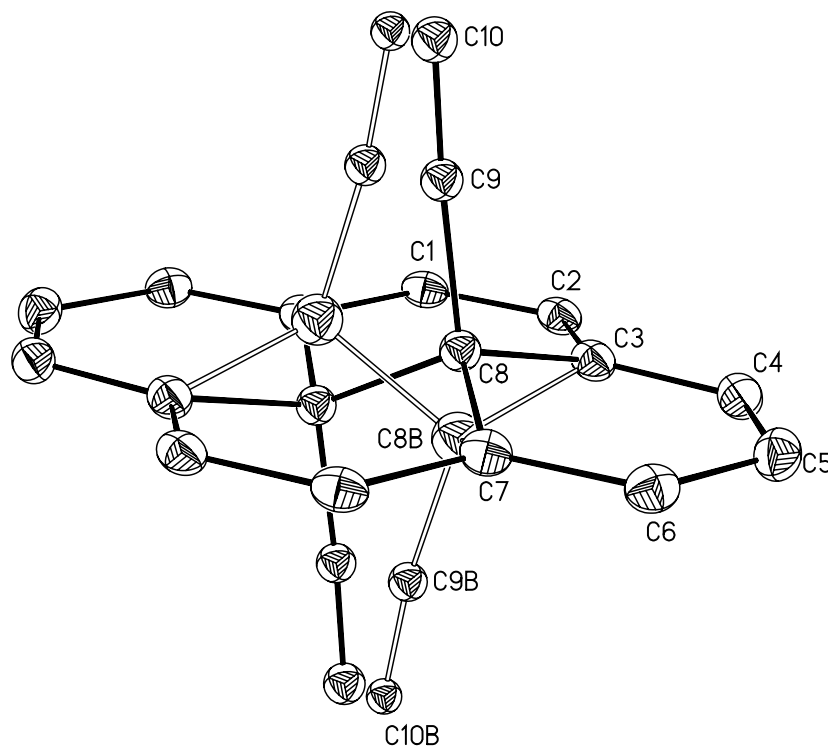
Single-Crystal X-ray Diffraction Laboratory
University of Idaho

X-ray structure report for diethynyl DHP 236



236

Brendan Twamley



Project name : Bt1228

1-26-08

Experimental:

Crystals of compound **1** were removed from the flask, a suitable crystal was selected, attached to a glass fiber and data were collected at 90(2) K using a Bruker/Siemens SMART APEX instrument (Mo K α radiation, $\lambda = 0.71073$ Å) equipped with a Cryocool NeverIce low temperature device. Data were measured using omega scans 0.3° per frame for 30 seconds, and a full sphere of data was collected. A total of 2400 frames were collected with a final resolution of 0.83 Å. Cell parameters were retrieved using SMART⁷² software and refined using SAINTPlus⁷³ on all observed reflections. Data reduction and correction for Lp and decay were performed using the SAINTPlus software. Absorption corrections were applied using SADABS.⁷⁴ The structure was solved by direct methods and refined by least squares method on F² using the SHELXTL program package.⁷⁵ The structure was solved in the space group P2(1)/n (# 14) by analysis of systematic absences. The central diethynyl group was disordered in two positions (85:15%) and these atoms (C8, C9, C10) were held isotropic. Mild bond length restraints were used to stabilize the minor component. All other non-hydrogen atoms were refined anisotropically. Ethynyl hydrogen atoms were geometrically placed and refined with a riding model. All other hydrogen atoms were located and refined. No decomposition was observed during data collection. Details of the data collection and refinement are given in Table 1. Further details are provided in the Supporting Information.

⁷² SMART: v. 5.632, Bruker AXS, Madison, WI, **2005**.

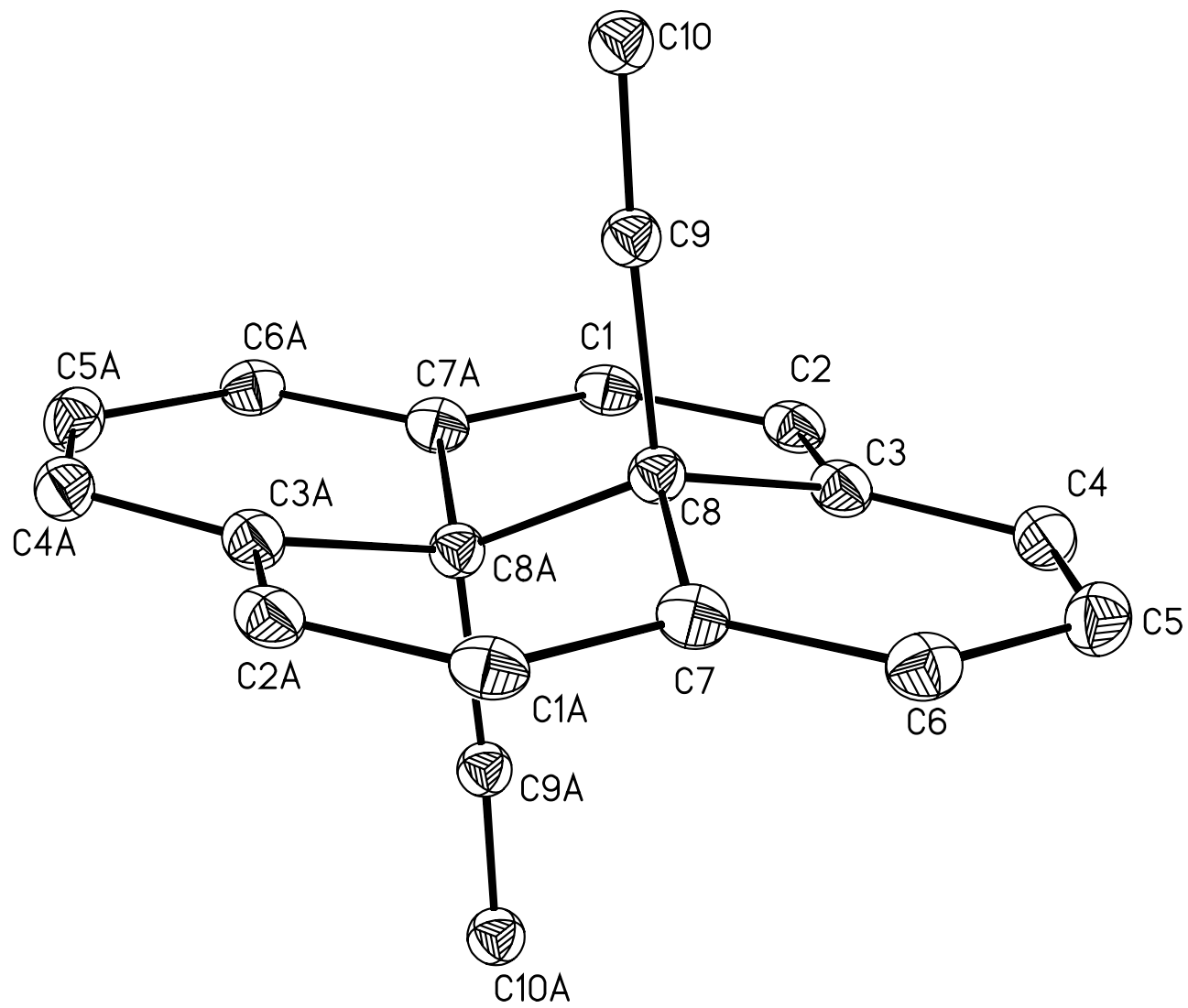
⁷³ SAINTPlus: v. 7.23a, Data Reduction and Correction Program, Bruker AXS, Madison, WI, **2004**.

⁷⁴ SADABS: v.2007/4, an empirical absorption correction program, Bruker AXS Inc., Madison, WI, **2007**.

⁷⁵ SHELXTL: v. 6.14, Structure Determination Software Suite, Sheldrick, G.M., Bruker AXS Inc., Madison, WI, **2004**.

Acknowledgement

The Bruker (Siemens) SMART APEX diffraction facility was established at the University of Idaho with the assistance of the NSF-EPSCoR program and the M. J. Murdock Charitable Trust, Vancouver, WA, USA.



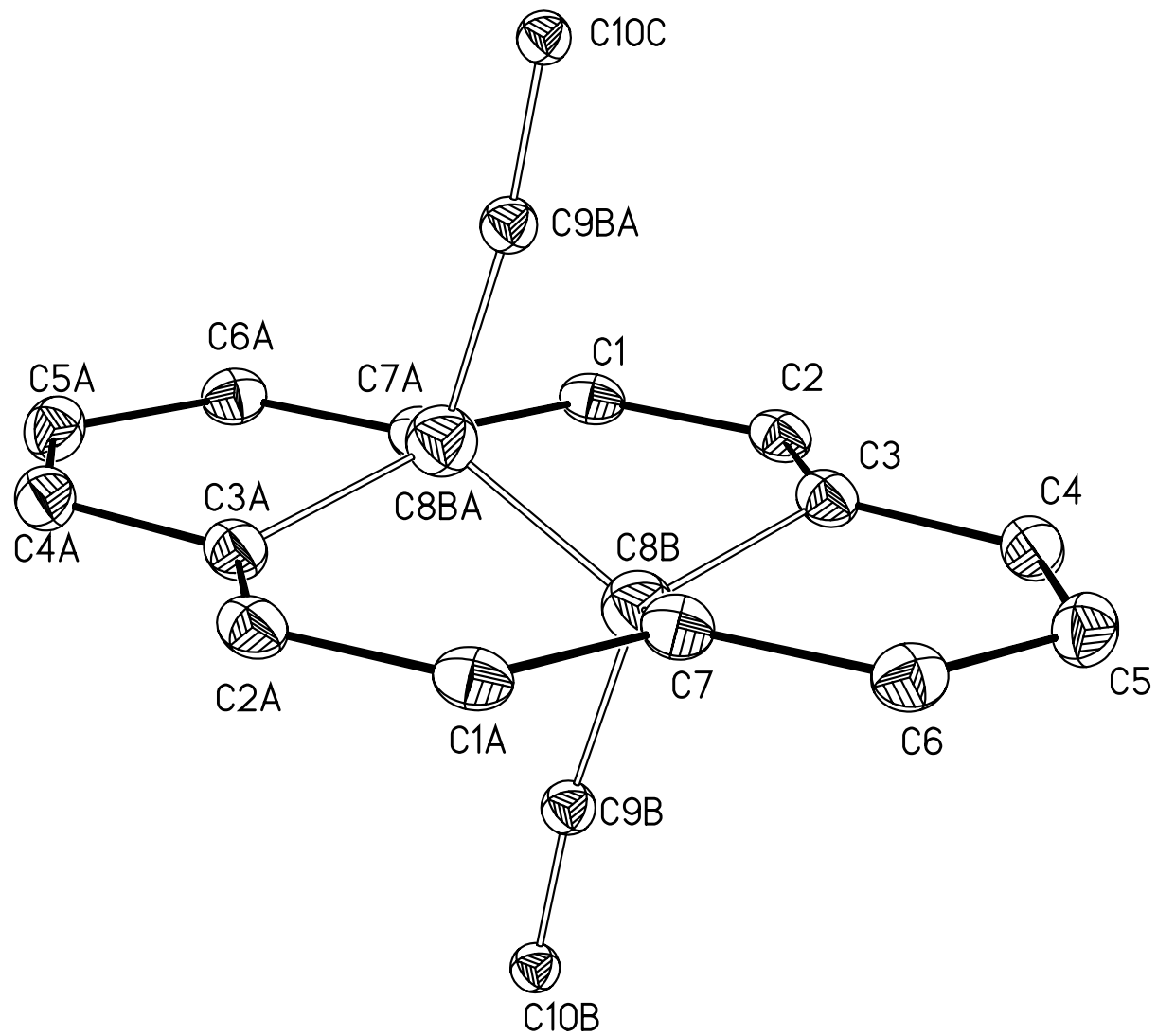


Table A. 87 Crystal data and structure refinement for diethynyl DHP 236.

Identification code	bt1228
Empirical formula	C ₂₀ H ₁₂
Formula weight	252.30
Temperature	90(2) K
Wavelength	0.71073 Å
Crystal system	Monoclinic
Space group	P2(1)/n
Unit cell dimensions	a = 6.9735(5) Å α = 90°. b = 6.8401(5) Å β = 93.252(1)° c = 13.5036(9) Å γ = 90°.
Volume	643.08(8) Å ³
Z	2
Density (calculated)	1.303 Mg/m ³
Absorption coefficient	0.074 mm ⁻¹
F(000)	264
Crystal size	0.54 x 0.10 x 0.05 mm ³
Crystal color and habit	green needle
Diffractometer	Bruker/Siemens SMART APEX
Theta range for data collection	3.02 to 25.24°.
Index ranges	-8 ≤ h ≤ 8, -8 ≤ k ≤ 8, -16 ≤ l ≤ 16
Reflections collected	9506
Independent reflections	1163 [R(int) = 0.0259]
Completeness to theta = 25.24°	100.0%
Absorption correction	Semi-empirical from equivalents
Max. and min. transmission	0.9963 and 0.9612
Solution method	XS, SHELXTL v. 6.14 (Bruker, 2003)
Refinement method	Full-matrix least-squares on F ²
Data / restraints / parameters	1163 / 4 / 108
Goodness-of-fit on F ²	1.058
Final R indices [I > 2σ(I)]	R1 = 0.0395, wR2 = 0.0971
R indices (all data)	R1 = 0.0467, wR2 = 0.1026
Largest diff. peak and hole	0.319 and -0.167 e.Å ⁻³

Table A. 88 Atomic coordinates ($\times 10^4$) and equivalent isotropic displacement parameters ($\text{\AA}^2 \times 10^3$) for 236 (bt 1228).

	x	y	z	U(eq)
C(1)	3085(2)	1866(2)	4635(1)	26(1)
C(2)	2019(2)	2938(2)	5282(1)	26(1)
C(3)	2656(2)	4714(2)	5688(1)	26(1)
C(4)	1639(2)	5873(2)	6318(1)	28(1)
C(5)	2346(2)	7664(2)	6667(1)	31(1)
C(6)	4069(2)	8439(2)	6363(1)	28(1)
C(7)	5217(2)	7427(2)	5732(1)	26(1)
C(8)	4763(2)	5254(2)	5534(1)	22(1)
C(9)	6001(2)	4075(3)	6249(1)	22(1)
C(10)	6935(3)	3181(3)	6855(2)	25(1)
C(8B)	4184(11)	5809(11)	5092(4)	35(2)
C(9B)	3457(13)	6492(14)	4080(6)	21(2)
C(10B)	2769(15)	7169(16)	3333(7)	18(3)

Table A. 89 Bond lengths [Å] and angles [°] for 236 (bt 1228)

C(1)-C(2)	1.388(2)	C(4)-C(3)-C(8)	118.08(14)
C(1)-C(7)#1	1.396(2)	C(2)-C(3)-C(8)	116.11(13)
C(1)-H(1)	0.987(17)	C(4)-C(3)-C(8B)	115.4(3)
C(2)-C(3)	1.395(2)	C(2)-C(3)-C(8B)	115.2(3)
C(2)-H(2)	0.995(16)	C(3)-C(4)-C(5)	121.79(14)
C(3)-C(4)	1.386(2)	C(3)-C(4)-H(4)	118.7(10)
C(3)-C(8)	1.541(2)	C(5)-C(4)-H(4)	119.4(10)
C(3)-C(8B)	1.563(5)	C(4)-C(5)-C(6)	121.93(15)
C(4)-C(5)	1.393(2)	C(4)-C(5)-H(5)	117.4(10)
C(4)-H(4)	0.995(17)	C(6)-C(5)-H(5)	120.5(10)
C(5)-C(6)	1.396(2)	C(7)-C(6)-C(5)	121.84(15)
C(5)-H(5)	0.996(18)	C(7)-C(6)-H(6)	119.7(9)
C(6)-C(7)	1.387(2)	C(5)-C(6)-H(6)	118.3(9)
C(6)-H(6)	0.999(18)	C(6)-C(7)-C(1)#1	125.18(14)
C(7)-C(1)#1	1.396(2)	C(6)-C(7)-C(8)	117.92(13)
C(7)-C(8)	1.540(2)	C(1)#1-C(7)-C(8)	116.30(13)
C(7)-C(8B)	1.556(5)	C(6)-C(7)-C(8B)	115.5(3)
C(8)-C(9)	1.495(2)	C(1)#1-C(7)-C(8B)	115.1(2)
C(8)-C(8)#1	1.537(3)	C(9)-C(8)-C(8)#1	109.66(17)
C(9)-C(10)	1.186(2)	C(9)-C(8)-C(7)	107.60(13)
C(10)-H(10)	0.9500	C(8)#1-C(8)-C(7)	109.19(16)
C(8B)-C(9B)	1.506(5)	C(9)-C(8)-C(3)	107.67(13)
C(8B)-C(8B)#1	1.617(18)	C(8)#1-C(8)-C(3)	109.30(16)
C(9B)-C(10B)	1.186(5)	C(7)-C(8)-C(3)	113.36(13)
C(10B)-H(10B)	0.9500	C(10)-C(9)-C(8)	176.6(2)
		C(9)-C(10)-H(10)	180.0
C(2)-C(1)-C(7)#1	122.38(14)	C(9B)-C(8B)-C(7)	113.9(6)
C(2)-C(1)-H(1)	119.7(9)	C(9B)-C(8B)-C(3)	114.3(6)
C(7)#1-C(1)-H(1)	118.0(9)	C(7)-C(8B)-C(3)	111.3(3)
C(1)-C(2)-C(3)	122.55(14)	C(9B)-C(8B)-C(8B)#1	106.0(6)
C(1)-C(2)-H(2)	119.5(9)	C(7)-C(8B)-C(8B)#1	105.4(5)
C(3)-C(2)-H(2)	118.0(9)	C(3)-C(8B)-C(8B)#1	104.9(5)
C(4)-C(3)-C(2)	125.22(14)	C(10B)-C(9B)-C(8B)	173.0(12)
		C(9B)-C(10B)-H(10B)	180.0

Symmetry transformations used to generate equivalent atoms:

#1 -x+1,-y+1,-z+1

Table A. 90 Anisotropic displacement parameters ($\text{\AA}^2 \times 10^3$) for 236 (bt 1228).

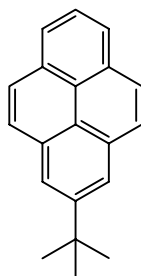
	U11	U22	U33	U23	U13	U12
C(1)	28(1)	24(1)	24(1)	3(1)	-6(1)	-4(1)
C(2)	21(1)	32(1)	24(1)	7(1)	-3(1)	-4(1)
C(3)	22(1)	31(1)	23(1)	5(1)	-1(1)	-2(1)
C(4)	22(1)	37(1)	25(1)	3(1)	0(1)	0(1)
C(5)	28(1)	37(1)	27(1)	-3(1)	1(1)	4(1)
C(6)	30(1)	28(1)	26(1)	-1(1)	-5(1)	1(1)
C(7)	27(1)	27(1)	23(1)	0(1)	-4(1)	-2(1)

Table A. 91 Hydrogen coordinates ($\times 10^4$) and isotropic displacement parameters ($\text{\AA}^2 \times 10^3$) for 236 (bt 1228).

	x	y	z	U(eq)
H(1)	2630(20)	560(30)	4414(12)	25(4)
H(2)	760(20)	2420(20)	5481(11)	26(4)
H(4)	340(20)	5430(20)	6499(12)	28(4)
H(5)	1530(20)	8420(30)	7113(13)	33(4)
H(6)	4430(20)	9790(30)	6578(12)	29(4)
H(10)	7682	2464	7340	30
H(10B)	2218	7711	2735	22

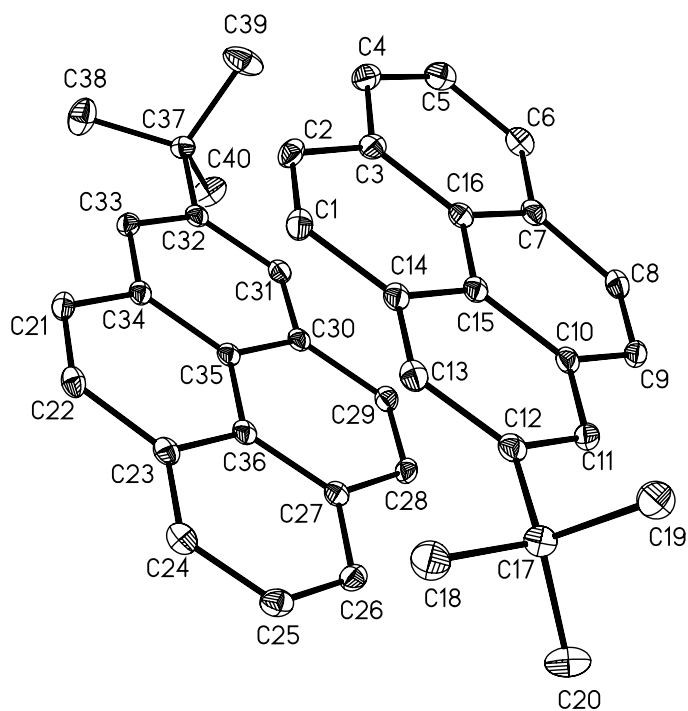
Single-Crystal X-ray Diffraction Laboratory
University of Idaho

X-ray structure report for pyrene 150



150

Brendan Twamley



Project name : bt957

8-18-06

Experimental:

Crystals of compound **1** were removed from the flask, a suitable crystal was selected, attached to a glass fiber and data were collected at 90(2) K using a Bruker/Siemens SMART APEX instrument (Mo K α radiation, $\lambda = 0.71073$ Å) equipped with a Cryocool NeverIce low temperature device. Data were measured using omega scans of 0.3 ° per frame for 5 seconds, and a full sphere of data was collected. A total of 2400 frames were collected with a final resolution of 0.83 Å. Cell parameters were retrieved using SMART⁷⁶ software and refined using SAINTPlus⁷⁷ on all observed reflections. Data reduction and correction for Lp and decay were performed using the SAINTPlus software. Absorption corrections were applied using SADABS.⁷⁸ The structure was solved by direct methods and refined by least squares method on F² using the SHELXTL program package.⁷⁹ The structure was solved in the space group P2(1)/c (# 14) by analysis of systematic absences. All non-hydrogen atoms were refined anisotropically. No decomposition was observed during data collection. Details of the data collection and refinement are given in Table 1. Further details are provided in the Supporting Information.

Acknowledgement

The Bruker (Siemens) SMART APEX diffraction facility was established at the University of Idaho with the assistance of the NSF-EPSCoR program and the M. J. Murdock Charitable Trust, Vancouver, WA, USA.

⁷⁶ SMART: v.5.630, Bruker Molecular Analysis Research Tool, Bruker AXS, Madison, WI, **2001**.

⁷⁷ SAINTPlus: v. 7.23a, Data Reduction and Correction Program, Bruker AXS, Madison, WI, **2004**.

⁷⁸ SADABS: v.2004/1, an empirical absorption correction program, Bruker AXS Inc., Madison, WI, **2004**.

⁷⁹ SHELXTL: v. 6.14, Structure Determination Software Suite, Sheldrick, G.M., Bruker AXS Inc., Madison, WI, **2004**.

Table A. 92 Crystal data and structure refinement for ^tBu-pyrene 150

Identification code	bt957	
Empirical formula	C ₂₀ H ₁₈	
Formula weight	258.34	
Temperature	90(2) K	
Wavelength	0.71073 Å	
Crystal system	Monoclinic	
Space group	P2(1)/c	
Unit cell dimensions	a = 11.5243(9) Å	α = 90°.
	b = 10.5760(8) Å	β = 95.2860(10)°.
	c = 22.9005(18) Å	γ = 90°.
Volume	2779.3(4) Å ³	
Z	8	
Density (calculated)	1.235 Mg/m ³	
Absorption coefficient	0.069 mm ⁻¹	
F(000)	1104	
Crystal size	0.50 x 0.31 x 0.28 mm ³	
Crystal color and habit	pale yellow block	
Diffractometer	Bruker/Siemens SMART APEX	
Theta range for data collection	1.77 to 25.25°.	
Index ranges	-13 ≤ h ≤ 13, -12 ≤ k ≤ 12, -27 ≤ l ≤ 27	
Reflections collected	41377	
Independent reflections	5033 [R(int) = 0.0329]	
Completeness to theta = 25.25°	100.0%	
Absorption correction	Semi-empirical from equivalents	
Max. and min. transmission	0.9808 and 0.9661	
Solution method	Bruker, 2003; XS, SHELXTL v. 6.14	
Refinement method	Full-matrix least-squares on F ²	
Data / restraints / parameters	5033 / 0 / 367	
Goodness-of-fit on F ²	1.034	
Final R indices [I > 2σ(I)]	R1 = 0.0462, wR2 = 0.1185	
R indices (all data)	R1 = 0.0546, wR2 = 0.1245	
Largest diff. peak and hole	0.352 and -0.174 e.Å ⁻³	

Table A. 93 Atomic coordinates ($\times 10^4$) and equivalent isotropic displacement parameters ($\text{\AA}^2 \times 10^3$) for 150 (bt 957).

	x	y	z	U(eq)
C(1)	969(1)	-146(1)	8231(1)	21(1)
C(2)	477(1)	-488(1)	7697(1)	22(1)
C(3)	622(1)	255(1)	7184(1)	20(1)
C(4)	84(1)	-47(1)	6631(1)	24(1)
C(5)	253(1)	702(2)	6149(1)	26(1)
C(6)	984(1)	1747(1)	6205(1)	24(1)
C(7)	1542(1)	2086(1)	6748(1)	20(1)
C(8)	2310(1)	3155(1)	6825(1)	21(1)
C(9)	2784(1)	3505(1)	7361(1)	19(1)
C(10)	2549(1)	2820(1)	7879(1)	18(1)
C(11)	2996(1)	3192(1)	8439(1)	19(1)
C(12)	2790(1)	2504(1)	8940(1)	19(1)
C(13)	2133(1)	1398(1)	8865(1)	20(1)
C(14)	1655(1)	990(1)	8315(1)	19(1)
C(15)	1843(1)	1720(1)	7812(1)	17(1)
C(16)	1337(1)	1352(1)	7247(1)	18(1)
C(17)	3279(1)	2985(1)	9545(1)	21(1)
C(18)	3147(2)	2011(2)	10027(1)	31(1)
C(19)	2627(1)	4187(2)	9691(1)	28(1)
C(20)	4580(1)	3292(2)	9540(1)	31(1)
C(21)	2352(1)	-3312(1)	7800(1)	19(1)
C(22)	2883(1)	-2875(1)	8310(1)	20(1)
C(23)	3611(1)	-1771(1)	8332(1)	19(1)
C(24)	4192(1)	-1310(1)	8852(1)	22(1)
C(25)	4861(1)	-221(1)	8852(1)	23(1)
C(26)	4964(1)	443(1)	8337(1)	21(1)
C(27)	4412(1)	16(1)	7806(1)	18(1)
C(28)	4509(1)	660(1)	7259(1)	19(1)
C(29)	3997(1)	203(1)	6749(1)	19(1)
C(30)	3323(1)	-944(1)	6725(1)	17(1)

C(31)	2797(1)	-1445(1)	6205(1)	18(1)
C(32)	2147(1)	-2560(1)	6184(1)	18(1)
C(33)	1990(1)	-3159(1)	6715(1)	18(1)
C(34)	2498(1)	-2696(1)	7252(1)	17(1)
C(35)	3190(1)	-1582(1)	7263(1)	16(1)
C(36)	3738(1)	-1112(1)	7800(1)	17(1)
C(37)	1588(1)	-3068(1)	5595(1)	20(1)
C(38)	1225(2)	-4450(2)	5637(1)	36(1)
C(39)	511(2)	-2282(2)	5405(1)	41(1)
C(40)	2434(2)	-3001(2)	5119(1)	34(1)

Table A. 94 Bond lengths [\AA] and angles [$^\circ$] for 150 (bt 957).

C(1)-C(2)	1.349(2)	C(11)-C(12)	1.3971(19)
C(1)-C(14)	1.441(2)	C(11)-H(11A)	0.9500
C(1)-H(1A)	0.9500	C(12)-C(13)	1.396(2)
C(2)-C(3)	1.436(2)	C(12)-C(17)	1.534(2)
C(2)-H(2A)	0.9500	C(13)-C(14)	1.396(2)
C(3)-C(4)	1.395(2)	C(13)-H(13A)	0.9500
C(3)-C(16)	1.423(2)	C(14)-C(15)	1.4202(19)
C(4)-C(5)	1.386(2)	C(15)-C(16)	1.423(2)
C(4)-H(4A)	0.9500	C(17)-C(18)	1.528(2)
C(5)-C(6)	1.389(2)	C(17)-C(19)	1.529(2)
C(5)-H(5A)	0.9500	C(17)-C(20)	1.534(2)
C(6)-C(7)	1.394(2)	C(18)-H(18A)	0.9800
C(6)-H(6A)	0.9500	C(18)-H(18B)	0.9800
C(7)-C(16)	1.419(2)	C(18)-H(18C)	0.9800
C(7)-C(8)	1.437(2)	C(19)-H(19A)	0.9800
C(8)-C(9)	1.347(2)	C(19)-H(19B)	0.9800
C(8)-H(8A)	0.9500	C(19)-H(19C)	0.9800
C(9)-C(10)	1.4365(19)	C(20)-H(20A)	0.9800
C(9)-H(9A)	0.9500	C(20)-H(20B)	0.9800
C(10)-C(11)	1.394(2)	C(20)-H(20C)	0.9800
C(10)-C(15)	1.4195(19)	C(21)-C(22)	1.350(2)

C(21)-C(34)	1.4371(19)	C(39)-H(39C)	0.9800
C(21)-H(21A)	0.9500	C(40)-H(40A)	0.9800
C(22)-C(23)	1.436(2)	C(40)-H(40B)	0.9800
C(22)-H(22A)	0.9500	C(40)-H(40C)	0.9800
C(23)-C(24)	1.398(2)		
C(23)-C(36)	1.4231(19)	C(2)-C(1)-C(14)	121.57(13)
C(24)-C(25)	1.386(2)	C(2)-C(1)-H(1A)	119.2
C(24)-H(24A)	0.9500	C(14)-C(1)-H(1A)	119.2
C(25)-C(26)	1.387(2)	C(1)-C(2)-C(3)	121.63(13)
C(25)-H(25A)	0.9500	C(1)-C(2)-H(2A)	119.2
C(26)-C(27)	1.396(2)	C(3)-C(2)-H(2A)	119.2
C(26)-H(26A)	0.9500	C(4)-C(3)-C(16)	118.95(14)
C(27)-C(36)	1.4227(19)	C(4)-C(3)-C(2)	122.83(13)
C(27)-C(28)	1.4386(19)	C(16)-C(3)-C(2)	118.21(13)
C(28)-C(29)	1.349(2)	C(5)-C(4)-C(3)	120.55(14)
C(28)-H(28A)	0.9500	C(5)-C(4)-H(4A)	119.7
C(29)-C(30)	1.4386(19)	C(3)-C(4)-H(4A)	119.7
C(29)-H(29A)	0.9500	C(4)-C(5)-C(6)	120.71(14)
C(30)-C(31)	1.390(2)	C(4)-C(5)-H(5A)	119.6
C(30)-C(35)	1.4245(19)	C(6)-C(5)-H(5A)	119.6
C(31)-C(32)	1.396(2)	C(5)-C(6)-C(7)	120.83(14)
C(31)-H(31A)	0.9500	C(5)-C(6)-H(6A)	119.6
C(32)-C(33)	1.3987(19)	C(7)-C(6)-H(6A)	119.6
C(32)-C(37)	1.5374(19)	C(6)-C(7)-C(16)	118.76(13)
C(33)-C(34)	1.3991(19)	C(6)-C(7)-C(8)	122.74(13)
C(33)-H(33A)	0.9500	C(16)-C(7)-C(8)	118.50(13)
C(34)-C(35)	1.4219(19)	C(9)-C(8)-C(7)	121.47(13)
C(35)-C(36)	1.4207(19)	C(9)-C(8)-H(8A)	119.3
C(37)-C(39)	1.523(2)	C(7)-C(8)-H(8A)	119.3
C(37)-C(38)	1.526(2)	C(8)-C(9)-C(10)	121.39(13)
C(37)-C(40)	1.529(2)	C(8)-C(9)-H(9A)	119.3
C(38)-H(38A)	0.9800	C(10)-C(9)-H(9A)	119.3
C(38)-H(38B)	0.9800	C(11)-C(10)-C(15)	119.33(13)
C(38)-H(38C)	0.9800	C(11)-C(10)-C(9)	122.35(13)
C(39)-H(39A)	0.9800	C(15)-C(10)-C(9)	118.32(13)
C(39)-H(39B)	0.9800	C(10)-C(11)-C(12)	122.17(13)

C(10)-C(11)-H(11A)	118.9	C(17)-C(20)-H(20B)	109.5
C(12)-C(11)-H(11A)	118.9	H(20A)-C(20)-H(20B)	109.5
C(13)-C(12)-C(11)	117.85(13)	C(17)-C(20)-H(20C)	109.5
C(13)-C(12)-C(17)	122.60(13)	H(20A)-C(20)-H(20C)	109.5
C(11)-C(12)-C(17)	119.55(13)	H(20B)-C(20)-H(20C)	109.5
C(14)-C(13)-C(12)	122.29(13)	C(22)-C(21)-C(34)	121.39(13)
C(14)-C(13)-H(13A)	118.9	C(22)-C(21)-H(21A)	119.3
C(12)-C(13)-H(13A)	118.9	C(34)-C(21)-H(21A)	119.3
C(13)-C(14)-C(15)	119.13(13)	C(21)-C(22)-C(23)	121.71(13)
C(13)-C(14)-C(1)	122.95(13)	C(21)-C(22)-H(22A)	119.1
C(15)-C(14)-C(1)	117.92(13)	C(23)-C(22)-H(22A)	119.1
C(10)-C(15)-C(14)	119.15(13)	C(24)-C(23)-C(36)	118.61(13)
C(10)-C(15)-C(16)	120.30(13)	C(24)-C(23)-C(22)	123.12(13)
C(14)-C(15)-C(16)	120.54(13)	C(36)-C(23)-C(22)	118.27(13)
C(7)-C(16)-C(15)	119.86(13)	C(25)-C(24)-C(23)	120.89(13)
C(7)-C(16)-C(3)	120.09(13)	C(25)-C(24)-H(24A)	119.6
C(15)-C(16)-C(3)	120.04(13)	C(23)-C(24)-H(24A)	119.6
C(18)-C(17)-C(19)	108.48(12)	C(24)-C(25)-C(26)	120.75(13)
C(18)-C(17)-C(12)	112.14(12)	C(24)-C(25)-H(25A)	119.6
C(19)-C(17)-C(12)	109.07(11)	C(26)-C(25)-H(25A)	119.6
C(18)-C(17)-C(20)	108.10(12)	C(25)-C(26)-C(27)	120.64(14)
C(19)-C(17)-C(20)	109.02(13)	C(25)-C(26)-H(26A)	119.7
C(12)-C(17)-C(20)	109.96(12)	C(27)-C(26)-H(26A)	119.7
C(17)-C(18)-H(18A)	109.5	C(26)-C(27)-C(36)	118.95(13)
C(17)-C(18)-H(18B)	109.5	C(26)-C(27)-C(28)	122.65(13)
H(18A)-C(18)-H(18B)	109.5	C(36)-C(27)-C(28)	118.40(12)
C(17)-C(18)-H(18C)	109.5	C(29)-C(28)-C(27)	121.37(13)
H(18A)-C(18)-H(18C)	109.5	C(29)-C(28)-H(28A)	119.3
H(18B)-C(18)-H(18C)	109.5	C(27)-C(28)-H(28A)	119.3
C(17)-C(19)-H(19A)	109.5	C(28)-C(29)-C(30)	121.83(13)
C(17)-C(19)-H(19B)	109.5	C(28)-C(29)-H(29A)	119.1
H(19A)-C(19)-H(19B)	109.5	C(30)-C(29)-H(29A)	119.1
C(17)-C(19)-H(19C)	109.5	C(31)-C(30)-C(35)	119.11(13)
H(19A)-C(19)-H(19C)	109.5	C(31)-C(30)-C(29)	123.07(12)
H(19B)-C(19)-H(19C)	109.5	C(35)-C(30)-C(29)	117.82(12)
C(17)-C(20)-H(20A)	109.5	C(30)-C(31)-C(32)	122.84(13)

C(30)-C(31)-H(31A)	118.6	C(38)-C(37)-C(32)	111.94(12)
C(32)-C(31)-H(31A)	118.6	C(40)-C(37)-C(32)	111.44(12)
C(31)-C(32)-C(33)	117.64(13)	C(37)-C(38)-H(38A)	109.5
C(31)-C(32)-C(37)	120.40(12)	C(37)-C(38)-H(38B)	109.5
C(33)-C(32)-C(37)	121.92(12)	H(38A)-C(38)-H(38B)	109.5
C(32)-C(33)-C(34)	121.93(13)	C(37)-C(38)-H(38C)	109.5
C(32)-C(33)-H(33A)	119.0	H(38A)-C(38)-H(38C)	109.5
C(34)-C(33)-H(33A)	119.0	H(38B)-C(38)-H(38C)	109.5
C(33)-C(34)-C(35)	119.56(12)	C(37)-C(39)-H(39A)	109.5
C(33)-C(34)-C(21)	122.33(13)	C(37)-C(39)-H(39B)	109.5
C(35)-C(34)-C(21)	118.10(12)	H(39A)-C(39)-H(39B)	109.5
C(36)-C(35)-C(34)	120.58(12)	C(37)-C(39)-H(39C)	109.5
C(36)-C(35)-C(30)	120.57(13)	H(39A)-C(39)-H(39C)	109.5
C(34)-C(35)-C(30)	118.85(12)	H(39B)-C(39)-H(39C)	109.5
C(35)-C(36)-C(27)	119.99(12)	C(37)-C(40)-H(40A)	109.5
C(35)-C(36)-C(23)	119.89(13)	C(37)-C(40)-H(40B)	109.5
C(27)-C(36)-C(23)	120.12(13)	H(40A)-C(40)-H(40B)	109.5
C(39)-C(37)-C(38)	108.69(14)	C(37)-C(40)-H(40C)	109.5
C(39)-C(37)-C(40)	109.13(13)	H(40A)-C(40)-H(40C)	109.5
C(38)-C(37)-C(40)	106.61(13)	H(40B)-C(40)-H(40C)	109.5
C(39)-C(37)-C(32)	108.95(12)		

Table A. 95 **Anisotropic displacement parameters ($\text{\AA}^2 \times 10^3$) for 150 (bt 957).**

	U11	U22	U33	U23	U13	U12
C(1)	20(1)	17(1)	28(1)	1(1)	10(1)	1(1)
C(2)	17(1)	16(1)	34(1)	-4(1)	10(1)	-2(1)
C(3)	14(1)	18(1)	29(1)	-5(1)	6(1)	3(1)
C(4)	19(1)	21(1)	33(1)	-9(1)	4(1)	0(1)
C(5)	25(1)	29(1)	25(1)	-8(1)	-1(1)	3(1)
C(6)	26(1)	25(1)	23(1)	1(1)	2(1)	5(1)
C(7)	18(1)	19(1)	24(1)	0(1)	3(1)	5(1)
C(8)	23(1)	18(1)	23(1)	4(1)	4(1)	3(1)

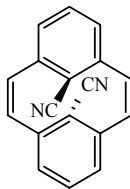
C(9)	18(1)	14(1)	27(1)	2(1)	4(1)	0(1)
C(10)	15(1)	14(1)	24(1)	1(1)	4(1)	3(1)
C(11)	16(1)	15(1)	26(1)	0(1)	2(1)	0(1)
C(12)	16(1)	19(1)	23(1)	0(1)	4(1)	4(1)
C(13)	19(1)	19(1)	22(1)	3(1)	7(1)	3(1)
C(14)	15(1)	16(1)	25(1)	1(1)	6(1)	3(1)
C(15)	14(1)	15(1)	23(1)	-1(1)	6(1)	3(1)
C(16)	15(1)	17(1)	25(1)	-2(1)	5(1)	5(1)
C(17)	20(1)	23(1)	21(1)	0(1)	1(1)	1(1)
C(18)	37(1)	32(1)	23(1)	1(1)	-3(1)	-1(1)
C(19)	31(1)	28(1)	24(1)	-5(1)	0(1)	2(1)
C(20)	22(1)	46(1)	26(1)	-4(1)	-2(1)	-2(1)
C(21)	20(1)	14(1)	24(1)	2(1)	6(1)	0(1)
C(22)	23(1)	18(1)	19(1)	4(1)	7(1)	4(1)
C(23)	17(1)	18(1)	21(1)	0(1)	5(1)	6(1)
C(24)	24(1)	25(1)	19(1)	2(1)	4(1)	5(1)
C(25)	22(1)	26(1)	21(1)	-6(1)	-1(1)	2(1)
C(26)	17(1)	19(1)	28(1)	-4(1)	3(1)	0(1)
C(27)	14(1)	16(1)	24(1)	-2(1)	4(1)	4(1)
C(28)	15(1)	15(1)	28(1)	1(1)	5(1)	-1(1)
C(29)	18(1)	19(1)	22(1)	4(1)	5(1)	1(1)
C(30)	14(1)	17(1)	21(1)	3(1)	4(1)	3(1)
C(31)	17(1)	20(1)	19(1)	5(1)	3(1)	3(1)
C(32)	14(1)	18(1)	21(1)	1(1)	3(1)	4(1)
C(33)	15(1)	16(1)	23(1)	0(1)	3(1)	0(1)
C(34)	15(1)	15(1)	21(1)	1(1)	5(1)	3(1)
C(35)	13(1)	15(1)	20(1)	0(1)	4(1)	4(1)
C(36)	14(1)	16(1)	21(1)	0(1)	5(1)	5(1)
C(37)	18(1)	22(1)	20(1)	0(1)	0(1)	0(1)
C(38)	55(1)	29(1)	24(1)	-3(1)	-1(1)	-12(1)
C(39)	36(1)	50(1)	34(1)	-16(1)	-15(1)	16(1)
C(40)	34(1)	44(1)	25(1)	-8(1)	7(1)	-11(1)

Table A. 96 Hydrogen coordinates ($\times 10^4$) and isotropic displacement parameters ($\text{\AA}^2 \times 10^3$) for 150 (bt 957).

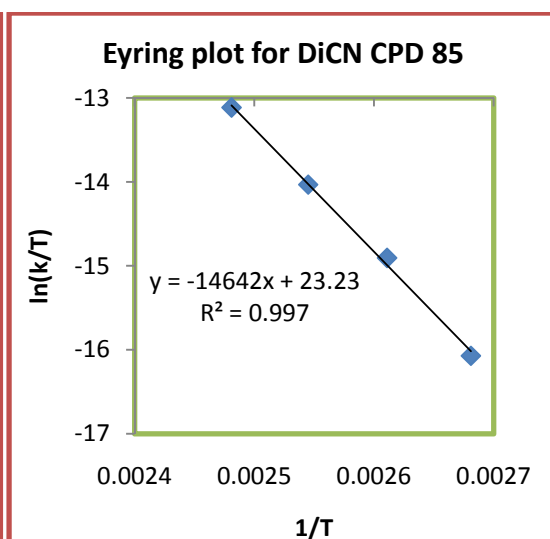
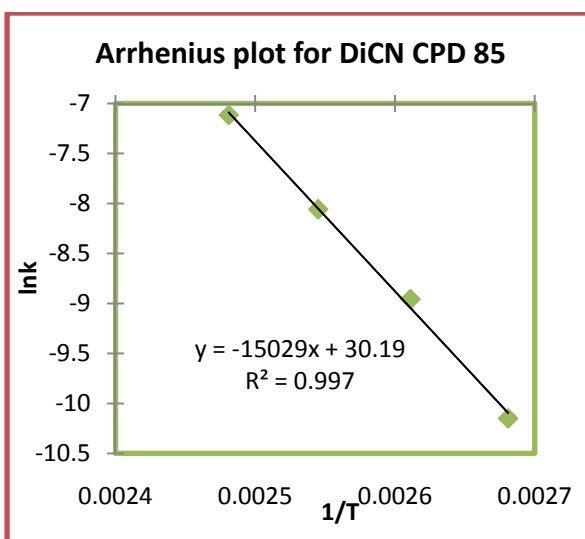
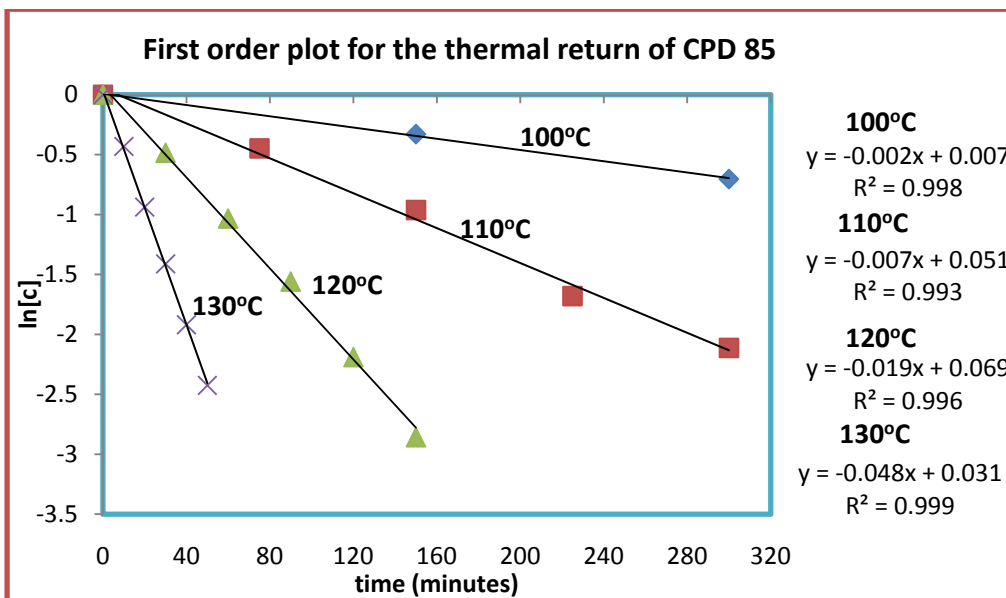
	x	y	z	U(eq)
H(1A)	860	-667	8560	25
H(2A)	23	-1239	7659	26
H(4A)	-401	-773	6584	29
H(5A)	-137	499	5777	32
H(6A)	1106	2237	5868	29
H(8A)	2487	3625	6492	25
H(9A)	3284	4220	7397	23
H(11A)	3457	3937	8481	23
H(13A)	2007	905	9200	23
H(18A)	3502	2340	10402	46
H(18B)	3536	1224	9932	46
H(18C)	2317	1846	10057	46
H(19A)	2957	4518	10071	42
H(19B)	1801	3990	9711	42
H(19C)	2706	4822	9386	42
H(20A)	4896	3553	9933	47
H(20B)	4678	3979	9262	47
H(20C)	4996	2540	9421	47
H(21A)	1872	-4042	7803	23
H(22A)	2771	-3310	8664	24
H(24A)	4127	-1749	9209	27
H(25A)	5253	75	9209	28
H(26A)	5415	1196	8347	25
H(28A)	4943	1424	7257	23
H(29A)	4083	651	6396	23
H(31A)	2885	-1010	5849	22
H(33A)	1526	-3902	6712	22
H(38A)	919	-4753	5249	55
H(38B)	621	-4526	5909	55

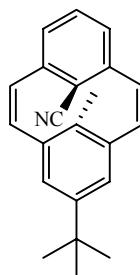
H(38C)	1903	-4959	5780	55
H(39A)	151	-2597	5028	61
H(39B)	737	-1395	5362	61
H(39C)	-48	-2347	5701	61
H(40A)	2062	-3356	4753	51
H(40B)	3137	-3487	5244	51
H(40C)	2645	-2117	5056	51

Appendix B Thermal closing data for cyclophanedienes

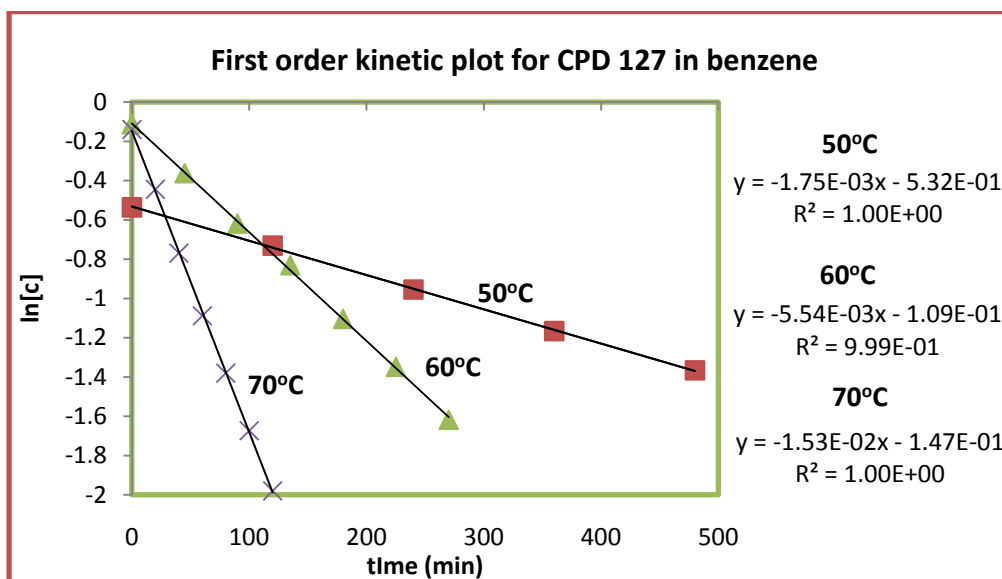
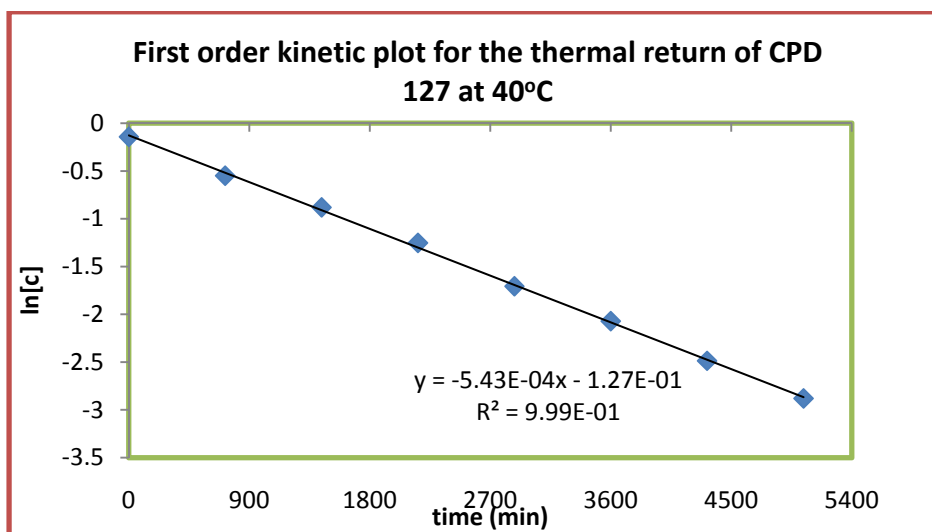


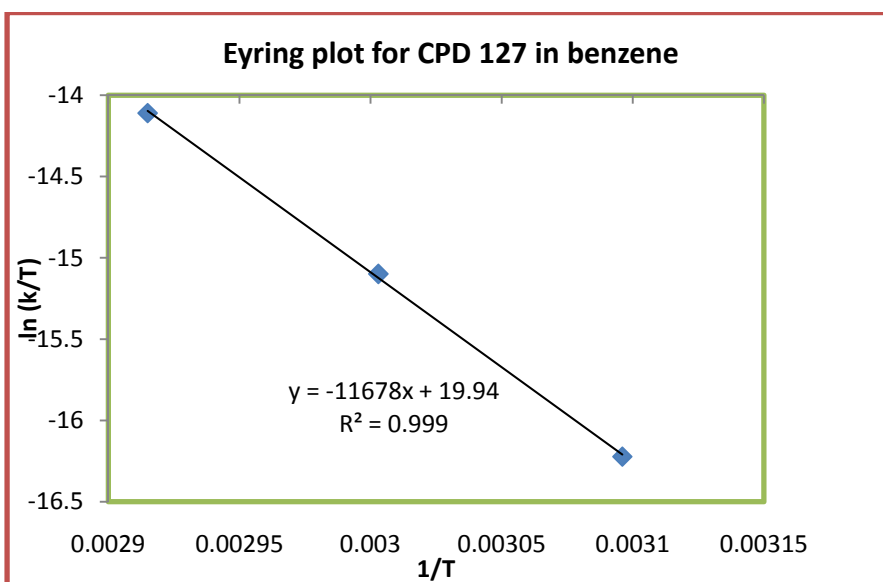
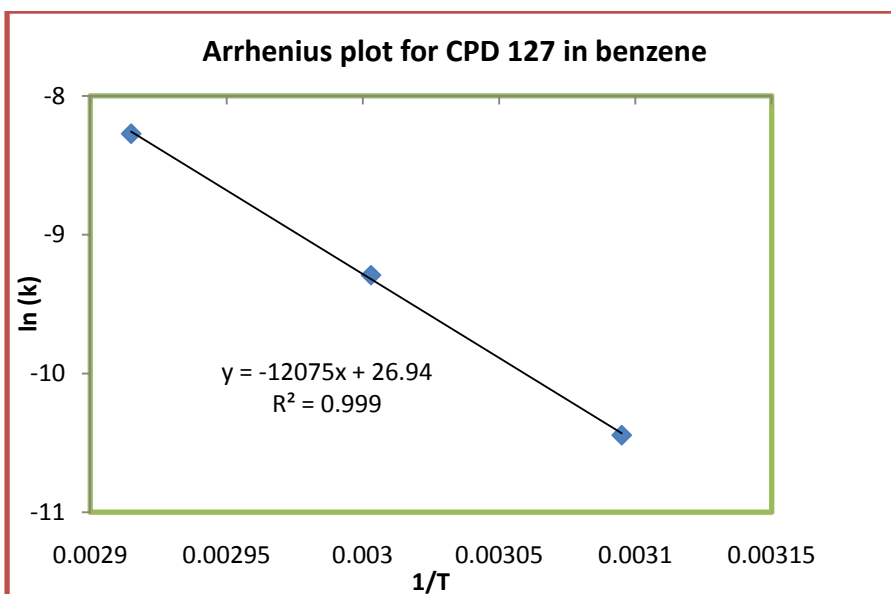
85

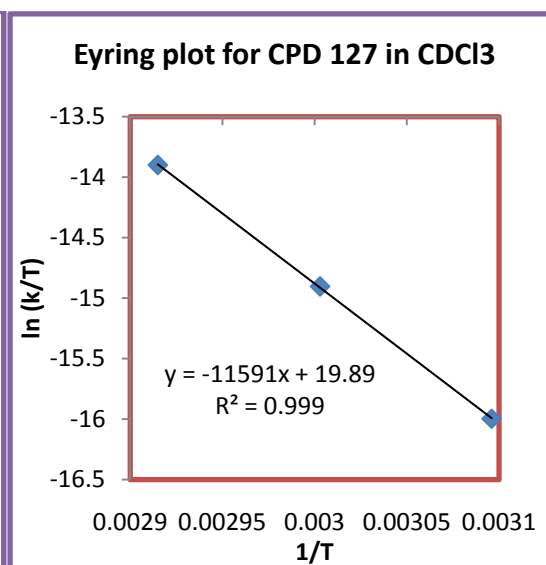
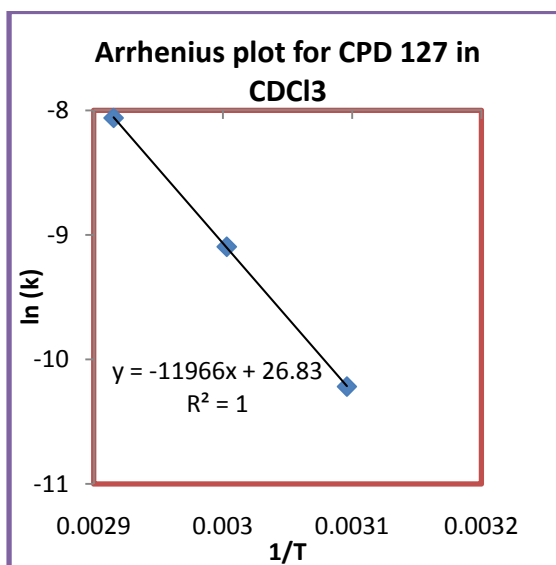
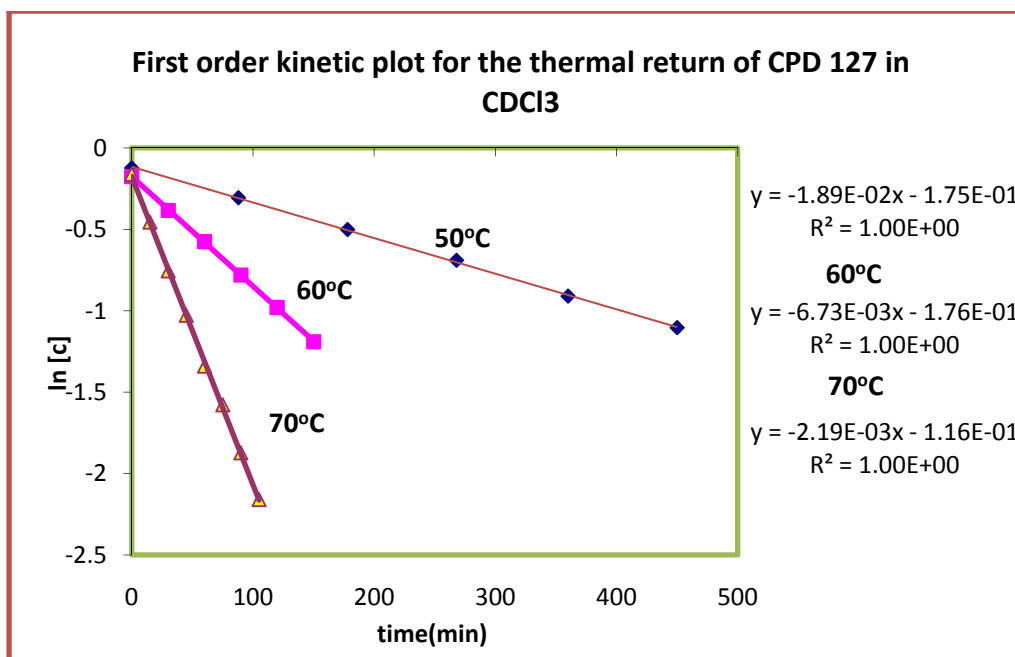


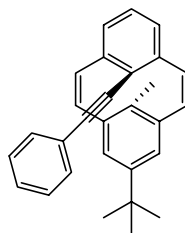


127

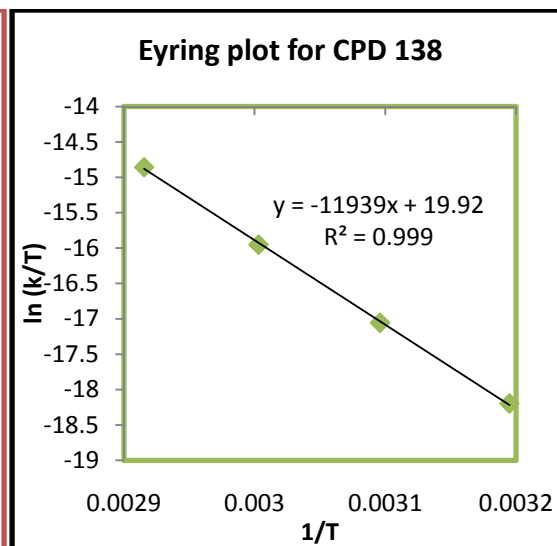
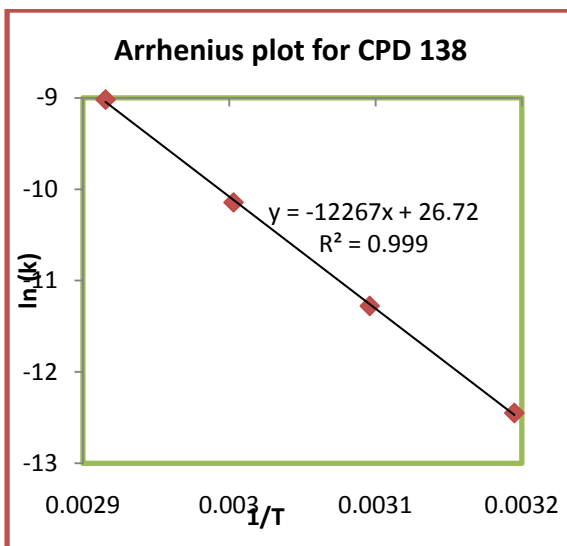
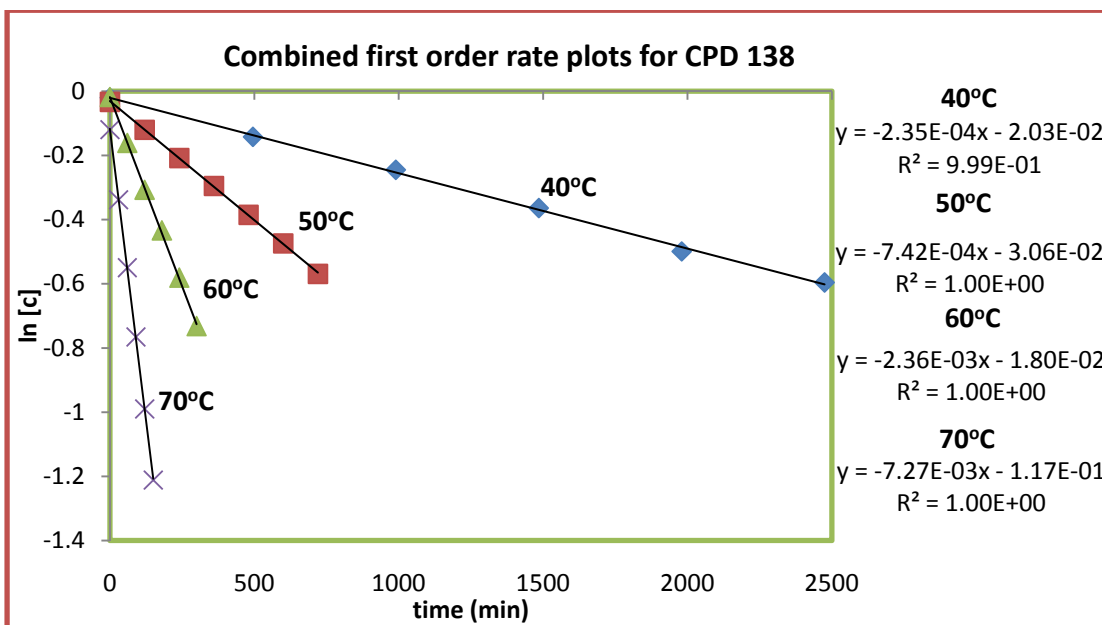


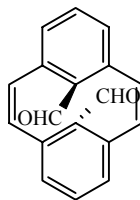




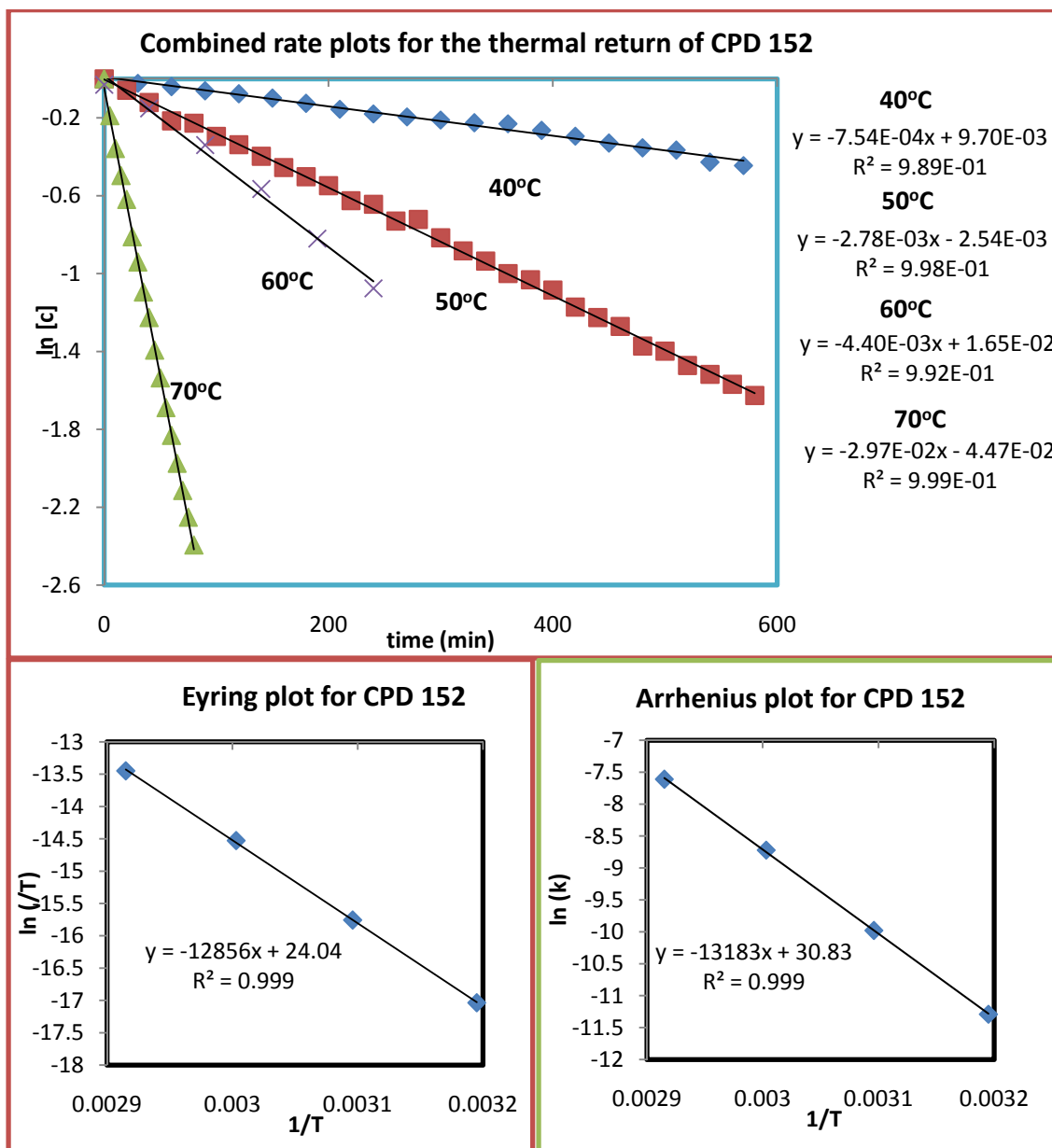


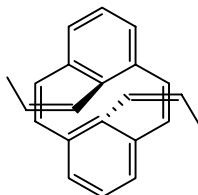
138



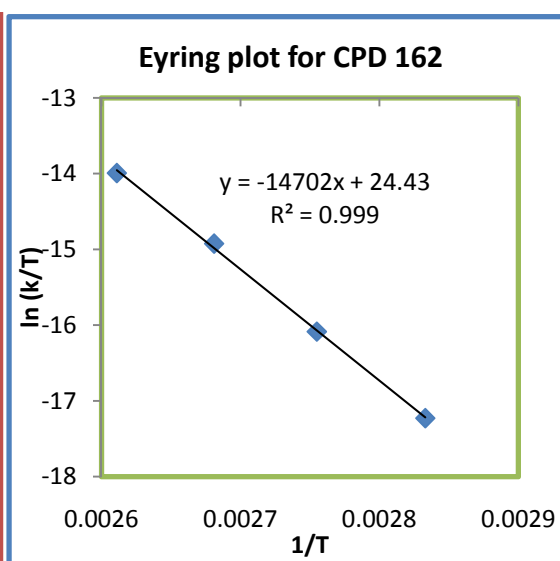
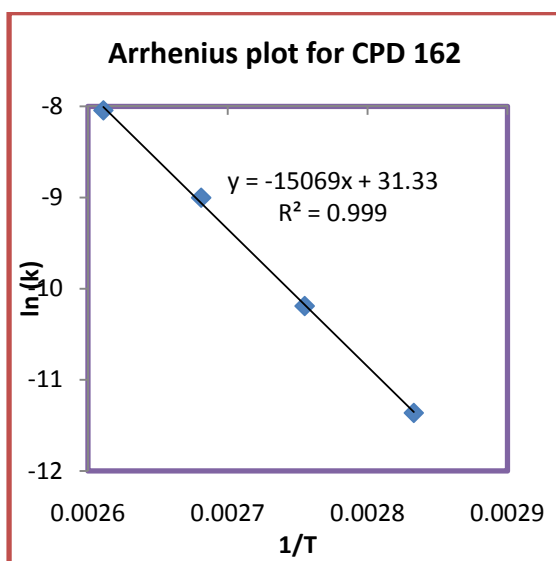
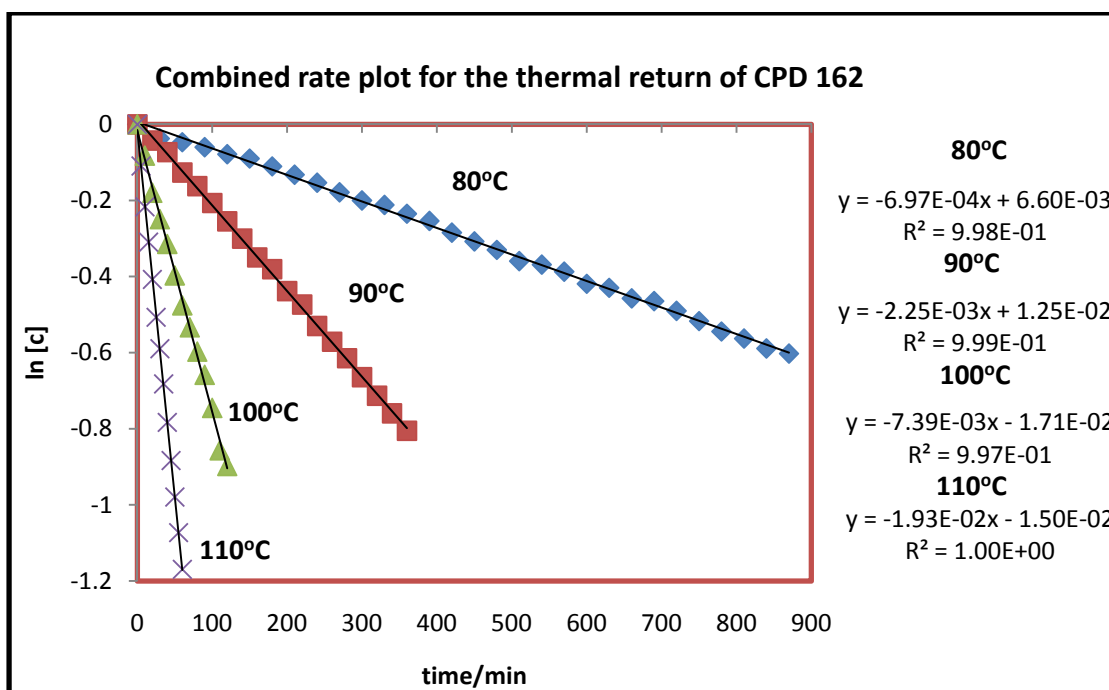


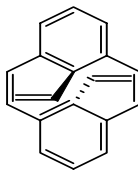
152



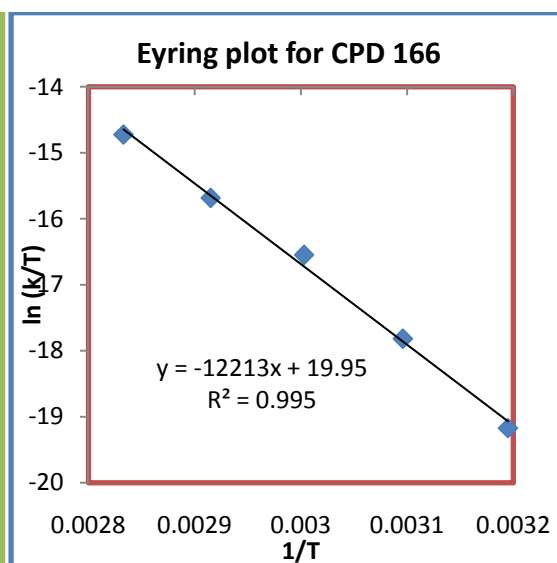
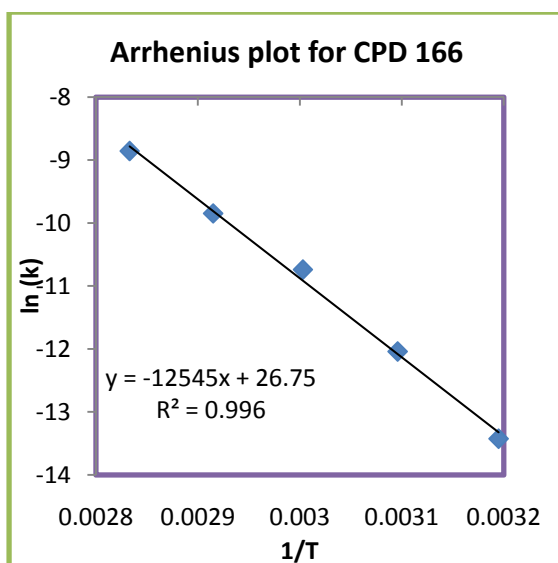
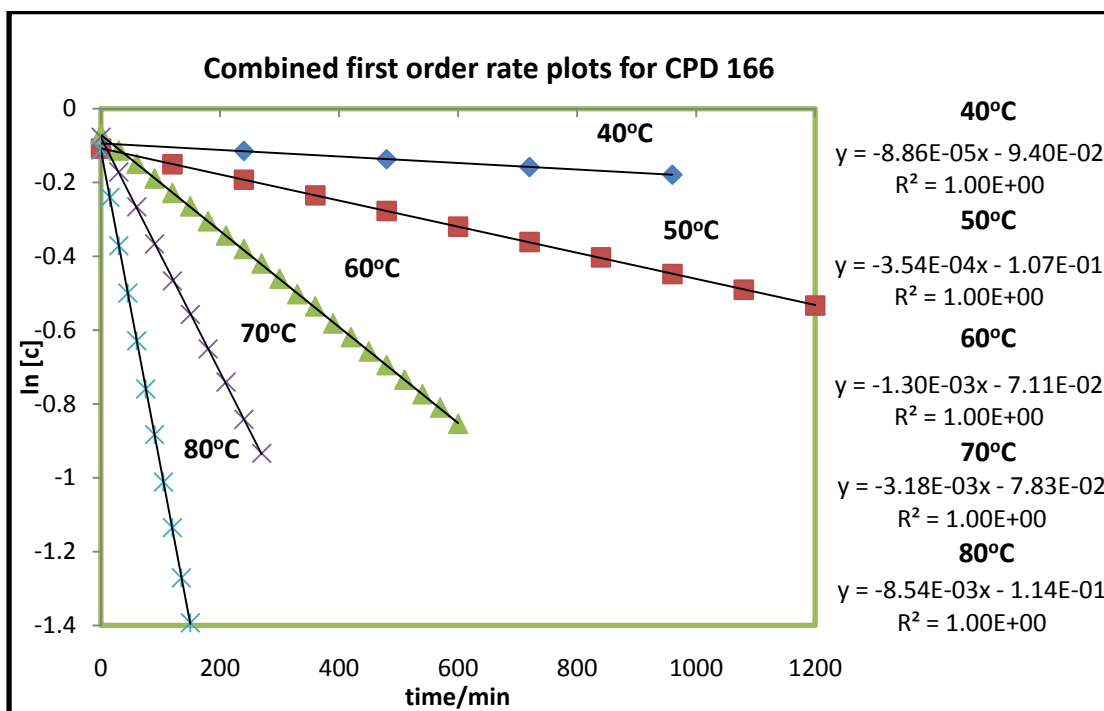


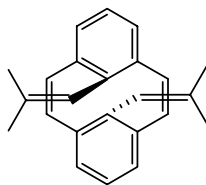
162



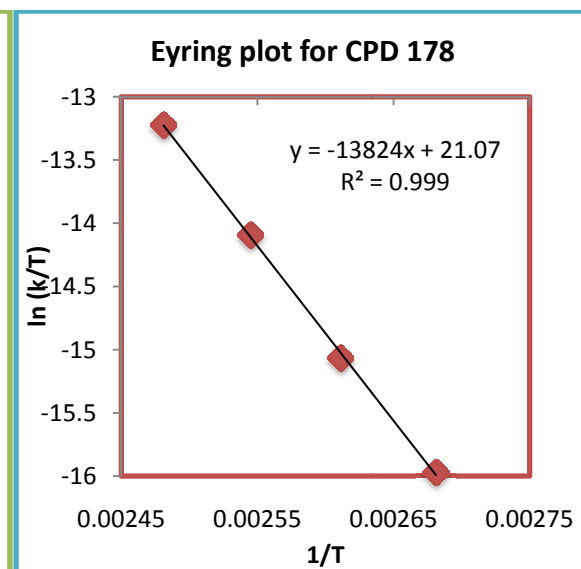
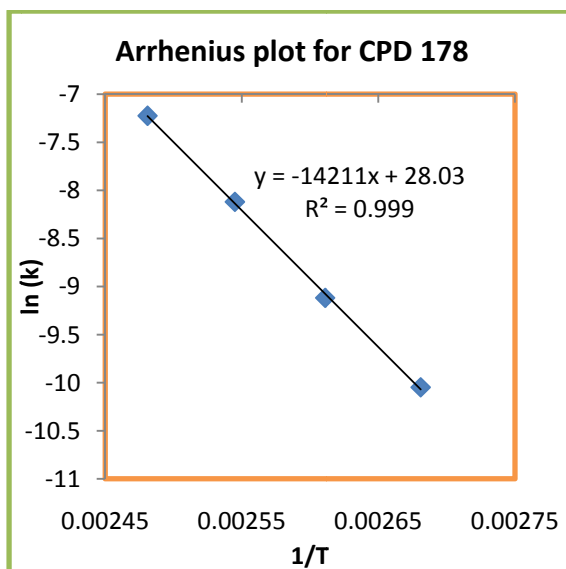
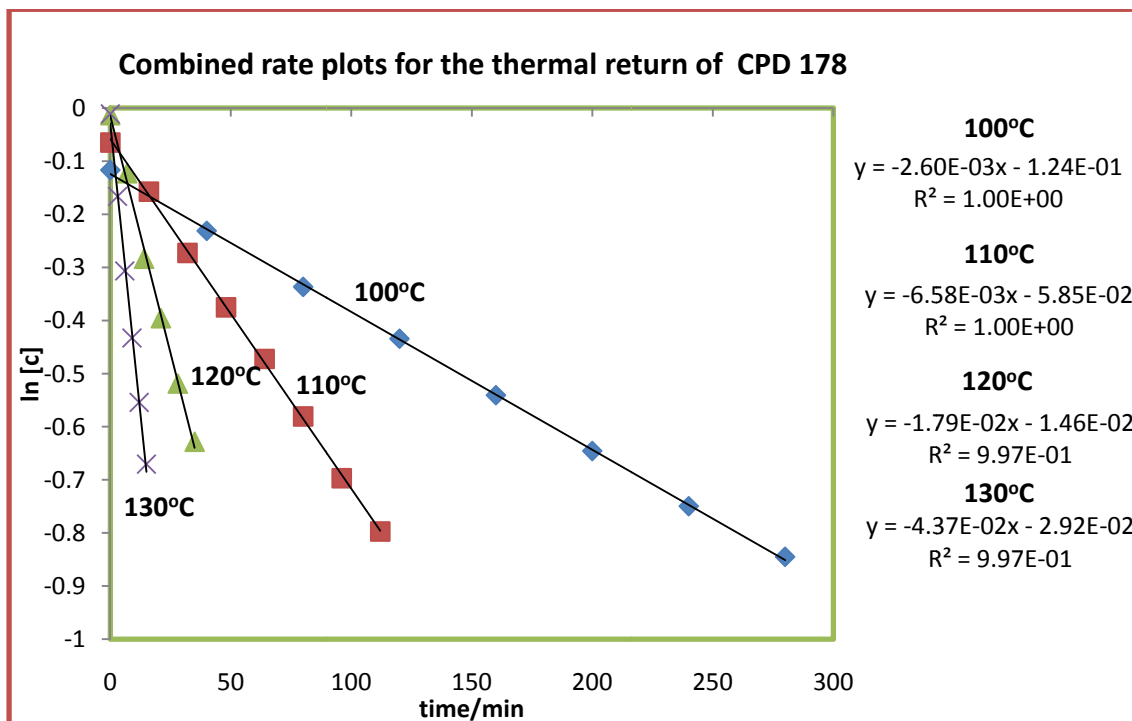


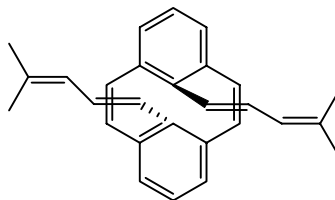
166



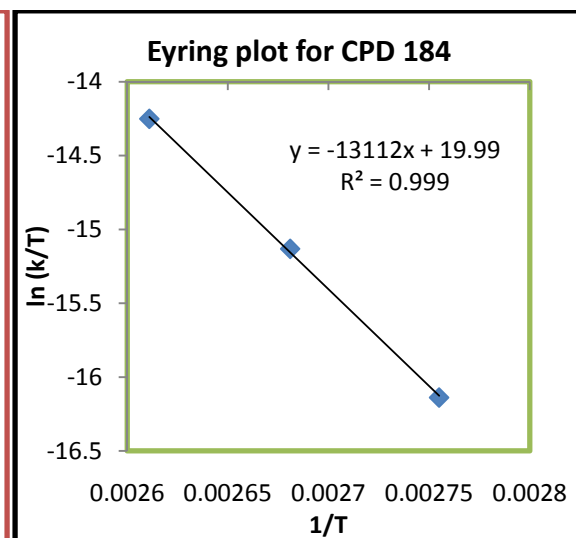
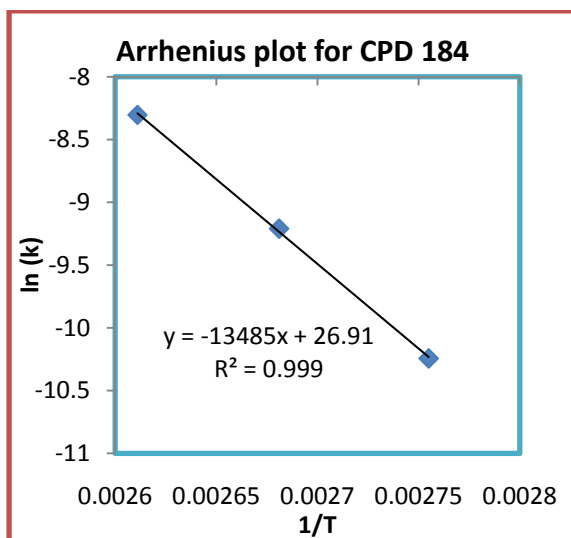
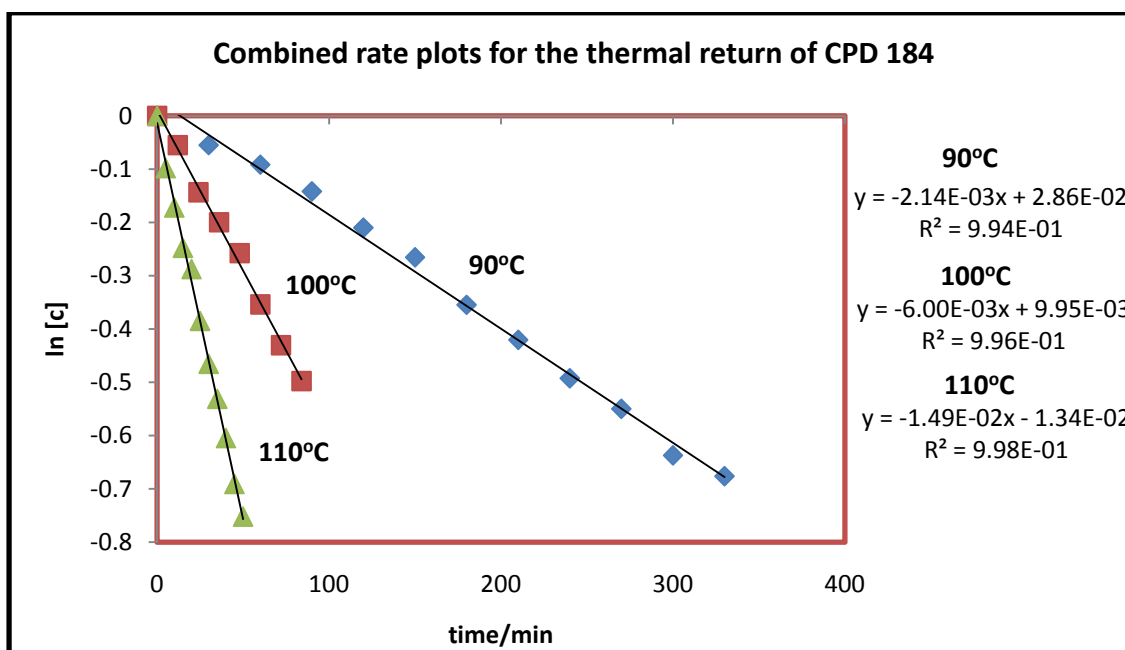


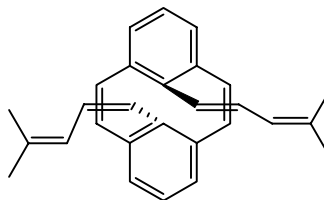
178



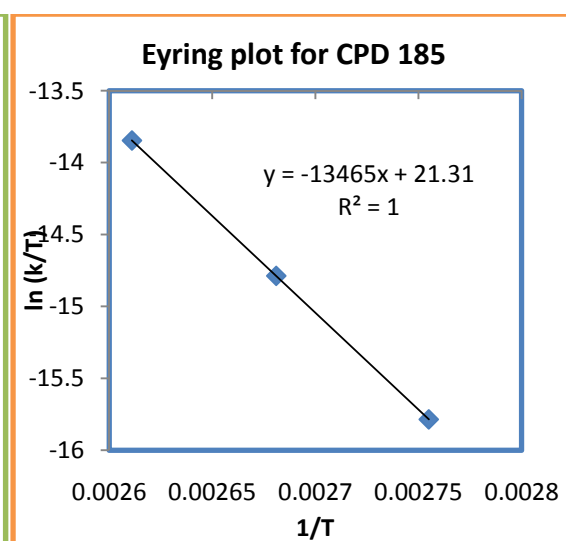
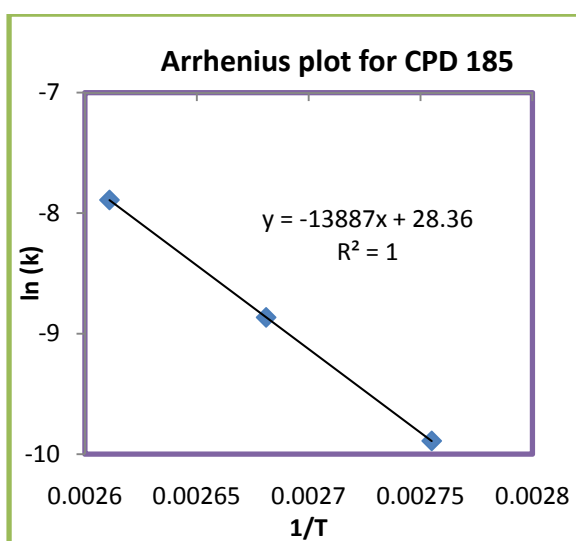
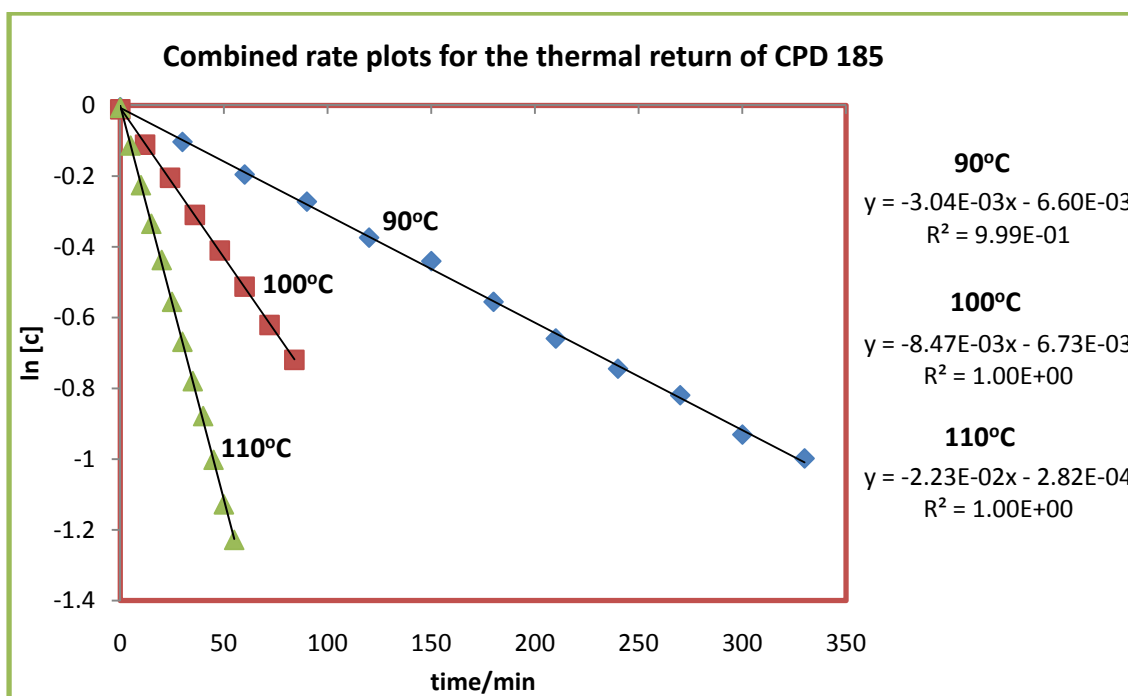


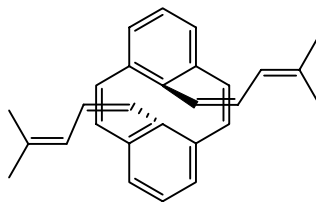
184



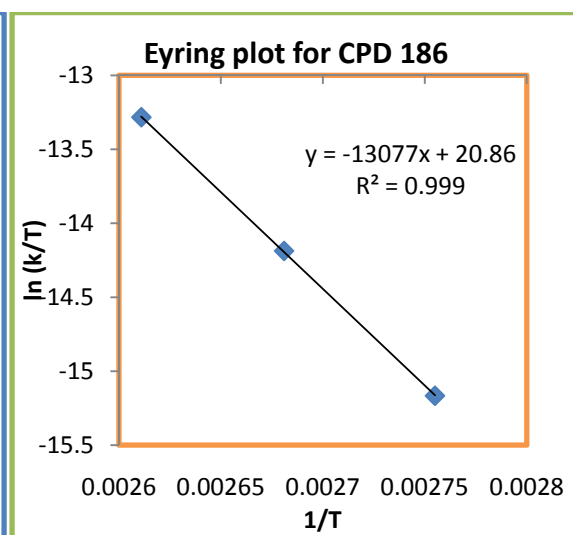
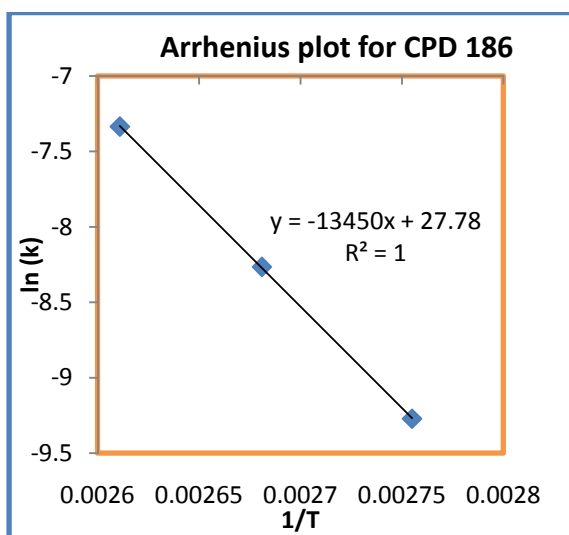
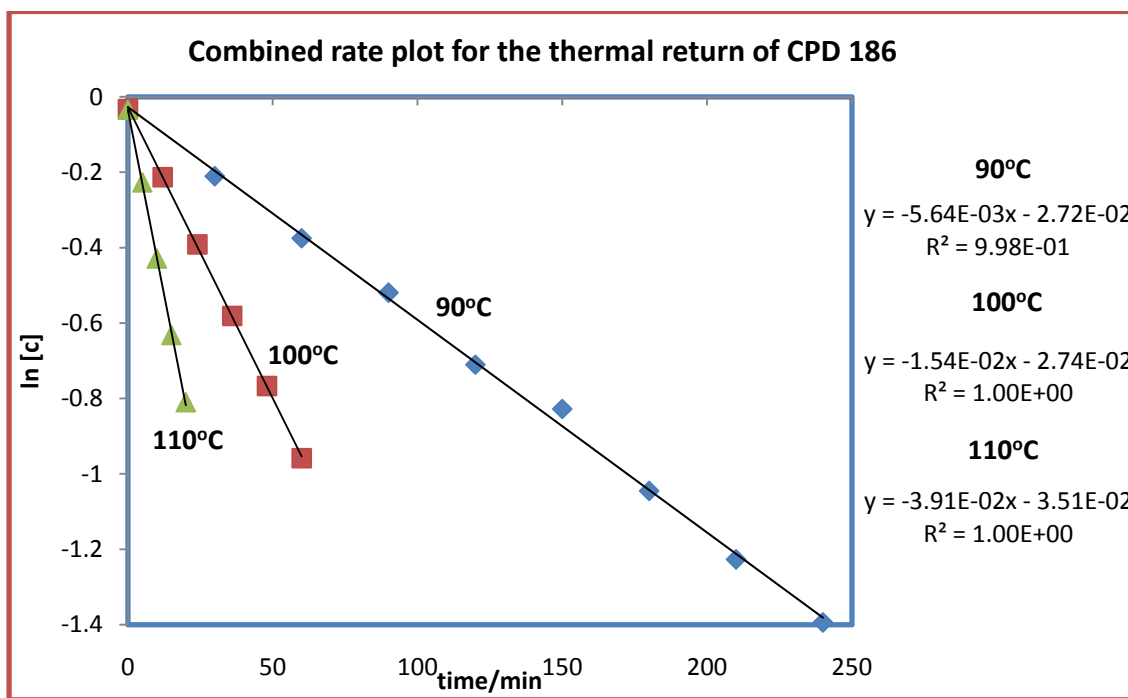


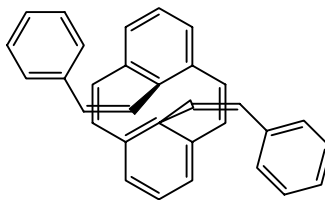
185



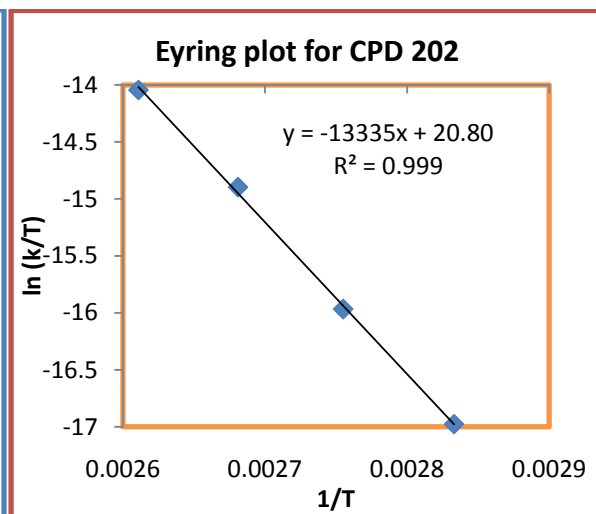
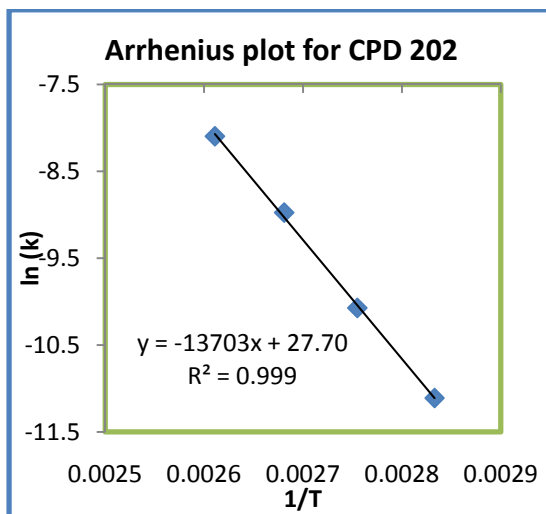
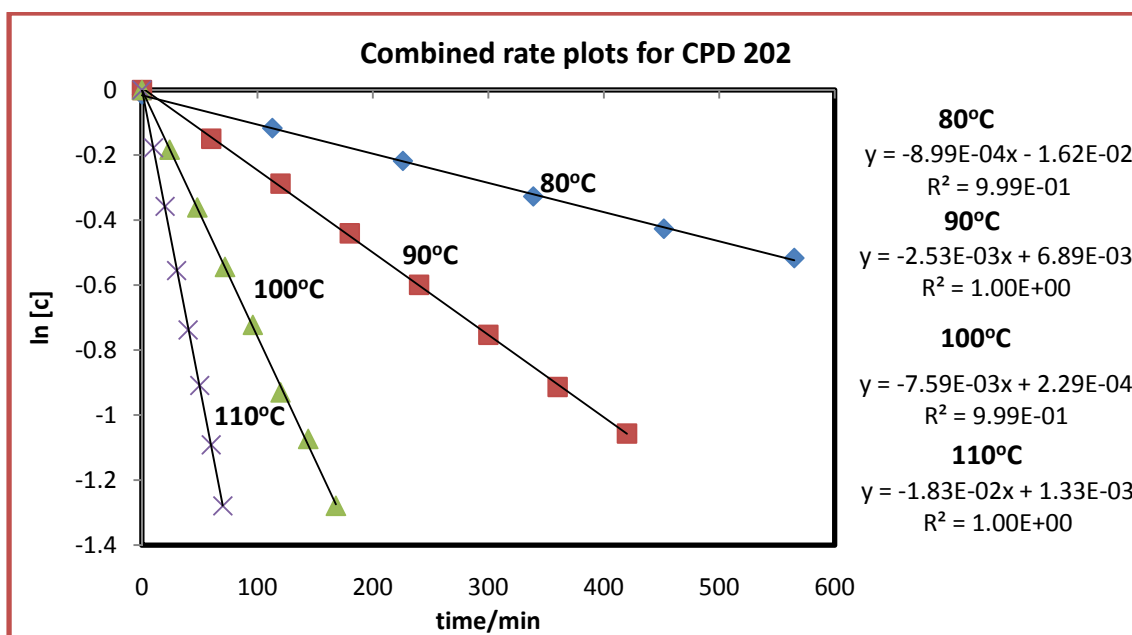


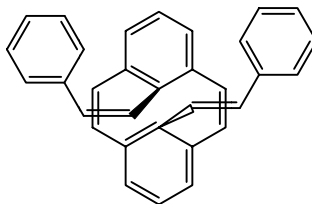
186



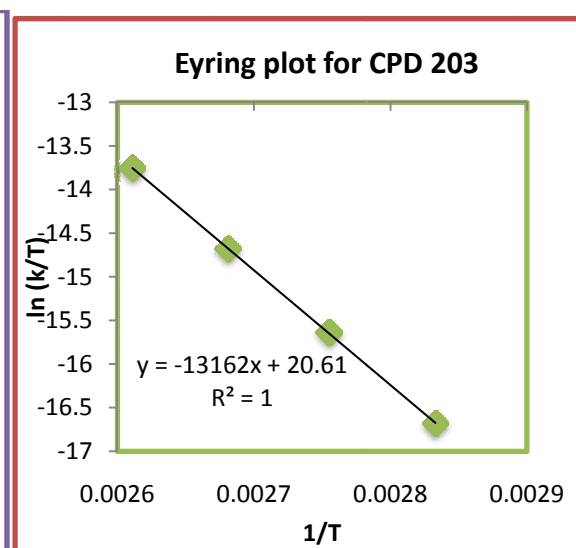
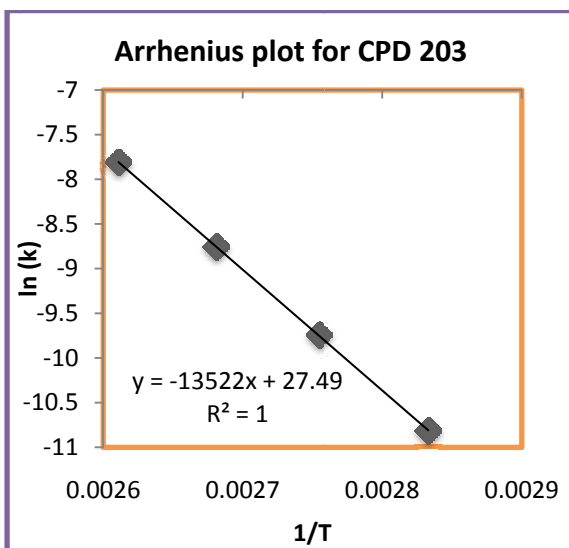
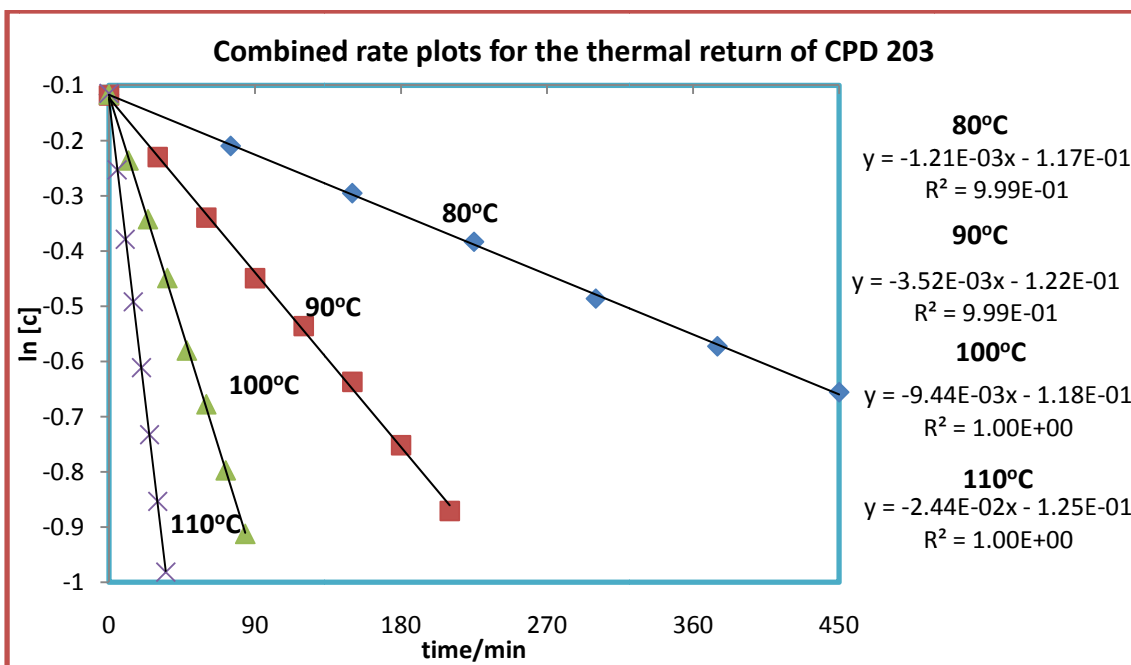


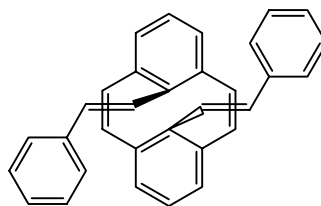
202



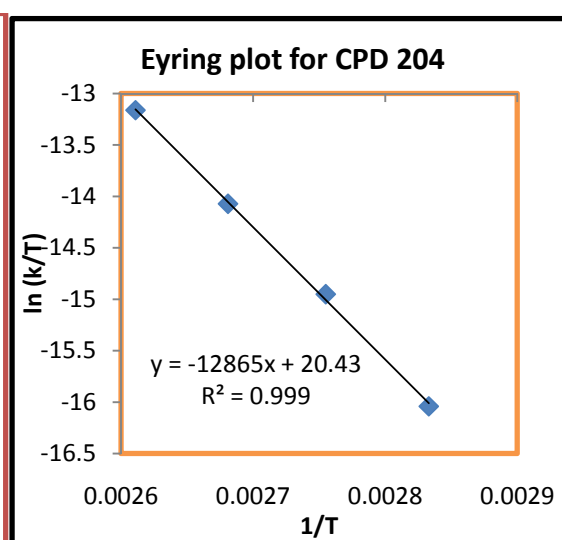
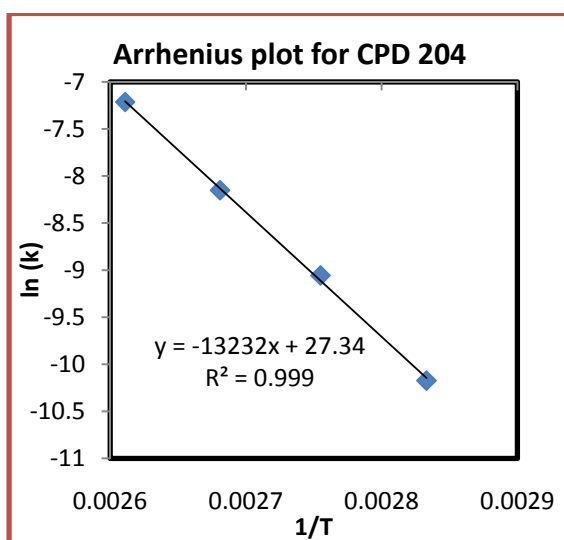
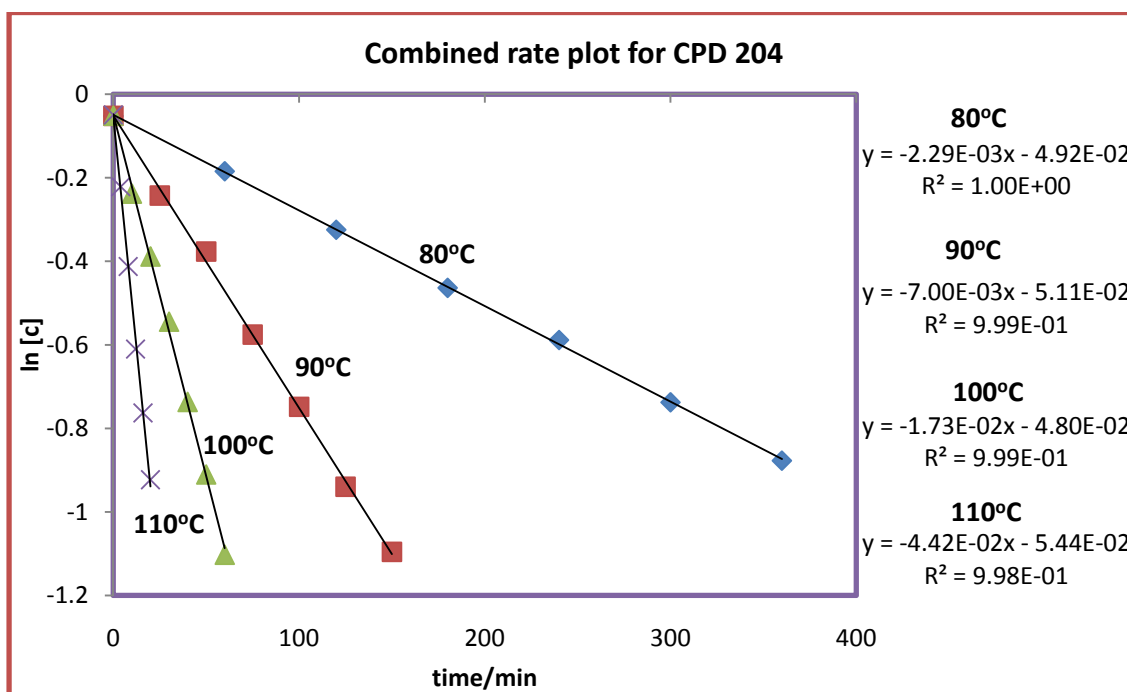


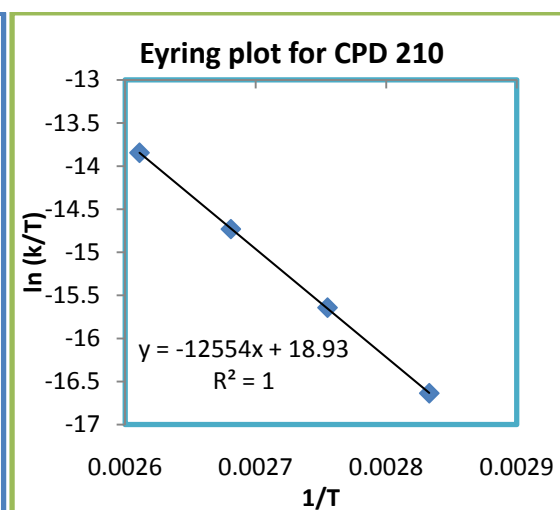
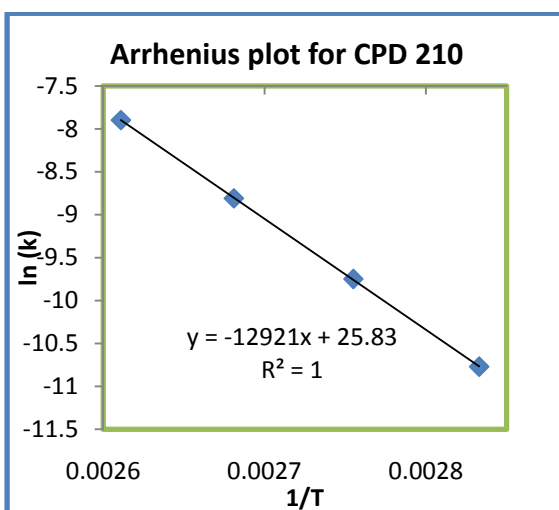
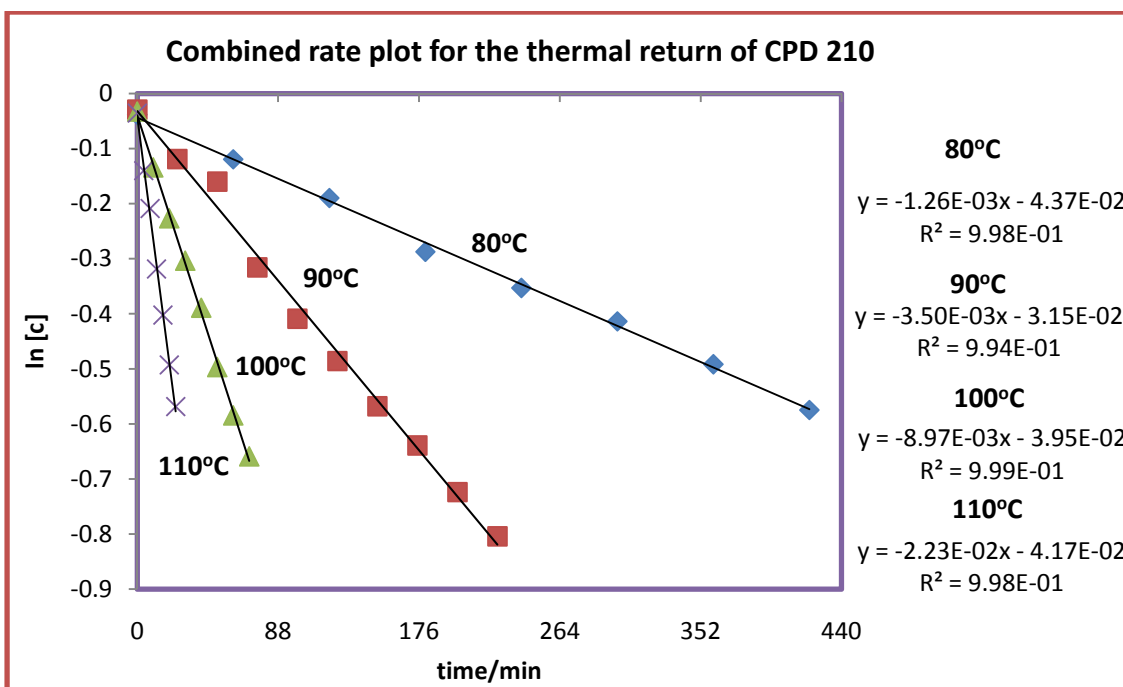
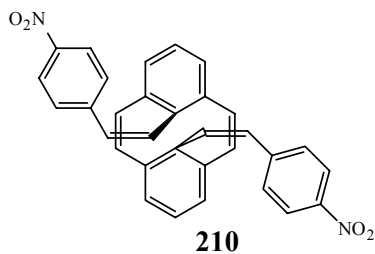
203

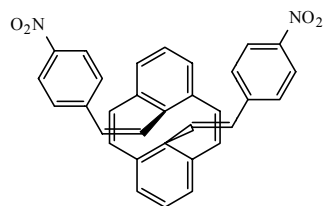




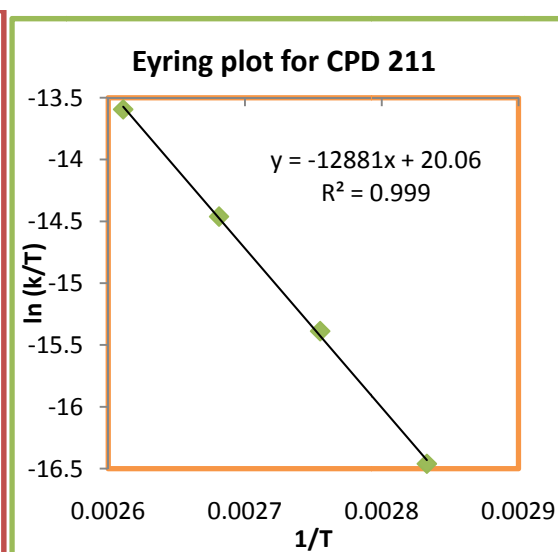
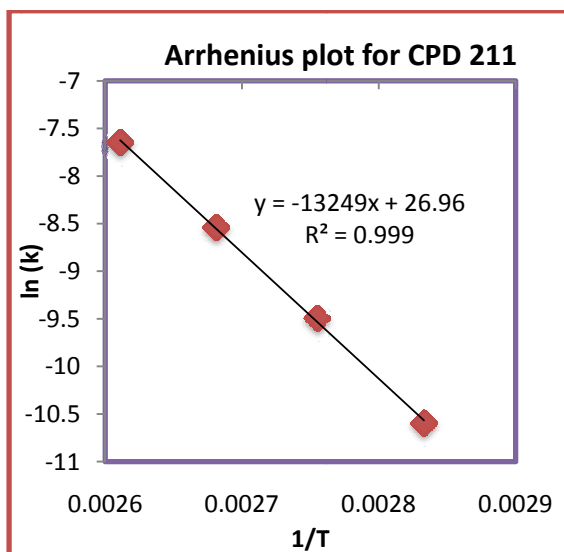
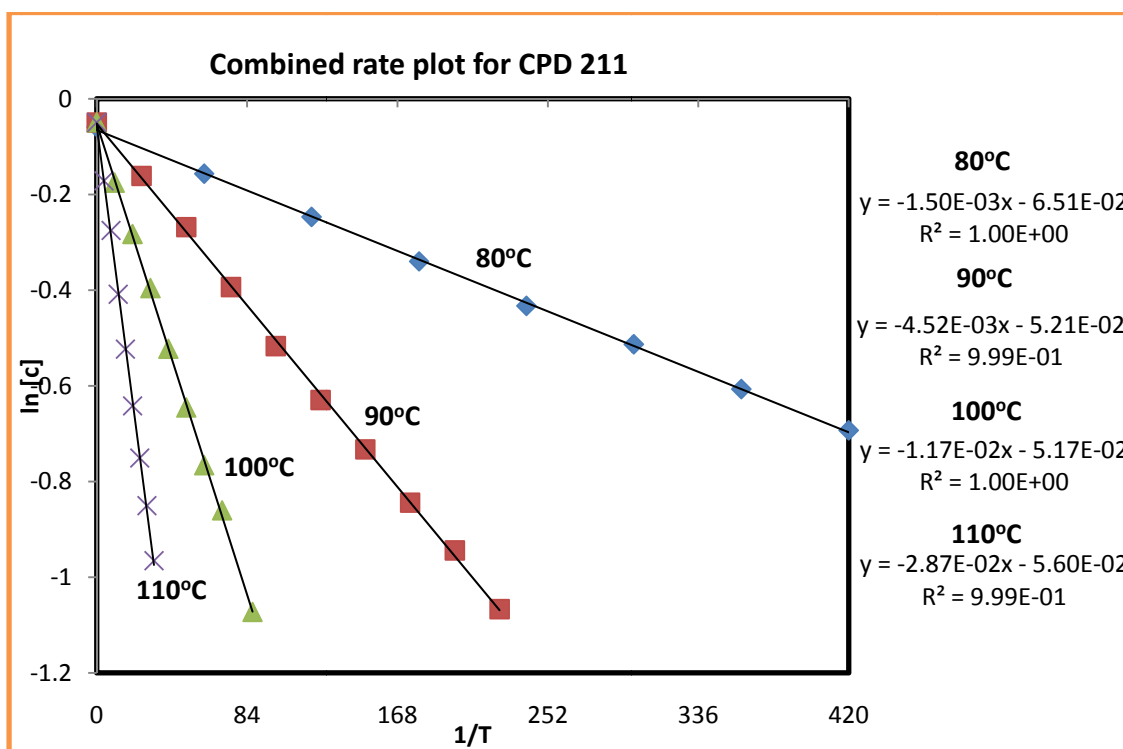
204

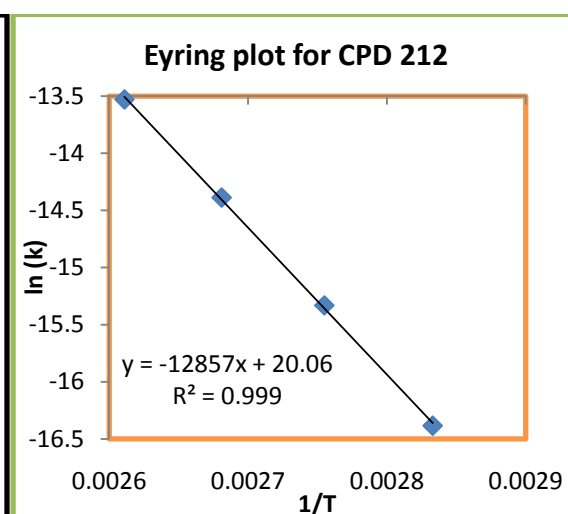
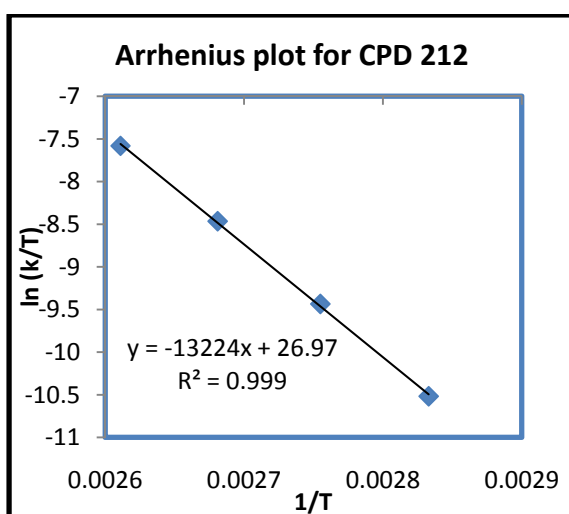
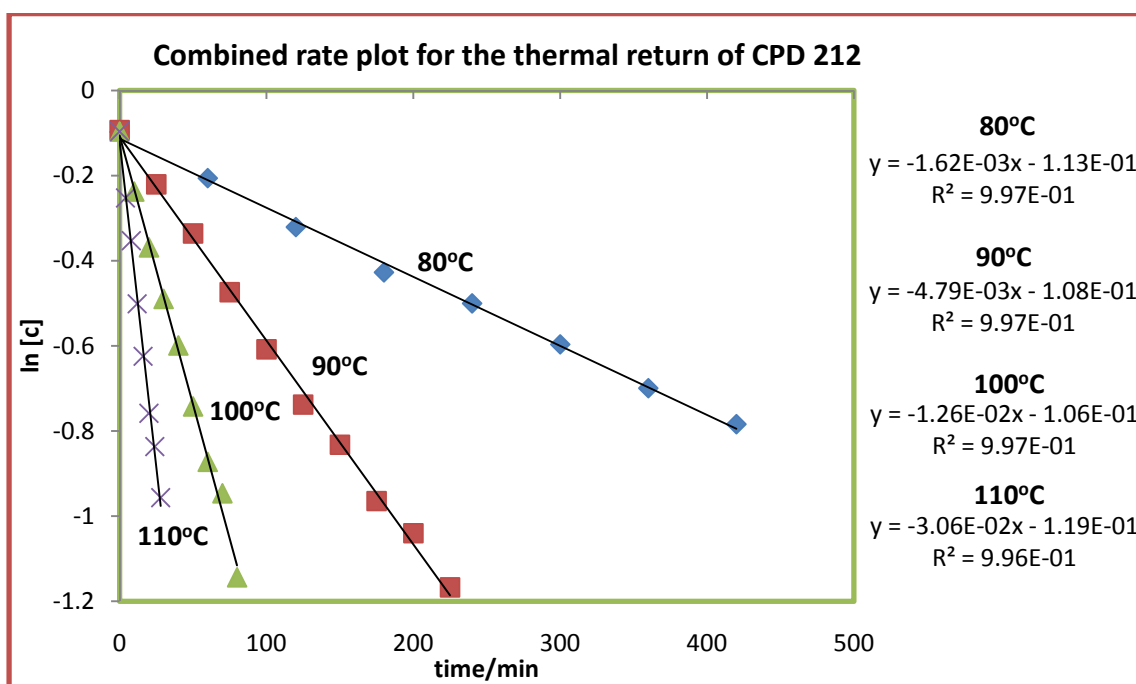
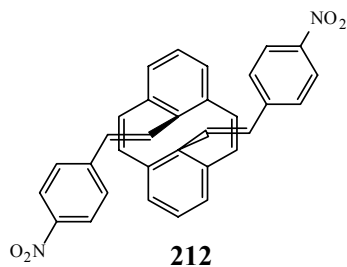


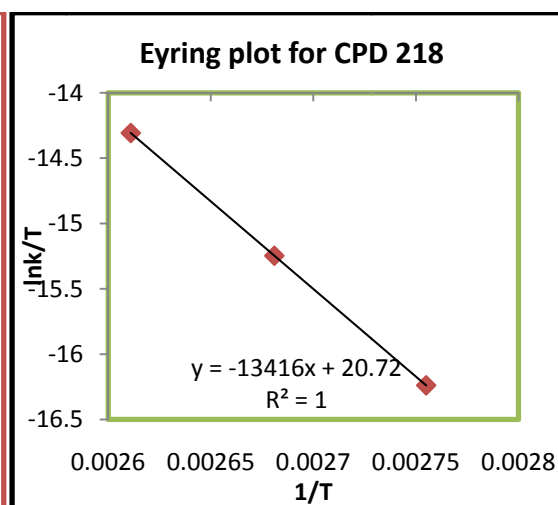
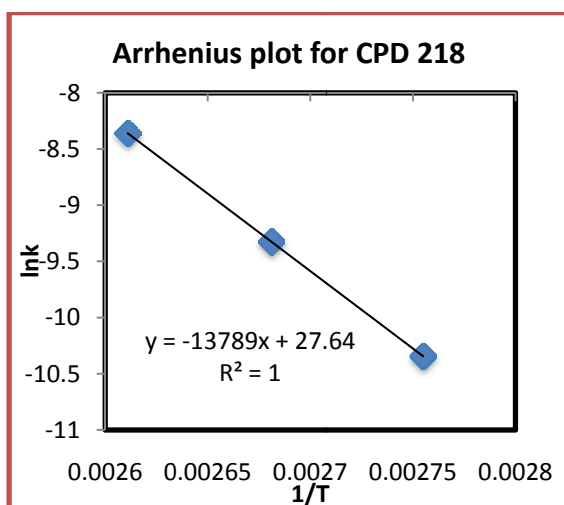
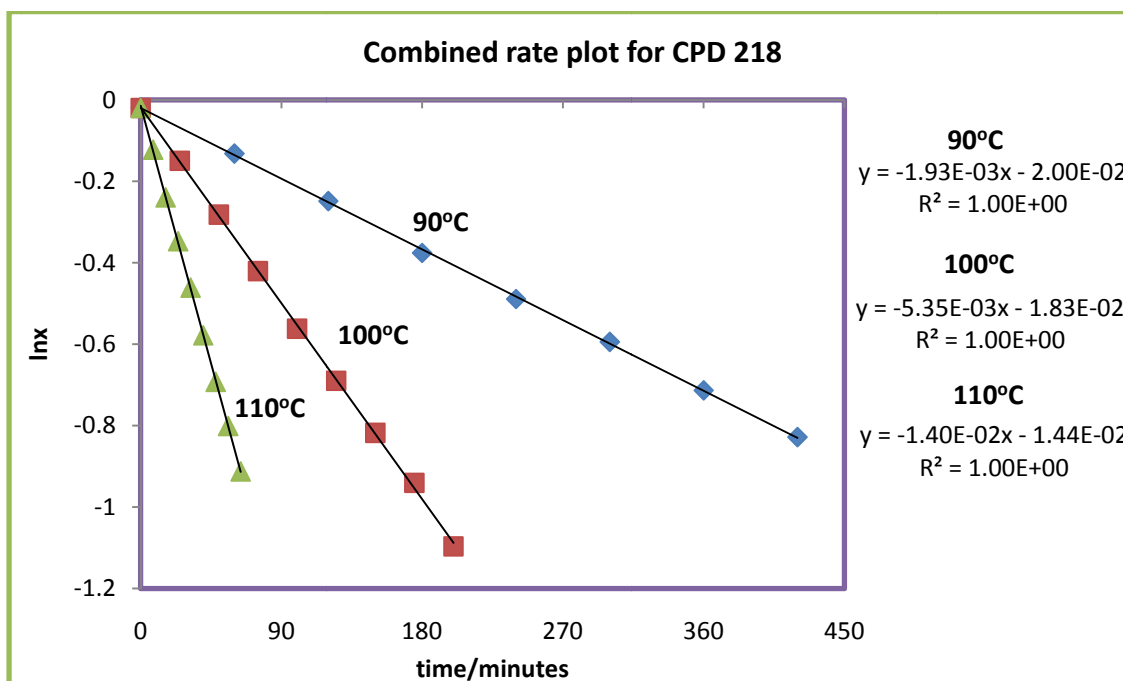
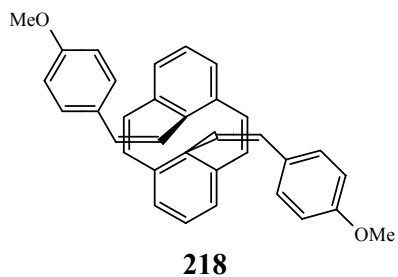


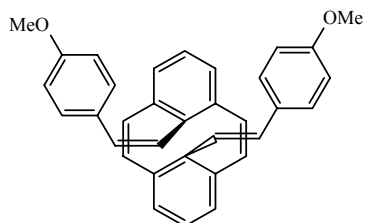


211

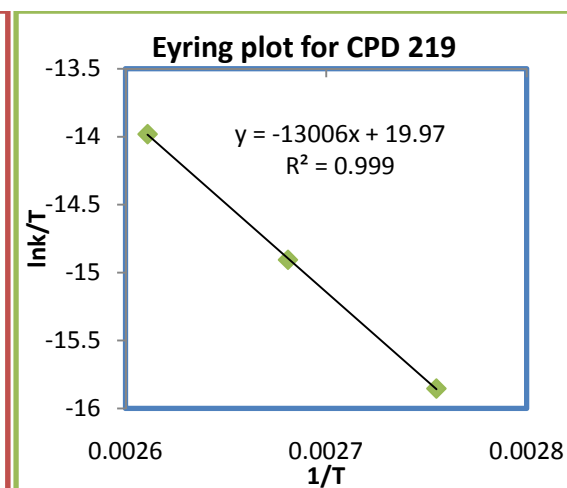
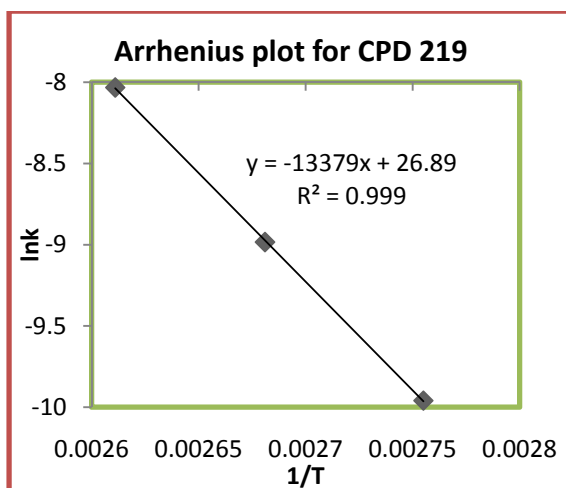
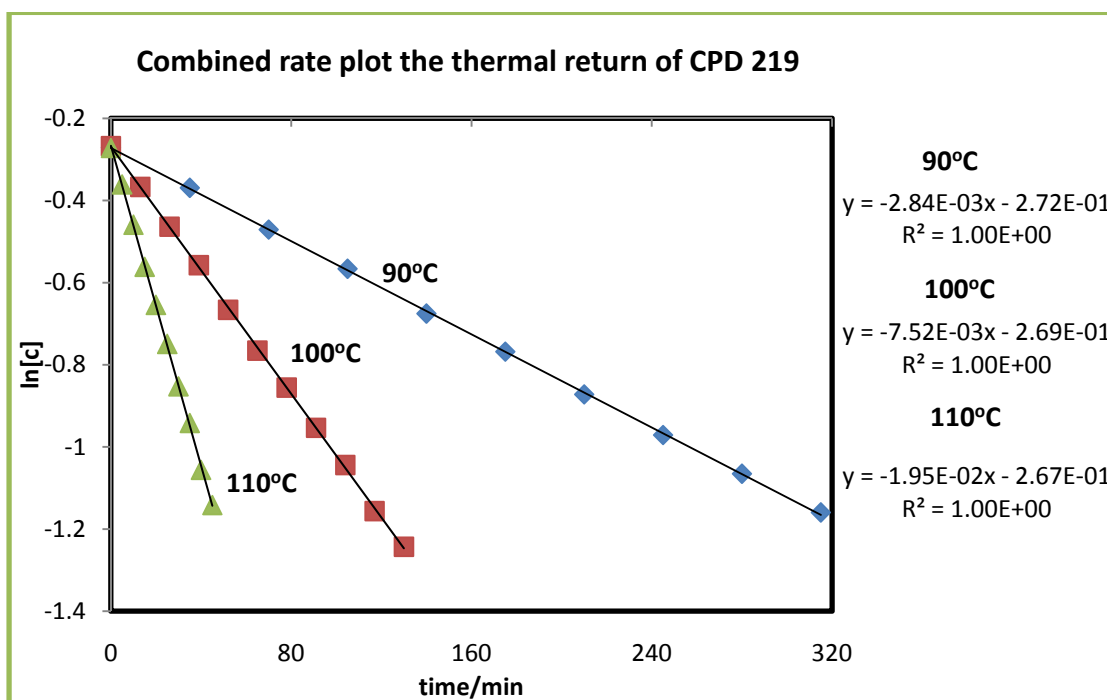


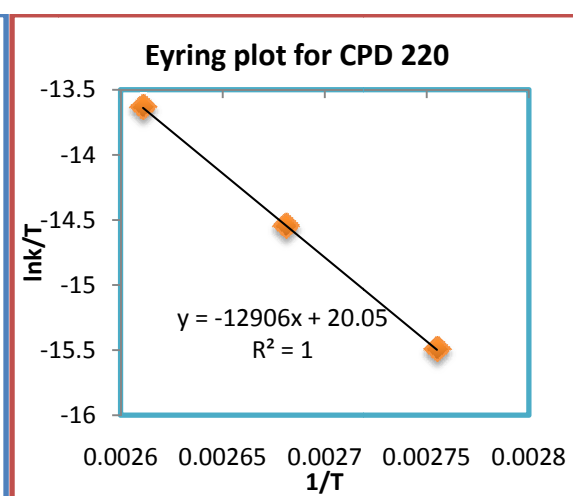
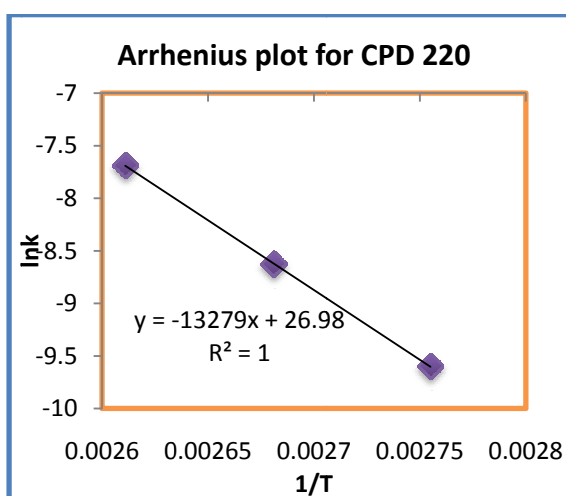
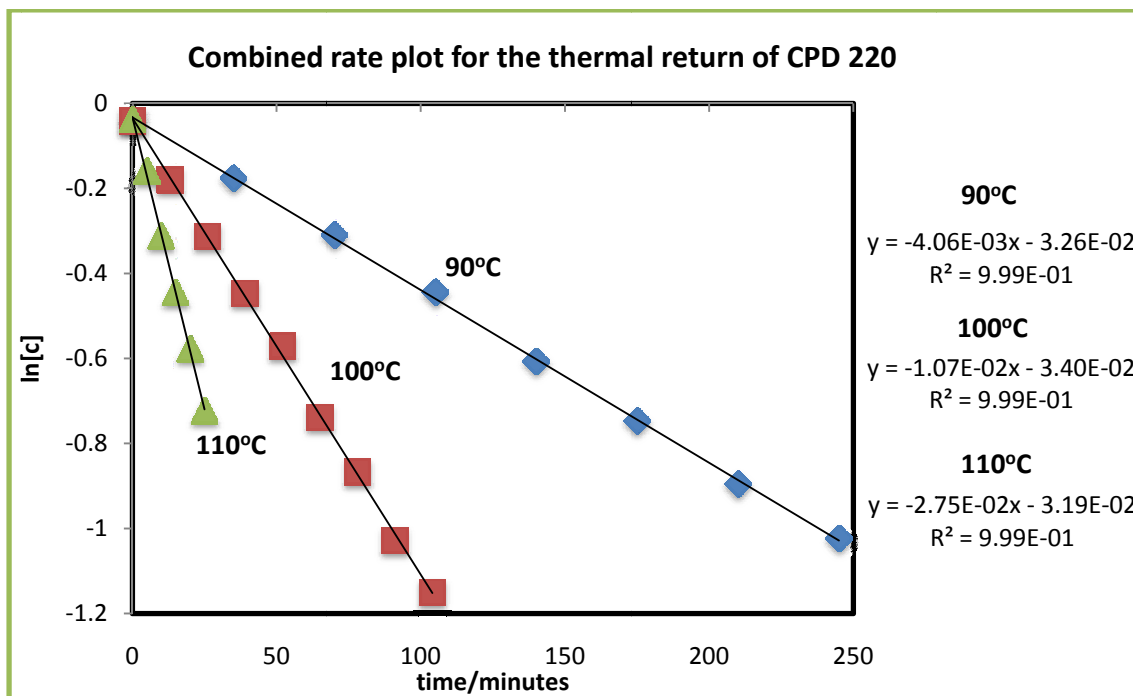
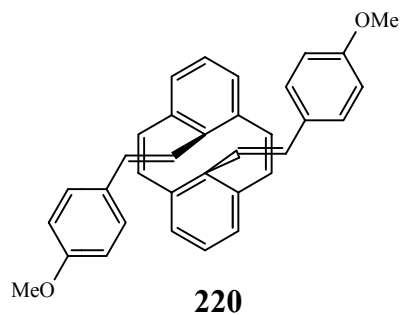


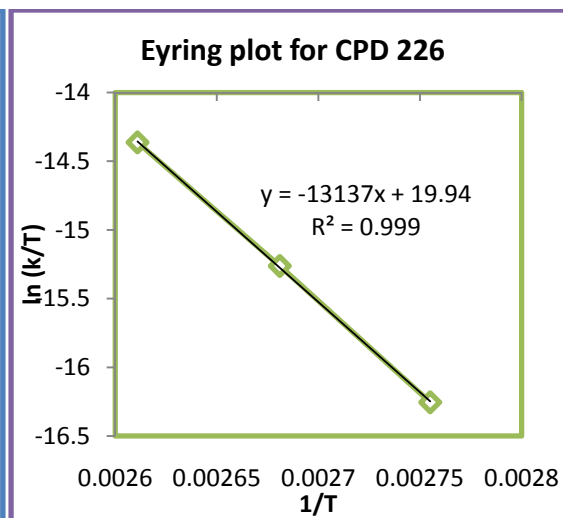
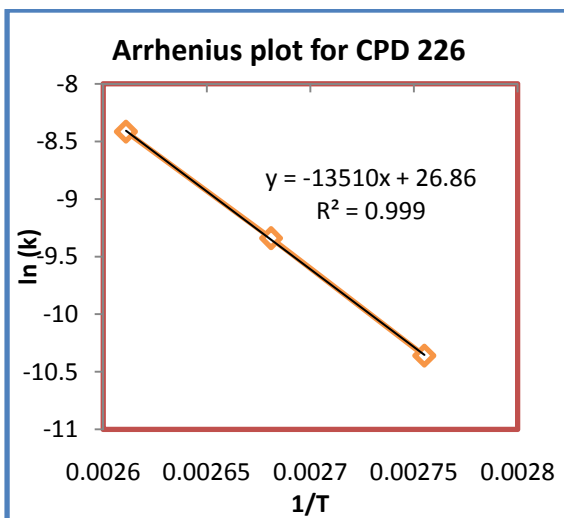
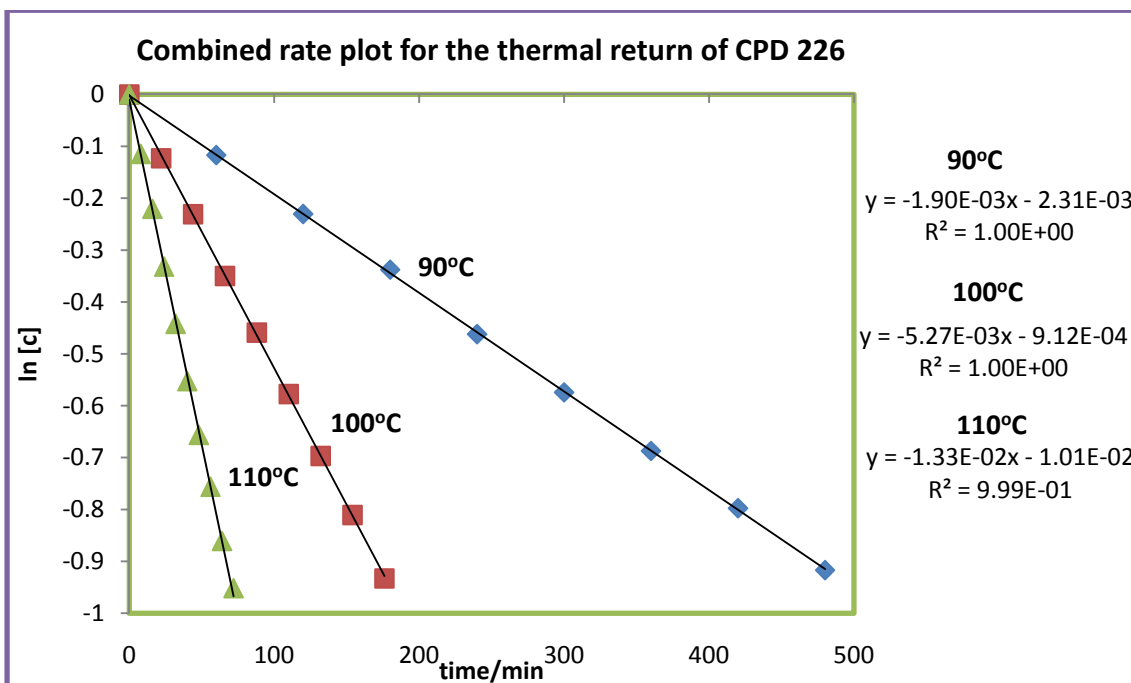
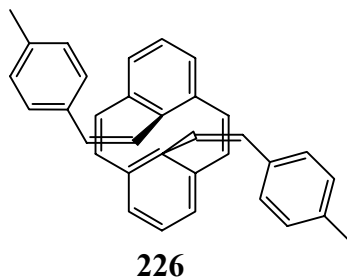


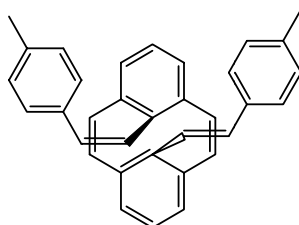


219

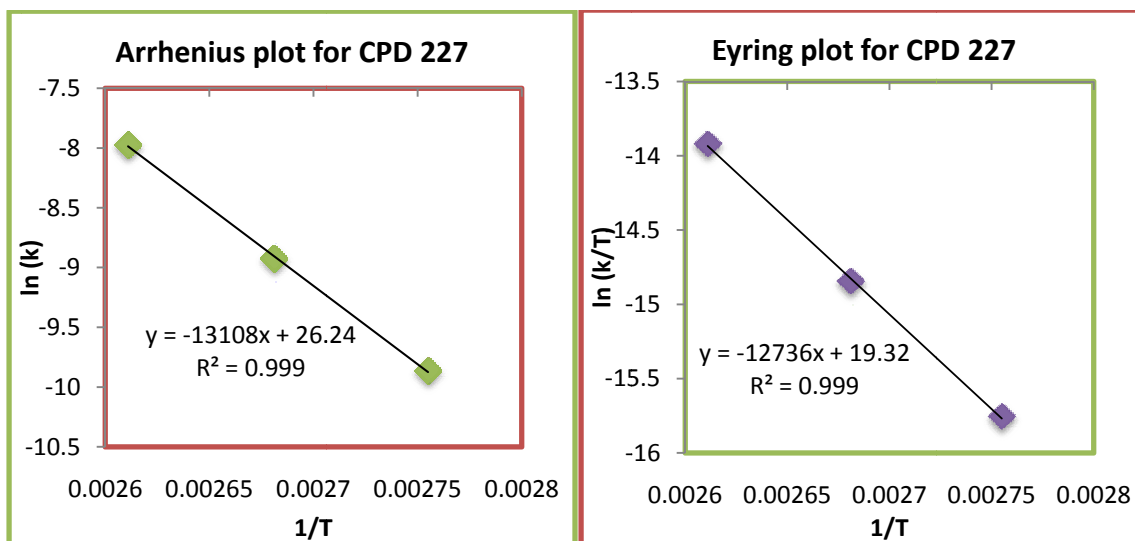
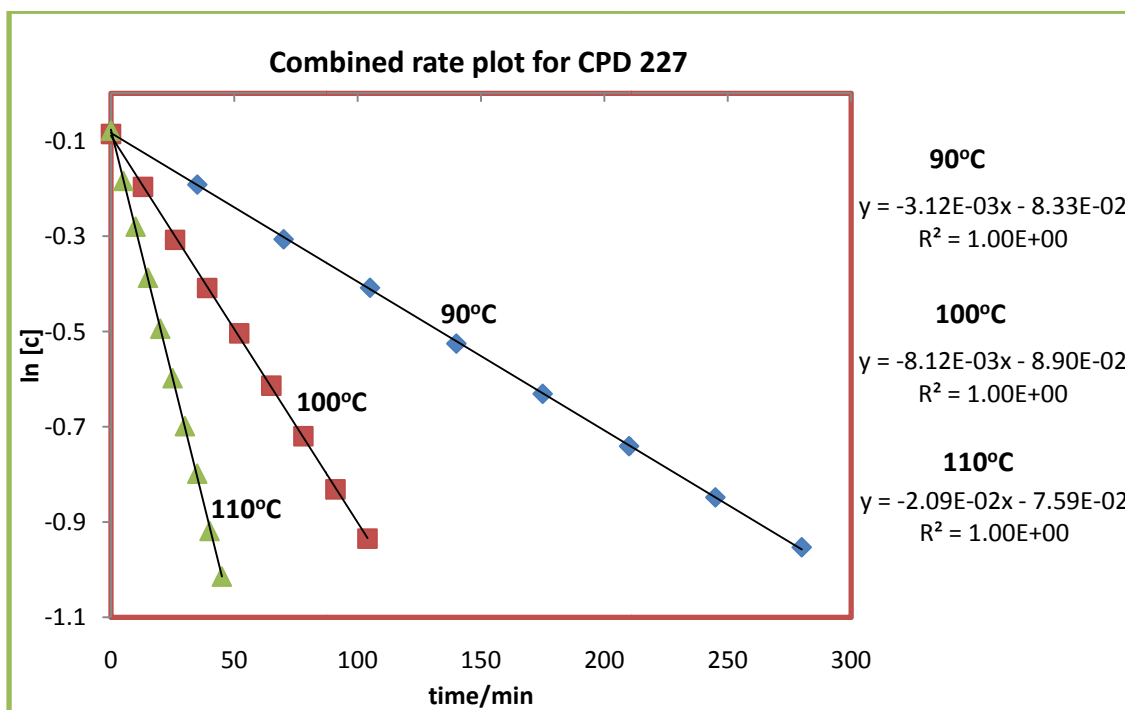


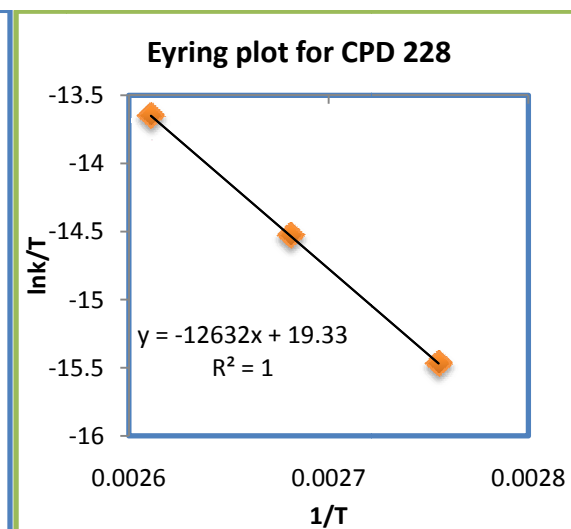
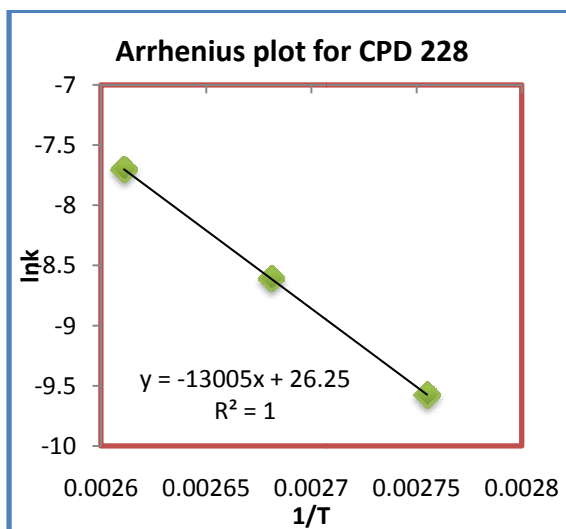
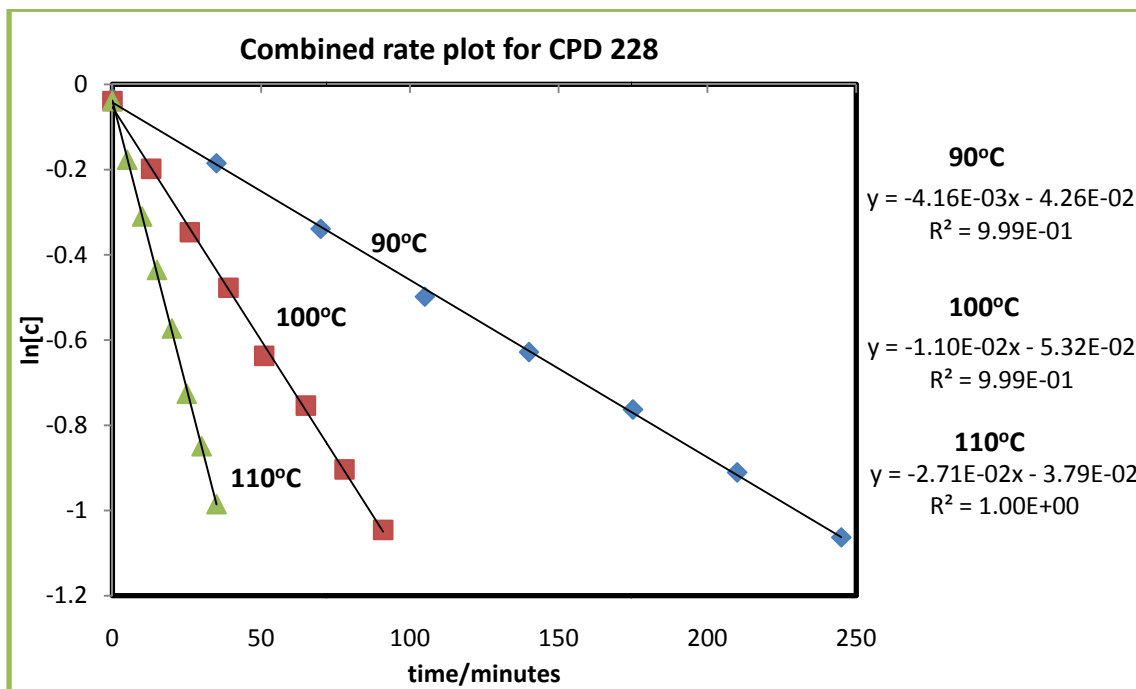
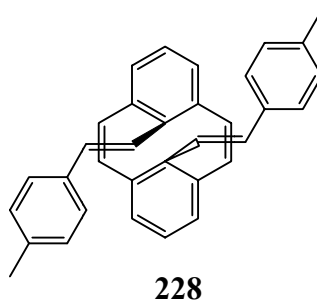


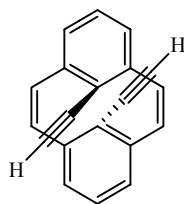




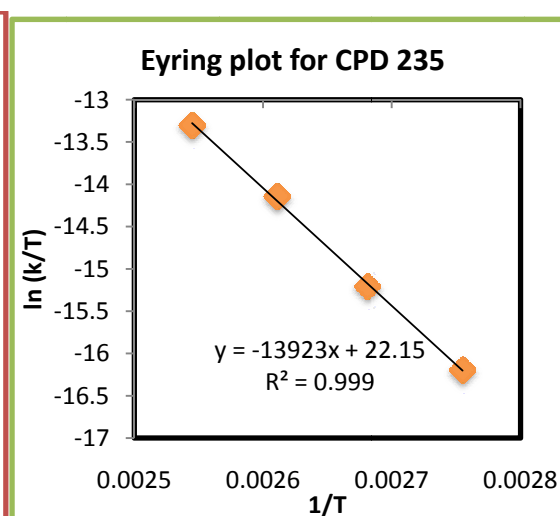
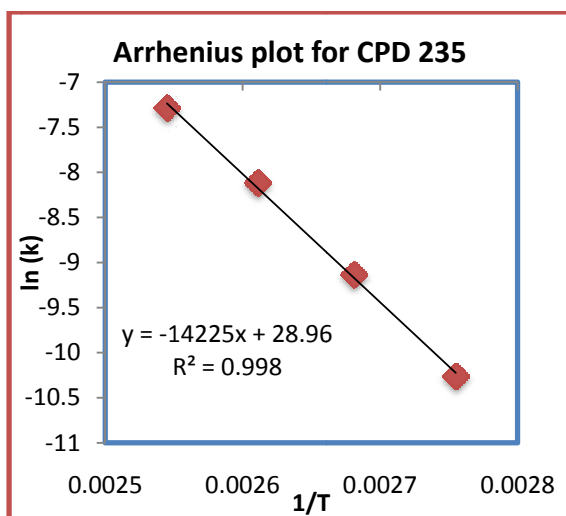
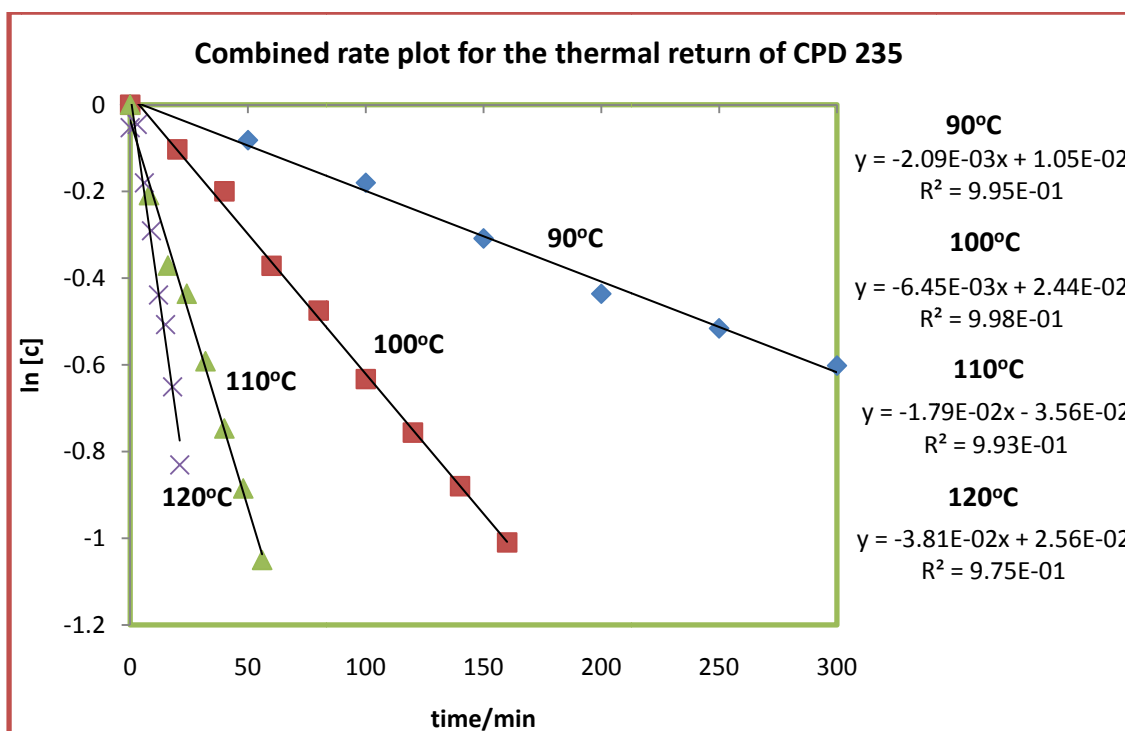
227

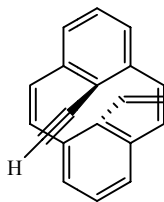




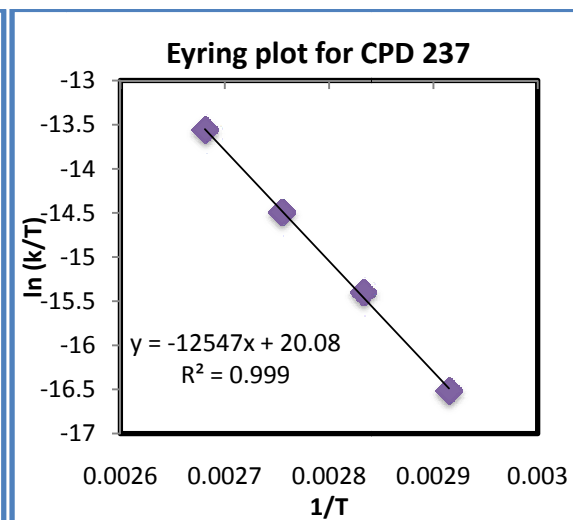
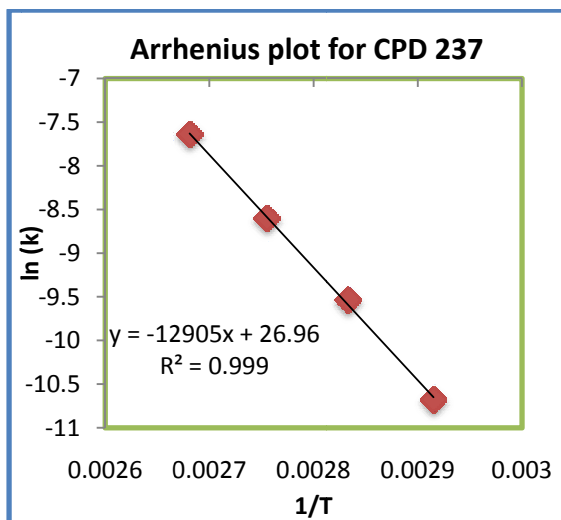
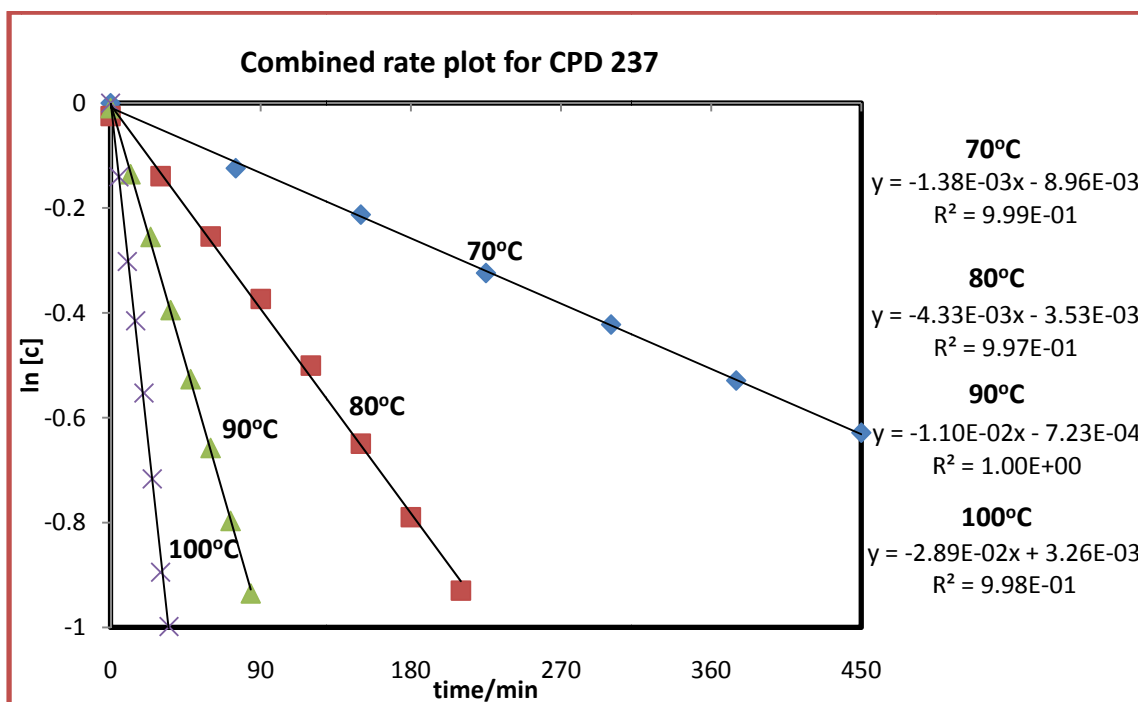


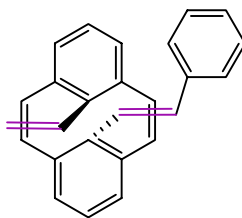
235



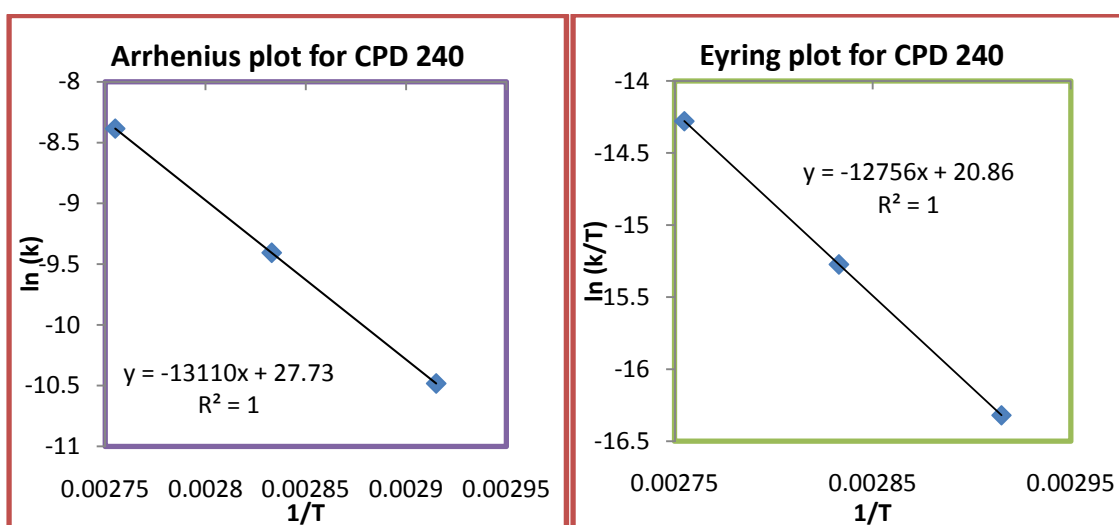
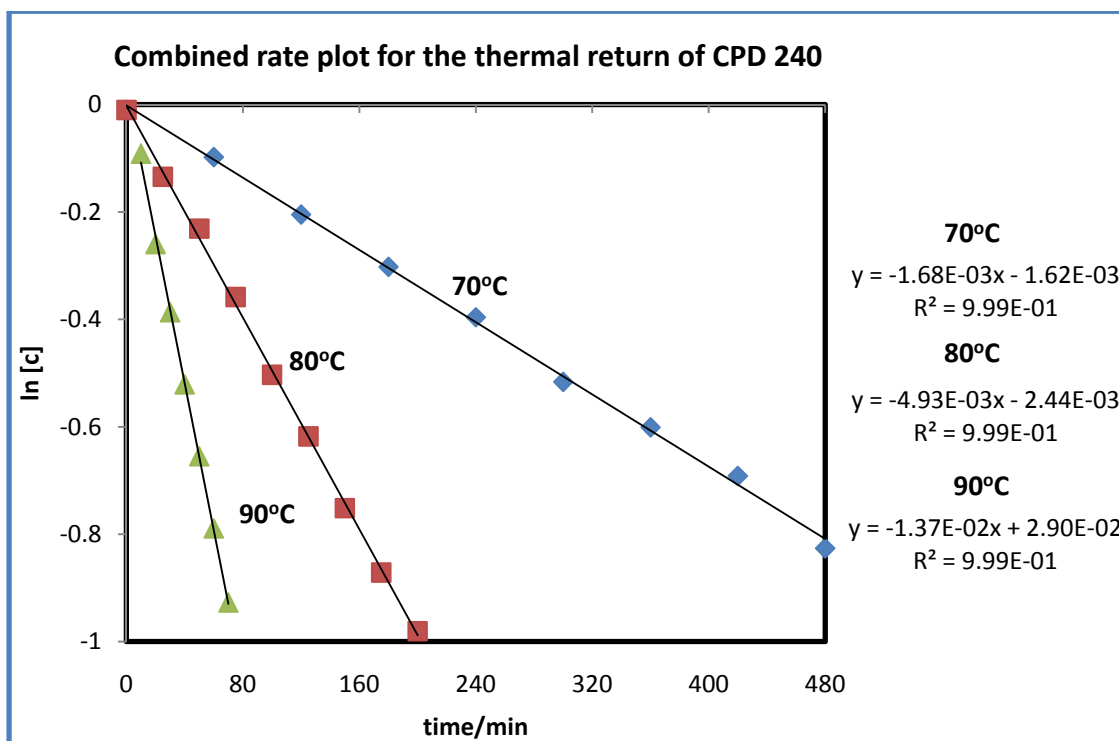


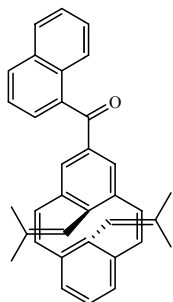
237



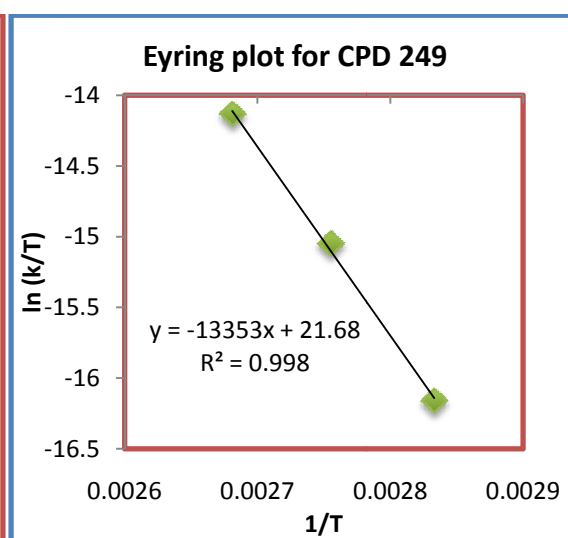
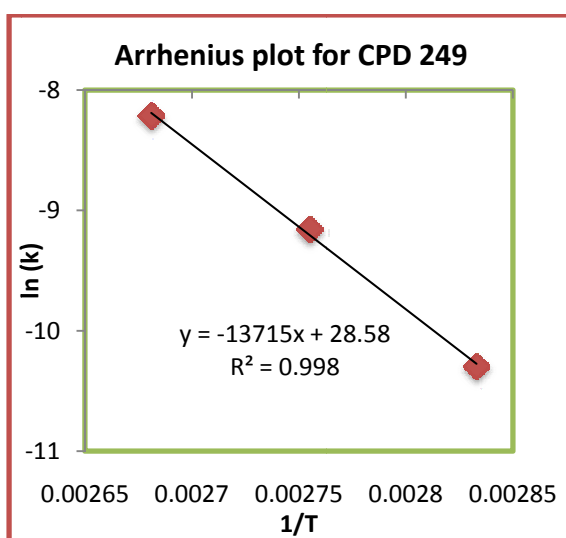
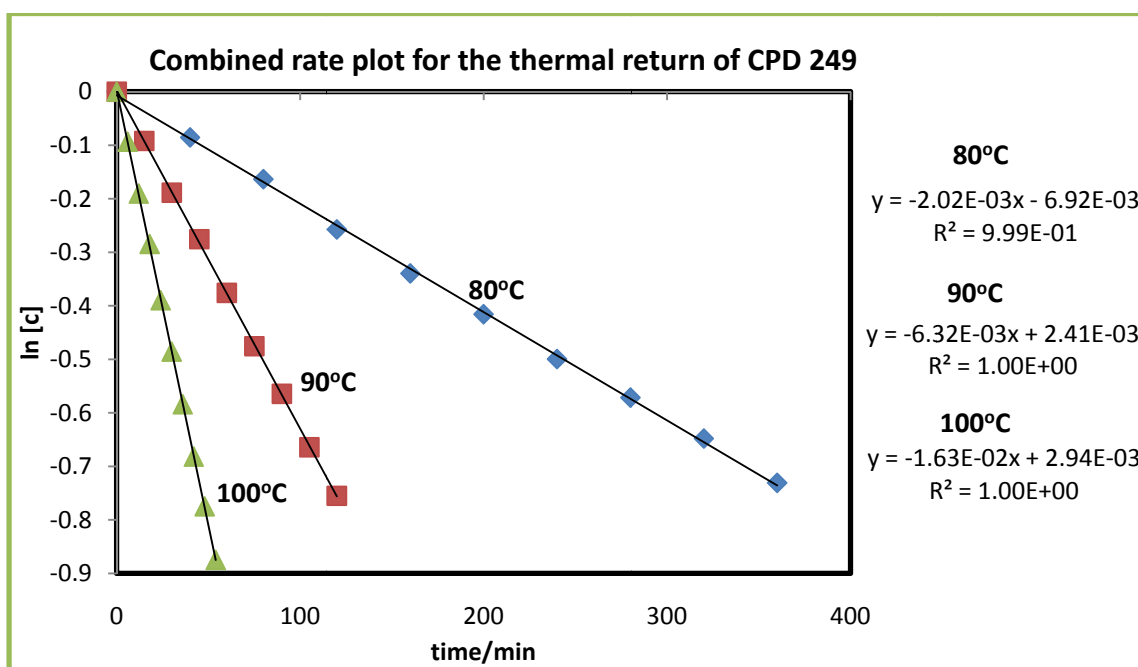


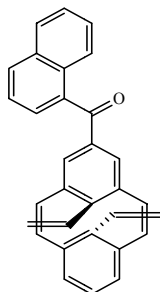
240



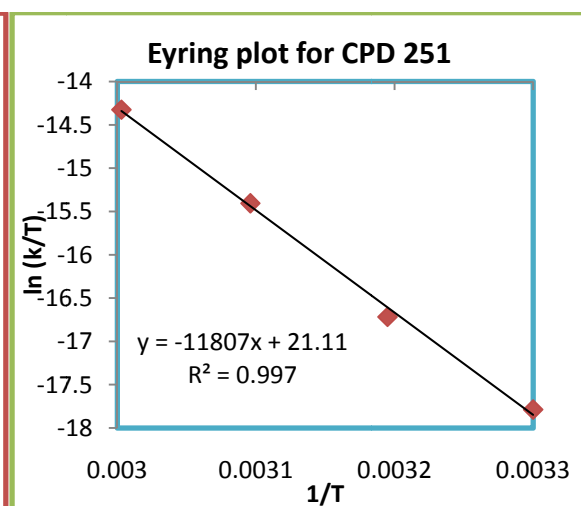
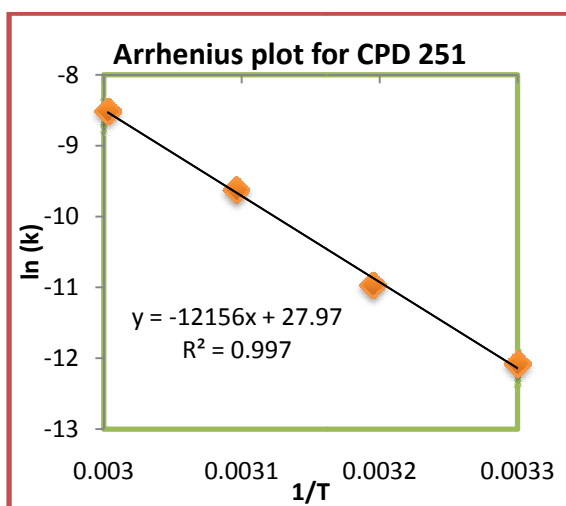
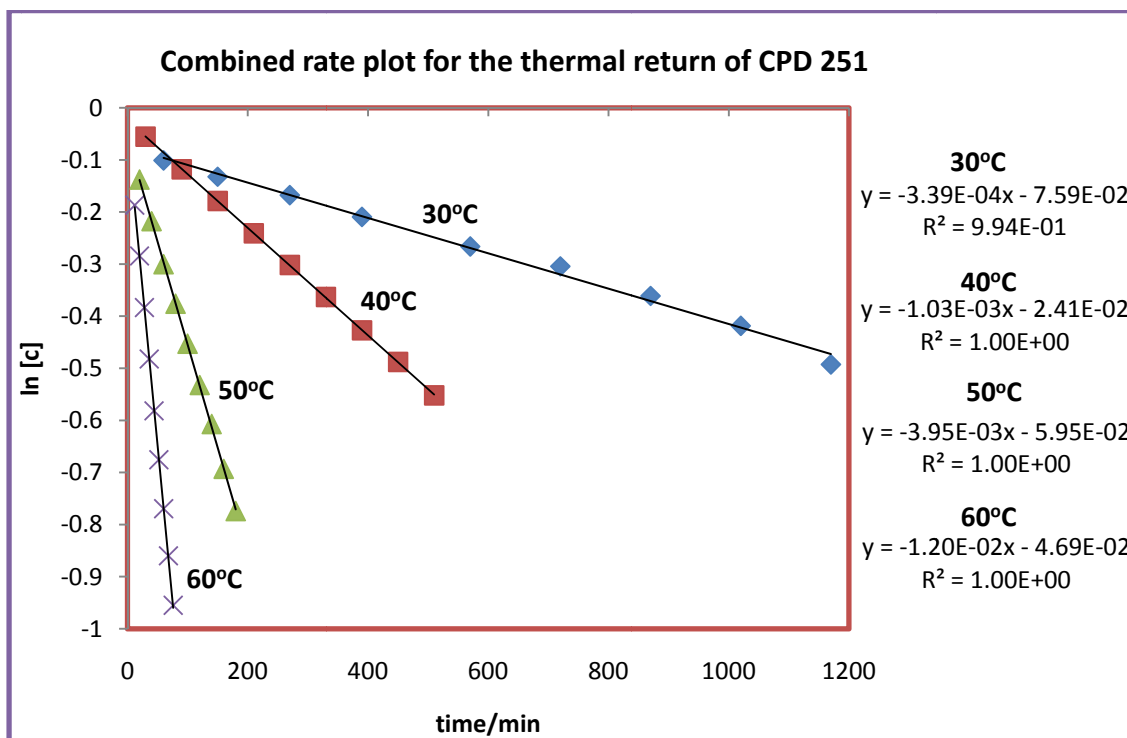


249

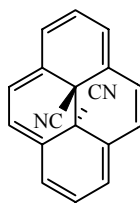




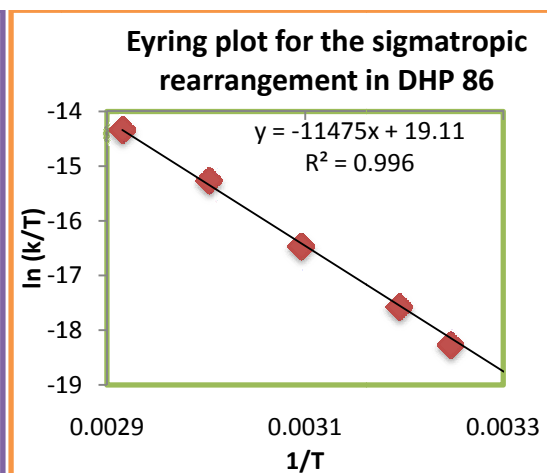
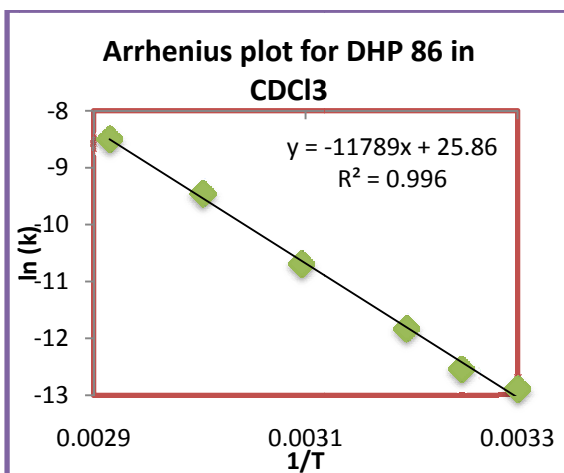
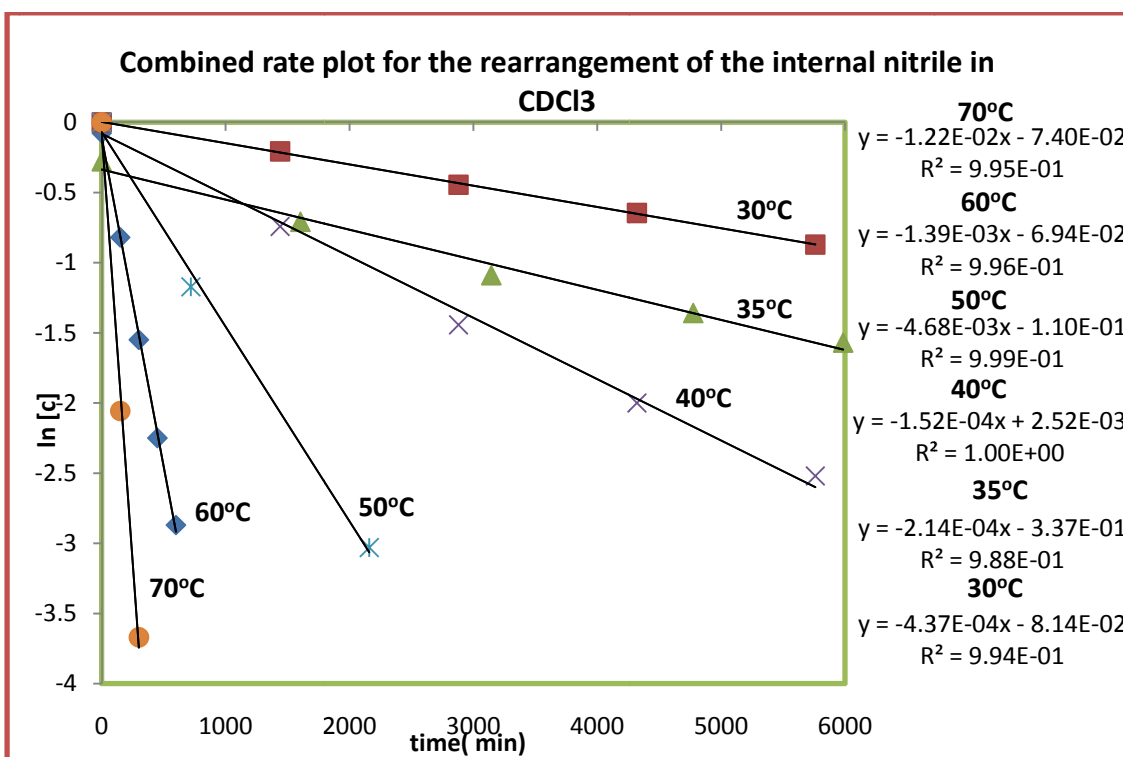
251

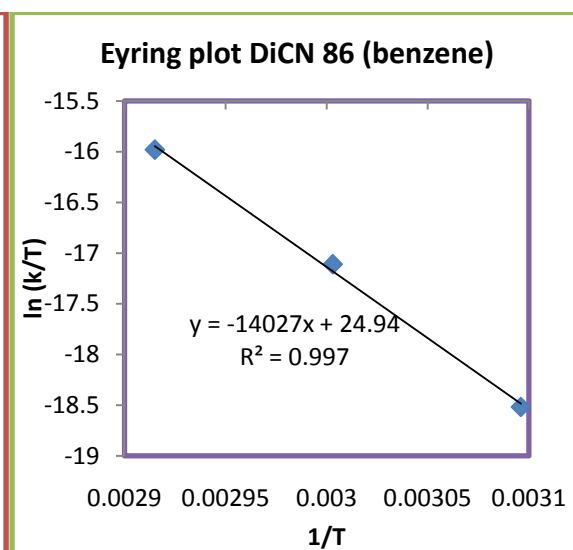
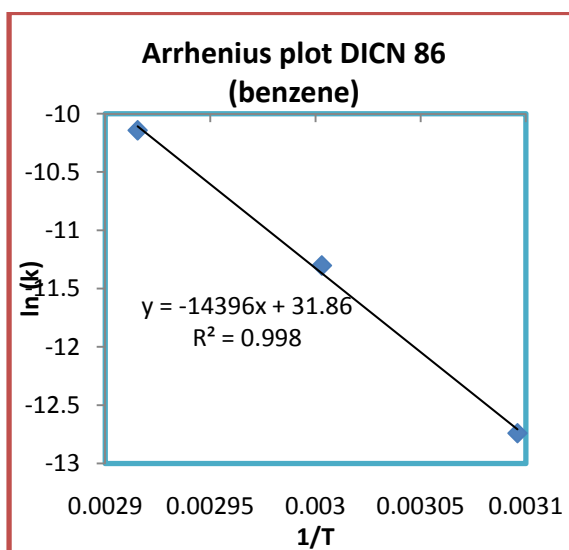
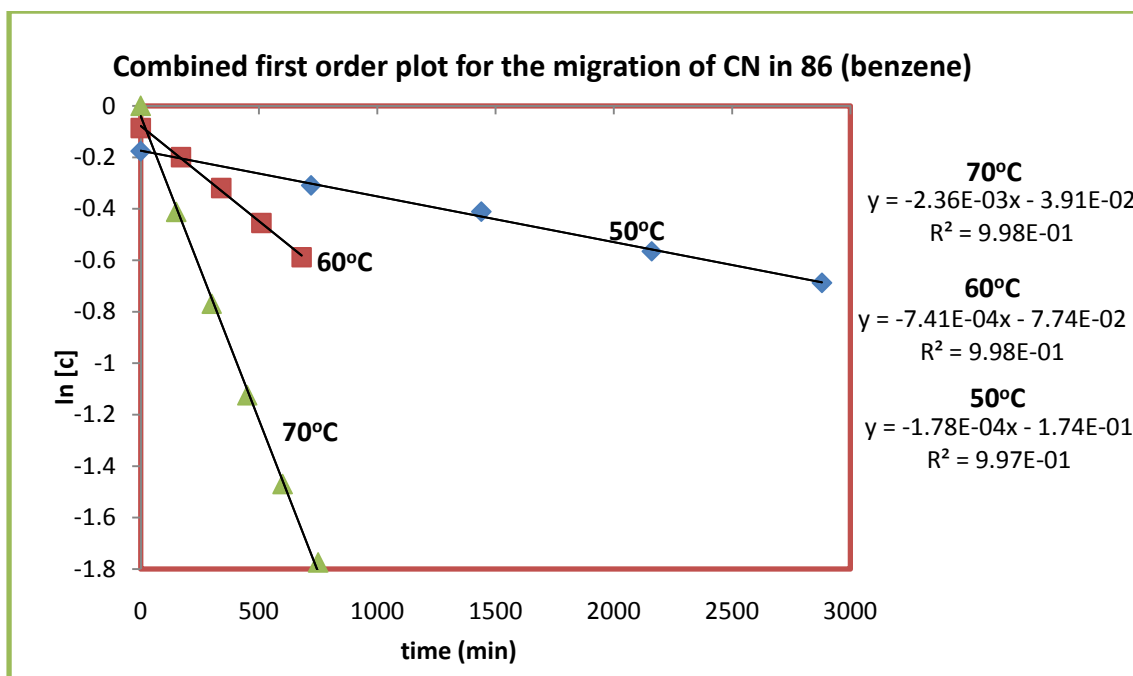


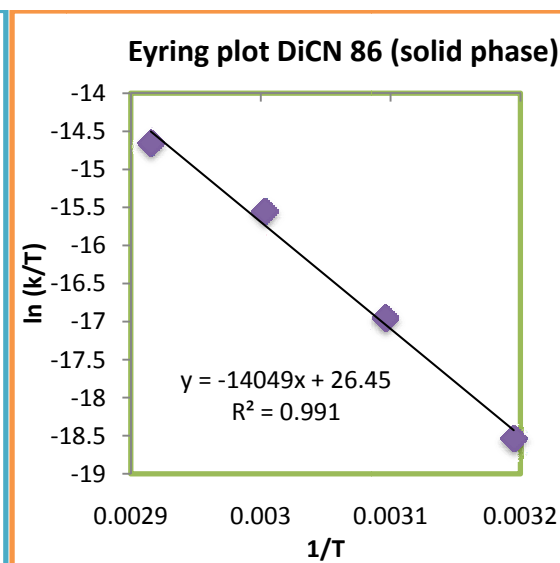
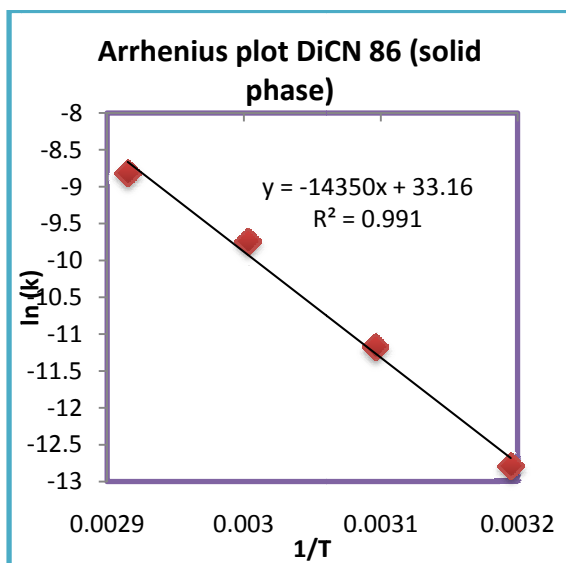
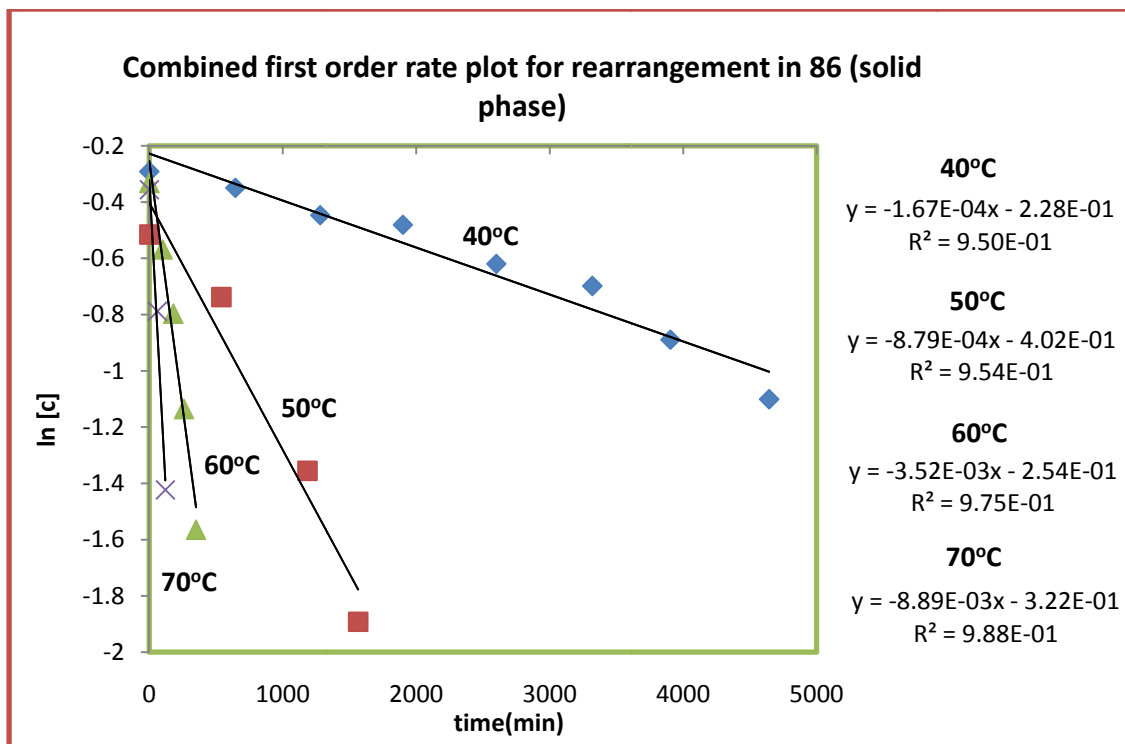
Appendix C: Sigmatropic rearrangement data for dicyano DHP 86



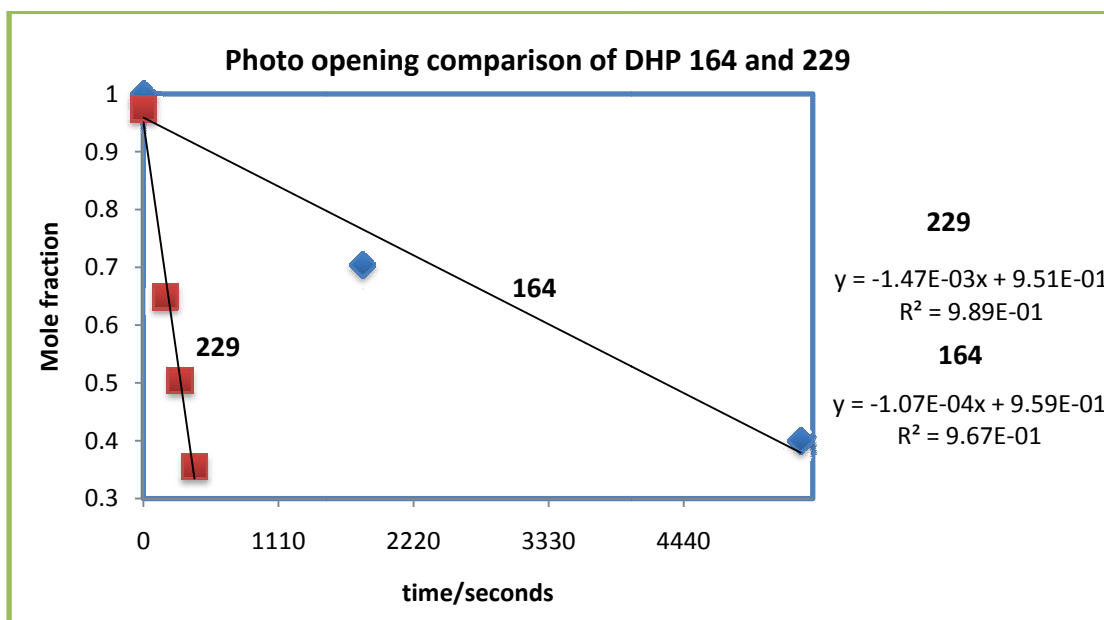
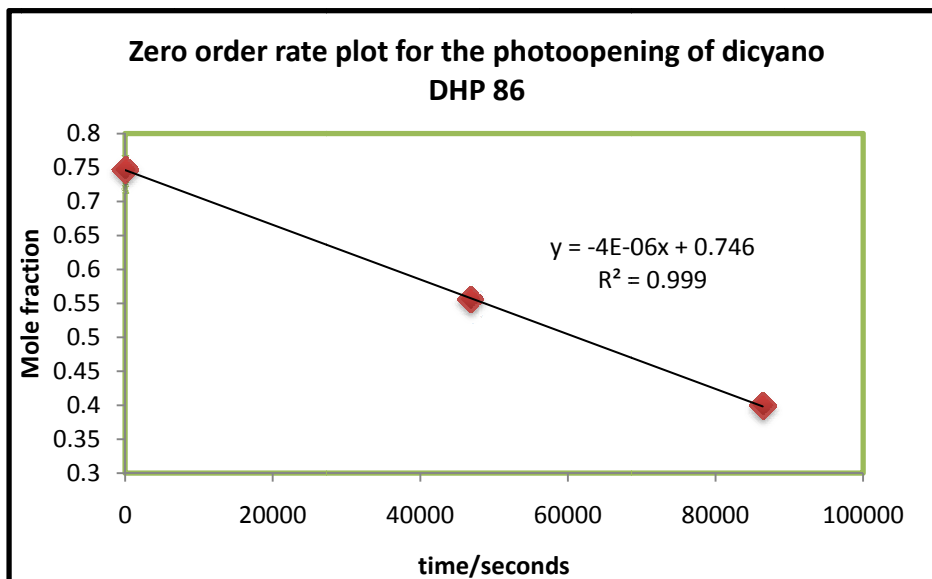
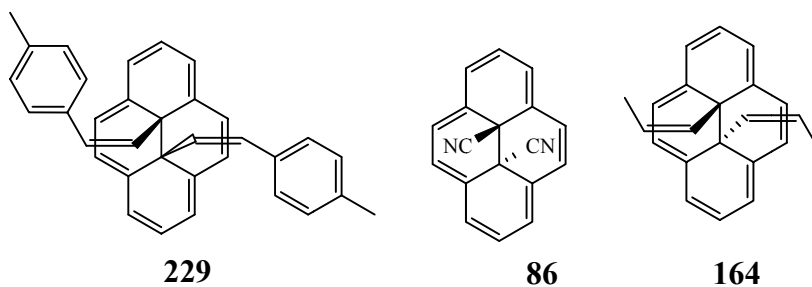
86

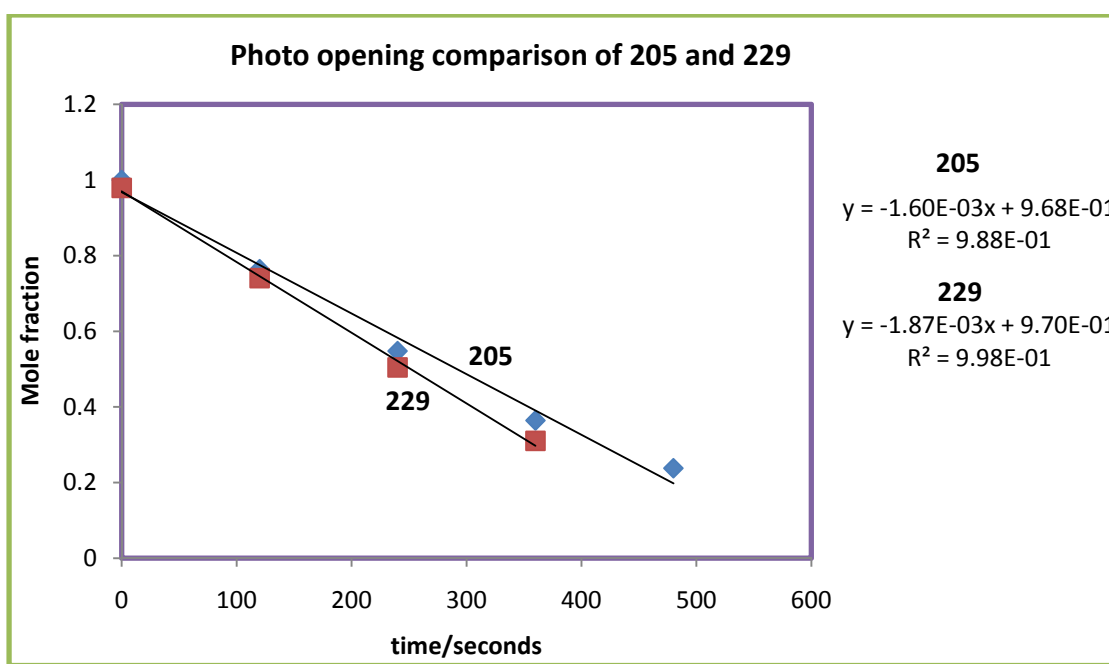
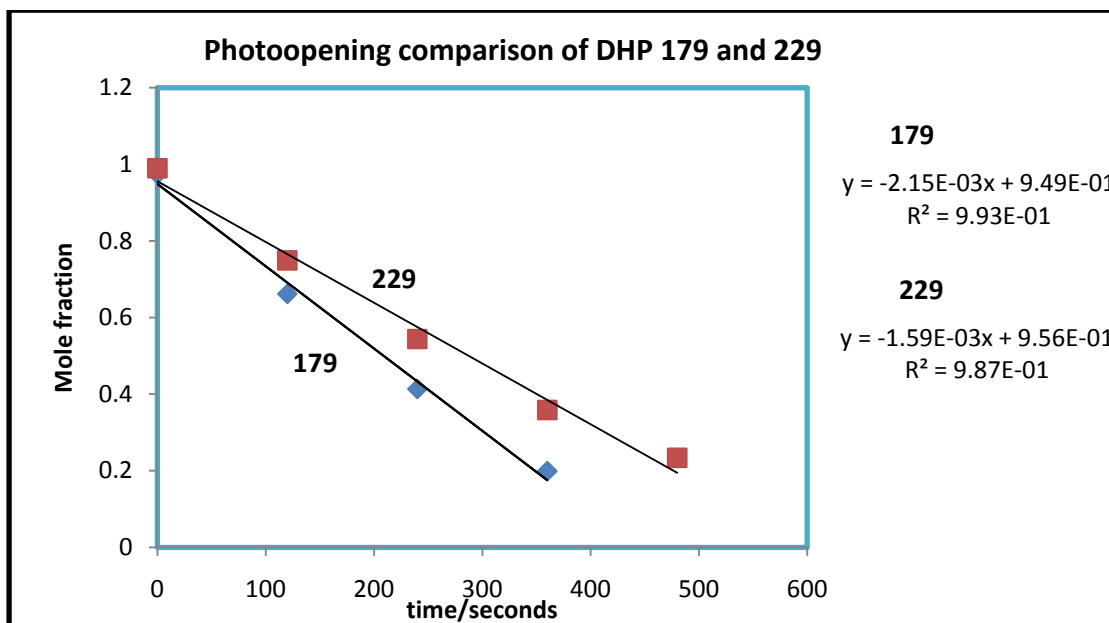
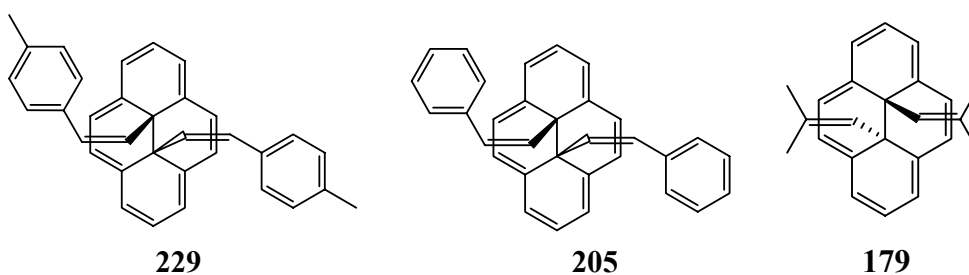


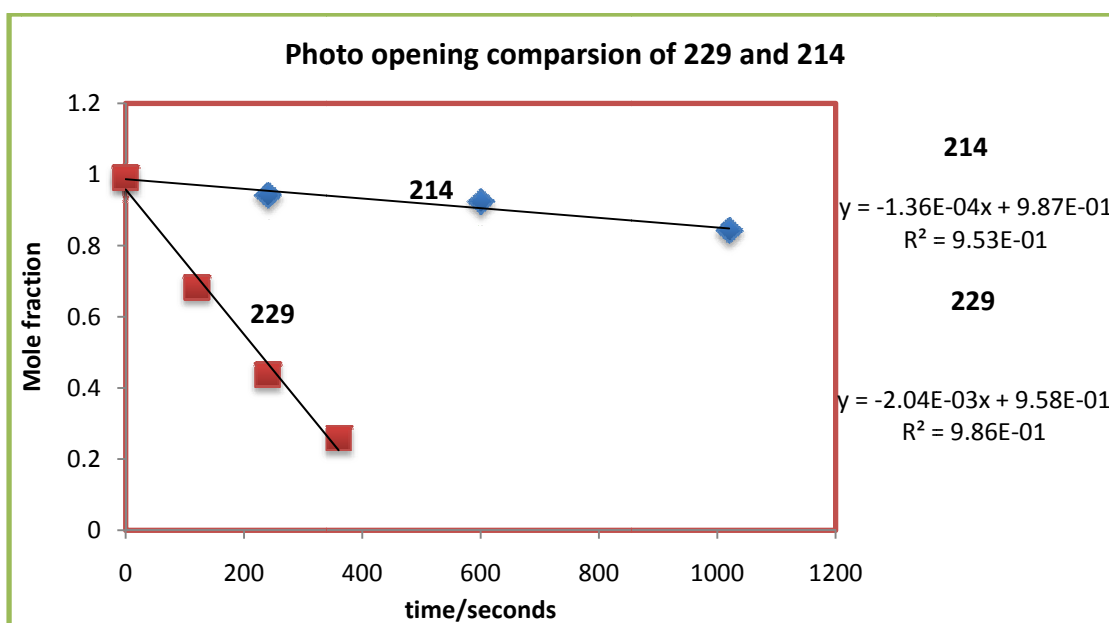
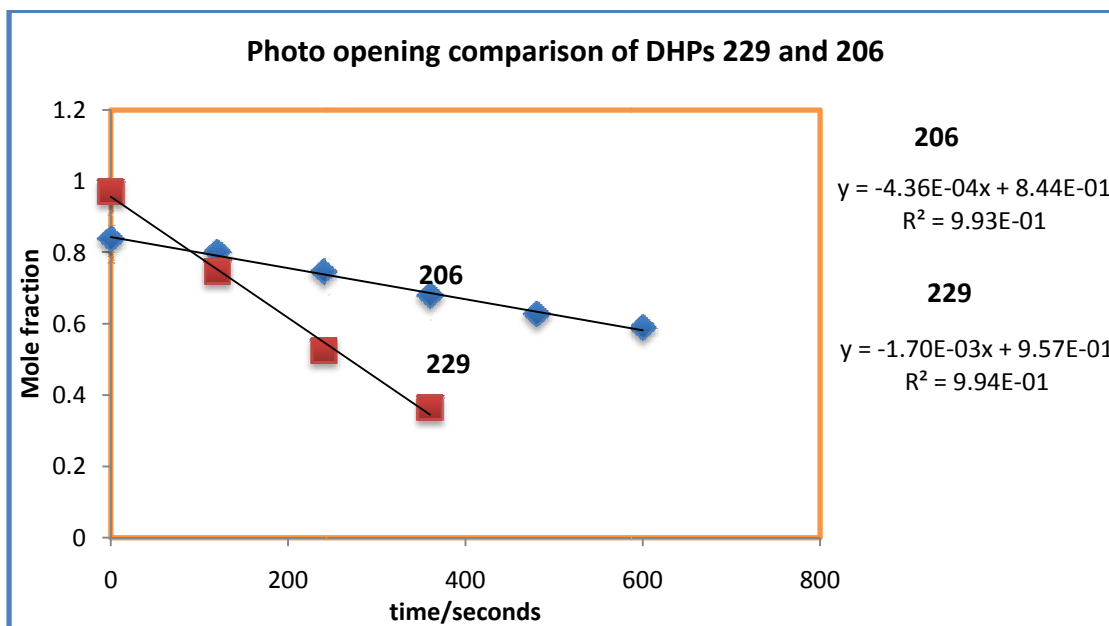
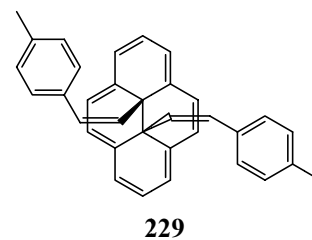
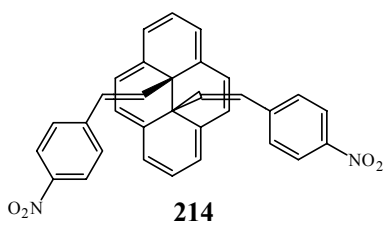
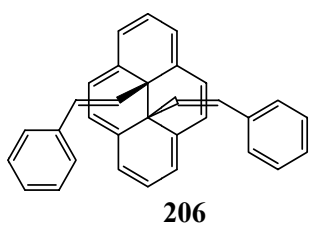


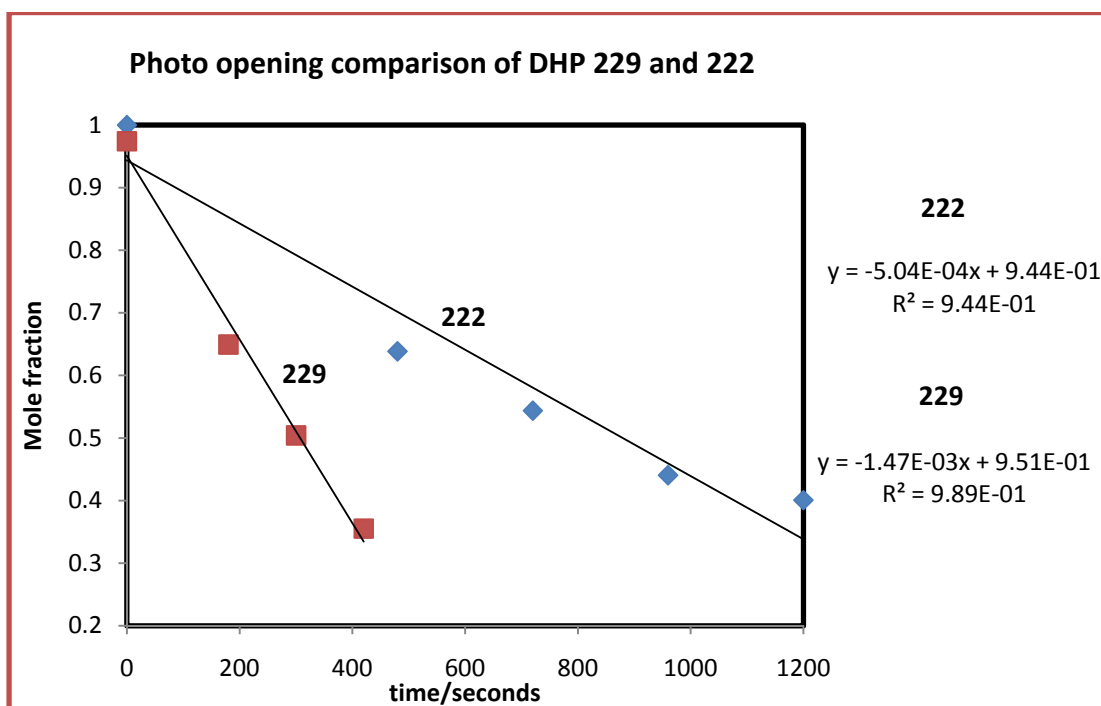
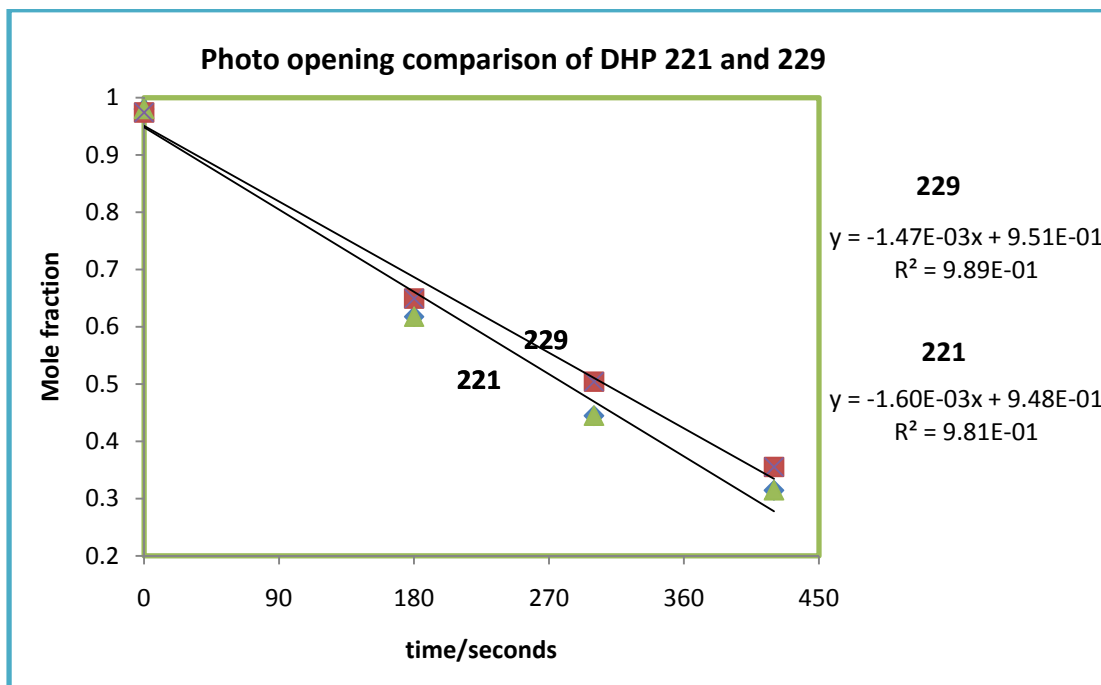
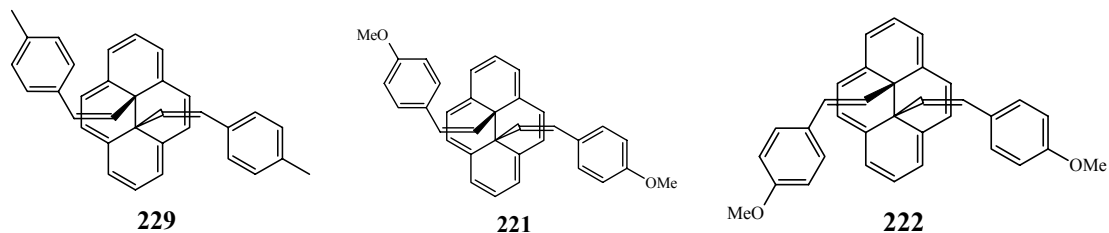


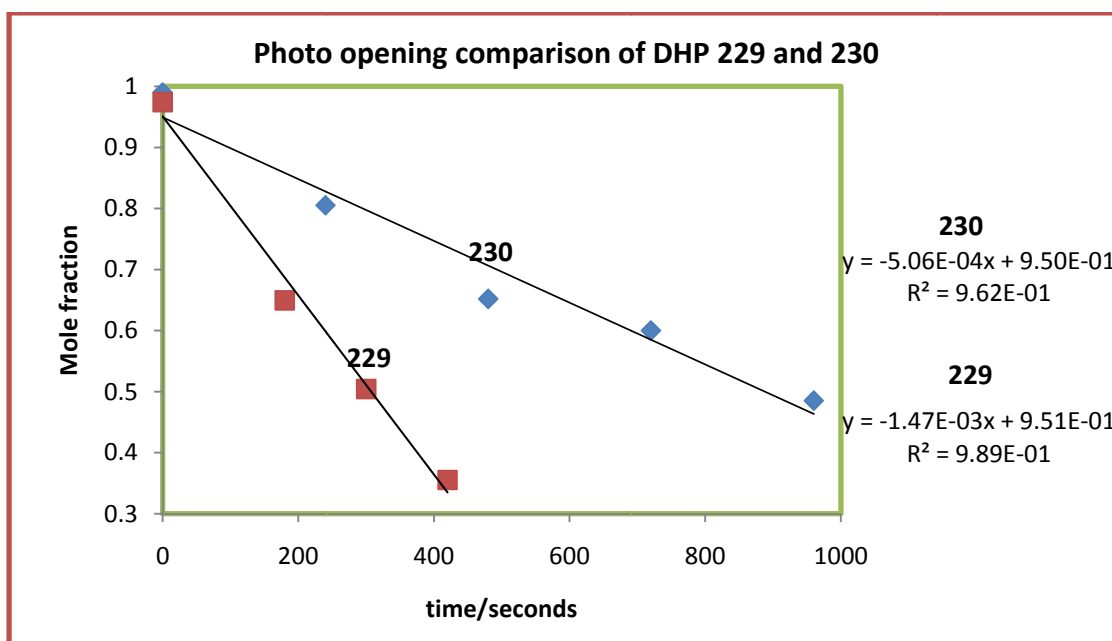
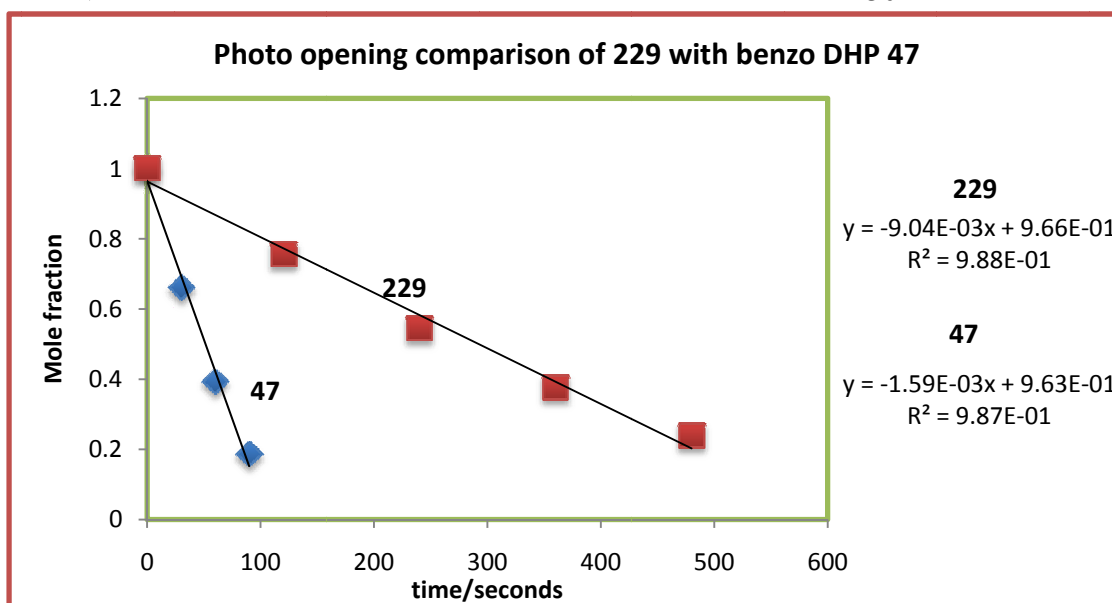
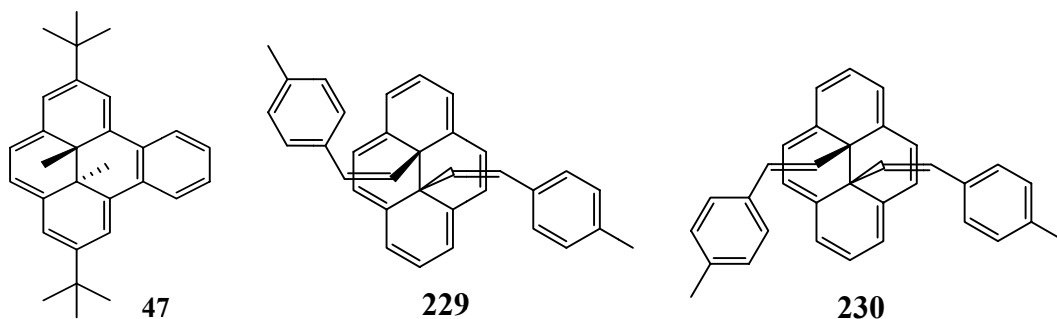
Appendix D Photoopening data for dihydropyrenes

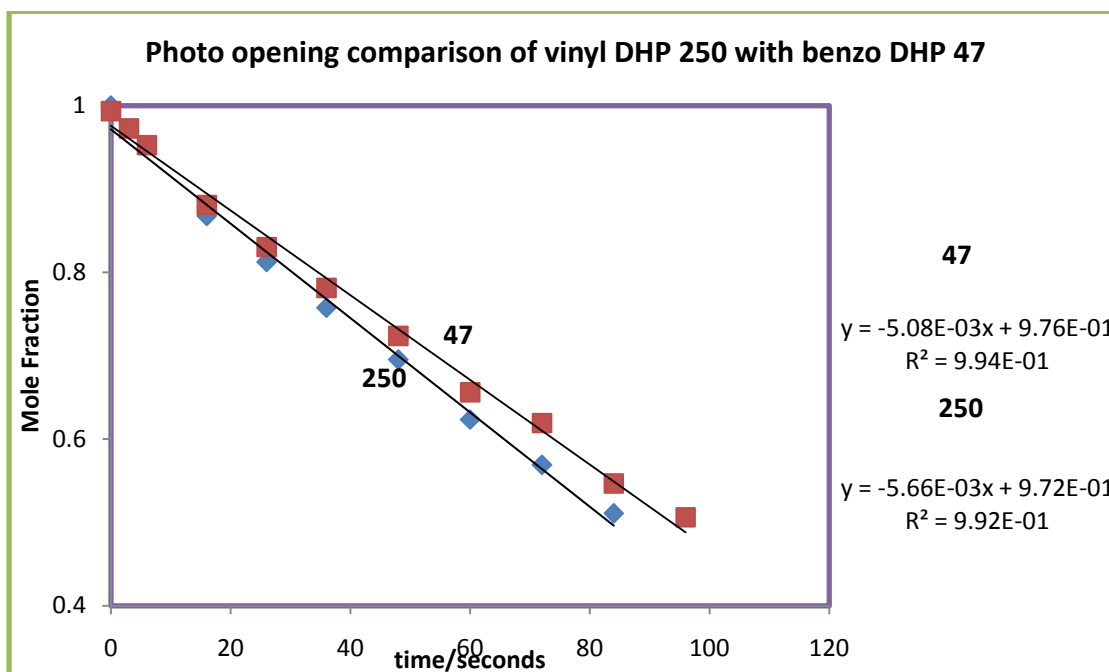
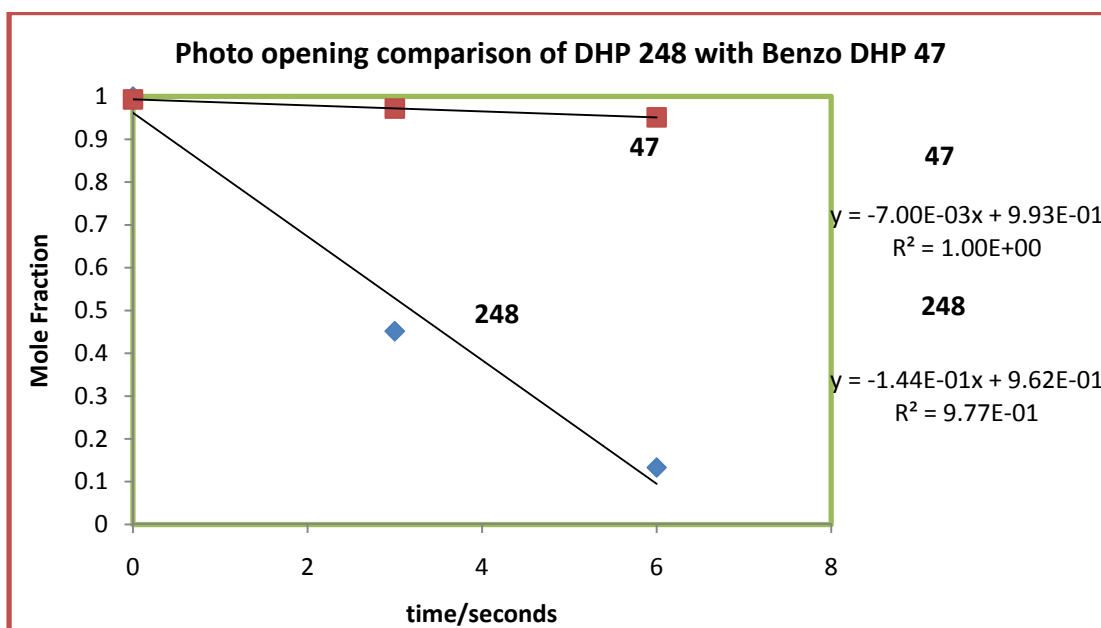
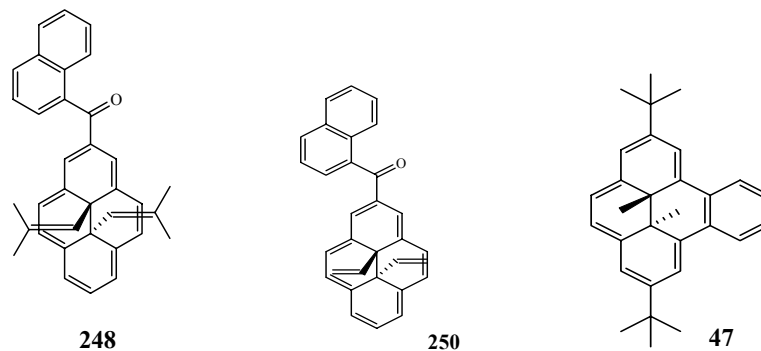


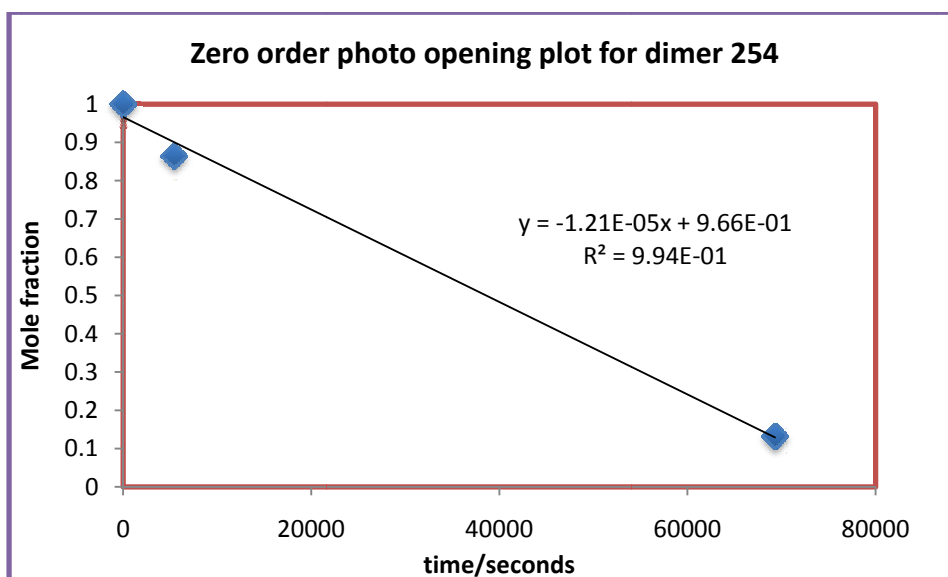
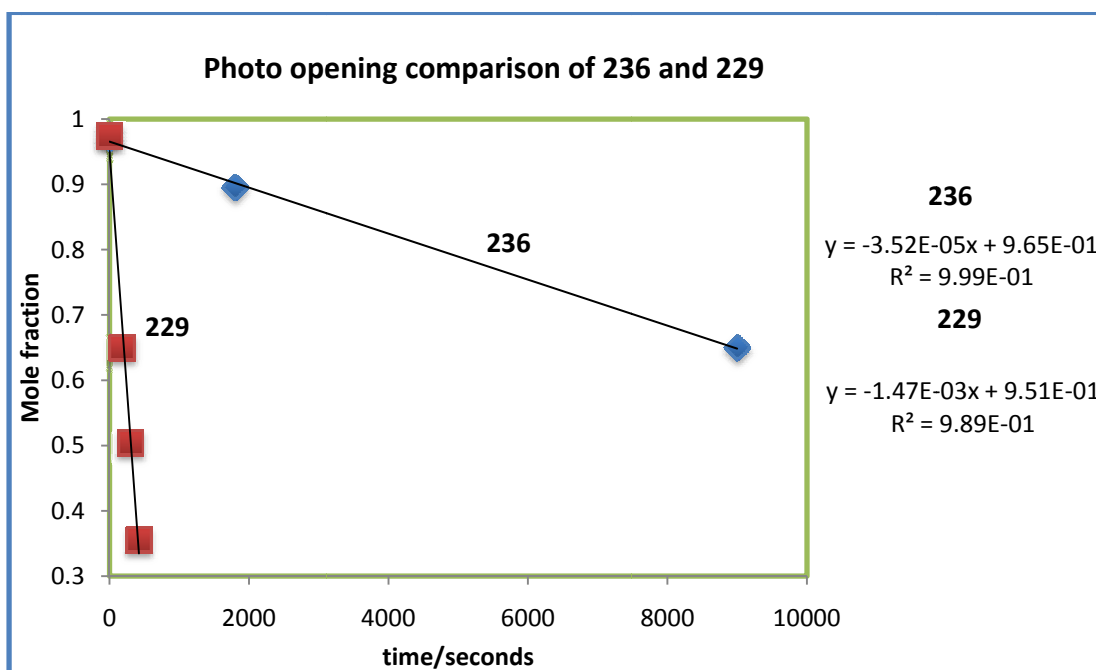
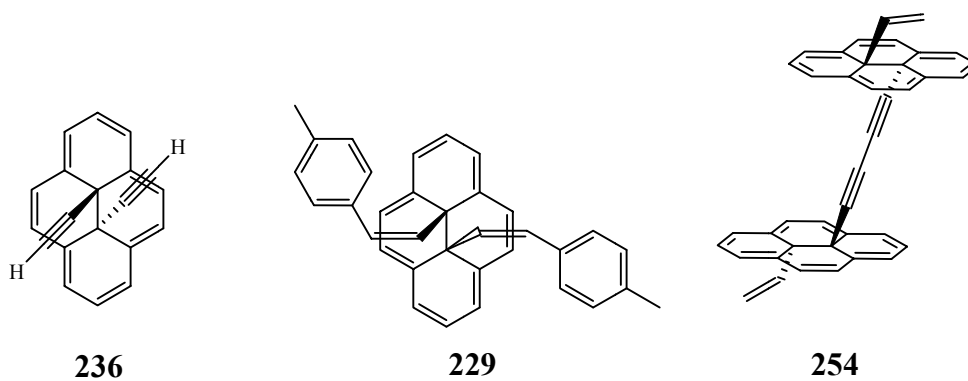




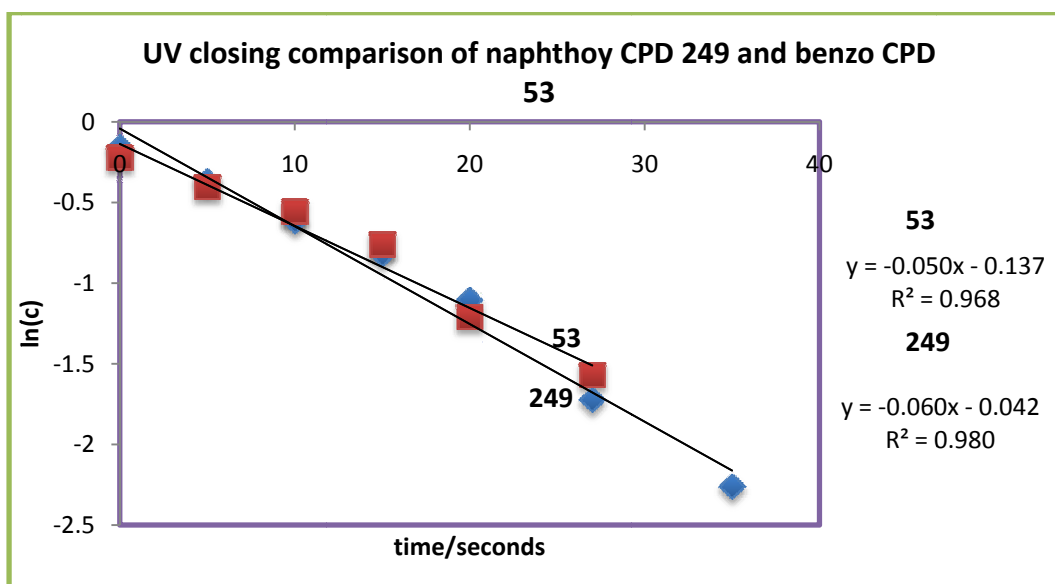
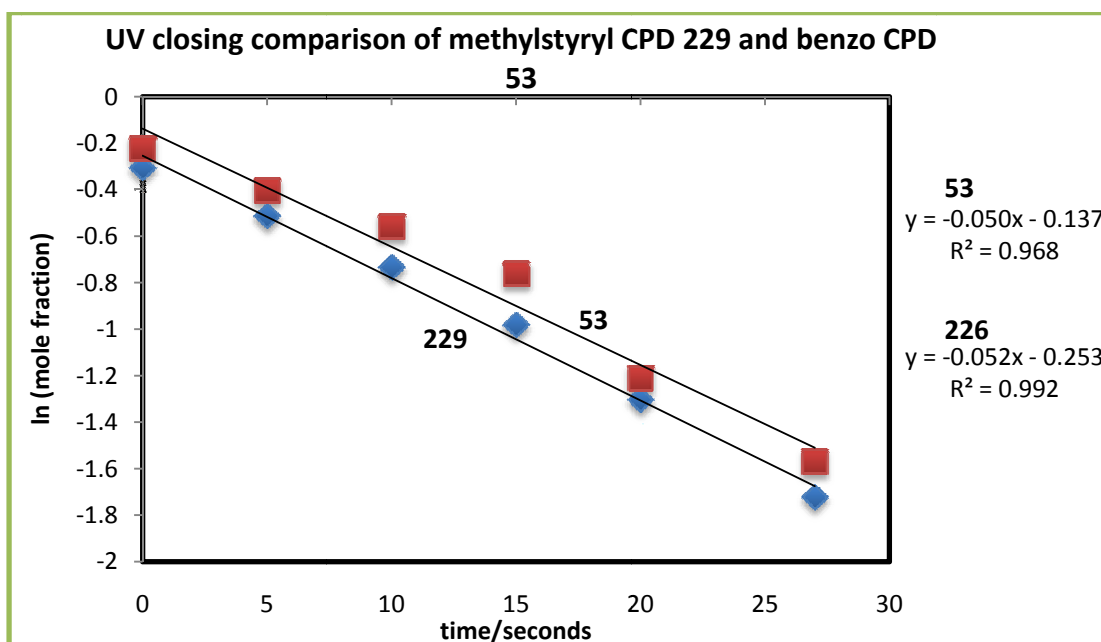
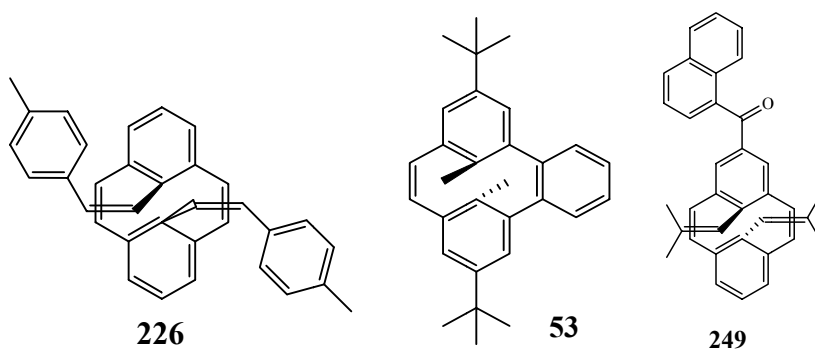


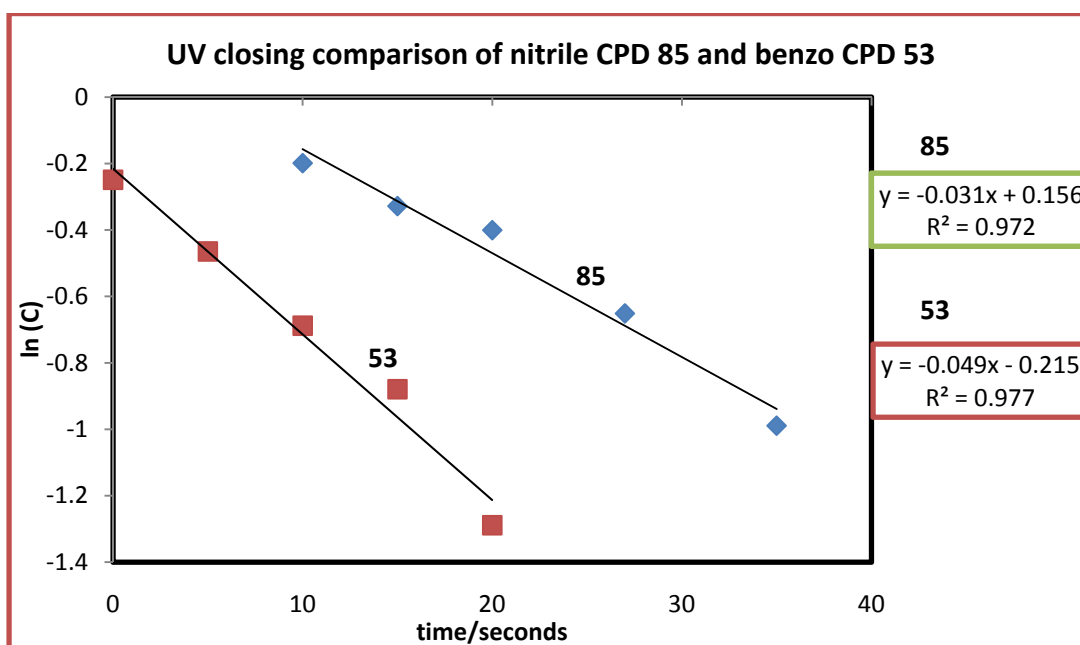
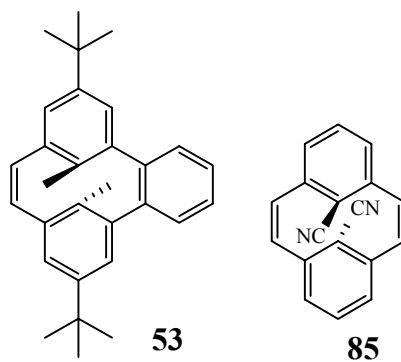




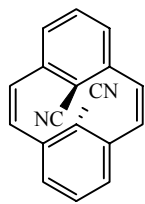


Appendix E: UV closing data for CPDs 53, 85, 226 and 249

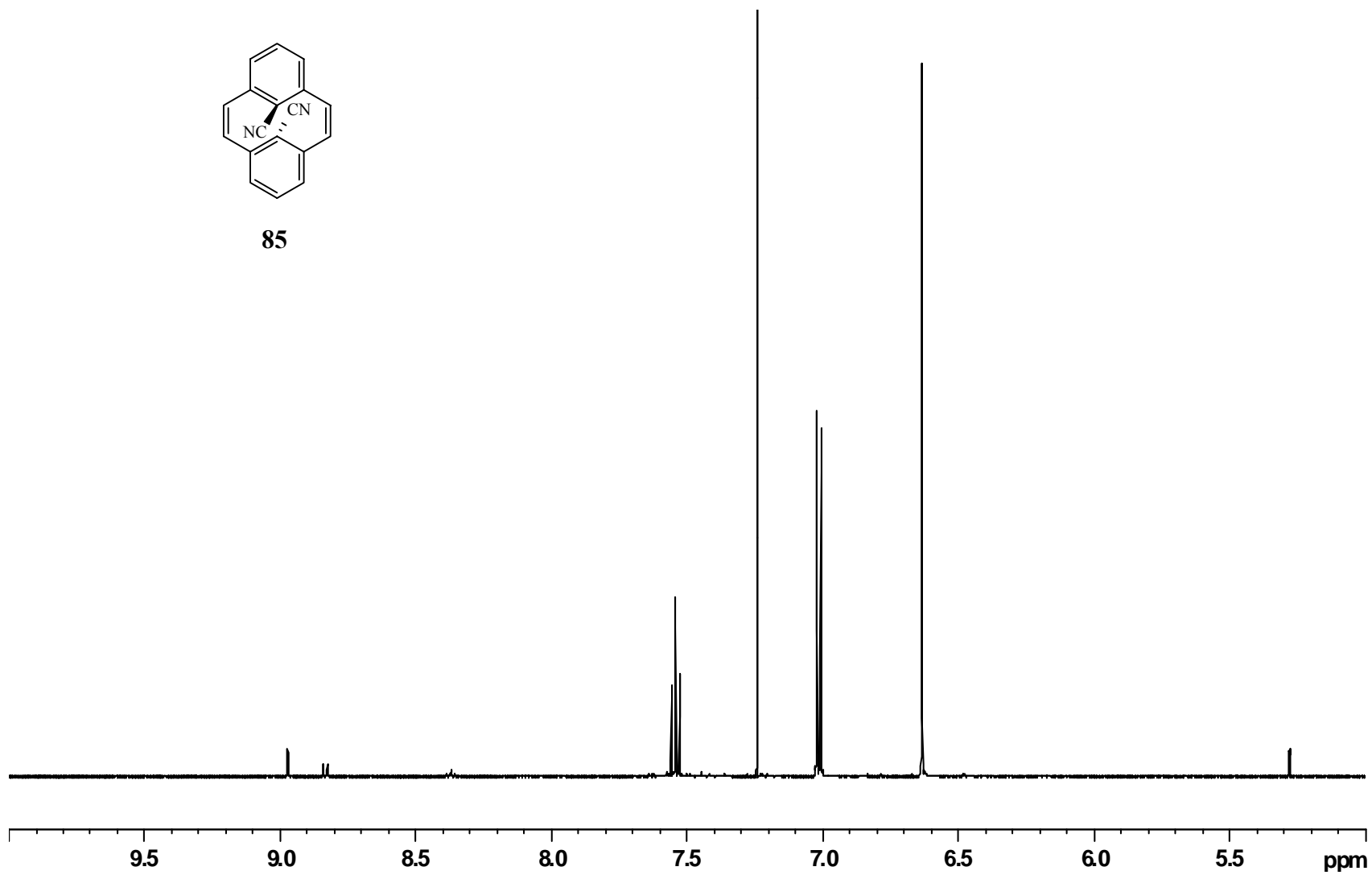


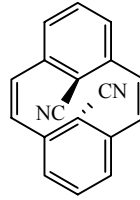


Appendix F: NMR spectra

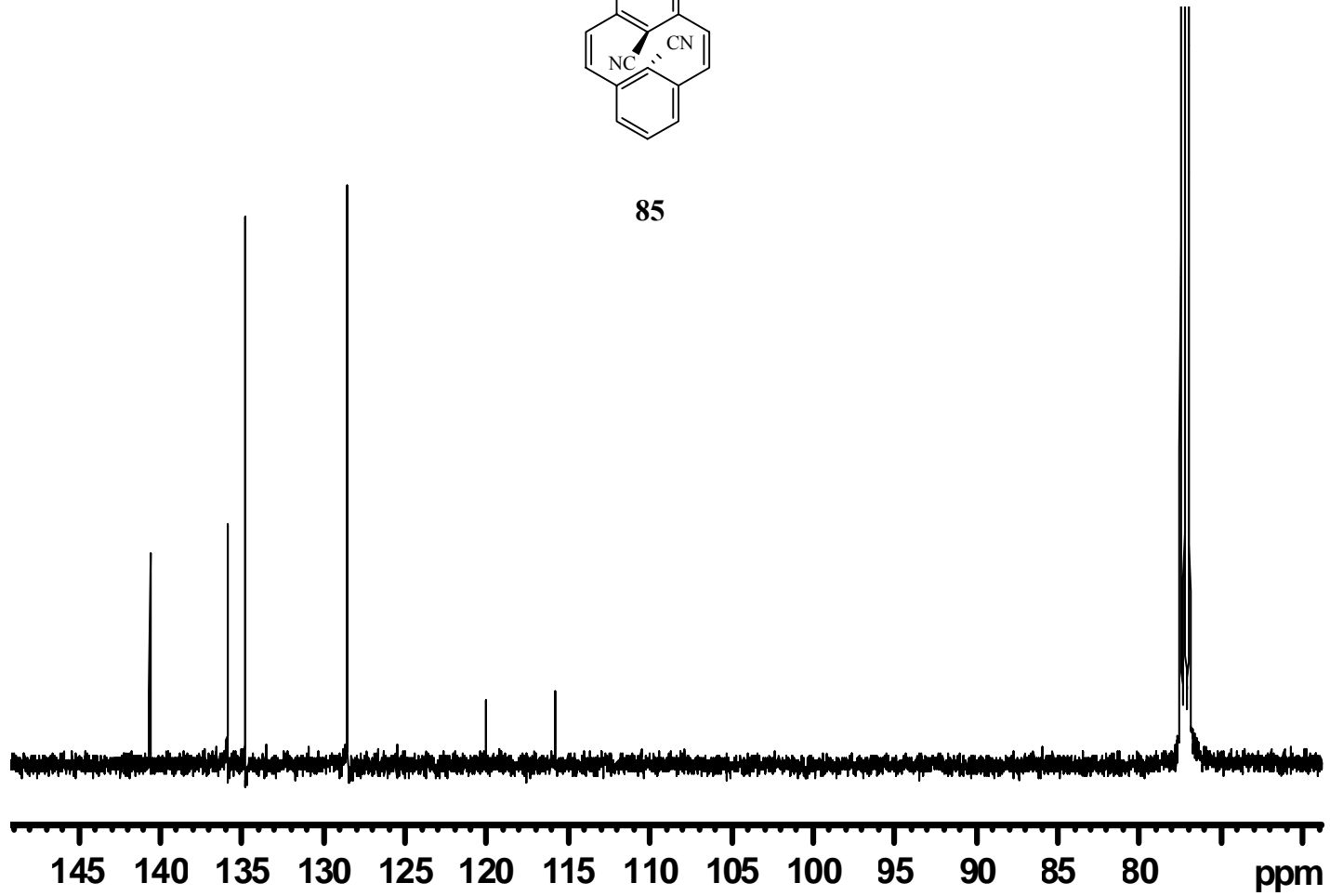


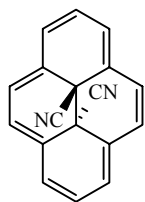
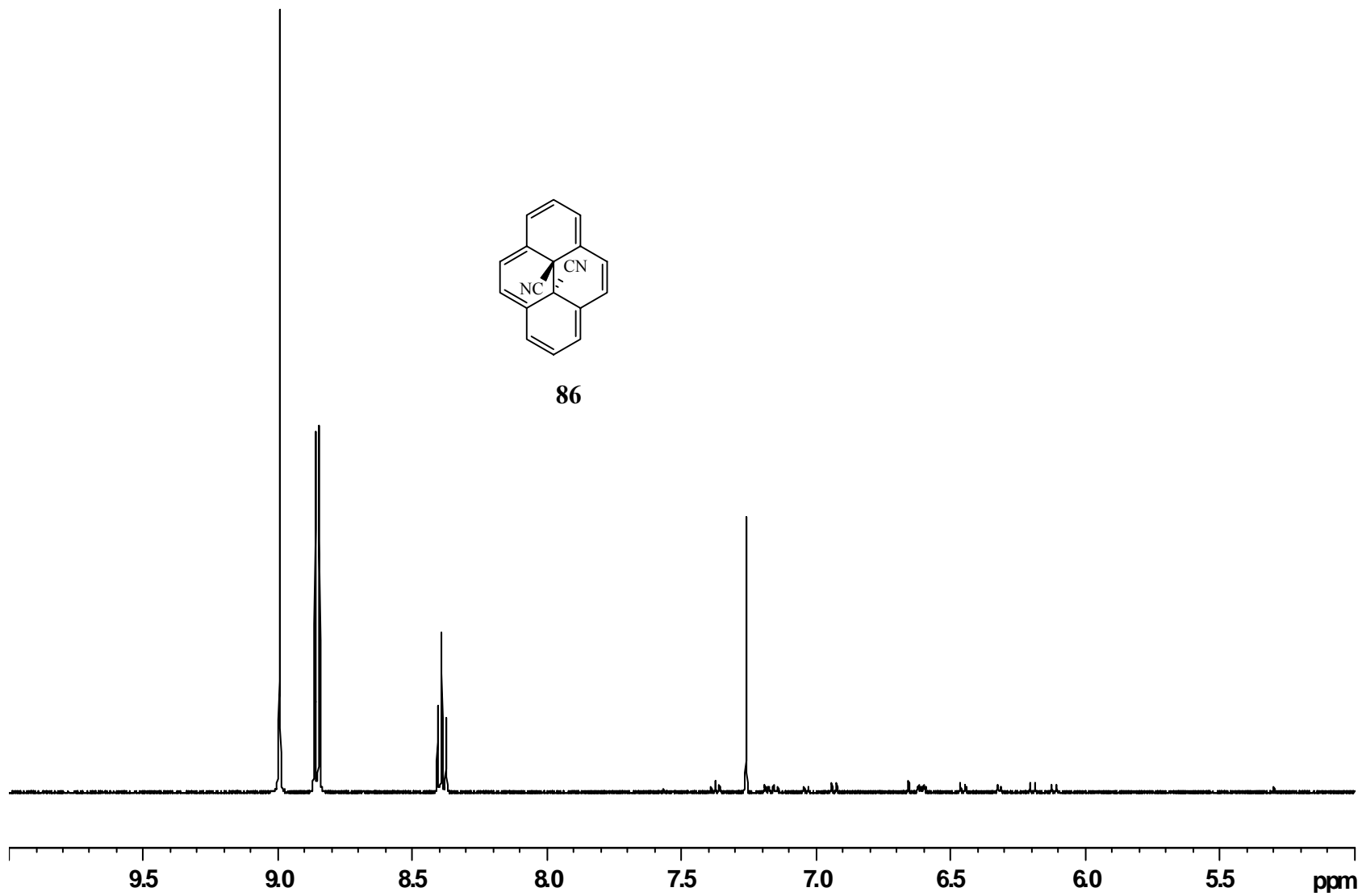
85

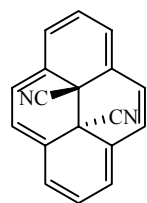




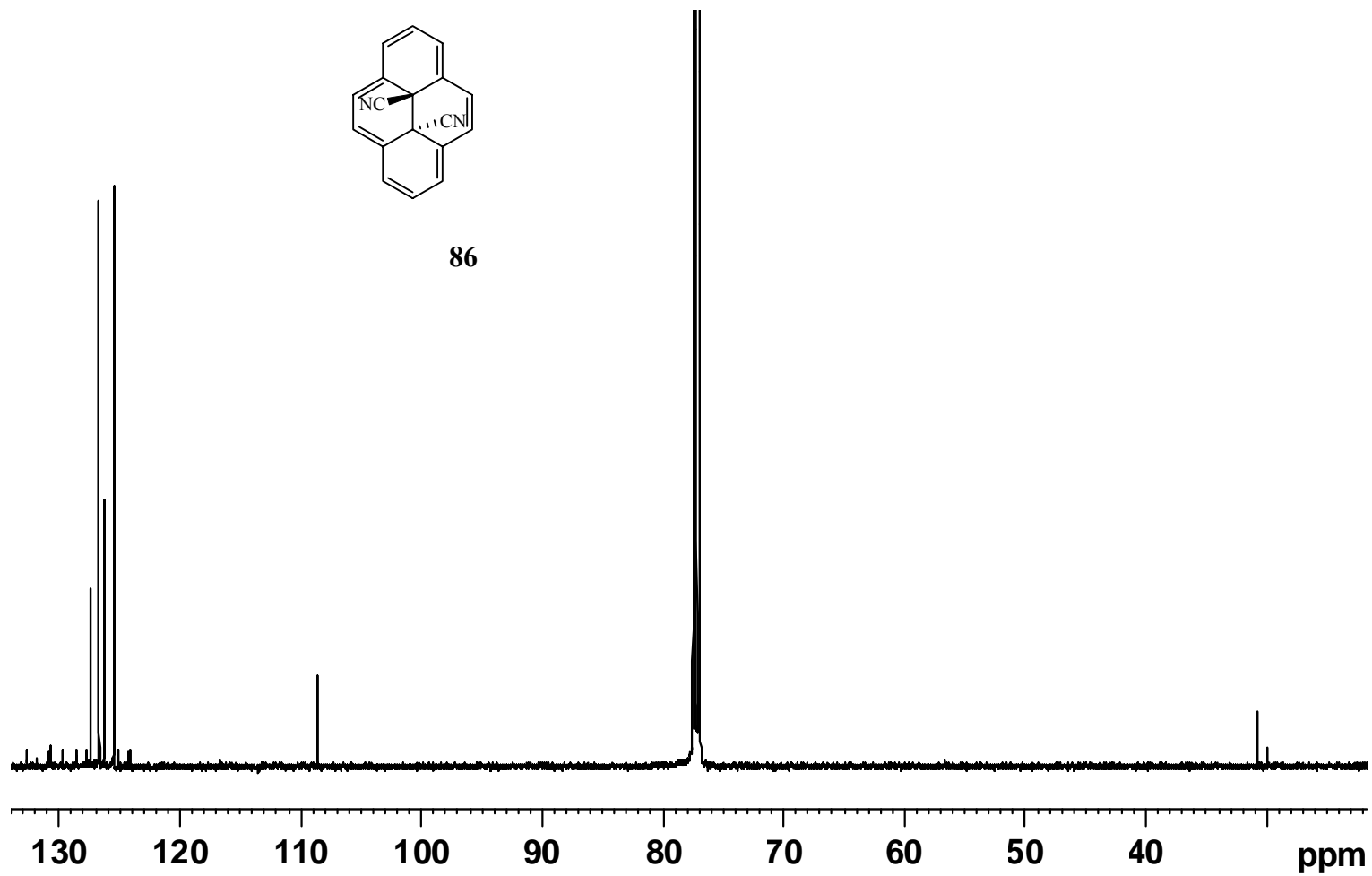
85

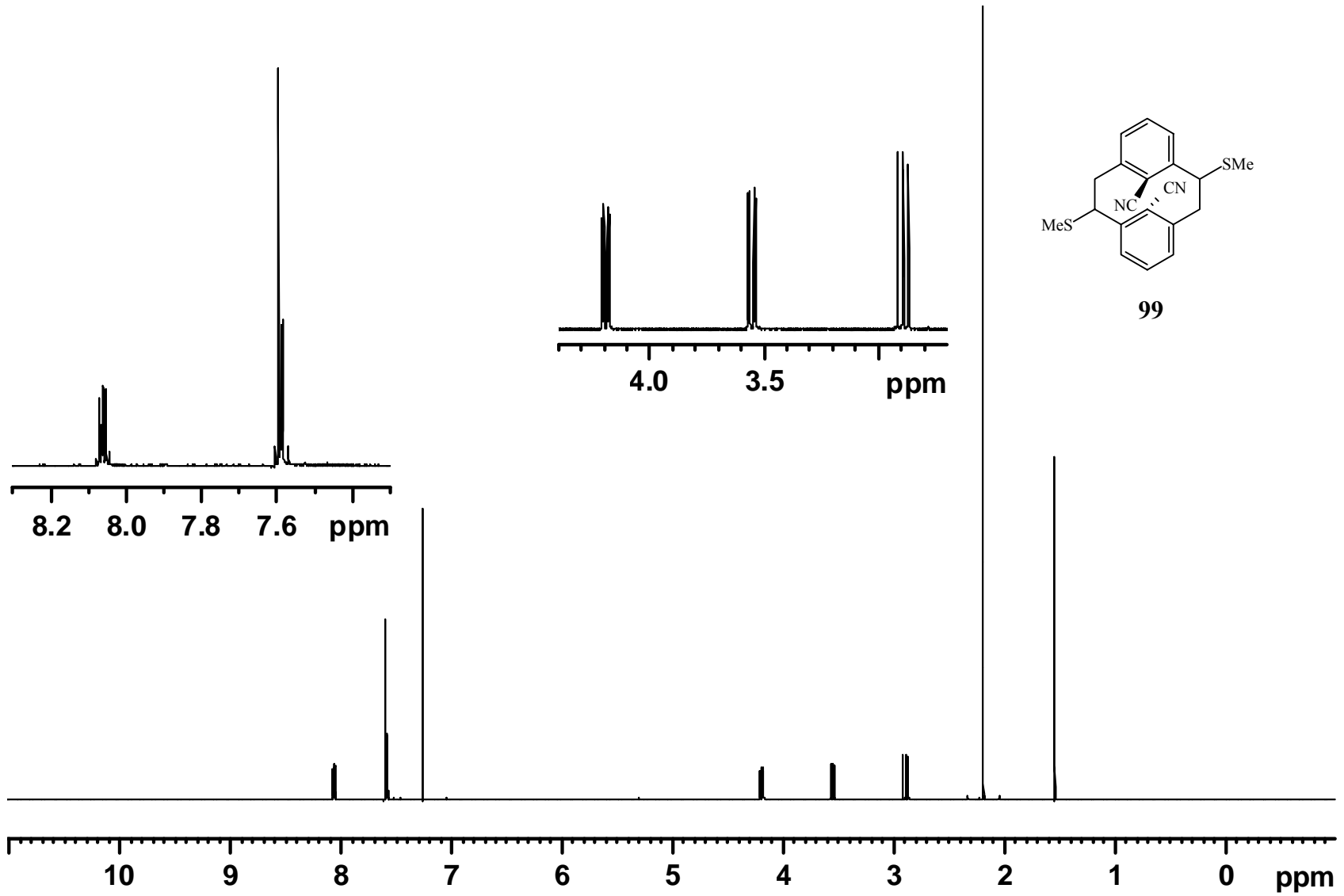


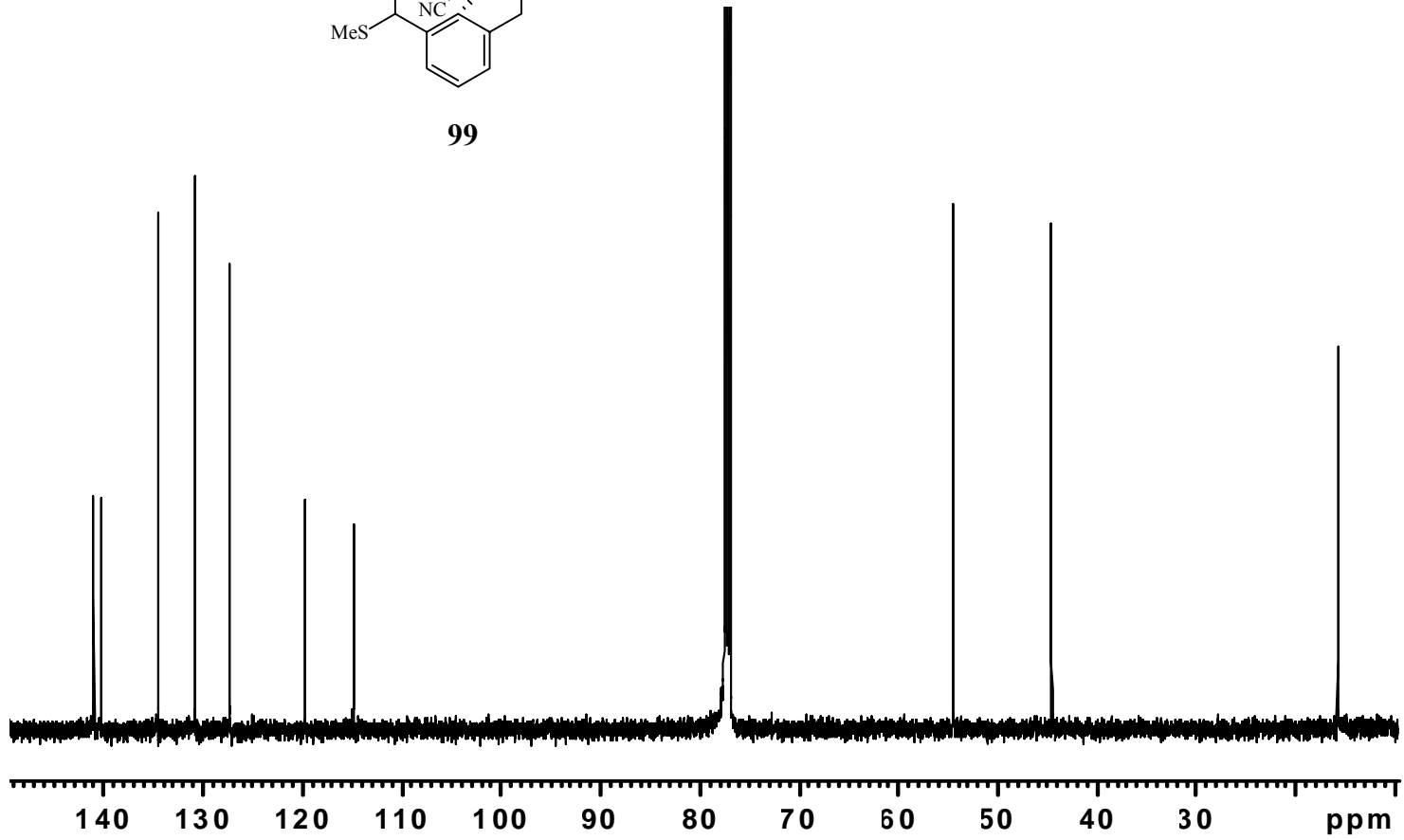
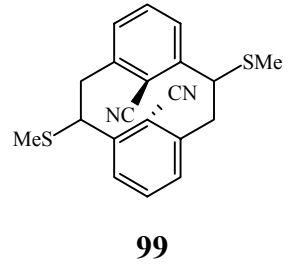
**86**

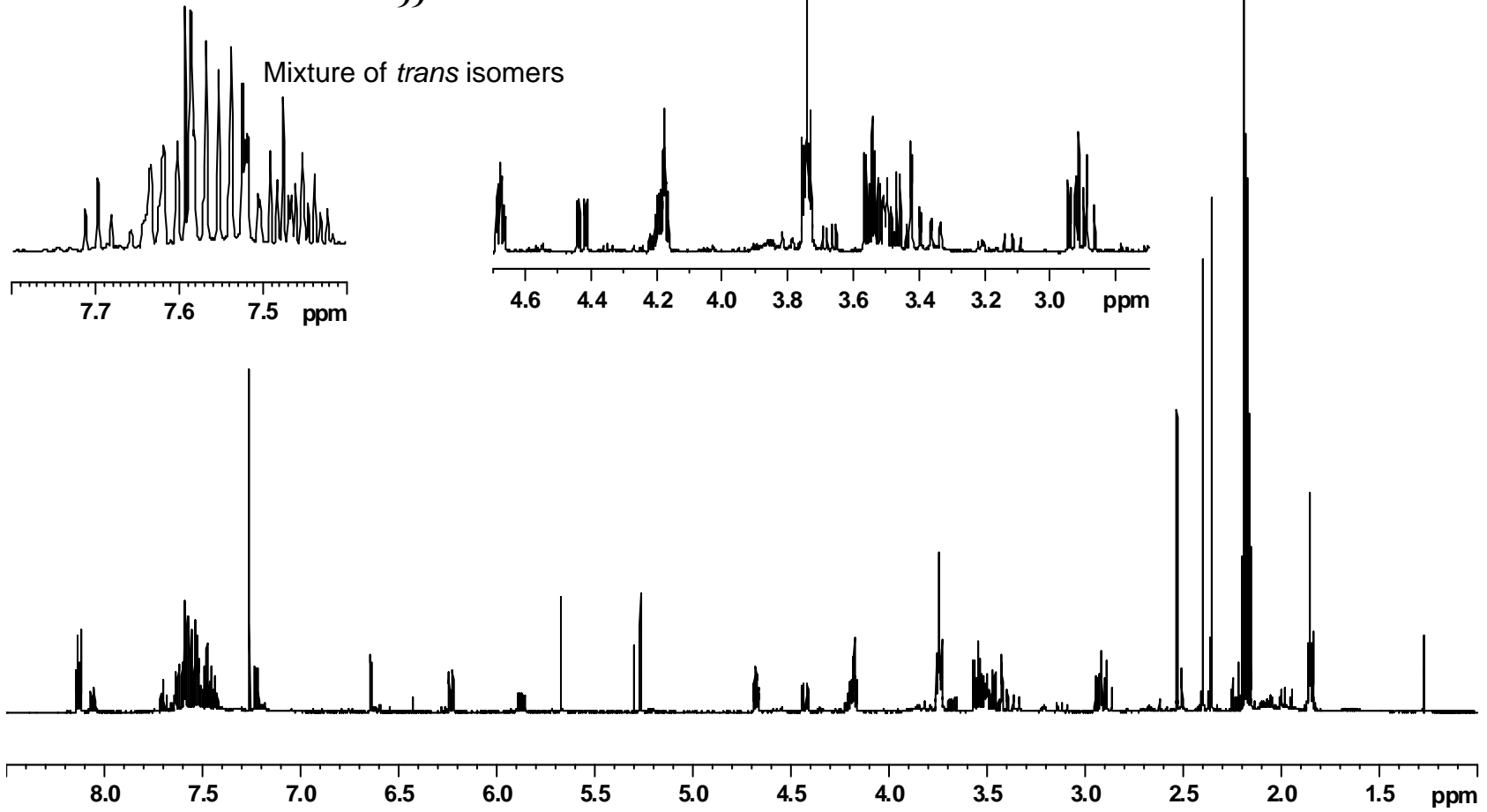
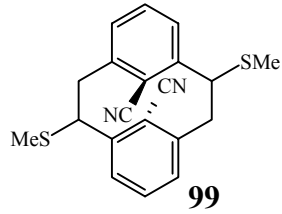


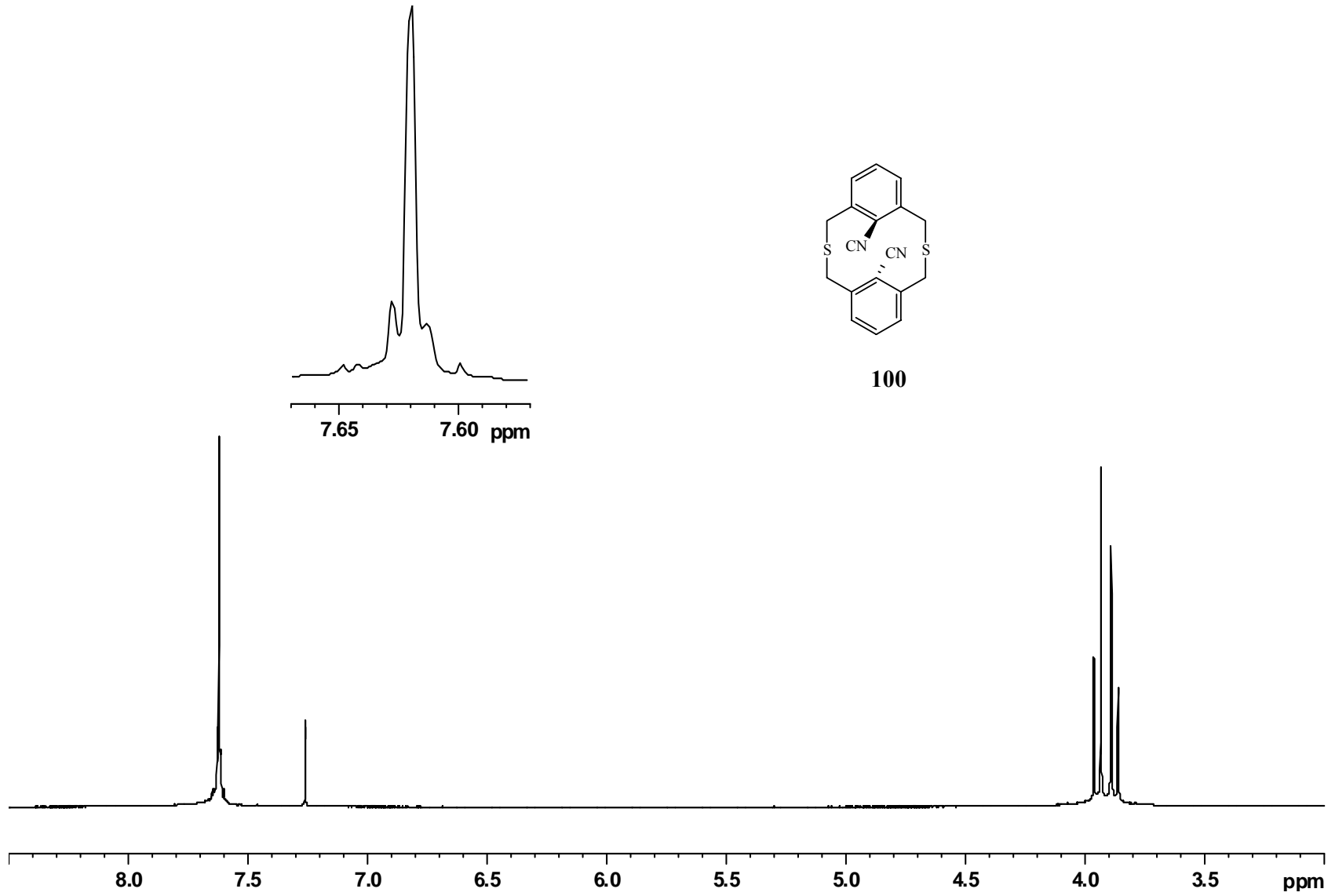
86

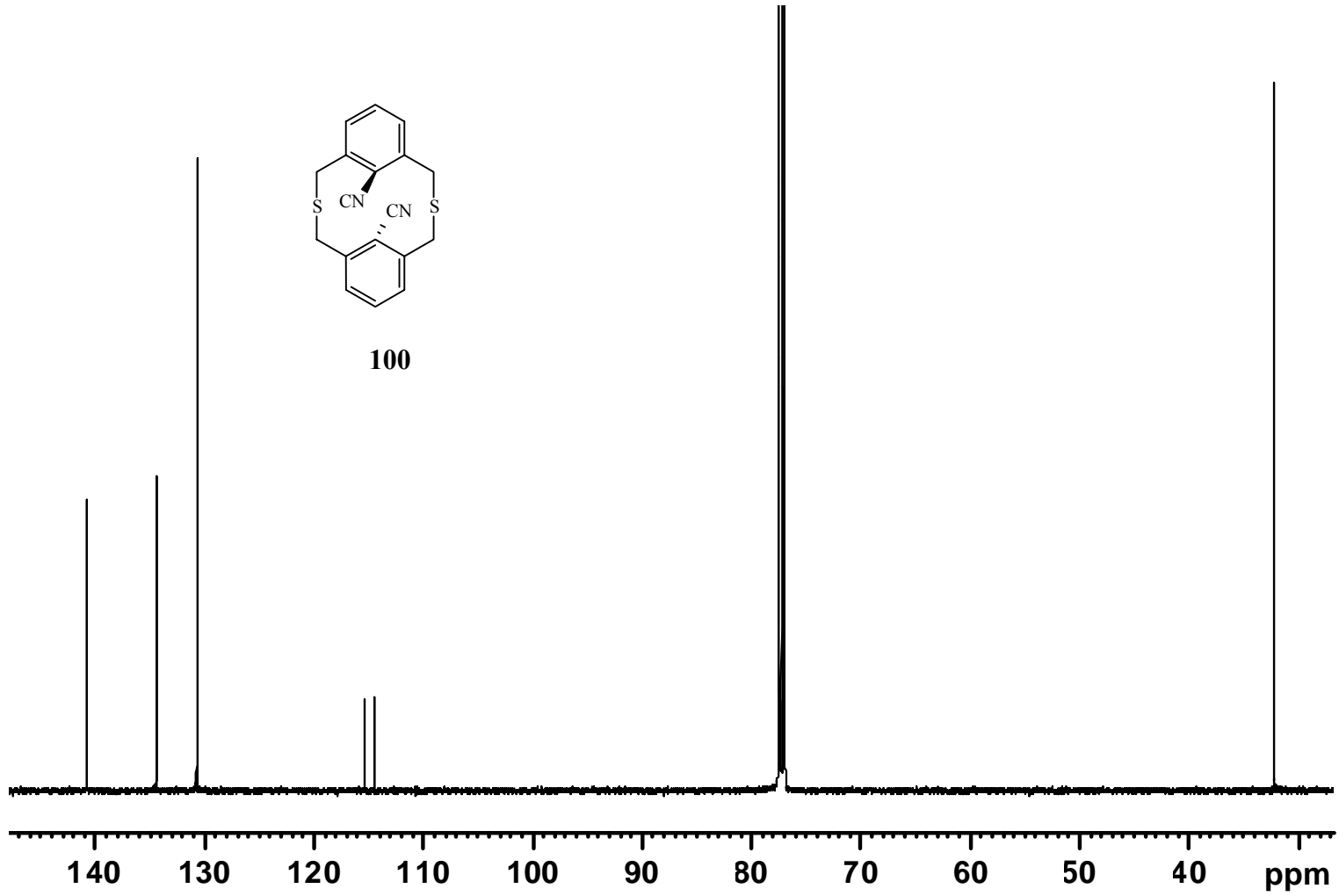


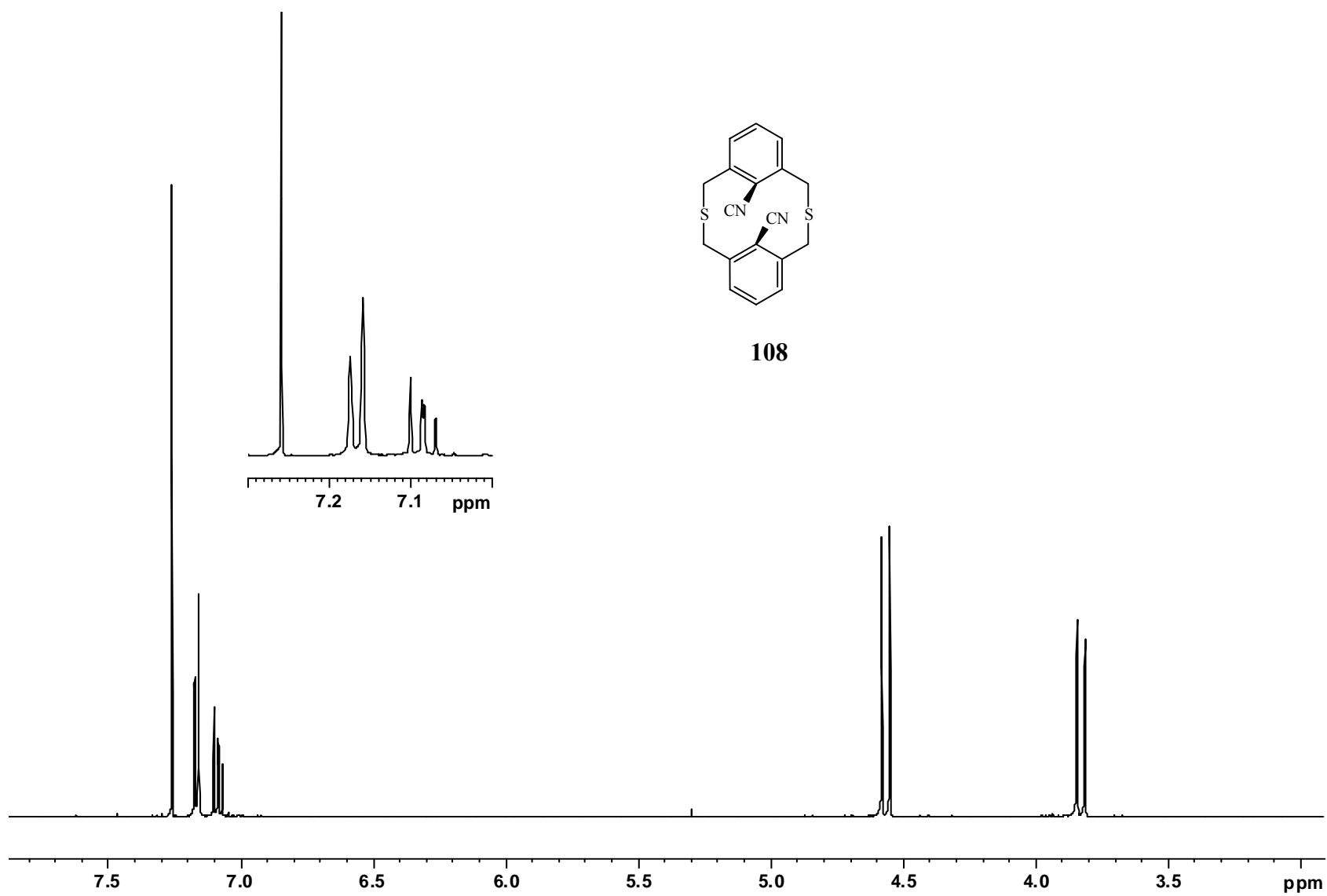


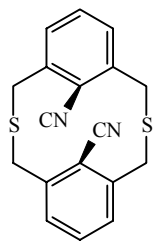
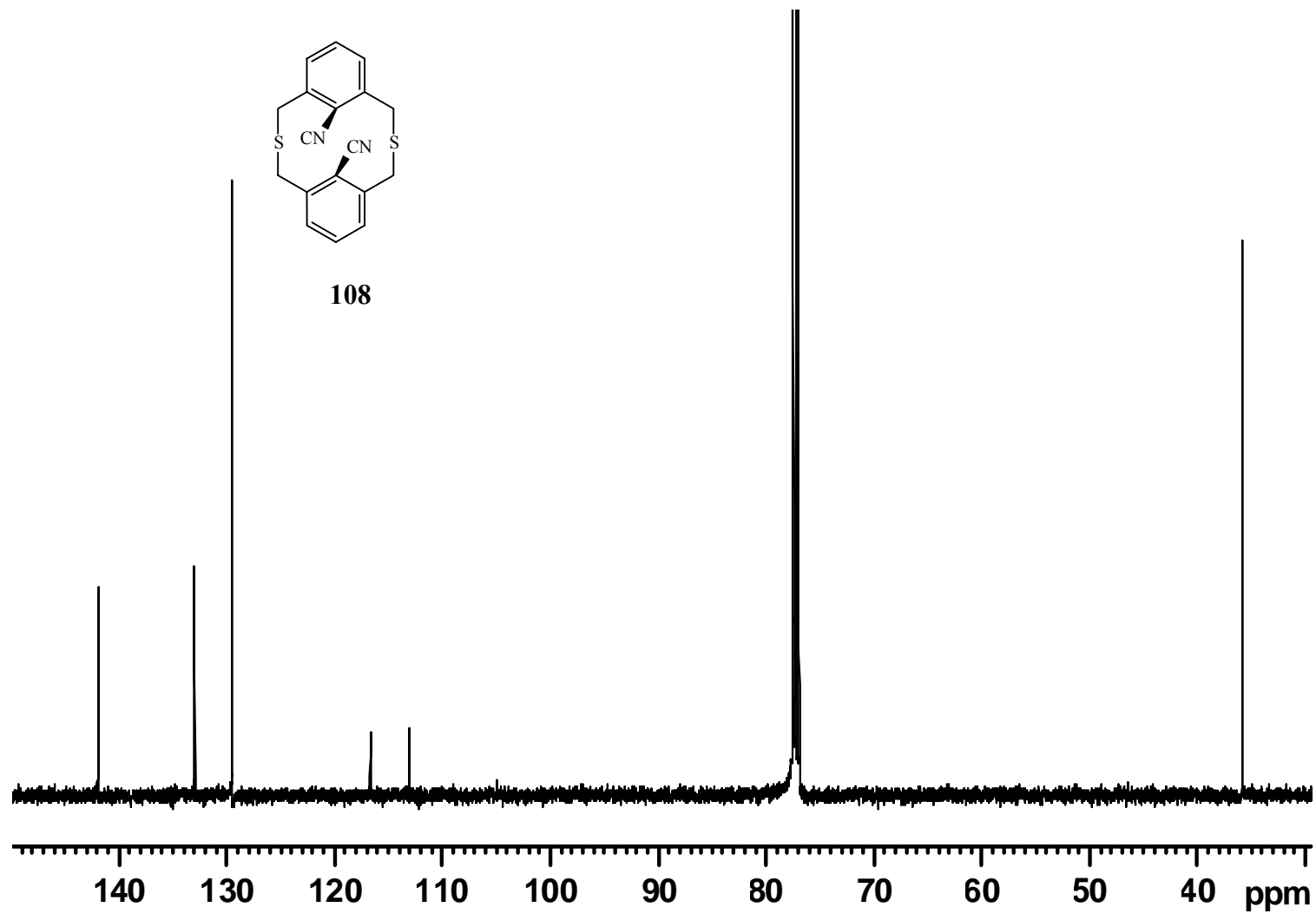


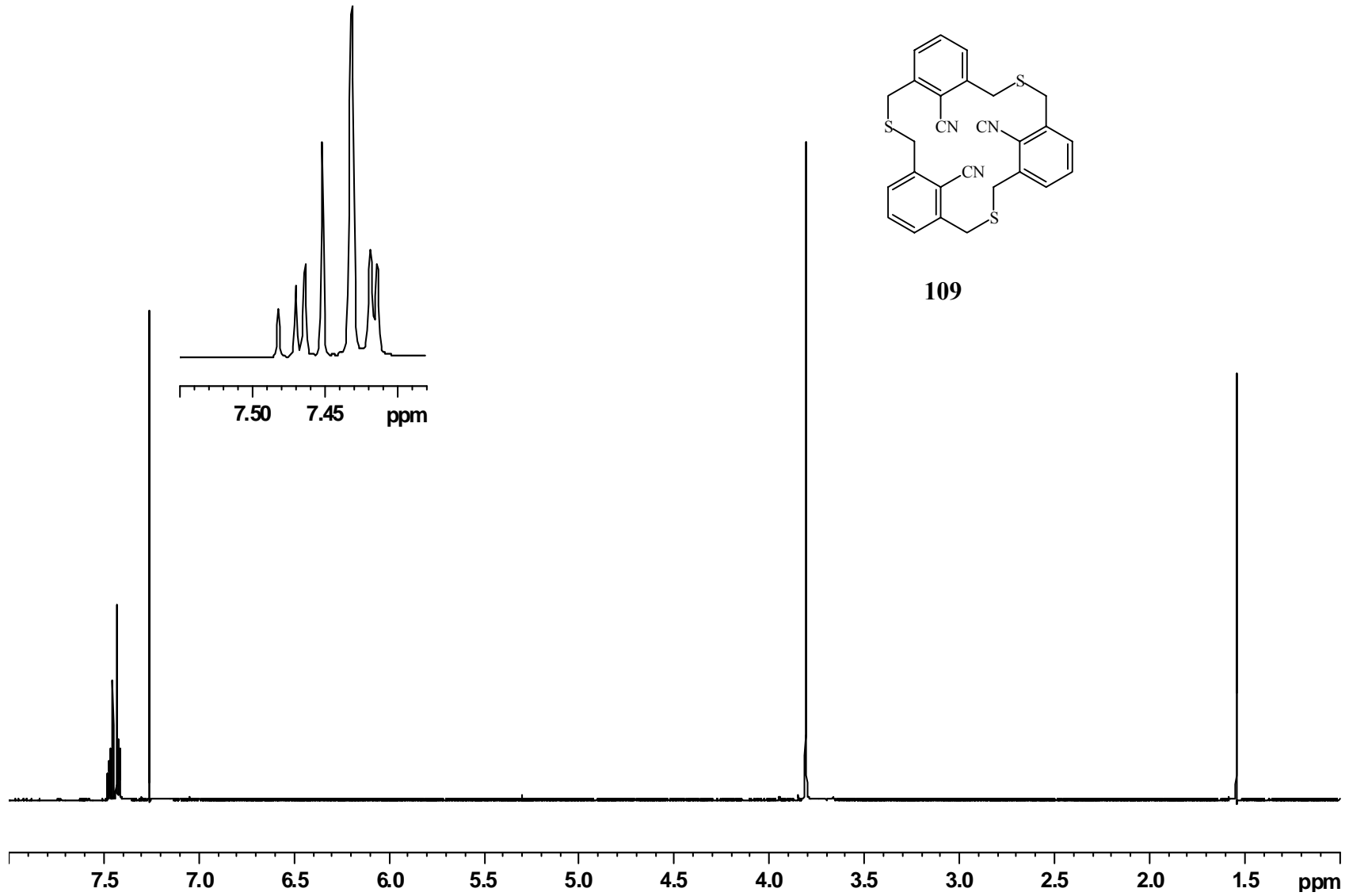


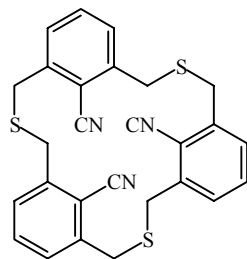
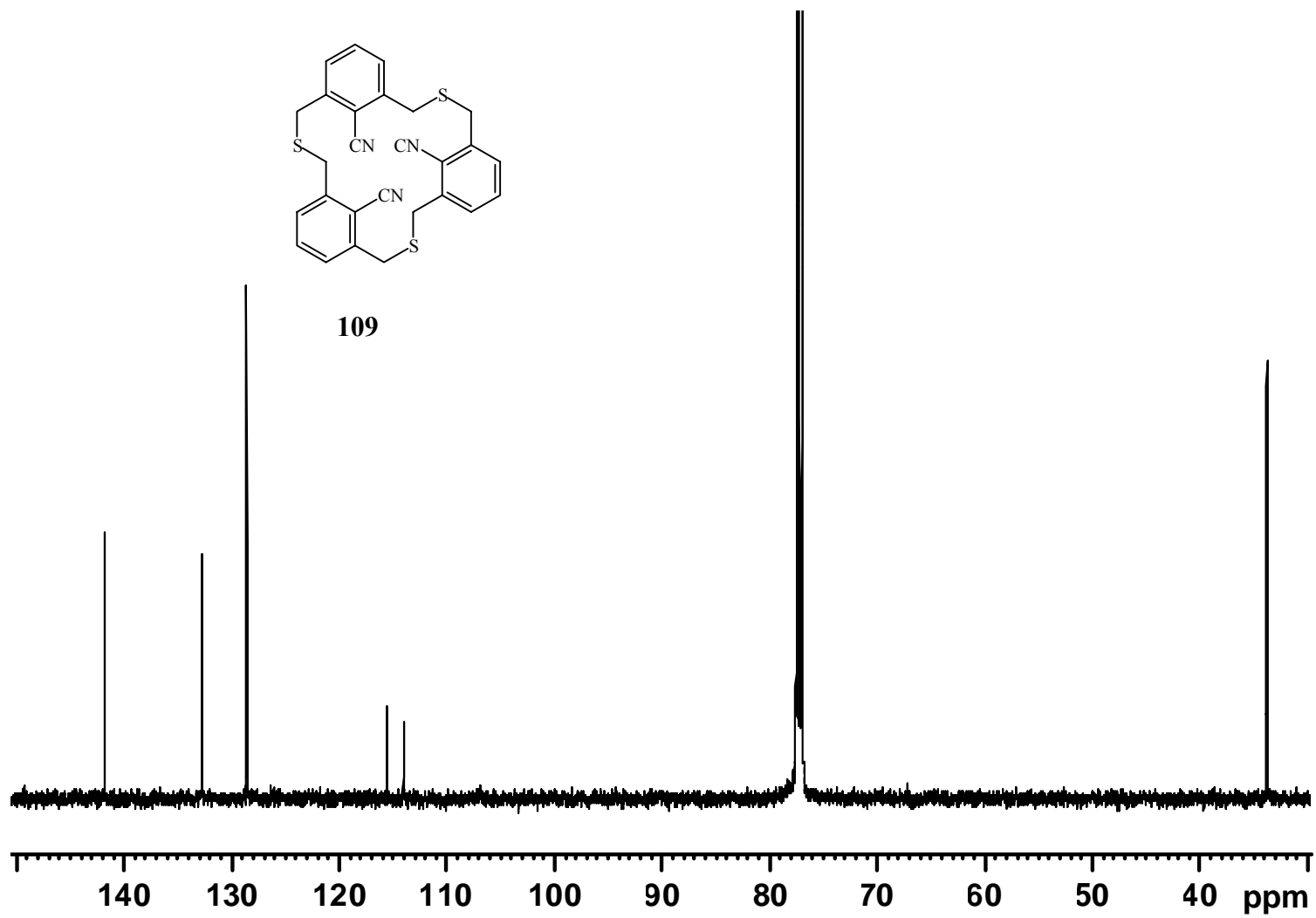


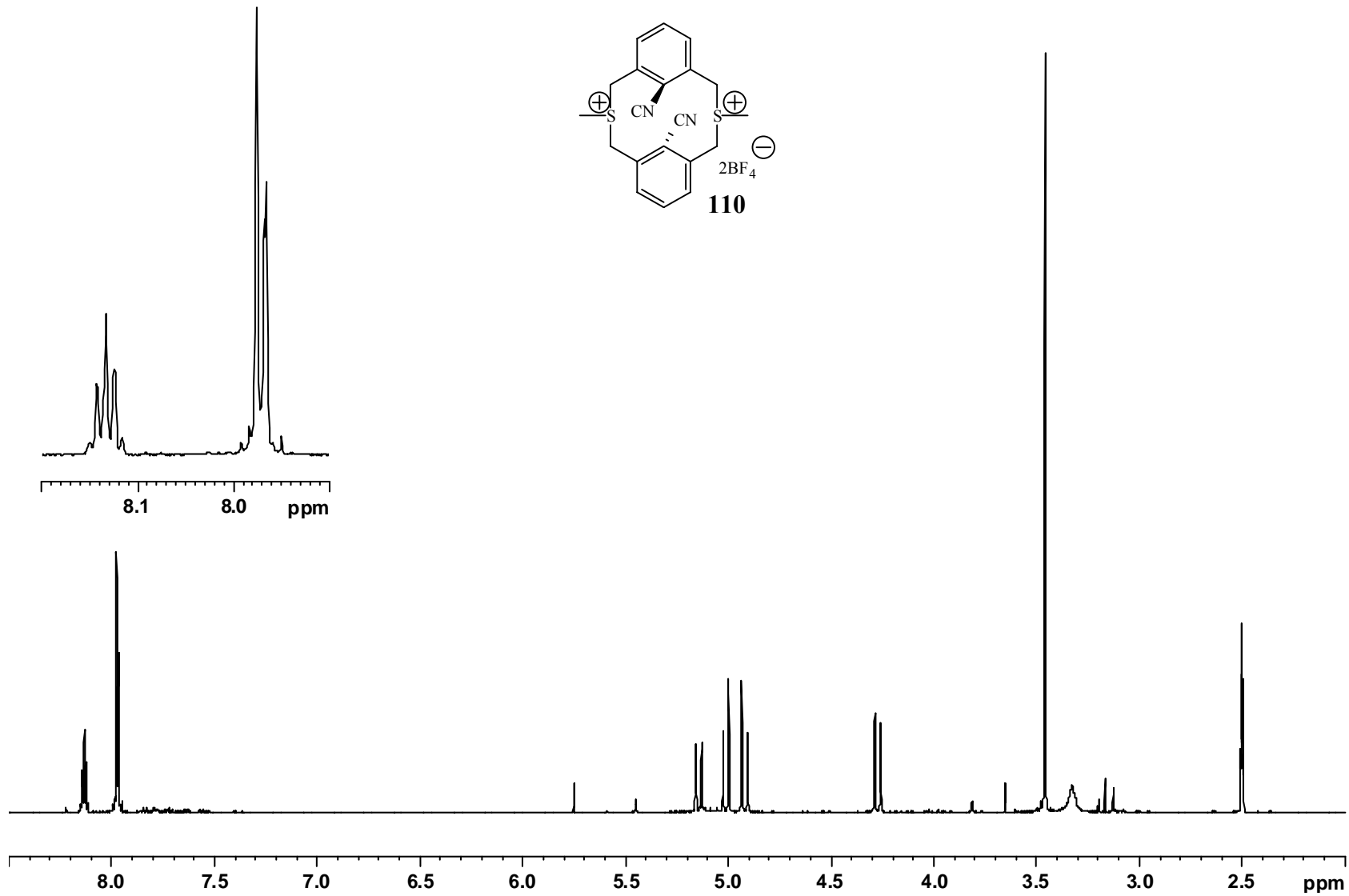


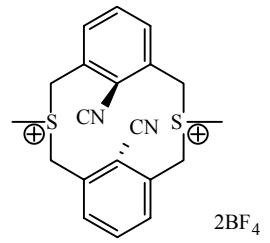
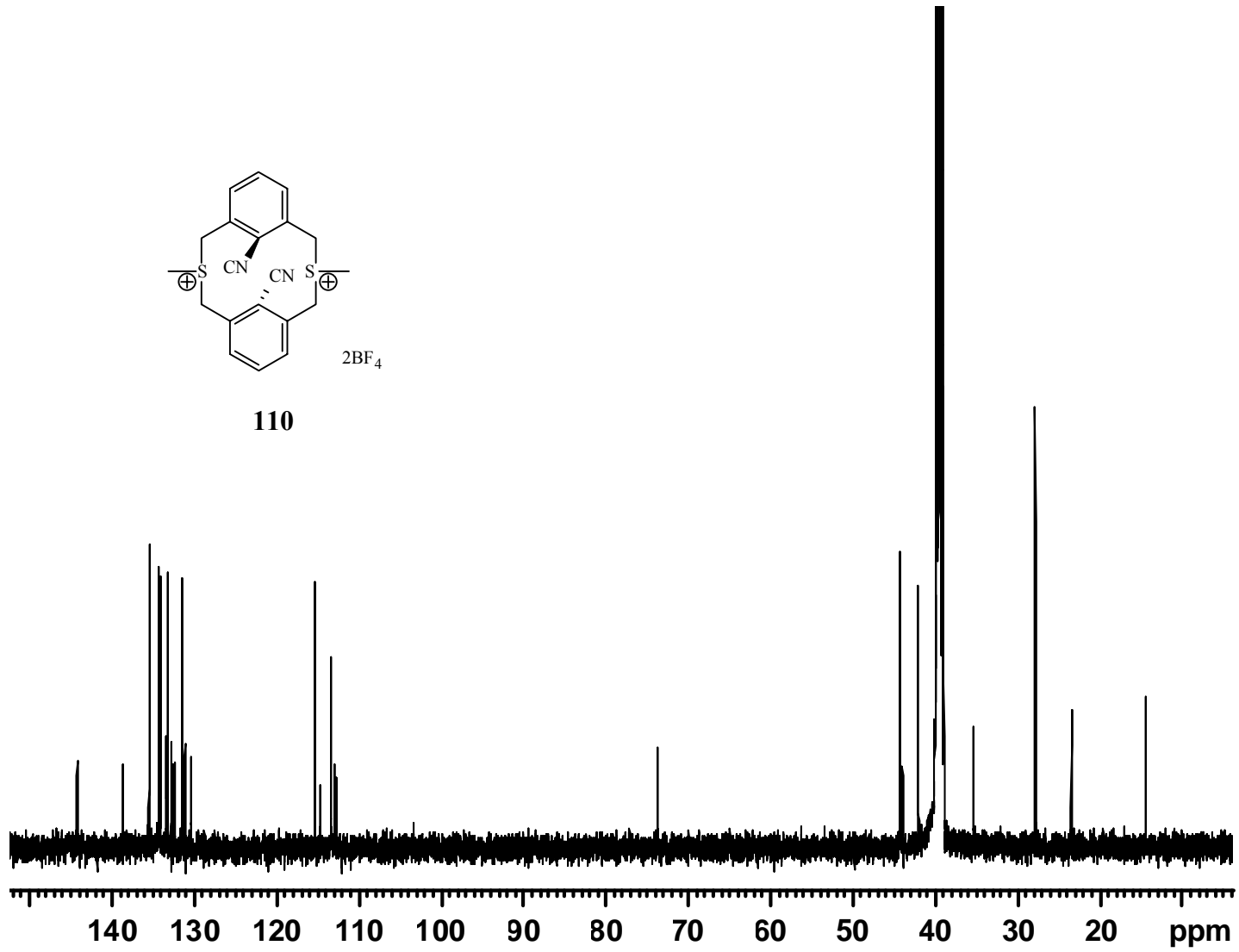


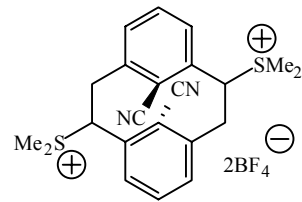
**108**



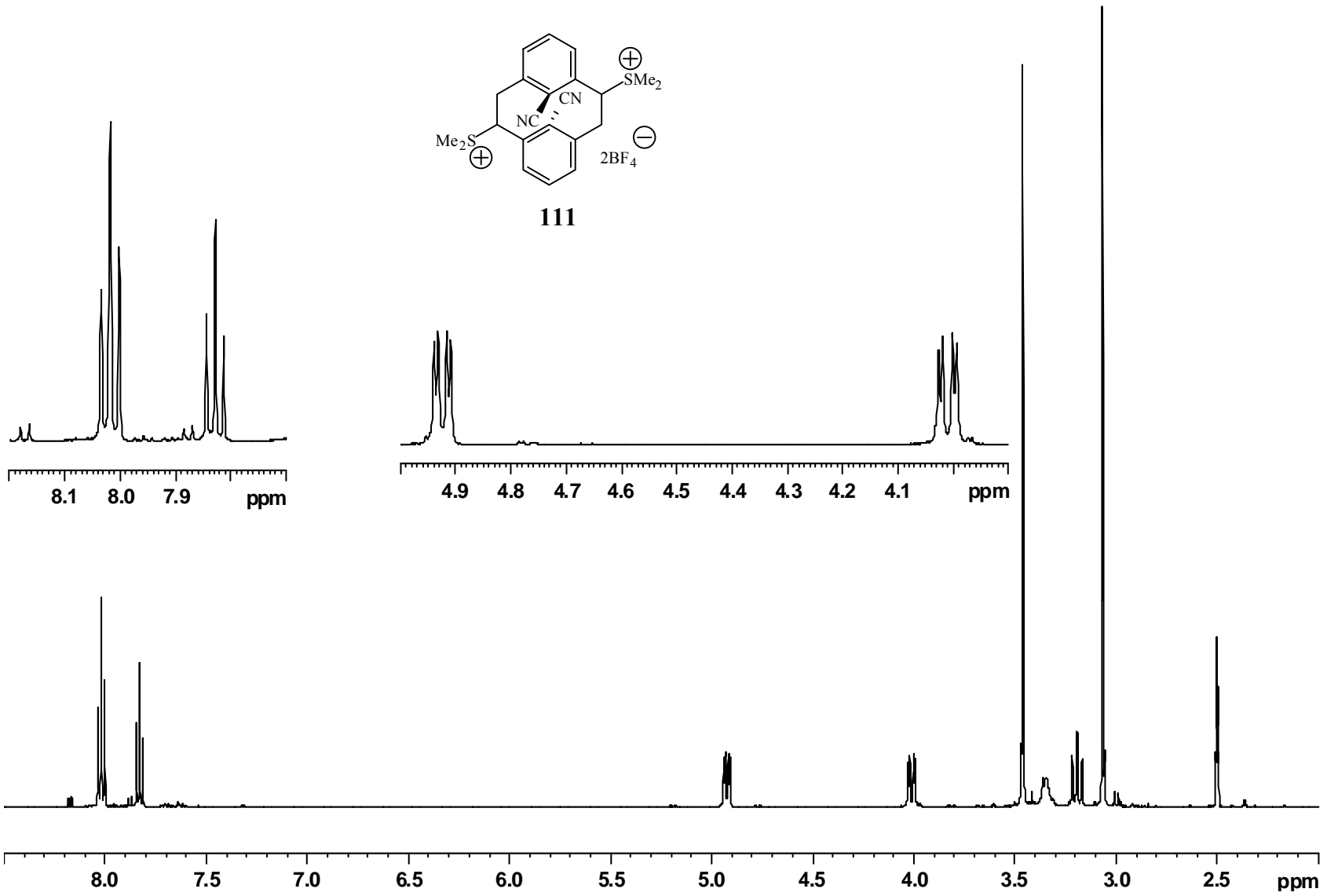
**109**

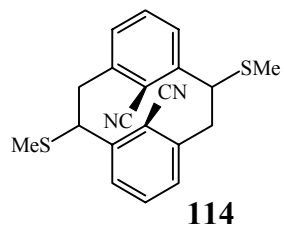


**110**

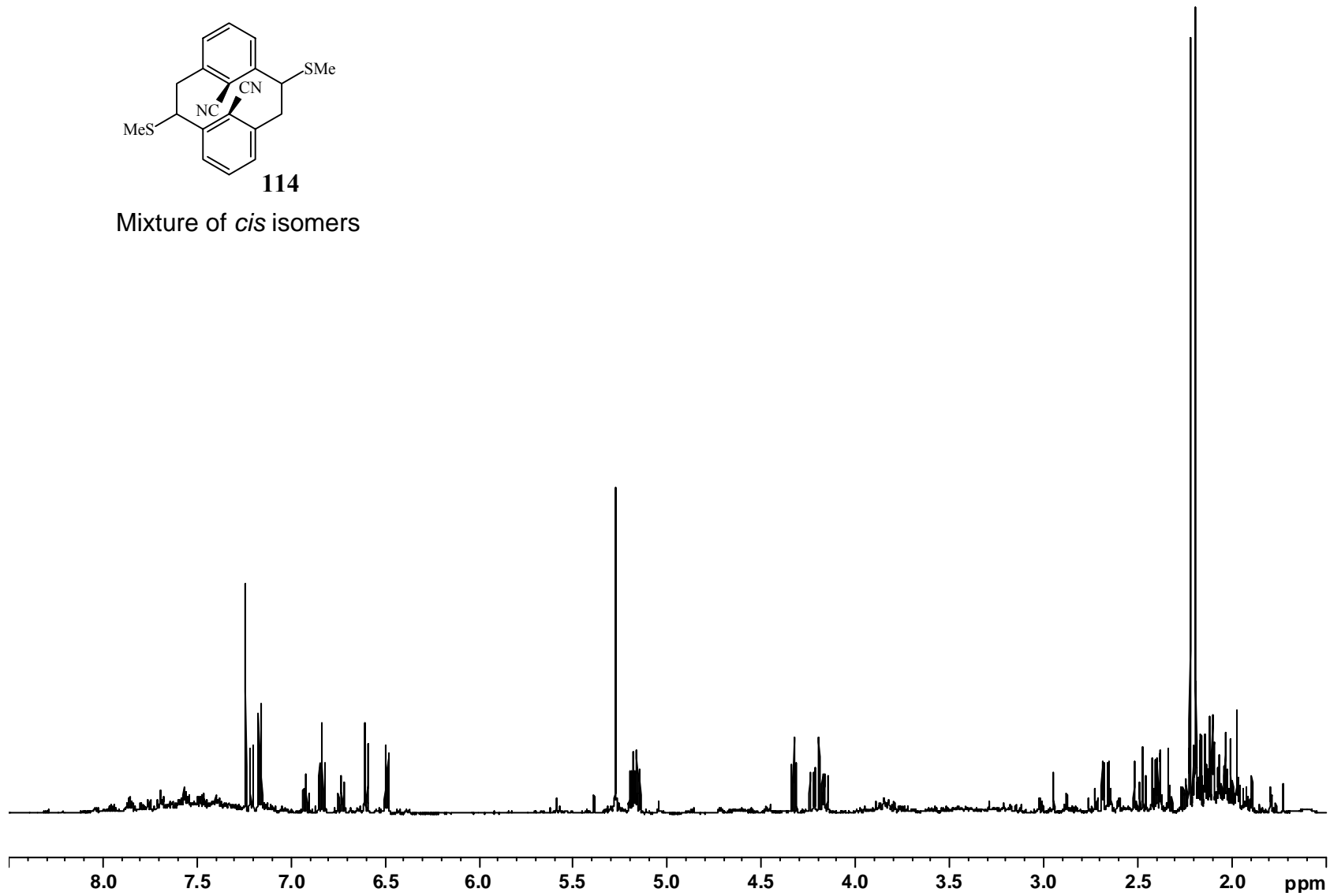


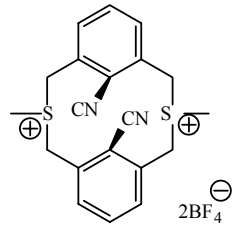
111



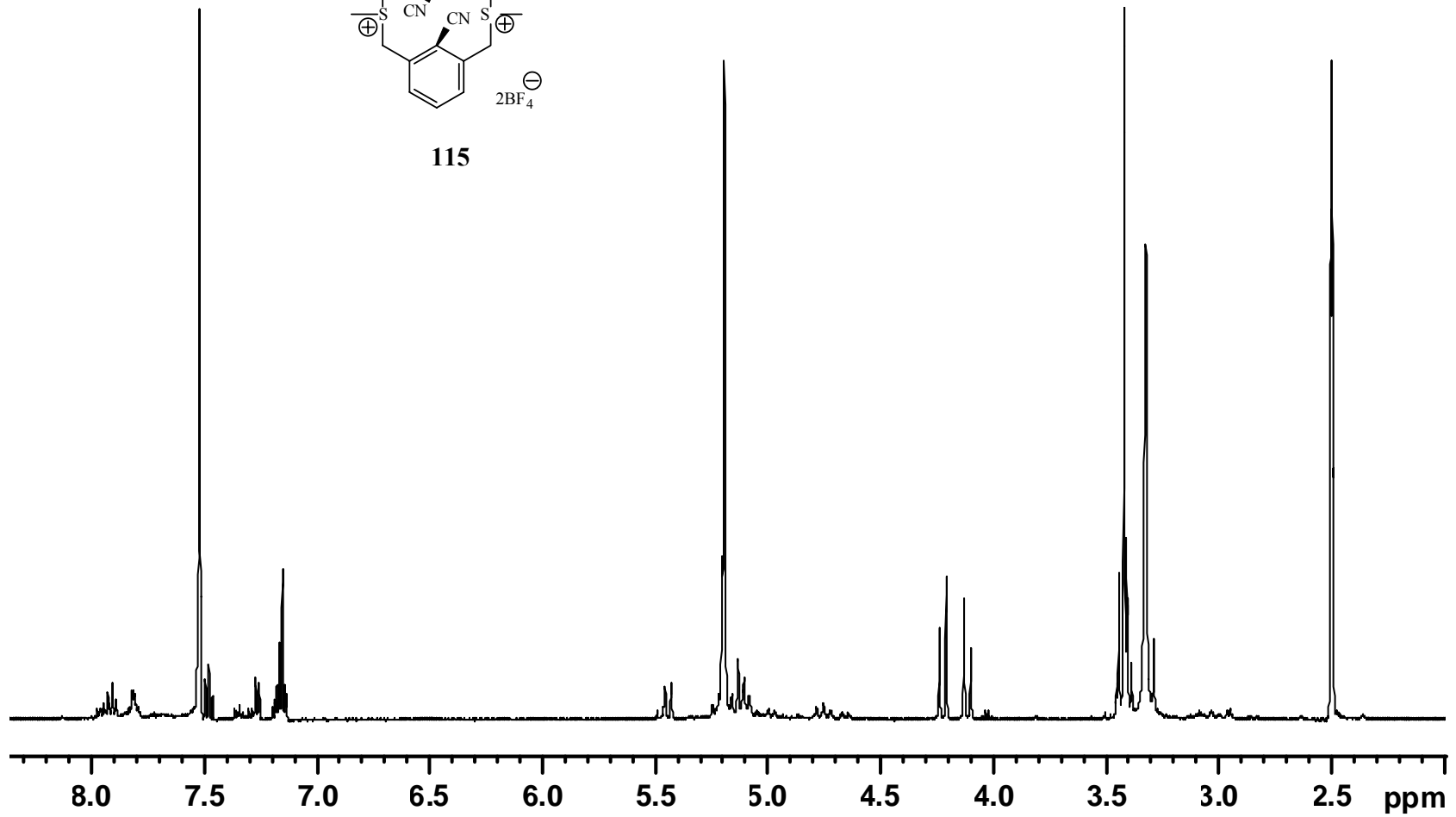


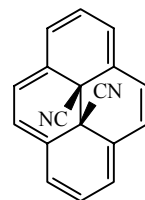
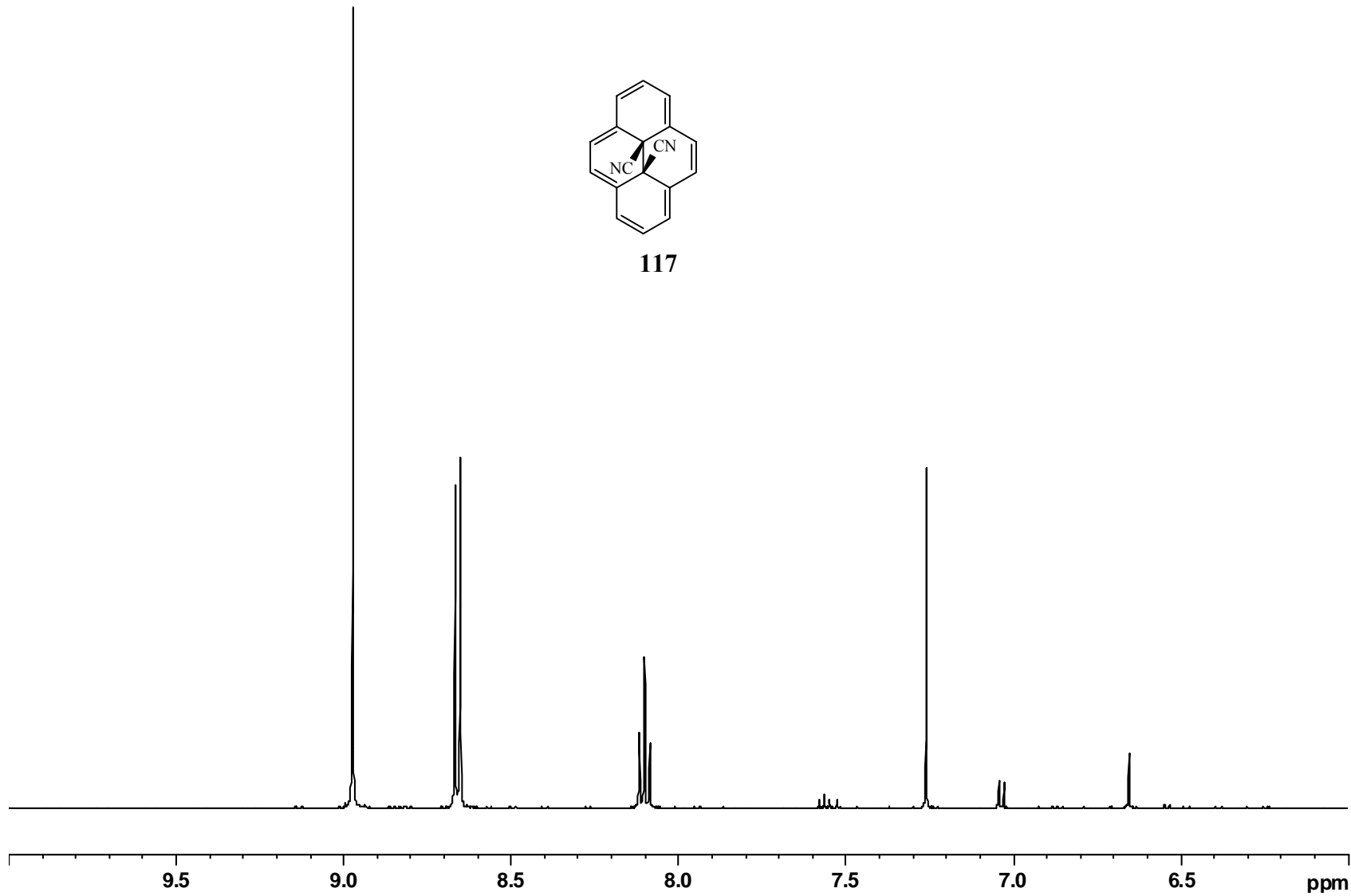
Mixture of *cis* isomers

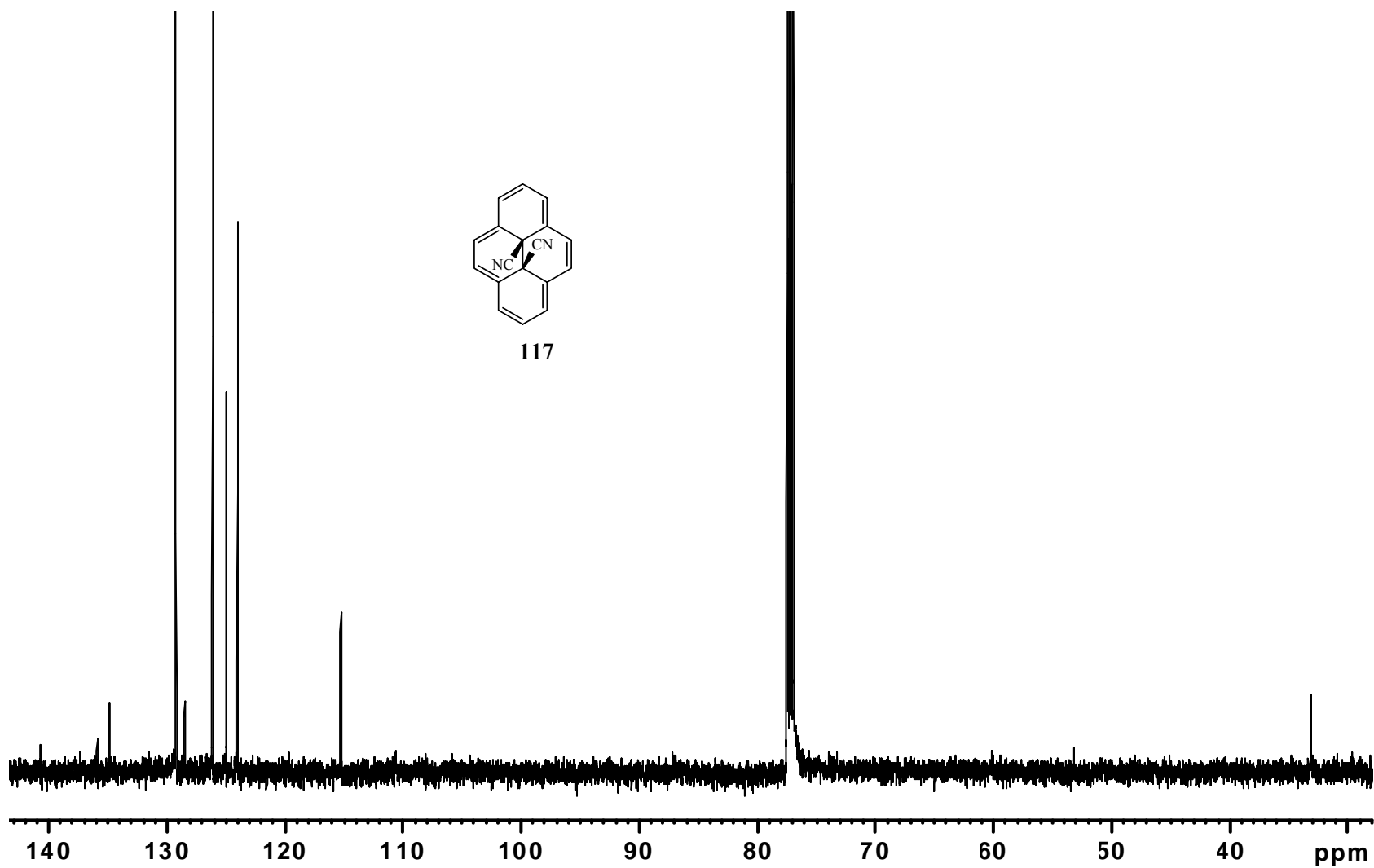


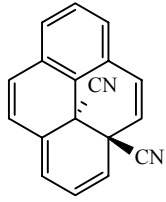


115

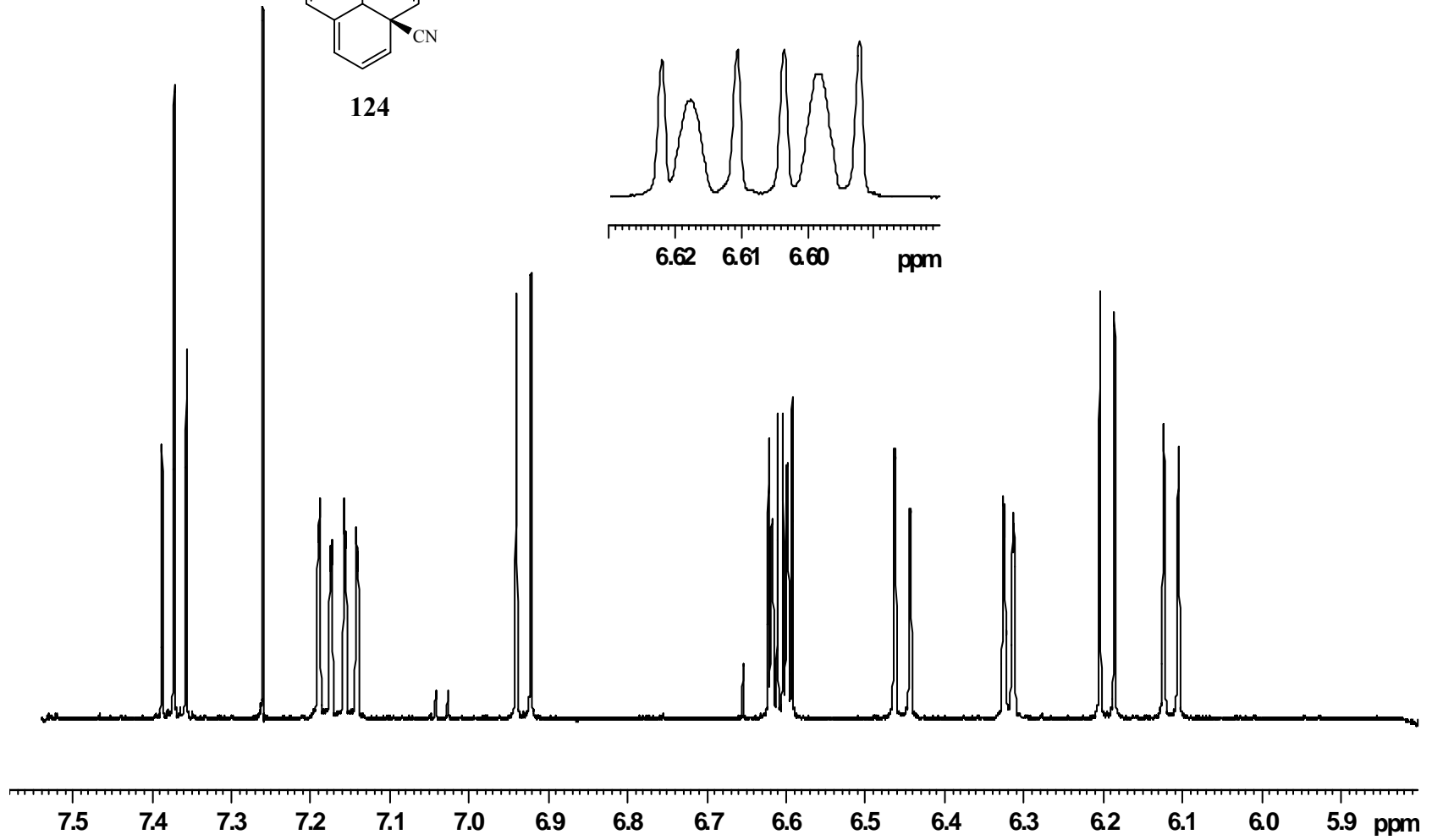


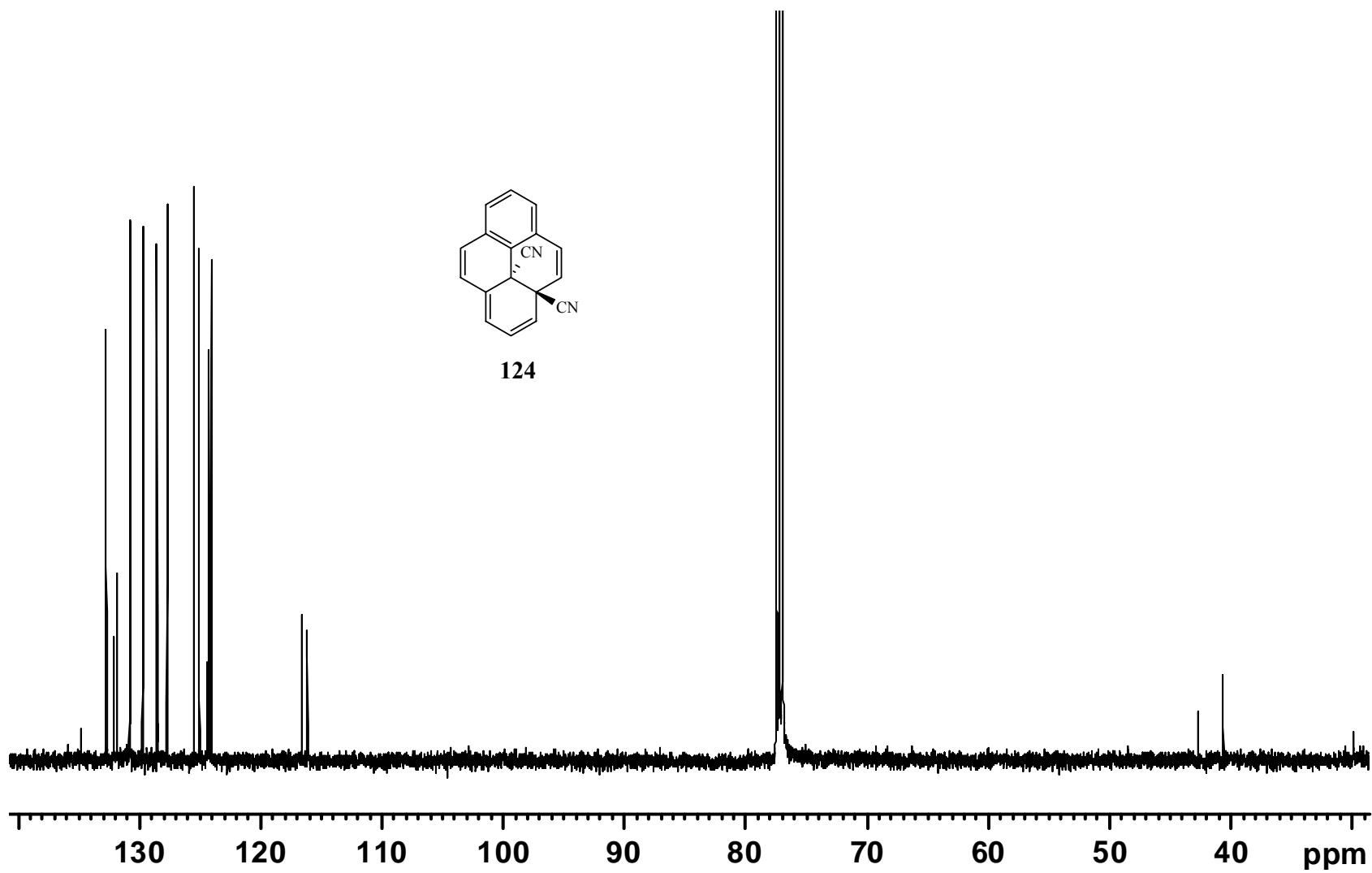
**117**

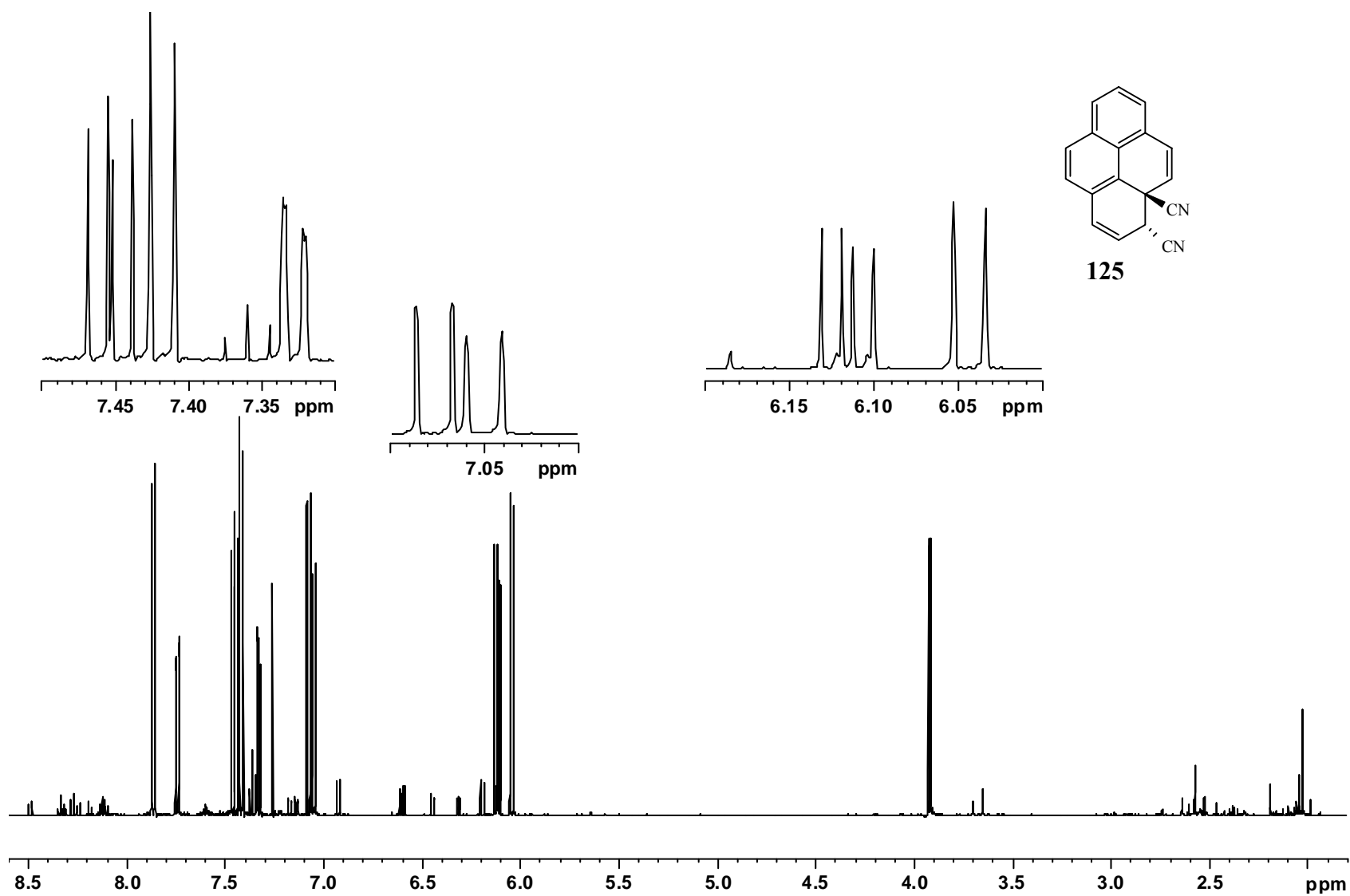


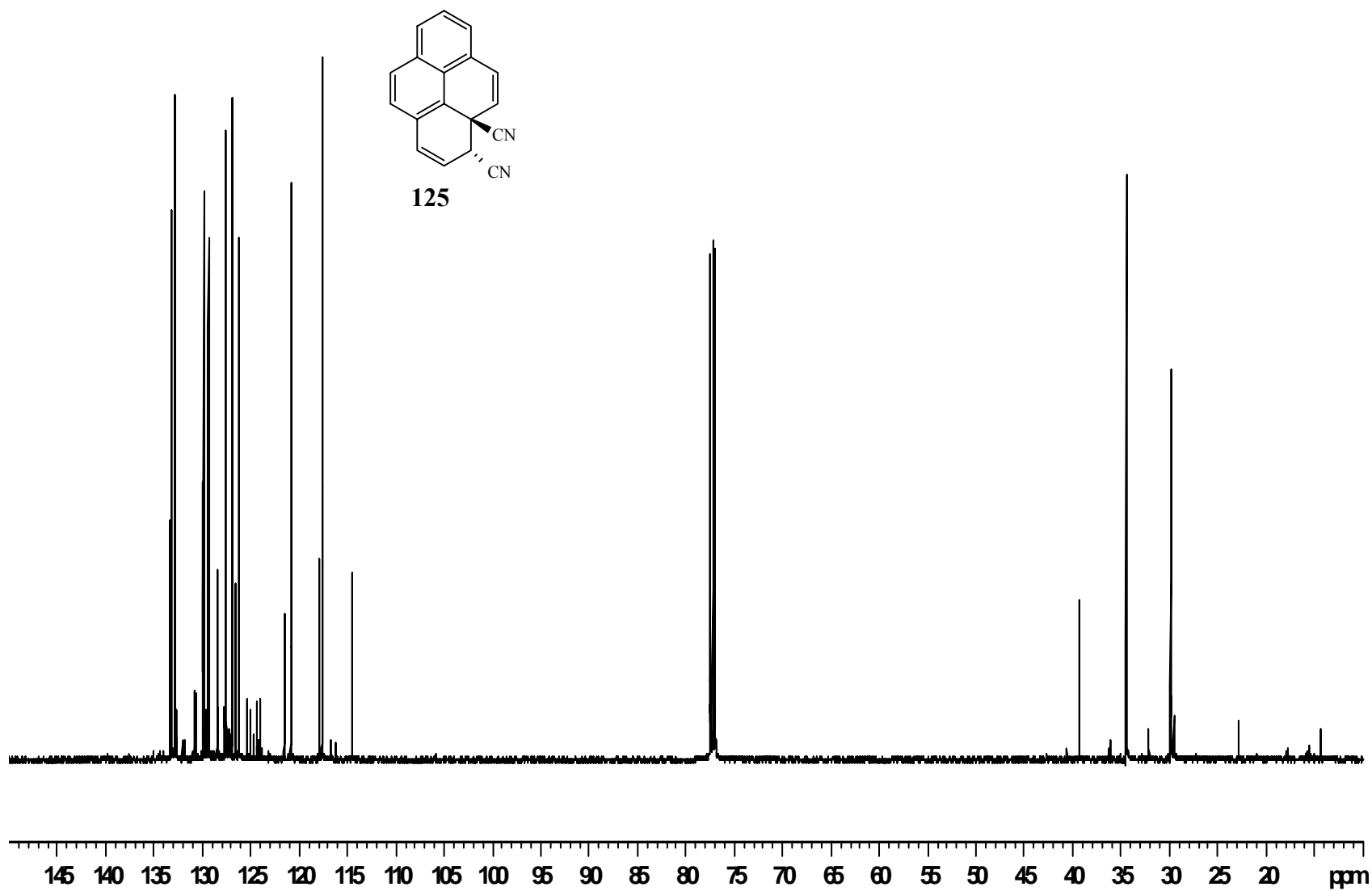


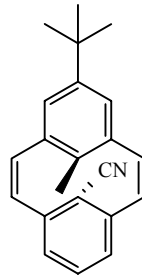
124



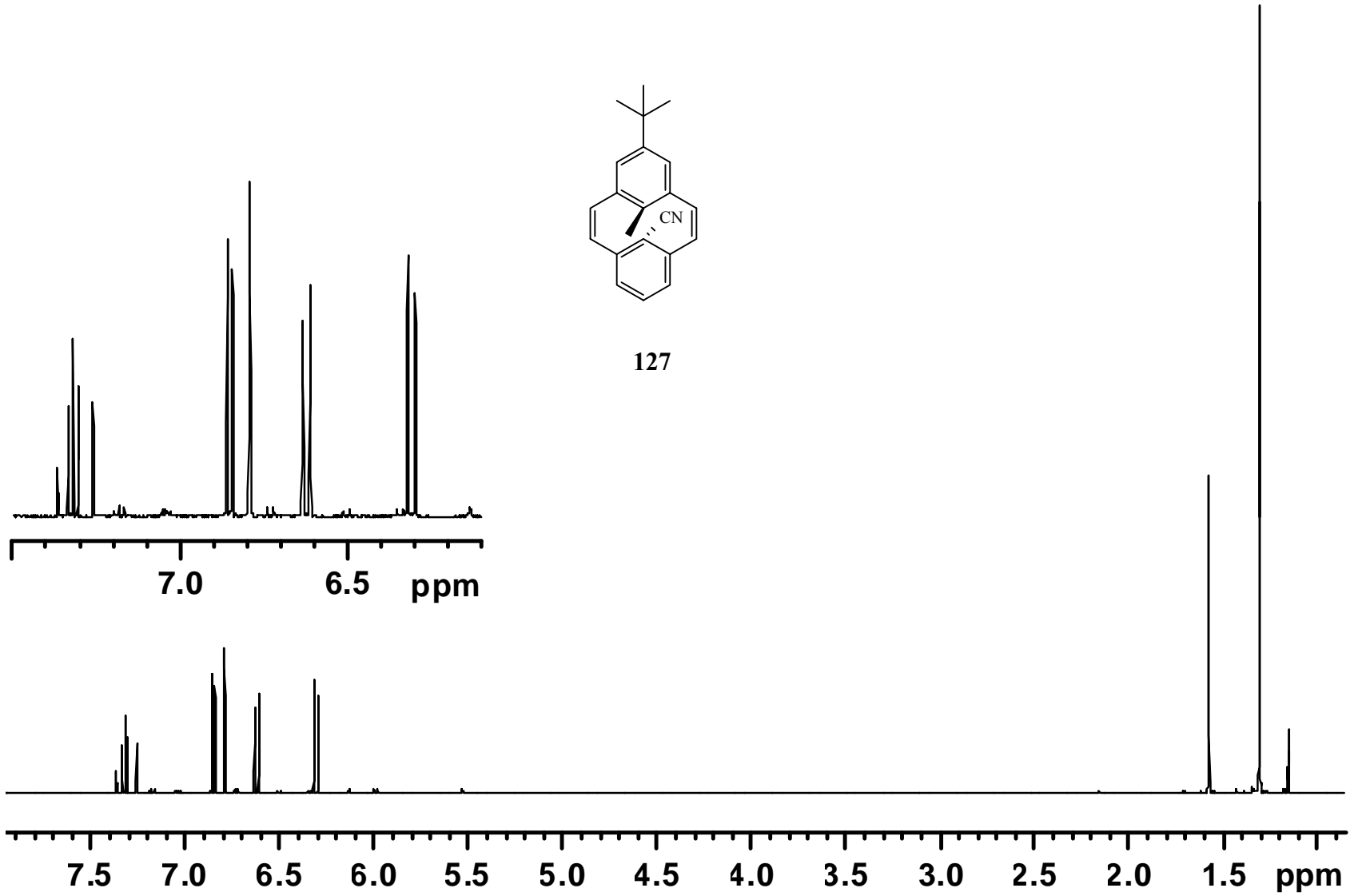


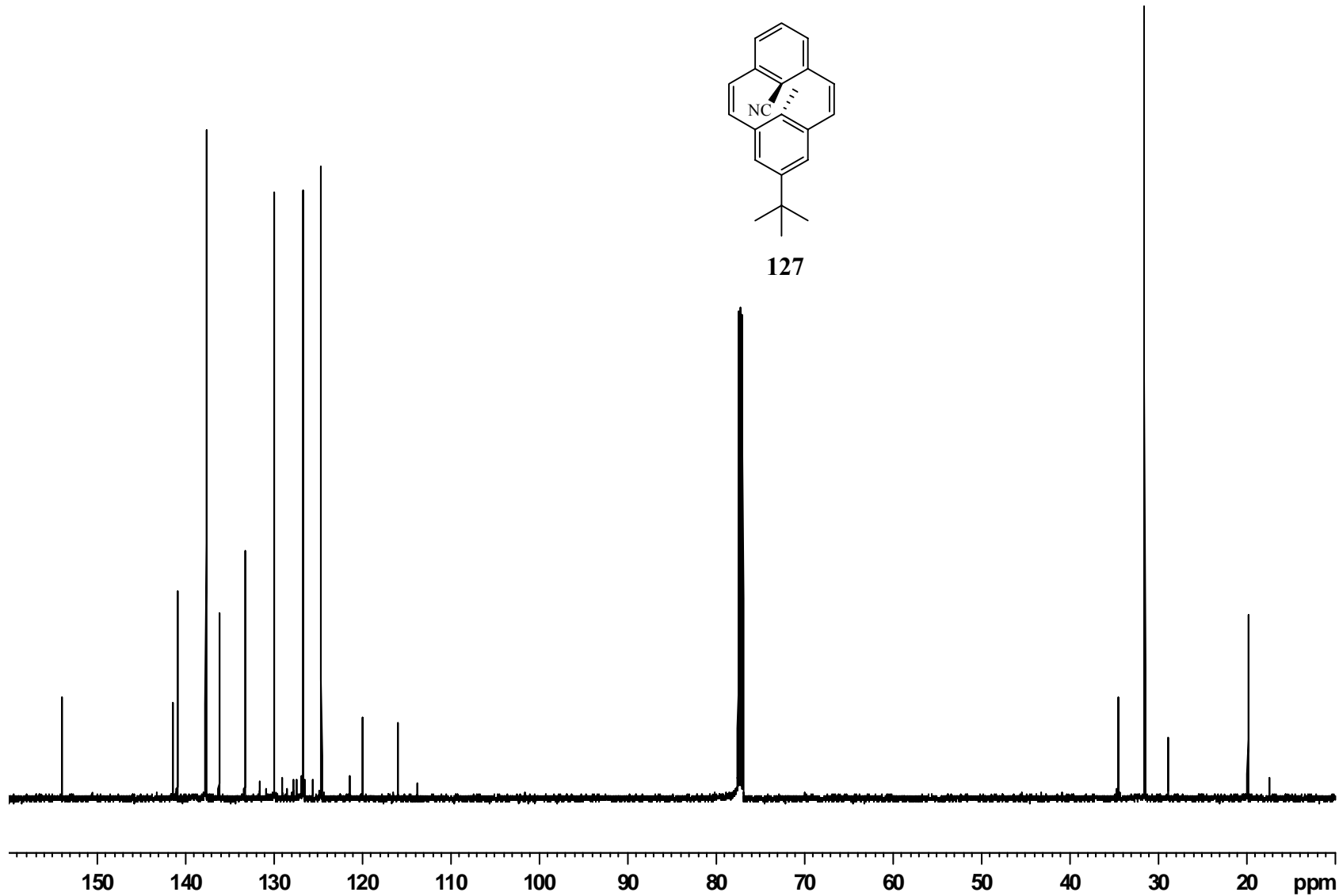


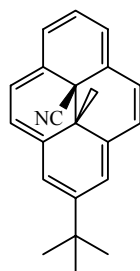




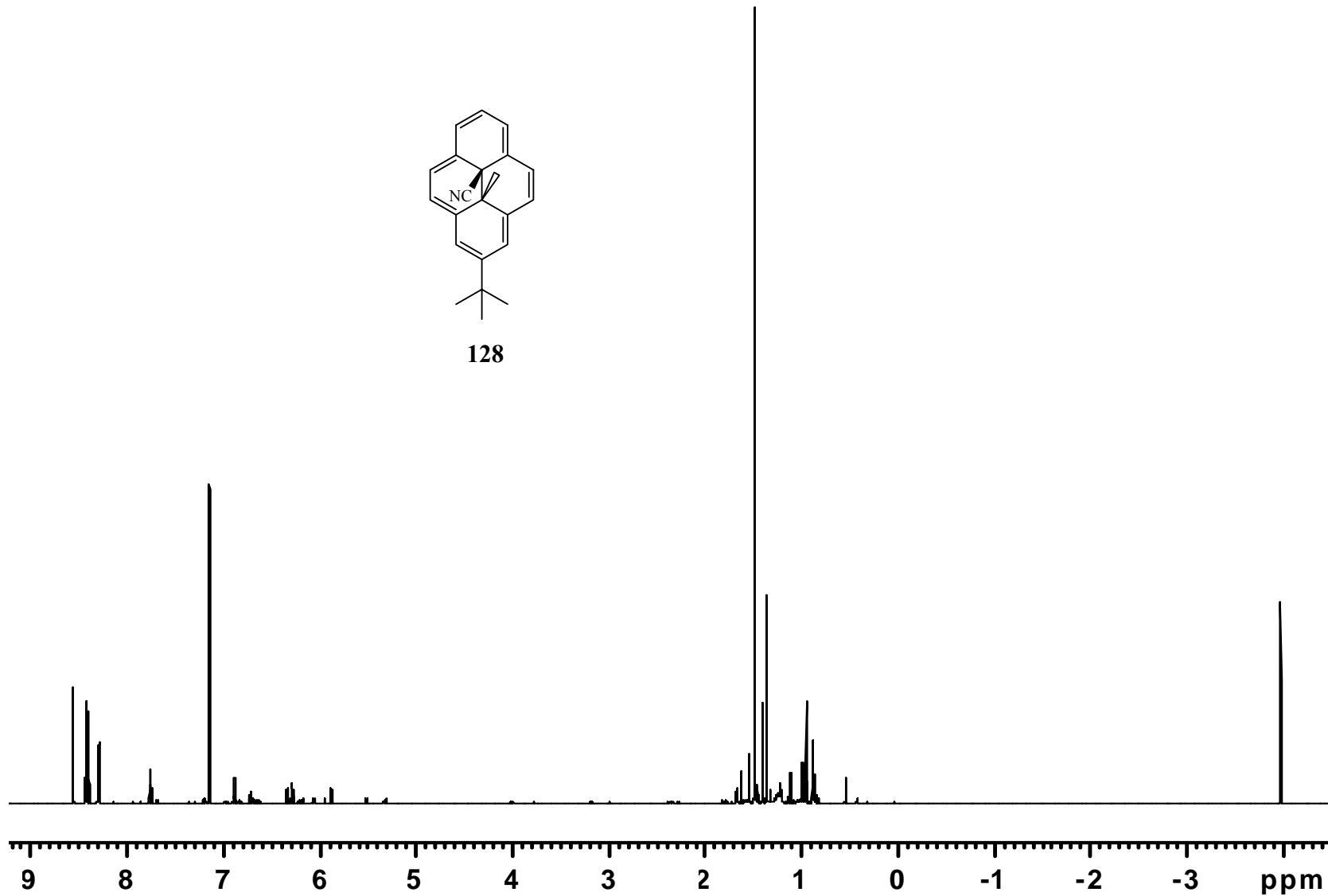
127

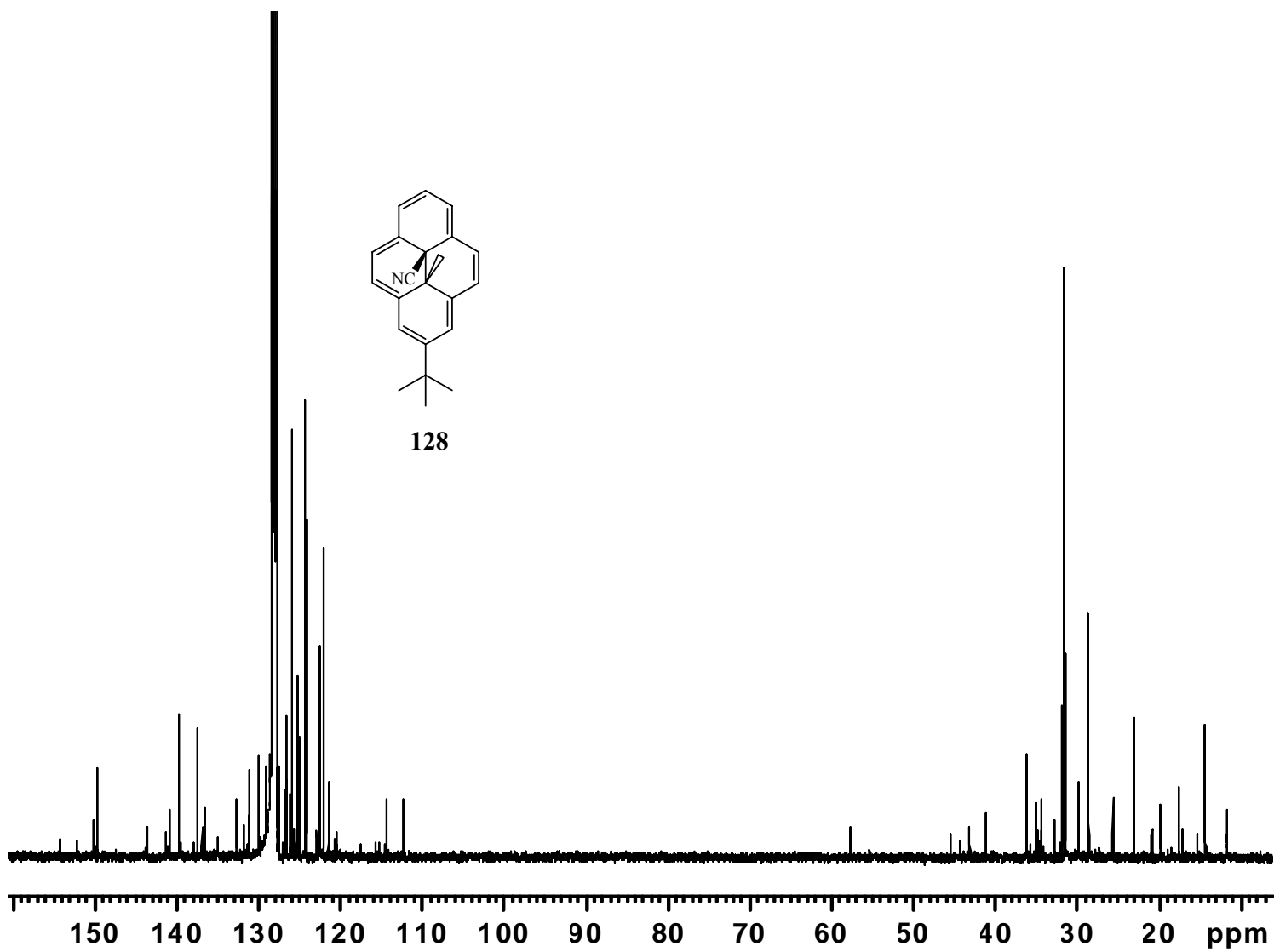


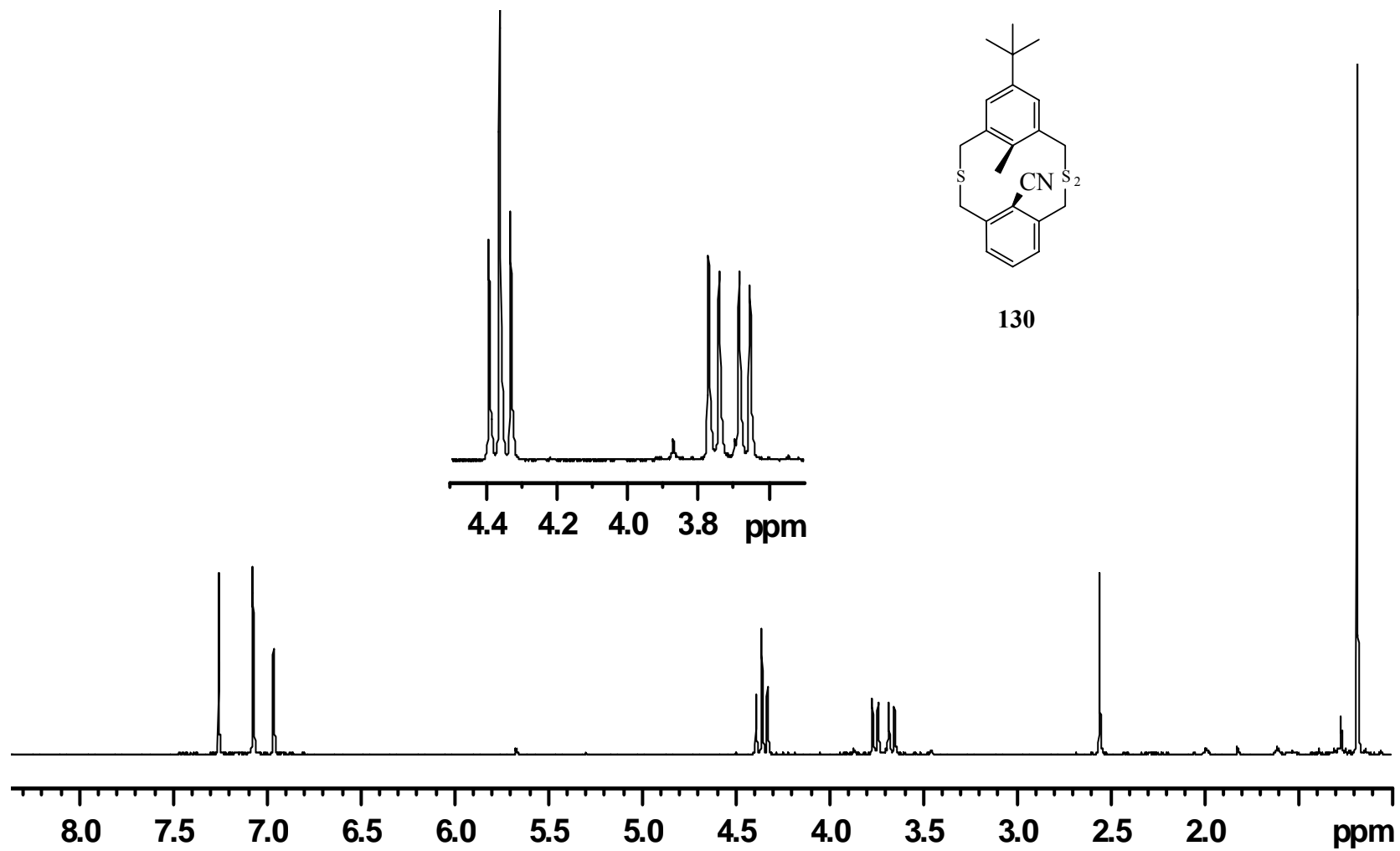


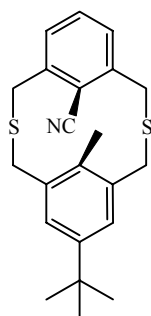


128

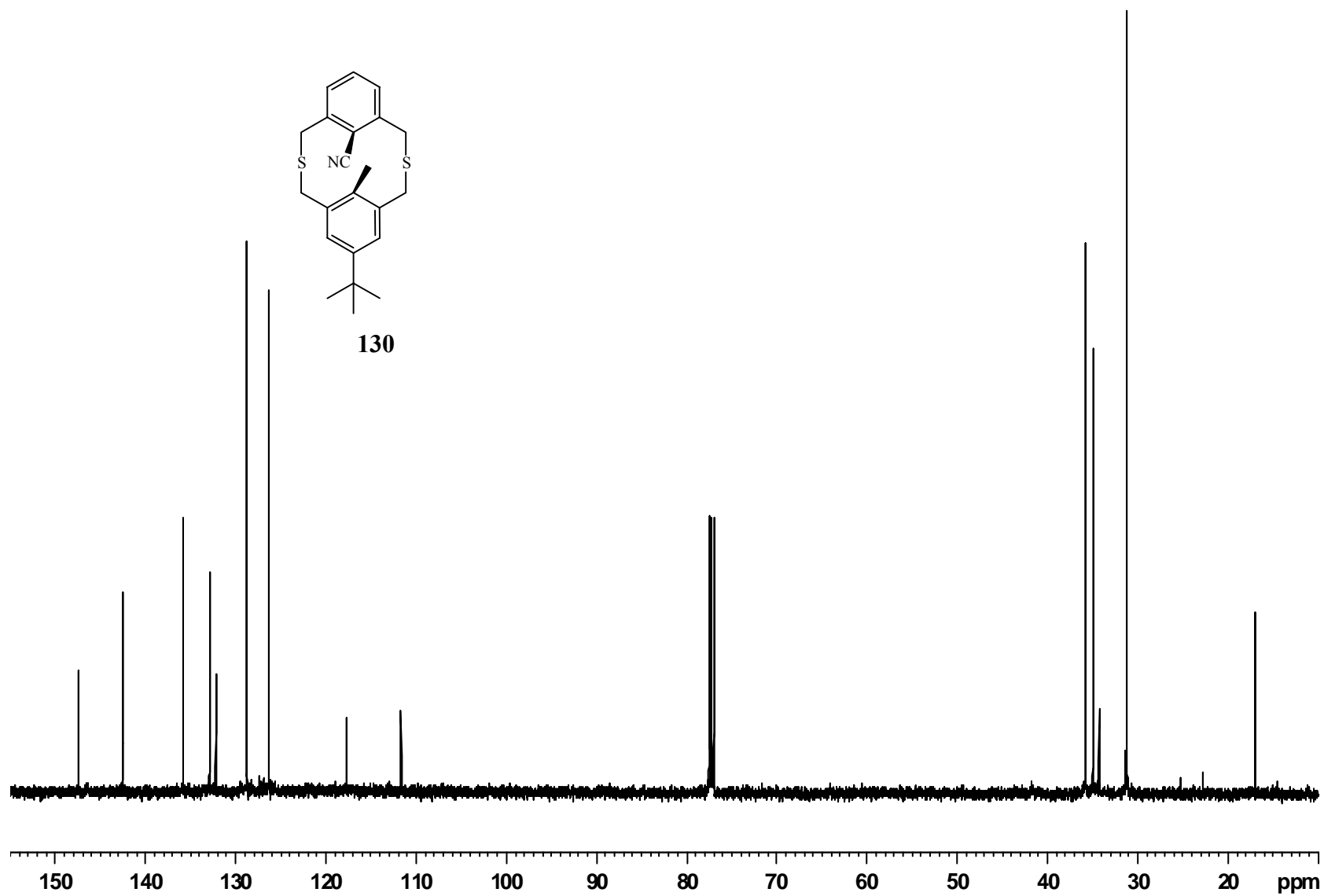


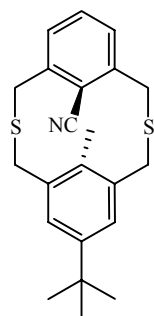
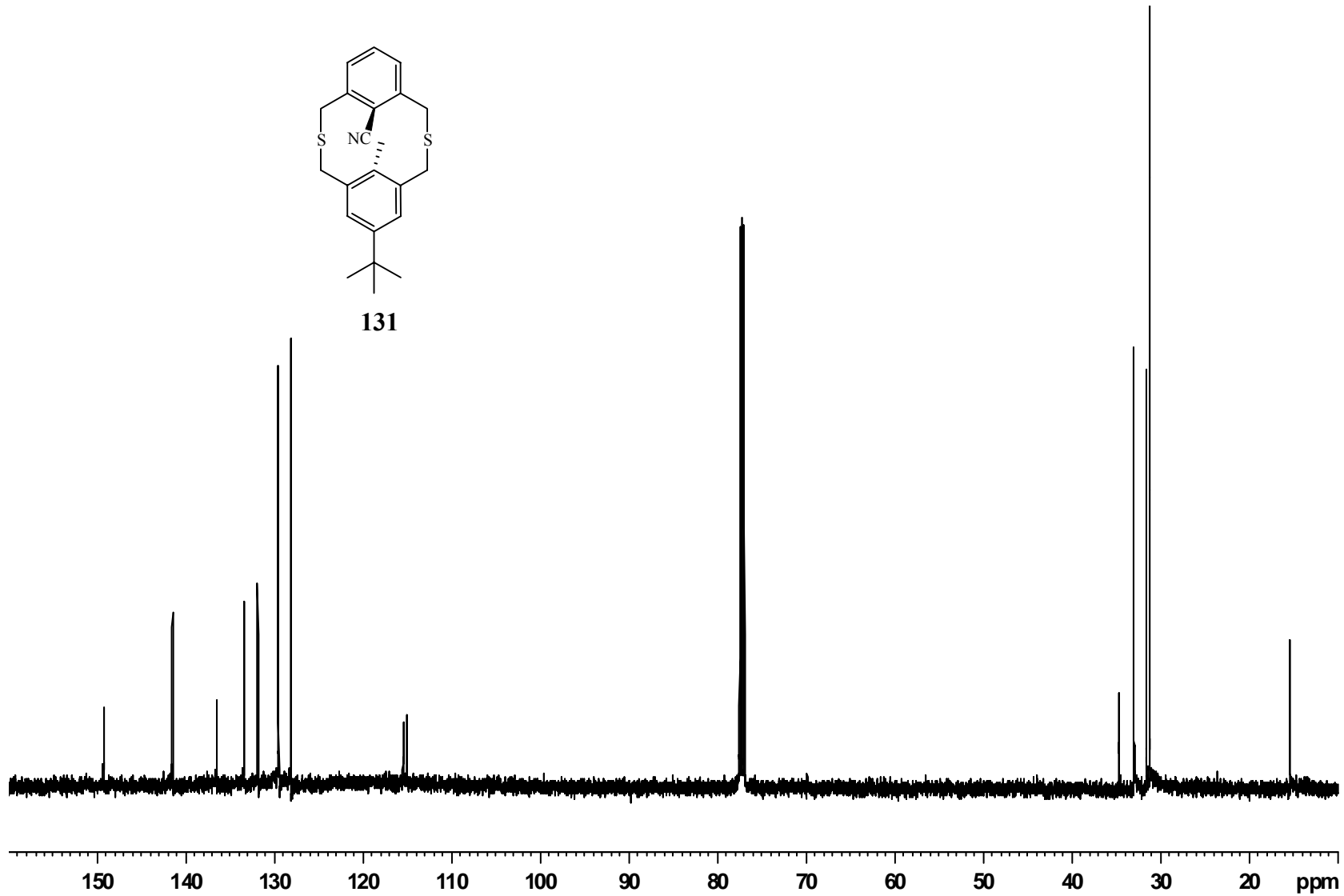


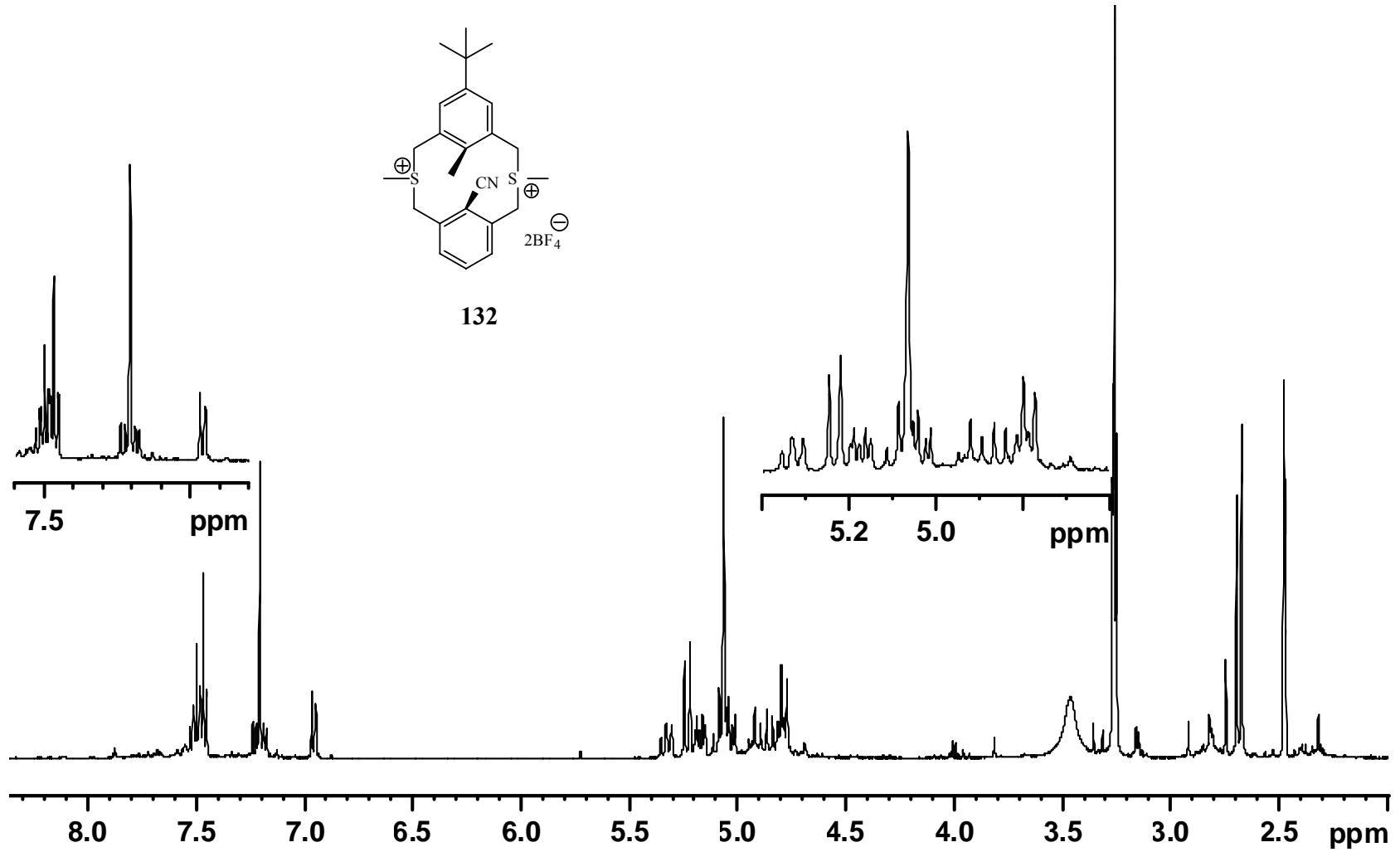


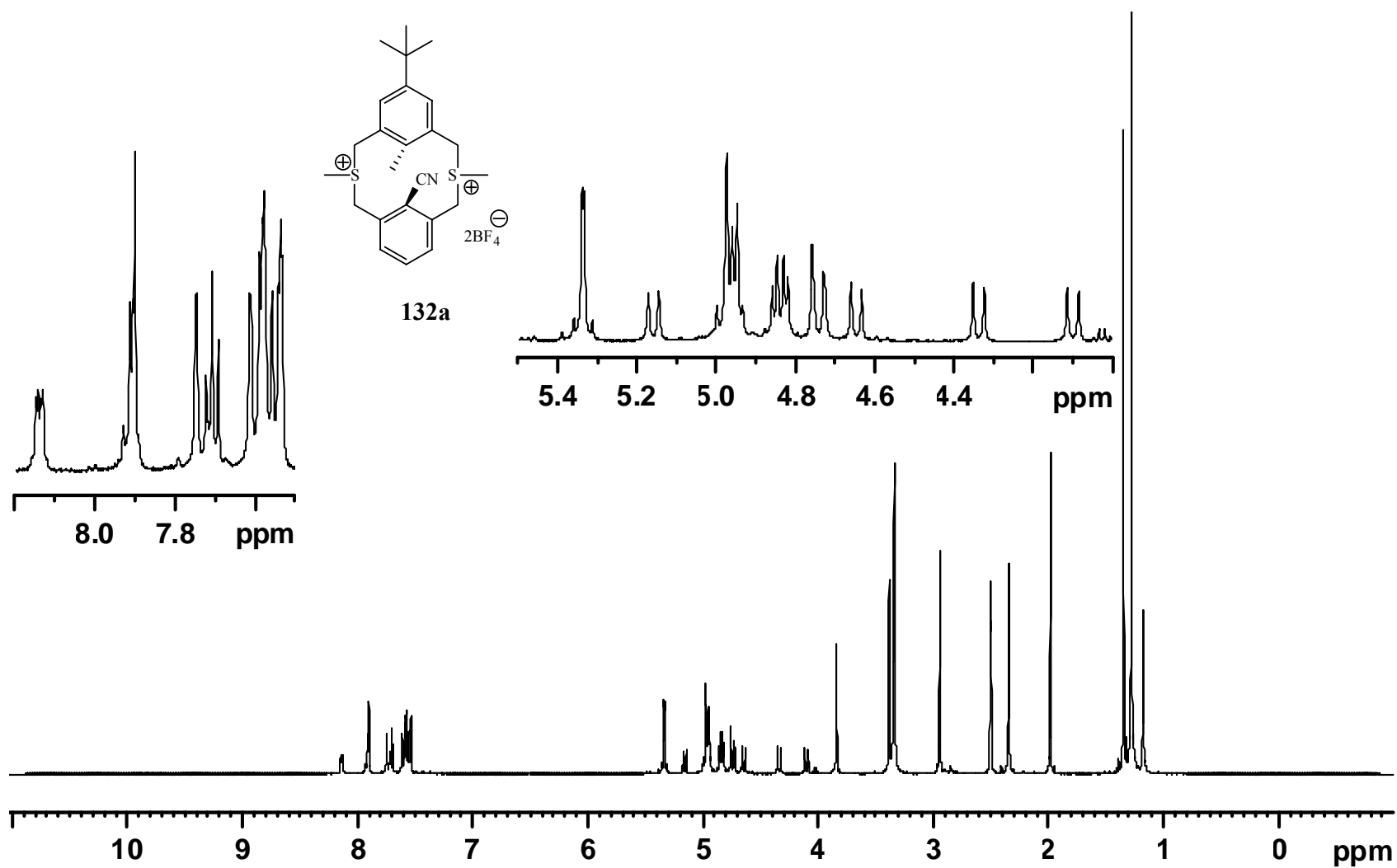


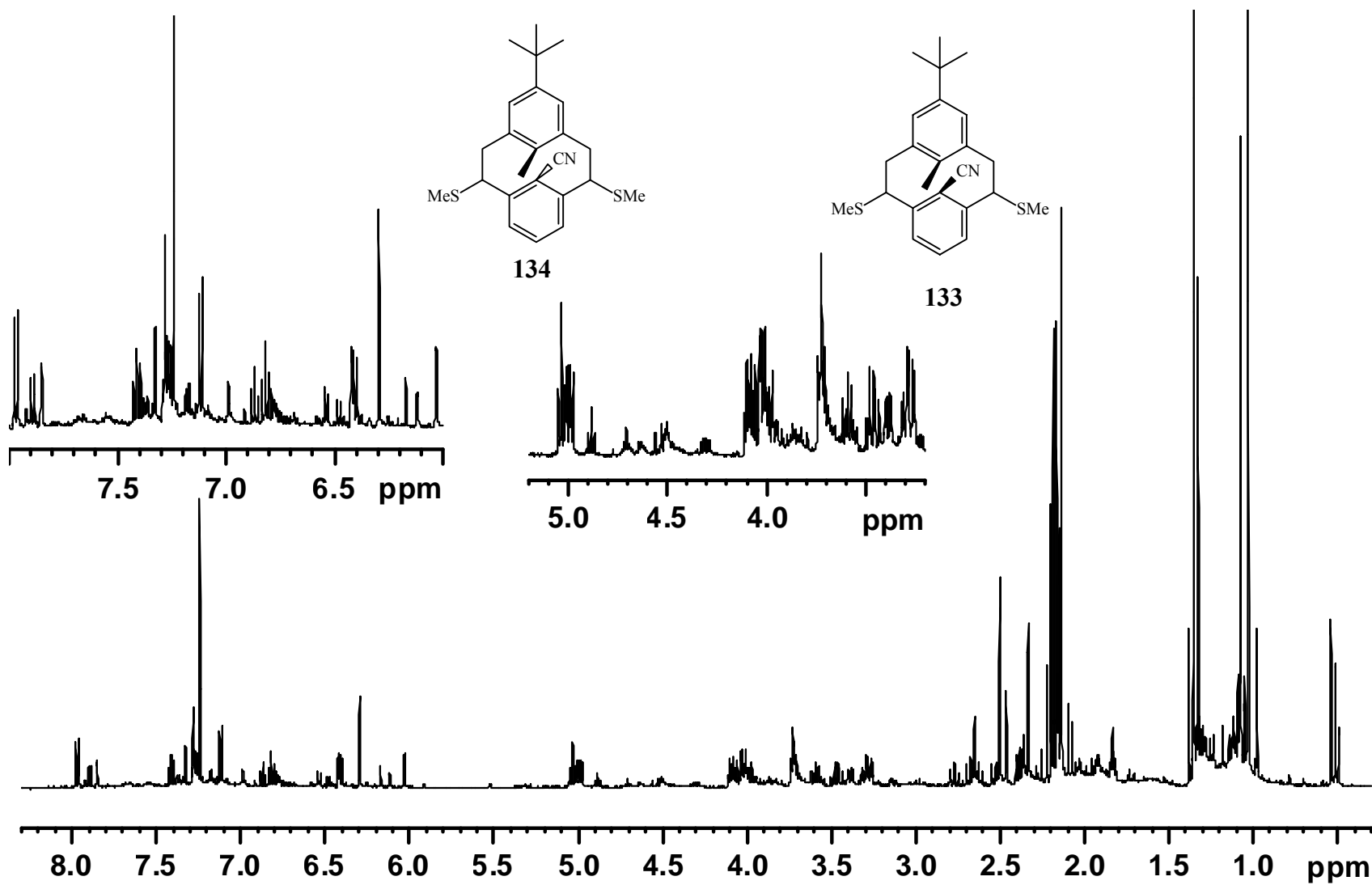
130

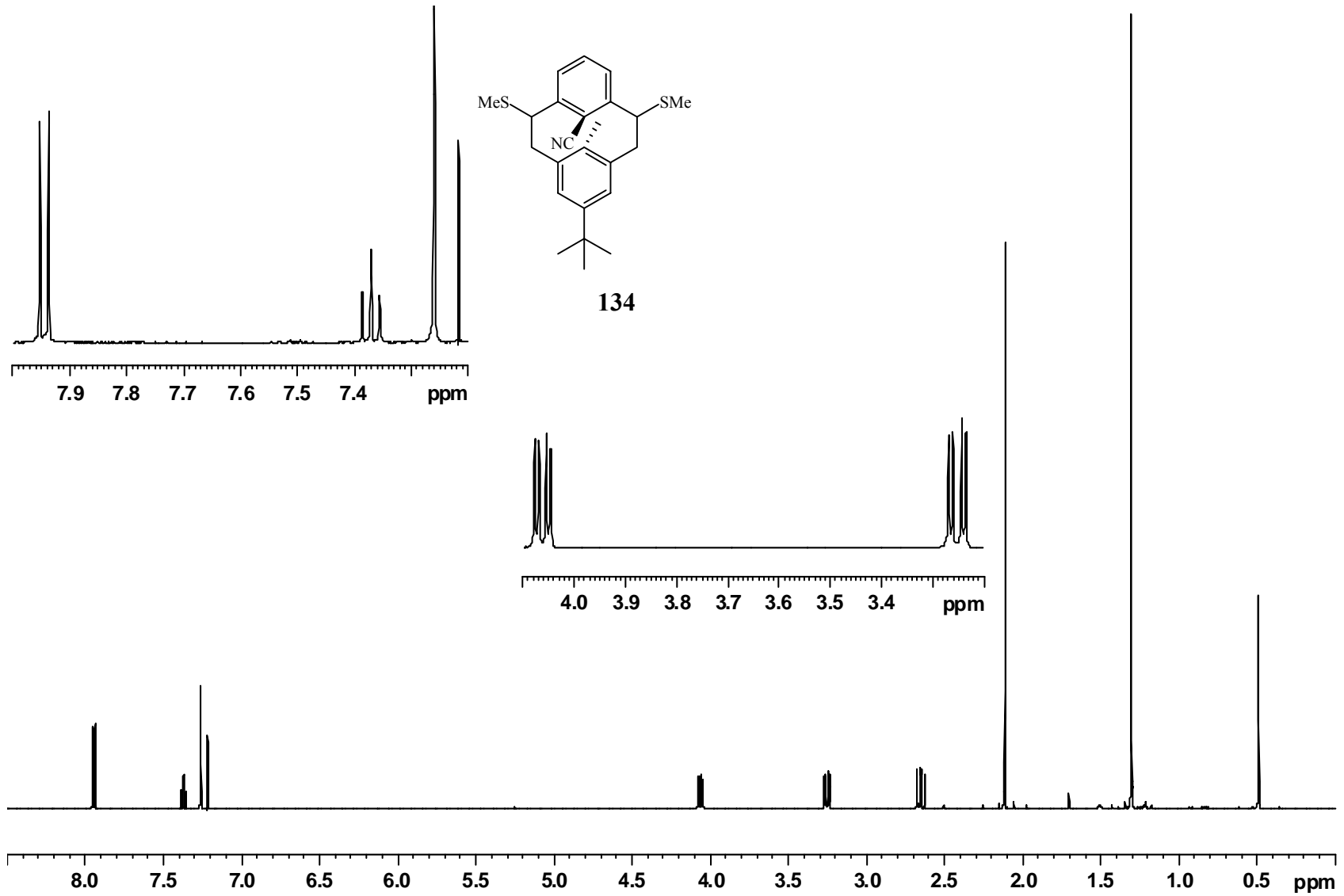


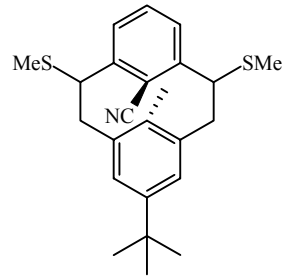
**131**



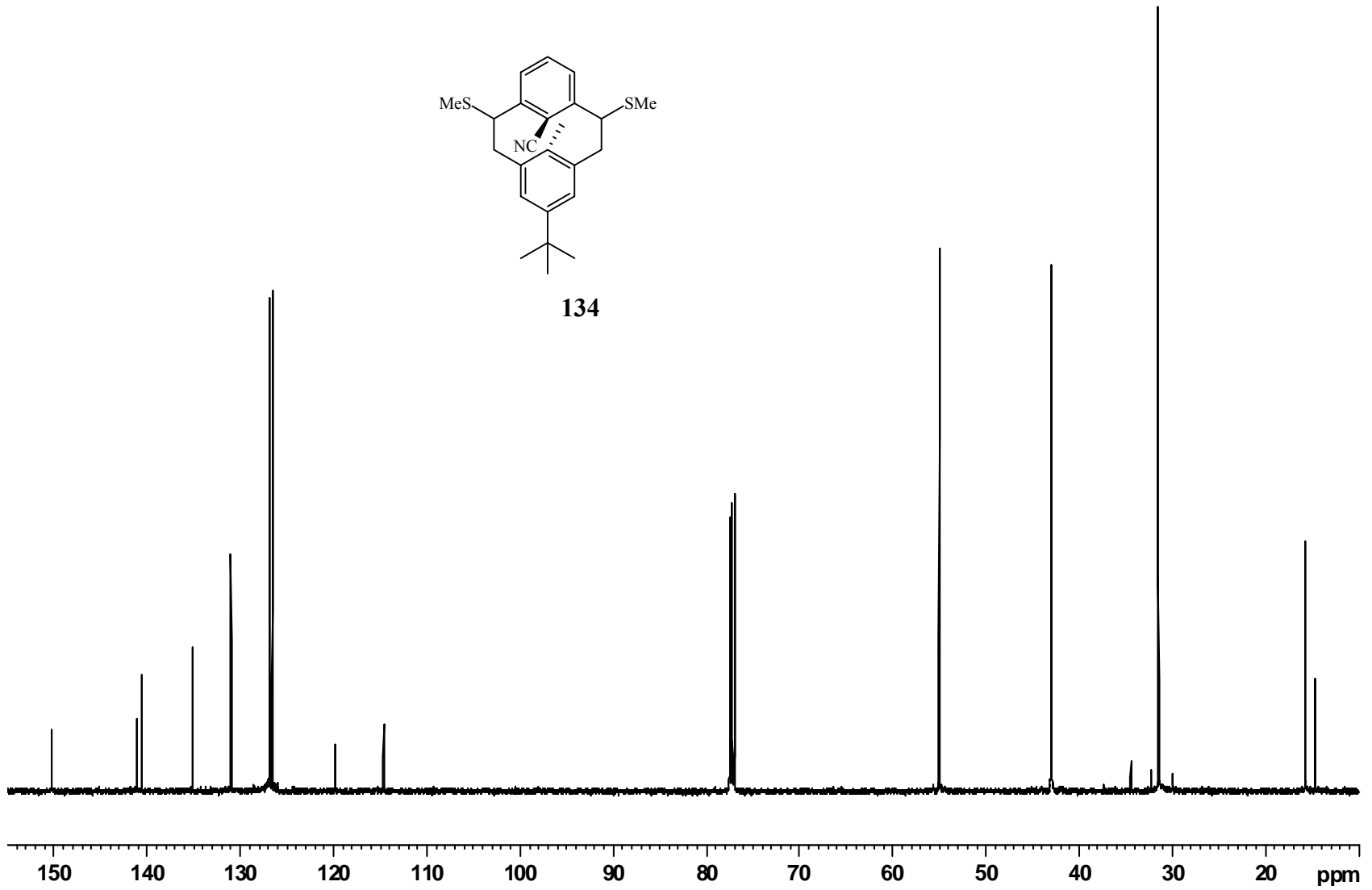




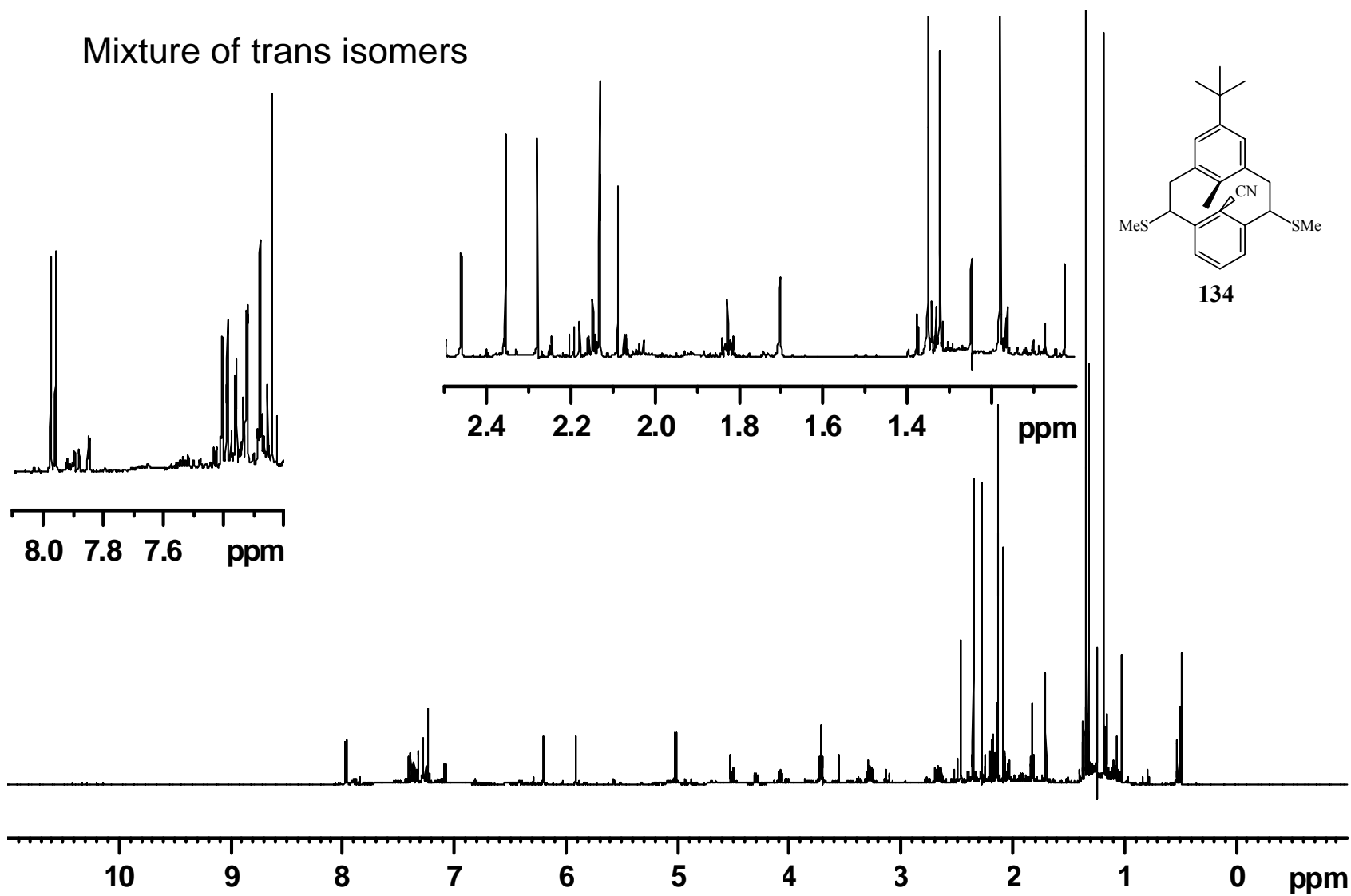


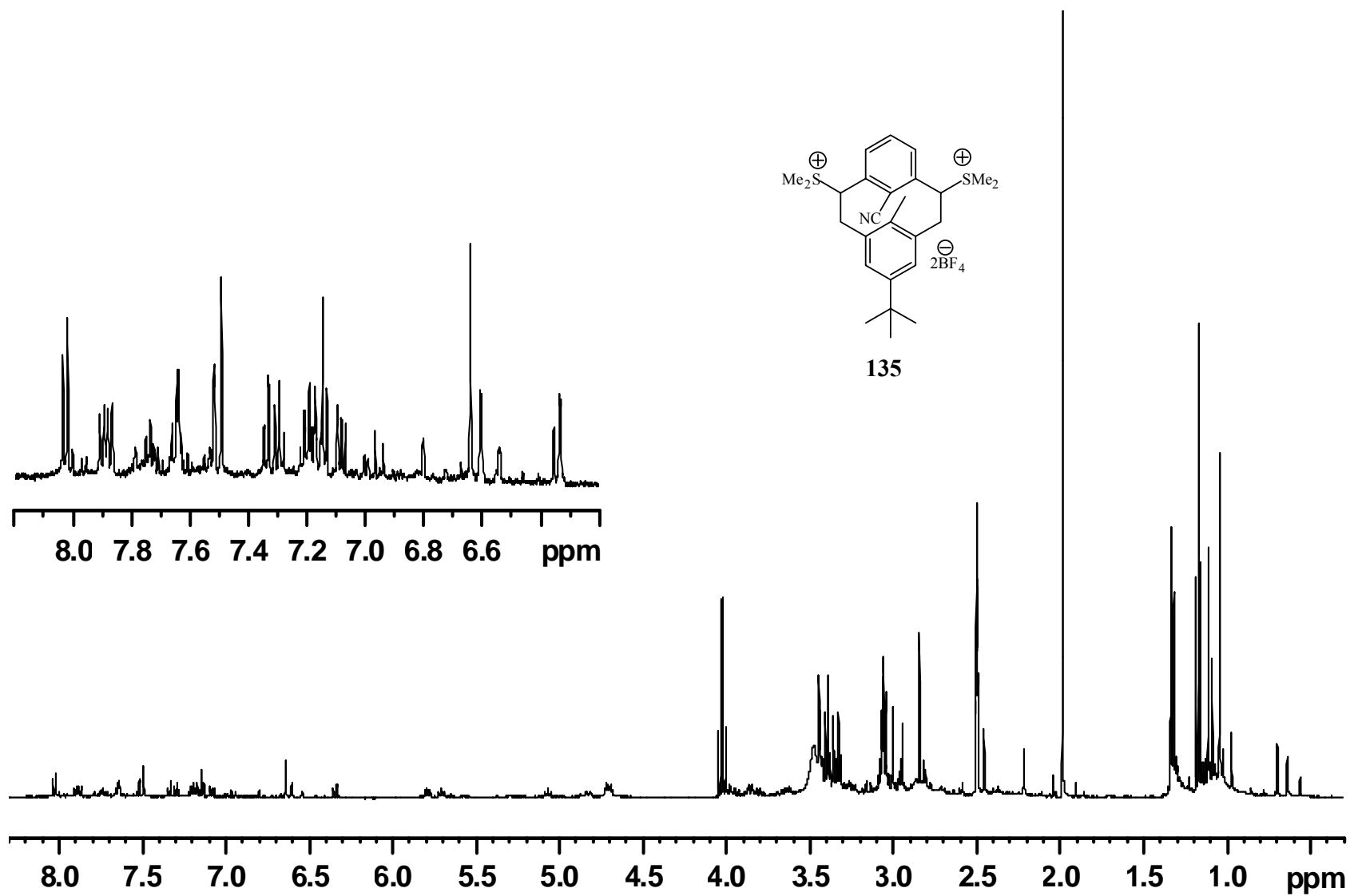


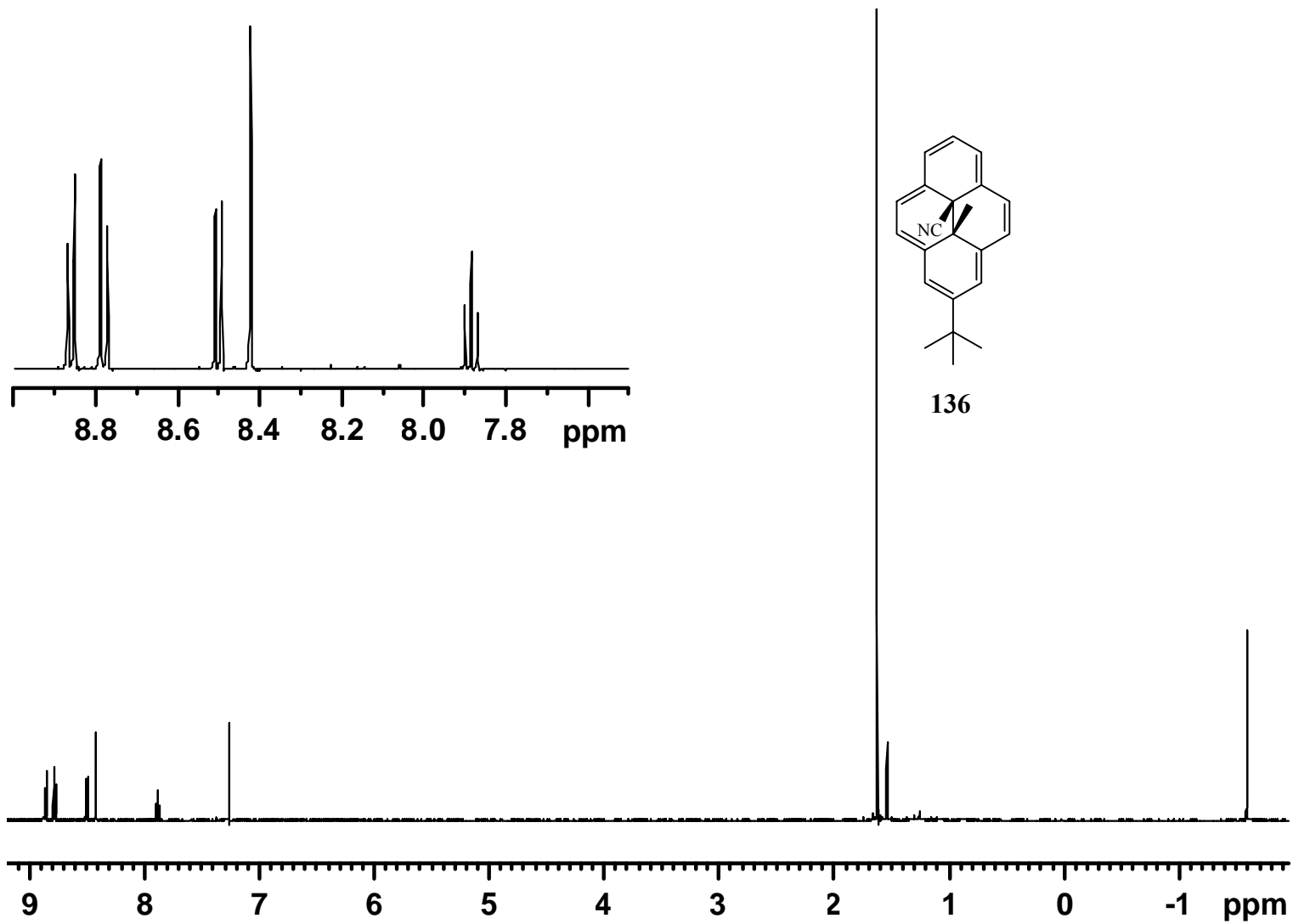
134

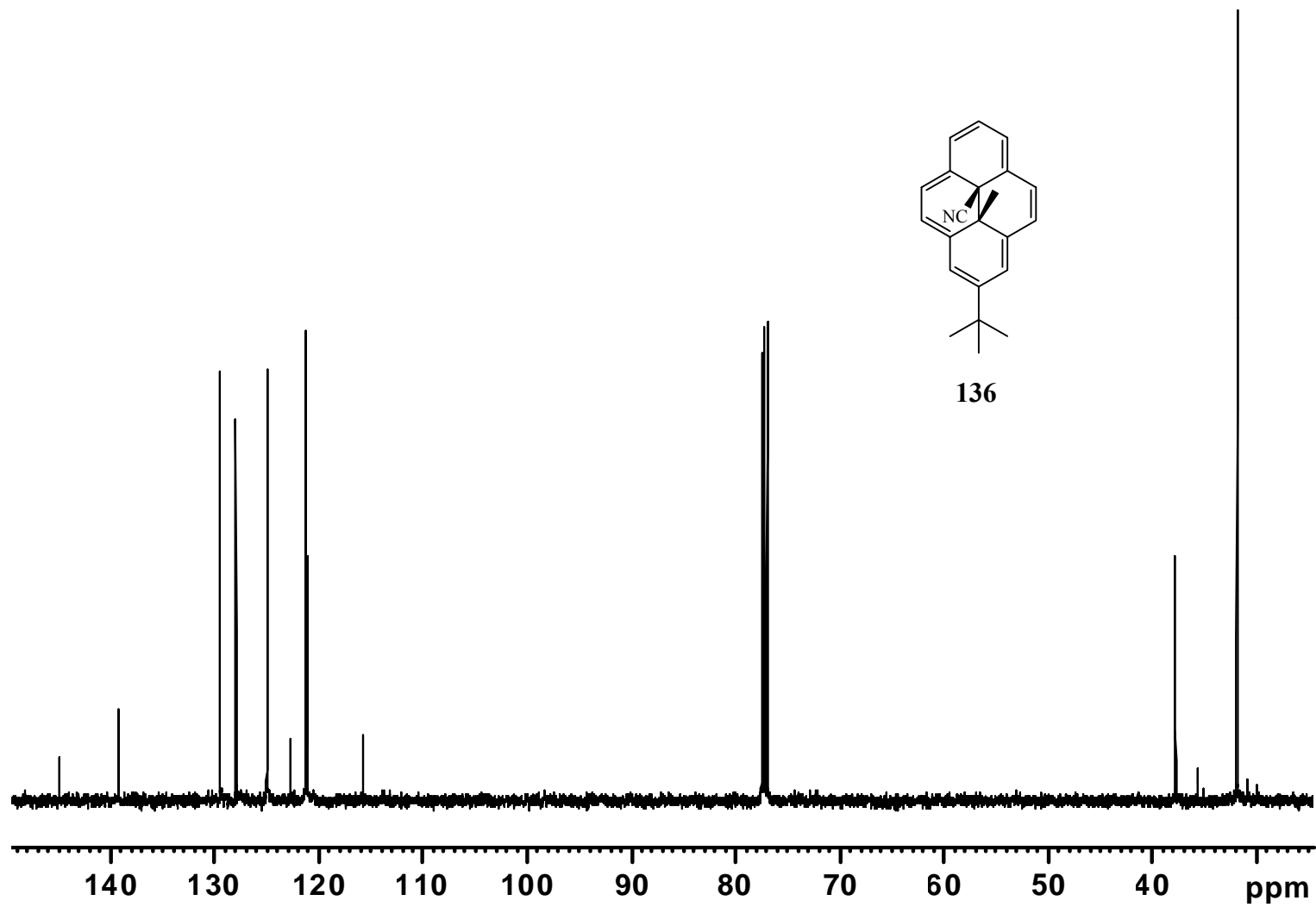


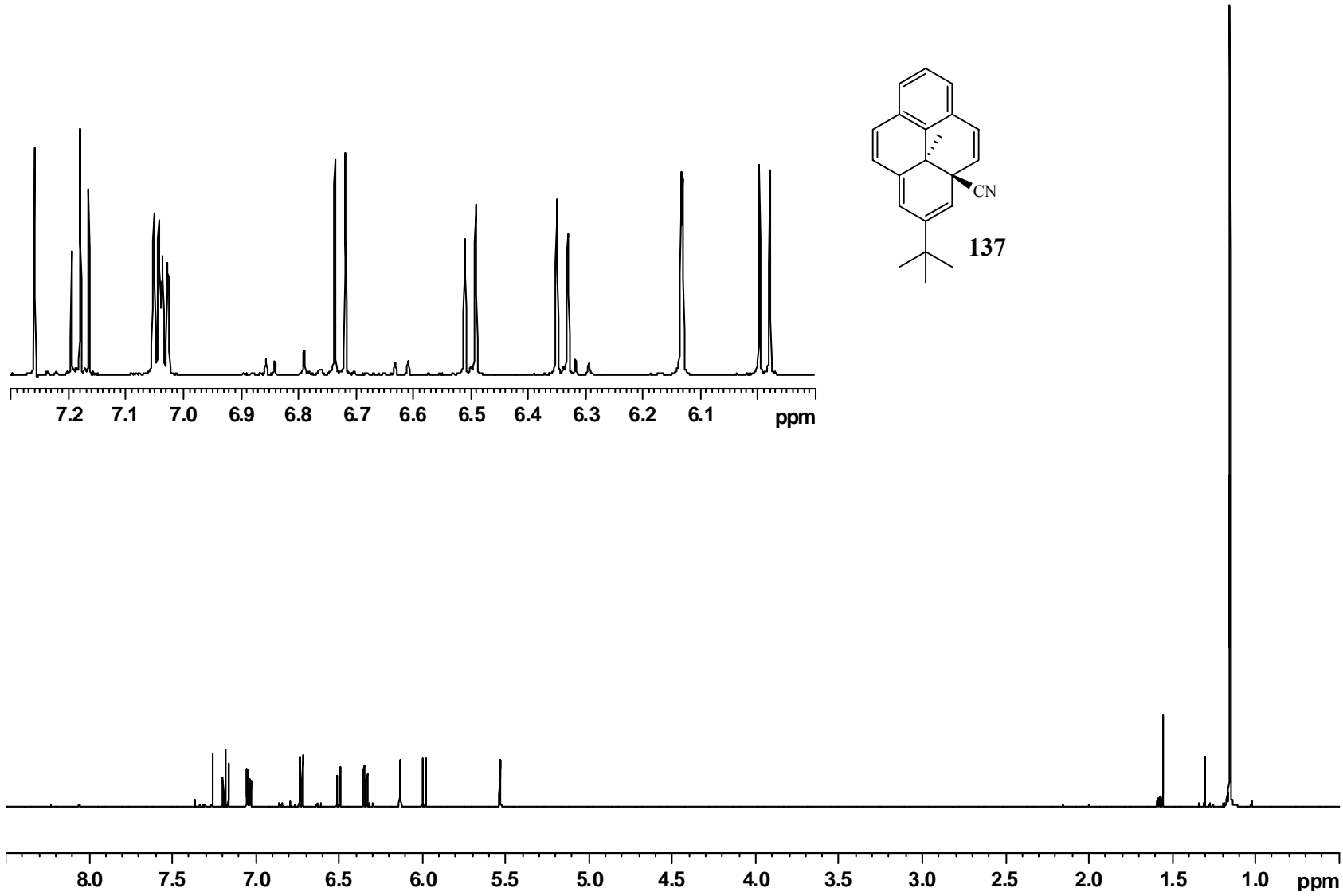
Mixture of trans isomers

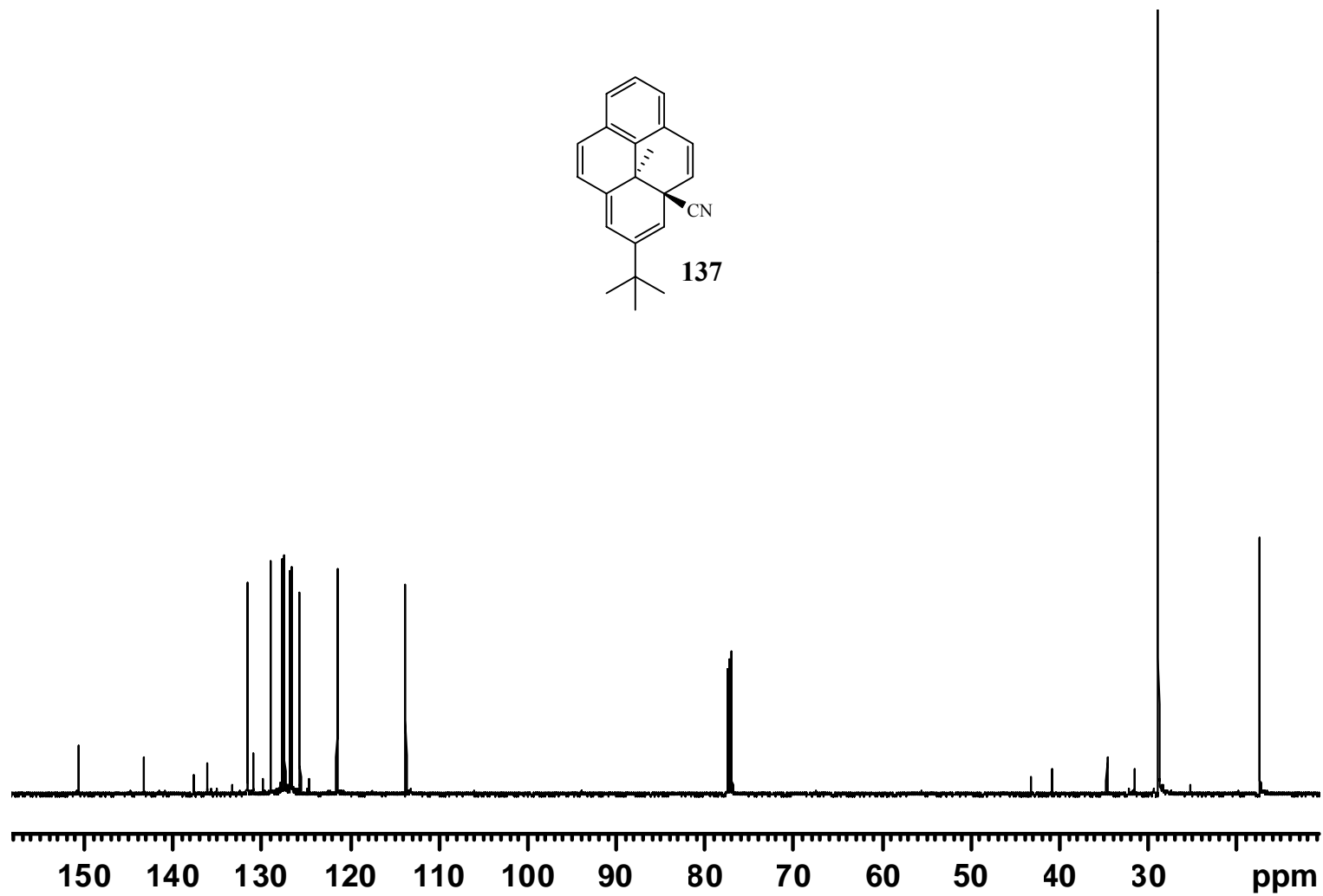
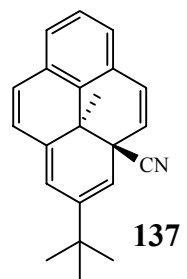


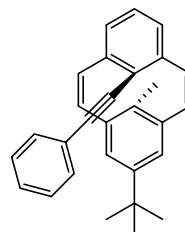
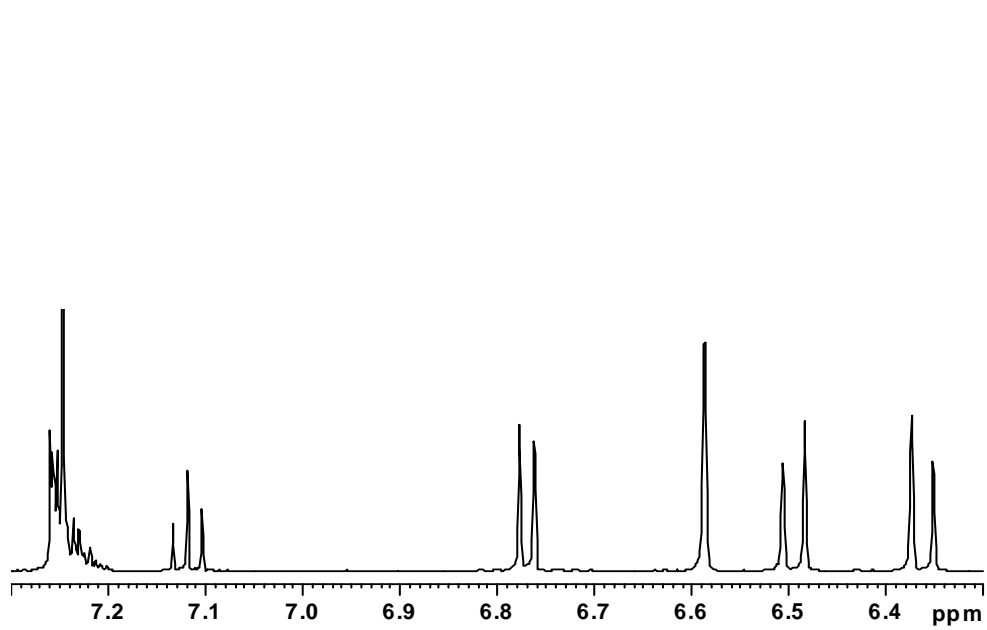




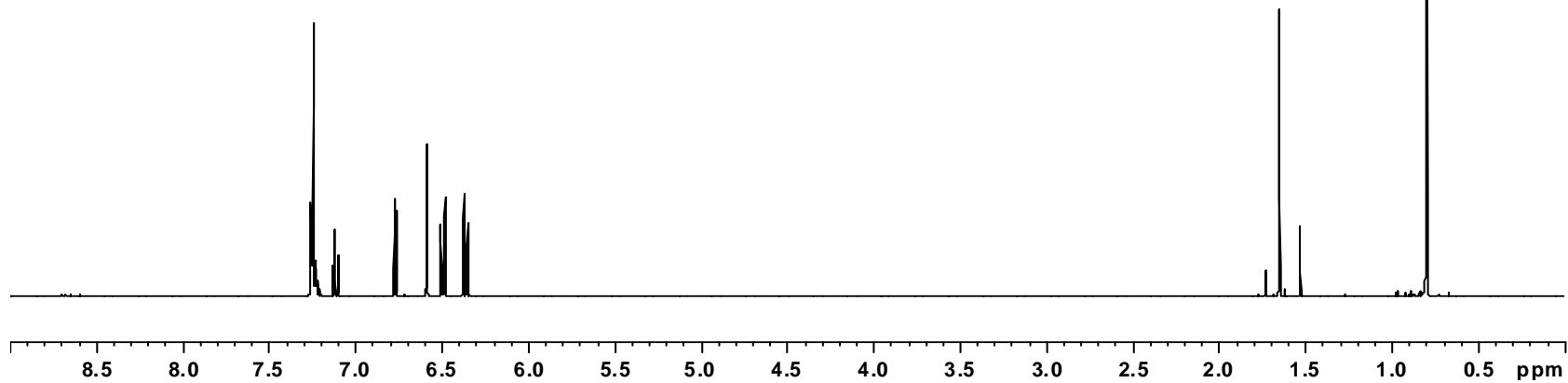


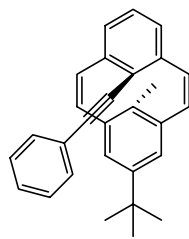




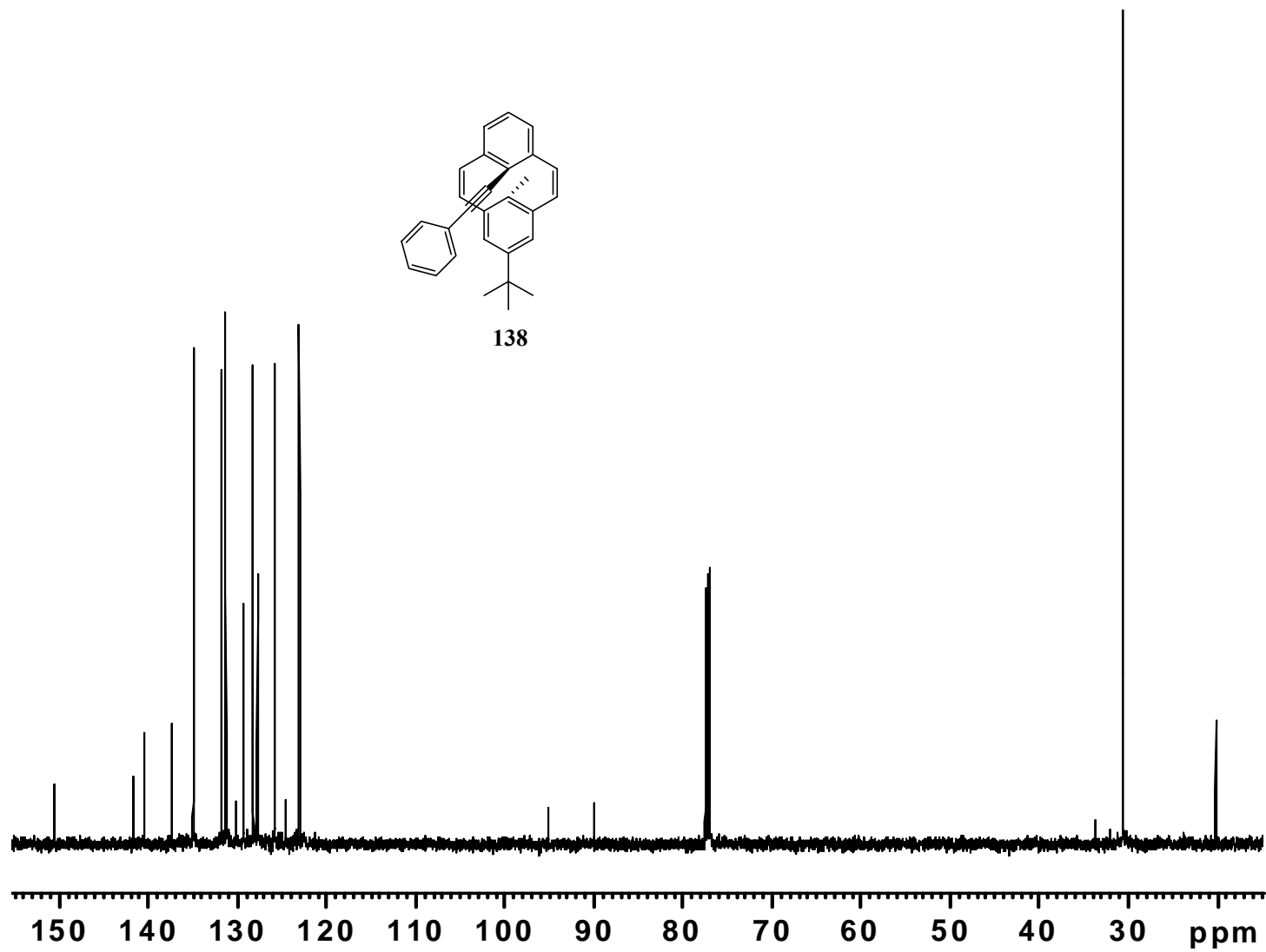


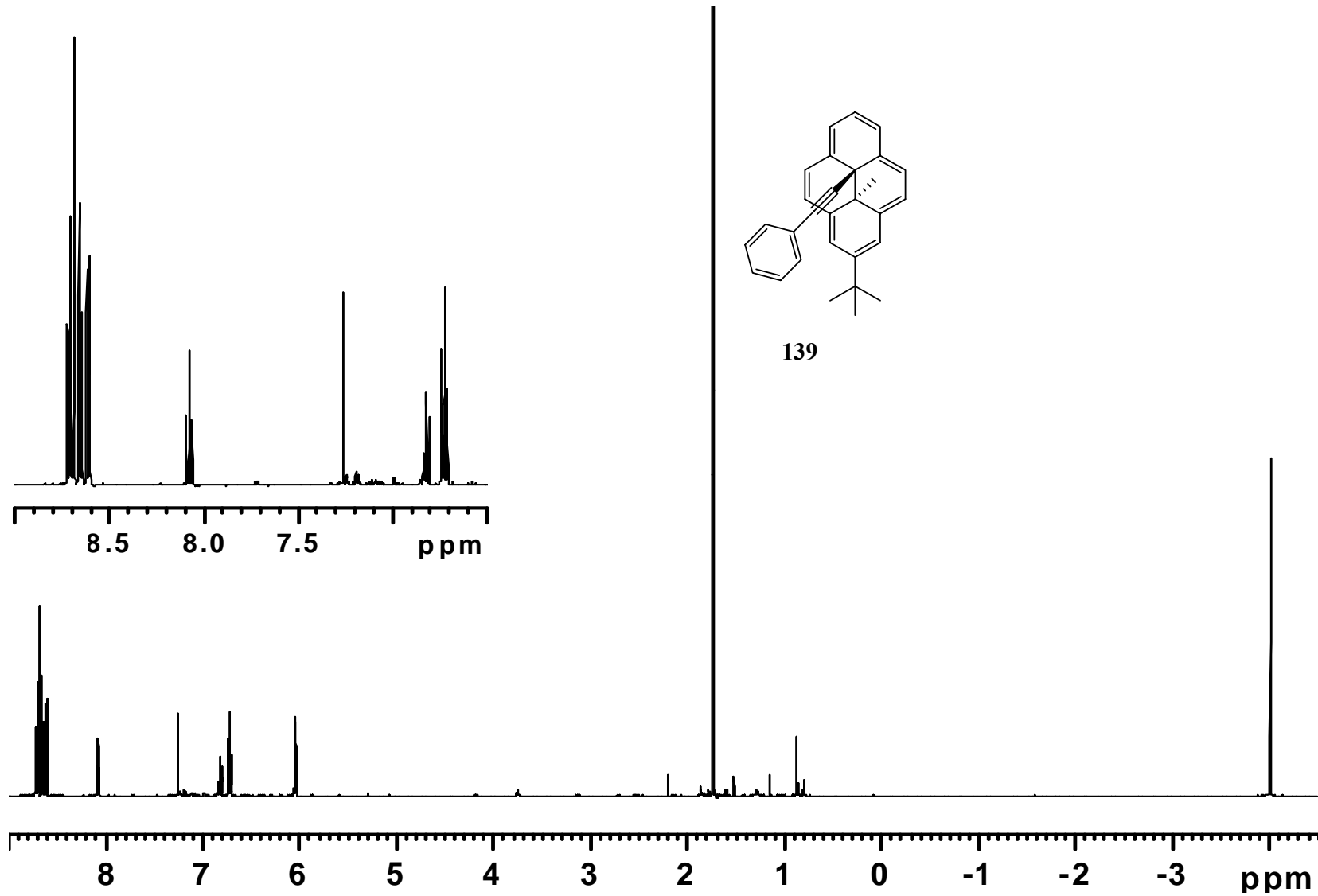
138

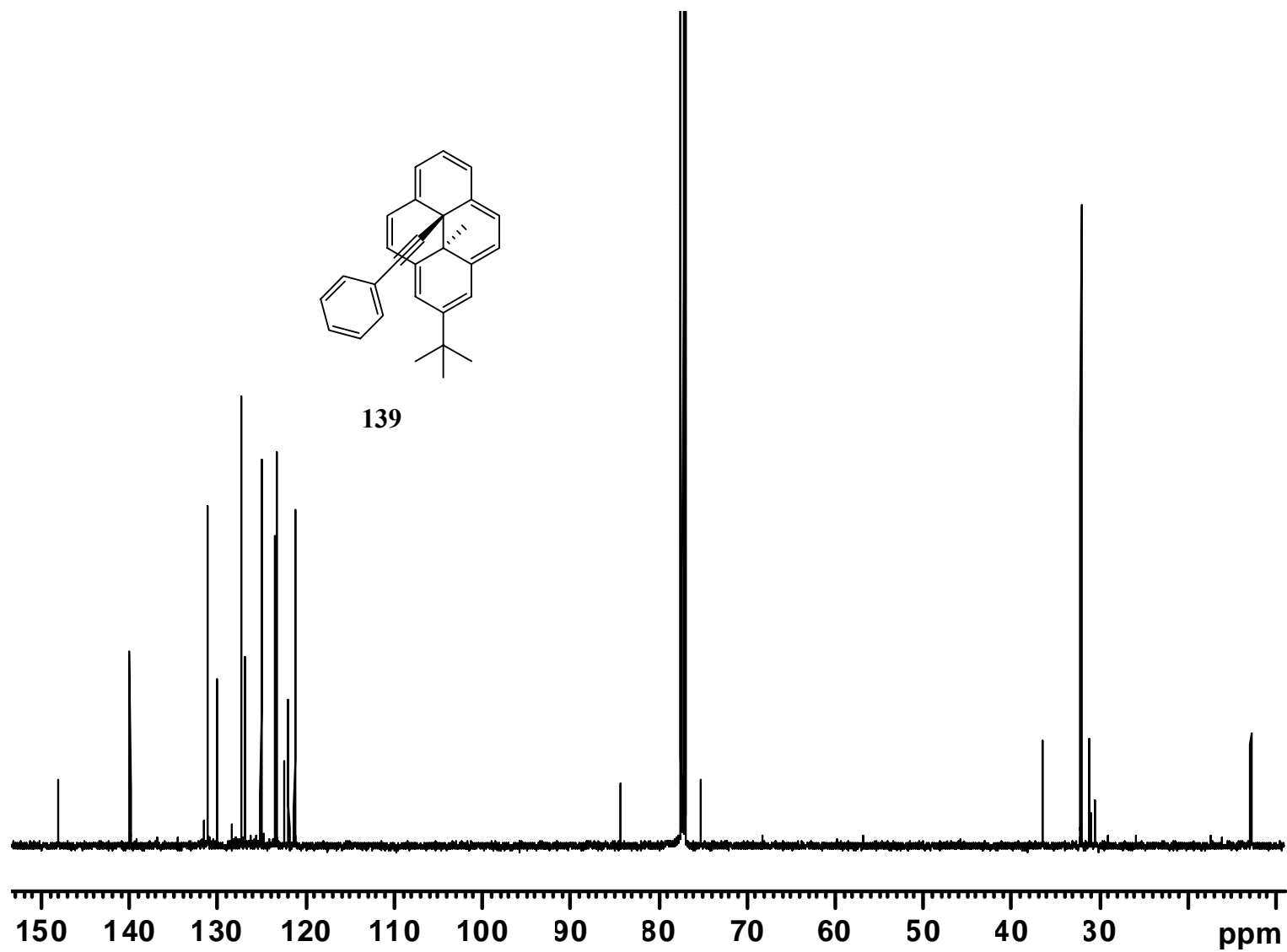


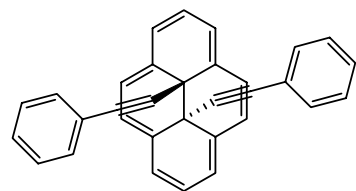


138

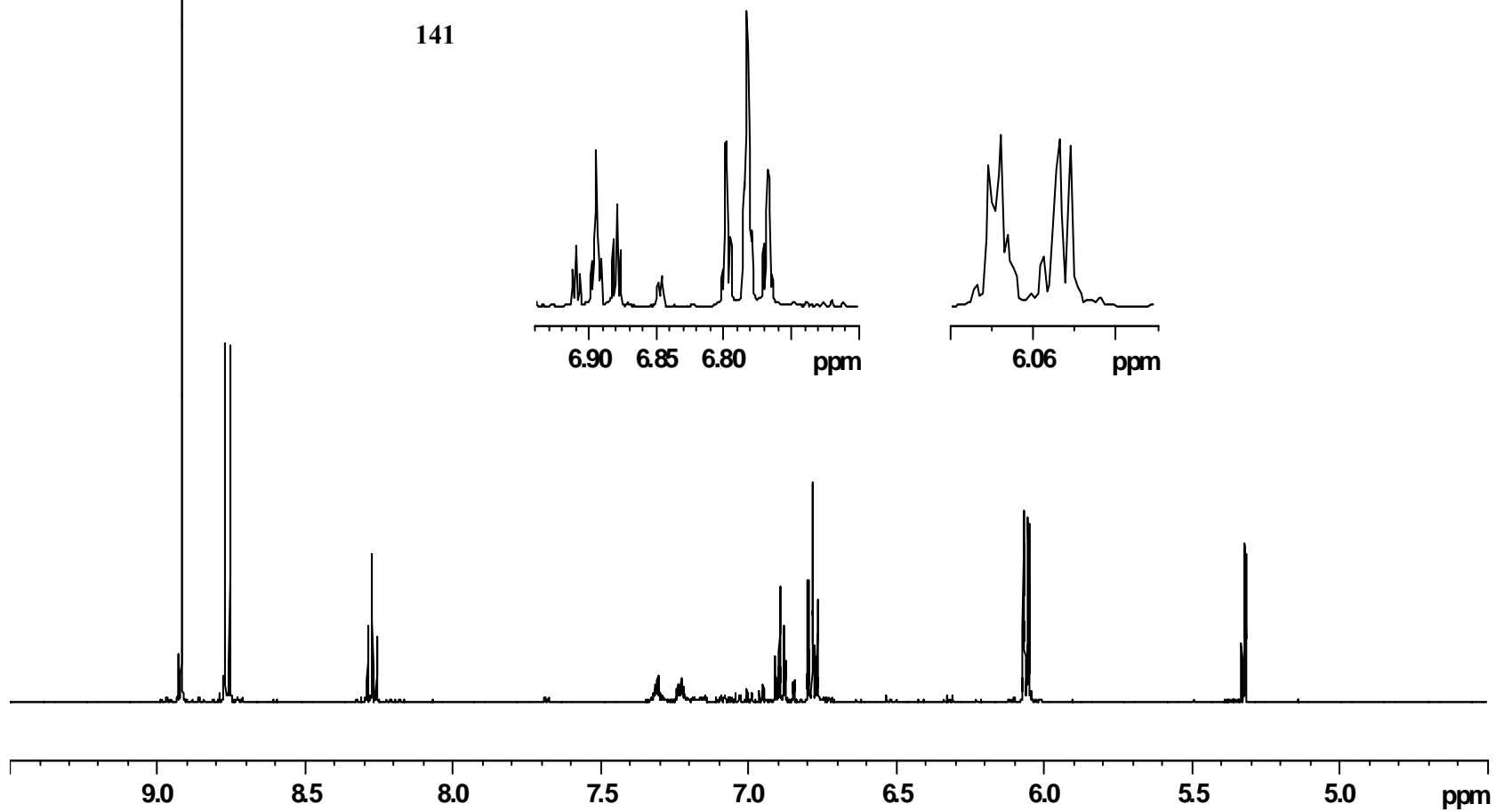


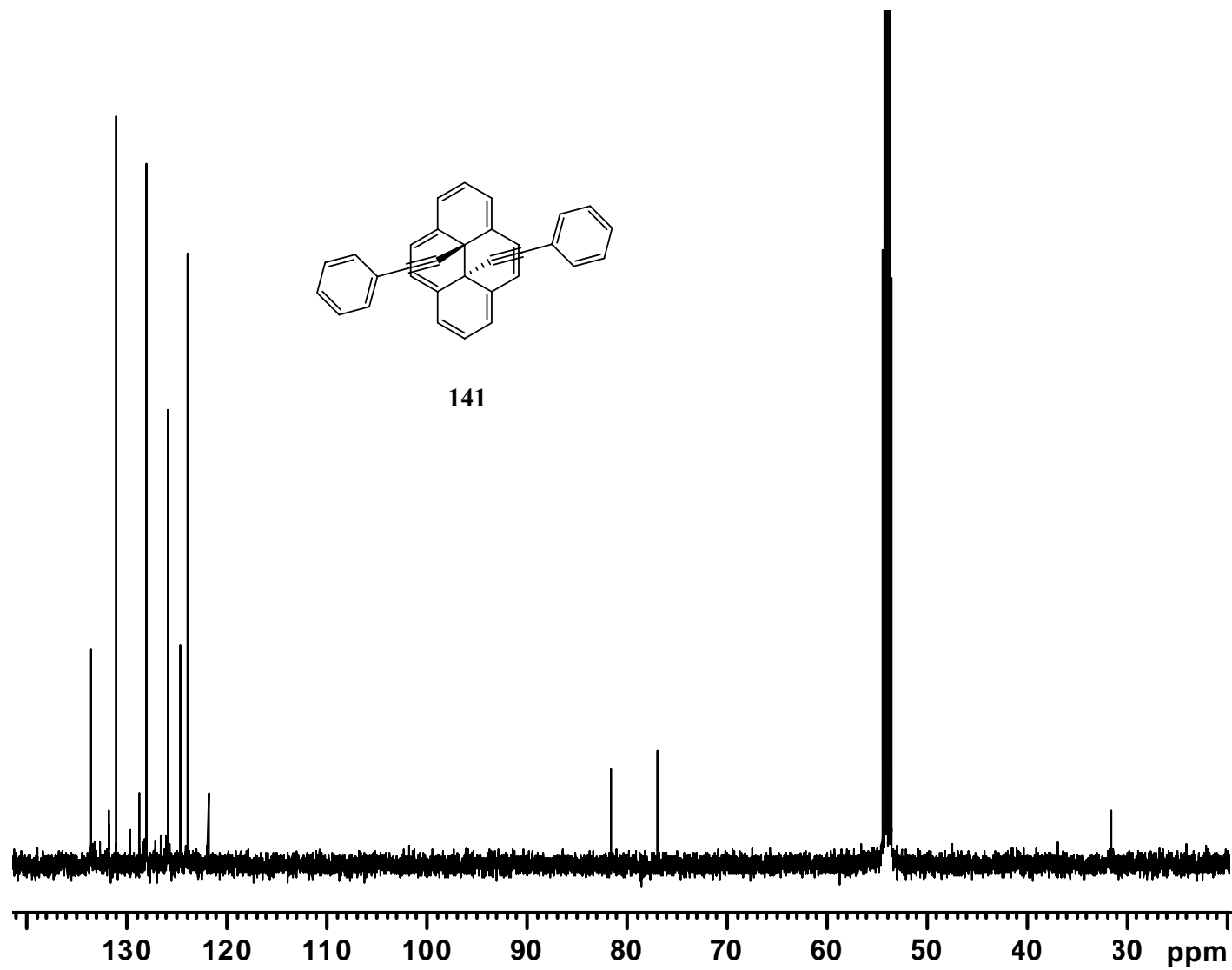


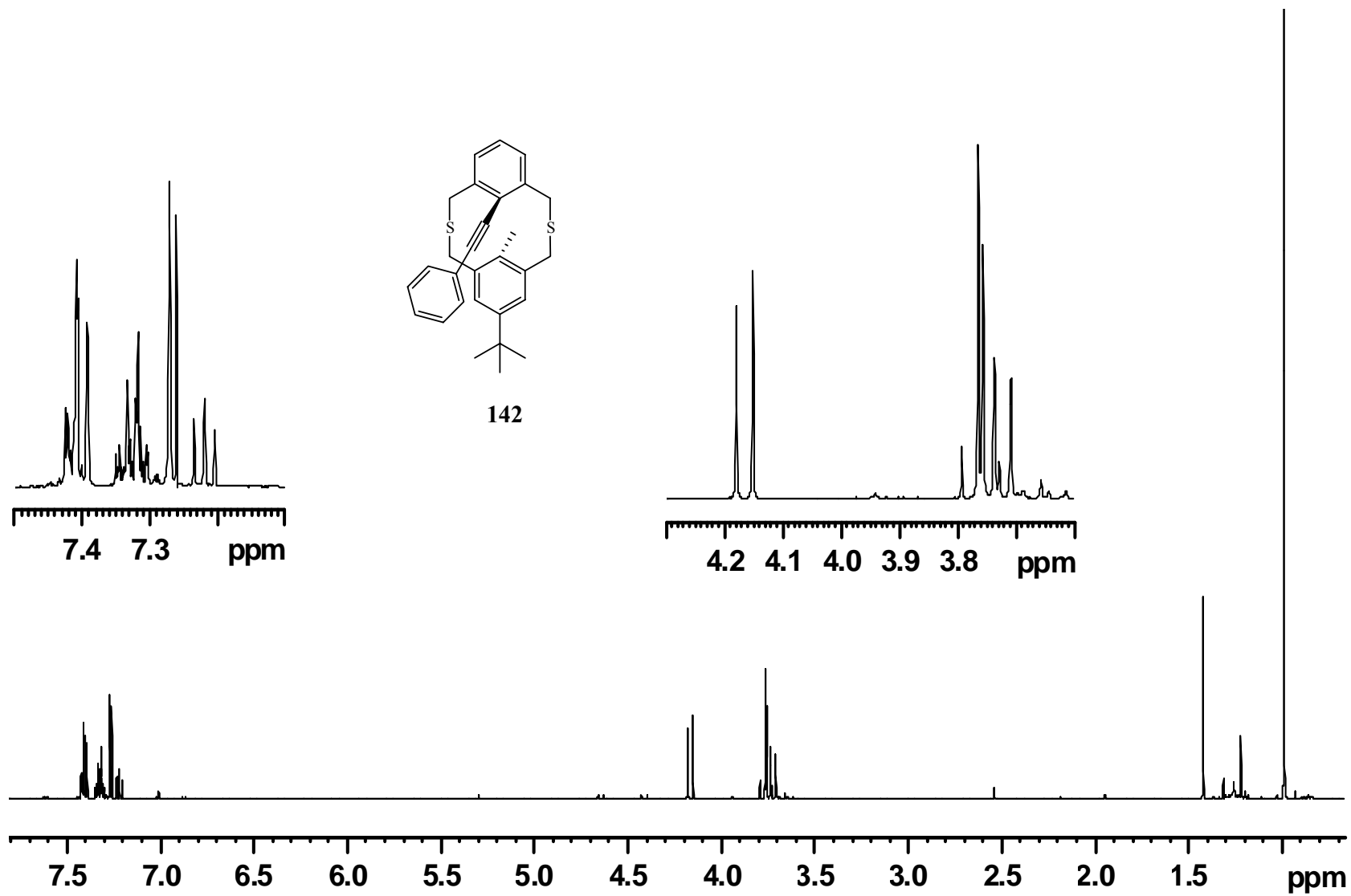


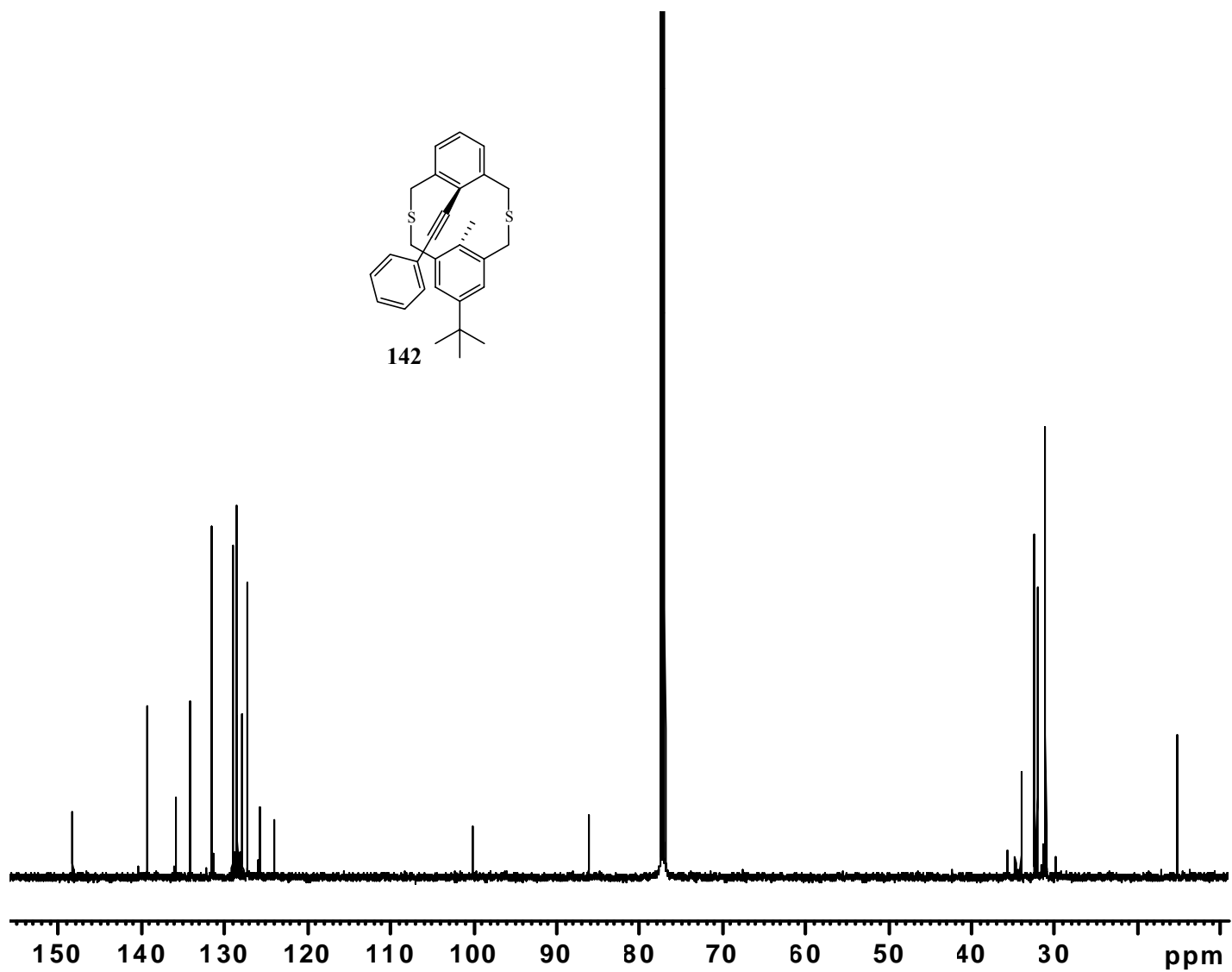
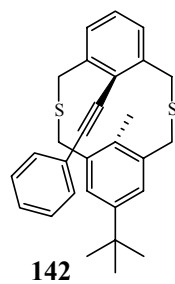


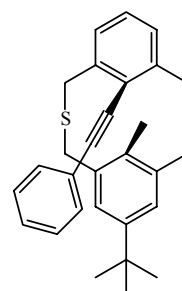
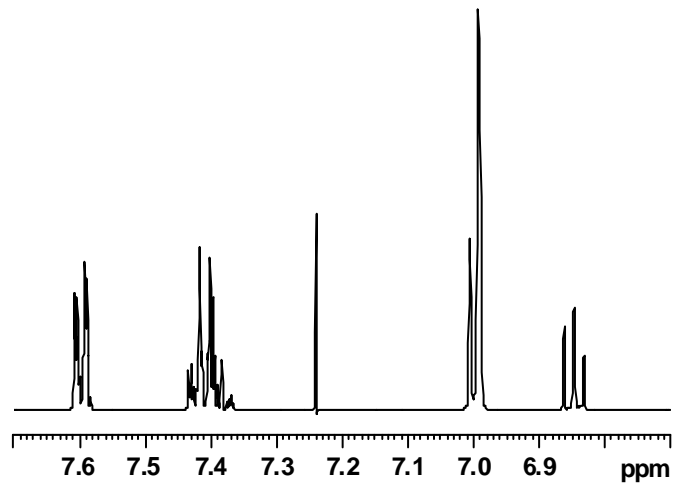
141



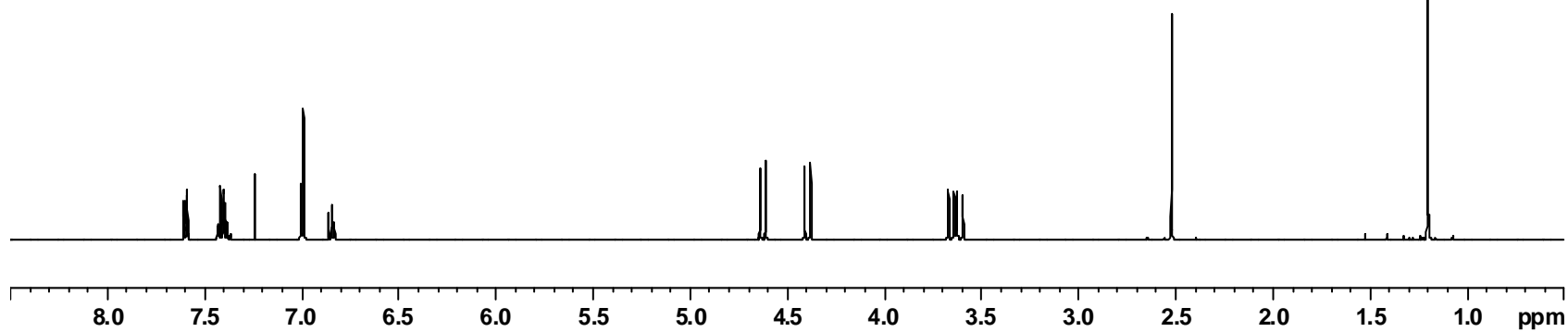
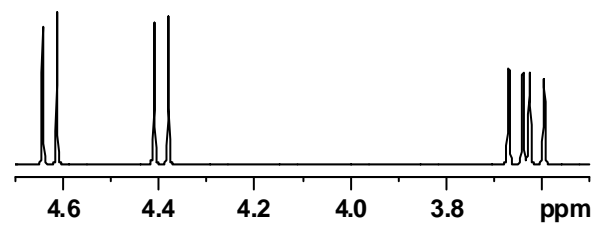


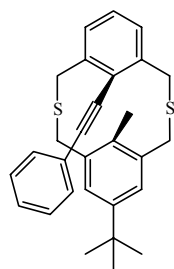




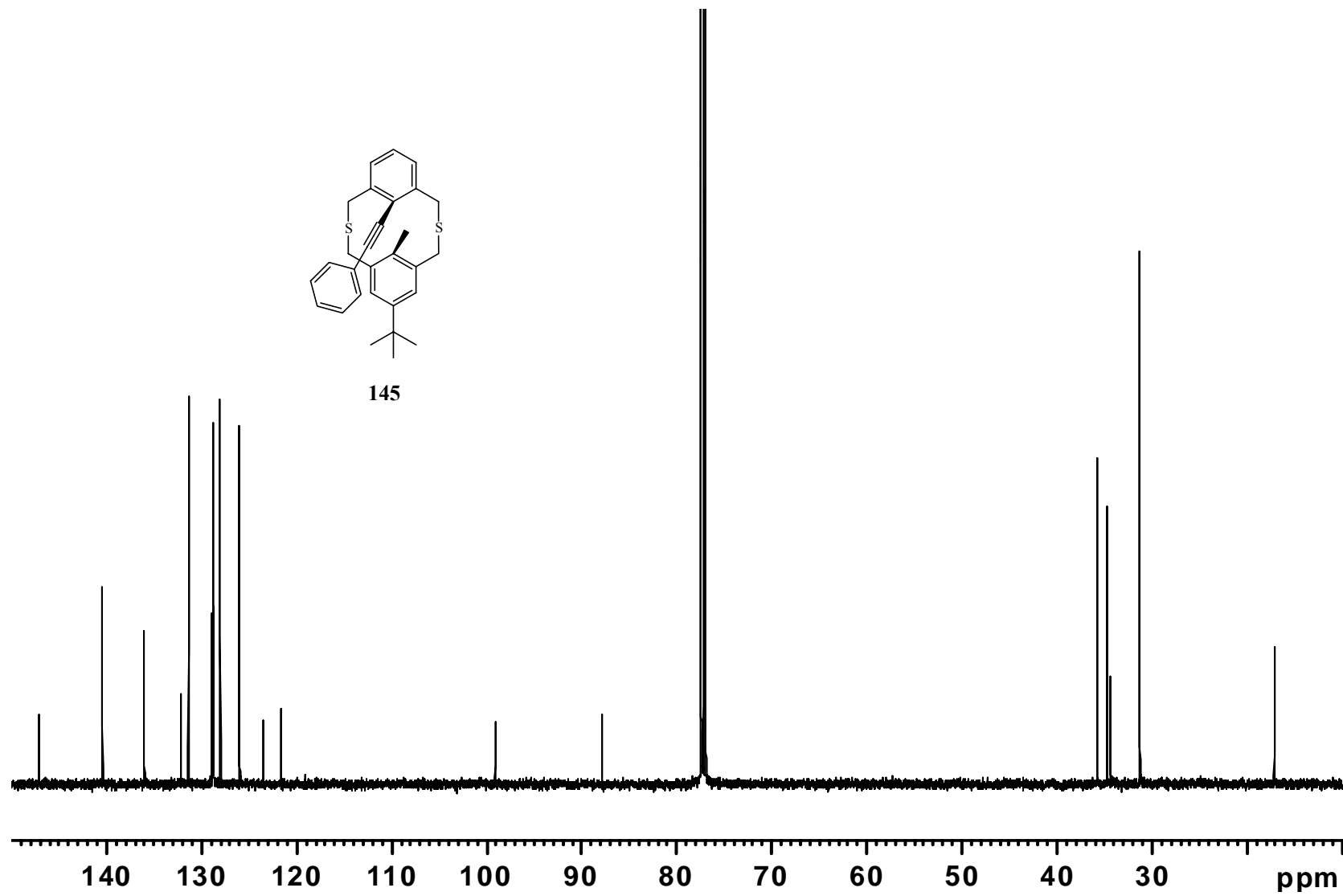


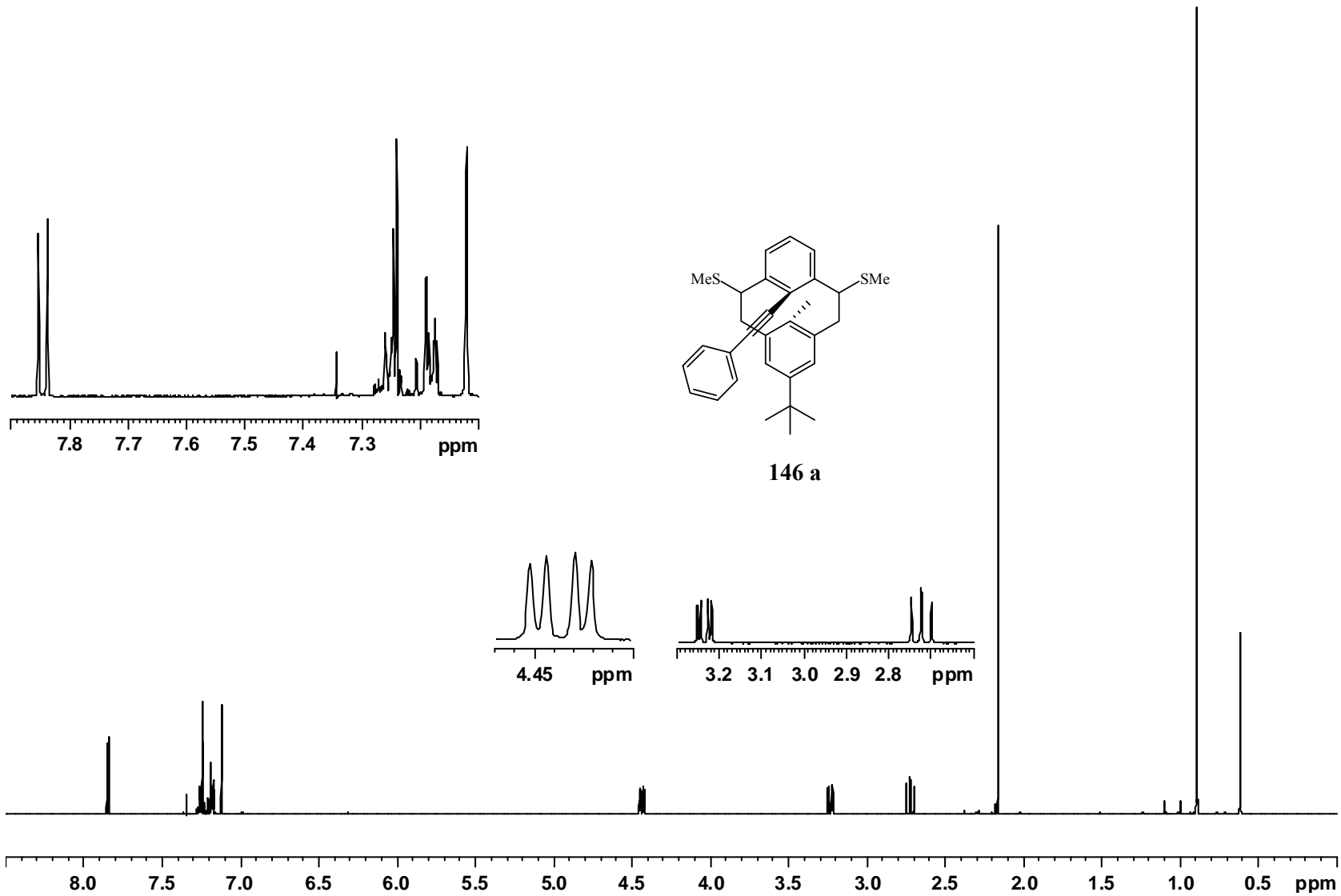
145

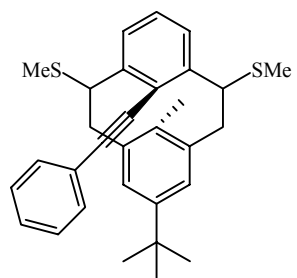
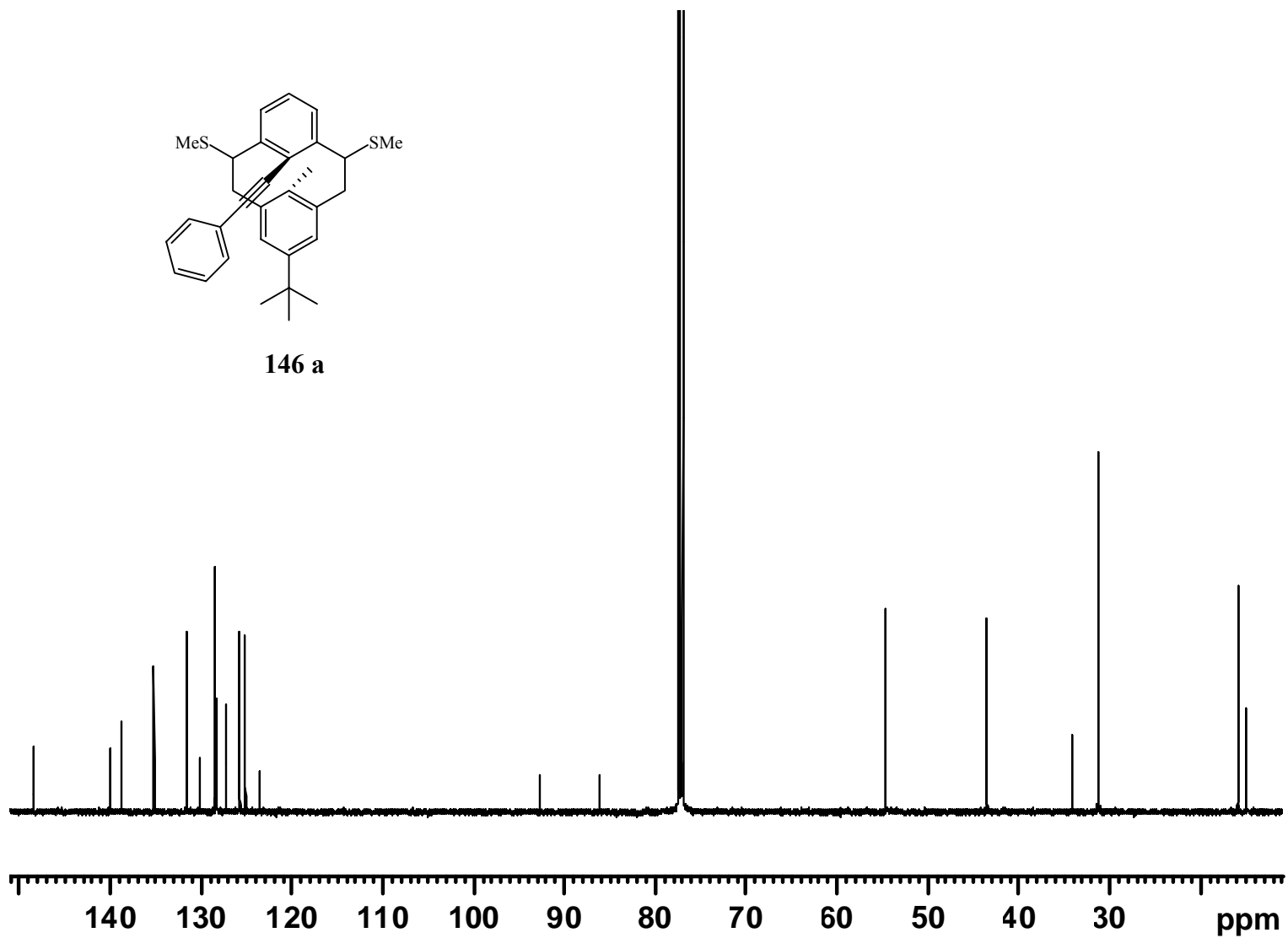


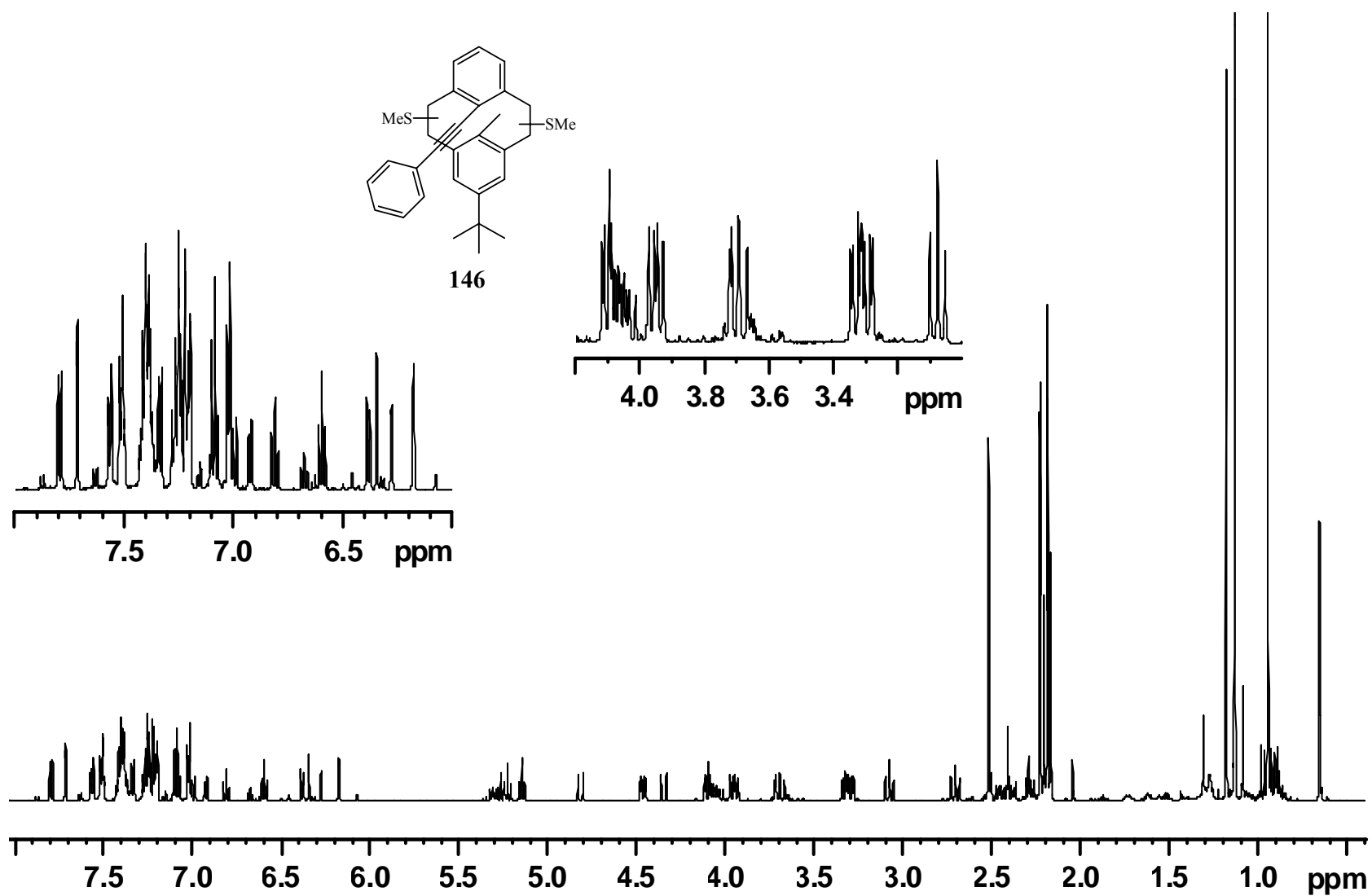


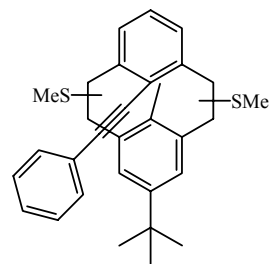
145



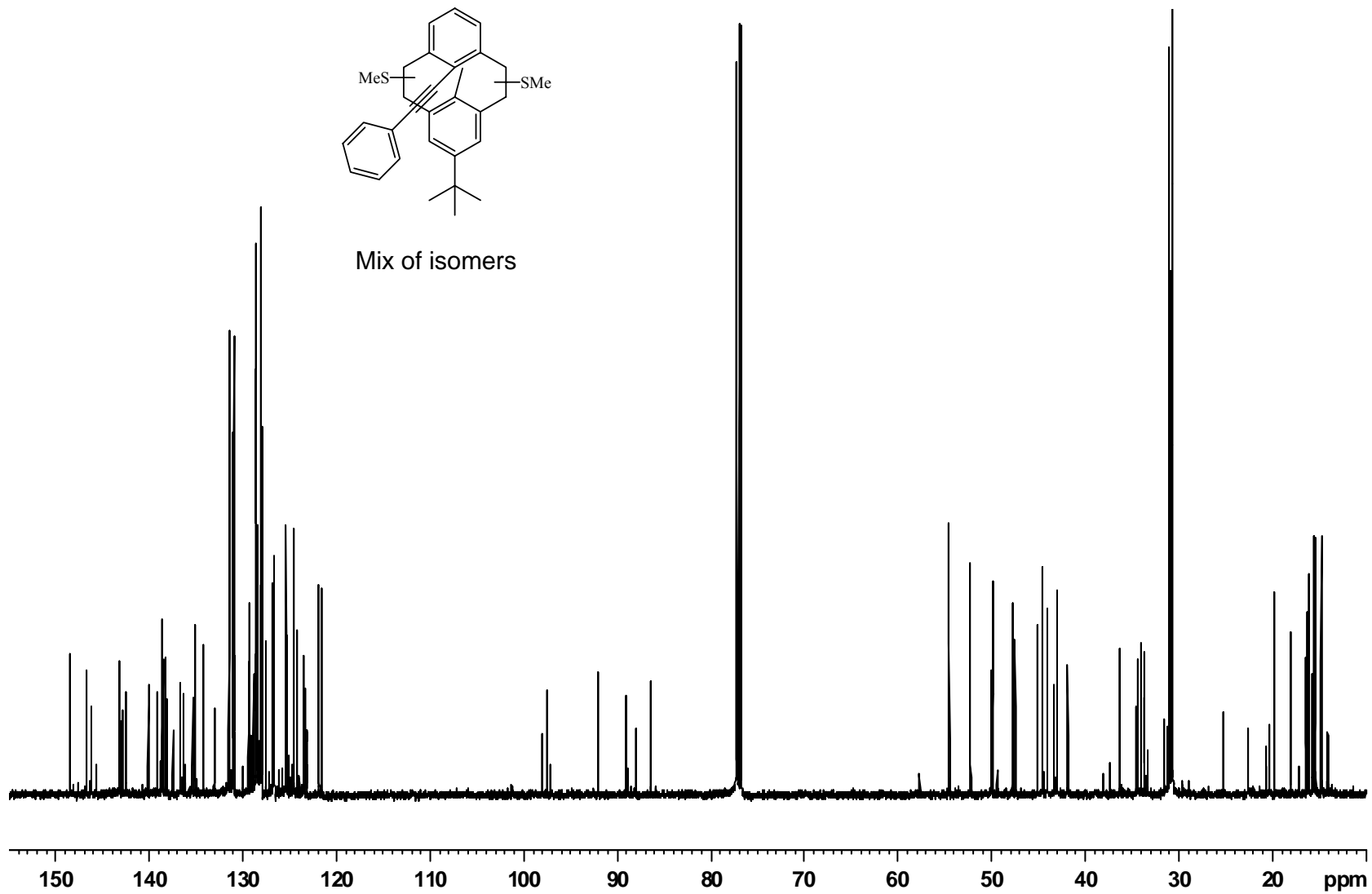


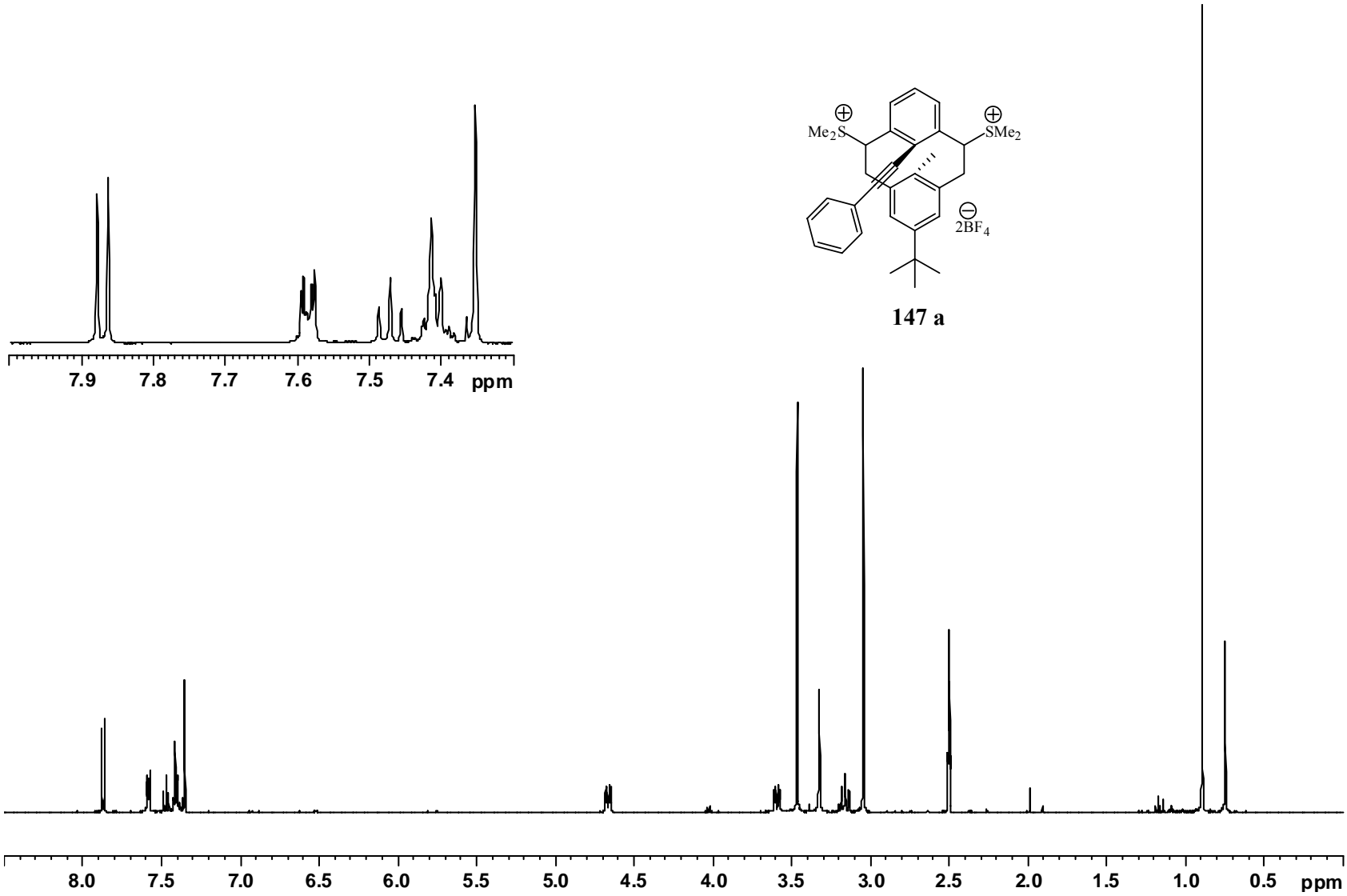
**146 a**

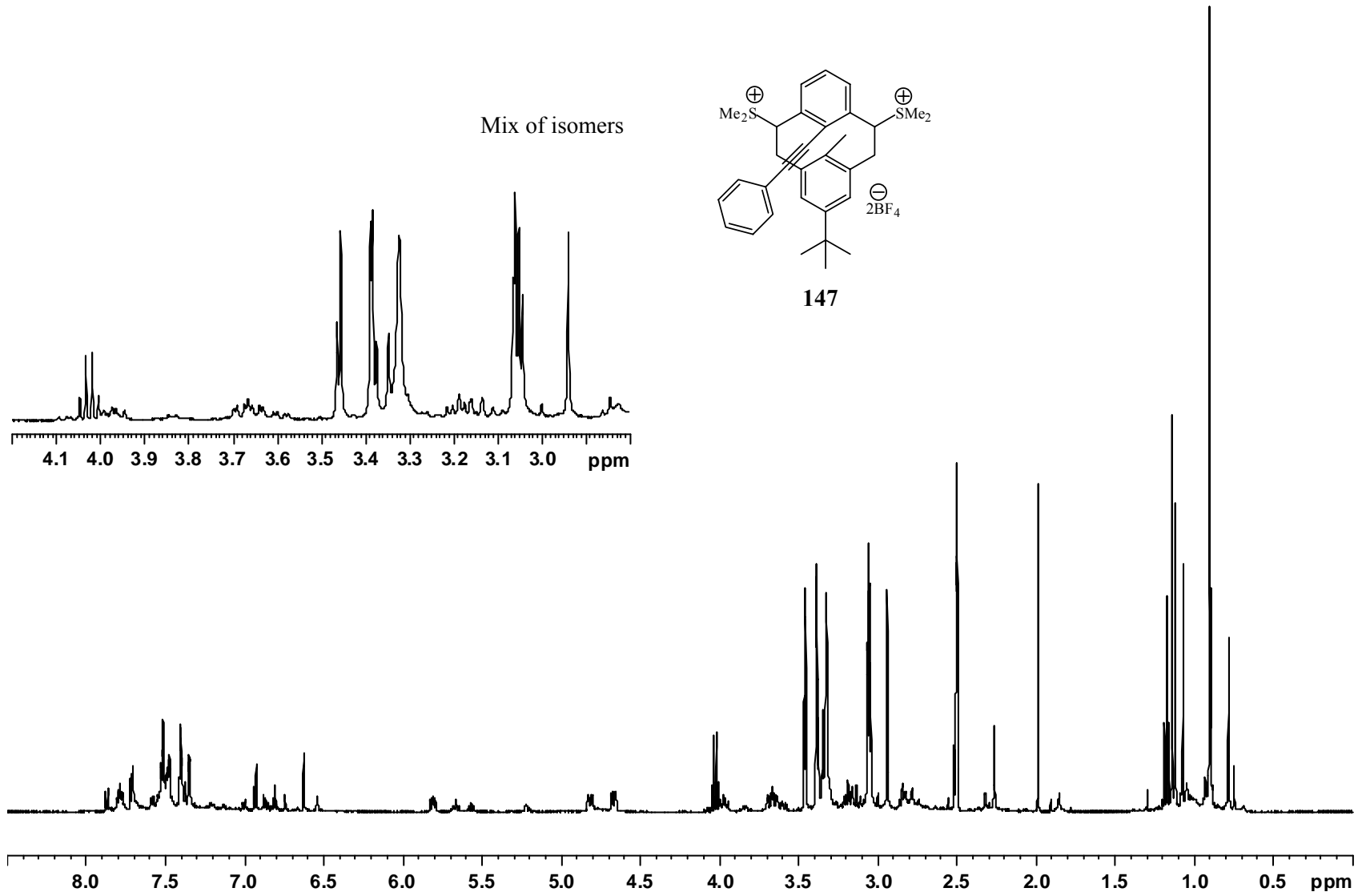


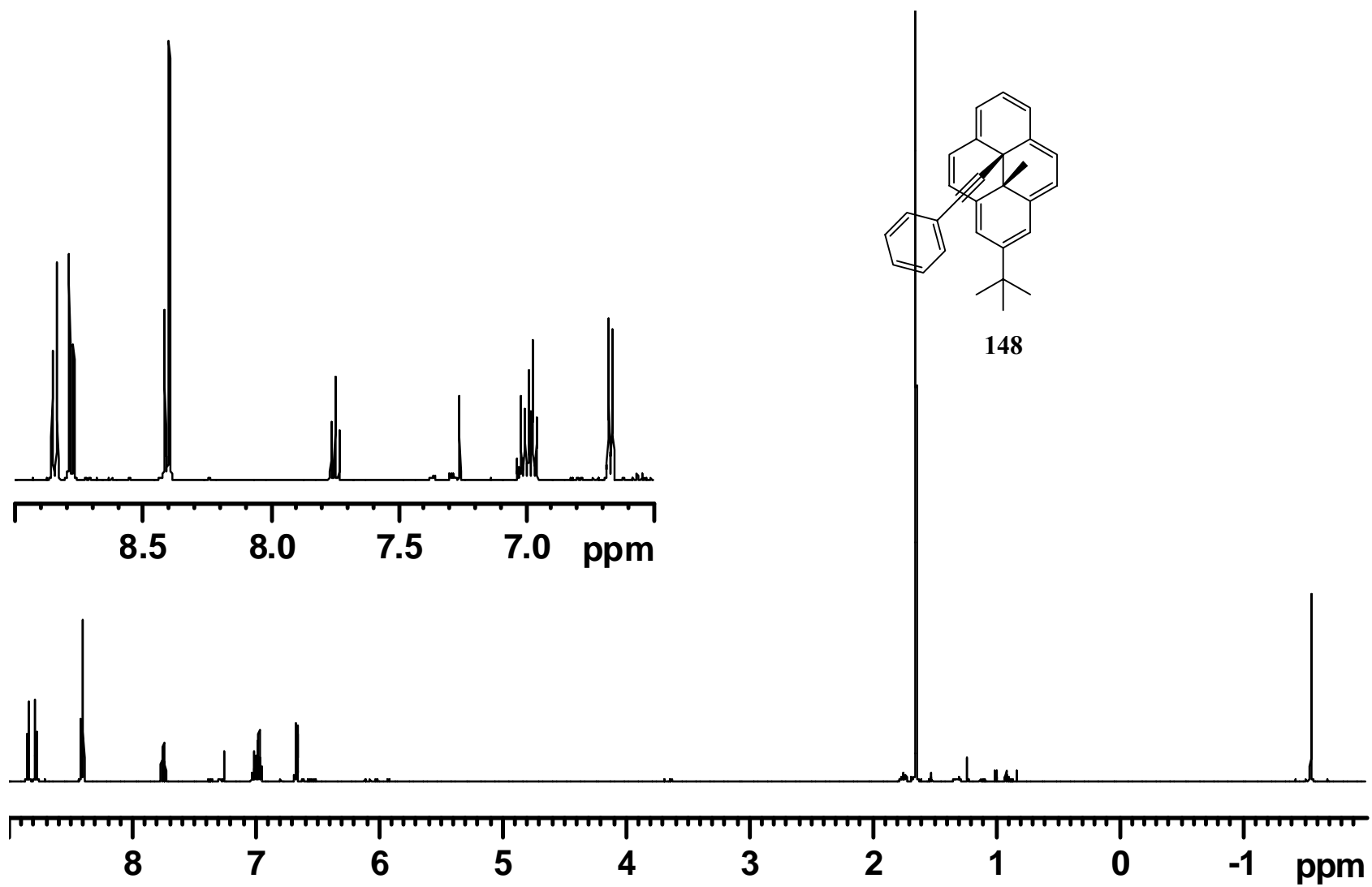


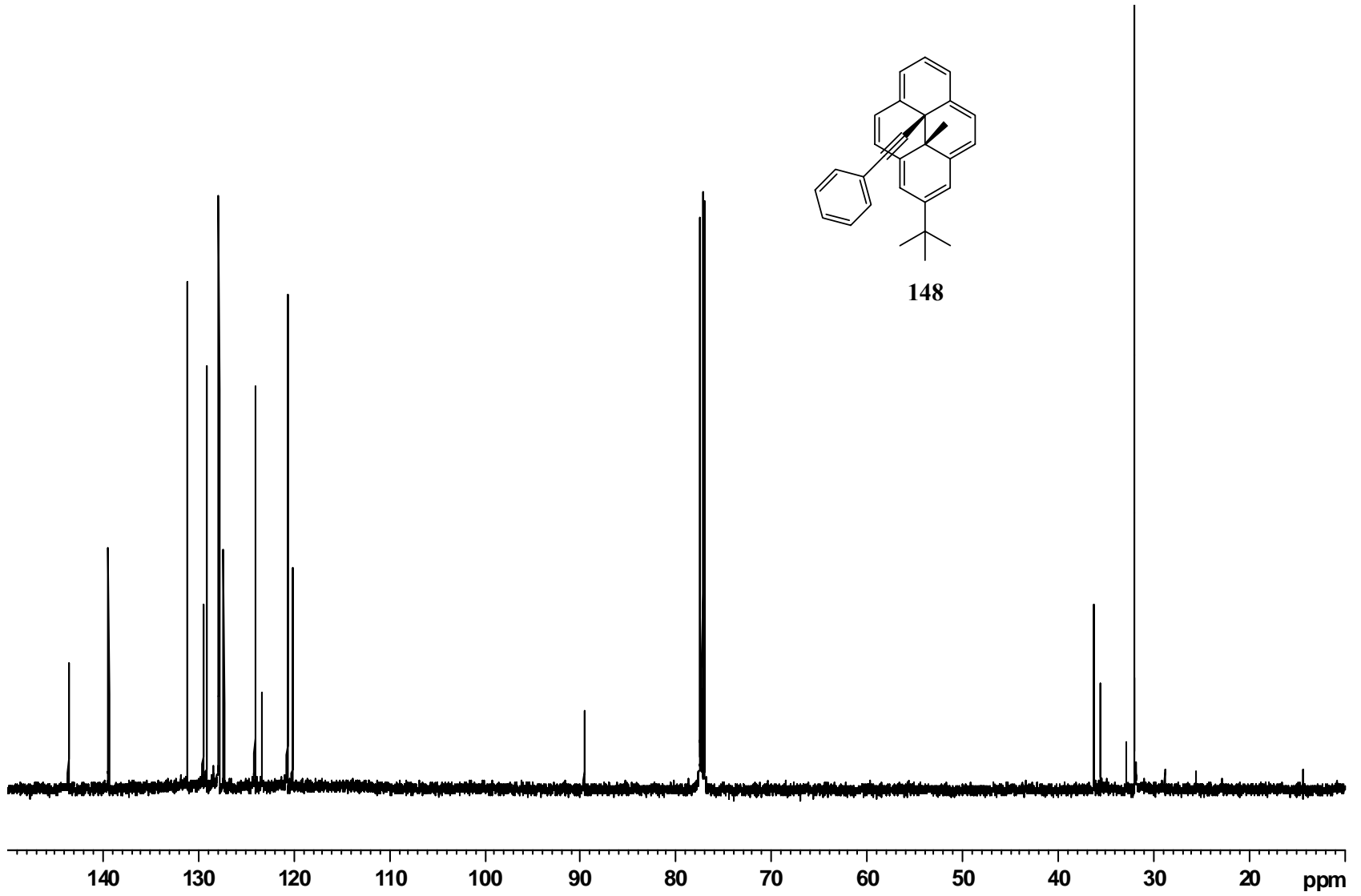
Mix of isomers

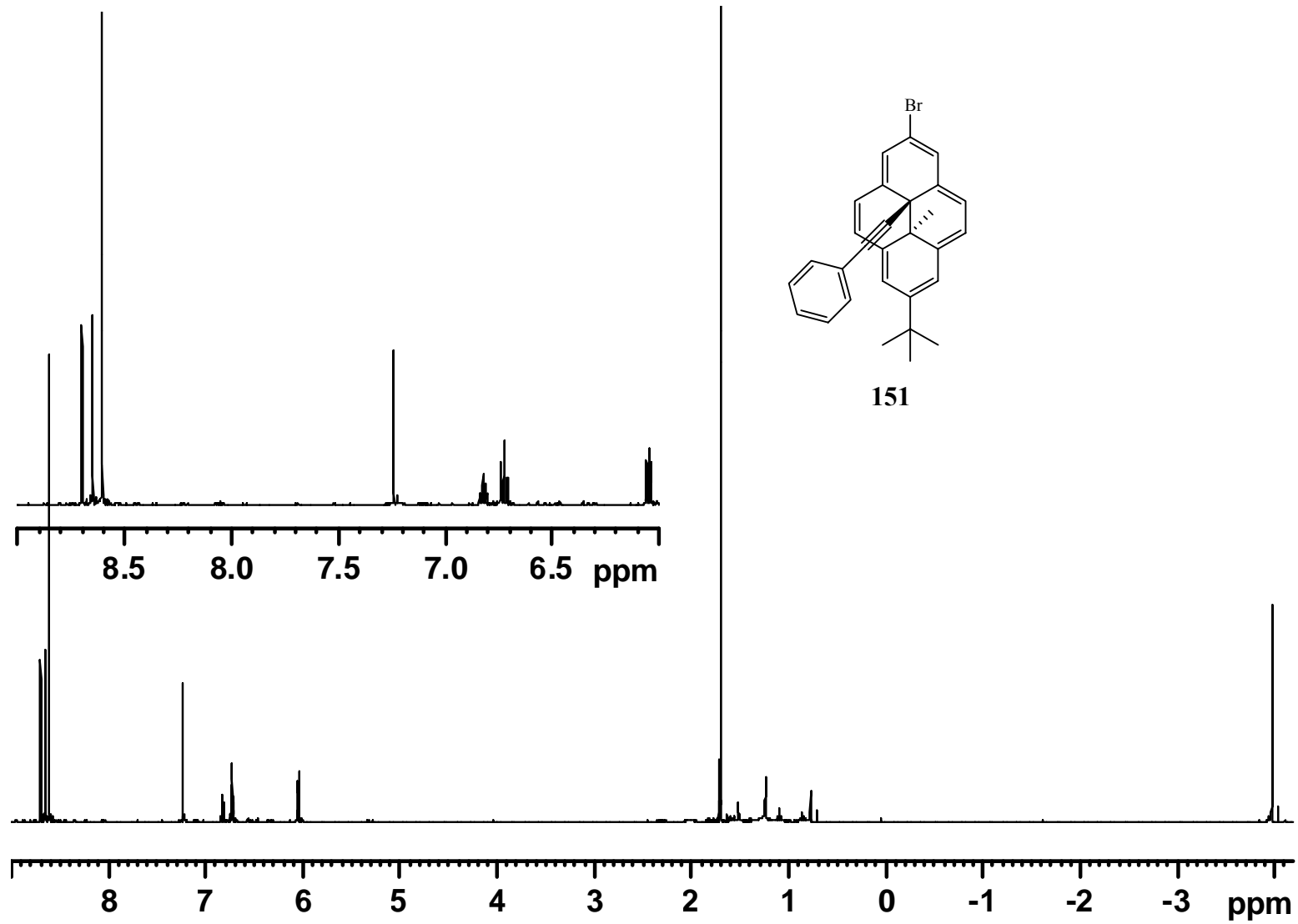


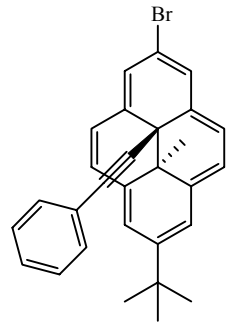




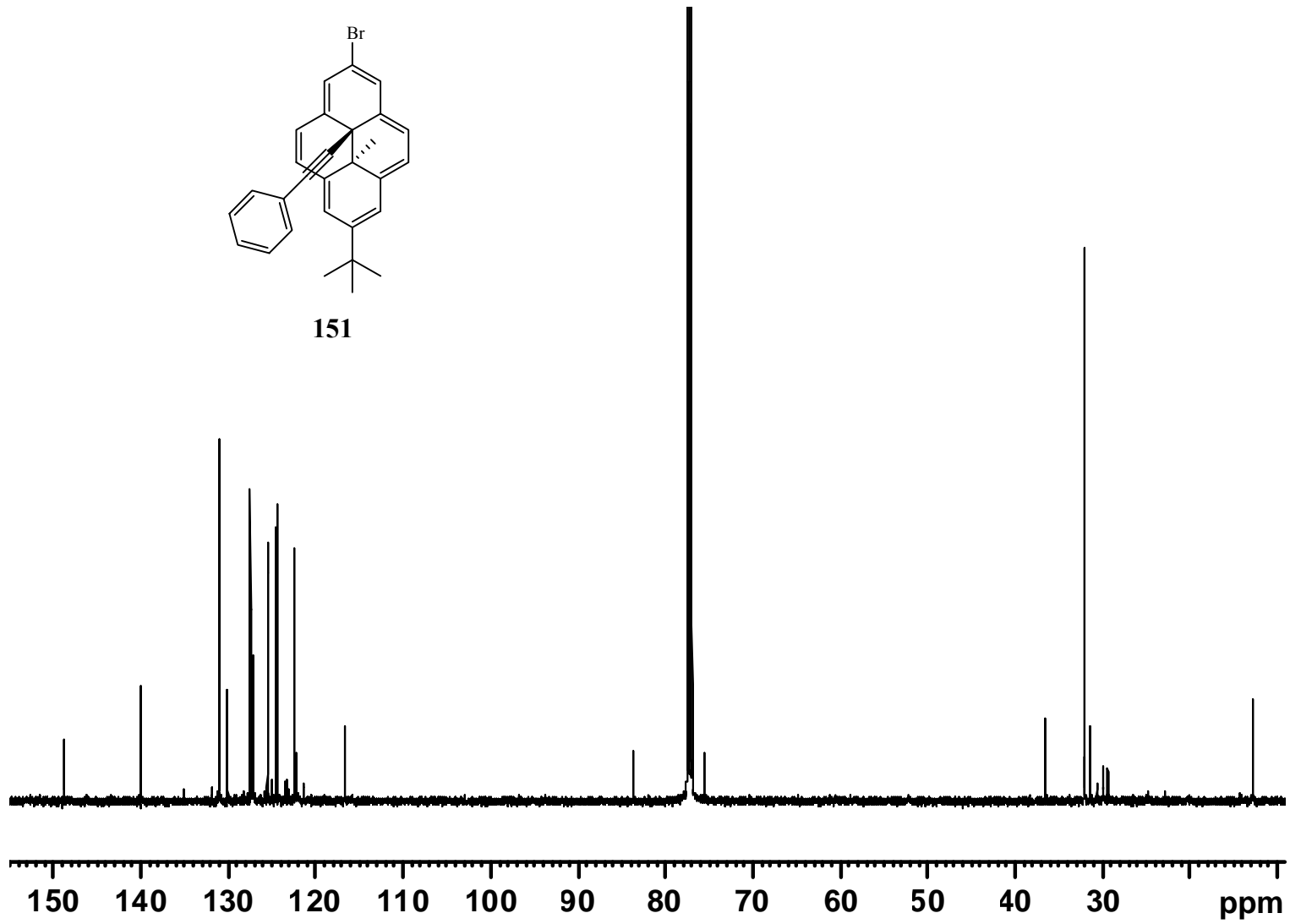


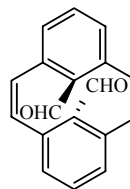




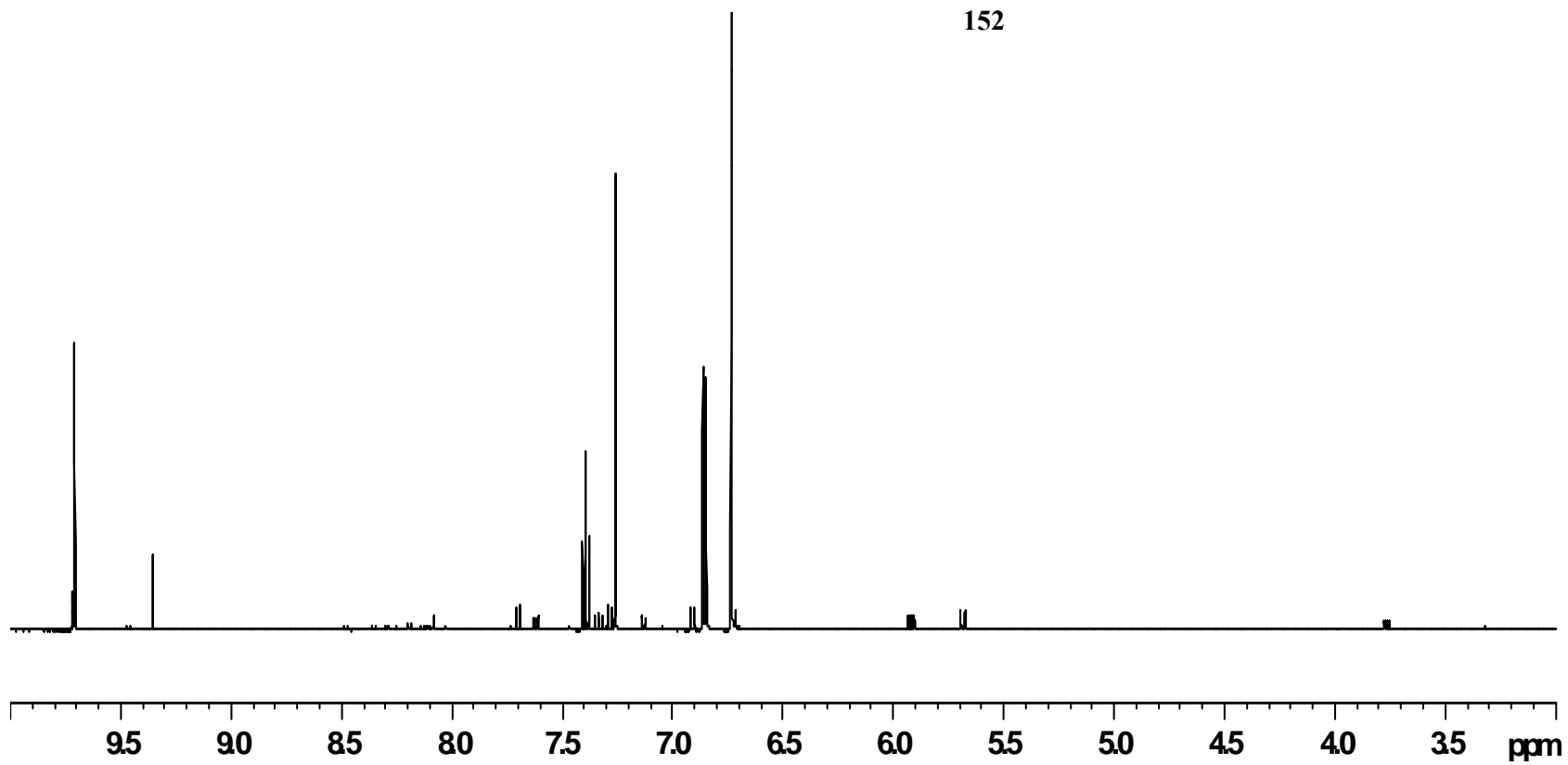


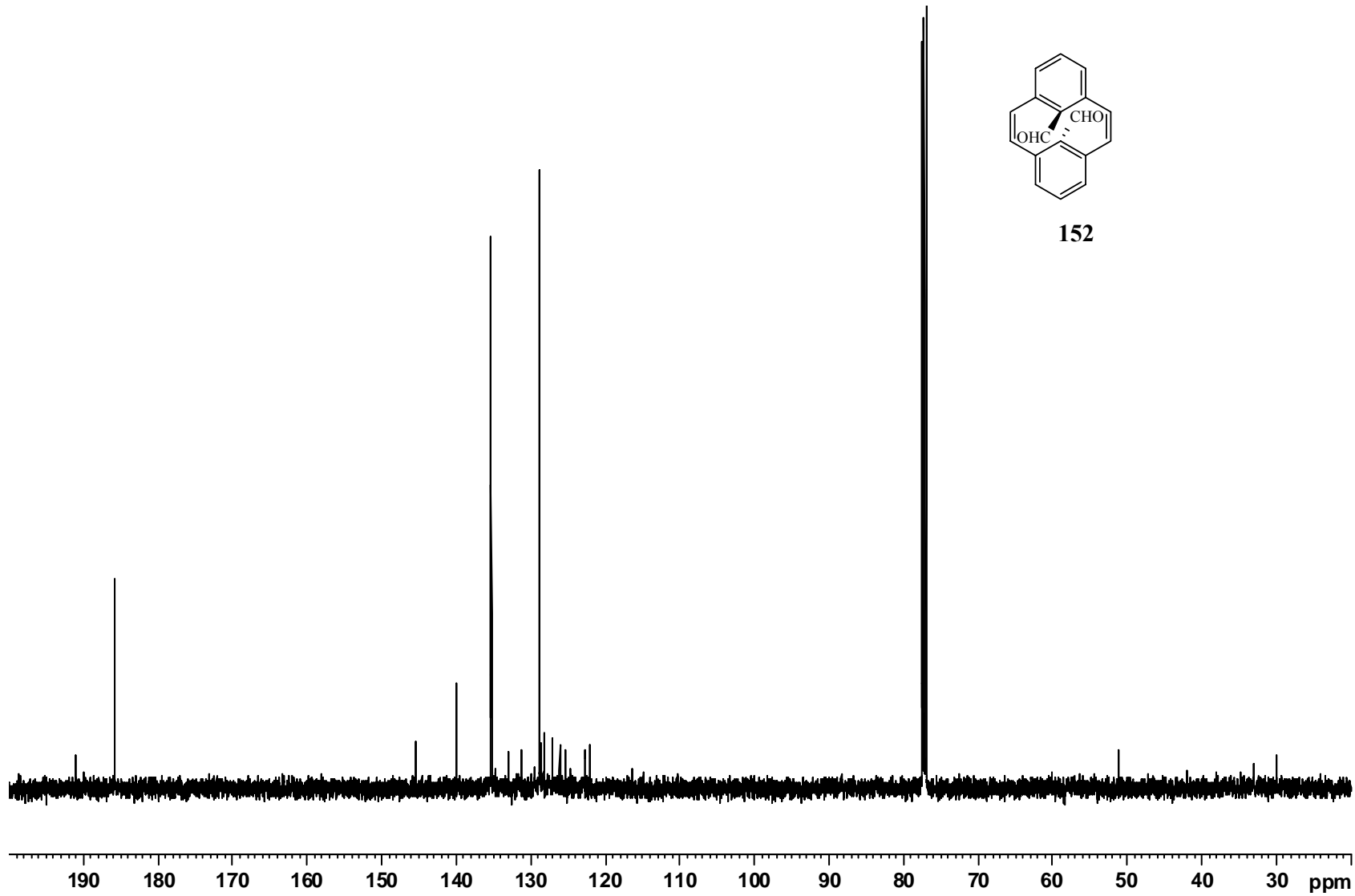
151

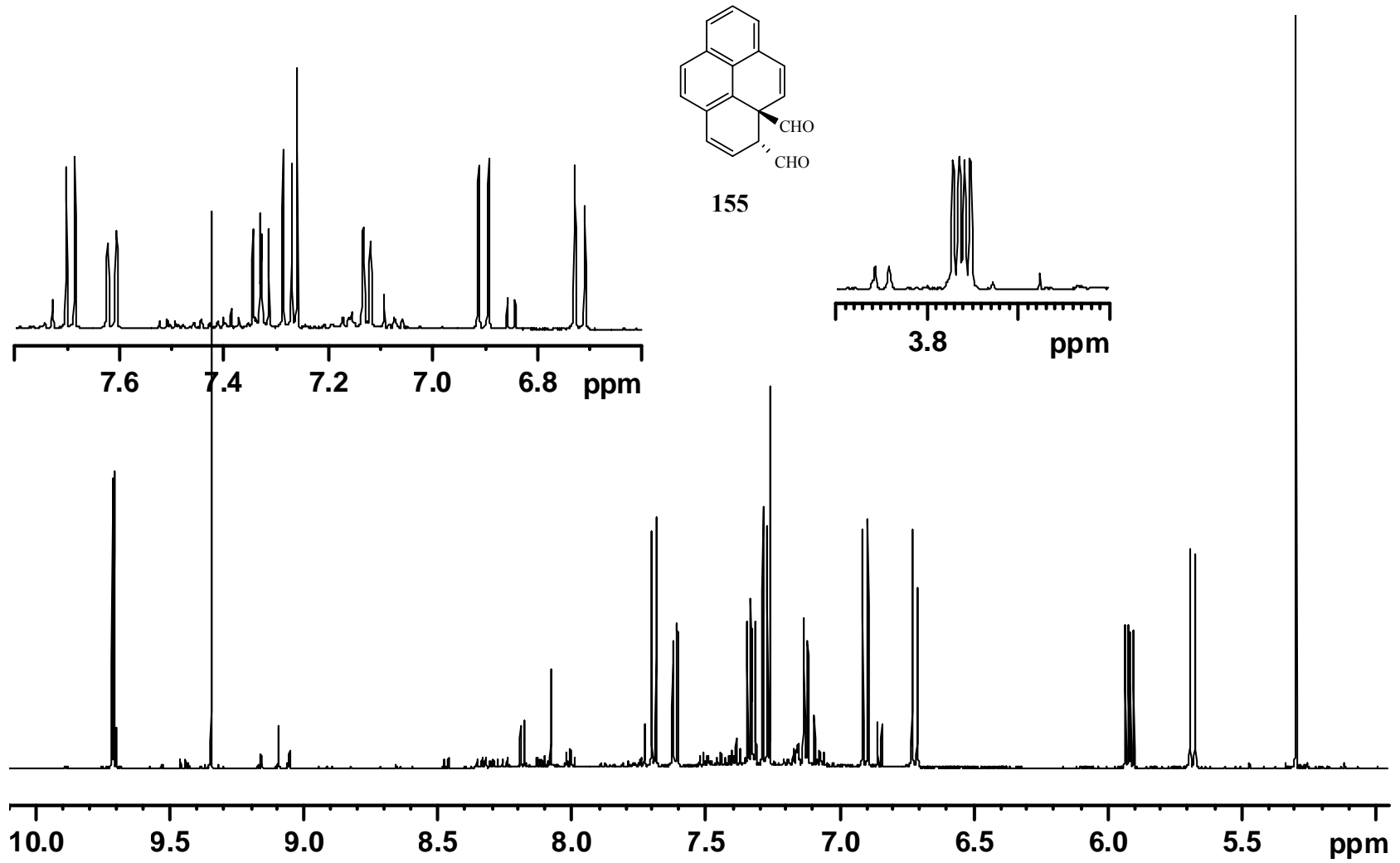


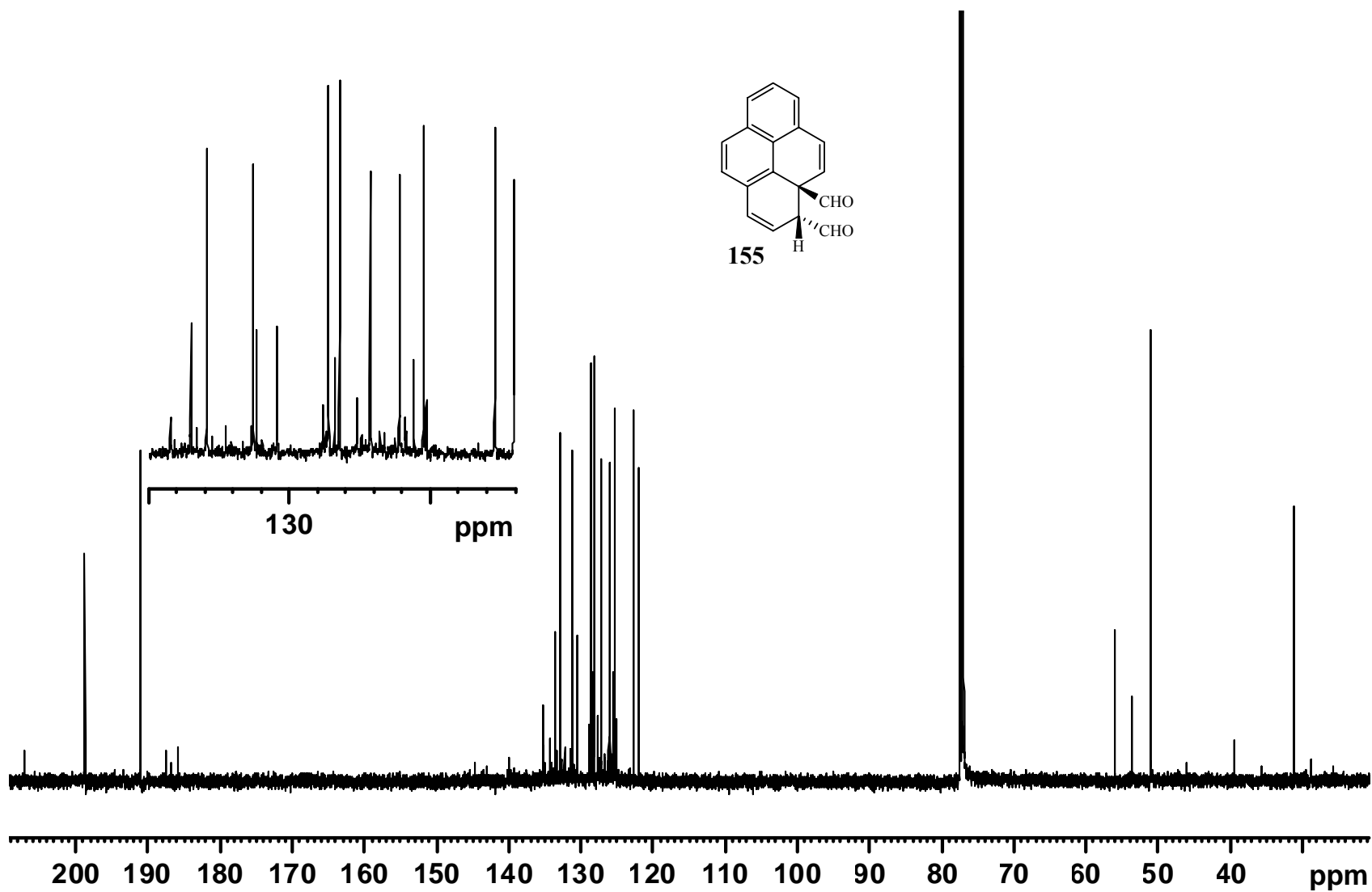


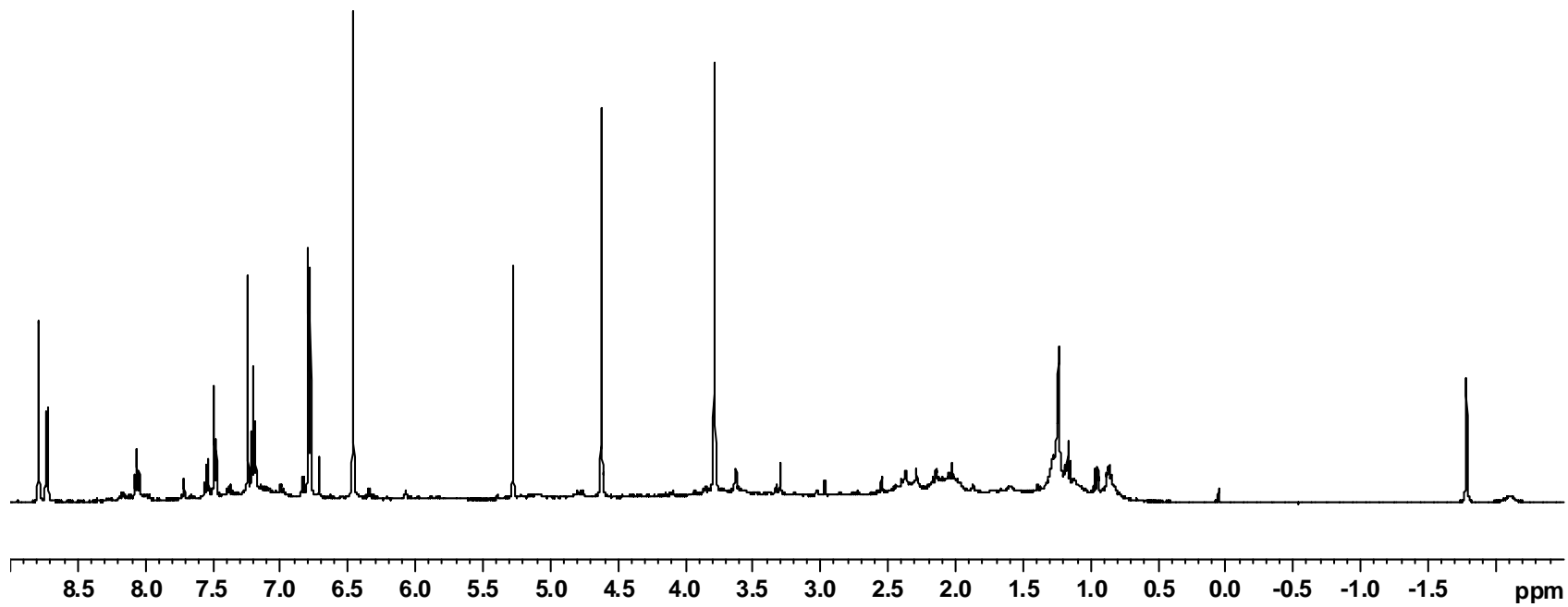
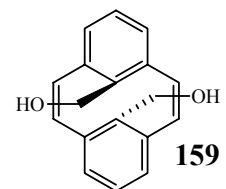
152

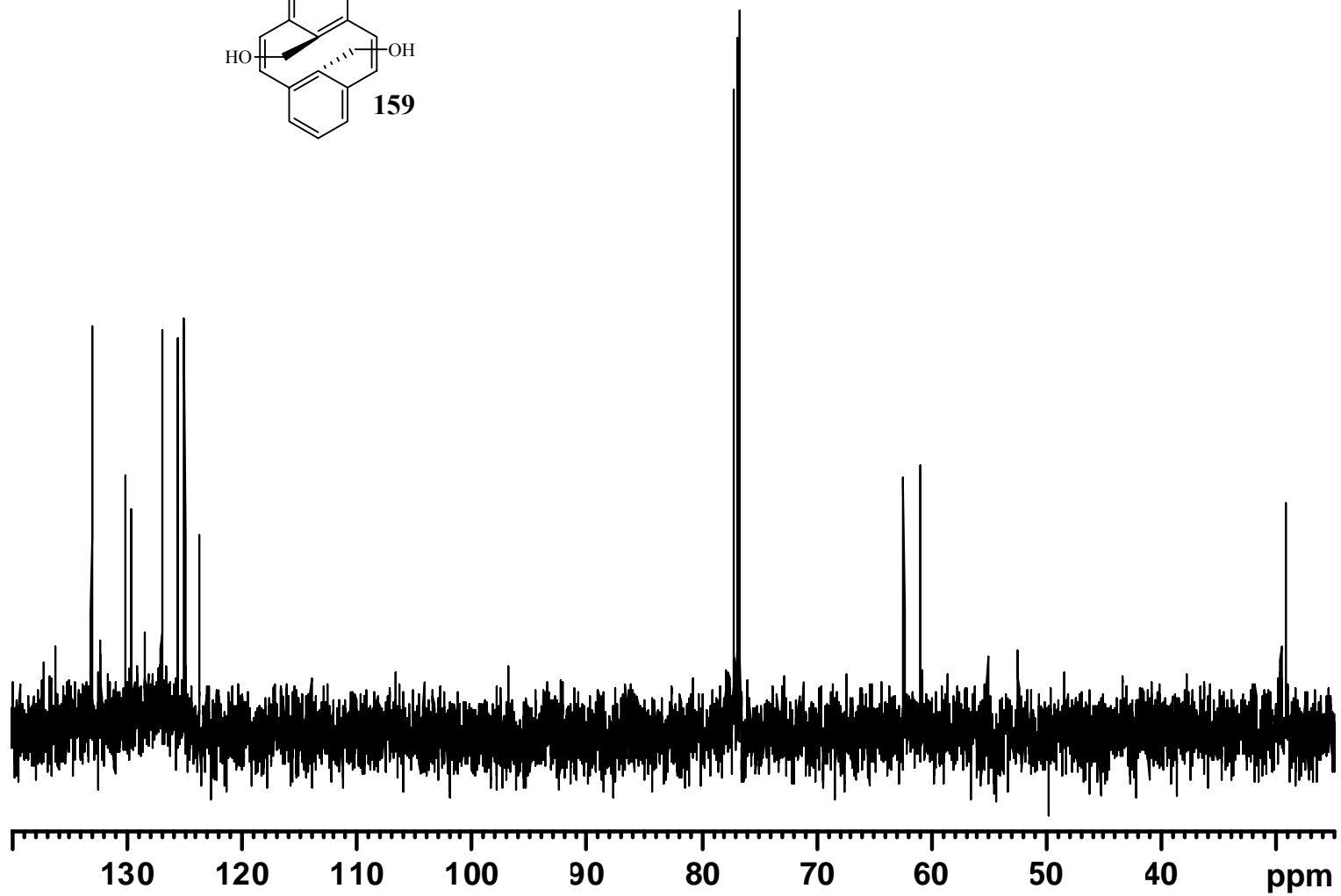
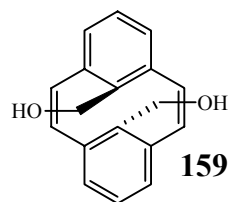


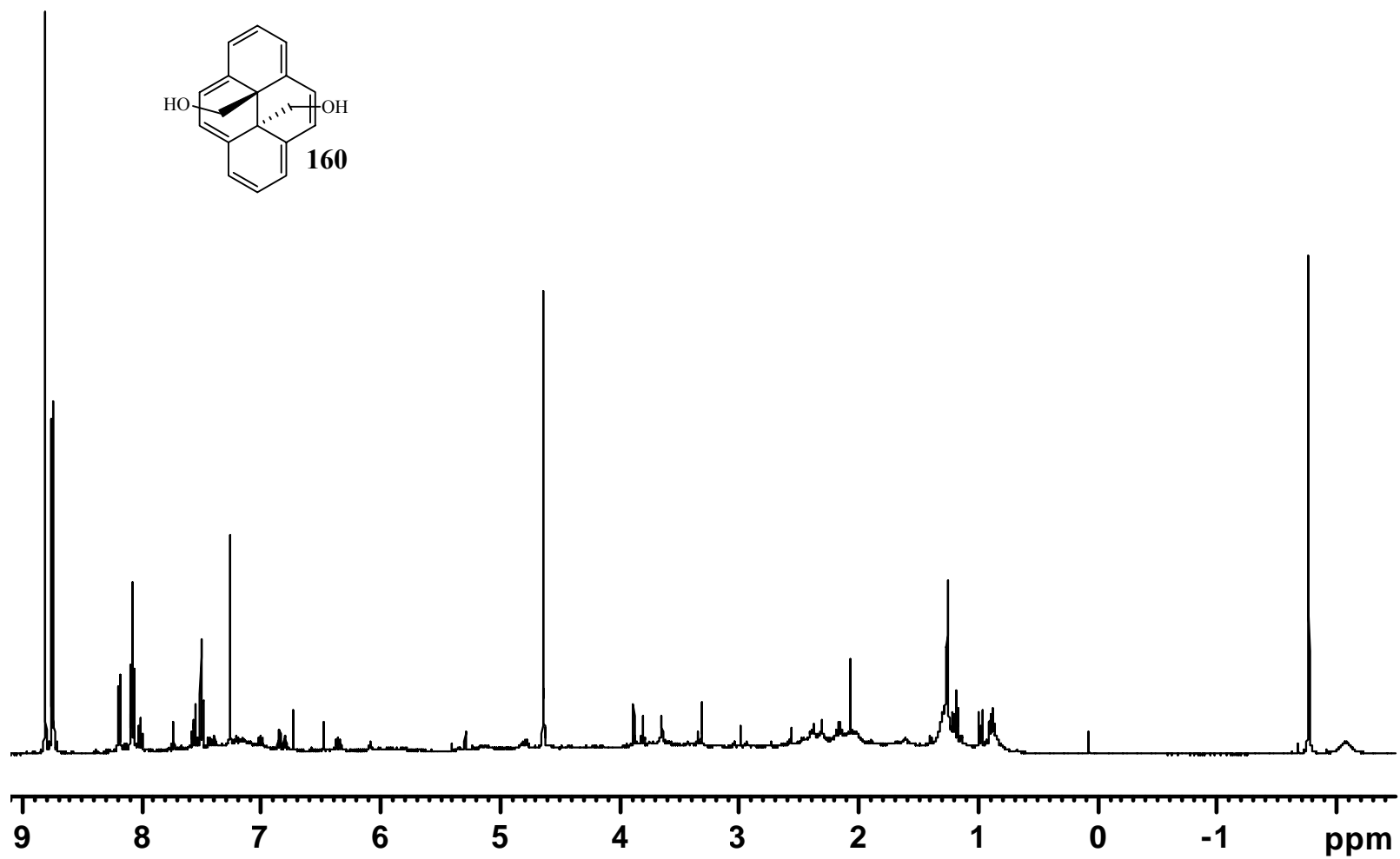


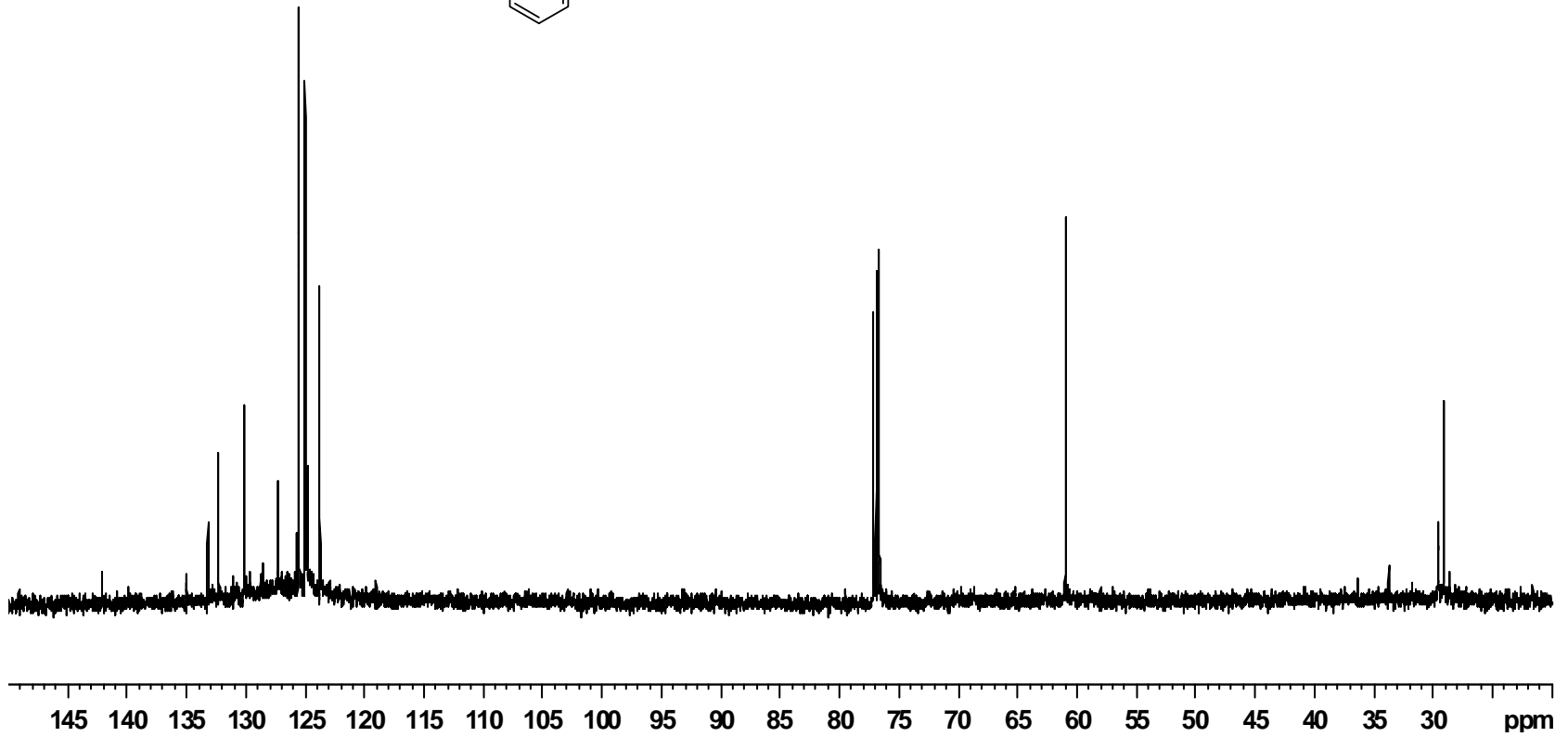
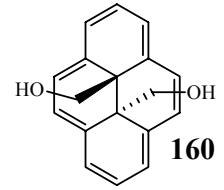


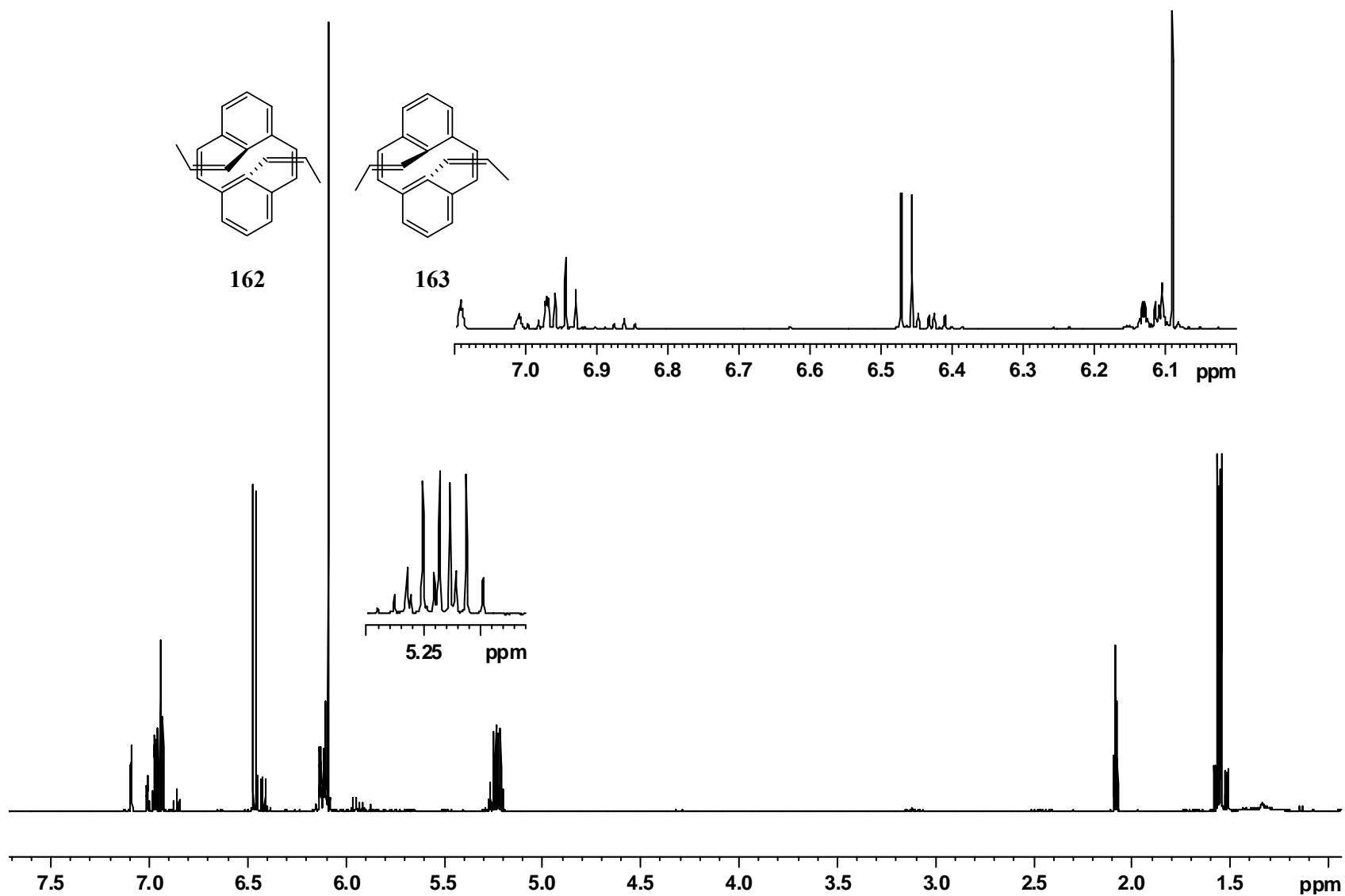


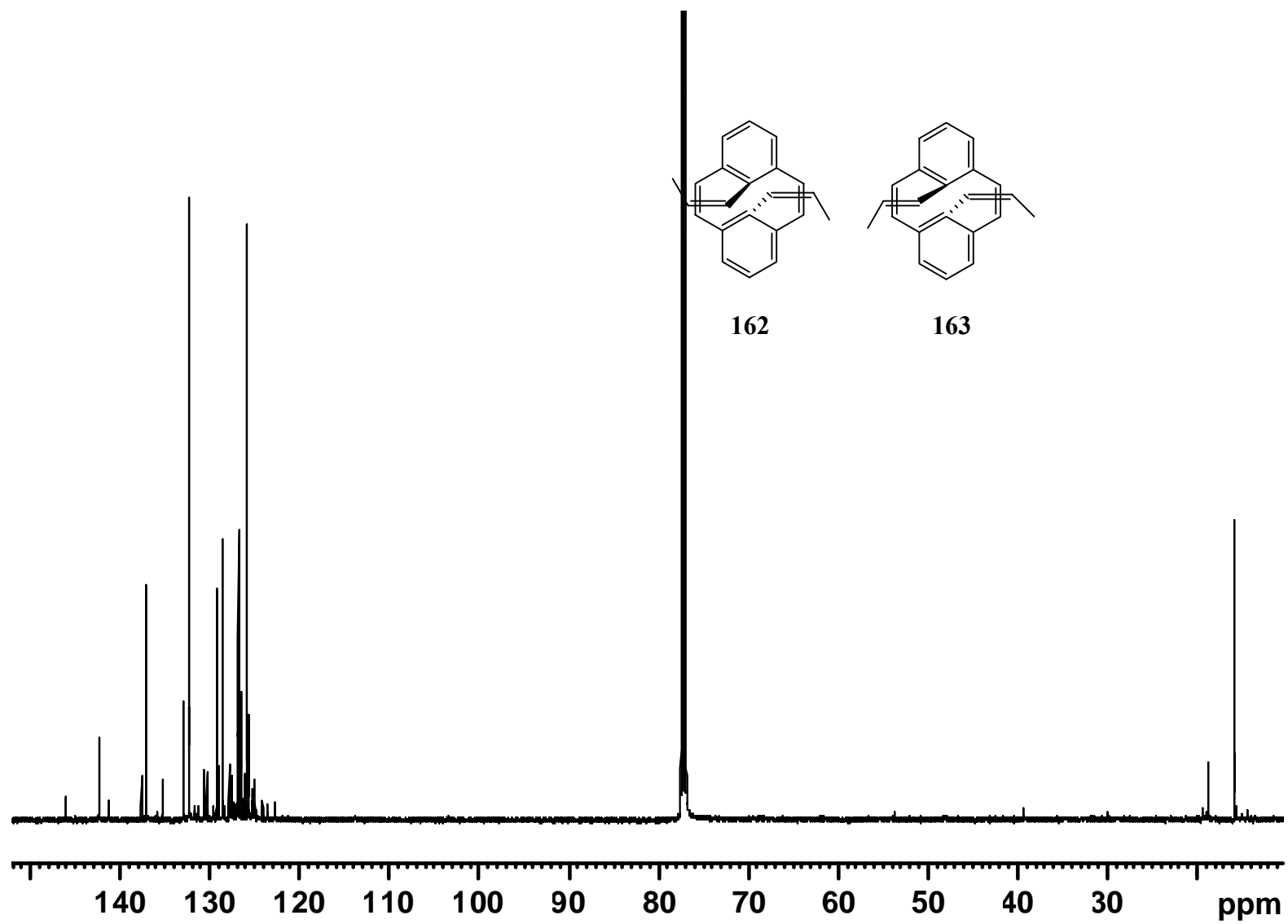


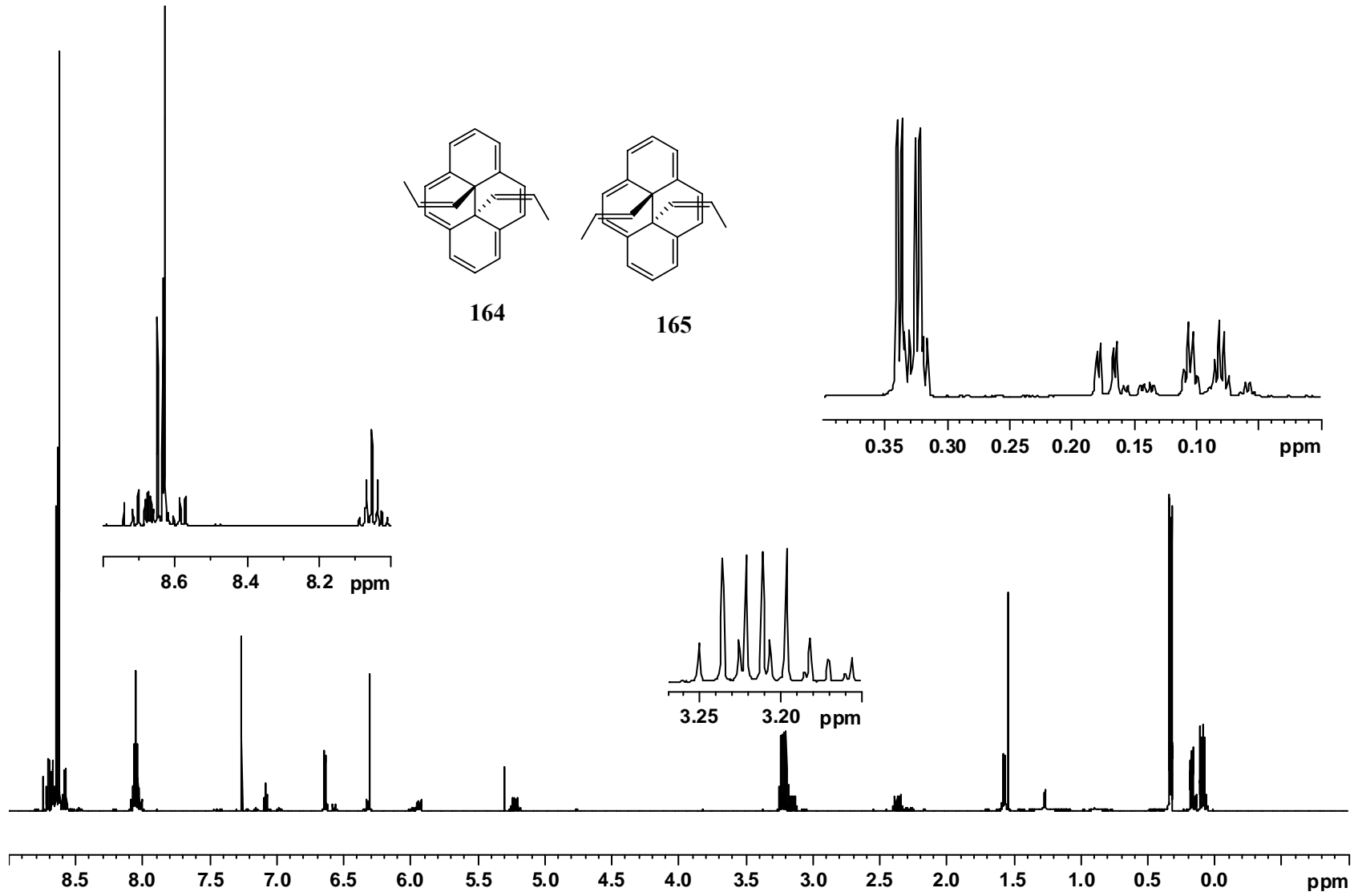


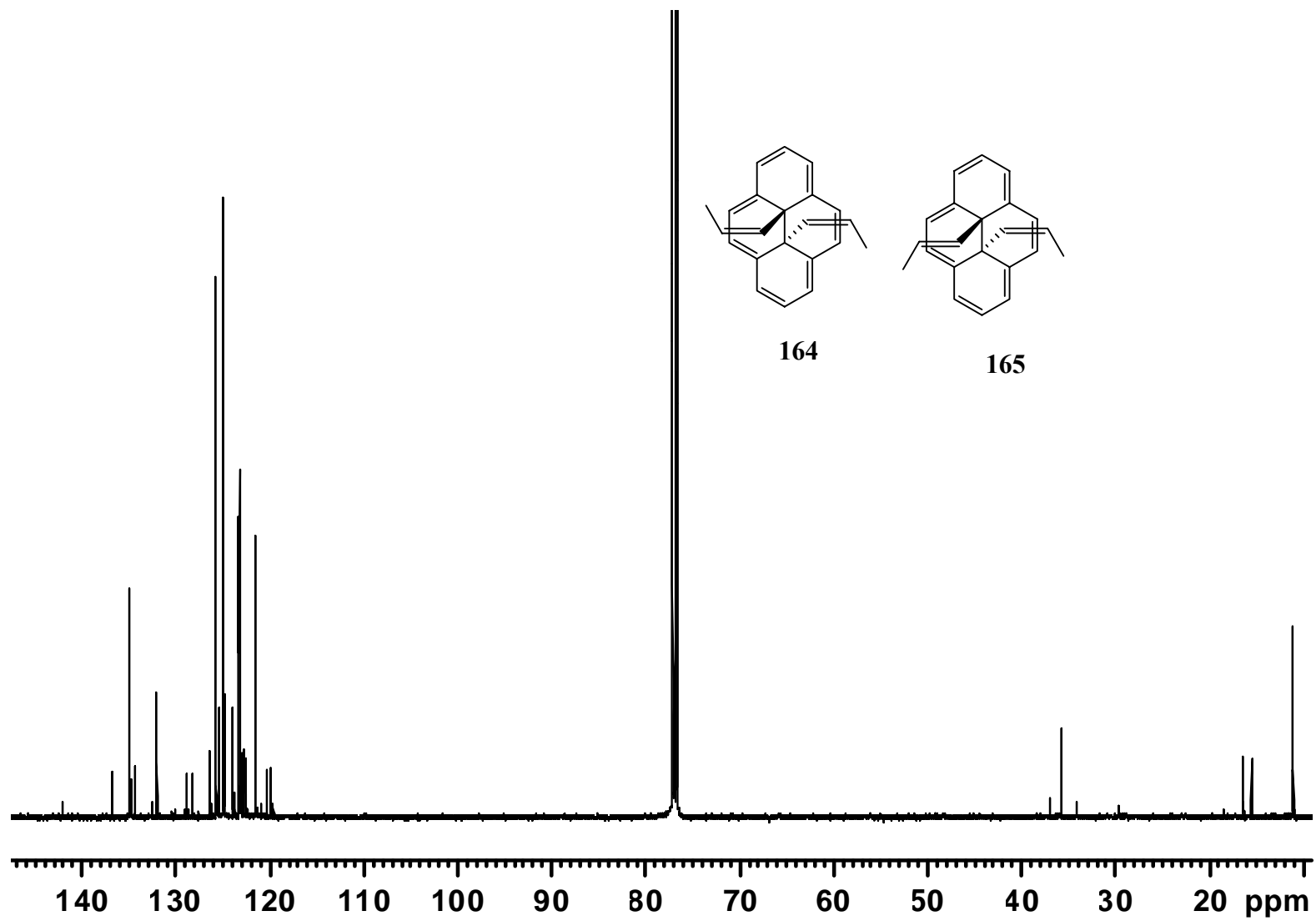


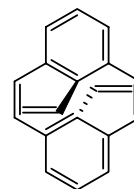




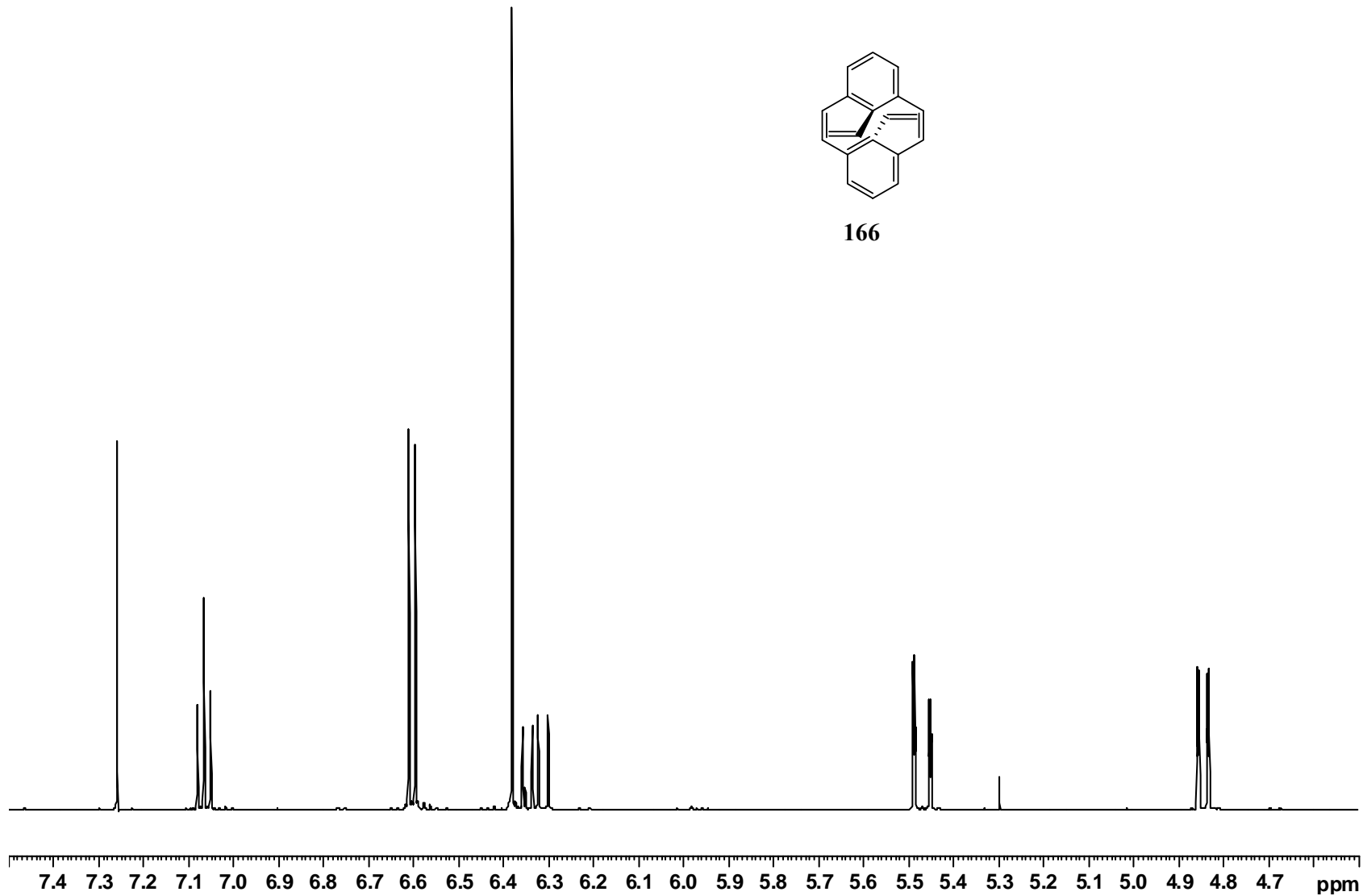


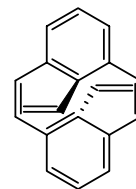




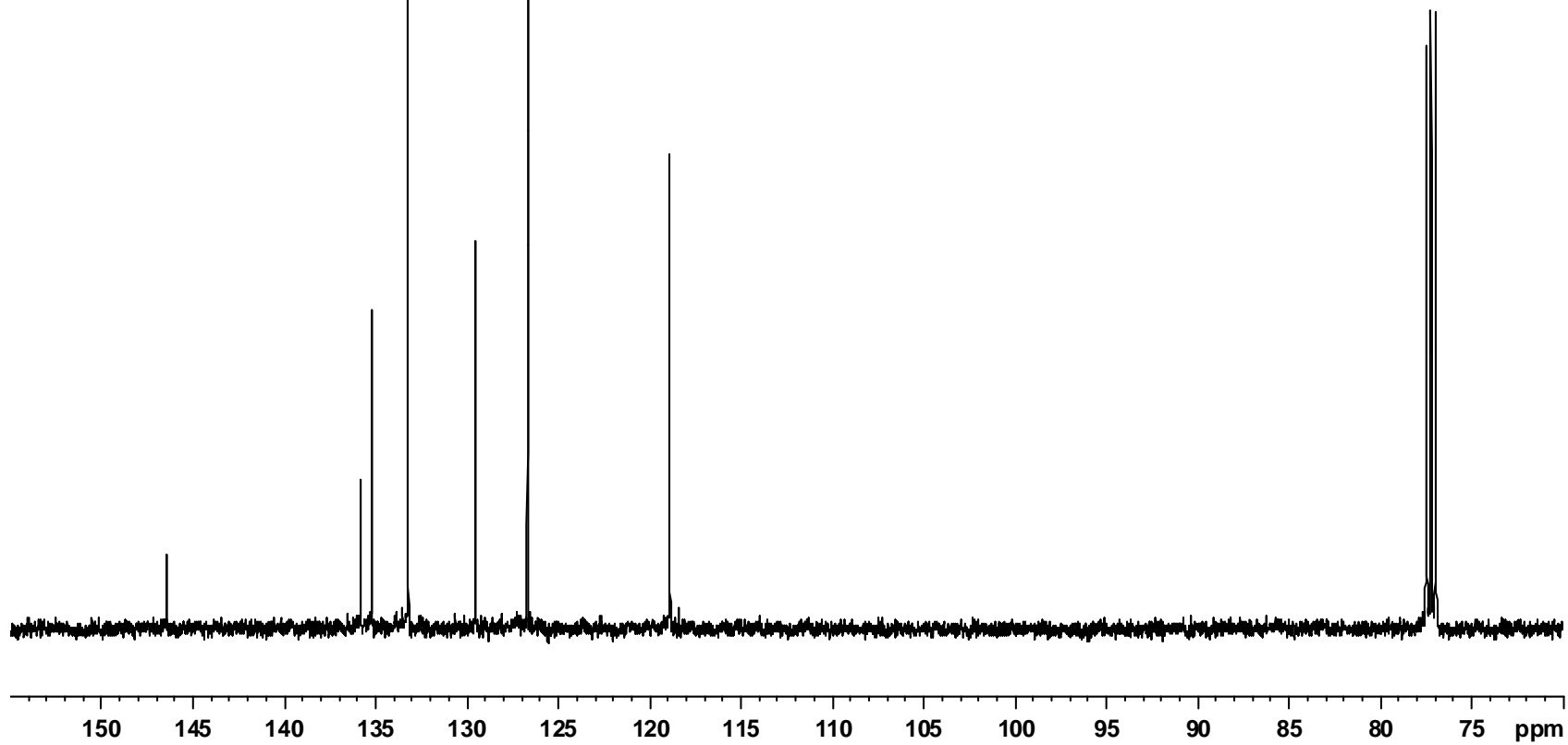


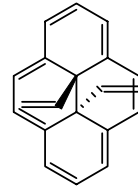
166



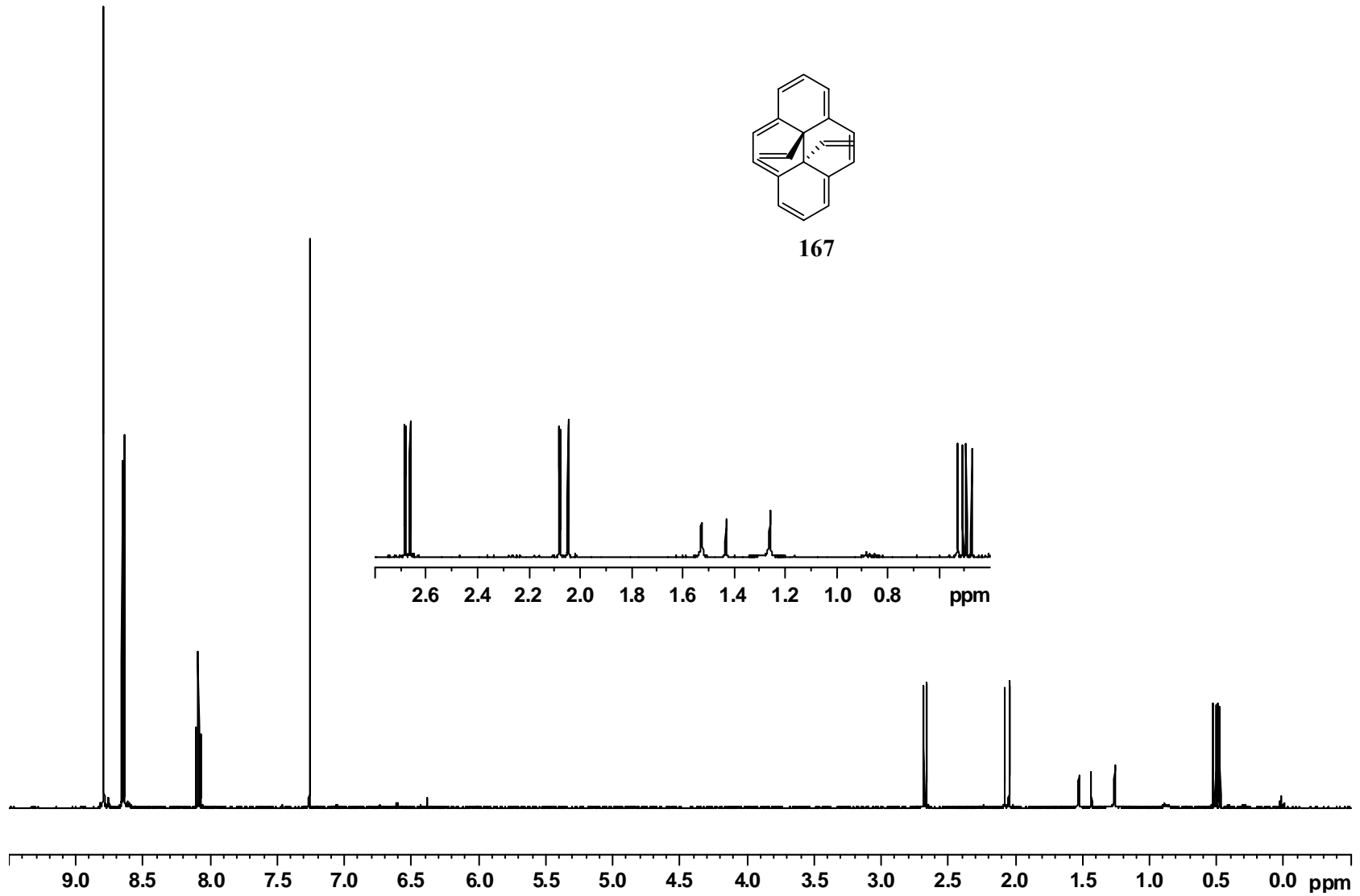


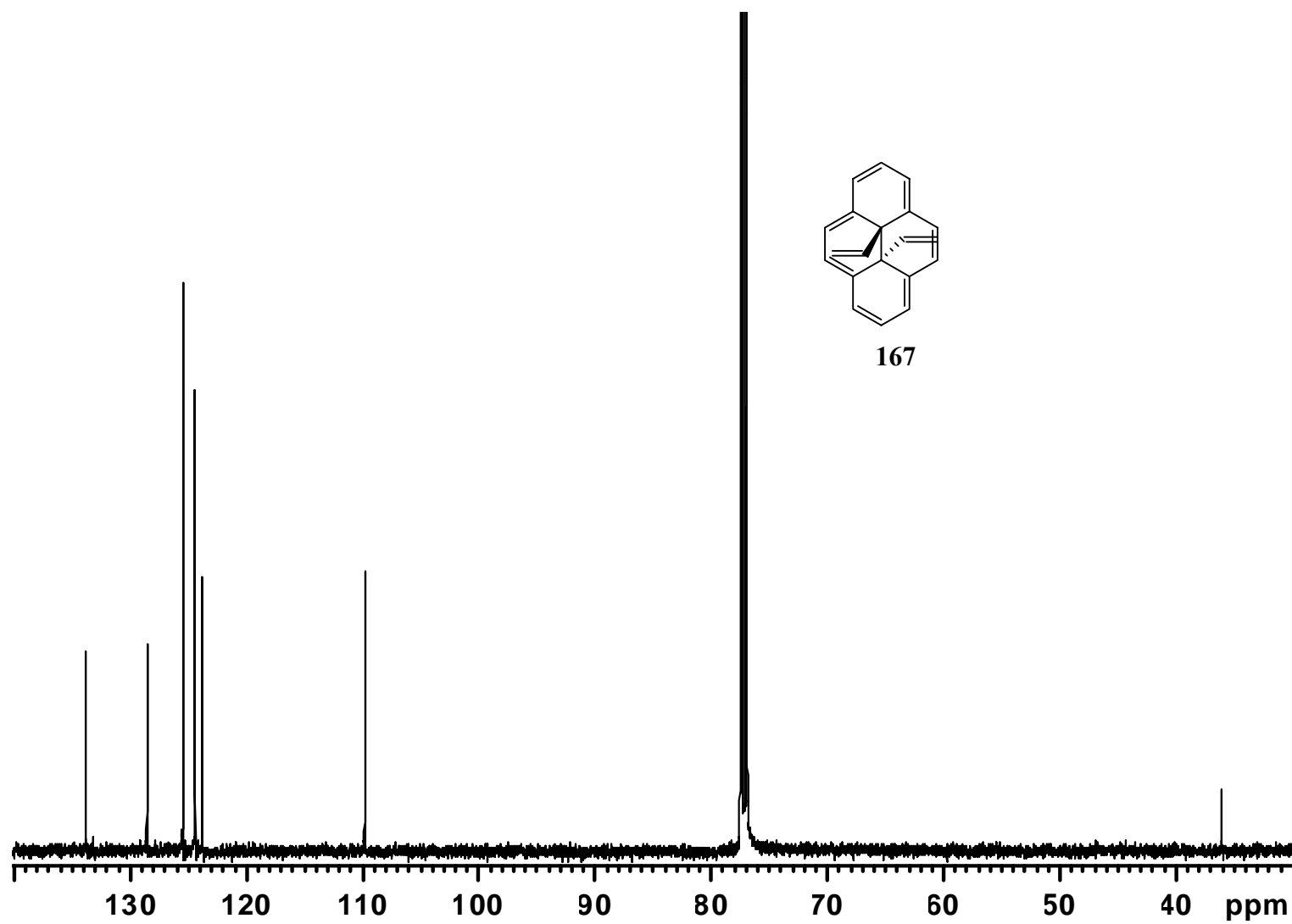
166

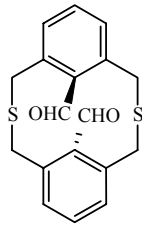




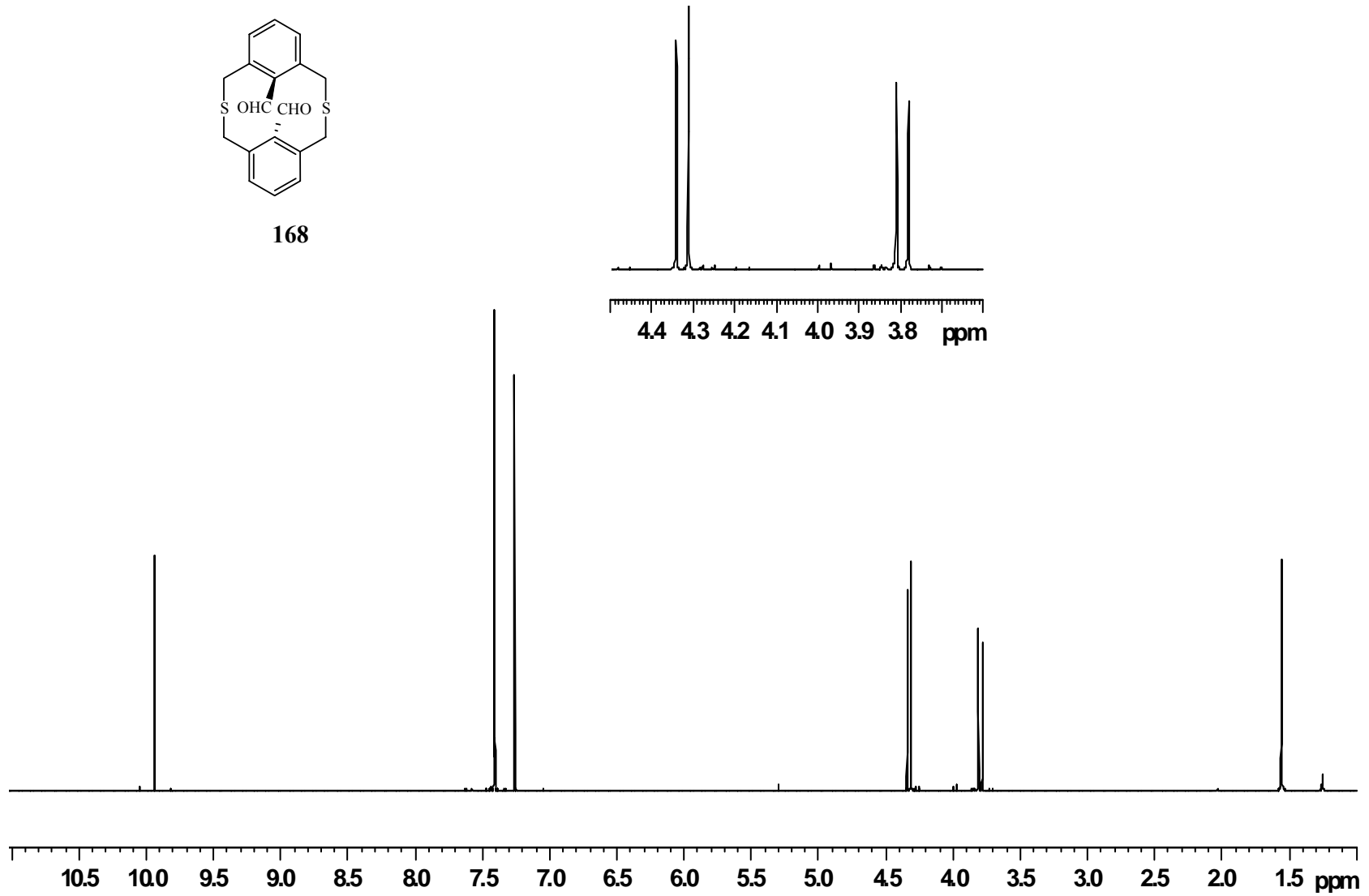
167

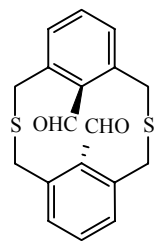




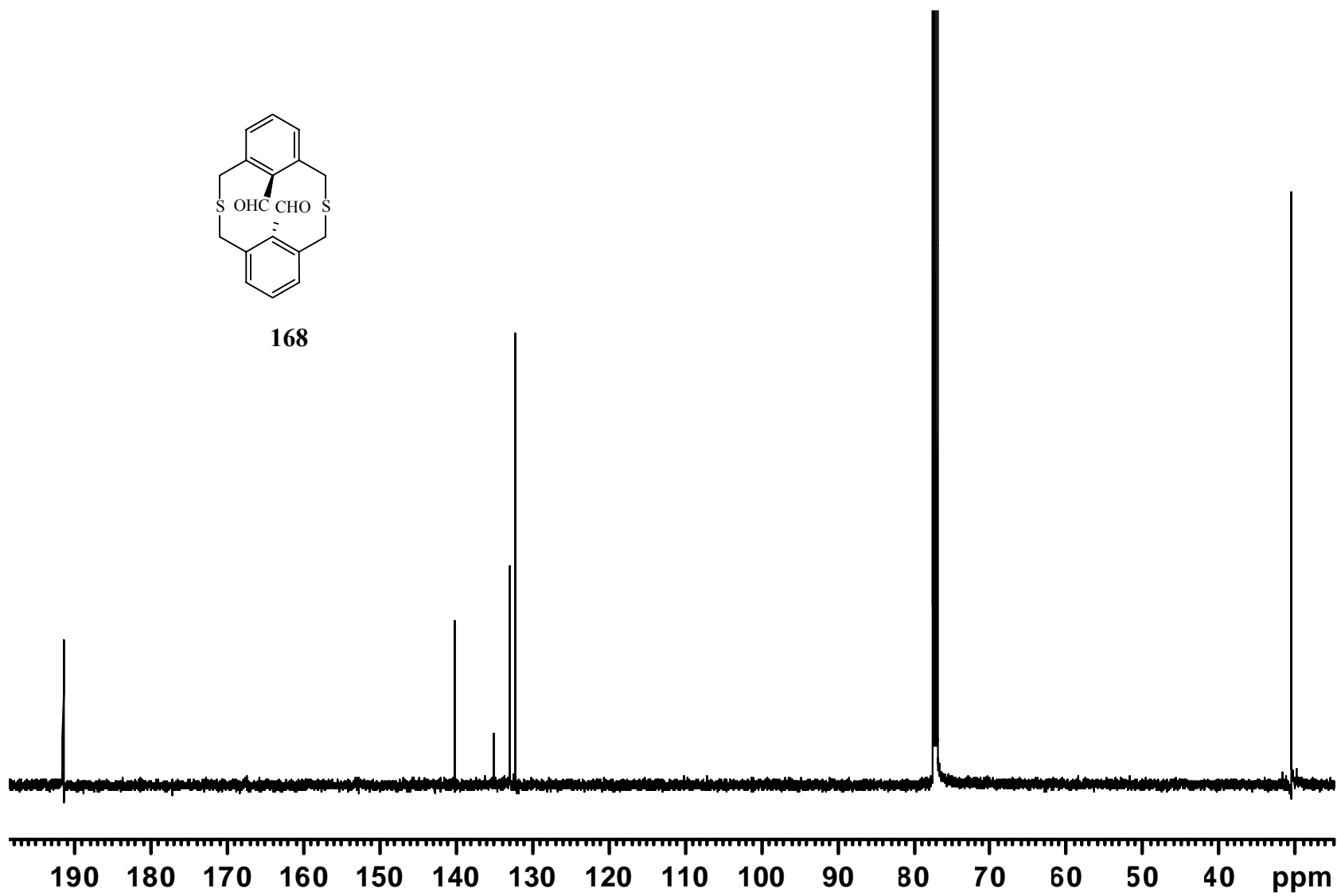


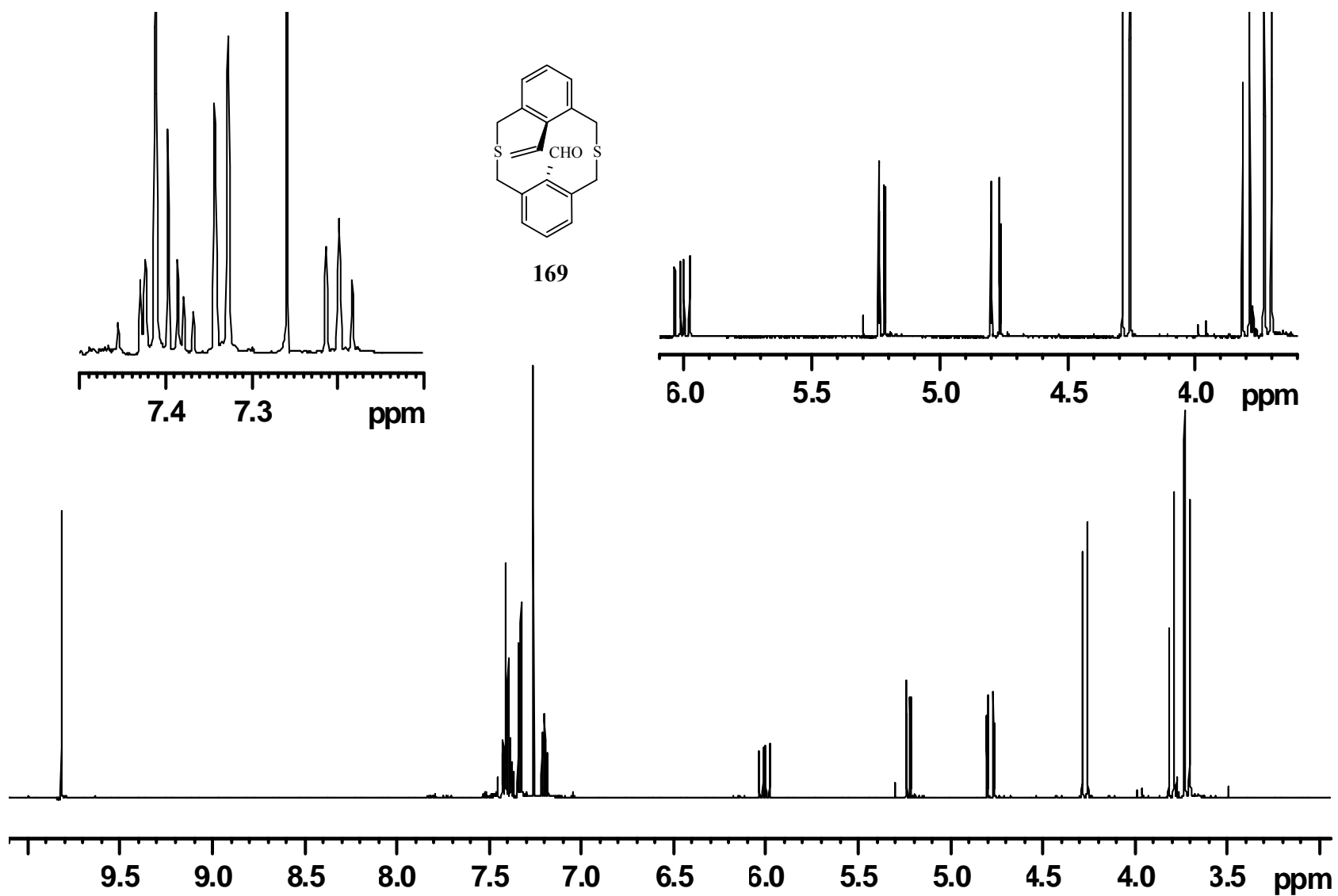
168

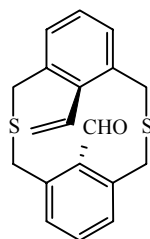
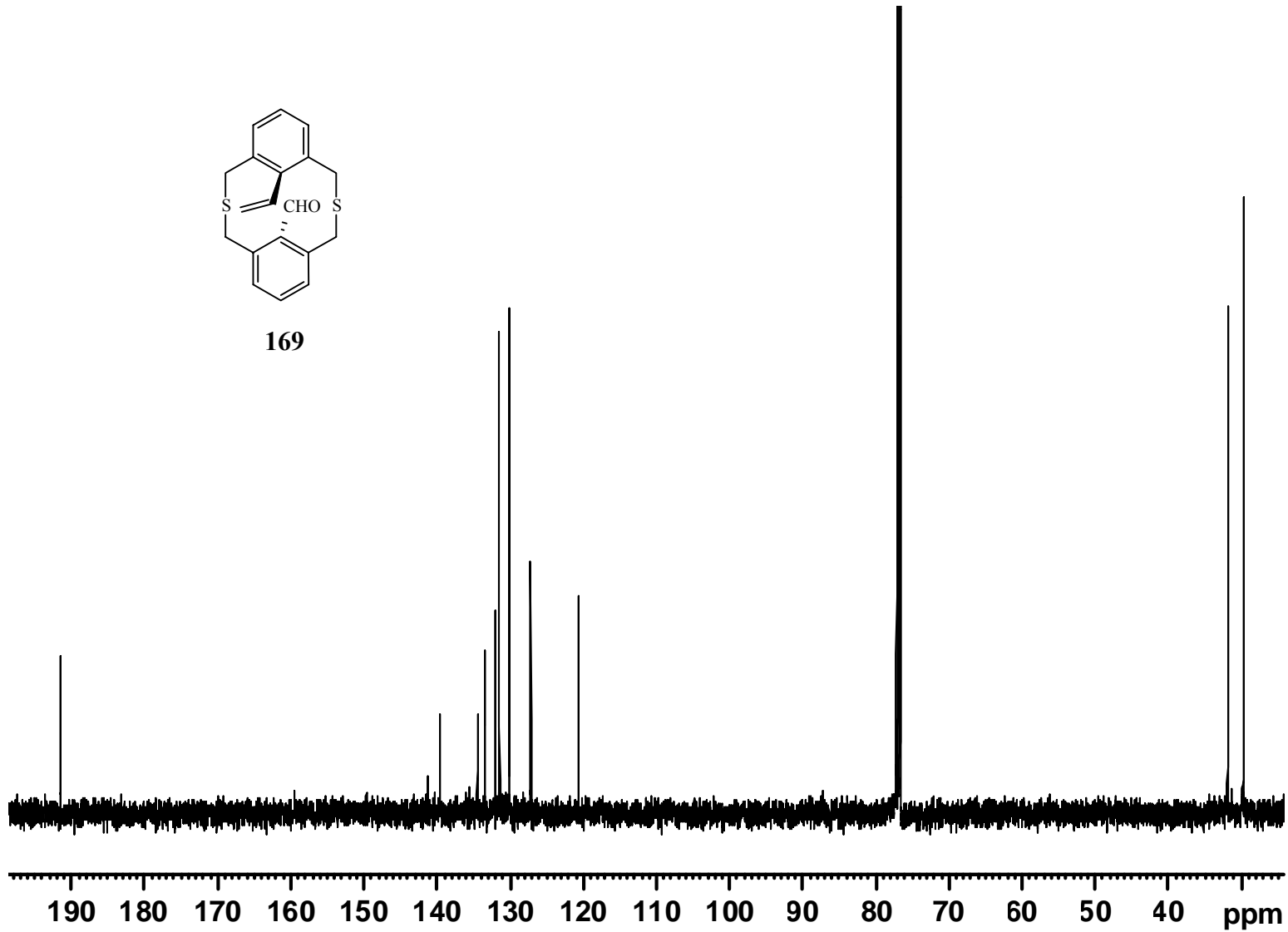


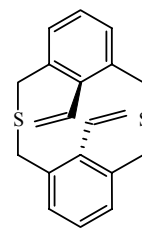
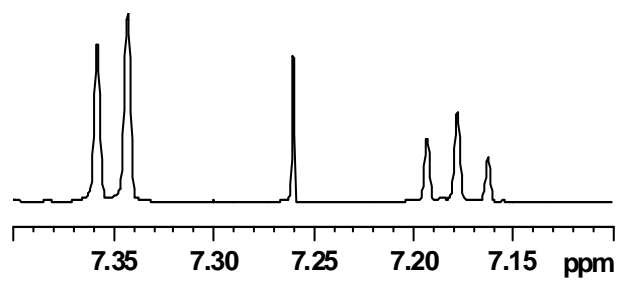


168

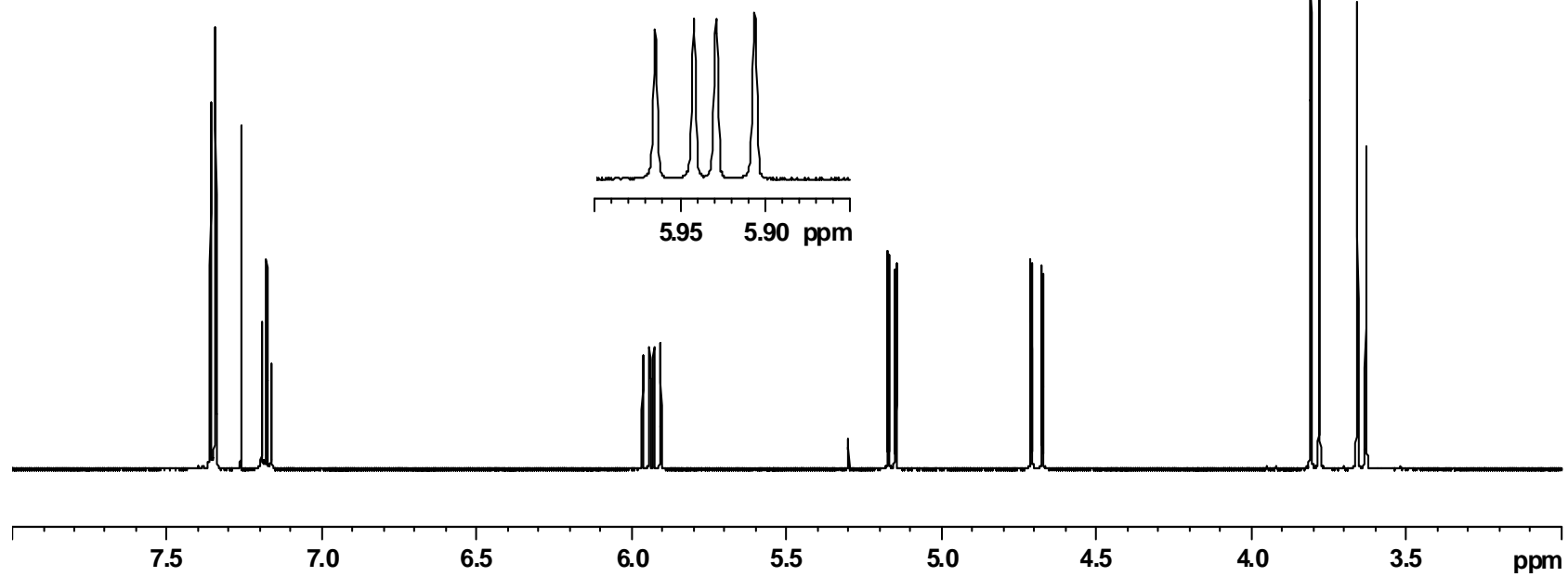


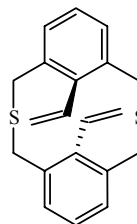


**169**

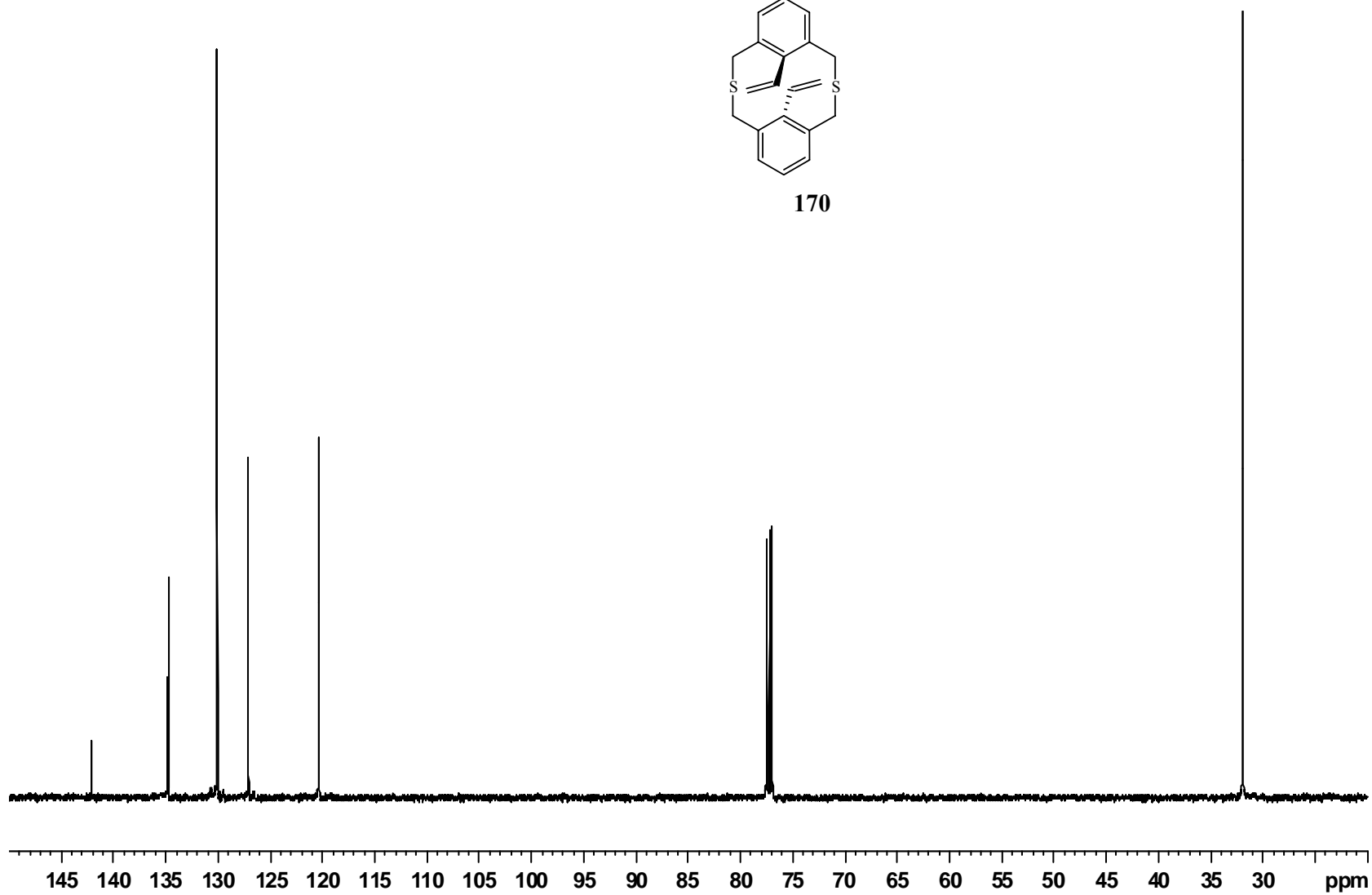


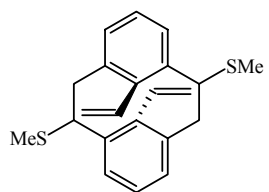
170



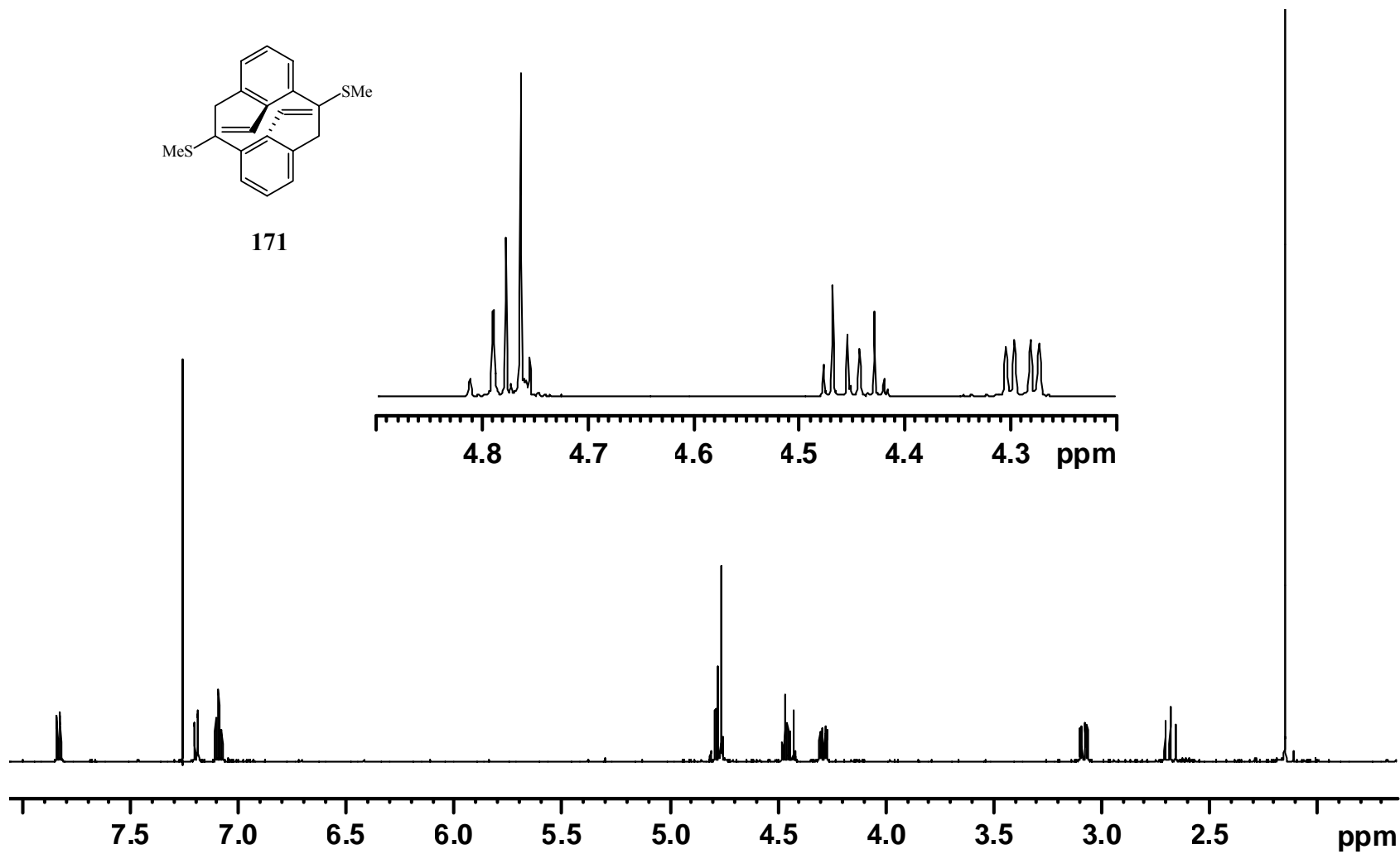


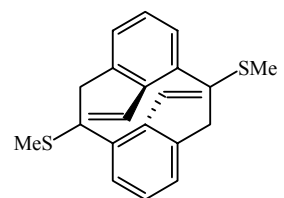
170



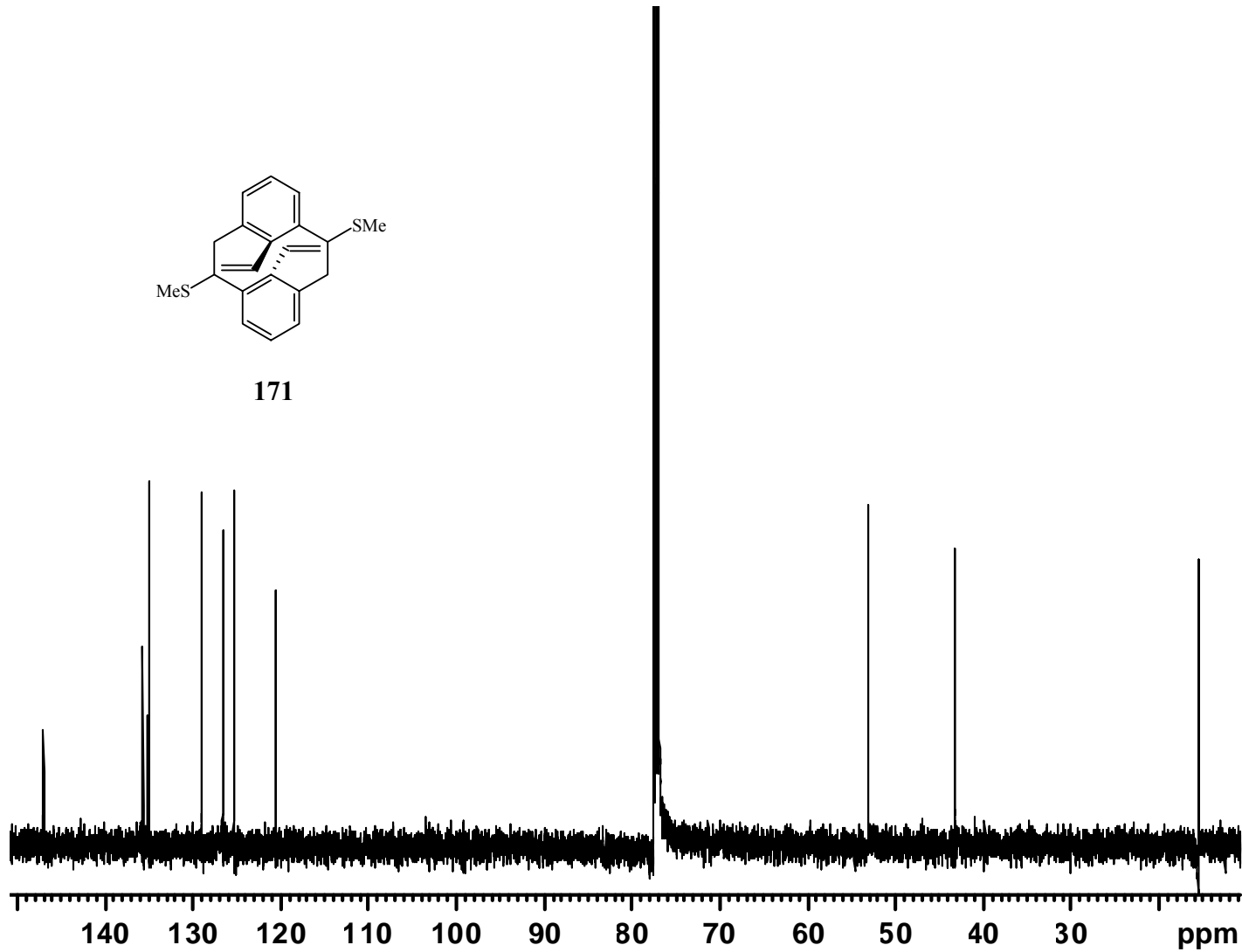


171

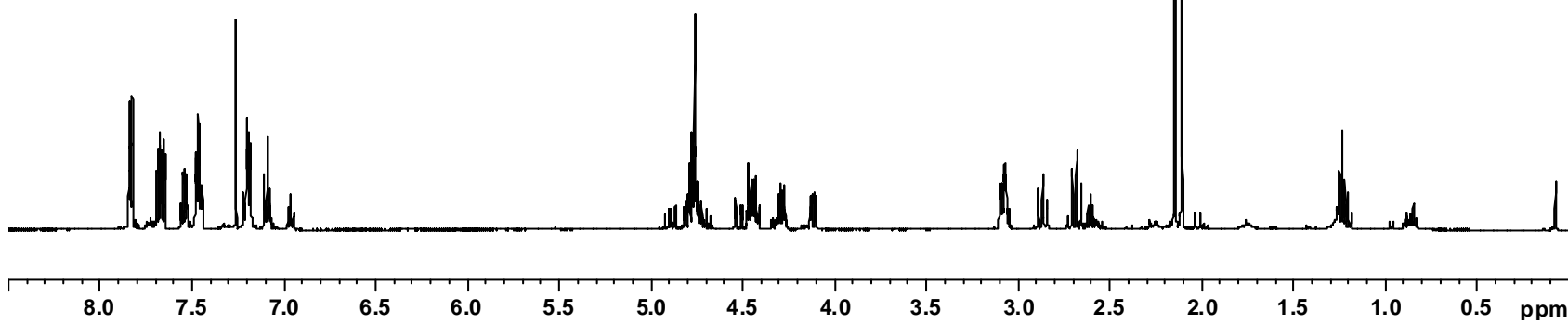
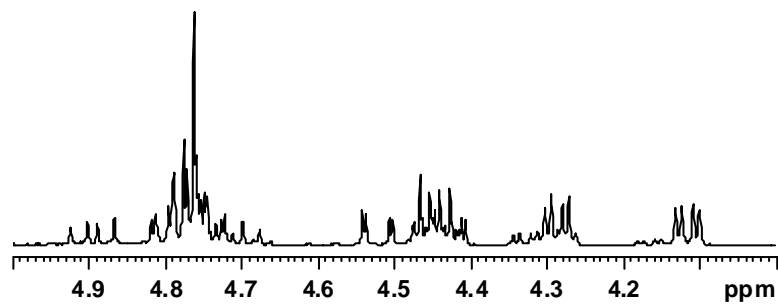
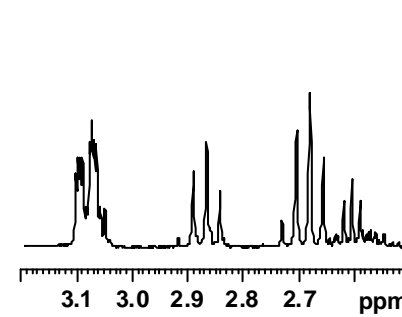
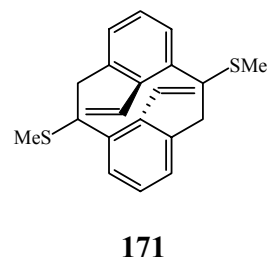
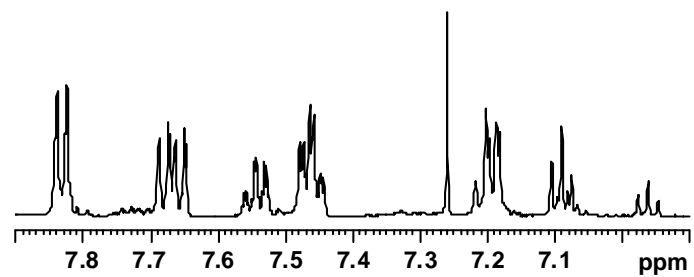


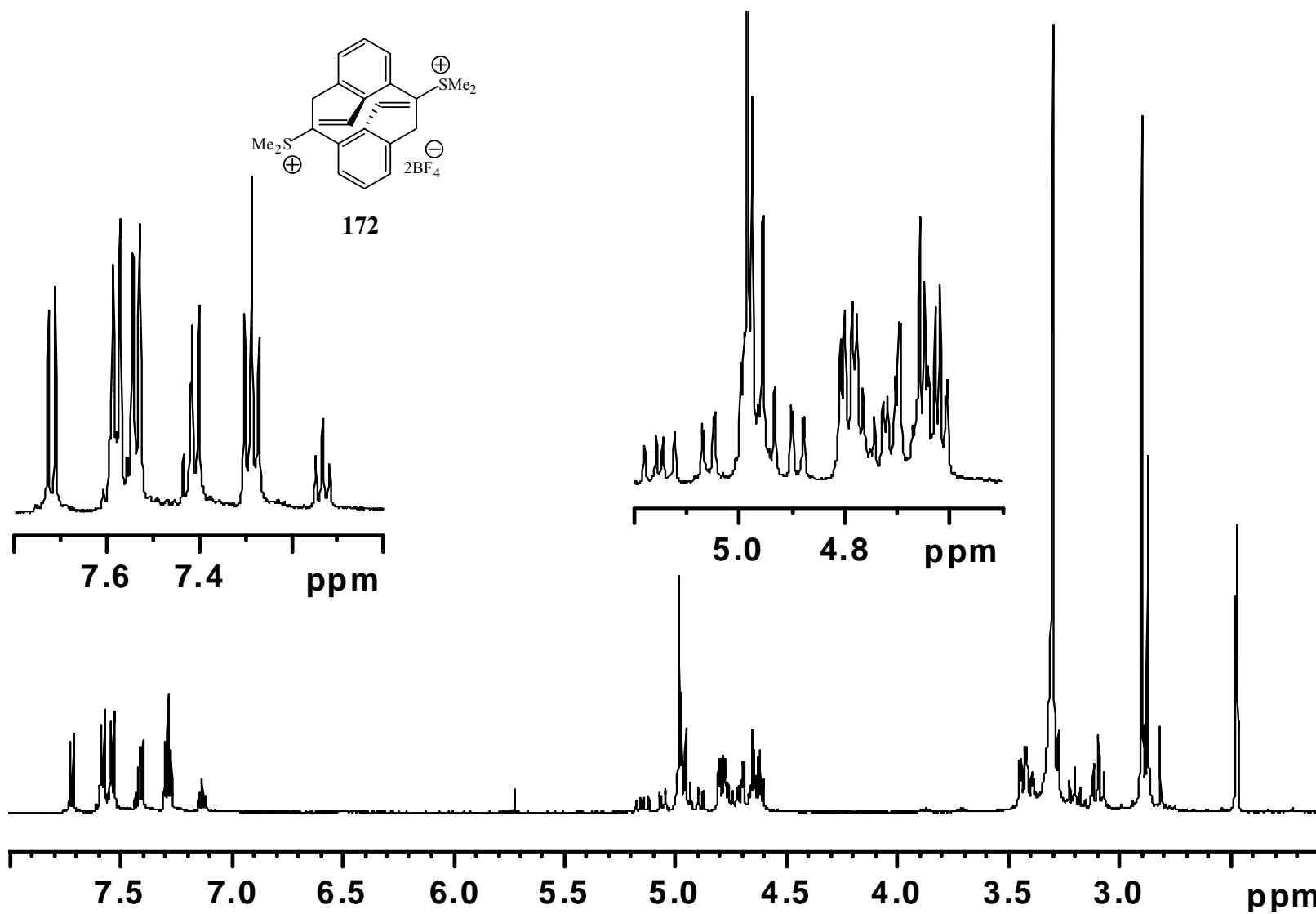


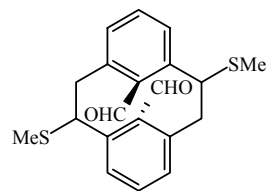
171



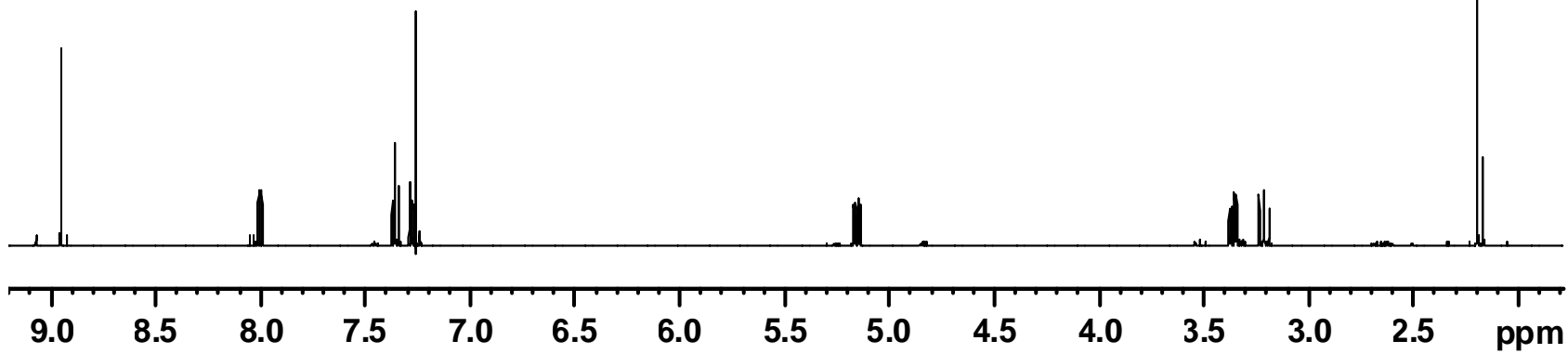
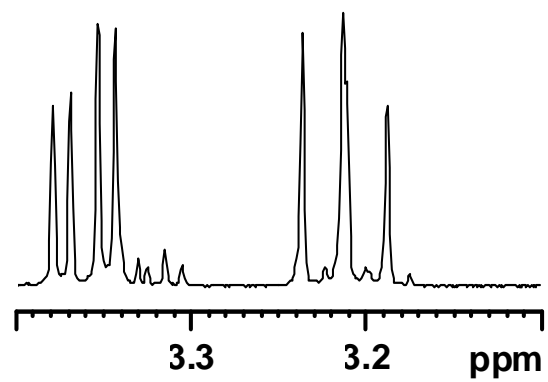
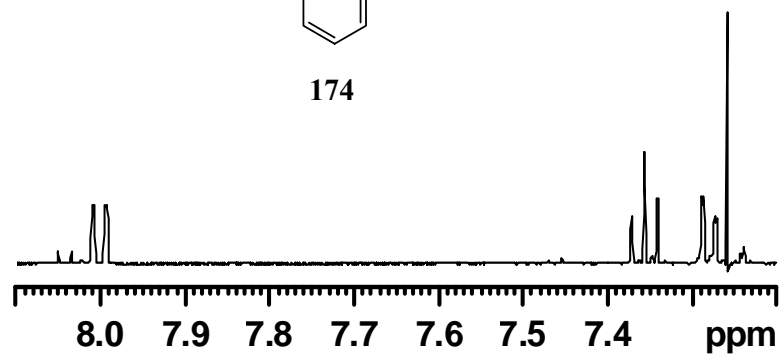
Mixture of isomers

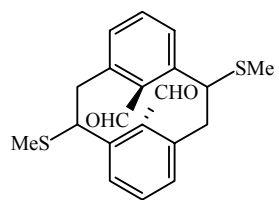




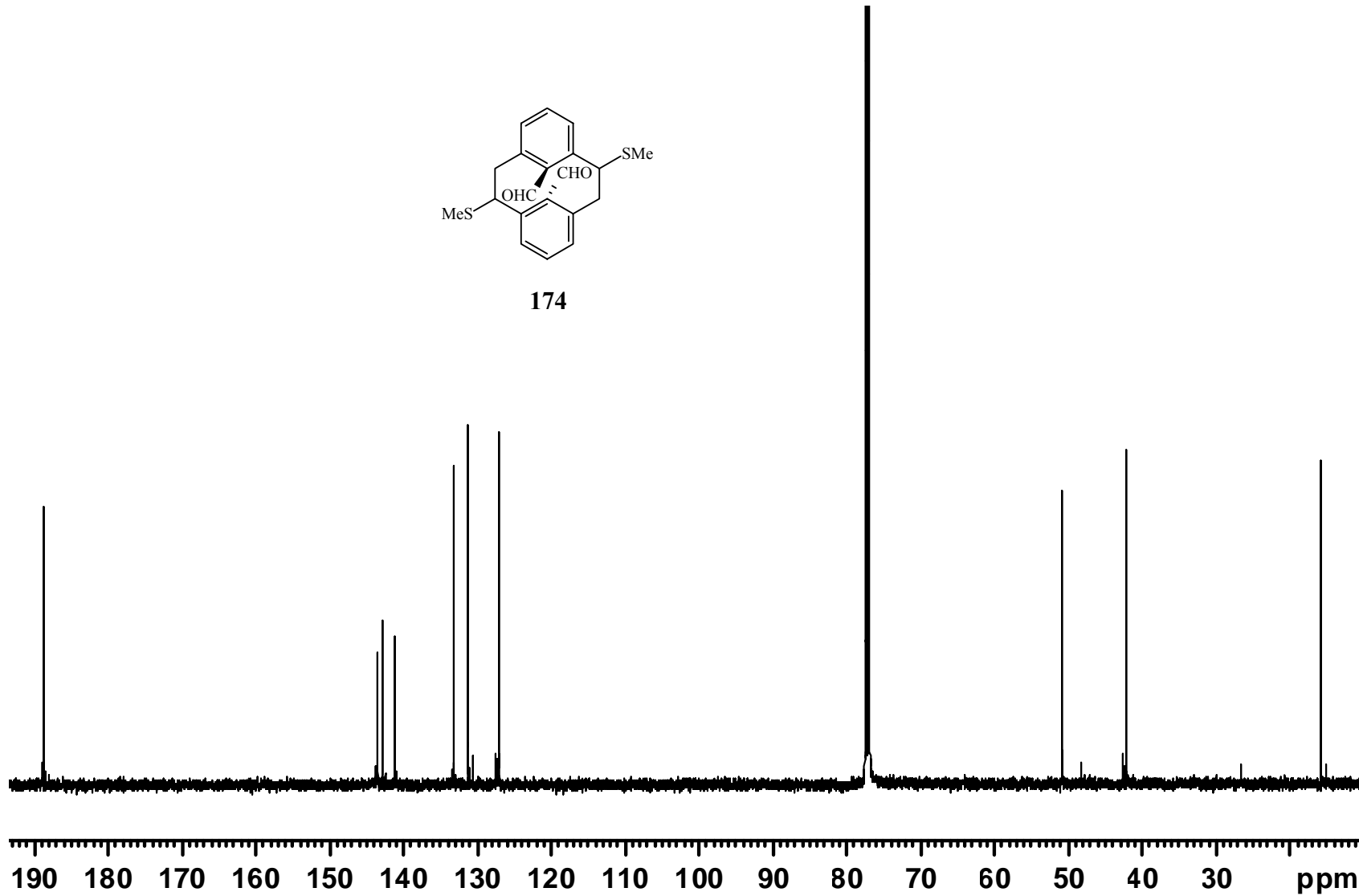


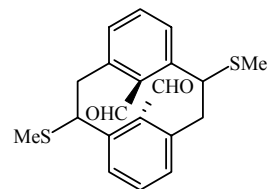
174



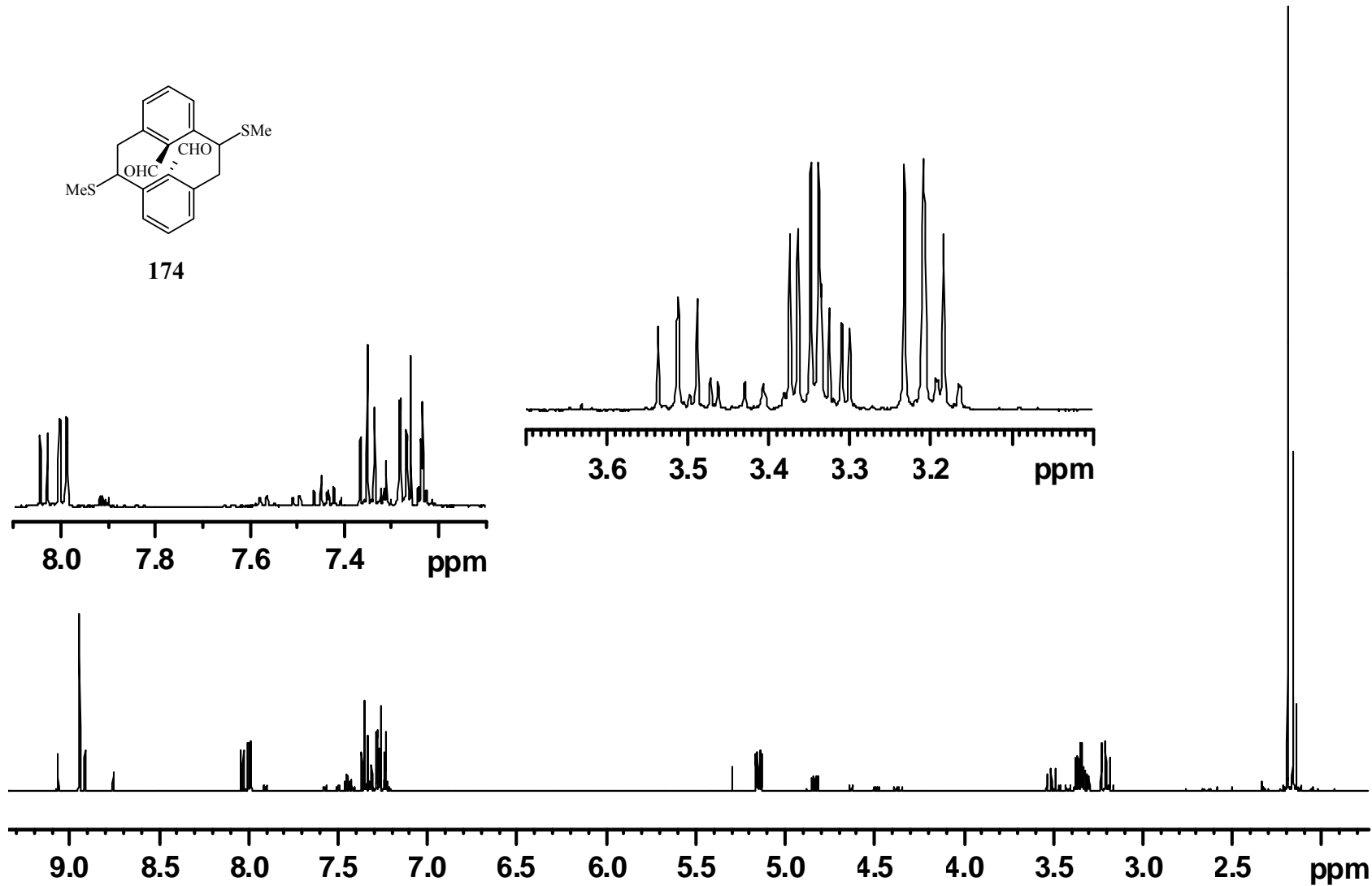


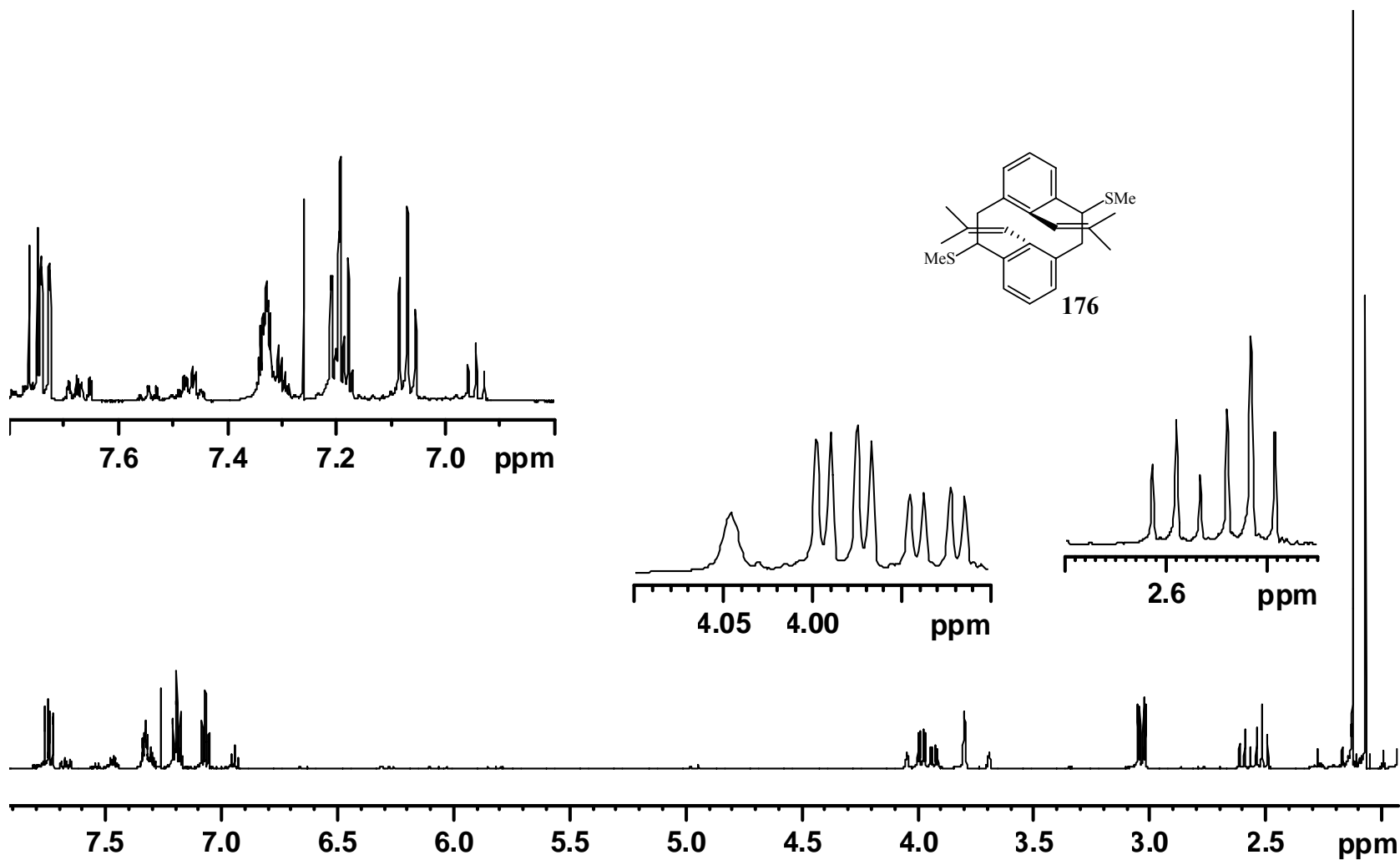
174

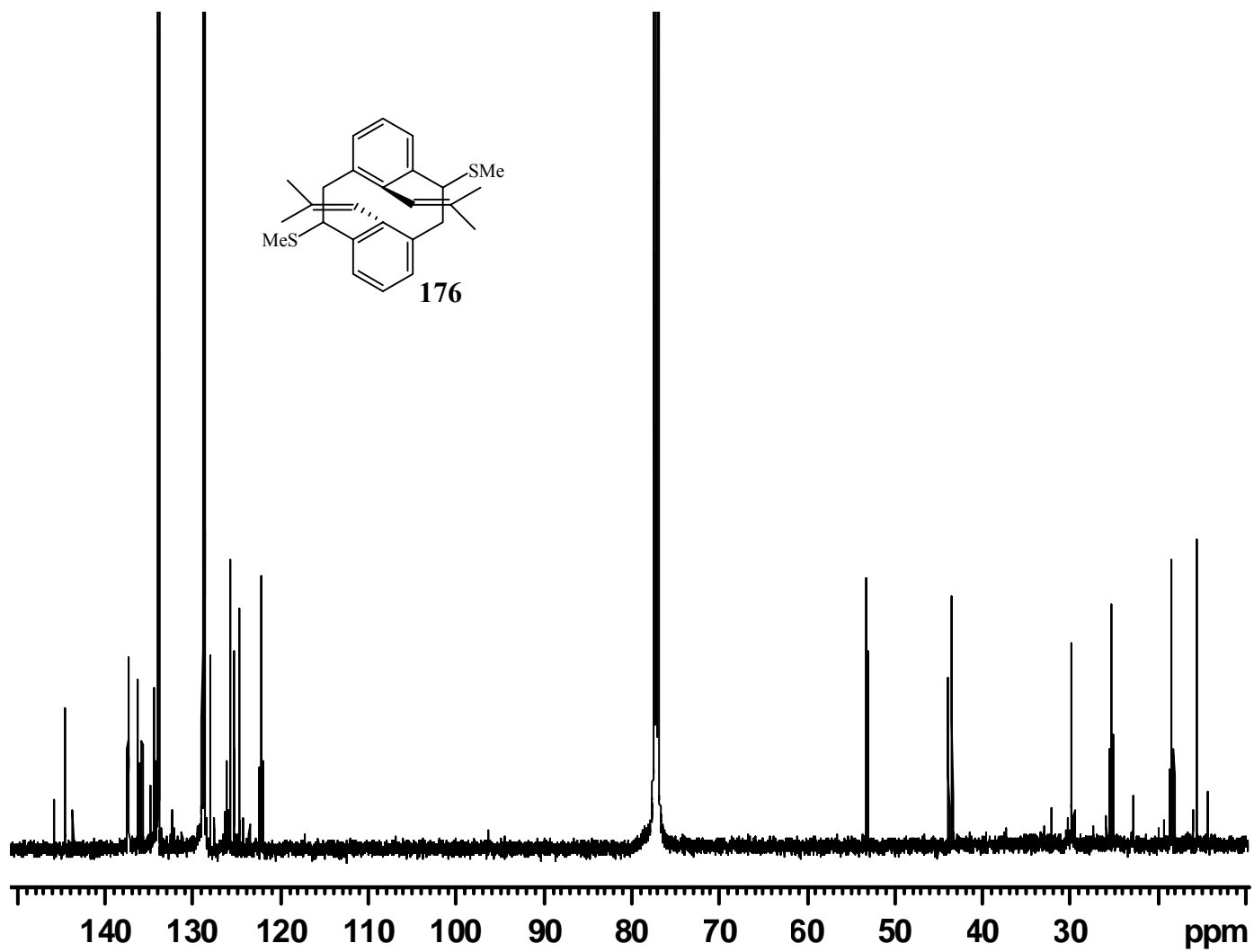


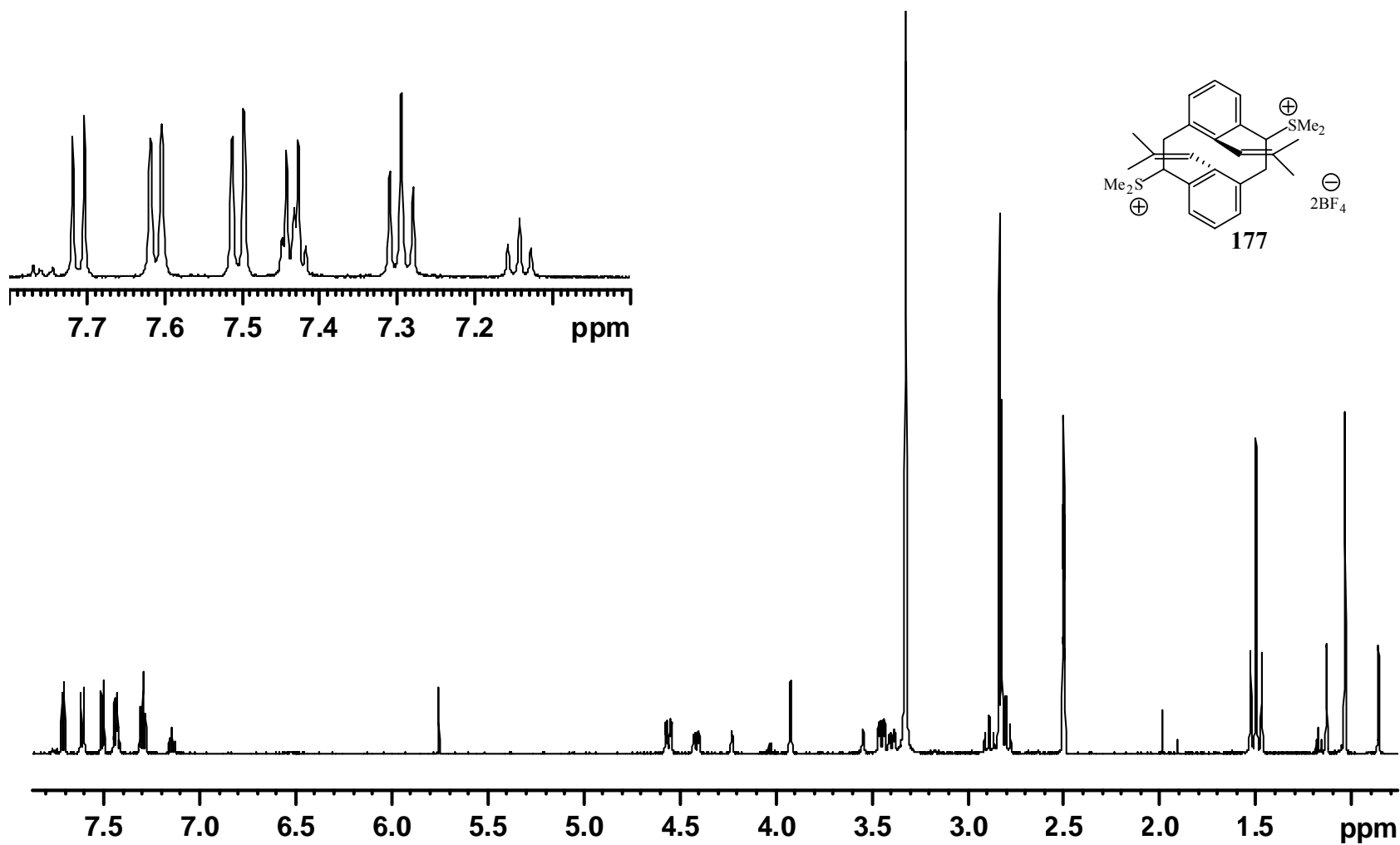


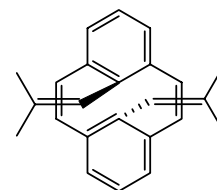
174



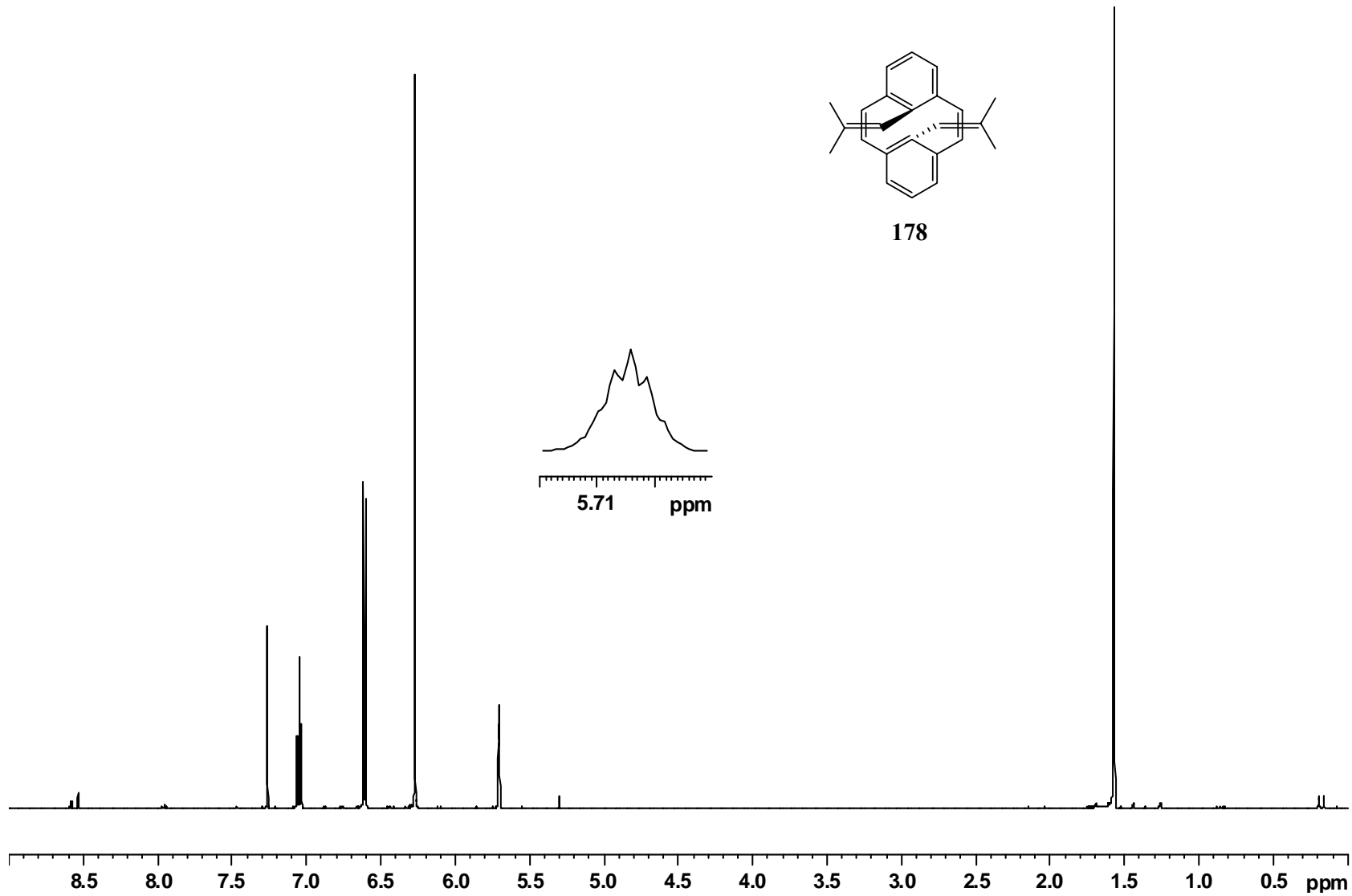


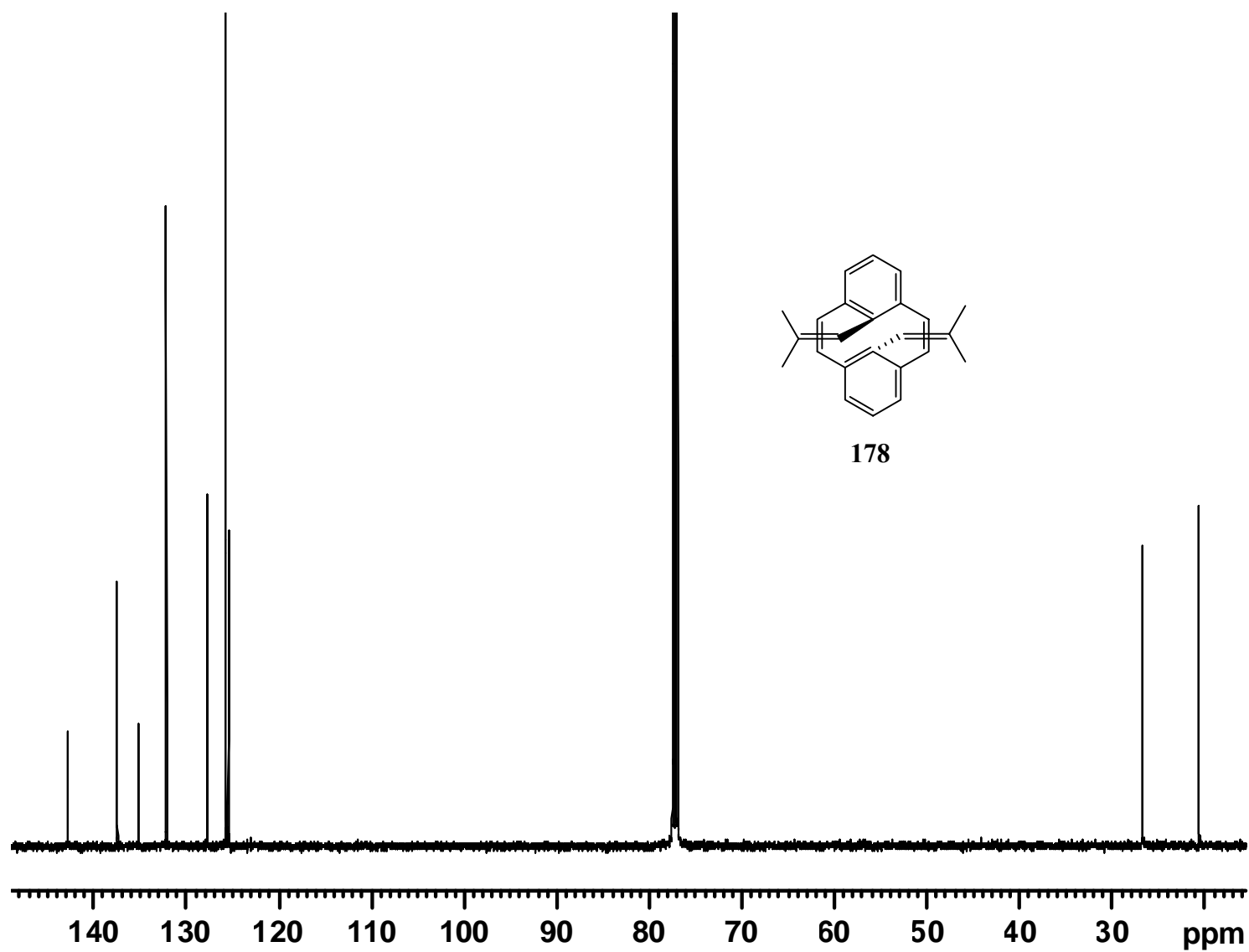


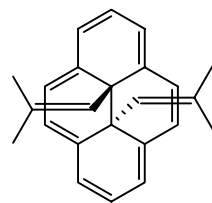




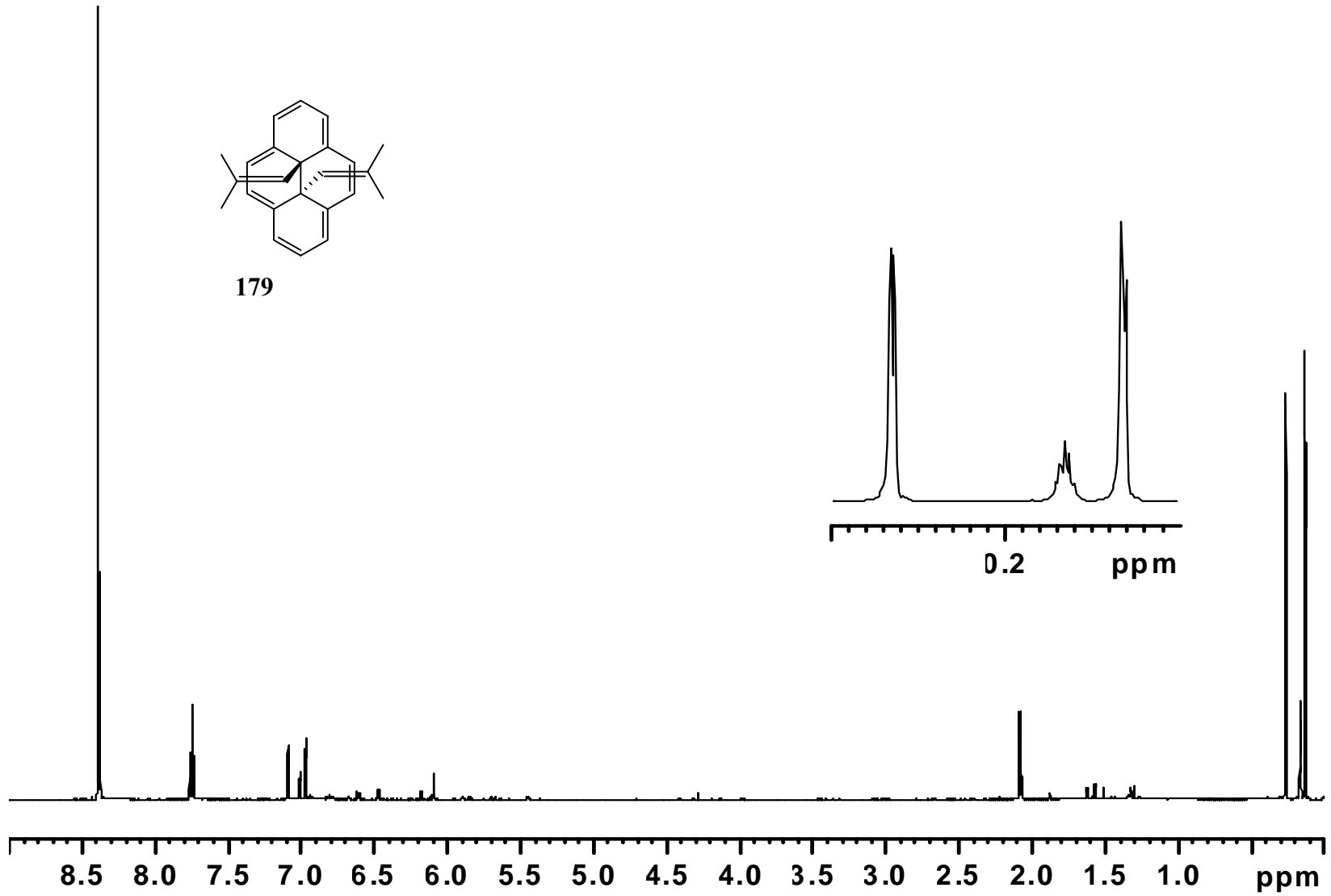
178

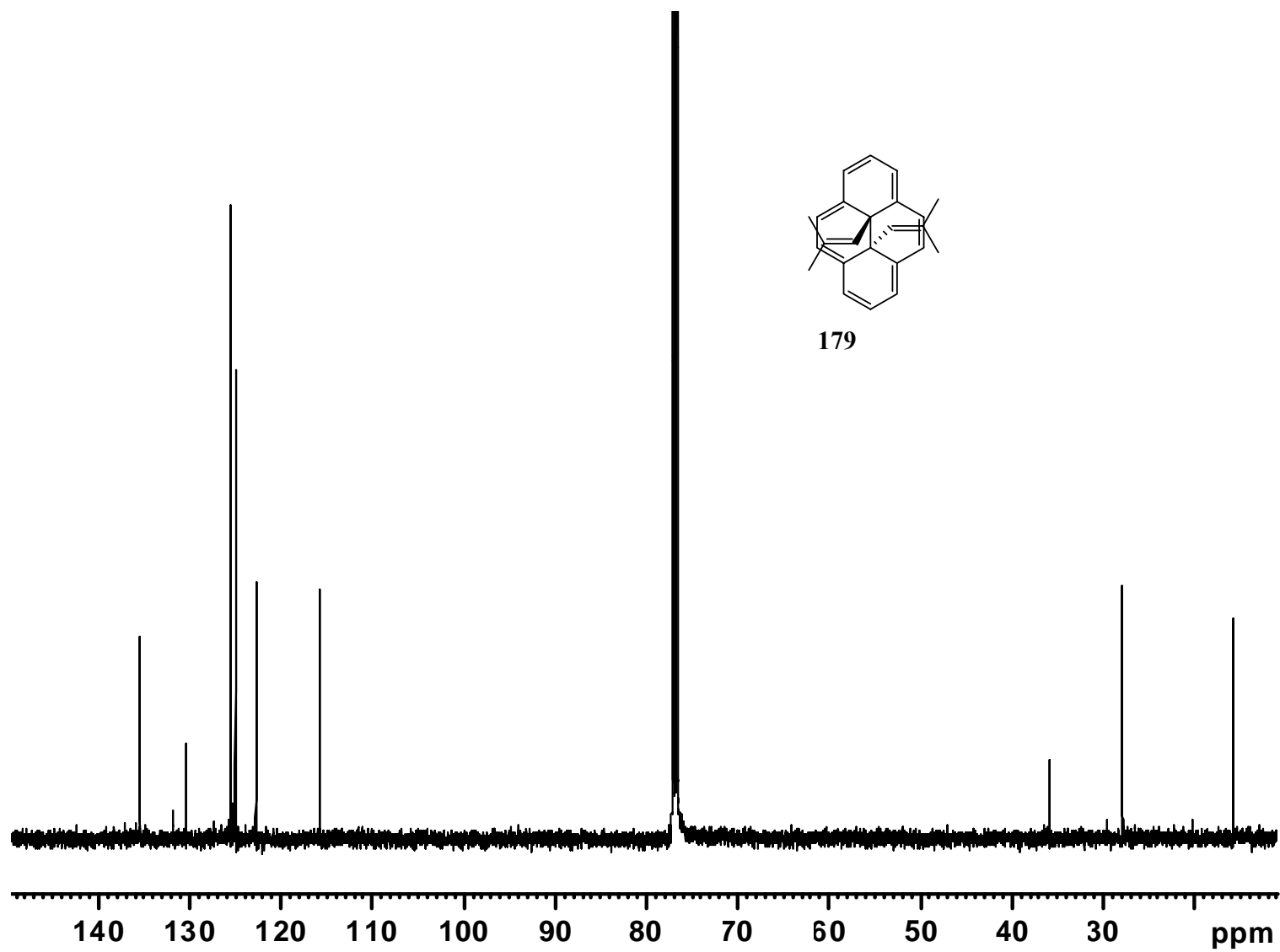


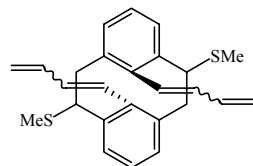
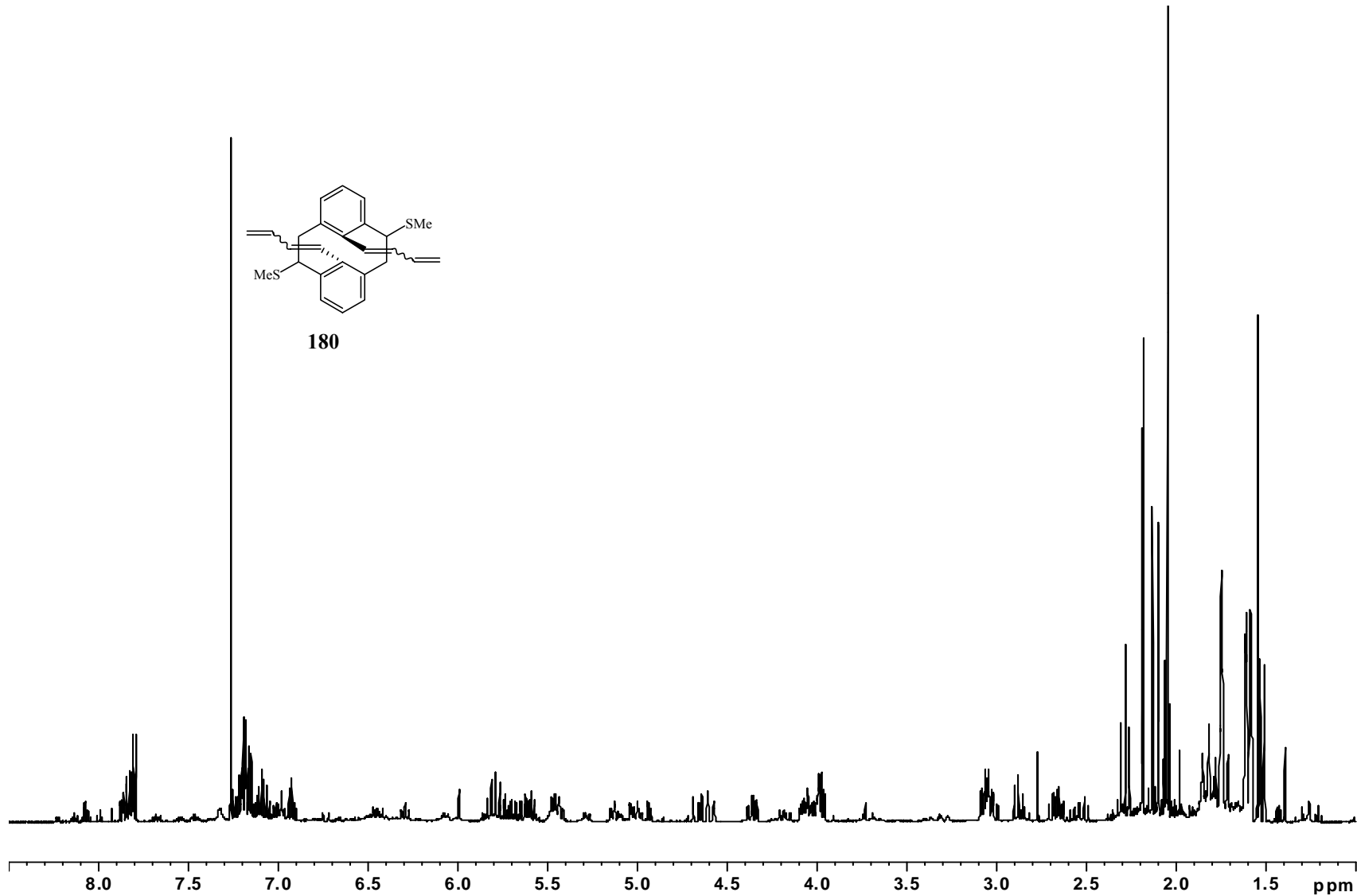


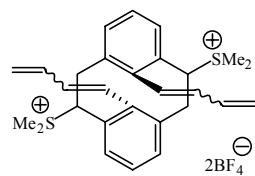


179

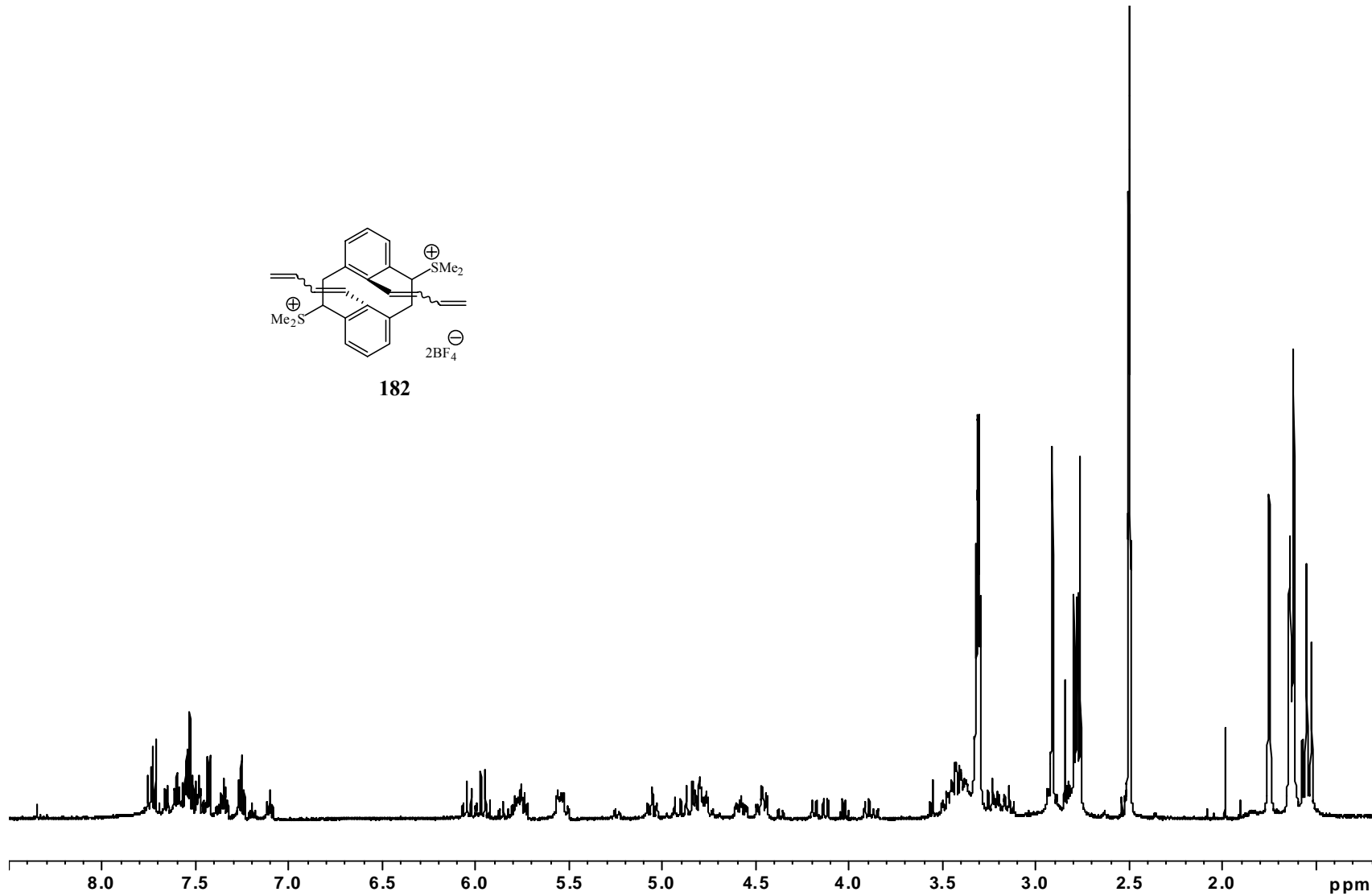


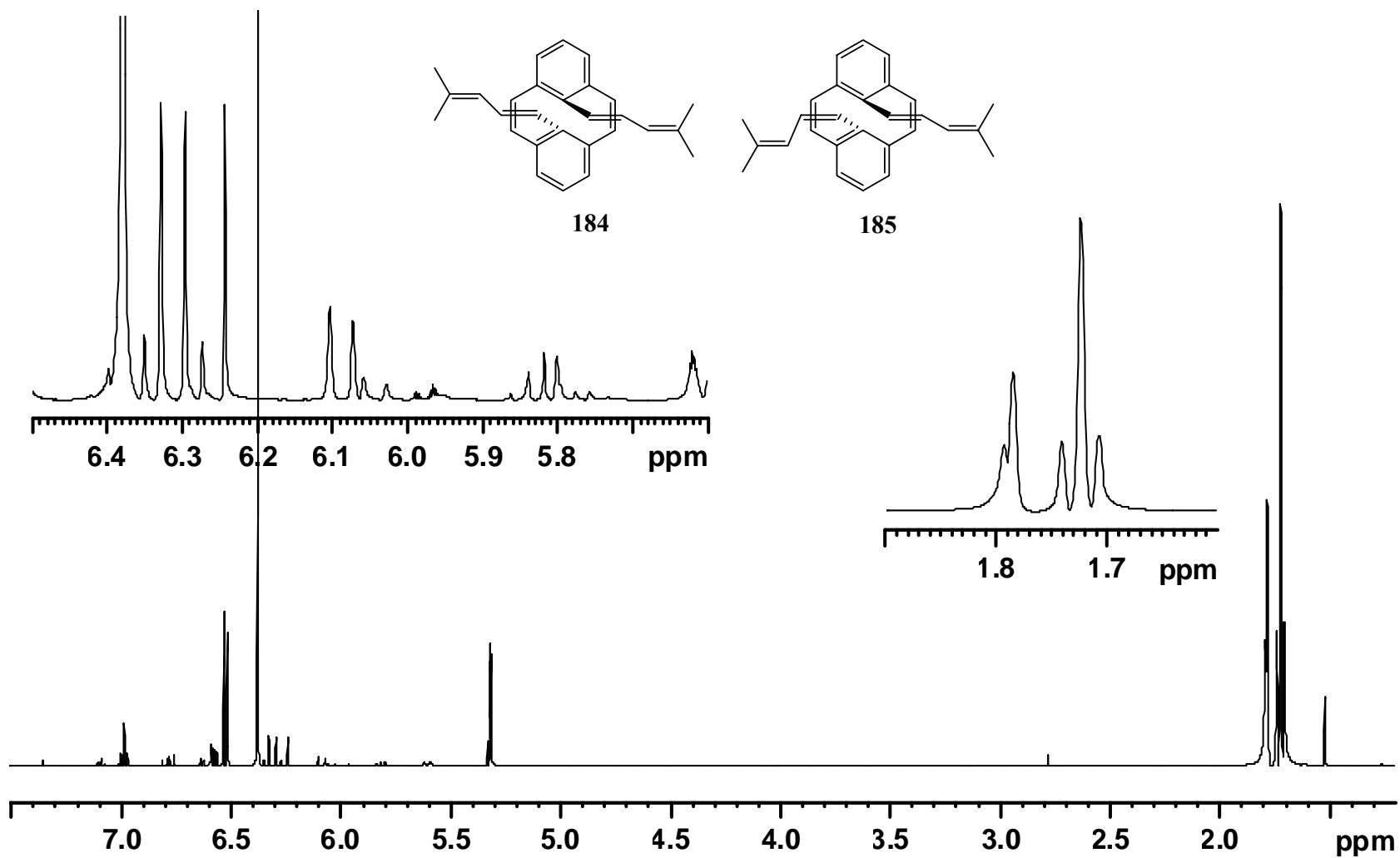


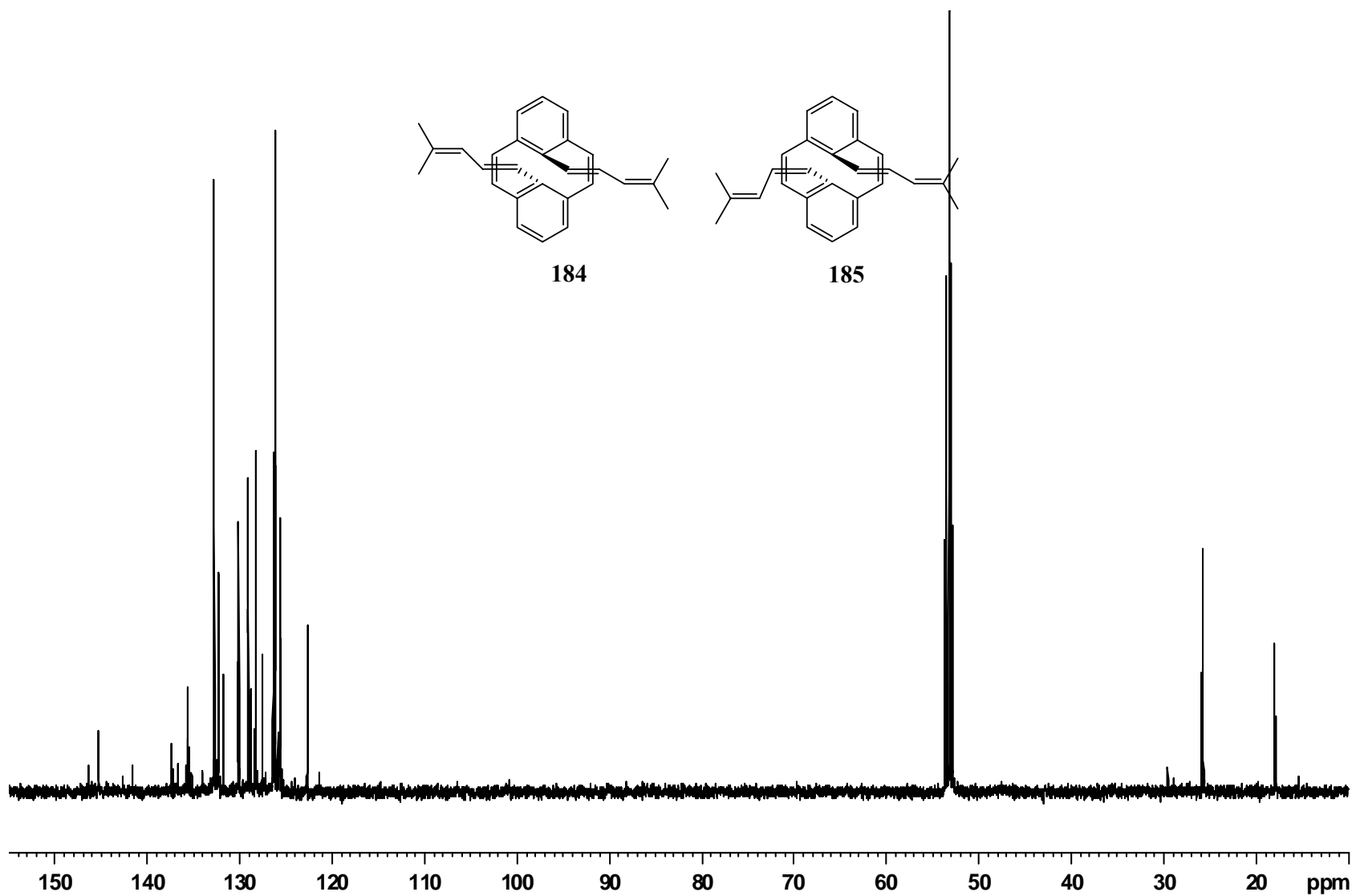
**180**

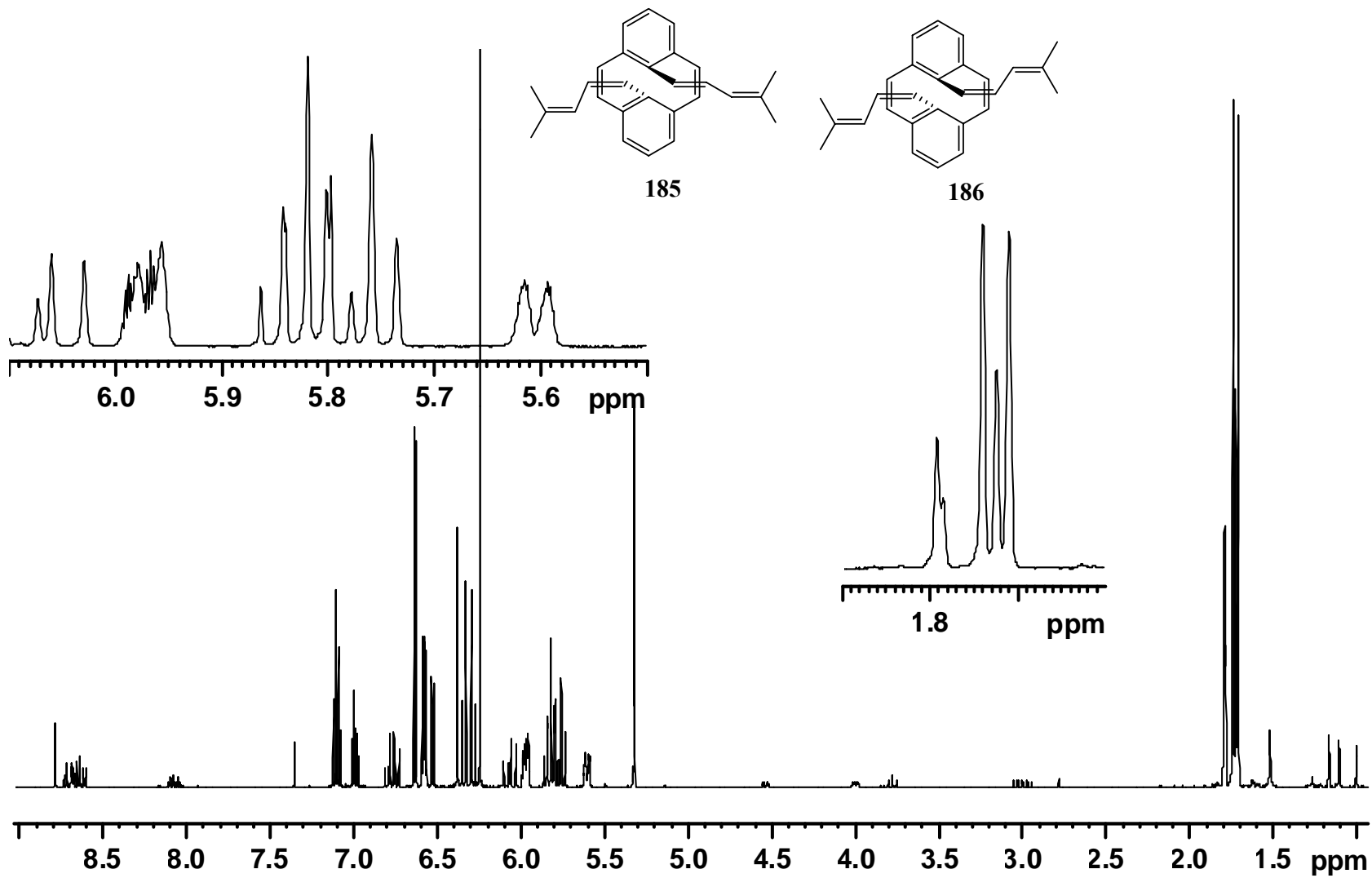


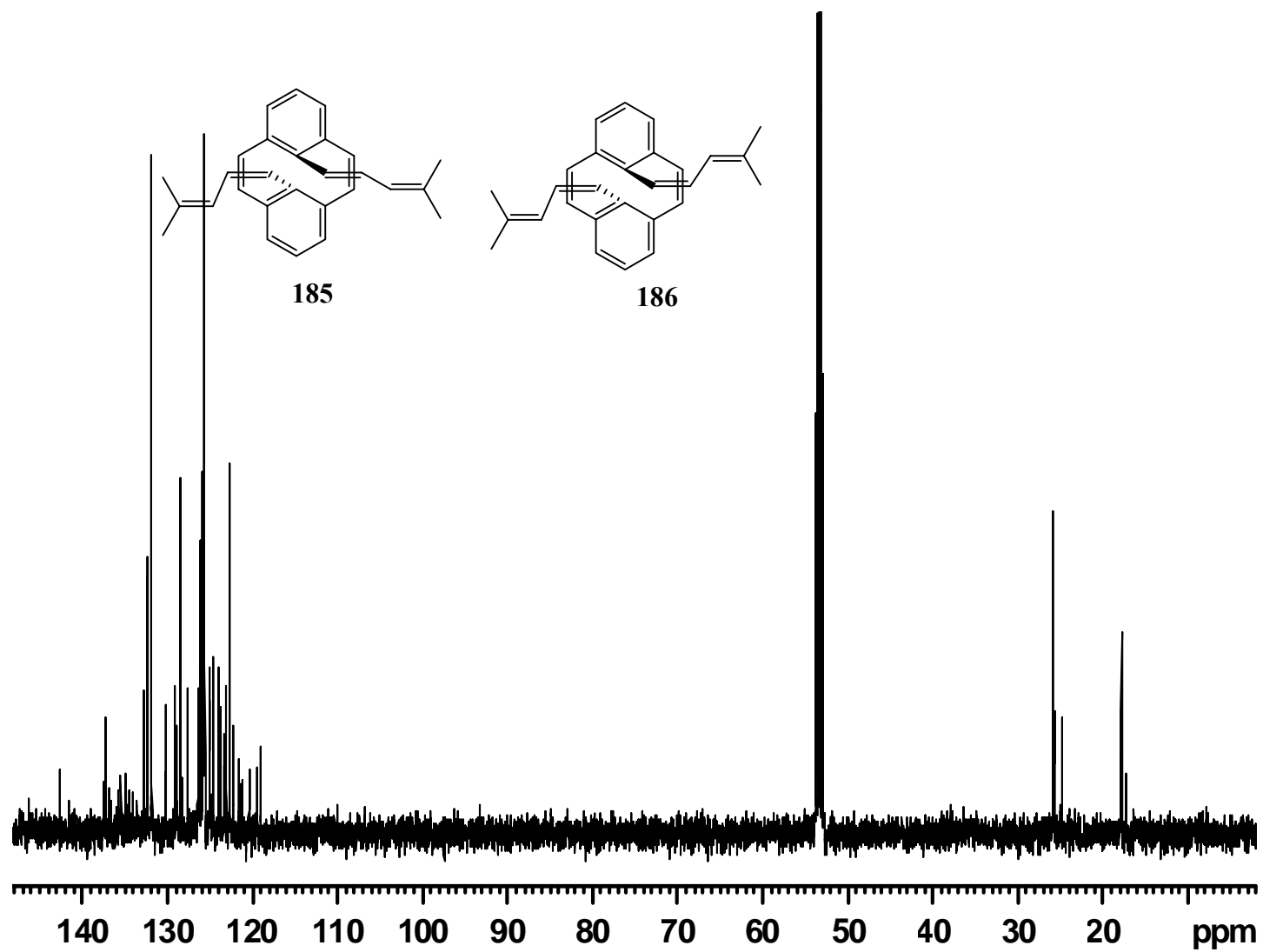
182

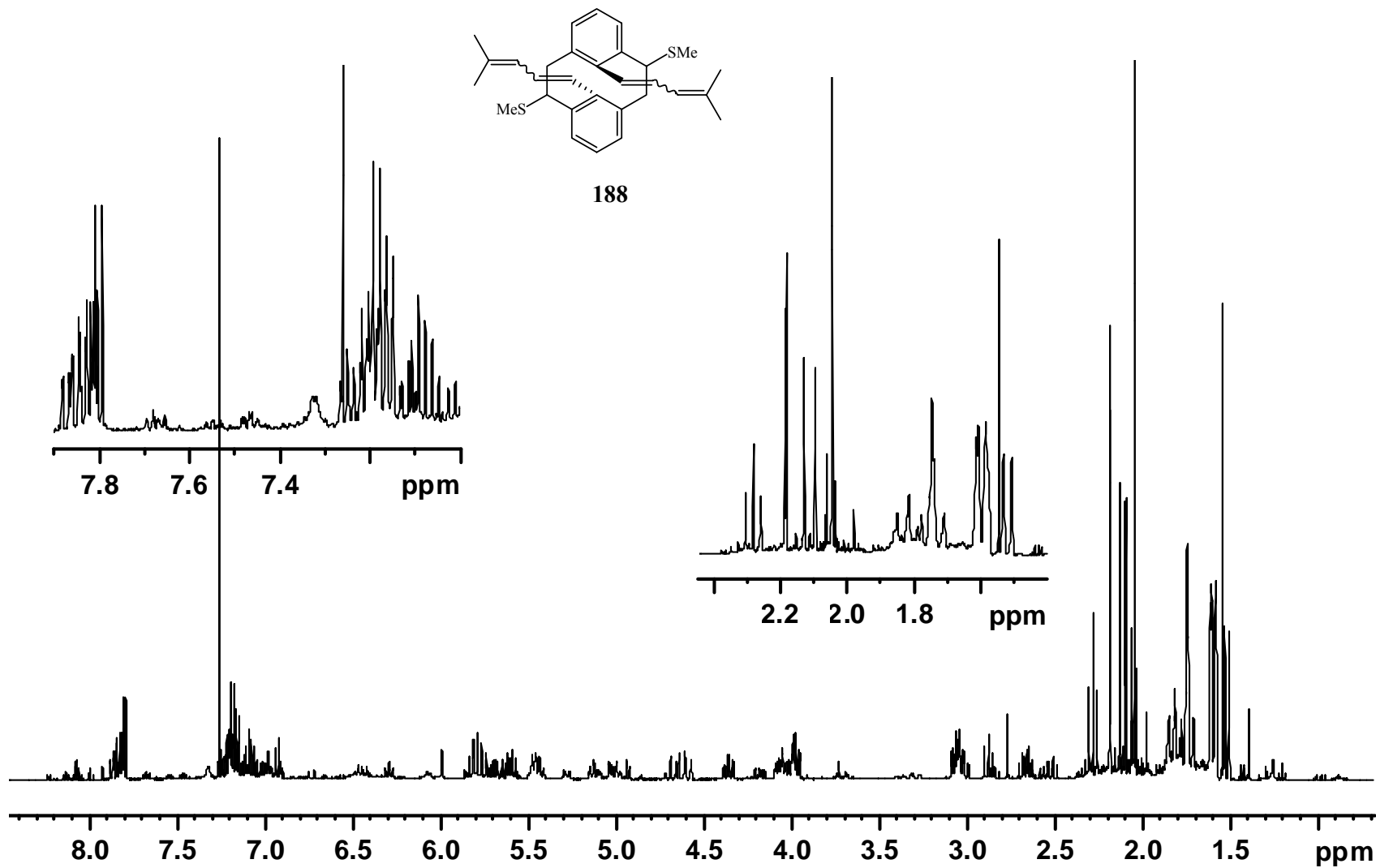


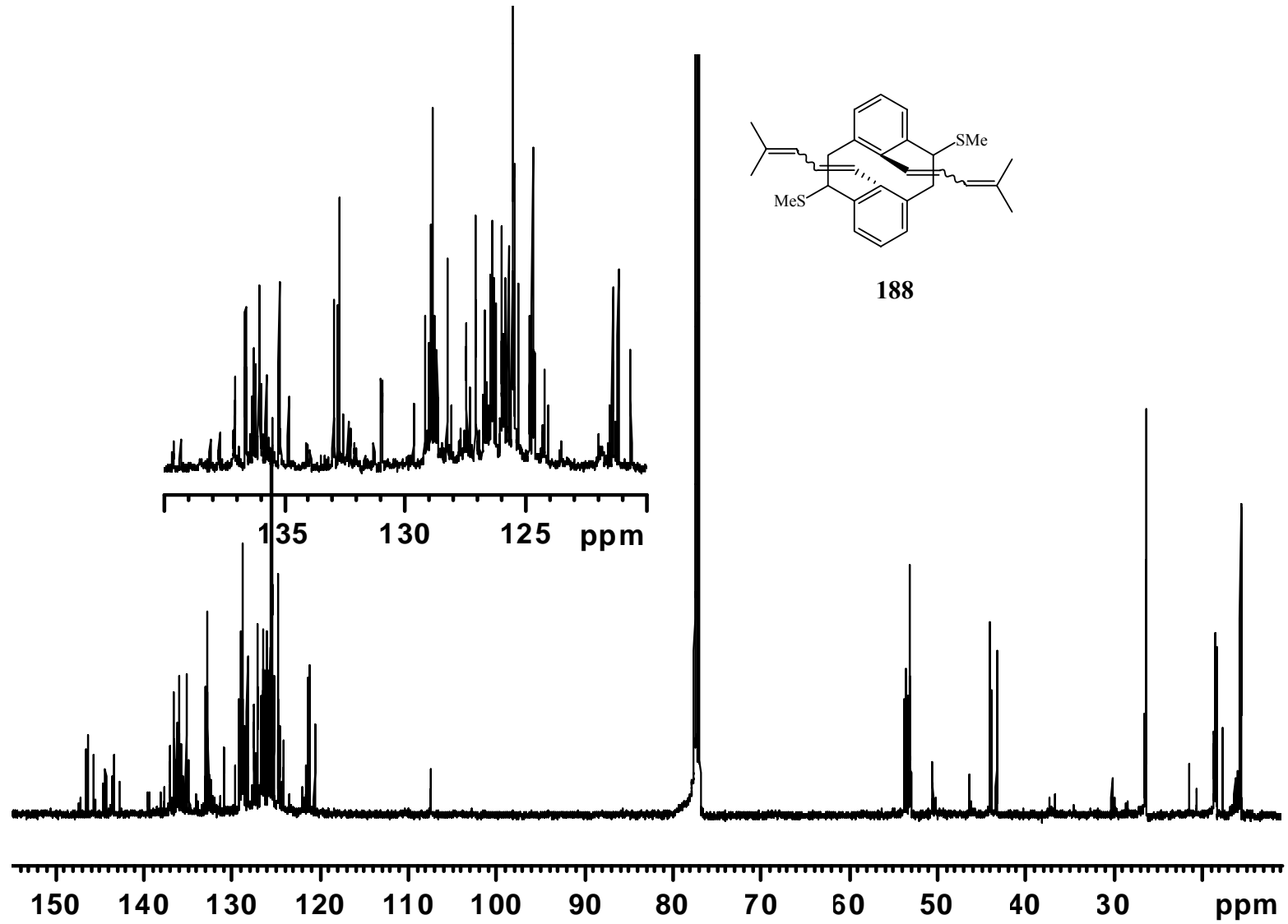


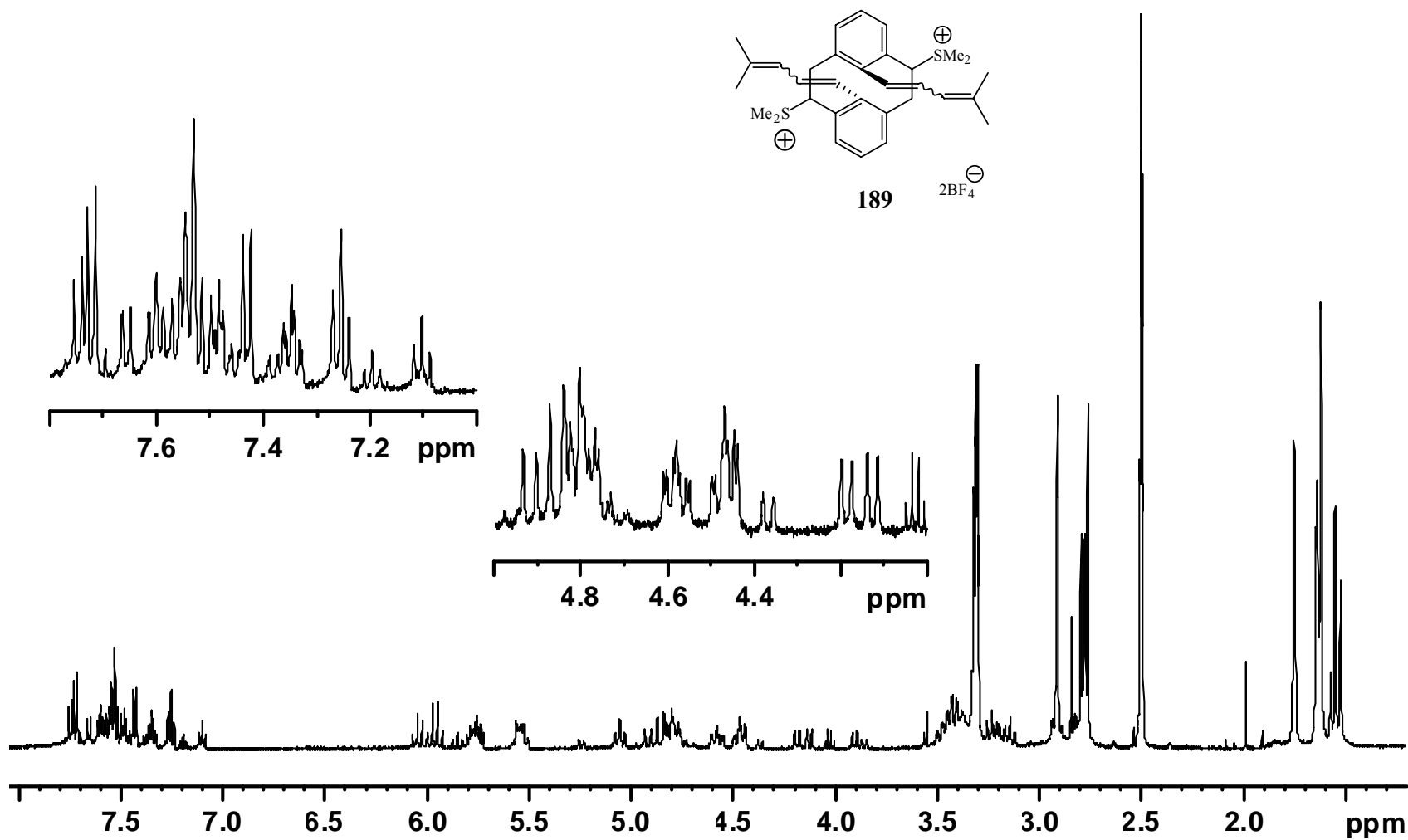


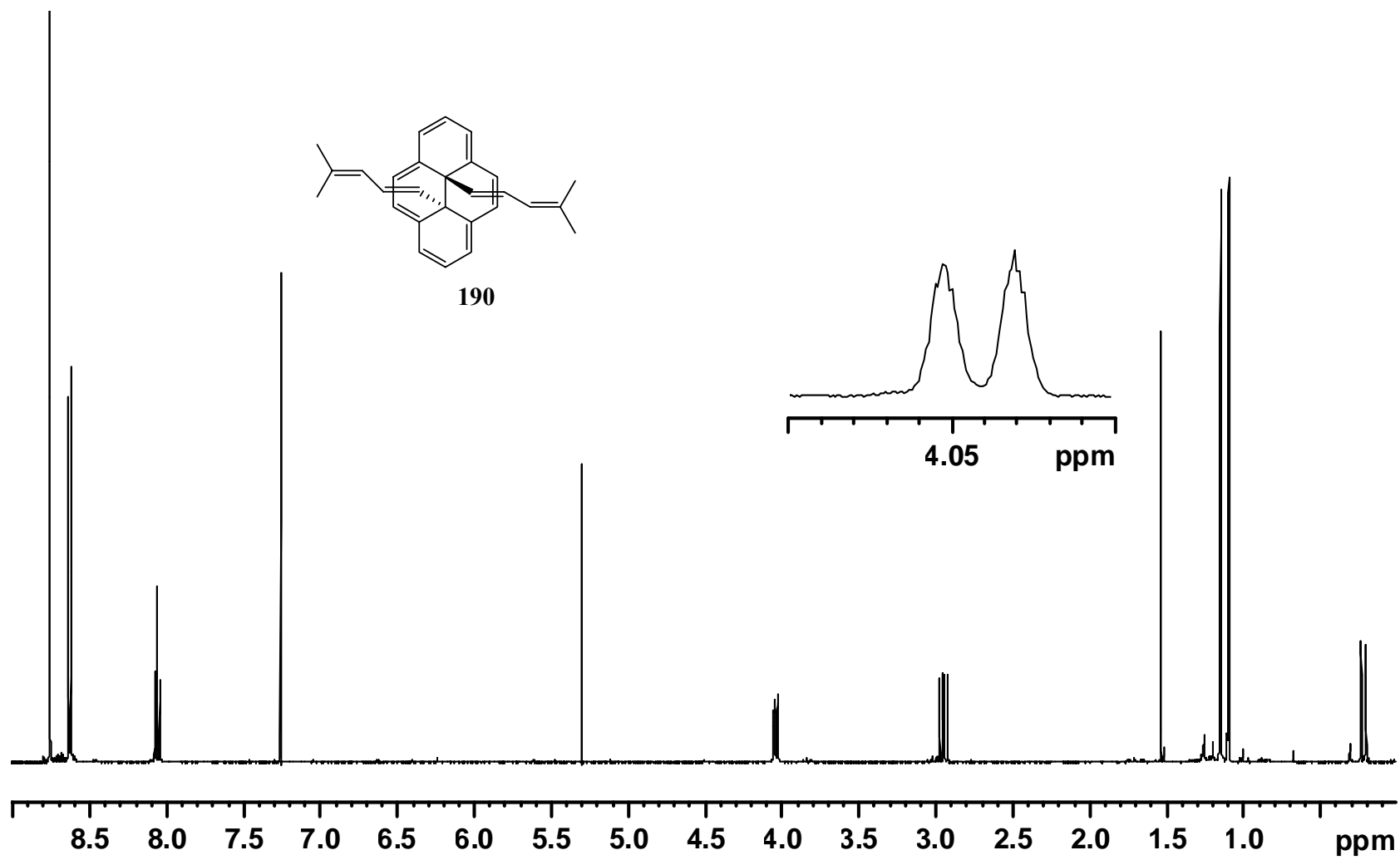


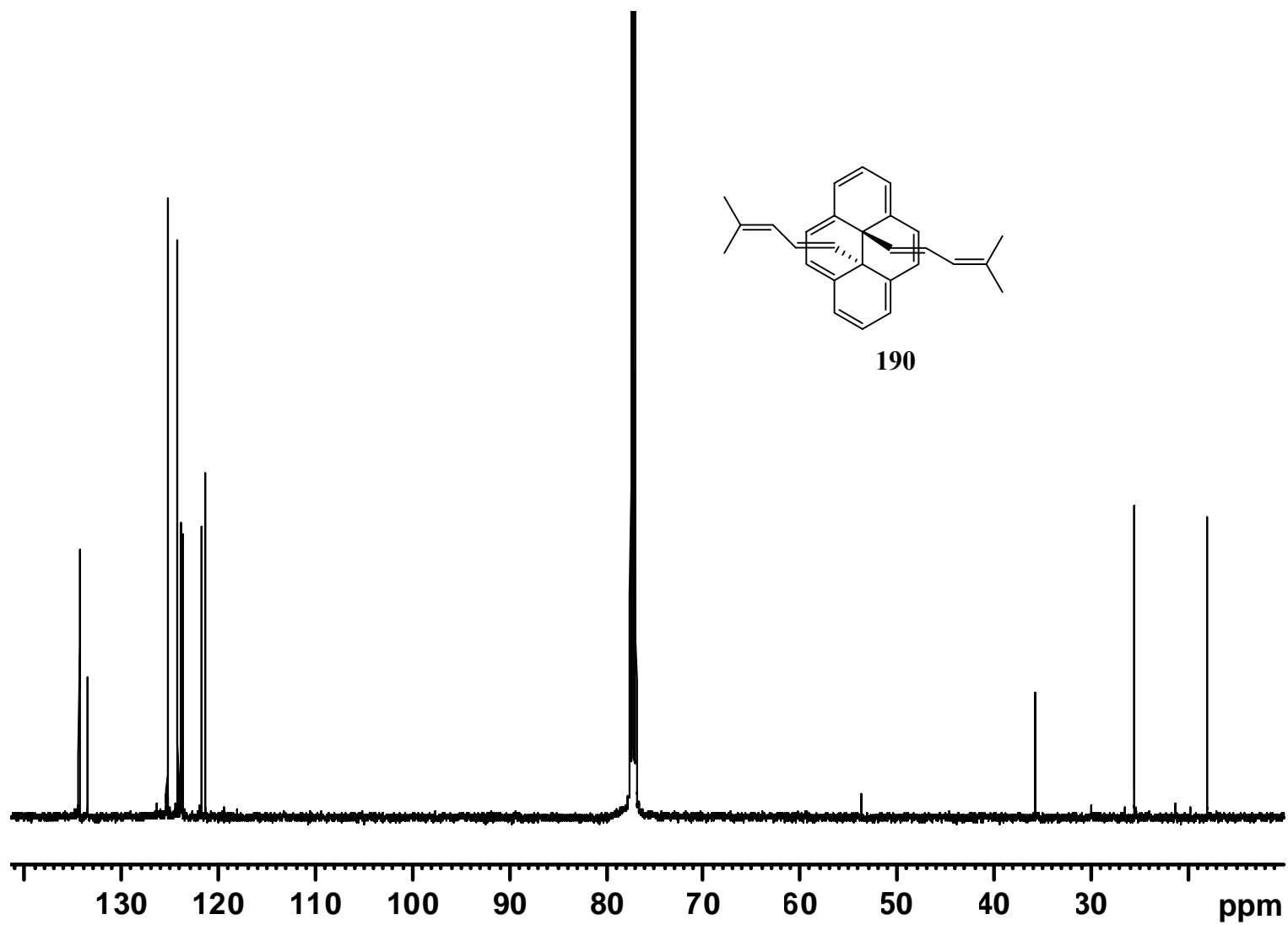


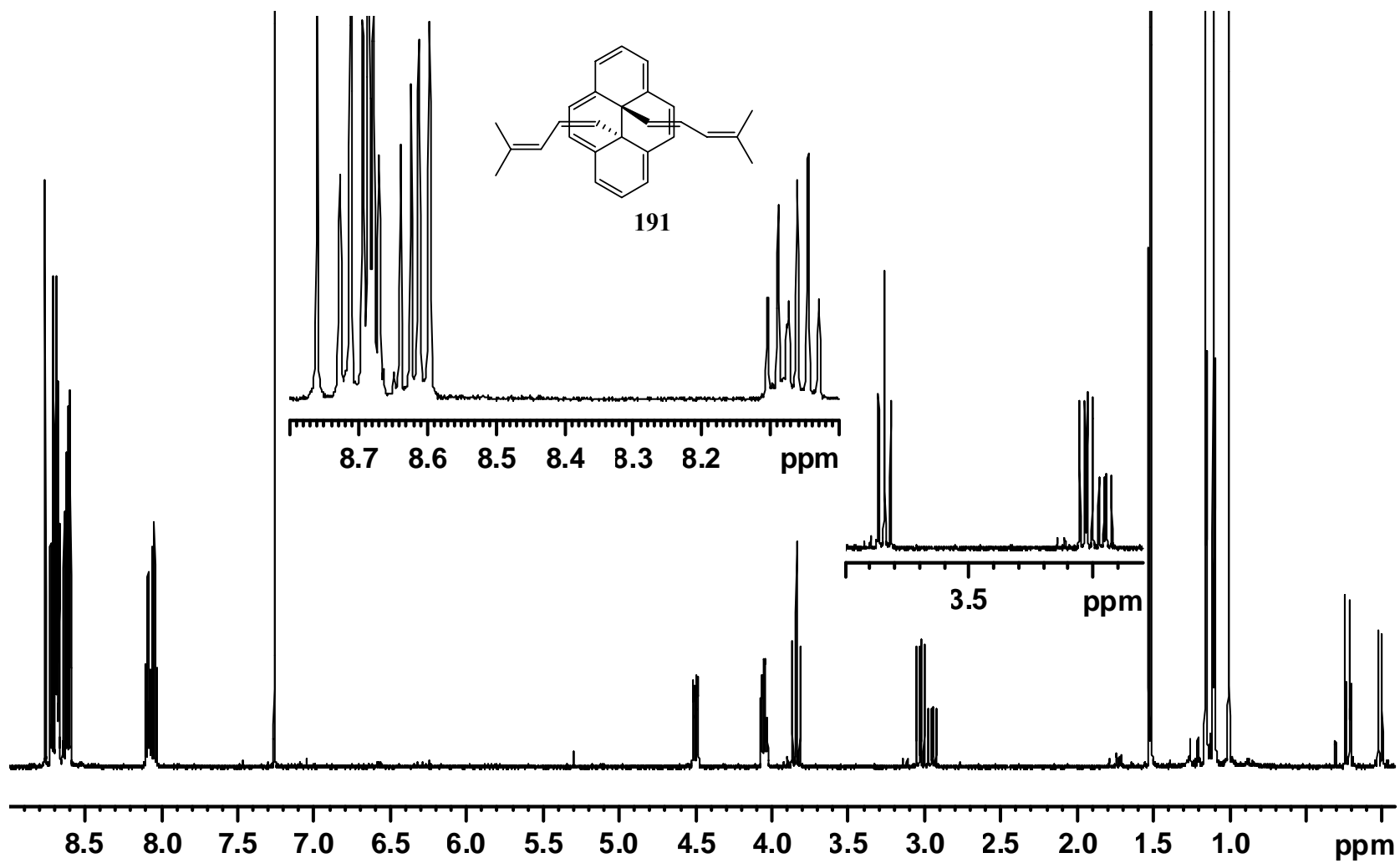


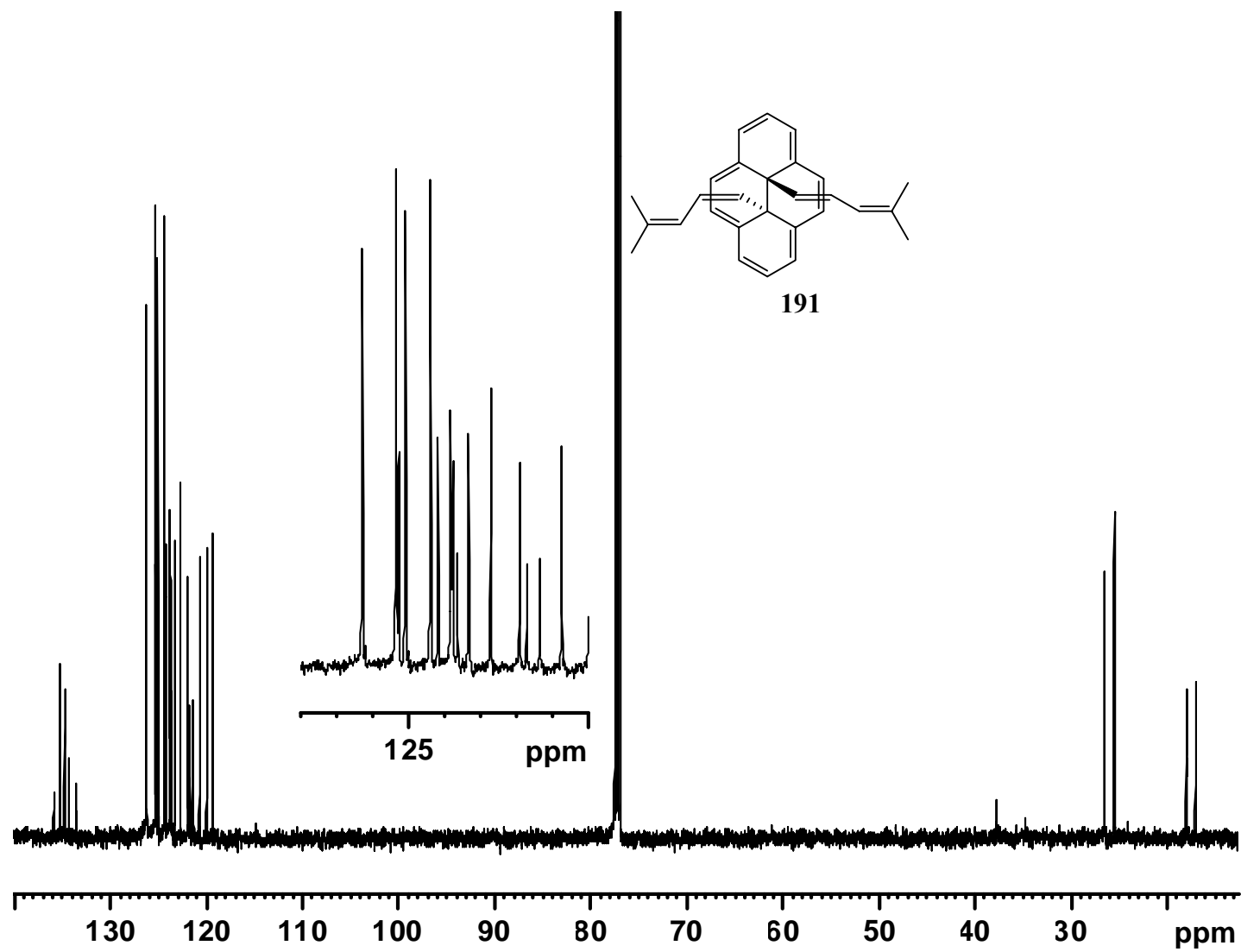


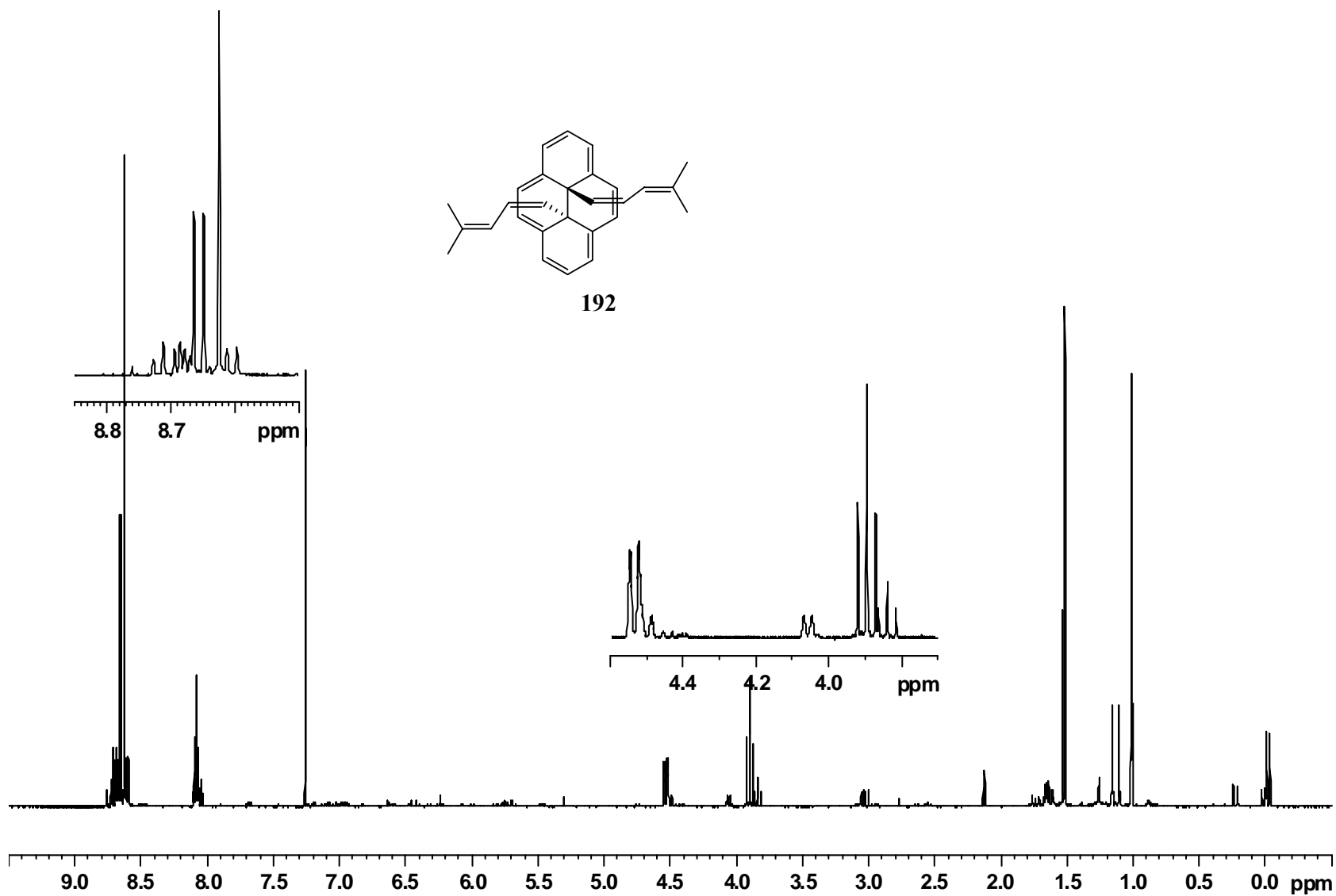


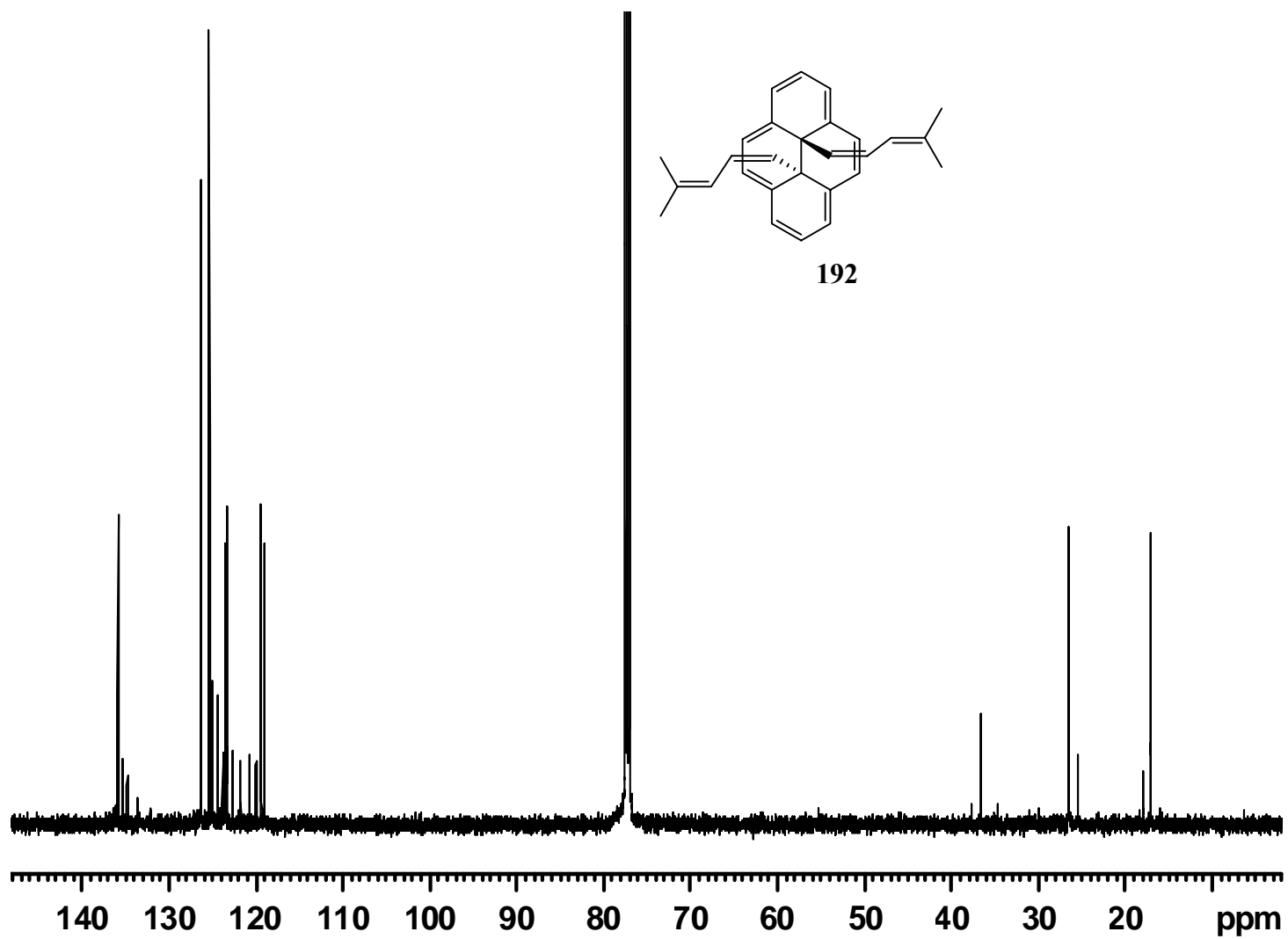


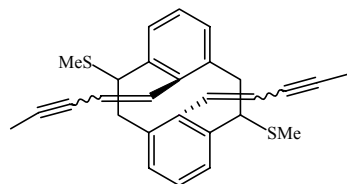
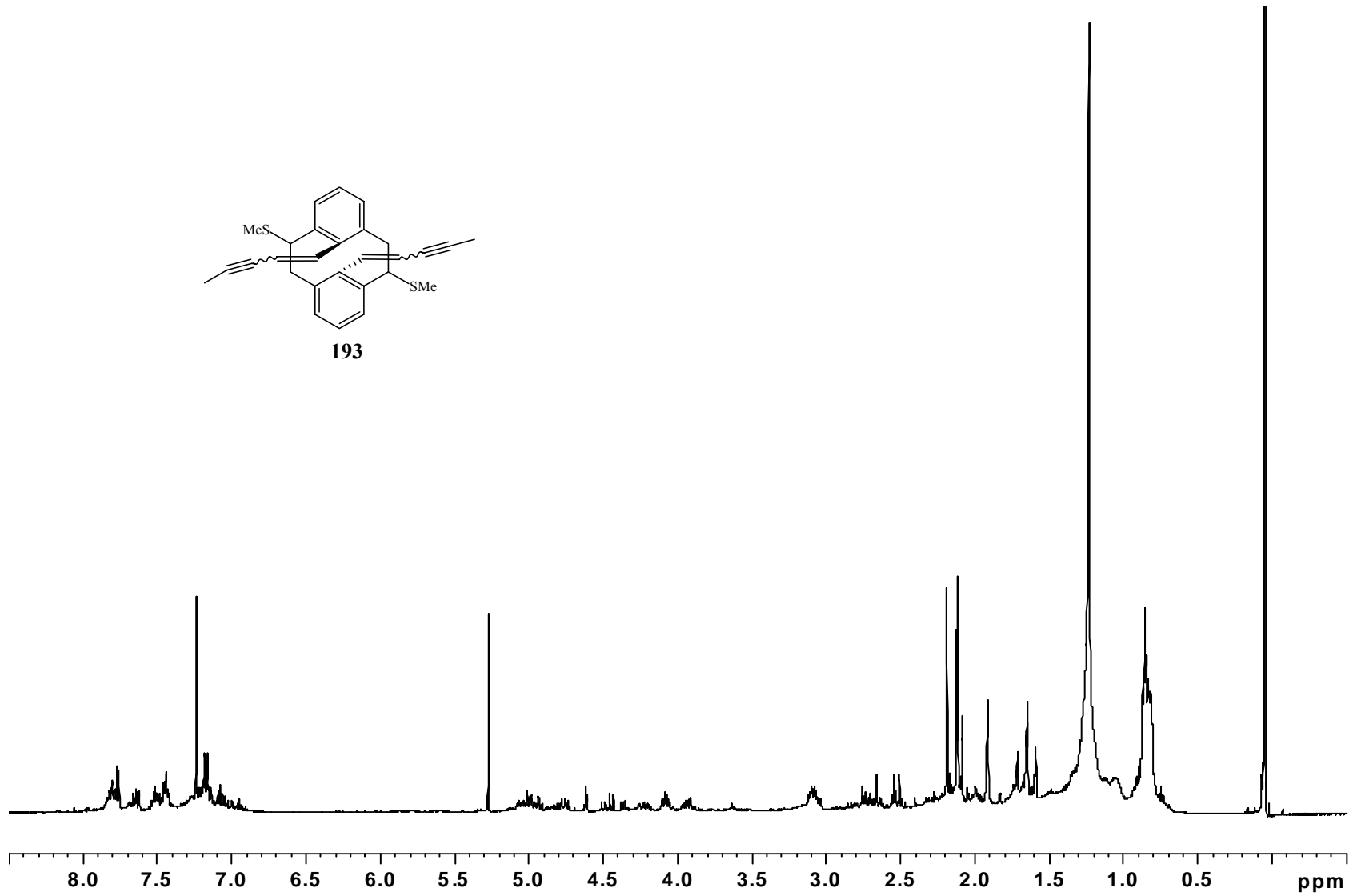


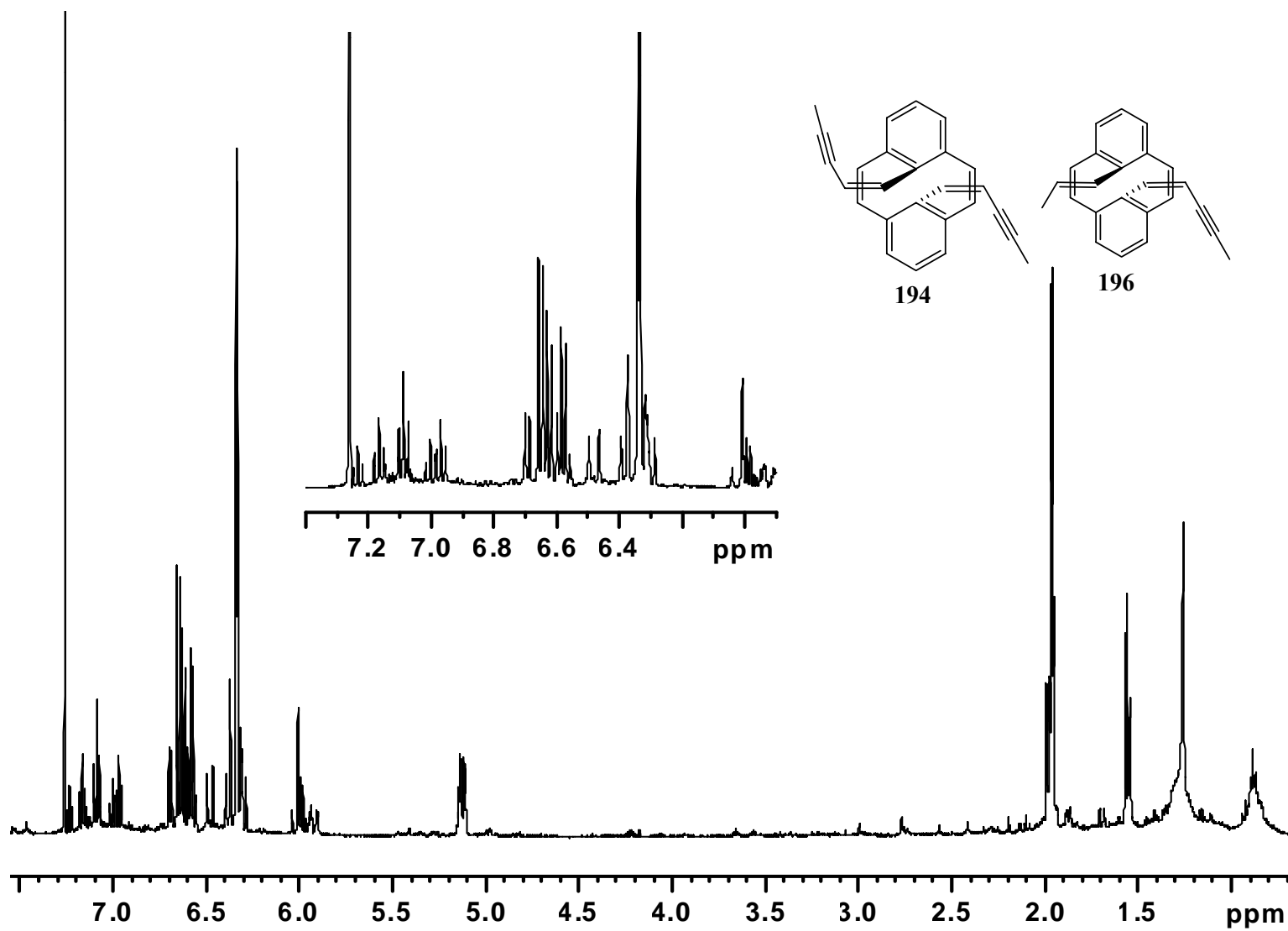


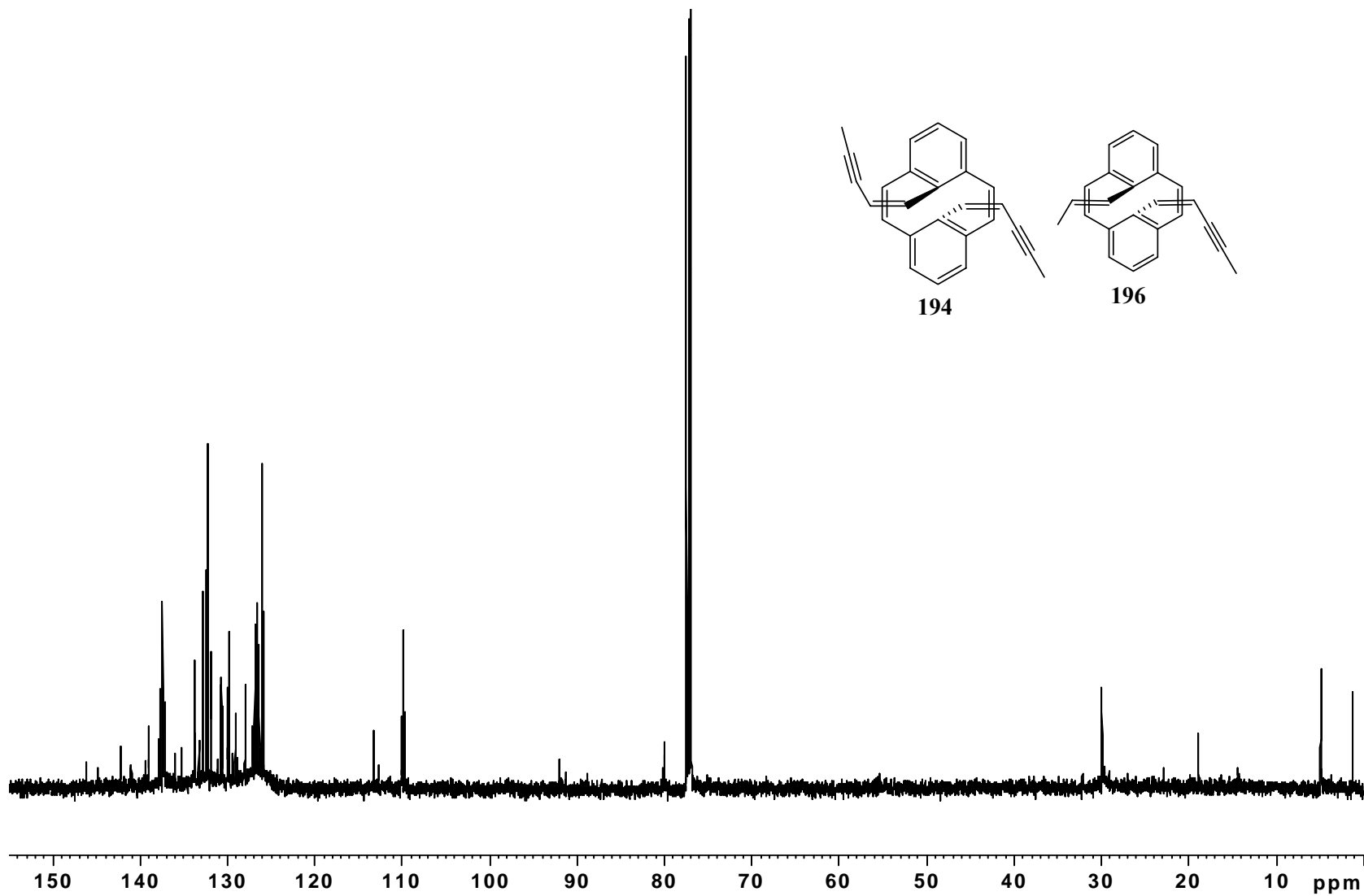


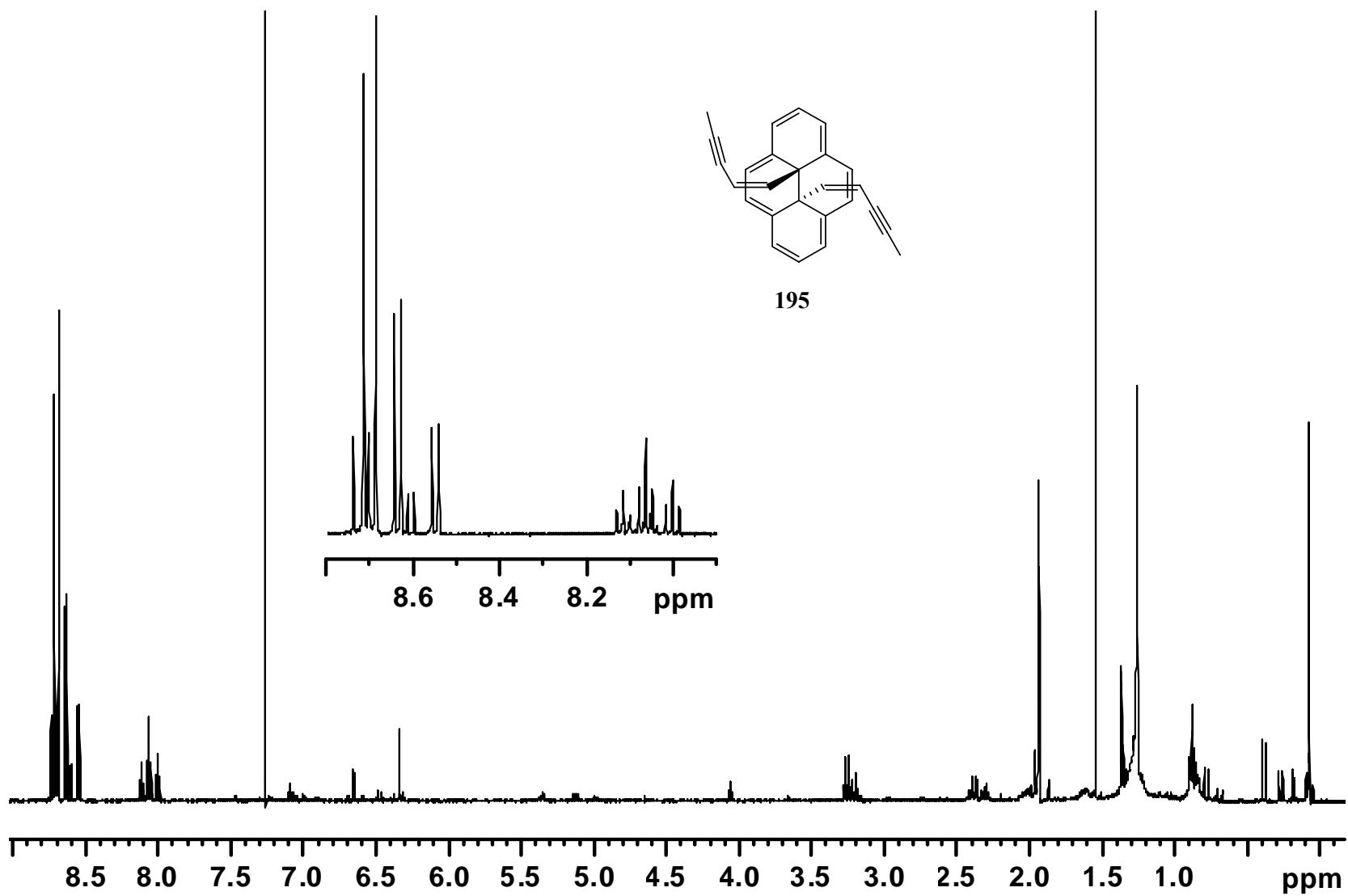


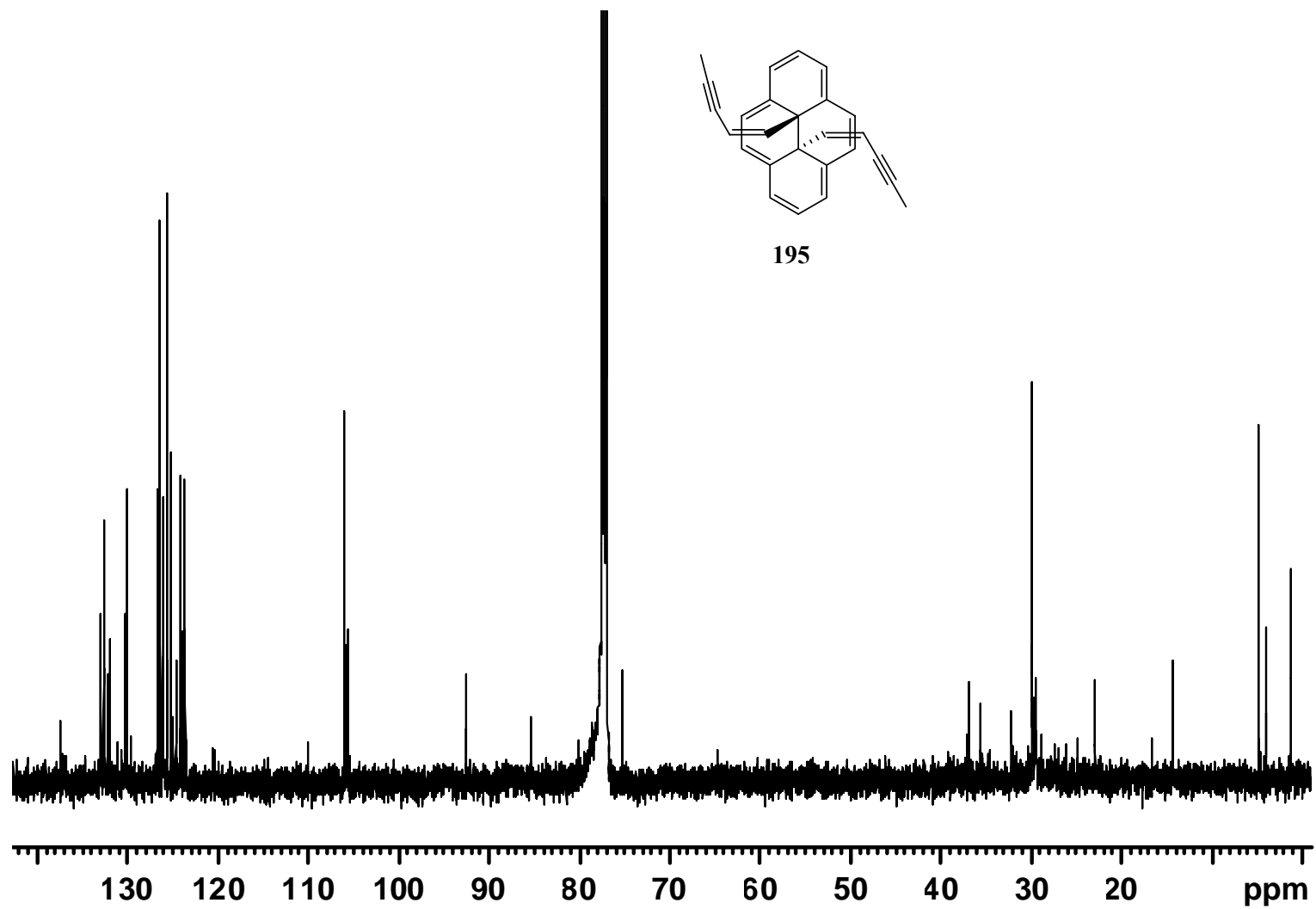


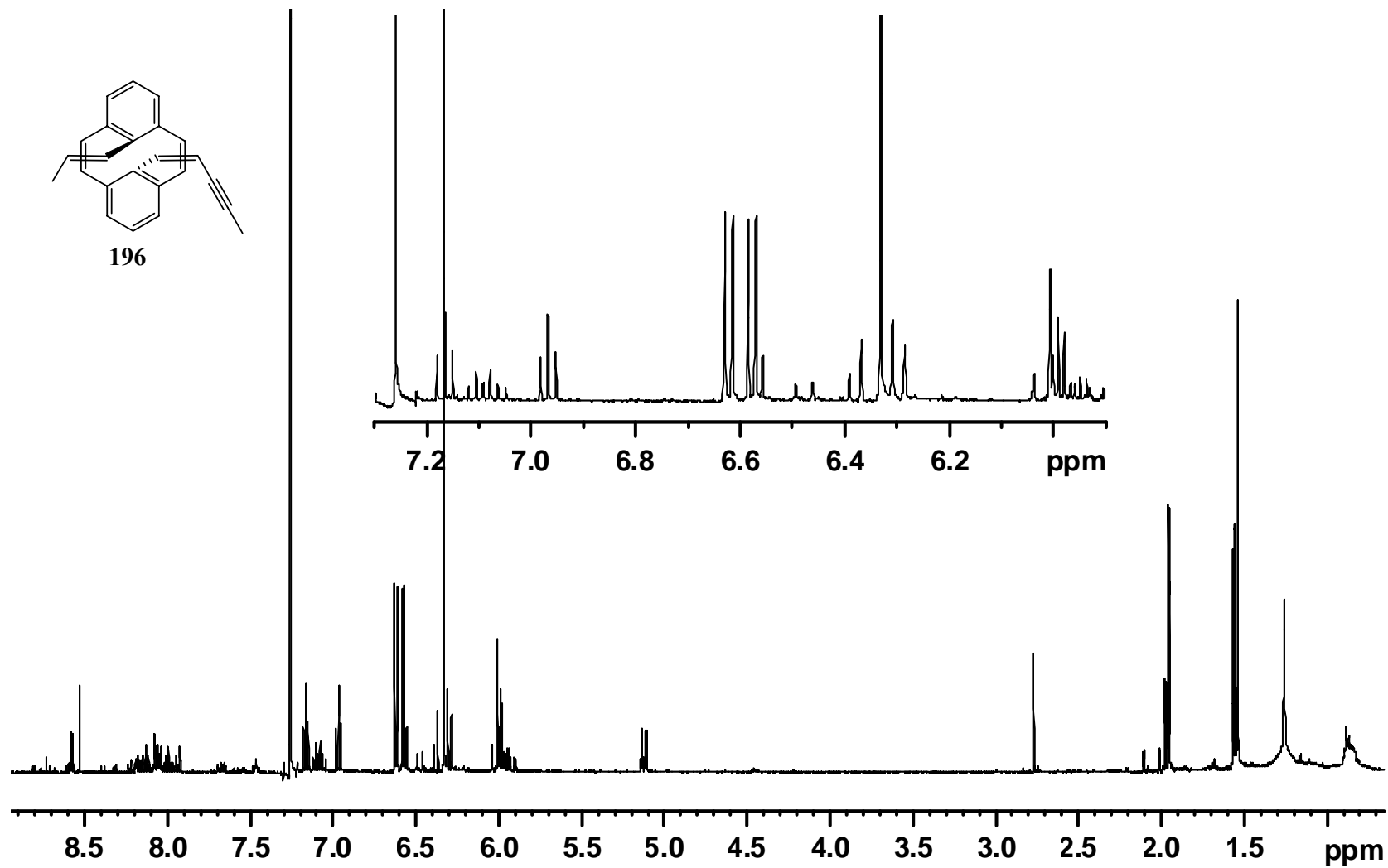
**193**

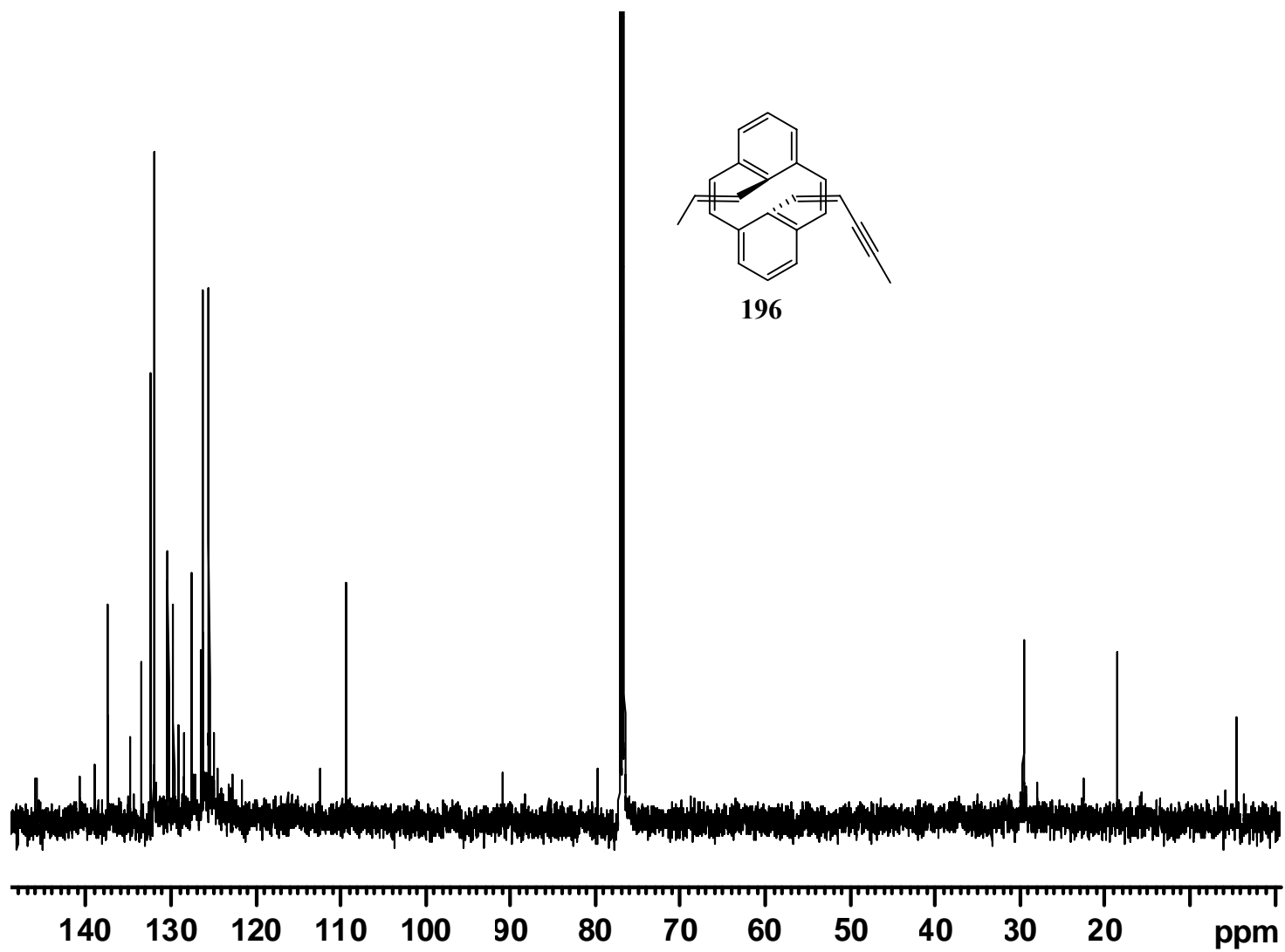


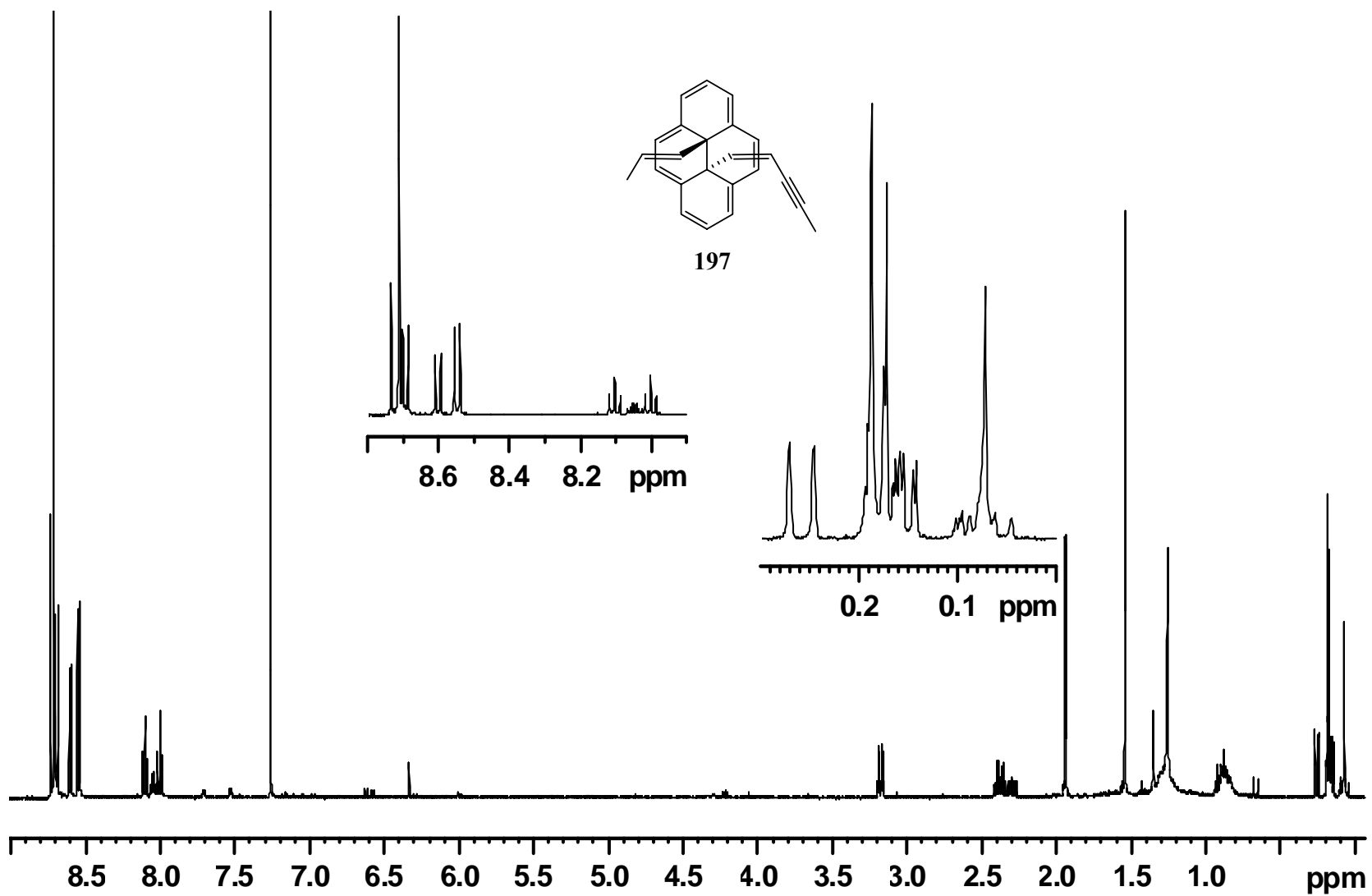


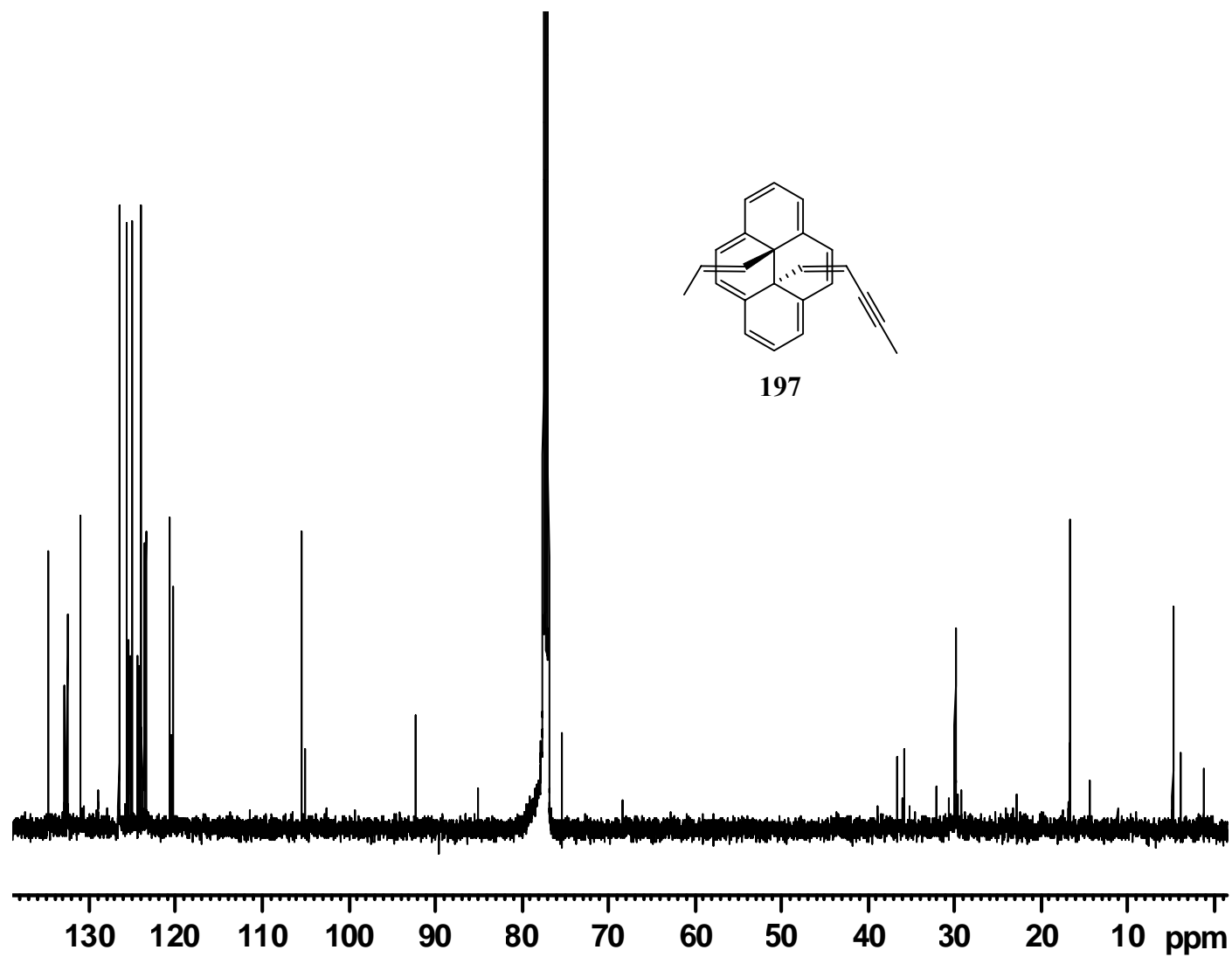


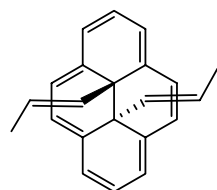




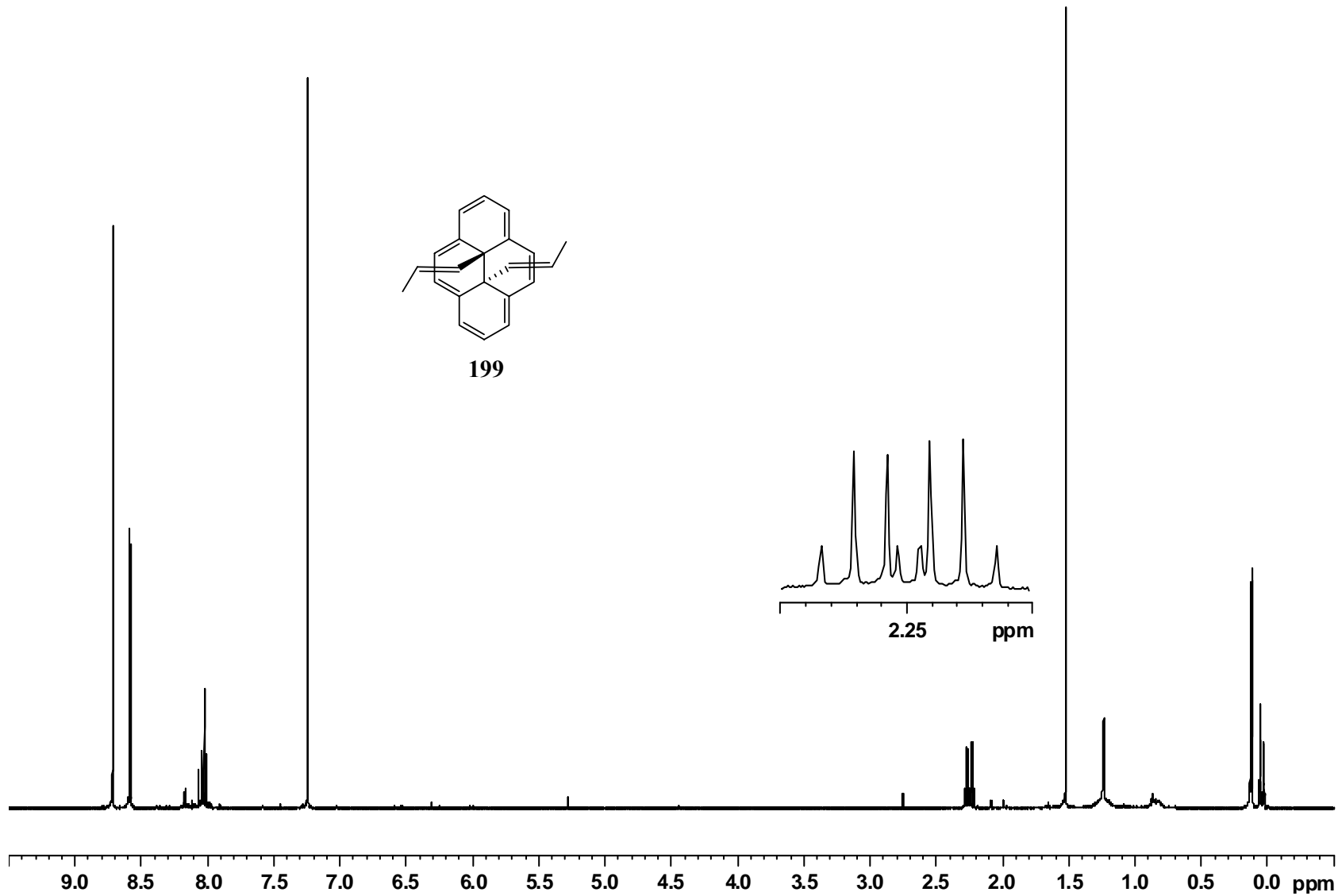


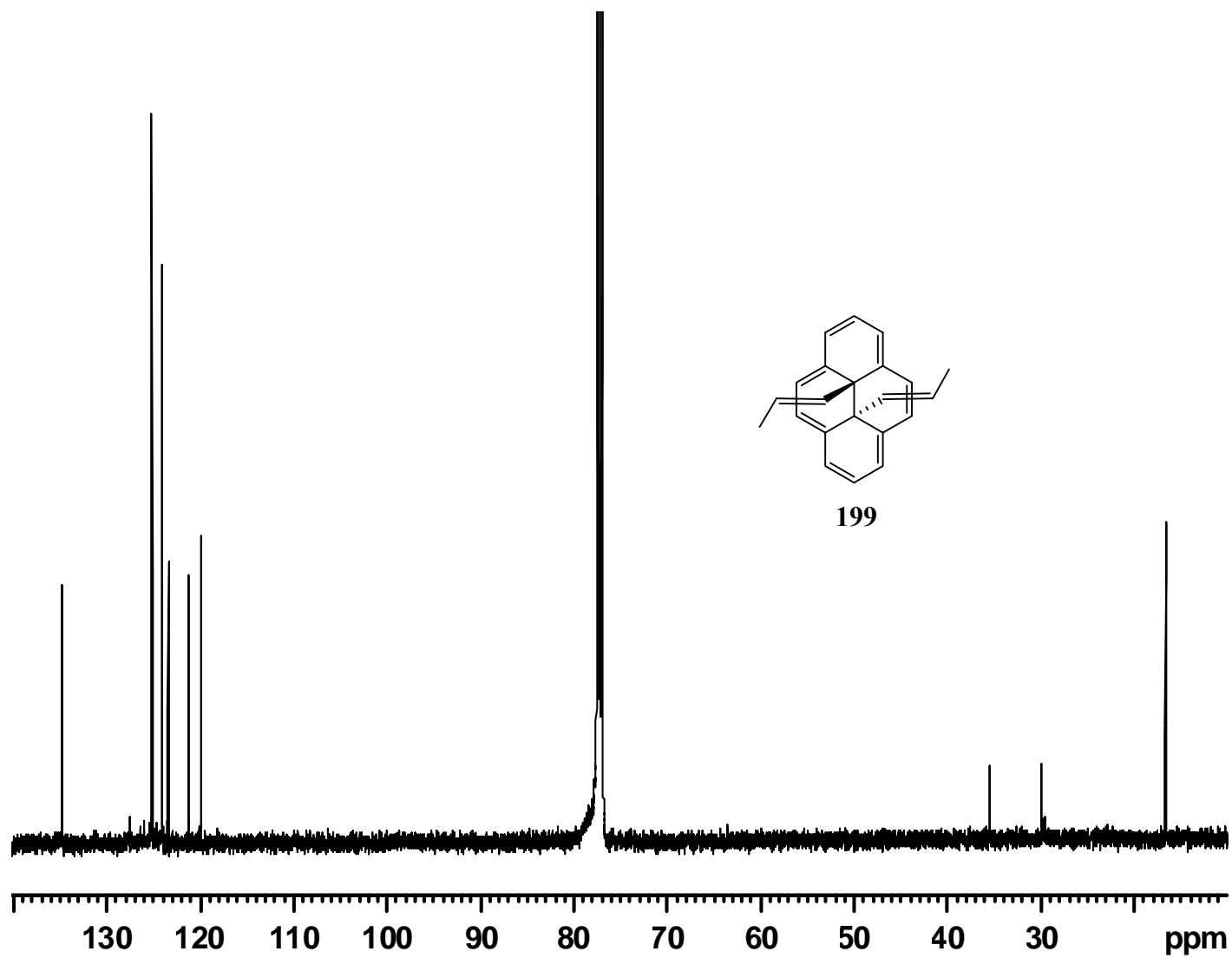


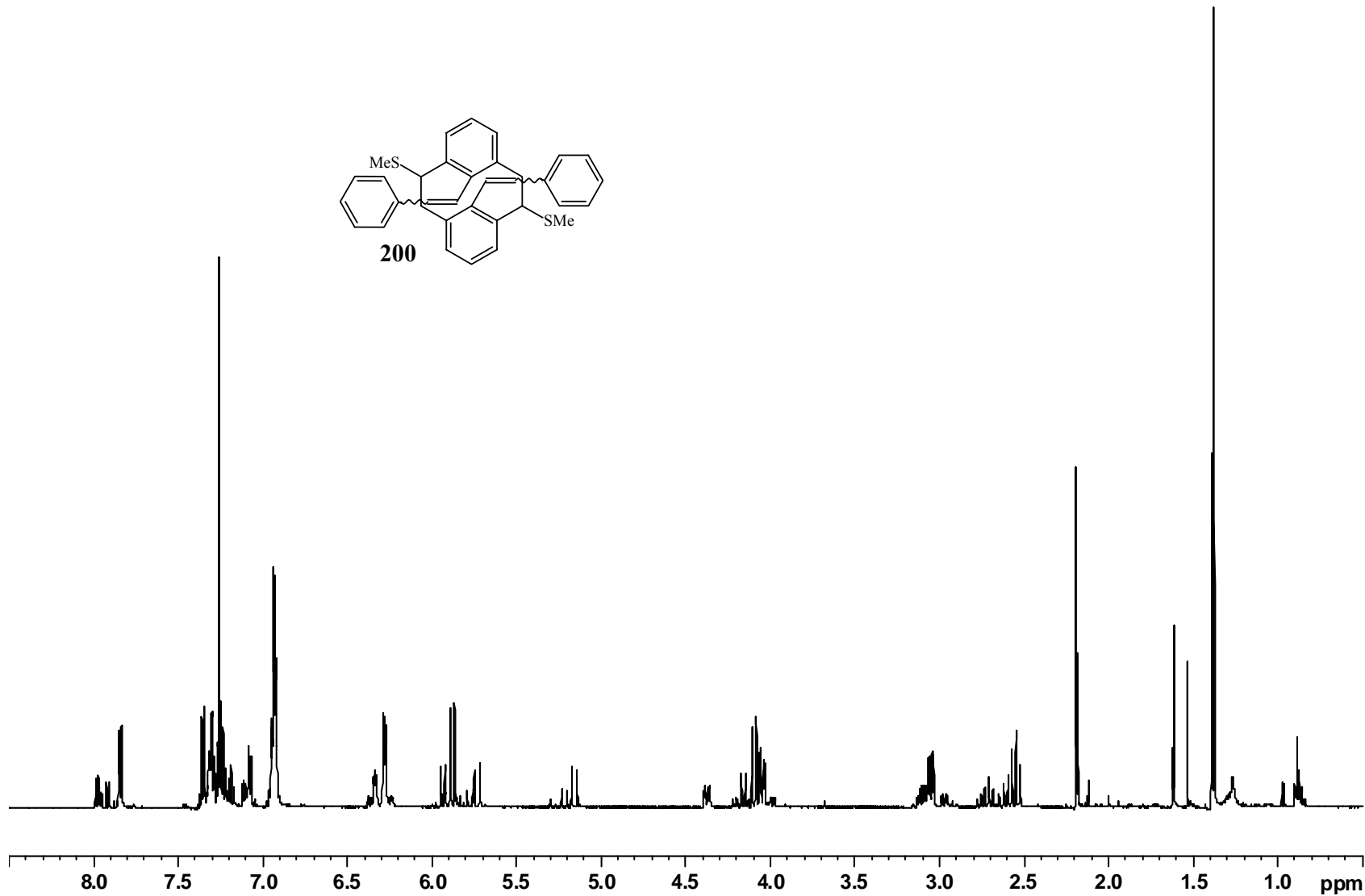
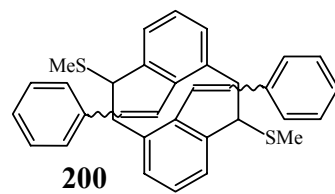


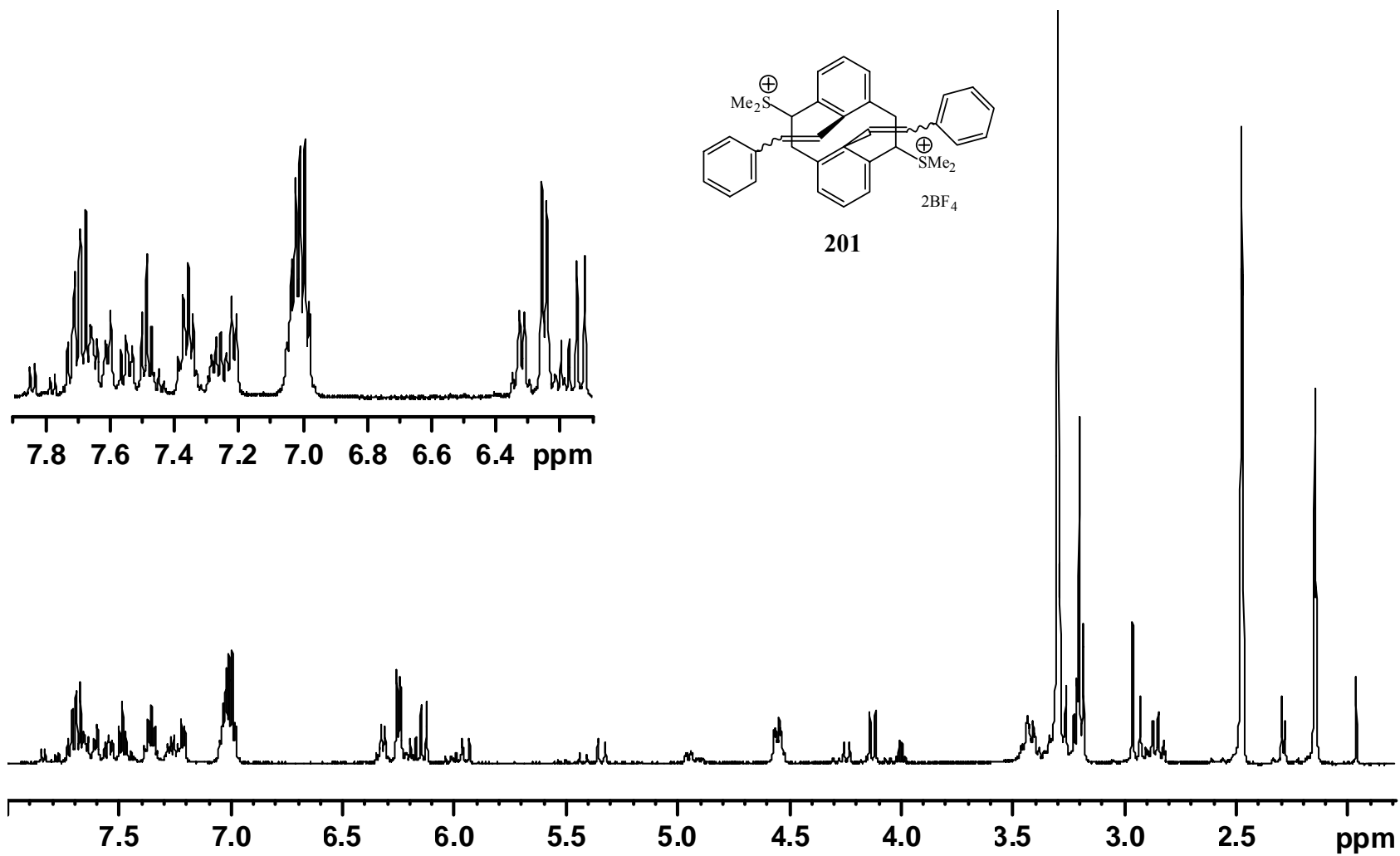


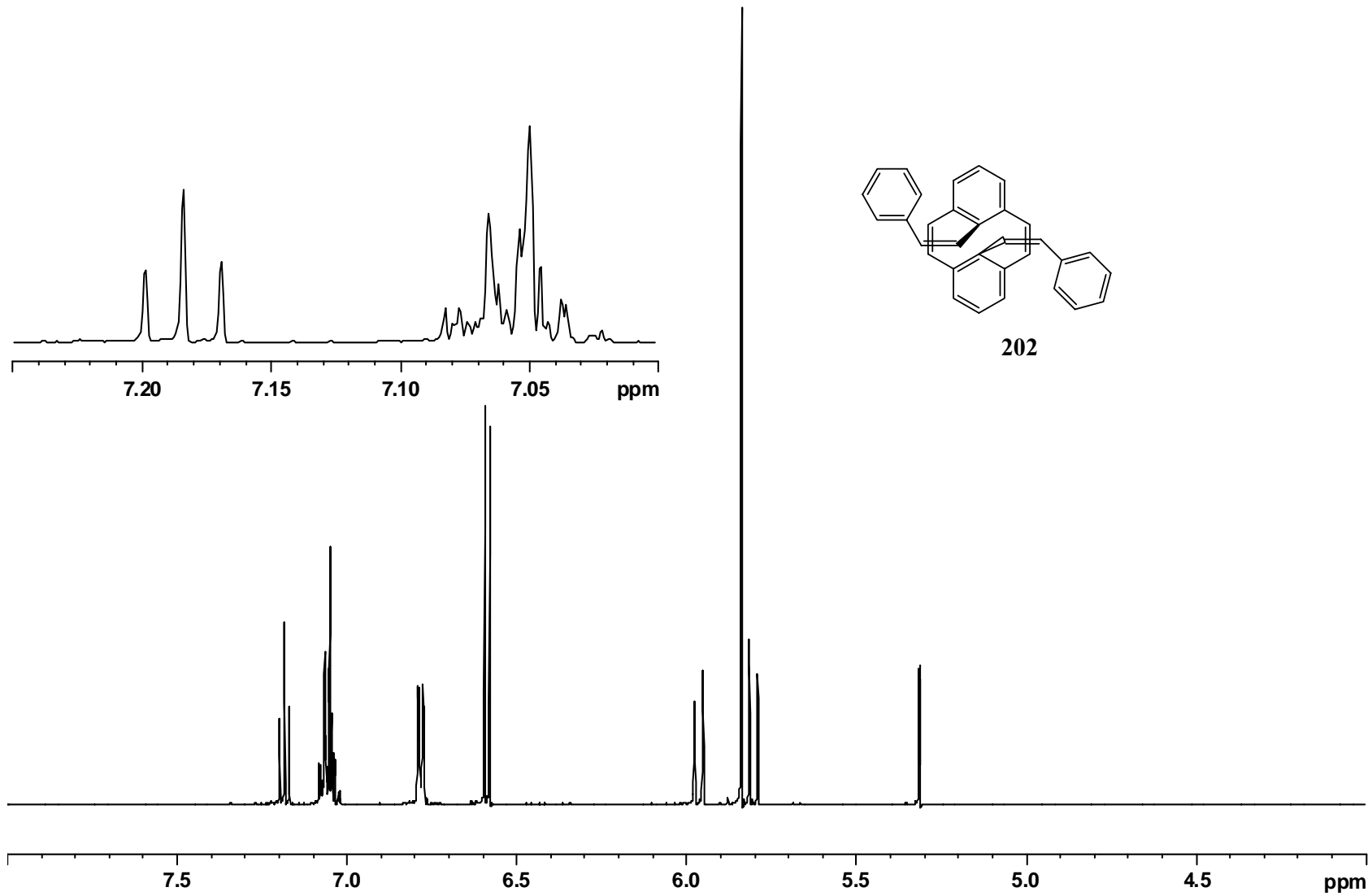
199

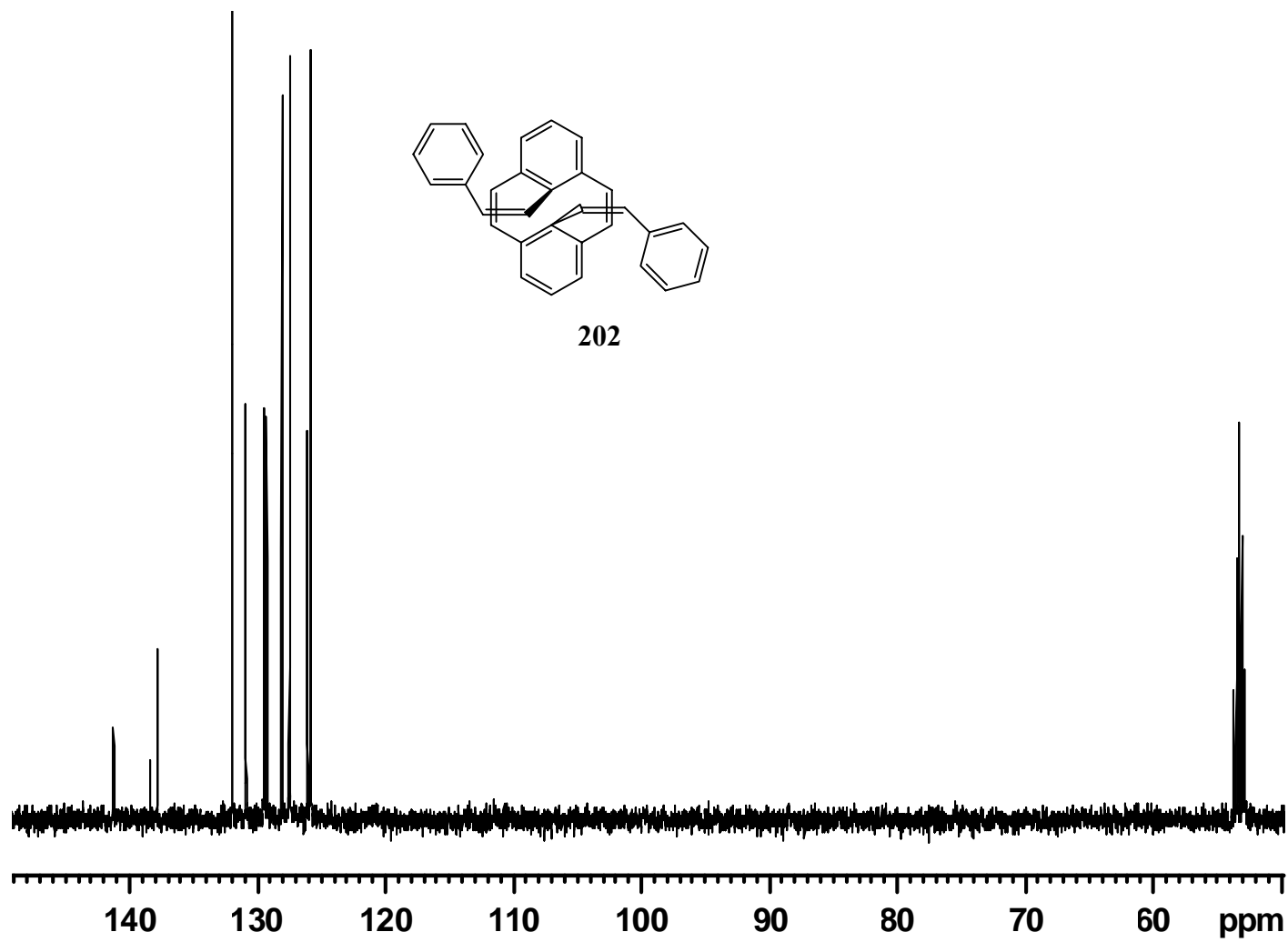


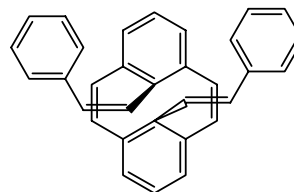




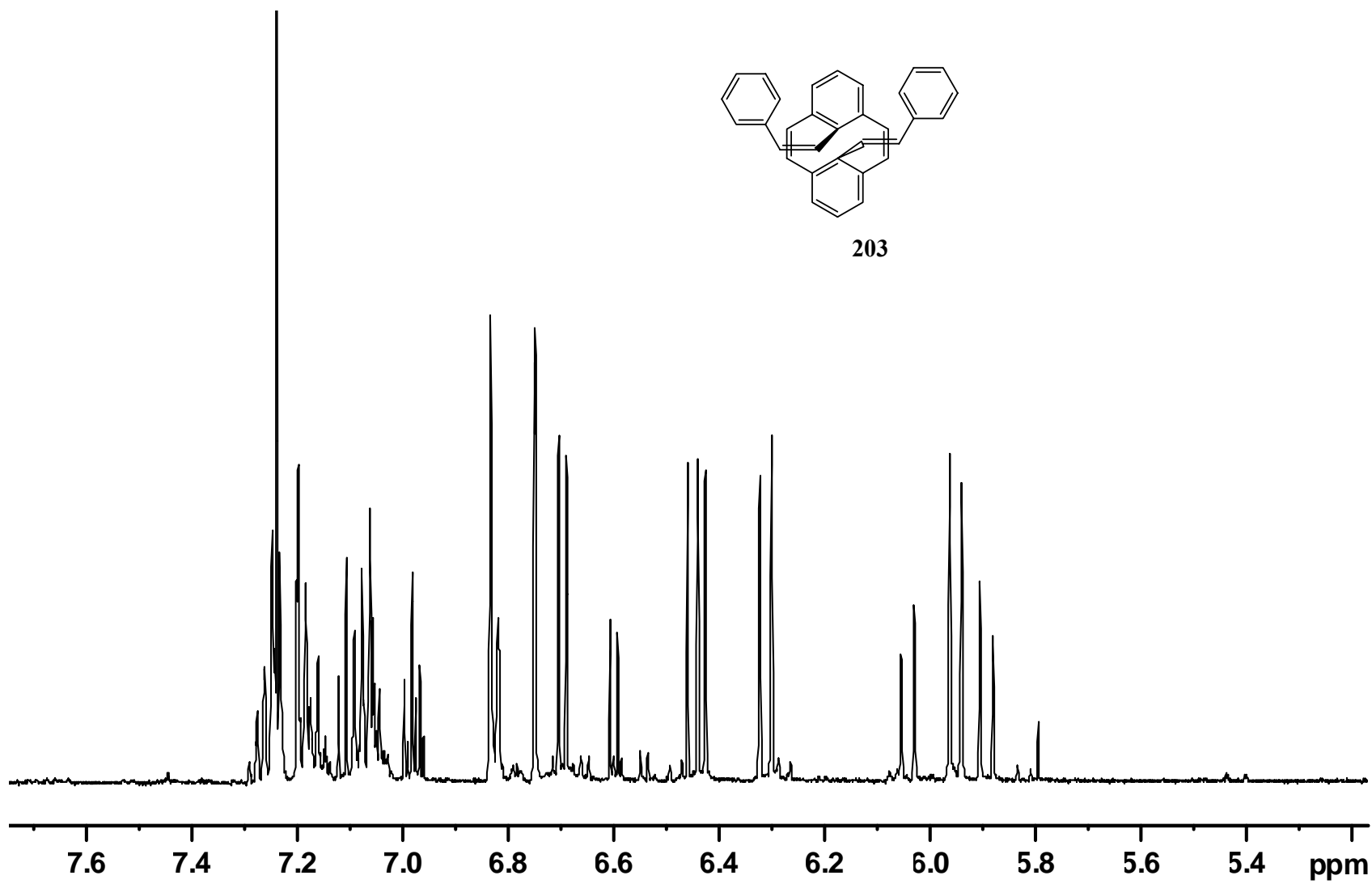


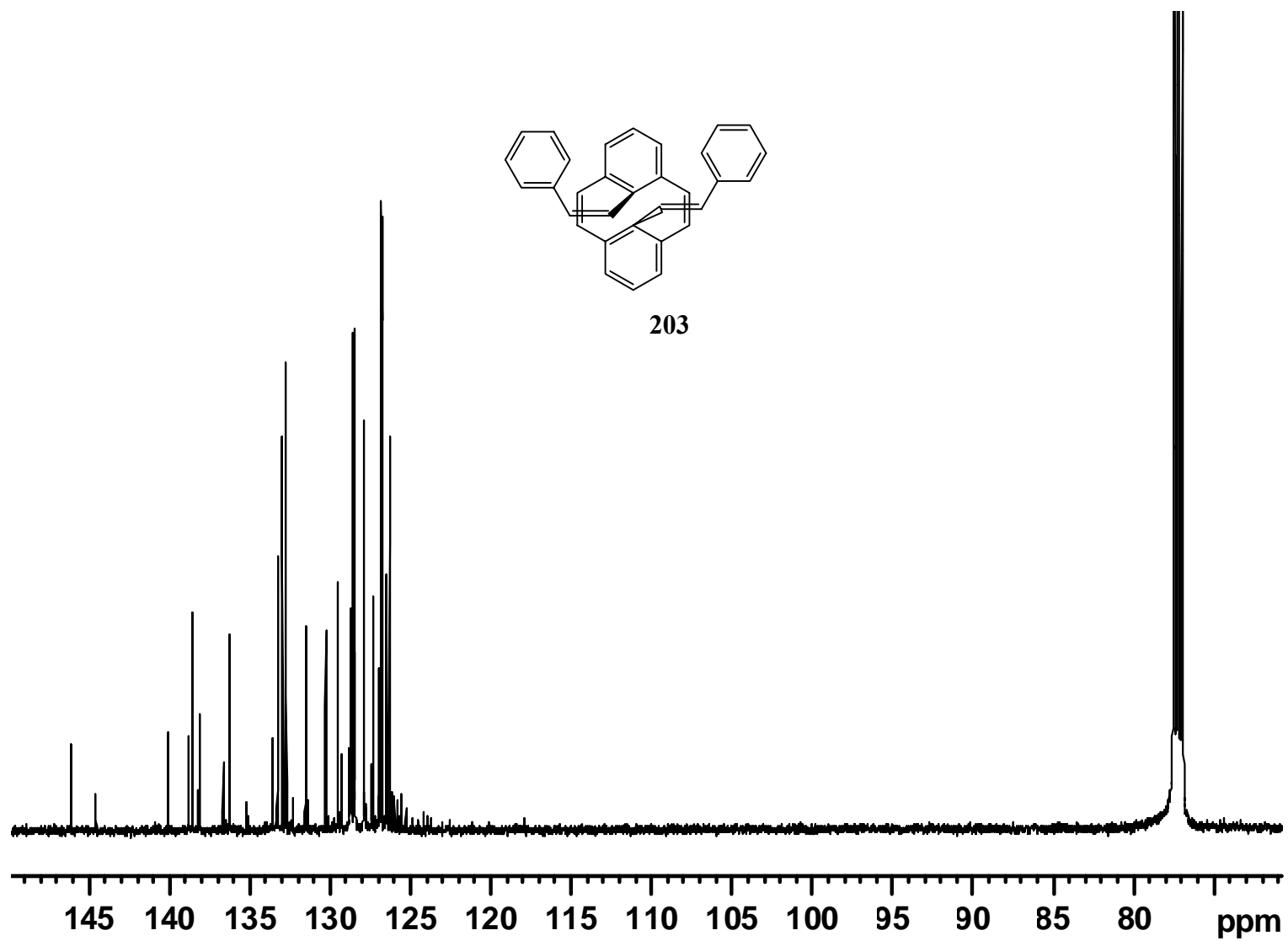


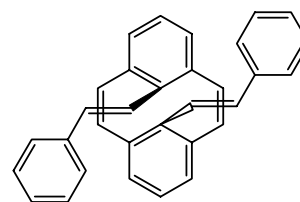
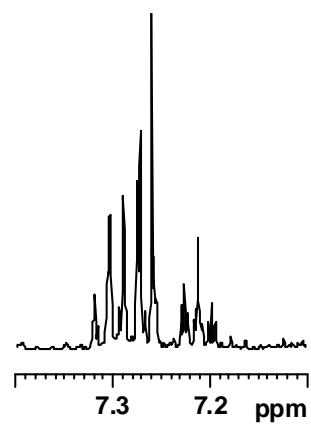




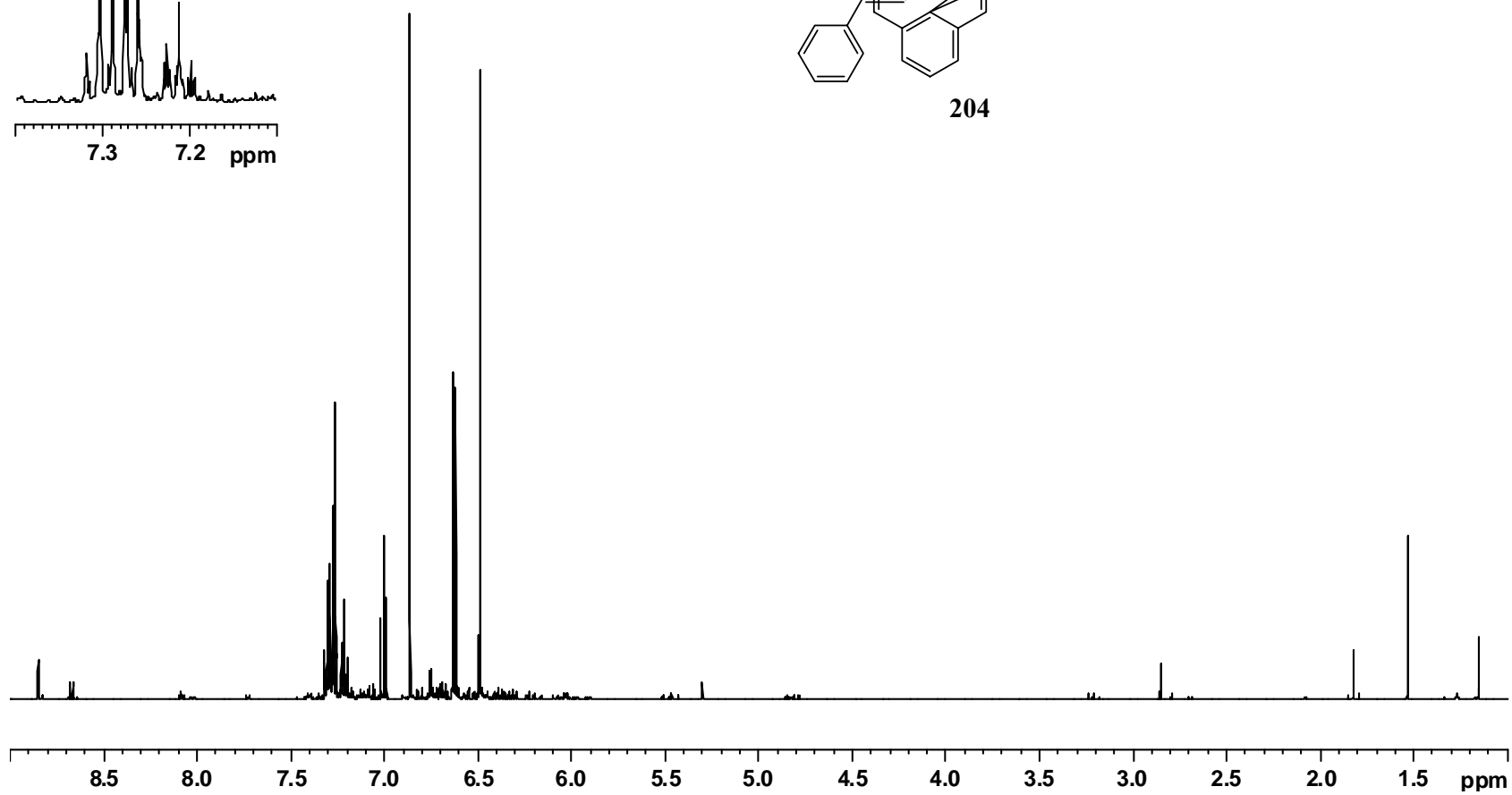
203

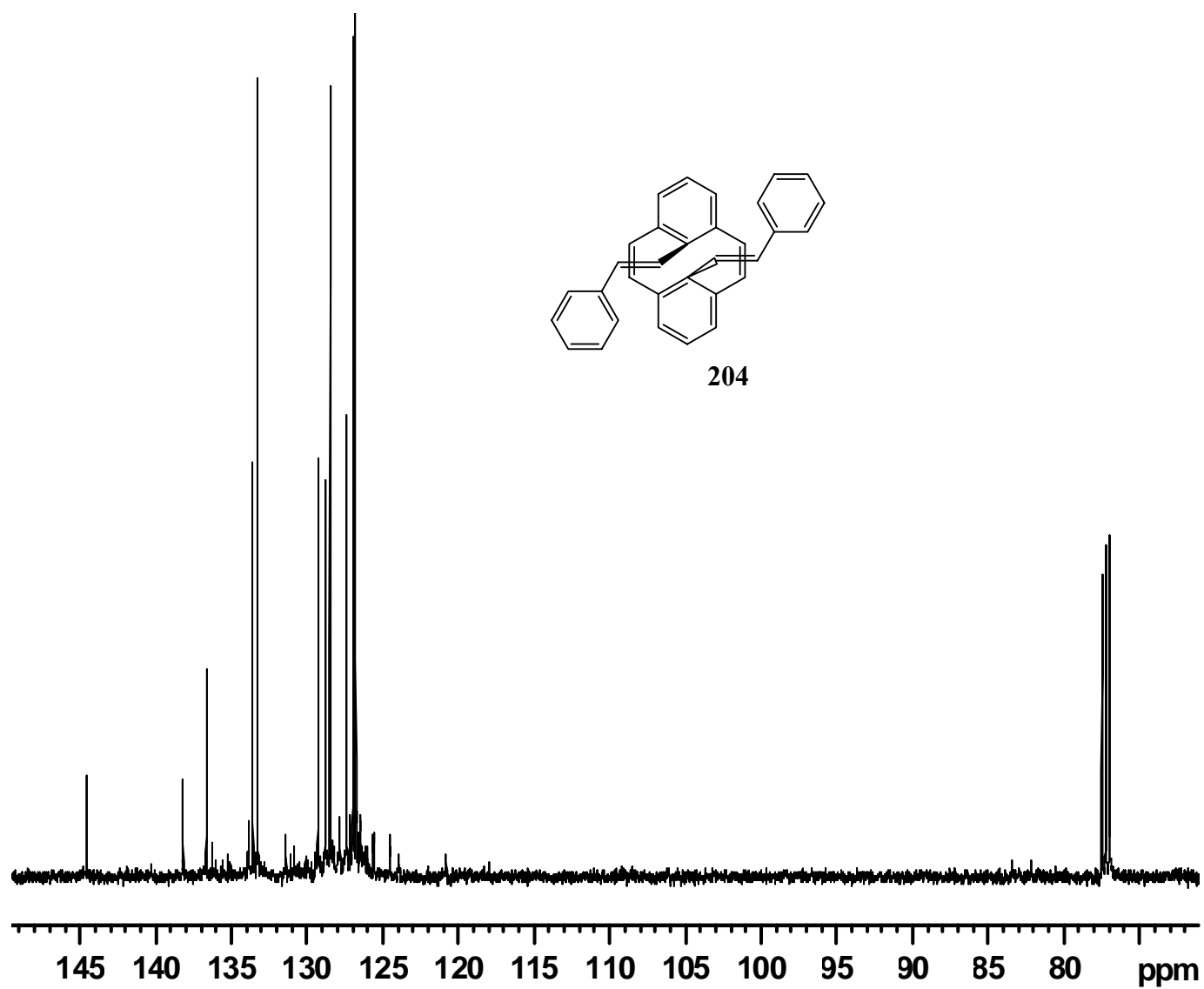


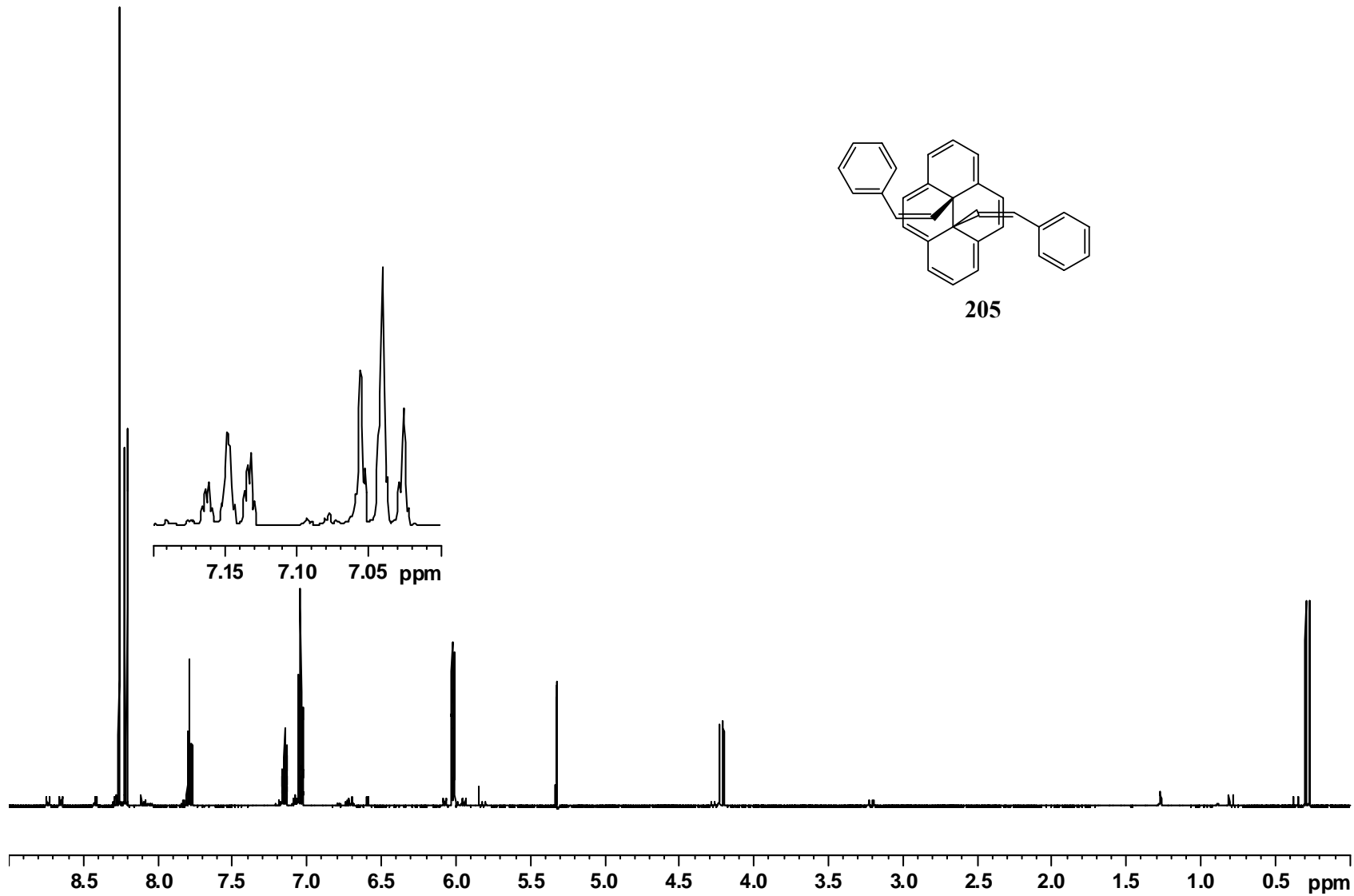


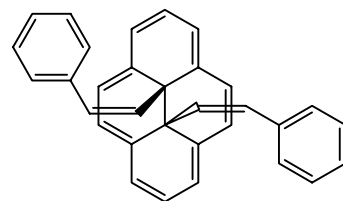


204

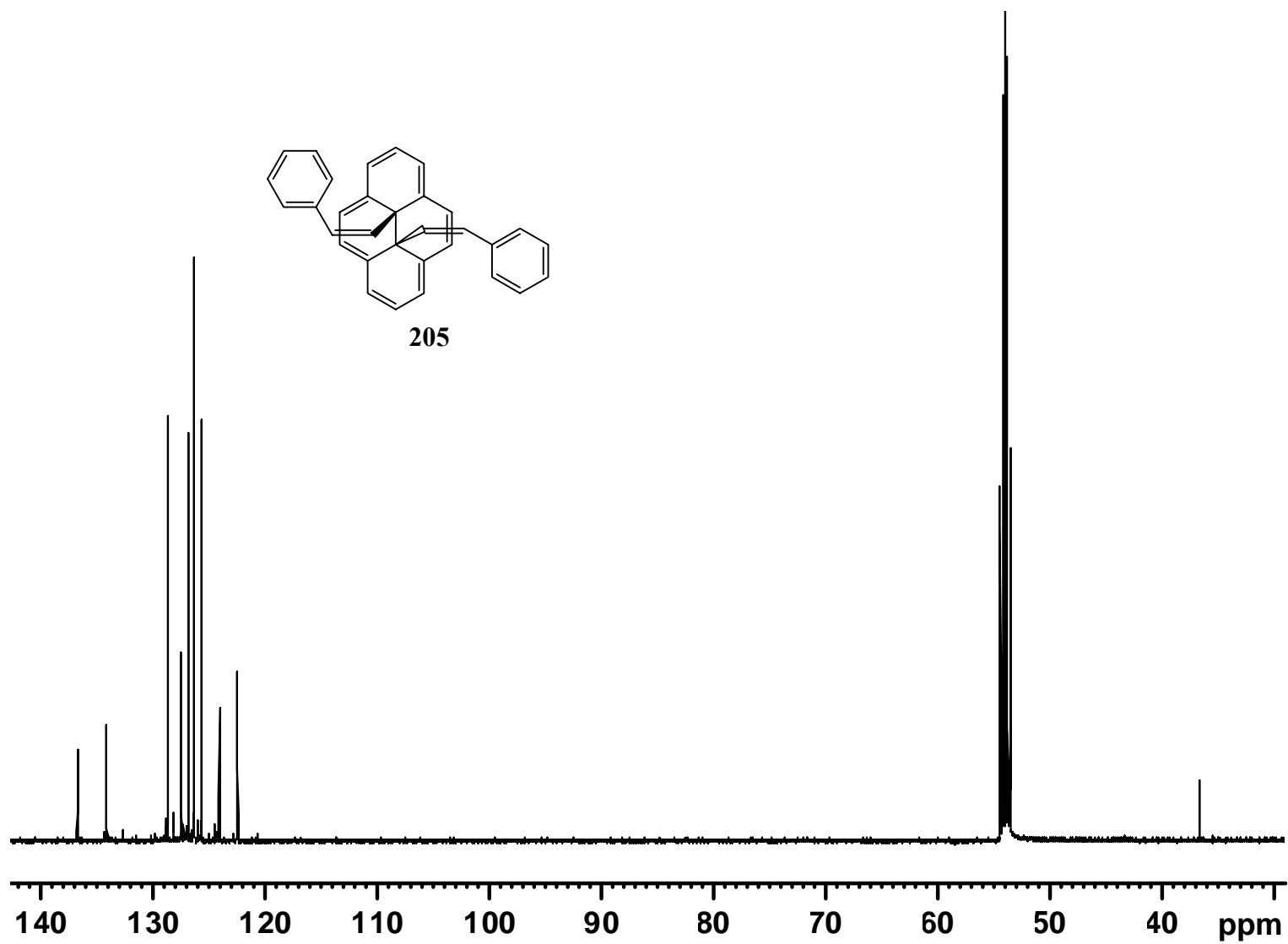


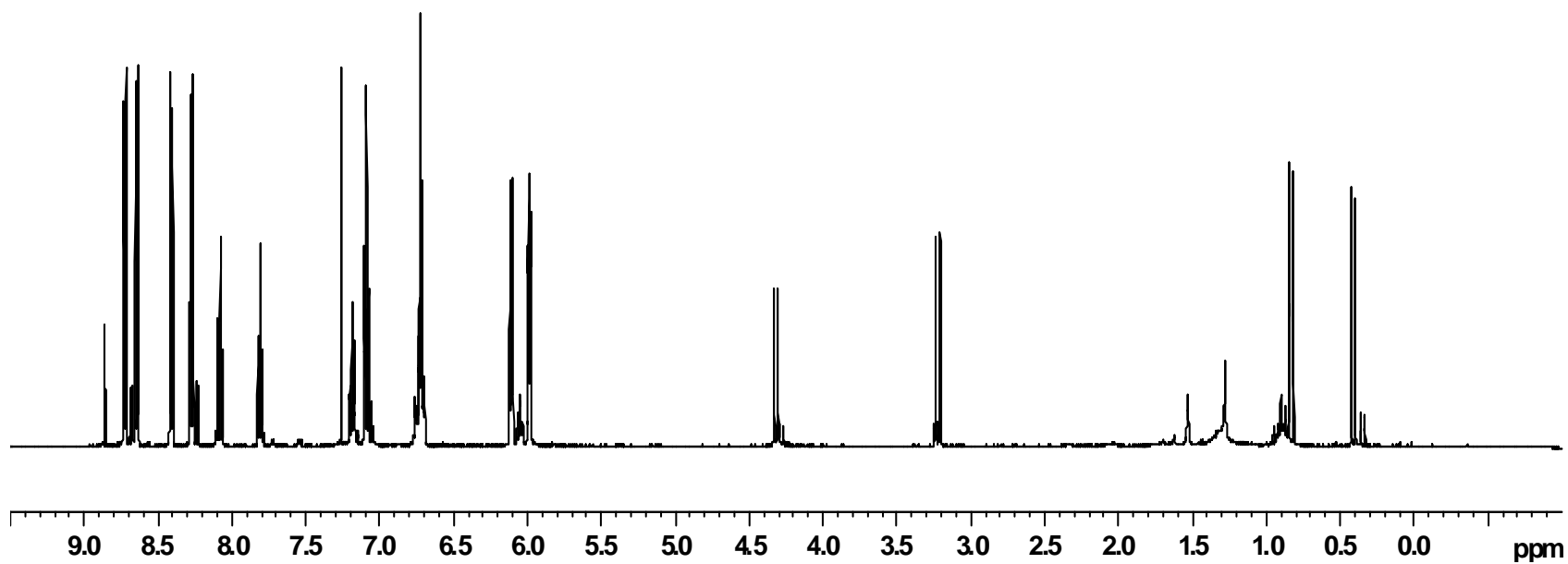
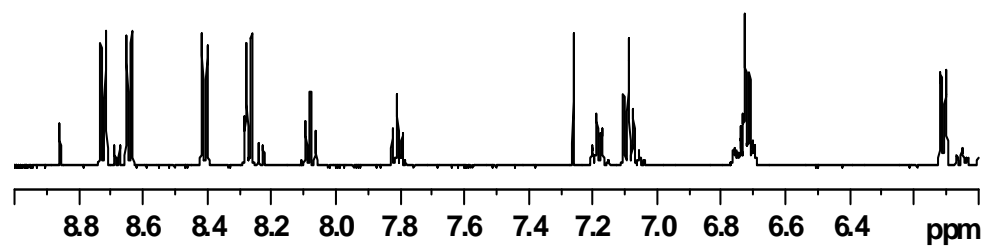
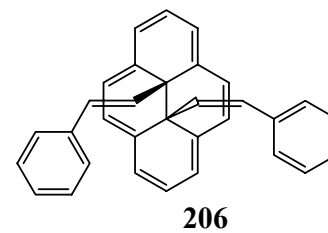


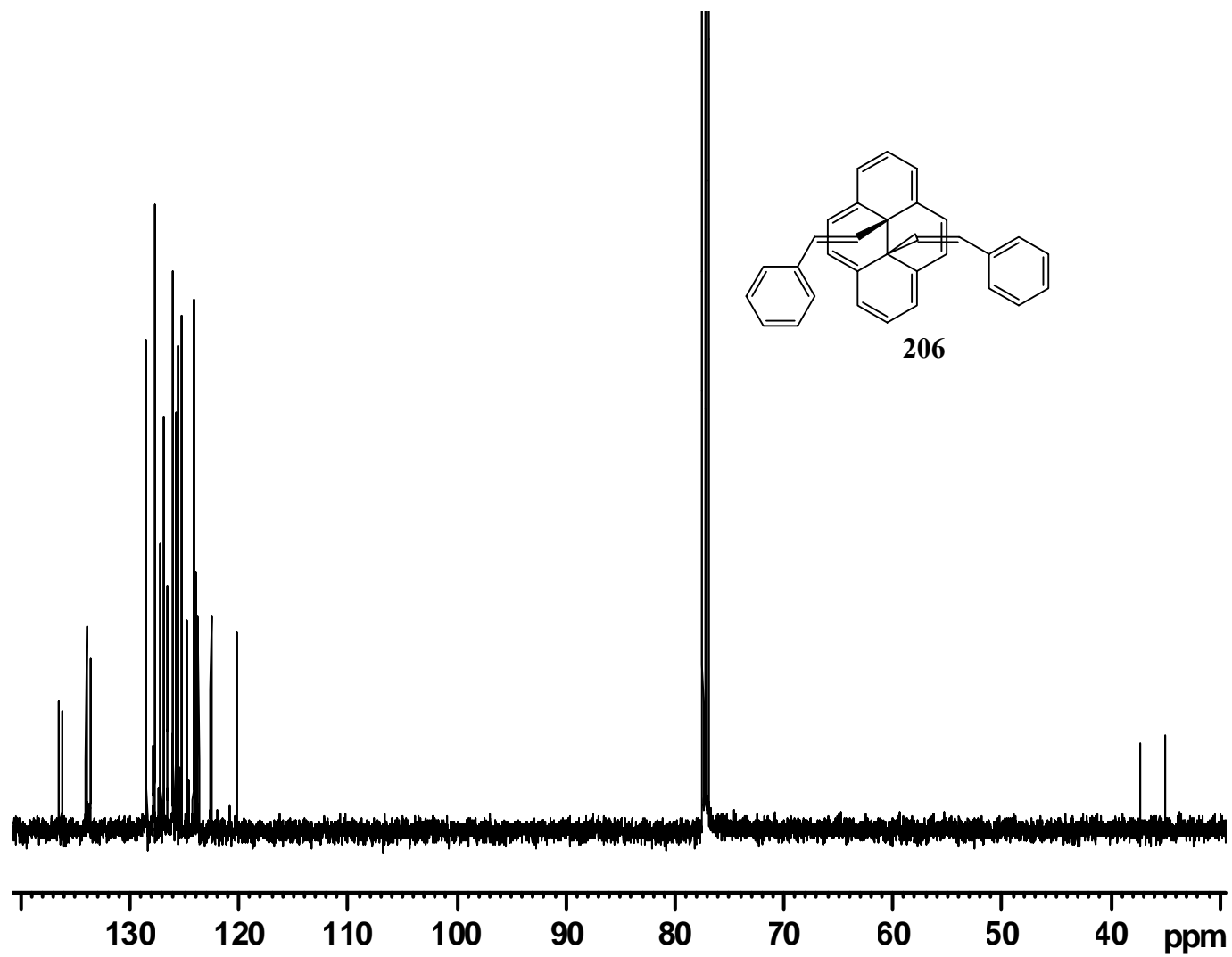


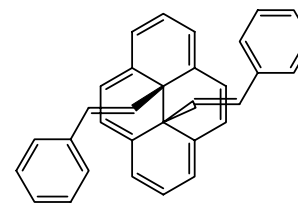


205

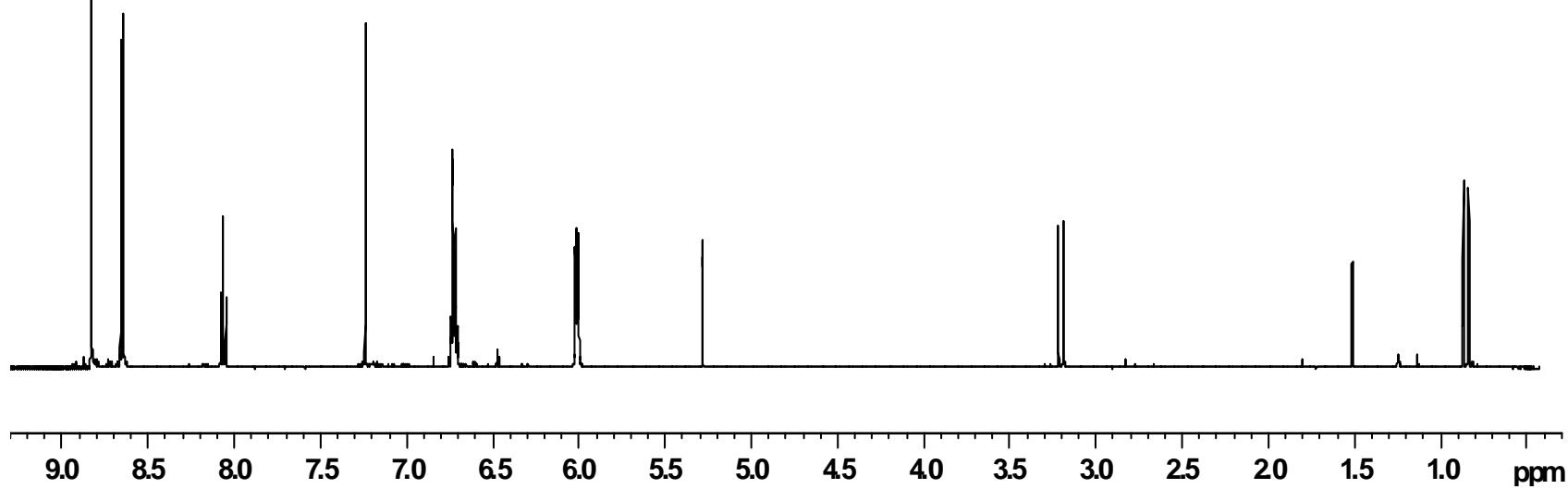
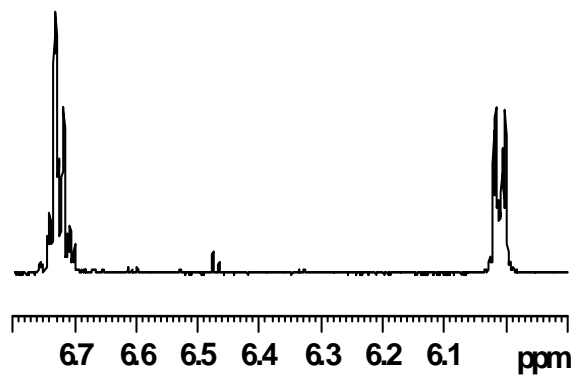


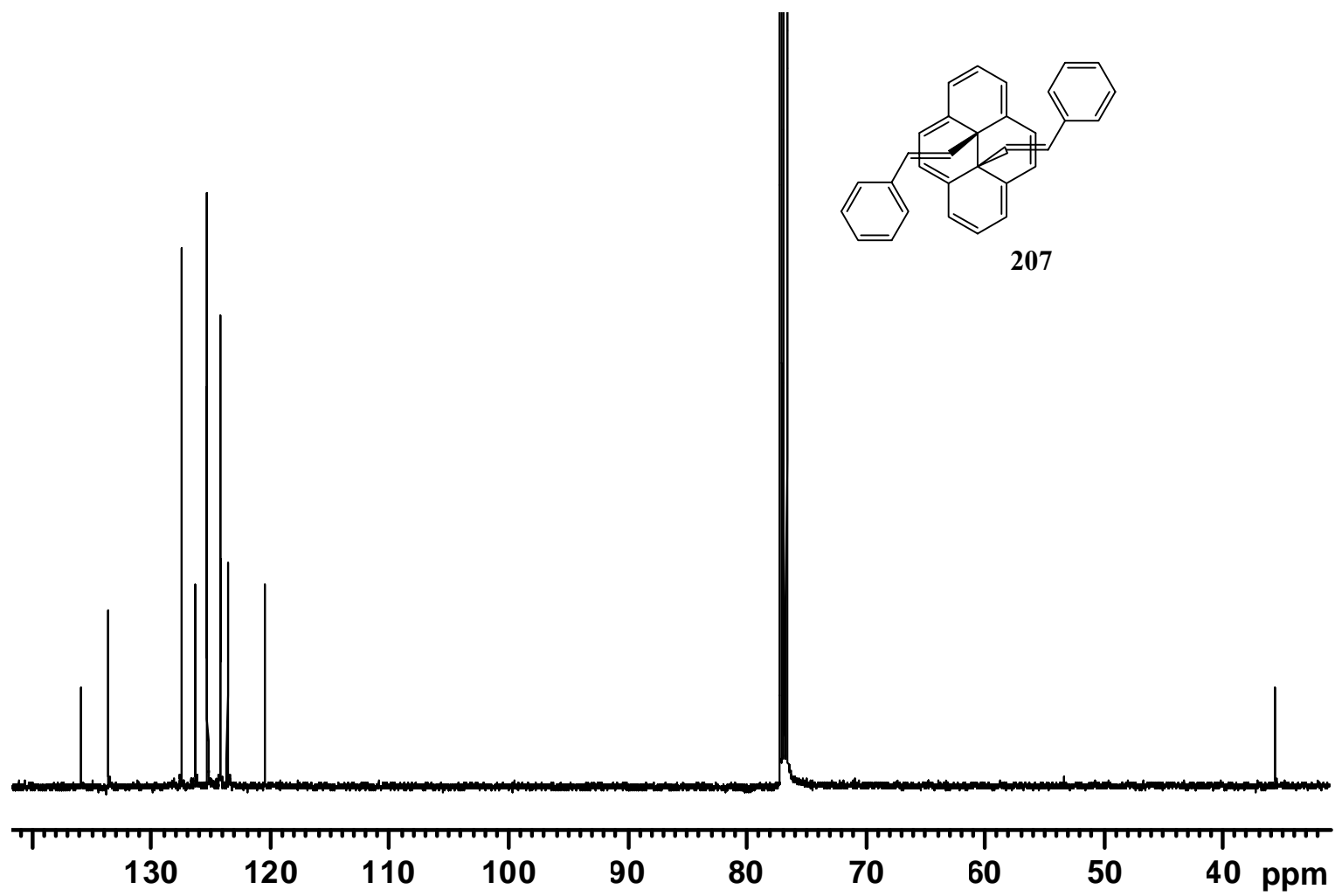


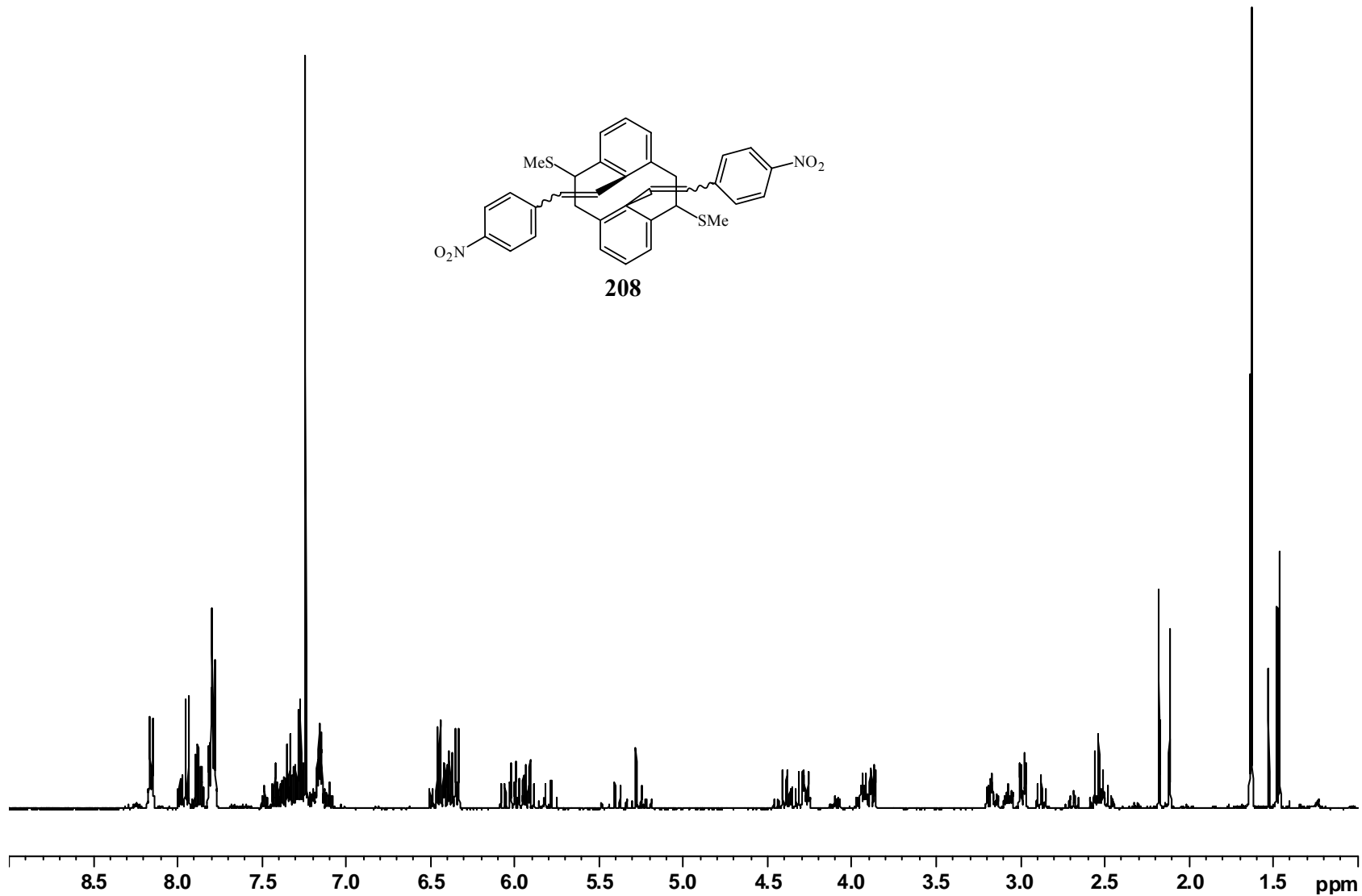
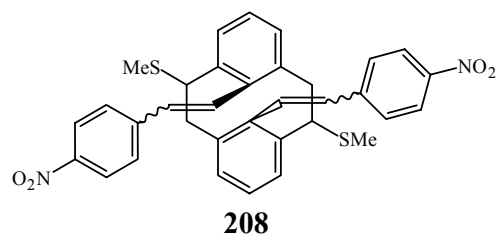


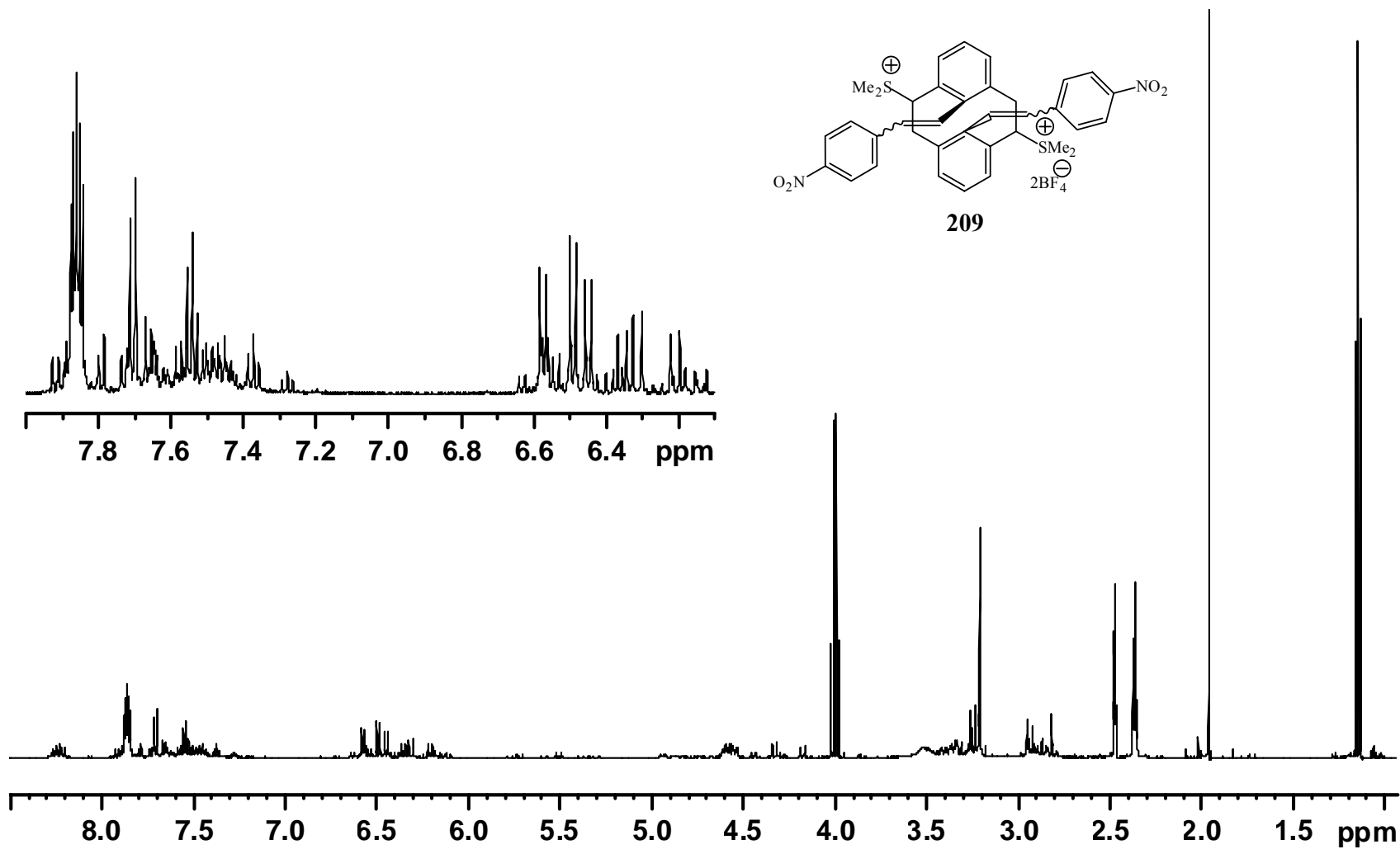


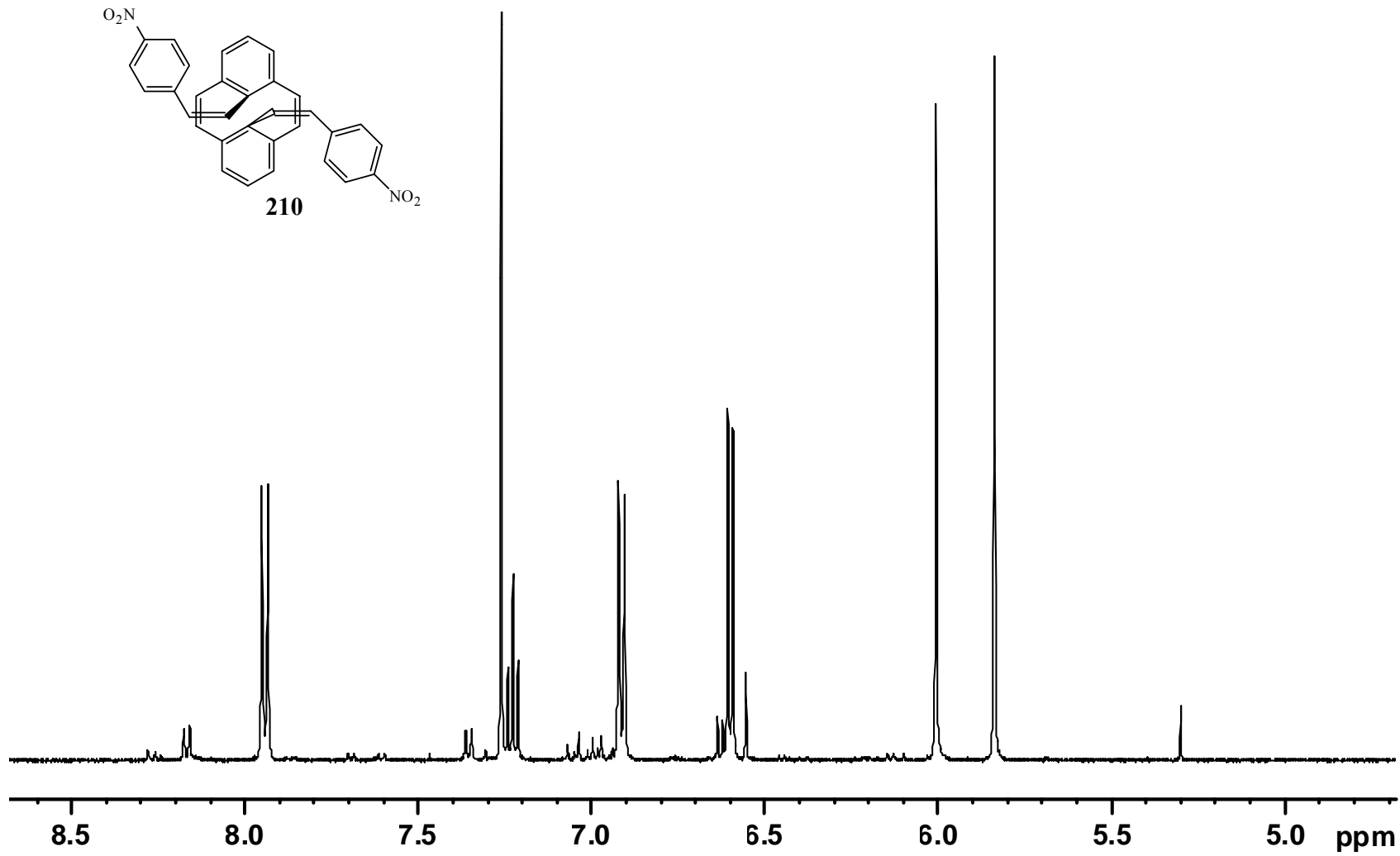
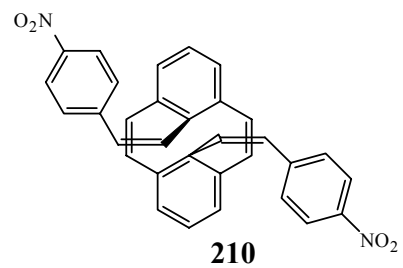
207

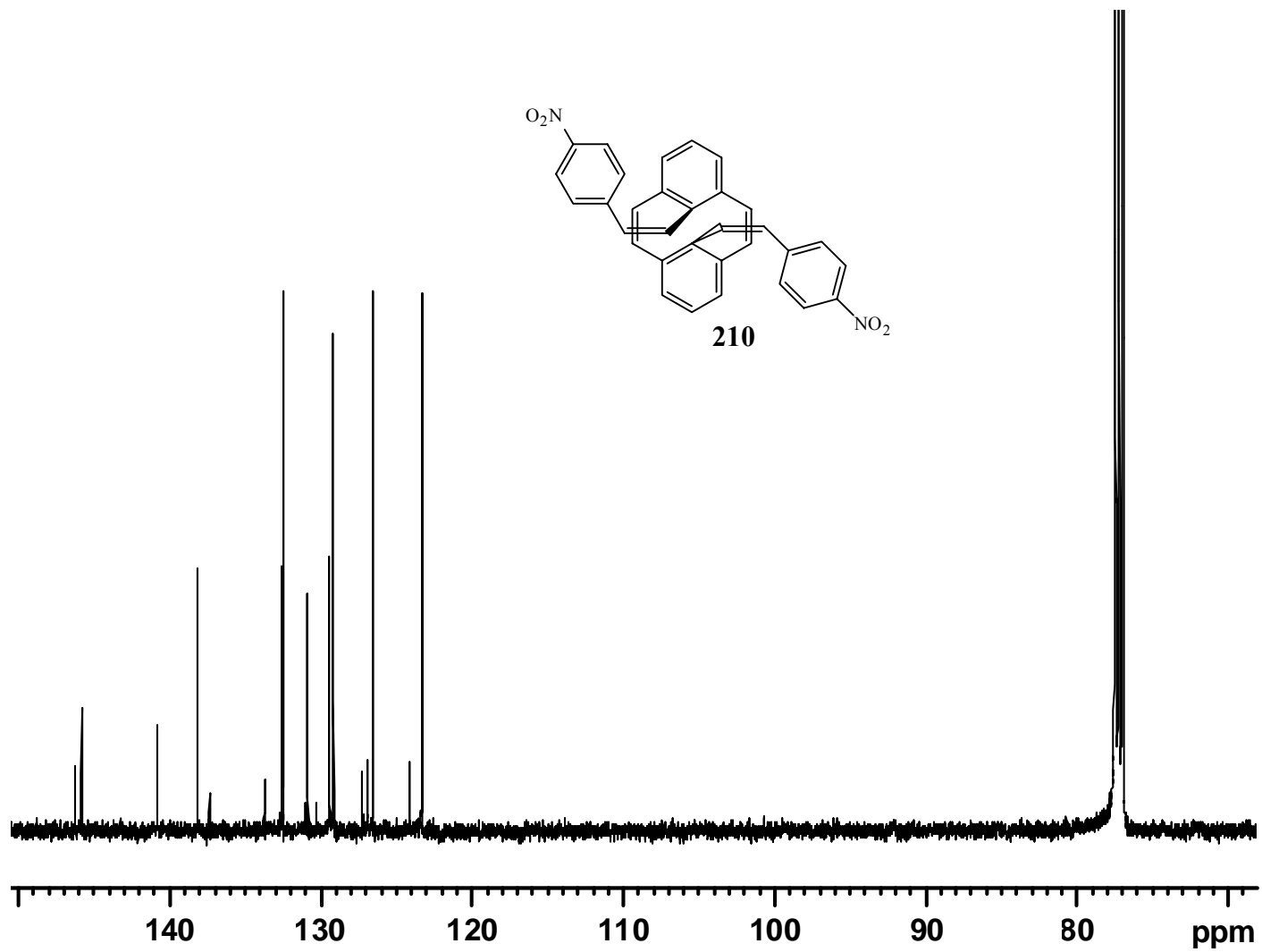


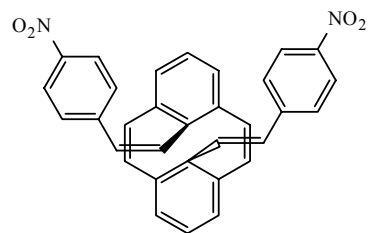




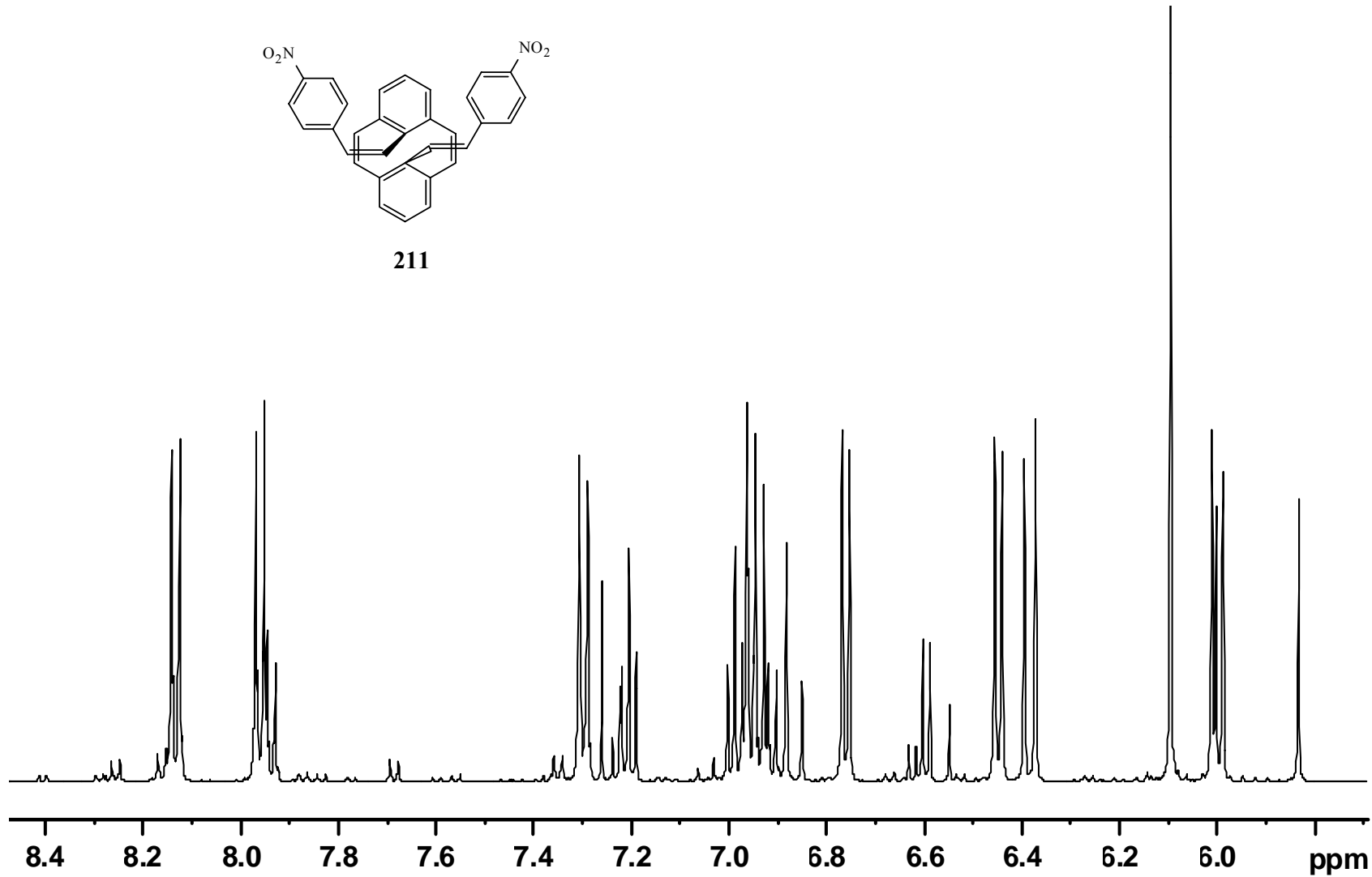


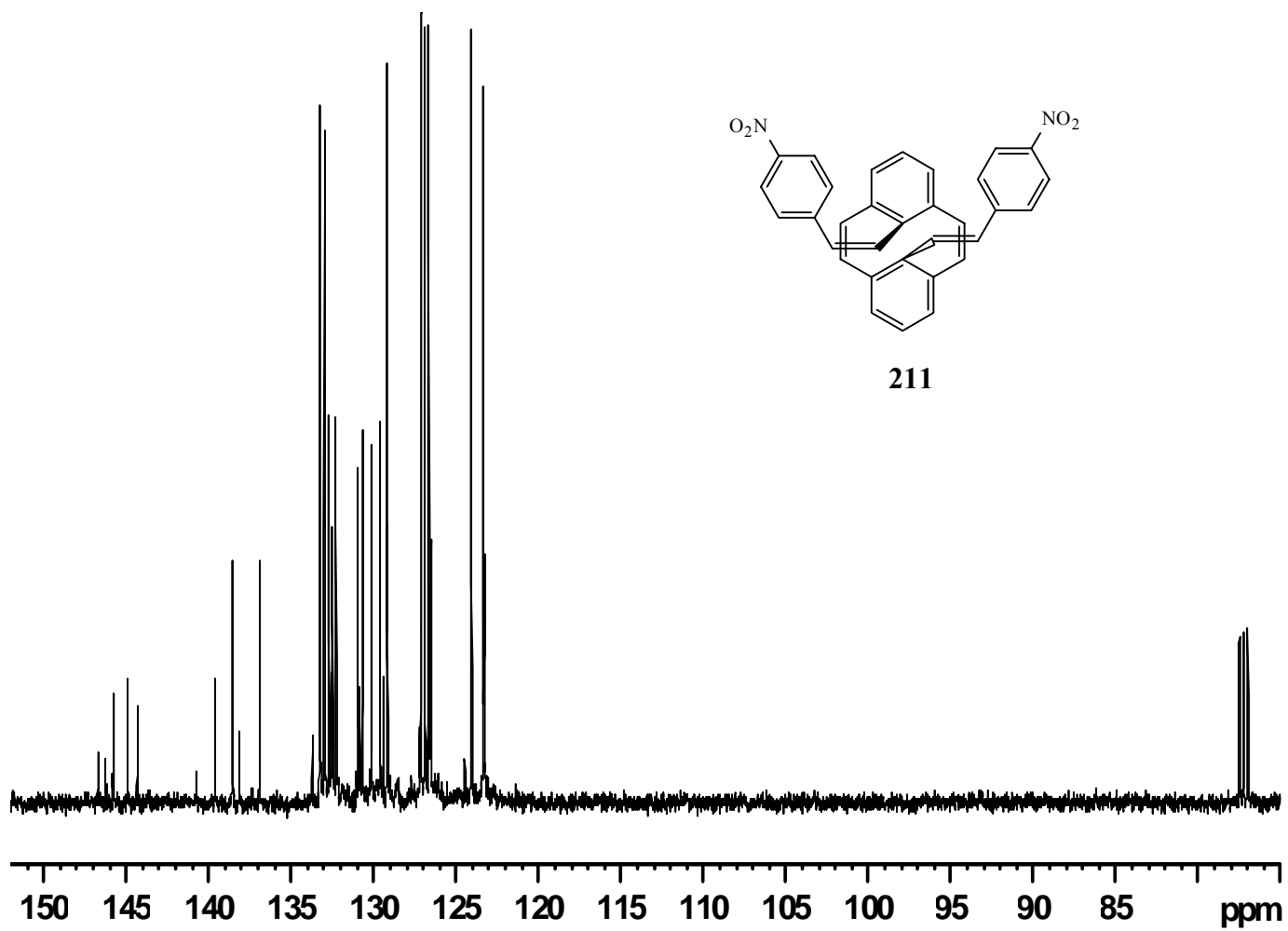


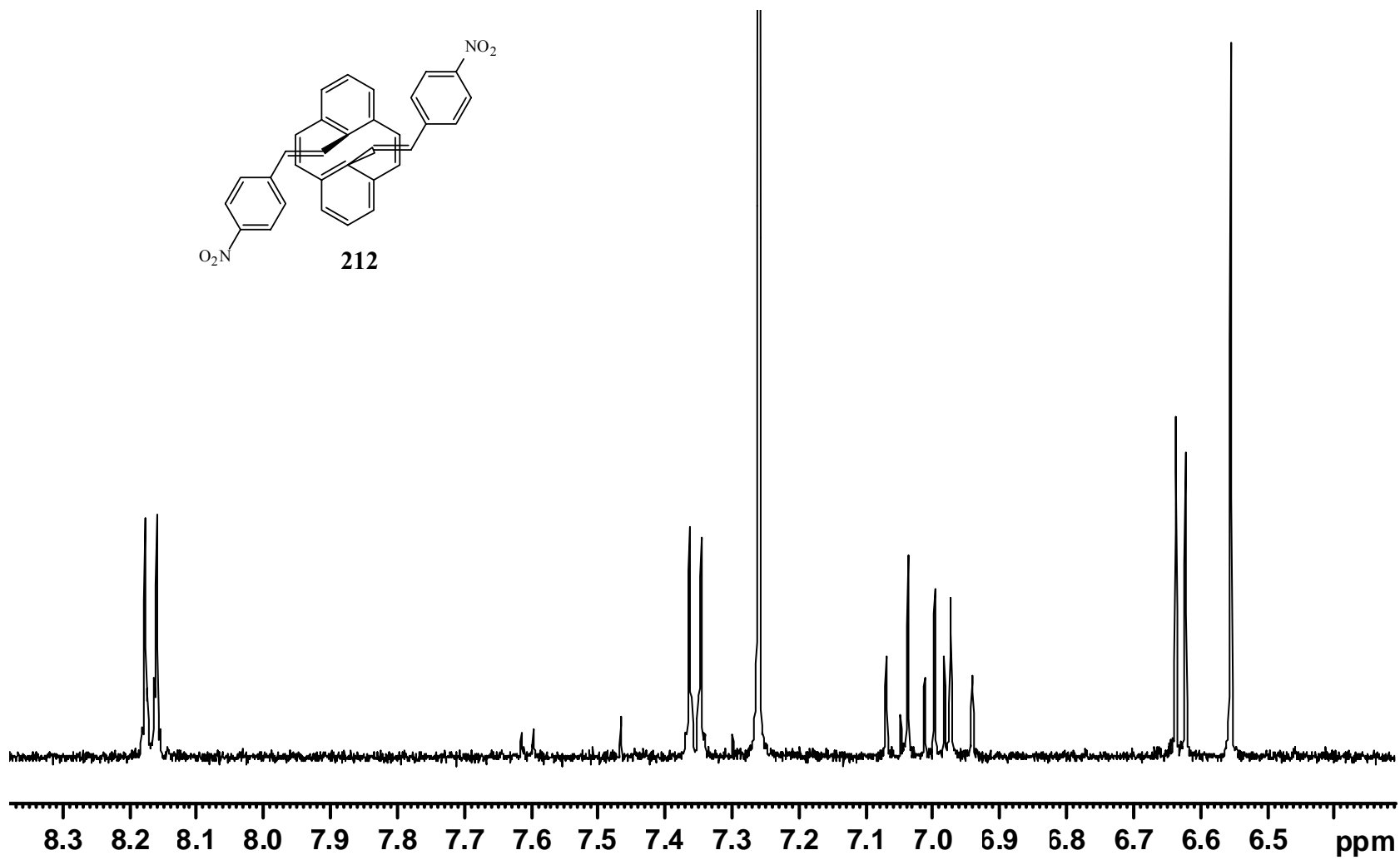
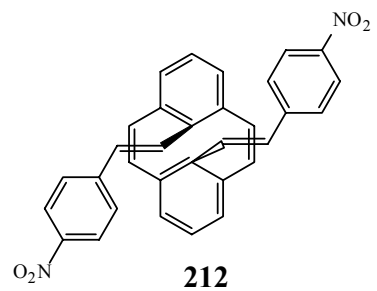


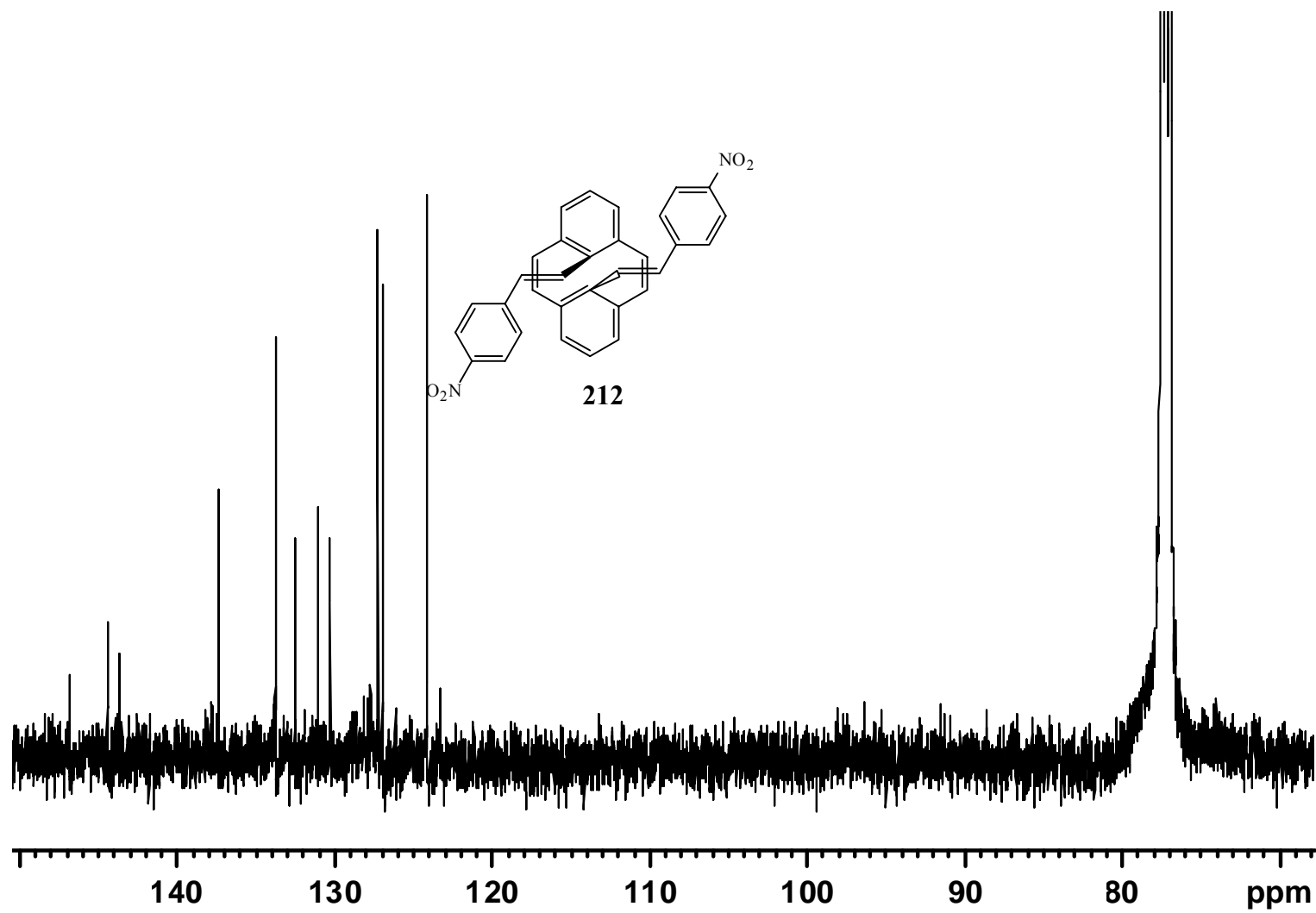


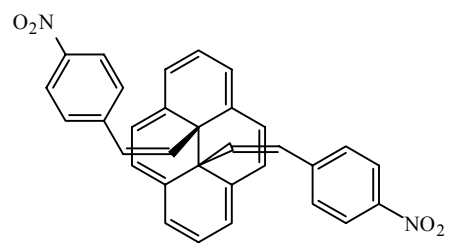
211



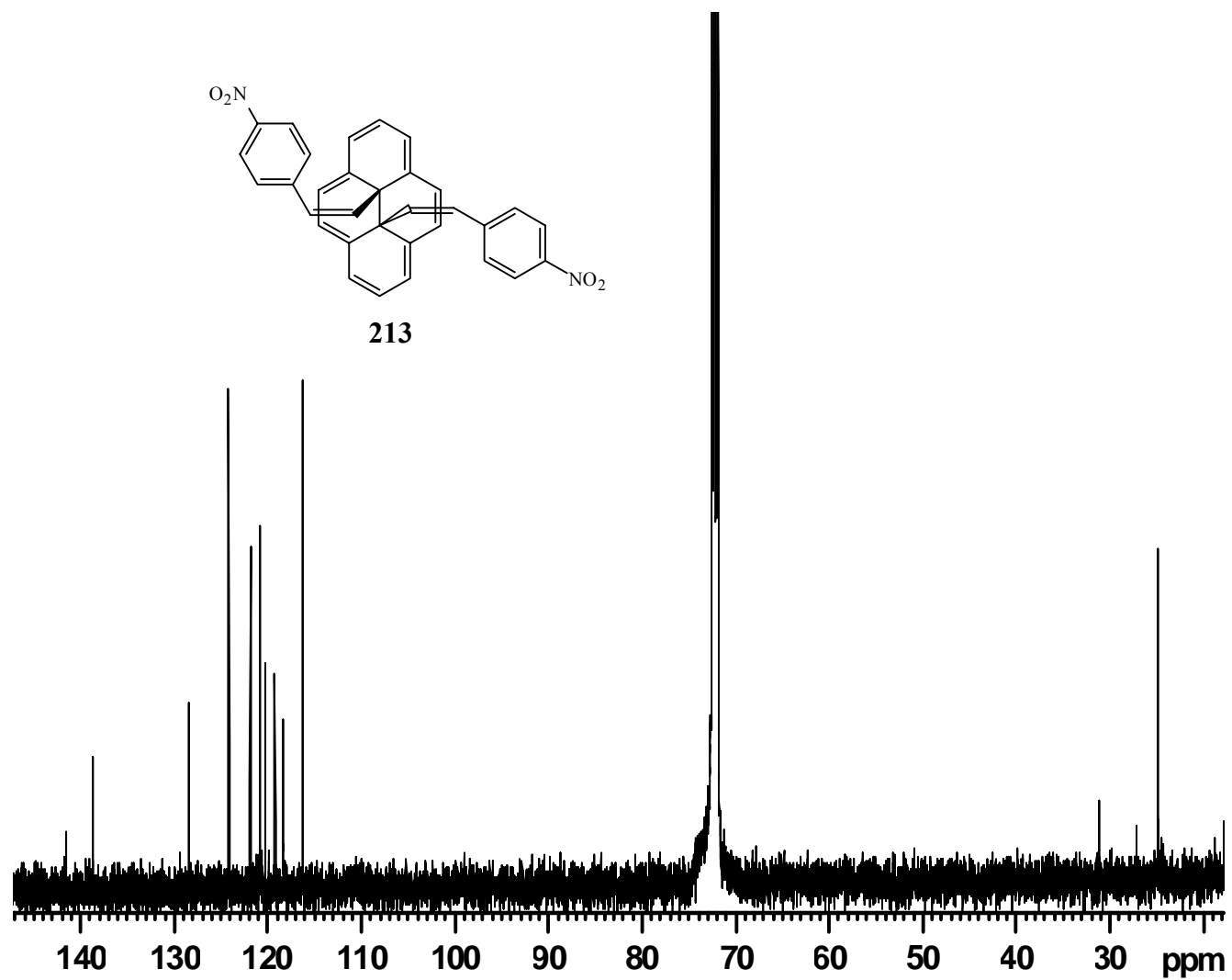


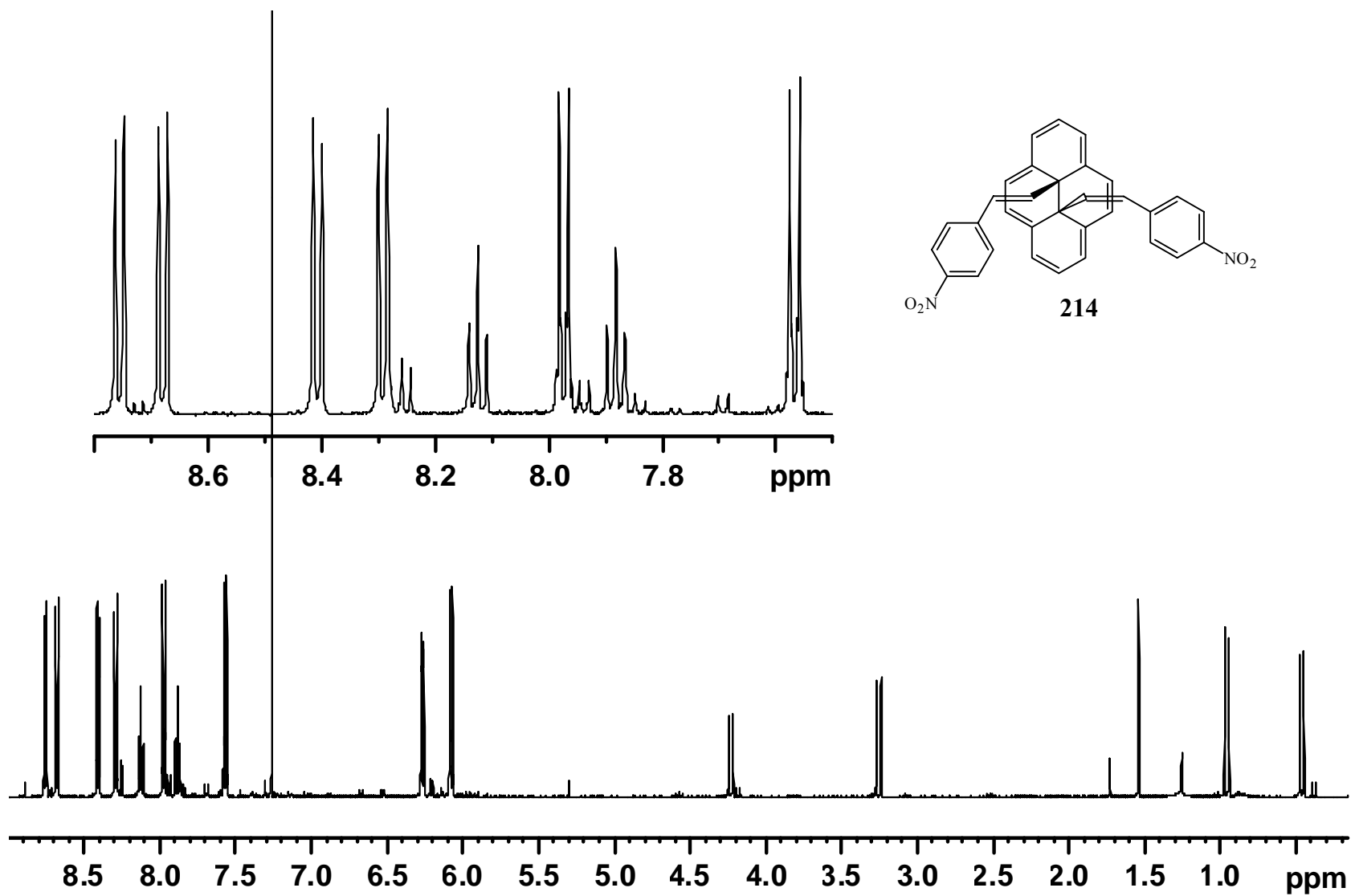


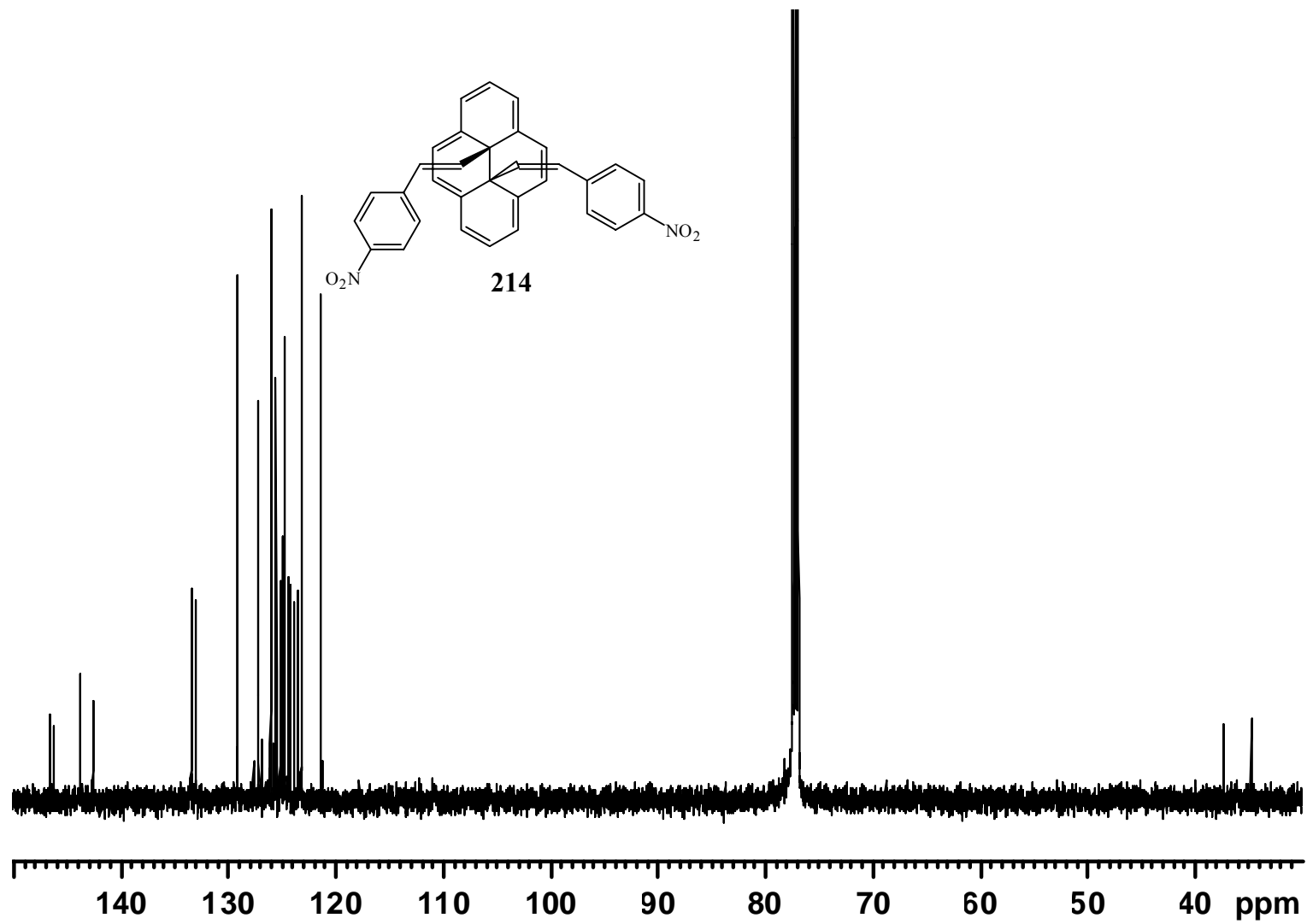


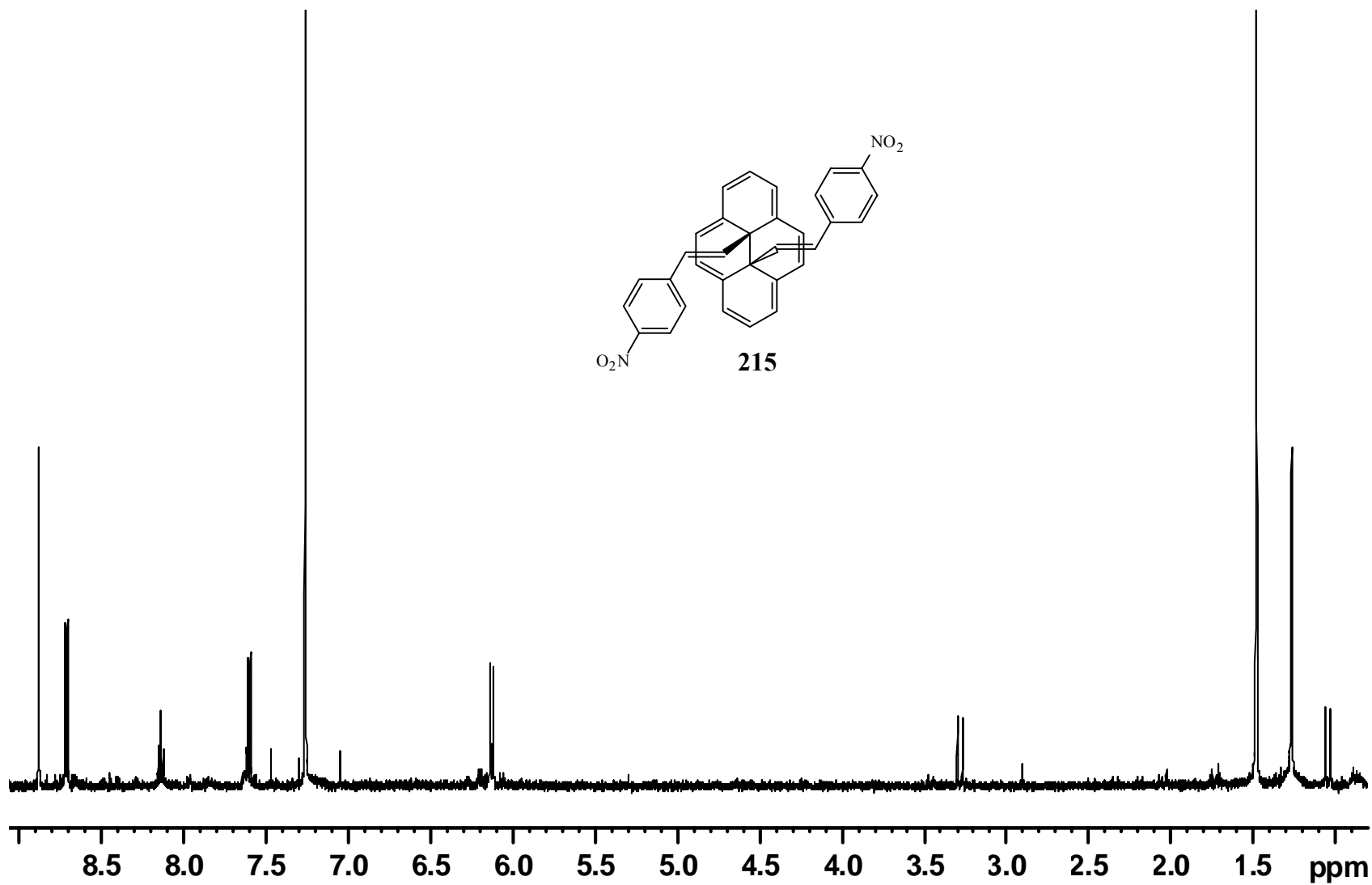
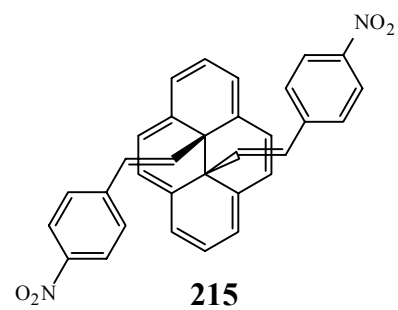


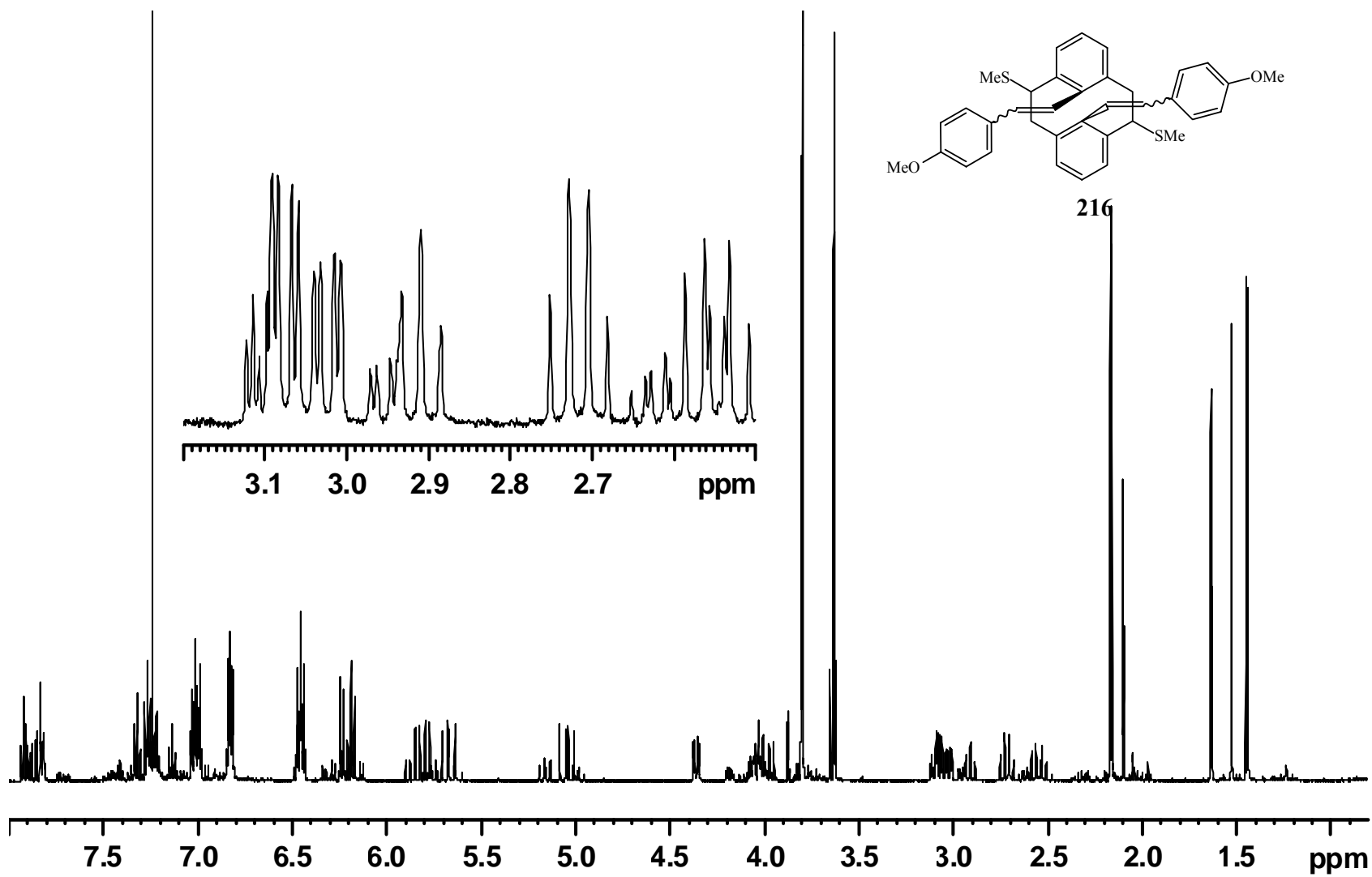
213

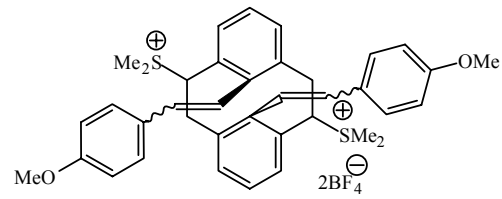




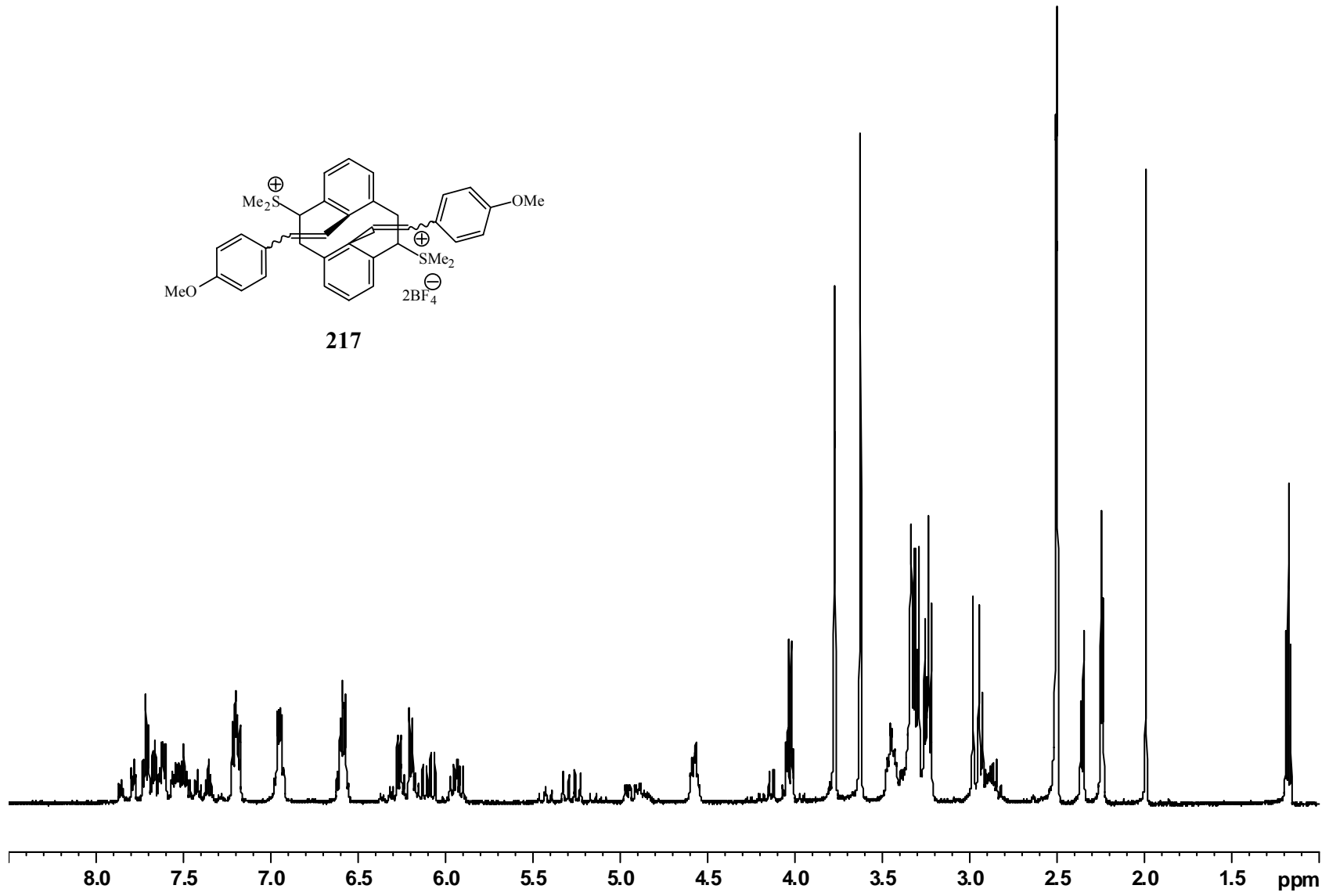


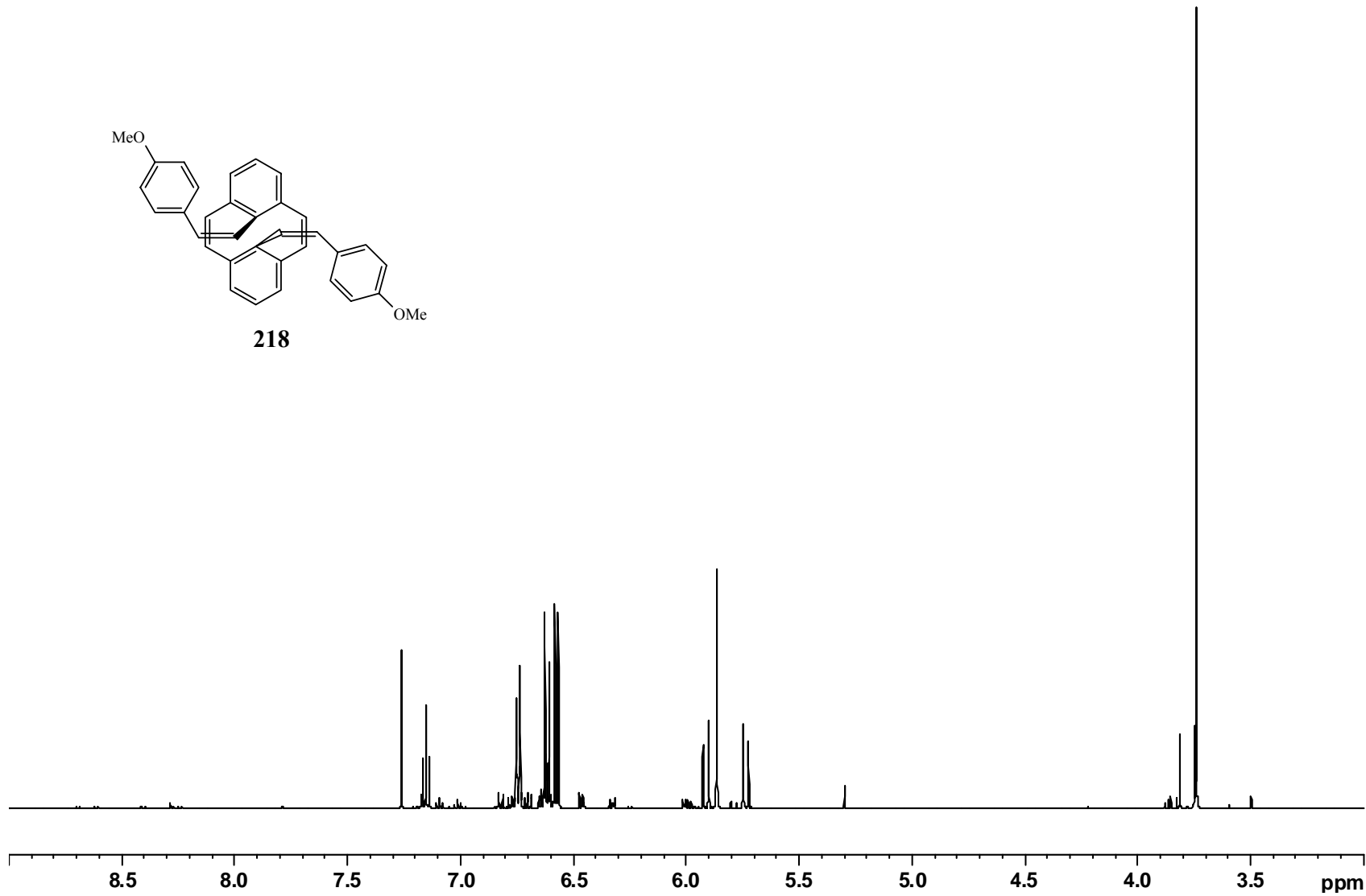
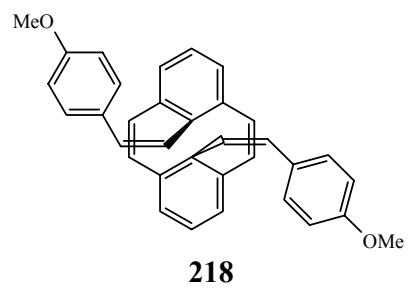


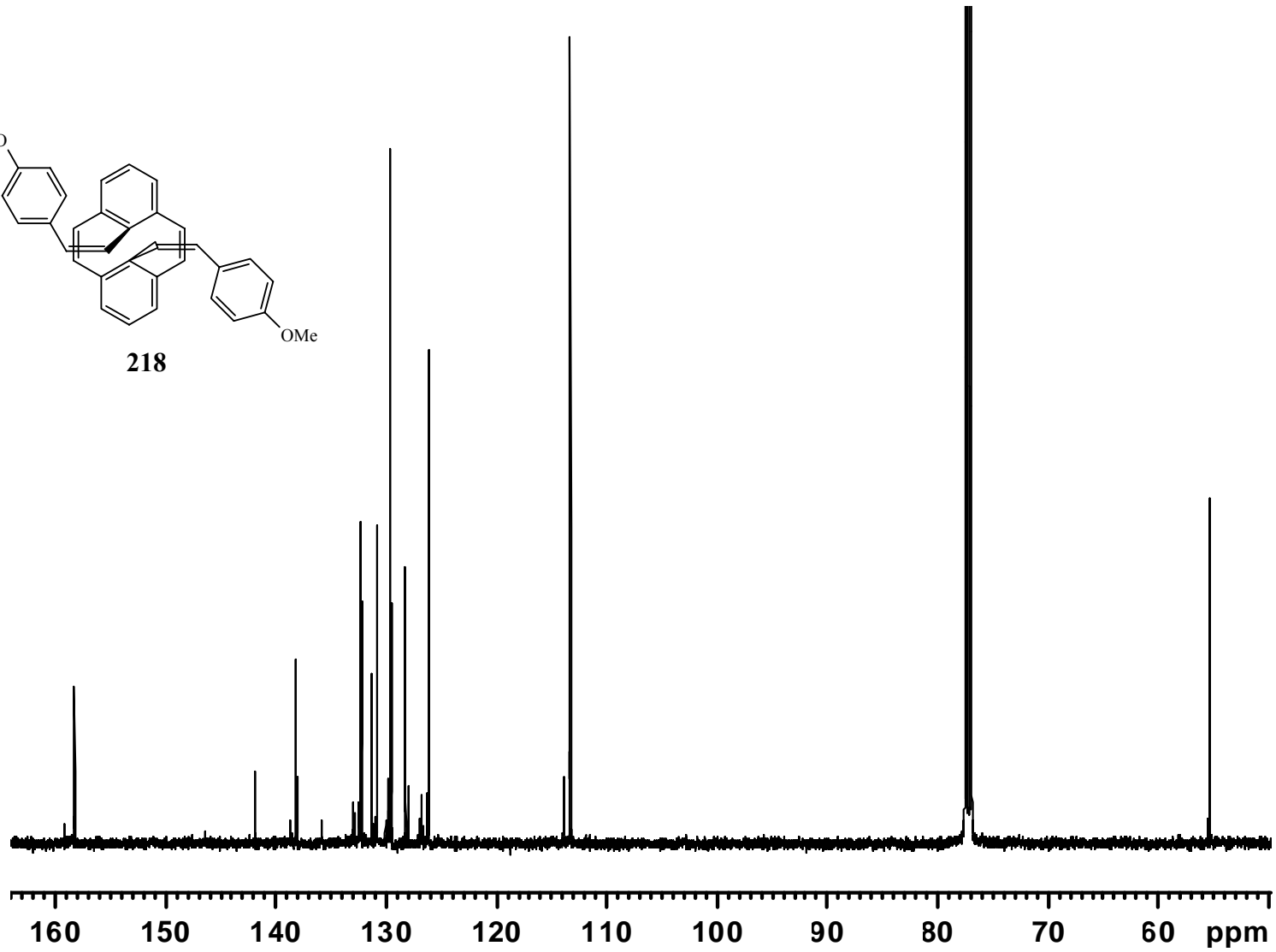
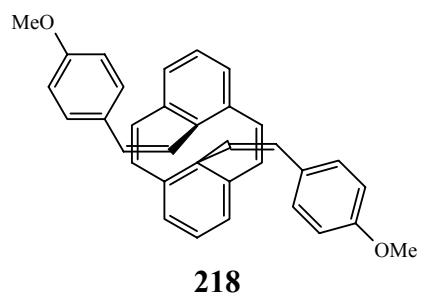


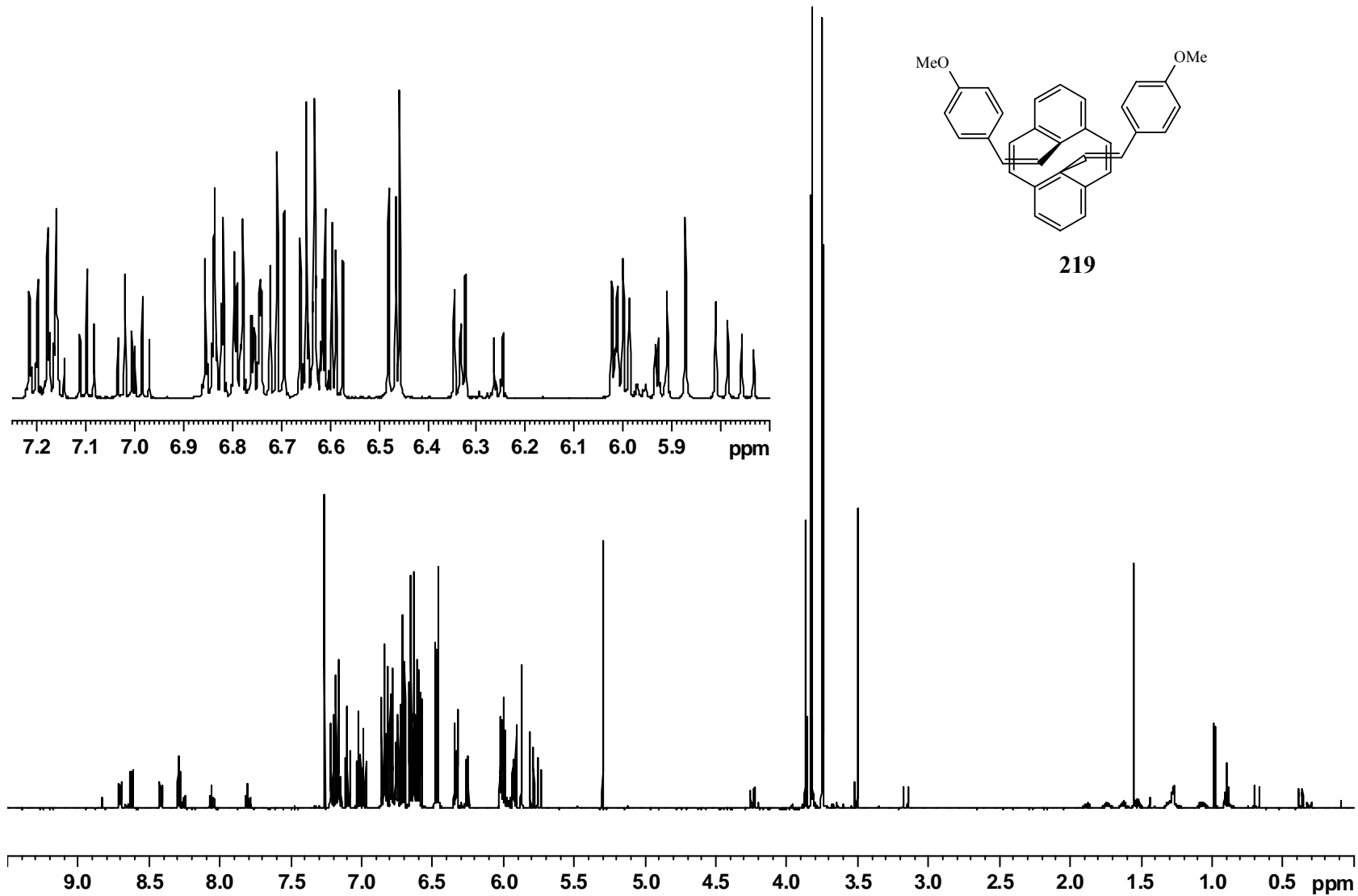


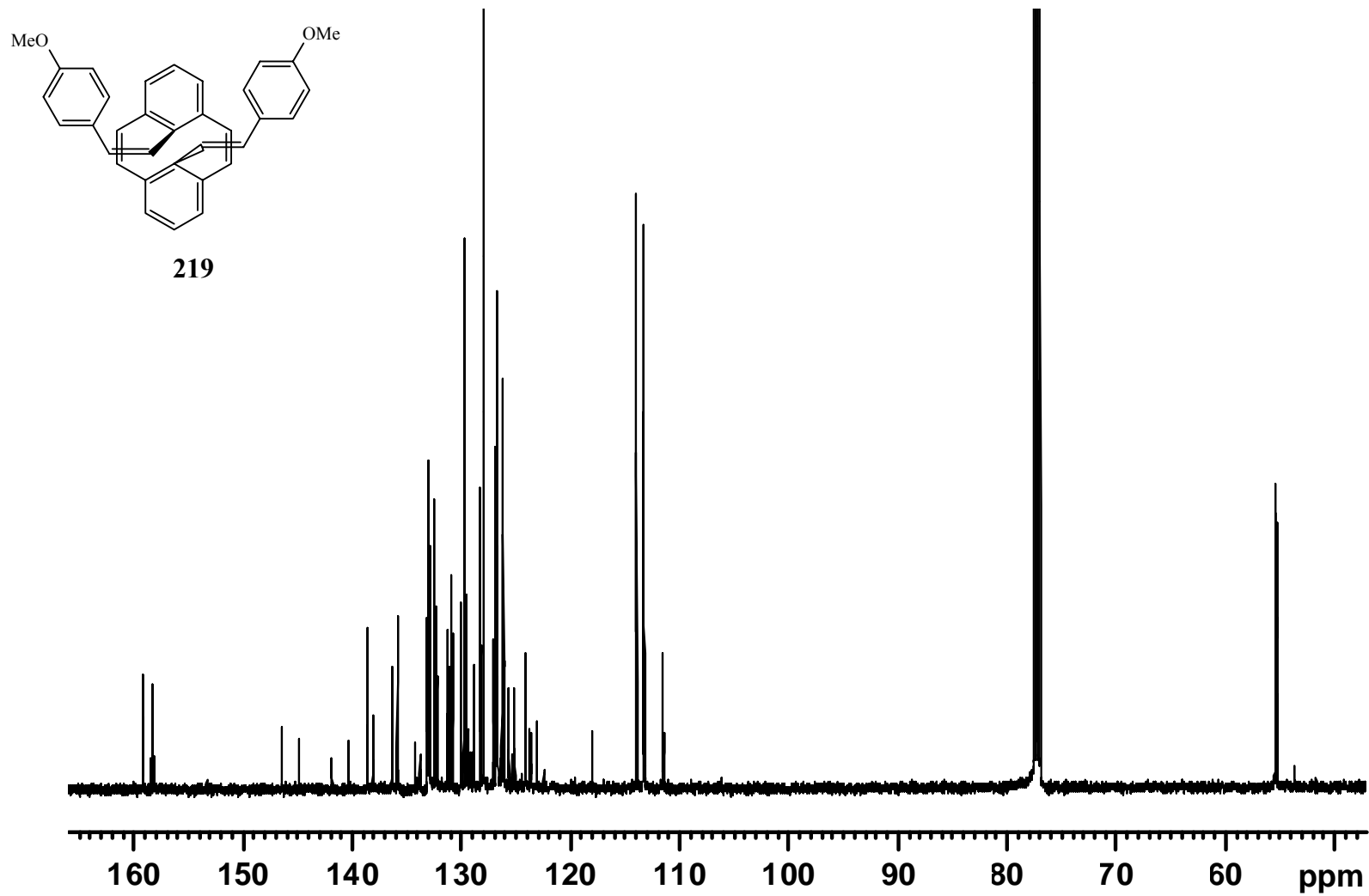
217

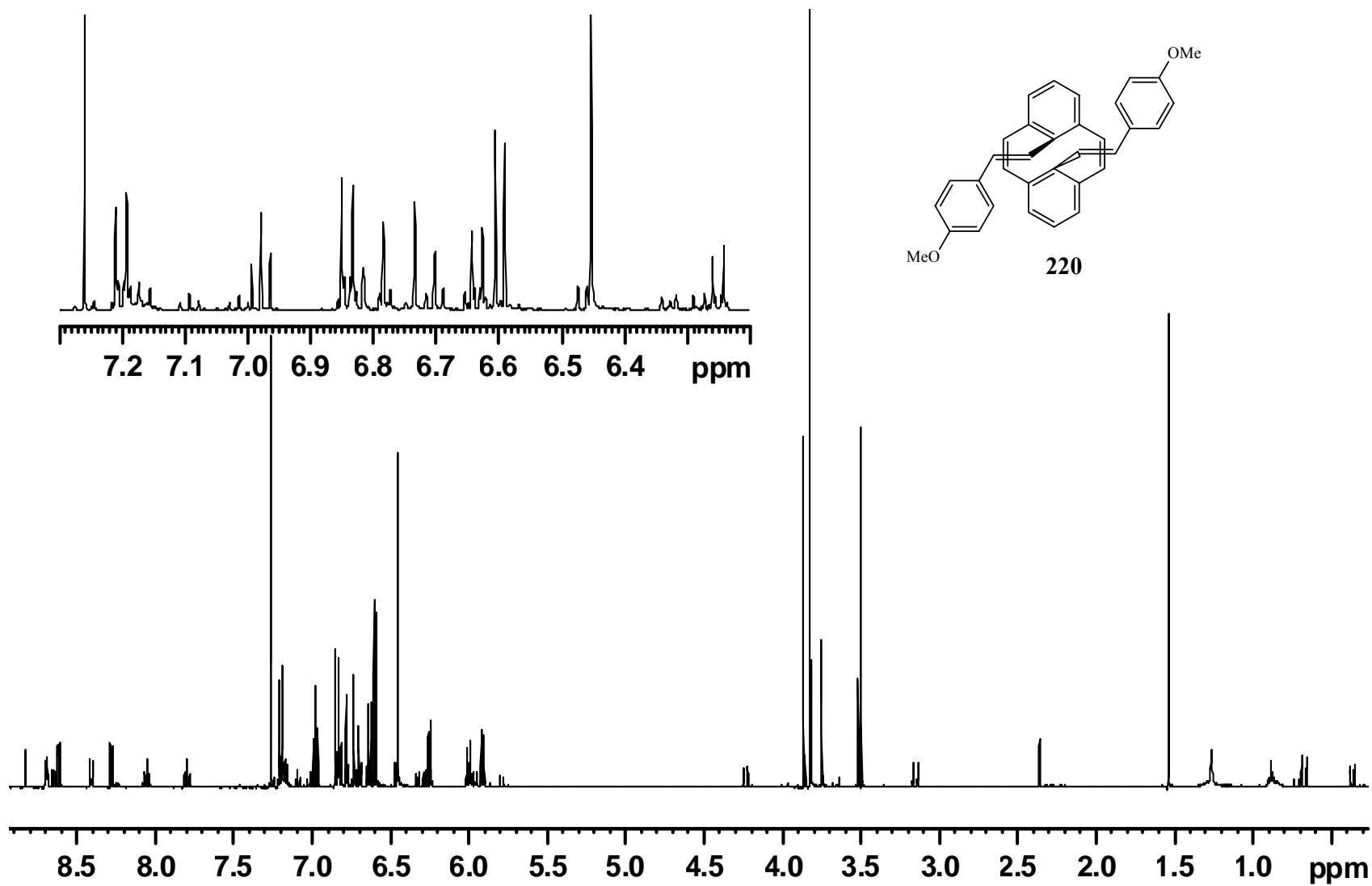


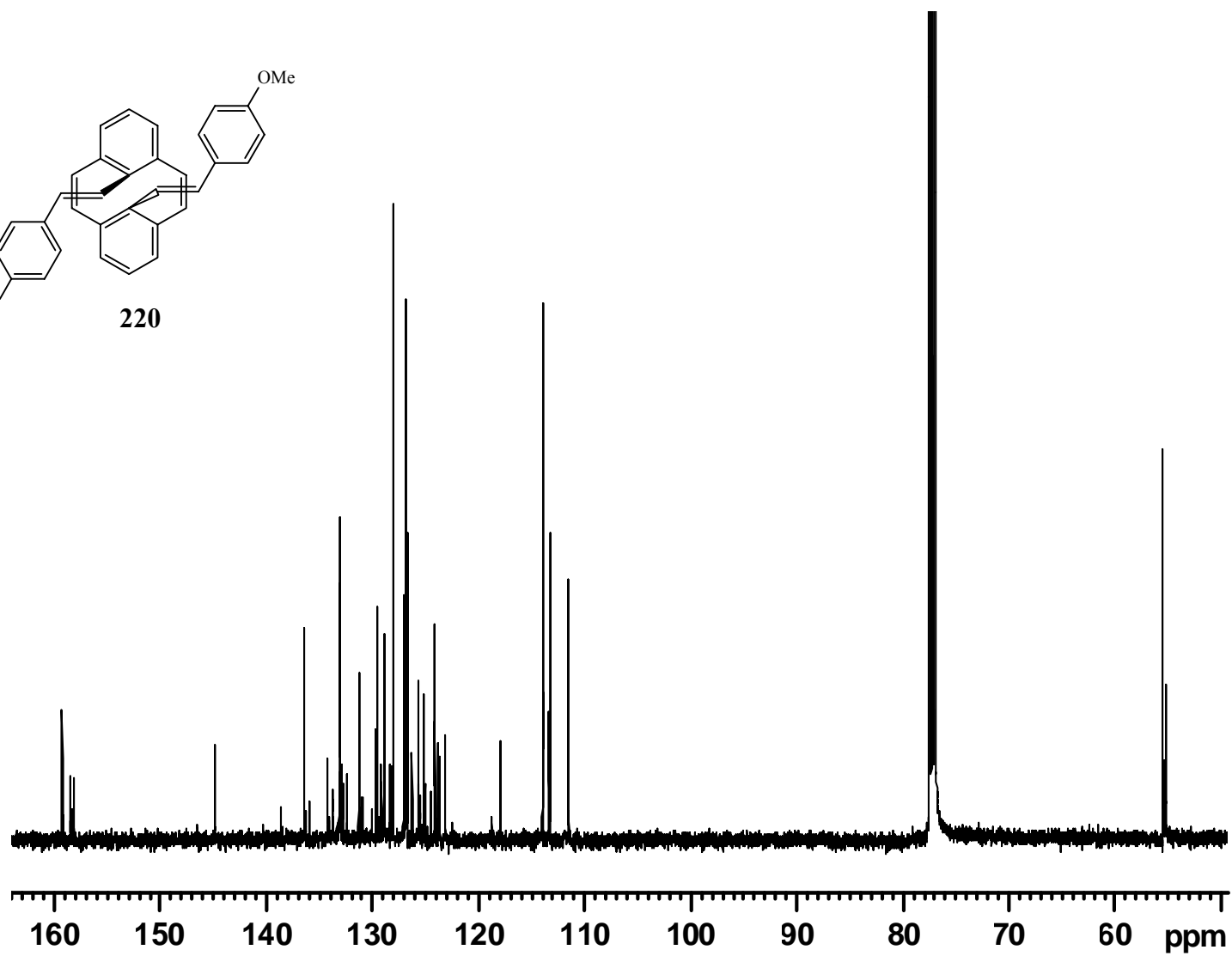
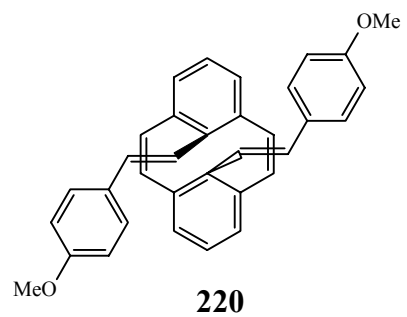


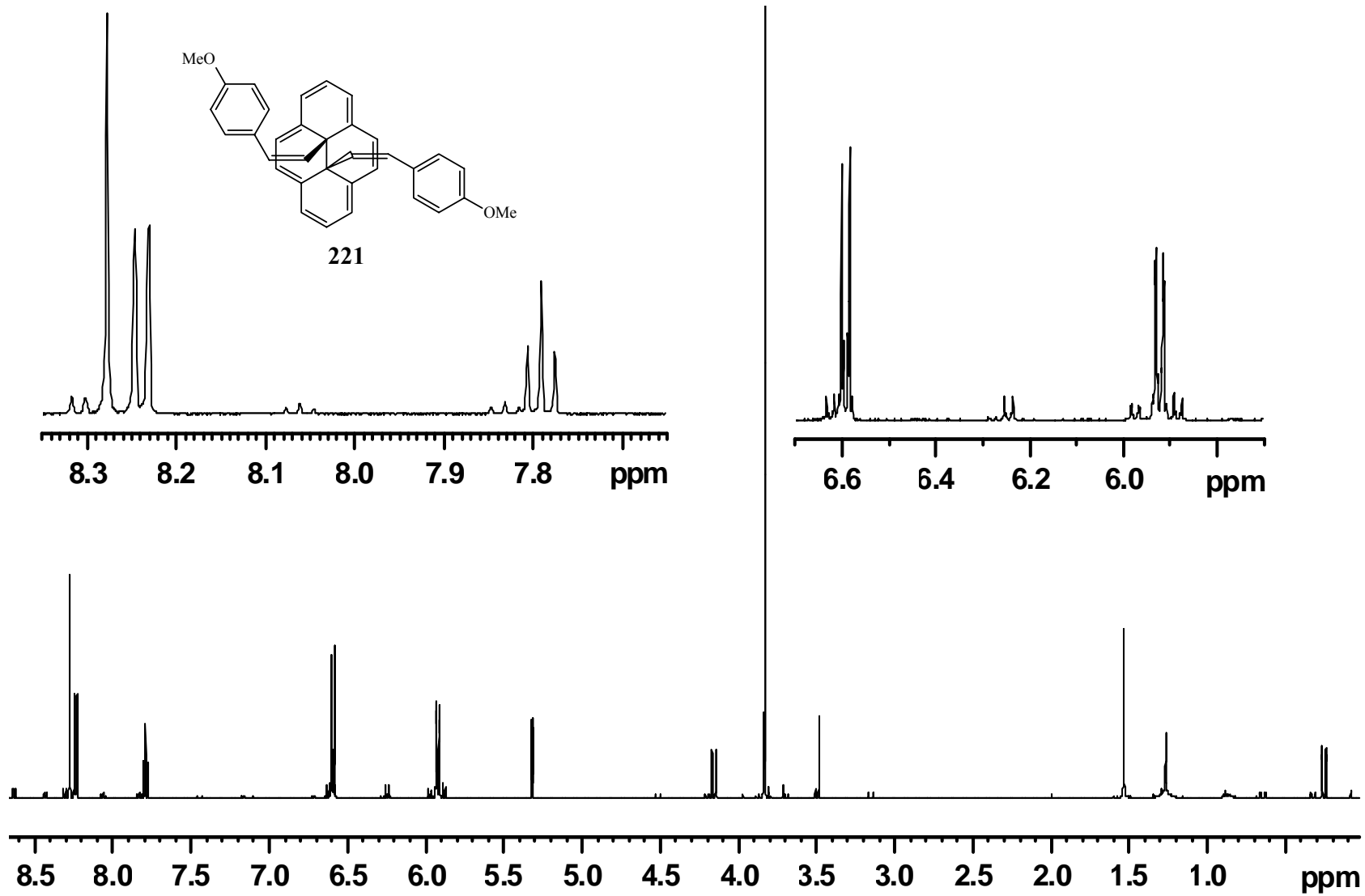


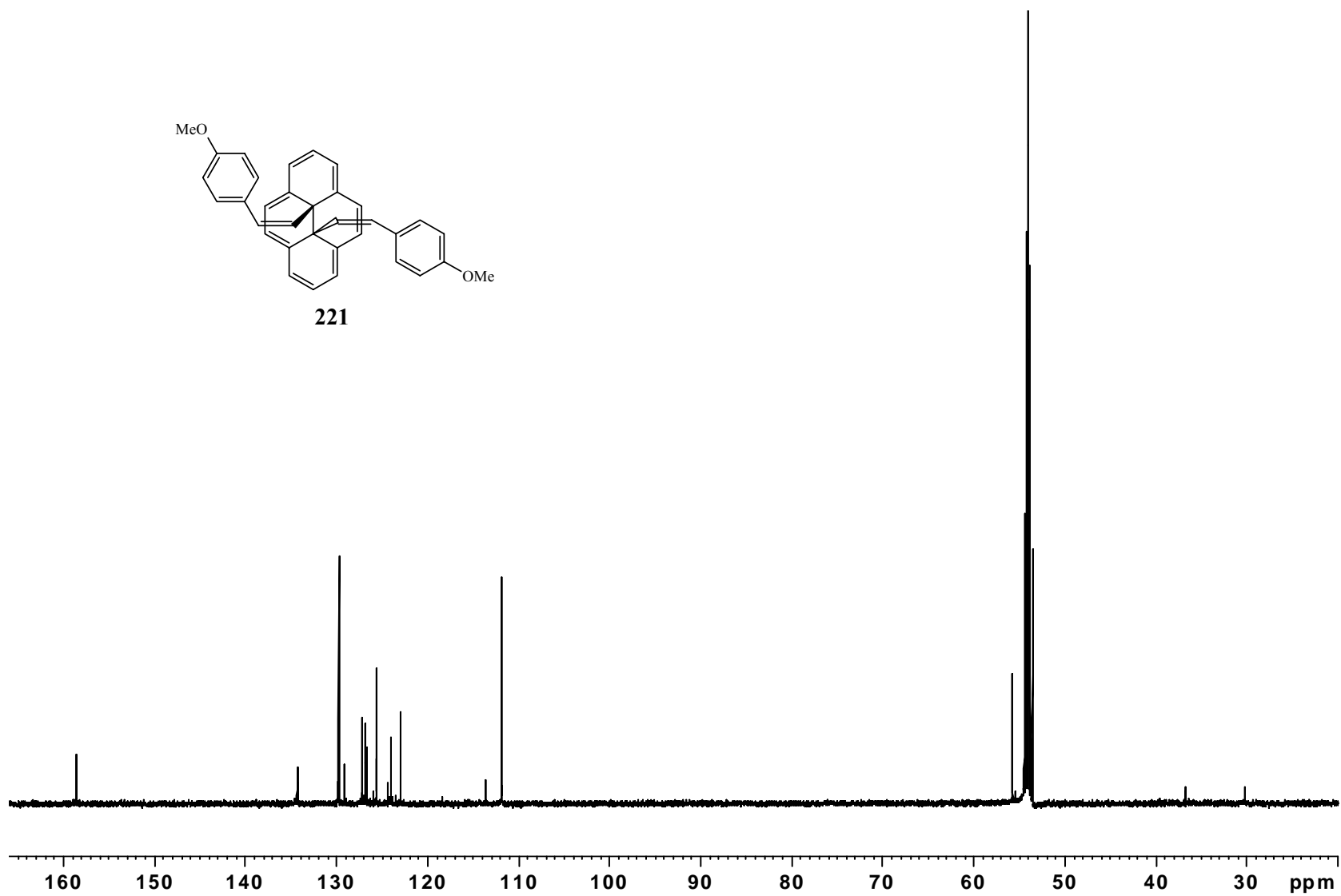
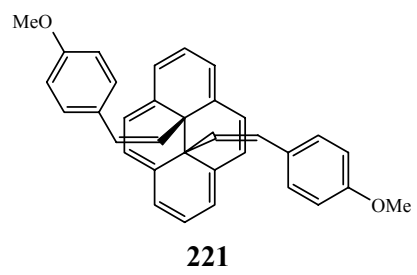


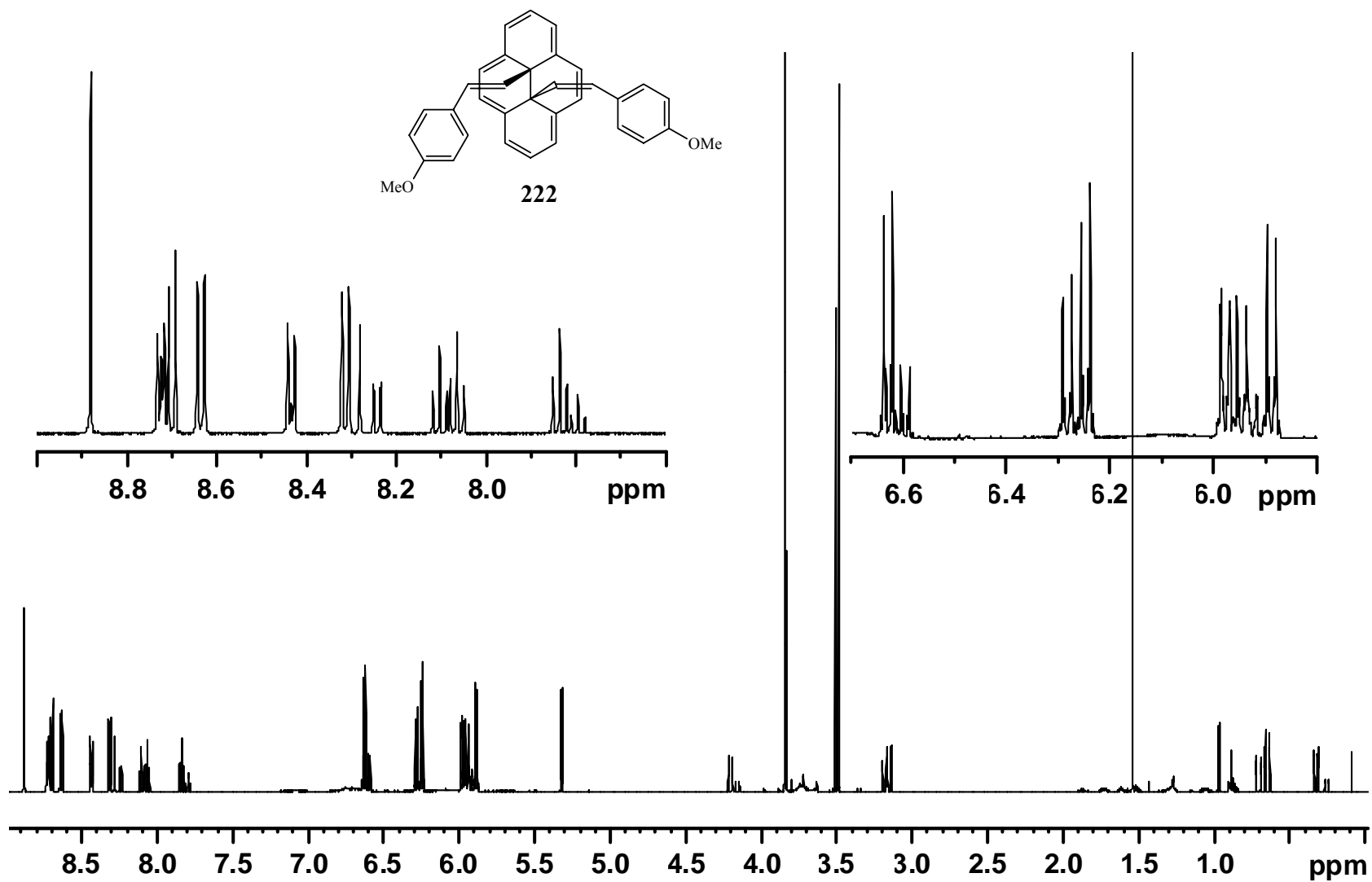


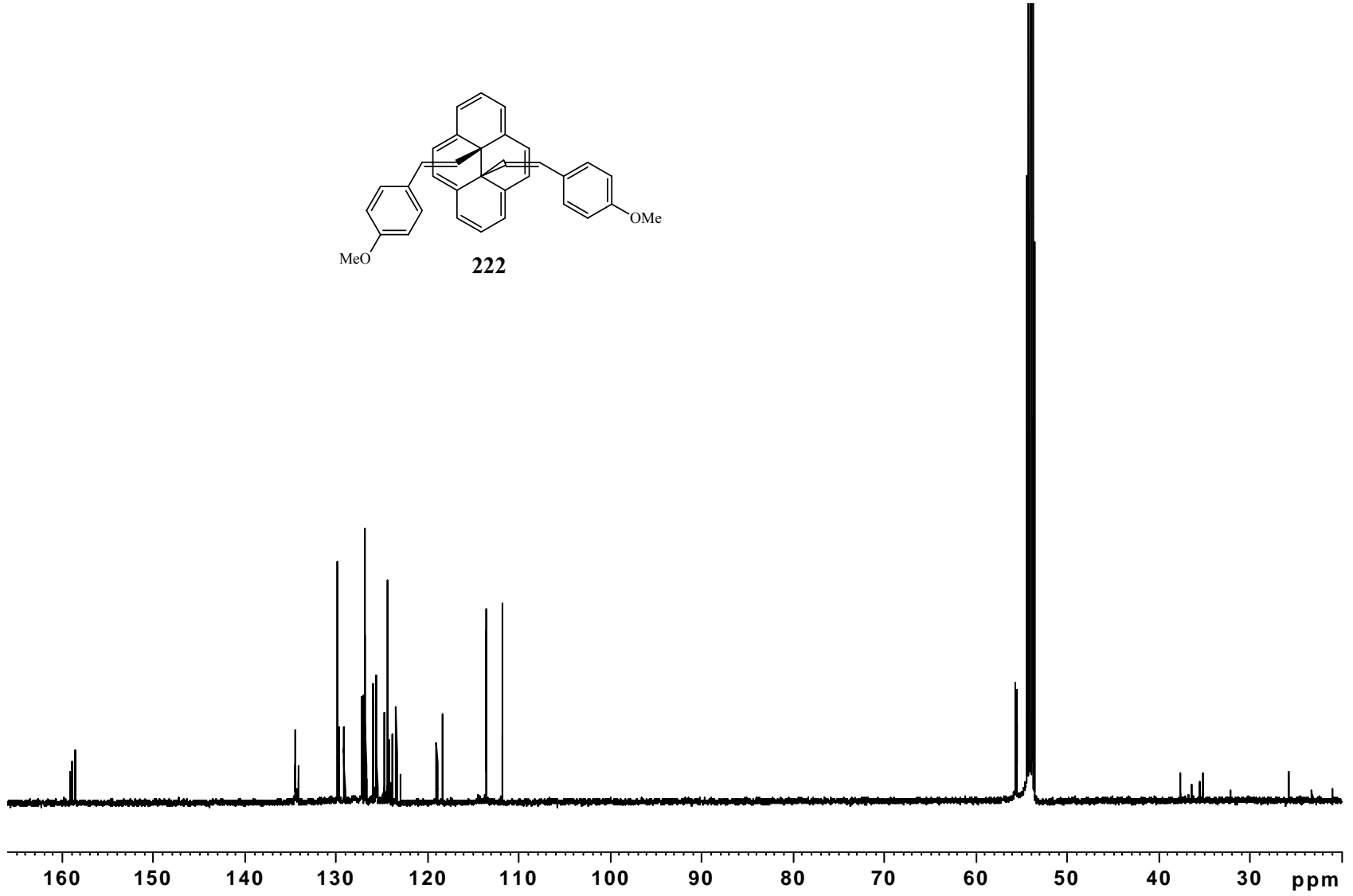
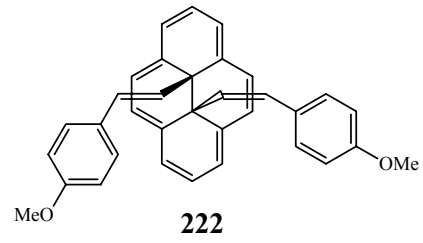


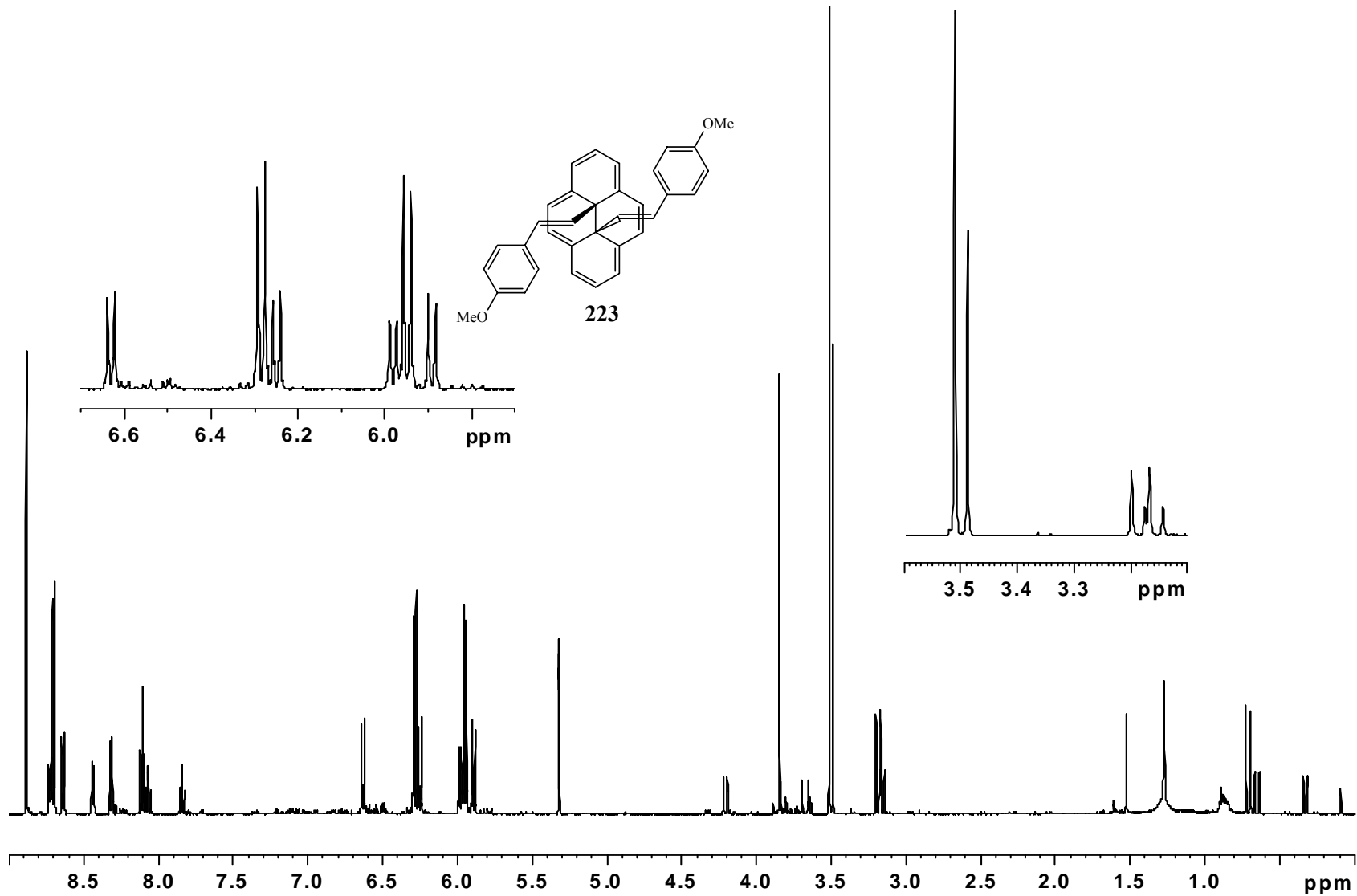


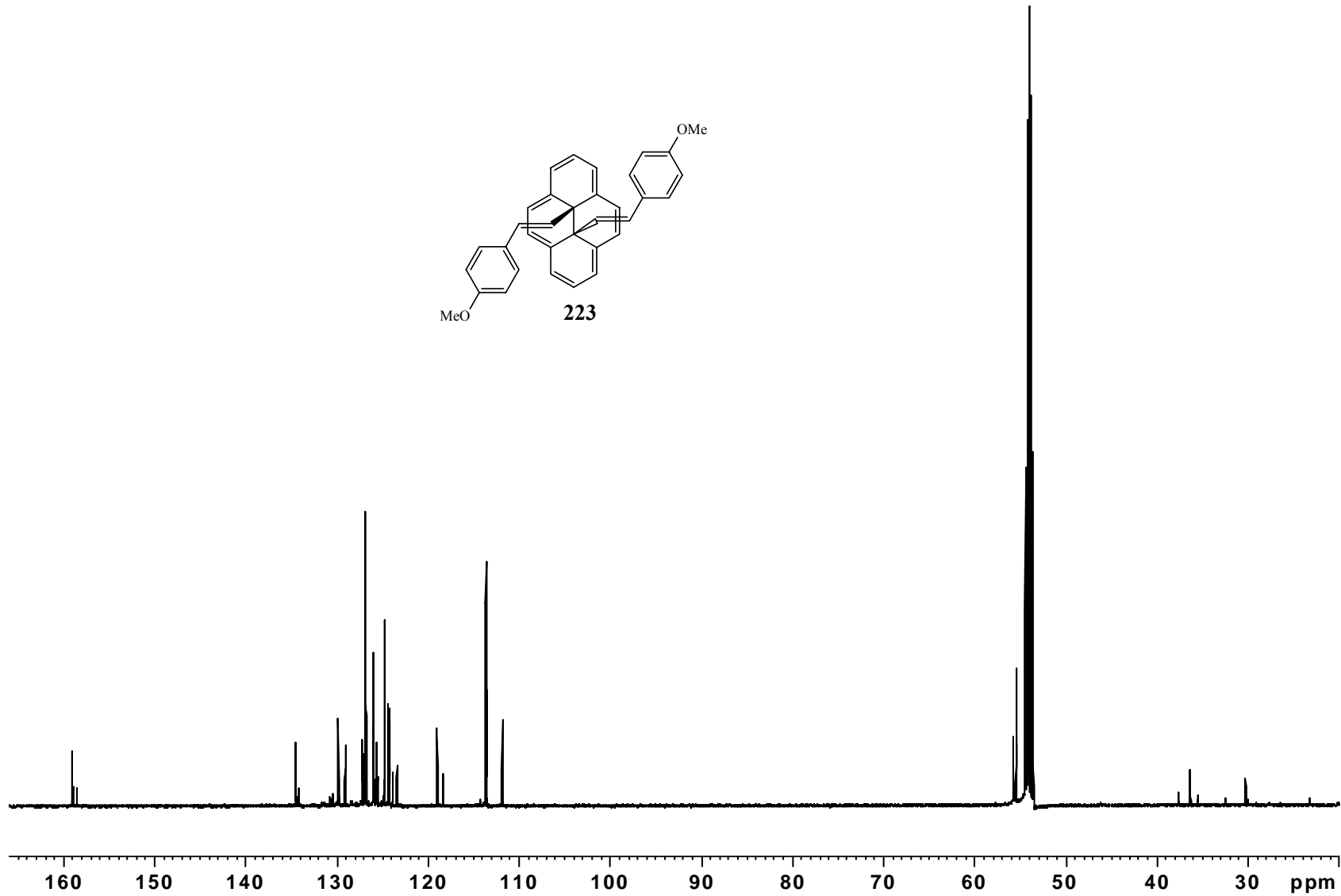
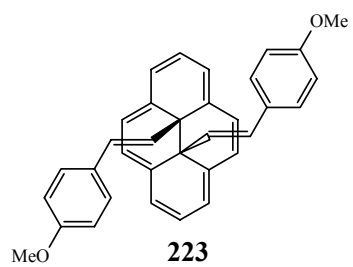


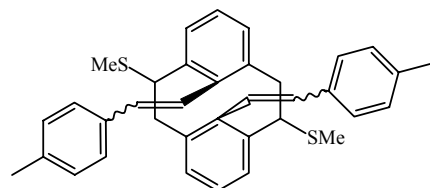




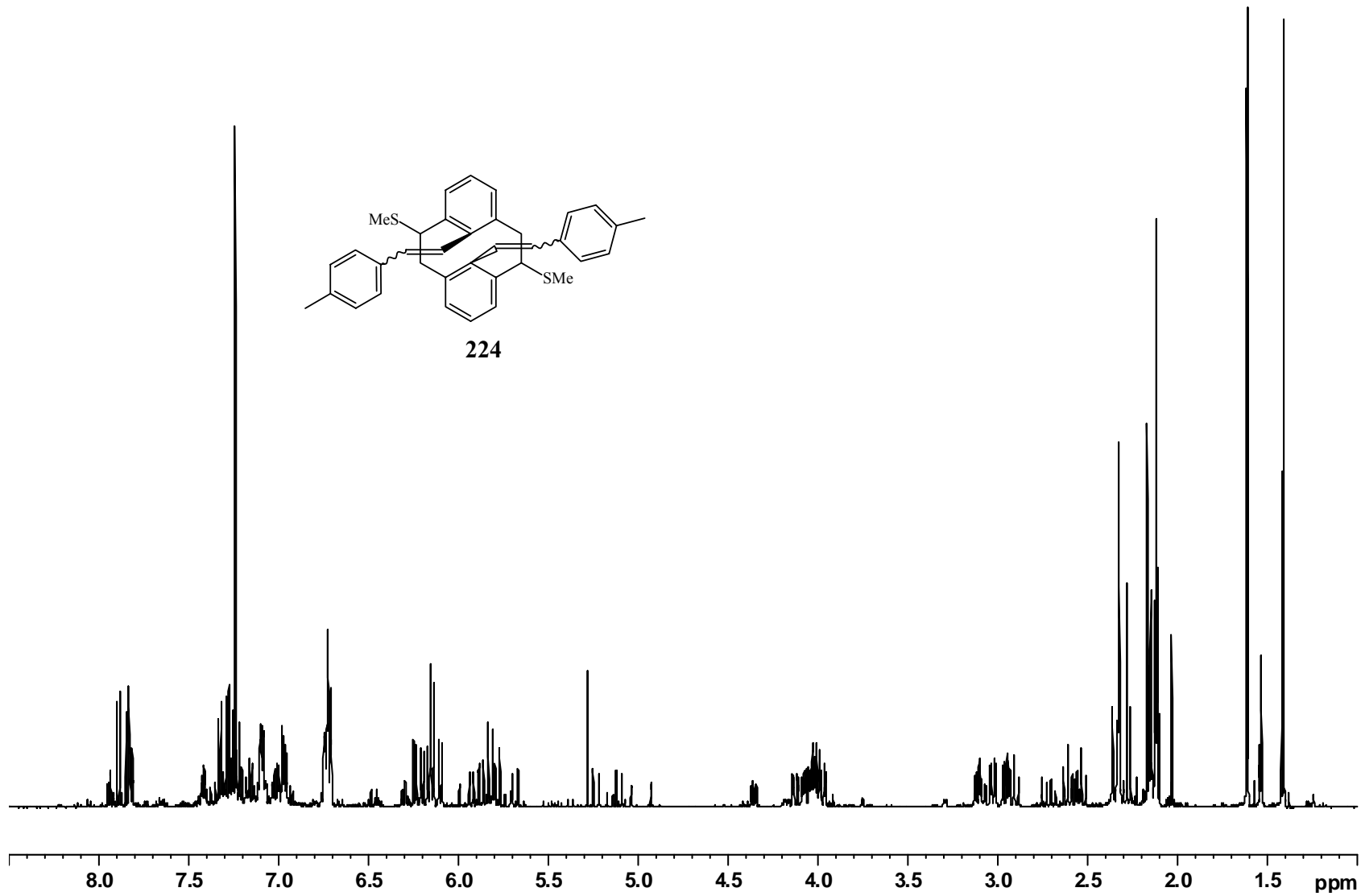


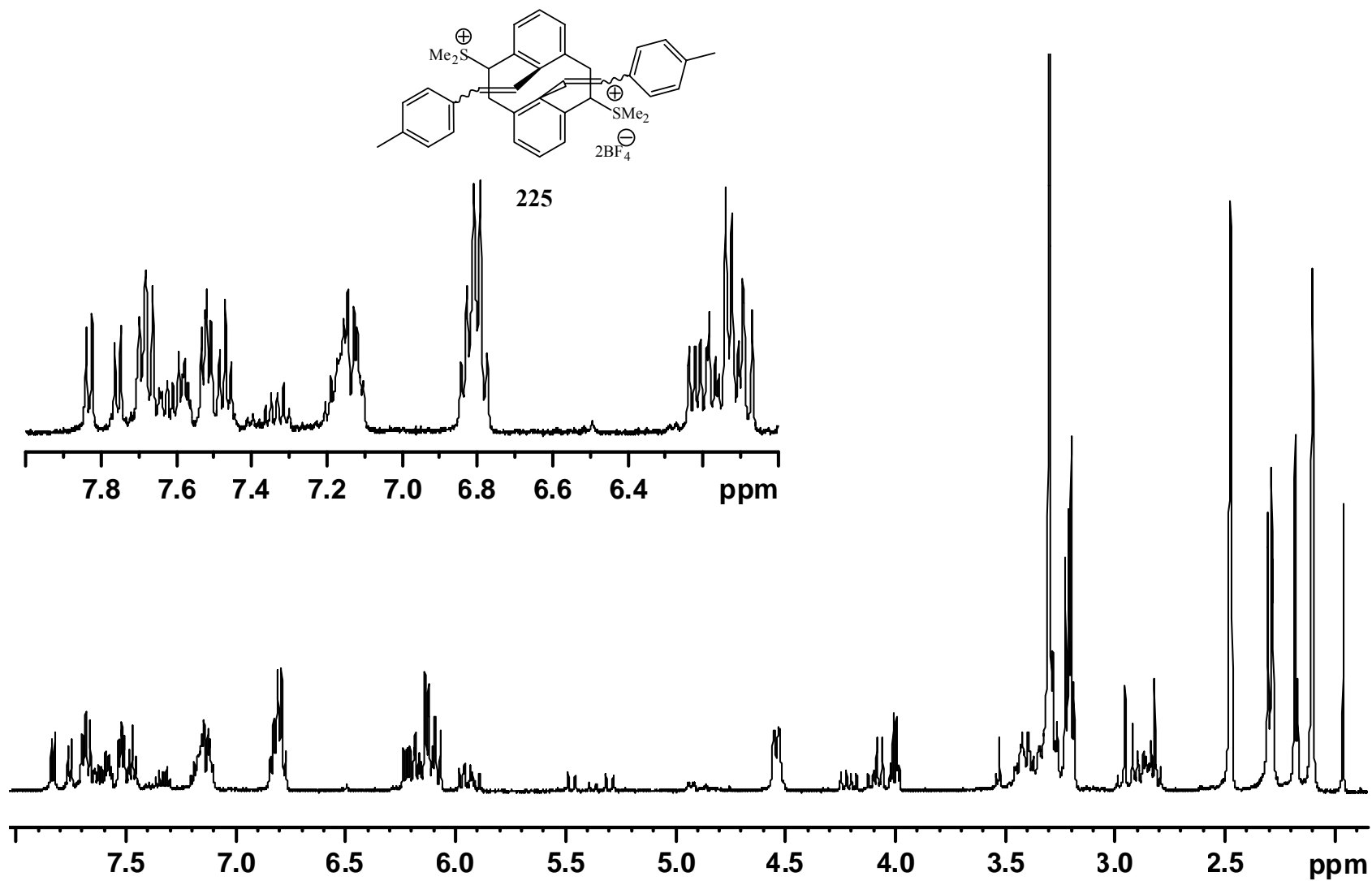


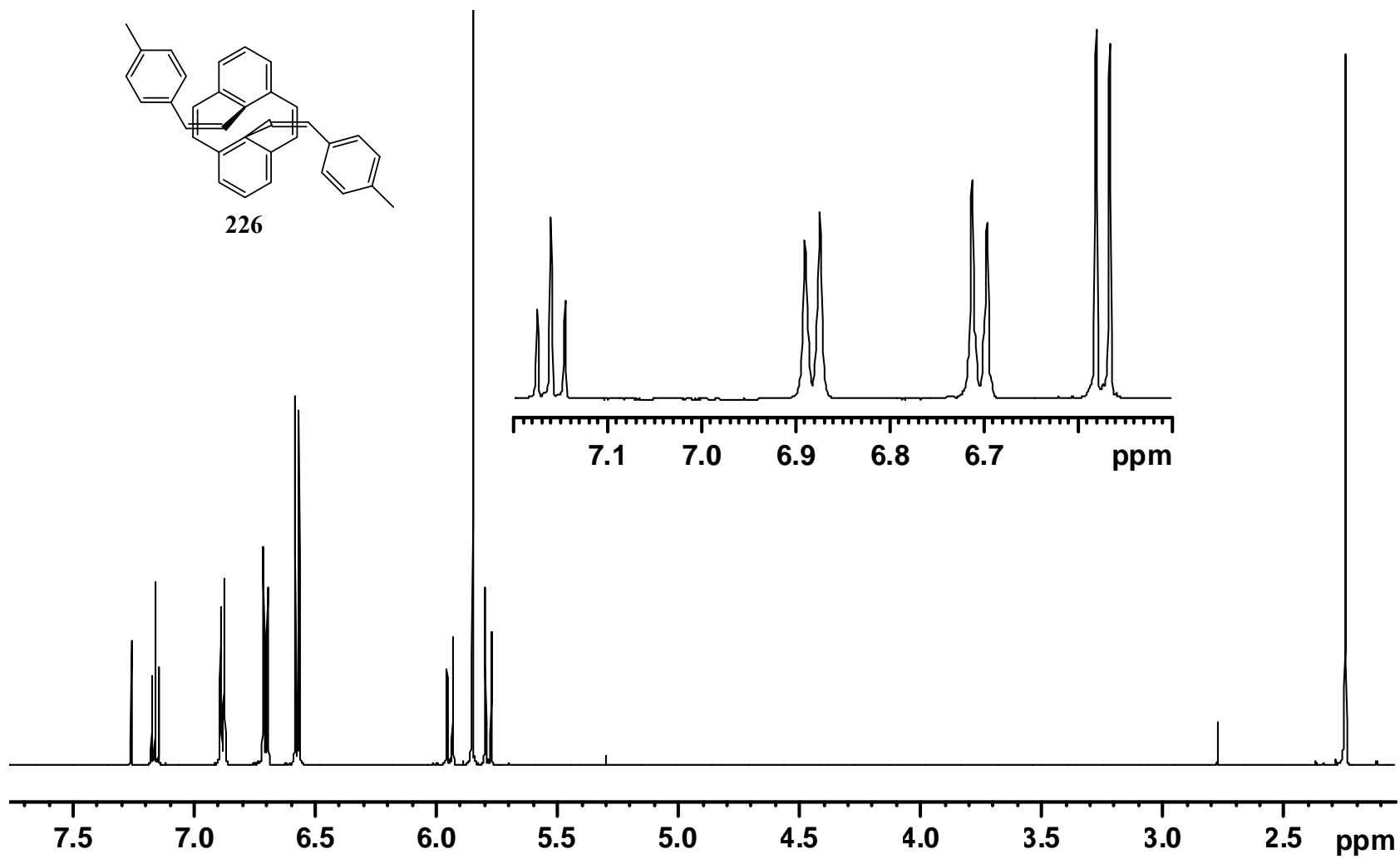


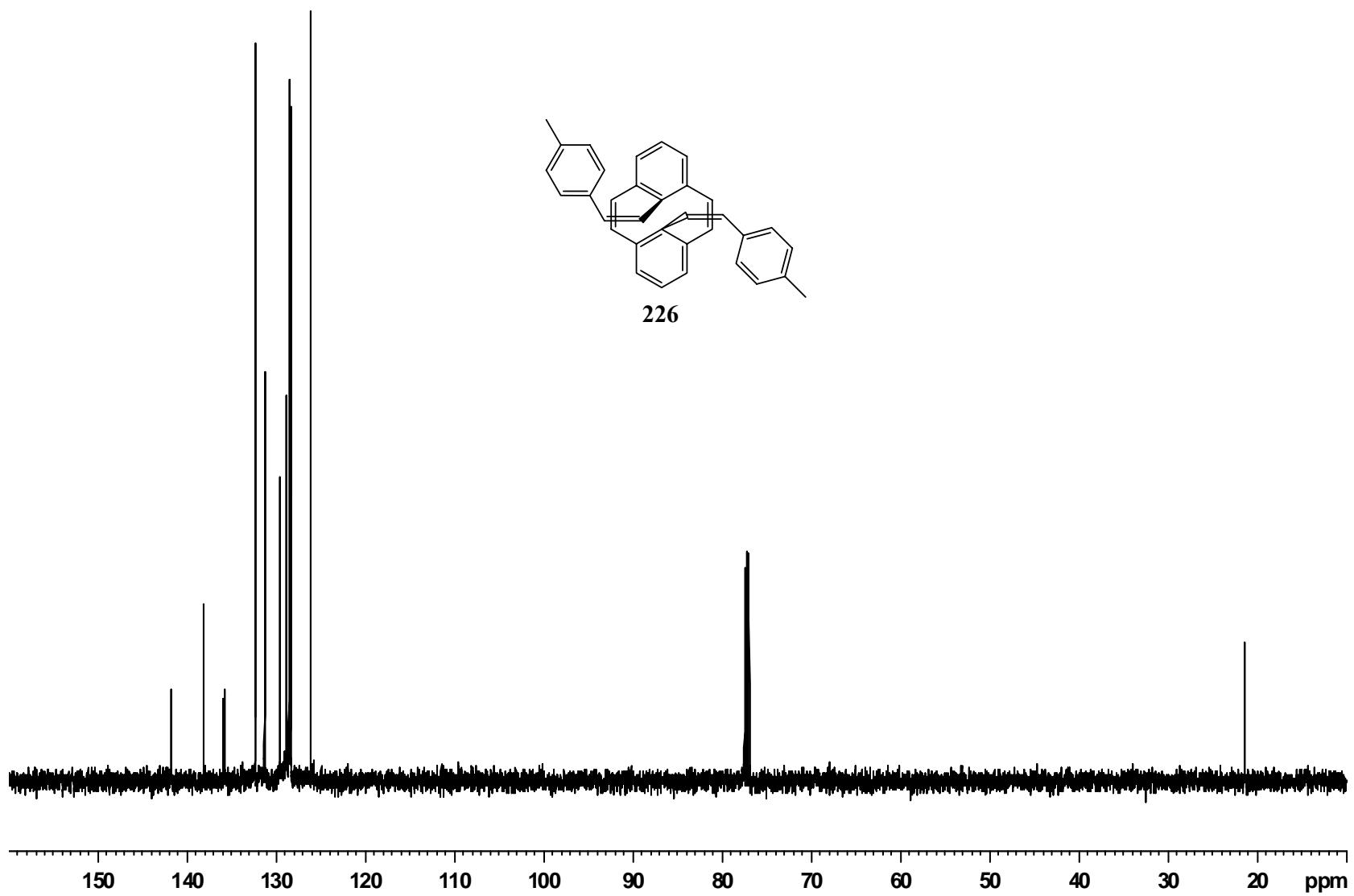


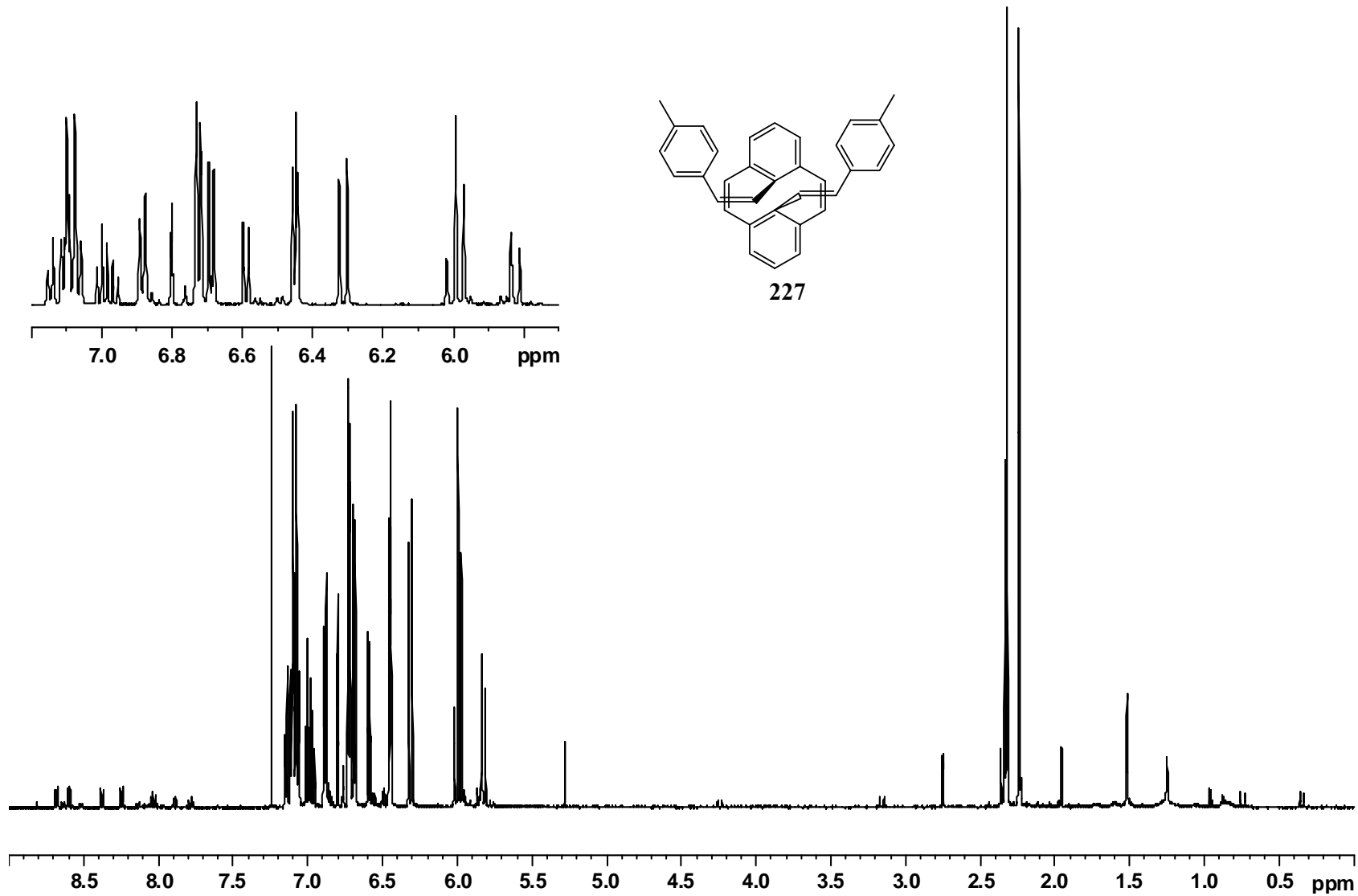
224

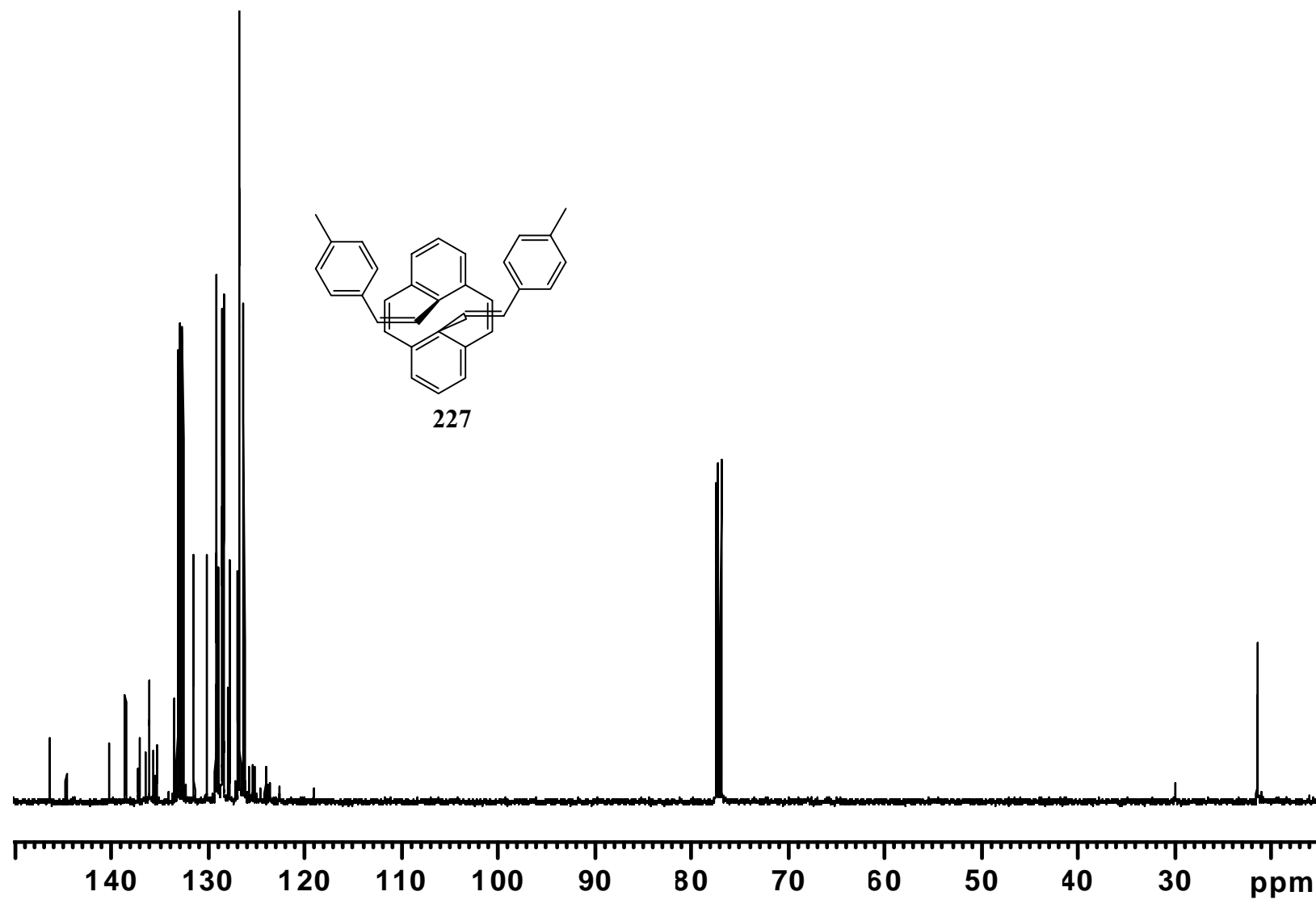


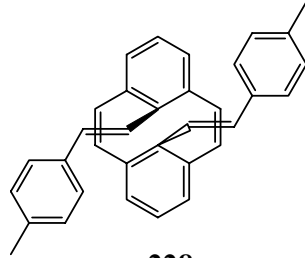




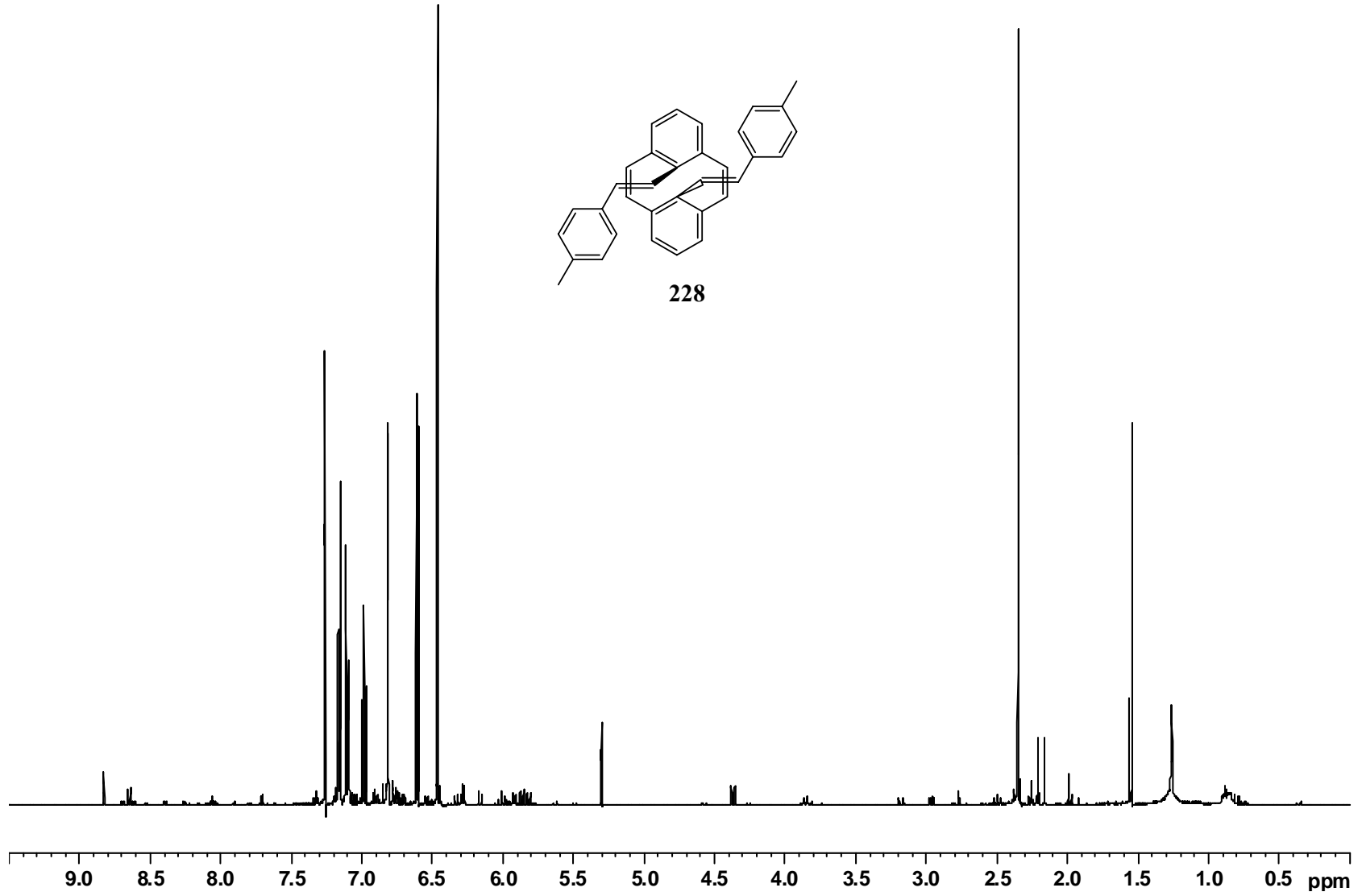


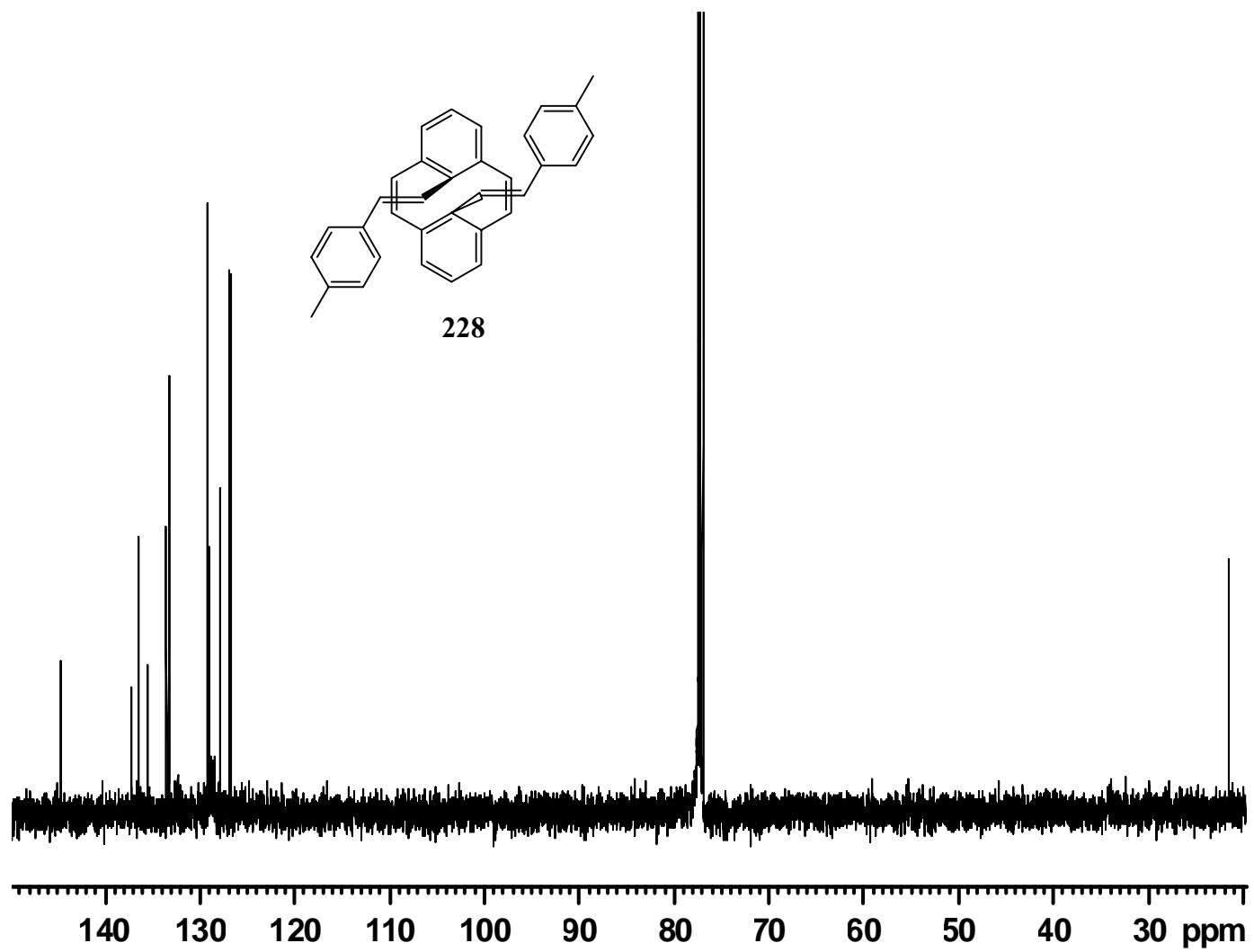


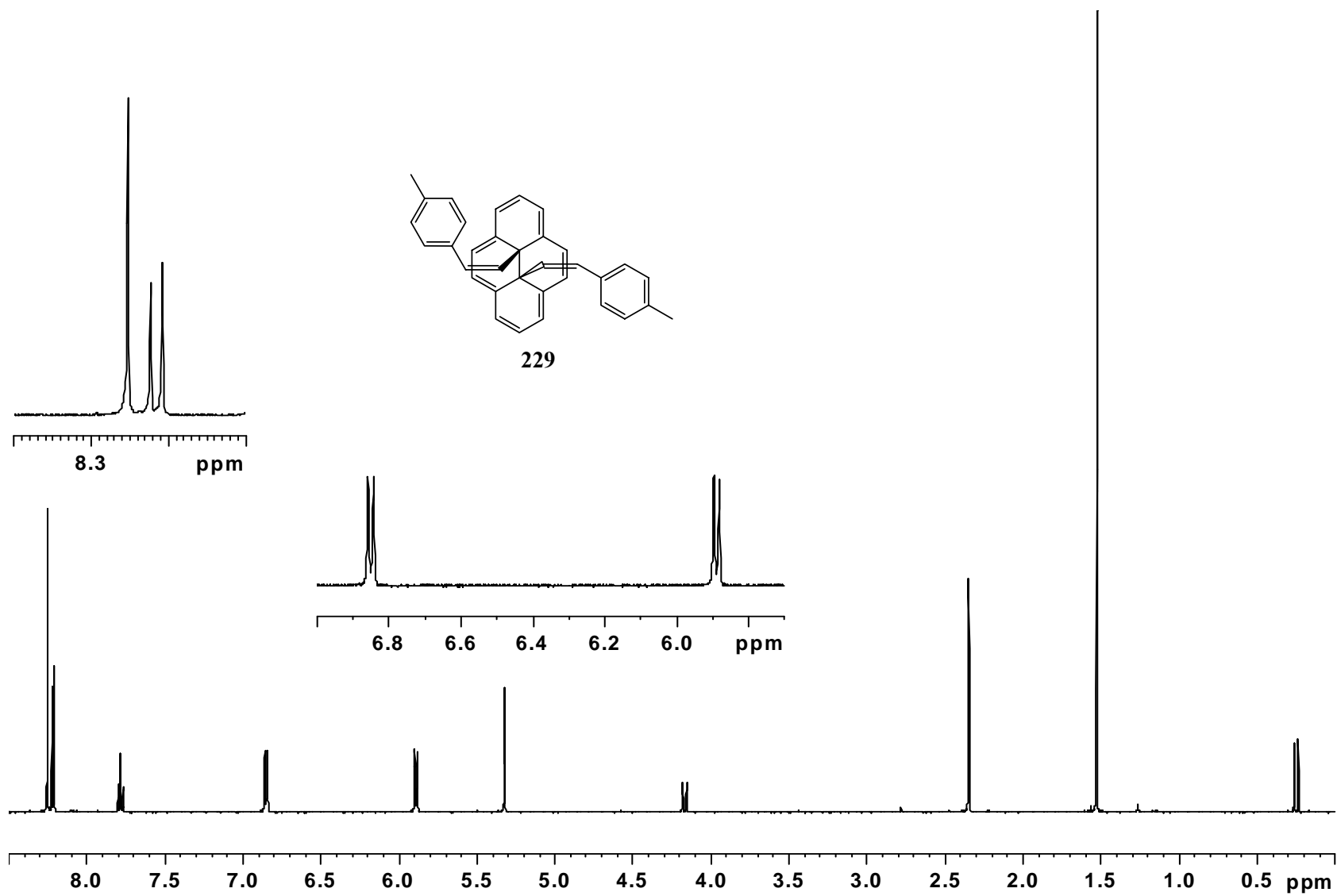


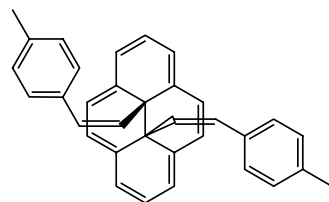


228

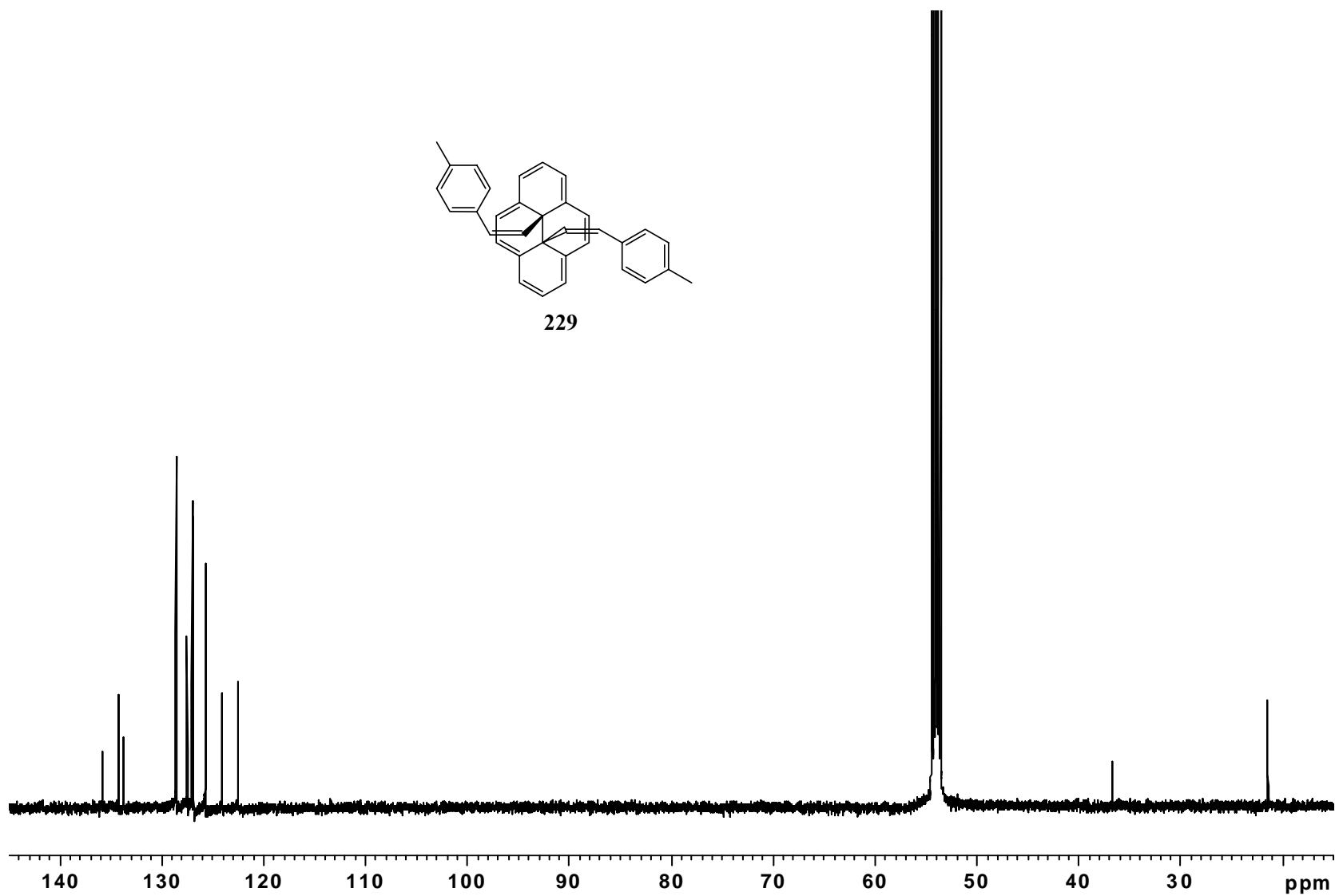


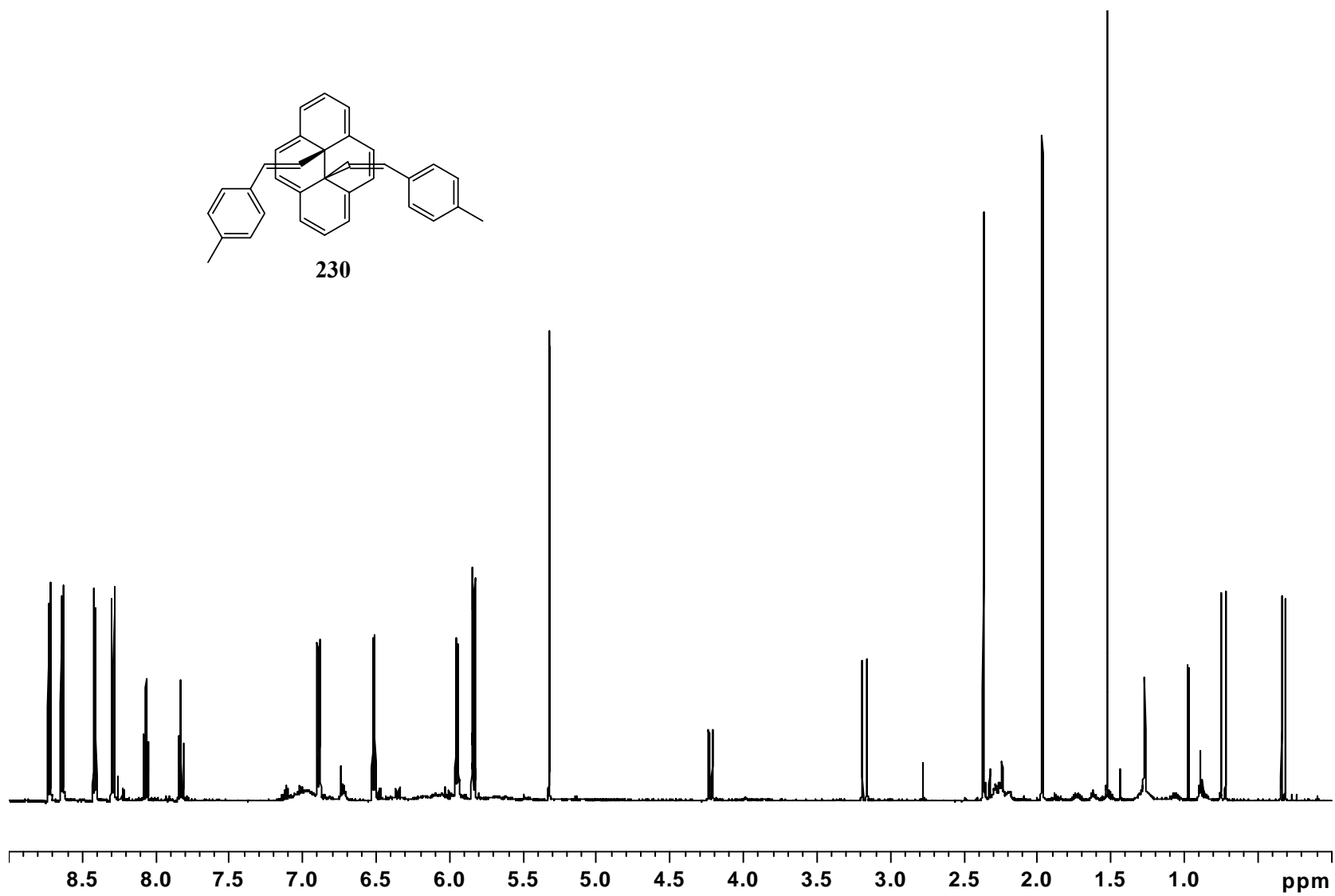
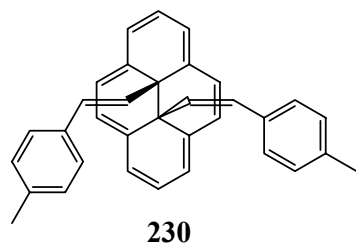


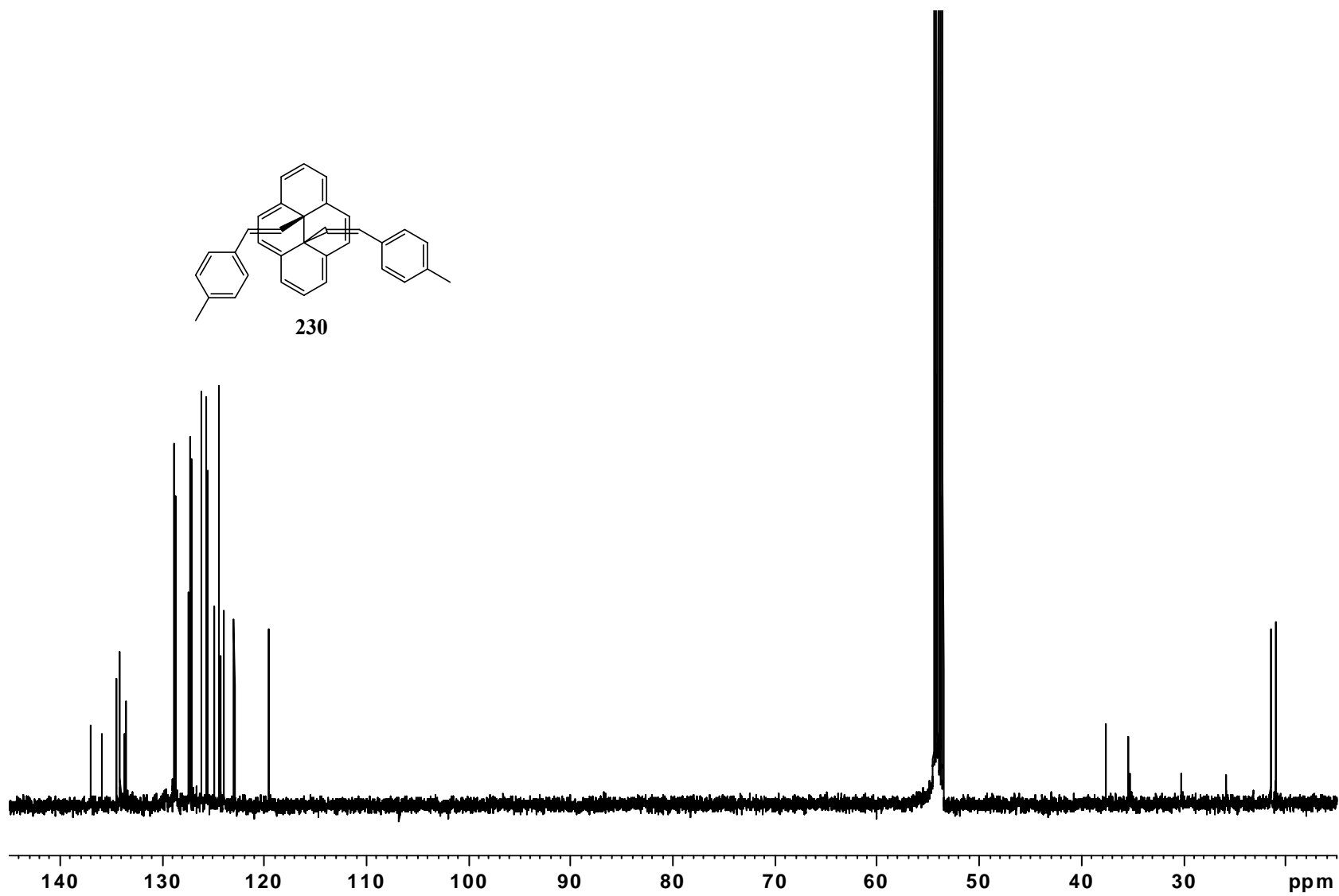
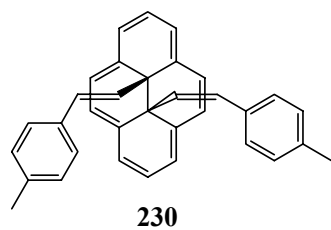


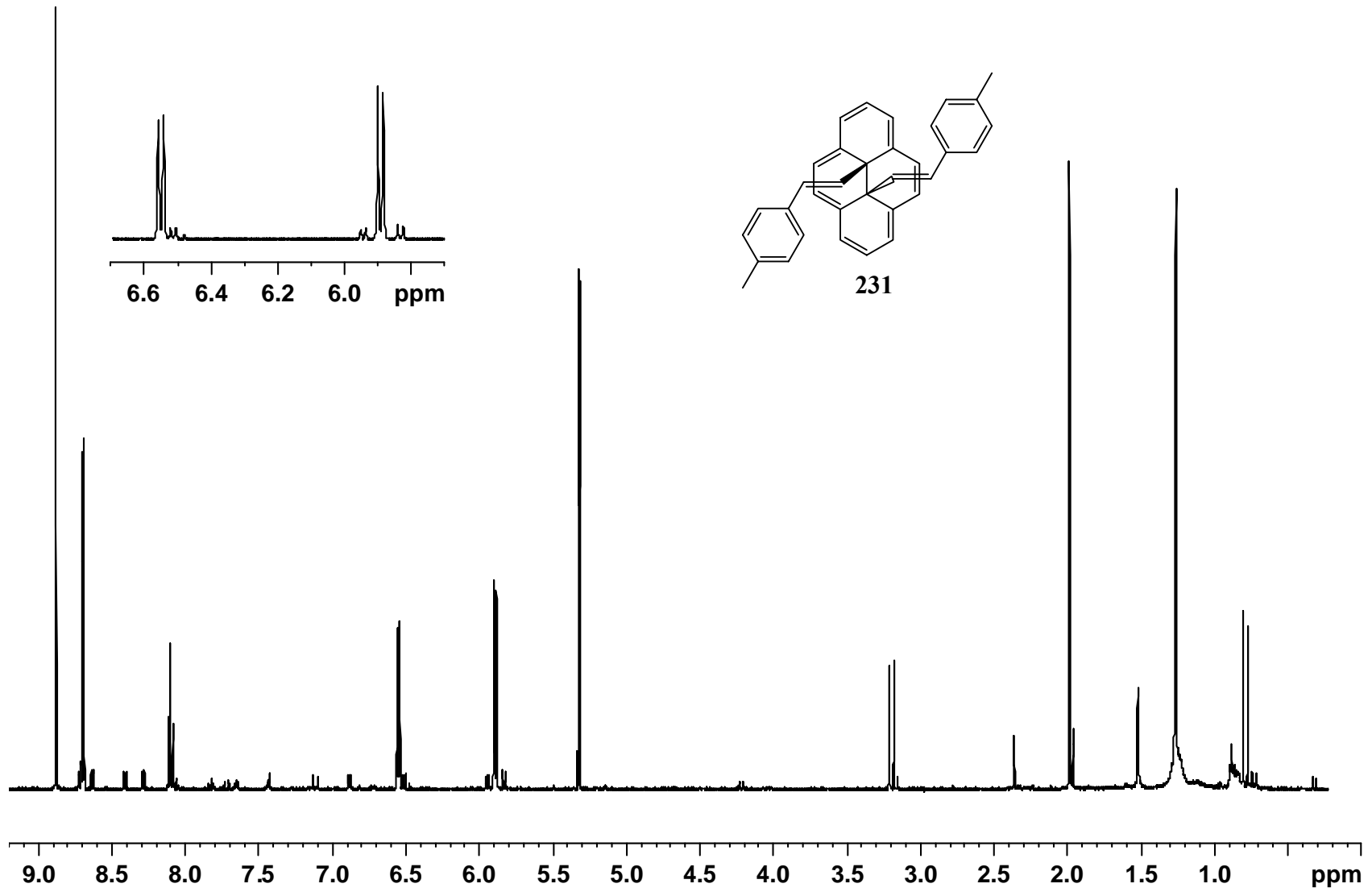


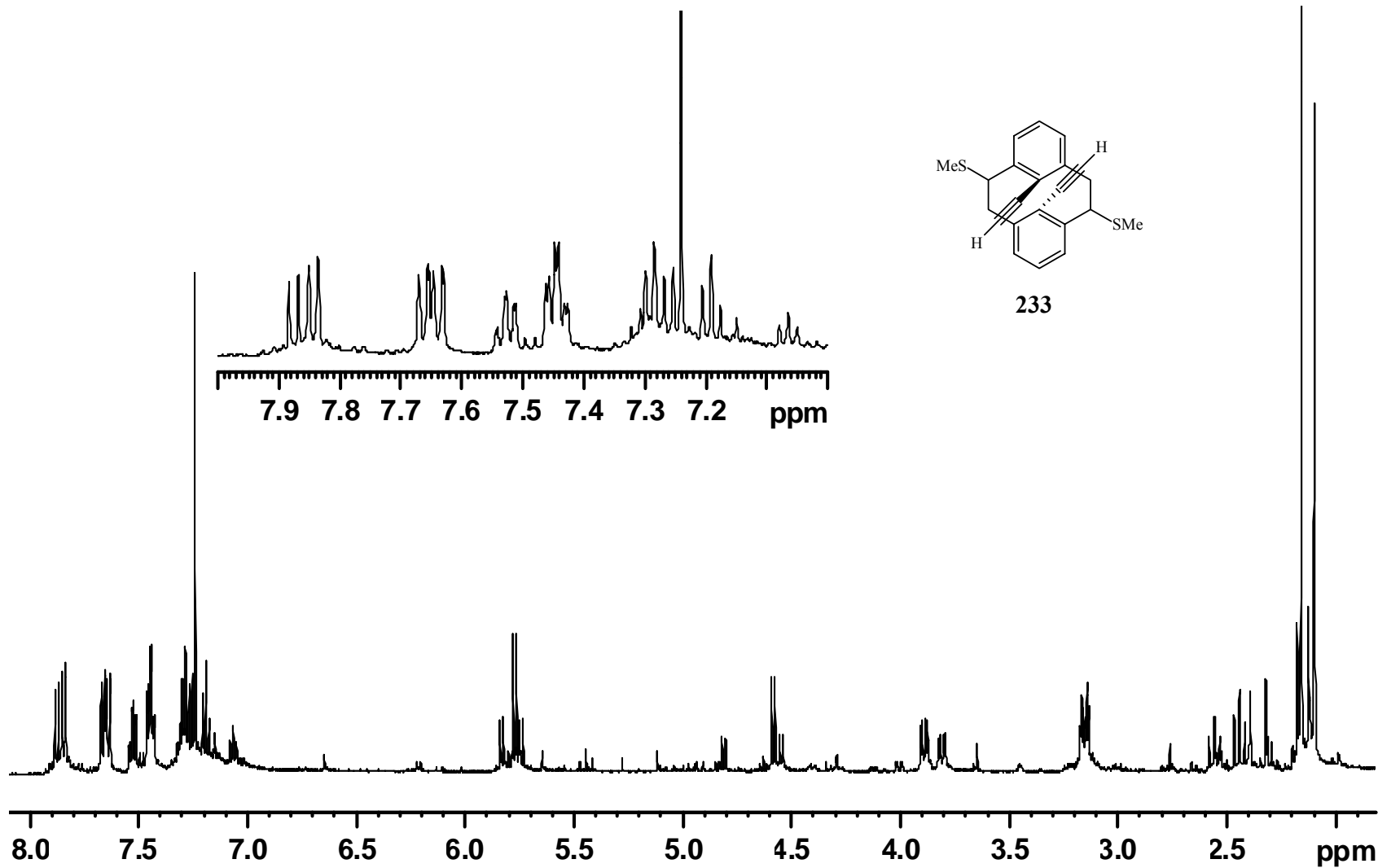
229

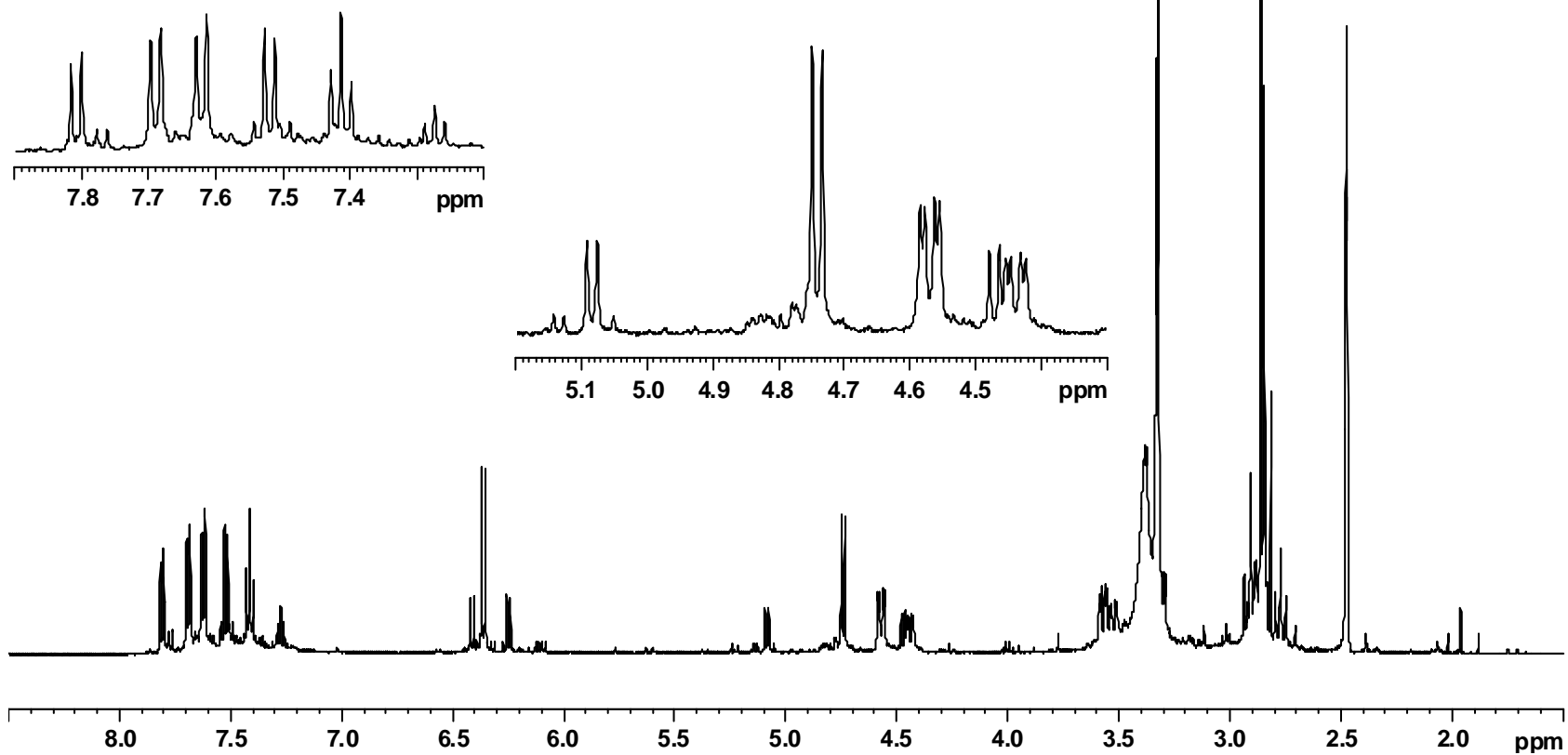
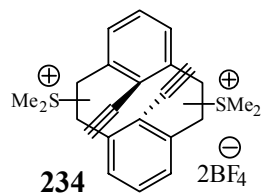


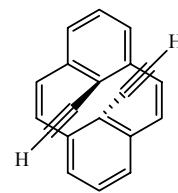




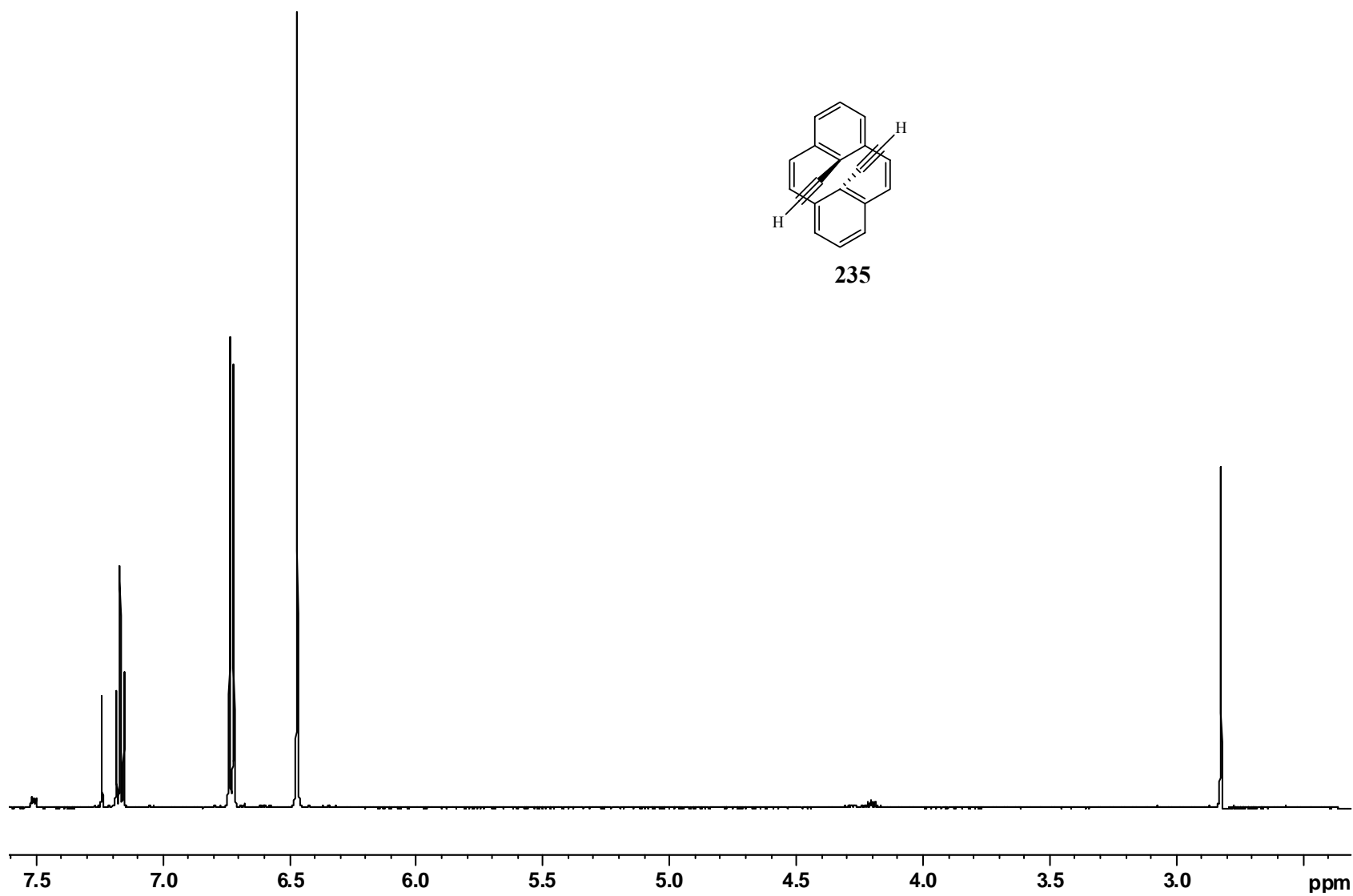


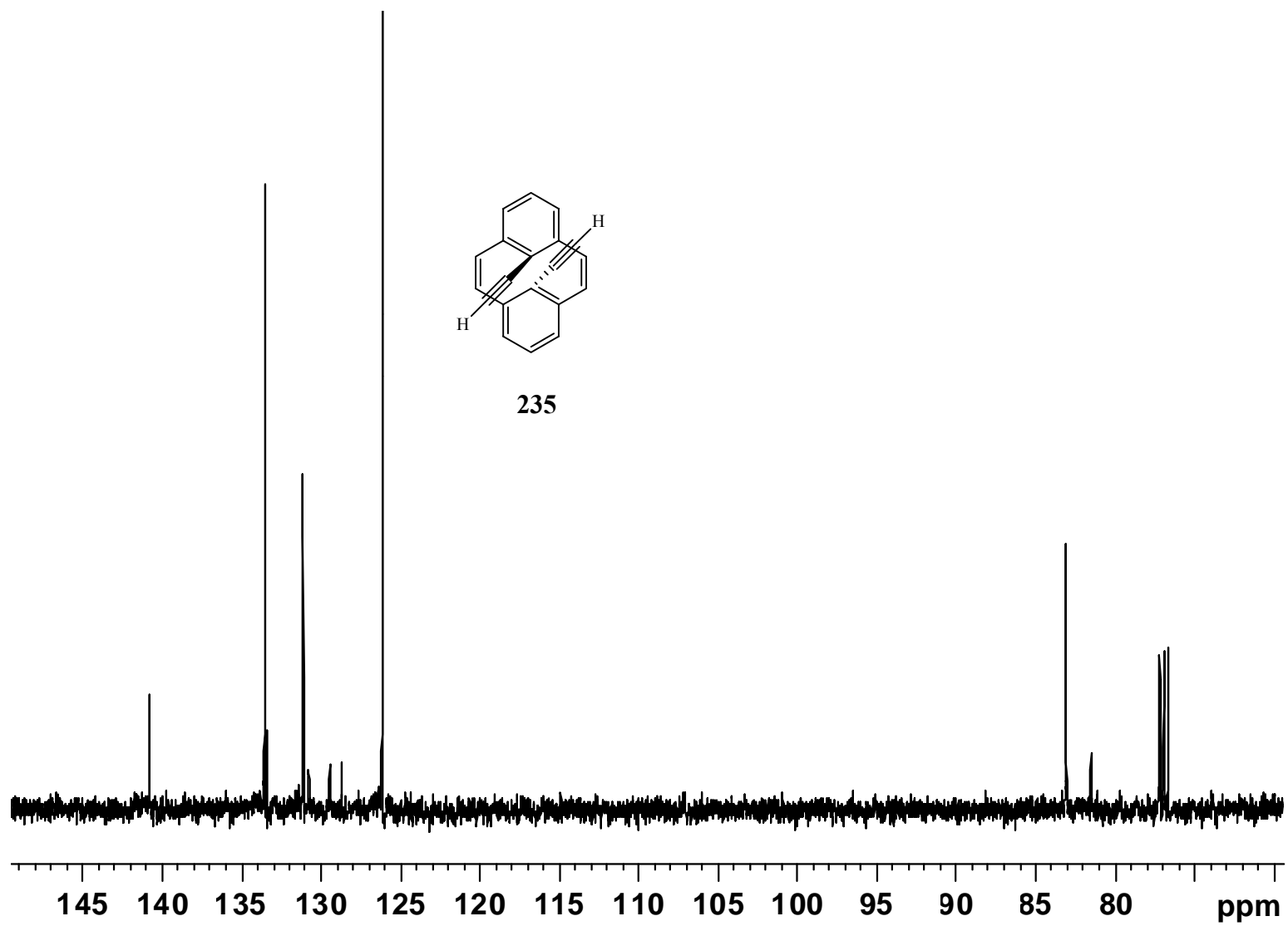


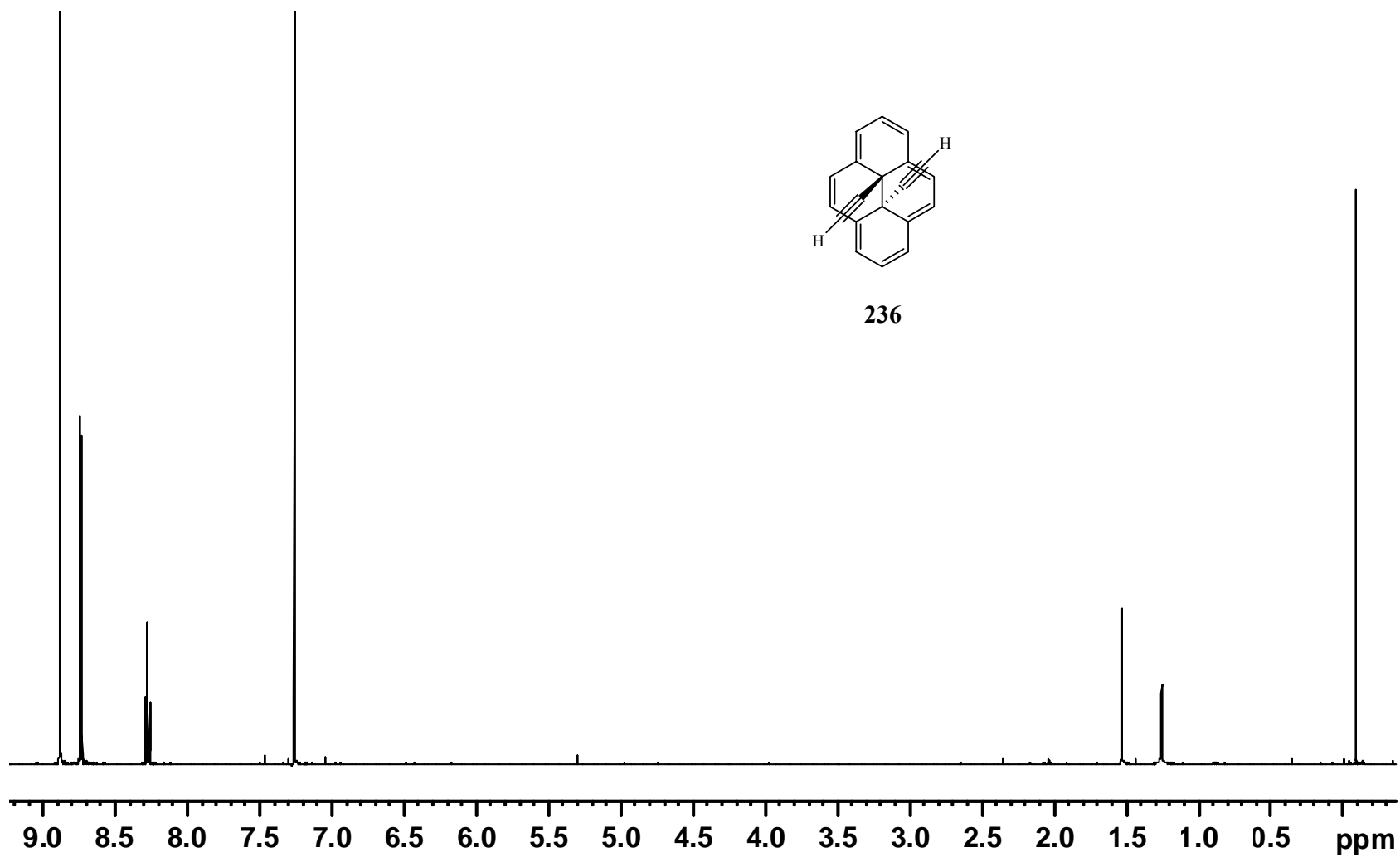


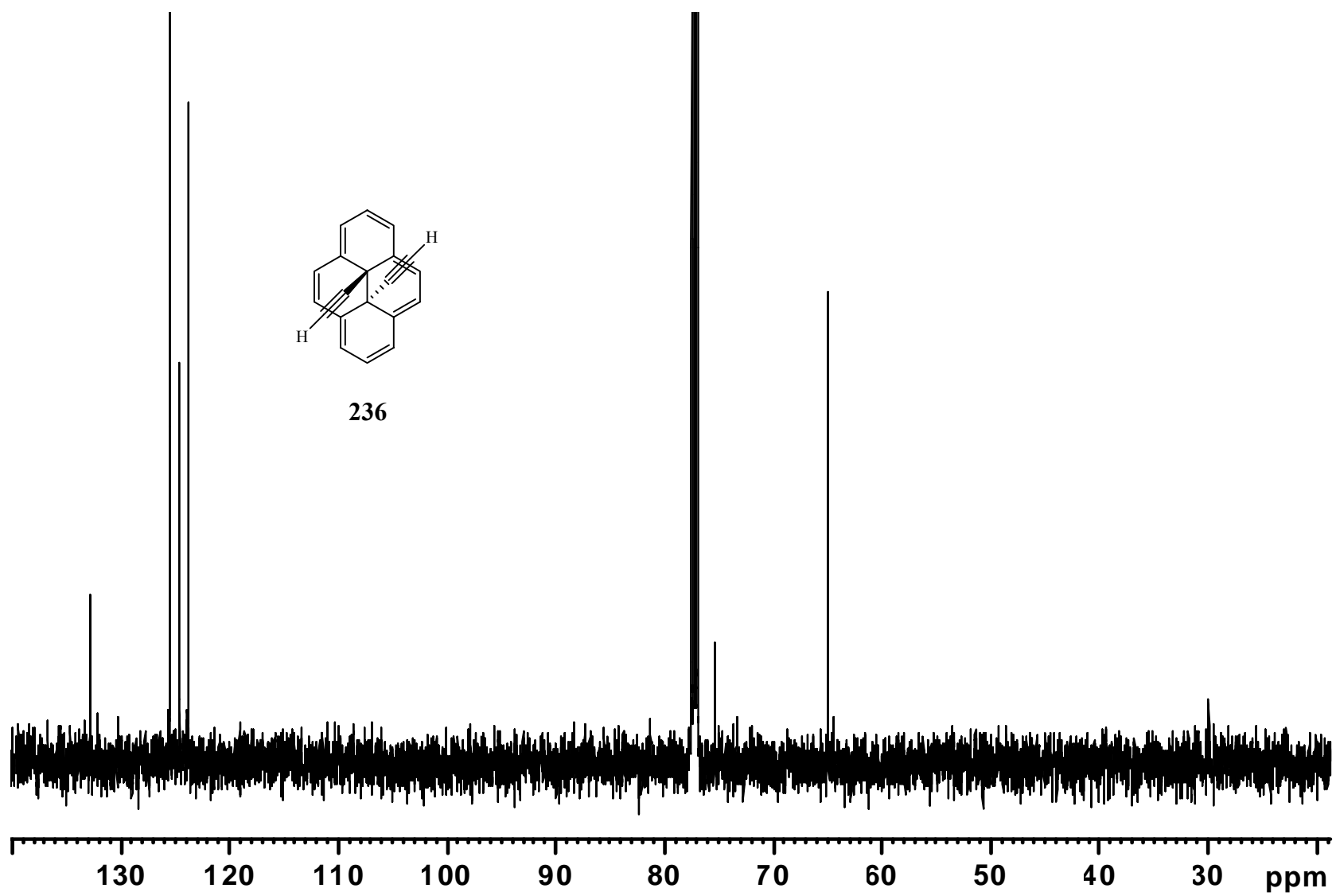


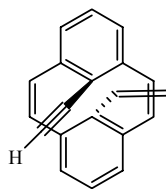
235



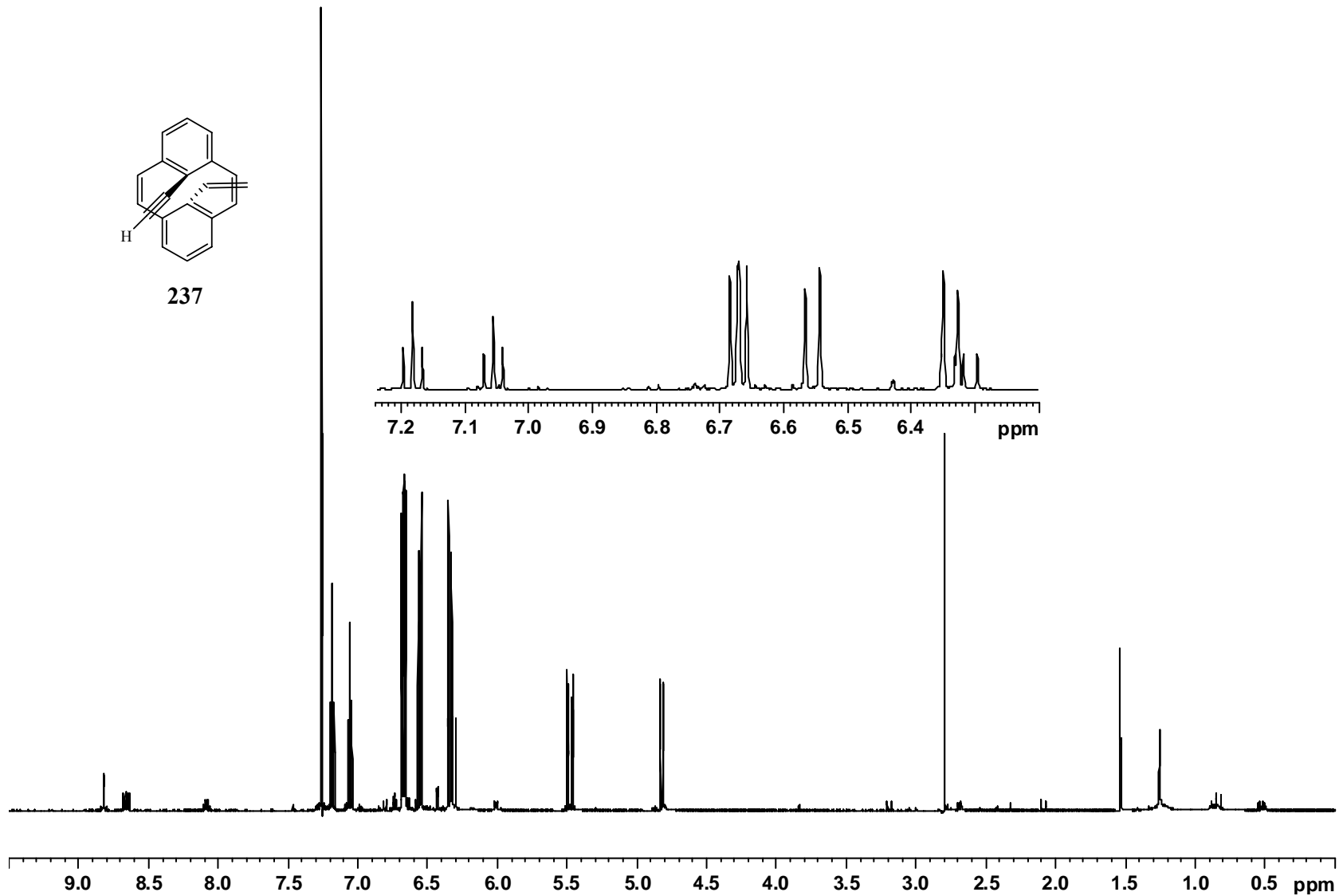


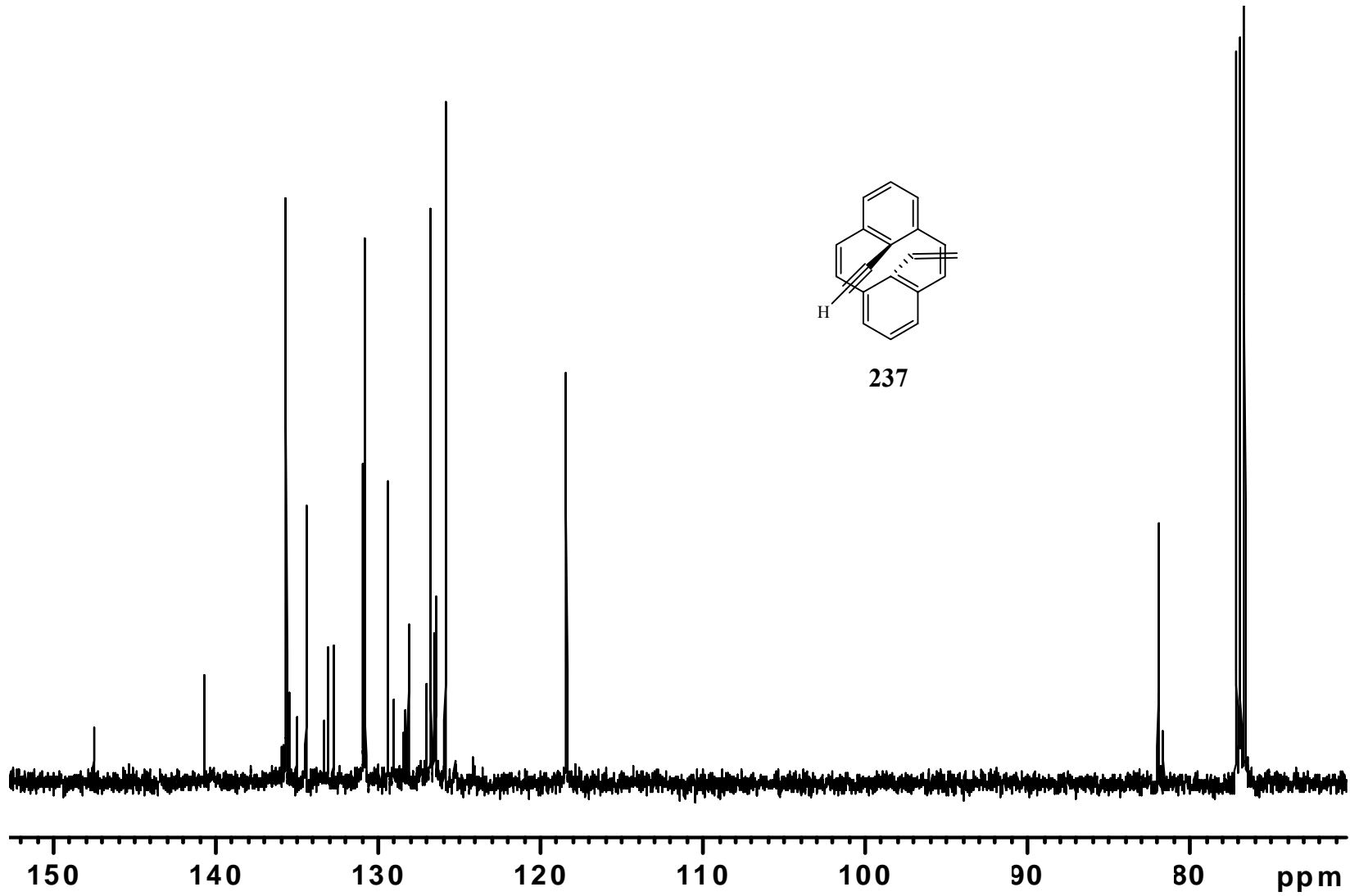


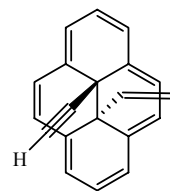
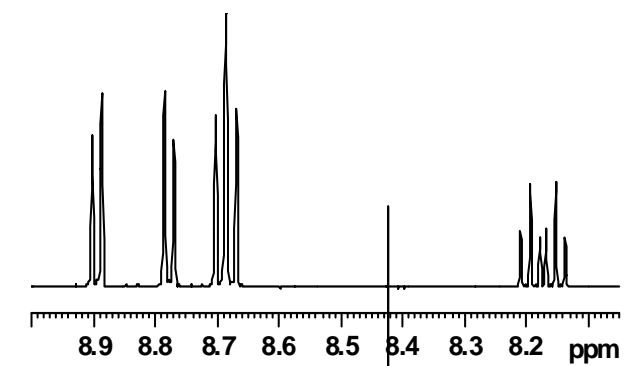




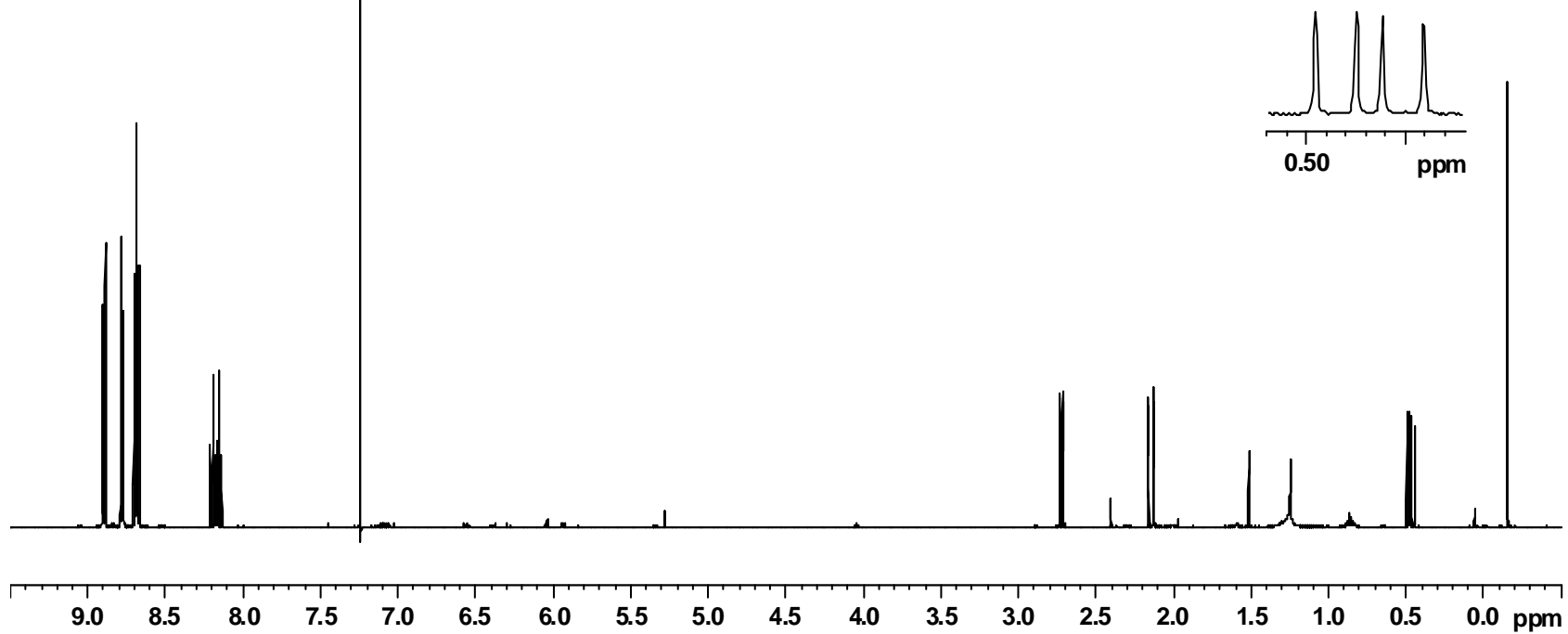
237

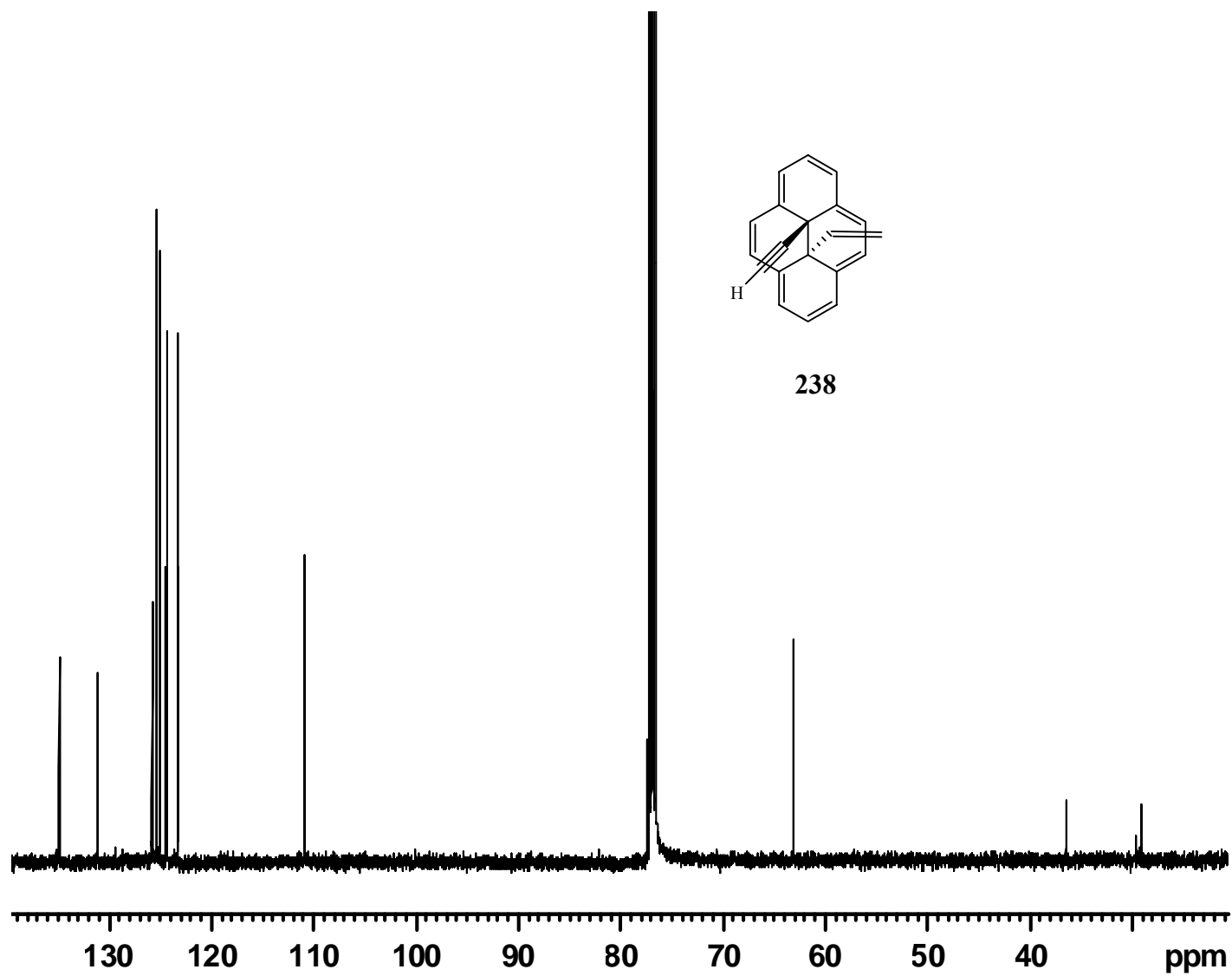


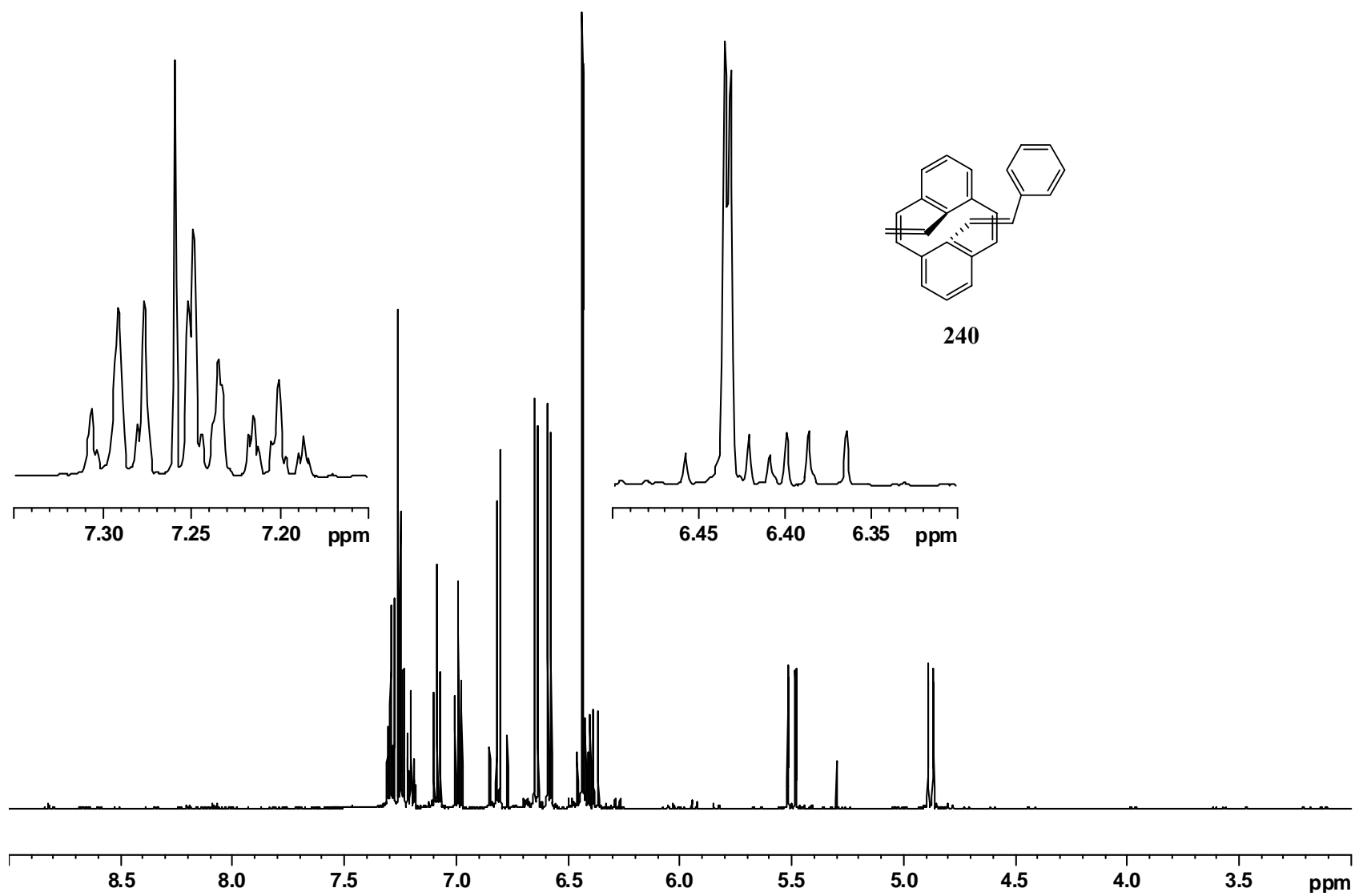


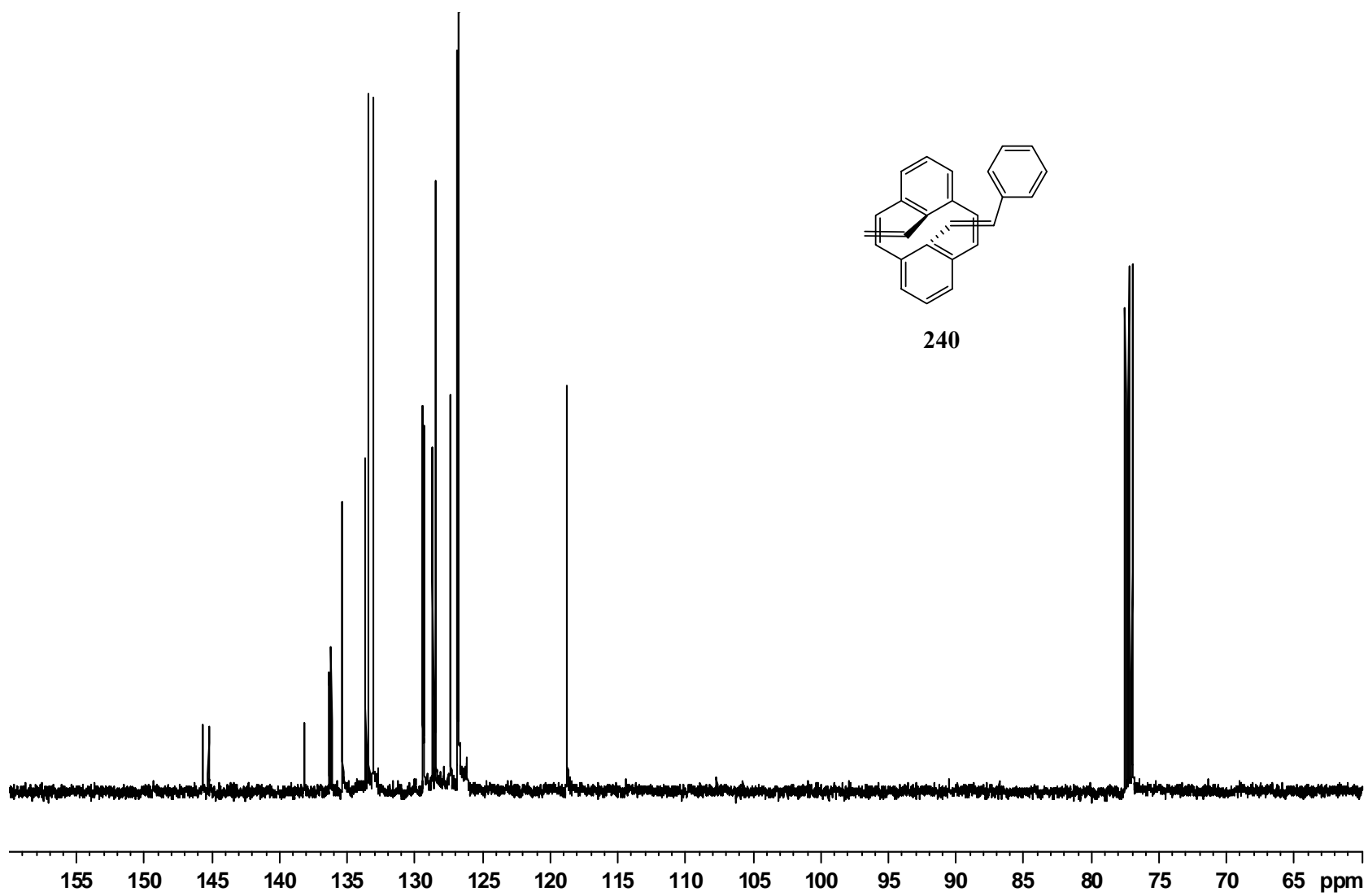


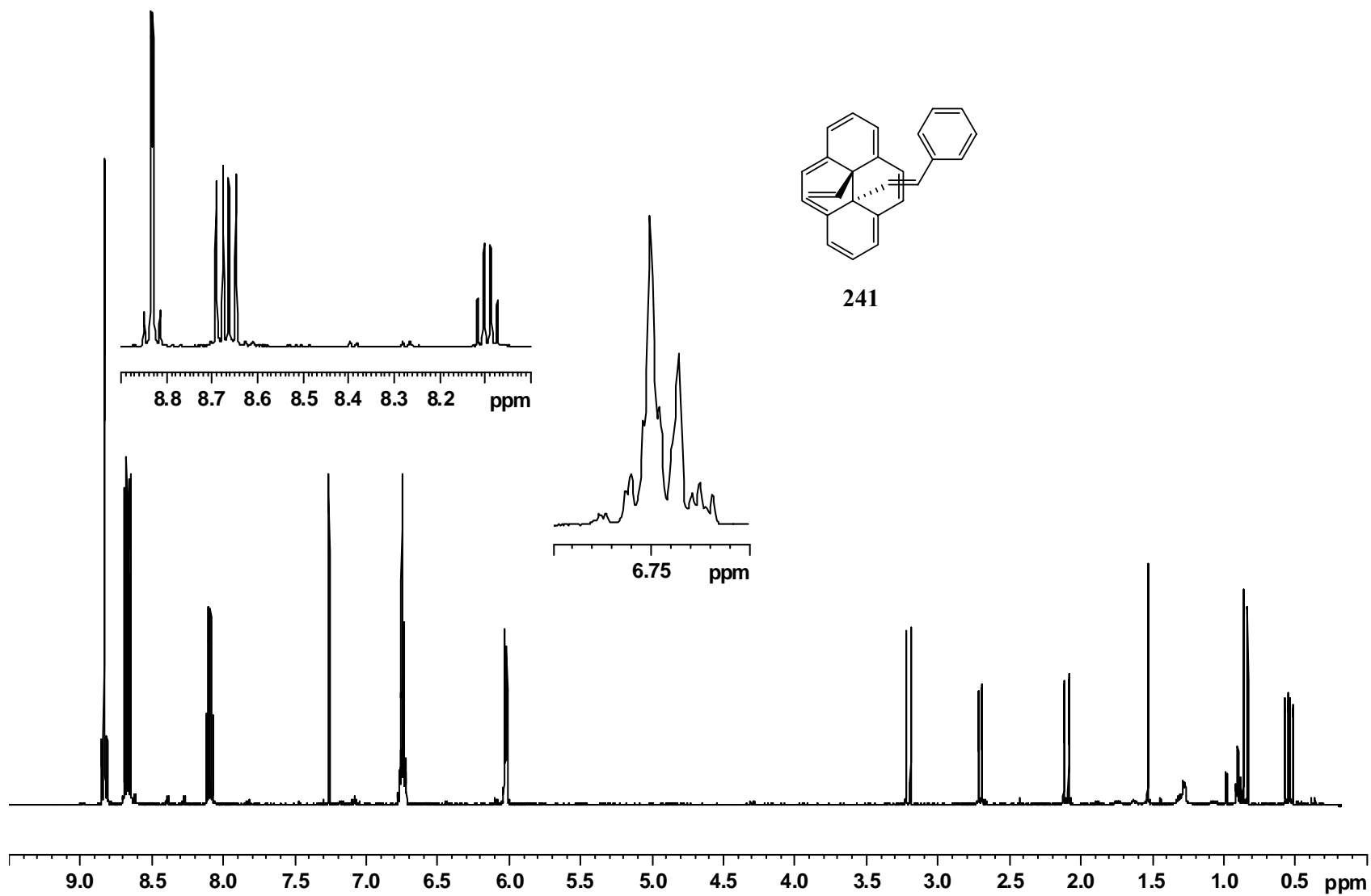
238

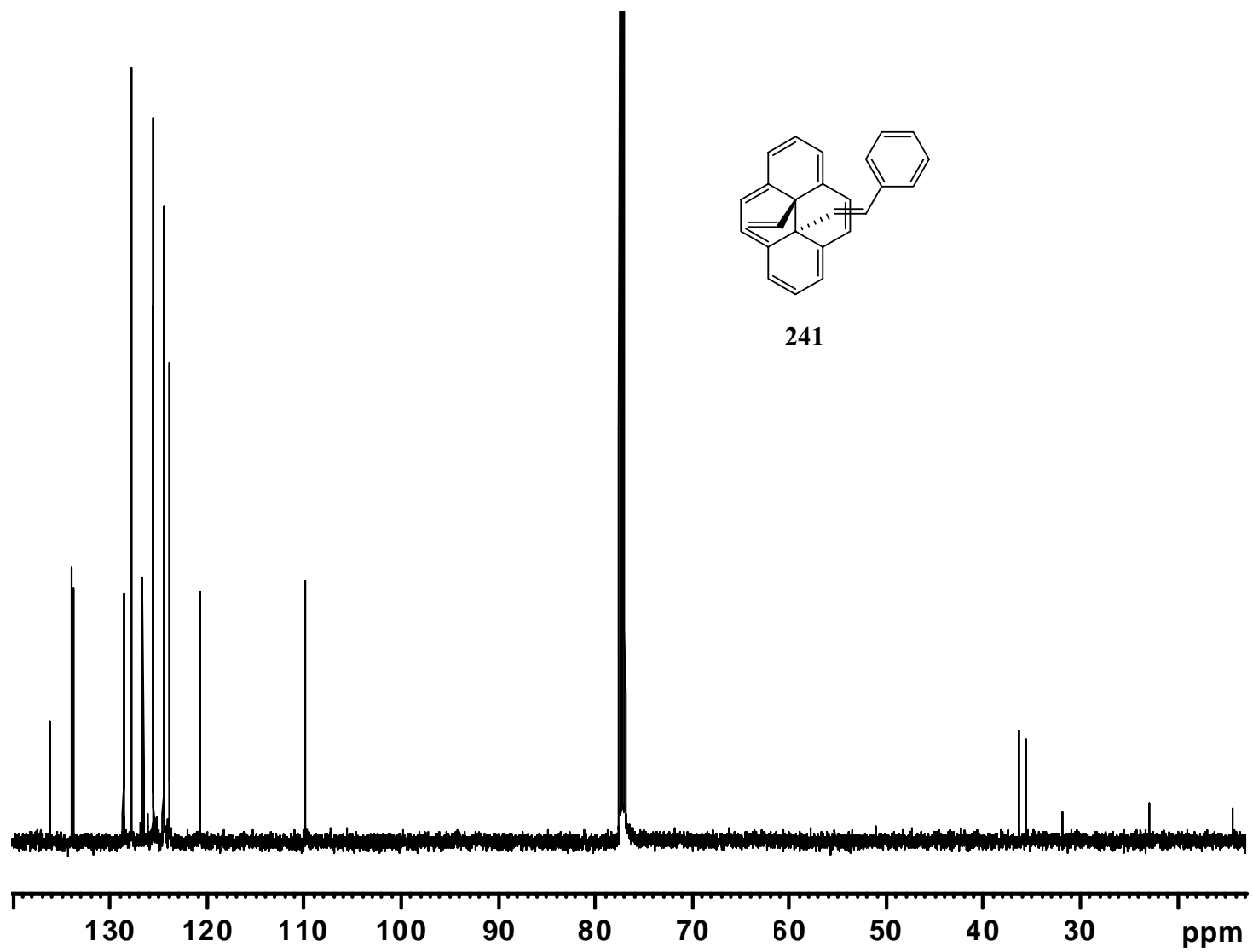


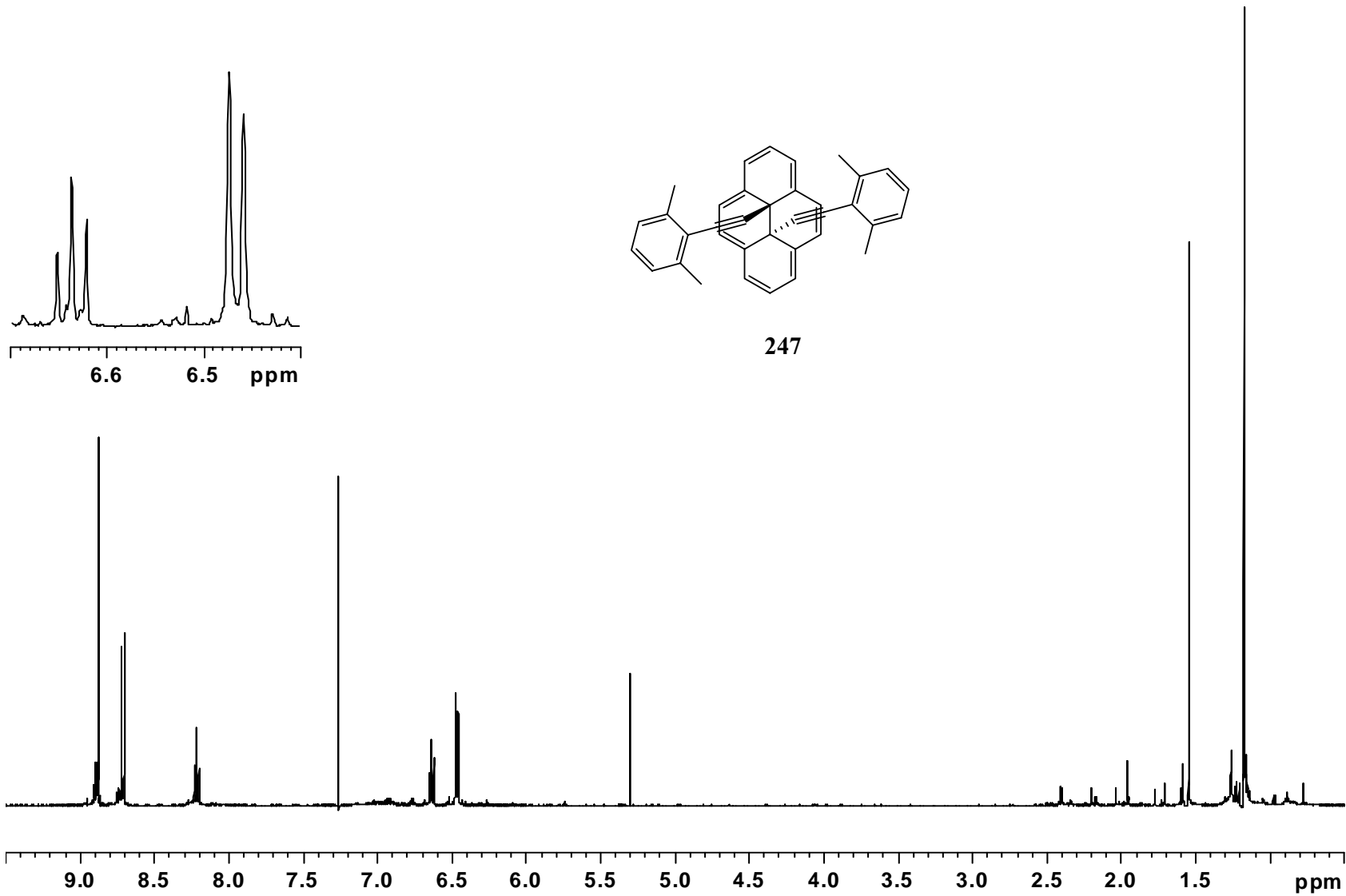


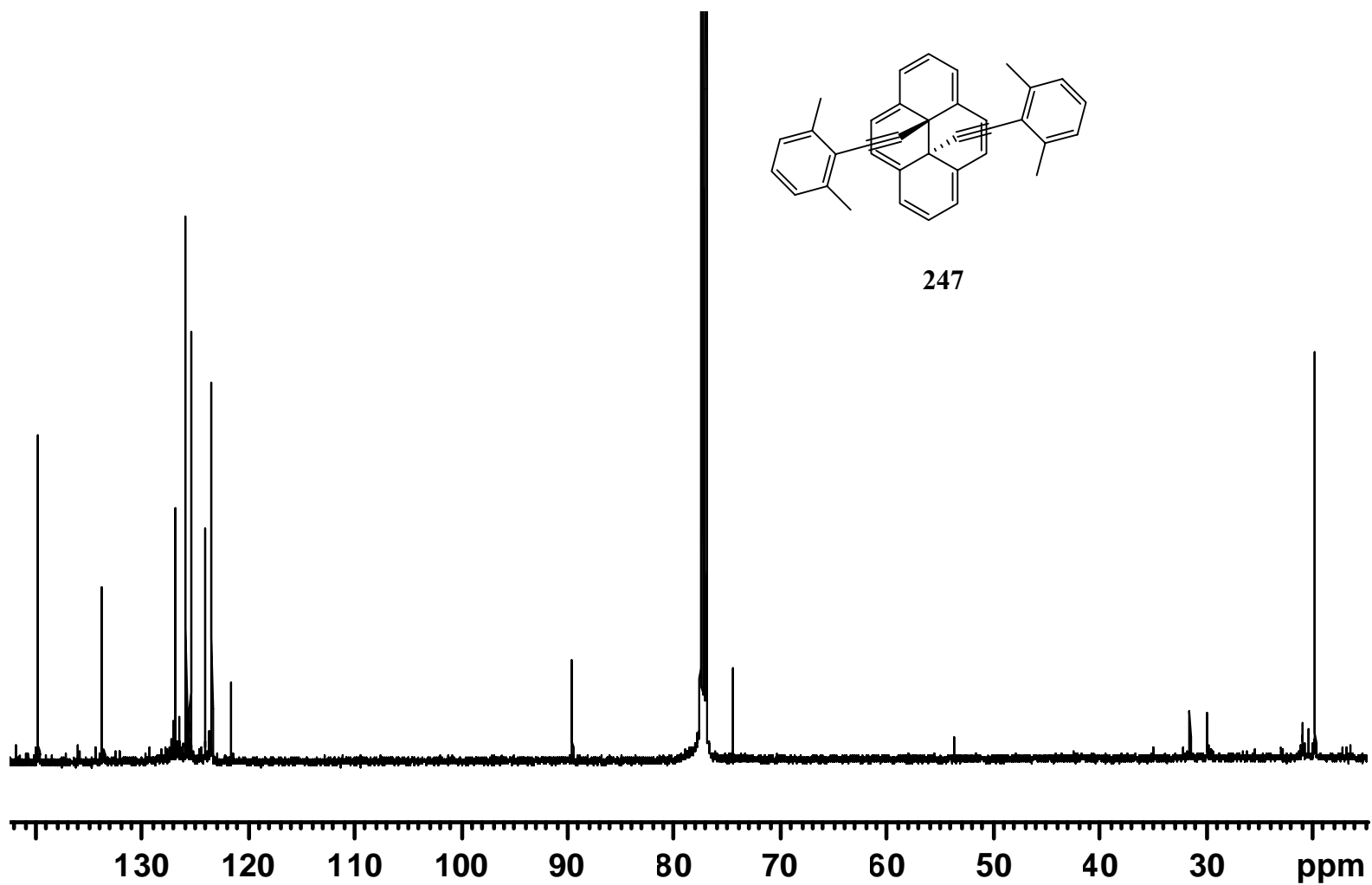


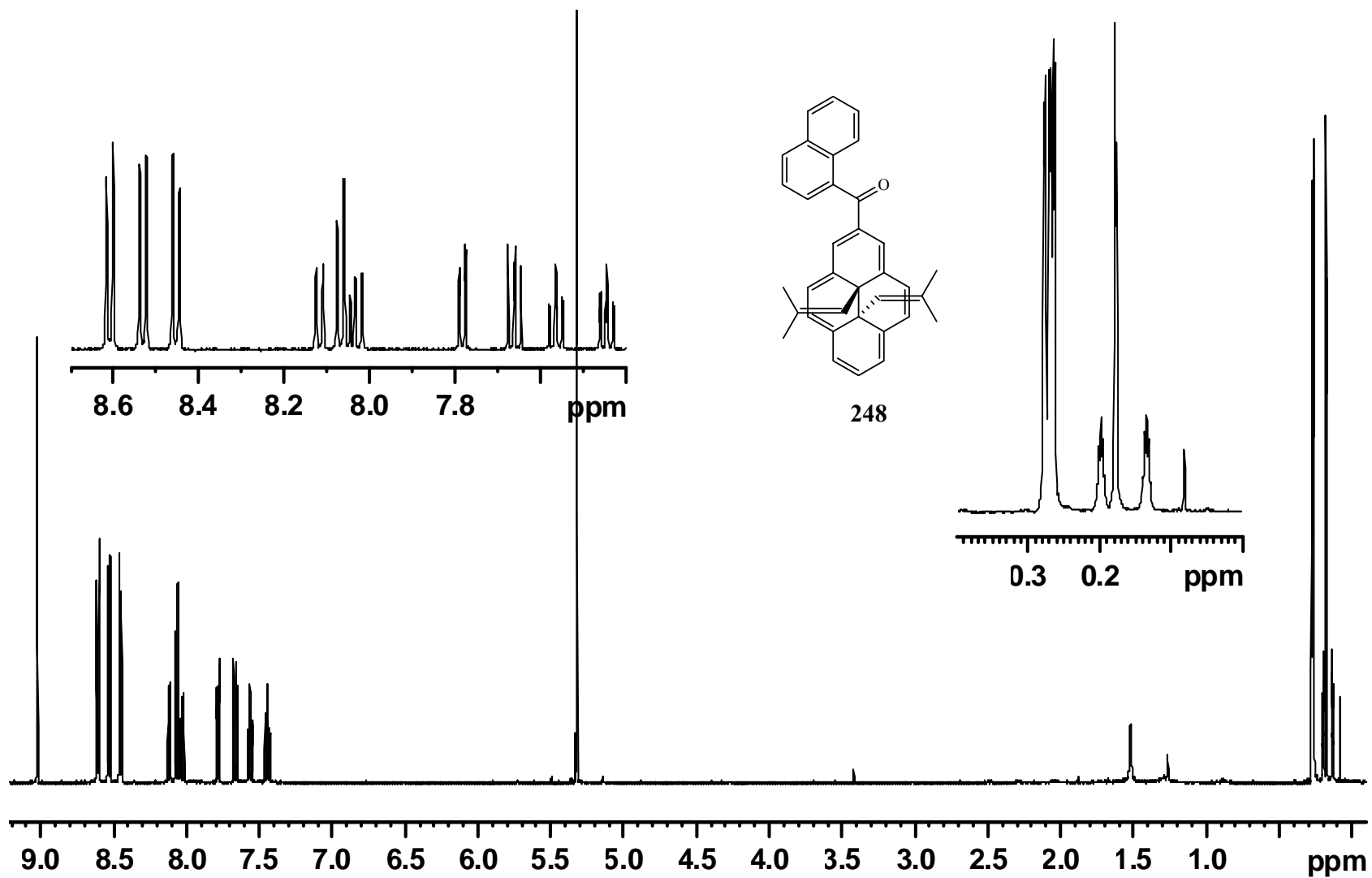


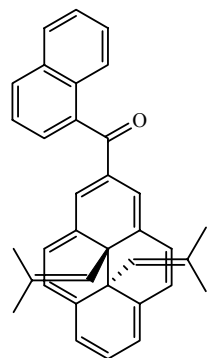




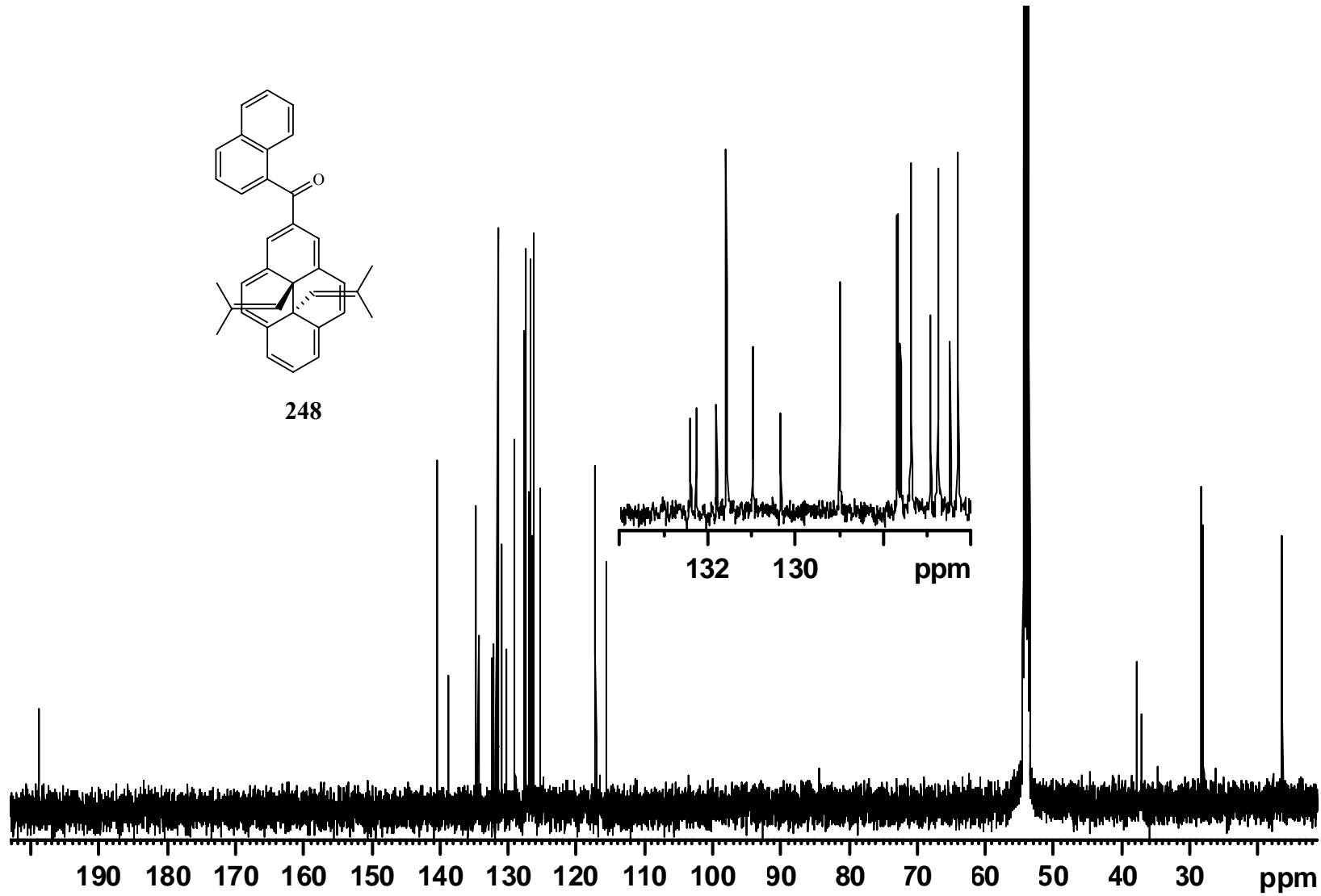


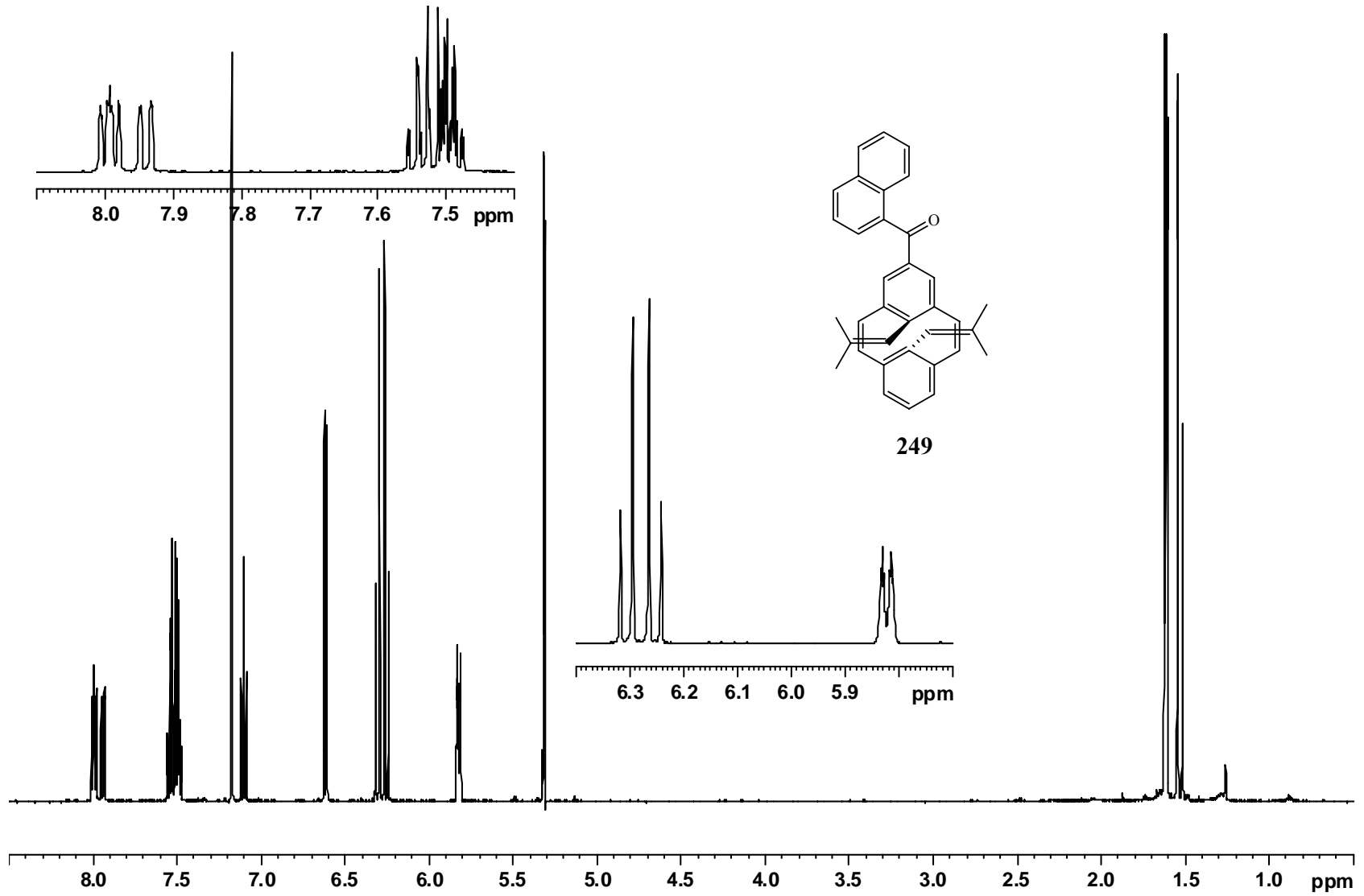


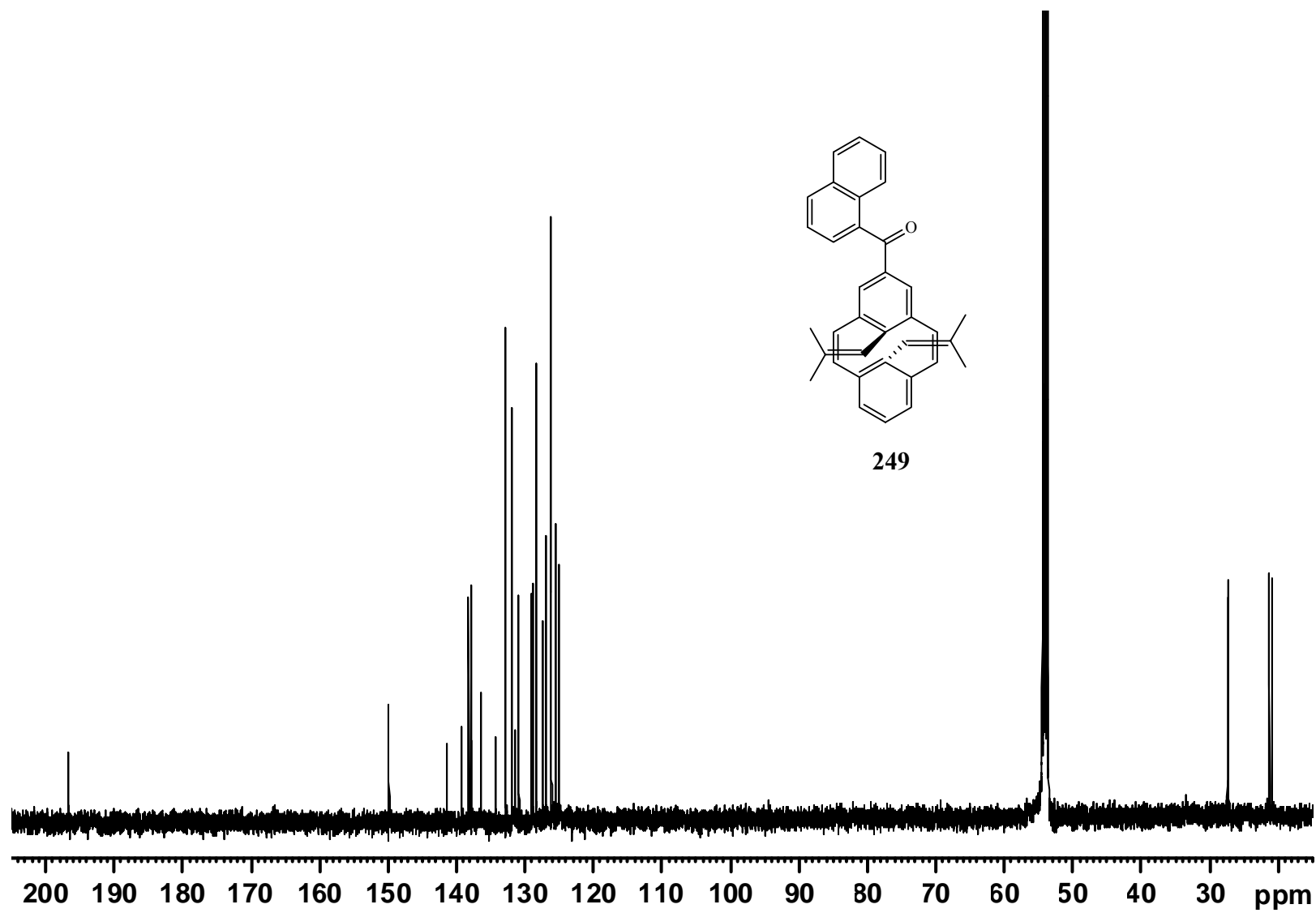


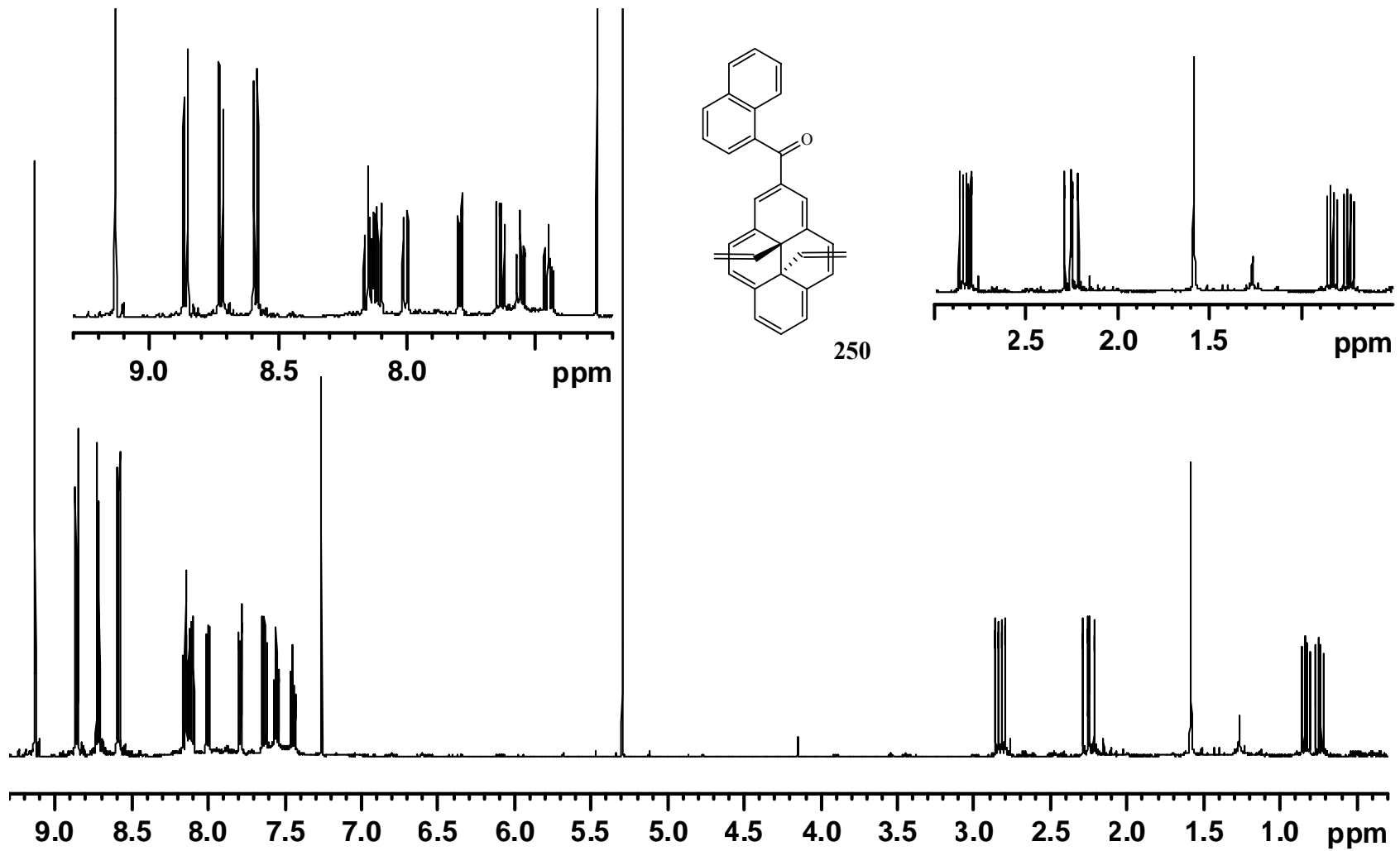


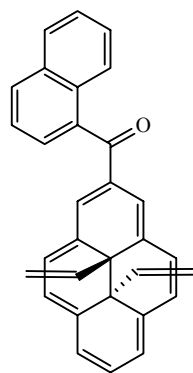
248



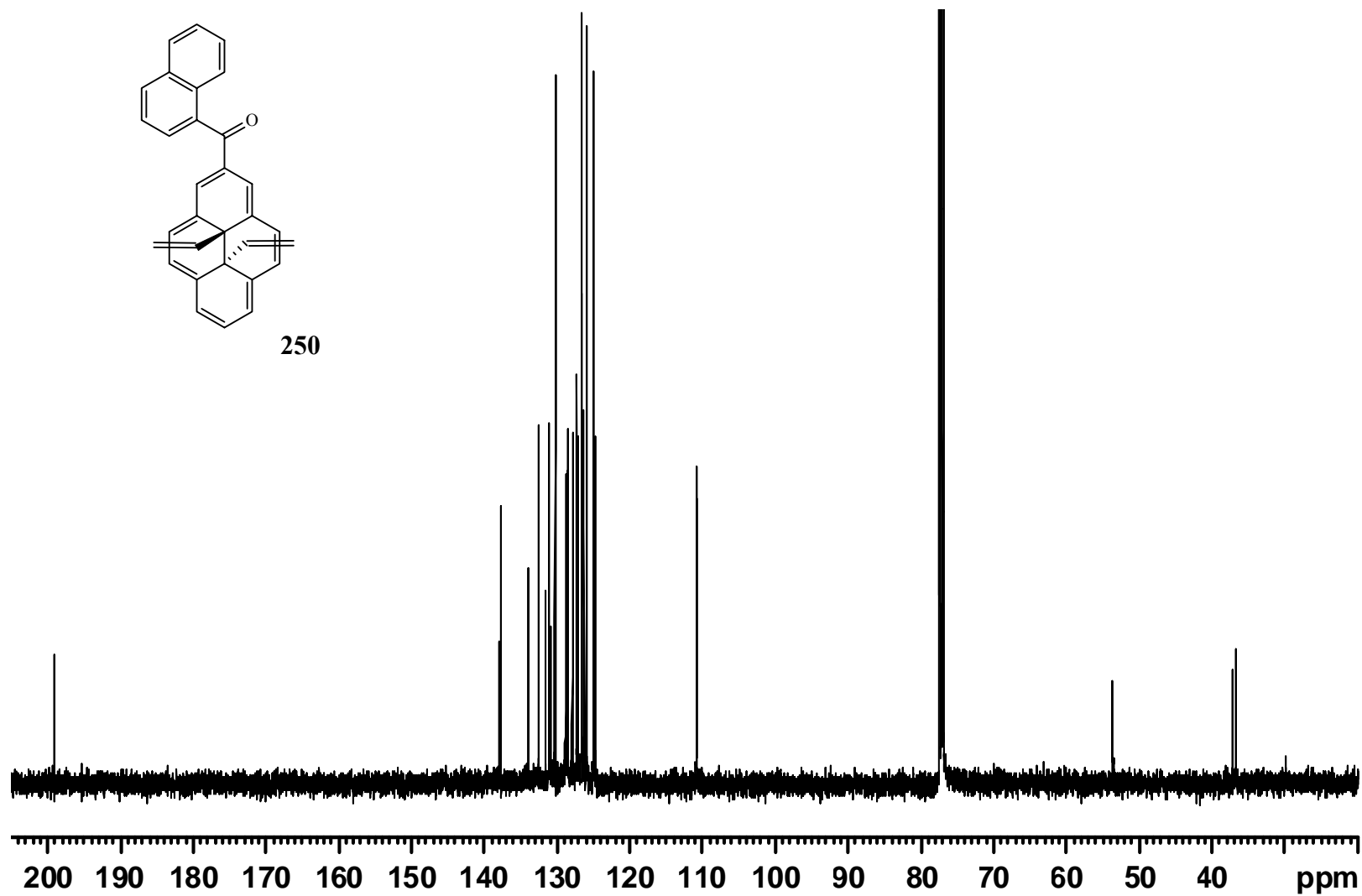


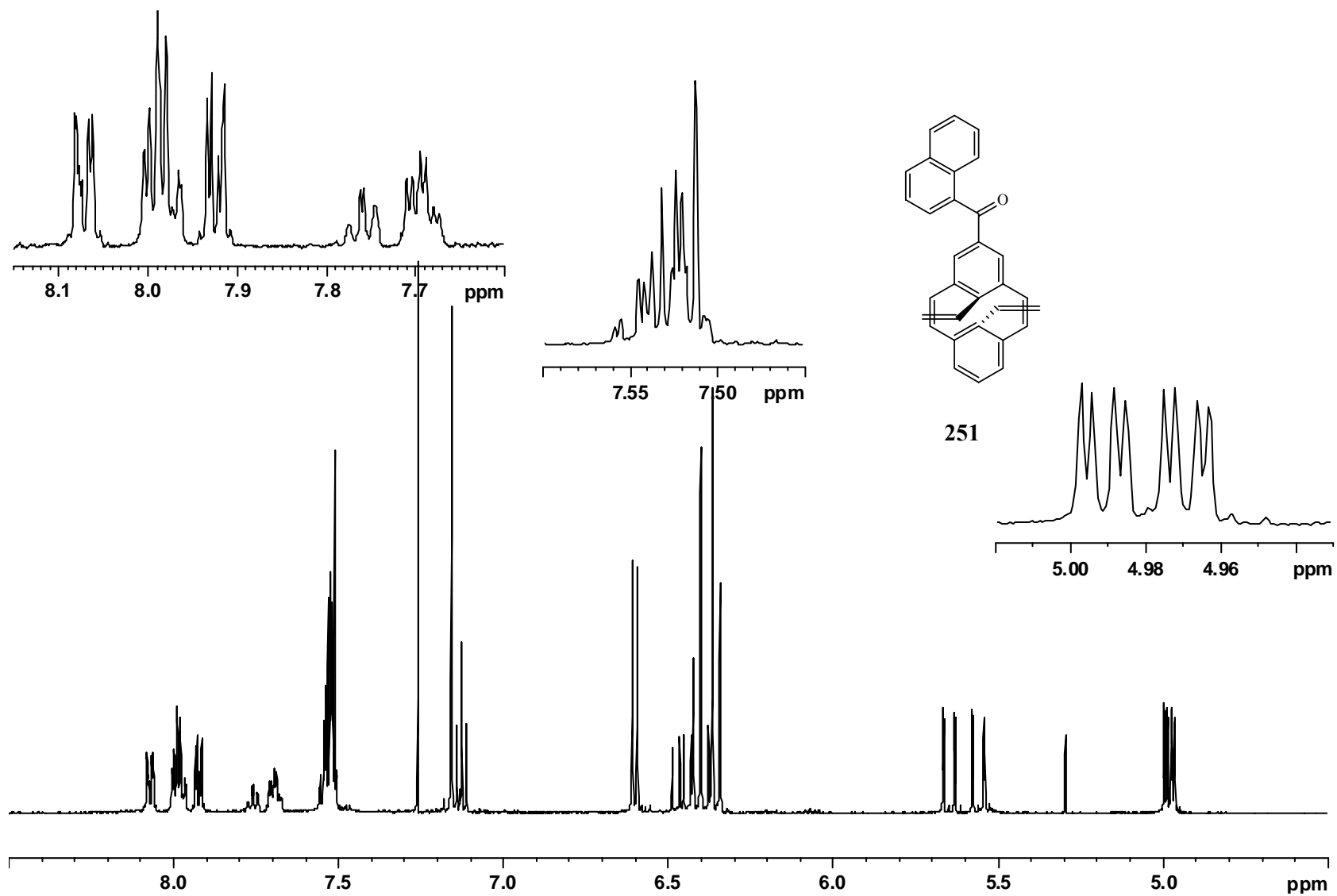


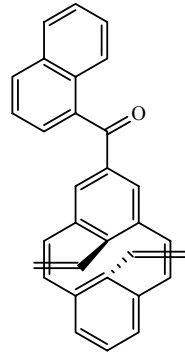




250







251

